AFML-TR-76-137
Volume I

12/NA

AD A039883

FRACTURE MECHANICS EVALUATION OF B-1 MATERIALS

Volume I
TEXT

ROCKWELL INTERNATIONAL
B-1 DIVISION
LOS ANGELES, CALIFORNIA

DDC

OCTOBER 1976

Approved for public release; distribution unlimited

AD NO.
DDC FILE COPY

AIR FORCE MATERIALS LABORATORY
AIR FORCE WRIGHT AERONAUTICAL LABORATORIES
AIR FORCE SYSTEMS COMMAND
WRIGHT-PATTERSON AIR FORCE BASE, OHIO 45433

NOTICE

When Government drawings, specifications, or other data are used for any purpose other than in connection with a definitely related Government procurement operation, the United States Government thereby incurs no responsibility nor any obligation whatsoever; and the fact that the government may have formulated, furnished, or in any way supplied the said drawings, specifications, or other data, is not to be regarded by implication or otherwise as in any manner licensing the holder or any other person or corporation, or conveying any rights or permission to manufacture, use or sell any patented invention that may in any way be related thereto.

This report has been reviewed by the Information Office (IO) and is releasable to the National Technical Information Service (NTIS). At NTIS, it will be available to the general public, including foreign nations.

This technical report has been reviewed and is approved for publication.

Allan W. Gunderson
ALLAN W. GUNDERSON
Engineering and Design Data
Materials Engineering Branch

Clayton L. Harmsworth
CLAYTON L. HARMSWORTH
Technical Manager
Engineering and Design Data

FOR THE COMMANDER

Albert Olevitch
A. OLEVITCH
Chief, Materials Engineering Branch
Systems Support Division

(AFSC 80-20)

Copies of this report should not be returned unless return is required by security considerations, contractual oblications, or notice on a specific document.

AIR FORCE - 18 APRIL 77 - 350

UNCLASSIFIED

SECURITY CLASSIFICATION OF THIS PAGE (When Data Entered)

REPORT DOCUMENTATION PAGE

READ INSTRUCTIONS BEFORE COMPLETING FORM

1. REPORT NUMBER: AFML-TR-76-137-Vol-1	2. GOVT ACCESSION NO.
	3. RECIPIENT'S CATALOG NUMBER
4. TITLE (and Subtitle): Fracture Mechanics Evaluation of B-1 Materials. I	5. TYPE OF REPORT & PERIOD COVERED: Documentary Report December 1970 to April 1975
	6. PERFORMING ORG. REPORT NUMBER: NA-74-862-Vol-1
7. AUTHOR(s): R. R. Ferguson, R. C. Berryman	8. CONTRACT OR GRANT NUMBER(s): F33657-70-C-0800
9. PERFORMING ORGANIZATION NAME AND ADDRESS: Rockwell International, B-1 Division, Los Angeles, California 90009	10. PROGRAM ELEMENT, PROJECT, TASK AREA & WORK UNIT NUMBERS
11. CONTROLLING OFFICE NAME AND ADDRESS: Aeronautical Systems Division (YHE), Wright-Patterson AFB, Ohio 45433	12. REPORT DATE: October 1976
	13. NUMBER OF PAGES: 744 Volume 1
14. MONITORING AGENCY NAME & ADDRESS (if different from Controlling Office): Air Force Materials Laboratory (MXE), Wright-Patterson AFB, Ohio 45433	15. SECURITY CLASS. (of this report): Unclassified
	15a. DECLASSIFICATION/DOWNGRADING SCHEDULE

16. DISTRIBUTION STATEMENT (of this Report)

Approved for public release; distribution unlimited

17. DISTRIBUTION STATEMENT (of the abstract entered in Block 20, if different from Report)

18. SUPPLEMENTARY NOTES

This report was prepared to document the materials evaluation efforts required to support the application of Fracture Mechanics Design Methodology to the B-1 Strategic Bomber.

19. KEY WORDS (Continue on reverse side if necessary and identify by block number)

Fracture Mechanics; Crack Growth; Fracture Toughness; Stress Corrosion; Materials Evaluation

20. ABSTRACT (Continue on reverse side if necessary and identify by block number)

A total of 1764 fracture mechanics tests ~~K_{IC}, K_c, K_{Iscc}, and da/dN~~ were conducted on fourteen alloys to develop property data for use in the B-1 design. Tests were performed on aluminum alloys 2024, 2124, 2219, 7049, 7050, 7075 and 7175; titanium alloy Ti-6Al-4V; steel alloys 9Ni-4Co-.20C, 9Ni-4Co-.30C and 300M; corrosion resistant steel PH13-8Mo; nickel alloy Inconel 718; and nickel-cobalt alloy MP 35 N. The effects of product form, heat-to-heat variability, grain orientation, and heat treat condition on fracture behavior were investigated. In addition, the fracture properties

over

DD FORM 1 JAN 73 1473 EDITION OF 1 NOV 65 IS OBSOLETE

UNCLASSIFIED

SECURITY CLASSIFICATION OF THIS PAGE (When Data Entered)

of welds in Ti-6Al-4V, PH13-8Mo and 9-4-.20 alloys and of diffusion bonds in Ti-6Al-4V were determined. Testing variables were temperature, specimen thickness, environment, cyclic frequency and R factor for the da/dN tests, temperature and specimen thickness for the K_c tests; temperature for the K_{Ic} tests; and environment for the K_{Iscc} tests.

The results of the tests are presented in tables and graphs in detailed and summarized forms. The effects of the various material and testing variables on fracture behavior are discussed.

ACCESSION for
NTIS White Section
DDC Buff Section
UNANNOUNCED
JUSTIFICATION
DISTRIBUTION/AVAILABILITY CODES
AVAIL. and/or SPECIAL
A

FOREWORD

This work was performed by Rockwell International under USAF Contract No. F33657-70-C-0800 in support of the application of fracture mechanics design requirement to the B-1 Strategic Bomber. The Air Force review team which directed this activity was headed by Mr. C. F. Tiffany, ASD/ENF and included the following personnel:

Mr. B. R. Meadows	B-1 SPO
Sgt. R. Bullock	B-1 SPO
Mr. M. A. Owens	B-1 SPO
Mr. H. W. Wood	AFFDL/FBE
Mr. N. G. Tupper	AFML/LLS
MR. A. W. Gunderson	AFML/MXE

The Rockwell International personnel primarily involved in this test effort included Mr. N. Klimmek, Dr. A. Summers, Mr. W. Padian, Mr. R. Ferguson, Mr. M. Katcher, Dr. L. Kasher, Mr. M. Harrigan, and Mr. J. Young, all of the Materials and Producibility Group, and Mr. G. Fitch of the Fatigue and Fracture Design Group.

The body of the report was assembled by Rockwell International as NA-74-862 to document this significant testing effort. Because of the wide scope of materials included and the general interest in the fracture mechanics data it was deemed appropriate to provide a wider distribution by releasing this document as an Air Force Materials Laboratory Technical Report.

The test program was conducted from December 1970 to December 1974. Testing in the program was performed by the Rockwell International Laboratories, Los Angeles, California; by the Air Force Materials Laboratory, WPAFB, Ohio; by the University of Dayton Research Institute, Dayton, Ohio; by the Lockheed California Company, Saugus, California, and by General Dynamics, Fort Worth, Texas.

TABLE OF CONTENTS

TABLE OF CONTENTS

TABLE OF CONTENTS

TABLE OF CONTENTS

LIST OF FIGURES

LIST OF FIGURES

LIST OF FIGURES

LIST OF TABLES

LIST OF TABLES

LIST OF TABLES

LIST OF TABLES

SECTION I INTRODUCTION

1.1 PROGRAM BACKGROUND

The B-1 supersonic bomber is unique in that it is the first military aircraft system to formally require application of the principles of fracture mechanics as an integral part of the entire air vehicle structural design process from initiation of the contract. The objective of the B-1 fracture mechanics requirement is to obtain significant improvements in aircraft safety and durability by modification of the conventional design, material and process selection and control and nondestructive inspection approaches used for primary structure in previous aircraft.

The fracture mechanics section of the Statement of Work as delineated in NA-71-958 requires that "a system of procedures and specifications sufficient to preclude utilization of material with inadequate toughness in critical areas" be developed and implemented. This requirement has had a significant impact on the selection and control of the materials and processes utilized for fabrication of B-1 primary structure. As shown schematically in Figure 1-1, the toughness of all materials for fracture critical parts is now controlled by Material Specifications while the toughness of certain designated critical parts is also verified after processing in accordance with the appropriate Material Processing Specification. All primary structure is now analysed using fracture mechanics analysis techniques in addition to conventional static and fatigue analyses in order to identify those parts to be designated as fracture critical.

At the inception of the B-1 program, only limited fracture mechanics test data was available pertaining to the materials of interest. Development of an extensive material properties data bank was one of the pacing items for conducting the design analyses and developing the Material and Processing Specifications. A comprehensive test program was, therefore, conducted by the Materials and Producibility Department to develop fracture mechanics test data for the aluminum, titanium and steel structural alloys used in the B-1 airframe. Additionally, the effects of the welding and diffusion bonding processes on fracture properties were evaluated for the appropriate alloys.

Testing to generate materials fracture mechanics data was initiated in December of 1970 and continued for the next four years reaching its peak during the years 1972 and 1973. In the latter part of 1971 an agreement was reached with the B-1 SPO Structural Review Committee which resulted in a plan which outlined materials testing requirements. This plan is shown in Appendix A of NA-71-958. Revisions were made to the plan during 1973 to update it to the evolving B-1 design. A total of 1804 tests were conducted including 1764 material property tests (K_{Ic}, K_c, K_{Iscc} and da/dN) and 40

fatigue crack growth spectrum loading tests to establish life-prediction models. The fatigue crack growth spectrum loading test results are described separately in References (a) and (b).

The material fracture mechanics data described in this report were used in conjunction with other available information (e.g., QC and literature data) to set allowable property limits for use in design. This report documents the results of all material property fracture mechanics tests and provides a record of data used in establishing design allowables.

1.2 PROGRAM OUTLINE

The material tests were conducted on a total of fourteen alloys: aluminum alloys 2024, 2124, 2219, 7049, 7050, 7075 and 7175 in selected tempers; titanium alloy Ti-6Al-4V; steel alloys 9Ni-4Co-.20C, 9Ni-4Co-.30C, and 300M; corrosion resistant steel PH13-8Mo; nickel base alloy Inconel 718; and a fastener material MP35N.

The effect of product form, heat-to-heat variability, and grain orientation on fracture behavior was investigated. In addition, the fracture properties of welds in Ti-6Al-4V, PH13-8Mo, and 9-4-.20 alloys and of diffusion bonds in Ti-6Al-4V were determined. Also, the effects of various heat treatments on the fracture behavior of Ti-6Al-4V and 9-4-.20 were investigated. Approximately 30% of the program effort was directed toward evaluations on thirty-one lots of Ti-6Al-4V alloy while another 30% of the effort was directed toward evaluations on seven or more lots each of 2024/2124, 9-4-.20 and PH13-8Mo.

Four types of fracture mechanics tests were conducted in the program -- K_{Ic}, da/dN, K_{Iscc} and K_c. K_{Ic} and da/dN data were obtained on nearly every lot of material, while K_c tests were generally run on only one lot of each alloy and K_{Iscc} tests on not more than two lots of each alloy. Testing temperatures for the K_{Ic}, K_c and da/dN tests ranged from -65F to 400F. The K_{Iscc} tests were conducted at room temperature, usually in an environment of a simulated fuel tank sump residue water, and occasionally in metal cleaning liquids. Most of the da/dN tests were in a low humidity air or a simulated sump residue water environment with limited testing in environments of laboratory air, 100% humidity, air, distilled water, JP-4, and metal cleaning liquids. For the da/dN tests, load R-factors were generally .08, .3 or .5, and cycling loading frequencies were generally 60 or 360 cpm.

The specimens used in the testing were of four types: CT, CCT, DCB and PTC (Figure 1-2). The DCB specimens were utilized for the K_{Iscc} determinations and were loaded to a constant deflection by means of bolts. The CCT specimen configuration was used for the K_c and da/dN tests on sheet

and welds in sheet, because CT sheet specimens buckle under these test conditions. The CT specimen configuration was used for the K_{Ic}, K_c and da/dN tests on bars, plates, forgings and extrusions since these product forms had adequate thickness to avoid buckling. The specimens used for the K_{Ic} and da/dN tests on weld joints in bars, plates, forgings, and extrusions were mostly of the PTC geometry, although a few were of the CT configuration.

Table 1-1 summarizes the testing in the program by listing for each alloy the product forms and number of material lots evaluated and the types and number of tests conducted.

Table 1-1

FRACTURE MECHANICS MATERIAL TEST PROGRAM SUMMARY

Materials	No. of Lots of Indicated Product Form					Number of Tests								Total Specimens
						K_{Ic}		K_c		K_{Iscc}	ΔK vs. da/dN			
	Sheet	Plate	Extru-sion	Rolled or Forged Bar	Forg-ing	CT	PTC	CT	CCT	DCB	CT	CCT	PTC	
Ti-6Al-4V	2	23	2		4	184	-	24	8	63	122	9	-	410
Ti-6Al-4V GTA Weld	1	6	1			11	38	-	2	29	5	2	36	123
2024/2124	2	8			2	86	-	17	11	19	55	16	-	204
2219		6	1		1	56	-	9	-	15	40	-	-	120
7075-T76xxx	2	5	1			50	-	10	5	9	25	8	-	107
7075-T73xxx			2		1	30	-	14	-	8	31	-	-	83
7049					3	10	-	4	-	13	14	-	-	41
7175					2	10	-	-	-	12	18	-	-	40
7050		1			1	12	-	-	-	2	6	-	-	20
HP-9Ni-4Co-0.20C		2		6	3	99	-	10	-	20	40	-	-	169
HP-9-4-20 GTA Weld		2			1	5	27	-	-	12	7	-	20	71
HP-9Ni-4Co-0.30C				2		32	-	-	-	-	20	-	-	52
PH13-8Mo			1	5	1	83	-	14	-	47	35	-	-	179
PH13-8Mo GTA Weld			1	1		8	14	-	-	21	4	-	8	55
300M					1	15	-	-	-	12	17	-	-	44
Inconel 718				1	1	20	-	-	-	8	14	-	-	42
MP35N				1		1	-	-	-	3	-	-	-	4
Total Specimens/Category						712	79	102	26	293	453	35	64	1,764

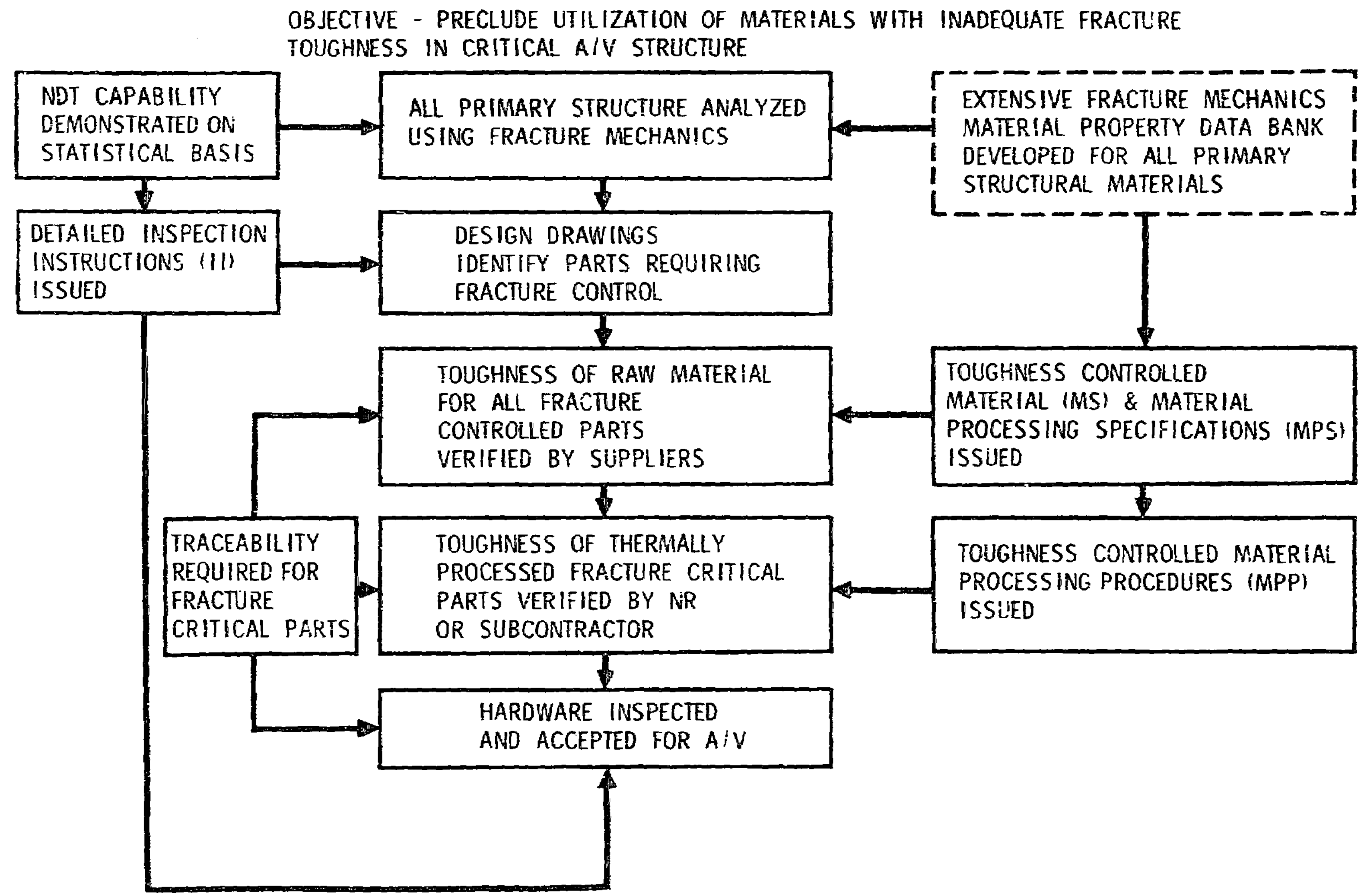

Figure 1-1 B-1 RDT&E Fracture Control System

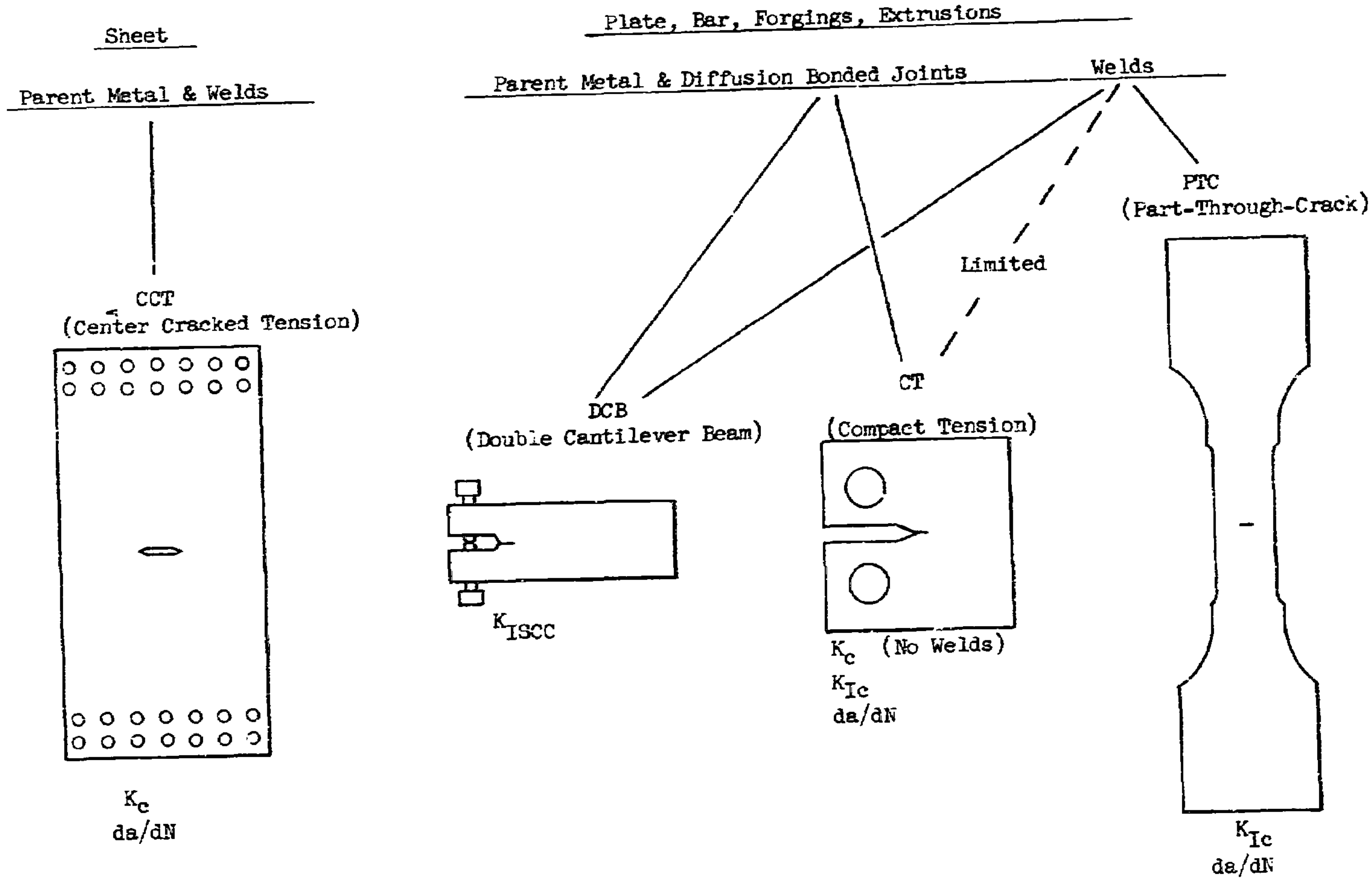

Figure 1-2 Specimen Configurations Used for the Various Tests and Alloy Prcluct Forms

SECTION 2 - MATERIALS: DESCRIPTIONS AND PROCESSING

2.1 MATERIAL AND SPECIMEN IDENTIFICATION SYSTEM

Tests were conducted on over 90 lots of alloy in the program. As each lot of material was received it was assigned a material number, which became the first number in the identification system of each specimen fabricated from that lot. The specimen numbering system, described below, provided precise traceability back to the specimen location in the original lot of material.

4	K	RW	9-32
Material Number (lot identification number)	Type of Test K = K_{Ic} or K_c N = da/dN E = K_{Iscc}	Specimen Orientation (Figure 2.1-1)	Identifies specimen location within a material lot (piece number on layout drawing)

For weldments, the specimen orientation is that of the parent metal in the specimen. For diffusion bond joints, two specimen orientations are shown in the specimen number separated by a slash number (e.g.,RW/TR) to show the orientation of the parent metal on each side of the joint.

2.2 TEST MATERIAL DESCRIPTION

The following information is presented in the indicated tables on the various lots of test materials. Coding is to the lot identification number (material number) in the tables.

Product Form and Size As Received Condition Procurement Specification Material Producer Heat Number	Table 2.2-1
Chemical Analysis	Table 2.2-2
Tensile Properties (Parent Metal)	Table 2.2-3
Tensile Properties (Weld Joints)	Table 2.2-4
Microstructures (Ti-6Al-4V Only)	Figure 2.2-1

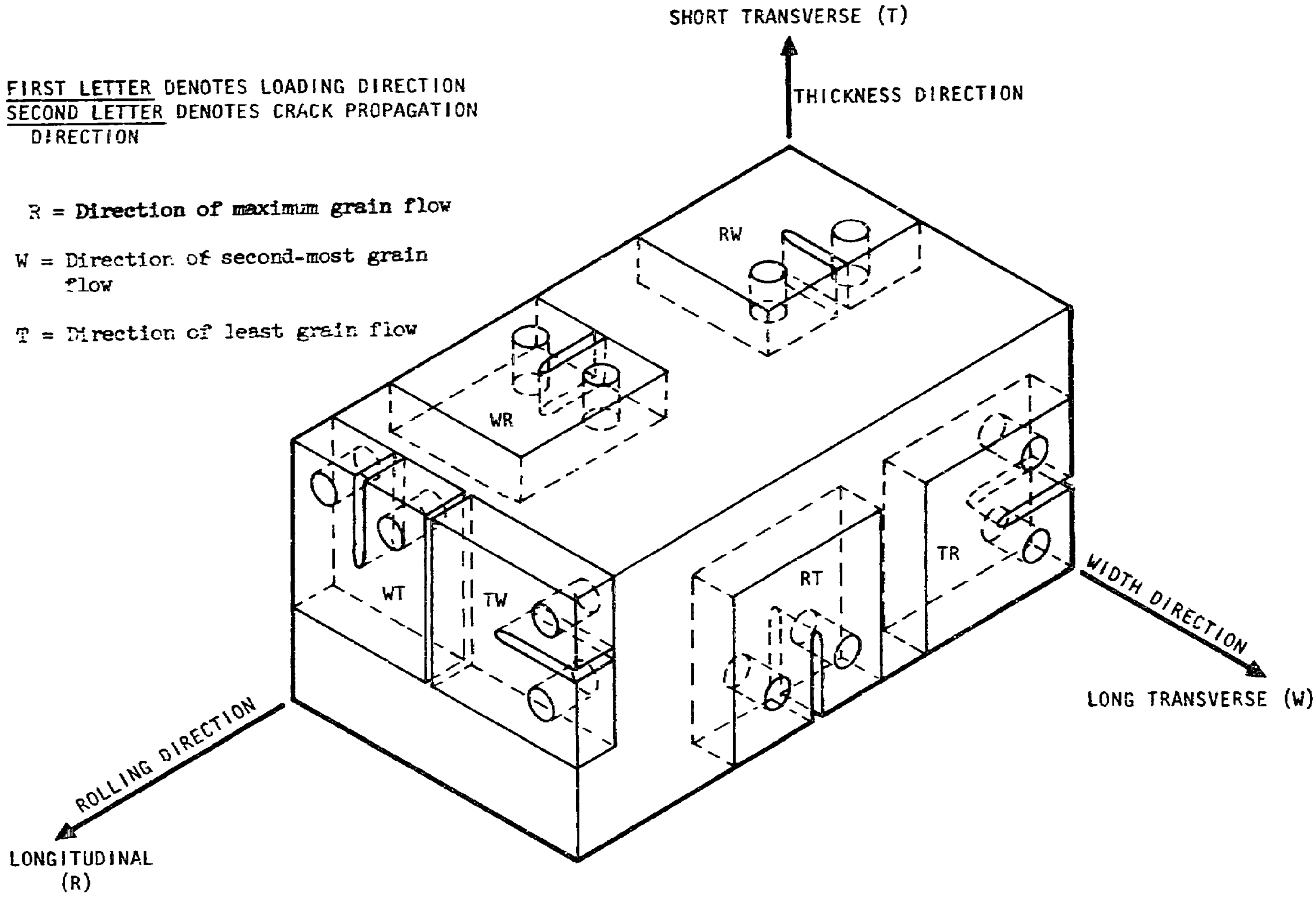

Figure 2.1-1 Specimen Orientation Relationships for Fracture Toughness Testing

The various lots of test material are grouped according to alloy in the tables. The alloys are arranged in the following sequence within a table:

Ti-6Al-4V	7050	PH13-8Mo
2024	7075	300M
2124	7175	Inconel 718
2219	9-4-20	MP 35N
7049	9-4-30	

Within an alloy, the various material lots are arranged in order of increasing material number.

When test results are presented in this report, the identification number of the material lot is given. By referring to this number in the above tables, a detailed description of the test material is available.

Table 2.2-1 (Page 1 of 8)

DESCRIPTION OF TEST MATERIALS

Matl. No.	6Al-4V TITANIUM ALLOY Form	Size	Condition	Procurement Specification	Producer	Heat No.
61-62	Plate	.625"	Mill Annealed (MA)	MIL-T-9046	TMCA	K6271
63	Plate	1-1/4"	Beta Processed +MA	MIL-T-9046	Carlson	HC442-1
64	Extrusion	24 Pounds/Foot	Beta Ext + MA	AMS4935	Harvey	BH-01
65	Plate	1.312"	Mill Annealed	MIL-T-9046	RMI	294773
66	Plate	1-1/2" x 16"	Beta Process + MA	XBMS 7-174	RMI	295500
67	Plate	1-1/2"	Recrystallization Annealed	ST0170LB0032	TMCA	K8294
68	Plate	2"	Mill Annealed	ST0170LB0032	RMI	295470-02
69	Plate	3-1/2"	Mill Annealed	ST0170LB0032	RMI	295470-01
70	Plate	1-1/2"	Recrystallization Annealed	ST0170LB0032	TMCA	K8574
71	Plate	1.312"	Annealed	MIL-T-9046	RMI	303816
72	Plate	1-1/2"	Recrystallization Annealed	ST0170LB0032	RMI	304610
74	Diffusion Bonded	billet of material	70 plate			
75	Extrusion	34 Pounds/Foot	Beta Extruded + Mill Annealed	DMS 1650	Harvey	BR-27

NOTE: Material 61-62 consisted of two plates from the same material lot. One plate was identified as material 61 and the other as material 62.

Table 2.2-1 (Page 2 of 8)

DESCRIPTION OF TEST MATERIALS

Matl. No.	6Al-4V TITANIUM ALLOY Form	Size	Condition	Procurement Specification	Producer	Heat No.
76	Plate	1-1/2"	Recrystallization Anneal	ST0170LB0032	Crucible	G50860
77	Plate	2-1/2"	Recrystallization Anneal	ST0170LB0032	Ladish*	K9540
78	Plate	.750" x 36" x 120"	Recrystallization Anneal	ST0170B0032	RMI	295891
79	Hand Forging	4" x 10" x 34"	Recrystallization Anneal	ST0170LB0037	Shultz**	C3696
80	Sheet	.100" x 25" x 144"	Mill Anneal	ST0170LB0032	TMCA	K8691
81	Sheet	.100" x 25" x 144"	Mill Anneal	ST0170LB0032	RMI	600135
82	Hand Forging	4" x 10" x 34"		ST0170LB0037	Shultz**	
84	Die Forging	575 Pounds	Recrystallization Anneal	ST0170LB0037	Alcoa	800060
85	Die Forging	350 POUNDS	Recrystallization Anneal	ST0170LB0037	Ladish	K9588
86	Plate	.375" x 72" x 88"	Recrystallization Anneal	ST0170LB0032	TMCA	N0548
87	Plate	1.500"	Recrystallization Anneal	ST017CLB0032	TMCA	K8577

* MCA Material Forged by Ladish

** Titanium West Material Forged by Shultz

Table 2.2-1 (Page 3 of 8)

DESCRIPTION OF TEST MATERIALS

Matl. No.	6AL-4V Titanium Form	Size	Condition	Procurement Specification	Producer	Heat No.
88	Plate	1.250"	Recrystallization Anneal	ST0170LB0032	RMI	304623
89	Plate	1.250"	Recrystallization Anneal	ST0170LB0032	TMCA	K8540
90	Plate	2.250"	Recrystallization Anneal	ST0170LB0032	RMI	304613
92	Plate	2.500"	Recrystallization Anneal	ST0170LB0032	TMCA	K9546
253	Plate	2.500"	Recrystallization Anneal	ST0170LB0032	RMI	890253
294	Plate	1.250"	Recrystallization Anneal	ST0170LB0032	RMI	890294
7406	Plate	2.000"	Recrystallization Anneal	ST0170LB0032	TMCA	K9892
7768	Plate	.750"	Recrystallization Anneal	ST0170LB0032	TMCA	K9983

Table 2.2-1 (Page 4 of 8)

DESCRIPTION OF TEST MATERIALS

2024-2124 ALUMINUM ALLOY

Matl. No.	Form	Size	Condition	Procurement Specification	Producer	Heat No.
1	Plate	3" x 48"	T351	QQ-A-250/4	Alcoa	610-571
2	Plate	3" x 36"	T351	QQ-A-250/4	Alcoa	632-821
3	Plate	3" x 48"	T351	QQ-A-250/4	Reynolds	DK50803-0
6	Plate	1-3/4" x	T351			
8	Plate	3-1/2" x 36"	T851	QQ-A-250/4	Kaiser	406721
9	Plate	3"	T851			
19	Hand Forgi g	3" x 18" x 23"	T852	ST0170LB0019	Premco	P922
27	Hand Forging	3" x 18" x 35"	T852	ST0170LB0019	Premco	P923
302	Sheet	.100" x 48"	T81	QQ-A-250/4	Kaiser	781921
303	Sheet	.100" x 48"	T81	QQ-A-250/4	Kaiser	740881
12 (2124	Plate	3" x 36"	T351	QQ-A-250/4	Alcoa	638-931
14 (2124	Plate	2" x 10" x 14"	T851	None	Kaiser	182745

Table 2.2-1 (Page 5 of 8)

DESCRIPTION OF TEST MATERIALS

Matl. No.	Form	Size	Condition	Procurement Specification	Producer	Heat No.
	2219 ALUMINUM ALLOY					
4	Plate	2" x 36"	T851	MIL-A-8920	Reynolds	7150190
7	Plate	1.750" x 48"	T851	MIL-A-8920	Reynolds	7150189
13	Plate	3.000" x 36"	T351	MIL-A-8920	Alcoa	641-041
16	Extruded Bar	1-3/4" x 7-1/2"	T8511	AMS 4162	Alcoa	K38362A1
17	Plate	2" x 48"	T351	MIL-A-8920	Alcoa	647-861
20	Hand Forging	6" x 12" x 48"	T852	QQ-A-367	Alcoa	724-509
304	Plate	3.000" x 36"	T851	ST0170LB0033	Alcoa	102-109
314**	Plate	2.55" x 112" x 604"	T851	ST0170LB0033	Reynolds	7350745
	7049 ALUMINUM ALLOY					
10	Die Forging		T73		Kaiser	DF4462
24	Die Forging	24 Pounds	T73	QQ-A-367	Harvey	9074-1
25	Hand Forging	3" x 24" x 48"	T7352	QQ-A-367	Alcoa	455-302
	7050 ALUMINUM					
23	Die Forging	24 Pounds	T73	QQ-A-367	Harvey	9075-1
28	Plate	4" x 24" x 24"	T73651	*	Alcoa	MK04964

*No Specification Established When Procured

** Trim material from a B-1 one piece wing lower cover

Table 2.2-1 (Page 6 of 8)

DESCRIPTION OF TEST MATERIALS

Matl. No.	Form	Size	Condition	Procurement Specification	Producer	Heat No.
	7075 ALUMINUM ALLOY					
5	Plate	2" x 48"	T7651	QQ-A-250/12		
15	Plate	.600" x 10" x 13"	T7651		Kaiser	902511
18	Plate	2" x 36"	T7651	ST0170LB0036	Reynolds	7153066
22	Die Forging	24 Pounds	T73	QQ-A-367	Harvey	9076-1
29	Extrusion	3" x 17" Shape	T73511	ST0170LB0041	Alcoa	K394140-1
30	Sheet	.100" x 48"	T76	ST0170LB0036	Kaiser	594491
301	Sheet	.100" x 42"	T76	ST0170LB0036	Kaiser	018051
306	Plate	2.500" x 48"	T7651	ST0170LB0036	Kaiser	032643
307	Plate	2.250" x 48"	T7651	ST0170LB0036	Kaiser	669561
309	Extruded Bar	3" x 8"	T76511	ST0170LB0031	Harvey	92-850901
311	Extrusion	3" x 17" Shape	T73511			A30349A-1
	7175 ALUMINUM ALLOY					
21	Die Forging	24 Pounds	T736	QQ-A-367	Harvey	9077-1
26	Hand Forging	6" x 13-1/2" x 48"	T73652		Alcoa	

Table 2.2-1 (Page 7 of 8)

DESCRIPTION OF TEST MATERIALS

Matl. No.	Form	Size	Condition	Procurement Specification	Producer	Heat No.
	HP-9Ni-4Co-0.20C STEEL					
31	Forged Bar	3" x 18" x 36"	Annealed	AMD-65-CD	Republic	3923286
33	Forged Bar	4" x 18" x 36"	Annealed	AMD-65-CD	Republic	3821290
37	Rolled Plate	2.50" x 33"	Annealed	ST0160LB0001	Republic	3821290
42	Forging	5000 Pounds	Annealed	ST0160LB0002	Wyman-Gordon**	3831586
43	Forged Bar	4" x 18" x 36"	Annealed	ST0160LB0002	Shultz*	3811379
46	Forged Bar	4" x 8"	Annealed	ST0160LB0002	Latrobe	61168
48	Forged Bar	4" x 18" x 36"	Annealed	ST0160LB0002	Shultz*	3811378
49	Forging	5000 Pounds	Annealed	ST0160LB0002	Wyman-Gordon**	3831586
52	Forging	130 Pounds	Annealed	LB0160-180	Shultz*	3831944
57	Rolled Plate	1.50"	Annealed	ST0160LB0001	Republic	3821290
59	Forged Bar	3 x 12"	Annealed	AMD-65-CD	Republic	3910462
	HP-9Ni-4Co-0.30C STEEL					
32	Forged Bar	3" x 18"	Annealed	AMD-65-CE	Republic	3911026
35	Forged Bar	3" x 18"	Annealed	AMD-65-CE	Republic	3932218

* Republic Material Forged by Shultz
** Republic Material Forged by Wyman-Gordon

Table 2.2-1 (Page 8 of 8)

DESCRIPTION OF TEST MATERIALS

Matl. No.	Form	Size	Condition	Procurement Specification	Producer	Heat No.
	PH13-8Mo STEEL					
36	Forged Bar	4" x 5"	Solution Treated	AMS 5629	Armco	3W0588
40	Rolled Bar	1-1/2" x 12"	Solution Treated	ST0160LB0005	Armco	2W0659
41	Extruded Bar	1-1/2" x 8"	Solution Treated	ST0160LB0005	Armco	WX0650
44	Forged Billet	22" Dia. x 6"	Solution Treated	AMS 5629	Reisner*	1X0644
50	Forged Bar	2-1/4" x 4"	Solution Treated	AMS 5629	Armco	1X0614
54	Rolled Bar	1-1/2" Dia.	Solution Treated	ST0160LB0013	Armco	2W0828
56	Rolled Bar	1-1/2" Dia.	Solution Treated	ST0160LB0013	Armco	1W0824
	300M STEEL					
39	Forged	3" x 36" x 72"	Annealed	MIL-S-8844	Republic	3831047
	INCONEL 718					
51	Forged Bar	4" x 8"	Solution Treated	LB0170-186	Reisner	91684
53	Die Forging	65 Pounds	185 ksi Min.	LB0170-186	Arcturus	92059
	MP 35N					
55	Bar	1-1/2" Dia.	Cold Worked	AMS 5758	S.P.S.	FT-181P

* Armco Material Forged by Reisner

Table 2.2-2 (Page 1 of 8)

6Al-4V TITANIUM ALLOY CHEMISTRY OF TEST MATERIALS

Matl. No.	Heat No.	C	Fe	N	Al	V	H	O_2	Ti	Source
61-62	K6271	.026	.23	.016	6.4	4.1	.003	.20	Bal.	TMCA
63	HC442-1	.017	.20	.012	6.3	4.1	.002	.14	Bal.	Carlson
64	BH-01	.024	.19	.012	6.5	4.1	.006	.15	Bal.	Harvey
65	294773	.020	.18	.012	6.2	4.2	.004	.16	Bal.	RMI
66	295500			XBMS7-174						Boeing
67	K8294	.220	.12	.011	6.0	4.0	.005	.08	Bal.	TMCA
68	295470-02	.010	.18	.010	6.4	4.3	.004	.12	Bal.	RMI
69	295470-01	.020	.17	.010	6.4	4.2	.005	.12	Bal.	RMI
70	K8574	.026	.06	.009	5.9	3.9	.004	.11	Bal.	TMCA
71	303816			MIL-T-9046						RMI
72	304610	.010	.20	.009	6.1	3.9	.005	.13	Bal.	RMI
74	Diffusion bonded billet of material 70 plate									
75	BR-27	.022	.16	.009	6.3	4.3	.006	.16	Bal.	Harvey
76	G-50860	.028	.13	.011	5.9	4.0	.006	.09	Bal.	Crucible
77	K9540	.010	.16	.011	6.5	4.2	.002	.15	Bal.	Ladish
78	295891	.03	.20	.009	6.4	4.0	.010	.14	Bal.	RMI
79	C3696	.011	.10	.012	6.1	4.1	.001	.10	Bal.	Shultz

NOTE: Material 61-62 consisted of two plates (both 5/8" thick) from the same material lot. One plate was identified as material 61 and the other as material 62.

Table 2.2-2 (Page 2 of 8)

6Al-4V TITANIUM ALLOY CHEMISTRY OF TEST MATERIALS

Matl. No.	Heat No.	C	Fe	N	Al	V	H	O2	Ti	Source
80	K8691	.022	.12	.012	6.4	4.1	.011	.14	Bal.	TMCA
81	600135	.030	.19	.011	6.1	3.9	.006	.13	Bal.	RMI
82	11775	.02	.14	.013	5.9	4.1	.001	.12	Bal.	Shultz
84	800060	.02	.17	.012	5.9	4.0	.011	.13	Bal.	Alcoa
85	K9583	.01	.16	.013	6.2	4.1	.003	.15	Bal.	Ladish
86	N0548	.03	.08	.012	5.8	4.0	.010	.12	Bal.	TMCA
87	K8577	.03	.09	.012	5.8	3.8	-	.11	Bal.	TMCA
88	304623	.02	.17	.010	6.1	3.9	.006	.11	Bal.	RMI
89	K8540	.02	.09	.007	5.9	3.8	-	.11	Bal.	TMCA
90	304613	.02	.21	.008	6.0	4.0	.012	.12	Bal.	RMI
92	K9546	.01	.19	.010	6.5	4.1	.002	.15	Bal.	TMCA
253	890253	.01	.18	.007	6.0	4.0	.006	.12	Bal.	RMI
294	890294	.01	.19	.009	6.1	3.9	.009	.12	Bal.	RMI
7406	K9892	.02	.16	.011	6.3	4.2	.004	.13	Bal.	TMCA
7768	K9983	.03	.18	.010	6.1	4.2	.004	.13	Bal.	TMCA
Weld Filler Wire		.05 Max	.25 Max	.03 Max	5.50-6.50	3.50-4.50	.01 Max	.12 Max	Bal	ST0170GB0001

Table 2.2-2 (Page 3 of 8)

CHEMISTRY OF TEST MATERIALS

Matl. No.	Heat No.	Si	Cr	Mn	Cu	Ti	Zn	Mg	Fe	Al	Source
	2024 ALUMINUM ALLOY										
1	610-571	0.11	0.02	0.61	4.27		0.04	1.60	0.26	Bal.	B-1
2	632-821	0.11	0.02	0.60	4.37		0.06	1.36	0.27	Bal.	B-1
3	DK50803-C	0.12	0.03	0.64	4.80		0.05	1.36	0.28	Bal.	B-1
6		0.20	0.03	0.54	4.95		0.05	1.20	0.20	Bal.	B-1
8	406721	0.08	0.03	0.62	4.46		0.04	1.60	0.25	Bal.	B-1
9		0.11	0.02	0.59	4.27		0.05	1.56	0.26	Bal.	B-1
19	P-922	0.12	0.01	0.59	4.44	0.03	0.08	1.59	0.17	Bal.	Premco
27	P-923	0.20	0.02	0.59	4.30	0.03	0.08	1.55	0.39	Bal.	Premco
302	781921	(Fed. Spec. QQ-A-250/4)									
303	740881	(Fed. Spec. QQ-A-250/4)									
	2124 ALUMINUM ALLOY										
12	638-931	0.03	0.01	0.49	5.10	0.01	0.01	1.40	0.25	Bal.	B-1
14	182745	0.13	0.01	0.46	4.80	0.05	0.06	1.80	0.29	Bal.	B-1

Table 2.2-2 (Page 4 of 8)

CHEMISTRY OF TEST MATERIALS

Matl. No.	Heat No.	Si	Cr	Mn	Cu	Ti	Zn	Mg	Fe	Al	V	Zr	Source
2219 ALUMINUM ALLOY													
4	7150190	0.27	0.01	0.31	6.76	0.08	0.04	0.01	0.08	Bal.	0.08	0.15	B-1
7	7150189	0.22	0.01	0.31	6.68	0.07	0.04	0.01	0.07	Bal.	0.09	0.17	B-1
13	641-041	0.21	0.04	0.40	6.30	0.05	0.08	0.01	0.25	Bal.	0.10	0.15	B-1
16	522951 (J)	0.22	0.04	0.40	5.90	0.04	0.08	0.02	0.20	Bal.	0.10	0.10	B-1
20	724-509	0.10	0.02	0.40	6.10	0.04	0.07	0.01	0.25	Bal.	0.10	0.10	B-1
304	102-109			(ST0170LB0033)									
314	7350745			(ST0170LB0033)									
7049 ALUMINUM ALLOY													
10	DF4462	0.12	0.17	0.07	1.33	0.03	8.01	2.11	0.20	Bal.	-	-	B-1
24*	9074-1	0.05	0.02	0.01	2.40	0.03	7.70	2.70	0.09	Bal.	-	0.12	B-1
25	455-302		(ASM 4111)										
7050 ALUMINUM ALLOY													
23	9075-1	0.03	0.03	0.01	3.10	0.03	5.90	2.60	0.34	Bal.	-	-	B-1
28	MK04964**												

* Zr Modified 7049

** New Alloy - Certification Not Supplied or Run

Table 2.2-2 (Page 5 of 8)

CHEMISTRY OF TEST MATERIALS

7075 ALUMINUM ALLOY

Matl. No.	Heat No.	Si	Cr	Mn	Cu	Ti	Zn	Mg	Fe	Al	Source
5	08901	0.23	0.20	0.08	1.44	0.06	5.35	2.73	0.23	Bal.	B-1
15	902511	0.06	0.21	0.09	1.10	0.04	5.50	2.80	0.40	Bal.	B-1
18	7153066	0.08	0.20	0.05	1.00	0.05	4.80	2.40	0.50	Bal.	B-1
22	9076-1	0.06	0.21	0.01	1.40	0.03	5.30	2.40	0.34	-	B-1
29	K39414D-1		(ST0170LB0041)								
30	594491		(ST0170LB0036)								
301	018051		(ST0170LB0036)								
306	032643		(ST0170LB0036)								
307	669561		(ST0170LB0036)								
309	92-850901		(ST0170LB0031)								
311	A30349A-1		(ST0170LB0041)								
7175 ALUMINUM ALLOY											
21	9077-1	0.05	0.21	0.01	1.10	0.03	5.40	2.50	0.32	Bal.	B-1
26	EOPR 4580*		(ST0170LB0043)								

(*) B-1 Engineering Purchase Order

Table 2.2-2 (Page 6 of 8)

CHEMISTRY OF TEST MATERIALS

HP-9Ni-4Co-0.20C

Matl. No.	Heat No.	Ni	Co	C	Cr	Mo	Mn	V	P	S	Si	Cu	Fe	Source
31	3923286	9.09	4.48	.20	.77	.94	.29	.09	.008	.008	.02	.17	Bal.	Republic
33	3821290	9.40	4.52	.19	.85	.94	.29	.10	.005	.005	.05	.17	"	Republic
37	3821290	9.40	4.52	.19	.85	.94	.29	.10	.005	.005	.05	.17	"	Republic
42	3831586	9.15	4.30	.19	.73	.98	.29	.10	.005	.004	.06	.16	"	Wyman-Gordon
43	3811379	9.20	4.42	.19	.74	.92	.29	.09	.009	.004	.10	.15	"	Shultz
46	61168	9.04	4.53	.20	.73	1.08	.20	.09	.008	.003	.05	.06	"	Latrobe
48	3811378	9.23	4.45	.19	.74	.93	.26	.10	.009	.005	.10	.15	"	Shultz
49	3831586	9.15	4.30	.19	.73	.98	.29	.10	.005	.004	.06	.16	"	Wyman-Gordon
52	3831944	9.30	4.57	.19	.81	1.00	.38	.10	.007	.002	.10	.20	"	Shultz
57	3821290	9.45	4.44	.20	.89	.97	.27	.10	.003	.005	.06	.12	"	Republic
59	3910462	9.00	4.50	.18	.77	.95	.20	.08	.006	.009	.02	.15	"	Republic
Weld Filler Wire		9.75-10.25	3.50-4.00	.014-.017	.90-1.05	.40-.50	.40-.55	.06-.10	.008 Max	.008 Max	.15-.25		Bal	ST-17 GB 0001

HP-9Ni-4Co-0.30C

Matl. No.	Heat No.	Ni	Co	C	Cr	Mo	Mn	V	P	S	Si	Cu	Fe	Source
32	3911026	7.55	4.45	.33	1.08	1.03	.27	.08	.007	.010	.06	.32	BAL	Republic
35	3932218	7.45	4.54	.31	.97	1.05	.30	.06	.005	.008	.03	.12	"	Republic

Table 2.2-2 (page 7 of 8)

.. CHEMISTRY OF TEST MATERIALS

PH13-8Mo

Matl. No.	Heat No.	Cr	Ni	Mo	Si	C	Mn	S	P	V	Al	N	Source
36	3W0588	12.77	8.18	2.18	.02	.04	.025	.004	.002		1.13	.004	Armco
40	2W0659	12.78	7.99	2.14	.01	.04	.020	.004	.003		1.15	.002	Armco
41	WX0650	12.68	8.17	2.18	.01	.04	.030	.004	.001		1.16	.003	Armco
		12.86	8.09	2.25	.04	.03	.025	.004	.007		1.12	.003	Atlas
44	1X0644	12.90	8.18	2.14	.02	.05	.020	.003	.004		1.22	.003	Reisner
50	1X0614	12.73	8.30	2.24	.02	.04	.020	.003	.001		1.17	.003	Armco
54	2W0828	12.69	8.15	2.13	.01	.04	.010	.004	.002		1.14	.002	Armco
56	1W0824	12.88	8.36	2.19	.01	.04	.010	.004	.002		1.22	.002	Armco
Weld Filler Wire		12.25-13.25	7.50-8.50	2.00-2.50	.10 Max	.05 Max	.10 Max	.010 Max	.008 Max		.90-1.35	.01 Max	ST0170GB 0001

Table 2.2-2 (Page 8 of 8)

CHEMISTRY OF TEST MATERIALS

300 M

Matl. No.	Heat No.	C	Mn	P	S	Si	Ni	Cr	Mo	V	Source
39	3831047	.42	.77	.008	.007	1.56	1.75	.88	.40	.08	Republic

INCONEL 718

Matl. No.	Heat No.	Co	Al	C	Cr	CB/Ta	Cu	Mn	Mc	Ni	Si	Ti	S	Fe	Source	P	B
51	81684	.16	.48	.04	18.1	5.24	.10	.10	3.15	53.5	.10	1.00	.005	18.2	Reisner	.01	.003
53	92059	.29	.53	.05	18.0	5.27	.10	.10	3.00	52.8	.10	1.06	.003	Bal.	Arcturus	.01	.003

MP35N

Matl. No.	Heat No.	C	Mn	Si	P	S	Cr	Ni	Mo	Ti	Fe	Co	Source
55	FT-181P		AMS 5758										

Table 2.2-3 (Page 1 of 16)

TENSILE PROPERTIES OF TEST MATERIALS

Matl. No.	6Al-4V TITANIUM Description	Condition	Test Direction	TUS, ksi	TYS, ksi	ELONG, %	RA, %
61 - 62	.625" Plate	Mill Annealed	L	148	138	13	24
			T	169	160	14	29
		Recrystallization Anneal	L	145	134	13	21
			T	166	153	14	21
		Diffusion Bonded	L	145	135	13	22
			T	165	153	14	26
		Beta Anneal	L	145	136	14	22
			T	161	150	14	24
		Solution Treated and Overaged	L	161	151	14	27
			T	164	160	15	31
63	1.250" Plate (Mill Beta Processed)	Mill Anneal	L	137	125	11	22
			T	128	139	9	18
		Recrystallization Anneal	L	133	116	13	30
			T	135	120	13	30
64	Extrusion (Beta Extruded)	Mill Anneal	L	139	127	14	24
			T	142	125	13	25
65	1.312" Plate	Mill Anneal	L	147	138	15	32
			T	148	139	15	34
		Recrystallization Anneal	L	141	129	15	34
			T	141	128	15	34

NOTE: Material 61-62 consisted of two plates from the same material lot. One plate was identified as material 61 and the other as material 62.

Table 2.2-3 (Page 2 of 16)

TENSILE PROPERTIES OF TEST MATERIALS

Matl. No.	6Al-4V TITANIUM Description	Condition	Test Direction	TUS, ksi	TYS, ksi	ELONG, %	RA, %
66	1.500" Plate (Mill Beta Processed)	Mill Anneal	L T	134 134	119 120	12 11	24 23
67	1.500" Plate	Recrystallization Anneal	L T	134 134	121 119	13 10	33 25
68	2.000" Plate	Mill Anneal	L T	131 135	119 126	14 14	26 27
		Recrystallization Anneal	L T	133 137	122 126	14 14	- -
69	3.500" Plate	Mill Anneal	L T	131 131	119 121	13 12	27 22
		Recrystallization Anneal	L T	129 127	118 116	16 15	31 31
70	1.500" Plate	Recrystallization Anneal	L T	138 135	124 122	12 12	28 30
71	1.500" Plate	Recrystallization Anneal	L T	144 137	135 126	14 11	25 22
72	1.500" Plate	Recrystallization Anneal	L T	133 134	117 122	15 15	33 34
74	Diffusion bonded billet of material 70 plate	As Bonded	L T ST	130 128 128	118 118 114	14 13 11	29 29 34

Table 2.2-3 (Page 3 of 16)

TENSILE PROPERTIES OF TEST MATERIALS

Matl. No.	6Al-4V TITANIUM Description	Condition	Test Direction	TUS, ksi	TYS, ksi	ELONG, %	RA, %
74	Diffusion Bonded Billet of Material 70 Plate	As Bonded Plus Four Diffusion Bond Thermal Cycles (DBTC)	L	128	116	14	27
			T	126	115	14	26
			ST	128	111	15	38
75	Extrusion (Beta Extruded)	Mill Annealed	L	139	123	11	27
			T	138	121	10	28
76	1.500" Plate	Recrystallization Anneal	L	127	113	12	19
			T	137	127	11	23
		Diffusion Bond Thermal Cycle (DBTC)	L	125	112	12	20
			T	128	120	8	18
77	2.500" Plate	Recrystallization Anneal	L	136	122	14	31
			T	135	122	12	29
			ST	137	120	11	23
		Diffusion Bonded	L	132	120	15	31
			T	132	119	14	28
			ST	130	117	14	30
78	.750" Plate	Recrystallization Anneal	L	136	125	15	28
			T	148	139	14	31
79	Hand Forging	Recrystallization Anneal	L	132	121	15	46
			T	136	128	14	42
			ST	135	125	15	37

Table 2.2-3 (Page 4 of 16)

TENSILE PROPERTIES OF TEST MATERIALS

Matl. No.	6Al-4V TITANIUM Description	Condition	Test Direction	TUS, ksi	TYS, ksi	ELONG, %	RA, %
80	.100" Sheet	Mill Anneal	L T	147 151	137 143	10 10	- -
81	.100" Sheet	Mill Anneal	L T	143 146	137 141	11 11	- -
82	Hand Forging	Recrystallization Anneal	L T	130 127	124 119	15 15	35 36
84	Die Forging	Recrystallization Anneal	L T	134 132	121 119	16 17	41 39
85	Die Forging	Recrystallization Anneal	L T	136 136	123 124	15 15	42 41
86	.375" Plate	Recrystallization Anneal	L T	138 140	122 129	20 15	41 30
87	1.500" Plate	Recrystallization Anneal	L T	130 129	121 120	14 11	28 34
88	1.250" Plate	Recrystallization Anneal	L T	139 134	127 123	13 10	26 31
89	1.250" Plate	Recrystallization Anneal	L	135	124	14	28

Table 2.2-3 (Page 5 of 16)

TENSILE PROPERTIES OF TEST MATERIALS

Matl. No.	6AL-4V Titanium Description	Condition	Test Direction	TUS, ksi	TYS, ksi	ELONG, %	RA, %
90	2.25 plate	Recrystallization Anneal	L	130	122	13	35
			T	131	123	14	39
92	2.50 Plate	Recrystallization Anneal	L	136	122	15	31
			T	136	124	14	29
253	2.50 Plate	Recrystallization Anneal	L	131	120	15	-
			T	132	122	14	-
294	1.25 Plate	Recrystallization Anneal	L	136	124	13	-
			T	137	124	10	-
7406	2.00 Plate	Recrystallization Anneal	L	141	126	12	23
			T	142	128	12	25
7768	.750 Plate	Recrystallization Anneal	L	144	126	12	26
			T	148	130	11	26

Table 2.2-3 (Page 6 of 16)

TENSILE PROPERTIES OF TEST MATERIALS

Matl. No.	2024 ALUMINUM ALLOY Description	Condition	Test Direction	TUS, ksi	TYS, ksi	ELONG, %	RA, %
1	3.000" Plate	-T851	L	71	66	8	20
			T	71	65	7	12
		-T62	L	69	59	11	20
			T	68	58	8	13
2	3.000" Plate	-T351	L	69	54	13	18
			T	68	48	14	16
			ST	56	44	3	7
		-T851	L	69	61	7	16
3	3.000" Plate	-T351	L	74	59	18	22
			T	71	51	13	15
			ST	60	47	4	5
		-T851	L	73	66	8	19
			T	72	65	6	12
			ST	66	63	2	3
6	1.750" Plate	-T351	L	73	57	20	24
			T	73	49	17	24
		-T851	L	72	65	9	21
			T	72	65	8	16
8	3.500" Plate	-T851	L	71	65	8	15
			T	70	64	6	11

Table 2.2-3 (Page 7 of 16)

TENSILE PROPERTIES OF TEST MATERIALS

Matl. No.	Description	Condition	Test Direction	TUS, ksi	TYS, ksi	ELONG, %	RA, %
	2024 ALUMINUM ALLOY						
9	3.000" Plate	T851	L	70	65	8	15
			T	71	64	6	11
19	3" x 18" x 23" Hand Forging	T852	L	69	58	10	26
			T	69	60	7	11
27	3" x 18" x 35" Hand Forging	T852	L	70	53	14	25
			T	68	54	9	13
302	.100" Sheet	T81	T	73	67	8	-
303	.100" Sheet	T81	T	73	68	8	-
	2124 ALUMINUM ALLOY						
12	3.000" Plate	T851	L	72	65	8	16
			T	73	67	8	19
			ST	69	63	4	9
14	2.000" Plate	T851	L	71	65	8	-
			T	71	66	7	-

Table 2.2-3 (Page 8 of 16)

TENSILE PROPERTIES OF TEST MATERIALS

Matl. No.	2219 ALUMINUM ALLOY Description	Condition	Test Direction	TUS, ksi	TYS, ksi	ELONG, %	RA, %
4	2.000" Plate	T851	L	68	50	12	28
			T	68	50	12	22
			ST	63	50	4	8
		T62	L	64	44	14	35
			T	63	43	12	26
7	1.750" Plate	T851	L	66	50	12	25
			T	66	48	10	17
13	3.000" Plate	T851	L	69	54	10	22
			T	68	53	10	18
			ST	66	53	7	10
16	1 3/4" x 7 1/2" Extruded Bar	T8511	L	66	51	12	-
			T	67	48	-	
20	6" x 12" x 48" Hand Forging	T852	L	65	51	12	-
			T	65	51	9	-
			ST	64	50	8	-
304	3.000" Plate	T851	L	67	53	10	-
			T	66	52	7	-
314	2.55" Plate	T851	L	69	52	10	-
			T	68	51	8	-

Table 2.2-3 (Page 9 of 16)

TENSILE PROPERTIES OF TEST MATERIALS

Matl. No.	7049 ALUMINUM ALLOY Description	Condition	Test Direction	TUS, ksi	TYS, ksi	ELONG, %	RA, %
10	Die Forging	T73	L	77	68	13	31
			ST	74	67	6	16
24	Die Forging	T73	L	80	74	12	
			T	77	70	6	-
			ST	74	69	4	-
25	Hand Forging	T7352	L	76	67	12	33
			T	73	64	9	13
			ST	74	62	9	-
	7050 ALUMINUM ALLOY						
23	Die Forging	T73	L	78	71	13	-
			T	76	68	7	11
			ST	74	66	4	5
28	4.000" Plate	T73651	L	77	68	10	27
			T	76	66	9	19
			ST	74	62	7	13

Table 2.2-3 (Page 10 of 16)

TENSILE PROPERTIES OF TEST MATERIALS

Matl. No.	7075 ALUMINUM ALLOYS Description	Condition	Test Direction	TUS, ksi	TYS, ksi	ELONG, %	RA, %
5	2.000" Plate	T7651	L	75	65	12	22
			T	77	66	10	17
		T7351	L	76	65	14	30
			T	77	66	13	24
15	.600" Plate	T7651	L	76	65	13	-
			T	74	64	12	–
18	2.000" Plate	T7651	L	74	63	13	25
			T	74	64	11	16
		T7351	L	70	58	14	23
			T	71	59	11	17
22	Die Forging	T73	L	75	67	13	
			T	72	62	10	18
			ST	70	61	6	10
29	Extrusion	T73511	L	77	66	13	31
			T	72	61	9	15
			ST	71	58	7	10

Table 2.2-3 (Page 11 of 16)

TENSILE PROPERTIES OF TEST MATERIALS

Matl. No.	7075 ALUMINUM ALLOY Description	Condition	Test Direction	TUS, ksi	TYS, ksi	ELONG, %	RA, %
30	.100" Sheet	T76	T	77	66	12	-
301	.100" Sheet	T76	T	75	66	12	
306	2.500" Plate	T7651	T	70	61	11	-
307	2.250" Plate	T7651	T	75	63	7	-
309	Extrusion	T76511	L	77	68	13	-
311	Extrusion	T73511	L	72	61	14	-
	7175 ALUMINUM ALLOY						
21	Die Forging	T736	L	78	70	13	
			T	75	66	9	
			ST	72	63	5	
26	Hand Forging	T73652	L	77	68	14	40
			T	74	64	10	25
			ST	67	53	9	17

Table 2.2-3 (Page 12 of 16)

TENSILE PROPERTIES OF TEST MATERIALS

Mat'l No.	9-4-20 Steel Description	Austenitize Temp	Quench	Delay	Sub-Zero	Temper	Orien-tation	TUS KSI	TYS KSI	% El	% El
31	3"x10"x36" Forged Billet	1525/1	Oil	None	-100/2	1050/4	L	196	182	19	69
		1525/2	Oil	None	-100/2	1050/2+2	L T	194 194	182 182	20 17	68 59
		1525/2	Oil	Over-night	---	1050/2+2	L T	193 192	177 176	19 18	67 61
		1500/2	Water	Over-night	---	1025/6	L T	196 196	183 184	20 18	68 63
		1500/2	Water	None	-100/3	1025/6	L T	196 196	185 186	19 18	68 62
		1525/2	Water	Over-night	---	1025/6	L T	196 194	184 183	18 16	67 63
		1550/2	Water	None	---	1050/2+2	L T	196 193	182 180	19 19	69 65
		1525/2	Water	Over-night	---	1050/2+2	L T	192 192	180 181	19 16	68 61
		1525/2	Water	None	---	1050/2+2	L T	197 198	182 181	17 16	65 59
33	4"x18"x36" Forged Billet	1525/2	Oil	--	-100/2	1025/4	L T ST	204 204 204	188 188 190	20 18 17	69 62 60
		1525/2	Air	--	-100/2	1025/6	L T	216 217	195 196	20 18	67 58
		1525/2	Air	--	-100/2	1050/4	L T	212 210	193 190	20 20	67 64

Table 2.2-3 (Page 13 of 16)

TENSILE PROPERTIES OF TEST MATERIALS

Mat'l No.	9-4-20 Steel Description	Austenitize Temp.	Quench	Delay	Sub-Zero	Temper	Orientation	TUS KSI	TYS KSI	% El	% RA
37	2½"x33"xL Plate	1525/2	Oil	--	-100/2	1025/4	L	200	189	15	65
							T	200	190	15	66
42	7" Dia. Die Forging Core	1525/2	Oil	--	-100/2	1025/4	L	207	194	15	57
							T	207	189	15	61
43	4"x18"36" Forged Billet	1525/2	Oil	--	-100/2	1025/4	L	211	186	16	57
							T	210	187	17	65
46	4"x18"x36" Forged Billet	1525/2	Oil	--	-100/2	1025/4	L	207	179	18	65
							T	209	178	17	62
							ST	208	180	17	61
		1525/2	Air	--	-100/2	1025/4	L	201	176	16	62
							T	202	177	18	68
48	4"x18"x36" Forged Billet	1525/2	Oil	--	-100/2	1025/4	L	206	187	16	63
							T	206	186	15	59
		1525/2	Air	--	-100/2	1025/4	L	205	180	17	60
							T	204	180	15	57
		1700/1	Air	--	-100/1	1025/4	L	204	186	16	68
		1525/1	Oil	--	-100/1	1025/12	L	198	185	16	64
		1650/4-900/1/2	Air	--	-100/1	1025/8	L	209	185	15	61
49	12" Dia. Die Forging Section	1525/2	Air	--	-100/2	1025/4	L	208	182	18	64
							T	207	183	16	58
52	5"x8"x8" Hand Forging	1525/2	Oil	--	-100/2	1025/4	T	209	198	14	58

TABLE 2.2-3 (Page 14 of 16)

TENSILE PROPERTIES OF TEST MATERIALS

MAT'L NO.	DESCRIPTION	AUSTENITIZE TEMP.	QUENCH	DELAY	SUB-ZERO	TEMPER	ORIEN-TATION	F_{TU} KSI	F_{TY} KSI	%EL.	%RA.
	9Ni-4Co-.20C										
57	1-1/2" Plate	1525/2	Oil	--	-100/2	1025/4	L	199	183	15	63
59	3"x8"x8" Forged Billet	1525/2	Oil	None	-100/2	1025/6	L T	204 204	185 185	17 17	67 66
	9Ni-4Co-.30C										
32	3 x 18 x 36 Forged Billet	1550/1	Oil	--	100/3	1000/2+2	L T	245 244	215 215	16 15	60 53
		1525/2	Oil	--	100/2	1000/5	L	241	207	16	56
		1525/2	Oil	--	100/2	1025/2+2	L	240	216	15	55
35	3 x 18 x 36 Forged Billet	1525/2	Oil	--	100/3	1050/4	L T	216 217	197 198	17 16	56 51
		1525/2	Oil	--	100/3	1000/4	L T	233 233	206 207	16 16	54 52
		1550/2	Oil	--	100/1	1025/2+2	L T	221 223	198 199	17 15	62 52
		1525/2	Air	--	100/3	1000/4	L T	235 237	210 212	17 15	56 48
		1525/2	Air	--	100/3	1050/4	L T	216 214	196 196	15 16	51 49

Table 2.2-3 (Page 15 of 16)

TENSILE PROPERTIES OF TEST MATERIALS

Matl. No.	PH 13-8 MO STEEL Description	Condition	Test Direction	TUS, ksi	TYS, ksi	ELONG, %	RA, %
36	4" x 5" Forged Bar	H950	L	216	204	12	47
			T	225	207	13	46
		H1000	L	212	201	13	48
			T	205	198	14	51
40	1-1/2" x 12" Rolled Bar	H1000	L	216	208	15	57
			T	219	215	13	55
41	1-1/2" x 8" Extruded Bar	H1000	L	221	214	13	51
			T	221	213	12	52
44	22" Dia. x 6" Forged Billet	H1000	L	208	191	9	26
			T	207	190	11	33
			TW	207	190	13	37
50	2-1/4" x 4"	H1000	L	219	212	12	57
			T	219	212	13	56
54	1-1/2" Dia. Bar	RH1000	L	222	215	14	54
		RH975	L	233	216	12	51
		RH950	L	236	217	13	52
56	1-1/2" Dia. Bar	RH1000	L	226	218	14	53
		RH975	L	231	219	14	53
		RH950	L	237	219	14	52

Table 2.2-3 (Page 16 of 16)

TENSILE PROPERTIES OF TEST MATERIALS

Matl. No.	300M STEEL Description	Condition	Test Direction	TUS, ksi	TYS, ksi	ELONG, %	RA, %
39	3" x 36" x 72" Hand Forging	280-300 UTS	L T	287 281	238 236	13 10	41 34
	INCONEL 718						
51	4" x 8" Forged Bar	Solution Treat 1850° - Age 1360° - 9 Hrs. F/C 1175° - Total Time 19 Hrs.	LT	192	160	39	20
53	Die Forging	1325F, 8 hrs, FC to 1150F (1325F + FC + 1150F = 18 hrs)	L LT	199 197	168 166	18 18	29 31
	MP 35N STEEL						
55	1-1/2" Dia. Bar	1000 F, 4 Hrs	L	236	233	13	57

TABLE 2.2-4

TENSILE PROPERTIES-WELD JOINTS

Mat'l No.	Material & Description	Heat Treat Preweld	Heat Treat Postweld	Joint Thickness	Weld Process	Weld Direction Transv.	Weld Direction Longit.	Break Location	TUS ksi	TYS ksi	Elong'n. %(2" gage)
	9Ni-4Co-.20C										
37	$2\frac{1}{4}$" Plate	190/210 TUS	950F-2 Hrs	.50 in.	GTAW	X	–	PM	207	177	19
	Ti-6Al-4V										
87	$1\frac{1}{2}$" Plate	RA Cond.	1100F-2 Hrs	.50	GTAW	X	–	PM	126	117	10
89	$1\frac{1}{4}$" Plate	RA Cond.	1100F-2 Hrs	.50	GTAW	X	–	PM	132	122	10
88	$1\frac{1}{4}$" Plate	RA Cond.	1100F-2 Hrs	.50	GTAW	X	–	PM	137	129	11
88	$1\frac{1}{4}$" Plate	RA Cond.	1100F-2 Hrs	.50	GTAW		X	--	142	134	11
--	Weld Metal	--	1100F-2 Hrs	.25	GTAW	-	-	--	142	130	10 (1" gage)
	PH13-8Mo										
41	$1\frac{1}{2}$ Extr Bar	Cond. A	1000F-4 Hrs	.25	GTAW	X	–	HAZ	204	184	8
	$1\frac{1}{2}$ Extr Bar	Cond. A	1000F-4 Hrs	.25	GTAW	–	X	--	218	177	11

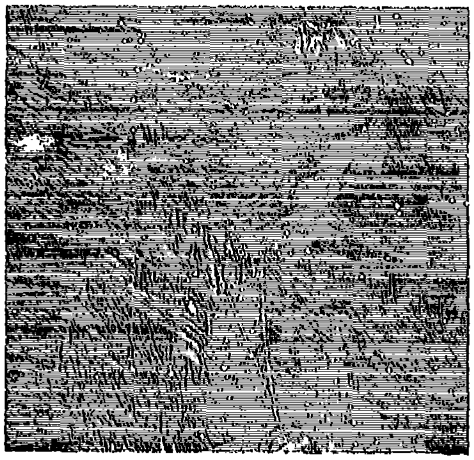

100X

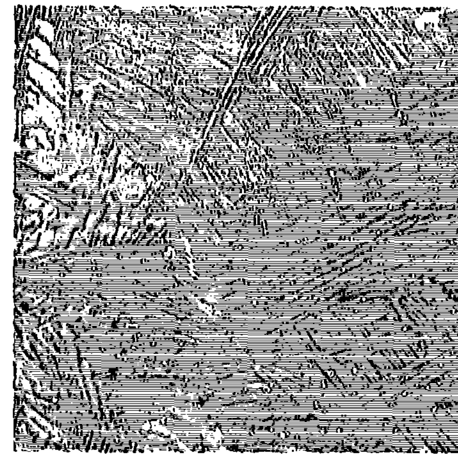

250X

MATERIAL NO. 62 .625 PLATE, BETA ANNEALED

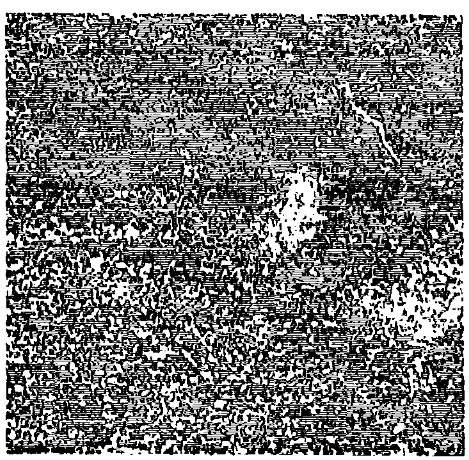

100X

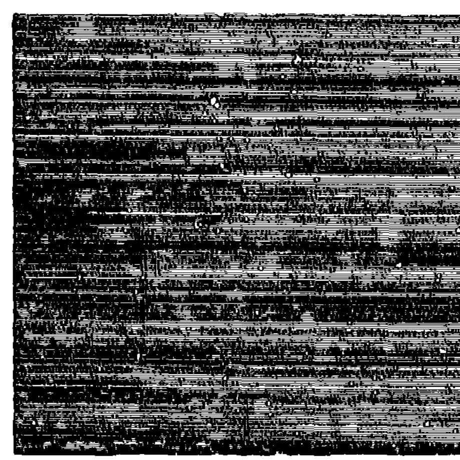

250X

MATERIAL NO. 62 .625 PLATE, SOLUTION TREATED AND OVERAGED

Figure 2.2-1 (page 1 of 15) TYPICAL 6Al-4V TITANIUM MICROSTRUCTURE

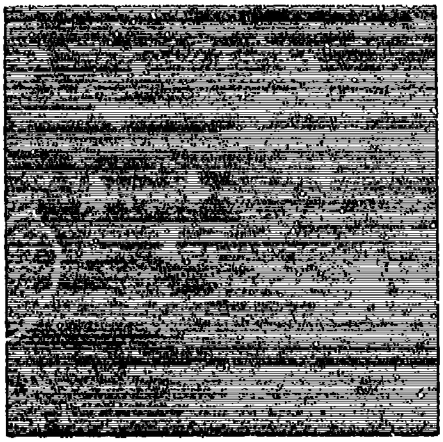

100X

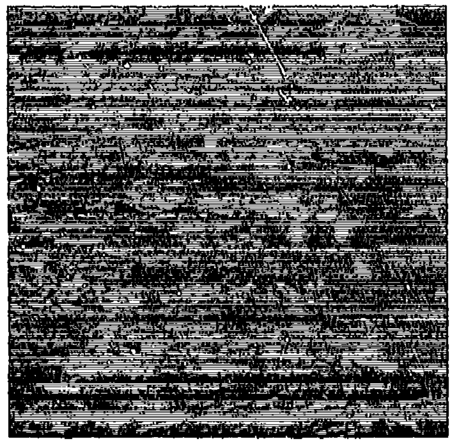

250X

MATERIAL NO. 62 .625 PLATE MILL ANNEALED

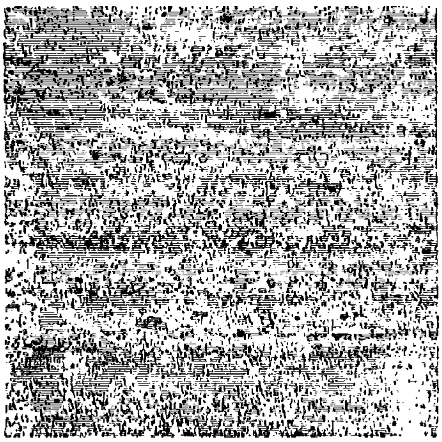

100X

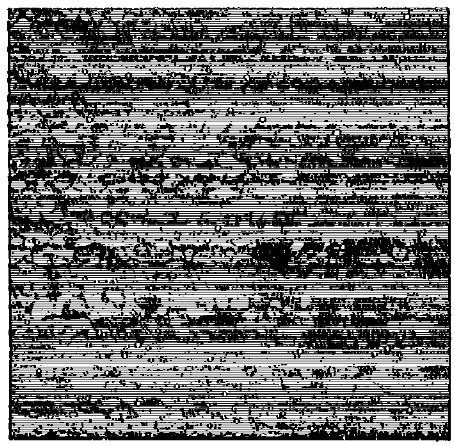

250X

MATERIAL NO. 62 .625 PLATE, DIFFUSION BOND TEMPERATURE AND PRESSURE CYCLE

Figure 2.2-1 (page 2 of 15) TYPICAL 6Al-4V TITANIUM MICROSTRUCTURE

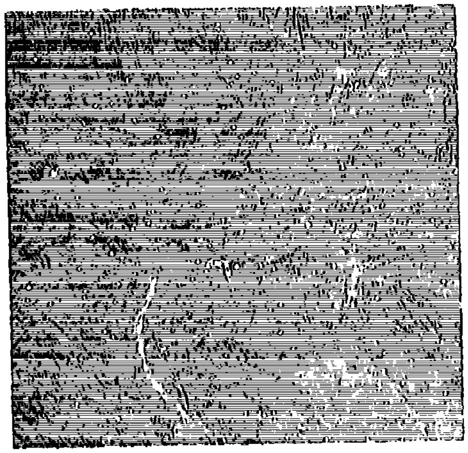

100X

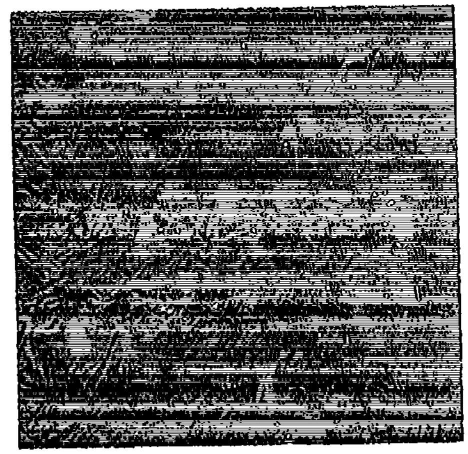

250X

MATERIAL NO. 63 1.25" PLATE, MILL BETA PROCESSED

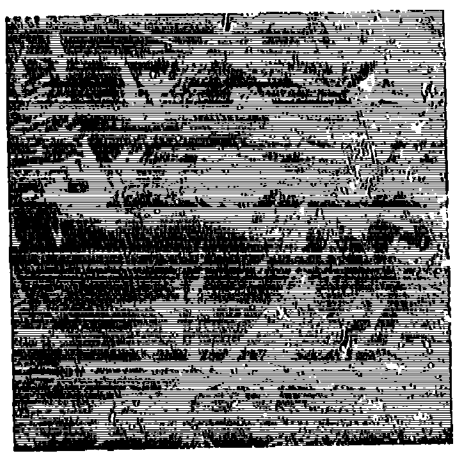

100X

500X

MATERIAL NO. 64 BETA EXTRUDED SHAPE AND MILL ANNEALED

Figure 2.2-1 (page 3 of 15) TYPICAL 6Al-4V TITANIUM MICROSTRUCTURE

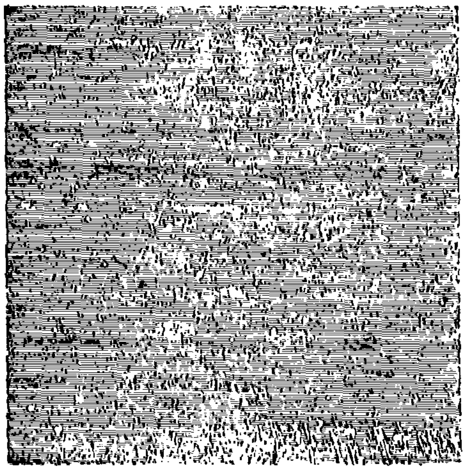

100X

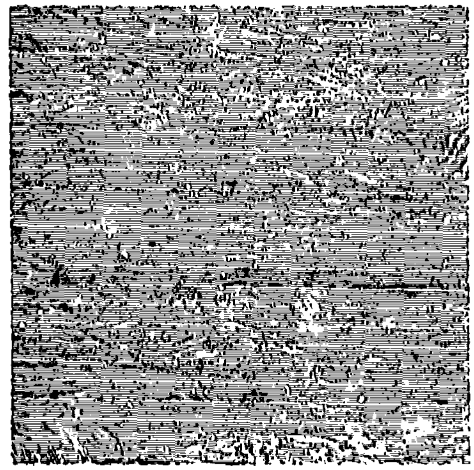

250X

MATERIAL NO. 65 1.312 PLATE, MILL ANNEALED

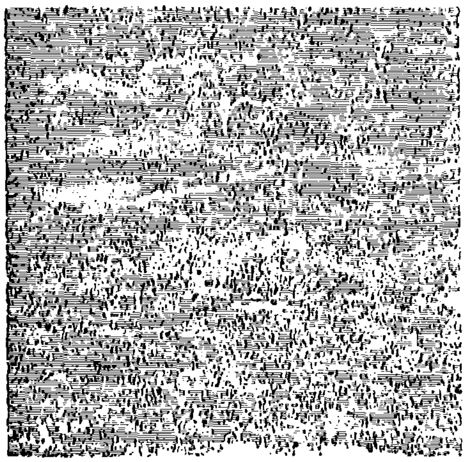

100X

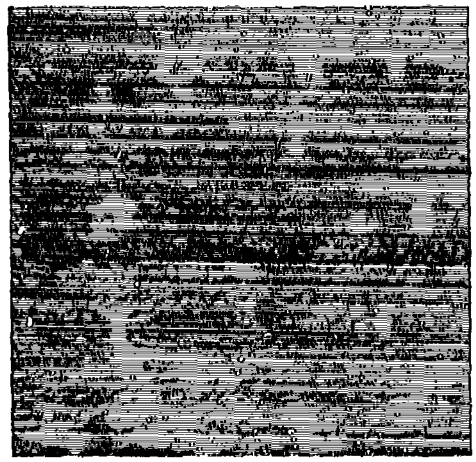

250X

MATERIAL NO. 65 1.312 PLATE, RECRYSTALLIZED ANNEALED

Figure 2.2-1 (page 4 of 15) TYPICAL 6Al-4V TITANIUM MICROSTRUCTURE

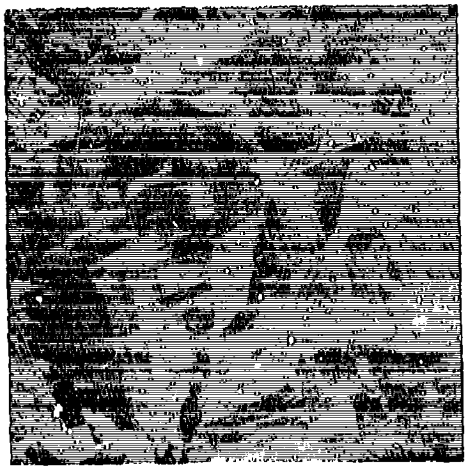

100X

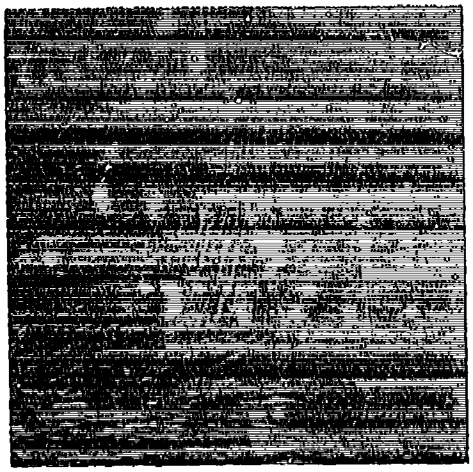

250X

MATERIAL NO. 66 1.250 PLATE, MILL BETA PROCESSED AND MILL ANNEALED

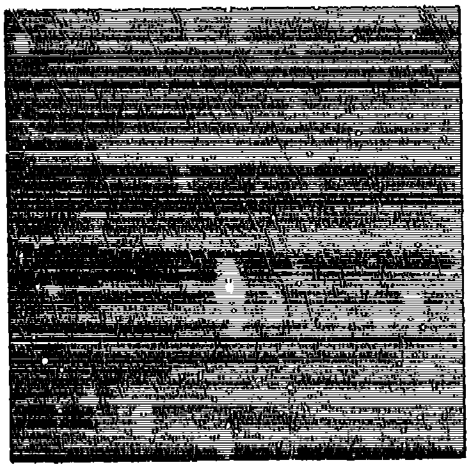

100X

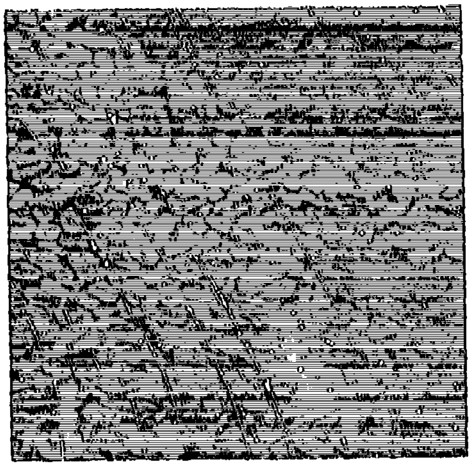

250X

MATERIAL NO. 67 1.500 PLATE, RECRYSTALLIZED ANNEALED

Figure 2.2-1 (page 5 of 15) TYPICAL 6Al-4V TITANIUM MICROSTRUCTURE

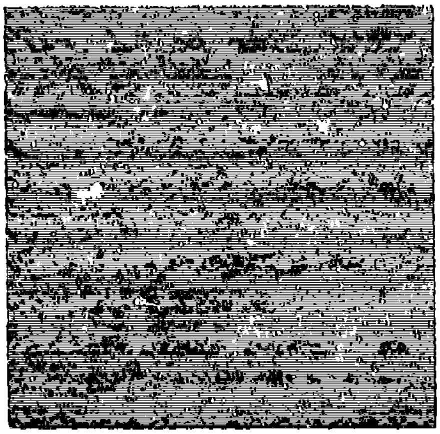

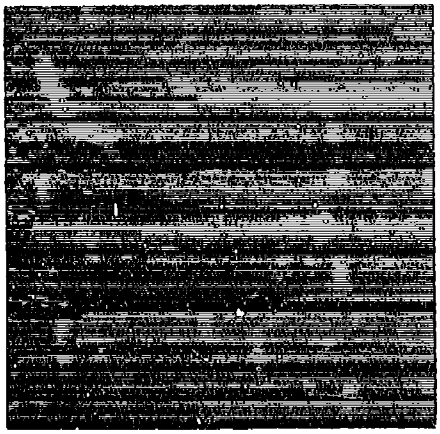

100X 250X

MATERIAL NO. 68 2.00" PLATE, RECRYSTALLIZED ANNEALED

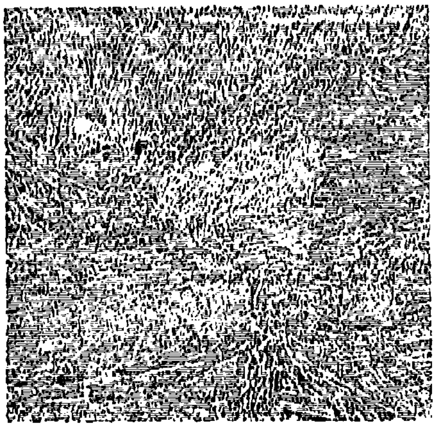

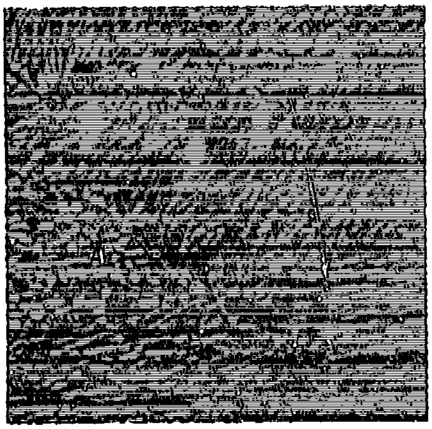

100X 250X

MATERIAL NO. 69 3.50" PLATE, RECRYSTALLIZED ANNEALED

Figure 2.2-1 (page 6 of 15) TYPICAL 6Al-4V TITANIUM MICROSTRUCTURE

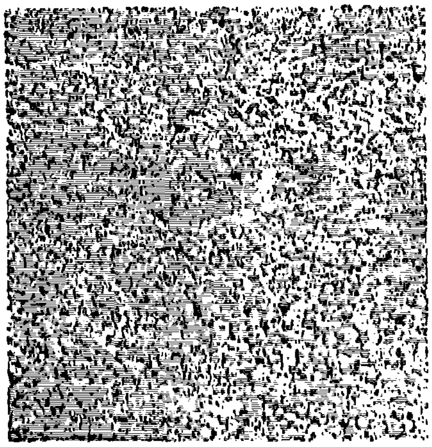

100X

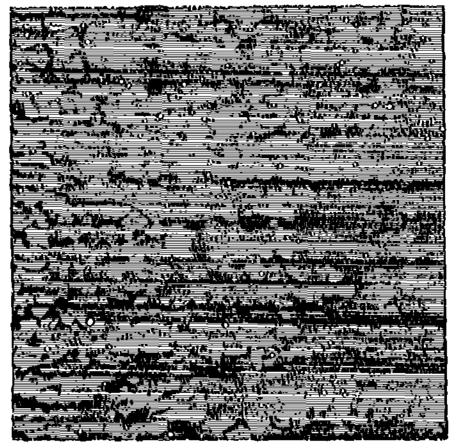

250X

MATERIAL NO. 70 1.50 PLATE, RECRYSTALLIZED ANNEALED

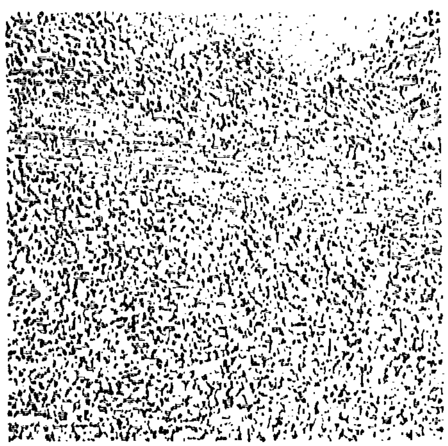

100X

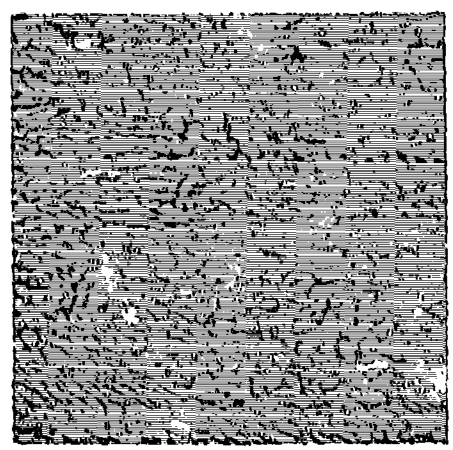

250X

MATERIAL NO. 71 1.312 PLATE, RECRYSTALLIZED ANNEALED

Figure 2.2-1 (page 7 of 15) TYPICAL 6Al-4V TITANIUM MICROSTRUCTURE

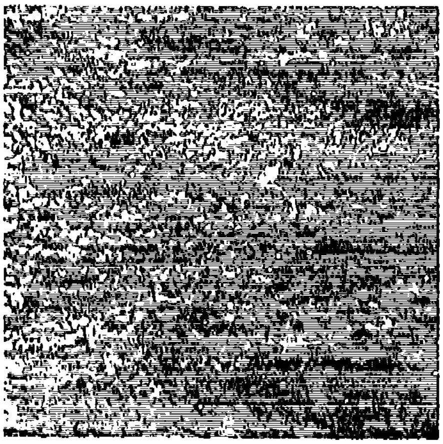

100X

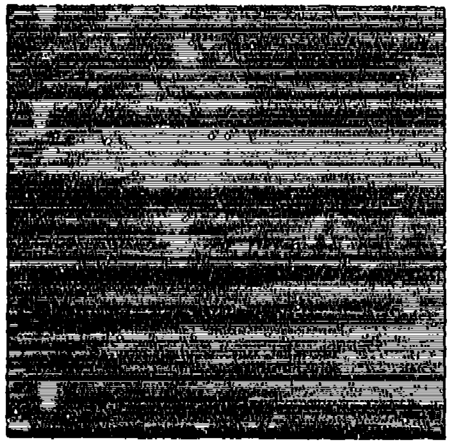

250X

MATERIAL NO. 72 1.500 PLATE, RECRYSTALLIZED ANNEALED

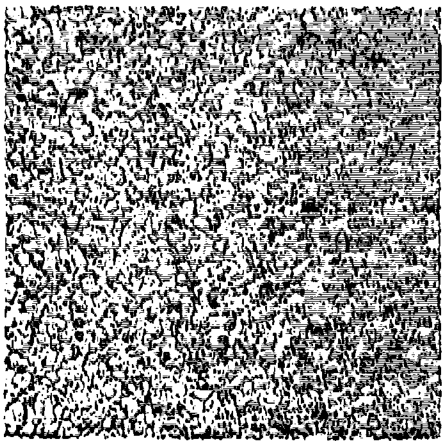

100X

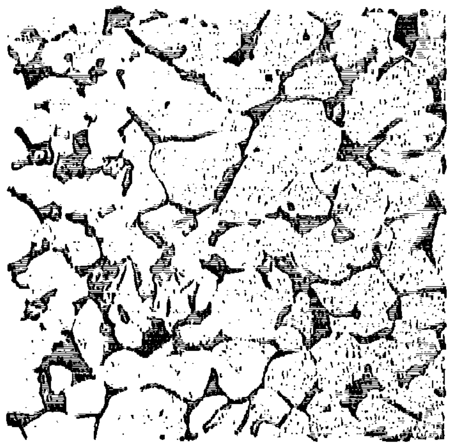

500X

MATERIAL NO. 74 1.500 PLATE, DIFFUSION BONDED (Material 74 is a Diffusion Bonded Billet of Material 70 Plate)

Figure 2.2-1 (page 8 of 15) TYPICAL 6Al-4V TITANIUM MICROSTRUCTURE

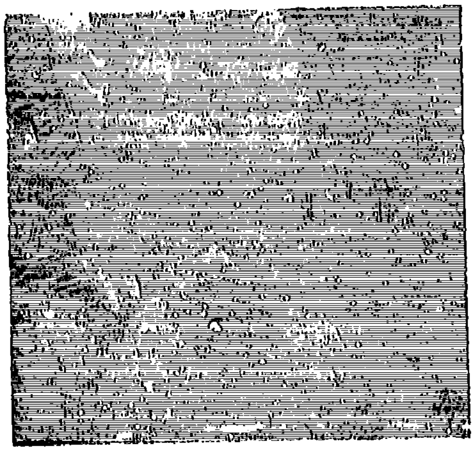

100X

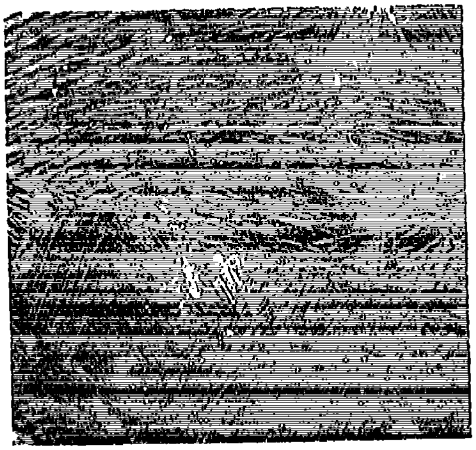

250X

MATERIAL NO. 75 BETA EXTRUDED SHAPE PLUS MILL ANNEALED

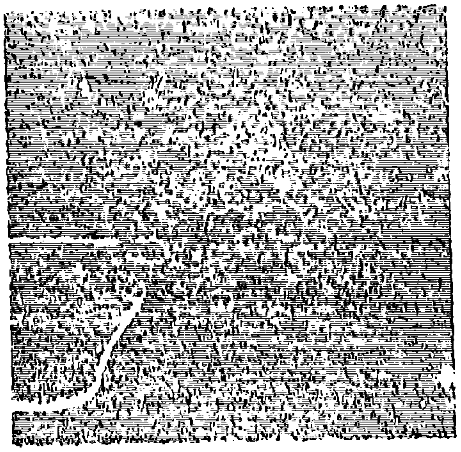

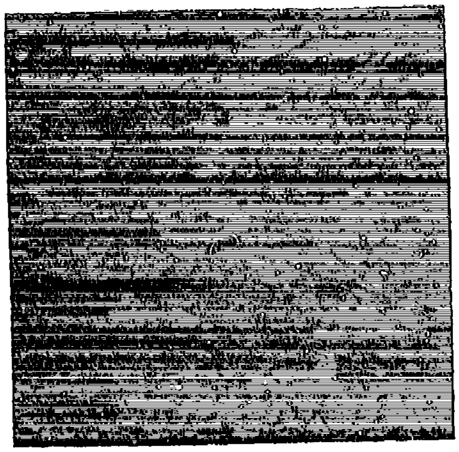

MATERIAL NO. 76 1.50" PLATE, RECRYSTALLIZED ANNEALED

Figure 2.2-1 (page 9 of 15) TYPICAL 6Al-4V TITANIUM MICROSTRUCTURE

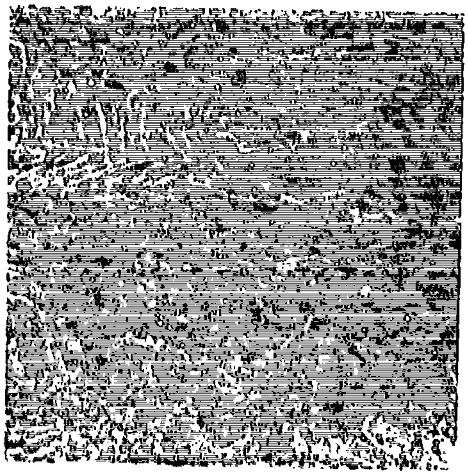

100X

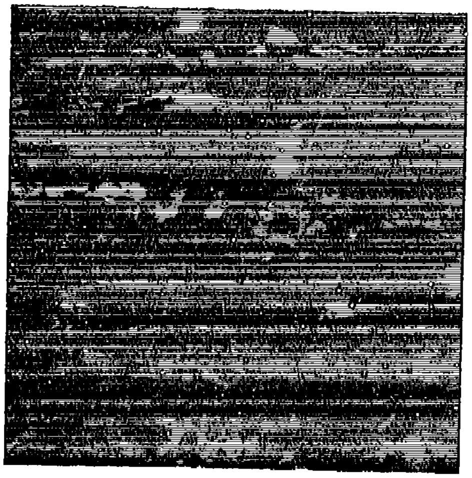

250X

MATERIAL NO. 77   2.500 PLATE, RECRYSTALLIZED ANNEALED

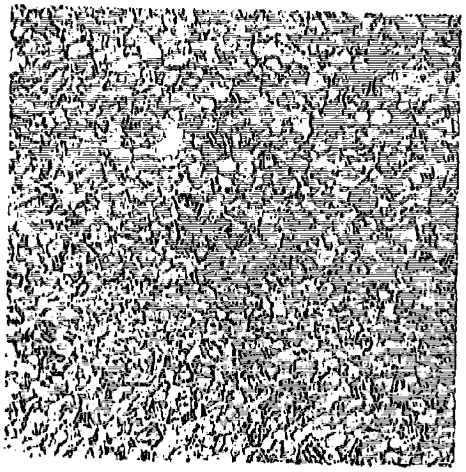

250X
RECRYSTALLIZED ANNEALED

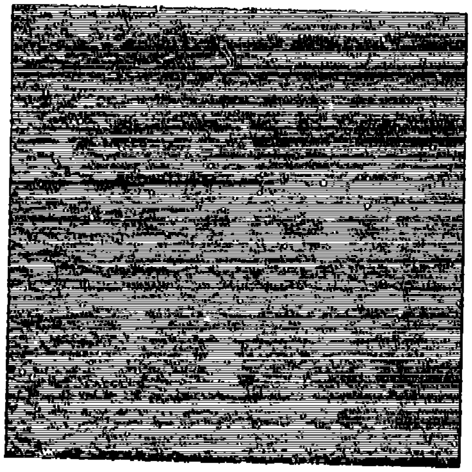

250X
MILL ANNEALED

MATERIAL NO. 78   .750 PLATE

Figure 2.2-1 (page 10 of 15) TYPICAL 6Al-4V TITANIUM MICROSTRUCTURE

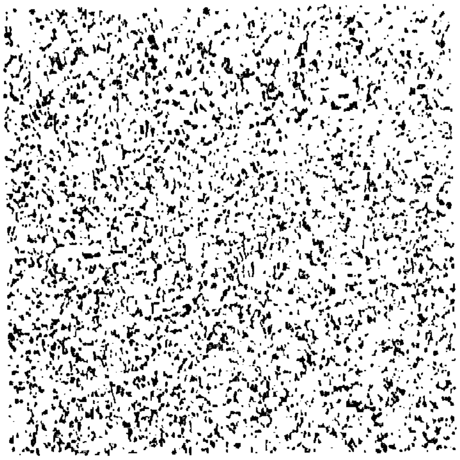

100X

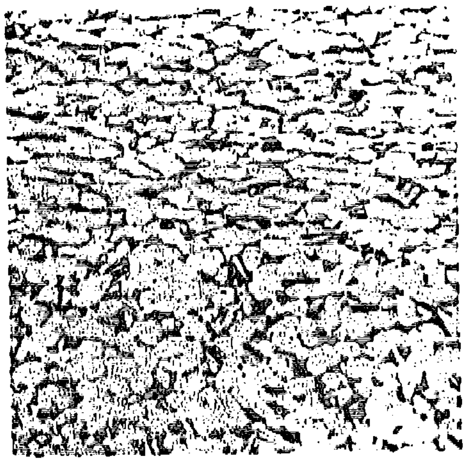

250X

MATERIAL NO. 79   4"x10"x34" FORGED BILLET, RECRYSTALLIZED ANNEALED

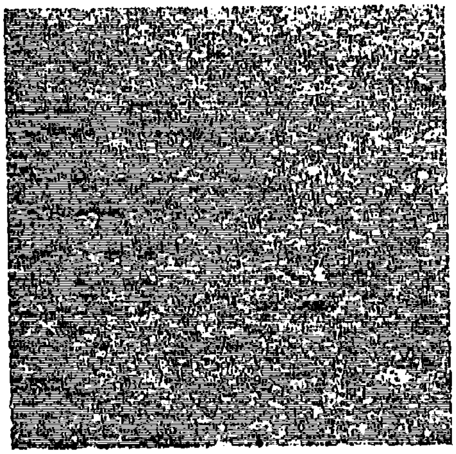

100X

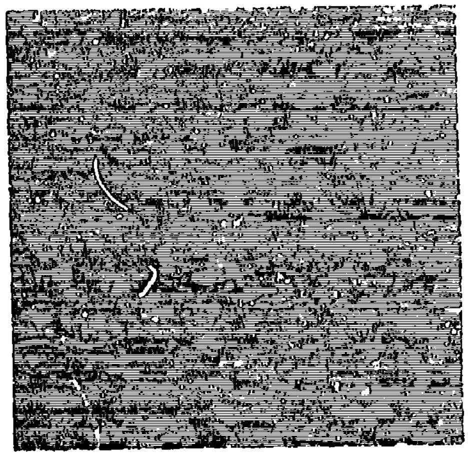

250X

MATERIAL NO. 80   .100" SHEET, MILL ANNEALED

Figure 2.2-1 (page 11 of 15) TYPICAL 6Al-4V TITANIUM MICROSTRUCTURE

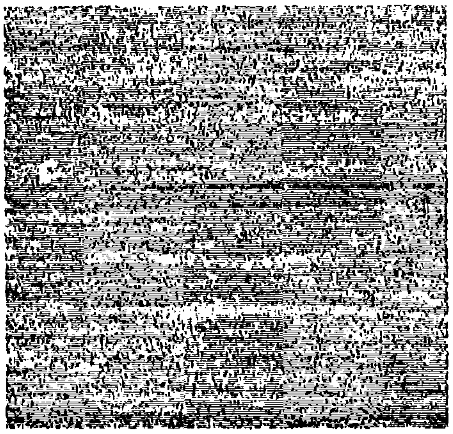

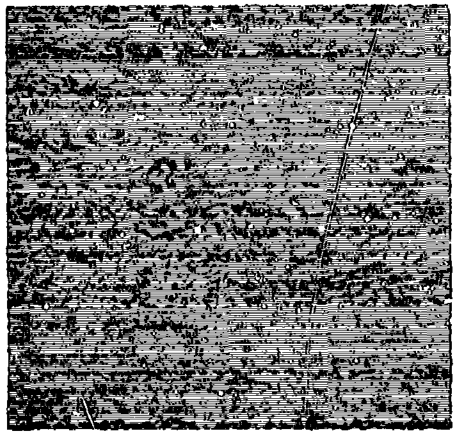

100X 250X

MATERIAL NO. 81 .100" SHEET, MILL ANNEALED

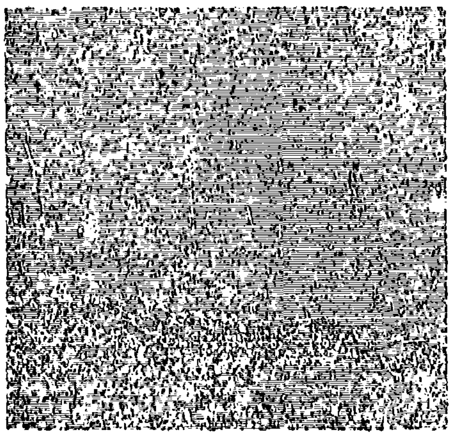

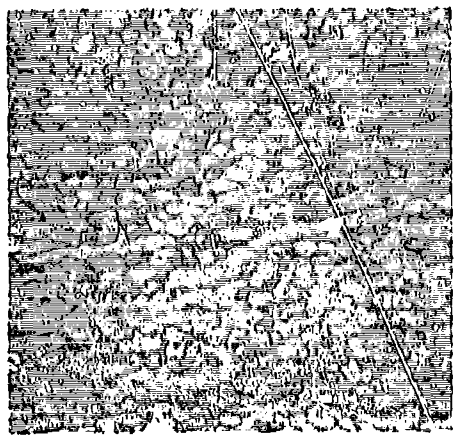

100X 250X

MATERIAL NO. 82 4"x10"x34" FORGED BILLET, RECRYSTALLIZED ANNEALED

Figure 2.2-1 (page 12 of 15) TYPICAL 6Al-4V TITANIUM MICROSTRUCTURE

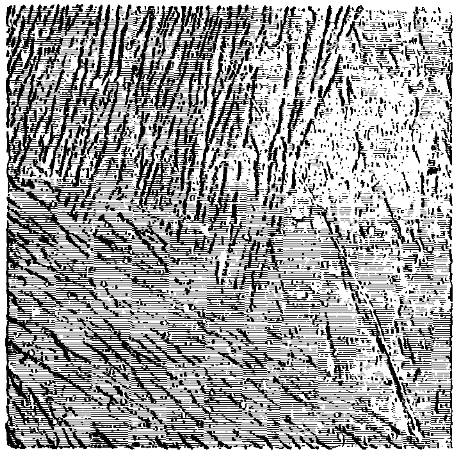

100X

250X

MATERIAL NO. 84 DIE FORGING, RECRYSTALLIZED ANNEALED

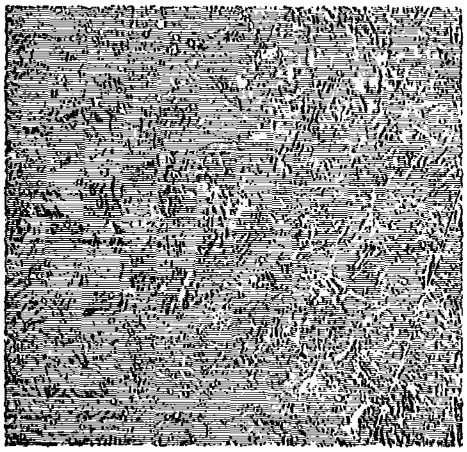

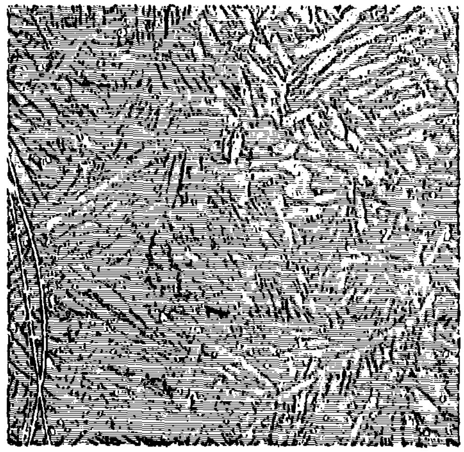

100X

250X

MATERIAL NO. 85 DIE FORGING, RECRYSTALLIZED ANNEALED

Figure 2.2-1 (page 13 of 15) TYPICAL 6Al-4V TITANIUM MICROSTRUCTURE

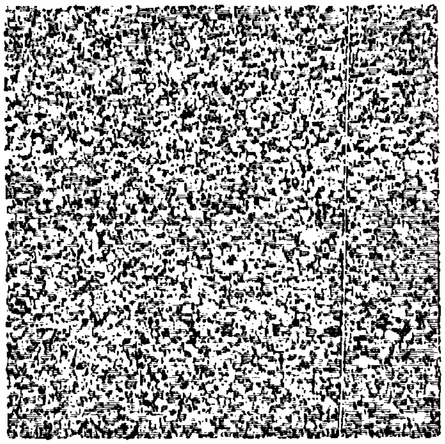

100X

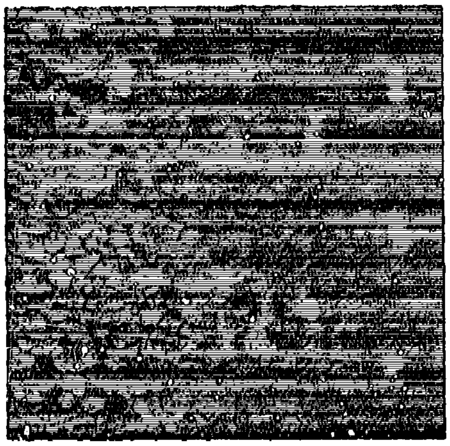

250X

MATERIAL NO. 86 .375 PLATE, RECRYSTALLIZED ANNEALED

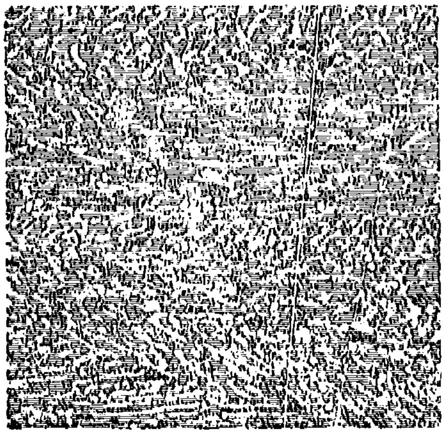

100X

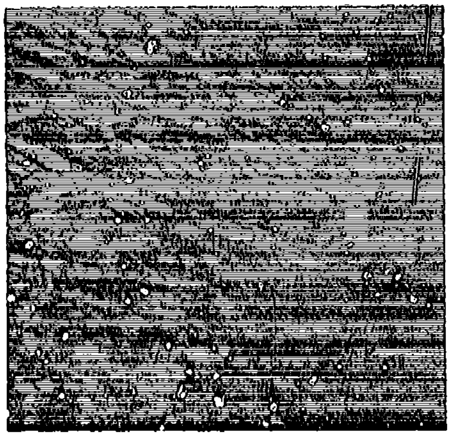

250X

MATERIAL NO. 253 2.500 PLATE, RECRYSTALLIZED ANNEALED

Figure 2.2-1 (page 14 of 15) TYPICAL 6Al-4V TITANIUM MICROSTRUCTURE

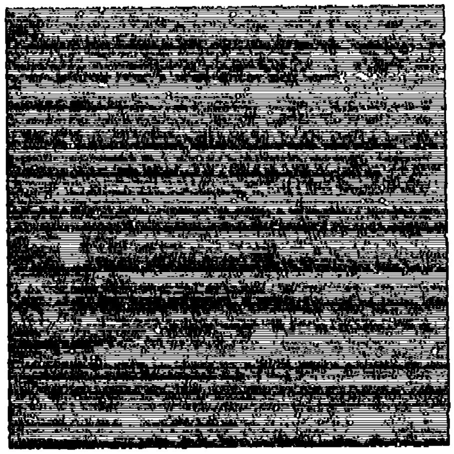

100X

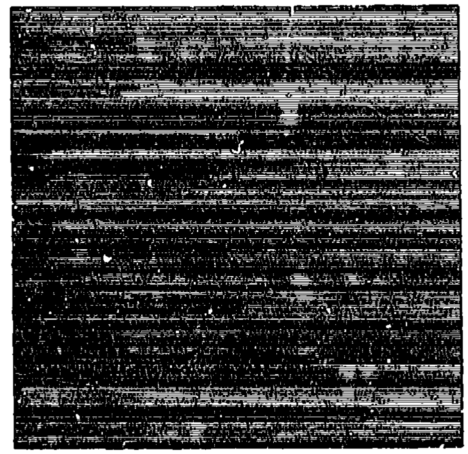

250X

MATERIAL NO. 294   1.25 PLATE, RECRYSTALLIZED ANNEALED

Figure 2.2-1 (page 15 of 15) TYPICAL 6Al-4V TITANIUM MICROSTRUCTURE

2.3 HEAT TREATMENT OR THERMAL PROCESSING

Most of the aluminum materials were procured in the heat treat condition in which they were to be tested. (When heat treating was performed after receival, standard temperatures and times per MIL-H-6088 were used). Heat treatment or processing cycles used on alloys other than aluminum are shown in Table 2.3-1. Thermal cycles shown in this table for the diffusion bond thermal cycle (DBTC) and diffusion bond (DB) conditions are broad enough to include all variations used in these processing cycles. More specific information is listed in Table 2.3-2 under the individual specimen number.

TABLE 2.3-1

HEAT TREATMENT OR PROCESS TIME-TEMPERATURE CYCLES

Alloy and Condition	Time-Temperature Cycle For Specified Condition
Ti-6Al-4V	
RA (Recrystallization Annealed)	Step 1 - Heated to just below the beta transus and held there to allow microstructural recrystallization (1700 to 1770F, 1 to 4 hrs.) Step 2 - One of the following - (a), (b) or (c) (a) Cooled to 1400F at 100F per hour or slower, cooled to below 900F in 45 minutes or less (b) Cooled to room temperature, reheated to 1400F and held for 1/2 hr. minimum, cooled to below 900F in 45 minutes or less (c) Cooled to 1400F, held at 1400F for 1 hr. minimum, cooled to below 900F in 45 minutes or less.
MA (Mill Annealed)	1350 to 1450F, 1/4 to 8 hrs.,AC
BA (Beta Annealed)	1900F, 1/2hr., AC; 1350F, 2 hrs., AC
STOA (Solution Treated and Over Aged)	1750F, 2 hrs., WQ; 1000F, 2 hrs., AC; 1300F, 2 hrs., AC
DB (Diffusion Bonded)	1700 or 1750F, 4 to 5 hrs. under 2000 psi pressure, slow cool in DB press (Table 2.3-2 lists specific cycles for this condition according to specimen number).
DBTC (Diffusion Bond Thermal Cycle)	1700 or 1750F, 1 to 6 hrs., no pressure applied, slow cool to below 600F (usually 100F/hr or slower) (Table 2.3-2 lists specific cycles for this condition according to specimen number).
DBT & PC (Diffusion Bond Thermal and Pressure Cycle)	1700F, 5 hrs. under 2000 psi pressure, slow cool in DB press (no bond joint in specimen).

HEAT TREATMENT OR PROCESS TIME-TEMPERATURE CYCLES

Alloy and Condition	Time-Temperature Cycle for Specified Condition
Ti-6Al-4V (Cont'd)	
TR (Thermal Repair)	1400F, 1 hr., AC
Hot Formed	1560F, 5 hrs. ; cooled about 17F/hr. to 1100F then da/dN specimens were furnace cooled to 500F and K_{Iscc} specimens were air cooled
9-4-.20 HT 190 to 210 ksi	(1650F, 1 to 1.5 hrs., AC) + (1525F, 1 to 1.5 hrs., AC or OQ) + (-100F, 1 to 1.5 hrs.,) + (1025 to 1075F, 4 hrs.)
9-4-.30 HT 220 to 240 ksi	(1650F, 1 to 1.5 hrs., AC) + (1550F, 1 to 1.5 hrs., AC or OQ) + (-100F, 1 to 1.5 hrs.,) + (1000 to 1075F, 4 hrs.)
300M HT 280 to 300 ksi	(1700F, 1.5 hrs., AC) + (1600F, 1.5 hrs., OQ) + (600F, 2 + 2 hrs.)
PH13-8Mo H 950, 975, 1000, RH 950, 975, 1000	Solution Treatment (Performed by Mill) H950, 975, 1000 - 1700F, AC RH 950, 975, 1000 - (1700F, AC) + (-100F, 5 hrs.) Aging Treatment H 950, RH 950 - 950F, 4 hrs. H 975, RH 975 - 975F, 4 hrs. H1000, RH1000 - 1000F, 4 hrs.
Inconel 718 Age Hardened	Material 51: (1850F, 1.5 hrs., OQ) + (1360F, 9 hrs., FC to 1175F and held at 1175F until total age time (1360F + FC + 1175F) was 19 hrs.). Material 53: (1750F, 1 hr., WQ)+ (1325F, 8 hrs., FC to 1150F at 100F/hr. and held at 1150F for 8 hrs.)
MP35N Age Hardened	1000F, 4 hrs.

Thermal cycles shown for 9-4-.20 and 9-4-.30 apply unless noted otherwise in the text.

TABLE 2.3-2

SPECIFIC TIME-TEMPERATURE CYCLES FOR Ti-6Al-4V
MATERIALS IN DB AND DBTC CONDITIONS

SPECIMEN NUMBER	CONDITION	TIME-TEMPERATURE CYCLE
62 NRW 4-34, 4-271 67 NWR 29-2, 29-3 77KRW YD 21, -22 Material 63, 65 and 92 specimens	DBTC	1700F, 4 to 6 hrs., FC to RT (100F/hr. or slower)
61 - 62 KWR 4-13, -14, -17 61 NRW 3-3	DBTC	1700F, 5 hrs., slow cool in DB press(insulation removed at 1000F)
Material 72 Specimens	DBTC except air cool from 1100F	1750F, 1 hr., FC 100F/hr. to 1100F, AC
70 NRW 39-14 77 NWR YD 1-15B 77 NWR YD 1-15A Material 72 Specimens	DBTC	1750F, 1 hr., FC to below 600F (100F/hr. or slower)
67 EWR 29-311, -312 70 EWR 39-131, -132 77 EWR 63P, Q 77 NRW LA 1-B	DBTC	1750F, 4 hrs., FC to below 600F (100F/ hr. or slower)
Material 74 Specimens	DBTC	First two cycles - 1750F, 5 hrs., slow cool (DB press) Third & fourth cycles - 1750F, 5 hrs., FC (laboratory furnace)
Material 74 specimens	DB	1750F, 5 hrs. under 2000 psi pressure, slow cool in DB press
All specimens not from Material 74	DB	1700F, 4 to 5 hrs. under 2000 psi pressure, slow cool in DB press

2.4 MATERIAL JOINING PROCEDURES

2.4.1 Gas Tungsten Arc (GTA) Welding Procedures

Weld joints and weld overlays in Ti-6Al-4V, 9-4-.20 and PH13-8Mo alloys were evaluated in the program. The joints in 0.10" sheet and all others prepared early in the program (total of 35 specimens) were machine welded. All other GTA welding was done manually. Preweld joint edge preparation was of the square type for 0.10" thick sheets, double-V for 0.125" thick plates, and single-U or double-U for material 0.250" or larger.

Manual welding was performed using a P and H Model DAR 200 power supply rated at 200 amps, with drooping characteristics and equipped with foot control. Welding torches were HW-20's rated at 200 amps. Straight polarity DC current with automatic high-frequency arc starting was used.

Parameters used in manual welding of joints having a double-U edge preparation were as follows:

Travel Speed	3 to 3.5 IPM
Filler Wire Diameter	0.045 to 0.062 in.
Argon Gas-Torch	12 to 15 CFH
Argon Gas-Backup	5 CFH
Amperage-Penetration Pass	195
Amperage-Filler Passes	160 to 180
Number of Weld Passes (average):	

0.12 in. Thick Joints - 6
0.25 in. Thick Joints - 14
0.50 in. Thick Joints - 20
0.75 in. Thick Joints - 44

Machine welding was done with a Miller direct current power source, Model ESR-150, or a Vickers Controlarc, 400 Amp-DC Welder, connected for straight polarity. An Airline stake welder was used to supply the torch drive mechanism and support the alignment and chill tooling for the weld specimens. The torch used was a Linde, Model HW 27. Typical parameters for machine welding of joints having a double-U edge preparation were as follows:

Material	Joint Thickness	Weld Pass No.	Amps	Volts	Travel IPM	Wire Dia/IPM	Torch Gas-CFH
9-4-20	0.56 in.	1	250	10	5	0.035/60	50
		2 to 18	280/ 300	10	5	0.035/60	40
Ti-6Al-4V	0.56 in.	1	195	8	5	0.045/12	25 + 25-Trailing Shield
		2 to 20	185/ 190	8	5	0.045/25	25 + 25-Trailing Shield
13-8	0.30 in.	1	220	10	6	0.035/60	60
		2 to 8	230/ 250	10	6	0.035/50	60

Copper hold-down and back-up bars (Figure 2.4-1, top) were used in both manual and machine welding. Hold-down bars were water-cooled to prevent excessive heat build-up, and were chamfered as shown in the Figure. Back-up bars not only helped cool the joint but also served as argon carriers, bleeding the gas to the weld underside for protection of that region.

Special copper blocks were placed against the joint ends (Figure 2.4-1, bottom) when welding manually. These reusable blocks improved the argon coverage in that area, allowing a full thickness, full length weld to and around the joint end without atmospheric contamination. Conventional run-on and run-off tabs were used in machine welding.

Titanium welds were protected during each pass by argon flowing from the torch, and by an argon-flushed trailing shield attached to the torch. This shield and the chamfered hold-down bars supporting it provided a gas-filled chamber which covered and protected the cooling weld.

If the material showed a tendency to warp, flatness was maintained by alternating the surfaces being welded. The specimen was turned over after each two or three weld passes, and subsequent passes run in the direction opposite to that of those run on the other surface.

Interpass temperature was held to 300°F maximum.

Welding electrodes were tungsten with 2 percent Thoria. Argon shielding gas per specification MIL-A-18455 was used in the torches and shielding tooling. Welding filler wire was purchased to specification ST0170GB0001.

Excess weld bead was removed by grinding, in the case of 0.1" sheets, or by machining off about 1/32" from the specimen surface, for thicker materials. These operations assured that the weld would be flush with the parent metal, and that no warpage would remain in the specimen.

Cross-sections of typical weld joints evaluated are shown in Figure 2.4-2.

2.4.2 Plasma Arc Weld (PAW) Techniques

One-half inch thick PAW joints in Ti-6Al-4V alloy were evaluated in the program. Joints were machine welded using equipment fabricated by Air Products Corporation, consisting of a Model MPW-400 torch, a Model DCCHF60R pilot power supply and a Model PDA 400 controller. The equipment is rated at 400 amps-DC. The welding power supply consists of two Model ESR-150, Miller DC power units connected in series. The torch was mounted on an Airline stake welder which provided a controllable motor drive and a mounting base for the fixture tooling.

Preweld joint edge preparation was of the square type. Joints were welded using run-on and run-off tabs. The weld underbead was enclosed in an argon-purged chamber. The torch surface of the weld was protected in the same manner as in GTA welding.

As the PAW process does not use filler wire, a concavity results from the keyhole pass. A second pass, GTAW, was therefore required to fill in that concavity.

PAW welding parameters were:

<u>Keyhole Mode</u> (First Pass)

- Welding Amperage - 185
- Pilot Arc Amperage - 25
- 1/8" Diameter Tungsten -2% Thoria Electrode
- 1/8" Diameter Gas Orifice
- Torch Gas - Orifice - 9 CFH Argon
  - Shield - 25 CFH Argon
- Torch Standoff - 0.31 in.
- Travel Speed - 4.5 IPM

GTA Mode (Second Pass)
Welding Amperage - 160
Torch Gas - Orifice - 1 CFH Argon
- Shield - 18 CFH Argon
Travel Speed - 4 IPM
Wire (0.035" diameter; 6 IPM-Feed)

Approximately 1/32" was machined from the specimen surfaces after completion of welding to make the weld flush with the parent metal and to remove any warpage left from the welding operation.

A macrograph showing the cross-section of a typical PAW joint is shown in Figure 2.4-2.

2.4.3 Diffusion Bonding Procedures (Figure 2.4-3)

Diffusion bond joints in Ti-6Al-4V were evaluated in the program. Diffusion bonding was performed at 1700 or 1750F for four to five hours under a pressure of 2000 psi with side restraint application. The bonding was performed in either a 300 ton press in the laboratory or a 500 ton press in the production facility. The cooling rate of the specimens from the bonding temperature was slow due to the mass of tooling employed.

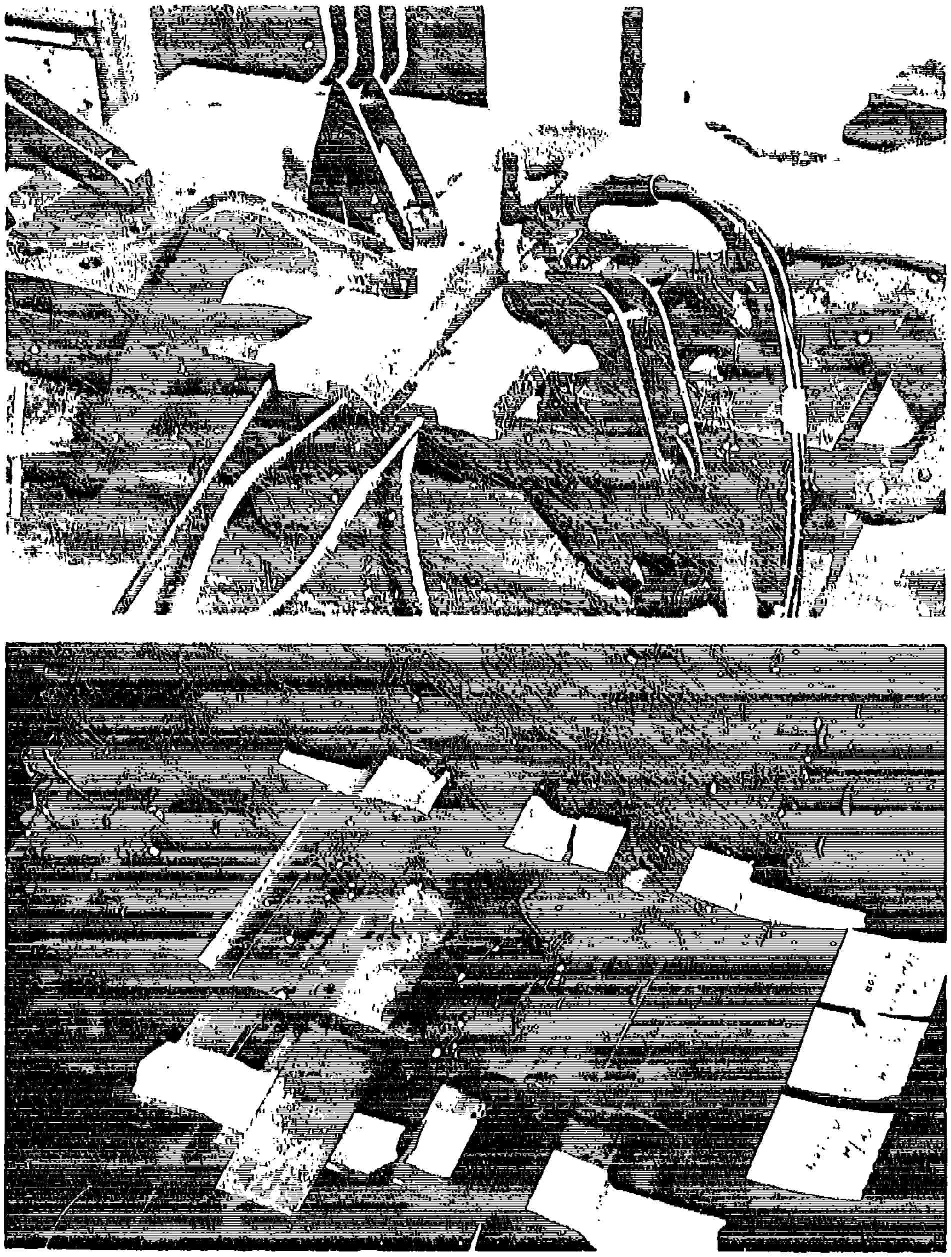

Figure 2.4-1 TIG Welding Setup For PTC Specimen
(Top View) Copper Hold-Down Bars In Position
(Bottom View) Copper Back-Up Bars In Position

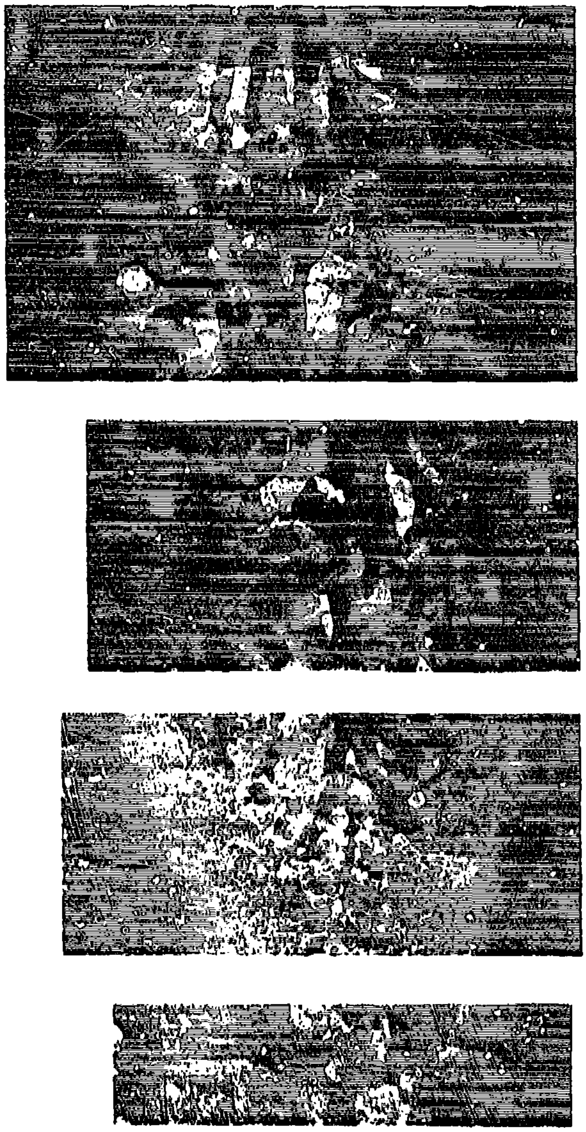

3/4-inch Thick GTAW Joint

1/2-inch Thick GTAW Joint

1/2-inch Thick PAW Joint
(Square Edge Preparation)

1/4-inch Thick GTAW Joint

(a) Ti-6Al-4V Alloy, 3.2X, Double-U Type
Edge Preparation Unless Noted

Figure 2.4-2 Macrographs Showing Transverse Cross-Sections of Typical Weld Joints.

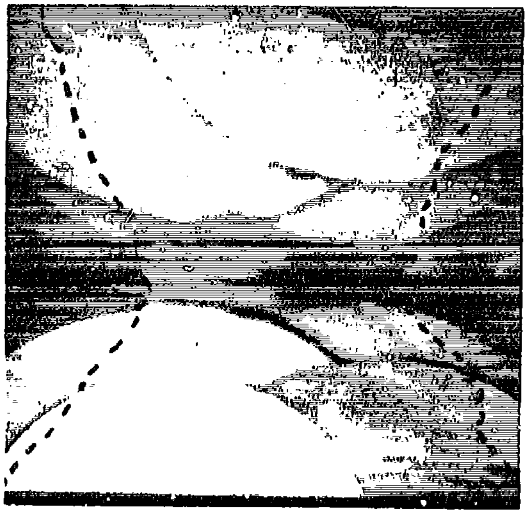

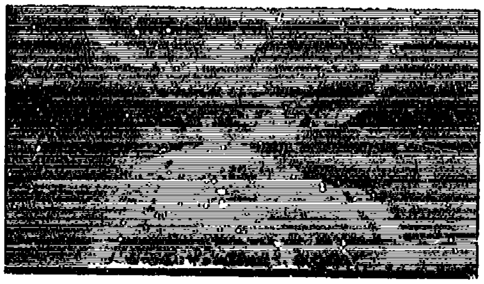

3.2X

6X 1/2-inch Thick GTAW Joints in 9-4-.20C Steel

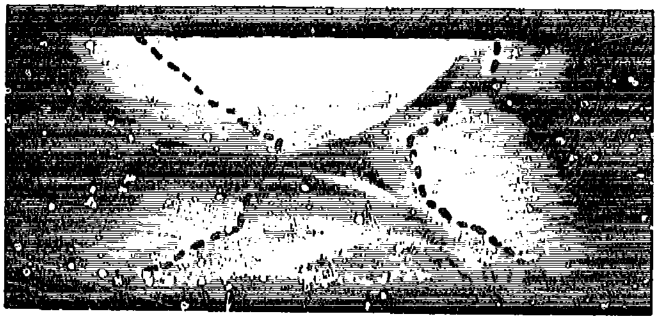

1/4-inch Thick GTAW Joint in 9-4-.20C Steel

6X

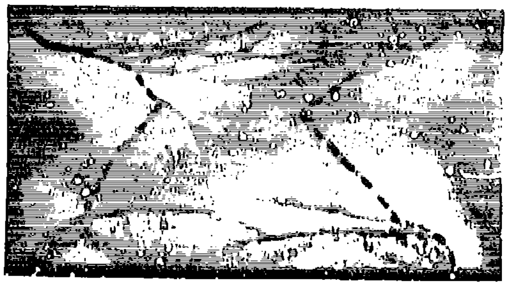

6X

1/4-inch Thick GTAW Joint in PH13-8Mo Steel

(b) Steel Alloys, Double-U Type Edge Preparation. Fusion Line Is Indicated By Dotted Line.

Figure 2.4-2 (Continued)

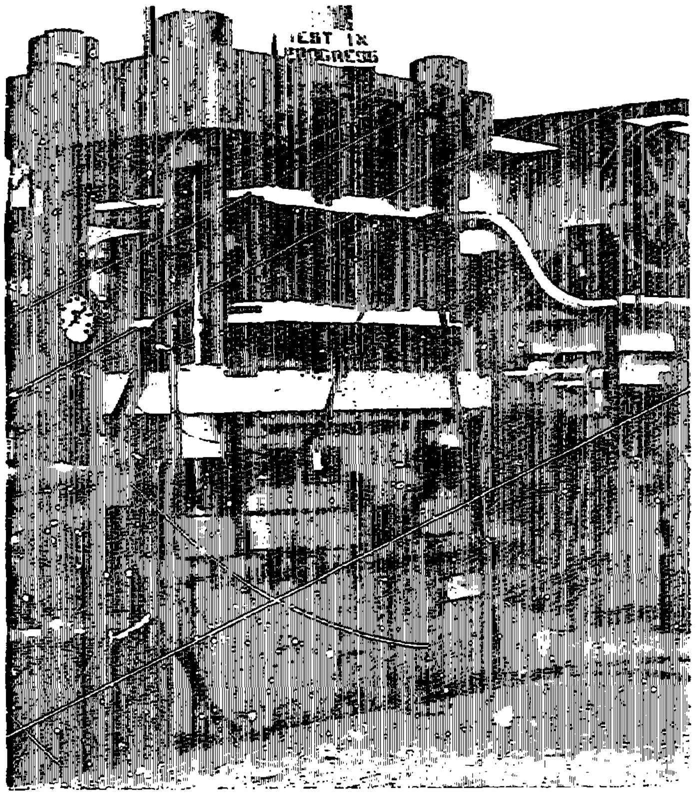

300 Ton Press With Retort-Ring Assembly In Place For Bonding Operation

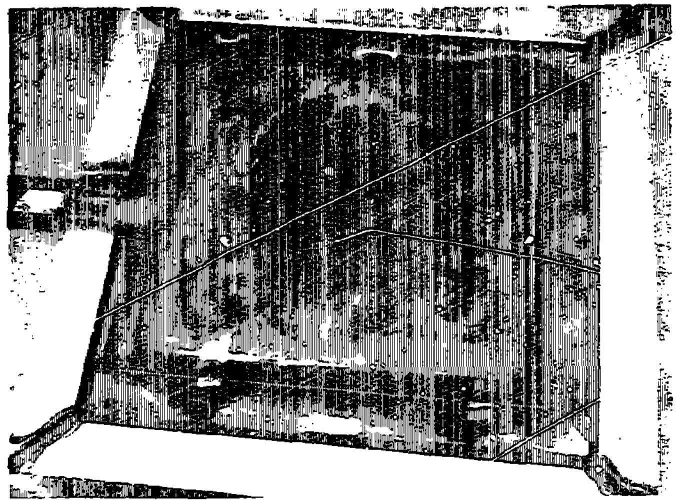

Retort With Top Removed Showing Internal Tooling Around Ti-6Al-4V Details

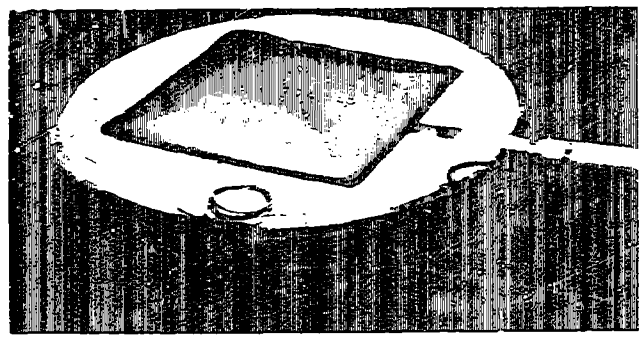

Retort In Side Restraint Ring

Figure 2.4-3 Diffusion Bonding Press and Assembly

SECTION 3 TEST SPECIMENS, EQUIPMENT AND ENVIRONMENTS

3.1 SPECIMEN CONFIGURATIONS AND PRECRACKING PROCEDURES

The specimen configurations used in this program were compact tension (CT), part-through-crack (PTC), center cracked tension (CCT) and double cantilever beam (DCB). CT specimens were used for K_{Ic}, K_c and da/dN tests, PTC specimens for K_{Ic} and da/dN tests, CCT for K_c and da/dN tests, and DCB for K_{Iscc} tests.

All precracking of specimens was performed at an R factor of .05.

3.1.1 CT Specimens (Figure 3.1-1, Tables 3.1-1, 3.1-2).

In general, thicknesses of CT specimens used in K_{Ic} tests were selected to satisfy the requirements of ASTM E399, i.e., thickness must be equal to or greater than 2.5 times the square of the ratio of toughness to tensile yield strength ($B \geq 2.5 \left|\frac{K_{Ic}}{Y.S}\right|^2$). It is generally accepted that compliance with this criterion will result in a plane strain stress state within the specimen during test.

The lengths of these specimens were selected, in general, to be equal to or greater than 6.8 times the square of the above ratio (i.e., $W \geq 6.8 \left|\frac{K_{Ic}}{Y.S}\right|^2$, (reference (d)\]. This length requirement keeps the ligament stress (the stress in the unfailed portion of the specimen) at crack initiation below 80% of the material yield strength and insures that the crack will propagate through an elastic stress field.

All other specimen dimensions (H, D, W_1, H_1, and N) were derived from the W dimension using ratios for the standard specimen described in ASTM E399. Specimens having B and W dimensions up to 2" and 8", respectively, were used in this program.

B dimensions of CT specimens used for K_c testing were selected to be in the range from 20 to 80% of that required for a plane strain stress state. (Specimens as thin as 0.11" were tested). W dimensions were selected to be large enough to keep the ligament stress below the material yield strength until the K_c load was reached.

Specimens used for da/dN testing were a modification of the ASTM E399 CT configuration, providing a longer crack growth length over which data could be generated. The crack notch was shortened so the a/W ratio after precracking would be .3 instead of .5. Some specimens also were used having an H/W ratio of .486 instead of .6 as specified in ASTM E399. For a given specimen height (2H), this change resulted in a longer W dimension and thus, a longer crack growth length. Most of the CT specimens

used for da/dN testing had a B dimension of 1.0 inch, a 2H dimension of 7.2 inches, and a W dimension of either 6.0 inches (-17 specimen of Table 3.1-1, H/W = .6) or 7.4 inches (-18 specimen of Table 3.1-2, H/W = .486).

CT specimens were usually fatigue precracked in three stages of decreasing loads. The K-level and crack extension during the final precracking stage of K_{Ic} and K_c specimens were controlled to meet ASTM E399 requirements. The K-level in final stage precracking of da/dN specimens was held slightly below the K-level which would be used in the testing.

3.1.2 PTC Specimen (Figure 3.1-2)

This configuration was used for most K_{Ic} and da/dN testing of welds (The CT geometry could not be used because required weld joint thicknesses were too thin to obtain a plane strain stress state during test. In addition, the small size of the PTC starter notch allowed accurate placement of the notch within the HAZ). PTC specimens were 30 inches long by 7.5 inches wide, with two reductions in width. These specimens were made up by welding two 12-inch by 7.5-inch reusable tabs to a 6-inch by 4-inch center section. This center section, which contained the weld to be tested, was further reduced in width .06 to .50" during finish machining. Two types of weldments were tested; butt weld joints and weld overlays (in which a surface depression in the parent metal was filled with weld metal).

Starter notches were 0.05 inches deep and 0.6 inches long (a few were 0.3 inches long) for K_{Ic} specimens and 0.10" long for da/dN specimens. In weld overlay specimens, the starter notch was located at the center of the weldment, while in butt weld joint specimens, the notch was located either at the center of the weld bead or at the fusion line. The starter notches were machined by the EDM process using a .010" thick radiused electrode.

PTC specimens were precracked in two to three stages of decreasing loads. K-levels during final stage precracking were kept below initial test K-levels for specimens to be used in da/dN testing and below the lesser of: 60% of the predicted K_{Ic} value or 0.2% E, for specimens used in K_{Ic} testing. All K_{Ic} specimens and a few da/dN specimens were precracked in three point bending by Rockwell International. Most da/dN specimens, however, were precracked in axial loading by Lockheed California Company. The K_{Ic} specimens were precracked a typical length of .07" at each end of the starter notches and the da/dN specimens, a typical length of .02". The size of typical flaws in K_{Ic} specimens after precracking are shown in Figure 3.1-3. Flaws in da/dN specimens after precracking were essentially semi-circular and had a typical radius of .07".

3.1.3 CCT Specimens (Figure 3.1-4).

CCT specimens were used to evaluate 0.10" sheet material and were 24" wide by 48 to 60" long with a 4" long starter notch in the center of the specimen. Four of the specimens fabricated from Ti-6Al-4V alloy contained a weld joint having a starter notch located at the edge of the weld bead. All other specimens were parent metal specimens.

The CCT specimens used in da/dN testing were precracked to a typical length of .25" at each end of the starter notch in stages of decreasing cyclic loads. In the final stage, cracks were extended a minimum length of .05" at a load slightly less than the intended initial test load.

The specimens used for K_c testing were fatigue precracked at least 0.1" at each end of the starter notch in one or two stages. Maximum K-levels in fatigue precracking of aluminum and titanium specimens were 10,000 and 17,500 psi $\sqrt{in}$, respectively.

In designing the CCT specimens, the following guidelines as suggested to ASTM Committee E-24.01 by Federsen, were used:

(1) Selection of notch and fatigue precrack length

$2a_o = W/6$

$2a_o = 2\,a_n + 2\,(\Delta a)$

$2a_n$ = mechanical notch length

Δa = length of fatigue precrack at each notch root

= the lesser of 0.10 inch or 2t (as a minimum)

t = thickness

(2) Selection of stress intensity factor levels for fatigue precracking

$$K_{max} \leq \frac{K_c}{4}$$

3.1.4 DCB Specimen (Figure 3.1-5).

This specimen was used for all K_{Iscc} tests. Each specimen was bolt-loaded to a constant deflection. The standard specimen for parent metal had a thickness of 1", a height of 2", and a length of 4.5" to 6".

A few tests were run using a much smaller specimen to evaluate some 1-1/2" diameter bar stock which was not large enough to make the standard specimen. The small specimen is a standard ASTM E399 K_{Ic} specimen (B = .5", W = 1:) with bolt holes added at the notch end for specimen loading.

Specimens used for tests on weld joints were essentially the same size as the standard parent metal specimen except that they had thicknesses as low as 1/8". Blocks 3/4" thick were welded onto the thinner test specimens to increase their cross sections to accommodate the loading bolts.

Specimens were precracked in three stages of decreasing loads to a minimum length of .12" (.20" typical). The K-level during the final .050" of crack growth was maintained below 50% of the estimated K_{Iscc} value to conform with ASTM proposed standards for K_{Iscc} testing. (Reference e).

Table 3.1-1

Dimensions of Compact Tension (CT) Specimens Having An H/W Ratio of .600
Used For K_c, K_{Ic} and Da/DN Tests
See Figure 3.1-1 For Configuration

Dash	Thickness		W	W_1	H	2H	H_1	D	N	C Dimension, ± .010	
No.	Min	Max	±0.005	±0.010	±0.005	±0.010	±0.005	+0.005 -0.000		da/dN Tests	K_c, K_{Ic} Tests
-1	0.063	0.500	1.000	1.250	0.600	1.200	0.275	0.250	1/16	0.175	0.375
-3	0.100	0.750	1.500	1.375	0.900	1.800	0.415	0.375	1/16	0.325	0.625
-5	0.125	1.000	2.000	2.500	1.200	2.400	0.550	0.500	1/8	0.475	0.875
-7	0.1875	1.250	2.500	3.125	1.500	3.000	0.6875	0.625	1/8	0.625	1.125
-9	0.1875	1.500	3.000	3.750	1.800	3.600	0.825	0.750	1/4	0.775	1.375
-11	0.250	1.750	3.500	4.375	2.100	4.200	0.9625	0.875	1/4	0.925	1.625
-13	0.250	2.000	4.000	5.000	2.400	4.800	1.100	1.000	3/8	0.950	1.750
-15	0.3125	2.500	5.000	6.250	3.000	6.000	1.375	1.250	3/8	1.250	2.250
-17	0.500	3.000	6.000	7.500	3.600	7.200	1.650	1.500	3/8	1.600	2.750
-19	0.250	4.000	8.000	10.000	4.800	9.600	2.200	2.000	3/8	2.150	3.750

Table 3.1-2

Dimensions of Compact Tension (CT) Specimens Having An H/W Ratio of .486
Used for Da/DN Tests
See Figure 3.1-1 for Configuration

Dash No.	Thickness Min.	Thickness Max.	W ±.005	W_1 ±.010	H ±.005	2H ±.010	H_1 ±.005	D +.005 -.000	N	C±.010
-2	0.063	0.500	1.235	1.485	0.600	1.200	0.275	0.250	1/16	0.312
-4	0.100	0.750	1.850	2.255	0.900	1.800	0.415	0.375	1/16	0.500
-6	0.125	1.000	2.470	2.970	1.200	2.400	0.550	0.500	1/8	0.687
-8	0.1875	1.000	3.090	3.715	1.500	3.000	0.6875	0.625	1/8	0.825
-10	0.1875	1.000	3.770	4.520	1.800	3.600	0.825	0.750	1/4	1.000
-12	0.250	1.000	4.330	5.205	2.100	4.200	0.9625	0.875	1/4	1.187
-14	0.250	1.000	4.940	5.940	2.400	4.800	1.100	1.000	3/8	1.375
-16	0.3125	1.000	6.180	7.430	3.000	6.000	1.375	1.250	3/8	1.625
-18	0.250	1.000	7.400	8.900	3.600	7.200	1.650	1.500	3/8	2.000

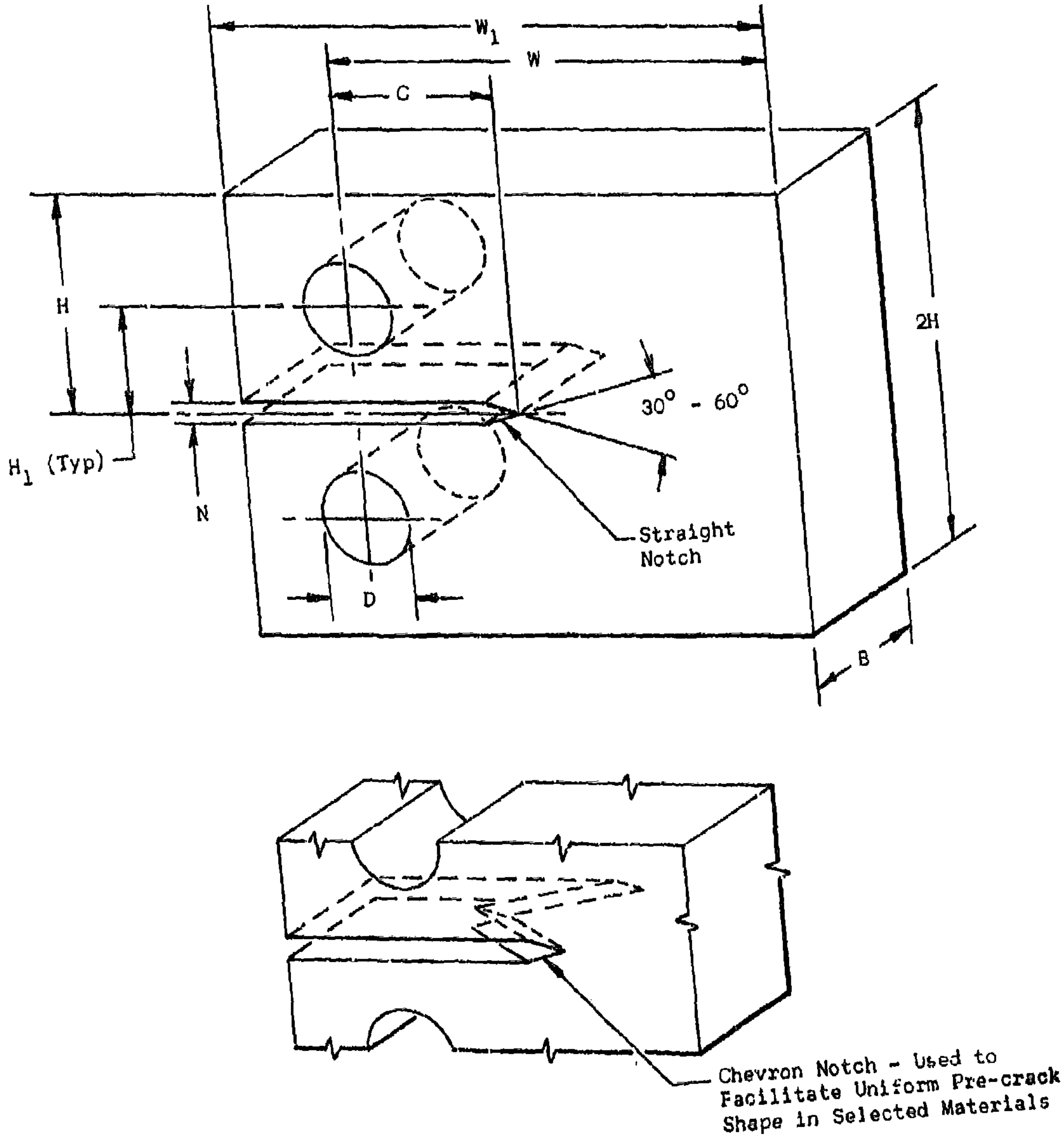

(a) Specimen for Parent Metal and Diffusion Bond Joints. Dimensions of the Various Specimen Sizes are Listed in Tables 3.1-1 and 3.1-2

Figure 3.1-1 Configuration of Compact Tension (CT) Specimen

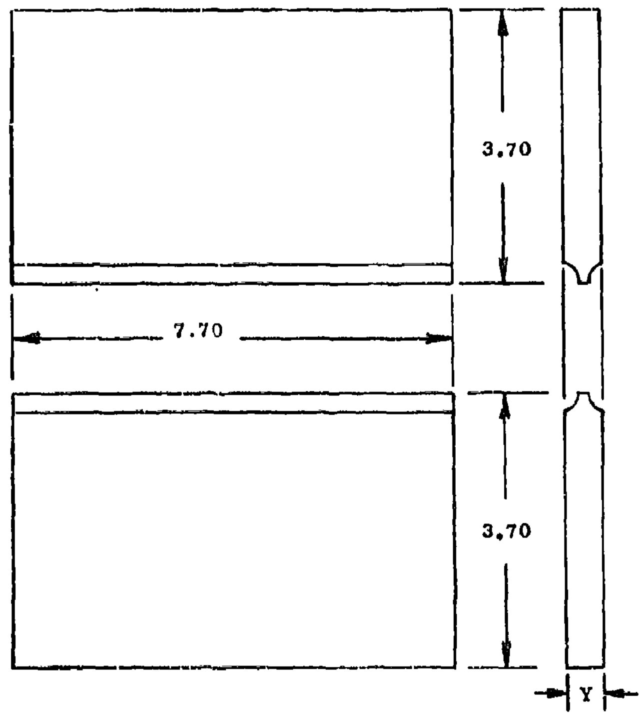

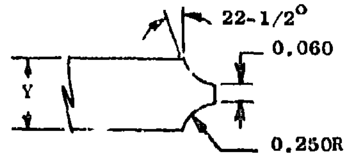

Double-U Edge Preparation, GTAW only

Notes:

1. The joints in three specimens (Ti-6-4) were prepared using the PAW Process. All others were prepared using the manual or machine GTAW process with double-U edge preparation.

2. The crack notch was located at the centerline of the weld.

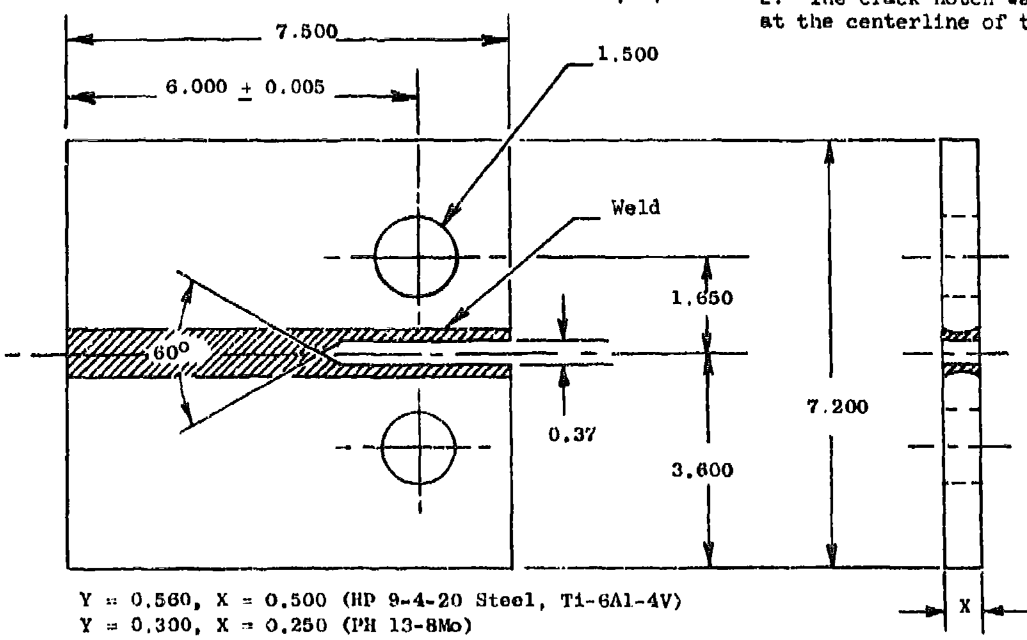

Y = 0.560, X = 0.500 (HP 9-4-20 Steel, Ti-6Al-4V)
Y = 0.300, X = 0.250 (PH 13-8Mo)

(b) Specimen for Butt Weld Joints

Figure 3.1-1 Cont'd

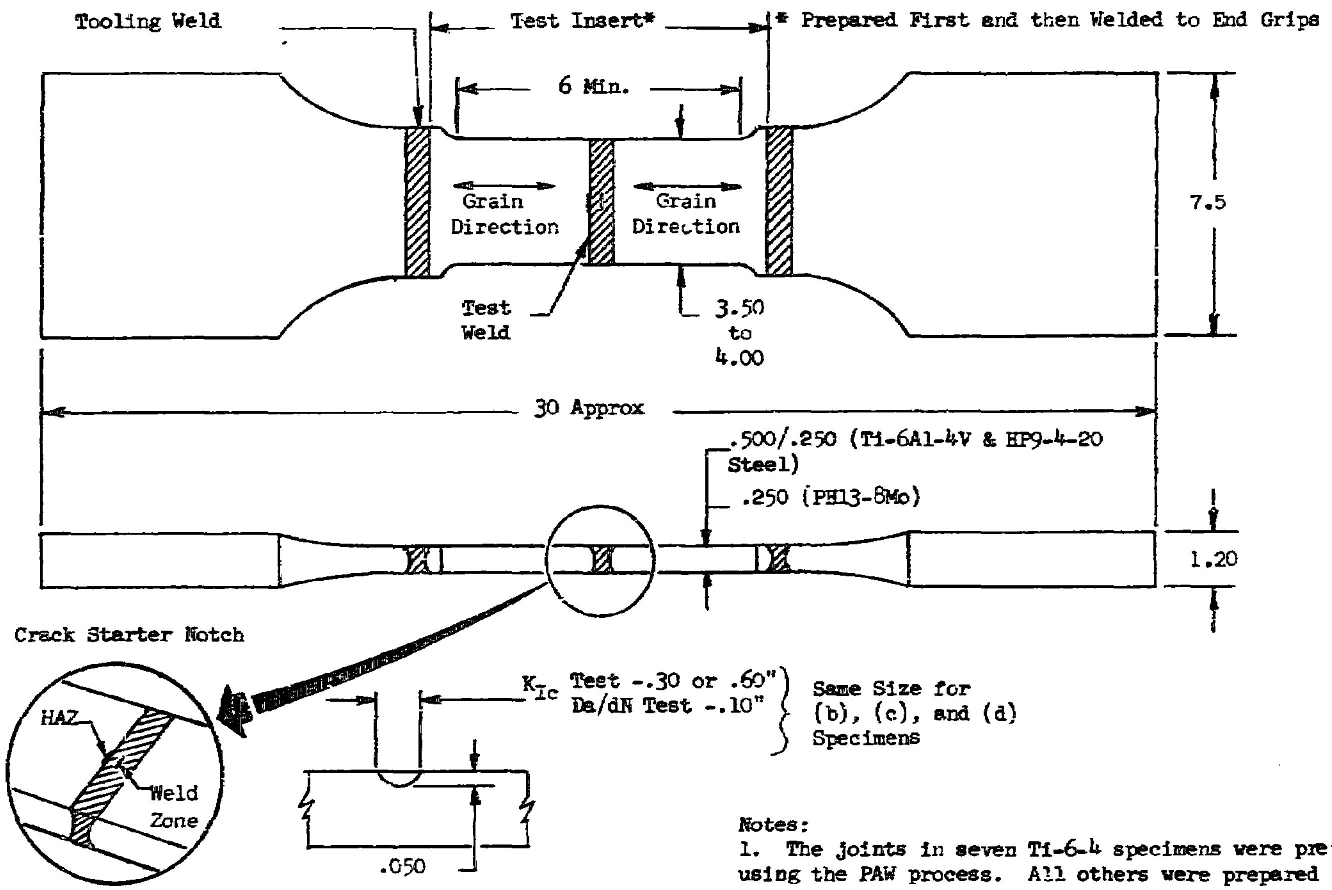

(a) Specimen For Transverse Butt Weld Joint

Notes:
1. The joints in seven Ti-6-4 specimens were prepared using the PAW process. All others were prepared using the GTAW process.

2. The edge preparation for four of the GTAW joints was of the single-U type. For all other GTAW joints, the edge preparation was of the double-U type.

3. GTA welding was performed both manually and by machine.

Figure 3.1-2 Configuration of Part-Through-Crack (PTC) Specimen

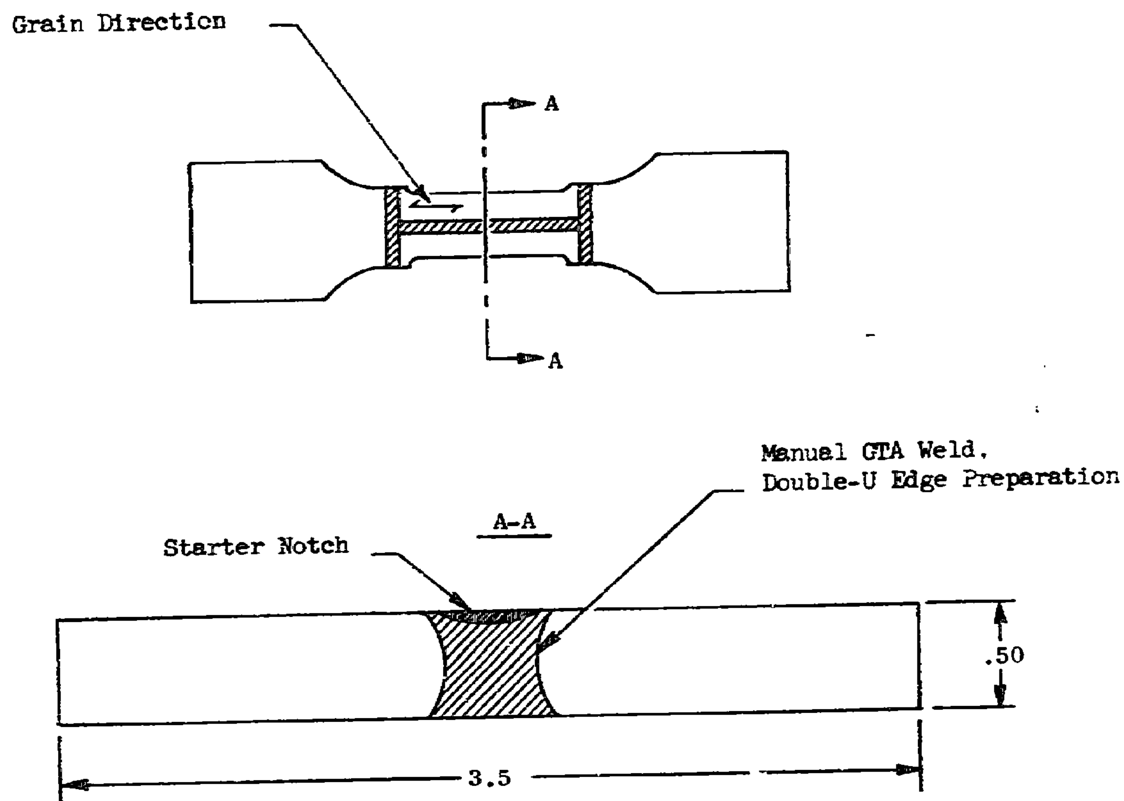

(b) Specimen for Longitudinal Butt Weld Joints (Two Specimens Used In K_{Ie} Tests)

Figure 3.1-2 Continued

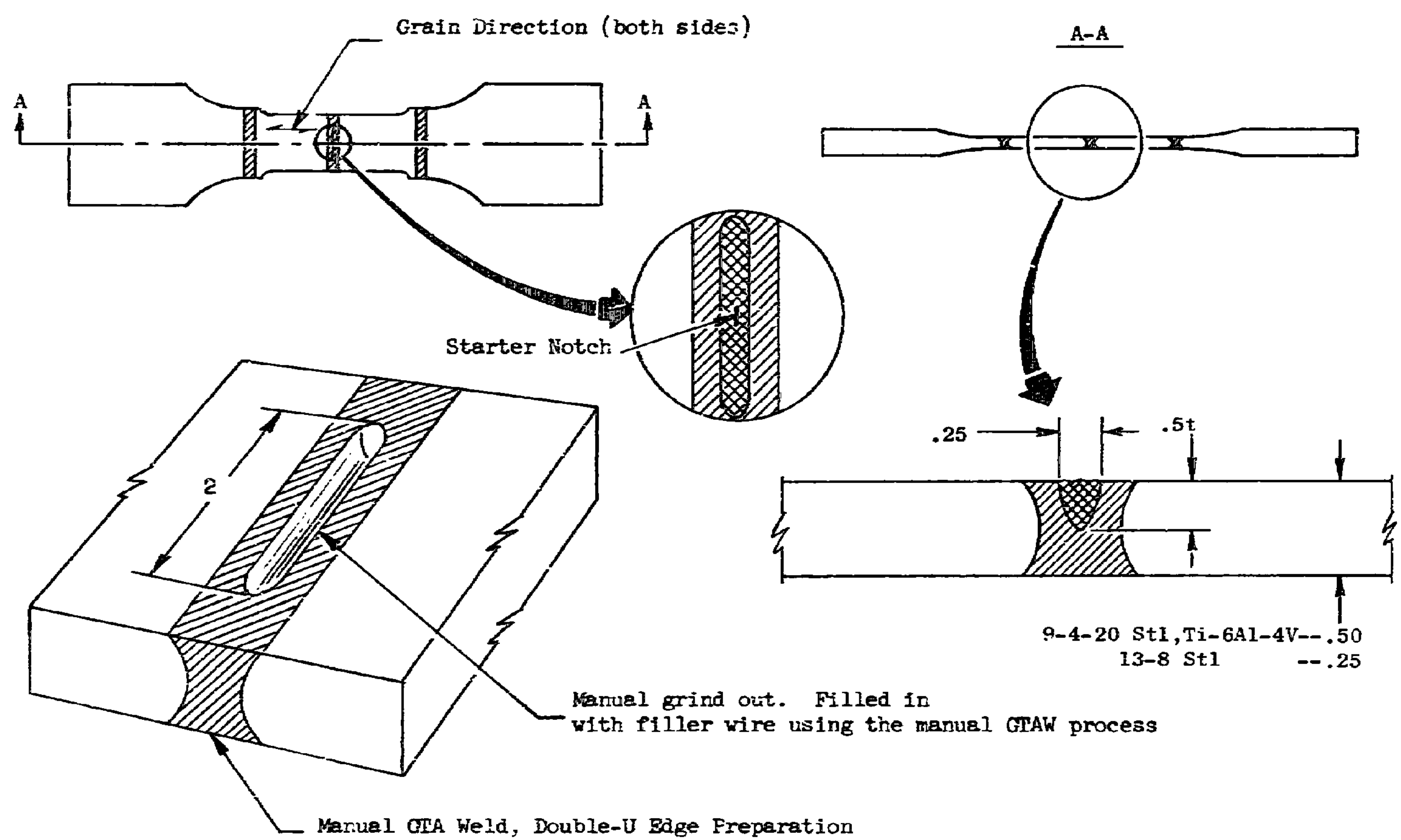

(c) Specimen for Butt Weld Joints Containing a Grindout Reweld Repair

Figure 3.1-2 Continued

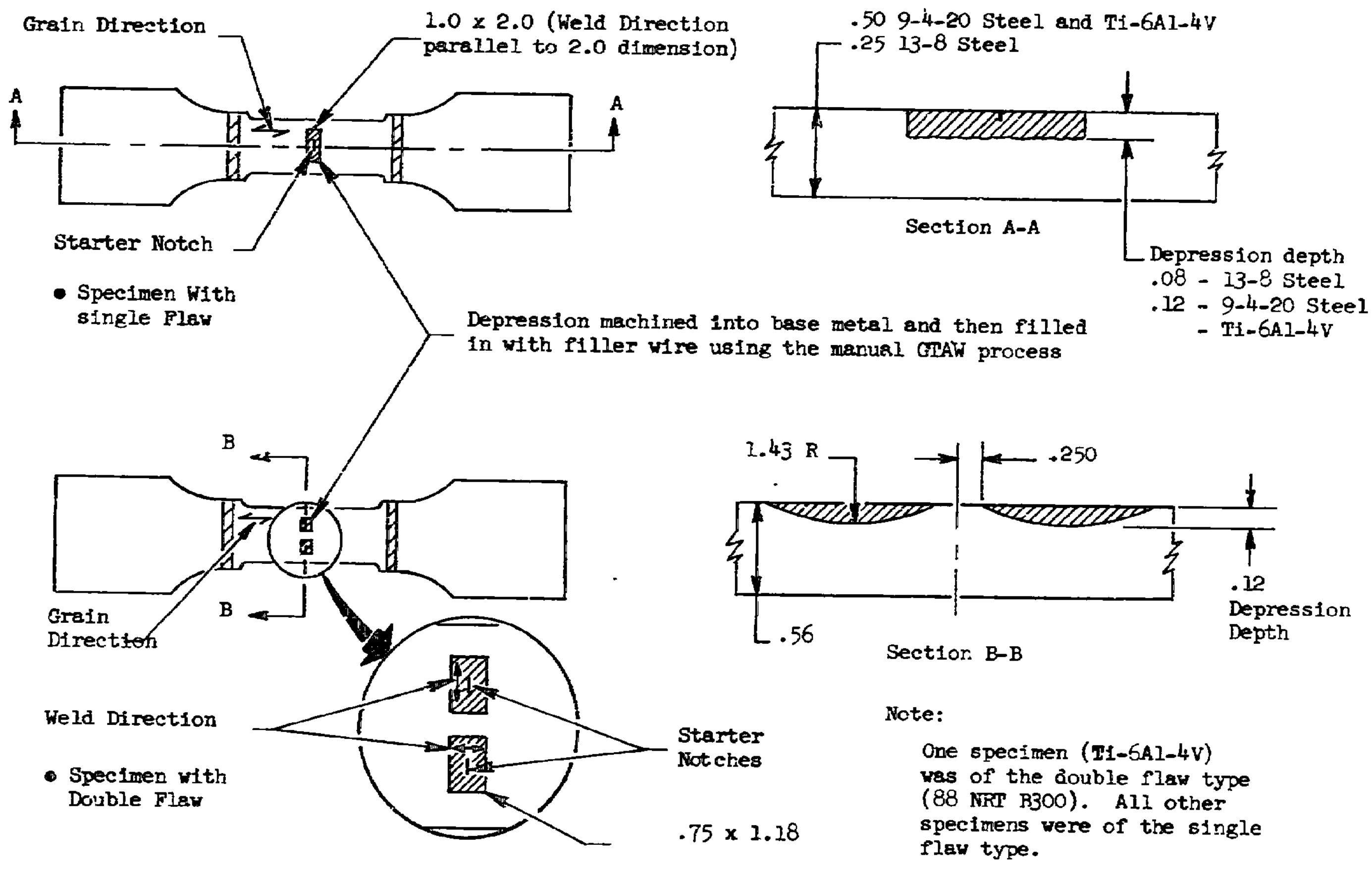

(d) Specimens for Weld Overlays

Figure 3.1-2 (Continued)

0.75-inch Thick Specimen

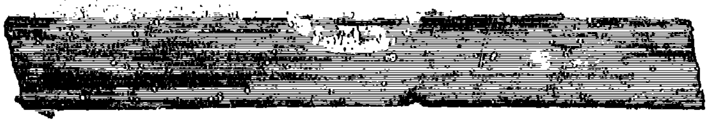

0.48-inch Thick Specimen

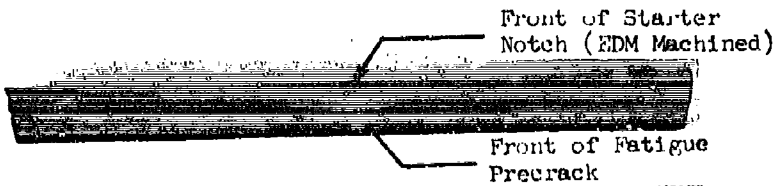

0.29-inch Thick Specimen

Figure 3.1-3 Fracture Faces on PTC Specimens Failed in K_{Ic} Testing, Showing Typical Precrack Size in Specimens of Various Thicknesses.

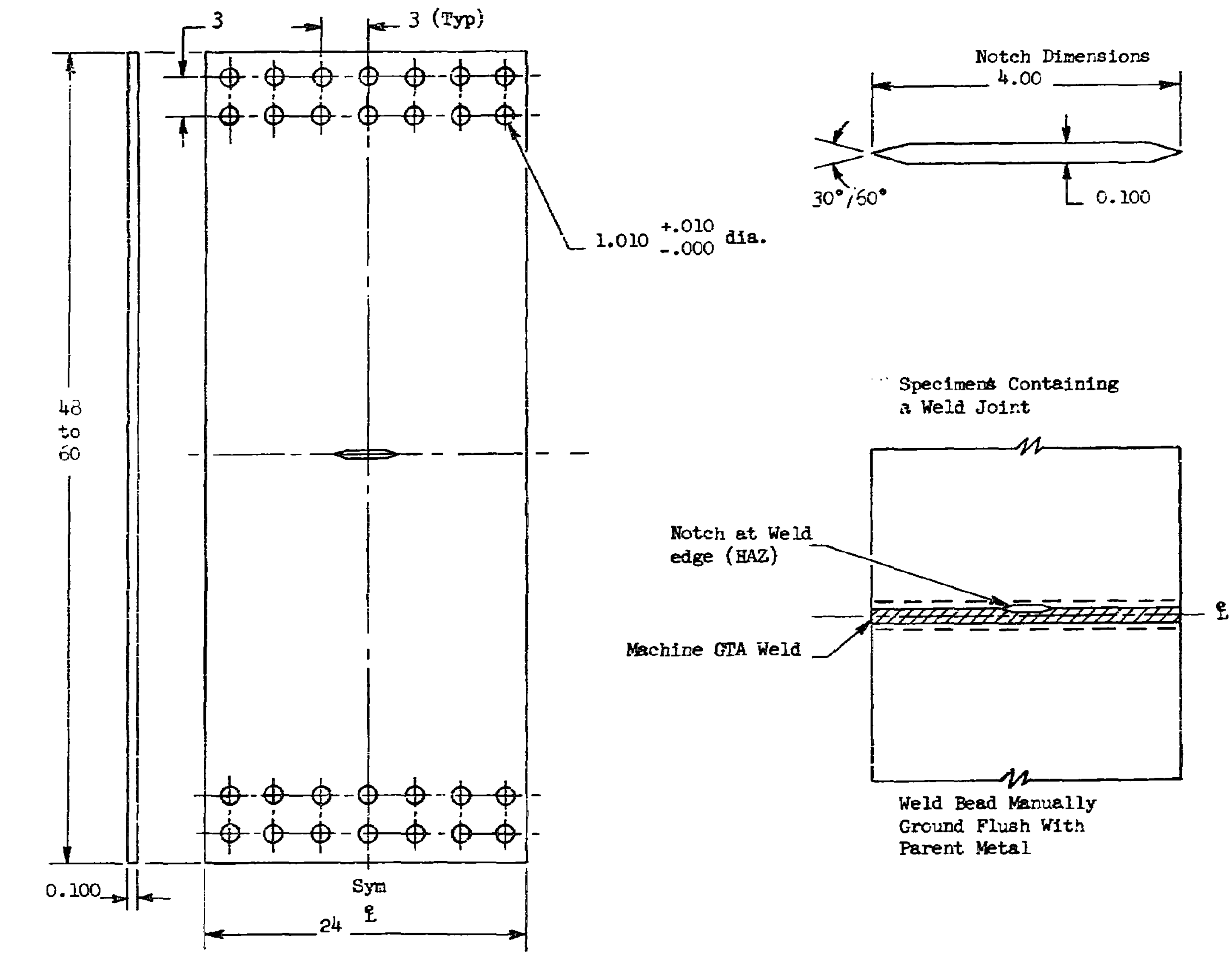

Figure 3.1-4 Configuration of Center Cracked Tension (CCT) Specimen

* Inconel 718, 300M and most PH13-8Mo Specimens had a notch depth of 1.500.
** Early Tests were run using 3/8 in. diameter bolts.

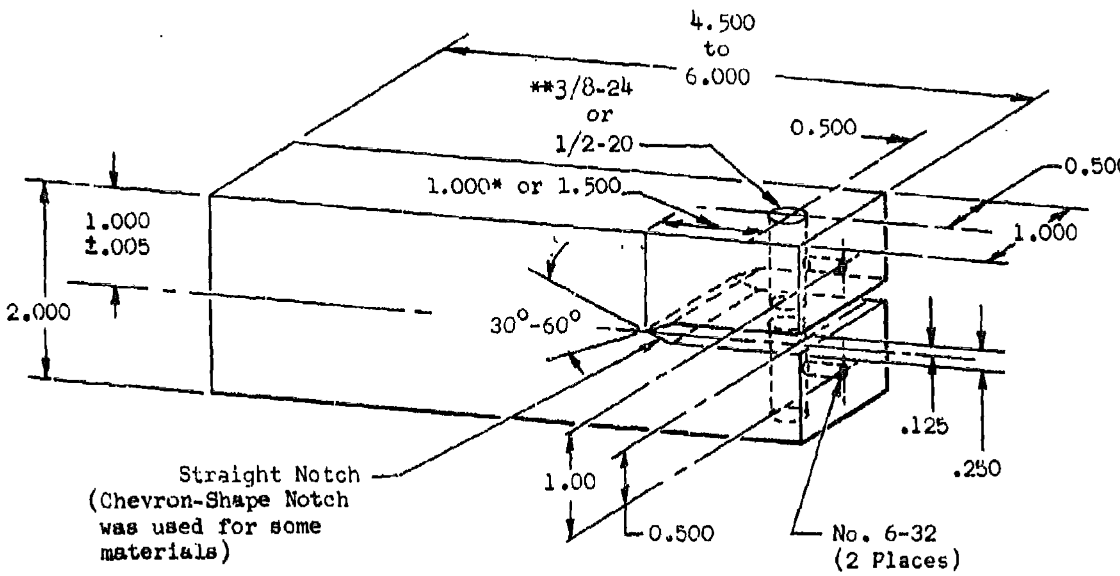

(a) Standard Specimen for Parent Metal and Diffusion Bond Joints

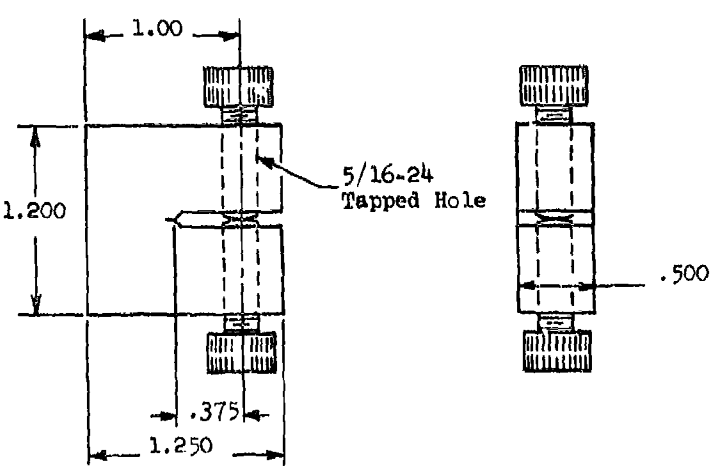

(b) Small Specimens for 1.500 Diameter Bar Stock

Figure 3.1-5 Configuration of Double Cantilever Beam (DCB) Specimens (K_{Iscc} Tests)

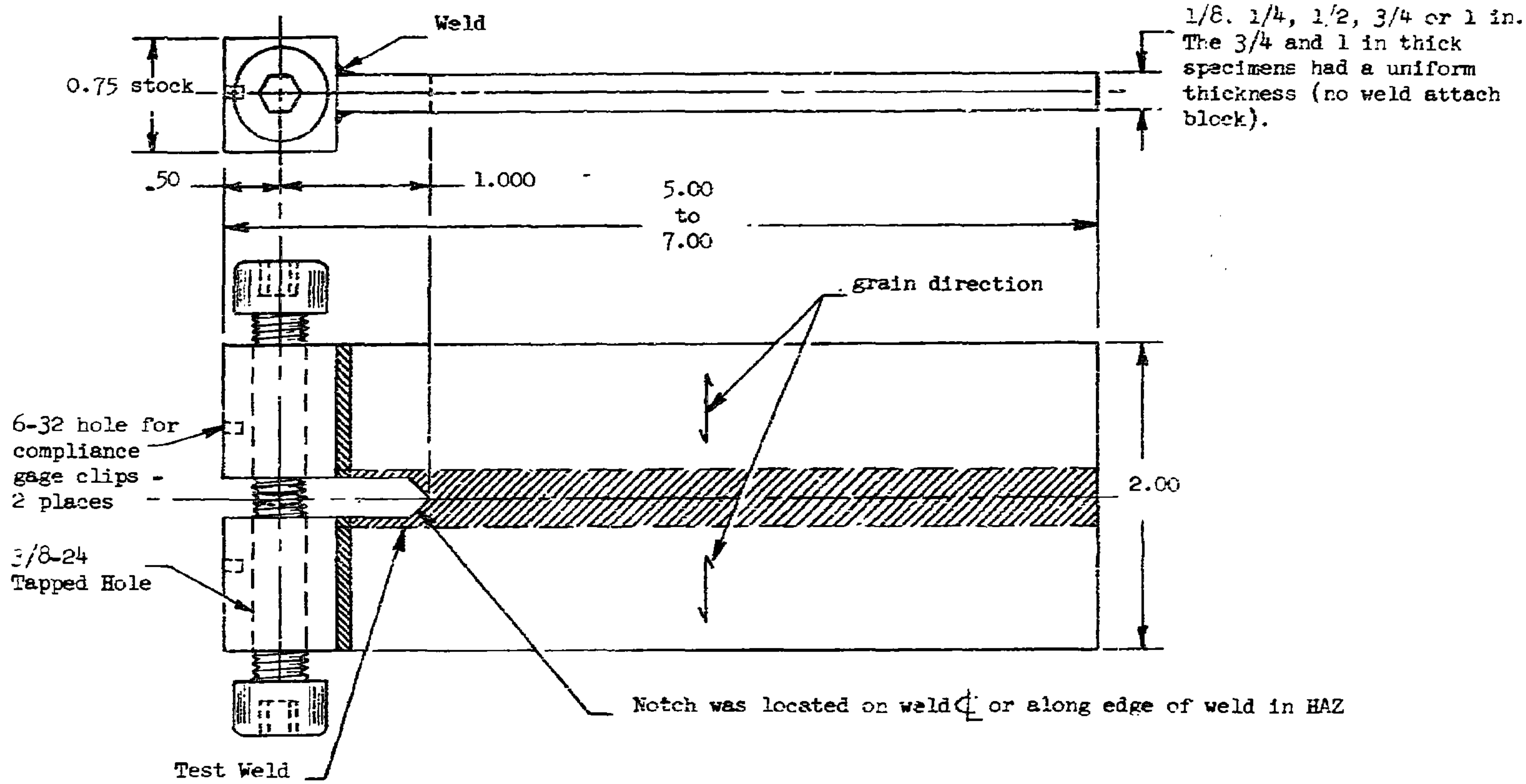

1. The joint in 3 specimens (Ti-6Al-4V) was prepared using the PAW process. All others were prepared using GTAW process.

2. Three of the GTAW joints (Ti-6Al-4V) were machine welded. All others were manually welded.

3. For GTAW joints, the joint edge preparation was of the double-V type for the 1/8 in. thick joints and of the double U type for all other thicknesses.

(c) Specimen for Butt Weld Joints

Figure 3.1-5 Continued

3.2 PRECRACKING AND TESTING EQUIPMENT

Each specimen was precracked in the laboratory in which it was to be tested. Precracking and testing was performed in Los Angeles at the B-1 Division of Rockwell International (RI); in Fort Worth Texas at the Convair Aerospace Division of General Dynamics (GD); and in Saugus, California, at the Lockheed-California Company (LCC). A few specimens were also precracked and tested by the University of Dayton Research Institute at the Wright-Patterson Air Force Base (WPAFB).

3.2.1 Static Test Specimens

Static tests consisted of K_{Ic} tests performed on CT and PTC specimens, K_c tests performed on CT and CCT specimens and K_{Iscc} tests performed on DCB specimens. All static testing was conducted at RI except for 16 K_{Ic} CT specimens which were tested at WPAFB.

3.2.1.1 Precracking Static Specimens (Figure 3.2-1).

Precracking CT and DCB specimens at RI was done either in conventional fatigue machines or in a bank of laboratory constructed electro-hydraulic fatigue frames. The conventional equipment included an Amsler Vibrophore Model 10 HFP 422, a BLH Sonntag SF-10V and a BLH IV 12. PTC specimens were precracked in 3-point bending on a BLH Sonntag SF-1. CCT specimens were precracked and tested, as one continuing operation, in an MTS Model 311.72.01 load frame equipped with an MTS Model 810 control console.

Before the start of the precracking operation, clear plastic scales ruled to .01" divisions were adhesively attached to the specimen sides adjacent to the crack plane. Crack growth was measured by observing the position of the crack trace tip along this scale using a binocular microscope, a transit scope (Bronson or Keuffel and Esser) or an alignment scope.

Precracking CT specimens at WPAFB was done in an MTS testing system, the length of the crack traces being measured with a sliding microscope.

3.2.1.2 Testing Static Specimens

Crack opening displacement (COD) on all static specimens in test was picked up by an MTS compliance gage which was mounted across the crack plane, either on grooves machined into the specimen end or on holding clips. These holding clips were variously attached to the specimen by means of screws or by welding or bonding in place.

An autographic curve of load versus COD was recorded on an X-Y recorder.

CT, PTC, and CCT specimens were all tested to failure in conventional testing equipment. DCB specimens, on the other hand, were exposed, at a constant crack opening displacement, to various environmental liquids.

Crack lengths on the fracture faces after testing of all specimens were measured using a hand magnifying glass and a scale with .01" graduations.

3.2.1.2.1 Testing CT, PTC and CCT Specimens (Figure 3.2-2).

At RI, CT specimens were tested in a 120,000-pound capacity Riehle Universal Test Machine. A Houston Instrument Series 2000 Recorder was used to record load versus crack opening displacement. At WPAFB CT specimens were tested in an MTS system.

PTC specimens were tested in an MTS Model 311.51.04 load frame (500 KIP capacity) controlled from an MTS Model 810 console.

CCT specimens were tested immediately on completion of the precracking cycles, as described in paragraph 3.2.1.1.

Testing at -65°F was done with a thermally insulated box enclosing the specimen and adjacent fixturing. Atomized liquid nitrogen, released into the box by a solenoid switch, maintained the specimen temperature at the set-point during testing.

Testing at 265°F was conducted in an electrically heated, circulating air type furnace which surrounded the specimen and adjacent fixturing.

3.2.1.2.2 Testing DCB Specimens (Figure 3.2-3).

DCB specimens were loaded using opposing bolts to obtain the appropriate deflection, as measured by a COD gage connected to a Houston Instrument Series 2000 Recorder. Immediately after loading, the specimens were immersed in the exposure medium, which was contained in a plastic tub of appropriate size. Crack trace lengths were periodically measured during the exposure period using a hand magnifying glass.

3.2.2 Fatigue Crack Growth Rate (FCGR) Test Specimens

Specimens used to monitor FCGR in this program were of the CT, PTC or CCT configuration. Some CT specimens were precracked and tested at WPAFB and at RI, and a number of PTC specimens were precracked and tested at RI. Most of the CT specimens, however, were precracked and tested at GD, while most PTC specimens and all CCT specimens were precracked and tested at LCC.

3.2.2.1 Precracking FCGR Specimens

Equipment used at RI for precracking was the same as that previously described for precracking CT and PTC specimens employed in static tests.

CT specimens tested at GD were precracked in a BLH IV 4 fatigue machine and those tested at WPAFB were precracked in an MTS Testing System.

CCT and PTC specimens tested at LCC were precracked in the same test fixtures used for actual da/dN testing of these specimens.

3.2.2.2 Testing FCGR Specimens (Figures 3.2-4, 3.2-5, 3.2-6, 3.2-7).

CT specimens tested at WPAFB and PTC specimens tested at LCC were tested in MTS Testing Systems. All other tests (all laboratories) were performed in laboratory constructed test frames of the electro-hydraulic closed-loop type. Basically, these frames employ load cells, hydraulic cylinders and pumps, servo-valves, servo-controllers and signal generators.

Frames for CT specimens tested at RI employed 4" diameter, 20 KIP capacity, hydraulic cylinders to apply loads to specimens. Microdot F210B wave form generators were used to program the desired load cycles and test frequencies. Servac 410.03 electro-hydraulic control systems (1% sensitivity at full scale) were used to obtain the mean and maximum load, and General Electric recording oscillographs were used to record minimum and maximum load.

On PTC specimens tested at LCC and on CT specimens tested at WPAFB, crack trace lengths during test were measured with the aid of a sliding microscope. On all other specimens (at all laboratories) clear plastic scales ruled to .01" divisions were adhesively attached to the specimen surface adjacent to the crack plane, and crack trace lengths were measured during testing by ovserving the position of the tip of the crack along the scale using a microscope, a transit scope or an alignment scope.

The elevated temperature (150, 265F) and sub-zero (-65F) tests were conducted in a thermally insulated box enclosing the specimen and adjacent fixturing. Cooling for the -65F tests was accomplished with a solenoid-controlled, atomized stream of liquid nitrogen injected into the chamber. Heating of the chamber during elevated temperature tests was accomplished by injecting a hot air stream into the box. Electric heaters were used to heat the air stream to appropriate test temperatures.

Room temperature environments (except lab air) were generally maintained only around the crack region of the specimens by enclosing that region between panels of clear plastic, thereby facilitating visual crack trace measurements without interruption of the test. Rubber rings or vacuum seal tape (General Sealant GS37, Prestite Type 587.3) were used to effect a seal between the panels and the specimen surfaces. On CT specimens seals across notch openings were accomplished using a soft rubber plug or vacuum seal tape.

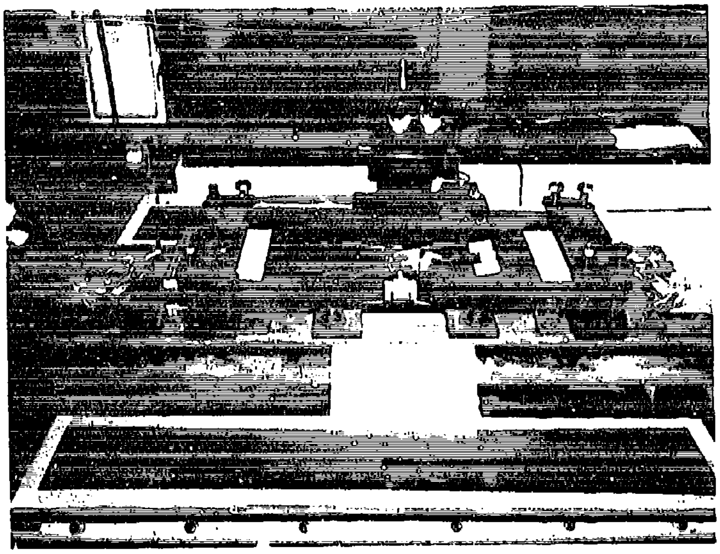

(a)

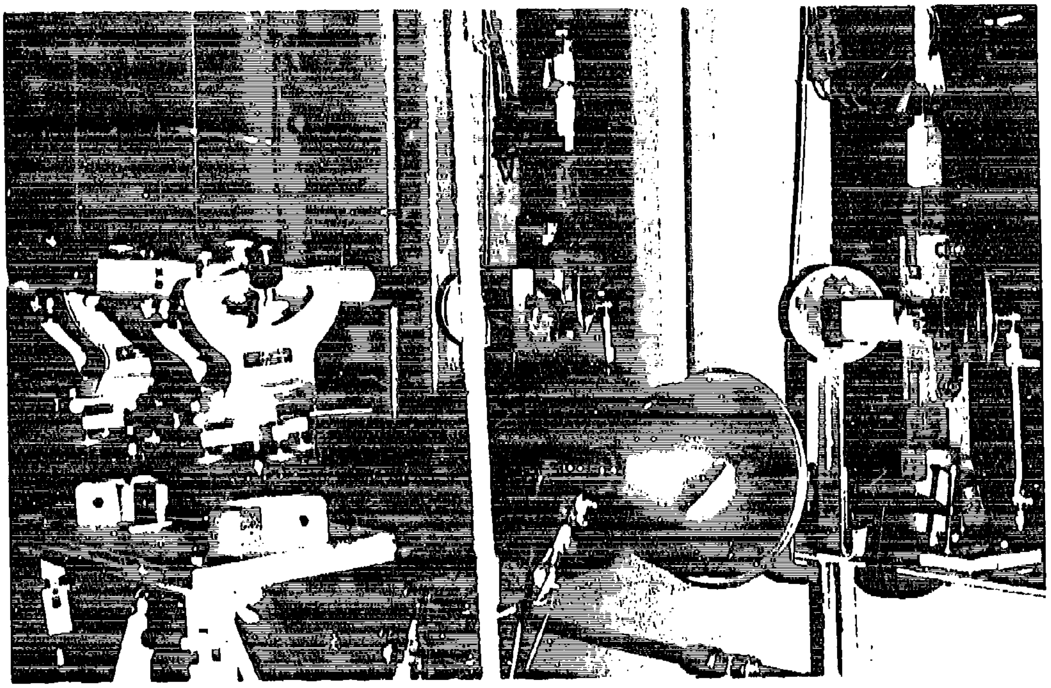

(b)

Figure 3.2-1 Setups At Rockwell International For Fatigue Precracking (a) PTC Specimen, (b) DCB K_{Iscc} Specimen

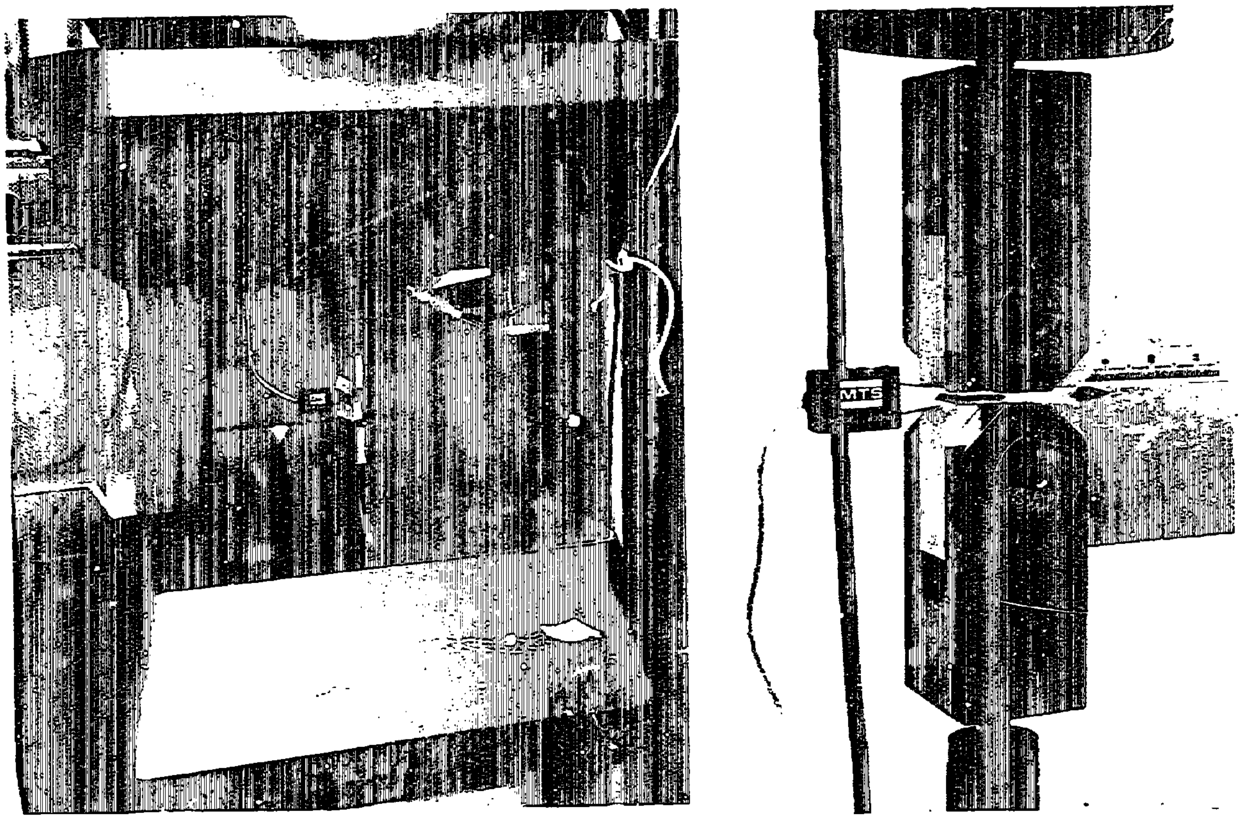

(a) (b)

Figure 3.2-2 Setups at Rockwell International for K_{Ic} and K_c Tests
(a) PTC Specimen (K_{Ic} Test) (b) CT Specimen (K_{Ic} and K_c Tests)
(c) CCT Specimen (K_c Test)

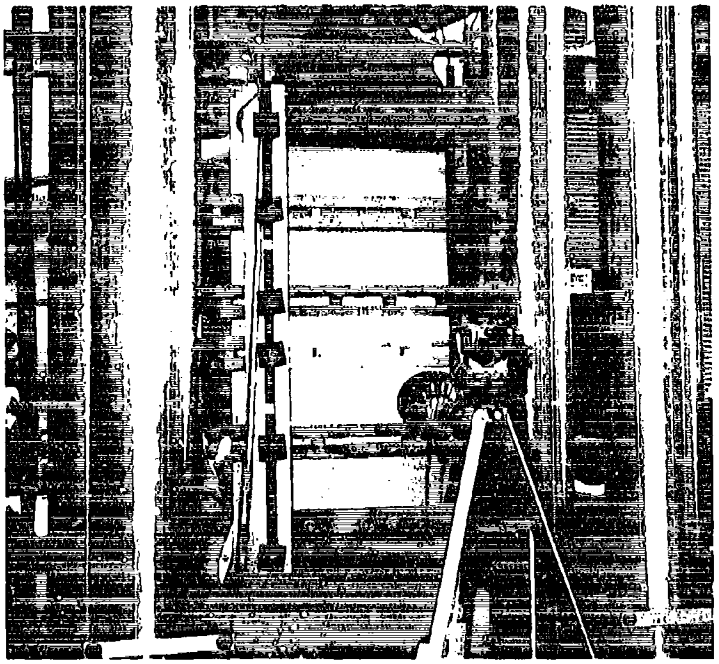

(c)

Figure 3.2-2 (Continued)

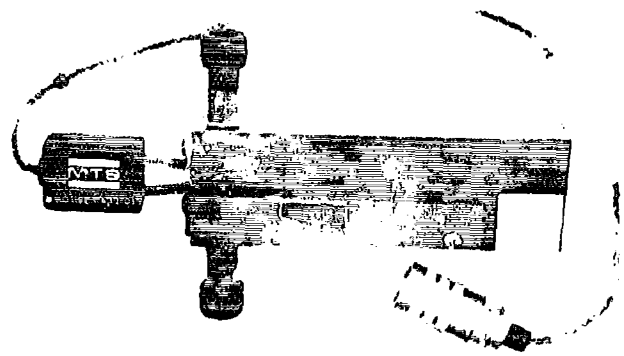

Specimen prepared for loading. Clip gage is in place for measuring Crack Opening Displacement.

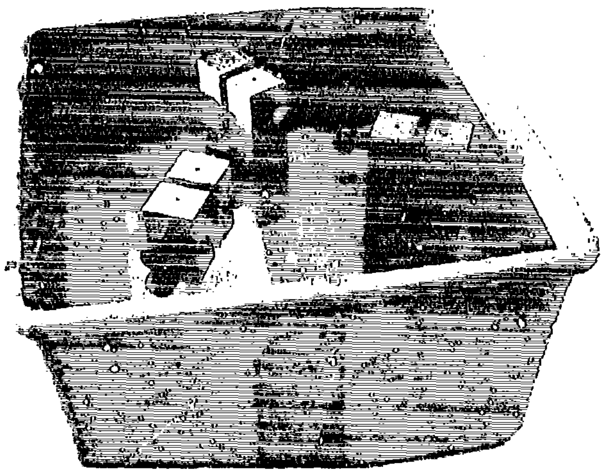

Specimens immersed in environmental liquid after loading. Only the bolt portion of the specimen was exposed to the air. Level of the bath was maintained to just below the bolts throughout the test.

Figure 3.2-3 Set-Up For K_{Iscc} Testing

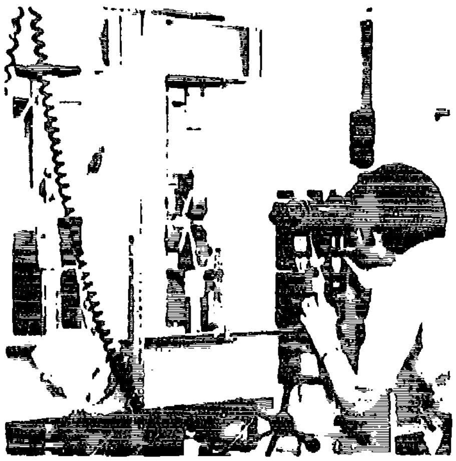

Overall View Of Specimens In The Testing Frame

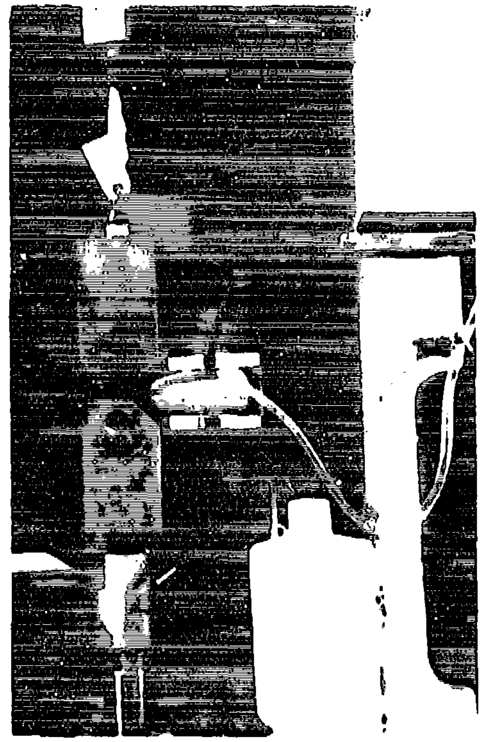

Close Range View Of Specimen and Fixturing

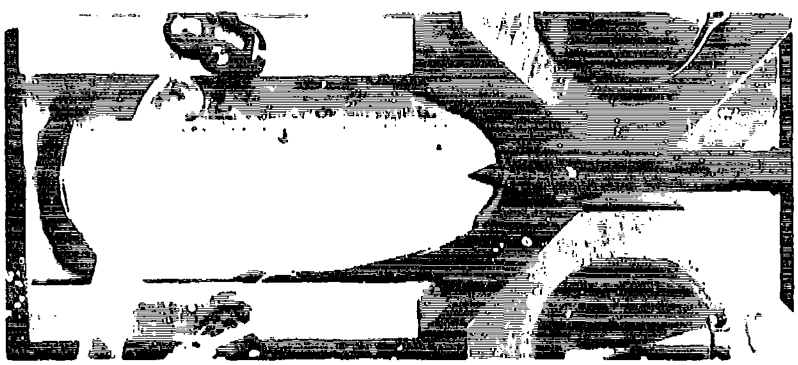

Close-Up View Of The Specimen Test Region

(a) CT Specimen

Figure 3.2-4 Setups At Rockwell International For FCGR Testing

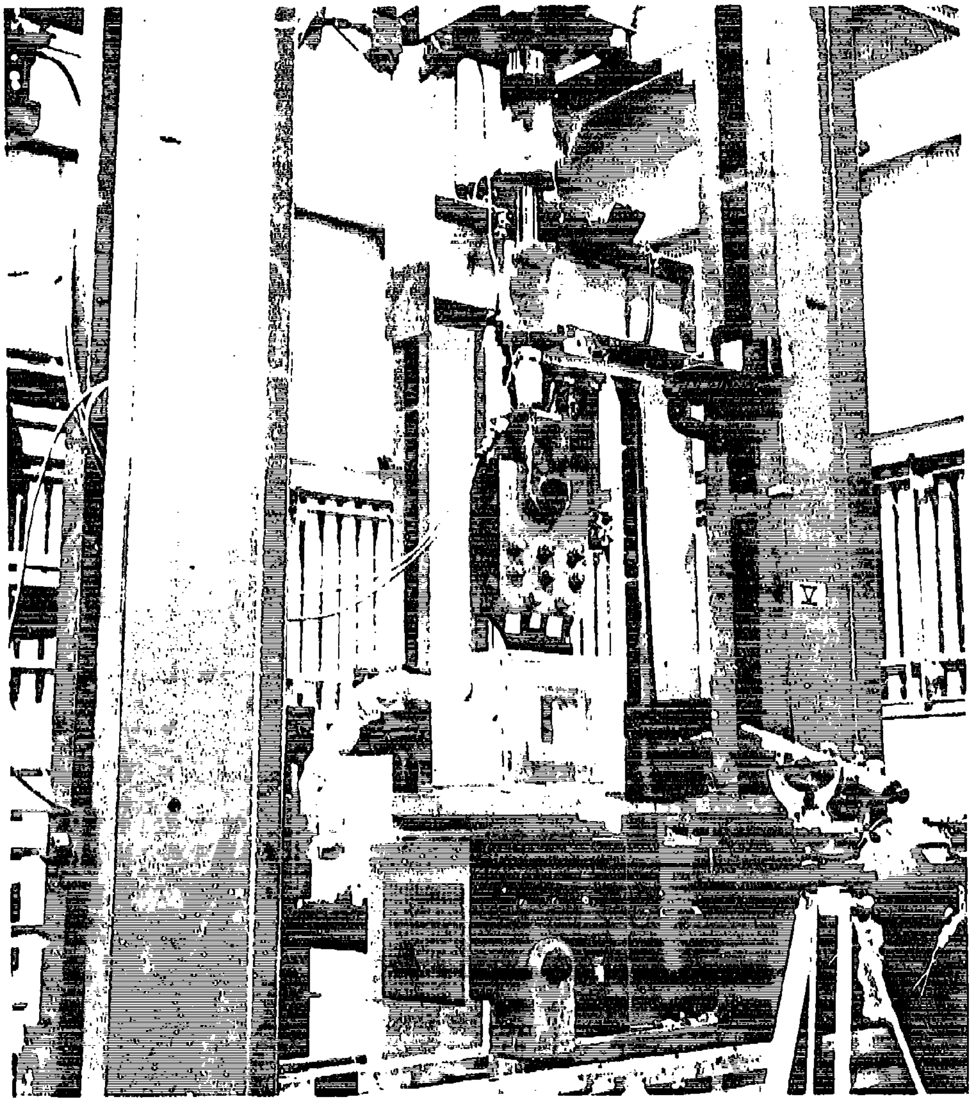

(b) PTC Specimen Being Tested at -65°F

Figure 3.2-4 (Cont'd)

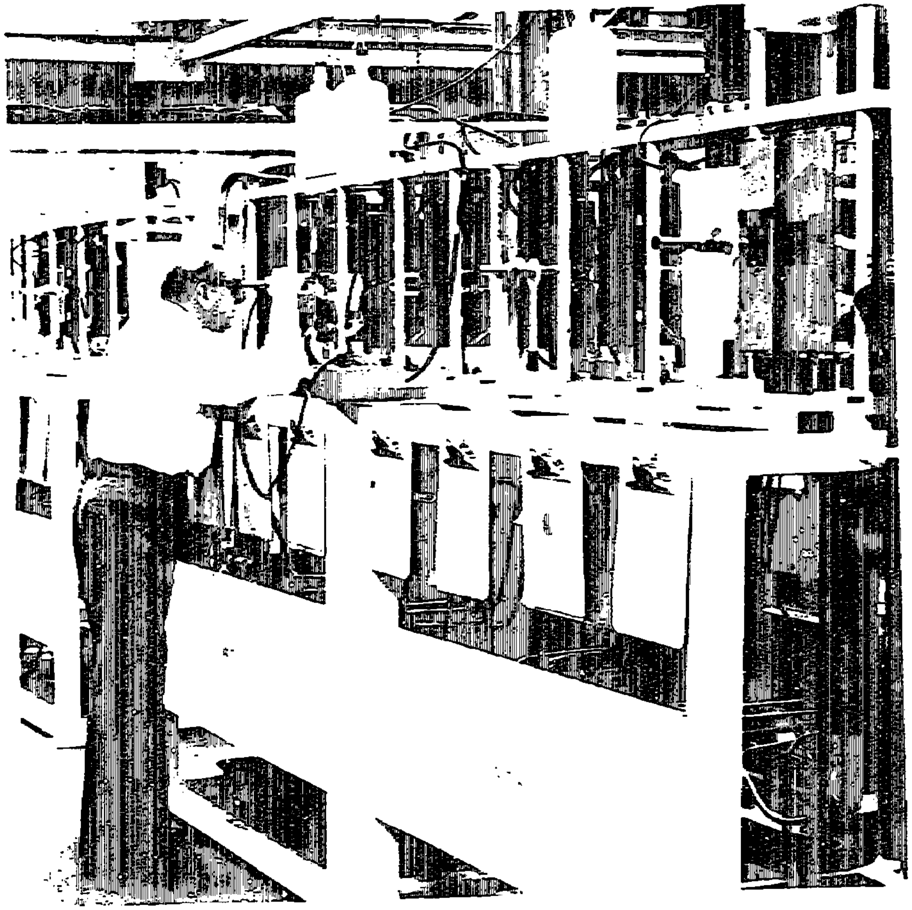

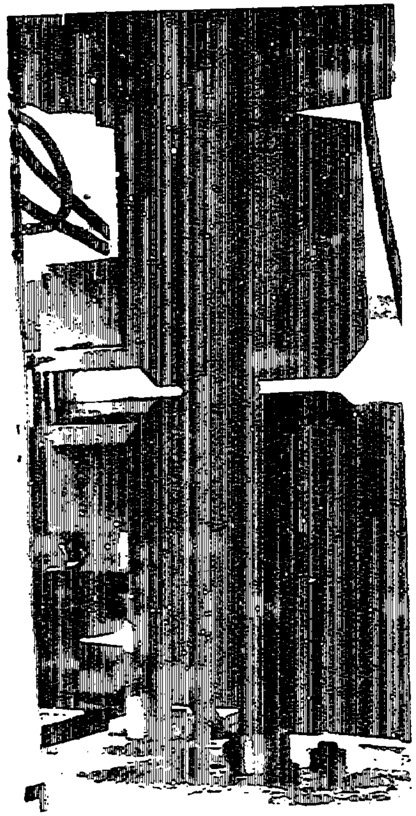

Figure 3.2-5 Setups At General Dynamics For FCGR Tests On CT Specimens

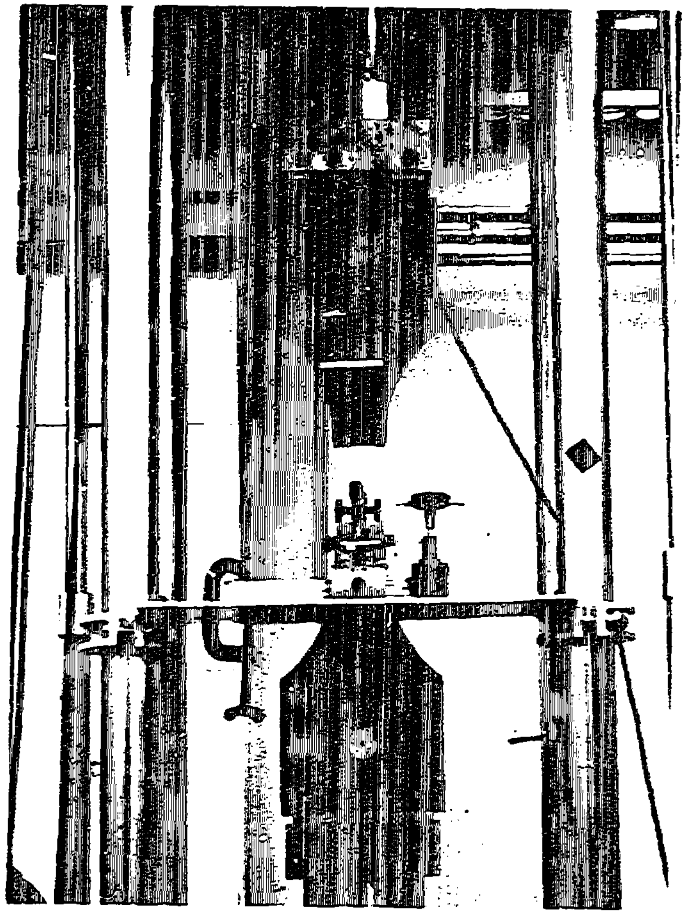

(a) PTC Specimen

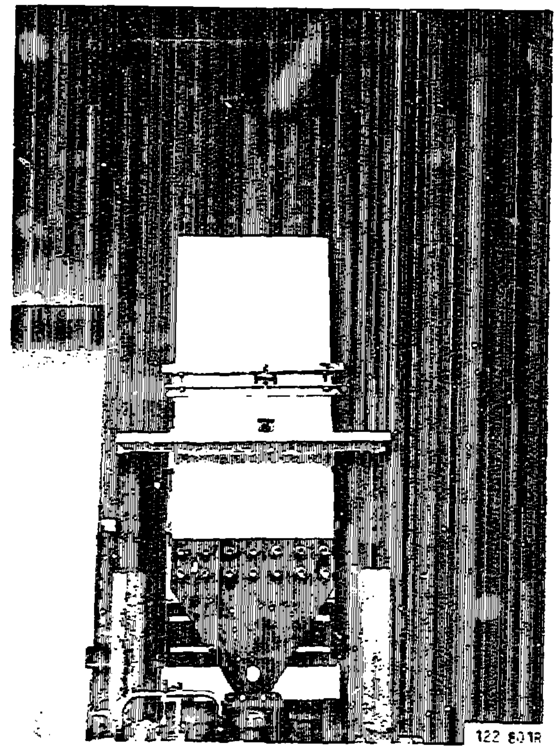

(b) CCT Specimen

Figure 3.2-6 Setups At Lockheed For FCGR Tests

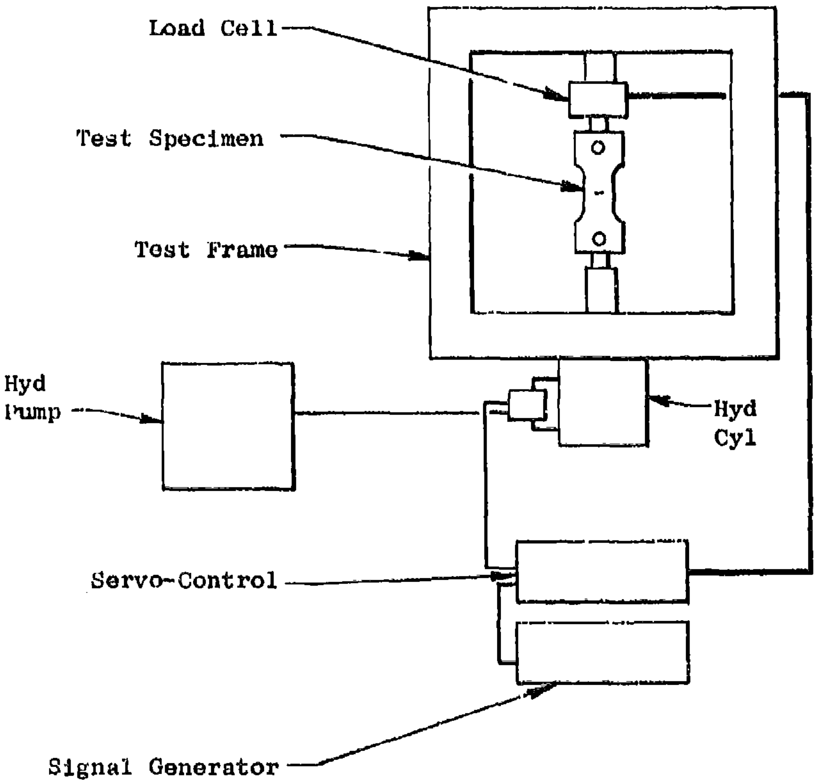

FIGURE 3.2-7

Schematic Of Laboratory Constructed Test Frame For FCGR Tests (Rockwell International, General Dynamics, Lockheed)

3.3 ENVIRONMENTS

Ten test environments were used in this program:

(1) Laboratory Air (LA) - The environment contained within the test facility, without control on humidity.

(2) Low Humidity Air (LHA) - A dry air environment of 10% or less relative humidity, as obtained by sealing the crack propagation zone within an enclosure containing freshly dried desiccant.

(3) 100% Humidity Air (100% Hum.) - A moist air environment obtained by sealing the crack propagation zone within an enclosure partially filled with commercially available distilled water. The liquid was not allowed to rise to the level of the crack propagation zone.

(4) Distilled Water (Dist H_2O) - A liquid environment of commercially available distilled water.

(5) Fuel Tank Sump Residue Water (STW) - A liquid environment of a .12% metal chloride solution consisting of distilled water with the following additions:

$CaCl_2$	50 PPM	$CrCl_3 \cdot 6H_2O$	1 PPM
$CdCl_2$	1000 PPM	$CuCl_3 \cdot 2H_2O$	1 PPM
$MgCl_2$	50 PPM	$FeCl_3$	5 PPM
NaCl	100 PPM	$MnCl_2 \cdot 4H_2O$	5 PPM
$ZnCl_2$	10 PPM	$NiCl_2 \cdot 6H_2O$	1 PPM
$PbCl_2$	1 PPM		

(6) Field Cleaning Solvent (FCS) - A liquid environment of a trisodium phosphate type cleaning solution consisting of 1 part MIL-C-25769 material to 8 parts water by volume.

(7) Shop Cleaning Solvent (SCS) - A liquid environment of an aliphatic naphtha per specification TT-N-95.

(8) Freon TF (FTF) - A liquid environment of a commonly used metal cleaning agent, Trichlorotrifluoroethane.

(9) Fuel - A liquid environment of JP-4 jet fuel saturated with distilled water.

(10) 90% Fuel + 10% Sump Tank Water (JP4 & STW) - A cyclic liquid environment of sump tank water then jet fuel, per (5) and (9) above. One complete environmental cycle consisted of 1.6 hours in STW followed by 14.4 hours in JP-4. Environmental cycling was continued throughout the duration of each test.

Da/DN testing was conducted in all ten environments, while K_{Iscc} testing was conducted only in STW, FCS, and SCS environments (numbers (5), (6), and (7). All K_{Ic} and K_c testing was conducted in a laboratory air environment (LA).

Environments (4) through (10) were applied to FCGR specimens by means of clear plastic chambers enclosing the crack propagation zone of the specimen. The chambers were equipped with inlet and outlet ports which allowed the liquid to flow through by gravity differential. In K_{Iscc} testing, the specimens were immersed vertically in the liquid environments to just below the level of the loading bolts.

SECTION 4: TEST PROCEDURES

4.1 TEST METHODS AND DATA ANALYSIS PROCEDURES

4.1.1 K_{Ic} Testing

4.1.1.1 K_{Ic} Testing of CT Specimens

K_{Ic} testing of compact tension specimens and analysis of test results was performed according to the procedures specified in ASTM E-399. The precracked specimens were loaded to failure in a tensile testing machine at a fixed cross-head separation rate. A load versus crack-opening-displacement (COD) curve was recorded during each test.

Crack opening displacement measurements were made at the crack notch opening across a 0.4" gage distance. On specimens having a W dimension of 2.5" or less, the deflections were measured 0.1" out from the specimen front surface, at clip gage mounting knife edges fastened to the specimen. On all other specimens, deflections were measured at the specimen front surface, at clip gage attachment knife edges machined into the specimen.

After completion of each test, length measurements were made on the specimen fracture face to determine the average length of the precrack (Figure 4.1-1). A K value was then calculated using the average length of the precrack and a P_Q load from the COD-load curve (Figure 4.1-2). This K value represented the K-level at which significant crack extension occurred. If all ASTM E-399 test validity requirements were met, this K value was then referred to as a valid toughness level (K_{Ic}). If the specimen failed one or more of the ASTM E-399 validity requirements, however, the resultant K value was appropriately identified by the accepted nomenclature of K_Q. Validity requirements per ASTM E-399 are listed below for the reader's convenience. None of the tests performed failed requirement (f).

(a) The minimum specimen thickness must be at least equal to 2.5 times the square of the ratio of K_Q to the yield stress.

$$B \geq 2.5\ (K_Q/\sigma_y)^2$$

(b) The maximum load must not exceed the P_Q load by more than 10%.

$$P_{max}/P_Q \leq 1.10$$

(c) Precrack requirements

(1) Length. The minimum precrack length along the entire crack front must not be less than the longer of (1) .050" or (2) five percent of the average crack length.

$$L \text{ (entire crack front)} \geq \text{the largest of (1) .050", (2) .05 a (average)}$$

(2) Shape. The difference between any two of the precrack length measurements must not exceed 5 percent of the average crack length.

$$(\text{Greatest of } a_1, a_3, a_4) - (\text{Smallest of } a_2, a_3, a_4) \leq 0.05 \text{ a (average)}$$

The length of either surface trace of the crack must be at least equal to 90 percent of the average crack length.

$$a_1, a_5 \geq 0.90 \text{ a (average)}$$

(3) Fatigue Stress Intensity. The maximum stress intensity during the final 2.5 percent extension of the crack (a_1, a_5) must be less than the smaller of (1) 0.6 K_Q or, (2) 0.002 E.

K_{max} precrack $<$ the smaller of (1) .6K_Q or, (2) .002 E

(e) The stress intensity loading rate must be between 30 and 150 ksi in/min

$$30 \text{ ksi} \sqrt{\text{in}}/\text{min} \leq \text{K rate} \leq 150 \text{ ksi} \sqrt{\text{in}}/\text{min}$$

(f) Slope angle of precrack shall not exceed 10°.

$$\text{Precrack angle} \leq 10°$$

4.1.1.2 K_{Ic} Testing of PTC Specimens

Precracked part-through-crack (PTC) specimens were loaded to failure at a loading rate of 200,000 pounds per minute. This procedure produced a K-loading rate within the range of 30 to 150 ksi $\sqrt{\text{in}}$ per minute, which was equivalent to the K-loading rate used for CT specimens. As in

the CT tests, a load versus crack-opening-displacement curve was recorded during each test. Crack opening displacement measurements were made across the center of the crack over a 0.4" gage distance.

After completion of each test, measurements were made on the specimen fracture face to determine the depth and surface length of the precrack. A P_Q load was then determined from the COD vs load curve in the same manner as was the P_Q load determined for CT specimens. This load and the precrack dimensions were used to calculate the K value at which significant crack extension had occurred. This resultant K value was then tested for validity per the following requirements:

$$\sigma_n \leq 0.9\ \sigma_{ys} \quad ; \quad B - a \geq 0.1\ (K/\sigma_{ys})^2$$ Reference (f)

where

σ_n = net stress at K test value   B = specimen thickness
σ_{ys} = yield strength   a = depth of precrack

All PTC toughness tests were found to satisfy the above validity requirements and, therefore, all test values obtained were identified as K_{Ic} values.

4.1.2 K_c Testing

4.1.2.1 K_c Testing of CT Specimens

Test procedures used for K_c testing of CT specimens were identical to those described for K_{Ic} testing of CT specimens with the following exceptions:

- Recording of the load versus COD curve in the test was continued to some point past the maximum load. In K_{Ic} testing, recording of this curve was discontinued after reaching the P_5 load.

- In specimens with large W dimensions and small B dimensions, buckling was minimized by sandwiching the specimens between lubricated side plates during test.

- On large specimens (W=8"), where COD at the crack opening on the specimen surface would exceed the deflection capacity of COD gage, the gage was mounted on metal clips which had been adhesively bonded to the side of the specimen.

- COD gages were also mounted on the sides of some specimens run at temperatures other than ambient to avoid contact of the gage with the thermal chamber walls.

Test data for each specimen were analyzed to determine a K_Q value, an R curve, a K_c value, and a critical Δa value. The K_Q value for each test was determined in the same manner as that described for K_{Ic} tests using CT specimens. The R-curve for each test, which is a plot of crack extension versus K-level, was developed in the following manner:

1. Eleven points are selected on the load vs COD curve, as illustrated in Figure 4.1-3.

2. The K-level and crack extension (Δ a) at each of these points are then calculated.

3. The resultant values of K and Δa are then plotted with Δa on the X axis and K on the Y axis.

The eleven points on the load vs COD curve used for developing the R curve were selected such that the K_c and critical Δa, corresponding to the K level and Δa at initial maximum load, would be included in the R curve calculations. In developing each R curve, the K level at each of the selected points on the load vs COD curve was calculated from specimen dimensions, load, and apparent crack length at that point. Apparent crack lengths were estimated using specimen compliance calculations, as described below;

- The specimen compliance (C) of a point on the load vs COD curve is the reciprocal of the slope of a straight line drawn from the origin of the load vs COD curve through that point.

- Compliance (C) is normalized by multiplying by the material modulus (E) and the specimen thickness (B).

- Using a table of normalized compliance (CEB) versus a/W ratios, the a/W ratio corresponding to that particular point on the load vs COD curve was established.

- Multiplying a/W by the known width, W, of the specimen, then provided the unknown, apparent crack length, a.

In actual data reductions adjustments were made to the calculated CEB values before using the a/W vs CEB tables. Inasmuch as the precrack length (a) could be accurately measured from the specimen fracture surface, the initial a/W could also be accurately established. The CEB value for this precrack length (the linear portion of load vs COD curve) was, therefore, corrected to the tabular value, and the same correction was applied to each subsequent CEB value on that curve to obtain the estimated a/W ratio.

If the crack slope angle exceeded 10° or if the ligament stress exceeded the yield strength of the material, a notation to this effect was included in the test report.

4.1.2.2 K_c Testing of CCT Specimens

CCT specimens were loaded to failure at rates between 70 and 110 KIPS per minute, to produce K-loading rates between 30 and 150 ksi $\sqrt{in}$ per minute (up to peak load). Side restraint bars were used to prevent buckling. A curve of load versus crack opening displacement (COD) was recorded for each test. COD was measured across the midpoint of the machined notch over a 0.50" gage length.

Test data for each specimen were analyzed to determine an R-curve, a K_c value and a critical Δa value, using the load vs COD curves in the same manner as described for K_c tests in CT specimens. One exception to that procedure was used, however, for CCT specimens — crack lengths in CCT specimens were estimated from compliance using empirically established calibration curves of 2a/W versus compliance. At least one specimen of each alloy was used as a standard to develop load vs COD calibration curves at various known crack lengths. (Crack length extensions between two successive measurements of compliance were accomplished by fatigue cracking).

Again if the crack slope angle exceeded 10° or if the ligament stress exceeded the yield strength, this was noted in reporting the test results.

4.1.3 K_{Iscc} Testing

4.1.3.1 General

Since the specimen utilized here is a constant deflection type, the stress intensity, K, decreases as the crack grows. Thus, when a specimen is loaded above the K_{Iscc} level, the crack will extend until the stress intensity, K, decreases to a point where the crack no longer grows. This approach as used in this program to test for K_{Iscc} is known as the crack arrest method. Stress intensity measured at arrest was taken as K_{Iscc}.

Specimens were loaded to desired stress intensity levels using loading bolts which were threaded through both sides of the specimen, meeting at the notch center. Bolts were torqued equally on both sides until the desired crack opening displacement was attained. Loading of the specimens was performed with corrodent in contact with the specimen precrack. During the course of each test crack growth was monitored by measuring the length of the crack traces on the specimen sides. K_I values and crack growth rates were then calculated as a function of test time based on the length of these crack traces. At completion of each test, the specimen was fractured open and crack length measurements were made at three positions on the crack front (0.25, 0.5, and 0.75B) to determine an average crack length for both the precrack and the stress corrosion crack. This average crack length was then used in calculating the K_{Iscc} value.

4.1.3.2 Specimen Loading

Crack opening displacements were measured to an accuracy of within 0.0001" during loading of the specimen. These measurements were made at the notch opening between 0.1" thick metal clips (knife edges) which were bolted to the front surface of the specimen. Crack tip contact with the liquid test environment during loading was effected by placing a few drops of the corrodent in the notch prior to loading. After loading was completed the specimens were immersed vertically into test baths such that only the portions of the specimens including and above the loading bolts were not exposed to the test medium.

For standard K_{Iscc} specimens, the deflections required to produce desired K levels were calculated using specimen dimensions and lengths of precrack traces. For the small K_{Iscc} (modified K_{Ic}) specimens, however, the loads required to produce desired K levels were first calculated using the ASTM E-399 equation, $P = KBW^{\frac{1}{2}}/f(a/W)$. The crack opening displacement required to produce the appropriate load in each specimen was then determined by loading the specimen to the calculated load in a tensile machine. The specimen was then reloaded to the experimentally determined displacement using loading bolts.

4.1.3.3 Crack Length Measurements

Crack trace lengths were measured prior to loading, and, generally, were remeasured subsequent to loading after the following time periods had elapsed: 1 hour; 4 hours; 1 day; 1 week; three weeks; and every three weeks, thereafter. Crack traces were measured to an accuracy of ± 0.005", on both sides of the specimen and the average of the two lengths was used to calculate growth rates (da/dt) and K levels as a function of test time. Most of the tests were run for a period of slightly over 1000 hours, although some tests were as short as 800 hours, and some were as long as 2200 hours.

Subsequent to completion of each test crack lengths were again measured to an accuracy of ± 0.005" on the fracture surface. Measurements were made at the center of the crack front (i.e., mid-thickness position) and midway between the center and each of the specimen sides (i.e., quarter-thickness positions). An average of these three measurements was then used as the crack length, a, in subsequent K level calculations. This procedure was used to determine the initial and final crack lengths for determining the initial and final K level test values.

Most of the K_{Iscc} specimens exhibited a single thumbnail precrack shape, wherein the crack length at the mid-thickness location was greater than that at either of the sides of the specimens. A few titanium weld specimens, however, exhibited a double thumbnail precrack shape, wherein maximum precrack lengths occurred at or about both quarter-thickness locations. In these cases, the average precrack length was determined by assuming a straight crack front and estimating the depth at which this straight crack front would have the same crack area as the actual crack had.

Opening of cracks after test completion was accomplished by wedging or by pulling the specimen arms apart in a tensile machine. In many cases, early in the test program, difficulty was encountered in establishing a line of demarcation between the stress corrosion crack and the crack extension area occurring during opening. In many additional cases, crack extension during the test had occurred only in the mid-thickness region of the specimen, so that crack trace measurements during the test could not be depended upon to reliably detect the occurrence of and to monitor the progress of stress corrosion cracking.

To circumvent these problems, a system of crack front marking was developed, wherein the crack surface was either heat tinted or ink stained prior to opening. Most of the specimens, other than aluminum alloys, were heat tinted at 900°F for 1 hour prior to opening. Sump tank water corrosion in the aluminum alloys was found to sufficiently define the end of the stress corrosion crack without the aid of marking. Field and shop cleaning solvents produced little or no corrosion in these alloys, however, so that the crack surfaces had to be stained with metal lay-out ink prior to opening. It should be noted that all crack surface marking was performed with the specimen in the unloaded condition.

4.1.3.3 Data Analysis Procedures

In some K_{Iscc} specimens of the steels, stress corrosion cracks deviated from the plane of the notch. On many of the 300M specimens, stress corrosion cracks, after growing straight for about .7", curved toward the 1" x 6" edge surface. On these specimens, the K_{Iscc} value was taken as being less than the K value at the point where the crack deviated 1/4" from the plane of the notch in the height direction of the specimen.

In some PH13-8Mo and 9-4-20 specimens, the stress corrosion crack or cracks grew from the precrack at an angle of 40 to 70° from the plane of the notch (crack forking occurred at end of precrack on some specimens). In these specimens the K_{Iscc} value was taken as being less than the initial loading K value.

For all tests the plane strain capability of the test specimen was calculated

$$\left(K = \frac{\sigma_y}{1.58} \sqrt{B}\right)$$

and compared with the K_{Iscc} value obtained in the test. K_{Iscc} values exceeding the plane strain capability of the test specimen were noted as obtained under mixed mode stress states. For such tests, the K_{Iscc} value for a plane strain stress state was reported as being greater than the plane strain capability of that test specimen.

4.1.4 Da/DN Testing

4.1.4.1 Da/DN Testing of CT Specimens.

In CT specimens used for da/dN testing cracks were generally grown in or near the plane of the notch to a maximum a/W ratio of approximately 0.8. Tests normally required 1.0×10^6 to 1.5×10^6 cycles to complete although a few tests were completed in as few as 5×10^5 cycles, while others required in excess of 3×10^6 cycles to completion.

All load schedules were tension-tension (positive R factor) and were selected for each specimen such that predicted growth rate in the range of $\sim 10^{-7}$ up to $\sim 10^{-2}$ in.per cycle would be obtained. Two main types of loading were employed for these tests; (1) constant load, constant amplitude; and (2) increasing load, constant amplitude; although some tests were conducted utilizing a third type of loading--that of decreasing load, constant amplitude. The constant load, constant amplitude test consisted of using a single load range (P_{max} to P_{min}) throughout the entire test, wherein delta K is increased with increasing crack length. This type of test provides a smooth and continuous set of data points on a da/dn curve, but generally requires longer testing times and is thus more costly than the increasing load, constant amplitude type of test. This latter method of testing consists of selecting a set of increasing load ranges (at a constant ratio of P_{min}/P_{max}) to provide data points within various growth rate regimes of the da/dn curve. Again, due to increasing crack lengths, delta K will be continuously increased at each given load range level, but discontinuities are introduced into the curve during each load change. Obviously, this method is less time consuming and costly, but can lead to some errors in interpretation of the data, particularly over the intervals between changes in load range. Finally, in some instances, growth rates were observed to be greater than anticipated so that load range levels had

to be decreased during test. This practice can invariably lead to retardation effects due to relatively large plastic zones at the crack tip when going from high to low loads. To avoid the influence of retardation effects on the da/dn curve, the crack had to be grown out of the plastic zone associated with the higher load before the data could again be considered valid. This, too, can lead to some errors in data interpretation due to the unknown nature of plastic zone sizes, i.e., where to resume valid data collection.

Crack trace measurements were made periodically on both sides of the specimen throughout the duration of each test. Observation and measurements were generally conducted after an average growth interval of 0.050" had occurred. Data recorded during each observation of a test included the following:

- Date
- R Factor (P_{min}/P_{max})
- Maximum load (P_{max})
- Cyclic Rate
- Total elapsed cycles (n)
- Change in number of cycles between observations (dn)
- Total crack length on both sides of specimen (a_1 and a_2)

Data sheets for each specimen included specimen identification (material number, reference test direction, and specimen number), test temperature and environment, testing facility identification, and critical specimen dimensions.

During most of the tests, a system of marking the crack front was employed to document the crack front shape subsequent to testing as determined by visual examination of the fracture surface. Mark loading was accomplished by periodically shifting to load levels of approximately 80% of the test load until a total crack extension of approximately 0.050" was recorded. Mark loading was usually done at a higher cyclic frequency than that used during testing, and the resultant set of fatigue striations, more closely spaced due to the lower load levels employed, clearly identified the crack front shape by bands. Mark loading data was not included in the data used to derive the da/dn curve for each specimen.

After completion of each test, the specimen was pulled apart in a tensile machine, if it had not fractured completely during test, and the fracture surfaces were examined to determine significant differences between crack lengths at the specimen surfaces and that at the mid-thickness position. This condition was found to be fairly common in most specimens at a/W ratios in excess of ~0.7. In only a few specimens (3 out of 465), however, were gross anomalies in crack front shape observed below this a/W ratio. As a result of these post-test examinations, and the high degree of crack front uniformity, no adjustments were made to apparent crack

lengths, as determined by crack trace measurements during tests, prior to use in computer reductions of data.

The above data for each specimen were submitted into a computer program written to reduce such data. The output of this program then indicated, for each observation, the crack length on each side of the specimen; the average crack length extension, da (*); together with the change in number of cycles between observations, dn; the computed growth rate, da/dn; the maximum and minimum loads; and the computed value of change in stress intensity, delta K. Also listed on each output were pertinent information with regard to testing variables, specimen dimensions and identification. This program was also written to plot da/dn vs. delta K for each observation on a log-log plot.

4.1.4.2 Da/DN Testing of CCT Specimens

In da/dN tests conducted on CCT specimens, cracks were grown to a length of about four inches from each end of a 4.4" long flaw (starter notch with precrack at both ends) located in the center of the 24" wide by .10" thick panel specimen. The length of the crack trace (2a) on both sides of the panels was measured periodically during fatiguing and the total number of load cycles was noted at the time of each measurement.

These tests were conducted with the objective of defining a FCGR curve for growth rates ranging from 2×10^{-7} to at least 3×10^{-5} inches per load cycle. By periodically increasing the test load, sufficient growth rate data over the range of interest was generated in approximately 400,000 cycles for each specimen. Each test was started at a load predicted to yield a crack growth rate of 2×10^{-7} inches per cycle. After several crack growth rate measurements were made at this initial fatigue load, the load was usually increased by about 15% and the cycling was continued at this load for an additional several measurements. This procedure was normally repeated six more times before terminating the test. The loading R factor was maintained constant throughout each test.

From the crack trace measurements made in the above tests, Δa and $\bar{a}$ values were calculated for each interval between crack trace measurements as follows:

$$\Delta a = (2\, a_{n+1} - 2\, a_n) / 2 , \quad \bar{a} = (2\, a_{n+1} + 2\, a_n) / 4$$

(*) $da = [(a_1^{\,f} - a_1^{\,o}) + (a_2^{\,f} - a_2^{\,o})] / 2$ where superscripts f and o indicate after and before each observation, respectively.

where

$2\,a_n$ = average value of crack length (crack tip to crack tip distance*) as obtained from measurements made on both sides of the specimen during nth observation

Δa = half the increase in crack length between successive observations

$\bar{a}$ = half the average crack length between succesive observations

The above values of Δa and $\bar{a}$ were then used to calculate for each interval between crack length measurements, an average crack growth rate ($\Delta a/\Delta N$) and an average ΔK based on the average crack length $\bar{a}$ value. Plots of $\Delta a/\Delta N$ versus ΔK were then prepared for each specimen. The length of the crack growth increments (Δa) represented by the points on these plots varied from about .05 to .50" with .15" being typical. In general, the length of the crack growth extensions (between crack trace measurements) increased as a test progressed and higher crack growth rates were encountered.

At the termination of each test, the ligament stress [net section stress = P/(W-2a)B] was calculated, and was found to be below the material yield strength in all specimens.

4.1.4.3 Da/DN Testing of PTC Specimens

In da/dN tests conducted on PTC specimens, a crack was grown from a semi-circular surface flaw through the thickness of the specimen, with testing being terminated as soon as breakthrough occurred on the back surface of the specimen.

Crack trace length (2c) on the specimen surface was monitored during fatiguing. After every .05" increment of crack growth ($\Delta 2c$) in the .25" thick specimens, and every .10" increment on thicker specimens, the crack front was marked for a crack extension of .01" ($\Delta 2c$) by changing the cycling conditions. The length of the crack trace was recorded as well as the number of load cycles whenever a change was made in the cycling parameters. After completion of the test, the crack face was exposed and photographed at 4 to 6X. Crack depths at the start and end of each crack growth increment, which were separated by marking bands as illustrated in Figure 4.1-4, was determined by measurements made on the photograph.

---

*

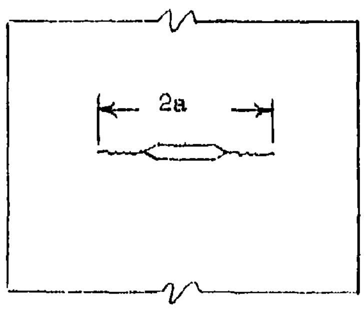

Fatigue loads were selected to develop crack growth data over the range from 2×10^{-7} to 3×10^{-5} inches per cycle. The initial test load was predicted to yield an initial growth rate of 2×10^{-7} inches per cycle. Usually the test load was increased about 10% for each succeeding crack growth increment in order to obtain data points over a wider range of growth rates than obtainable using the same test load. The loading R factor was maintained constant for all crack growth increments in a single specimen.

Marking of the crack front was accomplished by lowering the load by about 10% from the test load and changing to a different R factor than the one at which the test was being conducted. These changes produced a band on the fracture surface having a texture different from that of the fracture surface generated by the test cycling procedure.

For each crack growth increment, the average crack growth rate ($\Delta a/\Delta N$) and the average ΔK were calculated. Delta K was calculated from the specimen dimensions, applied load and crack size. The crack size used in the calculations was that at the mid-position of the crack growth increment. Plots were prepared of ΔK versus $\Delta a/\Delta N$ for each specimen.

The ligament stress (net section stress) in the specimen at test termination was calculated for each specimen and found to be below the material yield strength in all cases.

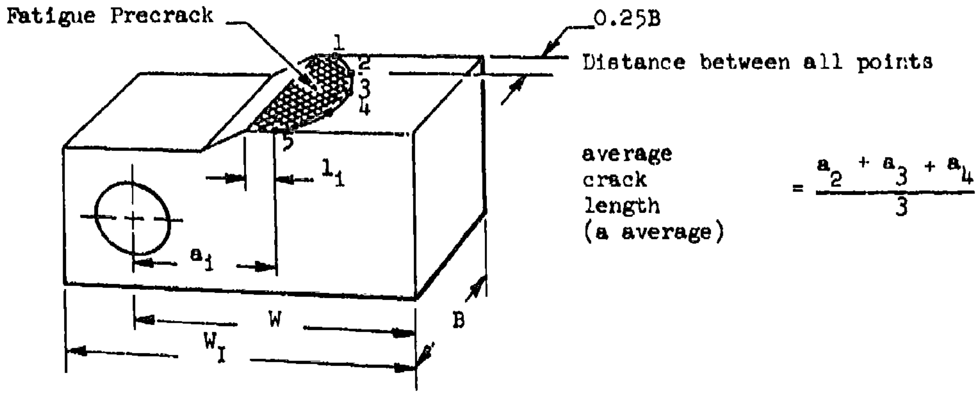

Figure 4.1-1 Position of Precrack Length Measurements on Compact Tension Specimen After Failure in K_{Ic} Test

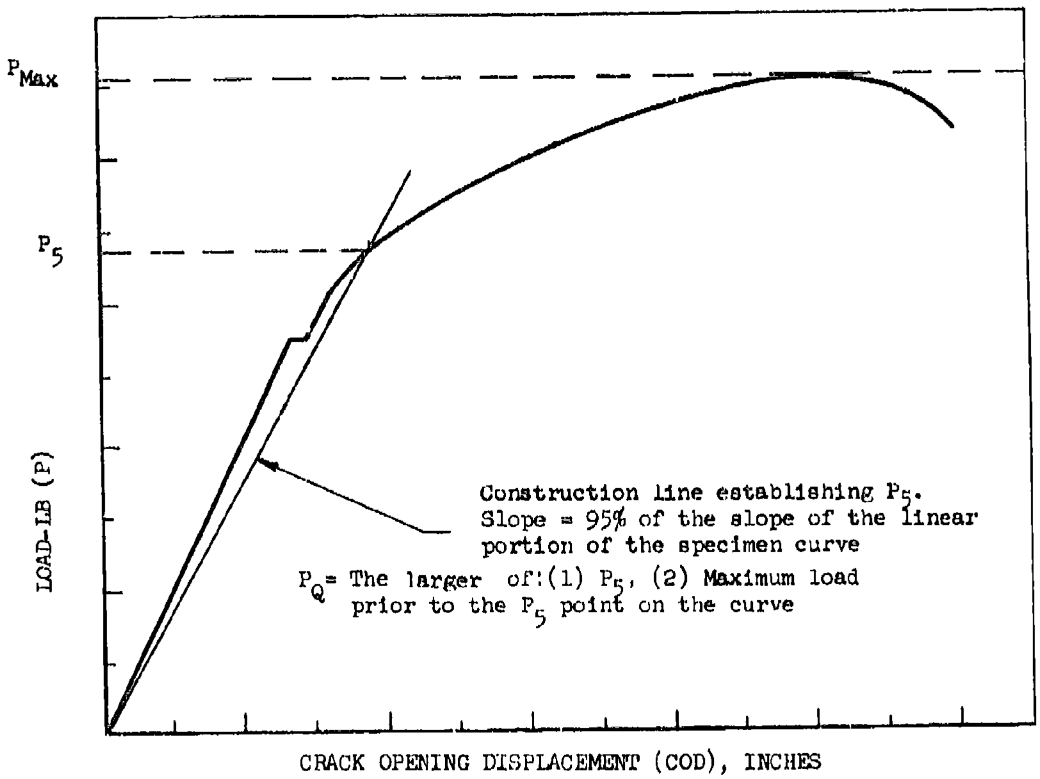

Figure 4.1-2 Location of Data Points on Load-COD Curve From K_{Ic} Test on Compact Tension Specimen

R Curves were developed as follows:

1. Eleven points were selected on load-COD curve as illustrated.

2. The crack length at each point was estimated from the specimen compliance. Compliance of nth point = $\frac{1}{\text{slope of line On}}$

3. The K-level at each point was calculated using the estimated crack length, the specimen dimensions and the load.

4. The K-level and crack extension for the eleven points were plotted to develop an R-curve.

The K-level and the crack extension at the initial maximum load are the K_c value and critical Δa, respectively.

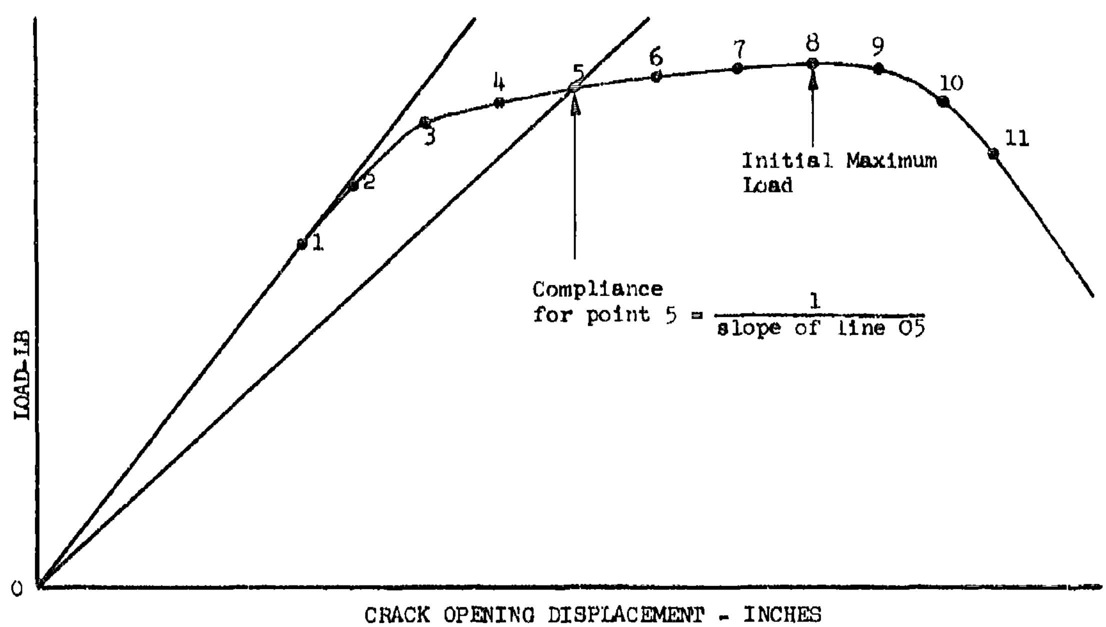

Figure 4.1-3 Location of Test Measurements on Load-COD Curve from K_c Test

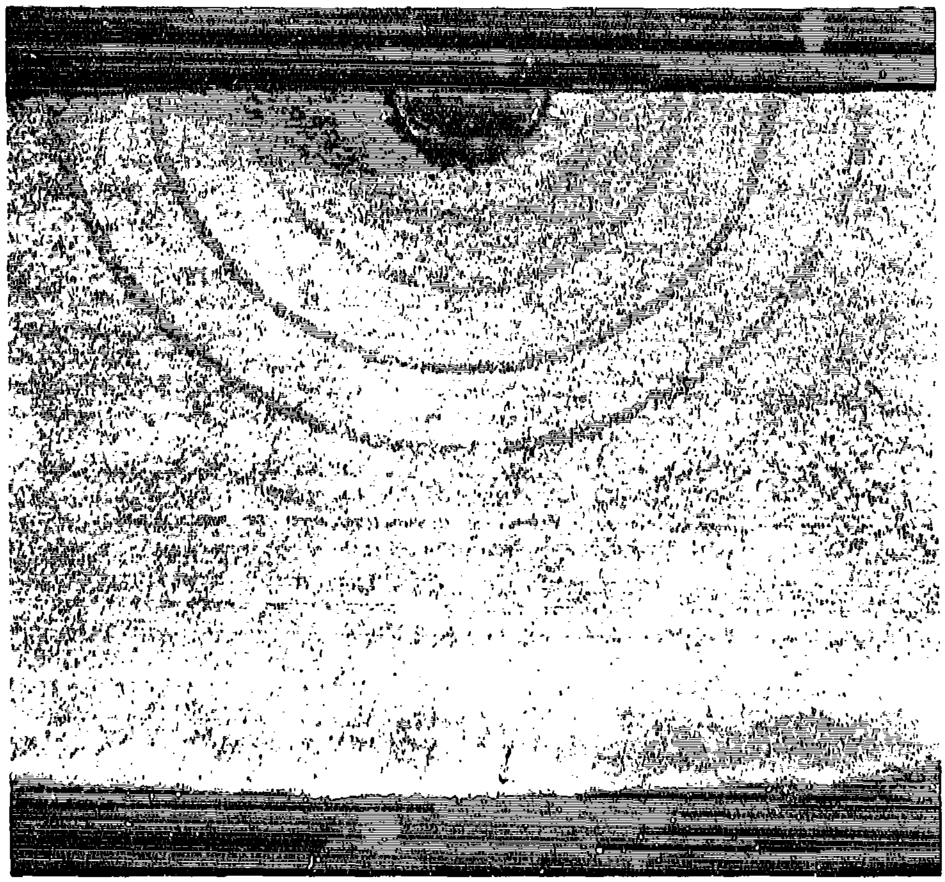

Figure 4.1-4 Fracture Face on a PTC Specimen (B=.46") Used in a Da/dN Test Showing Crack Front Marking Bands.

4.2.1 K_{Ic} and K_c Studies

K_{Ic} tests were conducted on all fourteen alloys included in this program while K_c tests were conducted on only seven of the alloys. Test temperatures ranged from -65°F to +400°F. Test matrices identifying product forms, and number of lots of each alloy tested together with the temperatures at which those tests were performed are shown in Tables 4.2-1 through -3.

K_c testing was limited to two steels, four aluminum alloys and Ti-6Al-4V. The principal variables evaluated in K_c testing of each alloy included the effects of specimen thickness, test temperatures, and grain direction on K_c values and R curves. In general, K_c tests were performed on specimens having thicknesses of 20, 40, 60 and 80% of the minimum thickness required for a plane strain stress state. In addition to room temperature K_c tests, -65°F tests were performed on the two steels and Ti-6Al-4V, and 265°F tests were performed on the aluminum alloys.

Much of the K_{Ic} testing was performed for the purpose of characterizing the various lots of test materials to ensure that they had reasonable toughness values before committing them to relatively expensive da/dN and K_{Iscc} testing. Additional K_{Ic} testing was performed for the purpose of identifying effects on toughness of variations in heat treatment, test temperature, and joining methods.

A study of heat treatment variation effects on K_{Ic} of 9-4-.20 steel was conducted, which included the following process variables: austenitizing temperature; cooling rates from austenitizing treatment; cooling temperature (the lowest temperature reached in the cooling cycle); holding times between austenitizing and tempering; and tempering time and temperature. The effects of variations in forging temperature on the toughness of this steel were also evaluated.

The effects of heat treatment on K_{Ic} of Ti-6Al-4V were evaluated including the MA, BA, STOA, RA and DBTC conditions. In addition, the effects of diffusion bonding on K_{Ic} were evaluated on several lots of this material.

Tests were performed on nine alloys to determine the effect of test temperature on K_{Ic}. In addition to tests at room temperature, tests were run at both -65°F and 265°F on Ti-6Al-4V, at 265°F on four aluminum alloys, at -65°F on three steel alloys and at -65°F and 400°F on Inconel 718.

Weldments were evaluated through K_{Ic} testing. Tests were performed on both weld joints and weld overlays. The weld overlay tests were performed to evaluate the effects of weld repairing by weld metal build-up on parent metal of a part which had been inadvertently machined undersize. Thicknesses of weld joints in Ti-6Al-4V ranged from 0.1" to 0.75", while 9-4-.20 steel they ranged from 0.25" to 1.5". In PH13-8Mo steel all welds were 0.25" thick. The GTAW process was used in preparing all but seven weld specimens. Thos seven weld specimens, all in Ti-6Al-4V, were prepared using the PAW process. With the exception of one specimen of Ti-6Al-4V and one of 9-4-.20 steel, which were tested with loads parallel to the joint direction, all specimens were tested with loads transverse to the joint direction. Toughnesses of both the HAZ and the weld bead of weld joints was examined in the testing.

Pre-weld and postweld thermal treatments for most weld specimens were those used or considered at one time for B-1 weldments. In some instances, however, welds were not postweld stress relieved, to simulate a weld repair procedure on the air vehicle where a postweld thermal treatment would not be feasible.

4.2.2 K_{Iscc} Studies

K_{Iscc} tests were conducted on thirteen of the fourteen alloys evaluated in this program. The only alloy not subjected to K_{Iscc} testing, 9-4-.30 steel, was included in the original test plan, but was deleted when the last fracture controlled part of 9-4-.30 was changed to 9-4-.20 steel. Most K_{Iscc} tests were performed in artificial fuel tank sump residue water (STW), while some tests were run on a spot check basis in field cleaning solvent (FCS) and shop cleaning solvent (SCS). Tests in the latter two environments were conducted to ensure that they would be less aggressive than STW. FCS and SCS tests were conducted on one lot in one direction only of each alloy selected for evaluation in these environments. Generally, duplicate to quadruplicate specimens were run for each test condition. A matrix for the K_{Iscc} studies of alloy forms, specimen orientations and environments involved in this phase of the testing is shown in Table 4.2-4.

4.2.2.1 Ti-6Al-4V

K_{Iscc} tests were conducted on four lots of plate and four lots of forgings in this material — all in the RA condition. Eight lots of plate were evaluated after exposure to a simulated diffusion bond thermal cycle. GTA butt weld joints having thicknesses from 1/8" through 1" and diffusion bond joints were also evaluated. In addition, material from the trim area of a hot formed B-1 wing pivot lug plate (P/N L1200021) was included in this evaluation.

4.2.2.2 Aluminum Alloys

K_{Iscc} tests were performed on the aluminum alloy product forms shown below. One lot of material was evaluated for each alloy and product form indicated except for 2024, wherein two forgings were evaluated:

2024 Forged Blocks	7050 Plate
2124 Plate	7075 Plate, Forging and Extrusion
2219 Plate	7175 Forging
7049 Forged Block	

4.2.2.3 Steels, Inconel 718, and MP 35 N

K_{Iscc} tests were performed on three lots of rolled bar, one extruded bar and one forged bar of PH13-8Mo. One lot of 9-4-.20 plate and one lot of 9-4-.20 bar were evaluated, while for 300M, Inconel 718, and MP 35 N one lot of bar of each alloy was evaluated. K_{Iscc} tests were also performed on weld joints of PH13-8Mo and 9-4-.20 steels.

4.2.3 Da/Dn Studies

Fatigue crack growth rate (da/dN) studies were conducted in this program to characterize the dynamic strength properties of the major aluminum alloys, steels, titanium alloy (Ti-6Al-4V) and nickel alloy (Inconel 718) which have been incorporated into B-1 structural designs. Tests were conducted on the product forms and material conditions considered to be representative of the fracture critical parts within the airframe whose design criterion is that of fatigue strength (crack growth resistance). The number of material lots of each product form for each alloy evaluated is shown in Table 4.2-5 together with the various test parameters used in their evaluation. The testing variables which were evaluated in this study are summarized below:

- Product Form
- Material Condition
- Cyclic Rate - 6, 60, 360 cpm (plus limited 540, 1800, 3600, 3800, and 7800 cpm)
- Test Temperature - -65F, R.T., 150F, 265F and 400F
- R Factor - 0.05, 0.08, 0.3, 0.5, and 0.7
- Environment - Low humidity air (LHA), Lab Air (LA), Sump tank residue water (STW), Jet fuel (JP4), Shop Cleaning solvent (SCS), Field cleaning solvent (FCS), Distilled water (Dist H_2O), 100% humidity (100% Hum.), Freon TF, and STW + Fuel
- Test Direction - RW, WR, TR, TW and RT

TABLE 4.2-1

TEST MATRIX FOR K_{Ic}/K_c STUDIES ON Ti-6Al-4V

	No. of Alloy Lots Evaluated					
	RT		-65F		265F	
	K_{Ic}	K_c	K_{Ic}	K_c	K_{Ic}	K_c
Sheet						
MA		2				
Plate						
RA	14	4	2	1	2	1
DBTC	4					
MA	4					
BA	1					
STOA	1					
Forgings						
RA	4					
Extrusion						
B extruded + MA	2					
DB Joints	4					
Butt Weld Joint	7	1	2			
Weld Overlay	1					

TABLE 4.2-2

TEST MATRIX FOR K_{Ic}/K_c STUDIES ON ALUMINUM ALLOYS

	No. of Alloy Lots Evaluated						
	2024	2124	2219	7049	7050	7075	7175
Plate							
K_{Ic}							
RT	6	2	4		1	5	
265F			1				
K_c							
RT	1		1				
265F			1				
Forgings							
K_{Ic}							
RT	2		1	3	1	1	2
265F	1						
K_c							
RT	1			1			
265F	1						
Extrusions							
K_{Ic}							
RT			1			1	
265F						1	
K_c							
RT						1	
265F						1	
Sheet							
K_c							
RT	2					2	

-- $_c/K_c$ STUDIES ON
STEELS, INCONEL 718 AND MP 35 N

	No. of Alloy Lots Evaluated					
	9-4-20	9-4-30	PH13-8Mo	300M	Inconel 718	MP 35 N
Rolled Bar						
K_{Ic}						
RT			3			1
-65F			2			
K_c						
RT			1			
-65F			1			
Forged Bar or Billet						
K_{Ic}						
RT	6	2	3	1	1	
-65F	2	1	2		1	
400F					1	
K_c						
RT	1					
-65F	1					
Die Forging						
K_{Ic}						
RT	2				1	
Extrusion						
K_{Ic}						
RT			1			
Plate						
K_{Ic}						
RT	1					
-65F	1					
Butt Weld Joint						
K_{Ic}						
RT	3		2			
-65F	2		2			
Weld Overlay						
K_{Ic}	1		1			

TABLE 4.2-4 TEST MATRIX FOR K_{Iscc} STUDIES

Alloy	Rolled or Extruded Bar			Forged Bar or Die Forging			Plate			Weld Joints
	RW or RT Orient.	WR	TR	RW	WR	TR or TW	RW	WR	TR or TW	
Ti-6Al-4V										ab
Cond RA (4 lots each of plate & forgings)					a	a	a	abc		
Exposed to DBTC (8 lots)							a	a		
Diffusion Bond Joint									a	
Hot Formed								a		
Aluminum										
2024 (2 lots)				ab	a	a				
2124							a	a	a	
2219							abc	a	[illegible]	
7049				abc	a	a				
7050							a	a	a	
7075	abc		a		a		abc		a	
7175				abc	a					
9-4-20				ab	a	a	a	a		ac
PH13-8Mo (5 lots)	abc	a								ab
300M				abc		a				
Inconel 718				ab	a	a				
MP35N	a									

Test Environments

(a) Sump Tank Residue Water
(b) Shop Cleaning Solvent
(c) Field Cleaning Solvent

TABLE 4.2-5

TEST MATRIX FOR FATIGUE CRACK GROWTH RATE STUDIES

Alloy	No. of Lots Evaluated: Bar	Forging	Sheet	Plate	Extr.	Test Conditions: Orientation	(cpm) Frequency	Environment	R Factor	Thickness, Inches	Temp, °F
2024 Al	-	2	2	2	-	RW, WR	6, 60, 360 1800, 7800	LHA, STW, Dist H_2O JP4, LA, SCS	.05, .08, .3, .5	.25, .5, 1.0	R.T., 150 265
2124 Al	-	-	-	2	-	RW, WR	60, 360	LHA, STW	.08, .3, .5	1.0	R.T.
2219 Al	-	1	-	5	1	RW, WR	6, 60, 360, 3800	LHA, STW Dist. H_2O LA, SCS, FCS	.08, .3, .5	.25, .5, 1.0	R.T., 150, 265
7049 Al	-	2	-	-	-	RW, WR	6, 60, 360	LHA, STW,	.08, .3, .5	.25, .5, 1.0	R.T.
7050 Al	-	1	-	1	-	RW, WR	60, 360	LHA, STW	.08, .3, .5	.5, 1.0	R.T.
7075 Al	-	1	2	5	3	RW, WR	6, 60, 360	LHA, STW, SCS, Freon TF,	.08, .3, .5	.25, .5, .6, .8, 1.0	R.T., 265
7175 Al	-	2	-	-	-	RW, WR	6, 60, 360	LHA, STW, SCS, FCS	.08, .3, .5	.25, .5, 1.0	R.T., 265
HP-9-4-.20 Steel	-	3	-	2	-	RW, WR	6, 60, 360, 540	LHA, STW, 100% Hum, SCS	.08, .3, .5, .7	.25, .5, .825, 1.0	-65, R.T.
HP-9-4-.30 Steel	-	2	-	-	-	RW, WR	6, 60, 360	LHA, STW	.08, .3, .5	.75, 1.0	-65, R.T.
300M Steel	-	1	-	-	-	RW, WR, TR	60, 360	LHA, STW	.08, .3, .5	1.0	-65, R.T.
PH13-8Mo Steel	-	1	-	-	1	RW, WR	6, 60, 360	LHA, STW, SCS	.08, .3, .5	.25, .5, 1.0	-65, R.T.

TABLE 4.2-5 (CONT'D)

Alloy	No. of Lots Evaluated					Test Conditions					
	Bar	Forging	Sheet	Plate	Extr.	Orientation	(cpm) Frequency	Environment	R Factor	Thickness"	Temp
Inconel 718	-	2	-	-	-	RW, WR, TR	60, 360	LHA, STW, SCS	.08, .5	.5, 1.0	R.T., 400
Ti-6Al-4V	-	4	2	18	2	RW, WR	6, 60, 360, 3600	LHA, STW, JP4, FCS, STW + JP4	.08, .3, .5, .7	0.1-1.38	-65, R.T. 150, 265
HP-9-4-.20 Welds	-	1	-	2	-	RW, RT	60, 360	LHA, STW, Dist. H_2O, 100% Hum.	.08, .3, .5	.25, .5, .75	R.T., -65
PH13-8Mo Welds	1	-	-	-	1	RW, RT	60, 360	LHA, STW, LA	.08, .3	.25	R.T., -65
Ti-6Al-4V Welds	-	-	1	6	1	RW, RT	60, 360	LHA, STW, SCS, Freon TF	.08, .3	.25, .5, .75, 1.0	R.T., -65
Ti-6Al-4V Diff. Bonds	-	-	-	5	-	RW/RW, WR/WR, TW/TW, WR/TR, RW/TR	60, 360, 1800	LHA, STW	.08, .3	1.0	R.T.

SECTION 5 APPLICABLE EQUATIONS

5.1 COMPACT TENSION SPECIMEN

Stress intensity factors (K) for the compact tension specimen were calculated using the following equation:

$$K = \frac{P}{B\sqrt{W}} f(a/W) \qquad \text{Reference (g)}$$

where:

P = load

W = specimen width

B = specimen thickness

a = crack length

f (a/W) per Table 5-1

A tabulation of CEB values versus a/W ratios, using the equations* below, was used in estimating K_c specimen crack lengths. Table 5-2, a shortened form of this table, is included for illustrative purposes.

$$\begin{pmatrix}\text{CEB} \\ \text{when COD is} \\ \text{measured at} \\ \text{load line}\end{pmatrix} = 876.15\,(a/W)^2 - 7321.06\,(a/W)^3 + 36613.85\,(a/W)^4 - 121388.44\,(a/W)^5 + 281690.79\,(a/W)^6 - 448778.77\,(a/W)^7 + 468035.62\,(a/W)^8 - 288782.77\,(a/W)^9 + 81638.6\,(a/W)^{10}$$

$$\begin{pmatrix}\text{CEB} \\ \text{when COD is} \\ \text{not measured} \\ \text{at load line}\end{pmatrix} = \begin{pmatrix}\text{CEB} \\ \text{when COD is} \\ \text{measured at} \\ \text{load line}\end{pmatrix} \times s/a$$

where:

C = specimen compliance = $\Delta COD/\Delta P$

E = modulus of elasticity

B = specimen thickness

a = effective crack length

s = distance from crack tip to COD measurement location

COD = crack opening displacement

P = load

* These equations are identical to those used in the preparation of Reference (h).

The following equation was used to calculate the maximum stress in the unfailed portion of a specimen ($\sigma = Mc/I + P/A$):

$$\text{Ligament Stress} = \frac{P}{BW\,(1-a/W)} \left[1 + 3\,\frac{(1+a/W)}{(1-a/W)} \right] \qquad \text{Reference (d)}$$

The maximum K-level at which a specimen was capable of maintaining a plane strain stress state was calculated using the following equation:

$$\text{Specimen plane strain K capability} = \frac{TY}{1.58}\sqrt{B} \qquad \text{Reference (g)}$$

where TY = tensile yield strength.

5.2 PART-THROUGH-CRACK SPECIMEN

The following equation was used to calculate the stress intensity factors for the specimens used in the K_{Ic} tests.

$$K = 1.1\sqrt{\pi}\;\sigma_g\,(a/Q)^{1/2}\,Mk \qquad \text{Reference (i)}$$

where

$$Q = \phi^2 - .212\,(\sigma g/\sigma_{ys})^2$$

$$\phi = \int_0^{\pi/2} \sqrt{1 - \left(\frac{c^2 - a^2}{c^2}\right)\sin^2\Theta}\;d\Theta$$

σ_g = gross area stress [P (load)/t (thickness) w(width)]

σ_{ys} = tensile yield strength

a = crack depth

c = 1/2 crack trace length

Mk = deep flaw magnification factor per Reference (j).

The above equation with the Mk factor deleted was used to calculate stress intensity factors for PTC specimens used in da/dN testing.

5.3 CENTER CRACKED TENSION SPECIMEN

Stress intensity factors were calculated using the following equation:

$$K = \frac{P}{WB}\left(\pi a \text{ secant } \frac{\pi a}{W}\right)^{1/2} \qquad \text{Reference (k)}$$

where

P = load

W = specimen width

B = specimen thickness

a = 1/2 total crack length as measured from crack tip to crack tip

Crack lengths were calculated from specimen compliance measurements using the empirically determined relationships in Table 5-3.

5.4 DOUBLE CANTILEVER BEAM SPECIMEN (K_{Iscc} TESTS)

For the standard DCB specimen, stress intensity factors were calculated using the following equation :

$$K_I = \frac{V_I \; EH \; [3H\,(a + 0.6H)^2 + H^3\,]^{1/2}}{4\,[(a + 0.6H)^3 + H^2\,a]} \qquad \text{Reference (1)}$$

where:

V_I = total deflection of the two arms of the test specimen at the centerline of the loading bolts.

E = modulus of elasticity

H = 1/2 specimen height

a = crack length measured from centerline of loading bolts

The following modulus of elasticity values were used in the above equation in calculating K_I values:

Alloys	E, 10^6 psi
7049, 7050, 7075, 7175	10.4
2024	10.6
2219	10.7
Ti-6Al-4V	16.2
PH13-8Mo	29.0
9-4-20	29.1
Inconel 718	29.6

Specimen arm deflections (V_2), measured at a distance of .6" in front of the centerline of the loading bolts, were converted to deflections at the bolt centerline (V_I) for use in the above K_I equation using the following equation:

$$V_I = V_2 \times \frac{a}{a + .6}$$

The above equation assumes that arm deflection increases linearly from the end of the crack and that the arms are hinged at the end of the crack. Load line deflection measurements on several specimens showed good agreement with calculated deflections using the above equation. Loading deflections and K_I levels vs. crack growth lengths for various initial K-levels are tabulated in Table 5-4 for illustrative purposes for the standard DCB specimen.

For the small DCB specimen (compact tension specimen with loading-bolt holes), the standard equation for the compact tension specimen $[K = \frac{P}{B\sqrt{W}} f(a/W)]$ was used for calculating the K_I level from the applied load.

The maximum K-level at which a specimen was capable of maintaining a plane strain stress state was calculated using the same equation as shown in Section 5.3 for CT specimens.

TABLE 5-1

VALUES OF f(a/W) USED IN STRESS INTENSITY
EQUATION FOR COMPACT TENSION SPECIMENS

a/W	f(a/W) H/W=0.486	f(a/W) H/W=0.600	a/W	f(a/W) H/W=0.486	f(a/W) H/W=0.600
0.300	6.60	5.85	0.500	10.31	9.60
0.305	6.67	5.90	0.505	10.44	9.75
0.310	6.74	5.96	0.510	10.58	9.90
0.315	6.81	6.02	0.515	10.72	10.05
0.320	6.88	6.08	0.520	10.86	10.21
0.325	6.95	6.15	0.525	11.01	10.37
0.330	7.02	6.22	0.530	11.17	10.54
0.335	7.10	6.28	0.535	11.33	10.71
0.340	7.17	6.35	0.540	11.49	10.89
0.345	7.25	6.42	0.545	11.66	11.07
0.350	7.32	6.50	0.550	11.83	11.26
0.355	7.41	6.57	0.555	12.01	11.46
0.360	7.49	6.65	0.560	12.20	11.66
0.365	7.57	6.73	0.565	12.40	11.87
0.370	7.66	6.81	0.570	12.60	12.08
0.375	7.74	6.89	0.575	12.81	12.30
0.380	7.82	6.97	0.580	13.02	12.54
0.385	7.91	7.06	0.585	13.25	12.77
0.390	8.00	7.14	0.590	13.48	13.02
0.395	8.09	7.23	0.595	13.73	13.28
0.400	8.18	7.32	0.600	13.98	13.54
0.405	8.27	7.42	0.605	14.25	13.82
0.410	8.36	7.51	0.610	14.52	14.10
0.415	8.45	7.61	0.615	14.80	14.39
0.420	8.55	7.70	0.620	15.10	14.70
0.425	8.64	7.80	0.625	15.41	15.01
0.430	8.74	7.91	0.630	15.73	15.34
0.435	8.84	8.01	0.635	16.07	15.68
0.440	8.94	8.12	0.640	16.42	16.03
0.445	9.04	8.23	0.645	16.78	16.40
0.450	9.15	8.34	0.650	17.16	16.78
0.455	9.25	8.45	0.655	17.55	17.17
0.460	9.36	8.57	0.660	17.96	17.58
0.465	9.47	8.69	0.665	18.39	18.00
0.470	9.58	8.81	0.670	18.83	18.44
0.475	9.70	8.93	0.675	19.29	18.89
0.480	9.82	9.06	0.680	19.77	19.36
0.485	9.94	9.19	0.685	20.27	19.86
0.490	10.06	9.32	0.690	20.79	20.36
0.495	10.18	9.46	0.695	21.33	20.88
			0.700	21.90	21.43

FOR SPECIMENS WHERE H/W = 0.486

$$f(a/W) = 30.96\ (a/W)^{1/2} - 195.8\ (a/W)^{3/2} + 730.6\ (a/W)^{5/2} - 1186.3\ (a/W)^{7/2} + 754.6\ (a/W)^{9/2}$$

FOR SPECIMENS WHERE H/W = 0.600

$$f(a/W) = 29.6\ (a/W)^{1/2} - 185.5\ (a/W)^{3/2} + 655.7\ (a/W)^{5/2} - 1017.0\ (a/W)^{7/2} + 638.9\ (a/W)^{9/2}$$

TABLE 5-2

VALUES OF CEB PARAMETER FOR VARIOUS a/W RATIOS
FOR COMPACT TENSION SPECIMEN WHERE H/W=.6

	CEB for Indicated Specimen W's and COD Measurement Locations				
a/W	All W's, COD at LL (Load Line)	All W's, COD at +.25W from LL	2.0" W, COD at +.60" from LL	2.5" W, COD at +.72" from LL	8" W, COD at -1.75" from LL
0.45	29.1	45.2	47.8	48.4	14.9
0.46	30.5	47.1	49.7	50.4	16.0
0.47	32.0	49.0	51.7	52.4	17.1
0.48	33.6	51.1	53.9	54.6	18.3
0.49	35.3	53.3	56.2	56.9	19.5
0.50	37.1	55.6	58.6	59.3	20.8
0.51	39.0	58.1	61.1	61.9	22.3
0.52	41.0	60.7	63.9	64.6	23.8
0.53	43.2	63.5	66.8	67.6	25.3
0.54	45.4	66.5	69.8	70.7	27.0
0.55	47.9	69.7	73.2	74.0	28.8
0.56	50.5	73.1	76.7	77.6	30.8
0.57	53.3	76.7	80.5	81.4	32.9
0.58	56.4	80.7	84.6	85.5	35.1
0.59	59.6	84.9	88.9	89.9	37.5
0.60	63.2	89.5	93.7	94.7	40.1
0.61	67.0	94.4	98.8	99.9	43.0
0.62	71.1	99.8	104.4	105.5	46.0
0.63	75.6	105.6	110.4	111.6	49.4
0.64	80.5	112.0	117.0	118.3	53.0
0.65	85.9	119.0	124.3	125.6	57.0
0.66	91.8	126.6	132.2	133.6	61.4
0.67	98.3	135.0	140.9	142.4	66.2
0.68	105.4	144.2	150.4	152.0	71.5
0.69	113.4	154.4	161.0	162.7	77.4
0.70	122.1	165.7	172.7	174.4	83.9

(WHEN CEB is at load line)

$$CEB = 876.16\,(A/W)^2 - 7321.06\,(A/W)^3 + 36613.85\,(A/W)^4 - 121388.44\,(A/W)^5 + 281690.79\,(A/W)^6 - 448778.77\,(A/W)^7 + 468035.62\,(A/W)^8 - 288782.77\,(A/W)^9 + 81636.6\,(A/W)^{10}$$

(WHEN CEB is not at load line)

$$CEB = \text{CEB at load line} \times \frac{d}{a}$$

WHERE a= Crack Length
d= Distance from crack tip to COD measurement location.

TABLE 5-3

EMPIRICALLY DETERMINED RELATIONSHIPS BETWEEN COMPLIANCE (C) AND 2a/W RATIO FOR 0.10 IN. x 24 IN. CCT SPECIMENS

C, IN 10^{-7} IN./LB. *	2a/W		
	2024-T81	7075-T76	Ti-6Al-4V, COND. A
2.5	---	---	.187
3.0	---	---	.225
3.5	.177	---	.266
4.0	.202	.176	.300
4.5	.224	.197	.337
5.0	.245	.223	.345
5.5	.266	.244	.416
6.0	.292	.265	.458
6.5	.317	.286	.500
7.0	.334	.311	.537
7.5	.351	.332	---
8.0	.338	.353	---

* C = Compliance = $\Delta COD/\Delta P$

(COD was measured across the crack at the specimen center. using a 0.5-in. gage length).

TABLE 5-4

LOADING DEFLECTIONS AND K_1 VERSUS CRACK LENGTH FOR STANDARD DCB SPECIMENS (K_{ISCC} TESTS)

(1.200" Initial Crack Length. H = 1.000")

Loading K_1, ksi $\sqrt{in}$ (1.200" crack length)	130	110	90	80	70	60	50	40	35	30	25	20	15
Loading Deflections (Inches)													
Alloys													
7049,7050,7075,7175									.0434	.0372	.0310	.0248	.0186
2024,2124									.0425	.0365	.0304	.0243	.0182
Ti-6Al-4V				.0636	.0557	.0477	.0398						
9-4-20	.0576	.0487	.0399	.0354	.0310								
Inconel 718	.0566	.0479	.0392										
K_1 (ksi $\sqrt{in}$) When Initial 1.200" Crack Grows To Noted Lengths													
Crack Growth Lengths													
1.250	123.7	104.6	85.6	76.0	66.6	57.0	47.5	38.1	33.2	28.5	23.8	19.0	14.3
1.300	117.8	99.6	81.5	72.4	63.4	54.3	45.3	36.2	31.7	27.2	22.7	18.1	13.6
1.350	112.3	94.9	77.7	69.0	60.4	51.8	43.2	34.5	30.2	25.9	21.6	17.3	13.0
1.400	107.2	90.6	74.2	65.9	57.7	49.4	41.2	33.0	28.8	24.7	20.6	16.5	12.4
1.450	102.4	86.6	70.9	62.9	55.1	47.2	39.4	31.5	27.5	23.6	19.7	15.8	11.8
1.500	97.9	82.8	67.8	60.2	52.7	45.1	37.7	30.1	26.3	22.6	18.8	15.1	11.3
1.550	93.8	79.3	64.9	57.6	50.5	43.2	36.1	28.8	25.2	21.6	18.0	14.4	10.8
1.600	89.9	76.0	62.2	55.2	48.4	41.4	34.6	27.6	24.2	20.7	17.3	13.8	10.4
1.650	86.2	72.9	59.6	53.0	46.4	39.7	33.2	26.5	23.2	19.9	16.6	13.3	9.9
1.700	82.7	70.0	57.3	50.9	44.5	38.1	31.8	25.5	22.2	19.1	15.9	12.7	9.5
1.750	79.5	67.2	55.0	48.9	42.8	36.7	30.6	24.5	21.4	18.4	15.3	12.2	9.2
1.800	76.4	64.6	52.9	47.0	41.2	35.2	29.4	23.5	20.5	17.6	14.7	11.8	8.8
1.850	73.6	62.2	50.9	45.2	39.6	33.9	28.3	22.6	19.8	17.0	14.2	11.3	8.5

NOTES:

1. Crack lengths are from centerline of loading bolts (load line)
2. Loading deflection in the above table is the total deflection of the two areas of the specimen measured 0.6" in front of the load line. Load line deflections are 2/3 of the listed values.
3. The following modulus of elasticity values were used in the program for K_1 calculations.

Alloys	E,10^6 psi
7049,7050,7075,7175	10.4
2024	10.6
2219	10.7
Ti-6Al-4V	16.2
PH13-8Mo	29.0
9-4-20	29.1
Inconel 718	29.6

4. In the program, the actual specimen dimensions (H, crack length) were used in calculating loading deflections and K values. The values in the above table, which are based on specimen nominal dimensions, are only for illustrative purposes and were calculated using equations in Section 5-4.

SECTION 6 - K_{Ic} AND K_c TEST DATA

6.1 TEST RESULTS

The individual test results and average values of tests for all K_{Ic} type testing are presented in Tables 6-1 thru 6-17. Average values of tests are also tabulated by themselves in Tables 6-18 thru 6-20 for comparison purposes. The actual arrangement of these tables is as follows:

Tabular Presentation of K_{Ic} Results

Alloy System	Individual Specimen and Average Value Results	Comparison of Average Value Results
Ti-6Al-4V	Tables 6-1 & 6-15 (welds)	Table 6-18
Aluminum Alloys	Tables 6-4 thru 6-8	Table 6-19
Steels, 718, MP35-N	Tables 6-9 thru 6-14, 6-16 (welds) & 6-17 (welds)	Table 6-20

Tables 6-1 through 6-11 also show K_c values to facilitate direct comparison with the K_{Ic} values.

The K_c test results (K_c values, critical Δa's and R-curves) are presented in Tables 6-21 through 6-28 and Figures 6-1 through 6-25 in accordance with the following arrangements:

Tabular or Graphical Presentation of K_c Test Results

Alloy System	Individual Specimen Results: K_c Values, Critical Δa's, Comparative R-Curve Points	Individual Specimen Results: R-Curves	Comparison of Average K_c Values
Ti-6Al-4V	Table 6-21	Fig. 6-1 thru 6-5	Fig. 6-18
Aluminum Alloys	Table 6-22 thru 6-26	Fig. 6-6 thru 6-15	Fig. 6-19 thru 6-23
9-4-.20, PH13-8Mo	Table 6-27 & 6-28	Fig. 6-16 & 6-17	Fig. 6-24 & 6-25

Some K_{Ic} tests using CT specimens did not meet all of the ASTM validity requirements and hence, K_Q values were obtained. K_Q values are designated in the test result tables by enclosing them in parentheses and attaching a superscript letter or letters, per the following code, to

indicate the validity requirement which was not met.

a - minimum thickness requirement $[B \geq 2.5 \quad (K_Q/TY)^2]$

b - load ratio requirement $(P_{max}/P_Q \leq 1.10)$

c - precrack requirements (length, shape, and/or fatigue maximum K level)

e - loading rate requirement (≥ 30 and ≤ 150 ksi $\sqrt{in}$ per minute)

K_Q values were included in the series of individual test results used in calculating average K_{Ic} values if it appeared that failure of the particular validity requirement or requirements had little effect on the test results.

6.2 DISCUSSION OF TEST RESULTS

6.2.1 Effect of CT Specimen Thickness (B) on K_Q Values (Table 6-29)

Some CT specimens used for K_{Ic} tests were too thin to produce a plane strain stress state at the crack tip. Test values from these specimens were therefore reported as K_Q values instead of the desired K_{Ic} values. (Inadequate specimen thickness occurred either because the as-received material was too thin to allow fabrication of a full-sized specimen, or the toughness of the material exceeded the predicted value). Inasmuch as K_Q values can not be used for direct comparison with K_{Ic} values, a method for estimating the toughness of materials which are too thin for valid K_{Ic} determinations is desirable. In the K_c phase of this program, K_c specimens were fabricated from materials of known K_{Ic} strengths, with thicknesses as small as 12% of that which would have been required for valid K_{Ic} tests. A review of the data obtained on these K_c specimens disclosed relationships between their K_Q values and the already known K_{Ic} values of the specimen materials. The ratio of these two values are shown in Table 6-29 opposite the specimen thicknesses. Also shown in this table is a column titled, "Specimen K_{Ic} Capability Ratio". This ratio is found by dividing the specimen plane strain capability value (which is a function of the material yield strength and the specimen thickness) by the known K_{Ic} value of the material.

K_Q values increased with decreasing specimen thickness. Except for specimens of PH13-8Mo, specimens having K_{Ic} capability ratios as low as .75 had K_Q values less than 11% above specimen material K_{Ic} values. For some materials, K_Q values from specimens having K_{Ic} capability ratios as low as .50 were less than 11% above specimen material K_{Ic} values.

6.2.2 K_{Ic} Characterization of Test Materials (Tables 6-18, 6-19 and 6-20)

Some test materials were procured prior to development of B-1 procurement specifications. In such instances, these materials were procured to the best available specification, e.g., Military, Federal, AMS. Also, in some instances, even after preliminary specifications had been prepared, it was necessary to waive K_{Ic} requirements before producers would accept orders due to inadequate existing toughness data. Later determinations revealed, however, that only three lots of material had K_{Ic} values appreciably below B-1 specification requirements.

K_{Ic} values of Ti-6Al-4V plate materials 61-62 and 65 were significantly below the K_{Ic} requirement of 70 ksi $\sqrt{in}$ in specification ST0170LB0032. These two materials were procured early in the program to Mil-T-9046 and had high oxygen content, which appeared to be the major cause of their low toughnesses. Test data on these materials were part of the supportive data for limiting oxygen content to 0.13% maximum in B-1 procurement specifications.

PH13-8Mo steel extrusion material 41 had a K_{Ic} value of 66 ksi $\sqrt{in}$ as compared to K_{Ic} requirements of 90 or 75 ksi $\sqrt{in}$ in B-1 procurement specifications. This material was procured on a best effort basis to the B-1 90 ksi $\sqrt{in}$ toughness specification. It was retained in the program because of the uncertainty of a realistic guaranteed K_{Ic} value for extrusions (due to inadequate existing toughness data for this product form). Current B-1 design does not require the use of PH13-8Mo extrusions.

6.2.3 Effect of Test Temperature on K_{Ic} Value (Table 6-30).

Of the five alloys tested at -65F, PH13-8Mo steel had the greatest percentage loss in K_{Ic} value when test temperature was decreased from ambient to -65F. The average ratio of K_{Ic} at -65F to that at room temperature (-65F K_{Ic}/RT K_{Ic}) from four lots of PH13-8Mo steel evaluated was .64. Similar ratios for Ti-6Al-4V, 9-4-.20, and 9-4-.30 alloys were in the range of .81 to .83, while Inconel 718 had a ratio of 1.06.

The magnitude of loss in toughness associated with decreasing test temperatures from ambient to -65F was seen to be less in weld joints of Ti-6Al-4V, PH13-8Mo, and 9-4-.20 than in their respective parent metals. The number of welded specimens tested at -65F was insufficient, however, to accurately define ratios of -65F K_{Ic} to RT K_{Ic} for welds.

The ratios of K_{Ic} values at 265F to those at room temperature for Ti-6Al-4V, 2024, 7075 and 2219 were 1.23, 1.19, 1.07 and .93, respectively. At 400F, the K_{Ic} value of Inconel 718 was 91% of its value at room temperature.

6.2.4 Ti-6Al-4V: Oxygen Content and Processing Effects on K_{Ic} (Tables 6-1, 6-15 and 6-18)

The various lots of Ti-6Al-4V test materials which varied in oxygen contents from .08 to .20%, showed a general trend of decreasing K_{Ic} value with increasing oxygen content. The lot of material having the highest oxygen content (Material 61-62) had the lowest K_{Ic} values for all heat treat conditions evaluated (RA, DBTC, BA, MA).

In general, beta processed materials were superior in toughness to alpha-beta processed materials. In material 61-62, the K_{Ic} value in the beta processed condition (BA) was 82 ksi $\sqrt{in}$ and in the alpha-beta processed condition was 51 ksi $\sqrt{in}$ (RA). This particular material had an oxygen content of .20%. In material lots having oxygen contents below .17%, the lowest K_{Ic} value for beta processed materials (four lots) was 90 ksi $\sqrt{in}$, as compared to 60 ksi $\sqrt{in}$ for alpha-beta processed materials in the RA condition (fifteen lots). Subjecting materials which originally had been alpha-beta processed and mill annealed to a subsequent RA or DBTC heat treat cycle produced significant increases in K_{Ic} values (materials 61-62 and 65). In material which had originally been beta processed plus mill annealed, no improvement in toughness resulted from these treatments (material 63). Toughnesses of alpha-beta processed material were essentially equivalent in the MA and STOA conditions(material 61-62). K_{Ic} values obtained on material tested in the DBTC condition (materials 61-62, 72, 77 and 92) were generally close to those obtained on the same material when it was tested in the RA condition (within test scatter).

Individual specimen K_{Ic} values of diffusion bonded joints ranged from 74 to 108 ksi $\sqrt{in}$ (materials 70, 77 and 90) as compared to a design allowable of 70 ksi $\sqrt{in}$ for bonded joints. The toughnesses of these joints were at least equal to the toughnesses of their respective parent metals in the RA condition. In those specimens with the diffusion bonded planes oriented perpendicular to the crack plane, the K_{Ic} values were equal to the parent metal in the RA condition in those of plate material 61-62, and were 80 ksi $\sqrt{in}$ or higher in those of .18" sheet (material MH05379, diffusion bonded).

K_{Ic} values of weld joints and weld overlays tested at room temperature varied from 62 to 87 ksi $\sqrt{in}$ (individual specimen values) as compared to a K_{Ic} design allowable of 60 ksi $\sqrt{in}$ for welds. K_{Ic} values of weld joints were at least 82% of their respective parent metal K_{Ic} values (average K_{Ic} values).

The toughness of the weld bead area and the HAZ of weld joints appeared to be about the same (material 88 and 89 tests).

Table 6-15 indicates that toughness was not affected appreciably by weld joint thickness (.25", .50", .75"), welding process employed (GTA, PAW), or postweld stress-relief process (1100/2hrs., 1200/1 hr., 1400/1hr.).

Toughness of a weld overlay in material 88 in the as-welded condition (B317, Table 6-15) was lower than were those of stress-relieved weld joints of the same specimen thickness (B307, B316). However, stress-relieving the weld overlay (B302) raised its toughness to a level greater than those of butt weld joints which had been similarly stress-relieved.

6.2.5 9-4-.20 Steel: Processing Effects on K_{Ic} (Tables 6-9, 6-16 and 6-20).

In material 52, no significant difference was found between the toughness of material which had been finish forged at 1700, 1800 or 1900F (Table 6-9, tenth page). Variations in heat treatment, on the other hand, were seen to affect material toughness. In material 48, for example, austenitizing at 1700F resulted in a 15% increase in toughness over that obtained when using the normal austenitizing temperature of 1525F (Table 6-9, eighth page). To determine if air cooling instead of oil quenching from the austenitizing temperature would affect toughness, tests were conducted on five lots of alloy (Table 6-9; material 33, 37, 46, 48 and 57). Two of the lots showed no toughness difference between the two quenching media (materials 37 and 48), while two lots showed a higher toughness in the air cooled condition (materials 46 and 57) and one lot showed a higher toughness in the oil quenched condition (material 33). The inconsistency in these results indicates that apparent differences in toughness resulting from either air cooling or oil quenching are due to data scatter. It was, therefore, concluded that either cooling method would be acceptable for section sizes capable of being through hardened with air cooling (thickness < 4 inches).

Material 48 test results indicated that ausbay quenching (hold at 900F for 1/2 hour on cooling) might result in a slight loss (less than 10%) of toughness from that obtainable by continuous cooling from the austenitizing cycle.

Material 31 was subjected to various time delays between quenching to room temperature and tempering. Subsequent tests did not reveal a significant difference between the toughness of material which was tempered immediately after quenching, that which was held at -100 for two hours before tempering, or that which had been held overnight at room temperature before tempering (Table 6-9, first page).

The toughness of oil quenched material 48 after a four hour tempering cycle was the same as that after a twelve hour tempering cycle at the same temperature. While tempering time had little effect on toughness, tempering temperature was seen to affect toughness. A 25F increase in tempering temperature from 1000 to 1025F resulted in an 18% increase in toughness of material 31. Further increasing the tempering temperature to 1050F resulted in a 6% increase in toughness over that resulting from a 1025F temper in both material 31 and material 33.

In summarizing the results of the heat treat study, material toughness was not significantly affected by quenching medium (air or oil), minimum cooling temperature (RT or -100F), tempering delay or tempering time (4 or 12 hours). Increasing the austenitizing and tempering temperatures on the other hand, resulted in improved material toughness.

K_{Ic} values of weld joint and weld overlay specimens tested at room temperature varied from 84 to 138 ksi $\sqrt{in}$. as compared to a K_{Ic} design allowable of 90 ksi $\sqrt{in}$ for welds. Only one test value was below the design allowable — that of a weld joint tested in the as-welded condition. This joint is not representative of B-1 welds in that all 9-4-.20 welds in the B-1 receive a post weld thermal treatment of 950F for 2 hours. Ratios of average K_{Ic} values of weld joints to average K_{Ic} values of their respective parent metals varied from .60 to .87.

Weld joint thickness in the range from .75" to .25" did not appear to have an effect on toughness. The highest K_{Ic} value (138 ksi $\sqrt{in}$) was obtained on a 1.5" thick joint.

The postweld thermal treatment of 950F for 2 hours appeared to have no significant effect on the toughness of weld beads in material 33, weld beads in material 37, or weld overlays in material 37. In material 57 joints, the toughness of the HAZ was lower in the as-welded condition than in the postweld thermal treated condition.

The K_{Ic} values of weld overlays were about the same as those of the weld bead area of weld joints of the same thickness (material 37 and 57 tests).

6.2.6 PH13-8Mo: Effect of Welding on K_{Ic} (Tables 6-17 and 6-20)

K_{Ic} values in butt weld joints and in weld overlays tested at room temperature varied from 79 to 100 ksi $\sqrt{in}$, as compared to a K_{Ic} design allowable of 80 ksi $\sqrt{in}$ for welds. K_{Ic} values of welds were at least equal to 90% of the average K_{Ic} values of their respective parent metals. Differences in K_{Ic} values of HAZ versus weld bead in weld joints, as-welded versus stress-relieved (950F, 2 hrs) weld overlays and weld overlays versus weld joints were all within replicate specimen testing scatter.

6.2.7 Effect of Testing Variables on R-Curves (Tables 6-21 thru 6-28 and 6-31, Figures 6-1 thru 6-17)

The effects of specimen thickness, orientation, and test temperature on the K-value of the R-curve at a given crack extension (R-curve K-level) are summarized in Table 6-31. WR oriented specimens had lower R-curve K-levels than comparable RW specimens.

Decreasing test temperatures were seen to result in decreased R-curve K-levels in four alloys, while levels were seen to increase in one alloy, 2219 aluminum, and remain unchanged in another, a 2024 aluminum alloy forging.

Decreases in specimen thickness in all materials except the 2024 forging were seen to result in increases in the R-curve K-levels. Specimen thickness decreases from 1.0" to 0.75" and 0.5" in the 2024 forging were not seen to affect the R-curve, but further decreasing the thickness to 0.25" did result in the normal K-level increase.

Varying the W dimension of CT specimens from 3.0 to 8.0" had no significant effect on R-curve K-levels of Ti-6Al-4V specimens (materials 71 and 78).

6.2.8 Relation of Specimen Fracture Features to R-Curves

An illustration of the fracture surface on a compact tension specimen is shown in Figure 6-26. As the crack grows from the precrack, the width of the shear lips increase but finally stabilize at a maximum width.

In 0.1" thick sheet specimens (Ti-6-4, 2024, 7075), fracture surfaces became 100% shear (slant fracture) within a crack extension of 0.2" from the precrack. The R-curves for these specimens had a parabolic shape with the greatest slope occurring at the initial portion of the curve, where the fracture was rapidly becoming 100% shear. The only difference between the fracture surfaces of the RW and WR specimens, which had lower R-curve, K-level, was that the fracture surface of the RW specimens became 100% shear within a shorter distance from the precrack than did the fracture surface of the WR specimens.

For compact tension specimens a comparison was made at a crack extension of 0.2" between the K-level on the specimen R-curve (Δa=0.2") and the shear fracture proportion on the specimen fracture face (Figure 6-26). For specimens of the same material with various thicknesses, the K-level from the R-curve correlated with the specimen shear fracture proportion. The specimens having the higher K value had a higher shear fracture proportion as illustrated in Figure 6-27 for PH13-8Mo. In general, for specimens of the same material, the shear fracture proportion at .2" crack extension increased with decreasing specimen thickness.

6.2.9 K_c Values (Figures 6-18 thru 6-25)

K_c values depend on the K-level of the R-curve and the critical Δa. While no significant effect of the specimen W dimension on the R-curve K-level was found to exist for the CT specimens, increasing the W dimension did result in an increase in the critical Δa and, thus, an increase in the K_c value (Figures 6-1 and 6-3). In specimens from two Ti-6Al-4V materials, increases of 30% and 100% in K_c values were obtained by increasing the W dimension from 3.0 or 3.5 to 8.0" (material 71, B=.5"; material 78, B=.76"; Figure 6-18).

In general, a decrease in specimen thickness resulted in an increase in critical Δa and K_c value. In those instances where Δa or K_c showed a drop in magnitude with a decrease in specimen thickness, the drop appeared to be within normal test scatter.

The highest K_c value obtained in the testing was 460 ksi $\sqrt{in}$, which was obtained on 9-4-.20 steel specimens having a .75" thickness and a W of 8.0". K_c values obtained on similar thickness specimens for PH13-8Mo (W=3.5), Ti-6Al-4V (W=8.0) and aluminum alloys (W=2.5 to 6.0) were 270, 200 and 90 to 60 ksi $\sqrt{in}$, respectively (Figures 6-18 thru 6-25). The maximum K_c values obtained on 0.1" thick sheet of Ti-6Al-4V, 7075-T76 and 2024-T81 alloys were 380, 108 and 70 ksi $\sqrt{in}$, respectively.

The K_c values of WR oriented specimens were lower than those of comparable RW specimens. For 7075-T73511 extrusion the K_c value of WR specimens was 40% of that of RW specimens (B=.75"). In the remaining test materials, WR values were in the range of 69 to 97% of the RW values (2219 plate, B=.5; 2024 sheet, B=.1; 7075 sheet and plate, B=.1 and .25).

K_c values at -65F were lower than those at room temperature. For Ti-6Al-4V (B=.62), 9-4-.20 (B=.38), and PH13-8Mo (B=.25), the K_c values at -65F were 80, 54 and 16%, respectively, of the room temperature values. The K_c values at 265F for 2219-T851 (B=.5), 7075-T73511 (B=.75) and 7075-T7651 (B=.25) exceeded the room temperature values by over 30%, whereas for 2024-T81 the two values were about the same (B=.5").

6.3 SUMMARY AND CONCLUSIONS

1) K_Q values from CT specimens with inadequate thickness for a plane strain stress state were seen to increase with decreasing specimen thickness. In general, K_Q values did not exceed K_{Ic} values of the test materials by more than 10% for specimen thicknesses as low as 60% of the required thickness to maintain a plane strain stress state within the specimen.

2) The ratio of the average K_{Ic} value at -65F to that at room temperature for Inconel 718, Ti-6Al-4V, 9-4-.30, 9-4-.20, and PH13-8Mo were 1.06, .83, .82, .81 and .64, respectively. The ratio of the average K_{Ic} value at 265F to that at room temperature for Ti-6Al-4V, 2024, 7075, and 2219 were 1.23, 1.19, 1.06 and .93, respectively. The K_{Ic} value of Inconel 718 at 400F was 90% of its room temperature value.

3) Ti-6Al-4V alloy showed a general trend of decreasing K_{Ic} value with increasing oxygen content. Beta processed material was superior to alpha-beta processed material in toughness. Subjecting alpha-beta processed materials in the mill annealed condition to an RA heat treatment improved their toughnesses.

4) In Ti-6Al-4V alloy, the K_{Ic} values of diffusion bonded joints were at least equal to those of their respective parent metals in an RA heat treat condition.

5) The K_{Ic} values obtained on those weld joints processed according to B-1 specifications met the K_{Ic} design allowable values for welds (welds in Ti-6Al-4V, PH13-8Mo and 9-4-.20 evaluated).

6) The heat treat study on 9-4-.20 steel showed toughness was not affected by quenching medium(air or oil), minimum cooling temperature (RT or -100F), tempering delay (< 1 or 18 hr) or tempering time (4 or 12 hrs.). Increases in austenitizing temperature (1525F to 1700F) and tempering temperature (1000 to 1050F) were shown to increase toughness. Variations in final forging temperatures from 1700 to 1900F were seen to have little effect on the toughness of this material.

7) R-curves for WR specimens were lower in K-level at a given crack extension than those of comparable RW specimens. Decreasing specimen thickness or increasing test temperature resulted in higher K-level R-curves for most of the alloys. Changes in the W dimension of CT specimens did not have a significant effect on the K-level of specimen R-curves.

8) K_c values from WR specimens were 3 to 60% lower than values from comparable RW specimens. Decreasing specimen thicknesses or increasing W dimensions of CT specimens increased K_c values. K_c values at -65F for Ti-6Al-4V and steels were 20 to 84% lower than those at room temperature. K_c values at 265F for aluminum alloys were up to 73% higher than those at room temperature.

Table 6-1 (Page 1 of 15)

Ti-6Al-4V ALLOY - K_{Ic}/K_c TEST RESULTS

Specimen No.	Nominal Dimensions, In B	Nominal Dimensions, In W	Orientation	Test Temp, F	Test Type	K_{Ic} (K_Q) or K_c In KSI $\sqrt{In}$ Individual Spec.	K_{Ic} (K_Q) or K_c In KSI $\sqrt{In}$ Average or Estimated Value	Specimen Plane Strain Capability K_I, KSI $\sqrt{In}$
Material 61-62, 5/8" Plate								
				MILL ANNEALED (MA)				
3-6,7,20, 4-50,52, 54	.63-.69	3.5	RW	RT	K_{Ic}	$(36)^b$,$(39)^b$,$(36)^b$, $(41)^b$,$(40)^b$,$(41)^b$	39	69-72
4-10,11, 51,53	.63-.65	3.5	WR	RT	K_{Ic}	29,$(30)^c$,36,33	32	80
				RECRYSTALLIZED ANNEALED BY LABORATORY (LAB RA)				
4-55,56, 57	.63	3.5	RW	RT	K_{Ic}	$(40)^b$,$(61)^b$,$(52)^b$	51	63
				AFTER DIFFUSION BOND THERMAL CYCLE (DBTC)				
4-13,14, 17	.63-.66	3.0	WR	RT	K_{Ic}	$(46)^b$,$(48)^b$,$(60)^b$	51	77-79
				AFTER DIFFUSION BOND THERMAL AND PRESSURE CYCLE (DBT&PC)				
3-26,27, 4-9	.55-.59	3.5	RW	RT	K_{Ic}	$(52)^{bc}$,$(59)^{bc}$,$(59)^{bc}$	54	63-65
3-21,24, 25	.65	3.0	RW	RT	K_{Ic}	$(49)^b$,$(53)^b$,$(52)^{bc}$		69
				BETA ANNEALED (BA) (1900F, .5 HR, AC: 1350F, 2 HR, AC)				
4-44,46, 48	.63	3.5	RW	RT	K_{Ic}	$(73)^{ab}$,$(93)^{ab}$,$(90)^{ac}$	82	68
4-45,49	.64	3.6	WR	RT	K_{Ic}	$(77)^{ab}$,$(89)^{ab}$	83	76

Table 6-1 (Page 2 of 15)

Ti-6Al-4V ALLOY - K_{Ic}/K_c TEST RESULTS

Specimen No.	Nominal Dimensions, In B	W	Orientation	Test Temp, F	Test Type	K_{Ic} (K_Q) or K_c In KSI $\sqrt{In}$ Individual Spec.	Average or Estimated Value	Specimen Plane Strain Capability K_I, KSI $\sqrt{In}$
Material 61-62, 5/8" Plate								
			SOLUTION TREATED AND OVER AGED (STOA) (1750F, 2 HR, WQ; 1000F, 2 HR, AC; 1300F, 2 HR, AC)					
4-38,40, 42	.63	3.5	RW	RT	K_{Ic}	$(44)^c$, 43, $(40)^b$	42	76
4-39,41, 43	.63	3.5	WR	RT	K_{Ic}	$(40)^b$, 44, $(44)^b$	43	80
Material 63, 1.25" Plate, Mill Beta Processed								
			MILL ANNEALED (MA)					
10-23,24	1.25	3.5	RW	RT	K_{Ic}	$(99)^{ac}$, $(100)^{ac}$	100	88
			AFTER DIFFUSION BOND THERMAL CYCLE					
10-20,16	1.22	3.5	RW	RT	K_{Ic}	$(108)^{ac}$, $(102)^{ac}$	105	81
10-17,19, 25	1.22	3.5	WR	RT	K_{Ic}	$(106)^{ac}$, $(106)^a$, $(103)^a$	105	84
Material 64, L-Shape Extrusion, Beta Extruded + Mill Annealed								
11-1,2	1.5	4.0	RW	RT	K_{Ic}	88, $(91)^c$	90	99
11-4,5	1.5	4.0	WR	RT	K_{Ic}	93, 92	93	97

Table 6-1 (Page 3 of 15)

Ti-6Al-4V ALLOY - K_{Ic}/K_c TEST RESULTS

Specimen No.	Nominal Dimensions, In B	Nominal Dimensions, In W	Orientation	Test Temp, F	Test Type	K_{Ic} (K_Q) or K_c In KSI $\sqrt{In}$ Individual Spec.	K_{Ic} (K_Q) or K_c In KSI $\sqrt{In}$ Average or Estimated Value	Specimen Plane Strain Capability K_I, KSI $\sqrt{In}$
Material 65, 1.312" Plate								
						MILL ANNEALED		
13-2,4	1.25	3.5	RW	RT	K_{Ic}	42, 42	41	98
13-10,29	1.25	3.5	RW	RT	K_{Ic}	(39)[c], (40)[c]		98
13-6	1.25	3.5	WR	RT	K_{Ic}	42	42	98
						RECRYSTALLIZED ANNEALED (RA)		
13-1,5, 8	1.25	3.5	RW	RT	K_{Ic}	56 , 59 , 64	60	91
13-3,7, 9	1.25	3.5	WR	RT	K_{Ic}	63 , 67 ,(56)[b]	62	91
Material 66, 1.5" Plate, Mill Beta Processed + Mill Annealed								
16-8,11, 13	1.25	3.5	RW	RT	K_{Ic}	(108)[a],(103)[a](104)[a]	105	84
16-9,10, 12	1.25	3.5	WR	RT	K_{Ic}	(95)[a],(95)[a],(97)[a]	96	85

Table 6-1 (Page 4 of 15)

Ti-6Al-4V ALLOY - K_{Ic}/K_c TEST RESULTS

Specimen No.	Nominal Dimensions, In B	Nominal Dimensions, In W	Orientation	Test Temp. F	Test Type	K_{Ic}, (K_Q) or K_c in KSI $\sqrt{In}$ Individual Specimens	K_{Ic}, (K_Q) or K_c in KSI $\sqrt{In}$ Average or Estimated Value	Specimen Plane Strain Capability K_I, KSI $\sqrt{In}$
Mat'l 67, 1.5" Plate, RA								
29-40,41	1.5	6.0	RW	RT	K_{Ic}	87,91	89	94
29-9,10AF	1.5	3.5	RW	RT	K_{Ic}	92,87		94
29-42	1.5	6.0	WR	RT	K_{Ic}	90	85	92
29-11,12AF	1.5	3.5	WR	RT	K_{Ic}	83,83		92
Mat'l 68, 2" Plate, RA								
32-1,4,5,7,9	1.8-2.0	6.0	RW	RT	K_{Ic}	$(97)^b,(88)^b,97,(90)^b,(89)^{bc}$	92	101-107
32-2,3,6,8	2.0	6.0	WR	RT	K_{Ic}	$106,102,(92)^b,101$	100	113
32-20	2.0	6.0	WR	-65	K_{Ic}	90	90	
32-19	2.0	6.0	RW	265	K_{Ic}	$(104)^{ab}$	104	86
32-21	2.0	6.0	WR	265	K_{Ic}	$(123)^a$	(123)	89
32-18A,18B	.26	6.0	RW	RT	K_c K_{Ic}	184,189 $(108)^{ab},(104)^{ab}$	186	39
Mat'l 69, 3.5" Plate, RA								
33-1,5,9	1.9	6.0	RW	RT	K_{Ic}	$(121)^{ace},(131)^{ac},(116)^{ac}$	123	104
33-3,8	2.0	6.0	WR	RT	K_{Ic}	$(116)^{ac},(111)^a$	114	108
Mat'l 70, 1.5" Plate, RA								
61665	1.5	3.0	RW	RT	K_{Ic}	$(68)^b$	68	96
61665	1.5	3.0	WR	RT	K_{Ic}	85	85	94

Table 6-1 (Page 5 of 15)

Ti-6Al-4V ALLOY - K_{Ic}/K_c TEST RESULTS

Specimen No.	Nominal Dimensions, In B	W	Orientation	Test Temp, F	Test Type	K_{Ic} (K_Q) or K_c In KSI $\sqrt{In}$ Individual Spec.	Average or Estimated Value	Specimen Plane Strain Capability K_I, KSI $\sqrt{In}$
Material 71, .5" Plate, RA								
25-5,6	.50	3.5	RW	RT	K_c K_{Ic}	137, 132 (77)ab, (72)ab	135	58
25-10,9	.50	5.0	"	"	K_c K_{Ic}	148, 141 (78)ab, (85)ab	145	58
25-14	.48	8.0	"	"	K_c K_{Ic}	176 (84)abc	176	57
25-13	.33	8.0	"	"	K_c K_{Ic}	190 (87)ab	190	47
25-3,4	.25	5.0	"	"	K_c K_{Ic}	174, 157 (91)abc, (92)ab	166	41

Table 6-1 (Page 6 of 15)

Ti-6Al-4V ALLOY- K_{Ic}/K_c TEST RESULTS

Specimen No.	Nominal Dimensions, In B	W	Orientation	Test Temp. F	Test Type	K_{Ic}, (K_Q) or K_c in KSI $\sqrt{In}$ Individual Specimens	Average or Estimated Value	Specimen Plane Strain Capability K_I, KSI$\sqrt{In}$
Mat'l 72, 1.5" Plate								
46-3,5,9, 47-9	1.5	4.0	RW	RT	COND RA K_{Ic}	83,79,(75)[b],82	78	91
46-14,15	1.2	4.0	RW	RT	K_{Ic}	(72)[b],(79)[b]		81
46-4,6, 47-7	1.5	4.0	WR	RT	K_{Ic}	94,(98)[a],92	95	95
47-10	1.5	4.0	RW	-65	K_{Ic}	(60)[b]	60	91
47-8	1.5	4.0	WR	-65	K_{Ic}	77	77	106
47-23	1.4	4.0	RW	265	K_{Ic}	(100)[ab]	(100)	69
47-5	1.4	4.0	WR	265	K_{Ic}	(120)[a]	(120)	72
46-14,15	1.2	4.0	RW	RT	K_c K_{Ic}	142,142 (72)[b],(79)[b]	142	81
46-16,17	.87	4.0	RW	RT	K_c K_{Ic}	165,166 (81)[ab],(81)[ab]	166	69
46-18,19	.62	5.0	RW	RT	K_c K_{Ic}	194,190 (87)[abc],(85)[ab]	192	59
46-20,21	.62	5.0	RW	-65	K_c K_{Ic}	151,177 (78)[abc],(82)[abc]	164	65
46-22,23	.25	8.0	RW	-65	K_c K_{Ic}	267,193 (101)[ab],(108)[abc]	230	42

Table 6-1 (Page 7 of 15)

Ti-6Al-4V ALLOY - K_{Ic}/K_c TEST RESULTS

Specimen No.	Nominal Dimensions, In B	Nominal Dimensions, In W	Orientation	Test Temp. F	Test Type	K_{Ic}, (K_Q) or K_c in KSI $\sqrt{In}$ Individual Specimens	Average or Estimated Value	Specimen Plane Strain Capability K_I, KSI $\sqrt{In}$
Mat'l 72, 1.5" Plate (Cont'd.)								
			EXPOSED TO DB THERMAL CYCLE EXCEPT AIR COOLED FROM 1100F					
46-10,12	1.5	4.0	RW	RT	K_{Ic}	(83)[b],(103)[a]	93	91
46-11,13	1.5	4.0	WR	RT	K_{Ic}	90,93	92	95
				EXPOSED TO DB THERMAL CYCLE				
46-75,77	1.5	4.0	RW	RT	K_{Ic}	(70)[b],(74)[b]	72	91
46-76,78	1.5	4.0	WR	RT	K_{Ic}	93,91	92	95
Material 75, T-Shape Extrusion, Beta Extruded + Mill Annealed (MA)								
59-2,3	1.60	4.0	WR	RT	K_{Ic}	95, 92	94	97
59-4,5	1.60	4.0	RW	RT	K_{Ic}	92, (91)[e]	92	99
Material 76, 1.5" Plate, RA								
61-41, 42 AF	1.37	6.0	RW	RT	K_{Ic}	80, 80	80	84
61-40, 43 AF	1.37	6.0	WR	RT	K_{Ic}	86, (77)[b]	82	98

Table 6-1 (Page 6 of 15)

Ti-6Al-4V ALLOY - K_{Ic}/K_c TEST RESULTS

Specimen No.	Nominal Dimensions, In B	Nominal Dimensions, In W	Orientation	Test Temp, F	Test Type	K_{Ic} (K_Q) or K_c In KSI $\sqrt{In}$ Individual Spec.	K_{Ic} (K_Q) or K_c In KSI $\sqrt{In}$ Average or Estimated Value	Specimen Plane Strain Capability K_I, KSI $\sqrt{In}$
Material 77, 2-1/2" Ring Rolled Plate								
					COND. RA			
YD1-1, 1-8, 5-6, 5-2, 3-1, 3-10	2.00	4.0	RW	RT	K_{Ic}	(79),(78),74,82,80,74	78	107
YD1-2, 1-9, 5-7, 5-3, 3-2, 3-11	2.00	4.0	WR	RT	K_{Ic}	(82), 75, 76, 85, 75, 69	77	108
				AFTER DB THERMAL CYCLE				
YD-21, 22	1.13	3.0	RW	RT	K_{Ic}	68, 69	69	85

Table C-1 (Page 9 of 15)

Ti-6Al-4V ALLOY - K_{Ic}/K_c TEST RESULTS

Specimen No.	Nominal Dimensions, In B	W	Orientation	Test Temp, F	Test Type	K_{Ic} (K_Q) or K_c In KSI $\sqrt{In}$ Individual Spec.	Average or Estimated Value	Specimen Plane Strain Capability K_I, KSI $\sqrt{In}$
Material 78, .75" Plate, RA								
76-1	.76	5	RW	RT	K_{Ic}	$(65)^b$		69
S	.75	-	RW	RT	K_{Ic}	49, 51	55	69
76-5,-6	.79	3	RW	RT	K_{Ic}	$(53)^b$, $(48)^b$		70
76-7,-8	.75 -.74	8	RW	RT	K_{Ic}	$(63)^b$, $(58)^b$		69-68
S	.75	-	WR	RT	K_{Ic}	58, 58	58	69
76-5,-6	.791	3.0	RW	RT	K_c	**111**, **108**	**110**	70
					K_{Ic}	$(53)^b$, $(48)^b$		
76-7,-8	.757-.745	8.0	RW	RT	K_c	**211**, **221**	**216**	69-68
					K_{Ic}	$(63)^b$, $(58)^b$		
Material 79, 4 x 10 x 34" Forged Block, RA								
77-6,25	2.0	6.0	RW	RT	K_{Ic}	$(105)^b$, $(108)^b$	107	108
77-7,26	2.0	6.0	WR	RT	K_{Ic}	$(120)^a$, 108	114	115

Table 6-1 (Page 10 of 15)

Ti-6Al-4V ALLOY - K_{Ic}/K_c TEST RESULTS

Specimen No.	Nominal Dimensions, In B	W	Orientation	Test Temp, F	Test Type	K_{Ic} (K_Q) or K_c In KSI $\sqrt{In}$ Individual Spec.	Average or Estimated Value	Specimen Strain Capability K_I, KSI $\sqrt{In}$	Plane
Material 80, .1" Sheet, Cond MA (CCT Specimens)									
84-1,2	.1	24	RW	RT	K_c	$(324)^f$, $(267)^f$	296	27	
84-15,16	.1	24	WR	RT	K_c	$(207)^f$, 213	210	29	
Material 81, .1" Sheet, Cond MA (CCT Specimens)									
94-2,3	.1	24	RW	RT	K_c	$(360)^f$, $(400)^{fg}$	(380)	27	
94-4,5	.1	24	WR	RT	K_c	368, $(367)^f$	368	28	
Material 82, 4 x 10 x 34" Forged Block, RA									
95-3,4	1.75	6.0	RW	RT	K_{Ic}	$(110)^a$, 102	106	104	
95-1,2	1.75	6.0	WR	RT	K_{Ic}	$(103)^a$, $(101)^a$	102	100	
Material 84, 600 Pound Die Forging, RA (B-1 P/N L3003380)									
103-5	1.79	4.0	RW	RT	K_{Ic}	78	81	102	
103-6	2.02	4.0	"	"	"	83		108	
103-7,8	1.75	3.5	WR	"	"	87, 90	89	99	
17375	1.50	3.0	TR	"	"	83	83	92	

f crack angle exceeds 10°

g Ligament stress exceeds yield strength

Table 6-1 (Page 11 of 15)

Ti-6Al-4V ALLOY - K_{Ic}/K_c TEST RESULTS

Specimen No.	Nominal Dimensions, In B	Nominal Dimensions, In W	Orientation	Test Temp, F	Test Type	K_{Ic} (K_Q) or K_c In KSI $\sqrt{In}$ Individual Spec.	K_{Ic} (K_Q) or K_c In KSI $\sqrt{In}$ Average or Estimated Value	Specimen Plane Strain Capability K_I, KSI $\sqrt{In}$
Material 85, 300 Pound Die Forging, RA (B-1 P/N L2100086)								
44S,125S, 135S	1.50	3.0	RW	RT	K_{Ic}	78, 73, 77	76	95
104S,114S	1.50	3.0	WR	"	"	77, 70	74	96
143S	1.50	3.0	TR	"	"	(105)a	105	95
Material 87, 1.5" Plate, RA								
S	-	-	RW	RT	K_{Ic}	82	82	-
S	-	-	WR	RT	K_{Ic}	82	82	-
Material 88, 1.25" Plate RA								
44181AS	1.0	3.0	RW	RT	K_{Ic}	78	78	-
44181AS	1.0	3.0	WR	RT	K_{Ic}	81	81	-
Material 90, 2.25" Plate, RA								
88A,B,C,DS	1.5	3.0	RW	RT	K_{Ic}	88, 84, 85, 86	86	94
88A,B,C,DS	1.5	3.0	WR	RT	K_{Ic}	94, 84, 89, 83	88	94
Material 92, 2-1/2" Ring Rolled Plate (Ladish Heat AK)								
					COND. RA			
AK7-2, 7-7, 9-1 9-6, 11-1 11-6	2.00	4.0	RW	RT	K_{Ic}	(69), (73), 72, (71), (72), 71	72	109

Table 6-1 (Page 12 of 15)

K_{Ic}/K_c TEST RESULTS

Specimen No.	Nominal Dimensions, In B	W	Orientation	Test Temp, F	Test Type	K_{Ic} (K_Q) or K_c In KSI $\sqrt{In}$ Individual Spec.	Average or Estimated Value	Specimen Plane Strain Capability K_I, KSI $\sqrt{In}$
				AFTER DB THERMAL CYCLE				
AK13, 16-30	1.11-1.37	3.0	WR	RT	K_{Ic}	69, 72, 69	70	79-88
Material 253, 2.5" Plate, RA								
5570-1, 2,3S		-	RW	RT	K_{Ic}	89, 87, 89	88	-
5570-1, 2,3S	-	-	WR	"	"	91, 81, 93	83	-
Material 294, 1.25" Plate, RA								
6163-1A 1B, 2A, 2B, 3A, 3BS	-	-	RW	RT	K_{Ic}	77,81,79,75,73,81	78	-
6163-1A 1B, 2A, 2B, 3A, 3BS	-	-	WR	RT	K_{Ic}	76,74,81,74,70,73	75	-
Material 7406, 2.00" Plate, RA								
S	-	-	RW	RT	K_{Ic}	70	70	-
S	-	-	WR	RT	K_{Ic}	69	69	-
Material 7768, .75" Plate, RA								
S	.75	-	RW	RT	K_{Ic}	(72)[a], (70)[a]	71	69
S	.75	-	WR	RT	K_{Ic}	(74)[a], (75)[a]	75	71

Table 6-1 (Page 13 of 15)

DIFFUSION BONDED Ti-6Al-4V - K_{Ic}/K_c TEST RESULTS

Specimen No.	Nominal Dimensions, In B	W	Orientation	Test Temp, F	Test Type	K_{Ic} (K_Q) or K_c In KSI $\sqrt{In}$ Individual Spec.	Average or Estimated Value	Specimen Plane Strain Capability K_I, KSI $\sqrt{In}$
Diffusion Bonded Billets of 5/8" Plate (Material 61)*								
10,11, 2	1.00	3.5	RW	RT	K_{Ic}	$(46)^{bc}$,$(49)^{bc}$,$(51)^{bc}$	49	85
3,4,9	1.00	3.5	WR	RT	K_{Ic}	$(65)^{cd}$,$(63)^{b}$,$(63)^{e}$	64	97
Material 74, Diffusion Bonded Billet of 1-1/2" Plate From Material 70								
				BOND JOINT, AS BONDED				
52-4,5, 6,7	1.50	4.0	TW/TW	RT	K_{Ic}	88,87,82,$(96)^{a}$	88	88
			BOND JOINT, AS BONDED + 2 DB THERMAL CYCLES					
53-4,5	1.50	4.0	TW/TW	RT	K_{Ic}	$(95)^{a}$, $(93)^{a}$	94	88
			BOND JOINT, AS BONDED + 4 DB THERMAL CYCLES					
54-4	1.50	4.0	TW/TW	RT	K_{Ic}	$(91)^{a}$, $(92)^{a}$	92	86
Diffusion Bond Joints, 2.5" Plate From Material 77								
LC-1,2	1.5	4.0	RW/RW	RT	K_{Ic}	88, 74	81	93
LB-1,2	1.5	4.0	TR/TR	RT	K_{Ic}	$(99)^{a}$, 81	90	91
Diffusion Bond Joints, 2.25" Plate FROM MAT'L 90								
C-1,2	1.5	4.0	RW/RW	RT	K_{Ic}	$(93)^{a}$, $(98)^{a}$	96	91
C-1,2	1.5	4.0	TR/TR	RT	K_{Ic}	$(106)^{a}$, $(108)^{a}$	107	87

* The bond plane in these specimens was parallel to the specimen side surfaces and was located at specimen mid-thickness.

Table 6-1 (Page 14 of 15)

DIFFUSION BONDED Ti-6Al-4V – K_{Ic}/K_c TEST RESULTS

Specimen No.	Nominal Dimensions, In B	Nominal Dimensions, In W	Orientation	Test Temp, F	Test Type	K_{Ic} (K_Q) or K_c In KSI $\sqrt{In}$ Individual Spec.	K_{Ic} (K_Q) or K_c In KSI $\sqrt{In}$ Average or Estimated Value	Specimen Plane Strain Capability K_I, KSI $\sqrt{In}$
Diffusion Bonded Billet of .180" Sheet (Material MH05379) **								
5379RW	1.50	3.0	RW	RT	K_{Ic}	80	80	90
5379WR	1.50	3.0	WR	"	"	83	83	99
5379RT, RT	1.50	3.0	RT	"	"	$(129)^{ab}$, $(132)^{ab}$	(131)	90
5379WT, WT	1.50	3.0	WT	"	"	$(102)^{ab}$, $(104)^{ab}$	103	99
Diffusion Bond Joints, 1.5" Plate (WR,RW) and 2.5" Plate (TR), Containing Bond Plane Anomalies								
				OXYGEN ENRICHED BOND PLANE, HEAVY				
1C1-1,2	1.24	2.5	RW/TR	RT	K_{Ic}	42, $(38)^{c}$	40	85
5A1-1,2	1.24	2.5	WR/TR	RT	K_{Ic}	$(33)^{c}$, 36	35	85
				OXYGEN ENRICHED BOND PLANE, MEDIUM				
1C6-1,2	1.25	2.5	RW/TR	RT	K_{Ic}	59, 57	58	84

** Bond Planes in these specimens were parallel to the specimen side surfaces in the specimens with RW and WR orientations and parallel to front and back edge surfaces in the specimens with RT and WT orientations.

Table 6-1 (Page 15 of 15)

DIFFUSION BONDED Ti-6Al-4V - K_{Ic}/K_c TEST RESULTS

Specimen No.	Nominal Dimensions, In B	Nominal Dimensions, In W	Orientation	Test Temp, F	Test Type	K_{Ic} (K_Q) or K_c In KSI $\sqrt{In}$ Individual Spec.	K_{Ic} (K_Q) or K_c In KSI $\sqrt{In}$ Average of Estimated Value	Specimen Plane Strain Capability K_I, KSI $\sqrt{In}$
Diffusion Bond Joints, 1.5" Plate (WR, RW) and 2.5" Plate (TR), Containing Bond Plane Anomalies (Cont'd.)								
FINE POROSITY IN BOND PLANE, DIA. .0015", FREQ. 10,000 PER IN^2								
1C5-1,-2	1.25	2.5	RW/TR	RT	K_{Ic}	70,69	70	84
1A5-1,-2	1.25	2.5	WR/TR	RT	K_{Ic}	62,63	63	85
MEDIUM POROSITY IN BOND PLANE, DIA. .002", FREQ. 2,500 PER IN^2								
1C3-1,-2	1.25	2.5	RW/TR	RT	K_{Ic}	80,77	79	84
5A3-1,-2	1.25	2.5	WR/TR	RT	K_{Ic}	(88)[a],(90)[a]	89	84
COARSE POROSITY IN BOND PLANE, DIA. .004", FREQ. 2,500 PER IN^2								
1C4-1,2	1.25	2.5	RW/TR	RT	K_{Ic}	76,82	79	84
5A4-1,2	1.25	2.5	WR/TR	RT	K_{Ic}	73,67	70	84

Table 6-2 (Page 1 of 5)

2024 AL - K_{Ic}/K_c TEST RESULTS

Specimen No.	Nominal Dimensions, In B	Nominal Dimensions, In W	Orientation	Test Temp. F	Test Type	K_{Ic}, (K_Q) or K_c in KSI $\sqrt{In}$ Individual Specimens	K_{Ic}, (K_Q) or K_c in KSI $\sqrt{In}$ Average or Estimated Value	Specimen Plane Strain Capability K_I, KSI$\sqrt{In}$
Material 1, 3" Plate, T851								
6-28,31,32	1.0	3.0	RW	RT	K_{Ic}	21, 22, 21	21	36
6-26,29,30	1.0	3.0	WR	RT	K_{Ic}	18, (19)[c], 18	18	35
6-34	1.0	2.5	TW	RT	K_{Ic}	(19)[c]	19	35
Material 1, 3" Plate, T62								
6-23,24	1.0	3.0	RW	RT	K_{Ic}	(33)[abc],(38)[abc]	36	32
6-21,22,25	1.0	3.0	WR	RT	K_{Ic}	(26)[cb],(23)[cb],(25)[c]	25	31
6-33, 35	1.0	2.5	TW	RT	K_{Ic}	(26)[c],(18)[cb]	22	31
Material 2, 3" Plate, T351								
7-1,2,3	2.0	6.0	RW	RT	K_{Ic}	(31)[c],(30)[b],(31)[c]	31	62
7-3,4,8	2.0	6.0	WR	RT	K_{Ic}	(34)[c], (29)[c], 29	31	61
7-9,10,11	1.25	2.5	TW	RT	K_{Ic}	22, 21, 21	21	48
Material 3, 3" Plate, T851								
8-141,142	0.49	6.0	RW	RT	K_{Ic}	(26)[b], (25)[b]	26	29
8-144,145,146	0.76-1.0	3.0	TW	RT	K_{Ic}	24, 23, 24	24	36-42

Table 6-2 (Page 2 of 5)

2024 AL - K_{Ic}/K_c TEST RESULTS

Specimen No.	Nominal Dimensions, In B	Nominal Dimensions, In W	Orientation	Test Temp. F	Test Type	K_{Ic}, (K_Q) or K_c in KSI $\sqrt{In}$ Individual Specimens	K_{Ic}, (K_Q) or K_c in KSI $\sqrt{In}$ Average or Estimated Value	Specimen Plane Strain Capability K_I, KSI $\sqrt{In}$
Material 6, 1.75" Plate, T851								
18-7,8,9,10	.76-1.0	3.0	RW	RT	K_{Ic}	23,(23)[b],(25)[c],23	24	36-41
18-5,6	.50	6.0	RW	RT	K_{Ic}	(27)[b], (28)[b]		29
18-3,4	.26	6.0	RW	RT	K_c K_{Ic}	54, 49 (31)[abc],(31)[abc]	51	21
18-1,2	.11	6.0	RW	RT	K_c K_{Ic}	57, 59 (45)[ac], (45)[ac]	58	14
Material 8, 3.5" Plate, T62								
26-22,21	1.75	5.0	RW	RT	K_{Ic}	(38)[c], (43)[c]	41	48
Material 9, 3.0" Plate, T851								
28-15,16,17, 18,19,20	0.63	2.5	RW	RT	K_{Ic}	(21)[b],(24)[b],(21)[b],(20)[b], (31)[ab], (22)[b]	23	33
28-21,22,23	0.63	2.5	WR	RT	K_{Ic}	18, 19, 19	19	32

Table 6-2 (Page 3 of 5)

2024 ALLOY

K_{Ic}/K_c TEST RESULTS

Specimen No.	Nominal Dimensions, In B	W	Orientation	Test Temp, F	Test Type	K_{Ic}, (K_Q) or K_c in KSI $\sqrt{In}$ Individual Specs.	Average or Estimated Value	Specimen Plane Strain Capability K_I, KSI $\sqrt{In}$
Mat'l 19, 3 x 18 x 23" Forged Block, T852								
64-1, 2, 3, 4	1.0	2.0	WR	R.T.	K_{Ic}	$(21)^c$, 21, 21, 20	21	38
64-5, 6, 7, 8, 9, 10	1.25	2.5	RW	R.T.	K_{Ic}	$(31)^c$, 26, 31, 27, $(30)^c$, $(25)^c$	28	41
64-11, 12	0.75	1.5	TR	R.T.	K_{Ic}	$(16)^{ec}$, $(18)^e$	18	33
64-26, 27, 28	1.25	2.5	RW	265	K_{Ic}	$(39)^a$, $(30)^c$, 31	33	37
64-29, 30	1.25	2.5	WR	265	K_{Ic}	$(26)^c$, 24	25	39
Mat'l 27, 3 x 18 x 35" Forged Block, T852								
75-62, 64	1.0	2.0	WR	R.T.	K_{Ic}	$(26)^c$, $(27)^c$	27	34
75-66, 68, 70	1.25	2.5	RW	R.T.	K_{Ic}	37, 37, 36	37	37
75-72, 74	1.0	2.5	RW	R.T.	K_c K_{Ic}	64, 44 $(40)^{ab}$, $(38)^a$	54	34
75-65, 67, 97	0.75	2.5	RW	R.T.	K_c K_{Ic}	64, 55, 50 $(40)^{ab}$, $(37)^{ab}$, $(35)^a$	56	29
75-69, 71	0.50	2.5	RW	R.T.	K_c K_{Ic}	60, 69 $(38)^{ab}$, $(38)^{ab}$	65	24

Table 6-2 (Page 4 of 5)

2024 ALLOY

K_{Ic}/K_c TEST RESULTS

Specimen No.	Nominal Dimensions, In B	Nominal Dimensions, In W	Orientation	Test Temp, F	Test Type	K_{Ic} (K_Q) or K_c In KSI $\sqrt{In}$ Individual Specimens	K_{Ic} (K_Q) or K_c In KSI $\sqrt{In}$ Average or Estimated Value	Specimen Plane Strain Capability K_I, KSI $\sqrt{In}$
Mat'l 27, 3 x 18 x 35" Forged Block, T852 (Cont'd)								
75-73, 75	0.50	2.5	RW	265	K_c K_{Ic}	66, 61 $(38)^{ab}$, $(37)^{ab}$	64	22
75-61, 63	0.38	2.0	WR	R.T.	K_c K_{Ic}	38, 38 $(26)^{ab}$, $(26)^{ab}$	38	21
75-76, 77	0.25	2.5	RW	R.T.	K_c K_{Ic}	77, 71 $(39)^{ab}$, $(35)^{ab}$	74	17

Table 6-2 (Page 5 of 5)

2024 ALUMINUM ALLOY - K_{Ic}/K_c TEST RESULTS

Specimen No.	Nominal Dimensions, In B	W	Orientation	Test Temp, F	Test Type	K_{Ic} (K_Q) or K_c In KSI $\sqrt{In}$ Individual Specimens	Average or Estimated Value	Specimen Plane Strain Capability K_I, KSI $\sqrt{In}$
Material 302, .1" Sheet, T81 (CCT Specimens)								
87-8,9	.10	24	RW	RT	K_c	64, 64	64	13
87-10,11, 12	.10	24	WR	RT	K_c	61, (60)^f, 59	60	13
Material 303, .1" Sheet, T81 (CCT Specimens)								
88-2,7,8	.10	24	RW	RT	K_c	(58)^f, (62)^f, (78)^f	66	14
88-10,12, 13	.10	24	WR	RT	K_c	47, 47, 44	46	14

^{f} crack angle exceeds 10°

Table 6-3

2124 ALLOY K_{Ic}/K_c TEST RESULTS

Specimen No.	Nominal Dimensions, In B	Nominal Dimensions, In W	Orientation	Test Temp, F	Test Type	K_{Ic}, (K_Q) or K_c in KSI $\sqrt{In}$ Individual Specimens	K_{Ic}, (K_Q) or K_c in KSI $\sqrt{In}$ Average or Estimated Value	Specimen Plane Strain Capability K_I, KSI $\sqrt{In}$
Mat'l 12, 3" Plate, T851								
35-123, 124 125	0.75	2.3	RW	R.T.	K_{Ic}	$(39)^a$, $(39)^a$, 32		36
11734 RW	0.50	1.5	RW	R.T.	K_{Ic}	$(32)^a$	33	29
35-38, 40 (AF)	0.62	2.0	RW	R.T.	K_{Ic}	29, 29		32
35-130, 131	0.75	2.5	WR	R.T.	K_{Ic}	25, 23	24	37
35-37, 39 (AF)	0.62	[illegible].0	WR	R.T.	K_{Ic}	23, 24		33
11734 RW	0.75	2.5	TW	R.T.	K_{Ic}	24	24	35
Mat'l 12, 3" Plate, Brake Bump Formed To 180" Radius In T351 And Then Aged To T851								
1171 RW	2.00	5.0	RW	R.T.	K_{Ic}	33	33	58
1171 TW	0.87	2.5	TW	R.T.	K_{Ic}	23	23	37
Mat'l 14, 3" Plate, T851								
41-1, 3, 5	0.75	2.0	WR	R.T.	K_{Ic}	22, 23, 23	23	36
41-2, 4, 6	0.75	2.0	RW	R.T.	K_{Ic}	25, 24, 25	25	36

Table 6-4 (Page 1 of 3)

2219 AL - K_{Ic}/K_c TEST RESULTS

Specimen No.	Nominal Dimensions, In B	Nominal Dimensions, In W	Orientation	Test Temp. F	Test Type	K_{Ic}, (K_Q) or K_c in KSI $\sqrt{In}$ Individual Specimens	K_{Ic}, (K_Q) or K_c in KSI $\sqrt{In}$ Average or Estimated Value	Specimen Plane Strain Capability K_I, KSI$\sqrt{In}$
Material 4, 2" Plate, T62								
9-22,26	1.5	5.0	RW	RT	K_{Ic}	(47)[c ea],(44)[bc a]	45	39
9-23,24,25,27	1.5	5.0	WR	RT	K_{Ic}	(30)[cba],(47)[cba],(40)[ca], (42)[cba]	42	39
Material 4, 2" Plate, T851								
9-30, 32, 12-16,17	1.5	5.0	RW	RT	K_{Ic}	(40)[a],39,(38)[c],(38)[c]	39	39
9-29,31	1.5	5.0	WR	RT	K_{Ic}	34,36	35	39
9-45,46,47	0.75	1.5	TW	RT	K_{Ic}	(25)[c], 25, 21	24	27
Material 7, 1.75" Plate, T851								
23-35,36	1.5	3.0	RW	RT	K_{Ic}	(40)[a],(40)[a]		39
27-63,64,65,66	1.5	5.0	RW	RT	K_{Ic}	(45)[a],(45)[a],(45)[a],(46)[a]	45	39
36-5,6	1.5	6.0	RW	RT	K_{Ic}	(46)[ab],(45)[ab]		39
27-37,38	1.5	3.0	WR	RT	K_{Ic}	34, 34		37
27-60,61,62	1.5	5.0	WR	RT	K_{Ic}	(39)[a], 37, 37	38	37
36-11,12	1.5	6.0	WR	RT	K_{Ic}	(39)[a], (39)[a]		37

Table 6-4 (Page 2 of 3)

2219 Al - K_{Ic}/K_c TEST RESULTS

Specimen No.	Nominal Dimensions, In B	Nominal Dimensions, In W	Orientation	Test Temp F	Test Type	K_{Ic} (K_Q) or K_c In KSI $\sqrt{In}$ Individual Specimens	K_{Ic} (K_Q) or K_c In KSI $\sqrt{In}$ Average or Estimated Value	Specimen Plane Strain Capability K_I, KSI $\sqrt{In}$
Material 7, 1.75" Plate T851 (Cont'd.)								
36-1,4	1.5	6.0	TW	265F	K_{Ic}	$(44)^{ba}$, $(43)^{cba}$	43	35
36-8,10	1.5	6.0	WR	265F	K_{Ic}	$(35)^{cba}$, $(33)^{cb}$	34	33
36-13,14	1.25	6.0	RW	RT	K_c K_{Ic}	>65, 72 $(46)^{abc}$, $(48)^{ab}$	72	35
36-16,17	0.87	6.0	RW	RT	K_c K_{Ic}	86, 80 (48) ceba, $(47)^{eba}$	83	30
36-21,23	0.50	6.0	RW	RT	K_c K_{Ic}	70, 87 $(44)^{ab}$, $(49)^{abe}$	79	22
26,28,	0.5	6.0	WR	RT	K_c K_{Ic}	63, 61, 62 $(37)^{a}$, $(43)^{bac}$, $(44)^{ba}$	62	
36-22,24	0.25	6.0	RW	RT	K_c K_{Ic}	104, 95 $(57)^{ba}$, $(48)^{bac}$	100	16
36-25,27	0.5	6.0	RW	265F	K_c K_{Ic}	102, 104 $(37)^{cba}$, $(37)^{ba}$	103	20
Material 13, 3" Plate T851								
37-8,9	2.0	8.0	RW	RT	K_{Ic}	$(37)^{c}$, 35	36	48
37-10,11	2.0	8.0	WR	RT	K_{Ic}	$(29)^{c}$, $(29)^{c}$	29	48
202	.87	2.0	TW	RT	K_{Ic}	25	25	31
Material 13, 3" Plate, Brake Bump Formed to 180" Radius in -T351 and then Aged to -T851 Cond.								
207-35	2.0	5.0	RW	RT	K_{Ic}	37	37	48
202-17	.87	2.0	TW	RT	K_{Ic}	21	21	31

Table 6-4 (Page 3 of 3)

2219 AL - K_{Ic}/K_c TEST RESULTS

Specimen No.	Nominal Dimensions, In B	W	Orientation	Test Temp, F	Test Type	K_{Ic} (K_Q) or K_c In KSI $\sqrt{In}$ Individual Specimens	Average or Estimated Value	Specimen Plane Strain Capability K_I, KSI $\sqrt{In}$
Material 16, Extruded Bar T851								
48-8,9, 10	1.7	6.0	RW	RT	K_{Ic}	$(55)^{ca}, (55)^{a}, (58)^{a}$	55	42
48-6,7	1.7	6.0	WR	RT	K_{Ic}	$(44)^{ca}, (45)^{a}$	45	40
Material 20, Hand Forging T851								
65-2,3,5	2.0	5.0	RW	RT	K_{Ic}	$(44)^{b}, (40)^{b}, 24$	36	46
65-4,5A	2.0	5.0	WR	RT	K_{Ic}	22, 39	31	46
65-7,8	1.6	3.0	TR	RT	K_{Ic}	$(32)^{c}, (32)^{c}$	32	40
Material 304, 3" Plate T851								
89-3	2.0	8.0	RW	RT	K_{Ic}	$(41)^{c}$	41	48
89-4,5	2.0	8.0	WR	RT	K_{Ic}	$34, (35)^{c}$	35	47

Table 6-5

7049 AE – K_{Ic}/K_c TEST RESULTS

Specimen No.	Nominal Dimensions, In B	Nominal Dimensions, In W	Orientation	Test Temp. F	Test Type	K_{Ic}, (K_Q) or K_c in KSI $\sqrt{In}$ Individual Specimens	K_{Ic}, (K_Q) or K_c in KSI $\sqrt{In}$ Average or Estimated Value	Specimen Plane Strain Capability K_I, KSI$\sqrt{In}$
Material 10, Forging, T73								
22-1, 4	1.0	3.5	RW	RT	K_{Ic}	(26), 28	27	43
Material 24, Die Forging, T73								
70-2,3	1.5	3.0	RW	RT	K_{Ic}	(50)[ca], (37)[c]	44	
Material 25, Forging, T73, 3 x 24 x 48								
71-15,16,17	2.0	4.0	RW	RT	K_{Ic}	(39)[c], 39, 38	38	58
71-18,19	1.25	4.0	RW	RT	K_{Ic}	(38)[b], (37)[b]		46
71-22,23	1.5	3.0	WR	RT	K_{Ic}	(20)[c]. (26)[c]	23	49
71-25	1.25	2.5	TR	RT	K_{Ic}	23	23	44
71-18,19	1.25	4.0	RW	RT	K_c K_{Ic}	55, 51 (38)[b], (37)[b]	53	46
71-20,21	.75	4.0	RW	RT	K_c K_{Ic}	83, 77 (39)[ba], (40)[ba]	80	36

Table 6-6

7050 AL — K_{Ic}/K_c TEST RESULTS

Specimen No.	Nominal Dimensions, In B	W	Orientation	Test Temp. F	Test Type	K_{Ic}, (K_Q) or K_c in KSI $\sqrt{In}$ Individual Specimens	Average or Estimated Value	Specimen Plane Strain Capability K_I, KSI $\sqrt{In}$
Material 28, 4" Plate, T73								
80-1,2,3	1.5	3.0	RW	RT	K_{Ic}	30,26,(29)[c]	28	53
80-4,5,6	1.5	3.0	WR	RT	K_{Ic}	26, 30, 27	28	51
80-7,8,9	1.5	3.0	TR	RT	K_{Ic}	25, 26, 25	25	48
Material 23, Die Forging, T73								
69-2,3	1.5	3.0	RW	RT	K_{Ic}	(45)[c], (45)[c]	45	55
69-4	1.4	2.5	TW	RT	K_{Ic}	(26)[c]	26	47

Table 6-7 (Page 1 of 7)

7075 AL K_{Ic}/K_c TEST RESULTS

Specimen No.	Nominal Dimensions, In B	Nominal Dimensions, In W	Orientation	Test Temp, F	Test Type	K_{Ic} (K_Q) or K_c In KSI $\sqrt{In}$ Individual Specimens	K_{Ic} (K_Q) or K_c In KSI $\sqrt{In}$ Average or Estimated Value	Specimen Plane Strain Capability K_I, KSI $\sqrt{In}$
Mat'l 5, 2" Plate, -T7351								
17-18,-20 -22	0.82	2.0	RW	RT	K_{Ic}	26, 27, 26	26	37
17-26,-28 -55	0.82	3.0	RW	RT	K_{Ic}	27, 27, 29	28	37
17-53,-54 -24	0.82	3.0	WR	RT	K_{Ic}	23, 23, 22	23	37
Mat'l 5, 2" Plate, -T7651								
17-56,-57 -58,-59	0.83	2.0	RW	RT	K_{Ic}	29, 28, 29, 28	29	38
17-27	0.81	3.0	RW	RT	K_{Ic}	26	26	37
17-17,-19 -21	0.81	2.0	WR	RT	K_{Ic}	22, 20, 22	21	38
17-23,-25	0.80	3.0	WR	RT	K_{Ic}	22, 22	22	37
Mat'l 15, 2.6" Plate, -T7651								
42-8,-10 -12	0.5	1.5	RW	RT	K_{Ic}	(32)[a], (32)[a], (32)[a]	32	30

Table 6-7 (Page 2 of 7)

7075 AL K_{Ic}/K_c TEST RESULTS

Specimen No.	Nominal Dimensions, In B	W	Orientation	Test Temp, F	Test Type	K_{Ic} (K_Q) or K_c In KSI $\sqrt{In}$ Individual Specimens	Average or Estimated Value	Specimen Plane Strain Capability K_I, KSI $\sqrt{In}$
Mat'l 15, 2.6" Plate, -T7651 (Cont'd)								
42-9,-11	0.5	1.5	WR	RT	K_{Ic}	26, 28	27	30
Mat'l 18, 2" Plate, -T7351								
51-65,-67 -69	1.0	3.0	RW	RT	K_{Ic}	32, 32, 30	31	36
51-66,-68	1.0	3.0	WR	RT	K_{Ic}	25, 26	25	37
51-75,-76	0.5	1.5	TR	RT	K_{Ic}	18, (18)^c	18	26
Mat'l 18, 2" Plate, -T7651								
51-135, -133,-134	0.75	2.0	RW	RT	K_{Ic}	28, 28, 28	28	34
51-38,-39	0.51	2.5	RW	RT	K_{Ic}	(28)^b, (27)^b		28
51-136,-137	0.75	2.0	WR	RT	K_{Ic}	23, 24	24	35
51-43,-44	0.38	1.0	TR	RT	K_{Ic}	15, 17	16	24

Table 6-7 (Page 3 of 7)

7075 AL K_{Ic}/K_c TEST RESULTS

Specimen No.	Nominal Dimensions, In B	Nominal Dimensions, In W	Orientation	Test Temp, F	Test Type	K_{Ic} (K_Q) or K_c In KSI $\sqrt{In}$ Individual Specimens	K_{Ic} (K_Q) or K_c In KSI $\sqrt{In}$ Average or Estimated Value	Specimen Plane Strain Capability K_I, KSI $\sqrt{In}$
Mat'l 13, 2" Plate, -T7651 (Cont'd)								
51-38,-39	0.51	2.5	RW	RT	K_c K_{Ic}	49, 48 (28)[b], (27)[b]	49	28
51-40,-45	0.38	2.5	RW	RT	K_c K_{Ic}	66, 60 (30)[ba], (28)[ba]	63	25
51-46	0.26	2.5	RW	RT	K_c K_{Ic}	63 (29)[bae]	63	20
51-48,-49	0.13	2.5	RW	RT	K_c K_{Ic}	74, 68 (42)[ba], (42)[ba]	71	14
51-52	0.26	2.5	WR	RT	K_c K_{Ic}	45 (23)[bae]	45	20
51-50,-51	0.26	2.5	WR	265F	K_c K_{Ic}	83, 73 (23)[ba], (23)[ba]	78	17
Mat'l 22, Forging, -T73								
68-2,-3	1.5	3.0	RW	RT	K_{Ic}	(45)[c], (45)[c]	45	52
68-4	1.4	2.5	TW	RT	K_{Ic}	(28)[c]	28	47

Table 6-7 (Page 4 of 7)

7075 AL

K_{Ic}/K_c TEST RESULTS

Specimen No.	Nominal Dimensions, In B	W	Orientation	Test Temp, F	Test Type	K_{Ic} (K_Q) or K_c In KSI $\sqrt{In}$ Individual Specimens	Average or Estimated Value	Specimen Plane Strain Capability K_I, KSI $\sqrt{in}$
Mat'l 29, Extrusion -T73511								
83-31,-33 -35	2.0	4.0	RW	RT	K_{Ic}	41, 37, 43		58
83-21,-23	1.6	4.0	RW	RT	K_{Ic}	37, (41)[b]	39	53
83-27,-29 -55	1.25	4.0	RW	RT	K_{Ic}	(39)[b], (37)[b], (38)[b]		47
83-19,-25	1.75	3.5	WR	RT	K_{Ic}	27, 26	28	52
83-20,-26	0.75	3.5	WR	RT	K_{Ic}	(29)[b], 28		53
83-37,-38	1.0	2.0	TR	RT	K_{Ic}	23, 21	22	39
83-30,-81	2.0	4.0	RW	265F	K_{Ic}	(46)[b], (42)[b]	44	51
83-52,-83	2.0	4.0	WR	265F	K_{Ic}	29, 29	29	47
83 -21	1.6	4.0	RW	RT	K_c K_{Ic}	56 37	56	53

Table 6-7 (Page 5 of 7)

7075 AL K_{Ic}/K_c TEST RESULTS

Specimen No.	Nominal Dimensions, In B	Nominal Dimensions, In W	Orientation	Test Temp, F	Test Type	K_{Ic} (K_Q) or K_c In KSI $\sqrt{In}$ Individual Specimens	K_{Ic} (K_Q) or K_c In KSI $\sqrt{In}$ Average or Estimated Value	Specimen Plane Strain Capability K_I, KSI $\sqrt{In}$
Mat'l 29, Extrusion -T73511 (Cont'd)								
83-27, -29 -55	1.25	4.0	RW	RT	K_c K_{Ic}	>73, 78, 59 $(39)^b$, $(37)^b$, $(38)^b$	69	47
33-22, -24	0.75	4.0	RW	RT	K_c K_{Ic}	112, 89 $(40)^{ba}$, $(42)^{ba}$	101	36
83-32, -34 -56	0.37	4.0	RW	RT	K_c K_{Ic}	>104, 88, 81 $(41)^{ba}$, $(44)^{ba}$, $(43.9)^{ba}$	91	25
83-28, -30	0.75	4.0	RW	265F	K_c K_{Ic}	>93, 134 $(43)^{ba}$, $(48)^{ba}$	134	31
83-20, -26	0.75	3.5	WR	RT	K_c K_{Ic}	40, 39 $(29)^b$, 28	40	37

Table 6-7 (Page 6 of 7)

7075 ALUMINUM ALLOY - K_{Ic}/K_c TEST RESULTS

Specimen No.	Nominal Dimensions, In B	W	Orientation	Test Temp, F	Test Type	K_{Ic} (K_Q) or K_c In KSI $\sqrt{In}$ Individual Specimens	Average or Estimated Value	Specimen Plane Strain Capability K_I, KSI $\sqrt{In}$
Material 30, .1" Sheet, T76 (CCT Specimens)								
85-6,8,9	.10	24	RW	RT	K_c	89, 87, (88)[f]	83	13
85-10, 11	.10	24	WR	RT	K_c	68, 70	69	13
Material 301, .1" Sheet, T76 (CCT Specimens)								
86-1,2,3	.10	24	RW	RT	K_c	(> 130)[f], 93, 114	114	13
86-5,6	.10	24	WR	RT	K_c	79, 78	79	13
Mat'l 306, 2.5" Plate -T7651								
91-1,-2 -3	1.25	2.5	RW	RT	K_{Ic}	31, 31, 31	31	43
91-6 ,-7	1.25	2.5	WR	RT	K_{Ic}	24, 23	24	43
91-10,-11	0.75	1.5	TR	RT	K_{Ic}	20, 20	20	33

[f] crack angle exceeds 10°

Table 6-7 (Page 7 of 7)

7075 AL K_{Ic}/K_c TEST RESULTS

Specimen No.	Nominal Dimensions, In B	W	Orientation	Test Temp, F	Test Type	K_{Ic} (K_Q) or K_c In KSI $\sqrt{In}$ Individual Specimens	Average or Estimated Value	Specimen Plane Strain Capability K_I, KSI $\sqrt{In}$
Mat'l 306, 2.5" Plate -T7651								
91-4,-5	1.25	2.5	RW	265F	K_{Ic}	$(30)^b$, $(31)^b$	31	37
91-8,-9	1.25	2.5	WR	265F	K_{Ic}	25, 27	26	37
Mat'l 307, 2.3" Plate -T7651								
92-1,-2 -3	1.25	2.5	RW	RT	K_{Ic}	29, 30, 30	30	44
92-4,-5	1.25	2.5	WR	RT	K_{Ic}	23, 23	23	44
92-6,-7	0.75	1.5	TR	RT	K_{Ic}	20, 19	20	34
Mat'l 309, Extrusion -T7651								
96-1,-2 -3	1.25	2.5	RW	RT	K_{Ic}	33, 33, 35	33	46
96-4,-5	1.25	2.5	WR	RT	K_{Ic}	21, 21	21	48

Table 6-8

7175 AL - K_{Ic}/K_c TEST RESULTS

Specimen No.	Nominal Dimensions, In B	W	Orientation	Test Temp. F	Test Type	K_{Ic}, (K_Q) or K_c in KSI $\sqrt{In}$ Individual Specimens	Average or Estimated Value	Specimen Plane Strain Capability K_I, KSI $\sqrt{In}$
Material 21, Forging, T736								
67-3	1.5	3.0	RW	RT	K_{Ic}	$(41)^c$	41	54
67-4	1.38	2.5	TW	RT	K_{Ic}	$(27)^c$	27	46
Material 26, Forging, T73652								
72-1,3,5	2.0	4.0	RW	RT	K_{Ic}	34, 37, 34	35	60
72-2,4,6	1.75	3.5	WR	RT	K_{Ic}	29, 24, 28	27	53
72-8, 9	1.0	2.0	TR	RT	K_{Ic}	25, $(20)^c$	23	33

Table 6-9 (Page 1 of 10)

9-4-20 Steel - K_{Ic}/K_c TEST RESULTS

Specimen No.	Nominal Dimensions, In B	W	Orien-tation	Test Temp. F	Test Type	K_{Ic}, (K_Q) or K_c in KSI $\sqrt{In}$ Individual Specimens	Average or Estimated Value	Specimen Plane Strain Capability K_I, KSI$\sqrt{In}$
Material 31, 3 x 10 x 36" Forged Billet								
			(A) + (B, oq or wq) + (-100F, 2 Hrs) + (1000F, 4 to 5 Hrs)					
5-17,-19,-23	2.0	6.0	RW	RT	K_{Ic}	139,(132)[e],(133)[e]	135	161
2-9	2.0	5.7	WR	RT	K_{Ic}	102	102	161
			(A) + (B, wq) + (over-night delay or -100F, 2 Hrs)* + (1025F, 6 Hrs)					
			Over-Night Delay*; 196 TU, 183 TY					
2-6	1.0	6.0	RW	RT	K_{Ic}	(160)[ab]	(160)	117
2-5	2.0	6.0	RW	RT	K_{Ic}	160	160	166
			-100F, 2 Hrs*; 196 TU, 185 TY					
2-1	2.0	6.0	RW	RT	K_{Ic}	159	159	166
			(A) + (B, wq) + (over-night delay or no delay)** + (1050F, 4 Hrs)					
			Over-Night Delay**; 192 TU, 180 TY					
2-3	2.0	6.0	RW	RT	K_{Ic}	165	165	163
2-4	1.0	6.0	RW	RT	K_{Ic}	(172)[ab]	(172)	115
			No Delay**; 197 TU, 182 TY					
2-12	1.0	6.0	RW	RT	K_{Ic}	(160)[ab]	(160)	115

Table 6-9 (Page 2 of 10)

9-4-20 Steel - K_{Ic}/K_c TEST RESULTS

Specimen No.	Nominal Dimensions, In B	Nominal Dimensions, In W	Orientation	Test Temp. F	Test Type	K_{Ic}, (K_Q) or K_c in KSI $\sqrt{in}$ Individual Spec.	K_{Ic}, (K_Q) or K_c in KSI $\sqrt{in}$ Average or Estimated Value	Specimen Plane Strain Capability K_I, KSI $\sqrt{in}$
Material 31 (Cont'd.)								
(A) + (B, oq) + (over-night delay or -100F, 2 Hrs)*** + (1050F, 4 Hrs)								
Over-Night Delay***, 193 TU, 177 TY								
2-10	2.0	6.0	RW	RT	KIc	(167)[ab]	167	161
-100F, 2 Hrs***, 195 TU, 182 TY								
5-22	2.0	6.0	RW	RT	KIc	(155)[e]	155	161
2-2	1.0	6.0	RW	RT	KIc	(170)[ab]	(170)	114

A - 1650F to 1700F, 1 to 2 Hrs, AC
B - 1500F to 1550F, 1 to 2 Hrs

Table 6-9 (Page 3 of 10)

9-4-20 Steel - K_{Ic}/K_c TEST RESULTS

Specimen No.	Nominal Dimensions, In B	W	Orientation	Test Temp. F	Test Type	K_{Ic}, (K_Q) or K_c in KSI $\sqrt{in}$ Individual Spec.	Average or Estimated Value	Specimen Plane Strain Capability K_I, KSI$\sqrt{in}$
Material 33, 4 x 18 x 36" Forged Billet, (1650F, 1 to 2 Hrs, ac) + (1525F, 1 to 2 Hrs, og* or ac*) + (-100F, 1 to 2 Hrs) + (Temper)								
						1025F, 4 to 6 Hrs (oq)*; 204 TU, 188 TY		
14-1, 7, 9	2.0	6.0	RW	RT	K_{Ic}	$(158)^e, (151)^e, 164$	158	168
14-3, 5, 11	2.0	6.0	WR	RT	K_{Ic}	$(146)^e, (144)^e, (146)^e$	145	168
14-13,14,15	1.0	3.0	TW	RT	K_{Ic}	$(134)^a, (134)^a, (140)^a$	136	119
14-16,17,18	1.0	3.0	TR	RT	K_{Ic}	$(130)^a, (131)^a, (122)$	128	119
						1025F, 6 Hrs (ac)*; 216 TU, 195 TY		
15-4, 7	2.0	6.0	RW	RT	K_{Ic}	$133, (135)^c$	134	175
15-1	2.0	6.0	WR	RT	K_{Ic}	$(126)^c$	126	175
						1050F, 4 Hrs (ac)*; 212 TU, 193 TY		
15-10, 13	2.0	6.0	RW	RT	K_{Ic}	$(145)^c, (139)^c$	142	172
15-16	2.0	6.0	WR	RT	K_{Ic}	$(134)^c$	134	170

Table 6-9 (Page 4 of 10)

9-4-20 Steel - K_{Ic}/K_c TEST RESULTS

Specimen No.	Nominal Dimensions, In B	W	Orien-tation	Test Temp. F	Test Type	K_{Ic}, (K_Q) or K_c in KSI $\sqrt{In}$ Individual Specimens	Average or Estimated Value	Specimen Plane Strain Capabili+-; K_I, KSI$\sqrt{In}$
Material 37, 2.5" Plate								
(A) + (B, oq) + (-100F, 2 Hrs) + (1025F, 5 Hrs); 200 TU, 189 TY								
31-4, 15	2.0	6.0	RW	RT	K_{Ic}	142, 101	121	169
31-3	2.0	6.0	WR	RT	K_{Ic}	(131)[c]	131	169
30-21,23, 31-11,12,13	2.0	6.0	RW	-65F	K_{Ic}	90,91,105,107,109	100	179
30-20,31-14,16	2.0	6.0	WR	-65F	K_{Ic}	92, 104, 96	97	179
(A) + (B, ac) + (-100F, 1.5 Hr) + (1025F, 4 Hrs + 1060F, 6 Hrs); 208 TU, 189 TY								
30-10, 18 AF	2.0	6.0	RW	RT	K_{Ic}	115, 132	124	169
30-19 AF	2.0	6.0	WR	RT	K_{Ic}	128	128	169
(A) + (B, ac) + (-130F, 1.5 Hr) + (1025 to 1075F, 4 Hrs); 206 TU, 186 TY								
30-11 AF	2.0	6.0	WR	RT	K_{Ic}	116	116	166

A - 1650F, 1 to 2 Hrs, ac
B - 1525F, 1 to 2 Hrs

Table 6-9 (Page [illegible] of [illegible])

9-4-20 Steel - K_{Ic}/K_c TEST RESULTS

Specimen No.	Nominal Dimensions, In		Orientation	Test Temp. F	Test Type	K_{Ic}, (K_Q) or K_c in KSI $\sqrt{In}$		Specimen Plane Strain Capability K_I, KSI$\sqrt{In}$
	B	W				Individual Specimens	Average or Estimated Value	
Material 42, Spindle Forging Core, B-1 P/N L2300380 (1650F, 2 hrs, ac) + (1525F, 2 hrs, oq) + (-100F, 2 hrs) + (1025F, 4 Hrs); 207 TU, 194 TY								
58-1, 3, 4	1.5-1.6	4.0	RW	RT	K_{Ic}	141, 142, 135	139	150-155
58-2	1.5	4.0	WR	RT	K_{Ic}	126	126	147

Table 6-9 (Page 6 of 10)

9-4-20 Steel - K_{Ic}/K_c TEST RESULTS

Specimen No.	Nominal Dimensions, In B	Nominal Dimensions, In W	Orientation	Test Temp. F	Test Type	K_{Ic}, (K_Q) or K_c in KSI $\sqrt{In}$ Individual Specimens	K_{Ic}, (K_Q) or K_c in KSI $\sqrt{In}$ Average or Estimated Value	Specimen Plane Strain Capability K_I, KSI $\sqrt{In}$
Material 43, 4 x 18 x 36" Forged Fillet (1650F, 2 Hrs, ac) + (1525F, 2 Hrs, oq) + (-100F, 2 Hrs) + (1025F, 4 Hrs); 211 TU, 186 TY								
60-2,54,56,58, 60,62	2.0	6.0	RW	RT	K_{Ic}	136,143,138,138,140,136	141	166
60-9, 65	1.6	8.0	RW	RT	K_{Ic}	(146)[a],144		148
60-4,6,8,52,64	2.0	6.0	WR	RT	K_{Ic}	127,127,127,126,121	126	167
60-17,18	1.6	3.0	TW	RT	K_{Ic}	114,116	115	151
60-13,14	.875	8.0	RW	-65F	K_{Ic}	(79)[bc],(82)[bc]	81	114
60-9,65	1.6	8.0	RW	RT	K_c K_{Ic}	225,232 (146)[c],144	229	148
60-10	1.3	8.0	RW	RT	K_c K_{Ic}	>241 (157)[ab]	>241	134
60-12	.87	8.0	RW	RT	K_c K_{Ic}	>267 (154)[abc]	>267	109
60-15,16	.38	8.0	RW	RT	K_c K_{Ic}	470, 477 (182)[ab],(163)[ab]	478	72
60-13,14	.87	8.0	RW	-65F	K_c K_{Ic}	136, 153 (79)[bc],(82)[bc]	145	114
60-63,82	.375	6.0	RW	-65F	K_c K_{Ic}	238,243 (93)[ab],(92)[ab]	241	76

Table 6-9 (Page 7 of 10)

9-4-20 Steel - K_{Ic}/K_c TEST RESULTS

Specimen No.	Nominal Dimensions, In B	Nominal Dimensions, In W	Orientation	Test Temp. F	Test Type	K_{Ic}, (K_Q) or K_c in KSI $\sqrt{In}$ Individual Specimens	K_{Ic}, (K_Q) or K_c in KSI $\sqrt{In}$ Average or Estimated Value	Specimen Plane Strain Capability K_I, KSI $\sqrt{In}$
Material 46, 3.7 x 7.7 x 96" Forged Billet (1650F, 2 Hrs, ac) + (1525F, 2 Hrs, oq or ac)* + (-100, 2 Hrs) + (1025F, 4 Hrs)								
				oq*, 207 TU, 179 TY				
73-4	2.0	6.0	RW	RT	K_{Ic}	$(135)^e$	135	160
73-1,2,3	2.0	6.0	WR	RT	K_{Ic}	$(120)^e, (133)^e, (121)^e$	125	160
73-14	1.5	6.0	RW	-65F	K_{Ic}	127	127	145
				ac*, 201 TU, 176 TY				
73-6	2.0	6.0	RW	RT	K_{Ic}	$(177)^{ea}$	177	157
73-5	2.0	6.0	WR	RT	K_{Ic}	$(152)^e$	152	158
73-12	2.0	6.0	RW	-65F	K_{Ic}	163	163	165
73-13	2.0	6.0	WR	-65F	K_{Ic}	132	132	166

Table 6-9 (Page 3 of 10)

9-4-20 Steel - K_{Ic}/K_c TEST RESULTS

Specimen No.	Nominal Dimensions, In B	Nominal Dimensions, In W	Orien-tation	Test Temp. F	Test Type	K_{Ic}, (K_Q) or K_c in KSI $\sqrt{in}$ Individual Specimens	K_{Ic}, (K_Q) or K_c in KSI $\sqrt{in}$ Average or Estimated Value	Specimen Plane Strain Capability K_I, KSI$\sqrt{in}$
Material 48, 4 x 18 x 36 Forged Billet								
				Heat Treatment A, 205 TU, 180 TY				
78-5, 7	1.75	6.0	RW	RT	K_{Ic}	122, 121	122	151
78-6, 8	1.75	6.0	WR	RT	K_{Ic}	107, 108	108	151
				Heat Treatment B, 206 TU 187 TY				
78-1, 3	1.75	6.0	RW	RT	K_{Ic}	121, 131	126	157
78-2, 4	1.75	6.0	WR	RT	K_{Ic}	114, (114)[c]	114	155
				Heat Treatment C, 198 TU, 185 TY				
78-9, 10	1.6	6.0	RW	RT	K_{Ic}	128, 123	126	148
				Heat Treatment D, 204 TU, 186 TY				
78-13, 14	1.6	6.0	RW	RT	K_{Ic}	141, 140	141	149
				Heat Treatment E, 209 TU, 185 TY				
78-11, 12	1.6	6.0	RW	RT	K_{Ic}	129, 128	129	148

A - (1650F, 1.5 Hr, ac) + (1525F, 1.5 Hr, ac) + (-100F, 1.5 Hr) + (1025F, 4 Hrs)
B - (" " ") + (" " oq) + (" ") + (" ")
C - (" " ") + (" " ") + (" ") + (" 12 Hrs)
D - (1700F, 4.5 Hr, ") + (1700F " ac) + (" ") + (" 4 Hrs)
E - (1650F, 4.5 Hr, ac to 900F & hold for 1/2 hr, ac) + (" ") + (" 8 Hrs), ausbay quench

Table 6-9 (Page 9 of 10)

9-4-20 Steel - K_{Ic}/K_c TEST RESULTS

Specimen No.	Nominal Dimensions, In B	Nominal Dimensions, In W	Orien-tation	Test Temp. F	Test Type	K_{Ic}, (K_Q) or K_c in KSI $\sqrt{In}$ Individual Specimens	K_{Ic}, (K_Q) or K_c in KSI $\sqrt{In}$ Average or Estimated Value	Specimen Plane Strain Capability K_I, KSI$\sqrt{In}$
Material 49, Spindle Forging, B-1 P/N L2300380, (1650F, 2 Hrs, ac) + (1525F, 2 Hrs, ac) + (-100F, 2 Hrs, ac) + (1025F, 4 Hrs), 208 TU, 182 TY								
79-1,2,3	2.0	6.0	RW	RT	K_{Ic}	141, 143, 147	144	163
79-4	2.0	6.0	WR	RT	K_{Ic}	116	116	164

Table 6-9 (Page 10 of 10)

9-4-20 Steel - K_{Ic}/K_c TEST RESULTS

Specimen No.	Nominal Dimensions, In B	Nominal Dimensions, In W	Orientation	Test Temp. F	Test Type	K_{Ic}, (K_c) or K_c in KSI $\sqrt{In}$ Individual Specimens	K_{Ic}, (K_c) or K_c in KSI $\sqrt{In}$ Average or Estimated Value	Specimen Plane Strain Capability K_I, KSI$\sqrt{In}$
Material 52, 5 x 8 x 8" Hand Forging, (1650F, 2 Hrs, ac) + (1525F, 2 Hrs, oq) + (-100F, 2 Hrs) + (1025F, 4 Hrs); 209 TU, 198 TY								
				1700F Final Forging Temperature				
1A, B	2.0	5.0	RW	RT	K_{Ic}	130, 121	125	177
				1800F Final Forging Temperature				
2A, B	2.0	5.0	RW	RT	K_{Ic}	115, $(120)^c$	117	177
				1900F Final Forging Temperature				
3A, B	2.0	5.0	RW	RT	K_{Ic}	125, 126	125	177
Material, 57, 1-1/2" Rolled Plate (1650F, 2 Hrs, ac) + 1525F, 2 Hrs, *) + (-100F, 2 Hrs.) + 1025F, 4 Hrs)								
				* Air Quench After Austenitizing				
A403	.500	3.987	RT	RT	K_{Ic}(PTC)	103	103	-
A454	1.497	5.998	RW	RT	K_{Ic}(CT)	132	132	143
				* OIL QUENCH AFTER AUSTENITIZING				
A404	.495	3.972	RT	RT	K_{Ic}(PTC)	108	108	-
A453	1.426	6.001	RW	RT	K_{Ic}(CT)	99	99	143

Table 6-10 (Page 1 of 2)

9-4-30 Steel - K_{Ic}/K_c TEST RESULTS

Specimen No.	Nominal Dimensions, In B	W	Orientation	Test Temp. F	Test Type	K_{Ic} (K_Q) or K_c in KSI $\sqrt{In}$ Individual Specimens	Average or Estimated Value	Specimen Plane Strain Capability K_I, KSI$\sqrt{In}$
Material 32, 3 x 18 x 36 Forged Block (1650-1700F, 1 to 2 Hrs, ac) + (1525F, 1 to 2 Hrs, oq) + (-100F, 2 Hrs) + (Temper)								
						1000F, 4 to 5 Hrs; 245 TU, 215 TY		
1-7, 8, 9	1.0	3.0	RW	RT	K_{Ic}	$(83)^e$, $(81)^e$ $(81)^e$	81	131
1-10, 11, 12	1.0	3.0	WR	RT	K_{Ic}	85 , 89, 92	89	120
4,5	1.0	3.0	RW	-65	K_{Ic}	66, 67	67	127
						1025F, 6 Hrs		
1-1, 2, 3	1.0	3.0	RW	RT	K_{Ic}	$(92)^e$, $(91)^e$, $(92)^e$	92	131
1-40, 41, 43	1.0	3.0	WR	RT	K_{Ic}	$(84)^e$, $(83)^e$, $(86)^e$	84	131
						1050F, 4 Hrs		
1-4, 5, 6	1.0	3.0	RW	RT	K_{Ic}	$(96)^e$, $(87)^e$, $(94)^e$	92	120
1-44,45,46	1.0	3.0	WR	RT	K_{Ic}	$(81)^e$, 88, 87	85	131

Table 6-10 (Page 2 of 2)

9-4-30 Steel - K_{Ic}/K_c TEST RESULTS

Specimen No.	Nominal Dimensions, In B	W	Orientation	Test Temp. F	Test Type	K_{Ic}, (K_Q) or K_c in KSI $\sqrt{In}$ Individual Specimens	Average or Estimated Value	Specimen Plane Strain Capability K_I, KSI$\sqrt{In}$
Material 35, 3 x 18 x 36" Forged Block (1650F, 1 to 2 Hrs, ac)+(1525 to 1550F, 1 to 2 Hrs, ac or oq)*+(-100F, 1 to 3 Hrs)+ +(Temper)								
				1000F, 4 Hrs (ac)*, 238 TU, 206 TY				
20-35, 37	1.0	3.0	RW	RT	K_{Ic}	107, 105	106	120
20-26	1.0	3.0	WR	RT	K_{Ic}	86	86	120
				1025F, 2+2 Hrs. (oq)*, 220 TU, 205 TY				
20-38,42,44,45	1.0	3.0	RW	RT	K_{Ic}	(121)[a],(121)[a],116,(127)[a]	121	120
20-32,34	1.0	3.0	WR	RT	K_{Ic}	93, 94	94	120
				1050F, 4 Hrs (ac)*, 216 TU, 197 TY				
20-40, 47	1.0	3.0	RW	RT	K_{Ic}	124, 123	124	120
20-28	1.0	3.0	WR	RT	K_{Ic}	102	102	120

Table 6-11 (Page 1 of 4)

PH 13-8 MO

K_{Ic}/K_c TEST RESULTS

Specimen No.	Nominal Dimensions, In B	W	Orien-tation	Test Temp. F	Test Type	K_{Ic}, (K_Q) or K_c in KSI $\sqrt{In}$ Individual Specimens	Average or Estimated Value	Specimen Plane Strain Capability K_I, KSI$\sqrt{In}$
Mat'l 36, 4"x5" Forged Bar, Cond H950								
24-52,-53,-54	1.0	3.5	RW	R.T.	K_{Ic}	(59)[c] (60)[c] (61)[c]	60	129
24-19,-20,-21	1.0	3.5	WR	R.T.	K_{Ic}	(60)[c] (53)[c] (58)[c]	57	131
		Cond H-1000						
24-49,-50,-51	1.0	3.5	RW	R.T.	K_{Ic}	95, 98, 91	95	127
24-16,-17,-18	1.0	3.5	WR	R.T.	K_{Ic}	(84)[c] 93 (9[illegible])[c]	90	125
Mat'l 40, 1½"x12" Rolled Bar, Cond. H-1000								
56-19,-22,-23	1.0	3.0	RW	R.T.	K_{Ic}	85, (83)[b], 95		132
56-36,-38	.75	3.5	RW	R.T.	K_{Ic}	(79)[b] 76	87	114
56-30,-32	.63	3.5	RW	R.T.	K_{Ic}	100 (93)[b]		105
56-26,-27	1.0	3.0	WR	R.T.	K_{Ic}	78, 72	75	136
56-20,-21	1.0	3.0	RW	-65	K_{Ic}	(44)[c] (42)[c]		136
56-75,-76	.77	4.0	RW	-65	K_{Ic}	44, 49	47	120
56-77,-78	.26	4.0	RW	-65	K_{Ic}	51, 54		69
56-24,-25	1.0	3.0	WR	-65	K_{Ic}	(44)[c] (43)[c]	44	141
56-36,-38	.75	3.5	RW	R.T.	K_c K_{Ic}	.105, 108 (79)[b] 76	107	114
56-30,-32	.63	3.5	RW	R.T.	K_c K_{Ic}	149, 139 100 (93)[b]	144	105

Table 6-11 (Page 2 of 4)

PH 13-8 MO

K_{Ic}/K_c TEST RESULTS

Specimen No.	Nominal Dimensions, In B	Nominal Dimensions, In W	Orientation	Test Temp. F	Test Type	K_{Ic}, (K_c) or K_c in KSI $\sqrt{In}$ Individual Specimens	K_{Ic}, (K_c) or K_c in KSI $\sqrt{In}$ Average or Estimated Value	Specimen Plane Strain Capability K_I, KSI$\sqrt{In}$
Mat'l 40, 1½"x12" Rolled Bar, Cond H-1000								
56-29,-31,-33,-34	.38	3.5	RW	R.T.	K_c K_{Ic}	262, 264, 280, >215 (103)ba (109)cba (107)ba (107)ba	269	81
56-35,-37	.25	3.5	RW	R.T.	K_c K_{Ic}	359, 307 (113)ab (115)ab	333	67
56-75,-76	.77	3.5	RW	-65	K_c K_{Ic}	44, 49 44, 49	47	120
56-77,-78	.26	4.0	RW	-65	K_c K_{Ic}	51, 54 51, 54	53	69
Mat'l 41, 1½"x8" Extruded Bar, Cond H-1000								
57-27,-29,-31,-33 -35,-37	1.0	3.0	RW	R.T.	K_{Ic}	70,71,70,61,61,66	67	135
57-24,-26,-28,-30 -32,-36	1.0	3.0	WR	R.T.	K_{Ic}	68,67,67,66,62,67	66	135
57-23,-25,-39,-41	1.0	3.0	RW	-65	K_{Ic}	48,52,(44)c,50	49	140
57-22,-34,-38,-40	1.0	3.0	WR	-65	K_{Ic}	50,(43)c,48,48	47	139

Table 6-11 (Page 3 of 4)

PH 13-8 MO

K_{Ic}/K_c TEST RESULTS

Specimen No	Nominal Dimensions, In B	Nominal Dimensions, In W	Orientation	Test Temp. F	Test Type	K_{Ic}, (K_Q) or K_c in KSI $\sqrt{In}$: Individual Specimens	K_{Ic}, (K_Q) or K_c in KSI $\sqrt{In}$: Average or Estimated Value	Specimen Plane Strain Capability K_I, KSI$\sqrt{In}$
Mat'l 41, 1 1/8"x8" Extruded Bar, Re-solutioned + H-1000								
57-71,-73,-80,-81	1.4 1.3	4.0	RW	R.T.	K_{Ic}	77, 72, 74, (73)[ca]	74	160-154
57-72,-78,-79	1.4 1.3	4.0	WR	R.T.	K_{Ic}	(70)[c], (63)[c], (72)[c]	70	159-154
Mat'l 44, 22" Diax6" Upset Forging, Cond H-1000								
62-1,-2,-3	1.38	4.0	RW	R.T.	K_{Ic}	(81)[eb] (79)[e] (78)[eb]	79	142
62-4,-5	1.38	4.0	WR	R.T.	K_{Ic}	82, (80)[b]	81	141
62-6,-7	1.36	3.0	TW	R.T.	K_{Ic}	(88)[b] 86	87	140
62-11,-12	1.38	4.0	RW	-65	K_{Ic}	54, 52	53	148
Mat'l 50, 2¼"x4" Forged Bar, Cond A								
81-6	1.63	3.0	RW	R.T.	K_{Ic}	(122)[ab]	122	118
81-5	1.63	3.0	WR	R.T.	K_{Ic}	(121)[ab]	121	118
Cond H-1000								
81-2,-4	1.63	3.0	RW	R.T.	K_{Ic}	117, 89	103	171
81-1,-3	1.63	3.0	WR	R.T.	K_{Ic}	88, 91	90	171
81-8,-9	1.63	3.0	WR	-65	K_{Ic}	53, 56	55	179

Table 6-11 (Page 4 of 4)

PH 13-8 MO K_{Ic}/K_c TEST RESULTS

Specimen No.	Nominal Dimensions, In B	Nominal Dimensions, In W	Orientation	Test Temp, F	Test Type	K_{Ic} (K_Q) or K_c In KSI $\sqrt{In}$ Individual Specimens	K_{Ic} (K_Q) or K_c In KSI $\sqrt{In}$ Average or Estimated V.	Specimen Plane Strain Capability K_I, KSI $\sqrt{In}$
Mat'l 54, $1\frac{1}{2}$" Dia Rolled Bar, Cond RH 950								
105-1,-2	0.5	1.0	RT	R.T.	K_{Ic}	61, 62	62	97
			Cond RH 975					
105-3,-4	0.5	1.0	RT	R.T.	K_{Ic}	76, 68	72	97
			Cond RH 1000					
105-5,-6	0.5	1.0	RT	R.T.	K_{Ic}	(114)[a] (108)[a]	111	96
Mat'l 56, $1\frac{1}{2}$" Dia Rolled Bar, RH 950								
108-1,-2	0.5	1.0	RT	R.T.	K_{Ic}	59, 57	58	98
			RH 975					
108-3	0.5	1.0	RT	R.T.	K_{Ic}	66	66	98
			RH 1000					
108-4	0.5	1.0	RT	R.T.	K_{Ic}	95	95	97

Table 6-12

300M STEEL K_{Ic}/K_c TEST RESULTS

Specimen No.	Nominal Dimensions, In B	Nominal Dimensions, In W	Orientation	Test Temp, F	Test Type	K_{Ic} (K_Q) or K_c In KSI $\sqrt{In}$ Individual Specs.	K_{Ic} (K_Q) or K_c In KSI $\sqrt{In}$ Average or Estimated V.	Specimen Plane Strain Capability K_I, KSI $\sqrt{In}$
Mat'l 39, Forging, 280-300 Ksi								
55-41, -42 -43, -44 -45	0.25	1.0	RW	RT	K_{Ic}	$(57)^c$, 56, 57, 54, 52	55	75
55-46, -47	0.25	1.0	WR	RT	K_{Ic}	49, 52	51	75
55-51, -52, -53, -54	0.25	1.0	TR	RT	K_{Ic}	54, 53, 55, 55	54	75

Table 6-13

INCONEL 718

K_{Ic}/K_c TEST RESULTS

Specimen No.	Nominal Dimensions, In B	W	Orientation	Test Temp. F	Test Type	K_{Ic}, (K_Q) or K_c in KSI $\sqrt{In}$ Individual Specimens	Average or Estimated Value	Specimen Plane Strain Capability K_I, KSI$\sqrt{In}$
Mat'l 51, 4x8 Forged Bar, HT 192 KSI								
82-3,-4	1.9	5.0	RW	R.T.	K_{Ic}	(215)[bac] (212)[ba]	(213)	140
82-1,-2	1.9	5.0	WR	R.T.	K_{Ic}	(131)[c] (137)[b]	134	140
82-7,-8	1.9	5.0	RW	-65	K_{Ic}	(213)[abc] (223)[ab]	(218)	148
82-5,-6	1.9	5.0	WR	-65	K_{Ic}	(146)[c] 142	144	148
82-11-,-12	1.9	5.0	RW	400°F	K_{Ic}	(190)[ba] (189)[cba]	(190)	134
82-9,-10	1.9	5.0	WR	400°F	K_{Ic}	(122)[c] 129	125	134
82-13,-14,-17	1.75	3.5	TR	R.T.	K_{Ic}	(129)[c] (100)[c] (95)[c]	108	134
82-16	1.75	3.5	TR	-65	K_{Ic}	(119)[c]	119	142
82-18,-15	1.75	3.5	TR	400°F	K_{Ic}	(94)[c] (93)[c]	94	129
Mat'l 53 Die Forging (B-1 P/N L4100006), HT 199 KSI								
98-5	2.10	5.0	RW	R.T.	K_{Ic}	(156)[ac]	156	154
98-4	2.10	5.0	WR	R.T.	K_{Ic}	(114)[c]	103	152
4,75	.75	2.0	WR	R.T.	K_{Ic}	(95)[a], (99)[a]		91

Table 6-14

MP35N ALLOY

K_{Ic}/K_c TEST RESULTS

Specimen No.	Nominal Dimensions, In		Orientation	Test Temp. F	Test Type	K_{Ic}, (K_Q) or K_c in KSI $\sqrt{In}$		Specimen Plane Strain Capability K_I, KSI$\sqrt{In}$
	B	W				Individual Specimens	Average or Estimated Value	
Mat'l 55, 1½" Dia. Bar, HT 236 KSI								
106-2	0.5	1.0	RT	R.T.	K_{Ic}	(129)[ba]	129	104

Table 6-15

Ti-6Al-4V WELD SPECIMENS - K_{Ic} TEST RESULTS

Spec. Thickness (in)	Weld Process	Postweld Stress Relief	Specimen Type	Notch Location	Test Temp (°F)	K_{Ic} or (K_Q), ksi $\sqrt{in}$ Individual Specs.	Avg.	Specimen Nos.
Plate, Mat'l 62, Mill Annealed (MA)								
						Butt Weld Joint		
.50	GTA, Mach	1100F,2 hrs	CT	Weld	RT	(68)ab, (70)ab, (75)ab, (76)ab	(72)	121-21-1,-2
Plate, Mat'l 70, RA Cond								
						Butt Weld Joint		
.50	GTA, Man'l	1100F,2 hrs	PTC	HAZ	RT	75	75	B408
Plate, Mat'l 76, RA Cond								
						Butt Weld Joint		
.75	GTA, Man'l	1200F,1 hr	PTC	HAZ	RT	64, 69	67	B428, 429
Plate, Mat'l 87, RA Cond								
						Butt Weld Joint		
.50	GTA, Man'l	1100F,2 hrs	PTC	HAZ	RT	74, 82, 71, 87, 79	79	B400, 401, 402, 403, 404
	GTA, Mach	1100F,2 hrs	CT	Weld	RT	(74)abc, (84)ab	(79)	B450, 451

Table 6-15 (Cont'd)

Spec. Thick-ness (in)	Weld Process	Postweld Stress Relief	Speci-men Type	Notch Loca-tion	Test Temp (°F)	K_{Ic} or (K_Q), ksi $\sqrt{in}$ Individual Specs.	Avg.	Specimen Nos.
Plate, Mat'l 88, RA Cond								
					Butt Weld Joint			
.50	GTA, Man'l	1200F, 1 hr	PTC	HAZ	RT	70	70	B313 (single U-joint)
		1400F, 1 hr	PTC	HAZ	RT	69	69	B311
		1100F, 2 hr	PTC	HAZ	RT	69,68,76,82,69,78,75,67	73	B410 thru B417
		1100F, 2 hr	PTC	HAZ	-65	80, 74	77	B437, 438
		1200F, 1 hr	PTC	Weld	RT	77	77	B316,(90° to weld ℄)
	GTA, Mach	1100F, 2 hr	CT	Weld	RT	(101)[ab], (98)[ab]	(100)	B452, 453
					-65	(80)	(80)	B457
	PAW, Mach	1100F, 2 hrs	PTC	HAZ	RT	80, 81, 67, 70	75	B418, 419, 420, 436
			CT	Weld	RT	(109)[ab], (110)[ab], (104)[ab]	(108)	B454, 455, 456
.25	GTA, Man'l	1100F, 2 hrs	PTC	HAZ	RT	62, 65	64	B430, 431
				Butt Weld Joint Containing a Grindout Reweld Repair				
.50	GTA, Man'l	None	PTC	Weld	RT	47	*	B306
		1200, 1 hr	PTC	Weld	RT	72	72	B307
						*Discarded, porosity in weld		
					Weld Overlay Specimen			
.50	GTA, Man'l	None	PTC	Weld	RT	67	67	B317
		1200F, 1 hr	PTC	Weld	RT	83	83	B302

Table 6-15 (Concluded)

Spec. Thickness (in)	Weld Process	Postweld Stress Relief	Specimen Type	Notch Location	Test Temp (°F)	K_{Ic} or (K_Q), ksi$\sqrt{in}$ Individual Specs.	Avg.	Specimen Nos.
Plate, Mat'l 89, RA Cond						Butt Weld Joint		
.50	GTA, Man'l	1100F, 2 hr	PTC	HAZ	RT	63, 87	75	B405, 407
				Weld	RT	78	78	B406
Sheet, Mat'l 80, Mill Annealed						Butt Weld Joint		
.10	GTA, Mach	1100, 2 hrs	CCT	HAZ	RT	K_c = 264*, >134	264	B432, 433
Extruded Bar, Mat'l 75, Mill Annealed (MA)						Butt Weld Joint		
.50	GTA, Mach	1100F, 2 hrs	PTC	HAZ	RT	70	70	B423
	GTA, Man'l	1100F, 2 hrs	PTC	HAZ	RT	82	82	B422
		1200F, 1 hr	PTC	HAZ	-65	81, 90	86	B434, 435

*Crack had traveled 1 inch away from the weld at onset of instability.

Table 6-16

HP 9Ni-4Co-.20C WELD SPECIMENS - K_{Ic} TEST RESULTS
NOTE: Specimens were Manually GTA Welded

Spec. Thickness (in)	Postweld Stress Relief	Specimen Type	Notch Location	Test Temp (°F)	K_{Ic} or (K_Q), ksi $\sqrt{in}$ Individual Specs.	Avg.	Specimen Nos.
4" Forged Block, Mat'l 33, HT 190-210 ksi							
					Butt Weld Joint		
1.50	950F, 2 hrs	CT	Weld	RT	(138)[bc]	(138)	A465
	None	CT	Weld	RT	(179)[ac]	(179)	A466
.50	950F, 2 hrs	PTC	HAZ	RT	93,101,101,104,92,98	95	A413,414,416,427,431,432
				-65	82	82	A417
1-1/2" Plate, Mat'l 57, HT 190-210 ksi							
					Butt Weld Joint		
.75	950F, 2 hrs	PTC	HAZ	RT	98, 90	94	A418, 419
.50	950F, 2 hrs	PTC	HAZ	RT	112,114,103,93,100,118	107	A400,401,402,407,408,412
				RT	97	97	A312 (Single U-Joint)
	None	PTC	HAZ	RT	84	84	A310
	950F, 2 hrs	PTC	HAZ	-65	98, 85	92	A422, 423
		PTC	Weld	RT	101	101	A411
		PTC	Weld	RT	92	92	A316 (90° to weld ℄)
		CT	Weld	RT	(187)[ab],(188)[ab],(183)[ab]	(186)	A450,451,452
.25	950F, 2 hrs	PTC	HAZ	RT	92, 91	92	A420, 421

Table 6-16 (Concluded)

HP 9Ni-4Co-.20C WELD SPECIMENS - K_{Ic} TEST RESULTS
NOTE: Specimens were Manually GTA Welded

Spec. Thickness (in)	Postweld Stress Relief	Specimen Type	Notch Location	Test Temp (°F)	K_{Ic} or (K_Q), ksi $\sqrt{in}$ Individual Specs.	Avg.	Specimen Nos.
2-1/2" Plate, Mat'l 37, HT 190-210 ksi							
				Butt Weld Joint Containing Grindout Reweld Repair			
.50	950F, 2 hrs	PTC	Weld	RT	92	92	A306
	None	PTC	Weld	RT	91	91	A307
				Weld Overlay Specimen			
.50	950F, 2 hrs	PTC	Weld	RT	97	97	A302
	None	PTC	Weld	RT	92	92	A303

Table 6-17

PH 13-8Mo WELD SPECIMENS - K_{Ic} TEST RESULTS

NOTE: Specimens were .25" in Thickness and were Manually GTA Welded

Postweld Stress Relief	Specimen Type	Notch Location	Test Temp (°F)	K_{Ic} or (K_Q), ksi $\sqrt{in}$ Individual Specs.	Avg.	Specimen Nos.
Rolled Bar, Mat'l 40, H-1000 Cond						
				Butt Weld Joint		
950F, 2 hrs	PTC	HAZ	RT	81, 84, 86, 100	88	C403, 404, 405, 406
			-65	88, 102	95	C409, 410
		Weld	RT	83	83	C407
			-65	98	98	C408
				Butt Weld Joint Containing a Grindout Reweld Repair		
None	PTC	Weld	RT	38 *	*	C300
				Weld Overlay Specimens		
None	PTC	Weld	RT	83	83	C304
950F, 2 hrs	PTC	Weld	RT	79	79	C306
Extruded Bar, Mat'l 41, Cond A						
				Butt Weld Joint		
1000F, 4 hrs	PTC	HAZ	RT	90, 95	93	C401, 402
	CT	Weld	RT	$(111)^{ab}, (139)^{ab}, (159)^{ab}, (150)^{ab}$	(140)	C452, 453, 454, 460
			-65	$(80)^{ab}, (103)^{ab}$	(91)	C450, 451

* Discarded - Lack of fusion in reweld

NOTE:
A preweld of H1000 and a postweld of 950F, 2 hrs. are being used for the welds in the B-1.

Table 6-18

Ti-6Al-4V - SUMMARY OF K_{Ic} VALUES

Product Form	Mat'l No.	Condition	Product Size or Weld Jt. Thickness (In)	O_2 Content	TU, KSI (L)	TY, KSI (L)	Estimated K_{Ic}, KSI $\sqrt{IN}$ RW or RT	WR	TW/TR
Beta Processed (Widmanstatten Transformed Beta Microstructure)									
Plate	61-62	BA	.625	.20	145	136	82	83	-
	63	DBTC	1.25	.14	-	-	105	105	-
		MA	1.25	.14	137	125	100	-	-
	66	MA	1.50	.06-.13	134	119	105	96	-
Extrusion	75	MA	T-Shape	.16	139	123	92	94	-
		Weld Joint	t = .5	-	-	-	76(HAZ)	-	-
	64	MA	L-Shape	.15	139	127	90	97	-
	Specification Requirement								
	Parent Metal (.20 O_2 max)						70	70	70
	Welds						60	60	60
Alpha-Beta Processed (Microstructure Consisting Mostly of Primary Alpha)									
Plate	61-62	MA	.625	.20	148	138	39	32	-
		STOA	.625	.20	161	151	43	42	-
		DBTC	.625	.20	-	-	54	51	-
		DB *	.625	.20	145	135	49	64	-
		RA	.625	.20	145	134	51	-	-
		Weld Joint	t = .5	-	-	-	72(Weld)	-	-
	65	MA	1.312	.16	147	138	41	42	-
		RA	1.312	.16	141	129	60	62	-
	77	RA	2.500	.15	136	122	78	77	-
		DBTC	2.500	.15	-	-	69	-	-
		DB Joint	2.500	.15	132	120	81(RW/RW)	-	90(TR/TR)

* The bend plane was perpendicular to the crack plane.

Table 6-18 (Cont'd)

Ti-6Al-4V - SUMMARY OF K_{Ic} VALUES

Product Form	Mat'l No.	Condition	Product Size or Weld Jt. Thickness (In)	O_2 Content	TU, KSI (L)	TY, KSI (L)	Estimated K_{Ic}, KSI $\sqrt{IN}$ RW or RT	WR	TW/TR
Alpha-Beta Processed (Microstructure Consisting Mostly of Primary Alpha)									
Plate (Cont'd)	92	RA	2.500	.15	136	122	72	-	-
		DBTC	2.500	.15	-	-	-	70	-
	78	RA	.75	.14	136	125	55	58	--
	7406	RA	2.000	.13	141	126	70	69	-
	7768	RA	2.00	.13	144	126	71	75	-
	72	RA	1.500	.13	133	117	78	95	-
		DBTC	1.500	.13	-	-	72	92	-
		DBTC (except ac to 1100°F)	1.500	.13	-	-	93	92	-
	68	RA	2.00	.12	133	122	92	100	-
	69	RA	3.500	.12	129	118	123	114	-
	253	RA	2.500	.12	131	120	88	88	-
	294	RA	1.250	.12	136	124	78	75	-
	90	RA	2.250	.12	130	122	86	88	-
		DB Joint	2.250	.12	128	117	96 (RW/RW)	-	107 (TR/TR)
	70-74	RA	1.500	.11	135	122	68	85	-
		DB Joint	1.500	.11	131	120	-	-	88 (TW/TW)
		Weld Joint	t = .5	-	-	-	75 (HAZ)	-	-
	87	RA	1.500	.11	130	121	82	82	-
		Weld Joint	t = .5	-	126	117	79 (Weld)	-	-
		Weld Joint	t = .5	-	126	117	79 (HAZ)	-	-
	88	RA	1.250	.11	139	127	78	81	-
		Weld Joint	t = .5	-	137	129	77 (Weld)	-	-
		Weld Joint	t = .5	-	137	129	72 (HAZ)	-	-
		Weld Joint	t = .25	-	-	-	64 (HAZ)	-	-

Table 6-18 (Conc'd)

Ti-6Al-4V - SUMMARY OF K_{Ic} VALUES

Product Form	Mat'l No.	Condition	Product Size or Weld Jt. Thickness (In)	O_2 Content	TU, KSI (L)	TY, KSI (L)	Estimated K_{Ic}, KSI $\sqrt{IN}$ RW or RT	WR	TW/TR
Alpha-Beta Processed (Microstructure Consisting Mostly of Primary Alpha)									
Plate (Cont'd)	89	RA	1.250	.11	135	124	-	-	-
		Weld Joint	t = .5	-	132	122	78 (Weld)	-	-
		Weld Joint	t = .5	-	132	122	75 (HAZ)	-	-
	76	RA	1.500	.09	127	113	80	82	-
		Weld Joint	t = .75	-	-	-	67 (HAZ)	-	-
	67	RA	1.500	.08	134	121	90	85	-
Specification Requirement Parent Metal & DB Joints (.09-.13 O_2; RA, DB, DBTC)							70	70	70
Welds							60	60	60
Forgings	82	RA	4 x 10 x 34	.12	130	124	106	102	-
	79	RA	4 x 10 x 34	.10	132	121	107	114	-
	85	RA	Die, 300 lbs	.15	136	123	76	74	105
	84	RA	Die, 600 lbs	.13	134	121	81	89	83
Specification Requirement (.09 -.13 O_2)							70	70	70

NOTES: Heat treat condition of weld joint specimens: Preweld: RA (except for material 75, which was MA). Postweld: Stress relieved at 1100 to 1400°F for 1 to 2 hours.

Weld filler wire was .12% O_2 maximum.

Table 6-19

ALUMINUM ALLOYS - SUMMARY OF K_{IC} VALUES

Alloy	Product Form	Condition	Product Size (In)	Material No.	TU, KSI (L)	TY, KSI (L)	Estimated K_{IC}, KSI $\sqrt{IN.}$		
							RW	WR	TW/TR
2024	Plate	T851	1.75	6	72	65	26	-	-
			3.00	1	71	66	21	18	19
			3.00	3	73	66	26	-	24
			3.00	9	70	65	23	19	-
		Specification Requirement					20	18	-
		T62	3.00	1	68	58	>32	25	22
			3.50	8	-	-	41	-	-
		Specification Requirement					25	19	-
		T351	3.00	2	69	54	31	29	21
	Forged Block	T852	3 x 18 x 23	19	69	58	28	21	18
			3 x 18 x 35	27	70	53	37	27	-
		Specification Requirement					23	19	17
2124	Plate	T851	3.00	12	72	65	32	24	24
			3.00	14	71	65	25	23	-
		Specification Requirement					25	20	20
2219	Plate	T851	1.75	7	66	50	43	36	-
			2.00	4	68	50	39	35	23
			3.00	13	69	54	35	29	25
			3.00	304	67	53	41	34	-
		Specification Requirement					33	30	20
	Plate	T62	2.00	4	64	44	45	42	-
	Forging	T852	6 x 12 x 48	20	65	51	36	31	32
		Specification Requirement					33	30	20
	Extrusion	T8511	1.7 x 7.5	16	66	51	<42	<40	-
		Specification Requirement					33	30	-

Table 6-19 (Cont'd)

ALUMINUM ALLOYS - SUMMARY OF K_{Ic} VALUES

Alloy	Product Form	Condition	Product Size (In)	Material No.	TU, KSI (L)	TY, KSI (L)	Estimated K_{Ic}, KSI $\sqrt{IN.}$ RW	WR	TW/TR
7049	Die Forging	T73	-	10	77	68	28	-	-
		T73	-	24	80	74	43	-	-
	Hand Forging	T7352	3 x 24 x 48	25	76	67	38	23	23
		Specification Requirement					30	25	25
7050	Plate	T73651	4.0	28	77	68	28	28	25
	Die Forging	T73	-	23	78	71	(45)	-	26
	NOTE: Specification K_{Ic} values have not been established. Current B-1 design does not use this alloy.								
7075	Plate	T7651	2.0	5	75	65	29	21	-
			2.0	18	74	63	28	24	16
			2.3	307	75	63	30	23	20
			2.5	306	70	61	31	24	20
			2.6	15	76	65	32	27	-
		Specification Requirement					27	23	18
	Plate	T7351	2.0	5	76	65	27	23	-
			2.0	18	70	58	31	25	18
		Specification Requirement					30	26	20
	Extrusion	T76511	3 x 8	309	77	68	33	21	-
		Specification Requirement					27	25	20
	Extrusion	T73511	3 x 17	29	77	66	39	28	22
		Specification Requirement					30	26	20
	Die Forging	T73		22	75	67	45	-	28
		Specification Requirement					30	26	20

Table 6-19 (Concluded)

ALUMINUM ALLOYS - SUMMARY OF K_{Ic} VALUES

Alloy	Product Form	Condition	Product Size (In)	Material No.	TU, KSI (L)	TY, KSI (L)	Estimated K_{Ic}, KSI $\sqrt{IN.}$ RW	WR	TW/TR
7175	Die Forging	T736		21	78	70	41	27	-
		Specification Requirement					33	28	25
		T73652		26	77	68	35	27	22
		Specification Requirement					33	28	25

Table 6-20

STEELS, INCONEL 718, MP 35N - SUMMARY OF K_{Ic} VALUES

Alloy	Product Form	Condition	Product Size or Weld Jt. Thickness (In)	Mat'l No.	TU, KSI(L)	TY, KSI(L)	Estimated K_{Ic}, KSI $\sqrt{IN}$ RW or RT	WR	TW/TR
9-4-20	Spindle Die Forgings	*	5000 lbs	42	207	194	139	126	-
		*	5000 lbs	49	208	182	144	116	-
	Specification Requirement						110	110	-
	Forgings	*	3 x 10 x 36	31	195	182	155	-	-
		*	4 x 18 x 36	33	204	188	158	145	128
		Weld Joint	t = 1.5	33	-	-	138(Weld)	-	-
		Weld Joint	t = .5	33	-	-	95(HAZ)	-	-
		*	4 x 18 x 36	43	211	186	141	126	115
		*	3.7 x 7.7 x 96	46	207	179	135	125	-
		*	4 x 18 x 36	48	206	187	126	114	-
		*	5 x 8 x 8	52	209	198	125	-	-
	Specification Requirement - Parent Metal Welds						120 90	120 90	120 90

*Heat Treatment (STO111LA0002): (1650F, 1 to 1.5 hrs, ac) + (1525F, 1 to 1.5 hrs, ac or oq) + (-100F, 1 to 1.5 hrs) + (1025 to 1075F, 4 to 6 hrs)

NOTE: HP9-4-.20 steel was welded in the 190 to 210 ksi heat treat condition. Postweld thermal treatment was 950F, 2 hrs.

Table 6-20 (Cont'd)

STEELS, INCONEL 718, MP 35N - SUMMARY OF K_{Ic} VALUES

Alloy	Product Form	Condition	Product Size or Weld Jt. Thickness (In)	Mat'l No.	TU, KSI(L)	TY, KSI(L)	Estimated K_{Ic}, KSI $\sqrt{IN}$		
							RW or RT	WR	TW/TR
9-4-20 (Cont'd)	Plate	*	2.5	37	208	189	124	128	-
		Weld Joint	t = .5	37	207	177	92(Weld)	-	-
		*	1.5	57	190-210	180-190	111	-	-
		Weld Joint	t = .75	57	-	-	94(HAZ)	-	
		Weld Joint	t = .5	57	-	-	97(Weld)	-	-
		Weld Joint	t = .5	57	-	-	105(HAZ)	-	-
		Weld Joint	t = .25	57	-	-	92(HAZ)	-	-
		Specification Requirement - Parent Metal Welds					120 90	120 90	120 90
9-4-30	Forging	**	3 x 18 x 36	32	220-240	190-210	92	85	-
		**	3 x 18 x 36	35	220	205	121	94	-
		Specification Requirement					90	90	90

*Heat Treatment (STO111LA0002): (1650F, 1 to 1.5 hrs, ac) + (1525F, 1 to 1.5 hrs, ac or oq) + (-100F, 1 to 1.5 hrs) + (1025 to 1075F, 4 to 6 hrs)

**Heat Treatment (STO111LA0002): (1650F, 1 to 1.5 hrs, ac) + (1550F, 1 to 1.5 hrs, ac or oq) + (-100F, 1 to 1.5 hrs) + (1000 to 1075F, 4 hrs)

NOTE: HP9-4-.20 steel was welded in the 190 to 210 ksi heat treat condition. Postweld thermal treatment was 950F, 2 hrs.

Table 6-20 (Cont'd)

STEELS, INCONEL 718, MP 35N - SUMMARY OF K_{Ic} VALUES

Alloy	Product Form	Condition	Product Size or Weld Jt. Thickness (In)	Mat'l No.	TU, KSI (L)	TY, KSI (L)	Estimated K_{Ic}, KSI $\sqrt{IN}$ RW or RT	WR	TW/TR
PH13-8Mo	Forged Bar	H950	4 x 5	36	216	204	60	57	-
	Rolled Bar	RH950	1.5 Dia	54	236	217	62	-	-
			1.5 Dia	56	237	219	58	-	-
	Specification Requirement						60	60	-
	Rolled Bar	RH975	1.5 Dia	54	233	216	72	-	-
				56	231	219	66	-	-
	Forged Bar	H1000	4 x 5	36	212	201	95	90	-
			22 Dia x 6	44	208	191	79	81	-
			2.25 x 4	50	219	212	103	90	-
	Rolled Bar	H1000	1.5 x 12	40	216	208	87	75	-
	Rolled Bar	Weld Joint	t = .25	40	-	-	83 (Weld)	-	-
	Rolled Bar	Weld Joint	t = .25	40	-	-	88 (HAZ)	-	-
	Rolled Bar	RH1000	1.5 Dia	54	222	215	111	-	-
	Rolled Bar	RH1000	1.5 Dia	56	226	218	95	-	-
	Extruded Bar	H1000	1.5 x 8	41	221	214	67	66	-
	Specification Requirement - Parent Metal*						75 or 90	75 or 90	75 or 90
	Welds						80	80	80

*Incoming PH13-8Mo is identified by either of two specification numbers, according to its toughness.

NOTE: PH13-8Mo was welded in the H1000 heat treat condition. The postweld thermal treatment was 950F, 2 hrs.

Table 6-20 (Conc'd)

STEELS, INCONEL 718, MP 35N - SUMMARY OF K_{Ic} VALUES

Alloy	Product Form	Condition	Product Size or Weld Jt. Thickness (In)	Mat'l No.	TU, KSI(L)	TY, KSI(L)	Estimated K_{Ic}, KSI $\sqrt{IN}$		
							RW or RT	WR	TW/TR
300M	Forged Block	HT 280-300 ksi	3 x 36 x 72	39	287	238	55	51	54
NOTE: Specification K_{Ic} values have not been established for 300M because this alloy is not being used for any B-1 fracture control parts.									
Inconel 718	Forged Bar	Age Hardened	4 x 8	51	192	160	(212)	134	108
	Die Forging	Age Hardened	80 lbs	53	199	168	156	114	97
	Specification Requirement						85	85	85
MP35N	Bar	Cold Worked and Aged	1.5 Dia	55	236	233	129	-	-
	Specification Requirement						90	-	-

TABLE 6-21

Ti-6Al-4V K_c TEST RESULTS (K_c VALUES, CRITICAL Δa's, COMPARATIVE R-CURVE POINTS)

SPECIMEN NO.	DIMENSIONS, INCHES B	W	ORIENTATION	TEST TEMP °F	K_c, KSI $\sqrt{in}$	CRITICAL Δa, INCHES	R-Curve K Value at Indicated Δa Δa= 0"	.1"	.2"	.3"	.4"	.6"	1.0"	2.0"	Figure No. of R-Curve
Mat'l 68 2" Plate, RA															
32-18A	0.26	6	RW	RT	184	.33	74	128	157	178	191				
-18B	0.26	6	RW	RT	189	.40	76	125	158	177	189				
Mat'l 71, 1/2" Plate, RA															
25-5	0.50	3.5	RW	RT	137	.31	58	87	113	136	147				6-1(a)
-6	0.50	3.5	RW	RT	132	.29	63	92	115	133	147				6-1(a)
25-10	0.50	5	RW	RT	148	.34	77	93	119	140					6-1(a)
25-14	0.48	8	RW	RT	176	.55	63	94	120	139	157	179			
25-9	0.50	5	RW	RT	141	.34	68	97	122	136	143				6-1(a)
25-13	0.33	8	RW	RT	190	.53	62	114	146	168	176	194			
25-3	0.25	5	RW	RT	174	.36	57	121	150	164	177				6-1(b)
-4	0.25	5	RW	RT	157	.30	56	121	143	157					6-1(b)
Mat'l 72, 1-1/2" Plate, RA															
46-14	1.25	4	RW	RT	142	.43	64	84	99	118	137				6-2(a)
-15	1.25	4	RW	RT	142	.46	67	91	103	118	133				6-2(a)
46-16	0.87	4	RW	RT	165	.44	68	94	115	139	158				6-2(a)
-17	0.87	4	RW	RT	166	.44	70	94	113	139	159				6-2(a)
46-18	0.62	5	RW	RT	194	.50	63	102	143	163	180				6-2(b)
-19	0.62	5	RW	RT	190	.43	63	107	142	170	184				6-2(b)

TABLE 6-21 (Cont'd)

Ti-6Al-4V K_c TEST RESULTS (K_c VALUES, CRITICAL Δa's, COMPARATIVE R-CURVE POINTS)

SPECIMEN NO.	DIMENSIONS, INCHES B	W	ORIEN-TATION	TEST TEMP ^oF	K_c, KSI $\sqrt{in}$	CRITICAL Δa, INCHES	R-Curve K Value at Indicated Δa: Δa= 0"	.1"	.2"	.3"	.4"	.6"	1.0"	2.0"	Figure No. of R-Curve
46-20	0.62	5	RW	-65	151	.44	68	89	105	129	146	164			6-2 (b)
-21	0.62	5	RW	-65	177	.48	69	96	127	151	167	187			6-2 (b)
46-22	0.25	8	RW	-65	267	1.09	58	109	144	167	181	199	248^f		6-2 (c)
-23	0.25	8	RW	-65	193	.44	73	134	160	175	189	205			6-2 (c)
Mat'l	76, 3/4" Plate, RA														
76-5	0.79	3	RW	RT	111	.25	39	75	100	115					6-3
-6	0.79	3	RW	RT	108	.32	38	68	88	103					6-3
76-7	0.75	8	RW	RT	211	.87	46	74	101	126	144	173			6-3
-8	0.75	8	RW	RT	221	.97	44	68	92	114	132	168	224		6-3
Mat'l	80, 0.1" Sheet, MA (CCT SPECIMENS)														
84-1	0.10	24	RW	RT	324	3.30	70^f	120^f	133^f	145^f	160^f	175^f	198^f	256^f	6-4 (a)
-2	0.10	24	RW	RT	267	2.11	90^f	120^f	130^f	153^f	160^f	180^f	212^f	260^f	6-4 (a)
84-15	0.10	24	WR	RT	207	1.18	75	130	142	154	163	178^f	188^f		6-4 (b)
-16	0.10	24	WR	RT	213	1.75	98	118	134	143	151	162	172	183	6-4 (b)
Mat'l	81, 0.1" Sheet, MA (CCT SPECIMENS)														
94-2	0.10	24	RW	RT	360	2.87	92^f	110^f	138^f	168^f	179^f	201^f	237^f	307^f	6-5 (a)
-3	0.10	24	RW	RT	400	3.10	73^f	106^f	139^f	165^f	190^f	205^f	245^f	325^{fg}	6-5 (a)
94-4	0.10	24	WR	RT	368	3.25	88	104	120	136	152	183	215	287	6-5 (b)
-5	0.10	24	WR	RT	367	3.05	68^f	96^f	125^f	157^f	157^f	178^f	212^f	292^f	6-5 (b)

NOTE: Specimen 84-2 was first used to develop a calibration curve of compliance versus crack length and had a crack length of 8.4" ($2a_o$) at the start of the K_c test.

^{f} Crack angle exceeds 10°

^{g} Ligament stress exceeds yield strength.

TABLE 6-22

2024 K_c TEST RESULTS (K_c VALUES, CRITICAL Δa's, COMPARATIVE R-CURVE POINTS)

SPECIMEN NO.	DIMENSIONS, INCHES B	W	ORIEN-TATION	TEST TEMP ^oF	K_c, KSI $\sqrt{in}$	CRITICAL Δa, INCHES	R-Curve K Value at Indicated Δa: Δa= 0"	.1"	.2"	.3"	.4"	.5"	.6"	.7"	Figure No. of R-Curve
Mat'l 6	1.75" Plate, -T851														
18-1	.11	6	RW	RT	57	.39	25	46	51	54	57				6-6 (a)
-2	.11	6	RW	RT	59	.36	19	45	52	57	60				6-6 (a)
18-3	0.26	6	RW	RT	54	.44	12	37	45	48	53	54			6-6 (b)
-4	0.26	6	RW	RT	49	.25	18	40	47	50	53	54			6-6 (b)
Mat'l 27	3 x 18 x 35" Forged Block - T852														
75-72	1.0	2.5	RW	RT	64	.25	31	47	58	67					6-7 (a)
-74	1.0	2.5	RW	RT	44	.09	20	44							6-7 (a)
75-65	0.75	2.5	RW	RT	64	.20	24	52	64						
-67	0.75	2.5	RW	RT	55	.16	22	47							
-97	0.75	2.5	RW	RT	50	.21	32	41	48						
75-69	0.5	2.5	RW	RT	60	.20	27	47	60						6-7 (a)
-71	0.5	2.5	RW	RT	69	.26	27	48	61	73					6-7 (a)
75-73	0.5	2.5	RW	265	66	.22	26	50	63	73					6-7 (b)
-75	0.5	2.5	RW	265	61	.24	26	43	56	67					6-7 (b)
75-76	0.25	2.5	RW	RT	77	.23	24	51	72	85					6-7 (a)
-77	0.25	2.5	RW	RT	71	.21	23	57	69	78					6-7 (a)
75-61	0.38	2.0	WR	RT	38	.15	23	34							
-63	0.38	2.0	WR	RT	38	.12	20	36							

TABLE 6-22 (cont'd)

2024 K_c-TEST RESULTS (K_c VALUES, CRITICAL Δa's, COMPARATIVE R-CURVE POINTS)

SPECIMEN NO.	DIMENSIONS, INCHES B	W	ORIENTATION	TEST TEMP °F	K_c, KSI $\sqrt{in}$	CRITICAL Δa, INCHES	R-Curve K Value at Indicated Δa: Δa= 0"	.1"	.2"	.3"	.4"	.5"	.6"	.7"	Figure No. of R-Curve
Material 302, .1" Sheet, - T81, (CCT Spec's)															
87-8	0.1	24	RW	RT	64	.53	42	51	57	60	62	64	65		6-8 (a)
-9	0.1	24	RW	RT	64	.62	40	51	56	59	61	63	64		6-8 (a)
87-10	0.1	24	WR	RT	61	.60	<20	40^{f}	49^{f}	53^{f}	56^{f}	59^{f}	61^{f}		6-8 (b)
-11	0.1	24	WR	RT	60	.56	41^{f}	49^{f}	52^{f}	56^{f}	58^{f}	59^{f}	61^{f}		6-8 (b)
-12	0.1	24	WR	RT	59	.46	28	45	51	55	57	59	60		6-8 (b)
Mat'l 303, .1" Sheet, -T81, (CCT Spec's)															
88-2	0.1	24	RW	RT	58	.56	35^{f}	44^{f}	53^{f}	55^{f}	57^{f}	58^{f}	59^{f}		6-9 (a)
-7	0.1	24	RW	RT	62	.53	28^{f}	43^{f}	52^{f}	58^{f}	60^{f}	62^{f}	63^{f}		6-9 (a)
-8	0.1	24	RW	RT	78	.81	31^{f}	47^{f}	55^{f}	63^{f}	67^{f}	70^{f}	73^{f}	75^{f}	6-9 (a)
88-10	0.1	24	WR	RT	47	.37	31	41	44	46	47				6-9 (b)
-12	0.1	24	WR	RT	47	.33	33	40	44	46	47				6-9 (b)
-13	0.1	24	WR	RT	44	.35	28	39	42	44	45				6-9 (b)

^{f}Crack angle exceeds 10°

NOTE: Specimens 88-2 and 88-7 were first used to develop compliance calibration curves and had crack lengths ($2a_o$) of 7.7 and 8.8", respectively, at the start of the K_c tests.

TABLE 6-23

2219 K_c TEST RESULTS (K_c VALUES, CRITICAL Δa's, COMPARATIVE R-CURVE POINTS)

SPECIMEN NO.	DIMENSIONS, INCHES B	W	ORIENTATION	TEST TEMP ^oF	K_c, KSI $\sqrt{in}$	CRITICAL Δa, INCHES	R-Curve K Value at Indicated Δa								Figure No. of R-Curve
							Δa= 0"	.1"	.2"	.3"	.4"	.5"	.6"	.7"	
Mat'l 7,	1.75" Plate,		- T851												
36-13	1.25	6	RW	RT	> 65	>.32	36	51	58	65					
-14	1.25	6	RW	RT	72	.46	34	52	59	64	69	74			
36-16	0.87	6	RW	RT	86	.55	34	54	62	70	77	83	88		6-10(a)
-17	0.87	6	RW	RT	80	.41	32	55	64	72	80	84	89		6-10(a)
36-21	0.50	6	RW	RT	70	.34	32	53	61	68					
-23	0.50	6	RW	RT	87	.44	34	56	69	78	86	90			
36-26	0.50	6	WR	RT	63	.36	24	44	53	60	64				
-28	0.50	6	WR	RT	61	.29	31	47	55	61	64				6-10(b)
-30	0.50	6	WR	RT	62	.26	37	50	59	63	65				6-10(b)
36-22	0.25	6	RW	RT	104	.48	37	66	80	89[f]	98[f]	104[f]			6-10(c)
-24	0.25	6	RW	RT	95	.58	32	52	66	76[f]	84[f]	90[f]	96[f]		6-10(c)
36-25	0.5	6	RW	265	102	.59	16	42	58	72	85	95[f]	103[f]	110[f]	6-10(d)
-27	0.5	6	RW	265	104	.66	23	44	58	70	82	92[f]	99[f]	107[f]	6-10(d)

[f] Crack angle exceeds 10°

TABLE 6-24

7049 K_c TEST RESULTS (K_c VALUES, CRITICAL Δa's, COMPARATIVE R-CURVE POINTS)

SPECIMEN NO.	DIMENSIONS, INCHES B	W	ORIEN-TATION	TEST TEMP ^oF	K_c, KSI $\sqrt{in}$	CRITICAL Δa, INCHES	R-Curve K Value at Indicated Δa								Figure No. of R-Curve
							$\Delta a=$ 0"	.1"	.2"	.3"	.4"	.5"	.6"		
Mat'l	25, Forging, T73, 3 x 24 x 48														
71-18	1.25	4	RW	RT	55	.33	22	41	47	52	57				6-11
-19	1.25	4	RW	RT	51	.27	36	40	46	52	56				6-11
71-20	0.75	4	RW	RT	83	.47	29	44	55	64	76[f]	85[f]			6-11
-21	0.75	4	RW	RT	77	.46	29	46	56	63	72[f]	78[f]			6-11

[f] Crack angle exceeds 10°

TABLE 6-25

7075-T76XX K_c TEST RESULTS (K_c VALUES, CRITICAL Δa's, COMPARATIVE R-CURVE POINTS)

SPECIMEN NO.	DIMENSIONS, INCHES		ORIENTATION	TEST TEMP ^oF	K_c, KSI $\sqrt{in}$	CRITICAL Δa, INCHES	R-Curve K Value at Indicated Δa								Figure No. of R-Curve
	B	W					Δa= 0"	.1"	.2"	.3"	.4"	.6"	.8"	1.0"	
Mat'l 18, 2" Plate, T7651															
51-38	.51	2.5	RW	RT	49	.22	26	35	45	51					6-12(a)
-39	.51	2.5	RW	RT	48	.23	26	35	44	52					6-12(a)
51-40	.38	2.5	RW	RT	66	.26	26	44	59						6-12(a)
-45	.38	2.5	RW	RT	60	.26	21	40	54	60					6-12(a)
51-46	.26	2.5	RW	RT	63	.20	16	49	63						6-12(b)
51-48	.13	2.5	RW	RT	74	.23	15	55	70	82					6-12(a)
-49	.13	2.5	RW	RT	68	.19	19	55	69	76					6-12(a)
51-52	.26	2.5	WR	RT	45	.20	20	35	45						6-12(b)
51-50	.26	2.5	WR	265F	83	.34	17	39	60	77	86				6-12(c)
-51	.26	2.5	WR	265F	73	.23	23	46	67	79	87				6-12(c)
Mat'l 30, .1" Sheet, T76 (CCT Specimens)															
85-6	.10	24	RW	RT	89	.47	39	70	78	83	88				6-13(a)
-8	.10	24	RW	RT	87	.48	30	60	75	81	85				6-13(a)
-9	.10	24	RW	RT	88	.39	48^f	71^f	79^f	84^f	90^f				6-13(a)
85-10	.10	24	WR	RT	68	.34	31	58	64	66					6-13(b)
-11	.10	24	WR	RT	70	.60	32	58	63	64	67	70			6-13(b)
Mat'l 301, .1" Sheet, T76 (CCT Specimens)															
86-1	.10	24	RW	RT	>130	>1.2	30^f	67^f	82^f	90^f	97^f	108^f	116^f	124^f	6-14(a)
-2	.10	24	RW	RT	93	.62	36	65	75	85	90	98			6-14(a)
-3	.10	24	RW	RT	114	1.20	38	61	72	80	89	98	103	109	6-14(a)

NOTE: Specimen 86-3 was first used to develop a compliance calibration curve and had a crack length of 8.4" ($2a_o$) at the start of the K_c test.

TABLE 6-25 (Cont'd)

7075-T76XX K_c TEST RESULTS (K_c VALUES, CRITICAL Δa's, COMPARATIVE R-CURVE POINTS)

SPECIMEN NO.	DIMENSIONS, INCHES		ORIEN-TATION	TEST TEMP ^oF	K_c, KSI $\sqrt{in}$	CRITICAL Δa, INCHES	R-Curve K Value at Indicated Δa								Figure No. of R-Curve
	B	W					Δa= 0"	.1"	.2"	.3"	.4"	.6"	.8"	1.0"	
86-5	.10	24	WR	RT	79	.41	30	65	70	75	79				6-14(b)
-6	.10	24	WR	RT	78	.37	35	65	70	75	79				6-14(b)

[f] Crack angle exceeds 10°

TABLE 6-26

7075-T73511 K_c TEST RESULTS (K_c VALUES, CRITICAL Δa's, COMPARATIVE R-CURVE POINTS)

SPECIMEN NO.	DIMENSIONS, INCHES B	W	ORIENTATION	TEST TEMP °F	K_c, KSI $\sqrt{in}$	CRITICAL Δa, INCHES	R-Curve K Value at Indicated Δa: Δa= 0"	.1"	.2"	.3"	.4"	.5"	.6"	.7"	Figure No. of R-Curve
Mat'l	29, Extrusion, -T73511														
83-21	1.63	4	RW	RT	56	.40	26	42	46	51	56				6-15(a)
83-27	1.25	4	RW	RT	>73	>.50	23	44	50	58	64	73			6-15(a)
-29	1.25	4	RW	RT	78	.67	29	41	47	54	59	65	72	78	6-15(a)
-55	1.25	4	RW	RT	59	.35	33	43	47	56	63	66	73		6-15(a)
83-22	0.75	4	RW	RT	112	.62	24	47	61	73	82	94[f]	110[f]		6-15(c)
-24	0.75	4	RW	RT	89	.42	24	41	61	71	87	103[f]			6-15(c)
83-32	0.37	4	RW	RT	>104	>.39	27	56	74	86	105				6-15(a)
-34	0.37	4	RW	RT	88	.32	24	58	73	86	93				6-15(a)
-56	0.37	4	RW	RT	81	.29	32	56	73	82					
83-28	0.75	4	RW	265	>93	>.31	23	54	69	90					6-15(c)
-30	0.75	4	RW	265	134	.55	24	57	73	91	109	126	140		6-15(c)
83-20	0.75	3.5	WR	RT	40	.23	18	32	37						6-15(b)
-26	0.75	3.5	WR	RT	39	.27	15	31	34						6-15(b)

[f] Crack angle exceeds 10°

TABLE 6-27

HP-9-4-20 K_c TEST RESULTS (K_c VALUES, CRITICAL Δa's, COMPARATIVE R-CURVE POINTS)

SPECIMEN NO.	DIMENSIONS, INCHES B	DIMENSIONS, INCHES W	ORIEN-TATION	TEST TEMP °F	K_c, KSI $\sqrt{in}$	CRITICAL Δa, INCHES	R-Curve K Value at Indicated Δa = 0"	.1"	.2"	.3"	.4"	.5"	.6"	.7"	Figure No. of R-Curve
Mat'l	43, 4 x 18 x 36" Forged Billet, HT 211 ksi														
60-9	1.63	8	RW	RT	225	.79	106	152	158	168	178	191	202	215	6-16(a)
-65	1.63	8	RW	RT	232	.85	95	149	157	167	179	189	202	214	6-16(a)
60-10	1.25	8	RW	RT	>241	>.58	106	163	175	191	209	227			6-16(a)
60-15	0.38	8	RW	RT	479	.82	132	197	252	305	345	385	419	448	6-16(c)
-16	0.38	8	RW	RT	477	.88	123	187	242	292	332	370	404	433	6-16(c)
60-13	0.87	8	RW	-65	136	.54	79	81	109	110	112	122	139		6-16(b)
-14	0.87	8	RW	-65	153	.94	45	65	84	107	109	113	128	131	6-16(b)
60-63	0.375	6	RW	-65	238	.57	93	121	148	182	201	224	243	258	6-16(b)
-82	0.375	6	RW	-65	243	.58	92	124	150	179	207	222	246	257	6-16(b)

TABLE 6-28

PH13-8Mo K_c TEST RESULTS (K_c VALUES, CRITICAL Δa's, COMPARATIVE R-CURVE POINTS)

SPECIMEN NO.	DIMENSIONS, INCHES B	DIMENSIONS, INCHES W	ORIEN-TATION	TEST TEMP °F	K_c, KSI $\sqrt{in}$	CRITICAL Δa, INCHES	R-Curve K Value at Indicated Δa: Δa= 0"	.1"	.2"	.3"	.4"	.5"	.6"		Figure No. of R-Curve
Mat'l	40, 1-1/2" x 12" Rolled Bar, H 1000														
56-36	0.75	3.5	RW	RT	105	.16	47	92	102						6-17(a)
-38	0.75	3.5	RW	RT	108	.25	49	90	98	112					6-17(a)
56-30	0.63	3.5	RW	RT	149	.29	72	112	132	150	160				6-17(b)
-32	0.63	3.5	RW	RT	139	.24	64	107	126	145	163				6-17(b)
56-29	0.38	3.5	RW	RT	262	.40	80	131	181	222	258	288			6-17(c)
-31	0.38	3.5	RW	RT	264	.39	80	138	186	229	266	294			6-17(c)
-33	0.38	3.5	RW	RT	280	.44	80	143	188	229	266	299			6-17(c)
-34	0.38	3.5	RW	RT	>215	>.30	81	130	177	215					
56-35	0.25	3.5	RW	RT	359	.43	85	152	222	281[f]	339[f]	376[f]			6-17(d)
-37	0.25	3.5	RW	RT	307	.41	84	159	219	264	302	334			6-17(d)
56-75	0.77	3.5	RW	-65	44	.00	44								
-76	0.77	3.5	RW	-65	49	.00	49								
56-77	0.26	4	RW	-65	51	.00	51								
-78	0.26	4	RW	-65	54	.00	54								

[f] Crack angle exceeds 10°

TABLE 6-29 Effect of Specimen Thickness (B) on K_Q Values for CT Specimens Used in K_C Tests, Various Alloys

Alloy	Product Form	Mat'l No	Orientation	B (Test Specimen) /B (K_{Ic}) Ratio *	Specimen K_{Ic} Capability Ratio **	P_{max} / P_Q Ratio	K_Q/K_{Ic} Ratio
Ti-6Al-4V Cond RA	Plate	68	RW	.26/1.42 = .18	.42	1.42	106/92 =1.15
		72	RW	.87/1.10 = .79	.88	1.39	81/78 =1.04
				.62/1.10 = .56	.76	1.64	86/78 =1.10
2024-T851	Plate	6	RW	.26/ .59 = .44	.75	1.40	31/28 =1.11
				.11/ .59 = .19	.50	1.06	45/28 =1.61
2024-T852	Forging	27	RW	1.00/1.21 = .83	.92	1.12	39/37 =1.05
				.75/1.21 = .62	.78	1.20	37/37 =1.00
				.50/1.21 = .41	.65	1.24	38/37 =1.03
				.25/1.21 = .21	.46	1.49	37/37 =1.00
			WR	.38/ .62 = .61	.78	1.15	26/27 = .96
2219-T851	Plate	7	RW	.87/2.02 = .43	.67	1.33	47/45 =1.04
				.25/2.02 = .12	.36	1.43	52/45 =1.16
			WR	.50/1.56 = .32	.53	1.23	41/38 =1.08
7075-T7651	Plate	18	RW	.38/ .49 = .77	.89	1.53	29/28 =1.03
				.26/ .49 = .53	.71	1.64	29/28 =1.04
				.13/ .49 = .26	.50	1.28	42/28 =1.50
			WR	.26/ .35 = .74	.83	1.50	23/24 = .96
7075-T73511	Extrusion	29	RW	.75/ .86 = .87	.92	1.53	41/39 =1.05
				.37/ .86 = .43	.64	1.64	43/39 =1.10

TABLE 6-29 Effect of Specimen Thickness (B) on K_Q

Values for CT Specimens Used in K_C Tests, Various Alloys (Cont'd)

Alloy	Product Form	Mat'l No	Orien-tation	$B\left(\text{Test Specimen}\right)/B\,(K_{Ic})$ Ratio *	Specimen K_{Ic} Capability Ratio **	P_{max}/P_Q Ratio	K_Q/K_{Ic} Ratio
PH13-8Mo, H1000	Bar	40	RW	.38/ .44 = .86	.93	1.63	106/87 =1.22
				.25/ .44 = .57	.77	1.90	114/87 =1.31
9-4-20, HT 190-210	Bar	43	RW	1.30/1.42 = .92	.92	1.25	157/141=1.11
				.87/1.42 = .61	.75	1.50	154/141=1.09
				.38/1.42 = .27	.50	1.93	172/141=1.22

* Ratio of the B dimension of the test specimen to the minimum B dimension required for a plane strain stress state.

** This is the ratio of the plane strain K level capability of the test specimen to the K_{Ic} value for the test material.

NOTES:

1. The P_{max}/P_Q ratios and the values of K_Q and K_{Ic} in the Table are average values.

TABLE 6-30 Effect of Test Temperature on The K_{Ic} Toughness of Various Alloys

Alloy	Form and Condition	Mat'l No	Orientation	Ratio of K_{Ic} (Test Temp) to K_{Ic} (Room Temp)*
	-65F Test Temperature			
Ti-6Al-4V	Parent Metal, Cond RA Plate	72	RW	60/78 = .77
		72	WR	77/95 = .81
		68	WR	90/100 = .90
				.83 Avg.
	1/2" Thick Weld Joints, Preweld-Cond RA Plate, Postweld - 1100 to 1400F, 1 to 2 hours	88	RT, HAZ	77/70 = 1.10
			RW, Weld	(80)/(100)= .80
	Extrusion, Postweld-1100 to 1200F 1 to 2 hours	75	RT, HAZ	86/82 = 1.05
PH13-8Mo	Parent Metal, H1000 Rolled Bar	40	RW	47/87 = .54
			WR	44/75 = .59
		50	WR	55/90 = .61
	Extruded Bar	41	RW	49/67 = .73
			WR	47/66 = .71
	Upset Forging	44	RW	53/79 = .67
				.64 Avg.
	1/4" Thick Weld Joint Rolled Bar, Preweld-H1000 Postweld -950F, 2 hrs.	[illegible]	RT, Weld	98/83 = 1.18
			RT, HAZ	95/88 = 1.08
	Extruded Bar, Preweld-Cond A Postweld-H1000	41	RW, Weld	(91)/(140)= .65

TABLE 6-30 Effect of Test Temperature on The K_{Ic} Toughness of Various Alloys (Cont'd)

Alloy	Form and Condition	Mat'l No	Orientation	Ratio of K_{Ic} (Test Temp) to K_{Ic} (Room Temp) *
	-65F Test Temperature (Cont'd)			
9-4-20	Parent Metal, HT 190-120 ksi Plate	37	RW	100/121 = .83
			WR	97/131 = .74
	Forged Block	43	RW	81/141 = .57
	Forged Block	46	RW **	127/135 = .94
			RW ***	163/177 = .92
			WR	132/152 = .87
				.81 Avg.
	1/2" Weld Joint, Preweld – HT 190-210 ksi Plate, Postweld-950F, 2 hours	57	RT, HAZ	92/107 = .86
	Forged Block, Postweld - 950F, 2 hours	33	RT, HAZ	82/95 = .86
9-4-30	Forged Block, HT 245 ksi	32	RW	67/82 = .82
Inconel 718	Forged Bar, HT 192 ksi	51	RW	(218)/(213) = 1.02
			WR	144/134 = 1.07
			TR	119/108 = 1.10
				1.06 Avg.
	265 Test Temperature			
Ti-6Al-4V	Plate, Cond RA	68	RW	104/92 = 1.13
			WR	(123)/100 = 1.23
		72	RW	(100)/78 = 1.28
			WR	(120)/95 = 1.26
				1.23 Avg.

** Oil quenched from the austenitizing cycle
*** Air cooled from the austenitizing cycle

TABLE 6-30 Effect of Test Temperature on The K_{Ic} Toughness of Various Alloys (Cont'd)

Alloy	Form and Condition	Mat'l No	Orientation	Ratio of K_{Ic} (Test Temp) to K_{Ic} (Room Temp) *
	265 Test Temperature (Cont'd)			
2024	Forged Block, T-852	19	RW WR	33/28 = 1.18 25/21 = 1.19 1.19 Avg.
2219	Plate, T851	7	RW WR	43/45 = .96 34/38 = .89 .93 Avg.
7075	Plate, T7651	306	RW WR	31/31 = 1.00 26/24 = 1.08 1.04 Avg.
7075	Extrusion, T73511	29	RW WR	44/39 = 1.13 29/28 = 1.04 1.09 Avg.
	400F Test Temperature			
Inconel 718	Forged Bar, HT 192 ksi	51	RW WR TR	(190)/(213)= .89 125/134 = .93 94/108 = .87 .90 Avg.

* K_{Ic} ratios are based on average test values. If K_Q values are used in the ratio. these are indicated by enclosing the value in parentheses.

TABLE 6-31

Effect of Changes in Test Parameters on R-Curve K Levels *

(K_c Testing Program)

Alloy, Product Form, and Condition	Material Number	Parameter Changed (Decrease in Thickness, B)	Resultant Effect On R-Curve K Level	Parameter Changed (Decrease In Test Temperature, °F)	Resultant Effect On R-Curve K Level	Parameter Changed (Orientation)	Resultant Effect On R-Curve K Level
Ti-6Al-4V Plate, RA	72	1.3 to 0.87 to .62 to .25	Increase	R.T. to -65 (B= 0.62)	Decrease	-	-
Sheet, MA	80, 81	-	-	-	-	RW to WR (B= 0.1)	Decrease
2024 Plate, -T851	6	2.6 to 0.11	Increase	-	-	-	-
Sheet, -T81	302, 303	-	-	-	-	RW to WR (B= 0.1)	Decrease
Forging, -T852	27	1.0 to .75 to .50 .50 to .25	No Change Increase	265 to R.T. (B= .5)	No Change	-	-
2219 Plate, -T851	7	1.3 to .87 to .50 to .25	Increase	265 to R.T. (B= .5)	Increase	RW to WR (B= 0.5)	Decrease
7049 Forging, -T73	25	1.3 to .75	Increase	-	-	-	-
7075 Plate, -T7651	18	.51 to .38 to .25 to .13	Increase	265 to R.T. (B= .26)	Decrease	RW to WR (B= 0.26)	Decrease
Sheet, -T76	30, 301	-	-	-	-	RW to WR (B= 0.1)	Decrease

* K level of the R-Curve at a given crack extension.

TABLE 6-31 (Cont'd)

Effect of Changes in Test Parameters on R-Curve K Levels

(K_c Testing Program)

Alloy, Product Form, and Condition	Material Number	Parameter Changed (Decrease in Thickness, B)	Resultant Effect On R-Curve K Level	Parameter Changed (Decrease In Test Temperature, °F)	Resultant Effect On R-Curve K Level	Parameter Changed (Orientation)	Resultant Effect On R-Curve K Level
7075 Extrusion, -T73511	29	1.6 to 1.2 to .75 to .37	Increase	265 to R.T. (B= .75)	Decrease	RW to WR (B= .75)	Decrease
9-4-.20 Forging, HT 190-210 ksi	43	1.6 to 1.3 to 0.38	Increase	R.T. to -65 (B= .87, .37)	Decrease	-	-
PH13-8Mo Rolled Bar, H1000	40	.75 to .63 to .38 to .25	Increase	-	-	-	-

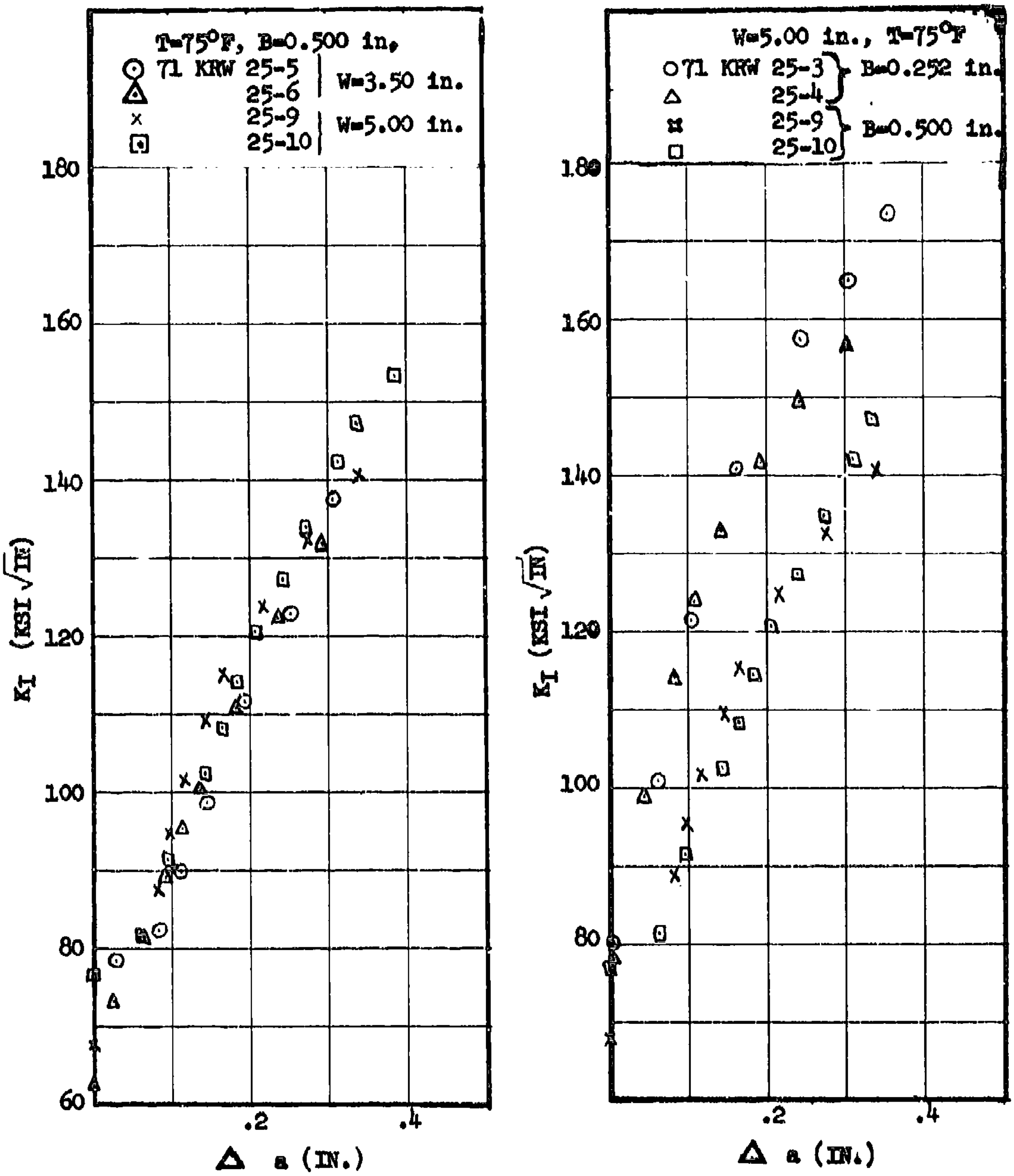

(a) Thickness of 0.500 Inch at Two Specimen Widths

(b) Thickness of 0.500 and 0.252 Inch

Figure 6-1 R-Curves for Ti-6Al-4V Plate, Material 71, RA Condition.

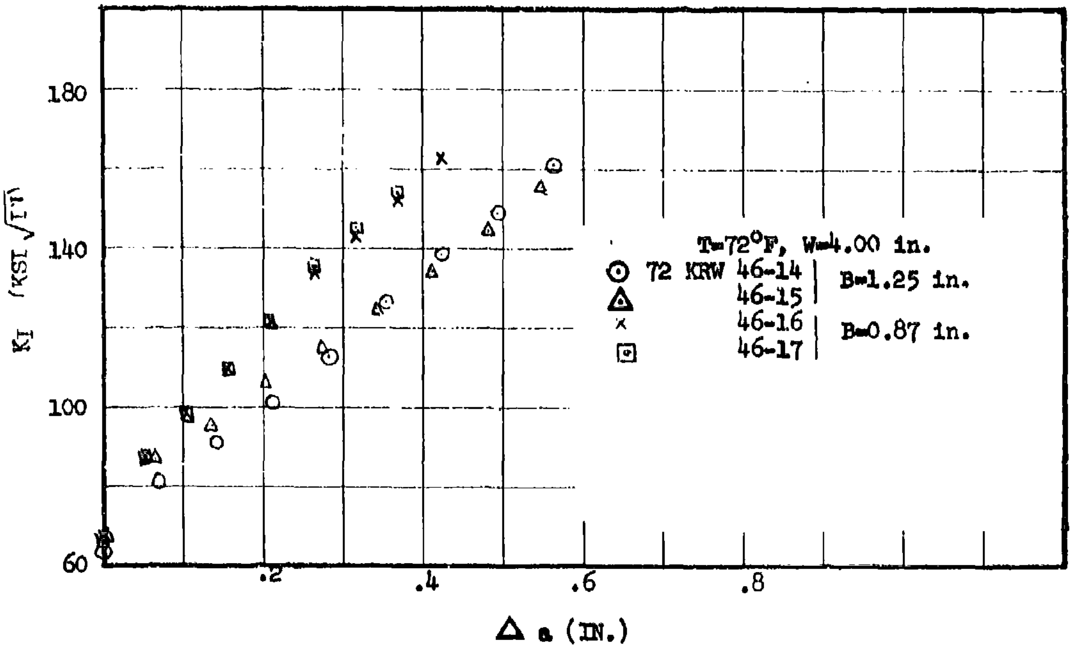

(a) Thicknesses of 1.25 and 0.87 Inches

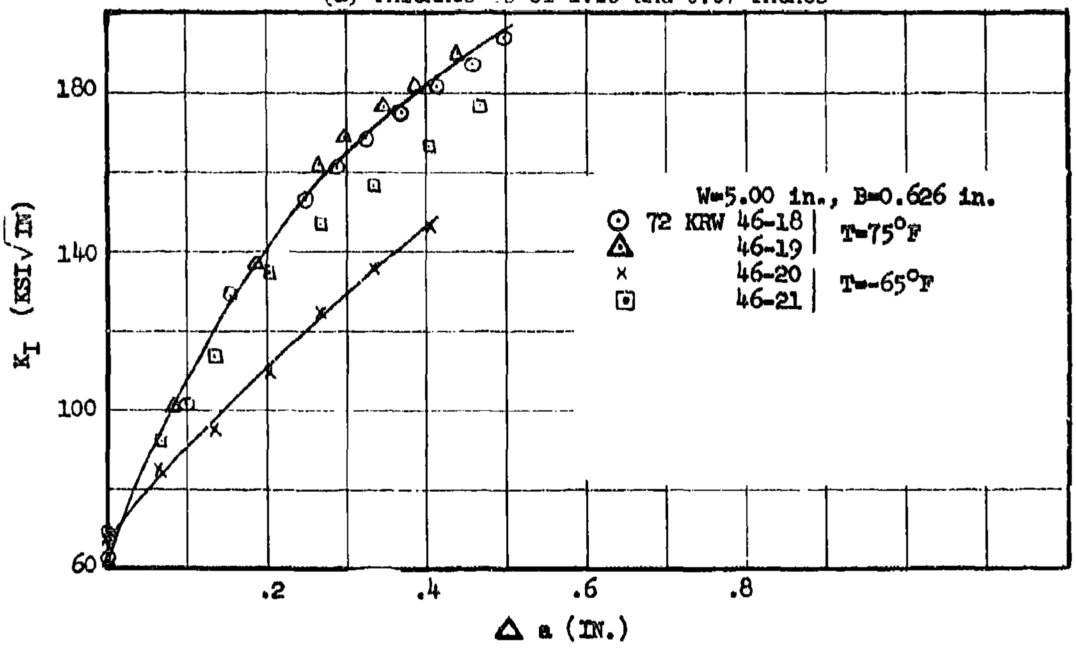

(b) Thickness of 0.626 Inches at 75°F and -65°F

Figure 6-2 R-Curves for Ti-6Al-4V Plate, Material 72, Condition RA (Page 1 of 2)

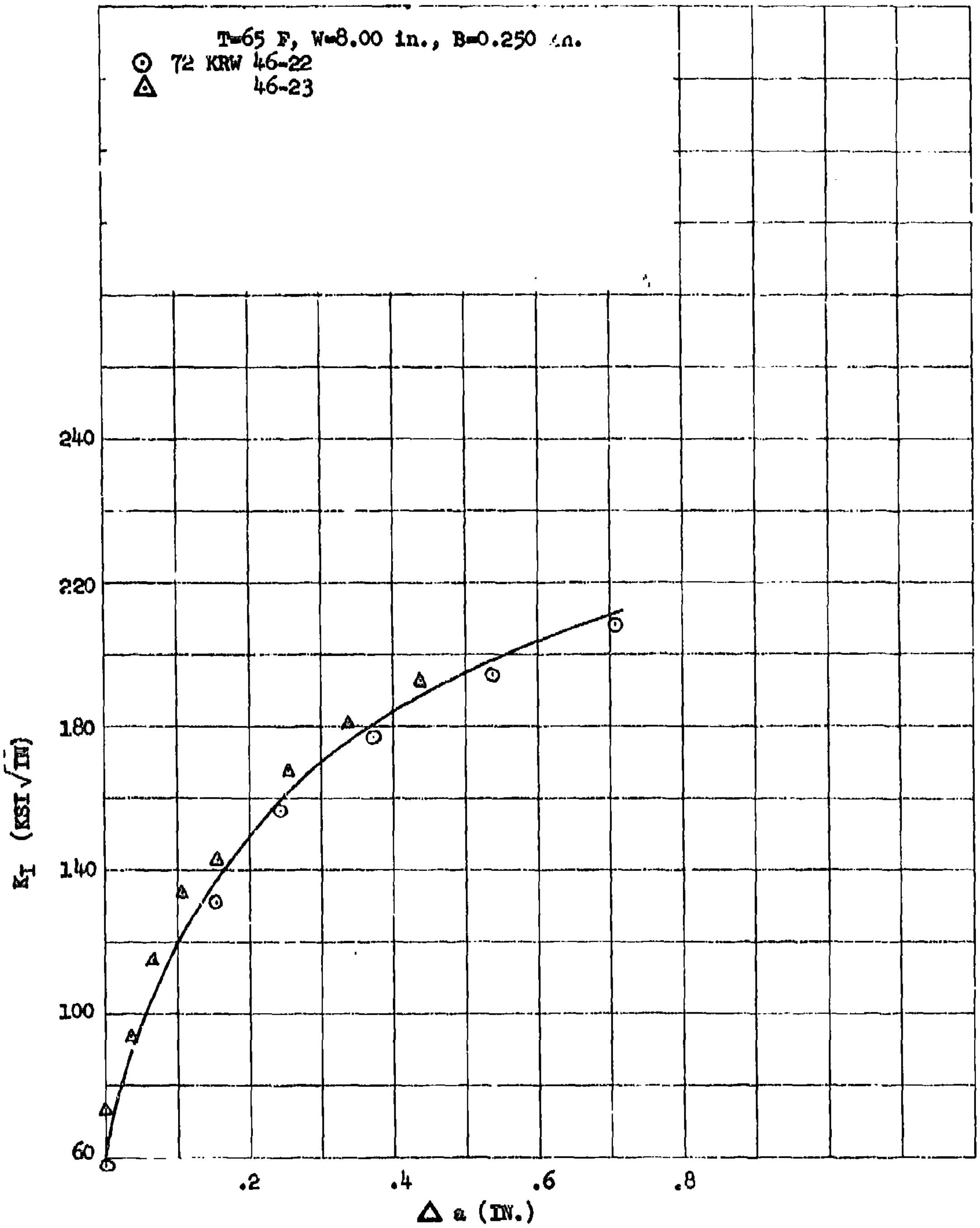

(c) Thickness of 0.250 Inches at -65°

Figure 6-2 (Cont'd) R-Curves for Ti-6Al-4V Plate, Material 72, Condition RA. (Page 2 of 2)

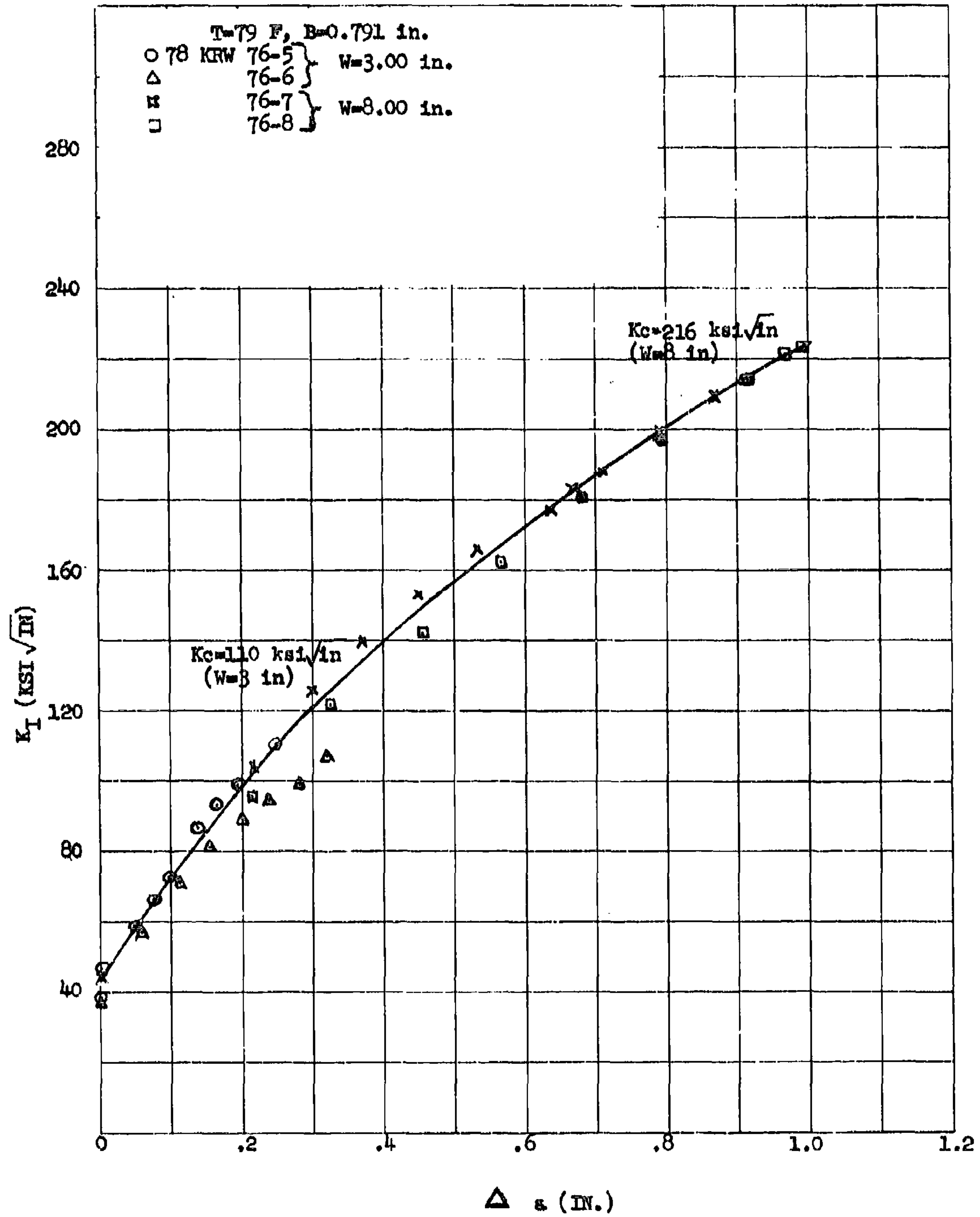

Figure 6-3 R-Curve for Ti-6Al-4V Plate, Material 78, Condition RA

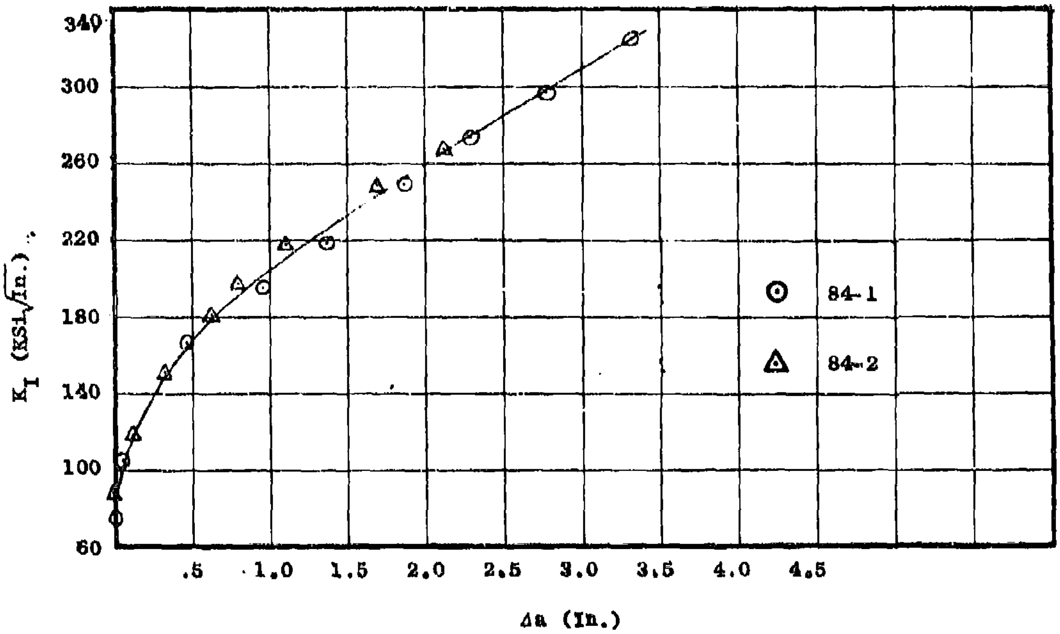

(a) RW Orientation

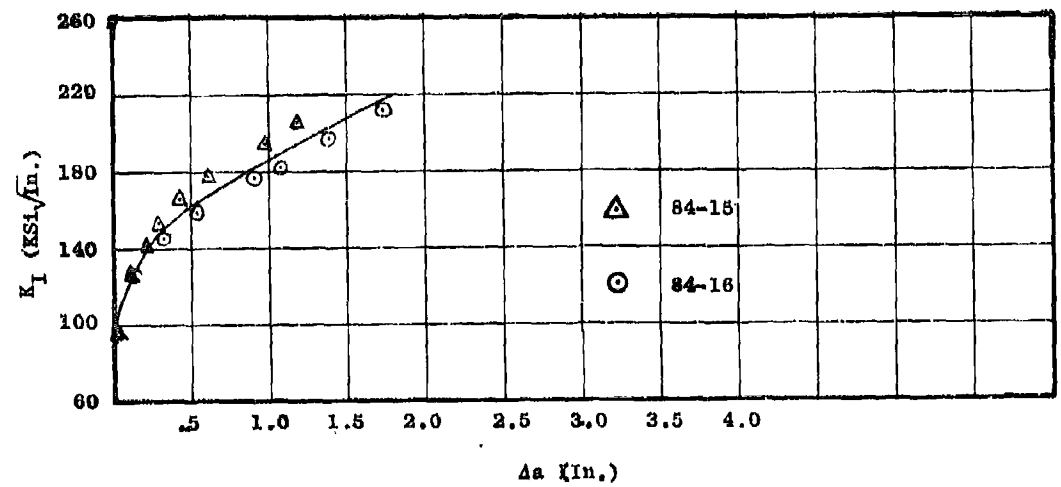

(b) WR Orientation

Figure 6-4 R-Curves for Ti-6Al-4V Sheet, Material 80, MA Condition

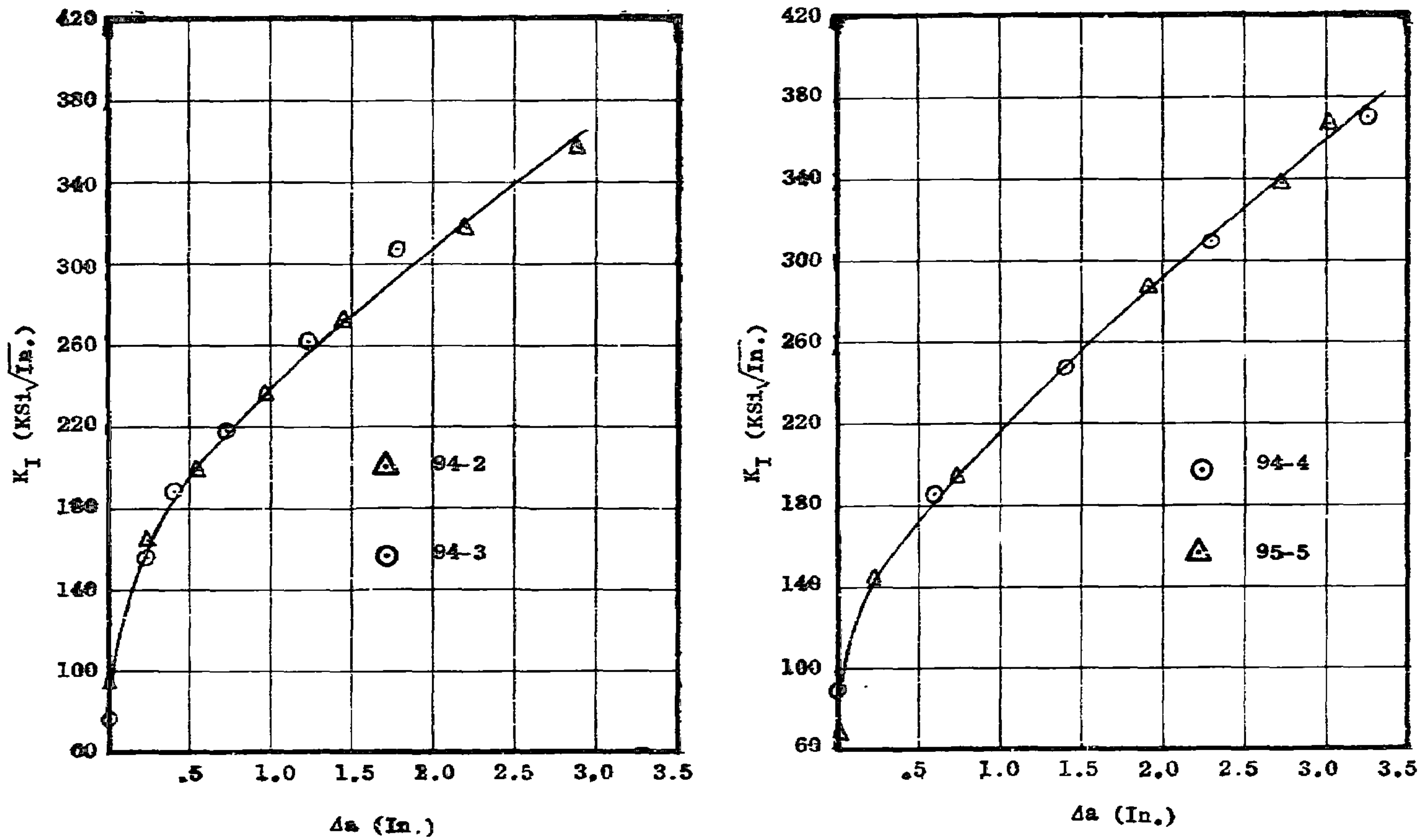

(a) RW Orientation

(b) WR Orientation

Figure 6-5 R-Curves for Ti-6Al-4V Sheet, Material 81, MA Condition

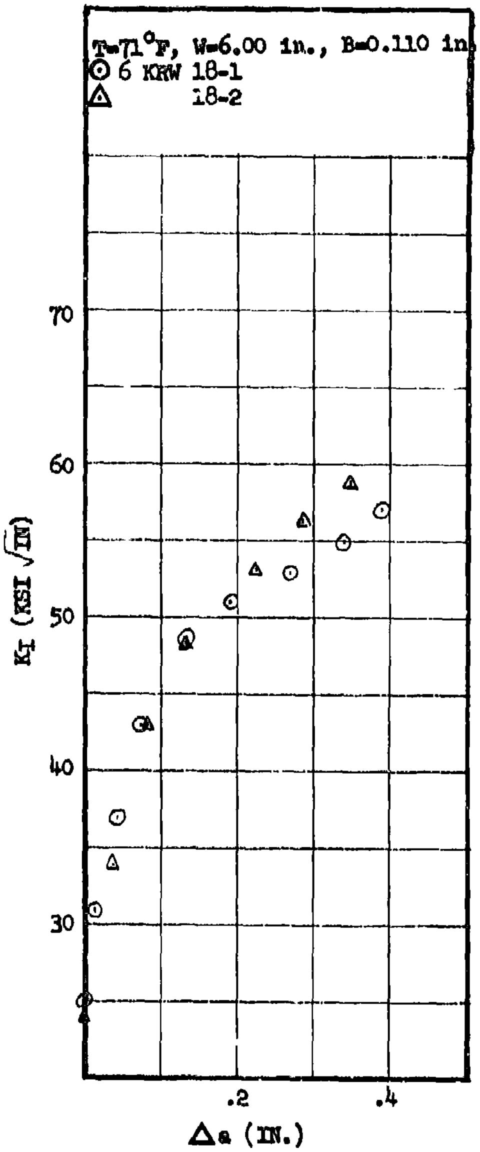

(a) Specimen Thickness of 0.110 In.

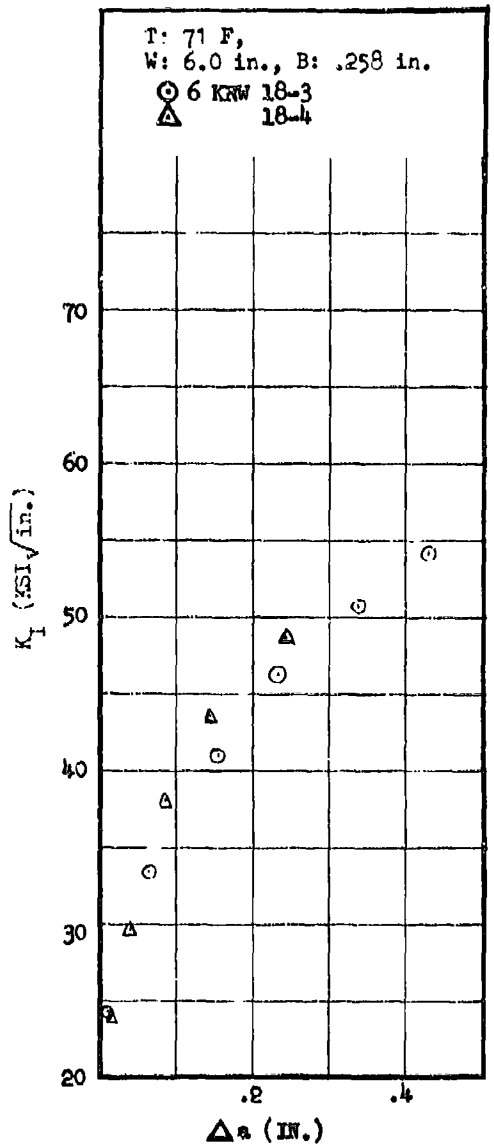

(b) Specimen Thickness of 0.258 In.

Figure 6-6 R-Curves for 2024-T851 Plate, Material 6.

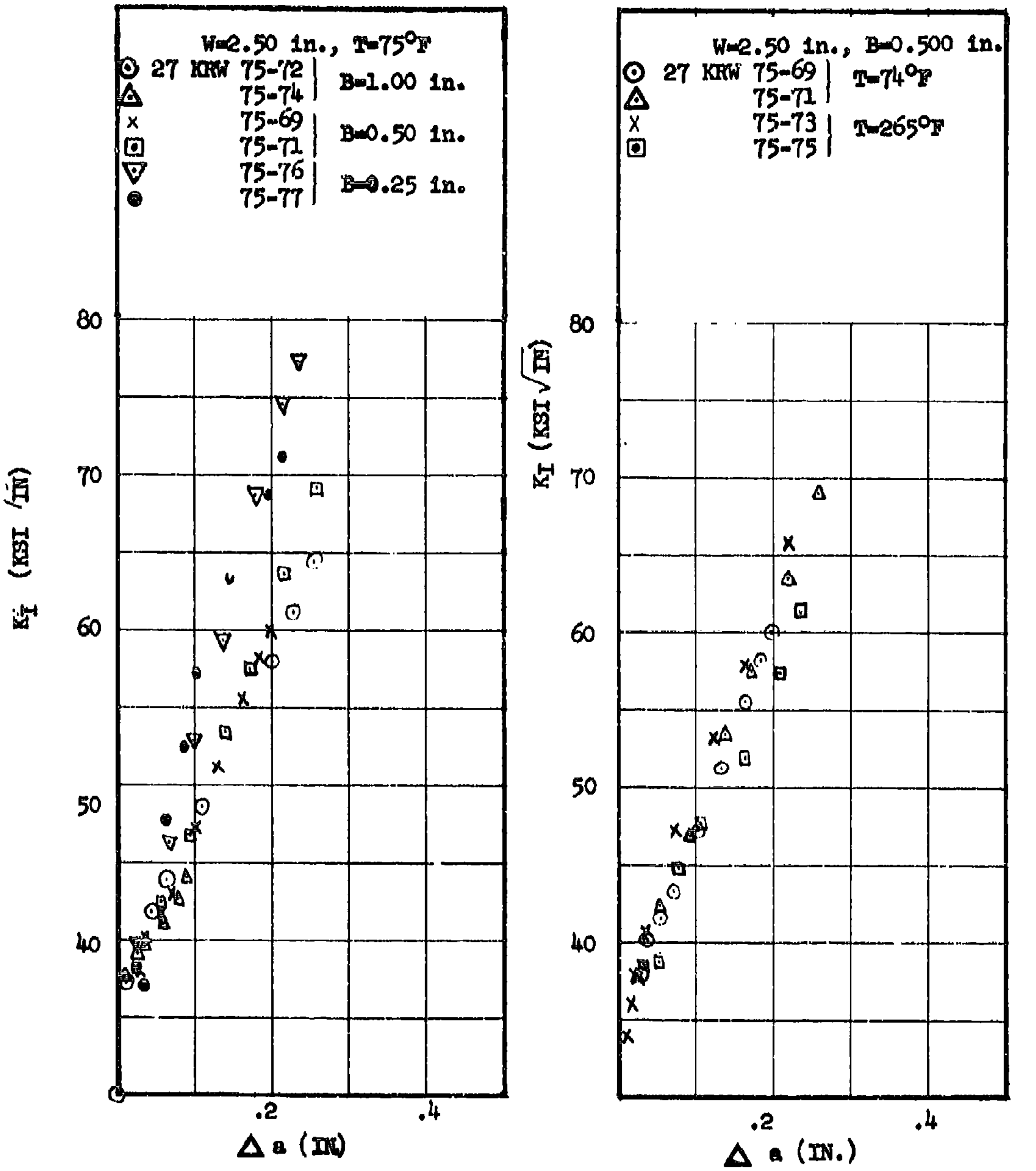

(a) Specimen Thickness of 1.00, 0.50 and 0.25 Inches

(b) Specimen Thickness of 0.50 Inches at 74°F and 265°F

Figure 6-7 R-Curves for 2024-T852 Hand Forging, Material 27.

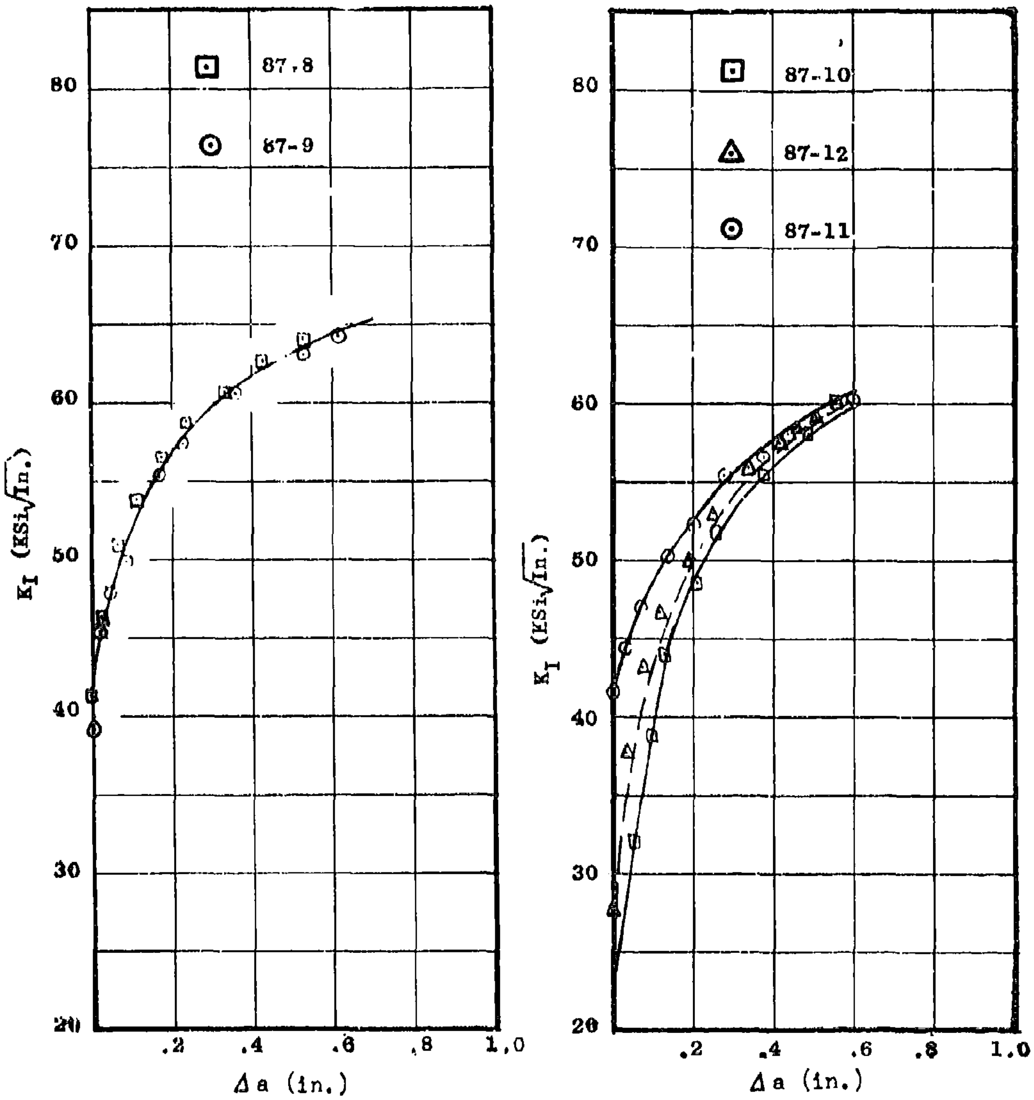

(a) RW Orientation

(b) WR Orientation

Figure 6-8 R-Curves for 2024-T81 Sheet, Material 302.

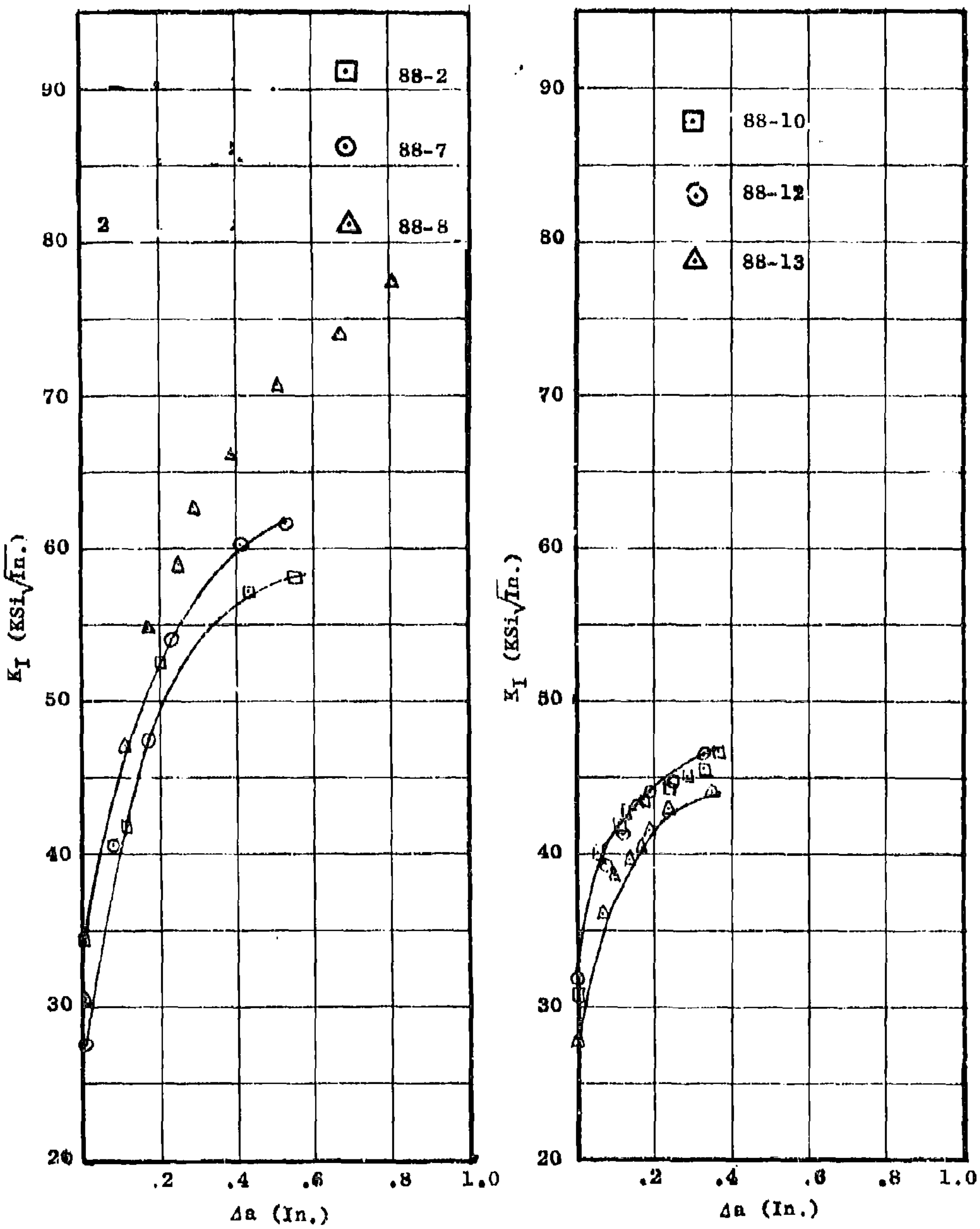

(a) RW Orientation (b) WR Orientation

Figure 6-9 R-Curves for 2024-T81 Sheet, Material 303.

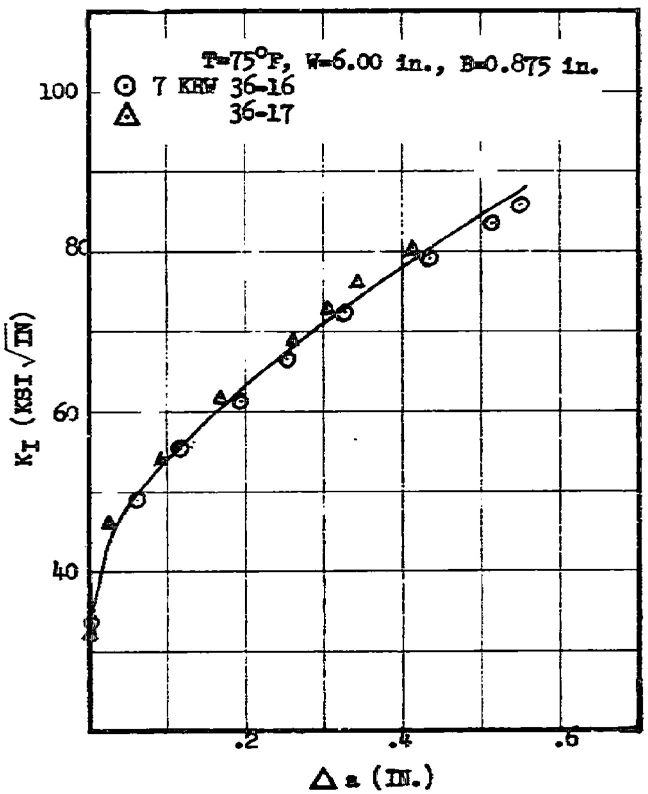

(a) RW Orientation at Thickness of 0.875 Inches

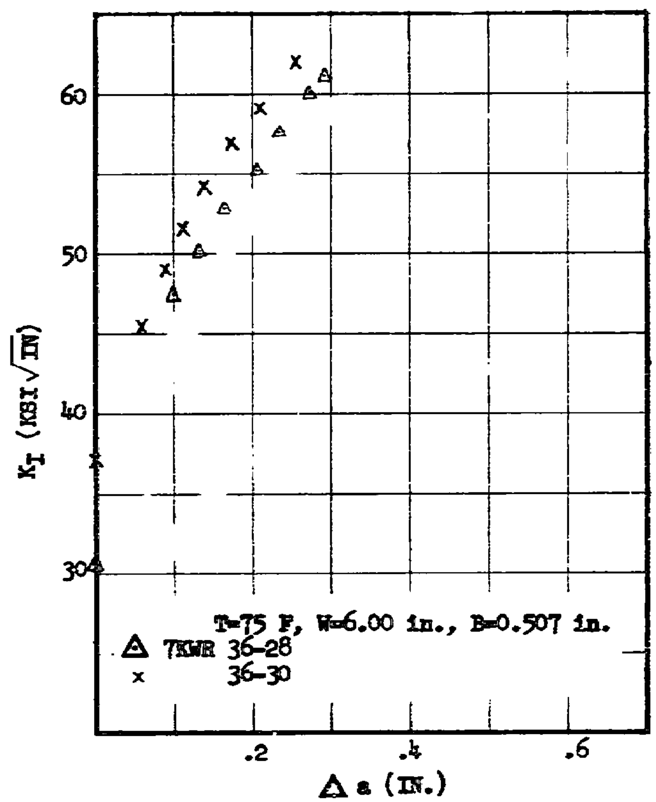

(b) WR Orientation at Thickness of 0.507 Inches

Figure 6-10 R-Curves for 2219-T851 Plate, Material 7. (Page 1 of 3)

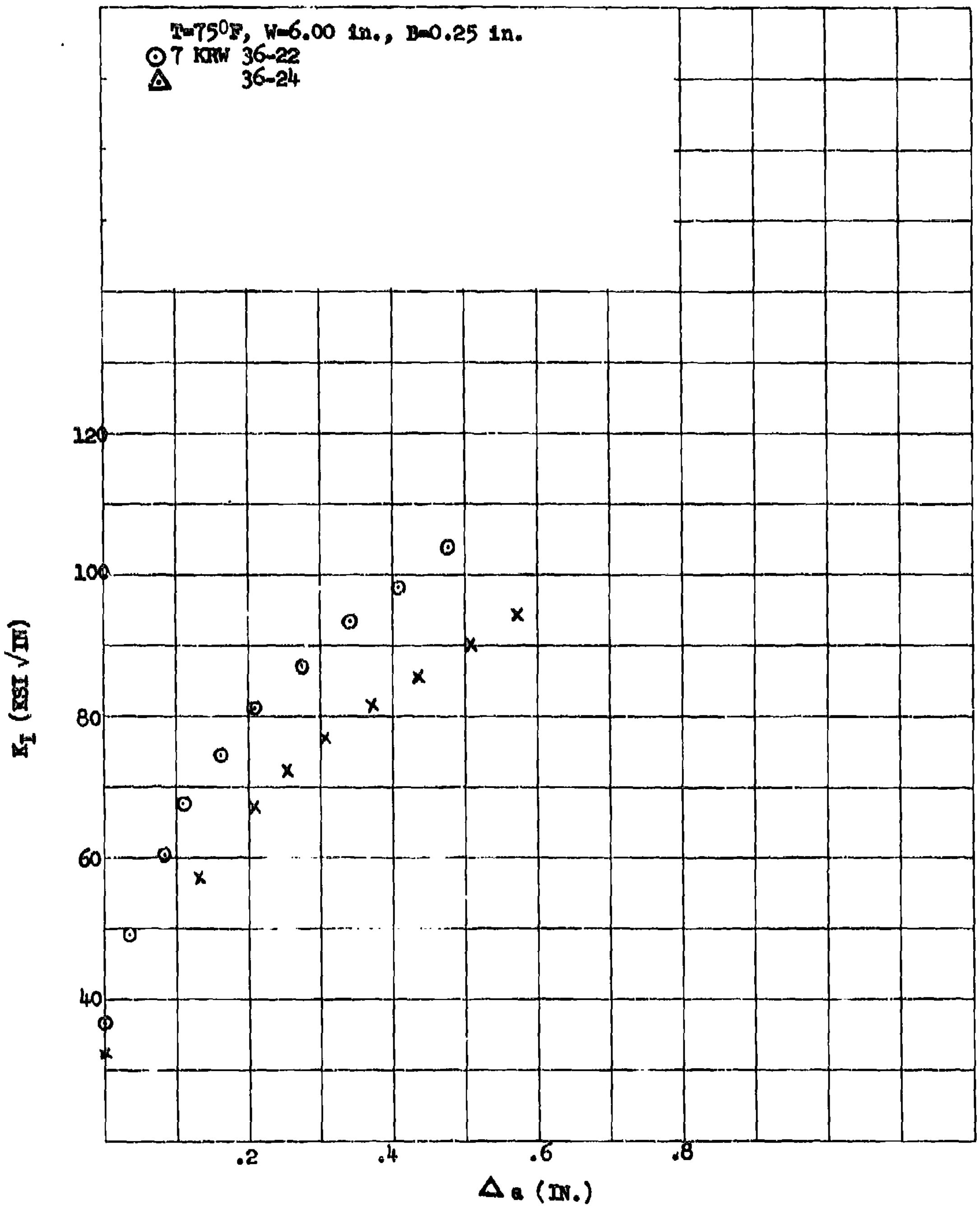

(c) RW Orientation at Thickness of 0.250 Inch

Figure 6-10 (Cont'd) R-Curves for 2219-T851 Plate, Material 7. (Page 2 of 3)

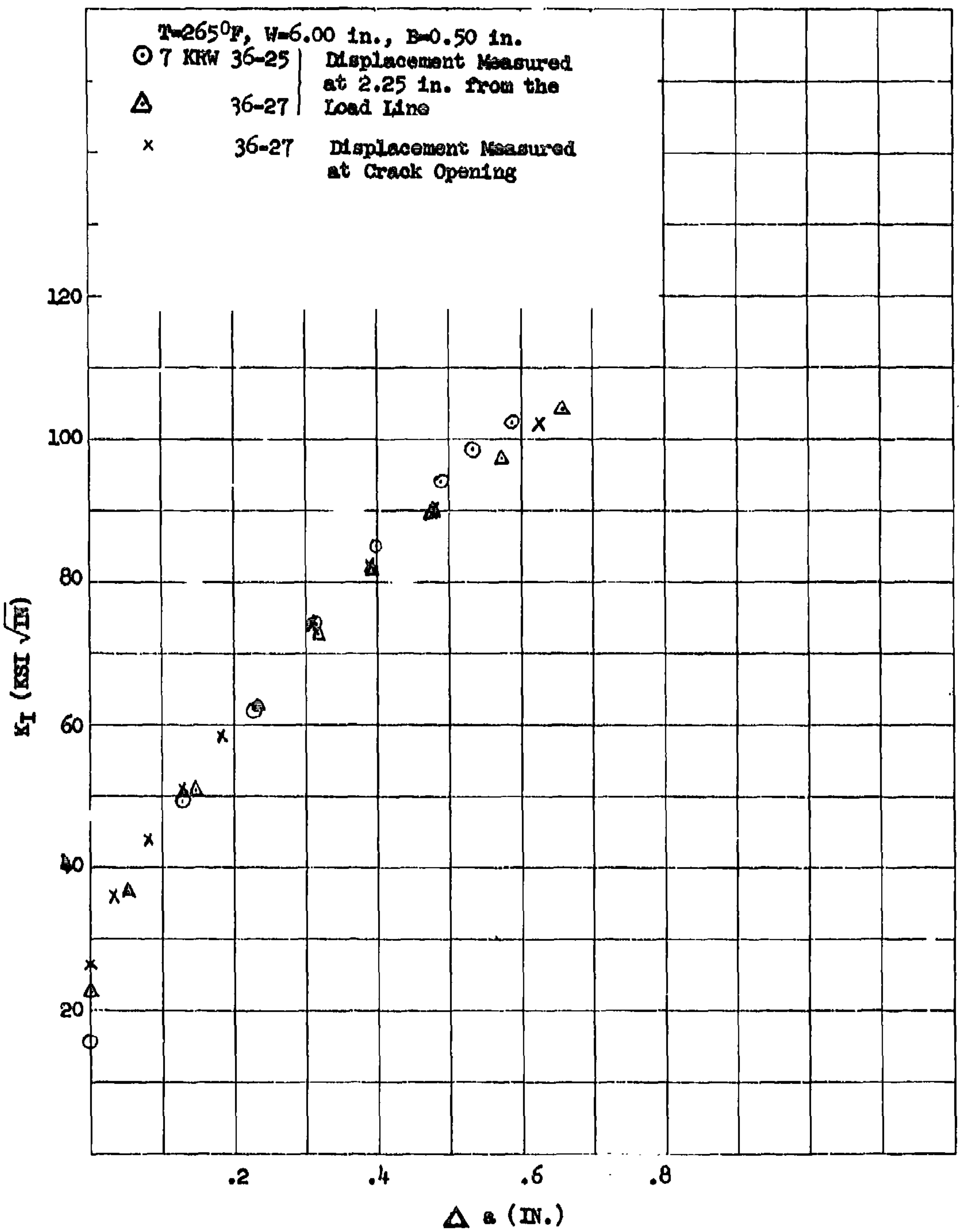

(d) RW Orientation at Thickness of 0.500 Inch and Temperature of 265°F

Figure 6-10 (Cont'd) R-Curves for 2219-T851 Plate, Material 7. (Page 3 of 3)

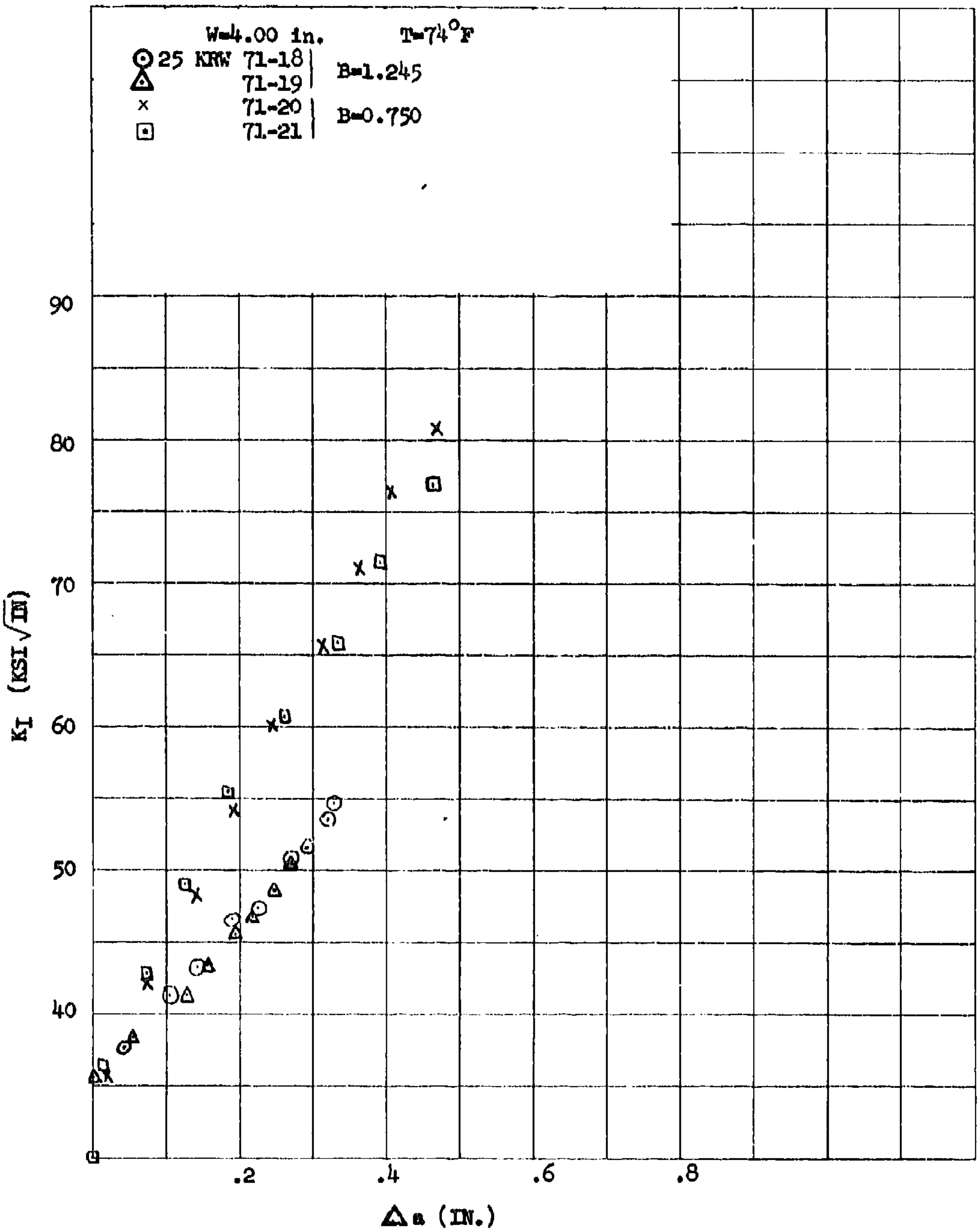

Figure 6-11 R-Curves for 7049-T73 Forging, Material 25.

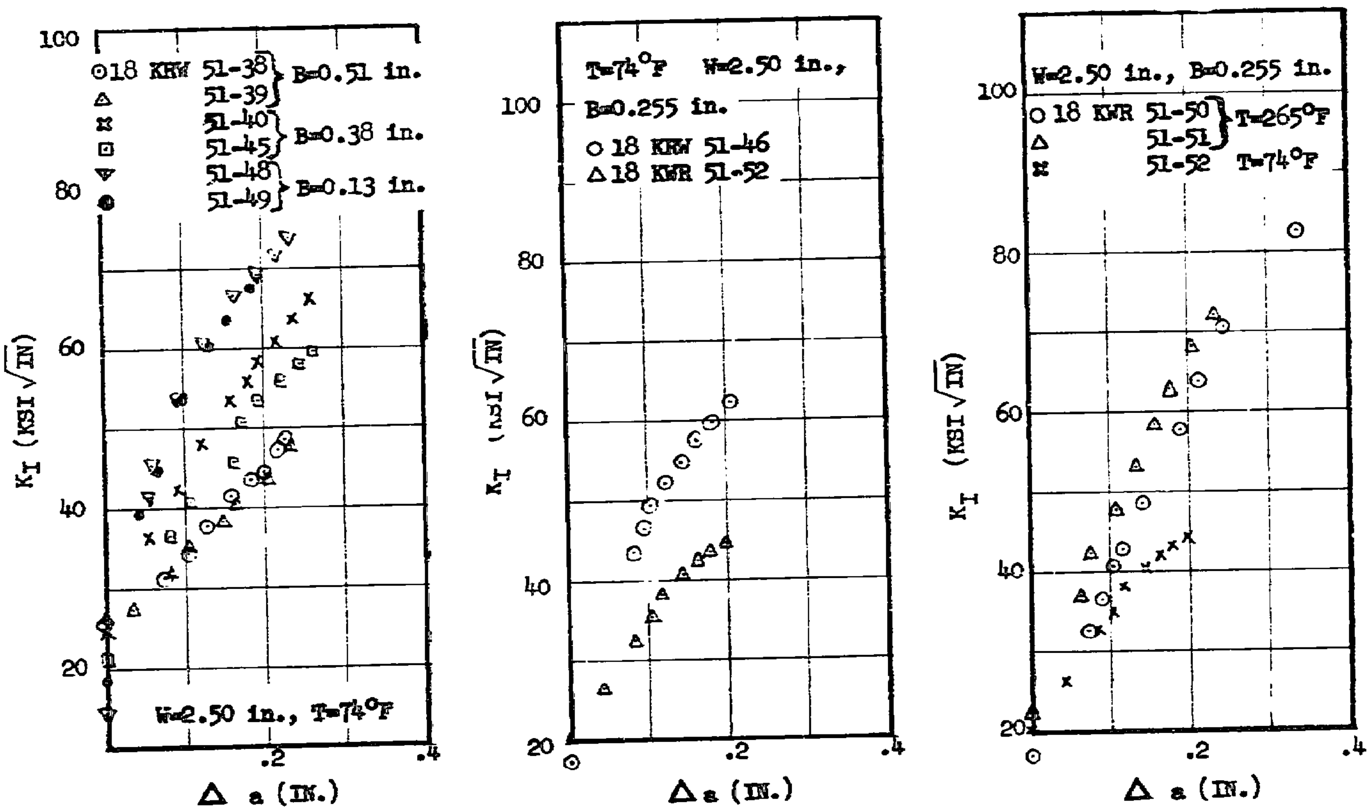

(a) RW Orientation at Thicknesses of 0.51, 0.38 and 0.13 Inches

(b) RW and WR Orientation at Thickness of 0.255 Inches

(c) WR Orientation at 74°F and 265°F

Figure 6-12 R-Curves for 7075-T7651 Plate

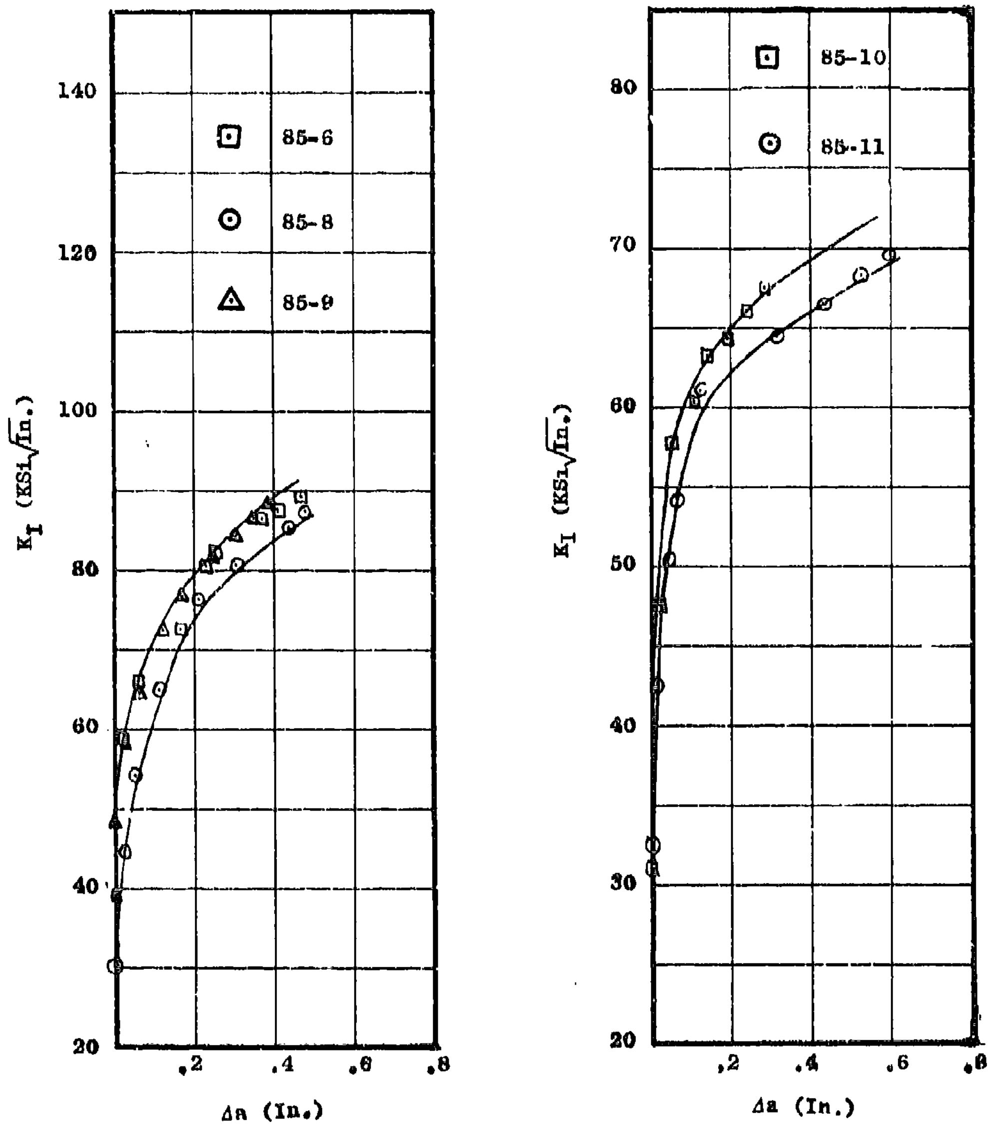

(a) RW Orientation

(b) WR Orientation

Figure 6-13 R-Curves for 7075-T76 Sheet, Material 30

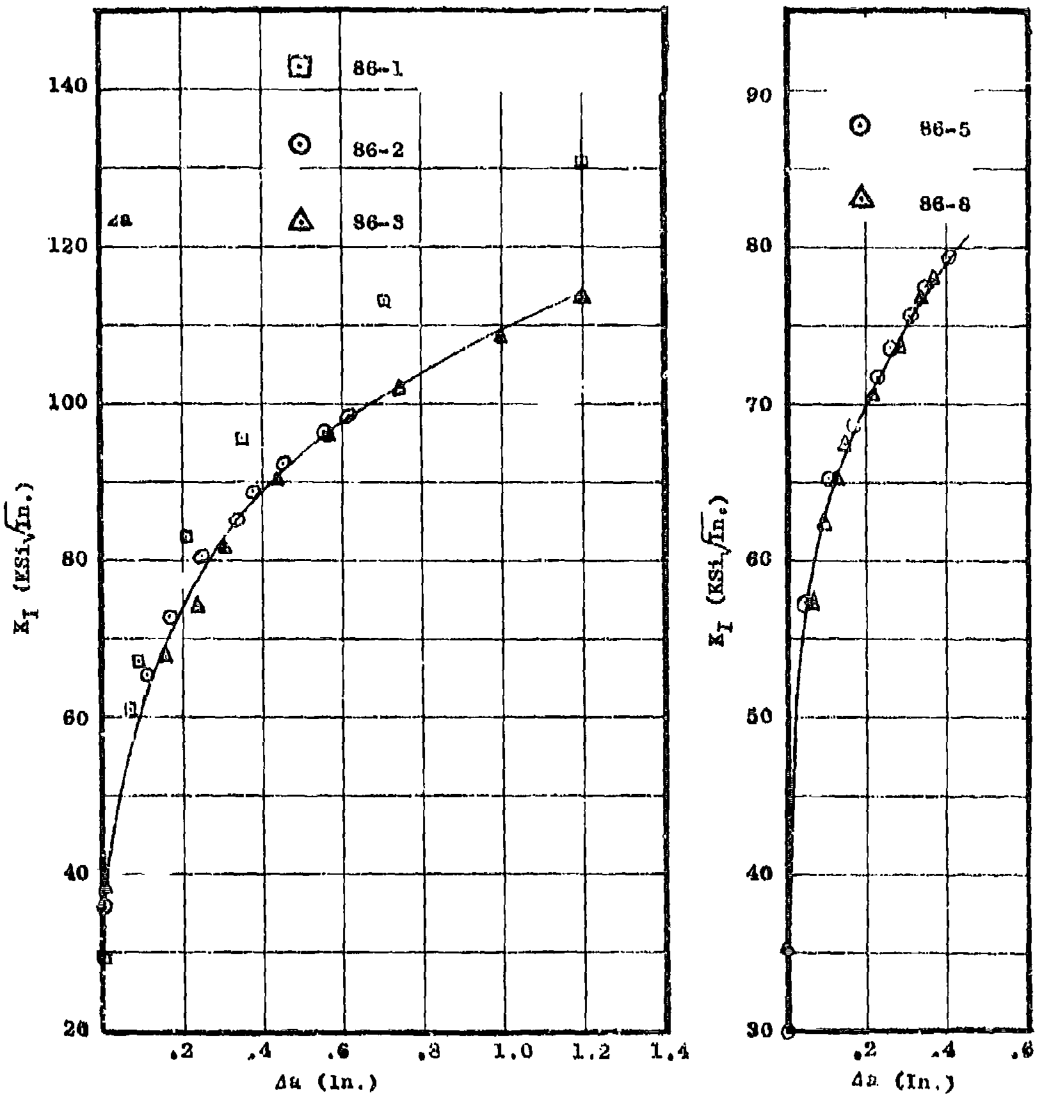

(a) RW Orientation (b) WR Orientation

Figure 6-14 R-Curves for 7075-T76 Sheet, Material 301

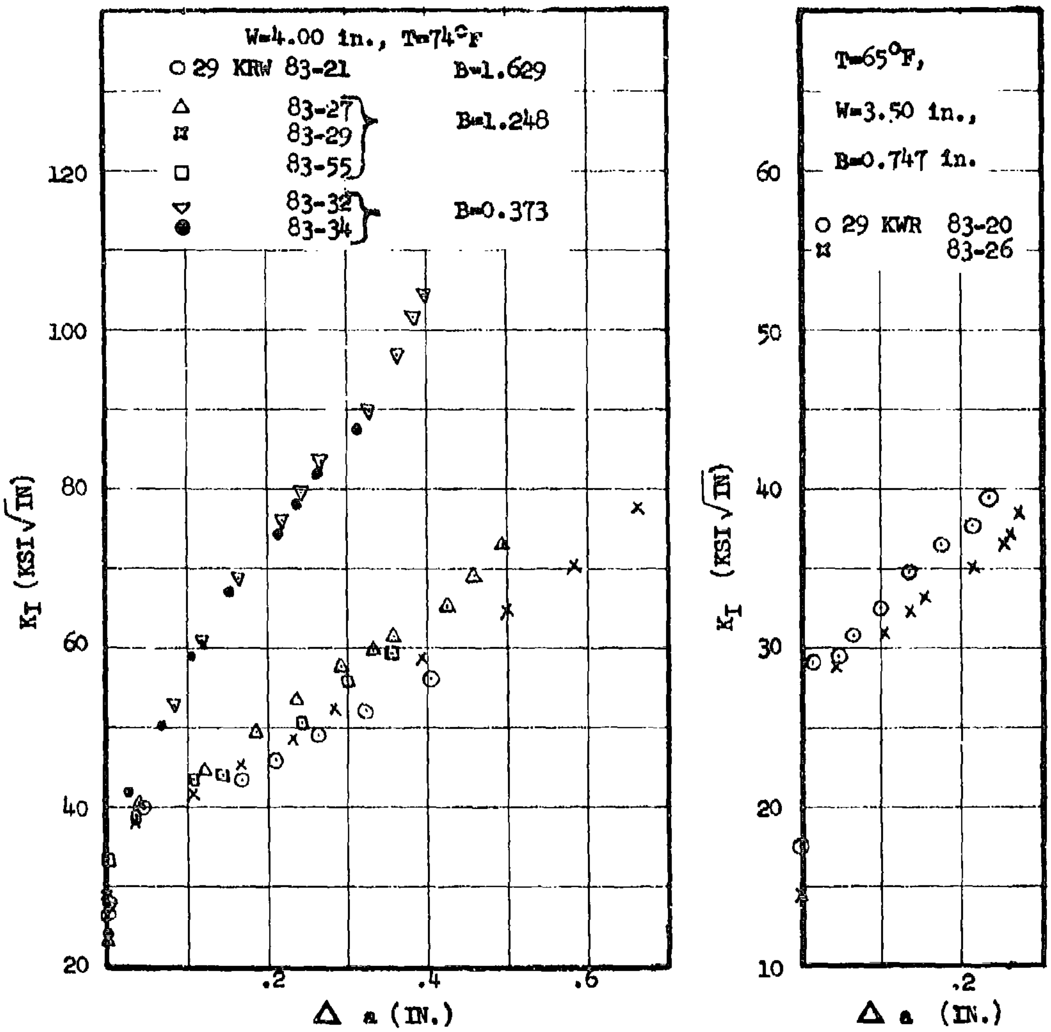

(a) RW Orientation at Thicknesses of 1.63, 1.25 and 0.37 Inches

(b) WR Orientation at Thickness of 0.747 Inches

Figure 6-15 R-Curves for 7075-T73511 Extrusion, Material 29. (Page 1 of 2)

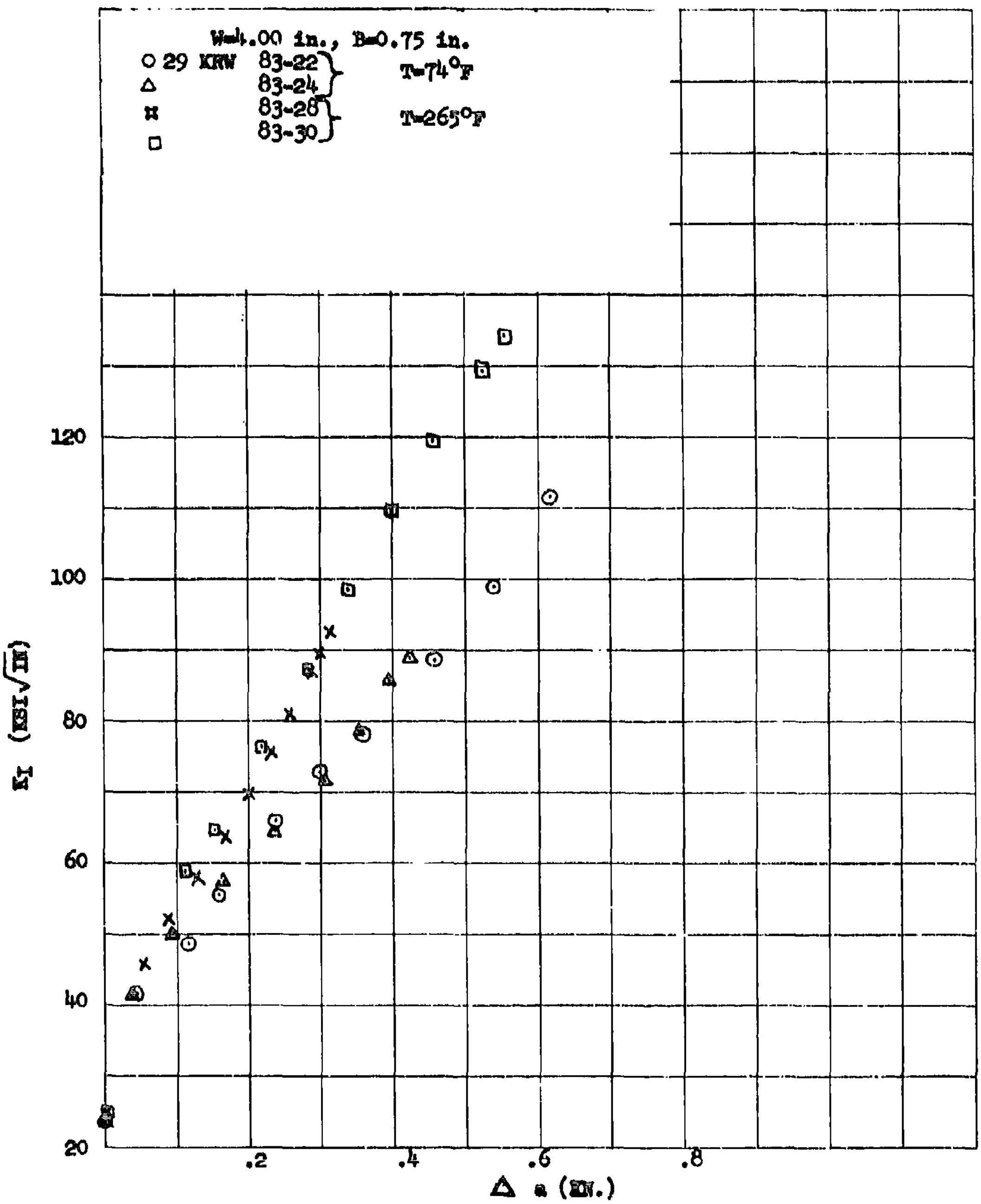

(c) RW Orientation at Thickness of 0.750 Inches and Test Temperatures of 74°F and 265°F

Figure 6-15 (Cont'd) R-Curves for 7075-T3511 Extrusion, Material 29. (Page 2 of 2)

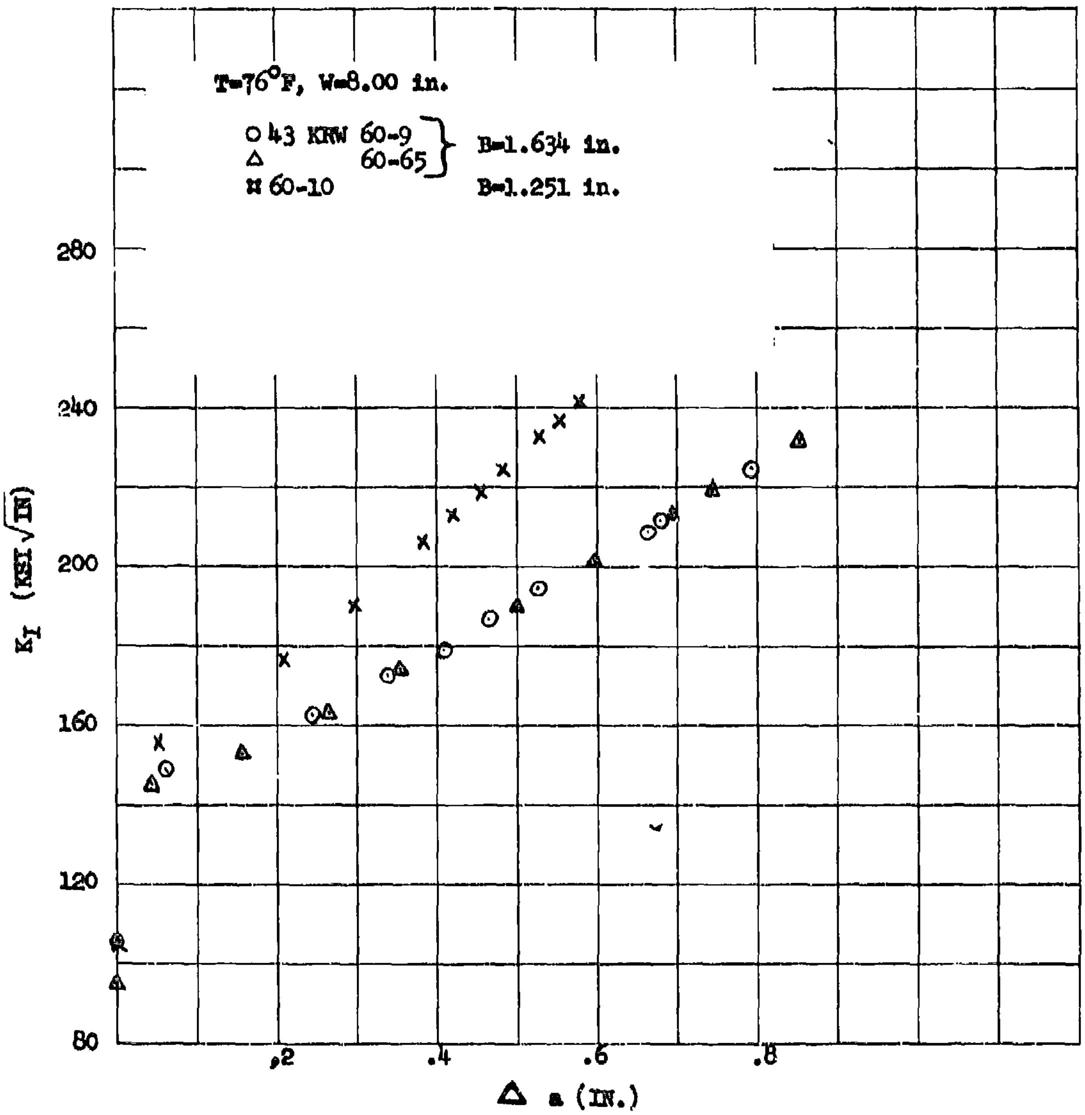

(a) Thicknesses of 1.634 and 1.251 Inches

Figure 6-16 R-Curves for HP 9Ni-4Co-.20C Forging, Material 43. (Page 1 of 3)

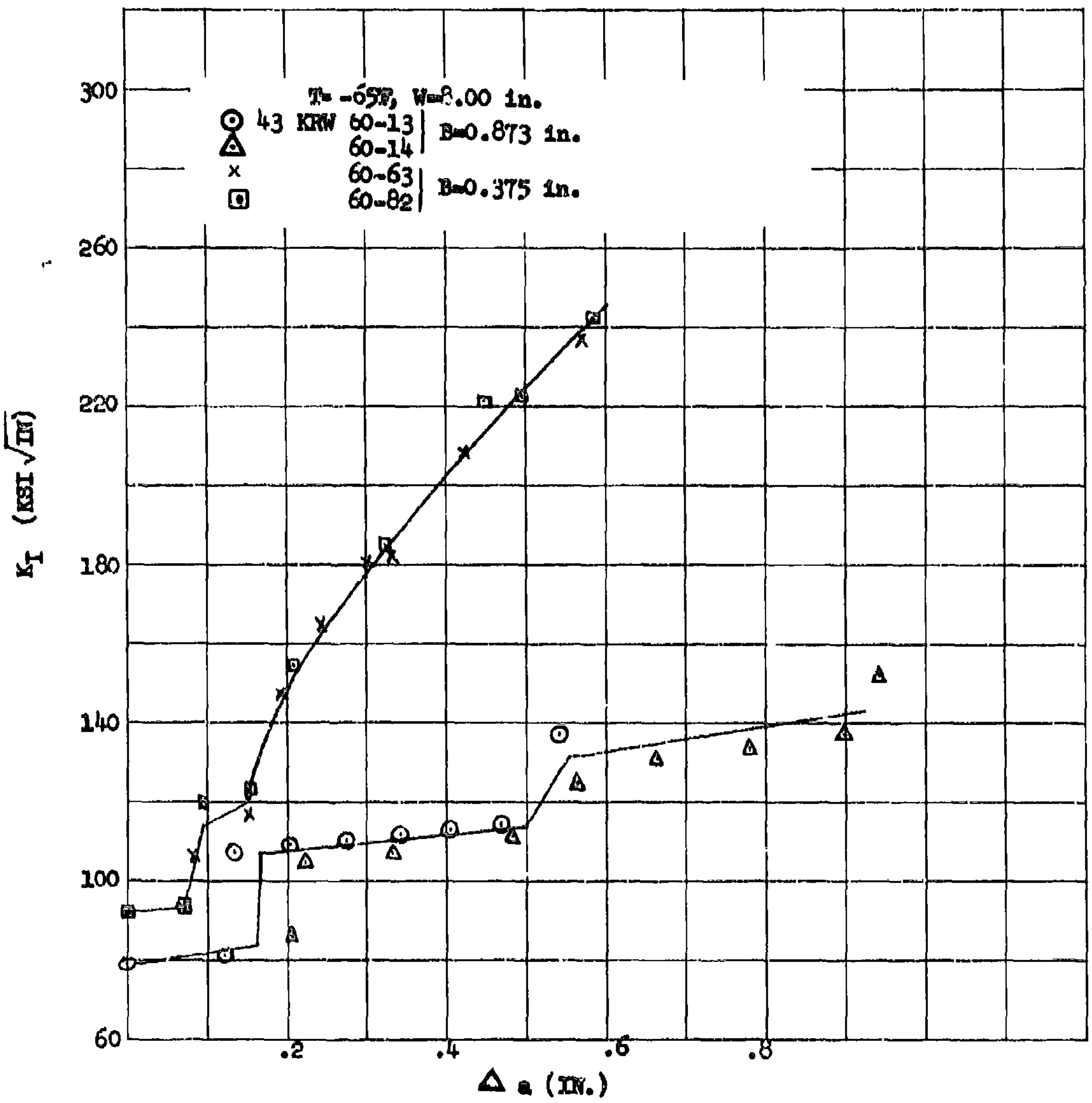

(b) Thicknesses of 0.873 and 0.375 Inches at -65°F

Figure 6-16 (Cont'd) R-Curves for HP 9Ni-4Co-.20C Forging, Material 43. (Page 2 of 3)

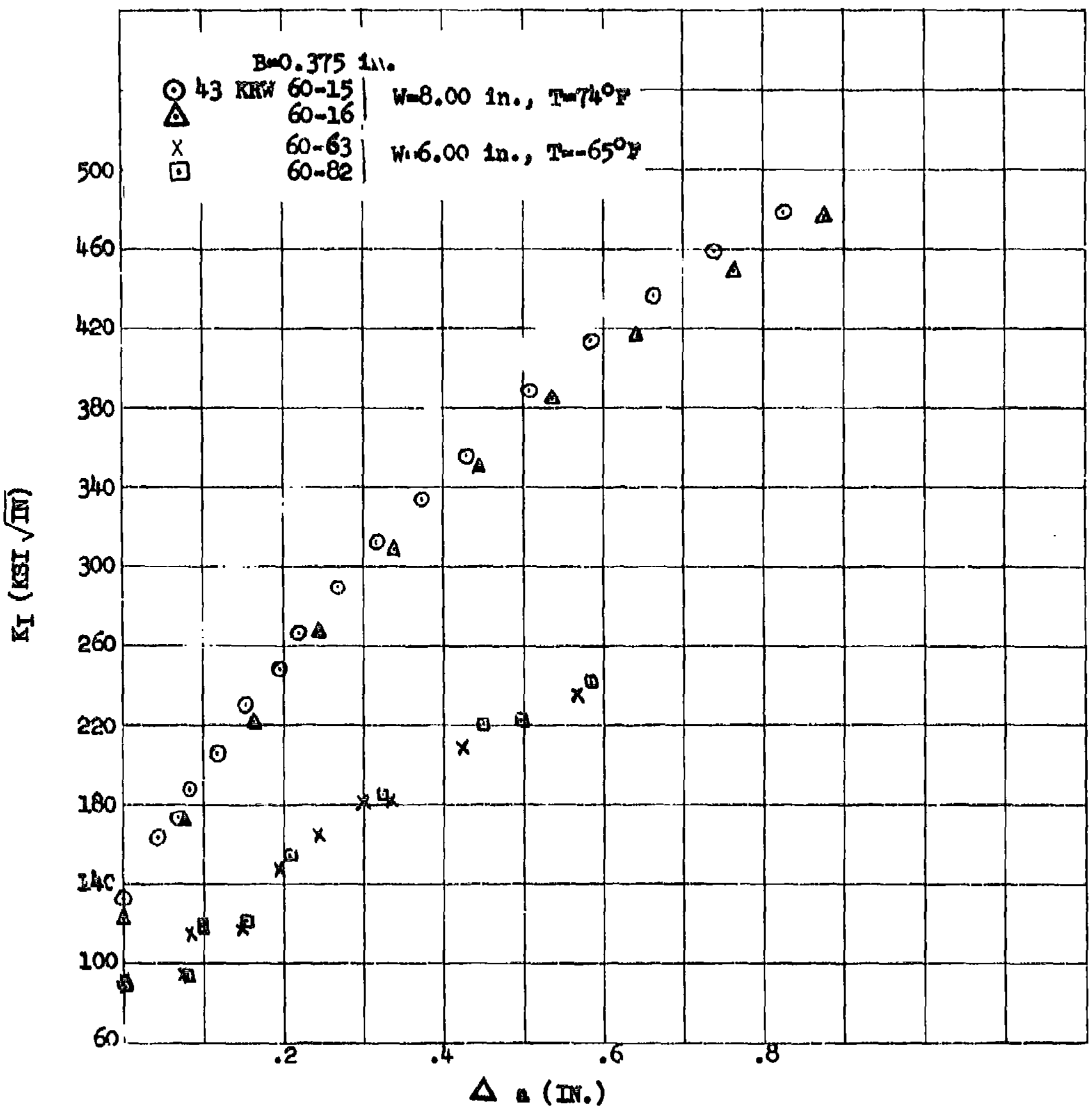

(c) Thickness of 0.375 Inches at 74°F and -65°F

Figure 6-16 (Cont'd) R-Curves for HP 9Ni-4Co-.20C Forging, Material 43. (Page 3 of 3)

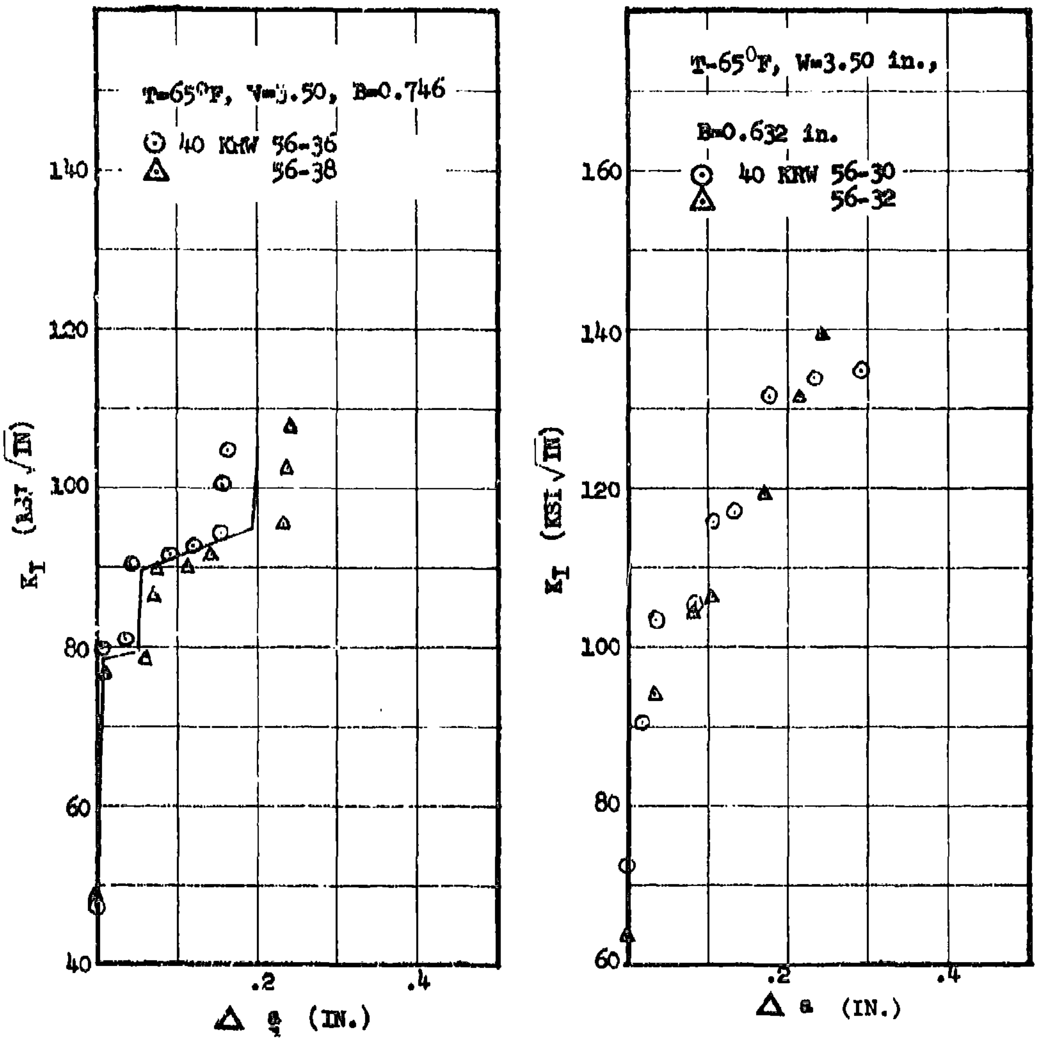

(a) Thickness of 0.746 Inches

(b) Thickness of 0.632 Inches

Figure 6-17 R-Curves for PH13-8Mo Rolled Bar, Material 40, H-1000 Condition. (Page 1 of 2)

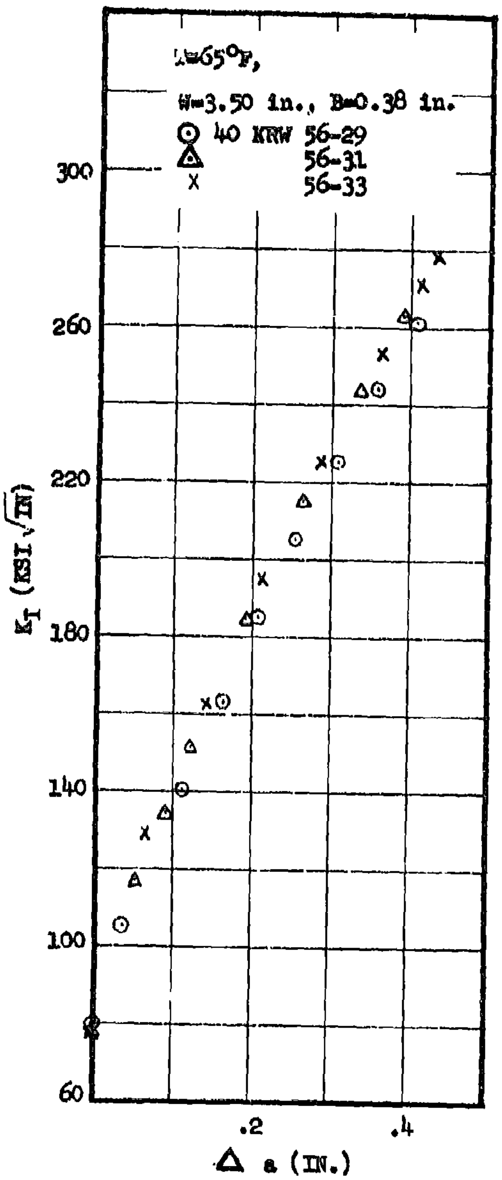

(c) Thickness of 0.380

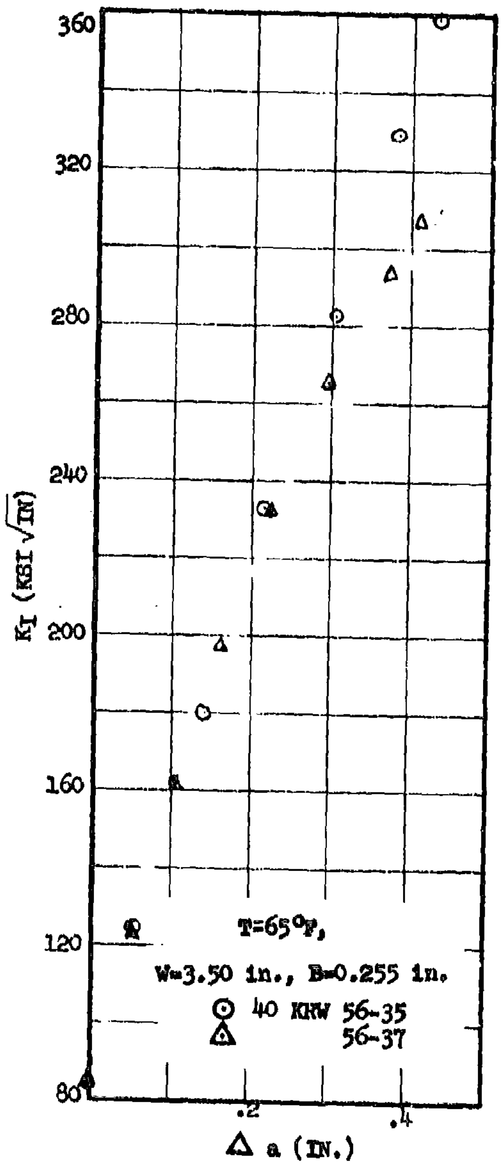

(d) Thickness of 0.255

Figure 6-17 (Cont'd) R-Curves for PH13-8Mo Rolled Bar, Material 40, H-1000 Condition. (Page 2 of 2)

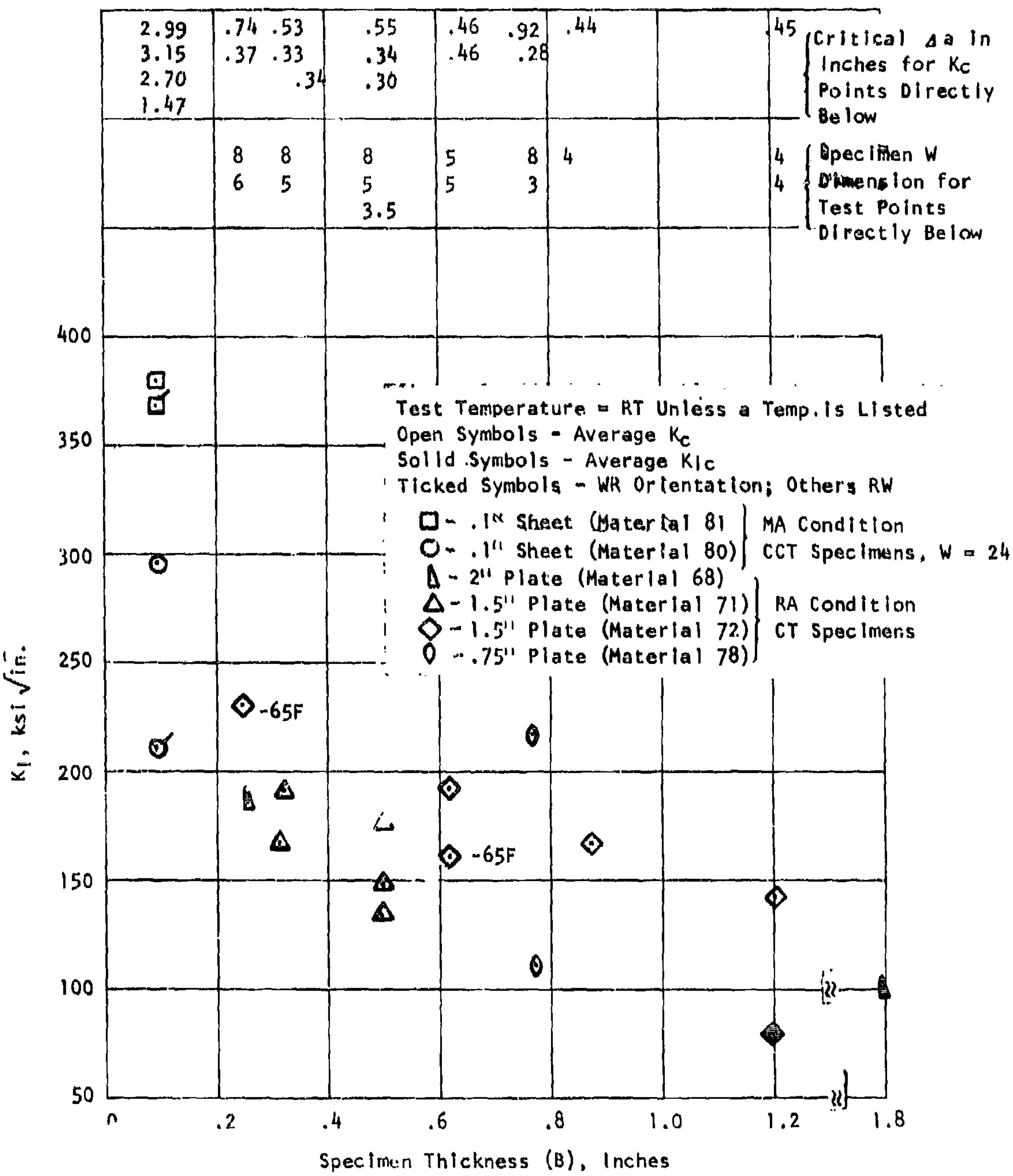

Figure 6-18. Effect of Specimen Thickness, Test Temperature and Grain Direction on K_c Values for Ti-6Al-4V Sheet and Plate

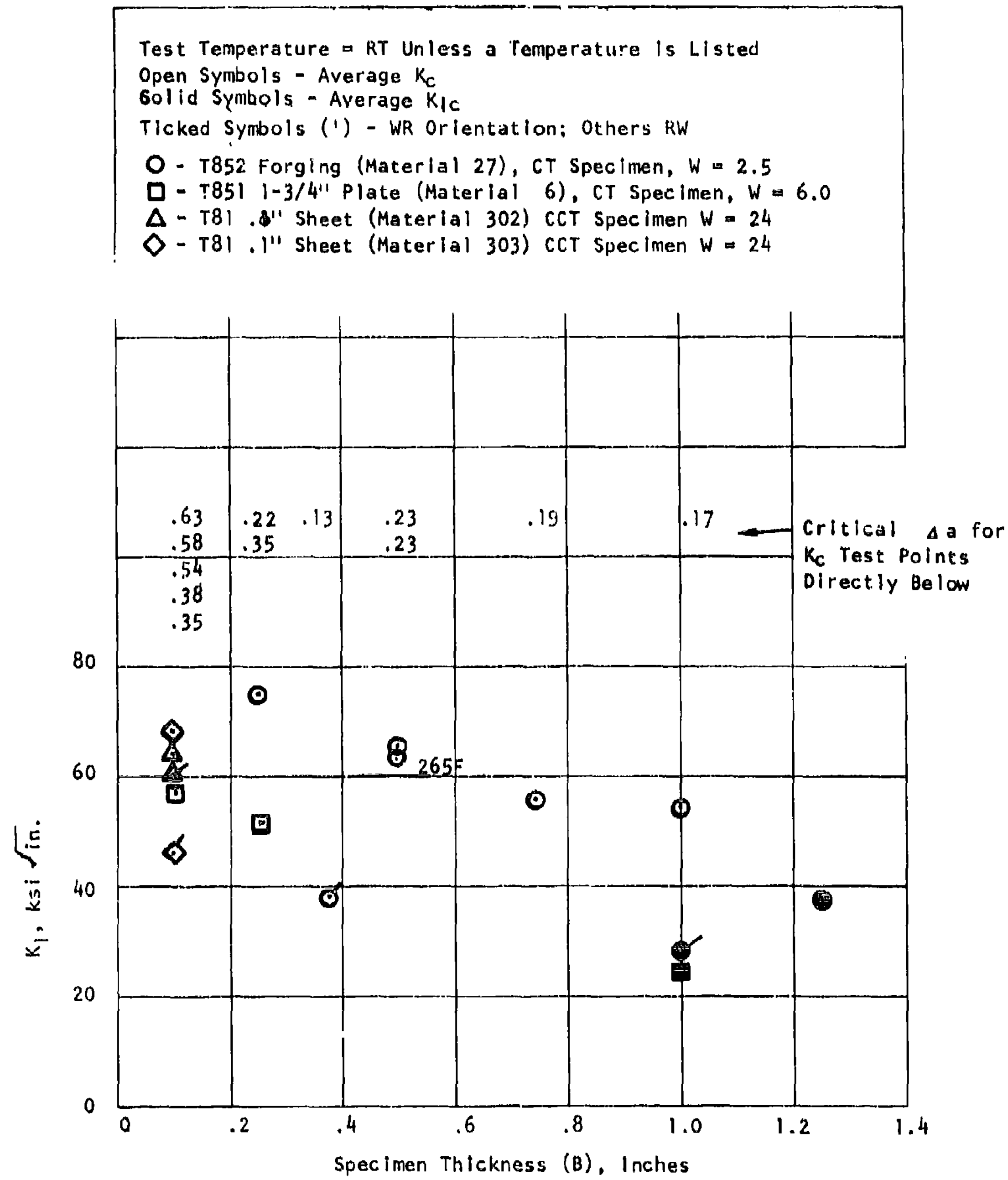

Figure 6-19. Effect of Specimen Thickness, Test Temperature and Grain Direction on K_c Values for 2024-T8XX Aluminum Alloy

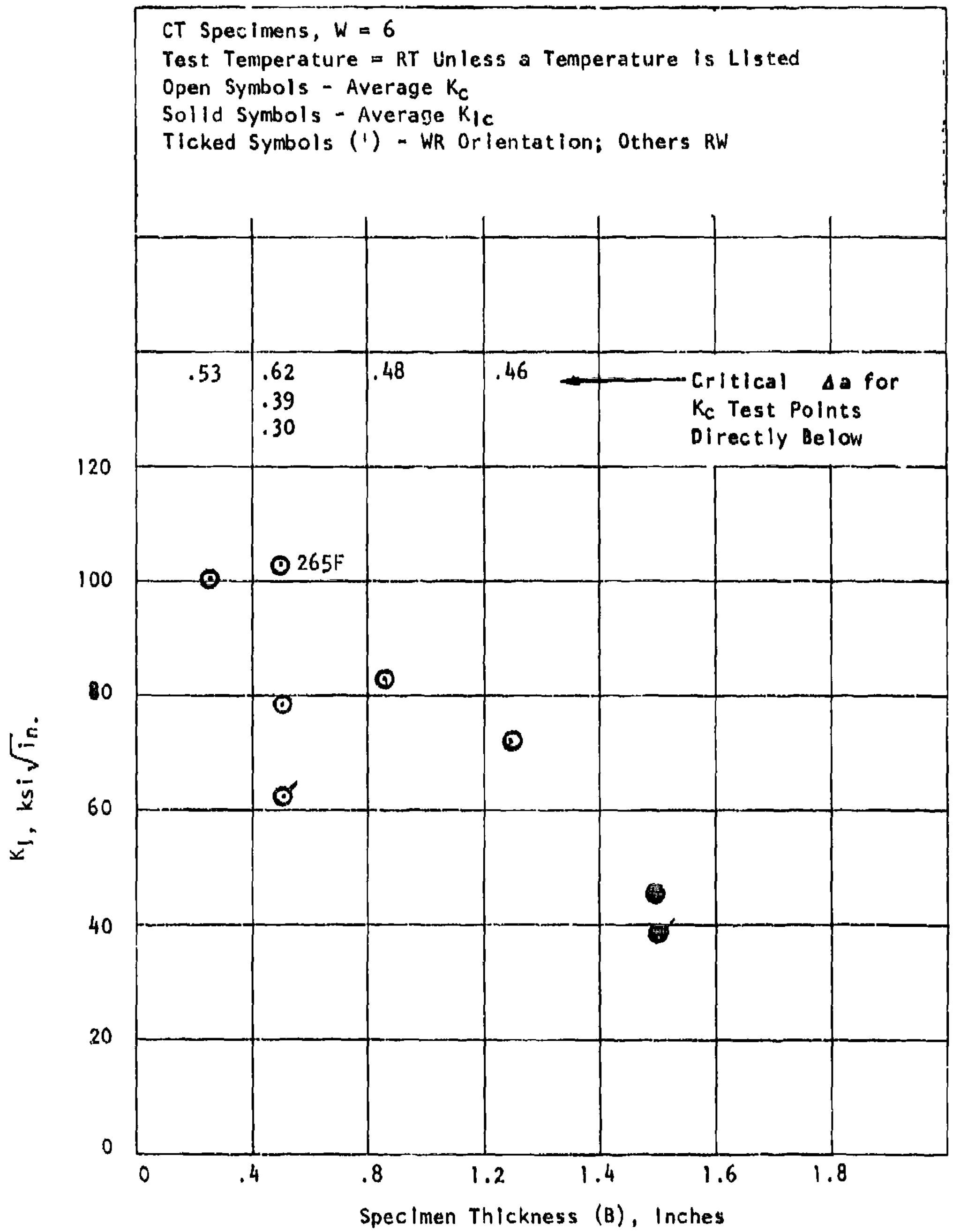

Figure 6-20. Effect of Specimen Thickness, Test Temperature and Grain Direction on K_c Values for 2219-T851 1-3/4" Plate Material 7

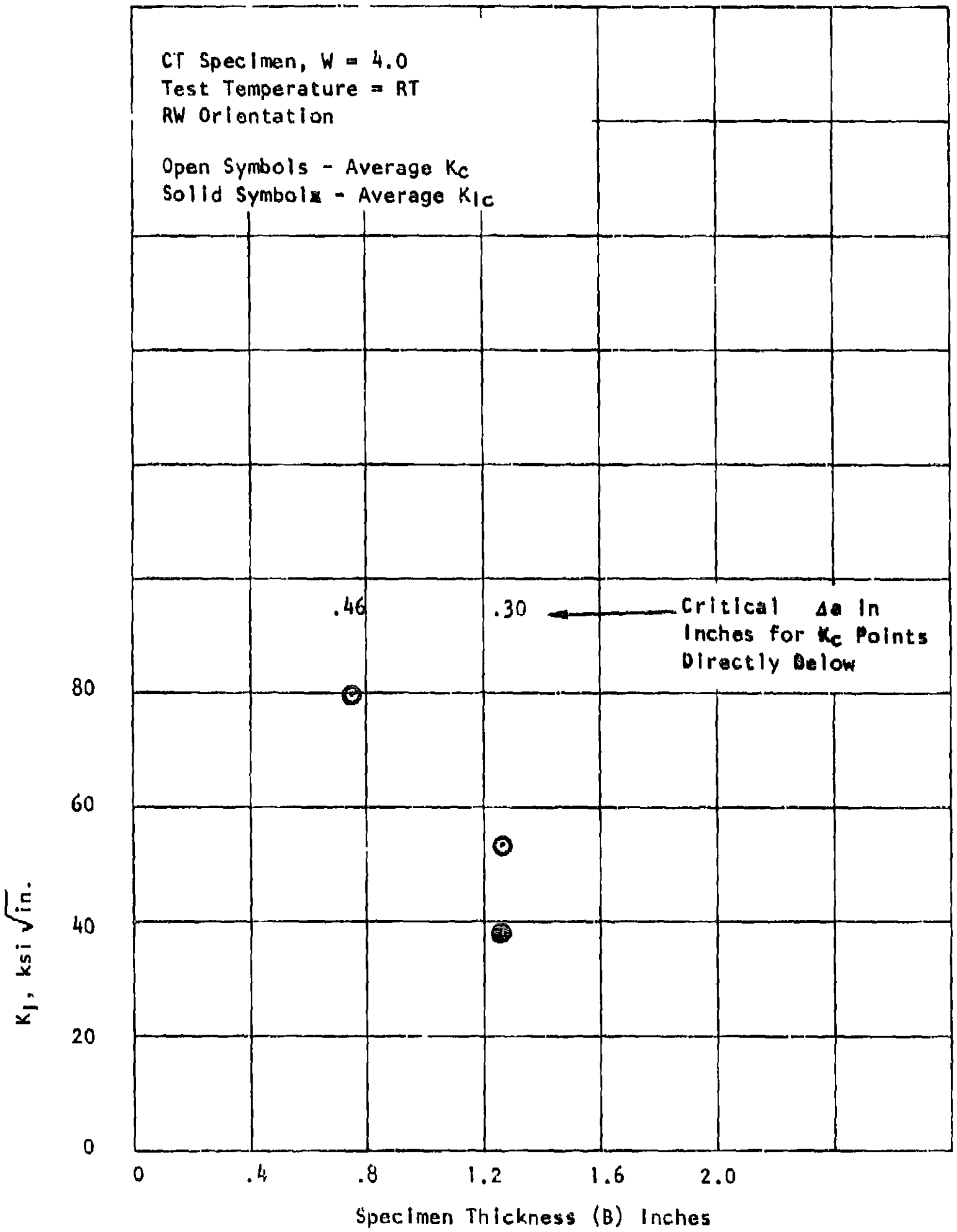

Figure 6-21. Effect of Specimen Thickness on K_c Values for a 7049-T73 Aluminum Alloy Forged Block (3 x 24 x 48", Material 25)

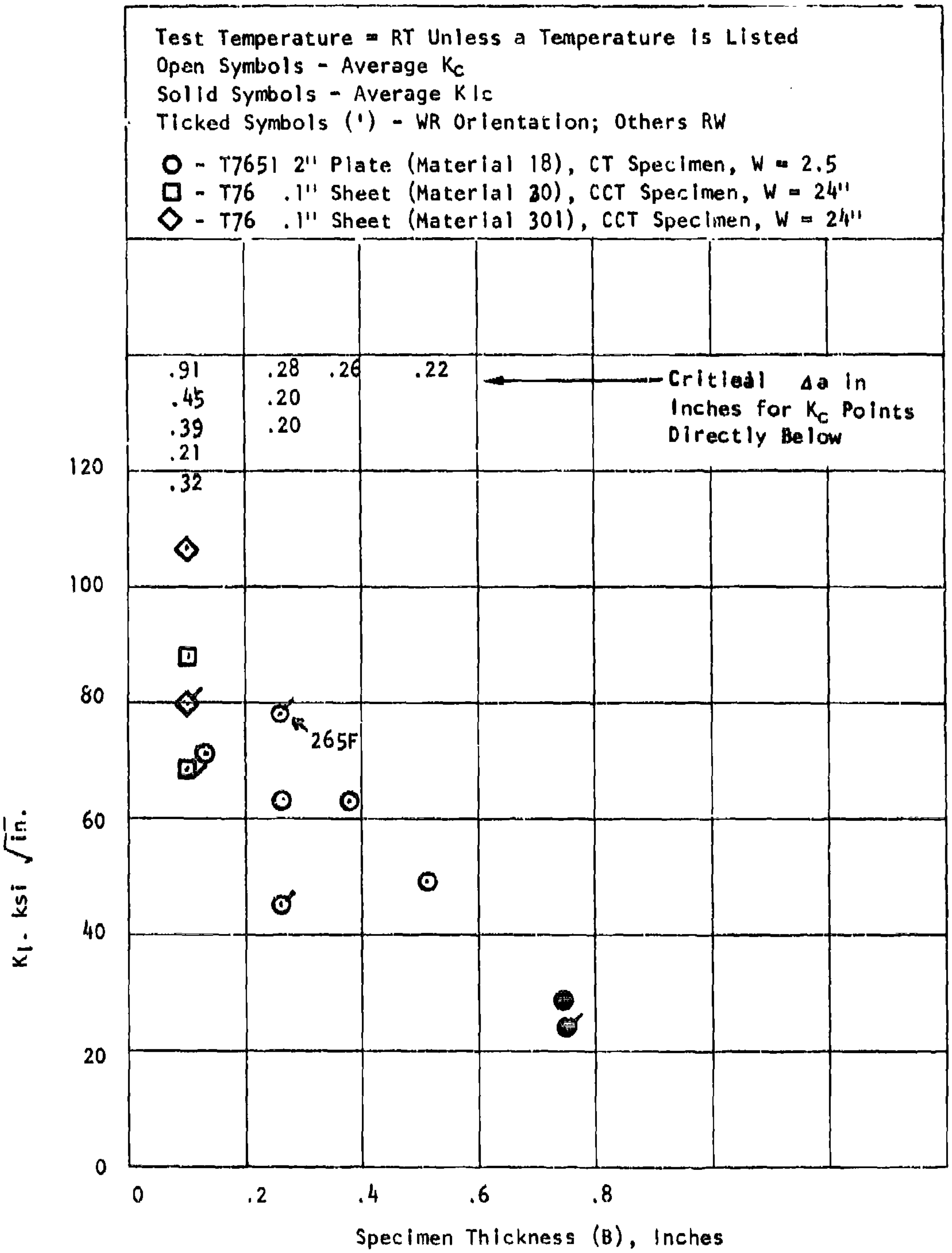

Figure 6-22. Effect of Specimen Thickness, Test Temperature, and Grain Direction on K_c Values for 7075-T76XX Aluminum Alloy

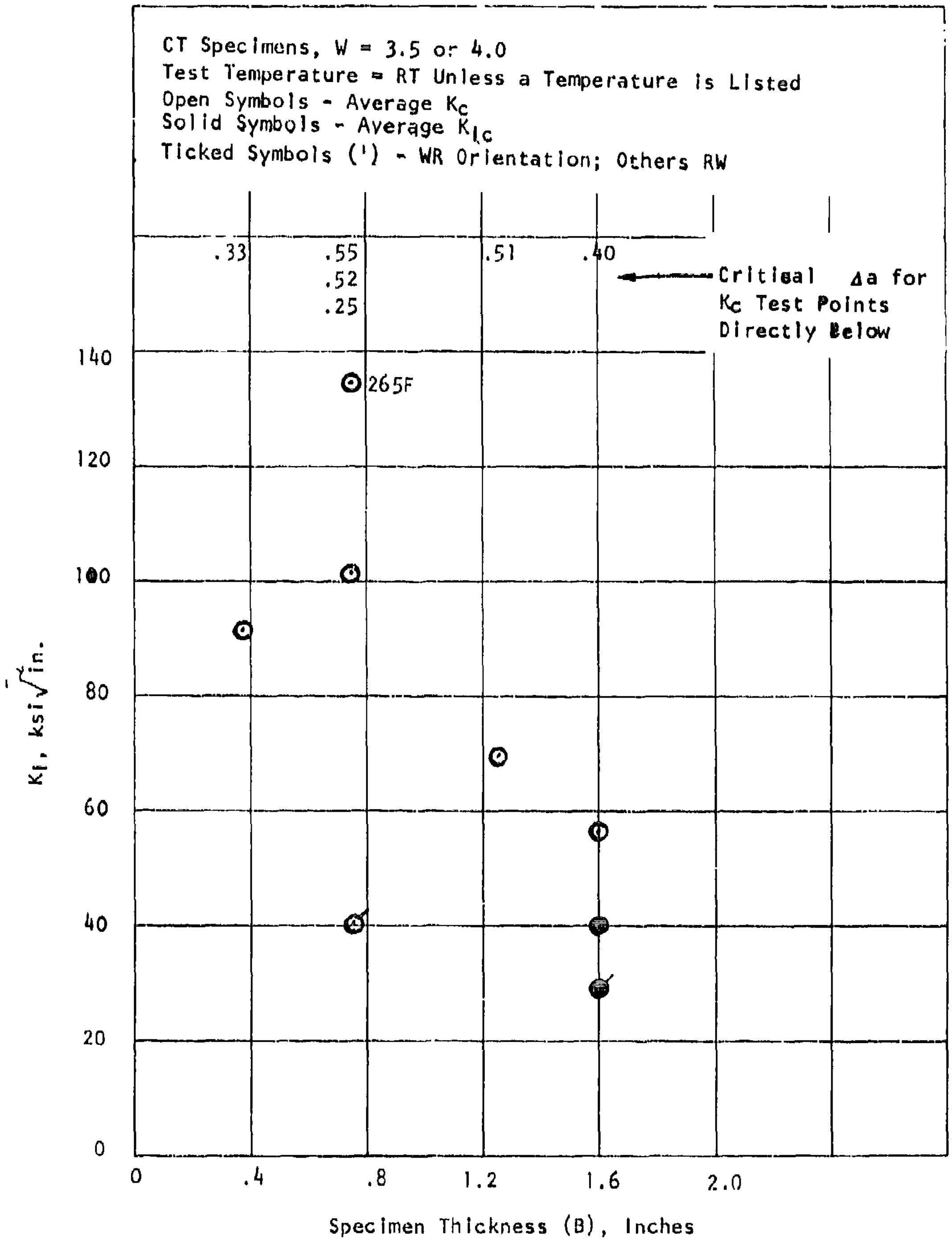

Figure 6-23. Effect of Specimen Thickness, Test Temperature and Grain Direction on K_c Values for a 7075-T73511 Extrusion (3 x 17", Material 29)

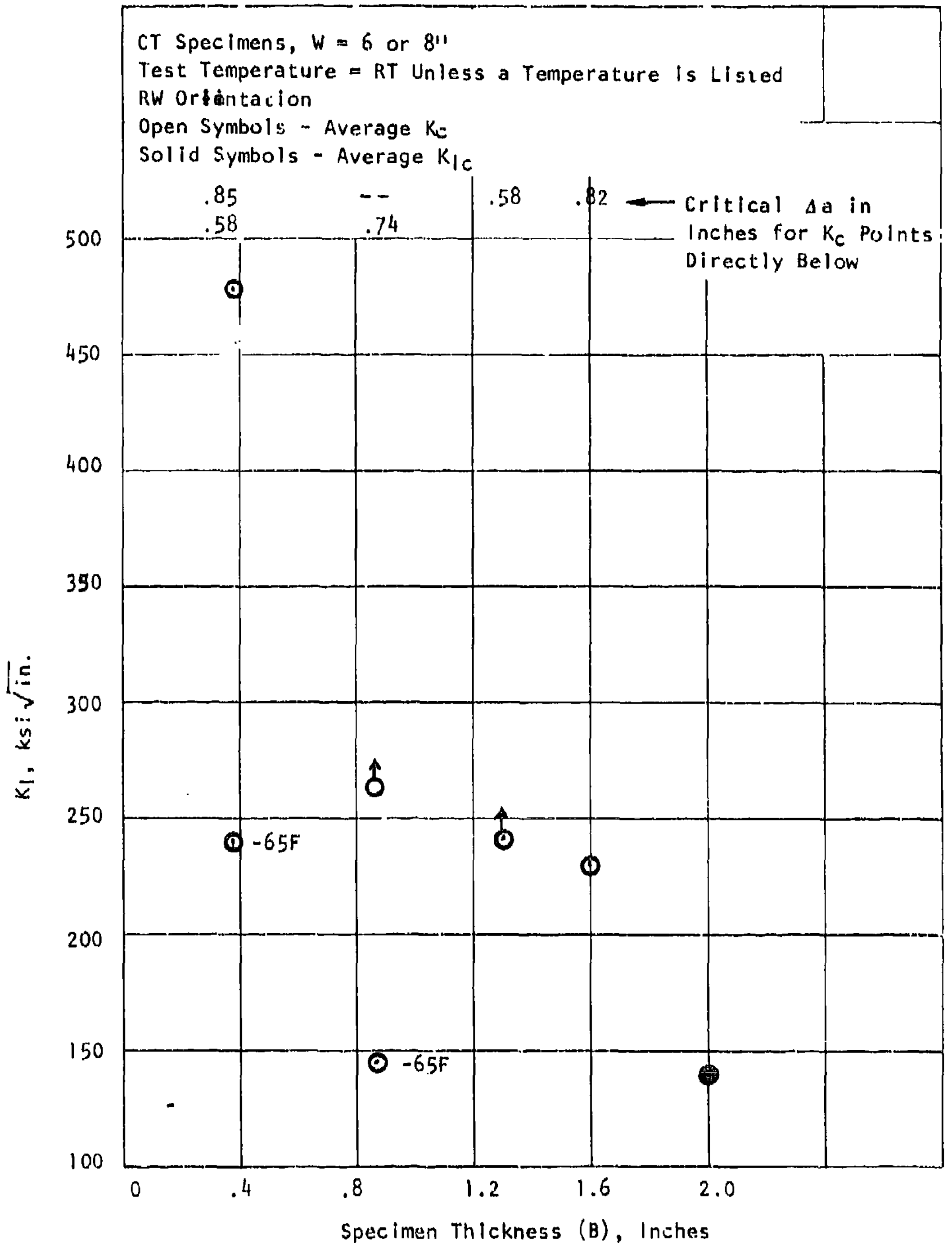

Figure 6-24 Effect of Specimen Thickness and Test Temperature on K_c Values for a 9-4-20 Steel Forged Billet (4 x 18 x 36", Material 43)

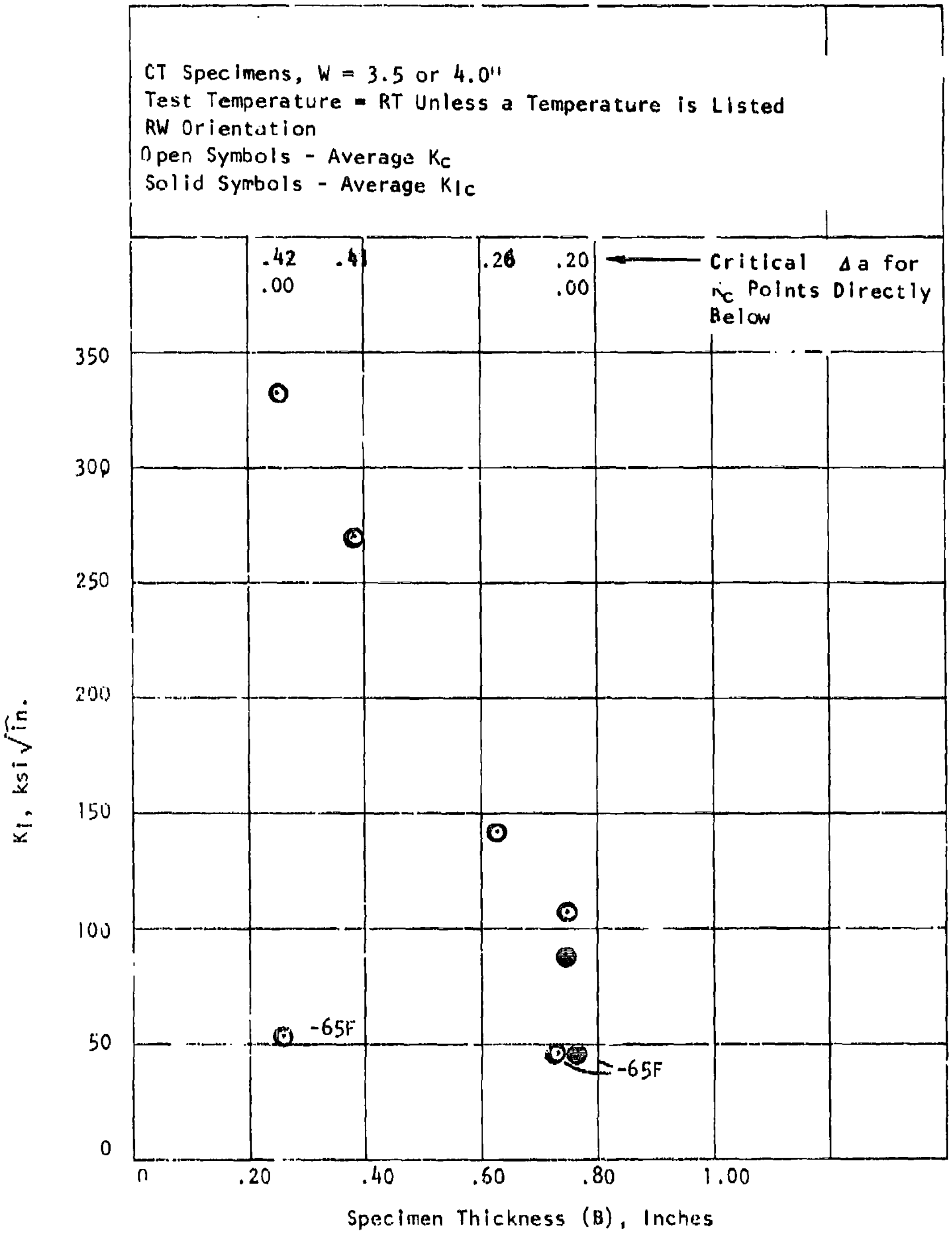

Figure 6-25 Effect of Specimen Thickness and Test Temperature on K_c Values for a PH13 ·°' Rolled Bar in the H1000 Heat Treat Condition (1.5 · ', Material 40)

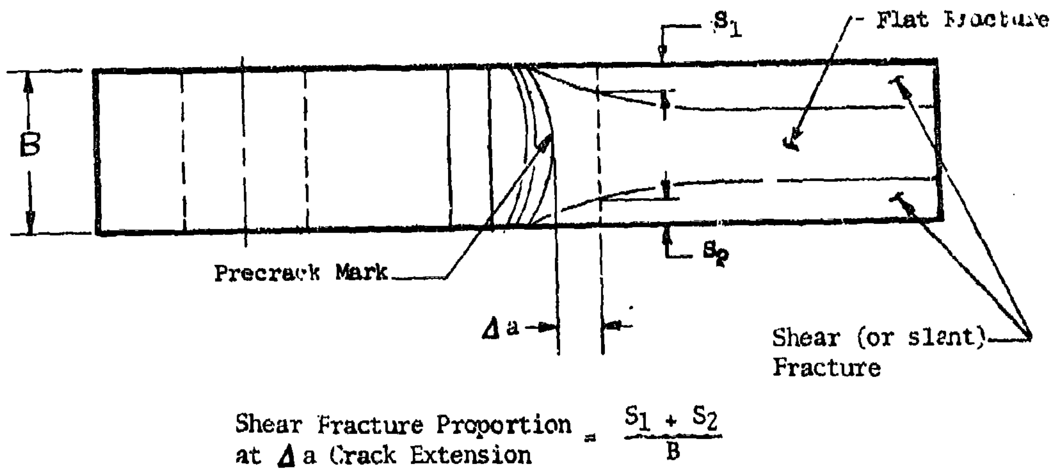

Figure 6-26 Typical Fracture Appearance of a Compact Tension Specimen

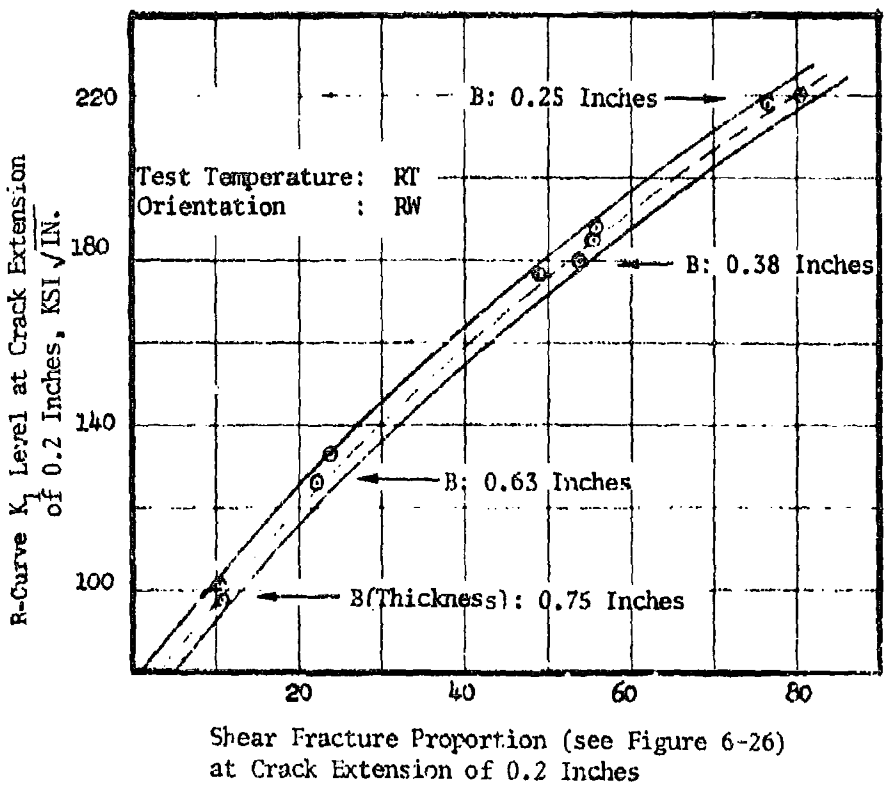

Figure 6-27 **Relationship between R-Curve K_1 Level and Fracture Appearance for PH13-8Mo K_c Specimens Having Different Thicknesses (Material 40)**

SECTION 7 - K_{ISCC} TEST DATA

7.1 TEST RESULTS

The individual test results for all K_{Iscc} type testing are presented in Tables 7-1 through 7-17, while average values of tests are shown in Tables 7-18 through 7-22. Graphical comparisons of these results are shown in Figures 7-1 through 7-4. The actual arrangement of these tables and figures is as follows:

Tabular or Graphical Presentations of Results

Alloy System	Individual Results	Average Value Results	Comparisons Of Results
Ti-6Al-4V	Tables 7-1 through 7-3	Table 7-18	Figure 7-1
Aluminum Alloys	Tables 7-4 through 7-10	Table 7-19	Figure 7-2
9-4-.20	Tables 7-11 through 7-12	Table 7-20	Figure 7-3
PH13-8Mo	Tables 7-13 through 7-14	Table 7-21	Figure 7-4
300M, Inconel 718, MP35N	Tables 7-15 through 7-17	Table 7-22	—

The tables containing individual specimen results present two types of data: (1) K_I level as a function of test time calculated from crack trace measurements, and (2) initial K_I, final K_I and total crack growth based on crack front measurements made on the fracture face after completion of the test. For most specimens, the K_I level calculated from crack trace measurements are higher than those calculated from crack front measurements. This difference is due to the curvature of the crack front which results in the crack length being greatest at the specimen mid-thickness position.

The time-dependent nature of K_{Iscc} results has been indicated in the tables by first presenting discrete K_I levels measured throughout the tests, followed by the times during the tests at which these measurements were made. The latter values have been enclosed in parentheses to avoid confusion. An example of such designation is as follows:

74 (0), 71 (5), 70 (30-862)

Initial K_I level of 74 ksi $\sqrt{in}$ at start of test, "0" hours.

At the end of 5 Hrs., crack growth had reduced the K_I level to 71 ksi $\sqrt{in.}$

At the end of 30 Hrs., crack growth had reduced the K_I level to 70 ksi $\sqrt{in.}$ No additional crack growth occurred during the test. Total test time was 862 hours.

The K_I levels and total crack growth based on crack front measurements are shown in the tables by first listing the initial K_I level (K_{Ii}), then the final K_I level (K_{If}), followed by the total crack growth (in inches) enclosed in parentheses, as illustrated in the following example:

74-62 (.18)

Initial K_I level of 74 ksi $\sqrt{in}$ at start of test (K_{Ii}).

A total of .18" of crack growth occurred during the test reducing the K_I level to 62 ksi $\sqrt{in}$ (K_{If}).

The K_I levels employed in some tests were above the specimens' capability to maintain a plane strain condition. In these cases $[B < 2.5\,(K_{Iscc}/TY)^2]$, a mixed mode stress state existed. In the tables of individual specimen test results, the plane strain K_I level capability of each specimen is listed to indicate whether the stress state in the specimen was plane strain or mixed mode.

In the summary tables of average test values, two values are listed in the K_{Iscc} column if the stress state in the specimen was mixed mode, as shown below:

>54, (93)[a]

In the above example the first value is the plane strain capability of the test specimen, while the second value enclosed in parentheses is the actual value obtained for the test. The superscript "a" indicates a mixed mode stress state. The ">" is shown to indicate that the value obtained from this test exceeded the plane strain capability of the test specimen.

7.2 DISCUSSION OF TEST RESULTS

7.2.1 Ti-6Al-4V (Tables 7-1 thru 7-3 and 7-18)

Stress corrosion cracking occurred in most of these specimens. Generally, the crack growth (obtained from crack front measurements) was in the range of .05 to .30" with the amount of crack growth greatest at specimen mid-thickness where the lateral restraint was the highest (Figure 7-5). A number of specimens had over .15" of crack growth at the center of the crack front and none at the specimen sides. Crack trace measurements could not be depended upon to indicate the occurrence of stress corrosion cracking.

The field cleaning solvent (FCS) and shop cleaning solvent (SCS) environments appeared to be slightly less aggressive than the sump tank water (STW) environment.

The tests did not show grain direction to have a major effect on stress corrosion cracking.

The average K_{Iscc} values in STW for plate (4 lots) and forgings (4 lots) in the RA condition were 61 and 59 ksi $\sqrt{in}$, respectively, suggesting that both product forms have about the same K_{Iscc} value. However, the lot to lot variation for forgings was greater than that for plate.

Exposure of Ti-6Al-4V to a diffusion bonding thermal cycle (DBTC) appears to increase its susceptibility to stress corrosion cracking over that of material in an RA condition. The average K_{Iscc} value for eight lots of plate after exposure to a DBTC was 56 ksi $\sqrt{in}$ as compared to 61 ksi $\sqrt{in}$ for four lots of plate evaluated in an RA condition (Table 7-18). One of the plate lots, material 72, had a K_{Iscc} value in a DBTC condition of 44 ksi $\sqrt{in}$. This is much lower than the lowest K_{Iscc} value of 53 ksi $\sqrt{in}$ obtained on the other seven lots of plate in the same condition, and the lowest value of 58 ksi $\sqrt{in}$ obtained for the four lots of plate evaluated in an RA condition. Apparently material 72 was abnormally susceptible to stress corrosion cracking in a DBTC condition.

The K_{Iscc} values for the diffusion bond joints in plate (material 74) and for the hot formed plate which had been slow cooled to 1100F, fell within the range of values obtained on plate in a DBTC condition.

In general, higher K_{Iscc} values were obtained on weld joints than were obtained on parent metal. This may be due to the fact that the lateral restraint in the 1/8, 1/4 and 1/2" thick weld joints was much less than in the 1" thick parent metal specimens causing the stress state in the welded specimens to be mixed mode (plane stress and plane strain) rather than plane strain, as in the parent metal specimens. That the susceptibility of the

alloy to stress corrosion cracking is dependent upon the degree of lateral restraint is indicated by the internal nature of the cracking in the specimens. The test results did not reveal any difference between the various post weld stress-relieving treatments on the corrosion cracking of welds (1100F - 2 hrs, 1200F - 1/2 to 1 hr, 1400F - 1/2 to 1 hr).

7.2.2 Aluminum Alloys (Tables 7-4 thru 7-10 and 7-19, Figure 7-2)

Crack growth occurred in about half of the specimens and did not exceed .23" in length. In most cases the crack growth was internal and did not extend to the specimen sides. Crack extension was greatest at specimen mid-thickness where the lateral restraint conditions were the highest.

The STW environment produced general corrosion and pitting of the specimen surfaces. Because of this general corrosion, it was difficult to determine the edge of the fatigue precrack on the fracture faces of some of the specimens with long test exposures. The SCS environment did not produce any visible surface corrosion and the FCS produced only a slight surface tarnish. The aggressiveness of the FCS and SCS environments with respect to stress corrosion cracking did not exceed that of the STW environment.

K_{Iscc} values for RW and WR oriented specimens were 20 ksi $\sqrt{in}$ or greater for all of the aluminum alloys evaluated. The lowest K_{Iscc} value obtained (13 ksi $\sqrt{in}$) was for the short transverse direction of 7075-T7651 plate. The highest K_{Iscc} values were obtained on 2219-T851 plate. Values for all directions for 2219-T851 plate were 27 ksi $\sqrt{in}$ or higher. K_{Iscc} values for 2124 were 23 ksi $\sqrt{in}$ or greater and for 2024, 21 ksi $\sqrt{in}$ or greater.

K_{Iscc} values as a percentage of the material K_{Ic} were above 64% for all alloys except for the longitudinal direction in 7049 alloy.

7.2.3 9-4-20 Steel (Tables 7-11, 7-12 and 7-20, Figure 7-3)

Stress corrosion cracking up to .31" in length occurred in all specimens tested in the STW environment. Cracking extended to the sides of the specimens in all except one case where the crack growth was only .03". In general, crack growth rates at the end of each test were under .0005 inches per hour based on crack trace measurements.

In some specimens the crack forked at the end of the precrack at the sides of the specimen but was normal in the interior (horizontal). On these specimens it appeared that cracking had occurred first in the interior on a horizontal plane, thus raising the stress on the remaining surface ligaments which then had cracked on 45 to 70° angles.

Both SCS and FCS environments were seen to be less aggressive than the STW environment. Cracking did not occur at all in the SCS environment, even at a K_I level of 91% of the material K_{Ic} value. In the STW environment the lowest K_{Iscc} value obtained for short transverse loading was 78 ksi $\sqrt{in}$ (69% of material K_{Ic}), and for the longitudinal and long transverse directions, 96 ksi $\sqrt{in}$ (75% of the material K_{Ic}).

K_{Iscc} values obtained for weld joints were generally lower than those for parent metal. However, the design allowable K_{Ic} value for welds is only 80 ksi $\sqrt{in}$ compared to 120 ksi $\sqrt{in}$ for parent metal. In relationship to the design allowable K_{Ic} value, the K_{Iscc} values for welds compare favorably with those for parent metal.

7.2.4 PH13-8Mo Steel (Tables 7-13, 7-14 and 7-21, Figure 7-4)

Many of the PH13-8Mo steel specimens did not show any evidence of stress corrosion cracking even when loaded to K_I levels above 80% of the material K_{Ic} value. In those specimens where stress corrosion cracking did occur, total crack growth was generally under 0.1".

K_{Iscc} values in the SCS and FCS environments were equal to or higher than those for the STW environment.

The results did not reveal any major effect of grain direction on stress corrosion cracking susceptibility.

The lowest K_I level at which cracks grew in specimens from rolled or forged bar in the H1000 heat treat condition was 72 ksi $\sqrt{in.}$ Crack growth at lower K_I levels occurred in specimens from an extruded bar that had an abnormally low K_{Ic} toughness (material 41). For all heat treat conditions, all lots of rolled and forged bar exhibited K_{Iscc} values greater than 79% of the material K_{Ic} value.

In general, K_{Iscc} values for weld joints were in the same range as those obtained on rolled or forged bar parent metal in the H1000 condition. However, it should be noted that the weld specimens were much thinner (1/8" and 1/4") than the 1" thick parent metal specimens making the degree of lateral restraint at the crack front much less than in the parent metal specimens.

7.2.5 300M Steel (Tables 7-15 and 7-22)

Extensive stress corrosion cracking (lengths over 0.7") occurred in the STW and FCS environments. In the SCS environment, corrosion crack lengths ranged from .19 to .27 inches. The test results show that the SCS environment is much less aggressive than the STW environment for which a K_{Iscc} value of 15 ksi $\sqrt{in}$ (28% of the material K_{Ic} value) was obtained.

7.2.6 Inconel 718 (Tables 7-16 and 7-22)

Cracking occurred in only one specimen of this alloy. Growth was .074" and did not extend to the specimen sides.

The results show that the K_{Iscc} value in STW is greater than 99 ksi $\sqrt{in}$ for a plane strain stress state for the test material. Tests were run at much higher K_I levels than this value without cracking occurring. However, it should be noted that the stress state in the specimens at the high K_I levels was mixed mode and not plane strain. Also, the K_I levels in these specimens would be less than the calculated value shown because some plastic bending of the specimen arms occurred in loading. The peak longitudinal surface stress in the arms exceeded the 0.2% yield strength of the test material at a loading K_I level of 138 ksi $\sqrt{in}$.

7.2.7 MP35N Alloy (Tables 7-17 and 7-22)

Two specimens were tested in a STW environment. Neither showed any evidence of stress corrosion cracking. One specimen was loaded to a K_I level of 86 ksi $\sqrt{in}$ and the other to a K_I level of 96 ksi $\sqrt{in}$. These K_I levels were selected to straddle the K_{Ic} design allowable of 90 ksi $\sqrt{in}$ for the alloy. The results show that the K_{Iscc} value for the test material exceeds 96 ksi $\sqrt{in}$.

7.3 SUMMARY AND CONCLUSIONS

1) The aggressiveness of the FCS and SCS environments was not seen to exceed that of the STW environment. For the non-corrosion resistant steels (300M, 9-4-20), the aggressiveness of the SCS environment was noticeably less than that of the STW environment.

2) The minimum K_{Iscc} value found for Ti-6Al-4V in an RA condition was 53 ksi $\sqrt{in}$ in tests on eight lots of plate and forgings. Ratios of K_{Iscc} to K_{Ic} for the eight lots of material varied from .52 to .78.

3) Sump tank residue water K_{Iscc} values for Ti-6Al-4V plate exposed to diffusion bond thermal cycles were on the average 5 ksi $\sqrt{in}$ lower than those for plate in an RA condition.

4) All the aluminum alloys, except 7049 alloy, had ratios of K_{Iscc} to test material K_{Ic} above .64. For 7049 alloy, the K_{Iscc}/K_{Ic} ratio for the longitudinal direction was .55.

5) For Inconel 718, PH13-8Mo, 9-4-20 and 300M alloys, the minimum ratios of K_{Iscc} to test material K_{Ic} were $>$ .78, .74, .69 and .28, respectively, for the STW environment.

6) K_{Iscc} values for 9-4-20 welds were lower than those for parent metal. For Ti-6Al-4V welds, K_{Iscc} values were at least equivalent to those for parent metal.

Table 7-1 (Page 1 of 5)

6-4 TITANIUM ALLOY K_{Iscc} TEST RESULTS

Specimen No.'s	Orientation	Environment	K_I (Test Time in Hrs), Specimen Crack Traces	K_{Ii} - K_{If} (Crack Growth, In), Crack Front Measurements	K_{Iscc}, KSI $\sqrt{In}$	Specimen Plane Strain Capability K_I, KSI $\sqrt{In}$
Mat'l 67, 1-1/2" Plate						
			Cond RA			
29-43	RW	STW	74(0), 71(5), 70 (30-862)	74 - 62(.18)	62	76
-45	RW	STW	73 (0-906)	67 - 67	>67	76
-46	RW	STW	70 (0), 69 (66-906)	70 - 63(.10)	63	76
-47	RW	STW	69 (0-906)	69 - 69	>69	76
					65	
			After DB Thermal Cycle			
29-311	WR	STW	75 (0), 72 (1-1082)	71 - 64(.10)	64	75
-312	WR	STW	60 (0), 56 (1-1003)	58 - 55(.06)	55	75
					60	
Mat'l 68, 2" Plate						
			Cond RA			
32-16	WR	STW	75 (0-1033)	71 - 61(.15)	61	80
-17	WR	STW	60 (0-1033)	57 - 55(.03)	55	80
					58	
			After DB Thermal Cycle			
32-13	WR	STW	75 (0-1), 67 (4-27), 66 (213-1011)	72 - 55(.29)	55	80
-14	WR	STW	60 (0), 59 (1-2), 58 (24-1003)	57 - 50(.13)	50	80
					53	
Mat'l 70, 1-1/2" Plate						
			After PB Thermal Cycle			
39-131	RW	STW	75 (0), 73 (1-1011)	73 - 69(.05)	69	79
-132	RW	STW	74 (0), 73 (1), 72 (4-1082)	71 - 66(.08)	66	79
					67	

Table 7-1 (Page 2 of 5)

6-4 TITANIUM ALLOY

K_{Iscc} TEST RESULTS

Specimen No.'s	Orientation	Environment	K_I (Test Time in Hrs), Specimen Crack Traces	K_{Ii} - K_{If} (Crack Growth, In), Crack Front Measurements	K_{Iscc}, KSI $\sqrt{In}$	Specimen Plane Strain Capability K_I, KSI $\sqrt{In}$
Mat'l 72, 1.5" Plate			Cond RA			
46-60	RW	STW	69 (0-1005)	69 - 69	>69	74
-61	RW	STW	68 (0-1005)	66 - 60(.10)	60	74
-62	RW	STW	67 (0-1005)	64 - 60(.08)	60	74
-59	RW	STW	62 (0-906)	60 - 55(.08)	55	74
					61	
46-54	WR	STW	81 (0), 80 (4-1005)	78 - 61(.27)	61	77
-55	WR	STW	76 (0), 73 (4-1005)	73 - 58(.24)	58	77
-53	WR	STW	76 (0), 75 (67-906)	74 - 62(.20)	62	77
-56	WR	STW	74 (0), 73 (4-1005)	71 - 62(.14)	62	77
					61	
47-71	WR	SCS	93 (0-1), 92 (7-985)	87 - 75(.17)	75	77
-65	WR	SCS	83 (0-1870)	83 - 63(.28)	63	77
					69	
46-58	WR	FCS	93 (0), 91 (1-1985)	89 - 70(.25)	[illegible]	77
			After DB Thermal Cycle Except AC From 1100F			
46-45	WR	STW	74 (0), 71 (67-906)	70 - 63(.11)	63	77
-47	WR	STW	71 (0), 61 (4), 60 (72-1005)	68 - 49(.36)	49	77
-49	WR	STW	69 (0-141), 68 (242-1173)	68 - 54(.25)	54	
					55	

Table 7-1 (Page 3 of 5)

6-4 TITANIUM ALLOY K_{Iscc} TEST RESULTS

Specimen No.'s	Orientation	Environment	K_I (Test Time in Hrs), Specimen Crack Traces	$K_{Ii} - K_{If}$ (Crack Growth, In), Crack Front Measurements	K_{Iscc}, KSI $\sqrt{In}$	Specimen Plane Strain Capability K_I, KSI $\sqrt{In}$
Mat'l T2, 1.5" Plate (Cont'd)						
			After DB Thermal Cycle			
46-46	WR	STW	75 (0), 48 (67-906)	74 - 44(.60)	44	77
-48	WR	STW	50 (0-1005)	48 - 48	>48	77
-50	WR	STW	45 (0), 44 (4-242), 43 (310-1005)	-----	-	77
-50RT*	WR	STW	74 (0), 41(5-1012)	72-40(.69)	40 / 44	77
Mat'l T6, 1.5" Plate						
			After DB Thermal Cycle			
61A	WR	STW	64 (0), 52 (1-864), 51 (1032-1368)	62 - 46(.33)	46	81
B	WR	STW	64 (0-1368)	61 - 61	>61	81
C	WR	STW	64 (0), 53 (1-1104)	63 - 45(.36)	45	81
D	WR	STW	63 (0-1104)	60 - 60	>60 / 53	81
Mat'l T7, 2-1/2" Ring Rolled Plate						
			Cond RA			
YD3-6	RW	STW	63(0-1169)	63-59(.08)	59	77
3-7	RW	STW	63(0-1169)	63-56(.11)	56	77
3-8	RW	STW	70(0-906)	69-60(.16)	60	77
3-9	RW	STW	70(0),69(66-168), 66(241-906)	70-60(.16)	60 / 59	77
			After DB Thermal Cycle			
63P	WR	STW	75 (0), 67 (1-1011	72 - 55(.28)	55	77
Q	WR	STW	60 (0-1003)	58 - 55(.06)	55 / 55	77
Mat'l T9, 4 x 10 x 34" Forged Block						
			Cond RA			
77-31	TR	STW	85 (0), 81 (1), 58 (20), 57 (73-1028)	81 - 57(.50)	57	79
-30	TR	STW	60 (0-1), 58 (4-1082)	58 - 55(.04)	55 / 56	79

* RT = Retest

Table 7-1 (Page 4 of 5)

6-4 TITANIUM ALLOY K_{Iscc} TEST RESULTS

Specimen No.'s	Orientation	Environment	K_I (Test Time in Hrs), Specimen Crack Traces	K_{Ii} - K_{If} (Crack Growth, In), Crack Front Measurements	K_{Iscc}, KSI $\sqrt{In}$	Specimen Plane Strain Capability K_I, KSI $\sqrt{In}$
Mat'l 82, 4 x 10 x 34" Forged Block						
			Cond RA			
95-10	WR	STW	75 (0), 70 (1-1006)	70 - 55(.26)	55	75
-11	WR	STW	60 (0-1006)	55 - 51(.09)	51	75
					53	
Mat'l 84, Die Forging						
			Cond RA			
103-3	TR	STW	75 (0), 73 (1-1011)	71 - 56(.25)	56	75
-4	TR	STW	60 (0), 56 (1-1003)	57 - 56(.02)	56	75
					56	
Mat'l 85, Die Forging						
			Cond RA			
104-3	TR	STW	75 (0-1011)	71 - 71	>71	78
-4	TR	STW	60 (0), 59 (1-1082)	57 - 57	>57	78
					>71	
Mat'l 253, 2.5" Plate						
			After DB Thermal Cycle			
1020A	WR	STW	71 (0), 69 (1-1104)	70 - 58(.20)	58	76
B	WR	STW	72 (0), 67 (1-1368)	71 - 54(.28)	54	76
C	WR	STW	71 (0-1368)	70 - 59(.17)	59	76
D	WR	STW	73 (0-1104)	71 - 61(.14)	61	76
					58	

Table 7-1 (Page 5 of 5)

6-4 TITANIUM ALLOY K_{Iscc} TEST RESULTS

Specimen No.'s	Orientation	Environment	K_I (Test Time in Hrs), Specimen Crack Traces	$K_{Ii} - K_{If}$ (Crack Growth, In), Crack Front Measurements	K_{Iscc}, KSI $\sqrt{In}$	Specimen Plane Strain Capability K_I, KSI $\sqrt{In}$
Mat'l 294, 1.25" Plate						
			After DB Thermal Cycle			
1022A	WR	STW	74 (0), 72 (1-213), 71 (523-1011)	71 - 62 (.14)	62	76
B	WR	STW	60 (0-1003)	57 - 55 (.04)	55	76
					58	
1.5" Plate, RA + Hot Formed (1560F, 5 hrs and cooled ~17F/hr to 1100F, AC), B-1 Wing Pivot Lug Plate, L1200021-004						
9012-1026A	WR	STW	85 (0), 66 (1-1028)	74 - 58 (.29)	58	76
B	WR	STW	60 (0), 57 (1-4), 56 (70-1082)	57 - 51 (.12)	51	76
					55	

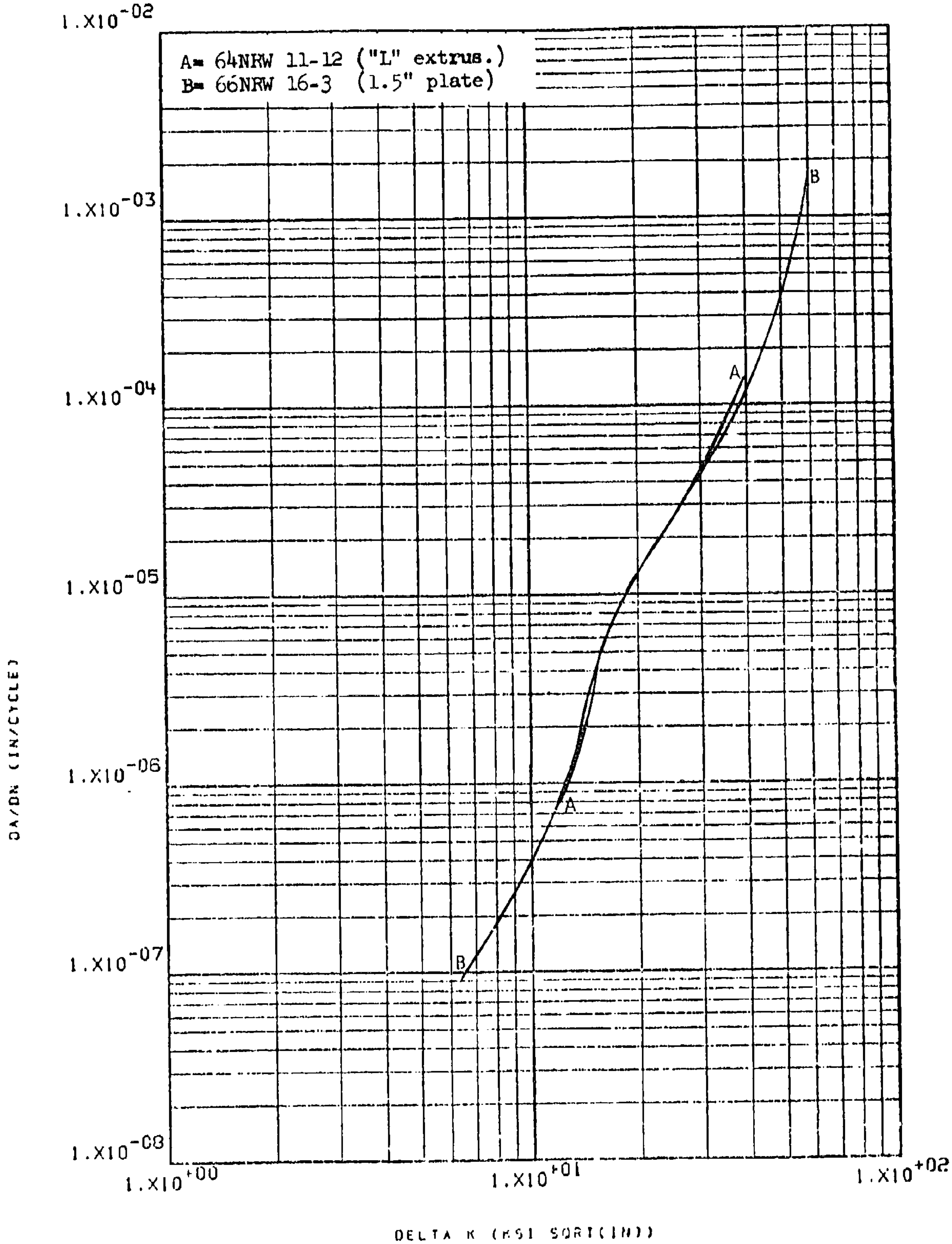

Figure 8.2.1.7-5 Effect of product form on LHA-FCGR at R.T., R=0.3, 360 cpm, RW direction in beta processed plus mill annealed Ti-6-4

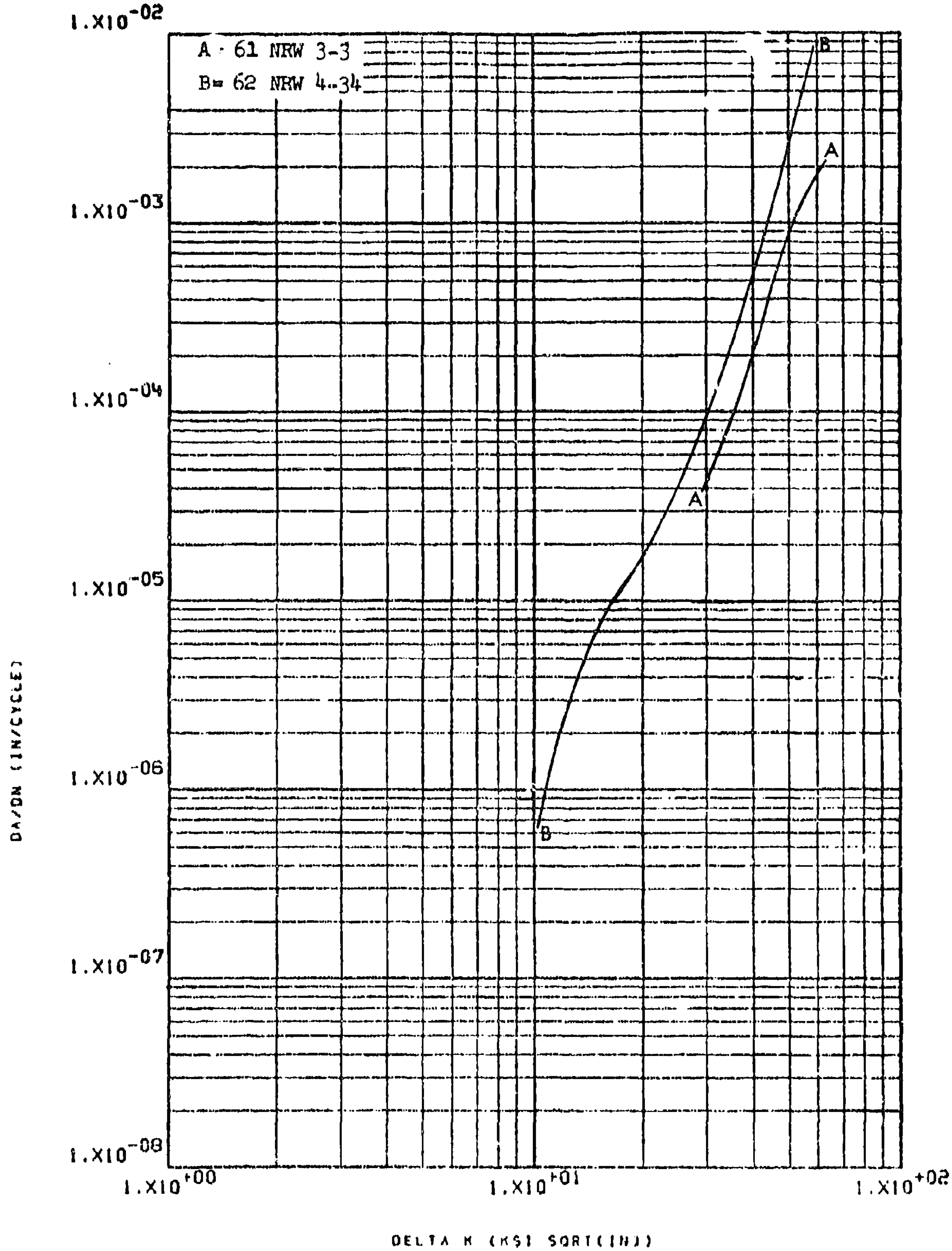

Figure 8.2.1.7-6 Effect of product form on LHA-FCGR at R.T., R=0.3, 60 cpm, RW direction in diffusion bond thermal cycled Ti-6-4 plate

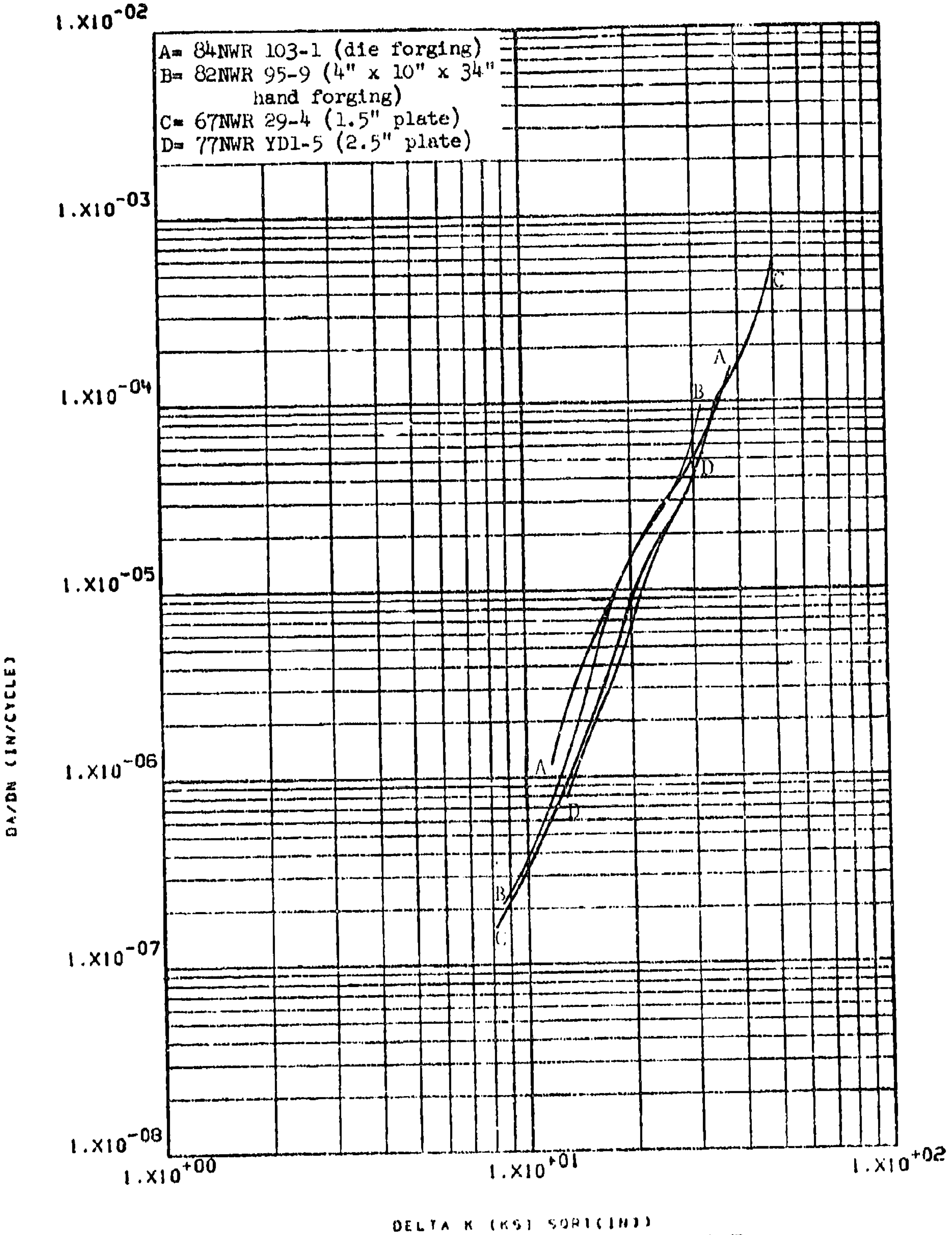

Figure 8.2.1.7-7 Effect of product form on STW-FCGR at R.T., R=0.08, 60 cpm, WR direction in recrystallization annealed Ti-6-4

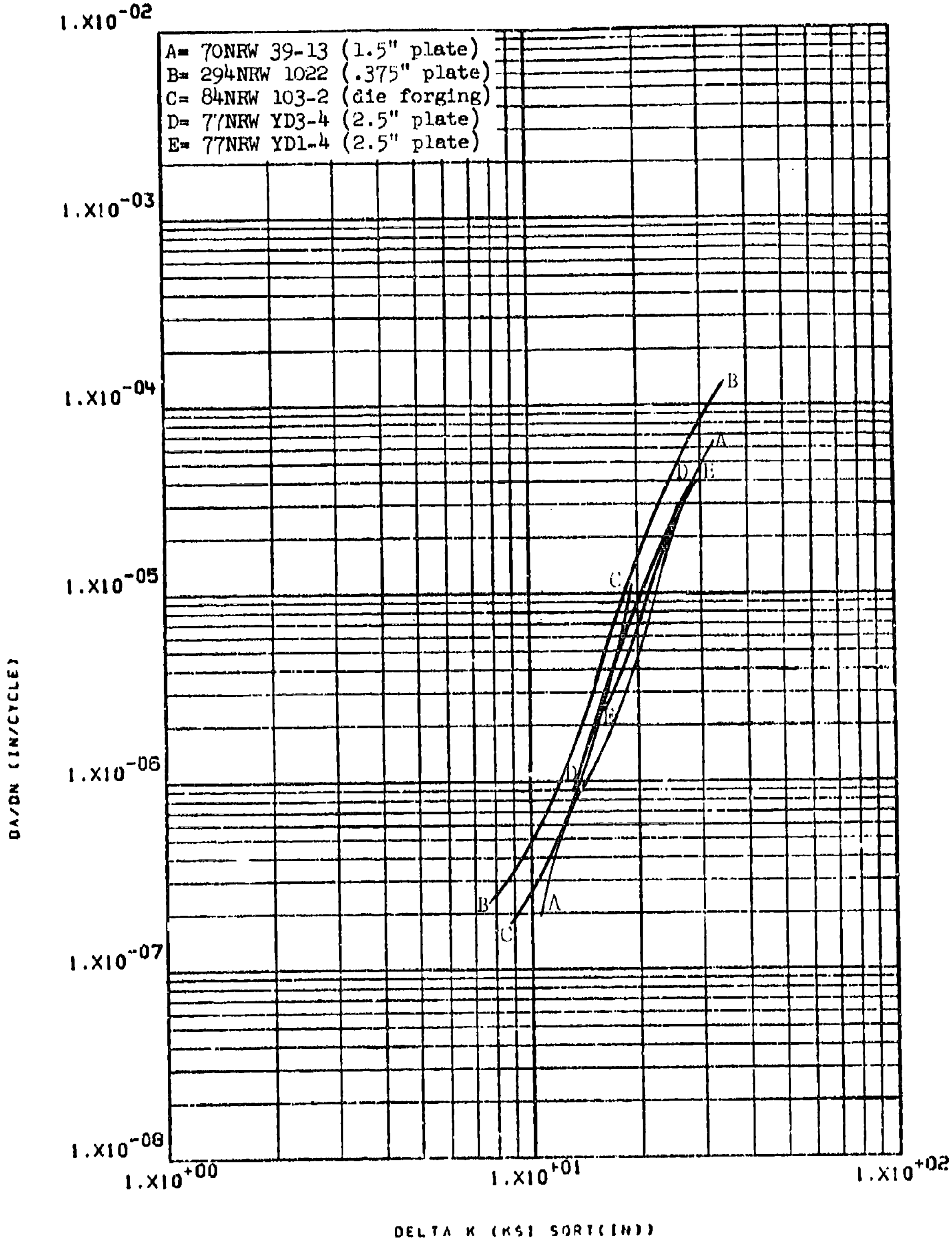

Figure 8.2.1.7-8 Effect of product form on STW-FCGR at R.T., R=0.08, RW direction in recrystallization annealed Ti-6-4

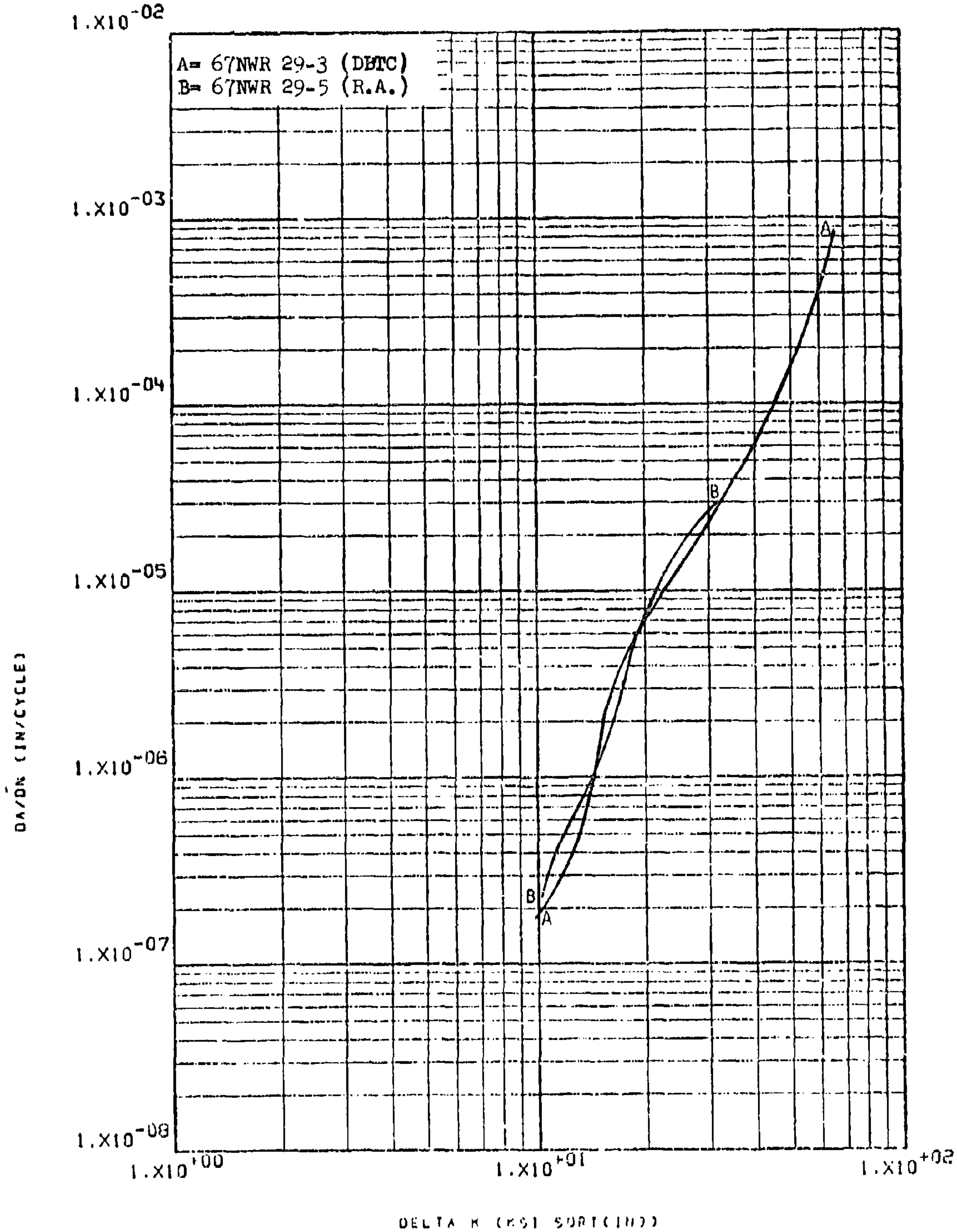

Figure 8.2.1.8-1 Effect of heat treat condition on LHA-FCGR at R.T., R=0.08, WR direction of 1.5" Ti-6-4 plate

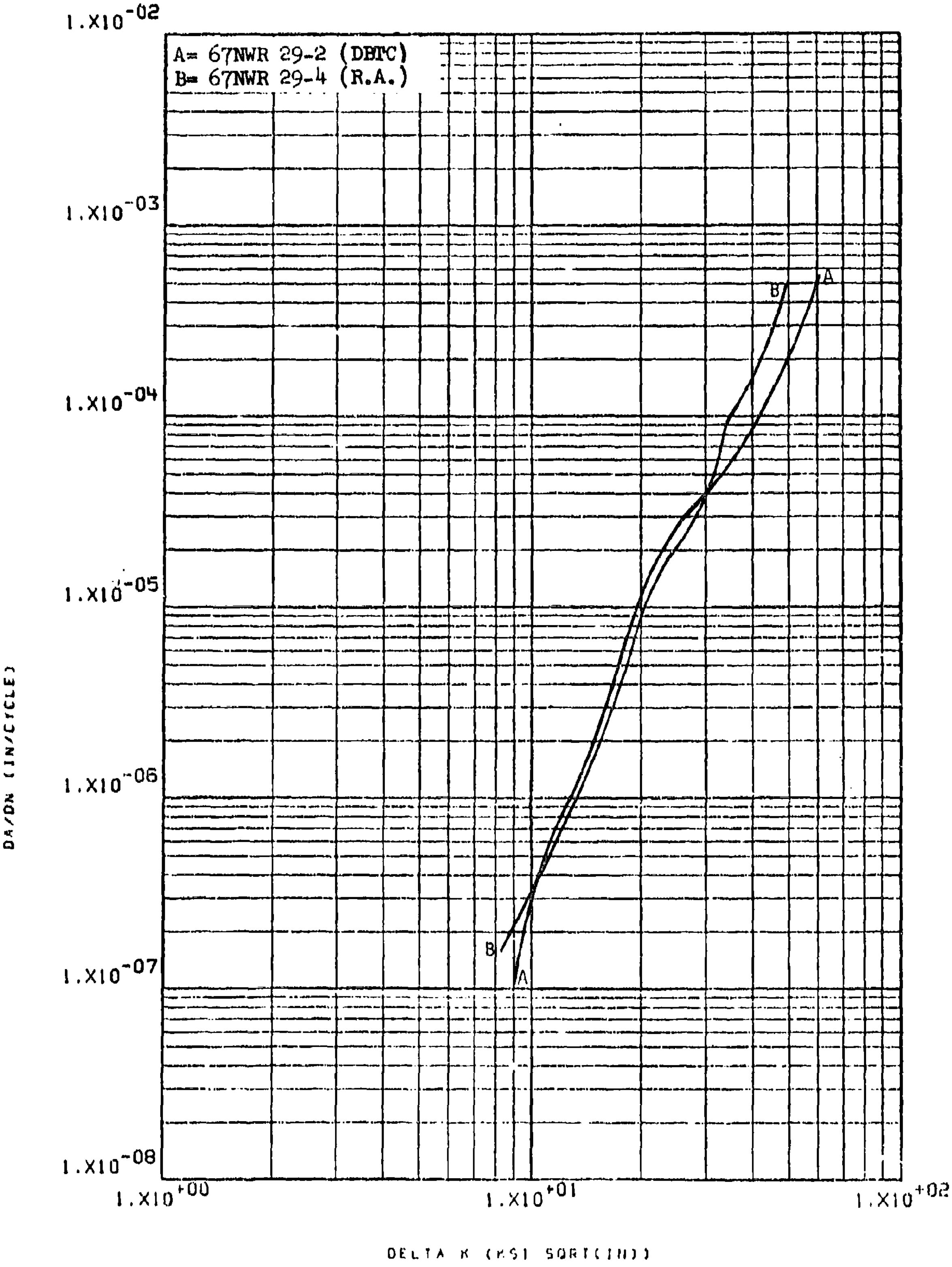

Figure 8.2.1.8-2 Effect of heat treat condition on STW-FCGR at R.T., R=0.08, 60 cpm, WR direction of 1.5" Ti-6-4 plate

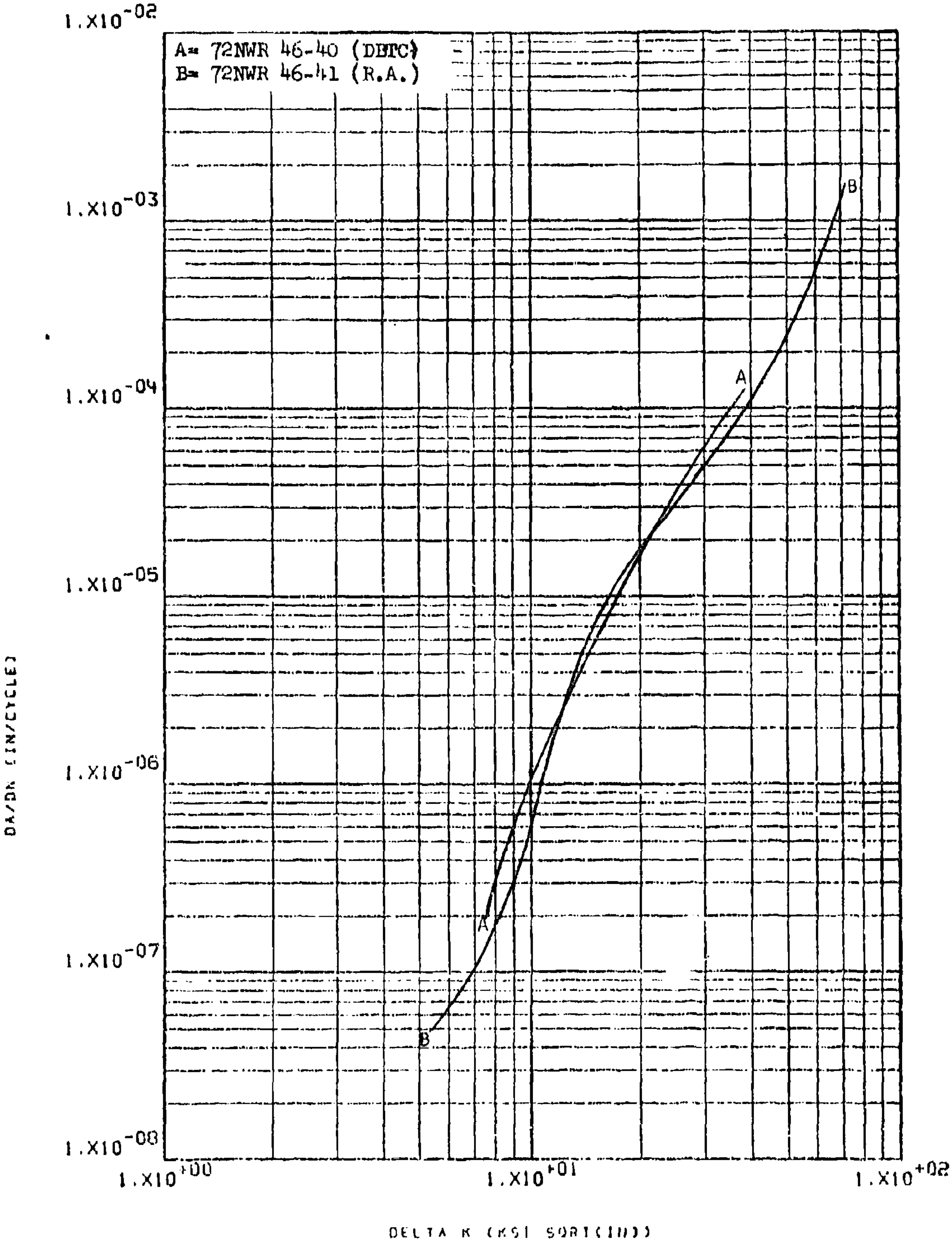

Figure 8.2.1.8-3 Effect of heat treat condition on STW-FCGR at R.T., R=0.08, 60 cpm, WR direction of 1.5" Ti-6-4 plate

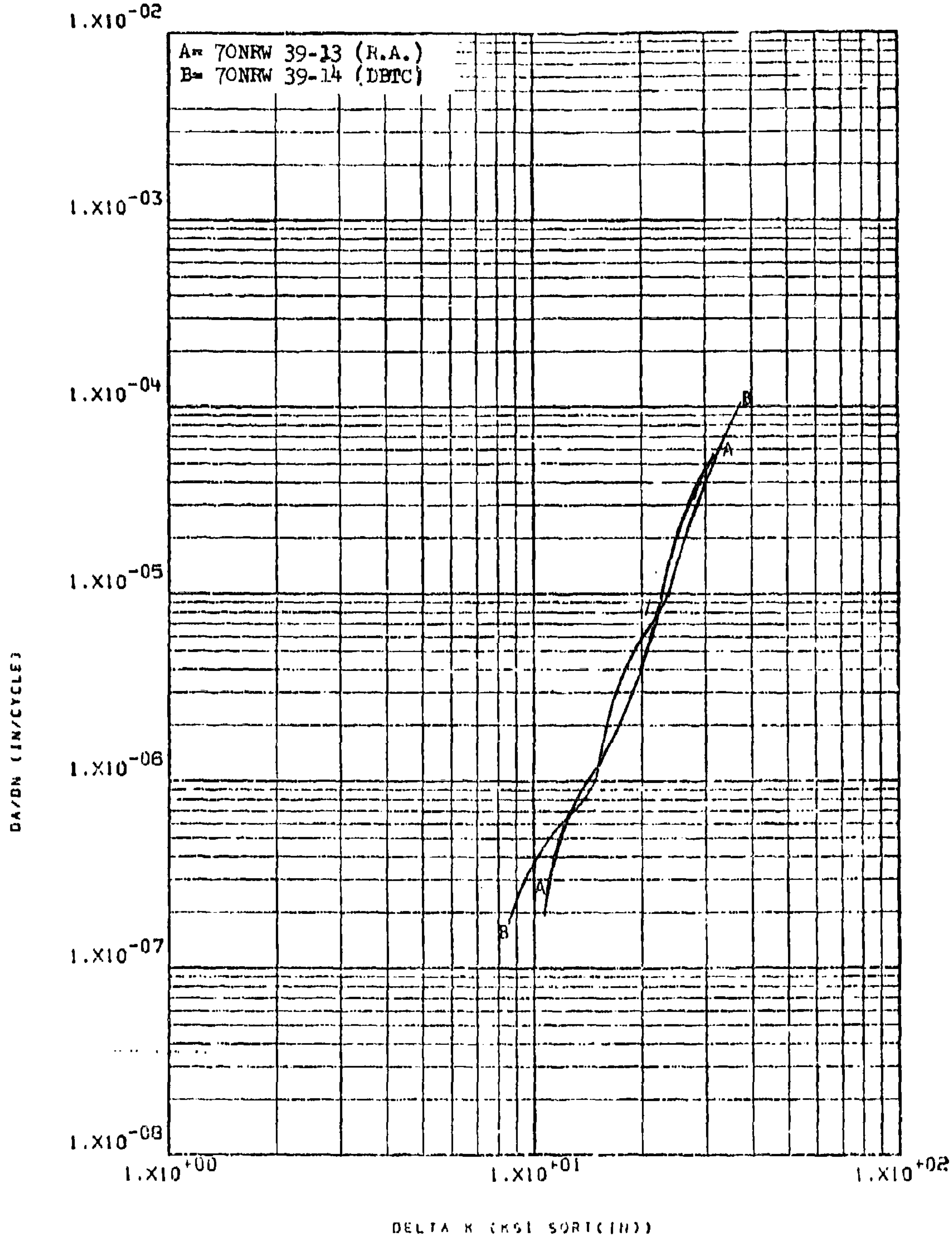

Figure 8.2.1.8-4 Effect of heat treat condition on STW-FCGR at R.T., R=0.08, 60 cpm, RW direction of 1.5" Ti-6-4 plate

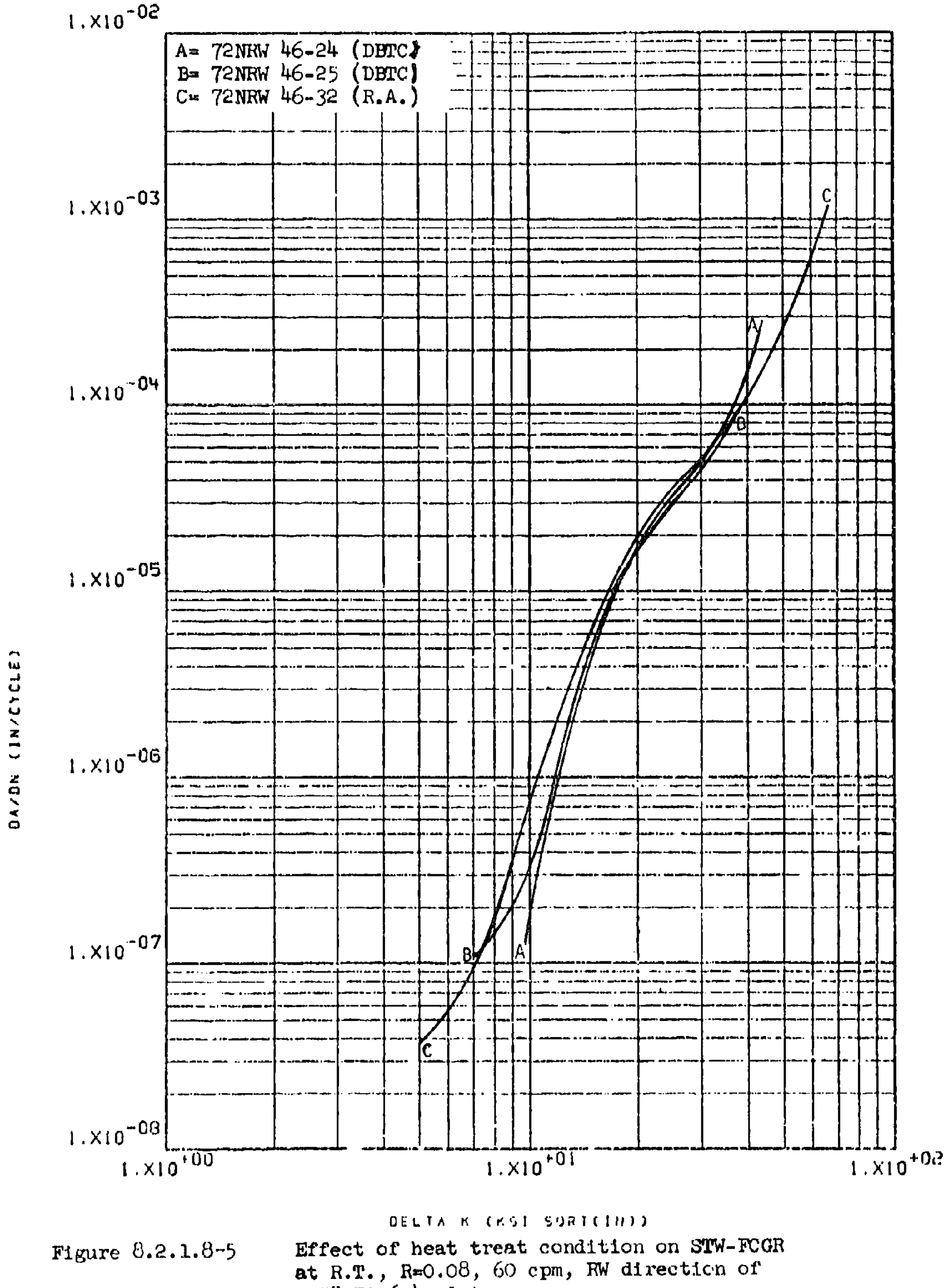

Figure 8.2.1.8-5 Effect of heat treat condition on STW-FCGR at R.T., R=0.08, 60 cpm, RW direction of 1.5" Ti-6-4 plate

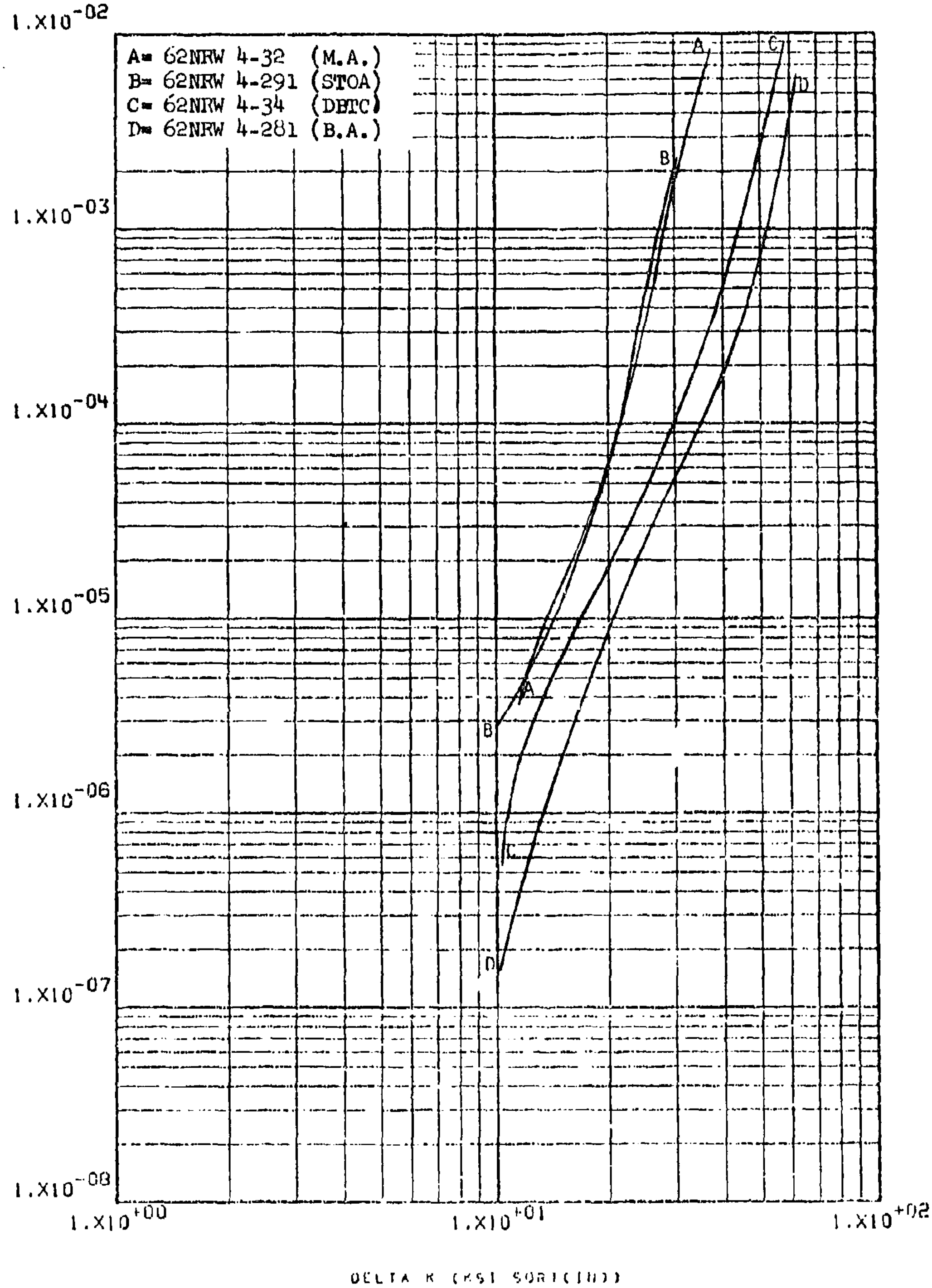

Figure 8.2.1.8-6 Effect of heat treat condition on LHA-FCGR at R.T., R=0.3, 60 cpm, RW direction in 0.625" Ti-6-4 plate

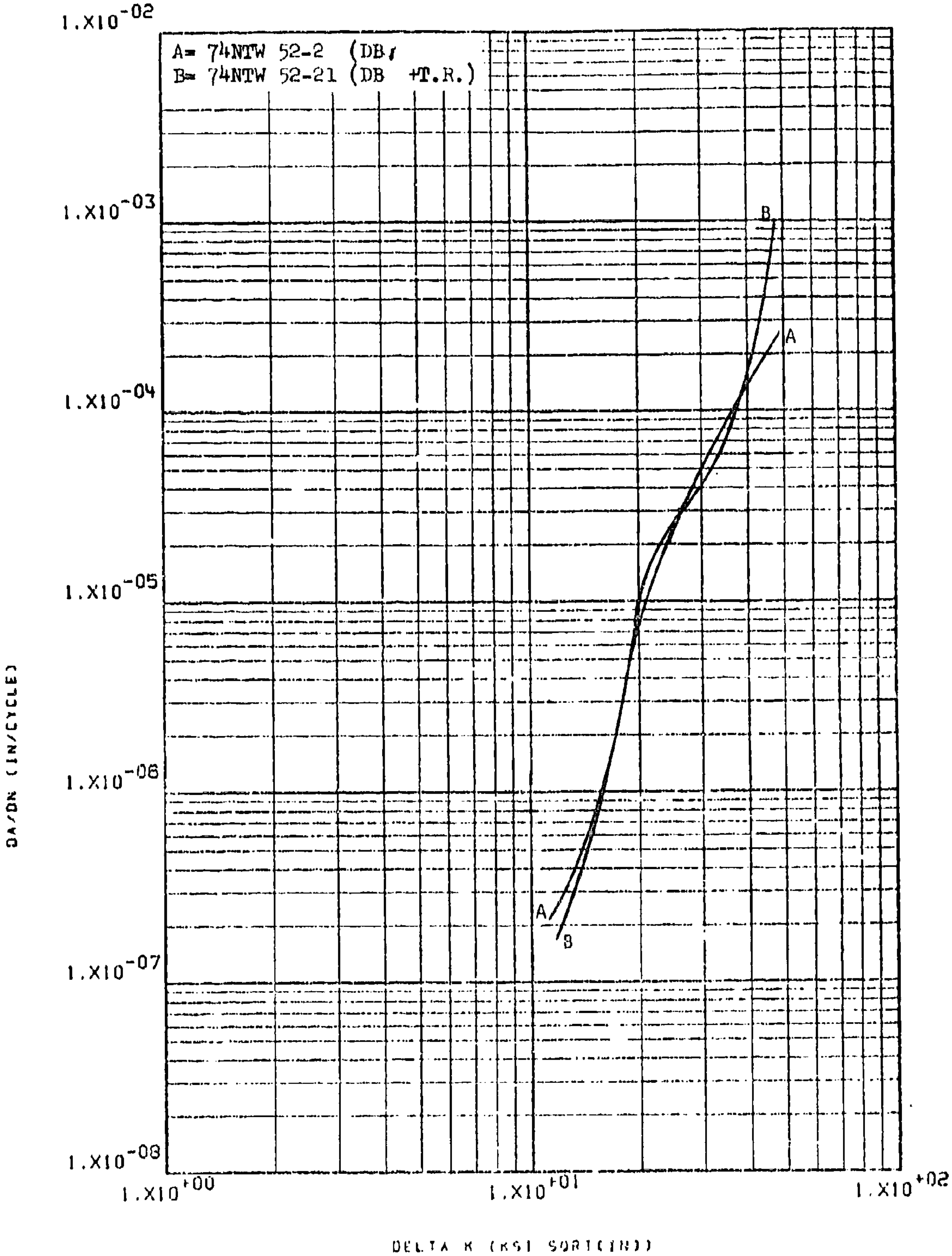

Figure 8.2.1.8-7 Effect of heat treat condition on STW-FCGR at R.T., R=0.08; 60 cpm. TW/TW direction in 1.5" Ti-6-4 diffusion bonded plate

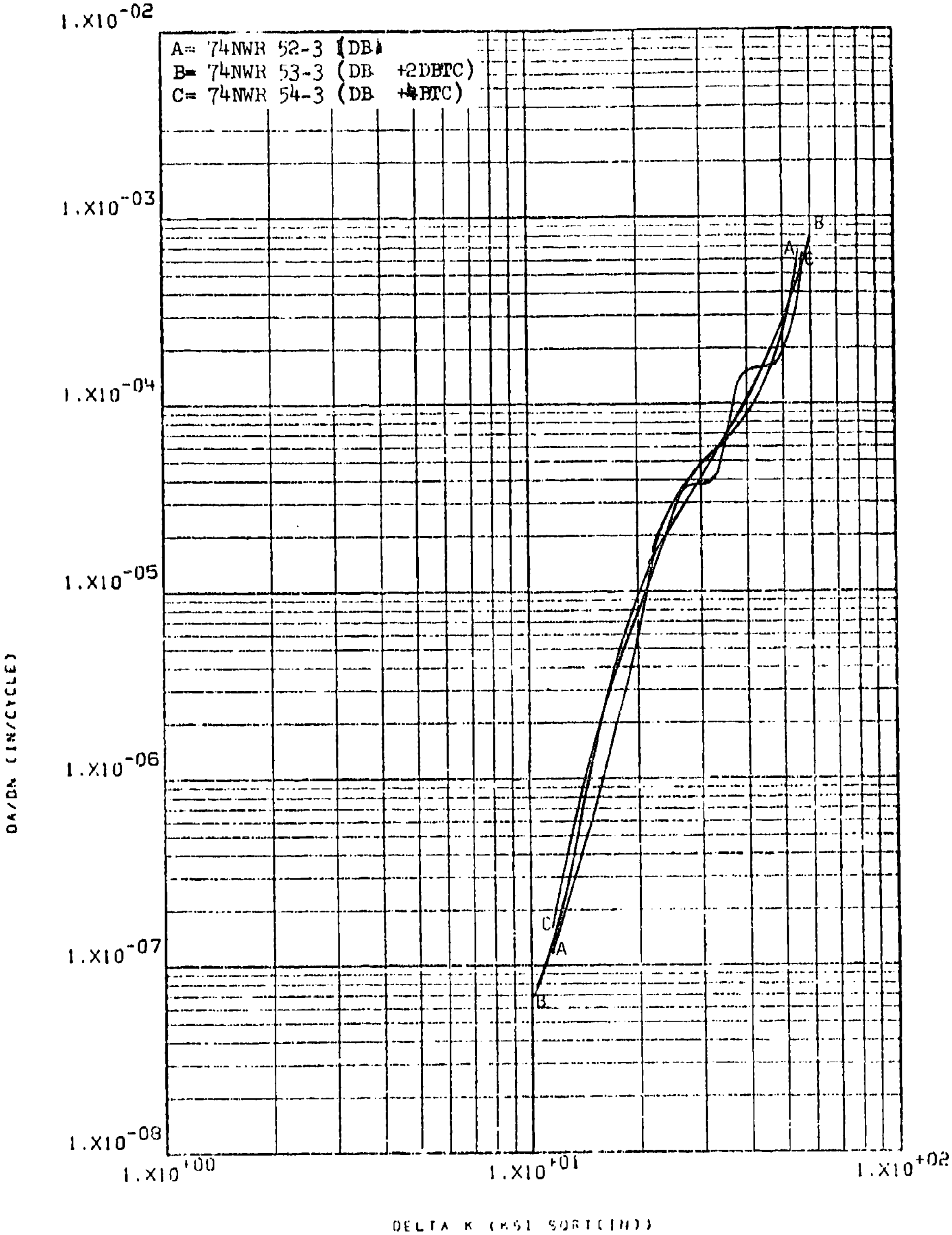

Figure 8.2.1.8-8 Effect of heat treat condition on STW-FCGR at R.T., R=0.08, 60 cpm, WR direction in 1.5" Ti-6-4 diffusion bonded plate

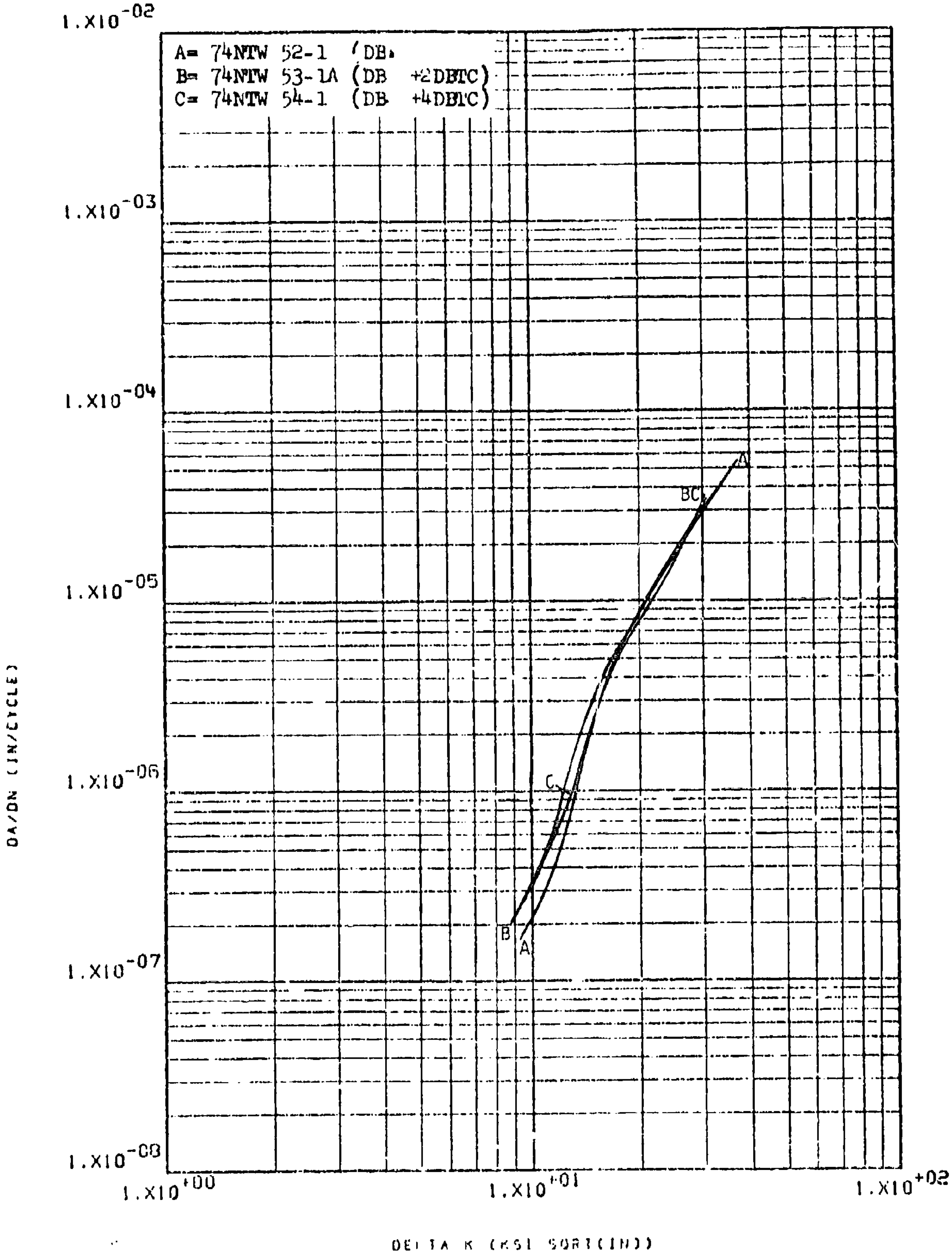

Figure 8.2.1.8-9 Effect of heat treat condition on LHA-FCGR at R.T., R=0.08, 360 cpm, TW/TW direction in 1.5" Ti-6-4 diffusion bonded plate

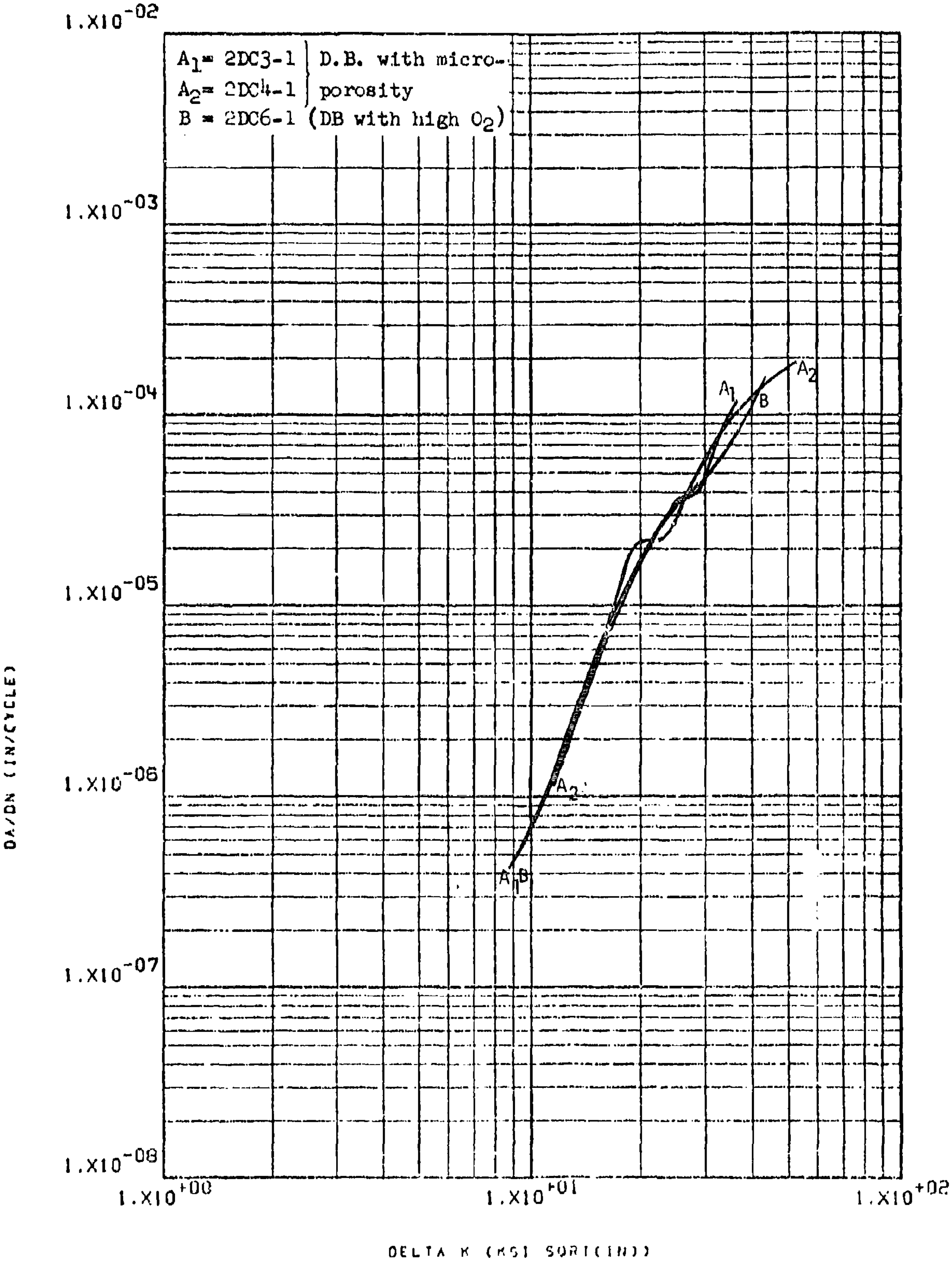

Figure 8.2.1.8-10 Effect of heat treat condition on STW-FCGR at R.T., R=0.08, 60 cpm, RW/TR direction in Ti-6-4 diffusion bonded plate.

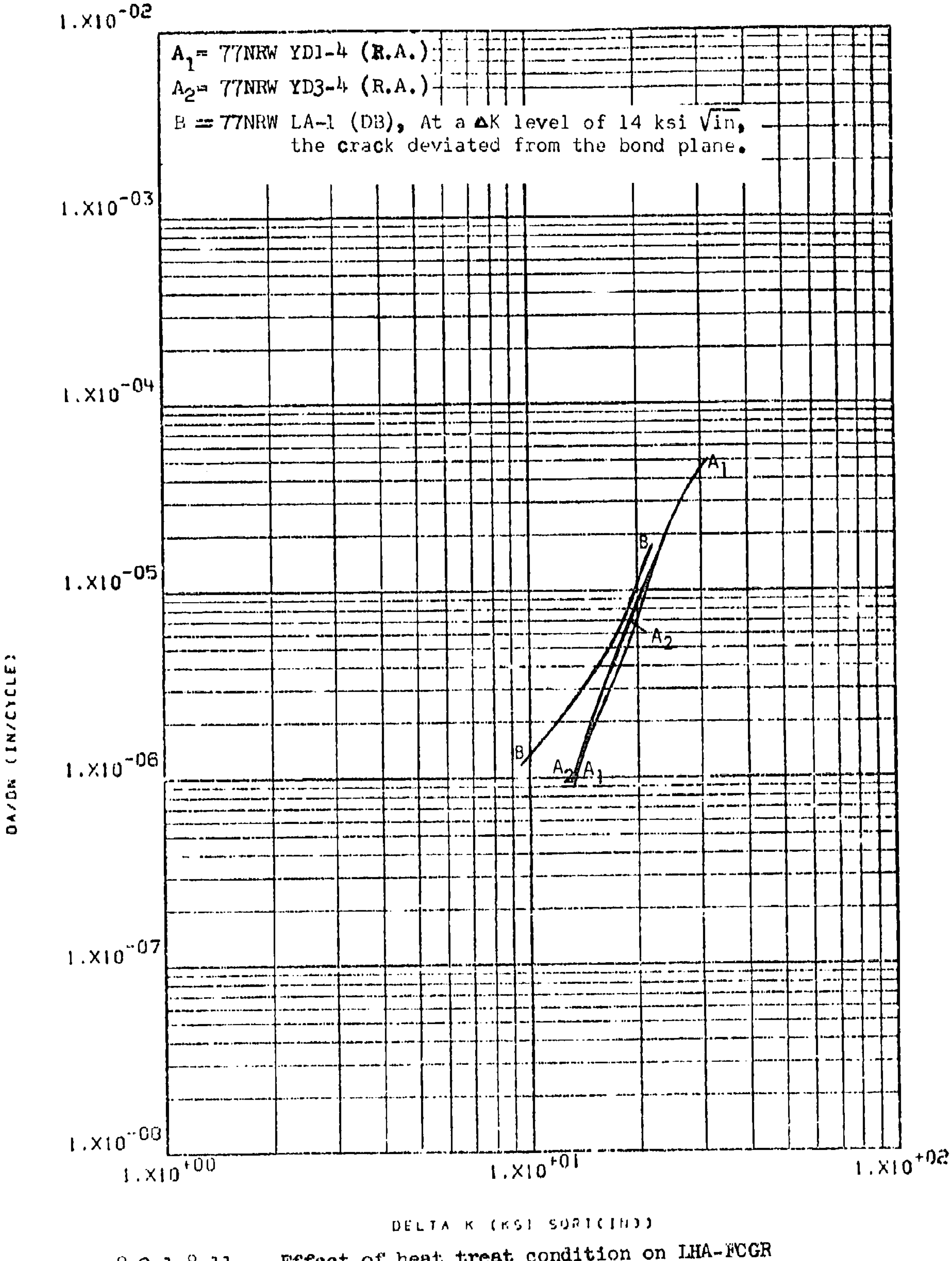

Figure 8.2.1.8-11 Effect of heat treat condition on LHA-FCGR at R.T., R=0.08, 360 cpm, RW direction in 2.5" Ti-6-4 plate

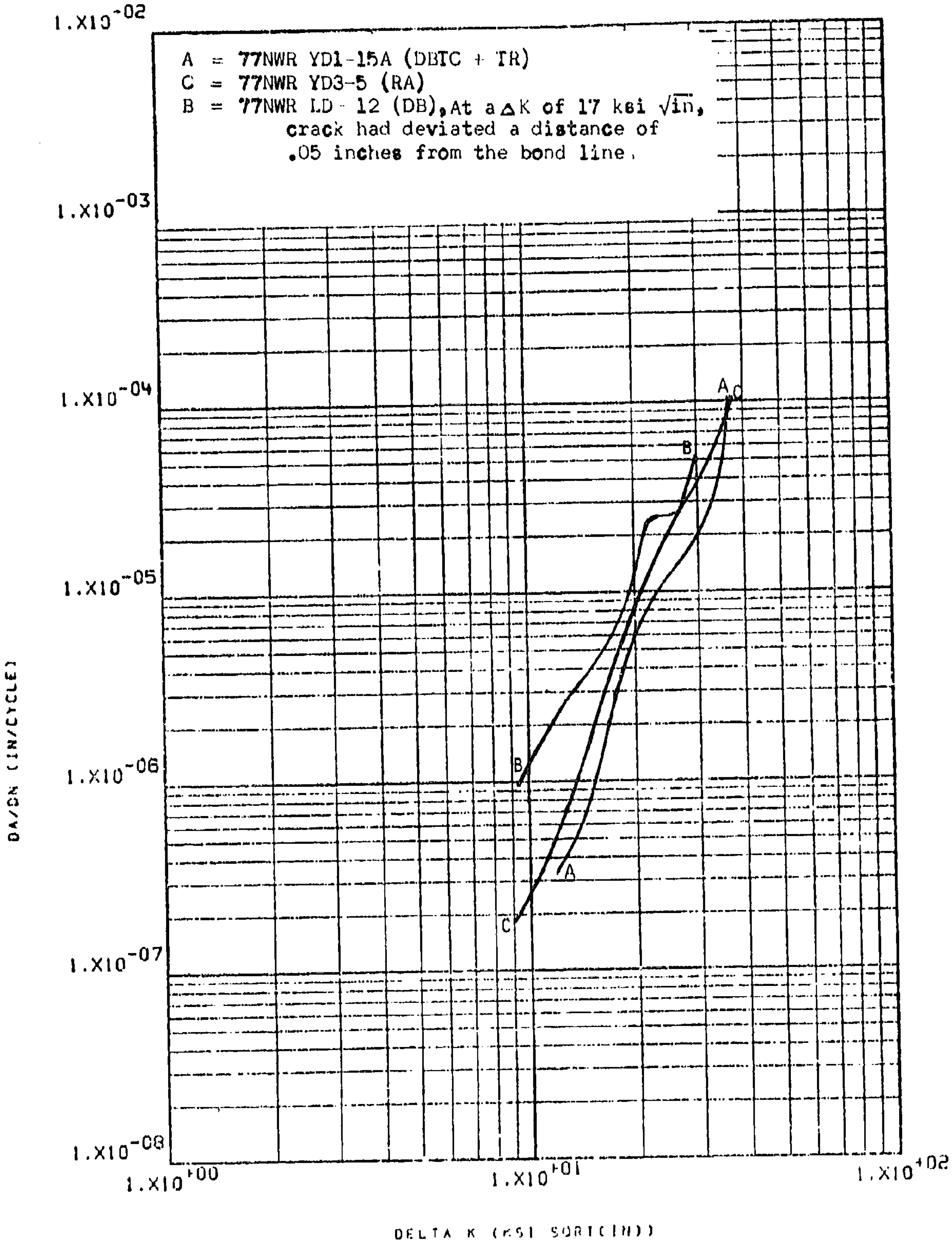

Figure 8.2.1.8-12 Effect of heat treat condition on STW-FCGR at R.T., R-0.08, 60 cpm, WR direction in 2.5" Ti-6-4 plate

8.2.2 Aluminum Alloy 2024

8.2.2.1 Cyclic Rate - The effects of changing cyclic frequency of tests on the growth rate characteristics of this material were seen to be inconsistent and essentially insignificant (Figure 8.2.2.1-1 through -4).

8.2.2.2 Test Temperature - The low humidity air growth rates of this alloy were seen to be substantially accelerated by increasing test temperatures from ambient to 265°F in both the RW and WR directions. (Figures 8.2.2.2-1 and -2). Sump tank water rates were similarly accelerated as temperature was increased from ambient to 150°F (Figure 8.2.2.2-3).

8.2.2.3 Specimen Thickness - Substantial accelerations in low humidity air growth rates were seen to result in this material when specimen thicknesses were reduced from 1.0 to 0.5 inch (Figure 8.2.2.3-1). Further decreasing the thickness to 0.25 inch, however, did not result in further acceleration of any significance.

8.2.2.4 R Factor - The low humidity air crack growth rates of this alloy were seen to be substantially accelerated by increasing the R factor from 0.08 to 0.3 (Figure 8.2.2.4-1) and to 0.7 (Figure 8.2.2.4-2). Sump tank water growth rates were also accelerated as R was increased from 0.08 to 0.5 (Figure 8.2.2.4-3).

8.2.2.5 Environment - No significant differences in growth rates were observed in either of the 3 inch thick plates when measured in low humidity air, distilled water, sump tank water, and jet fuel (Figures 8.2.2.5-1 and -2). Growth rates in the 23 inch long forging were similarly unchanged as the test environment was changed from low humidity air to sump tank water, (Figure 8.2.2.5-3) while in the WR direction of the 35 inch long forging a slight acceleration in growth rates was observed (Figures 8.2.2.5-3 and -4).

8.2.2.6 Test Direction - Low humidity air growth rates of both heats of 3 inch plate and of the 23 inch long forging were essentially unchanged as the direction of test was changed from RW to WR (Figures 8.2.2.6-1 and -2). In the 35 inch long forging, however, growth rates in the WR direction were seen to be significantly greater than those in the RW direction in both low humidity air and sump tank water (Figures 8.2.2.6-3 and -4).

8.2.2.7 Product Form - Four different lots of material were evaluated in the RW direction for this alloy consisting of two heats of 3" thick plate and two 3" x 18" x L forged blocks (L=23" & 35"). Low humidity air growth rates were seen to be significantly greater in the plate stock than in the forged block when tested at 360 cpm (Figure 8.2.2.7-1). The magnitude of difference between the rates in plates and forgings was diminished as the test frequency was decreased from 360 to 60 cpm, where growth rates of one

of the forged blocks (L=35") were essentially equivalent to the growth rates in the two plates (Figure 8.2.2.7-2). Growth rates in the second block (L=23") were seen to be somewhat slower. In sump tank water at 60 cpm the growth rates in both plates and in the 23" long forging were seen to be essentially equivalent to each other, all being substantially greater than those in the 35" long forging (Figure 8.2.2.7-3). In the WR direction at 360 cpm the low humidity air growth rates of both plates were seen to be equivalent to each other and substantially greater than the rates of either of the two forged blocks (Figure 8.2.2.7-4). At low levels of ΔK, rates in the 23" long forging were significantly greater than those in the 35" long forging, but this difference was seen to diminish as ΔK was increased, until at approximately 15 ksi$\sqrt{in}$ the rates became essentially equivalent. (Figure 8.2.2.7-4).

8.2.2.8 **Heat Treat Condition - Not evaluated**

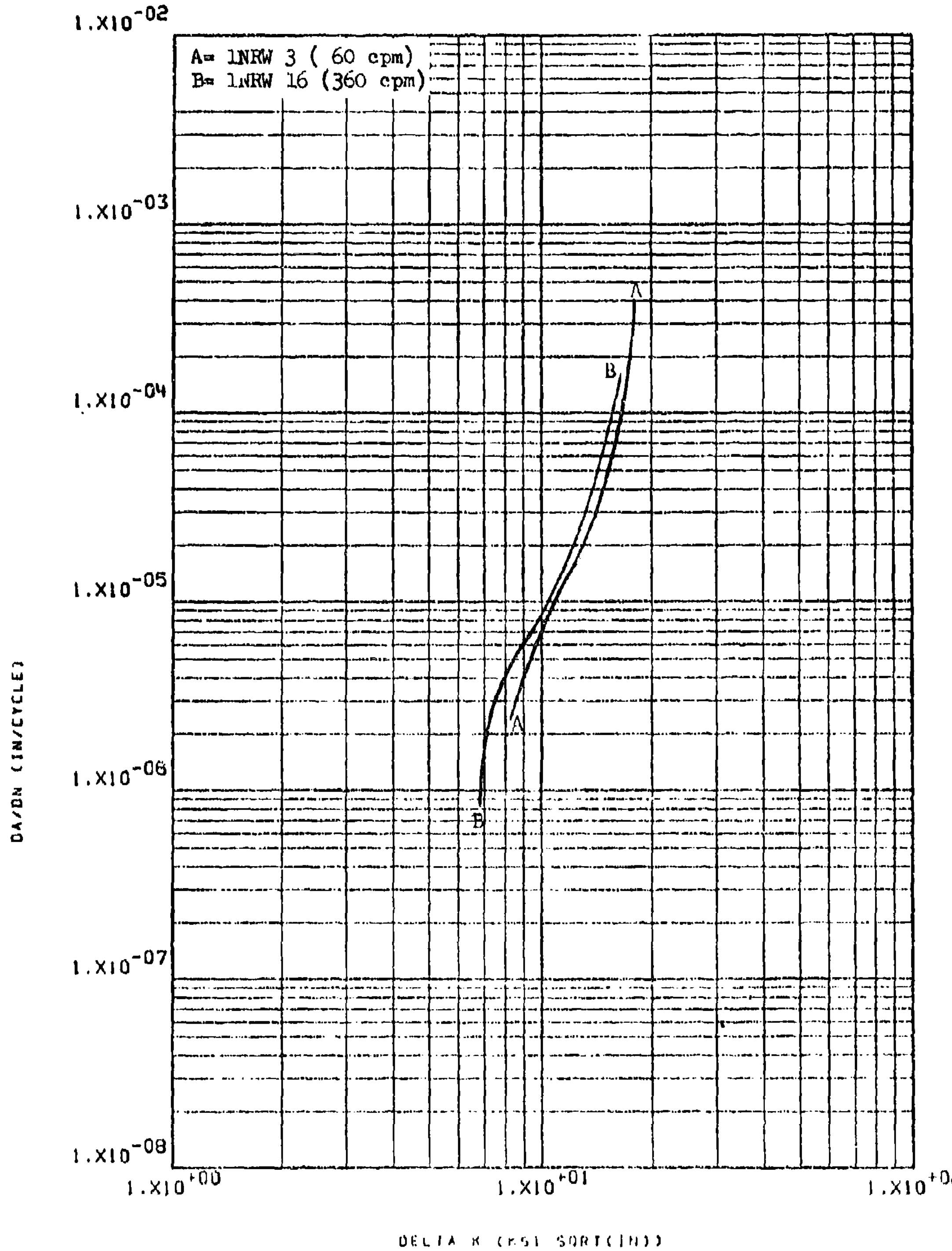

Figure 8.2.2.1-1 Effect of cyclic rate on LHA-FCGR at R.T., R= 0.08, RW direction, in 2024-T851 3" plate

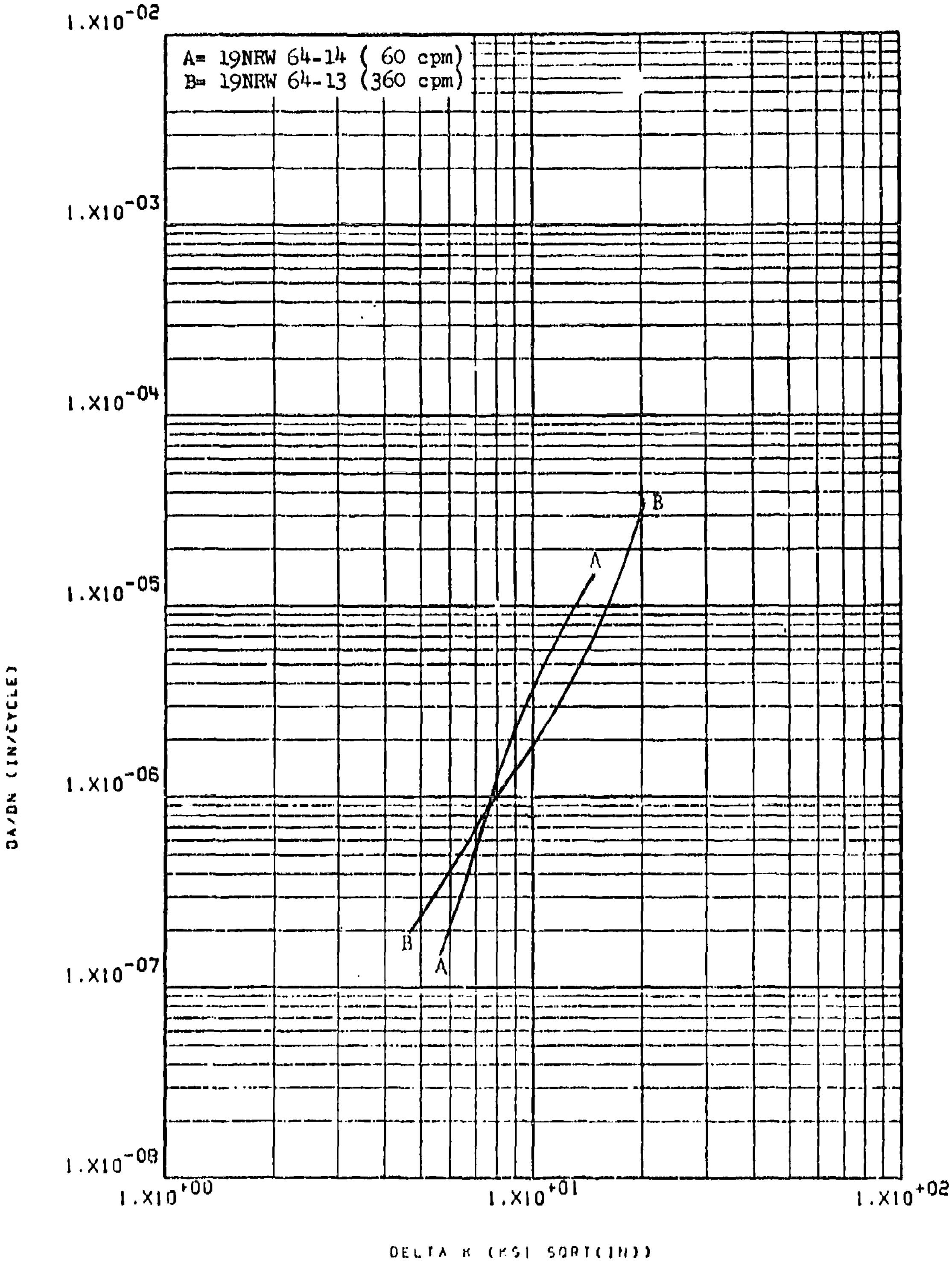

Figure 8.2.2.1-2 Effect of cyclic rate on LHA-FCGR at R.T., R= 0.08, RW direction, in 2024-T852 3" x 18" x 23" forging

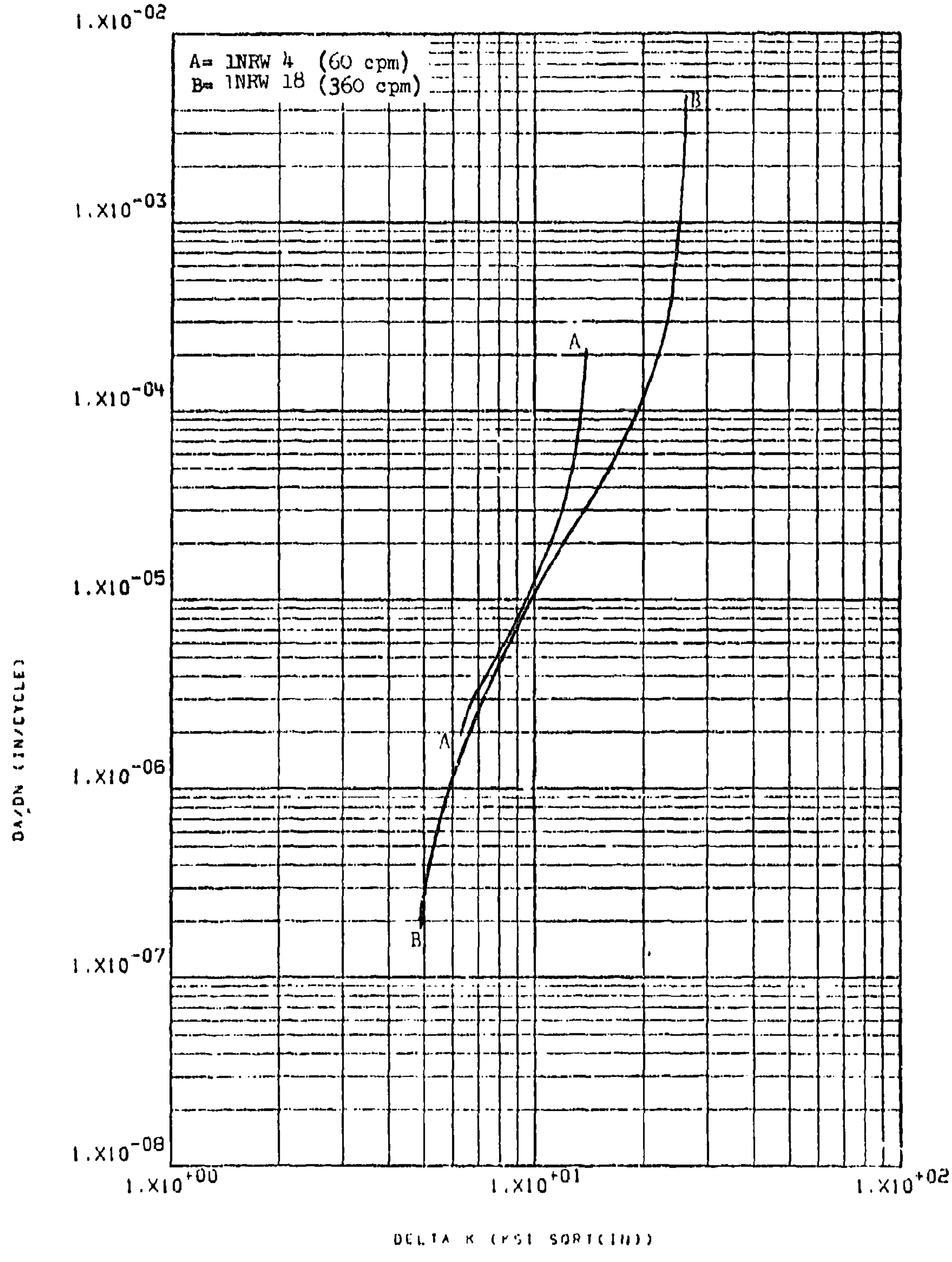

Figure 8.2.2.1-3 Effect of cyclic rate on IHA-FCGR at R.T., R= 0.3, RW direction, in 2024-T851 3" plate

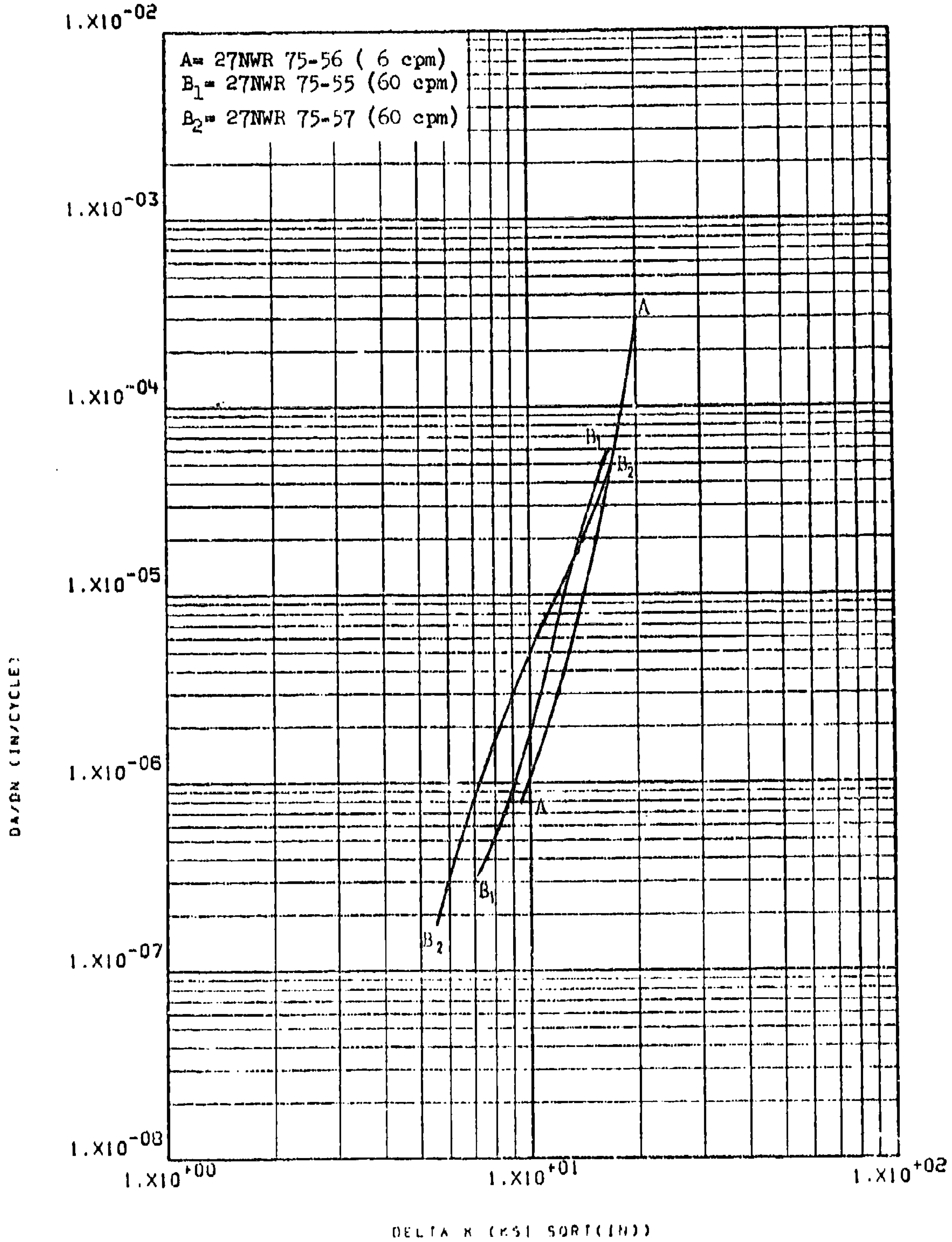

Figure 8.2.2.1-4 Effect of cyclic rate on STW-FCGR at R.T., R= 0.08, WR direction, in 2024-T852 3" x 18" x 35" forging 8-80

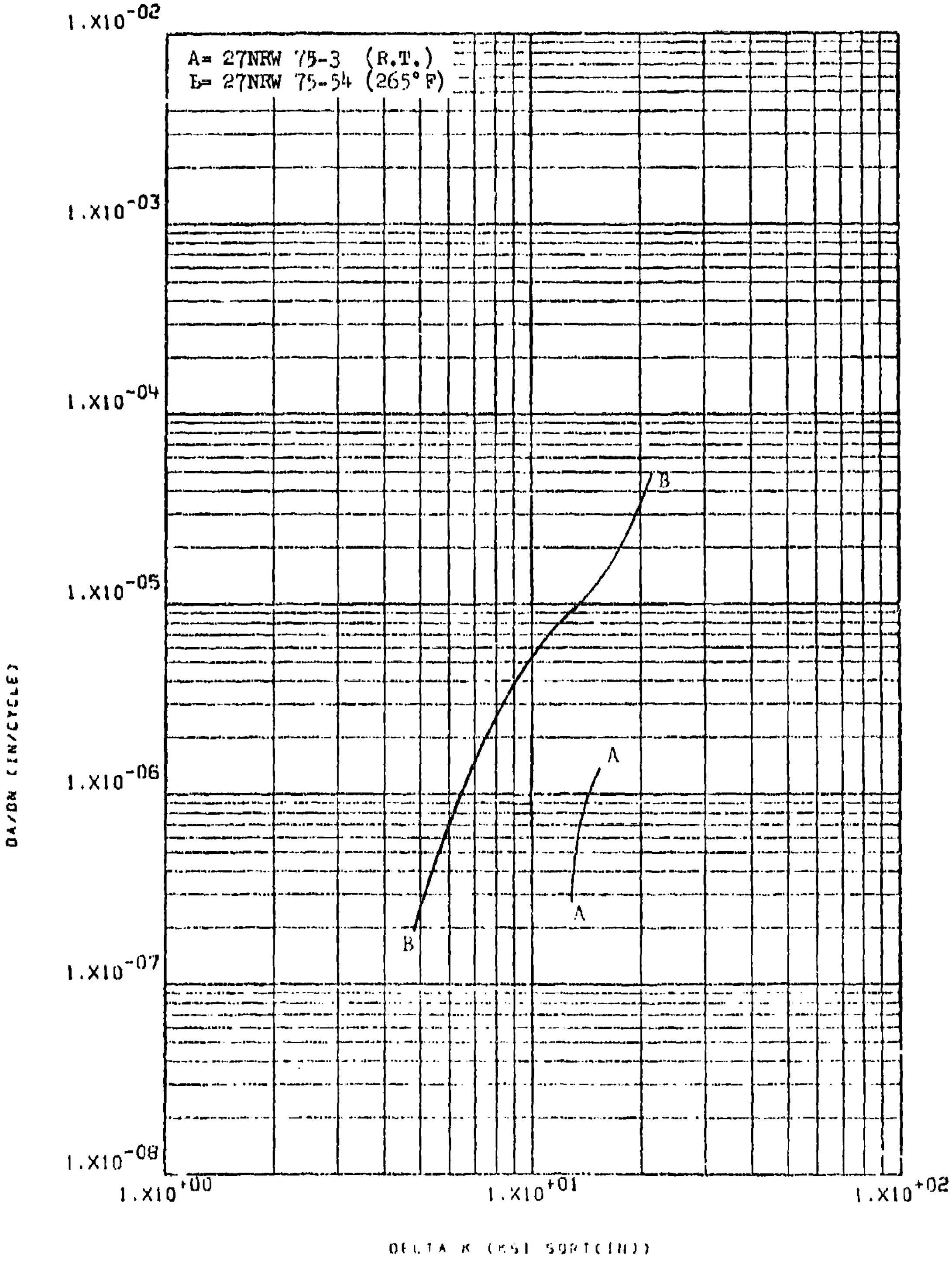

Figure 8.2.2.2-1   Effect of temperature on LHA-FCGR at R=0.08 8 81 360 cpm, RW direction, in 2024-T852 3" x 18" x 35" forging

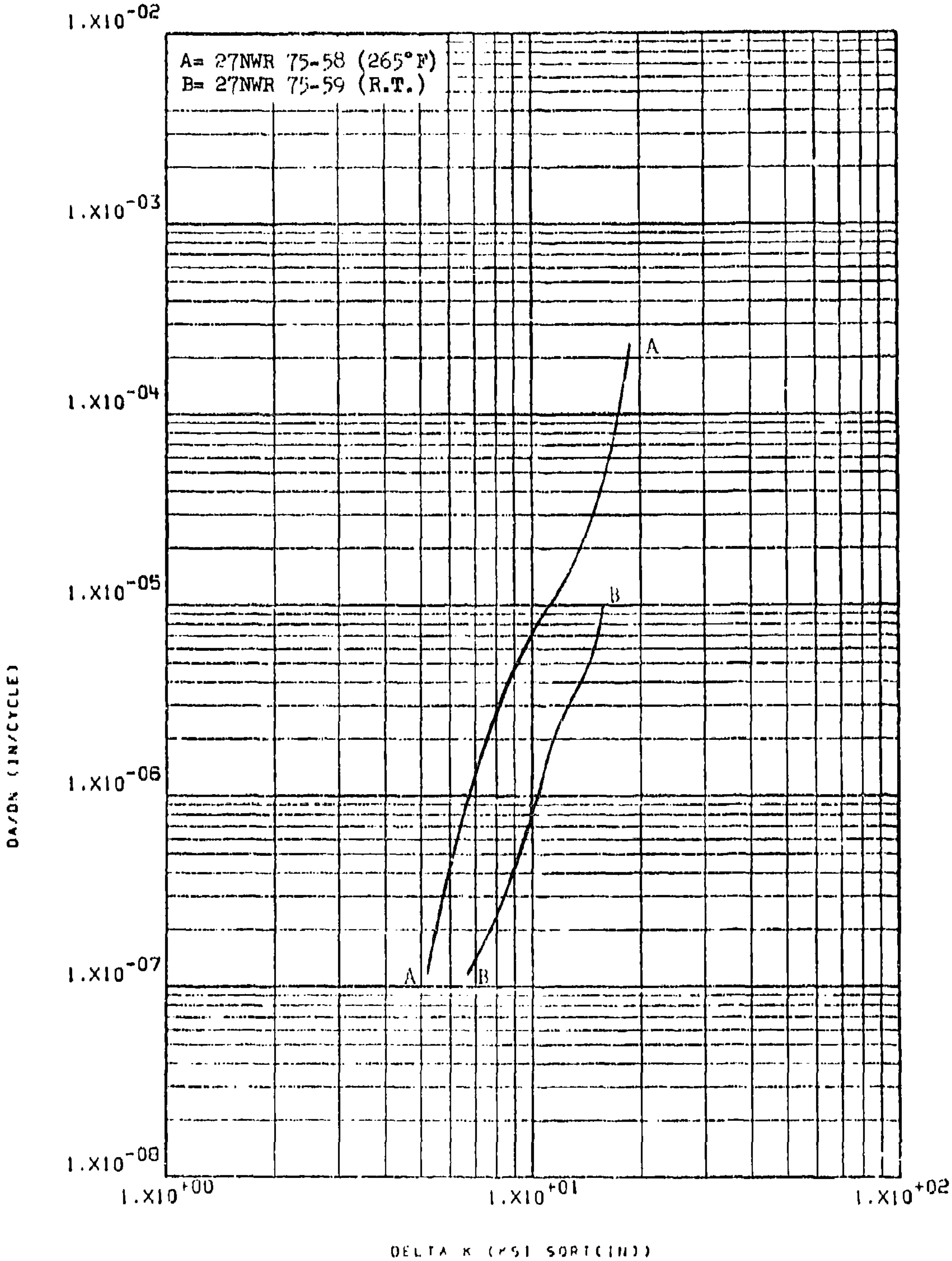

Figure 8.2.2.2-2 Effect of temperature on LHA-FCGR at R=0.08, 360 cpm, WR direction, in 2024-T852 3" x 18" x 35" forging

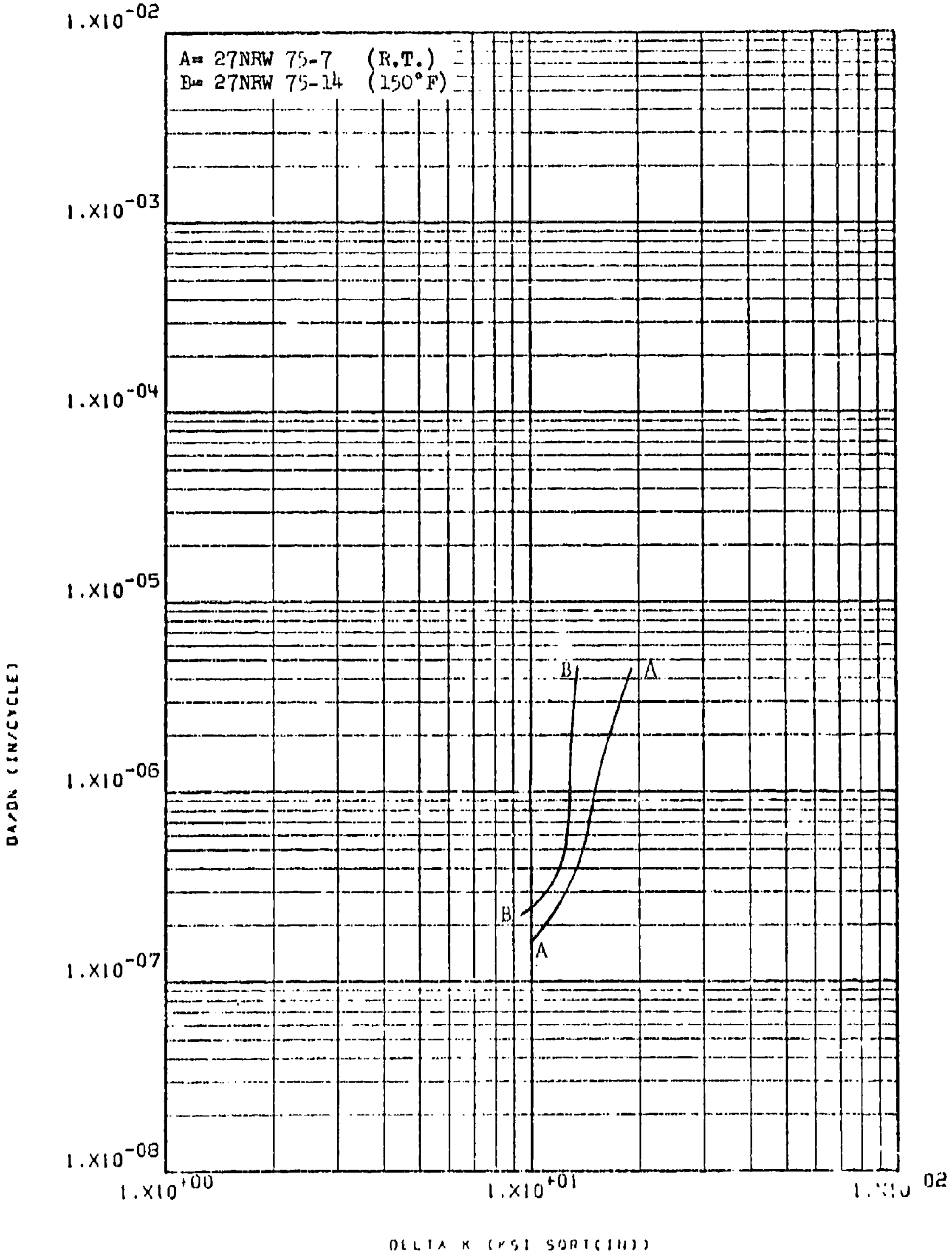

Figure 8.2.2.2-3 Effect of temperature on STW-FCGR at R=0.08, 60 cpm, RW direction, in 2024-T852 3" x 18" x 35" forging 8-83

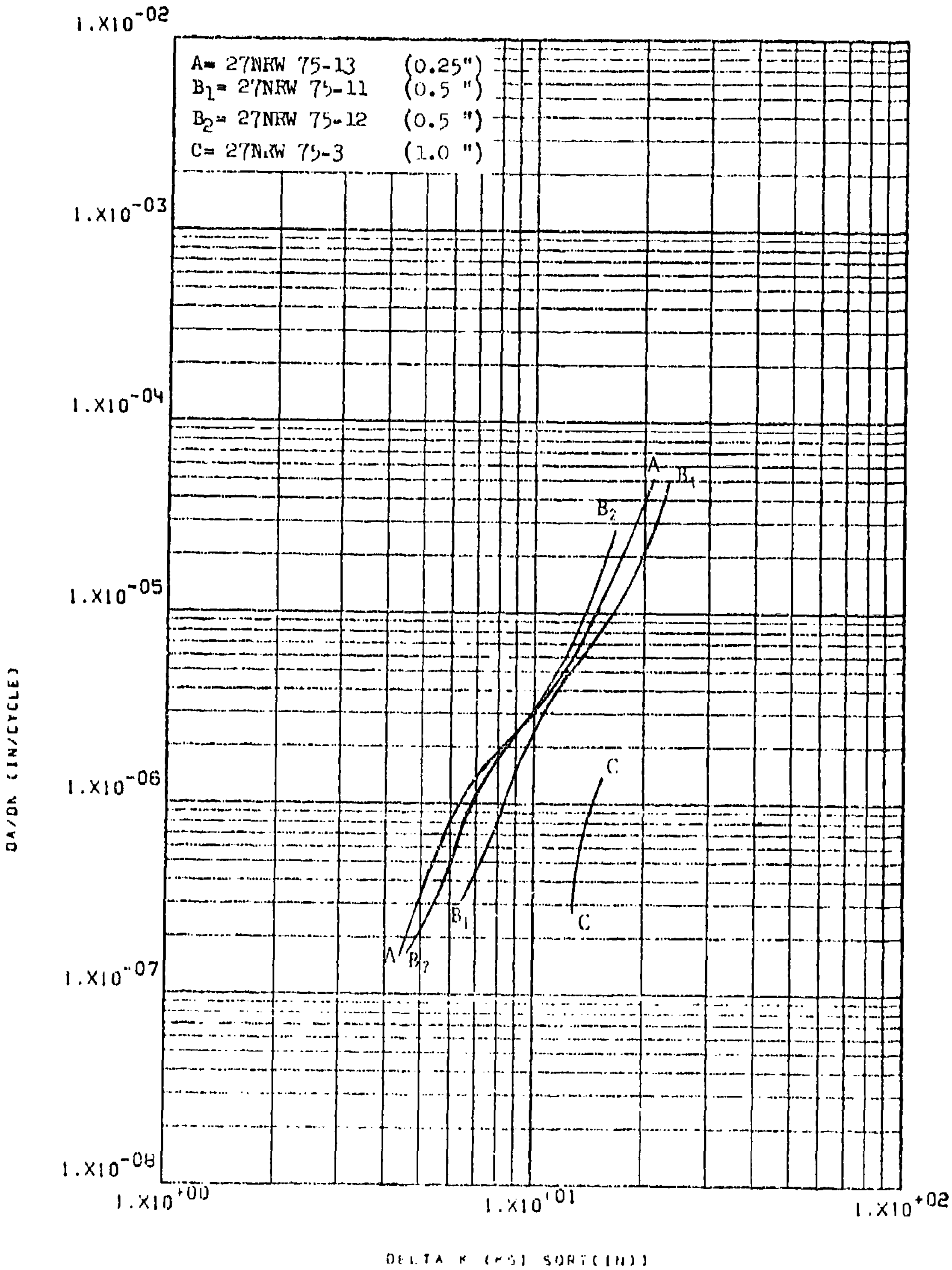

Figure 8.2.2.3-1 Effect of specimen thickness on LHA-FCGR at R.T., R=0.08, 360 cpm, RW direction, in 2024-T852 3" x 18" x 35" forging

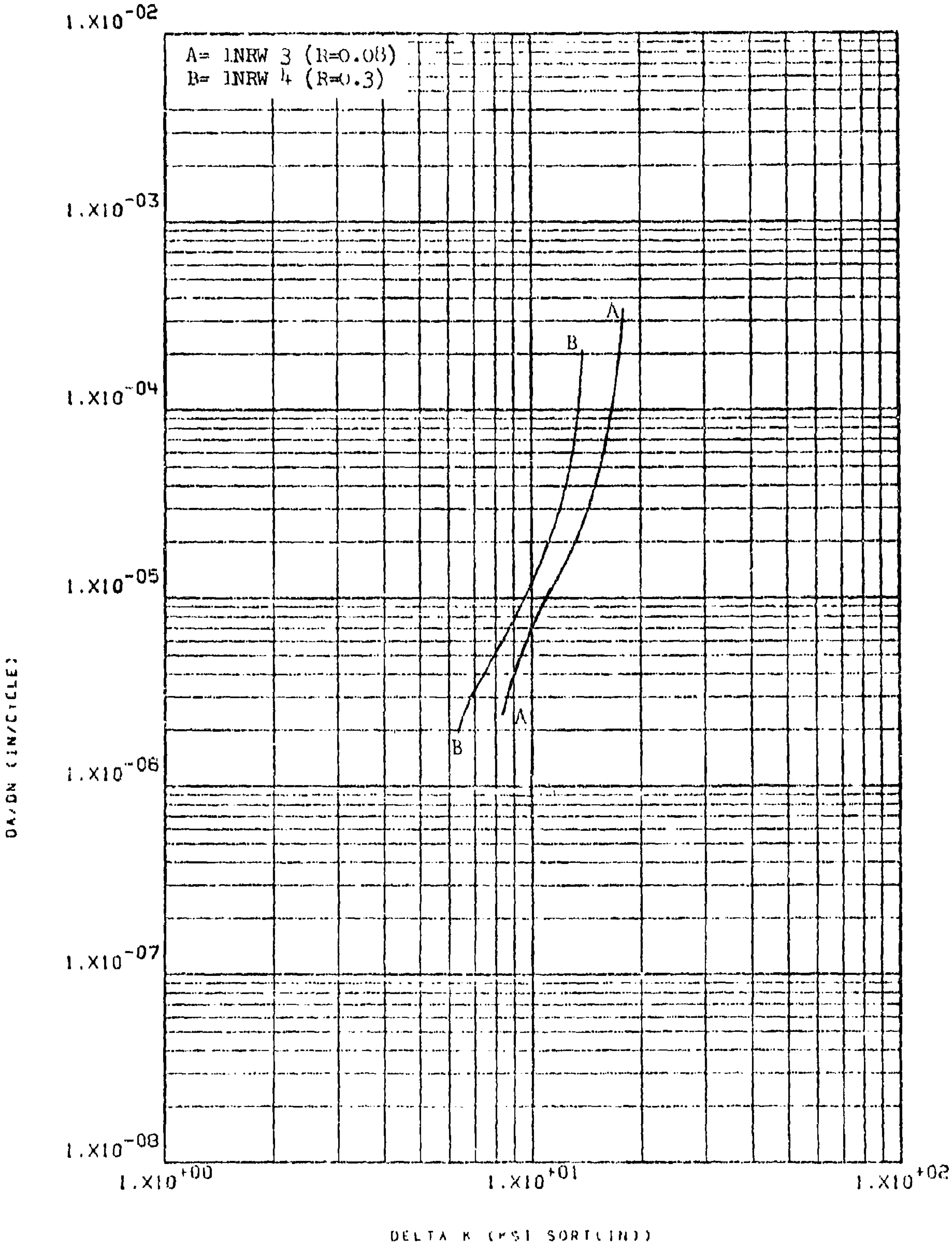

Figure 8.2.2.4-1 Effect of R factor on LHA-FCGR at R.T., 60 cpm, RW direction, in 2024-T851 3" plate

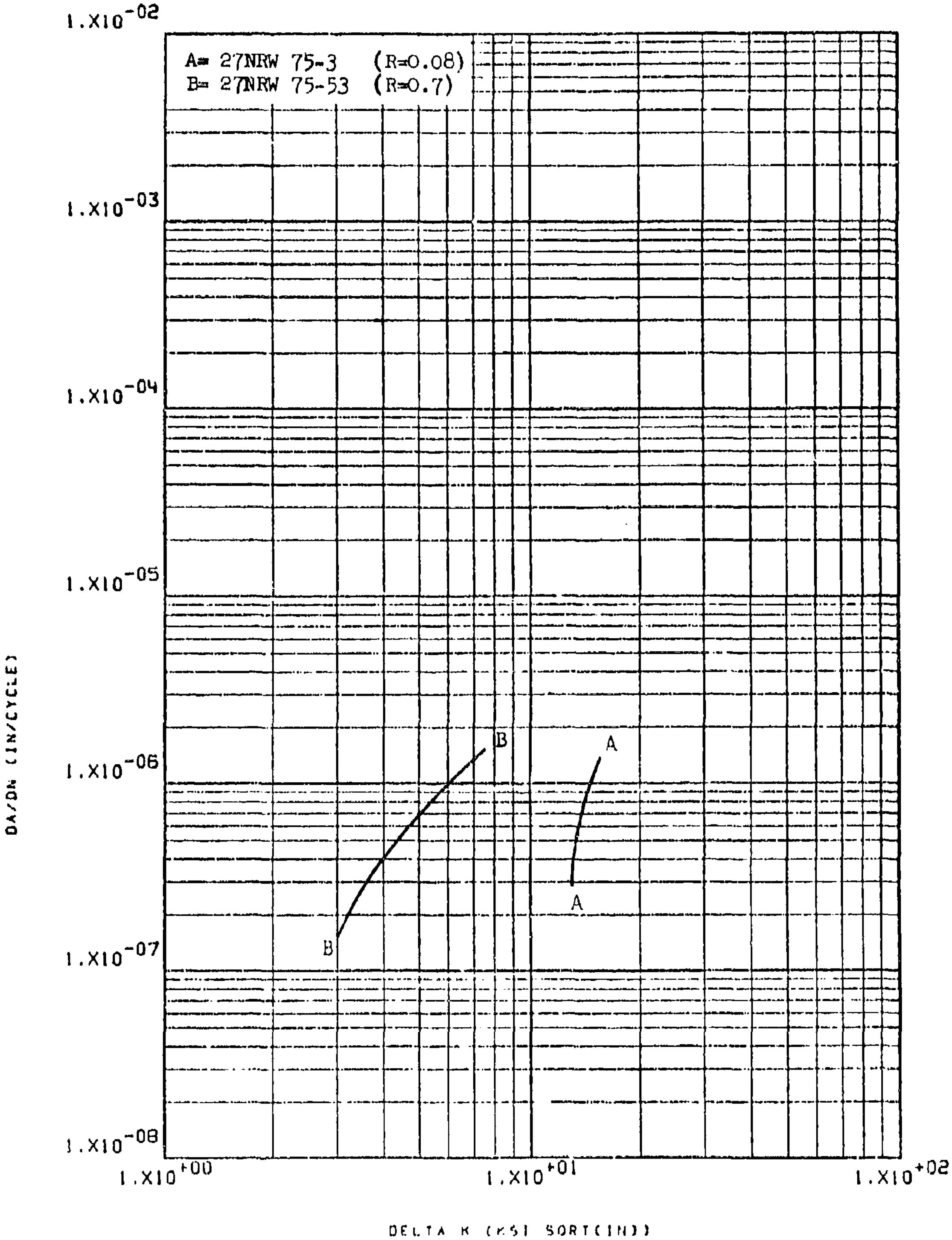

Figure 8.2.2.4-2 Effect of R factor on LHA-FCGR at R.T., 360 cpm, RW direction, in 2024-T852 3" x 18" x 35" forging

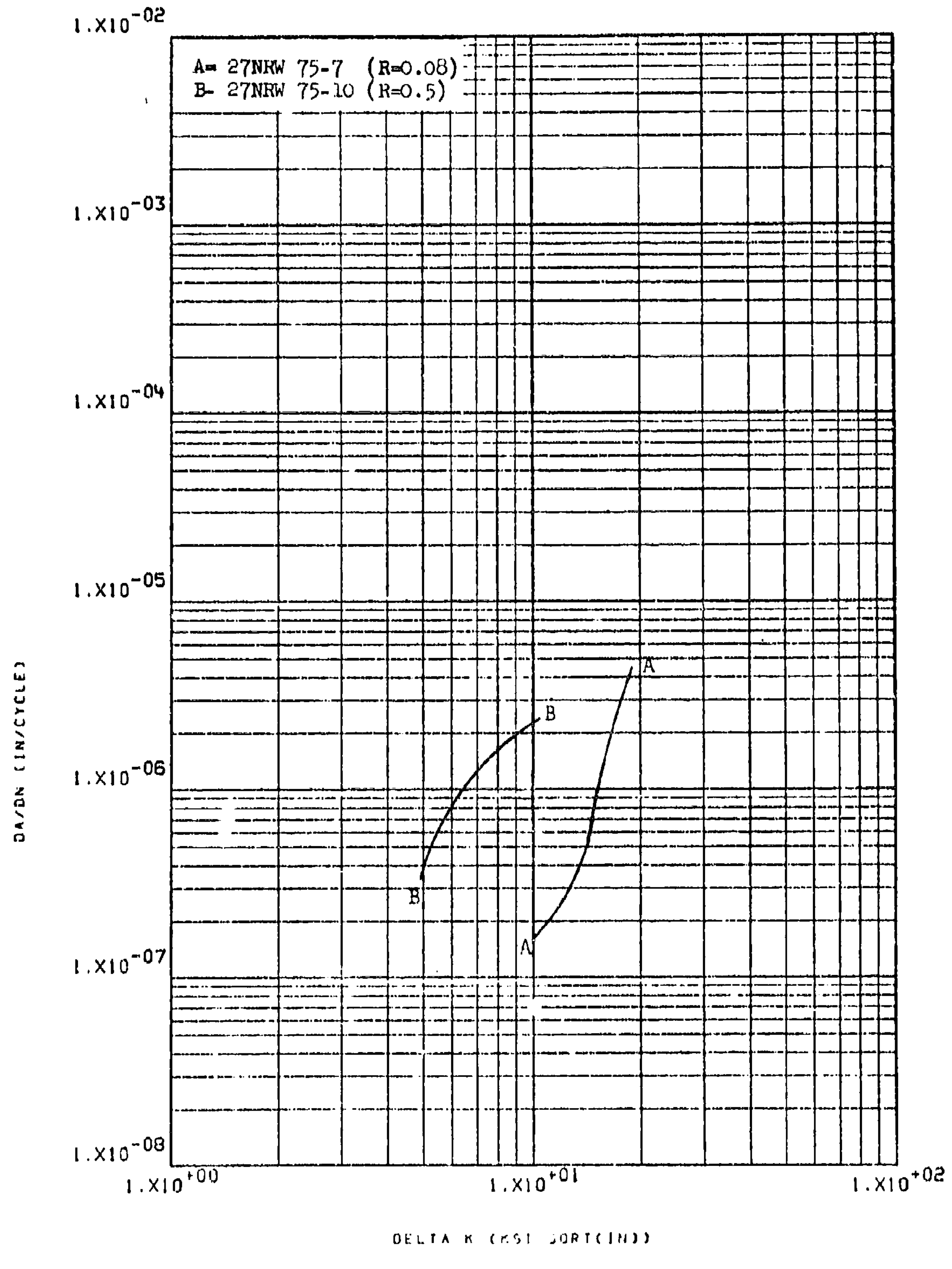

Figure 8.2.2.4-3 Effect of R factor on STW-FCGR at R. T., 60 cpm, RW direction, in 2024-T852 3" x 18" x 35" forging

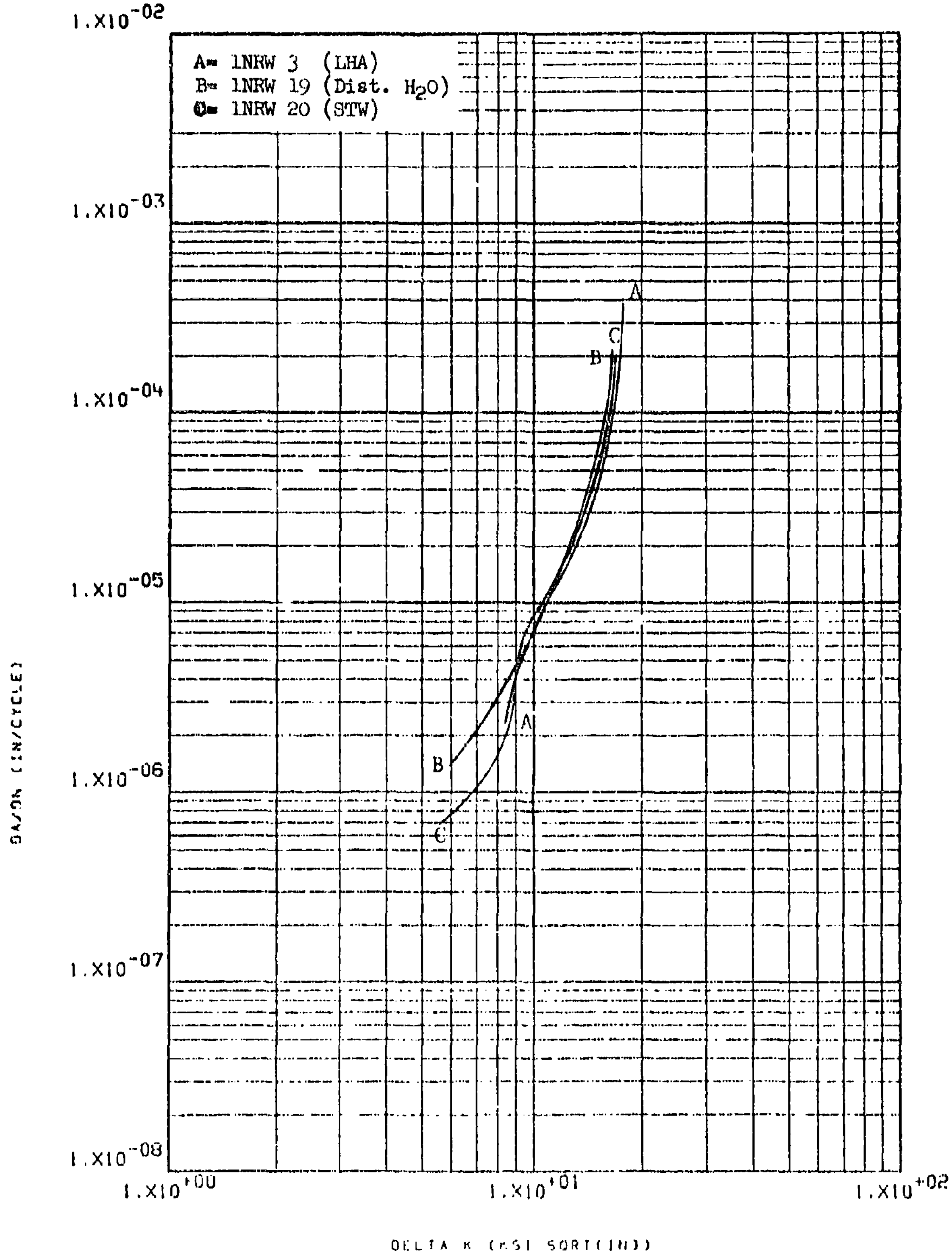

Figure 8.2.2.5-1 Effect of environment on FCGR at R.T., R=0.08, RW direction, in 2024-T851 3" plate

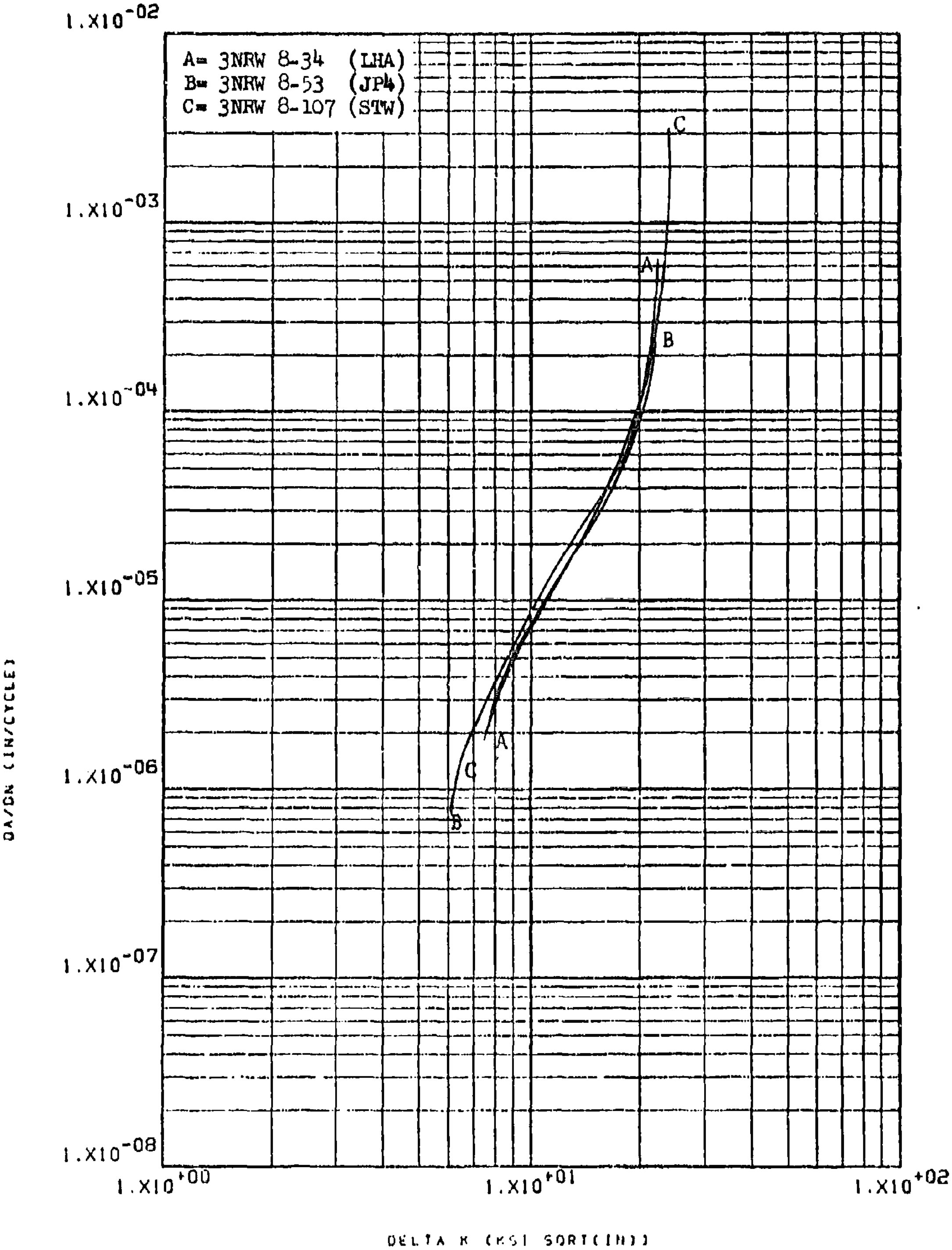

Figure 8.2.2.5-2 Effect of environment on FCGR at R.T., R=0.08, 60 cpm, RW direction, in 2024-T851 3" plate

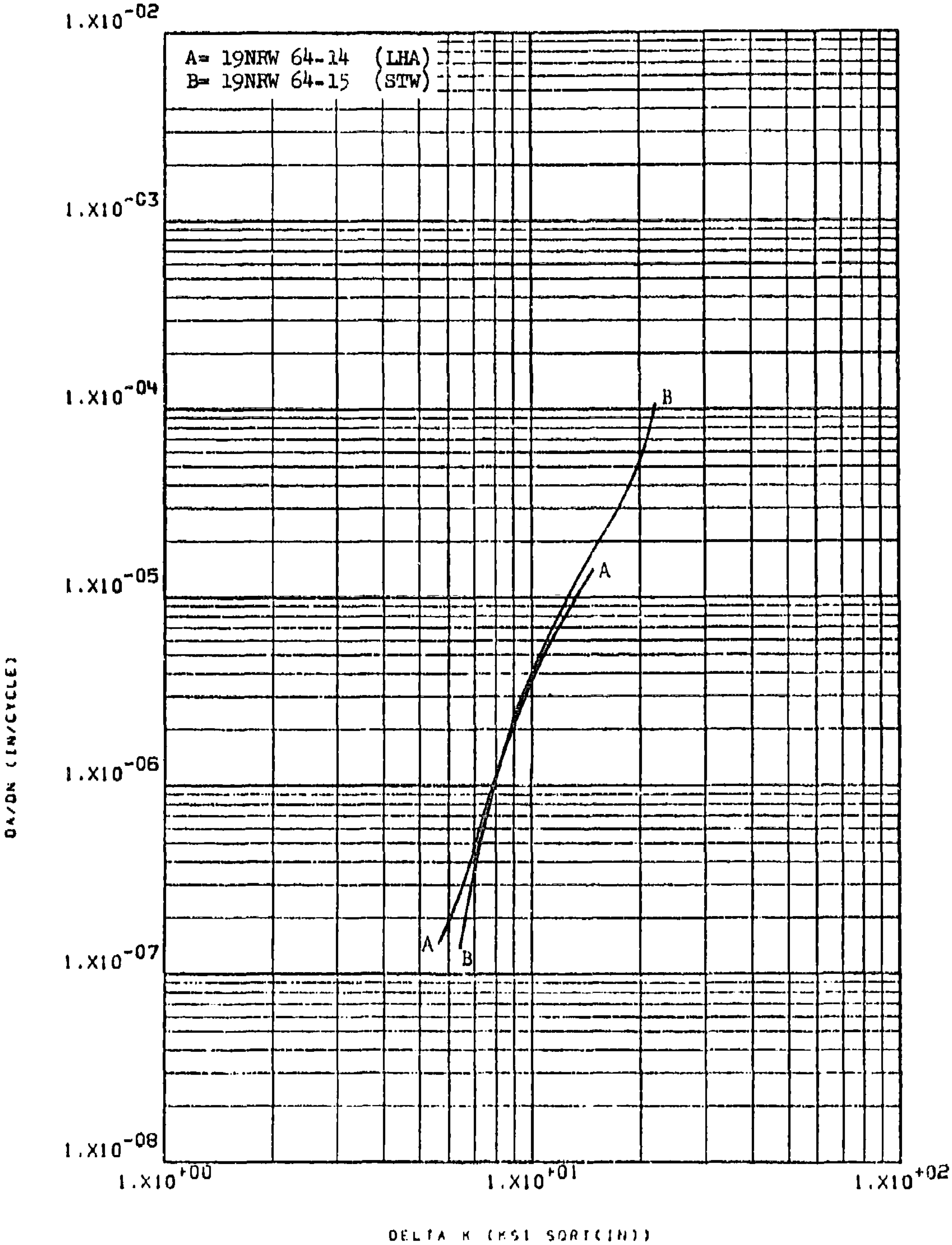

Figure 8.2.2.5-3 Effect of environment on FCGR at R.T., R=0.08, 60 cpm, RW direction, in 2024-T852 3" x 18" x 23" forging

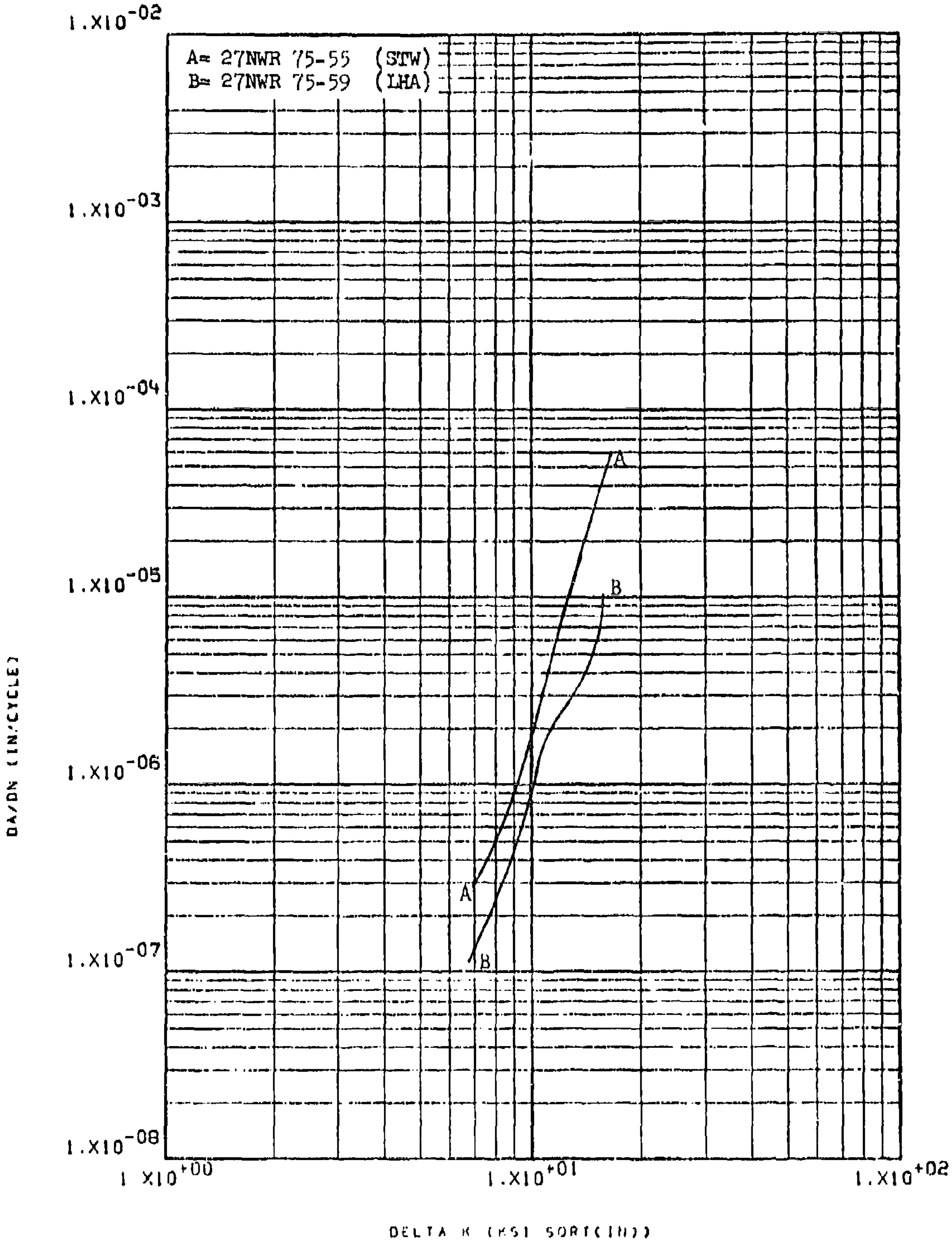

Figure 8.2.2.5-4 Effect of environment on FCGR at R. T., R=0.08, WR direction, in 2024-T852 3" x 18" x 35" forging

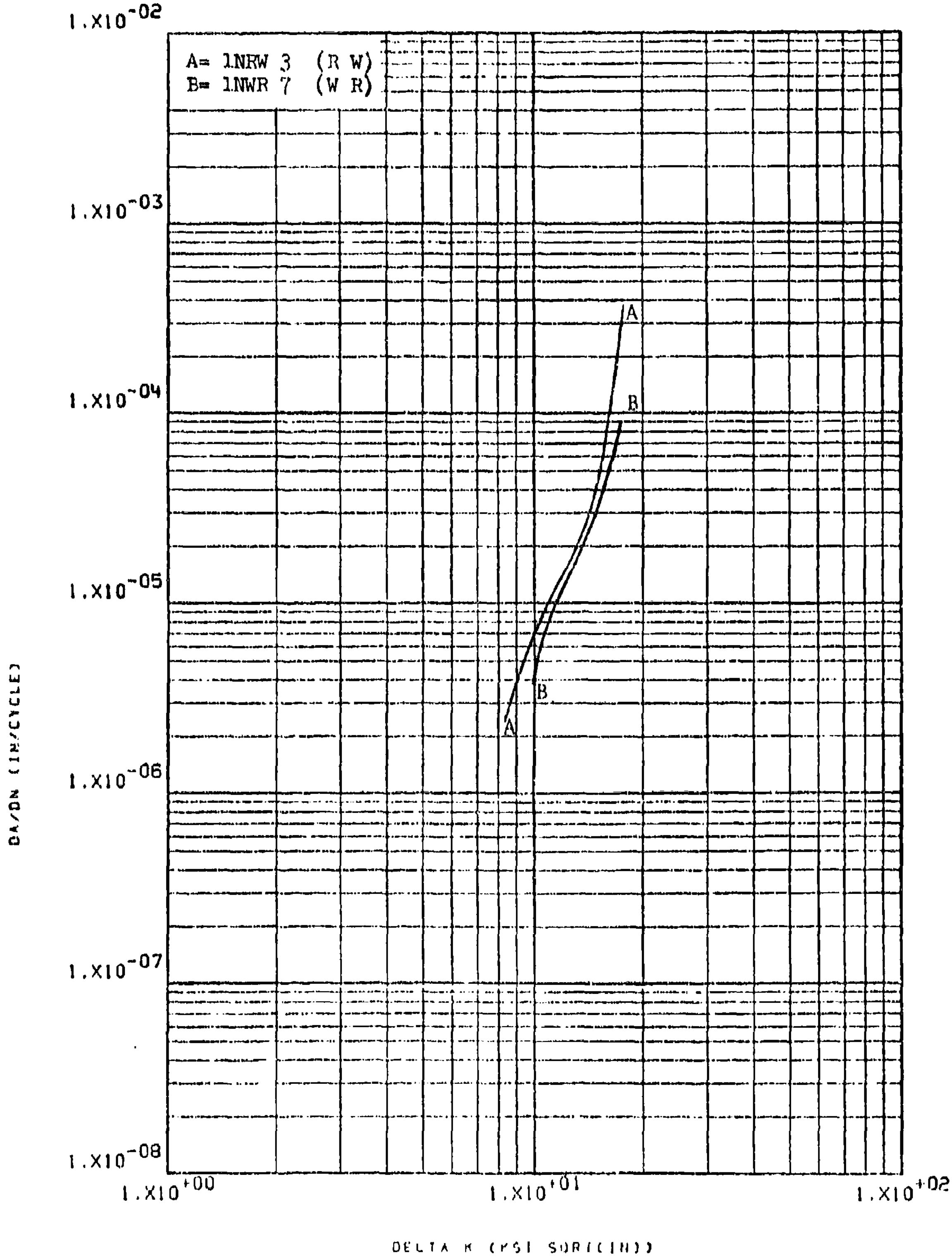

Figure 8.2.2.6-1 Effect of test direction on LHA-FCGR at R.T., R-0.08, 60 cpm, in 2024-T851 3" plate 8-92

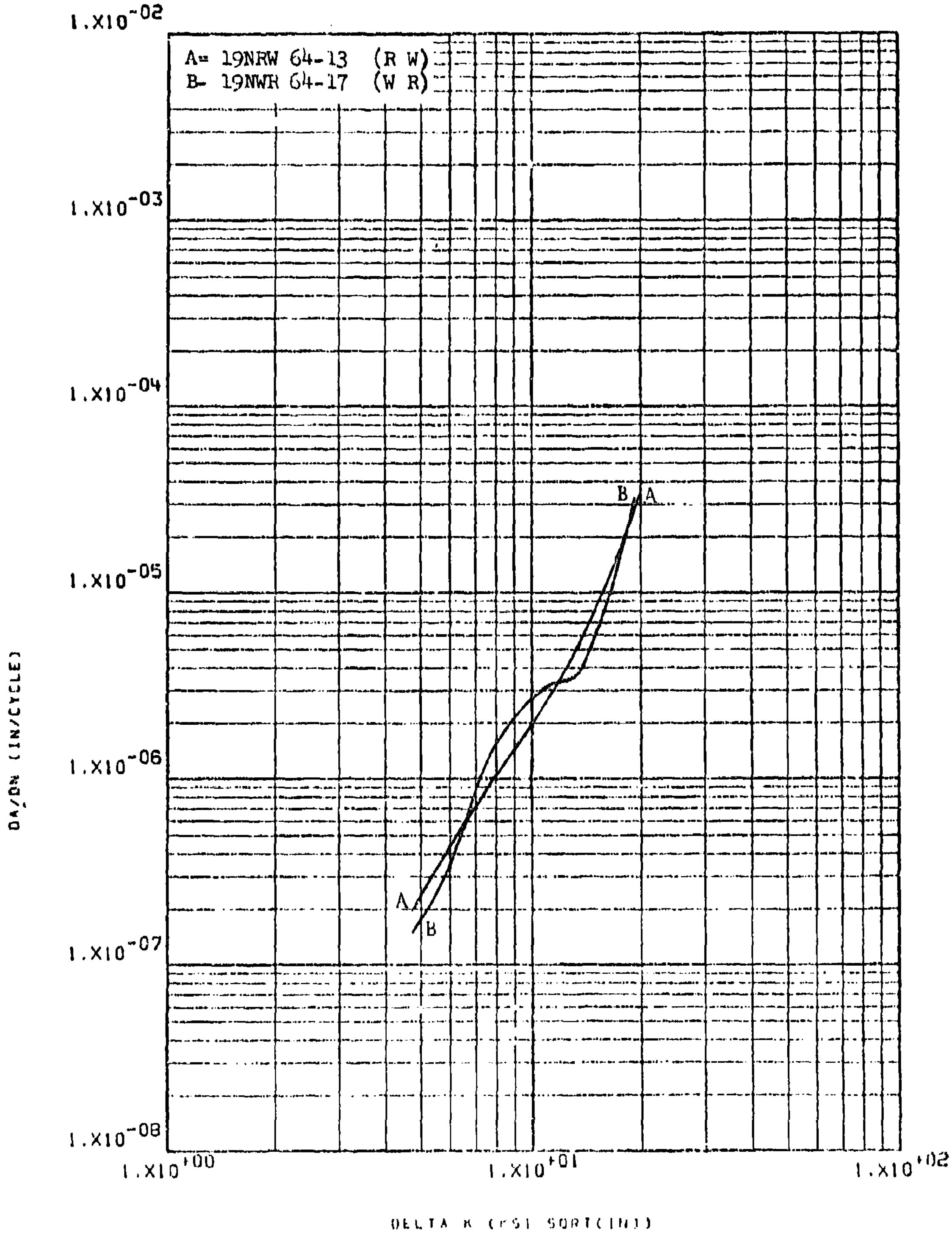

Figure 8.2.2.6-2 Effect of test direction on IMA-FCGR at R.T., R-0.08, 360 cpm, in 2024-T852, 3" x 18" x 23" forging

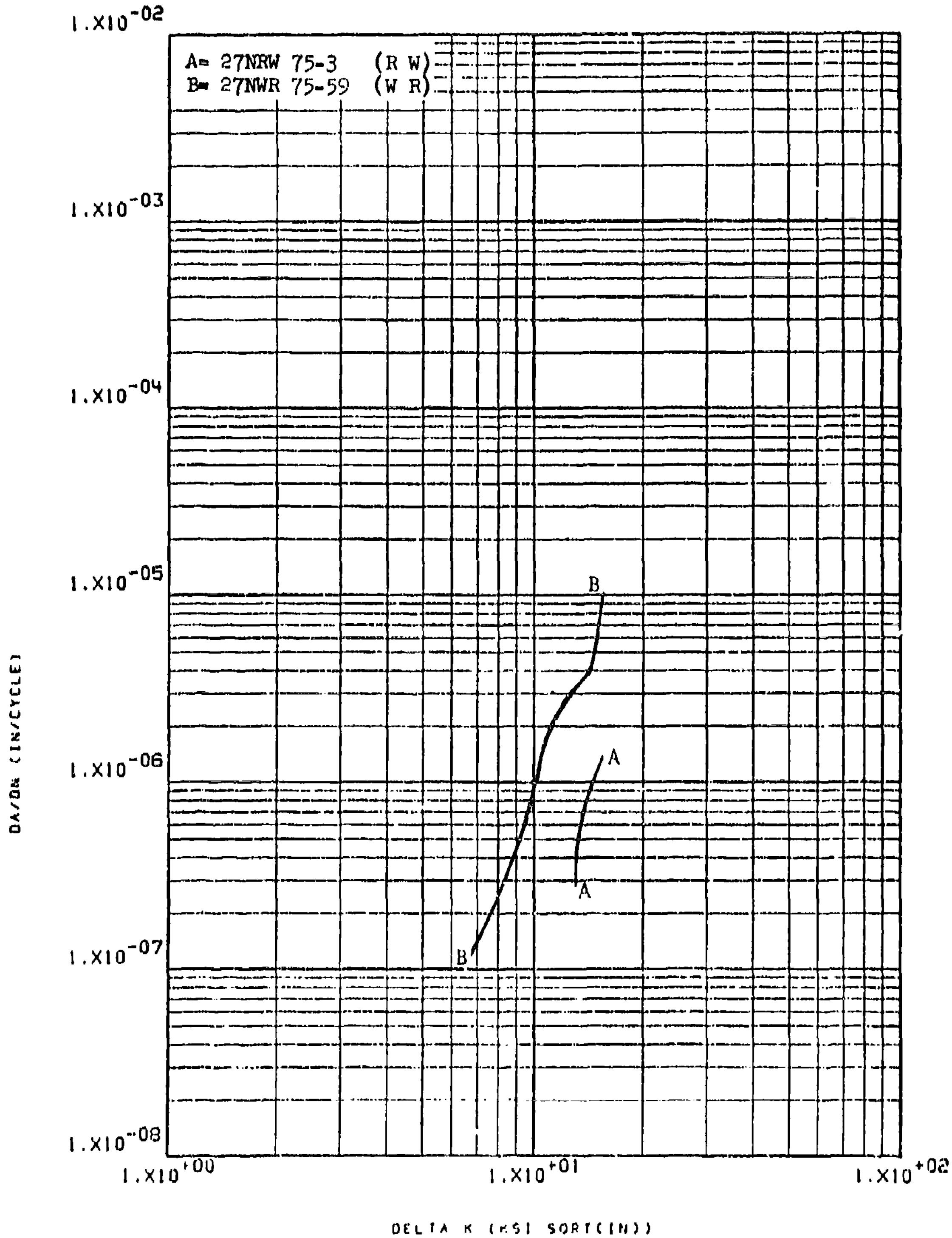

Figure 8.2.2.6-3 Effect of test direction on LHA-FCGR at R.T., R=0.08, 360 cpm, in 2024-T852 3" x 18" x 35" forging

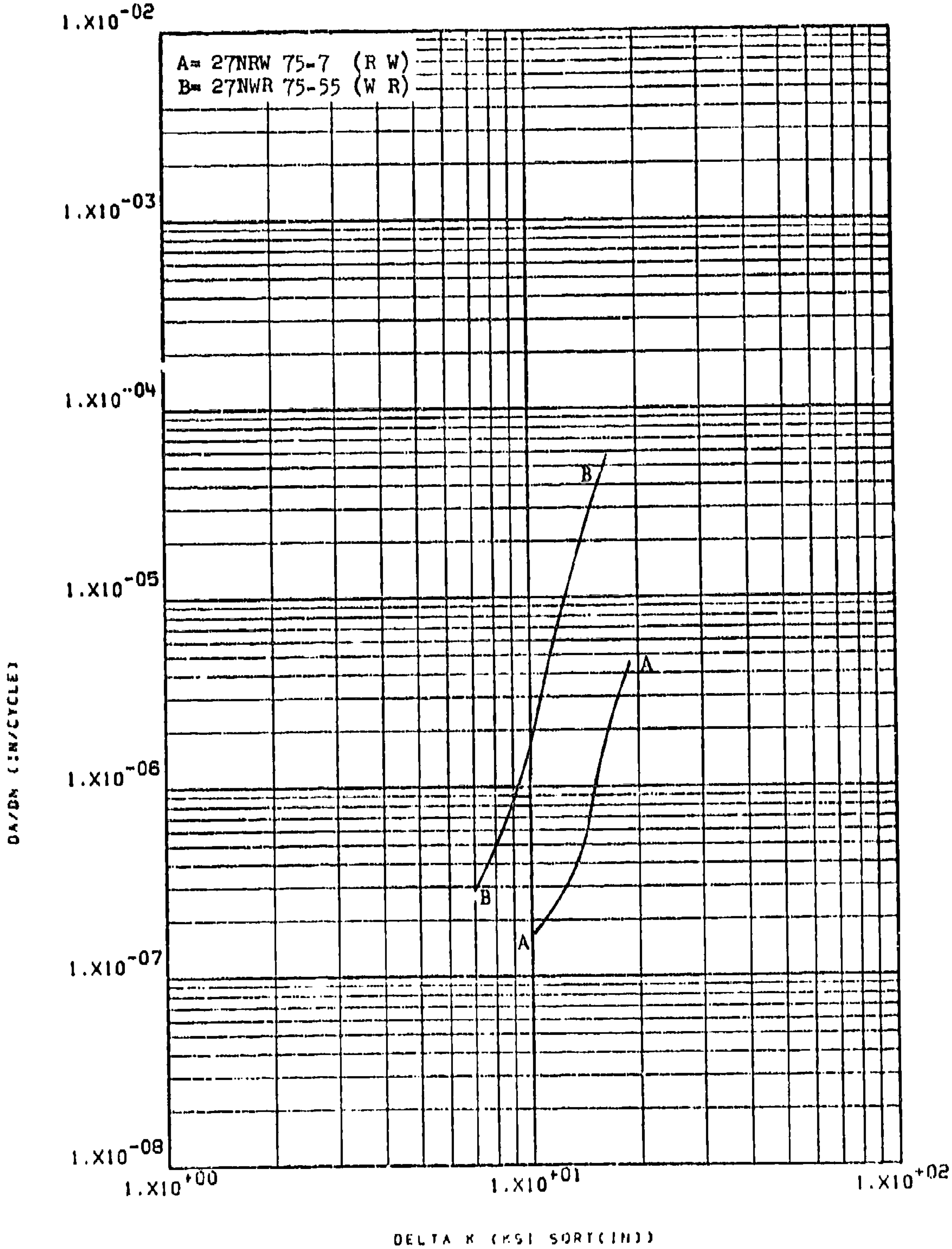

Figure 8.2.2.6-4 Effect of test direction on STW-FCGR at R.T., R=0.08, 60 cpm, in 2024-T852 3" x 18" x 35" forging

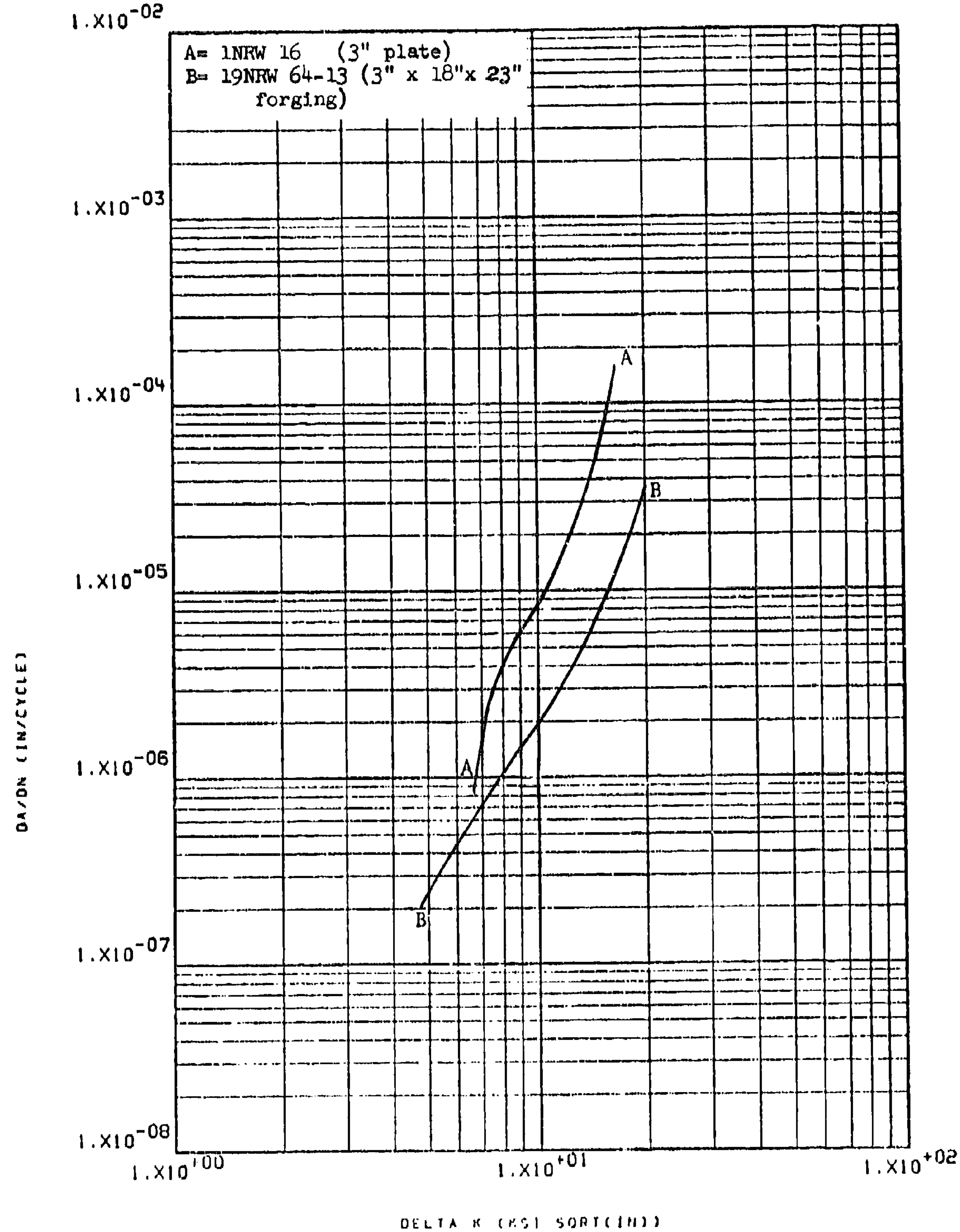

Figure 8.2.2.7-1 Effect of product form on LHA-FCGR at R.T., R= 0.08, 360 cpm, RW direction, in 2024 Al.

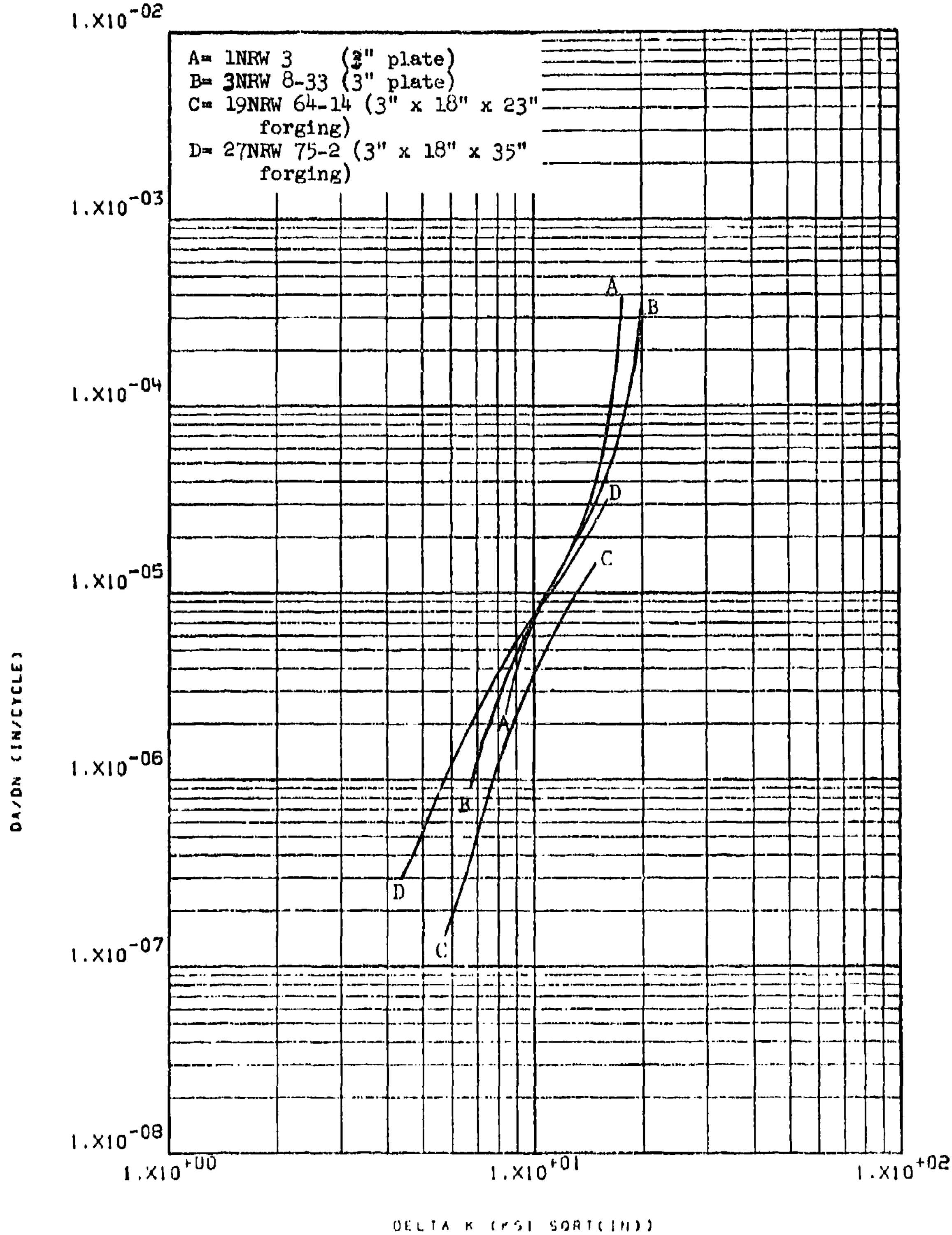

Figure 8.2.2.7-2 Effect of product form on LHA-FCGR at R.T., R= 0.08, 60 cpm, RW direction, 2024 Al.

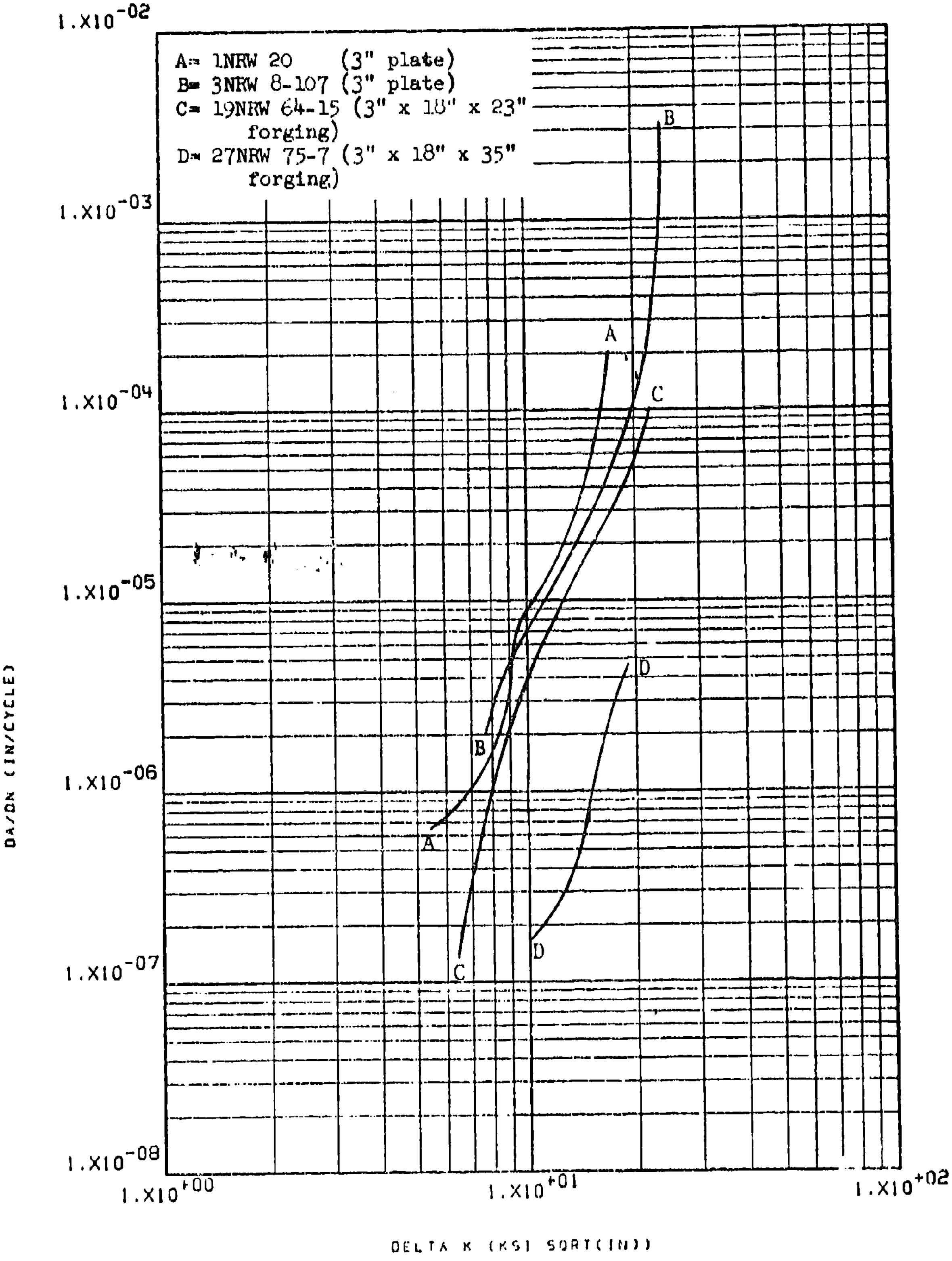

Figure 8.2.2.7-3 Effect of product form on STW-FCGR at R.T., R= 0.08, 60 cpm, RW direction, in 2024 Al.

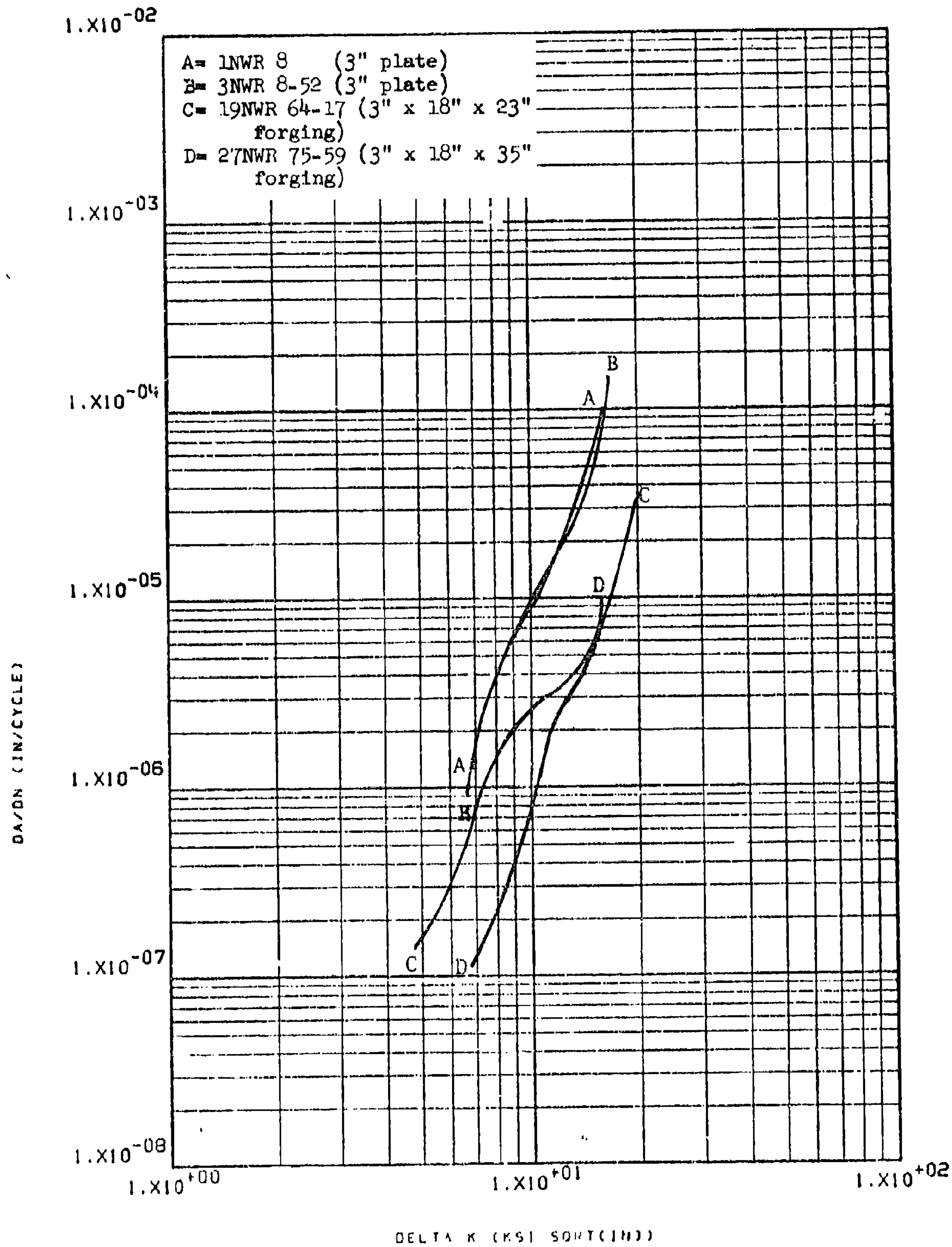

Figure 8.2.2.7-4 Effect of product form on LHA-FCGR at R.T., R= 0.08, 360 cpm, WR direction, in 2024 Al.

8.2.3 Aluminum Alloy 2124

8.2.3.1 Cyclic Rate - Low humidity air growth rates were seen to be significantly increased as cyclic frequency was decreased from 360 to 60 cpm (Figure 8.2.3.1-1).

8.2.3.2 Test Temperature - Not evaluated

8.2.3.3 Specimen Thickness - Not evaluated

8.2.3.4 R Factor - The crack growth rates of this alloy in low humidity air were seen to increase as the R factor was increased from 0.08 to 0.3 and then to 0.5 (Figure 8.2.3.4-1).

8.2.3.5 Environment - Crack growth rates in this material were seen to be only slightly, but inconsistently changed as the test environment was changed from low humidity air to sump tank water in both the RW and WR directions (Figures 8.2.3.5-1 and -2).

8.2.3.6 Test Direction - In low humidity air the growth rates of this alloy were significantly greater in the WR direction than in the RW direction (Figure 8.2.3.6-1). This effect was seen to be less significant in sump tank water (Figure 8.2.3.6-2).

8.2.3.7 Product Form - The low humidity air growth rates in this alloy were seen to be measurably greater in 3" thick plate than in 2" thick plate (Figure 8.2.3.7-1).

8.2.3.8 Heat Treat Condition - Not evaluated.

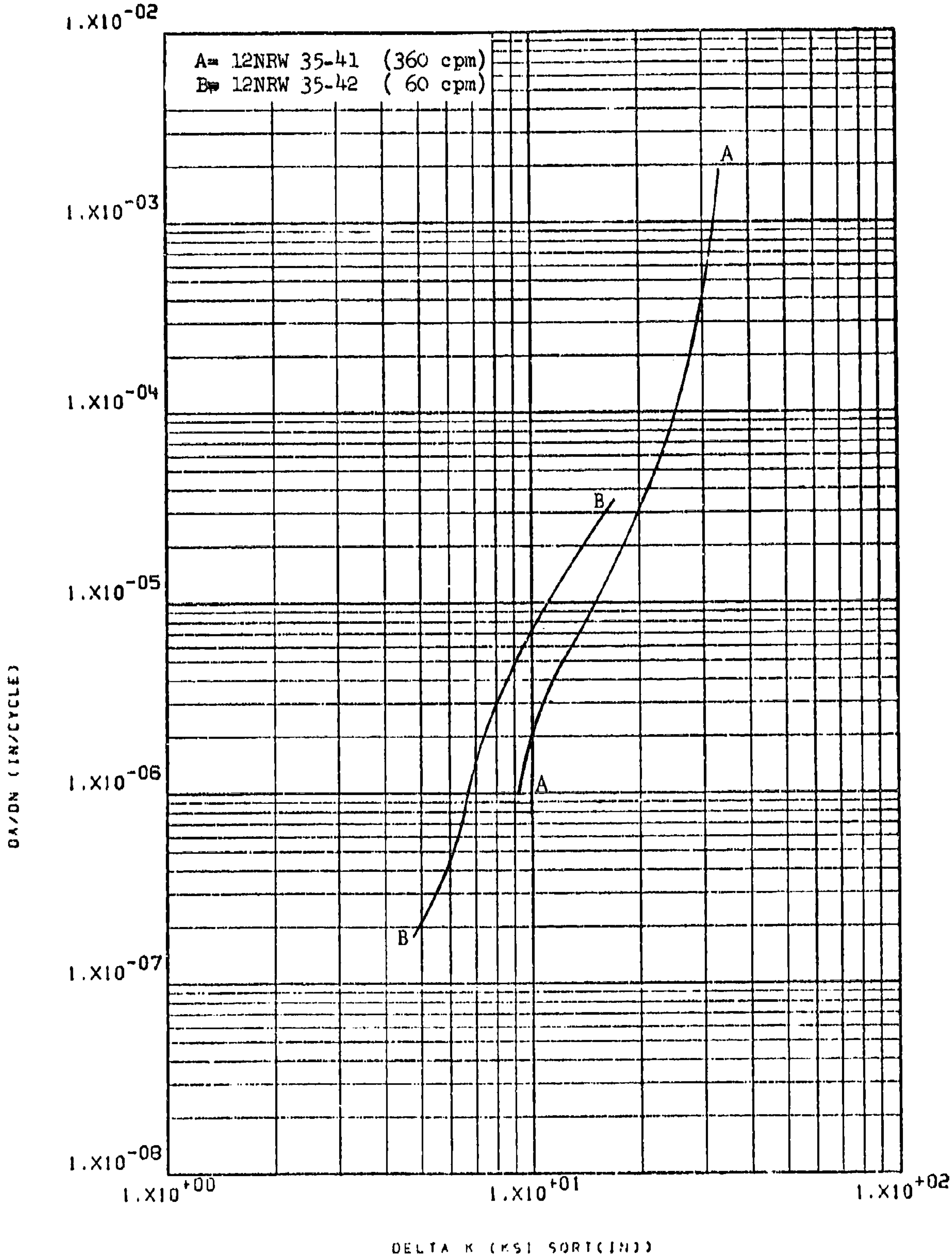

Figure 8.2.3.1-1 Effect of cyclic rate on LHA-FCGR at R.T., R=0.08, RW direction, in 2124-T851 3" plate

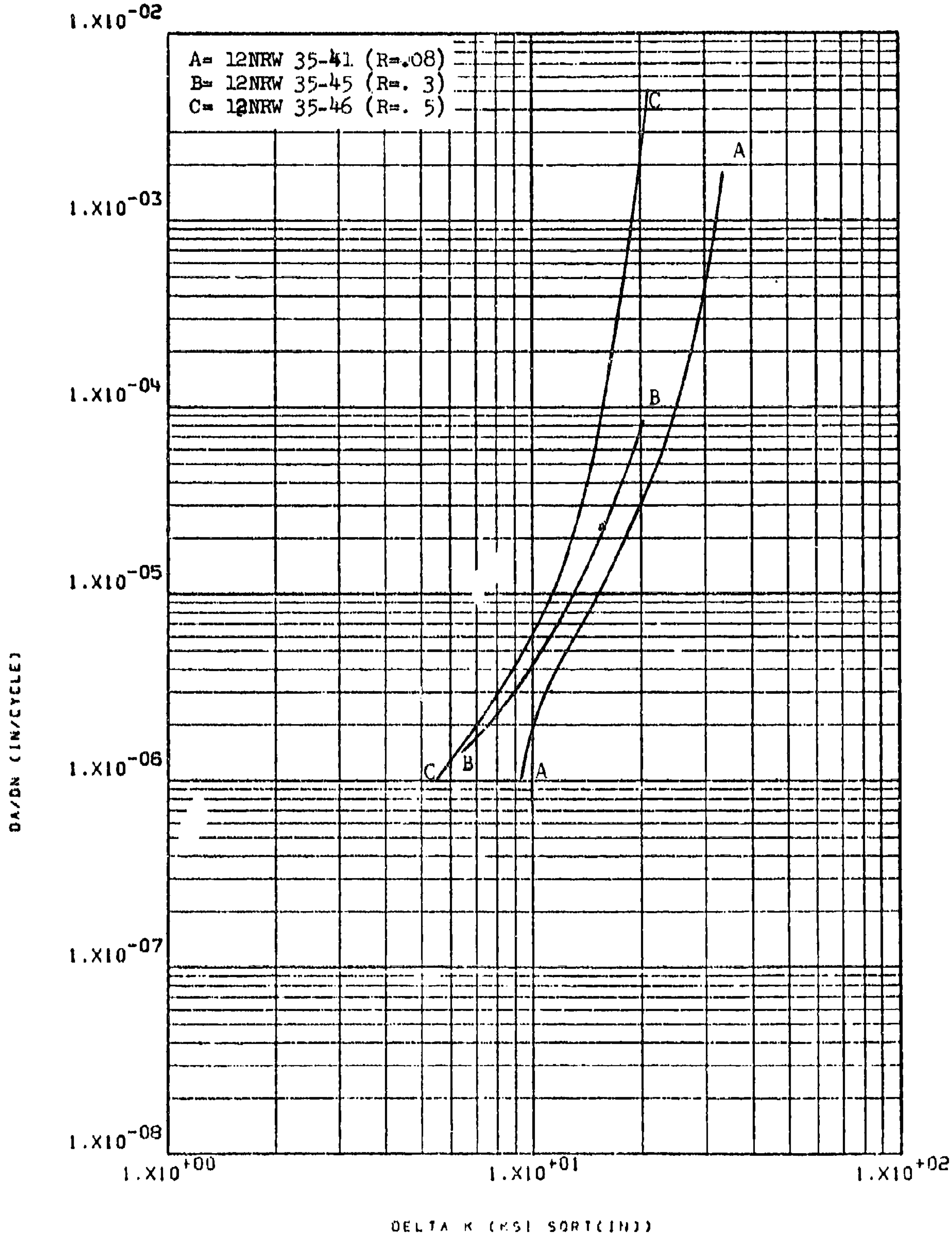

Figure 8.2.3.4-1 Effect of R factor on LHA-FCGR at R.T., 360 cpm, RW direction, in 2124-T851 3" plate

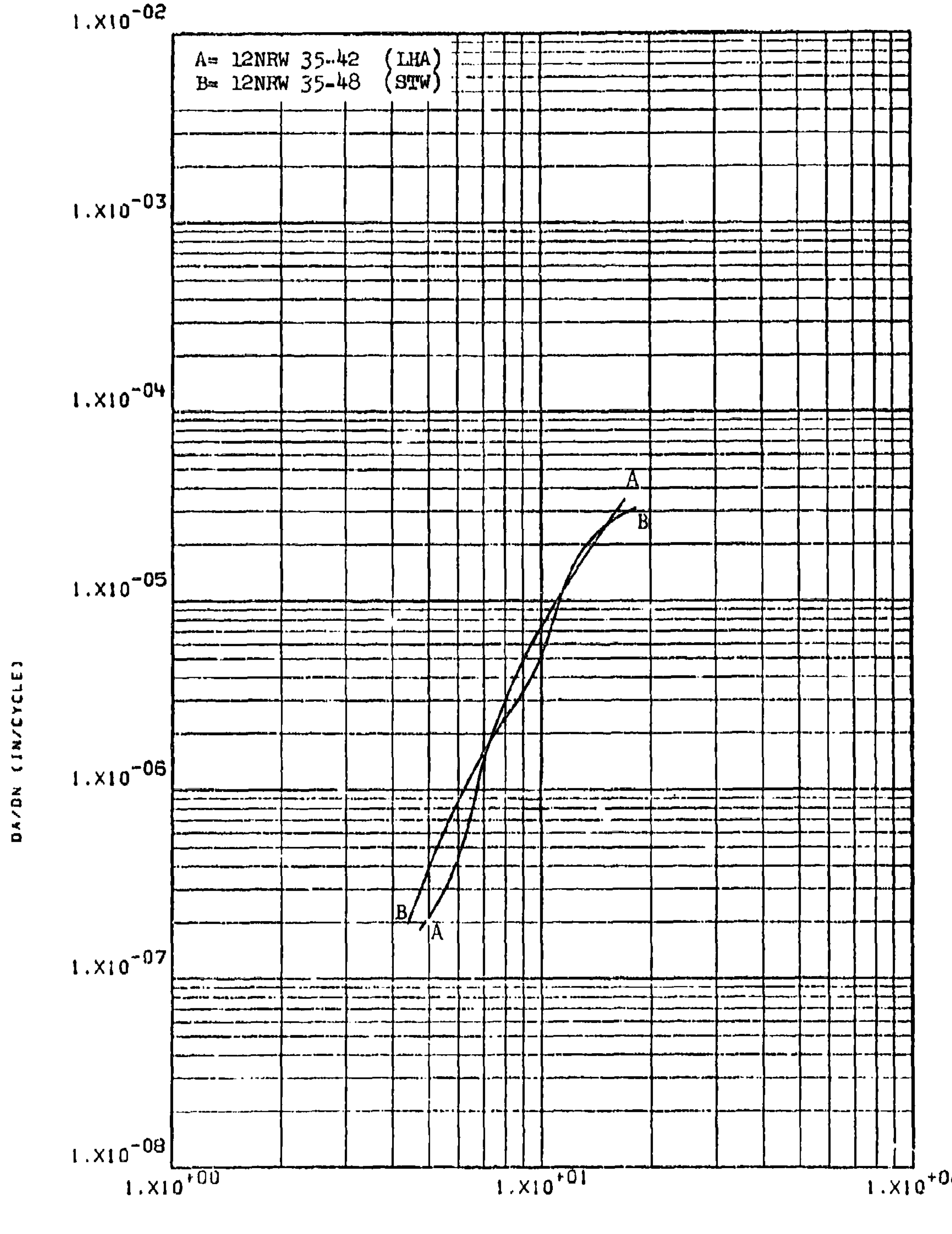

Figure 8.2.3.5-1 Effect of environment on FCGR at R.T., R=0.08, RW direction, in 2124-T851 3" plate

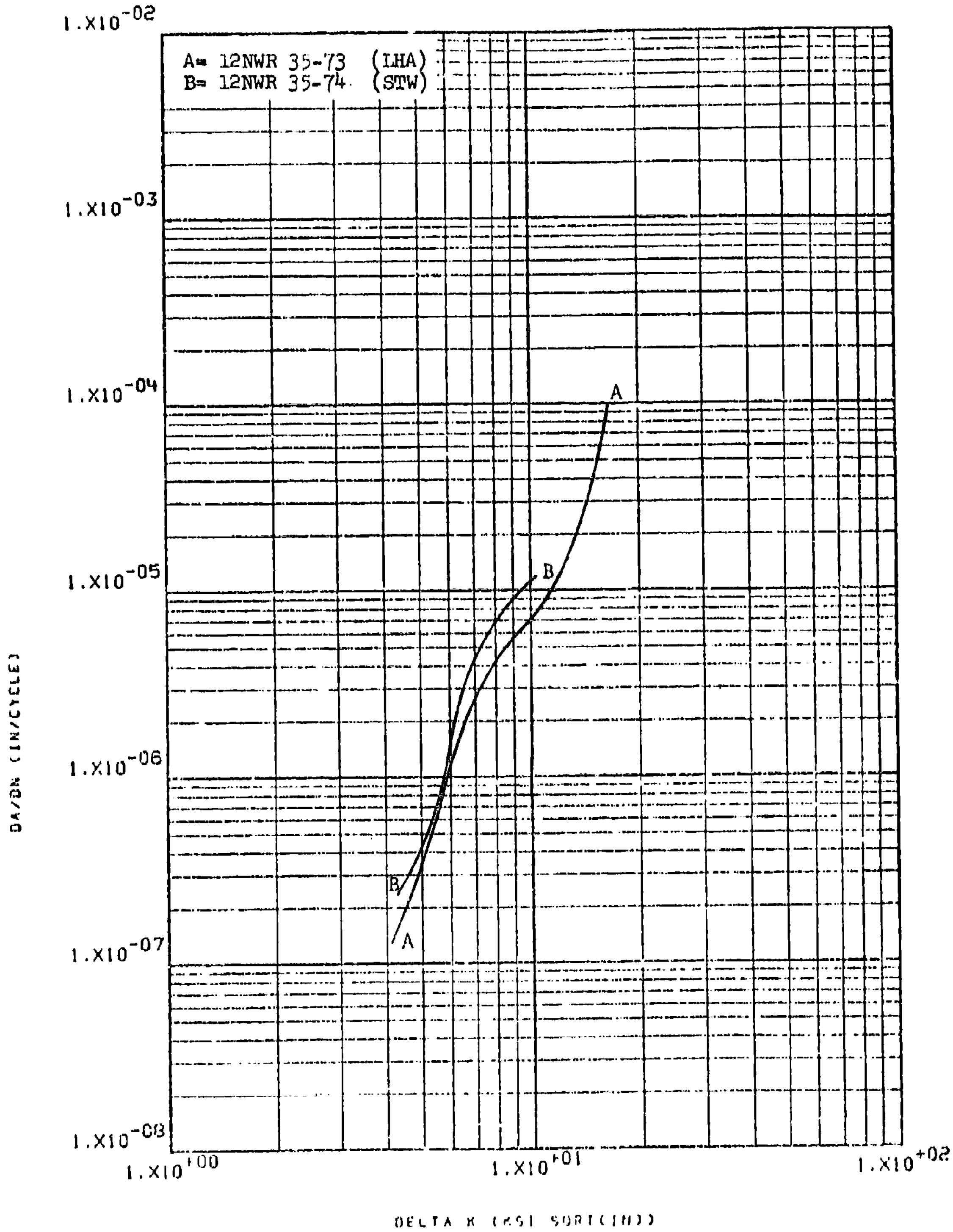

Figure 8.2.3.5-2 Effect of environment on FCGR at R.T., R=0.08, WR direction, in 2124-T851 3" plate

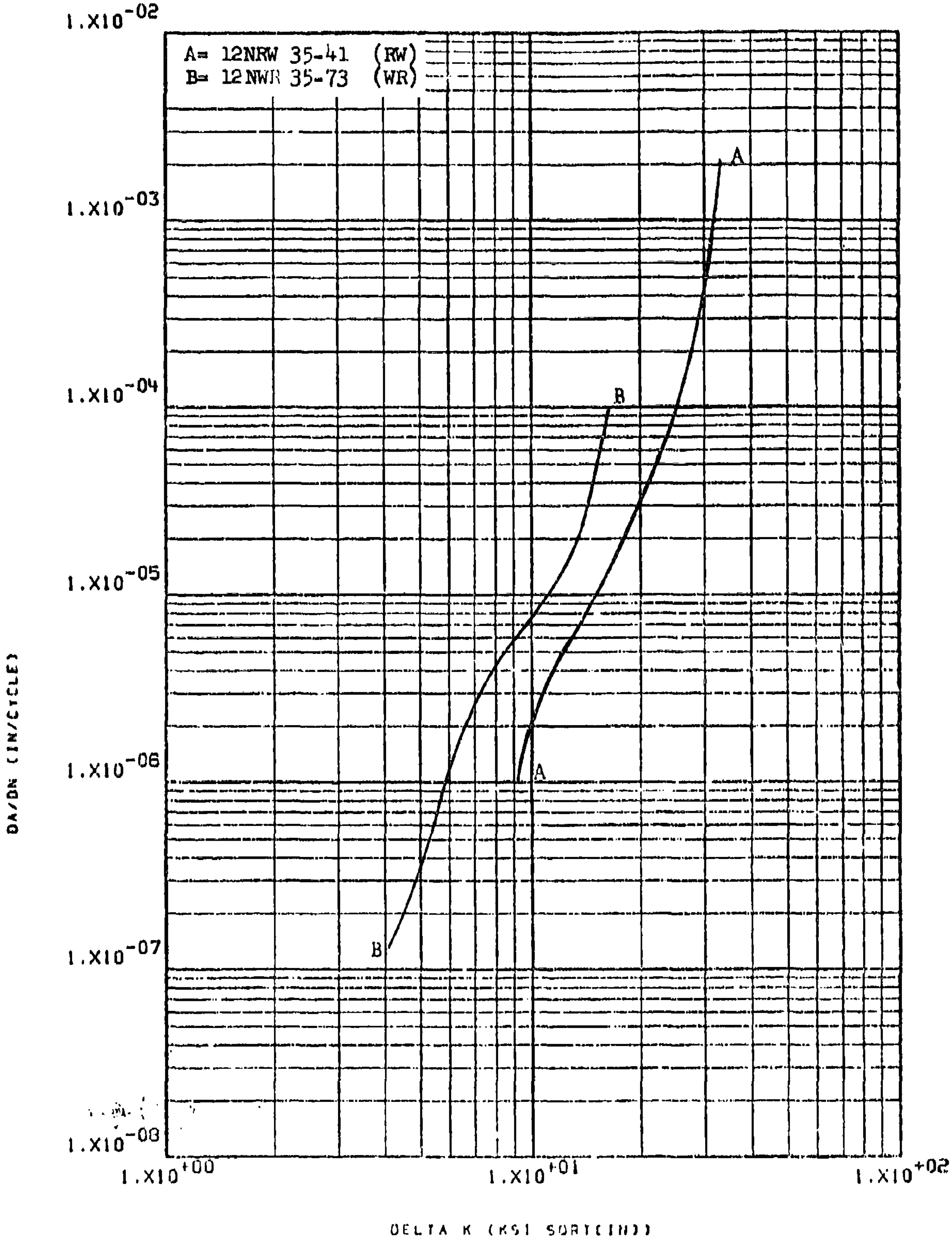

Figure 8.2.3.6-1 Effect of test direction on LHA-FCGR at R.T., 360 cpm, R=0.08, in 2124-T851 3" plate

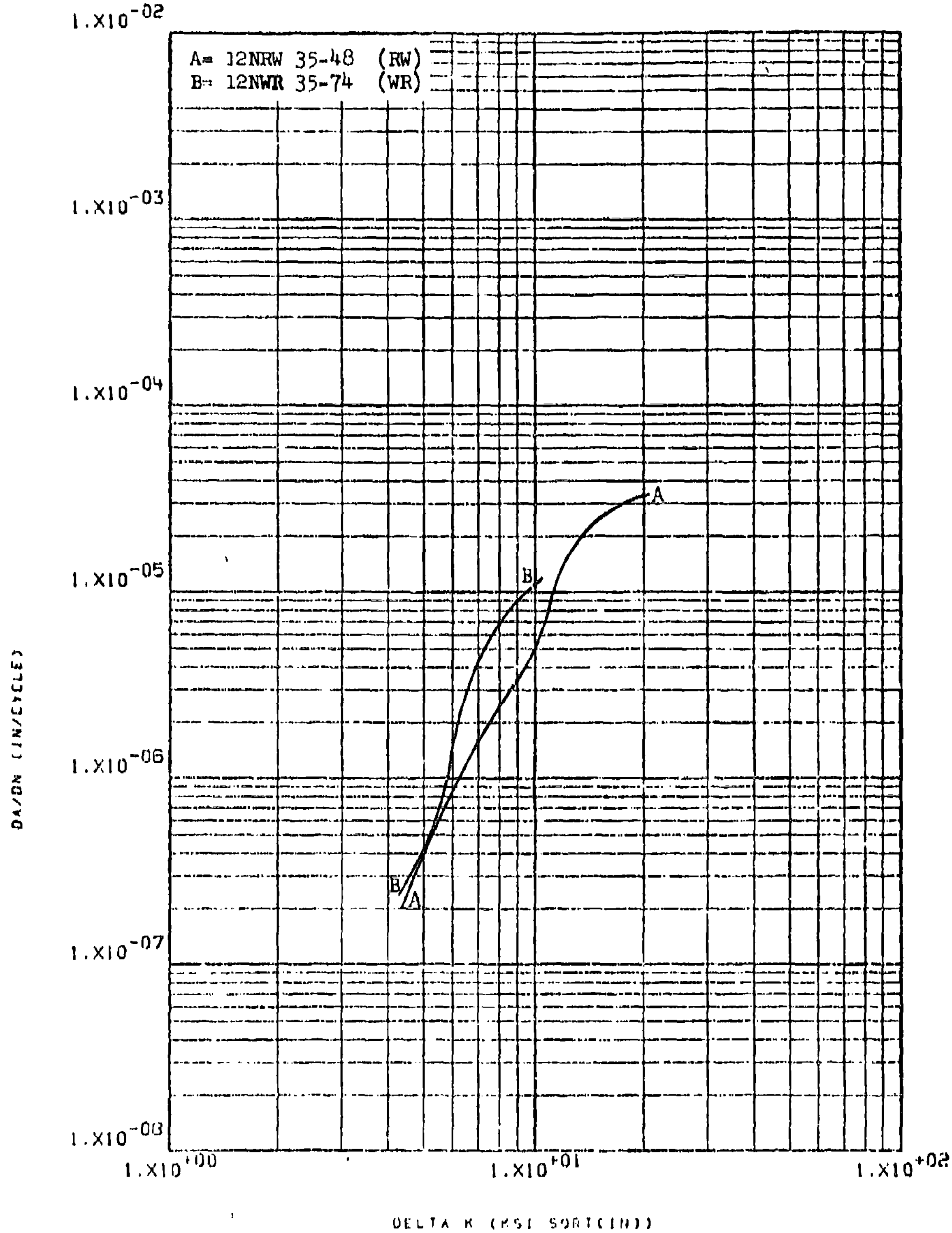

Figure 8.2.3.6-2 Effect of test direction on STW-FCGR at R.T., 60 cpm, R=0.08, in 2124-T851 3" plate

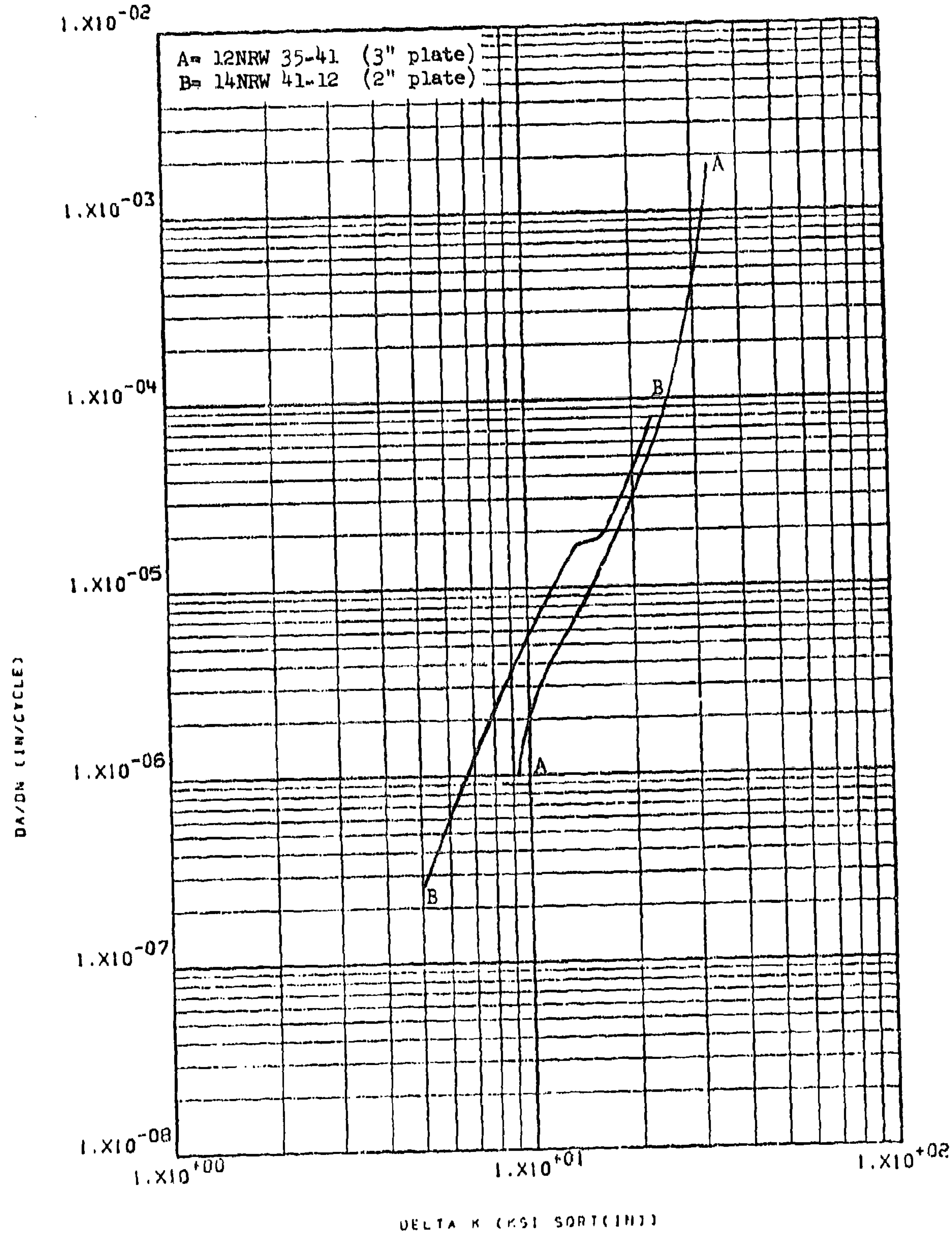

Figure 8.2.3.7-1 Effect of product form on LHA-FCGR at R.T., R=0.08, 360 cpm, RW direction, in 2124 Al.

8.2.4 Aluminum Alloy 2219

8.2.4.1 Cyclic Rate - Low humidity air growth rates were seen to be significantly increased as the cyclic frequency of test was decreased from 360 to 60 cpm (Figure 8.2.4.1-1). No further increases in rates were observed, however, when the frequency was further dropped from 60 to 6 cpm, nor were rates decreased when the frequency was increased from 360 to 3800 cpm (Figure 8.2.4.1-2). In sump tank water, rates were seen to increase when the frequency was decreased from 60 to 6 cpm (Figure 8.2.4.1-3).

8.2.4.2 Test Temperature - The low humidity air growth rates of this material were seen to be substantially greater at 265°F than at ambient temperature in both the RW and WR directions (Figures 8.2.4.2-1 and -2).

8.2.4.3 Specimen Thickness - Growth rates were seen to be essentially unaffected by varying specimen thickness from 0.25" to 0.5" to 1.0" (Figure 8.2.4.3-1).

8.2.4.4 R Factor - Increasing the R factor from 0.08 to 0.3 was seen to result in significant acceleration of growth rates in this material (Figures 8.2.4.4-1 and -2). In low humidity air further increasing R to 0.5 did not result in a further increase in growth rates, (Figure 8.2.4.4-1) whereas in sump tank water, further acceleration of growth rates did result (Figure 8.2.4.4-2).

8.2.4.5 Environment - The growth rates of this material in plate thicknesses up to 2" were seen to be essentially equivalent in low humidity air, distilled water, shop cleaning solvent, field cleaning solvent and sump tank water (Figures 8.2.4.5-1 through -3). At an R factor of 0.5 in the RW direction, however, and at R=0.08 in the WR direction growth rates were seen to be slightly greater in sump tank water than in low humidity air (Figures 8.2.4.5-4 and -5). Similar increases in growth rates when changing from low humidity air to sump tank water were seen to occur in 3" thick plate (Figure 8.2.4.5-6) and in extruded stock (Figures 8.2.4.5-7 and -8) at R=0.08.

8.2.4.6 Test Direction - There were no significant differences observed between the growth rates in the RW and WR directions of plate stock at thicknesses up to 2", as measured in low humidity air at ambient temperature (Figures 8.2.4.6-1 and -2) and 265°F (Figure 8.2.4.6-3) and in sump tank water at ambient temperature (Figure 8.2.4.6-4). In 3" thick plate stock, however, and in extrusions the growth rates were seen to be slightly greater in the WR direction than in the RW direction, when measured in low humidity air (Figures 8.2.4.6-5 and -6) and in sump tank water (Figure 8.2.4.6-7).

8.2.4.7 Product Form - Crack growth rates of this alloy were seen to be essentially unaffected by product form, as demonstrated by relatively narrow scatter bands for each condition tested (Figures 8.2.4.7-1 through -5).

8.2.4.8 Heat Treat Condition - Not evaluated.

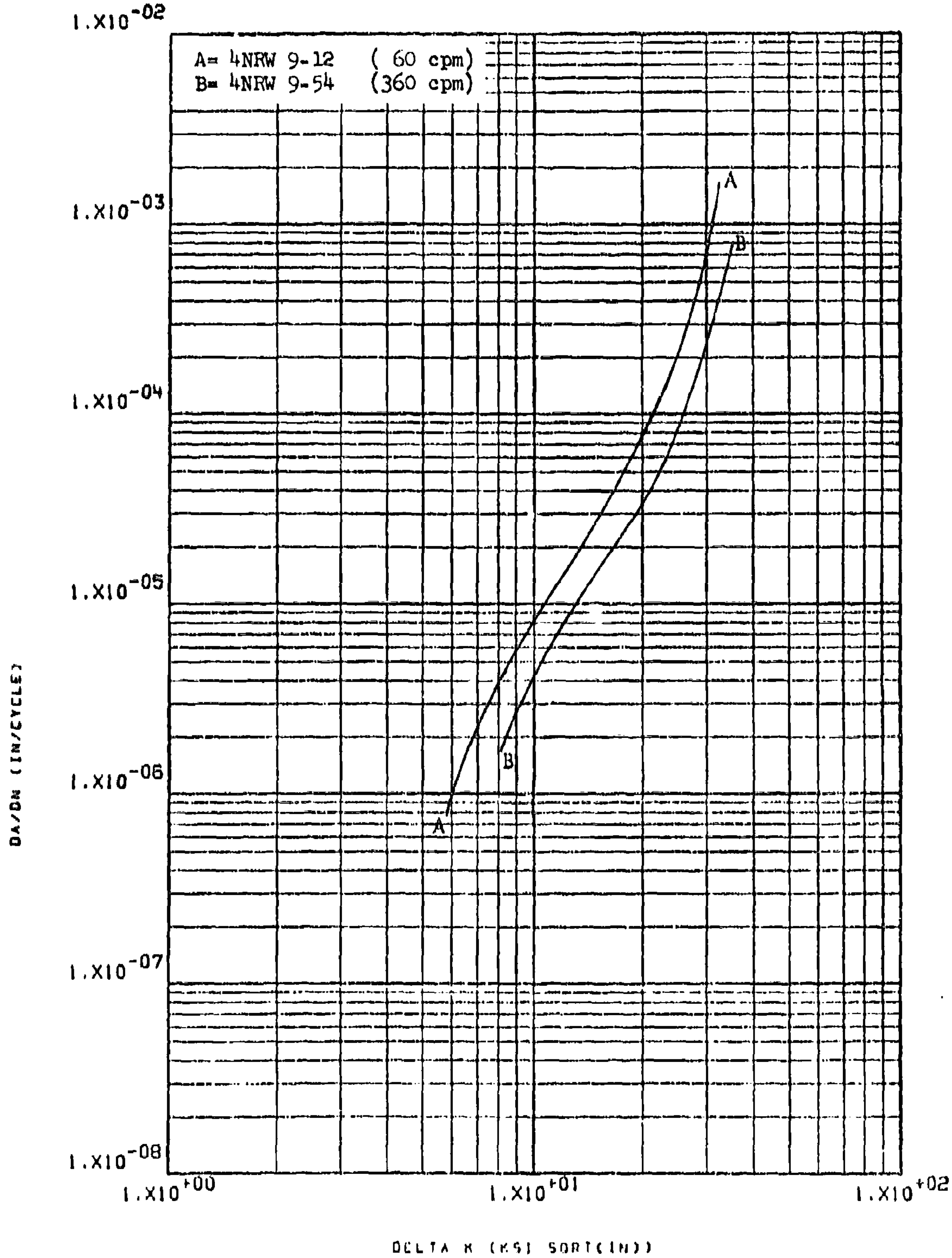

Figure 8.2.4.1-1 Effect of cyclic rate on LHA-FCGR at R.T., R=0.08, RW direction, in 2219-T851 2" plate

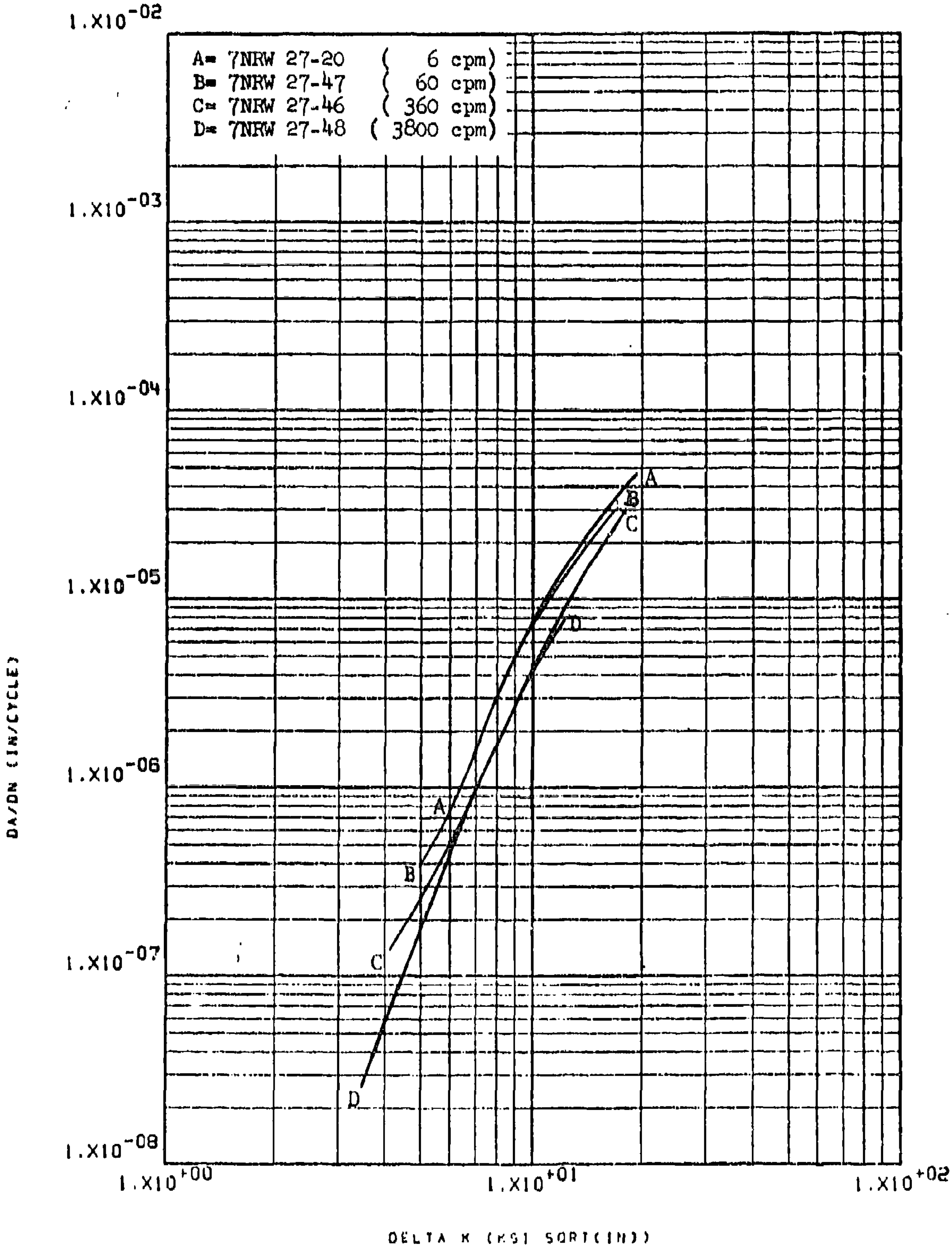

Figure 8.2.4.1-2 Effect of cyclic rate on LHA-FCGR at R.T., R=0.08, RW direction, in 2219-T851 1.75" plate

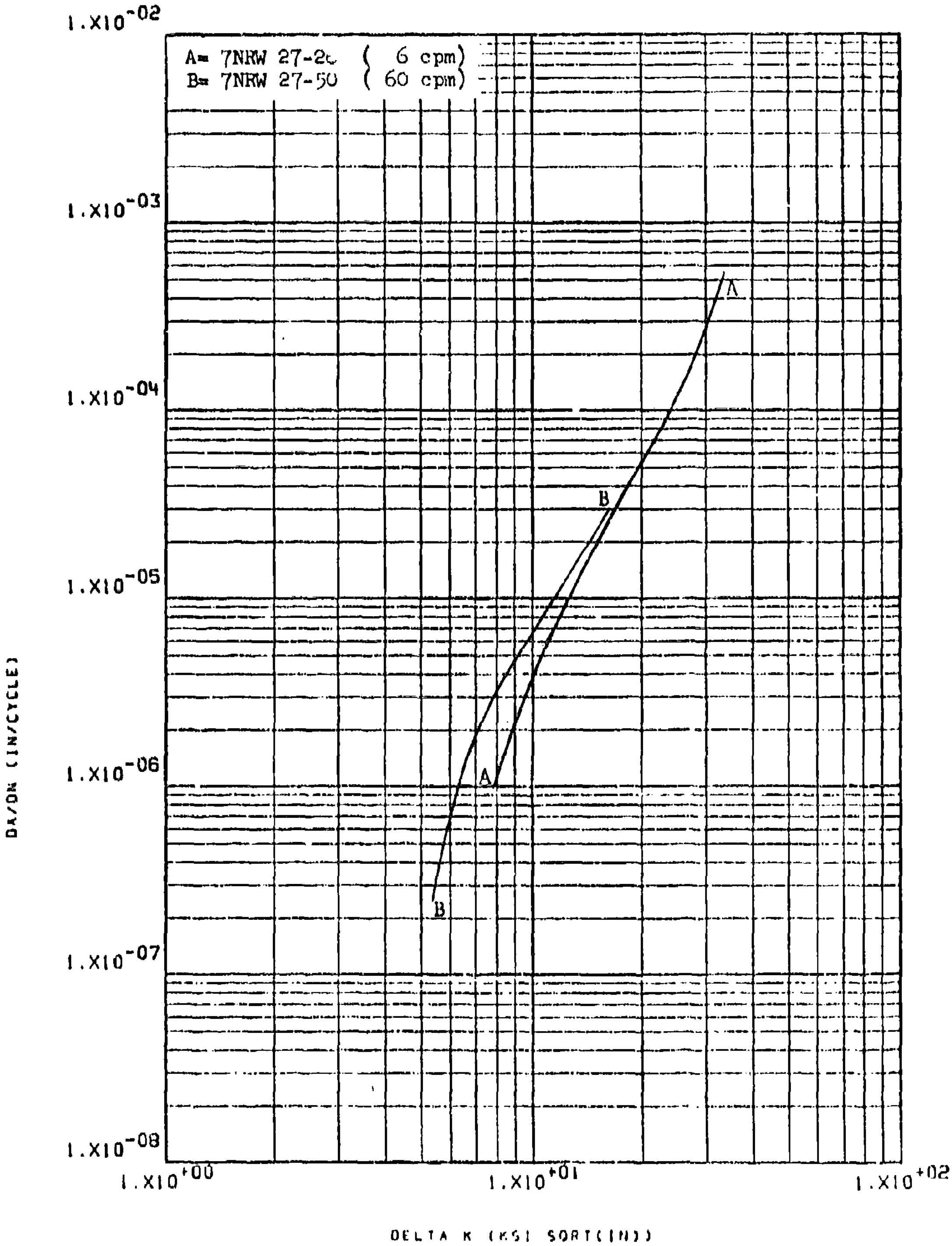

Figure 8.2.4.1-3 Effect of cyclic rate on STW-FCGR at R.T. R=0.08, RW direction, in 2219-T851, 1.75" plate

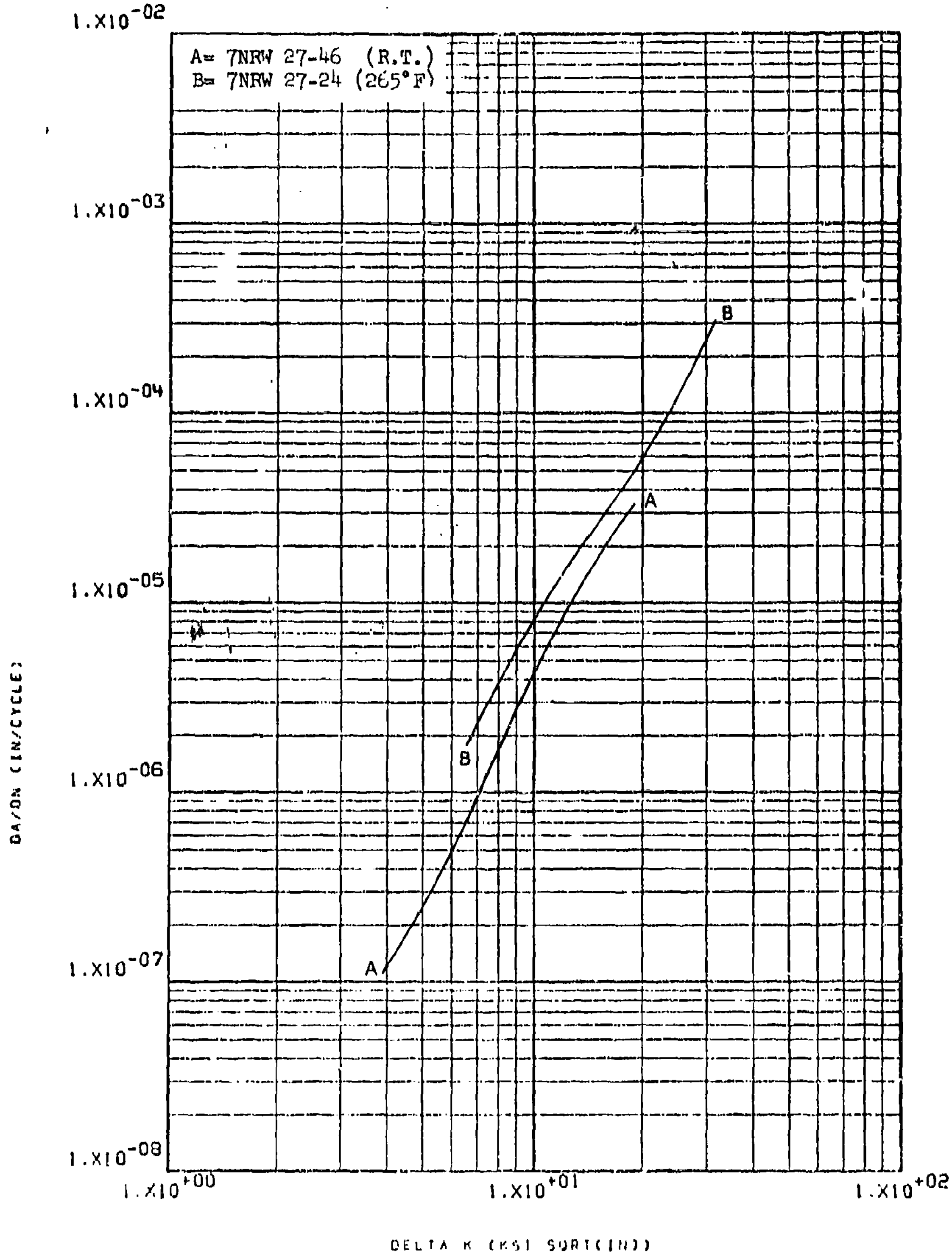

Figure 8.2.4.2-1 Effect of temperature on LHA-FCGR at R=0.08, 360 cpm, RW direction, in 2219-T851, 1.75" plate

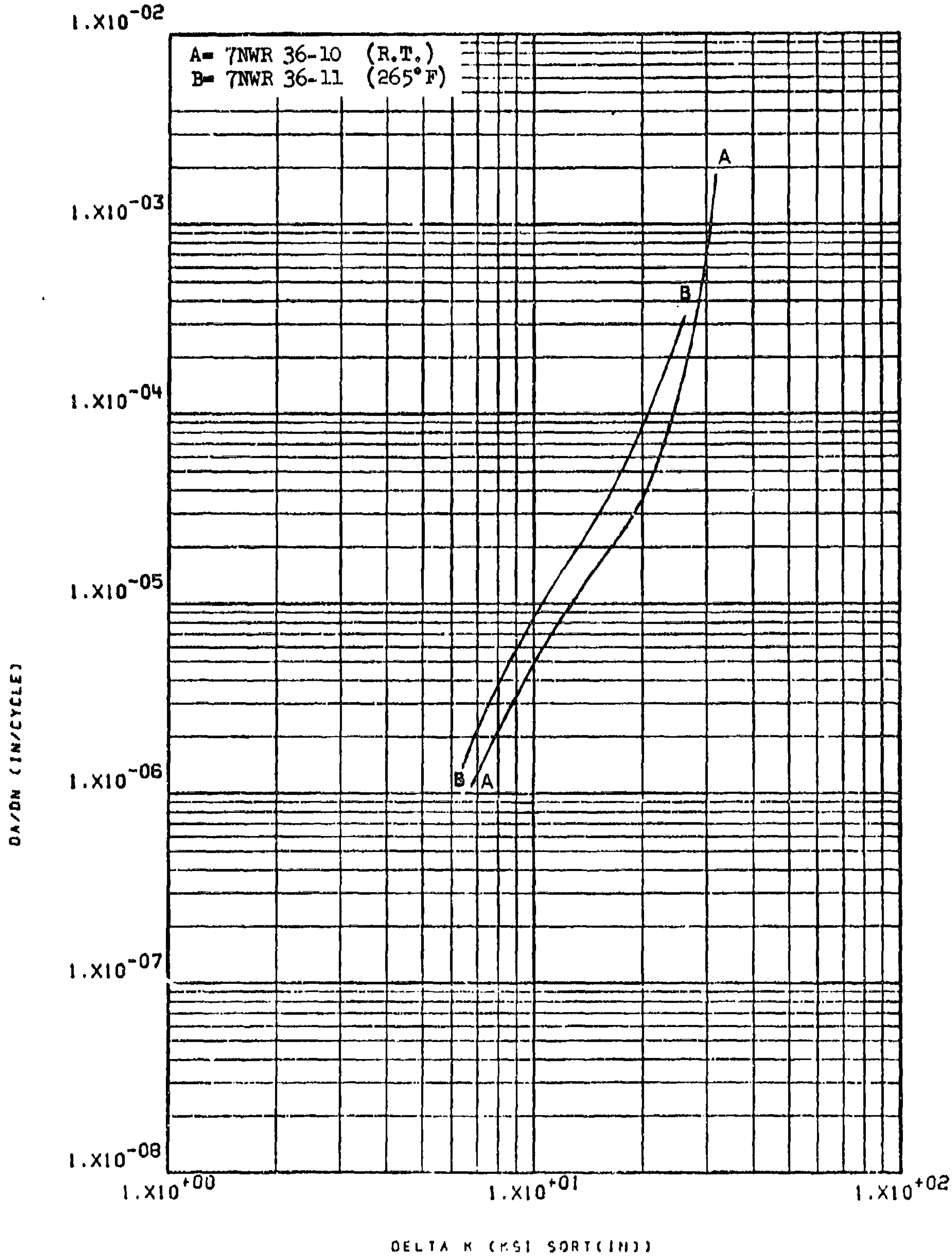

Figure 8.2.4.2-2 Effect of temperature on LHA-FCGR at R=0.08, 360 cpm, WR direction, in 2219-T851 1.75" plate

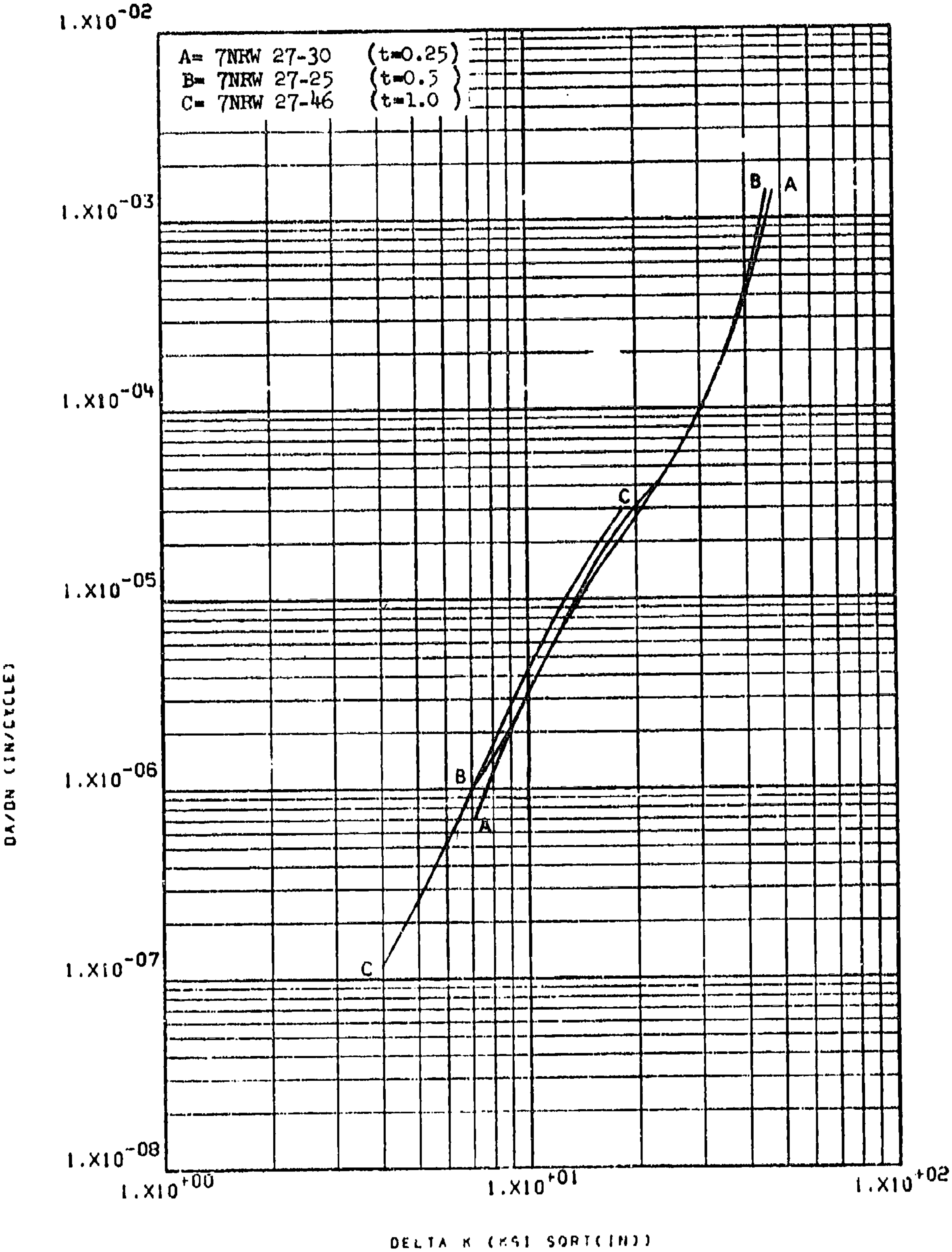

Figure 8.2.4.3-1 Effect of specimen thickness on LHA-FCGR at R.T., R=0.08, 360 cpm, RW direction, in 2219-T851 1.75" plate

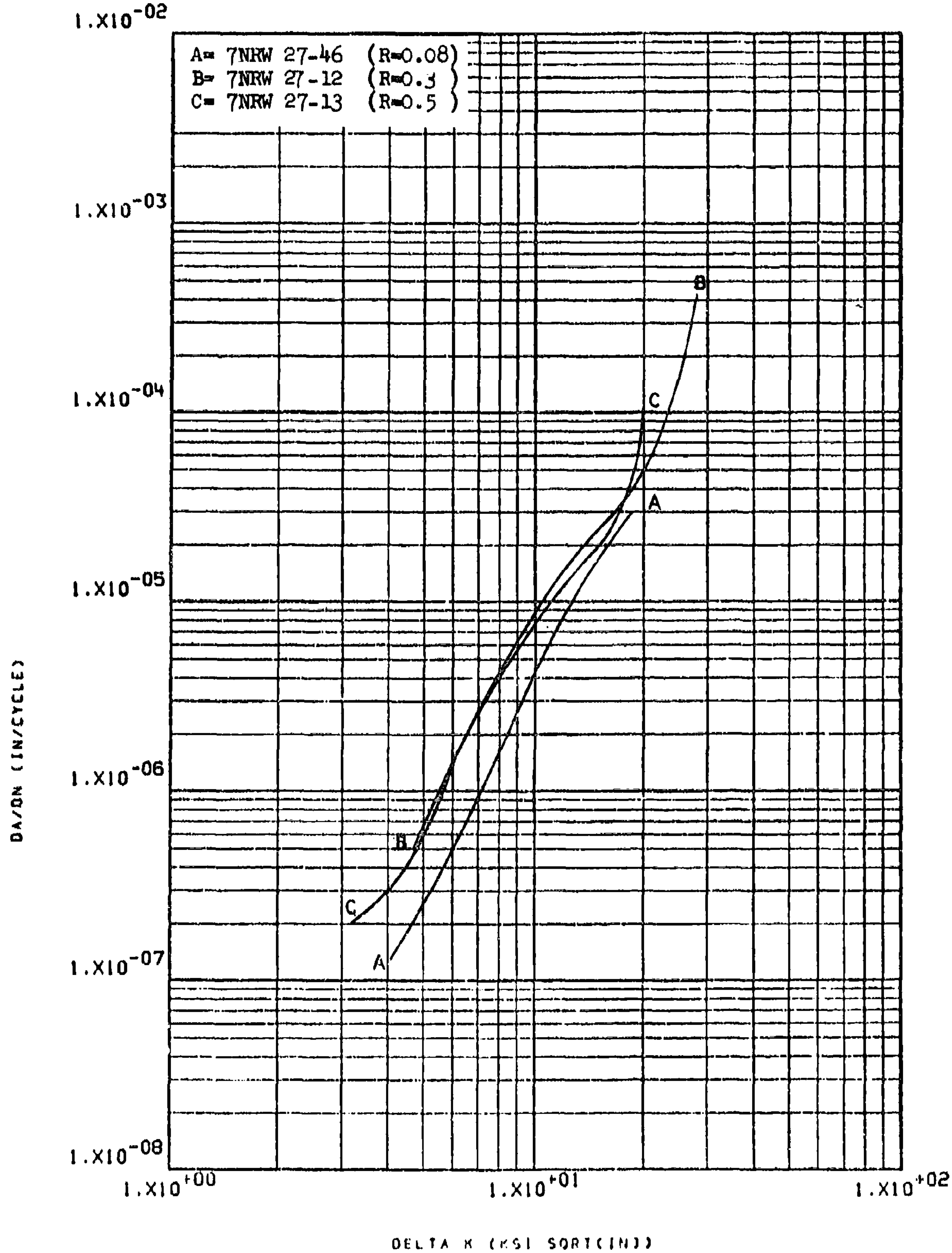

Figure 8.2.4.4-1 Effect of R factor on LHA-FCGR at R.T., 360 cpm, RW direction in 2219-T851 1.75" plate

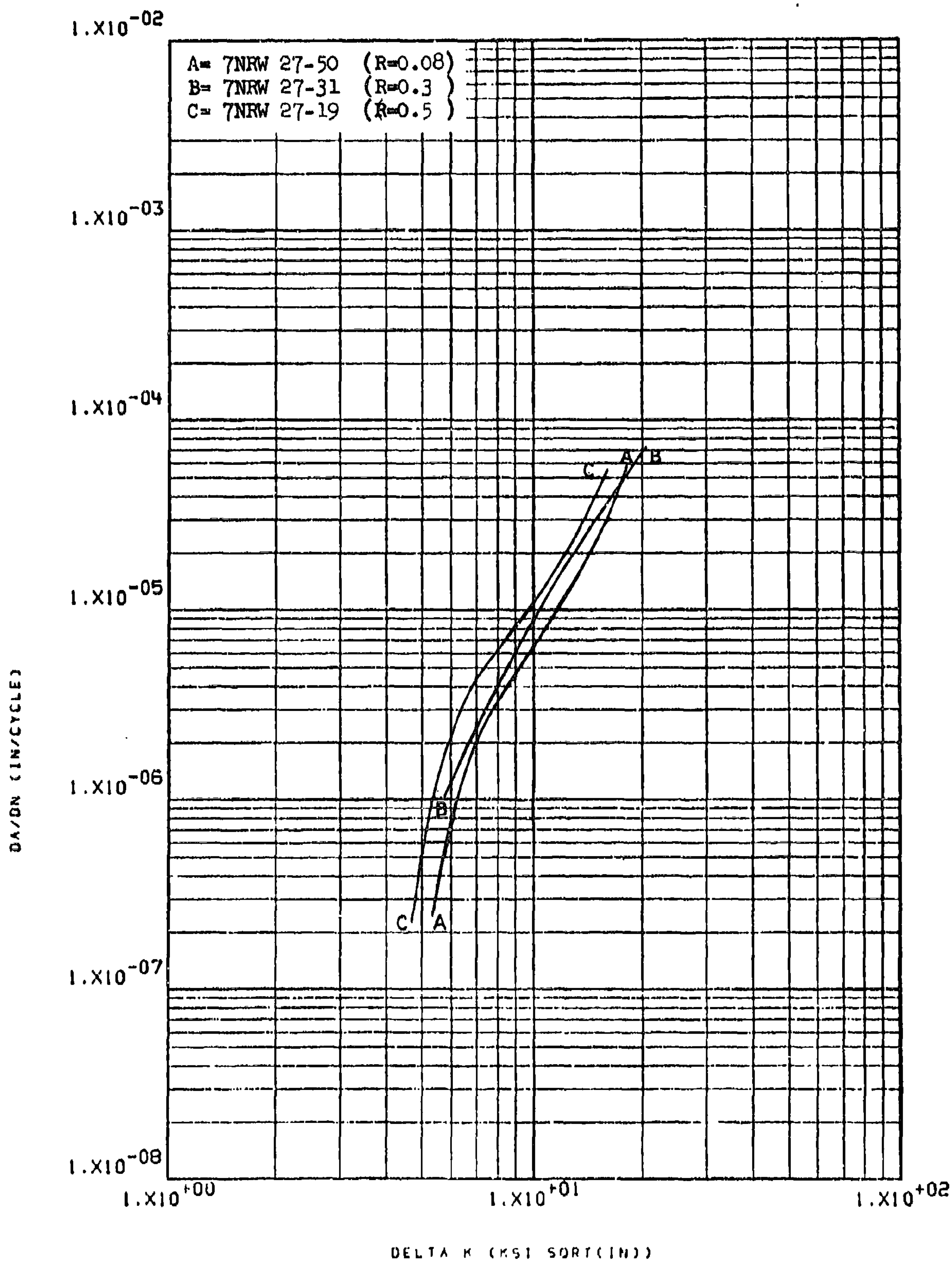

Figure 8.2.4.4-2 Effect of R factor on STW-FCGR at R.T., 60 cpm, RW direction, in 2219-T851 1.75" plate

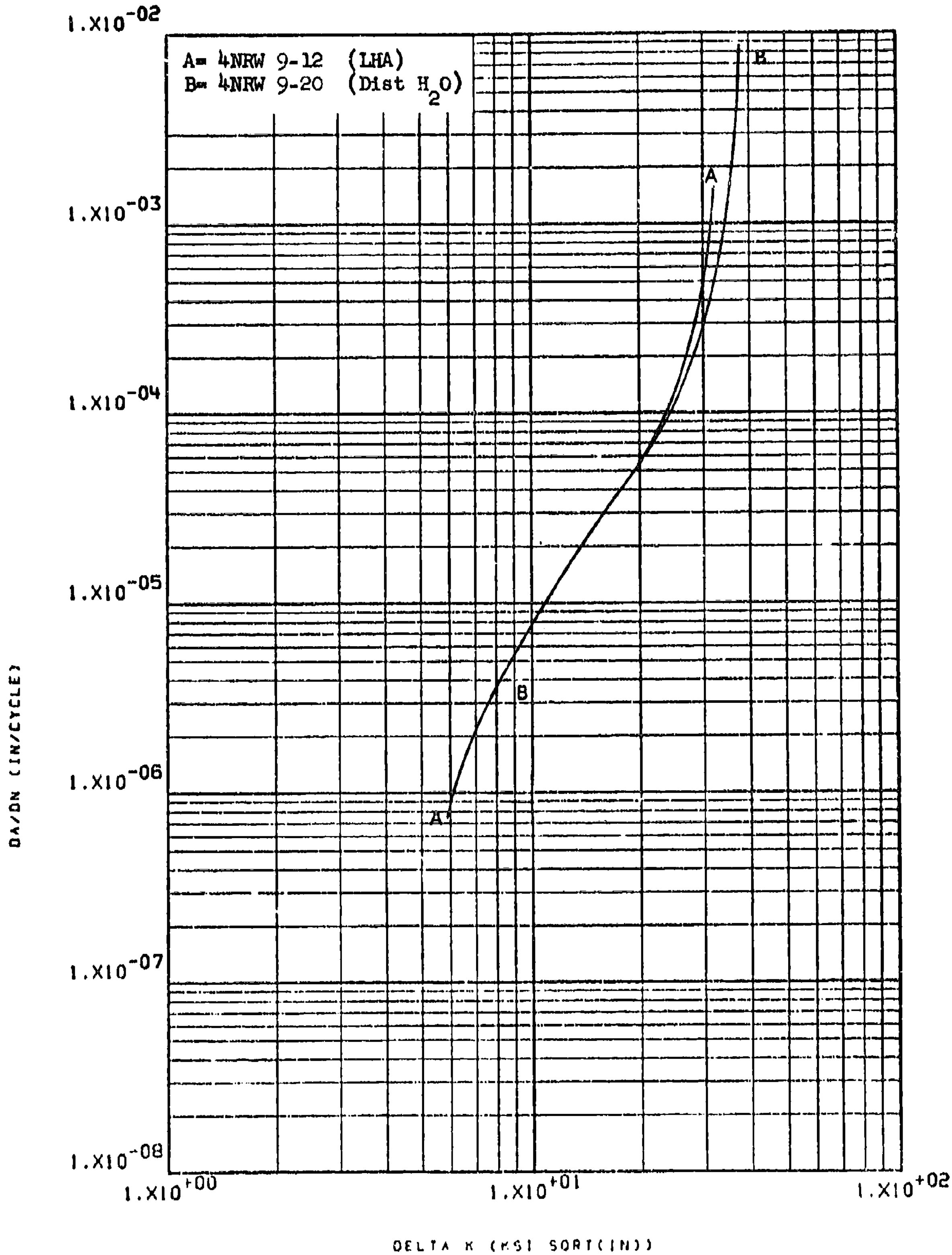

Figure 8.2.4.5-1 Effect of environment on FCGR at R.T., R=0.08, 60 cpm, RW direction, in 2219-T851 2" plate

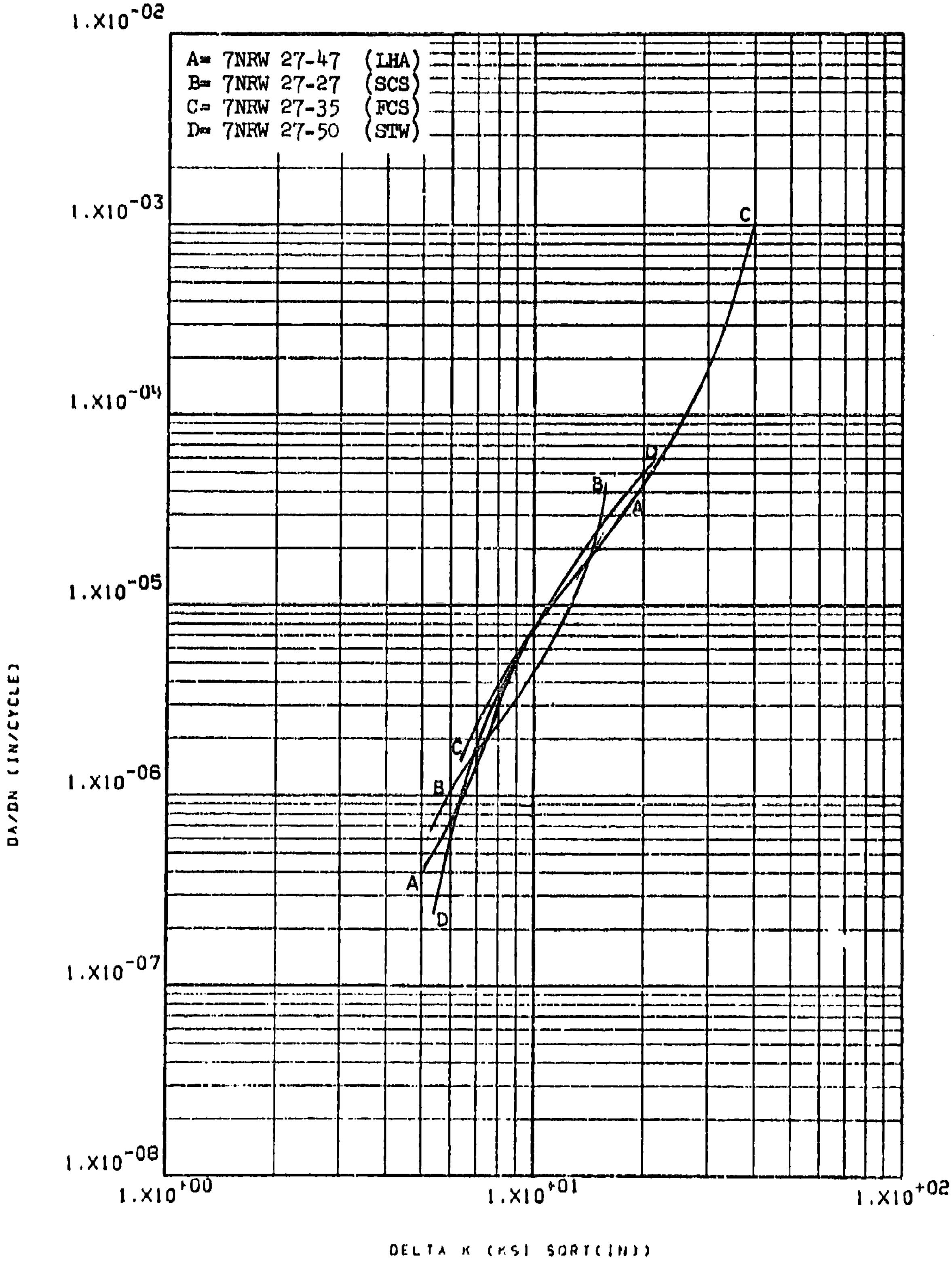

Figure 8.2.4.5-2 Effect of environment on FCGR at R.T., R=0.08, 60 cpm, RW direction, in 2219-T851 1.75" plate

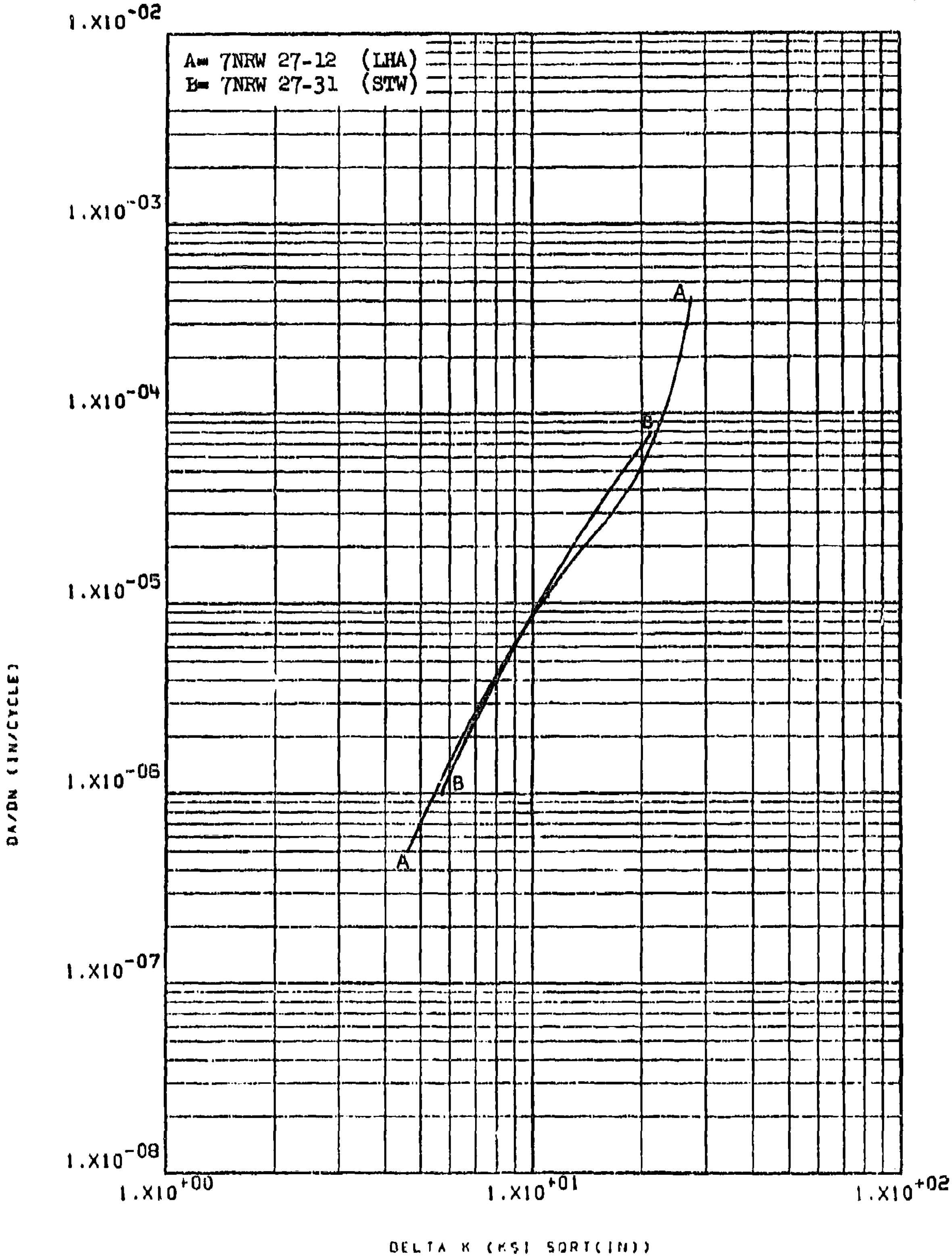

Figure 8.2.4.5-3 Effect of environment on FCGR at R.T., R=0.3, RW direction, in 2219-T851 1.75" plate

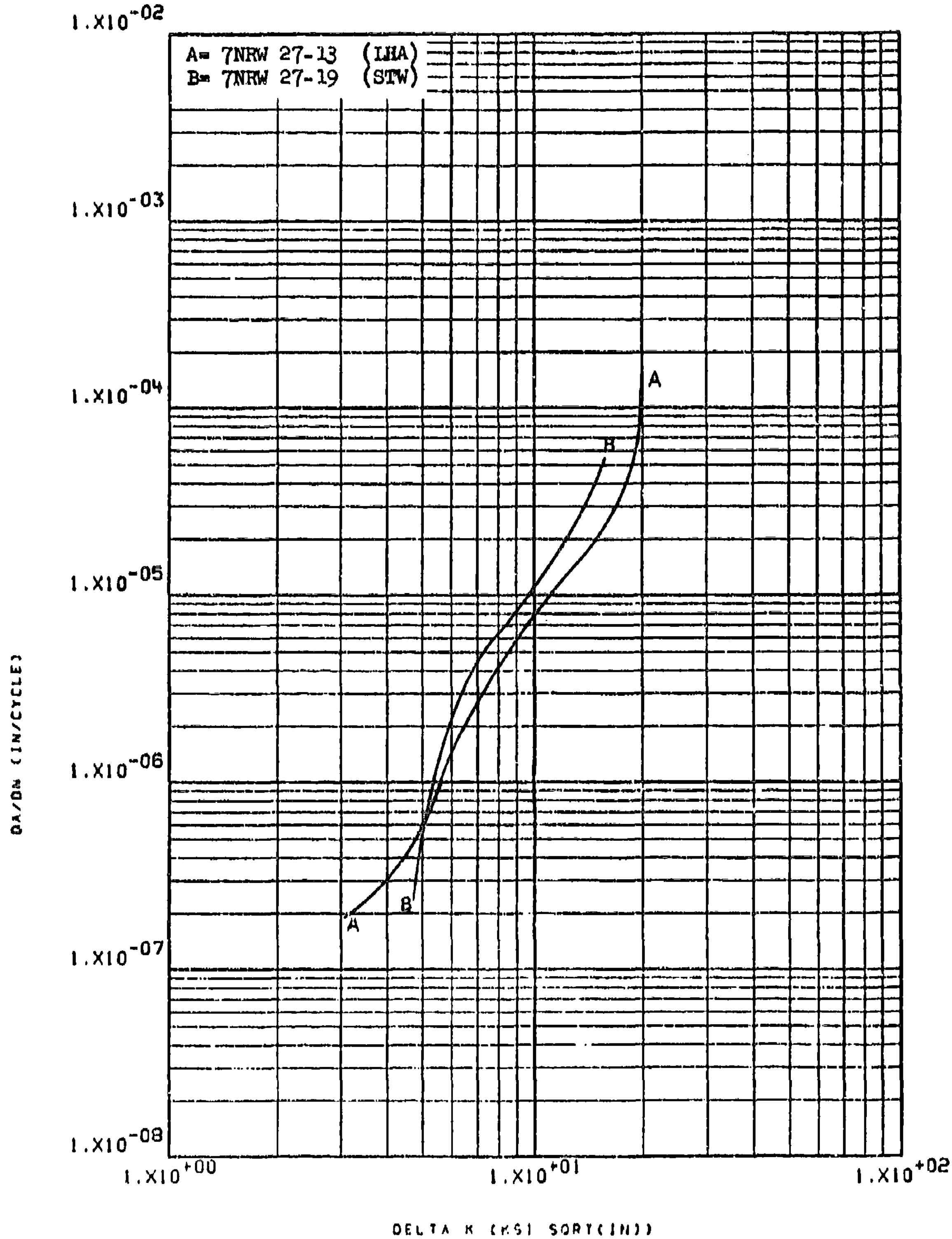

Figure 8.2.4.5-4 Effect of environment on FCGR at R.T., R=0.5, RW direction, in 2219-T851 1.75" plate

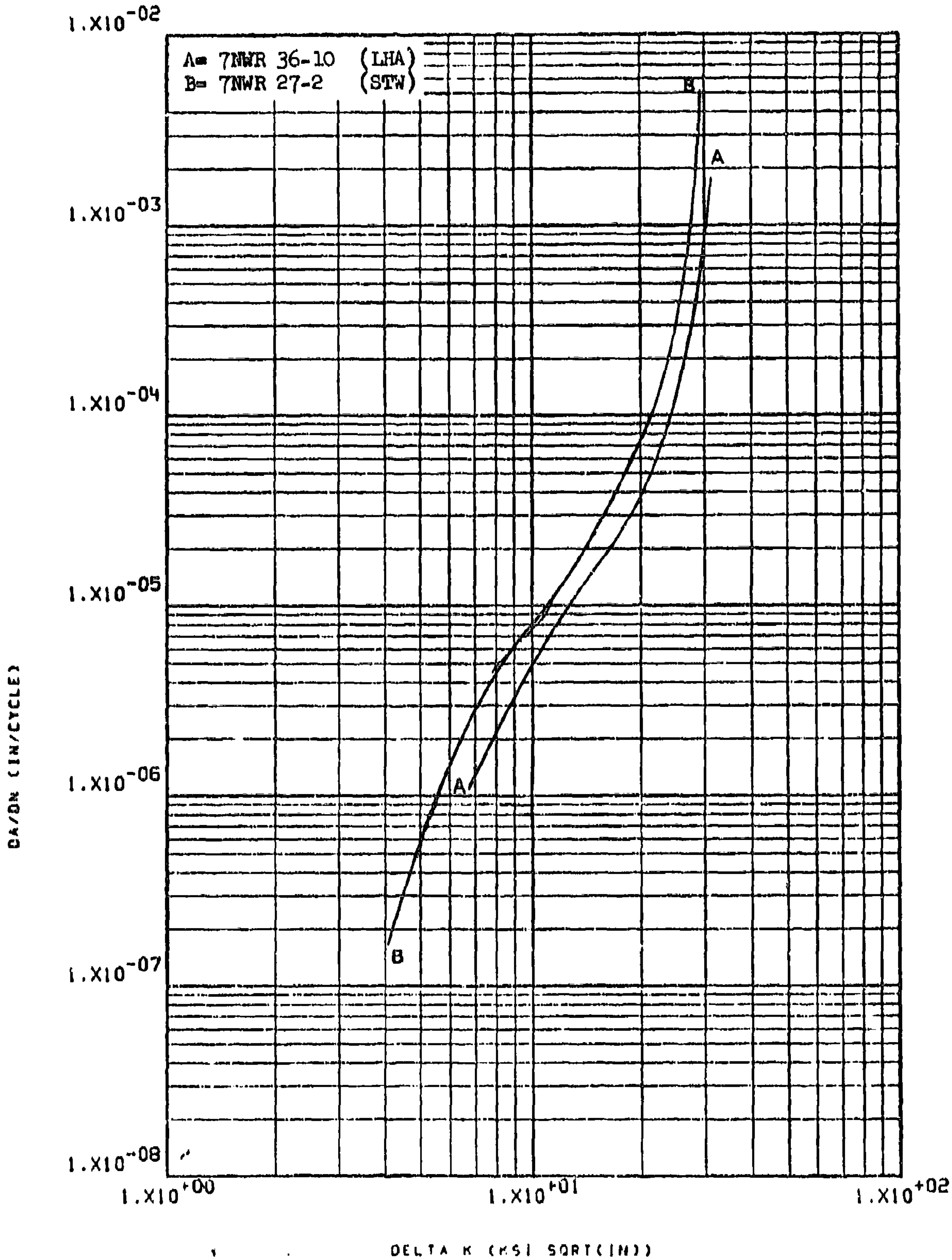

Figure 8.2.4.5-5 Effect of environment on FCGR at R.T., R=0.08, WR direction, in 2219-T851 1.75" plate

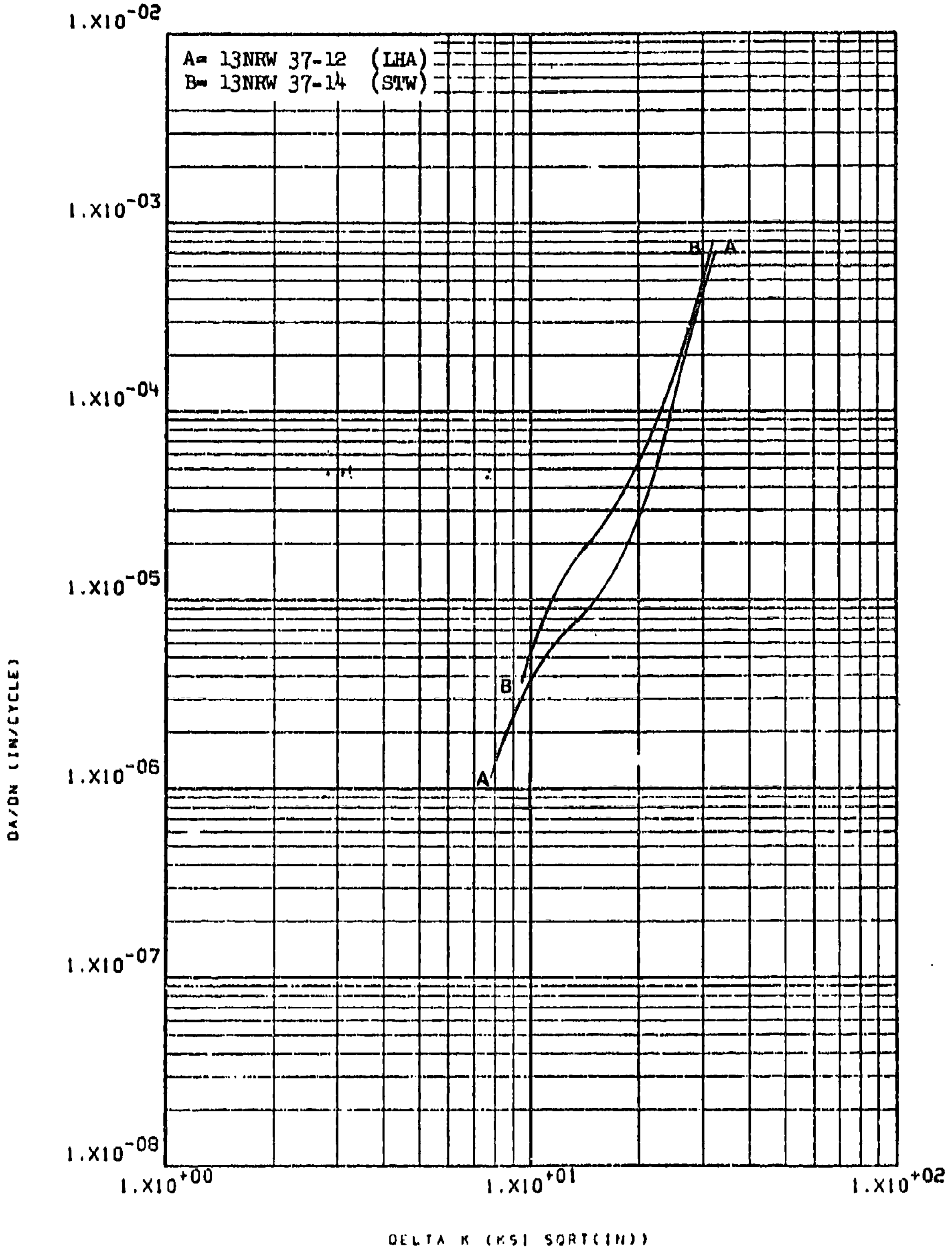

Figure 8.2.4.5-6 Effect of environment on FCGR at R.T., R=0.08, RW direction, in 2219-T851 3" plate

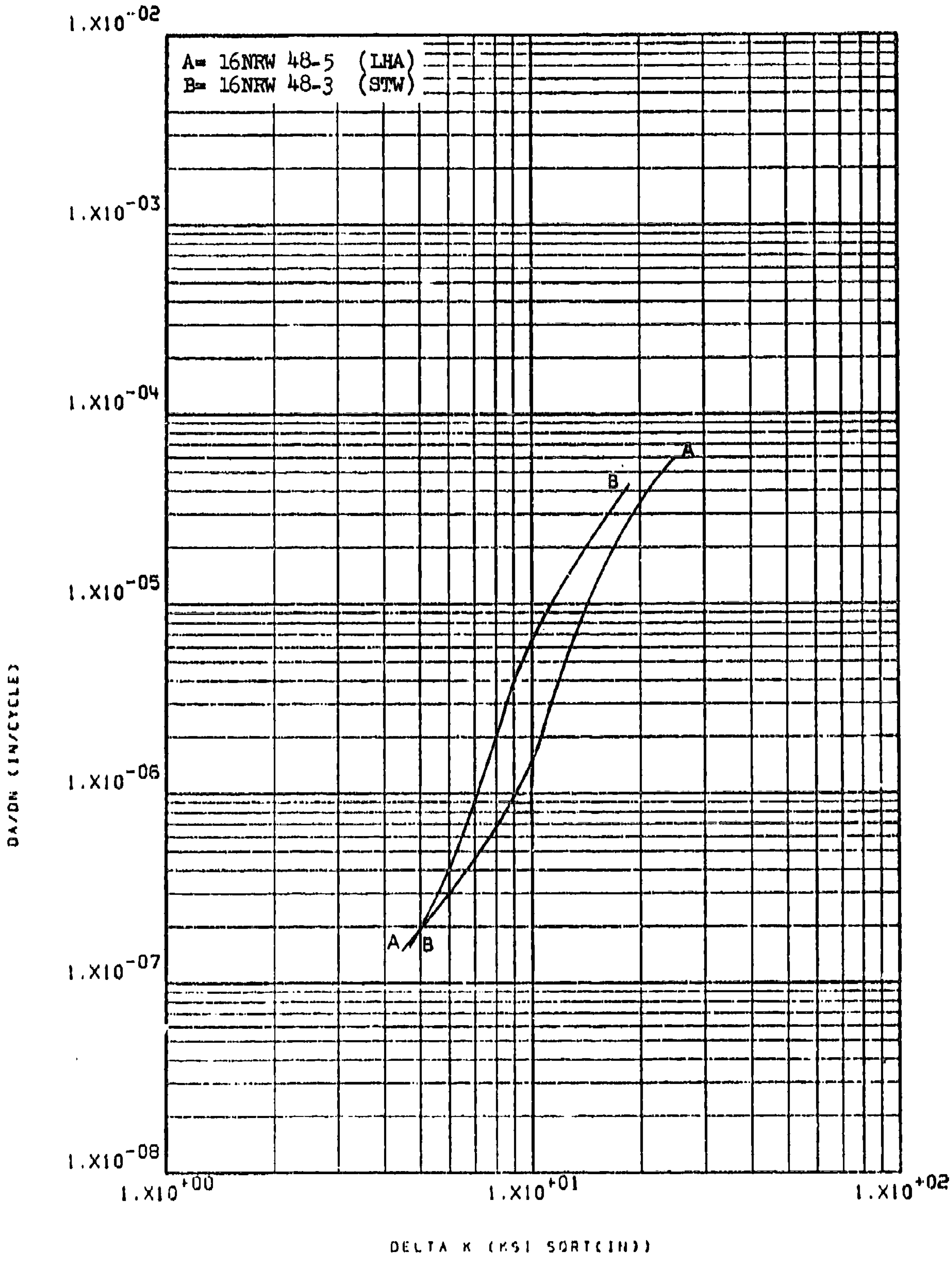

Figure 8.2.4.5-7 Effect of environment on FCGR at R.T., R=0.08, RW direction, in 2219-T8511 1.7" x 7.5" extrusion

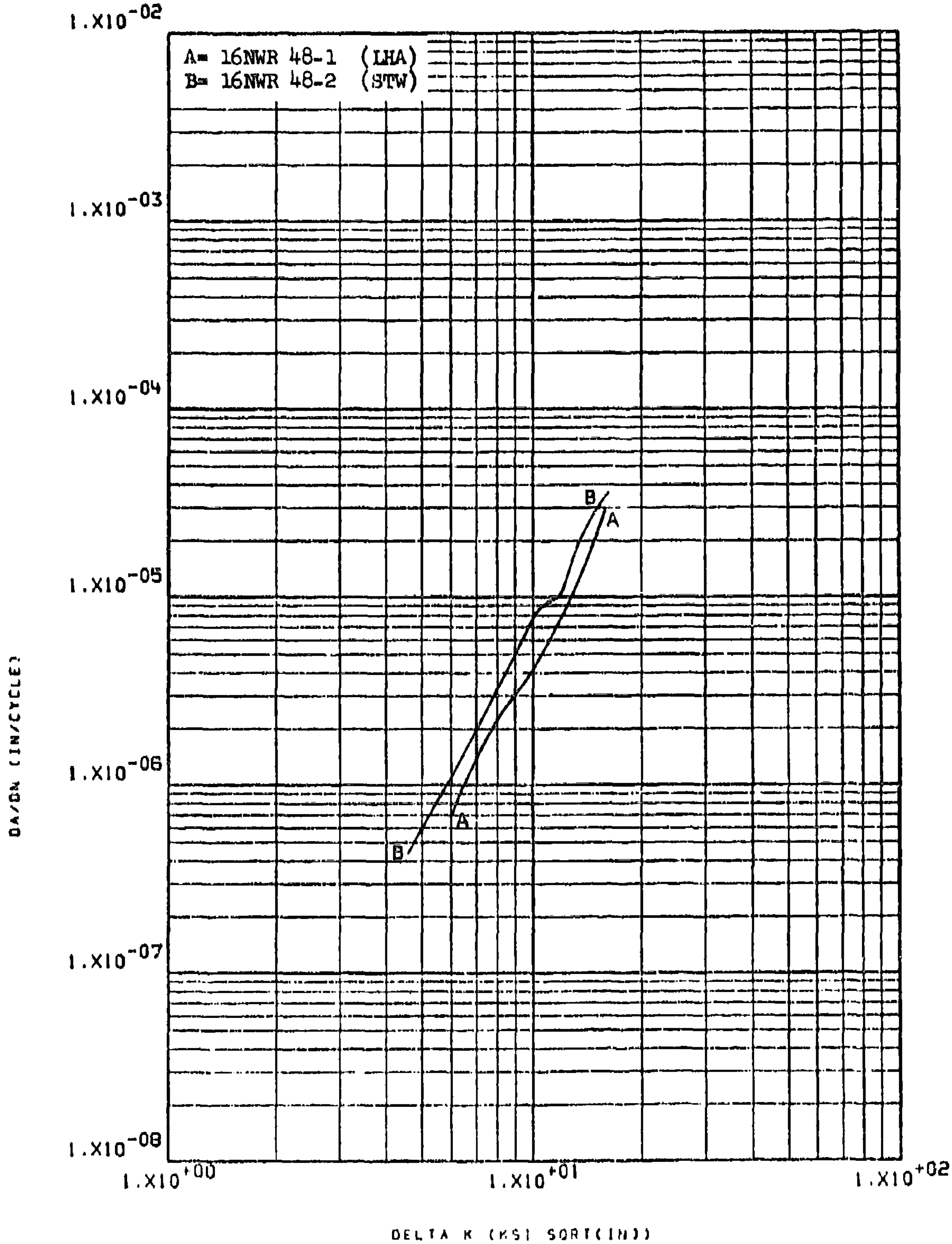

Figure 8.2.4.5-8 Effect of environment on FCGR at R.T., R=0.08, WR direction, in 2219-T8511 1.7" x 7.5" extrusion

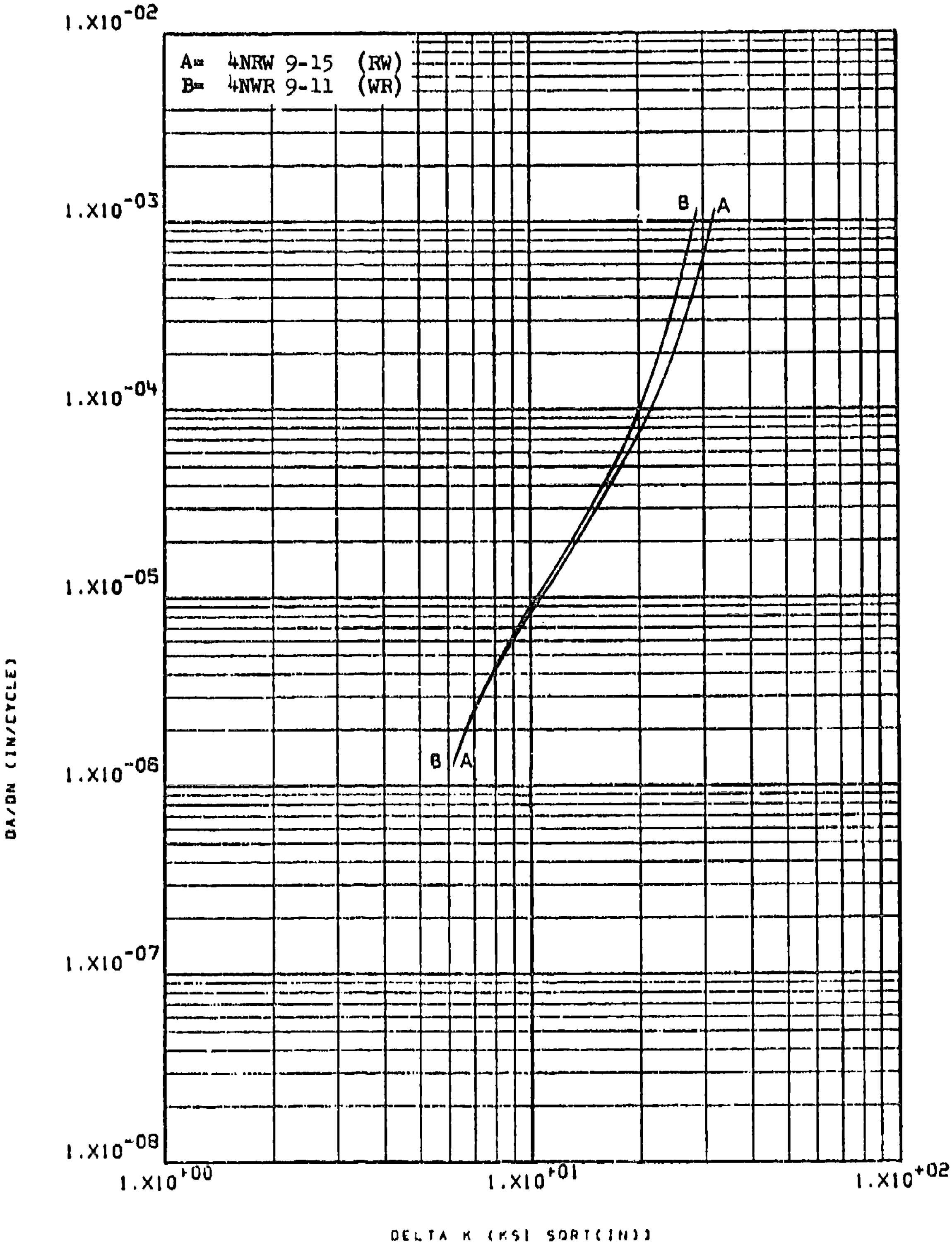

Figure 8.2.4.6-1 Effect of test direction on LHA-FCGR at R.T., R=0.08, 360 cpm, in 2219-T851 2" plate

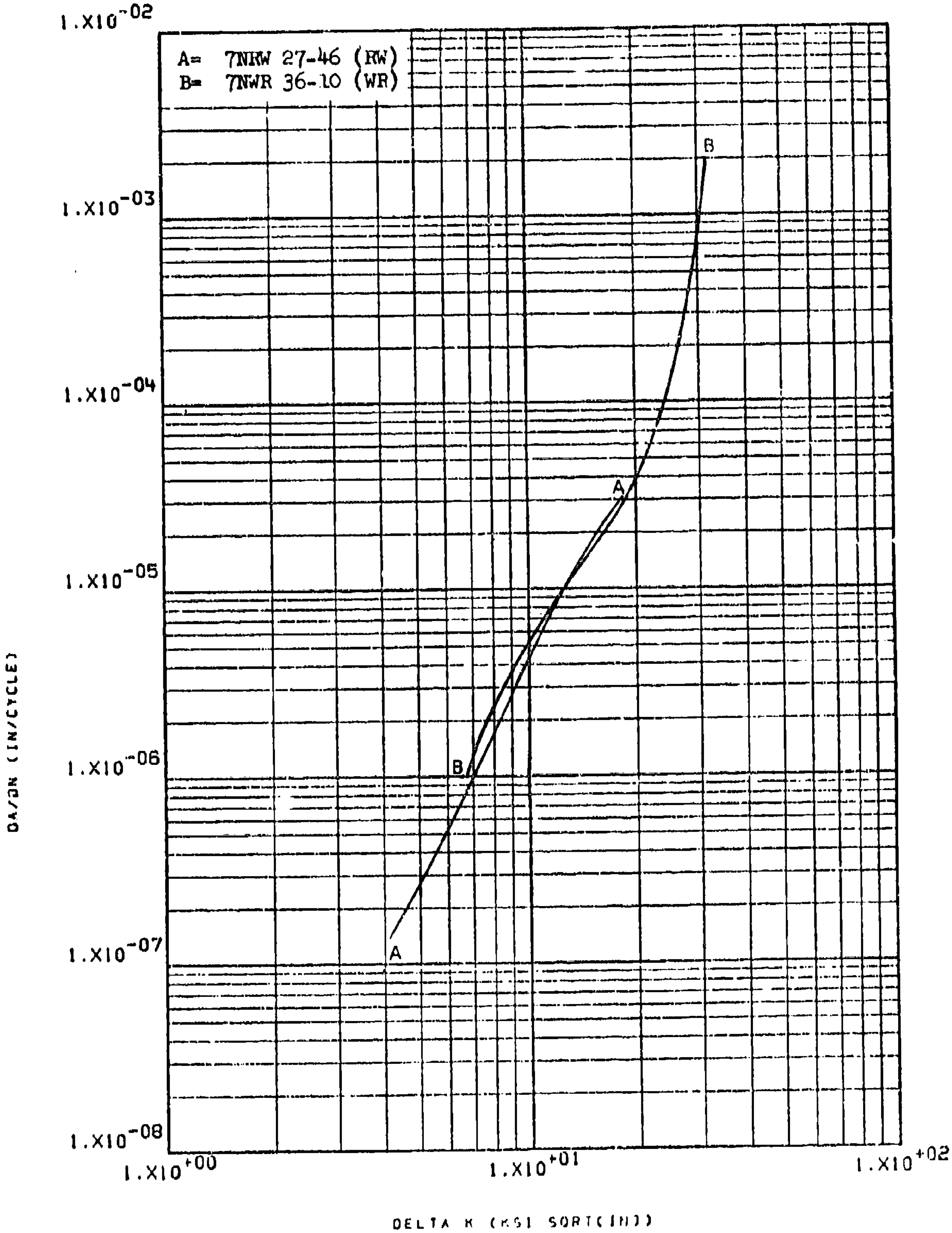

Figure 8.2.4.6-2 Effect of test direction on LHA-FCGR at R.T., R=0.08, 360 cpm, in 2219-T851 1.75" plate

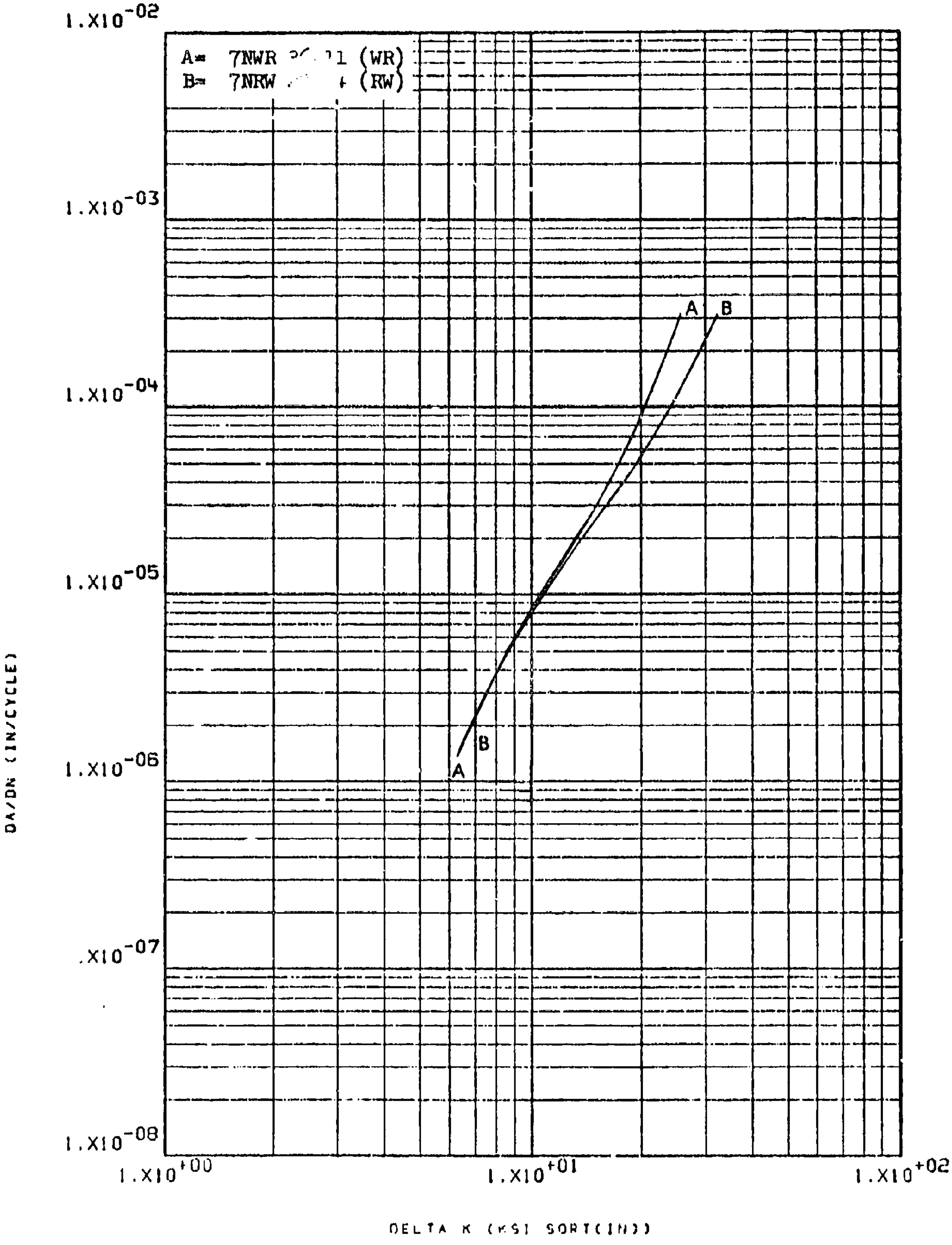

Figure 8.2.4.6-3 Effect of test direction on LHA-FCGR at 265°F, R=0.08, 360 cpm , in 2219-T851 1.75" plate

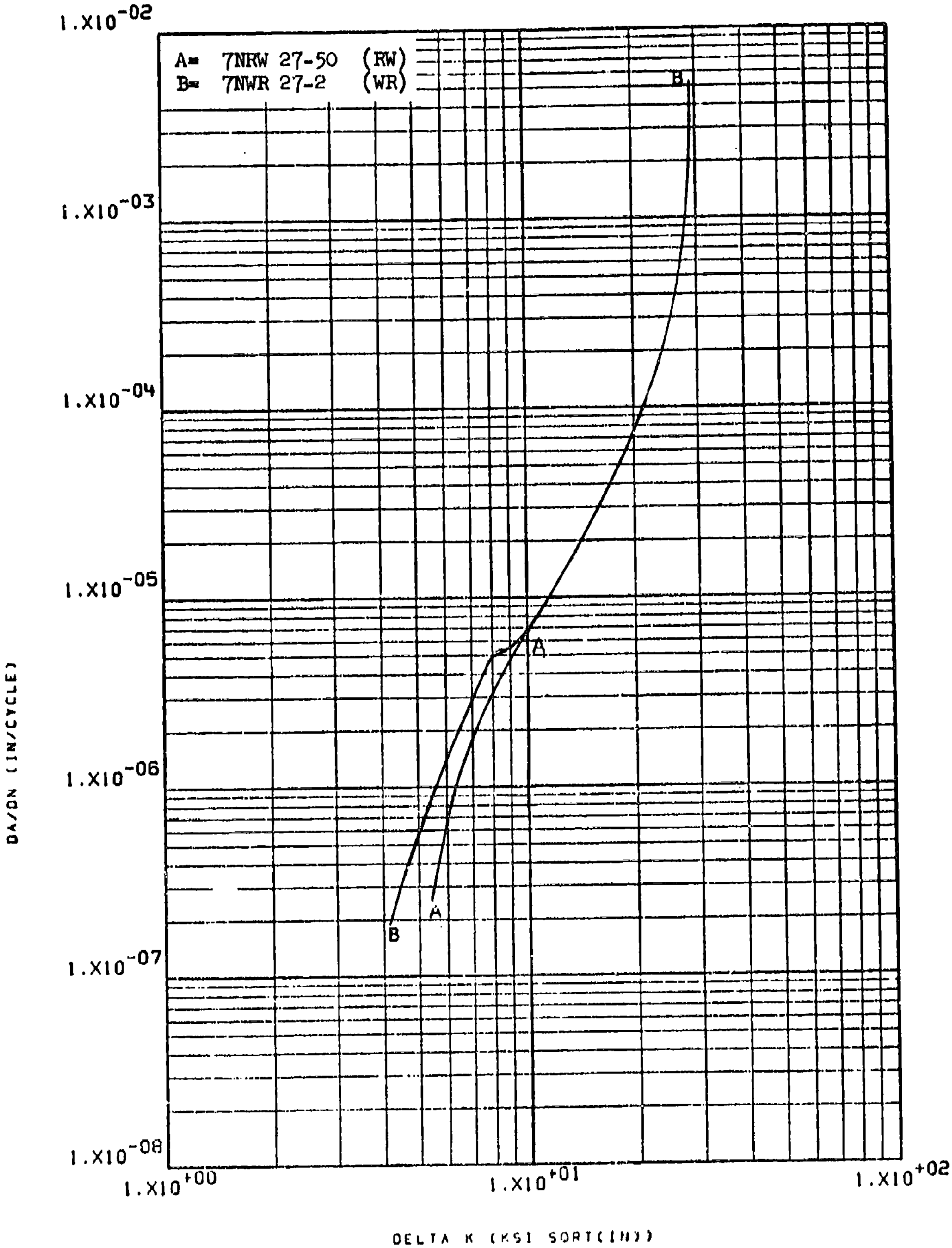

Figure 8.2.4.6-4 Effect of test direction on STW-FCGR at R.T., R=0.08, 60 cpm, in 2219-T851 1.75" plate

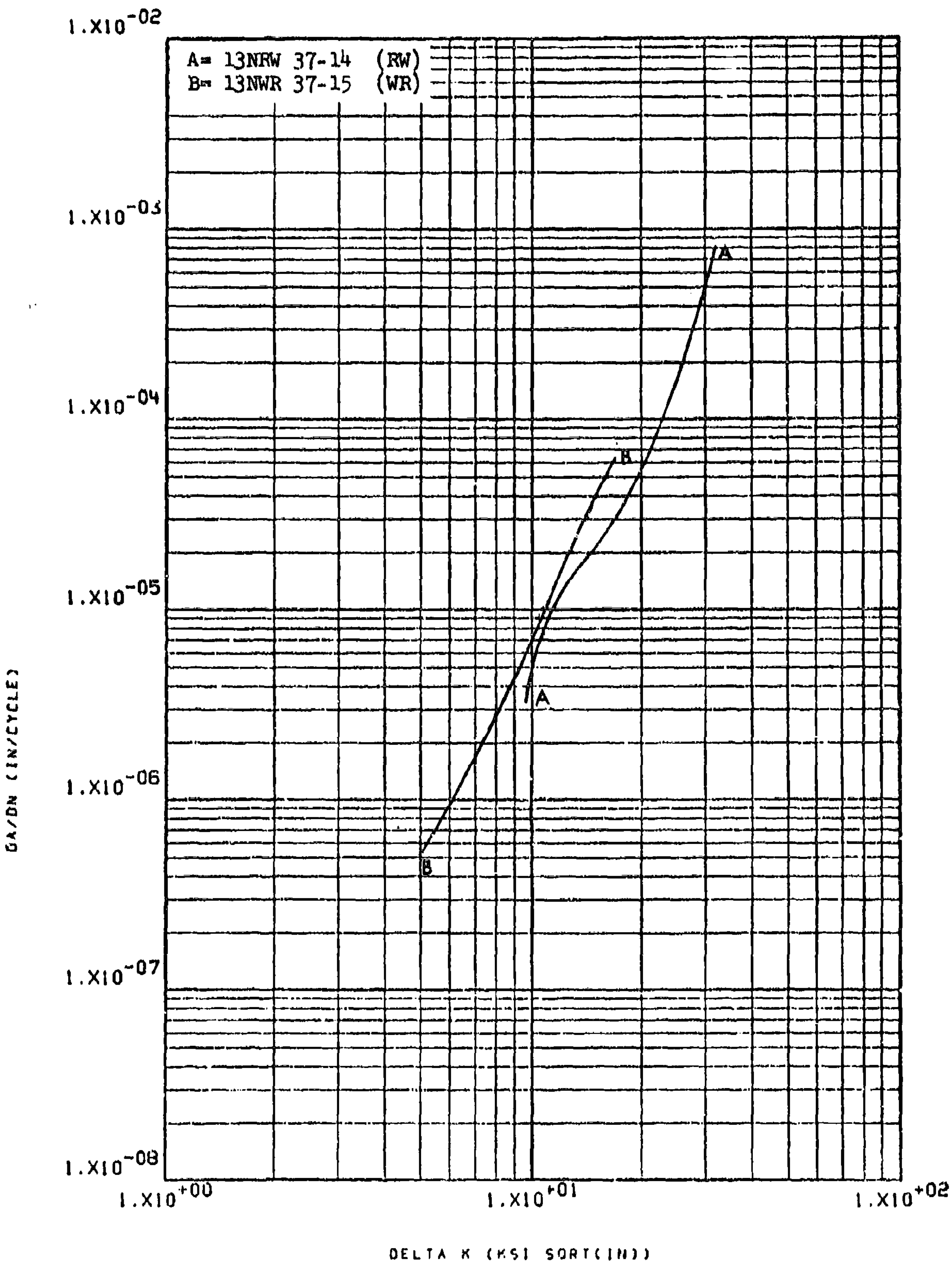

Figure 8.2.4.6-5 Effect of test direction on STW-FCGR at R.T., R=0.08, 60 cpm, in 2219-T851 3" plate

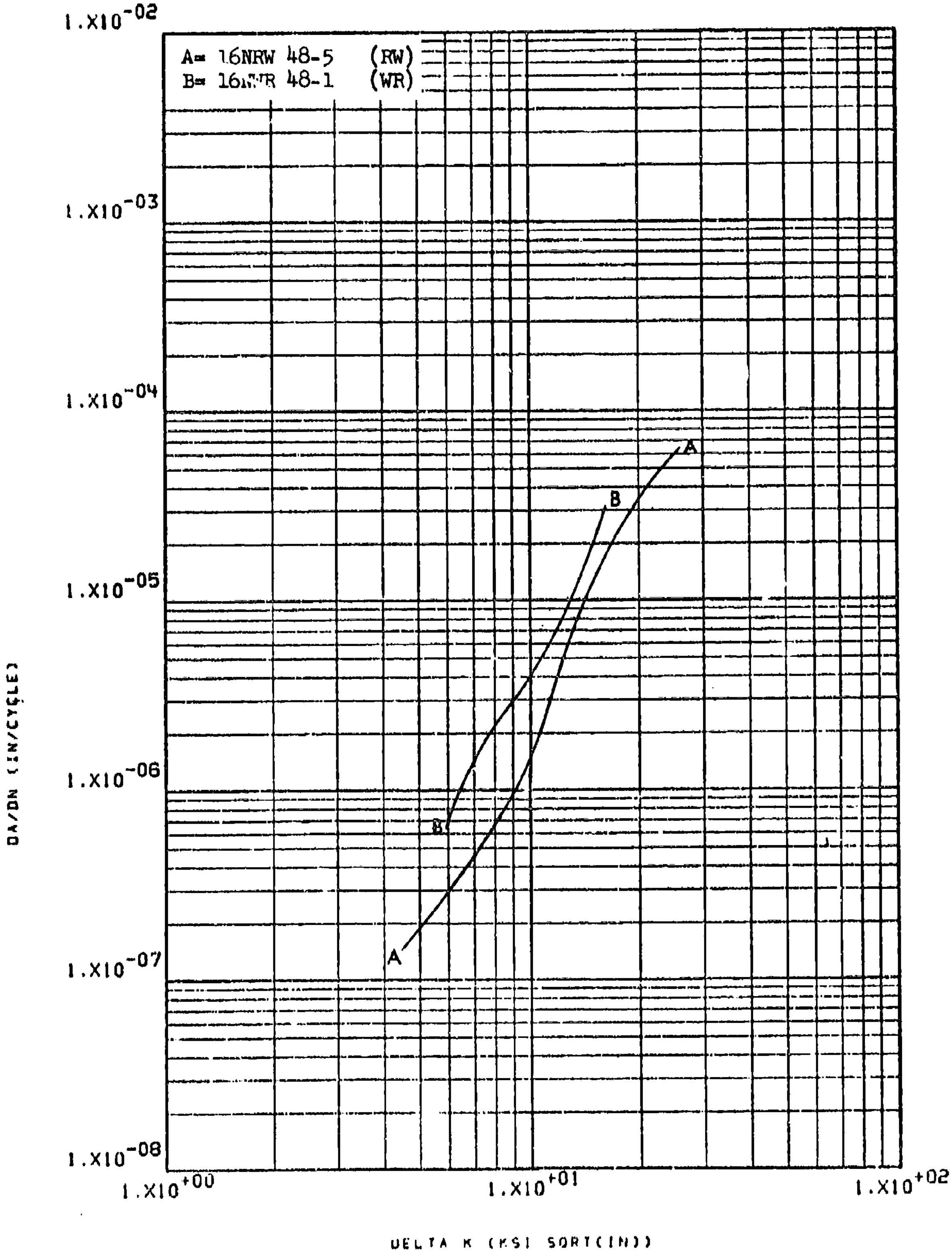

Figure 8.2.4.6-6 Effect of test direction on LHA-FCGR at R. T., R=0.08, 360 cpm, in 2219-T8511 1.7" x 7.5" extrusion

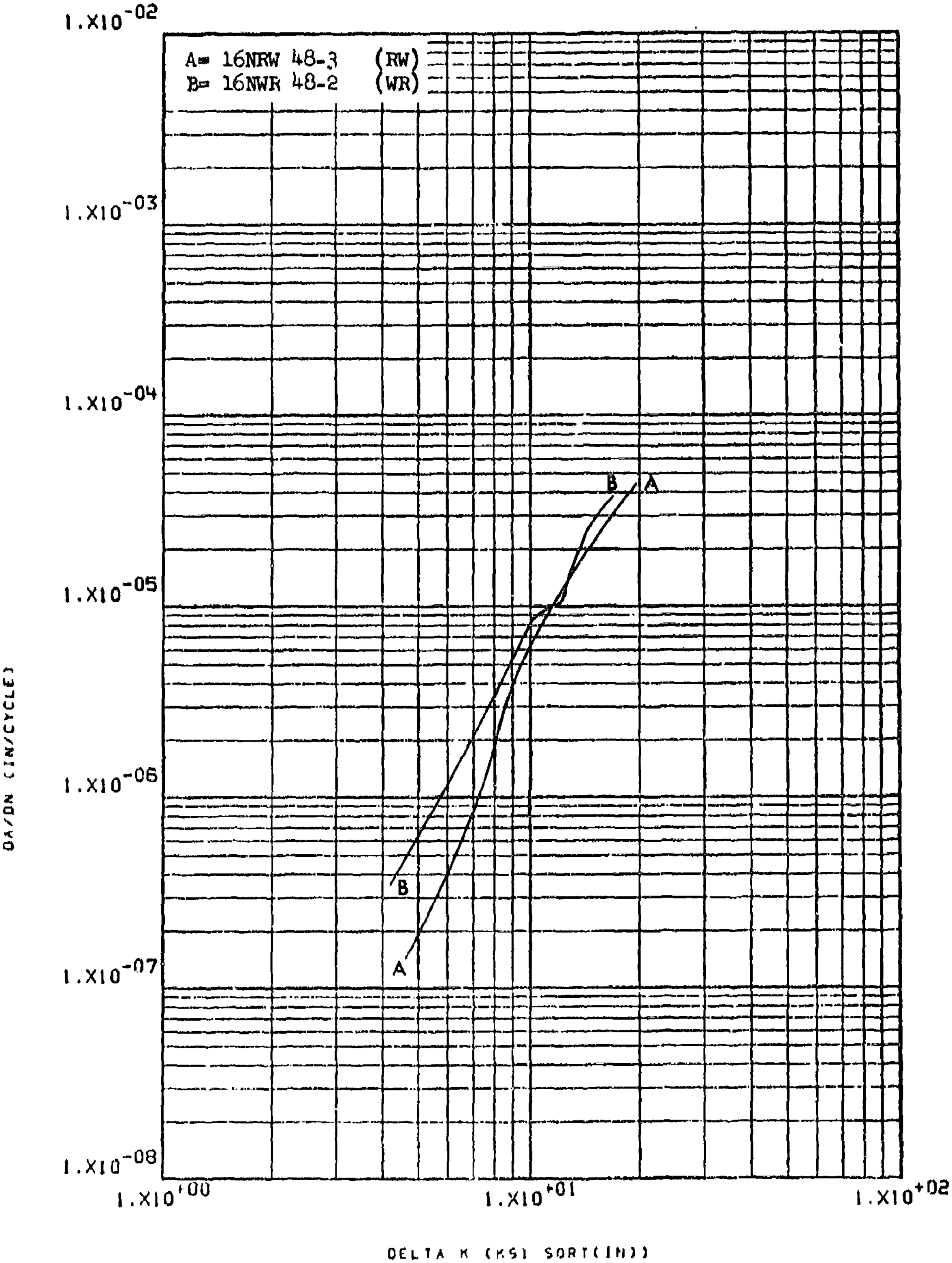

Figure 8.2.4.6-7 Effect of test direction on STW-FCGR at R.T., R=0.08, 60 cpm, in 2219-T8511 1.7" x 7.5" extrusion

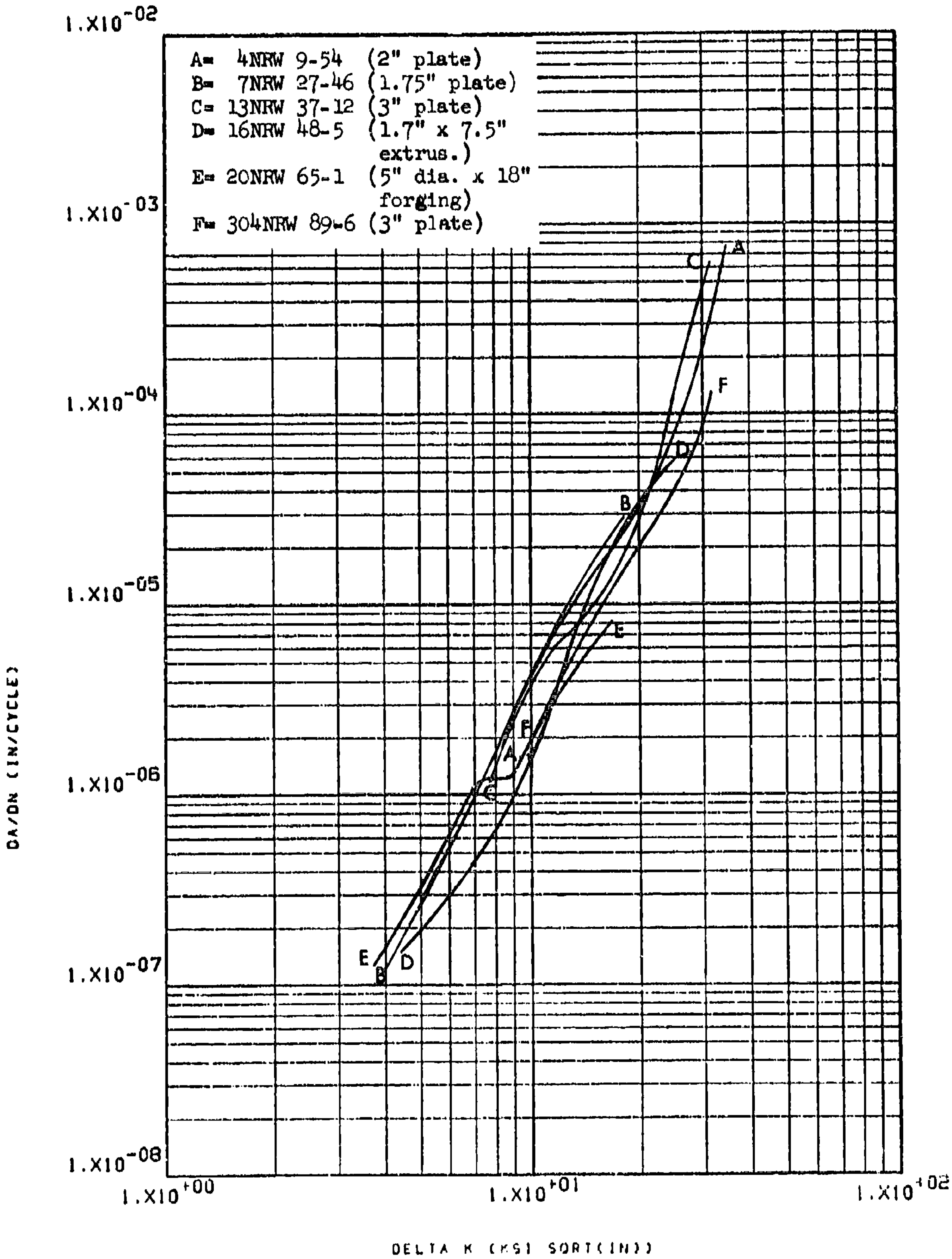

Figure 8.2.4.7-1 Effect of product form on LHA-FCGR at R.T., R=0.08, 360 cpm, RW direction, in 2219 Al.

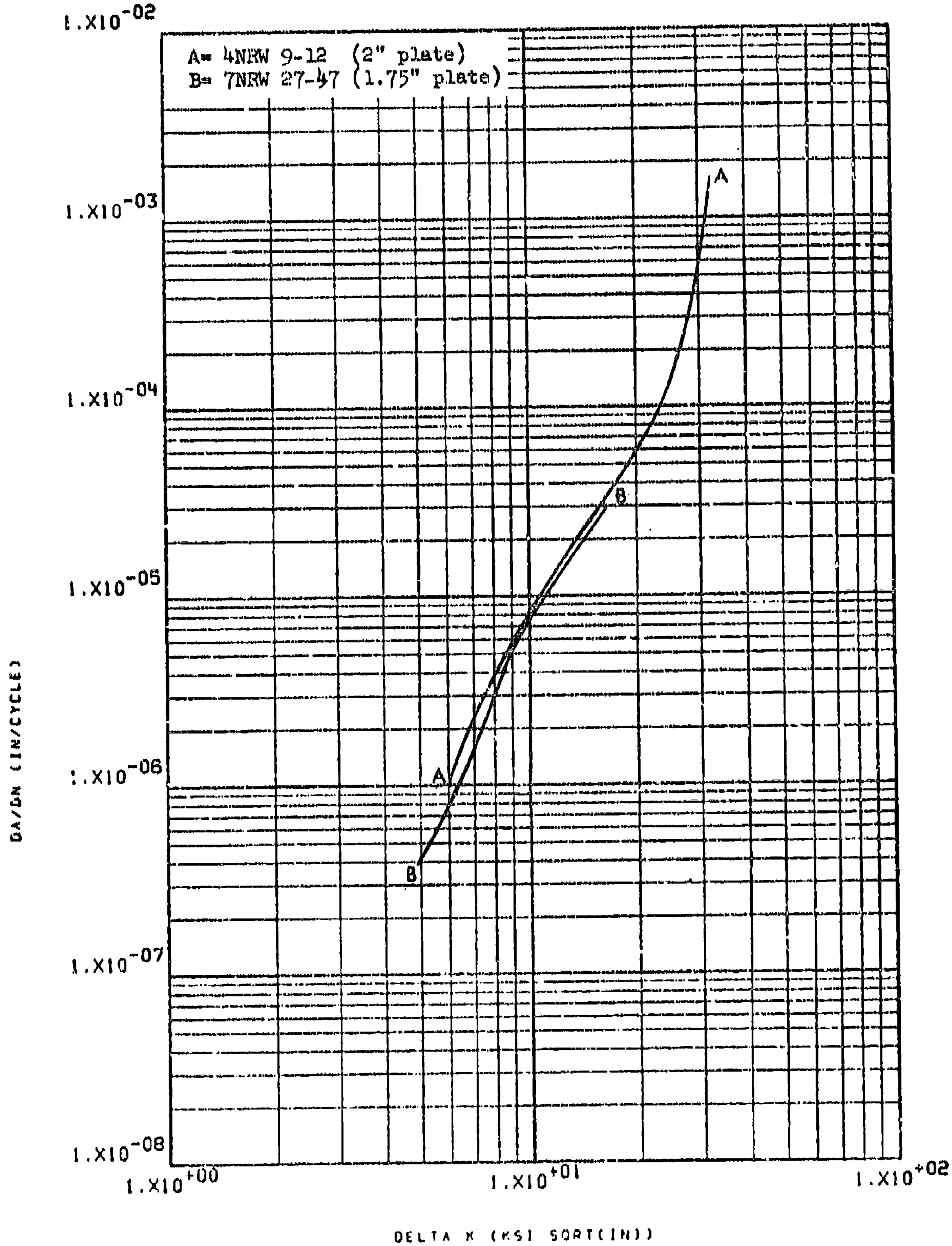

Figure 8.2.4.7-2 Effect of product form on LHA-FCGR at R.T., R=0.08, 60 cpm, RW direction, in 2219 Al.

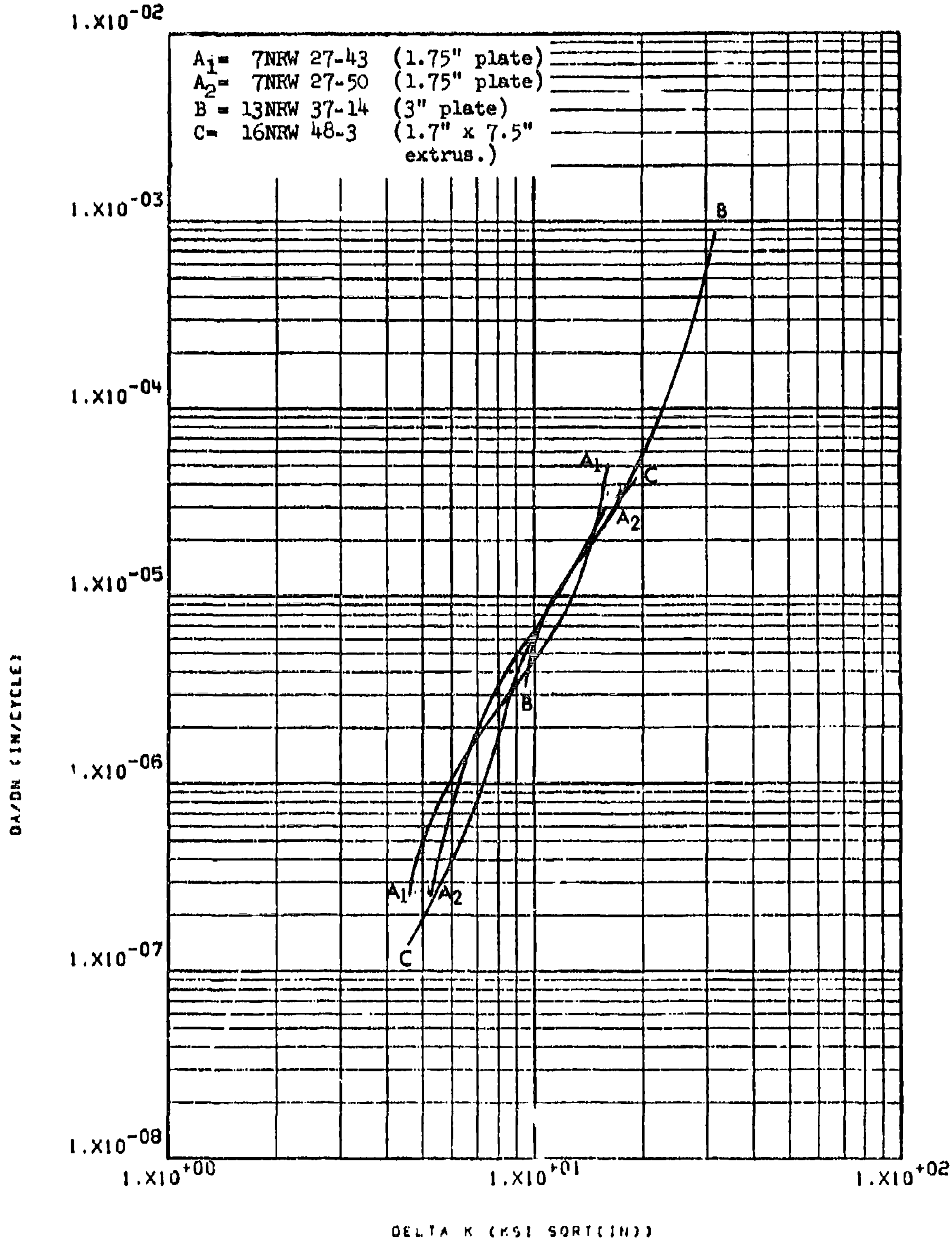

Figure 8.2.4.7-3 Effect of product form on STW-FCGR at R.T., R=0.08, 60 cpm, RW direction, in 2219 Al.

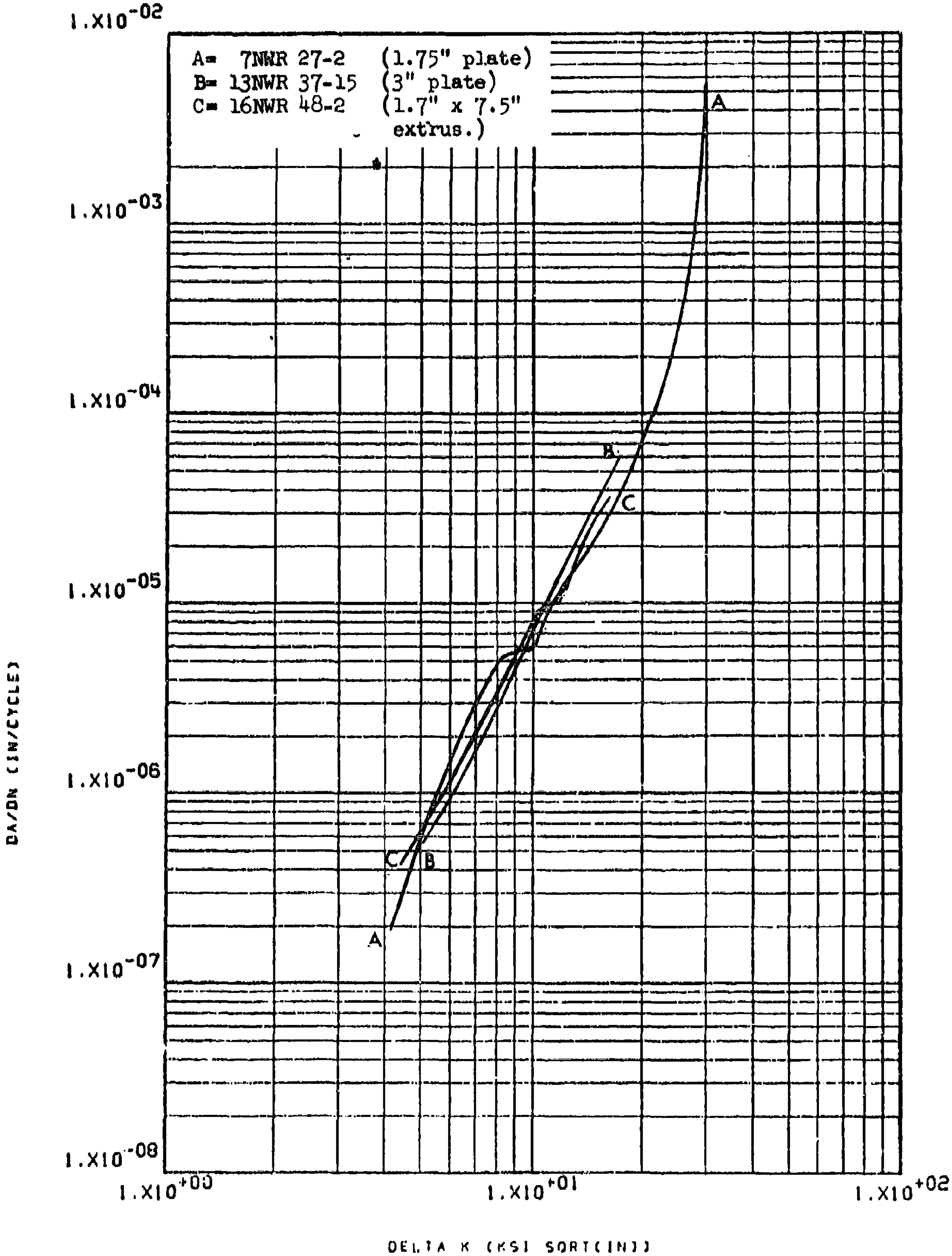

Figure 8.2.4.7-4 Effect of product form on STW-FCGR at R.T., R=0.08, 60 cpm, WR direction, in 2219 Al.

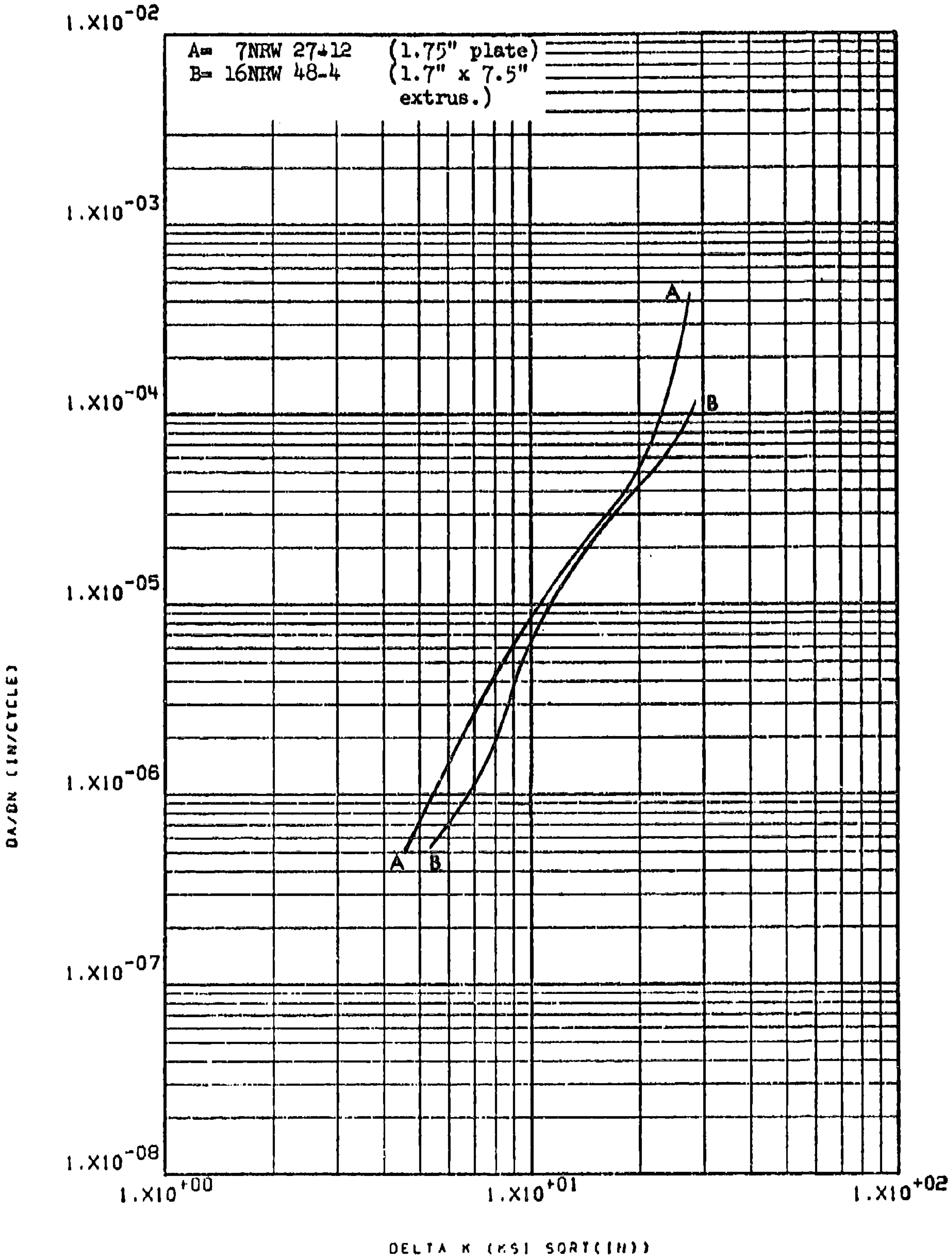

Figure 8.2.4.7-5 Effect of product form on LHA-FCGR at R.T., R=0.3, 360cpm, RW direction, in 2219 Al.

8.2.5 Aluminum Alloy 7049

8.2.5.1 Cyclic Rate - The crack growth rate of this material was seen to be about 1-1/2 orders of magnitude greater in sump tank water at a cyclic frequency of 6 cpm than at 60 cpm, when at low levels of delta K (5 ksi $\sqrt{in}$). As delta K is increased, however, the difference between these rates decreased until at ~11 ksi $\sqrt{in}$ they were seen to be essentially equivalent (Figure 8.2.5.1-1).

8.2.5.2 Test Temperature - Not evaluated.

8.2.5.3 Specimen Thickness - At delta K levels up to ~15 ksi $\sqrt{in}$ the crack growth rates of this material in low humidity air were seen to be greater in 1.0 inch thick specimens than in 0.5 inch and 0.25 inch thick specimens, where the rates were essentially equivalent. Above delta K ~ 15 ksi $\sqrt{in}$ the growth rates in all three thicknesses were seen to be equivalent (Figure 8.2.5.3-1).

8.2.5.4 R Factor - Increasing the R factor from 0.08 to 0.3 in this material was seen to result in a significant increase in crack growth rates in both low humidity air and sump tank water (Figures 8.2.5.4-1 and -2). Still further increases in growth rates were seen to result when R was increased from 0.3 to 0.5.

8.2.5.5 Environment - At very low levels of delta K (3-5 ksi $\sqrt{in}$) the crack growth rates of this material in low humidity air and sump tank water were seen to be essentially equivalent at R factors of 0.08, 0.3, and 0.5 (Figures 8.2.5.5-1 through -3). As delta K was increased above 5 ksi $\sqrt{in}$, the growth rate curves were seen to diverge with the rate in sump tank water becoming substantially greater than in low humidity air, for all three R factors.

8.2.5.6 Test Direction - The crack growth rate of this material in sump tank water was seen to be significantly greater in the RW direction than in the WR direction (Figure 8.2.5.6-1). This effect became less pronounced as delta K was increased until at delta K ~13 ksi $\sqrt{in}$ the rates were approximately equal.

8.2.5.7 Product Form - Not evaluated.

8.2.5.8 Heat Treat Condition - Not evaluated.

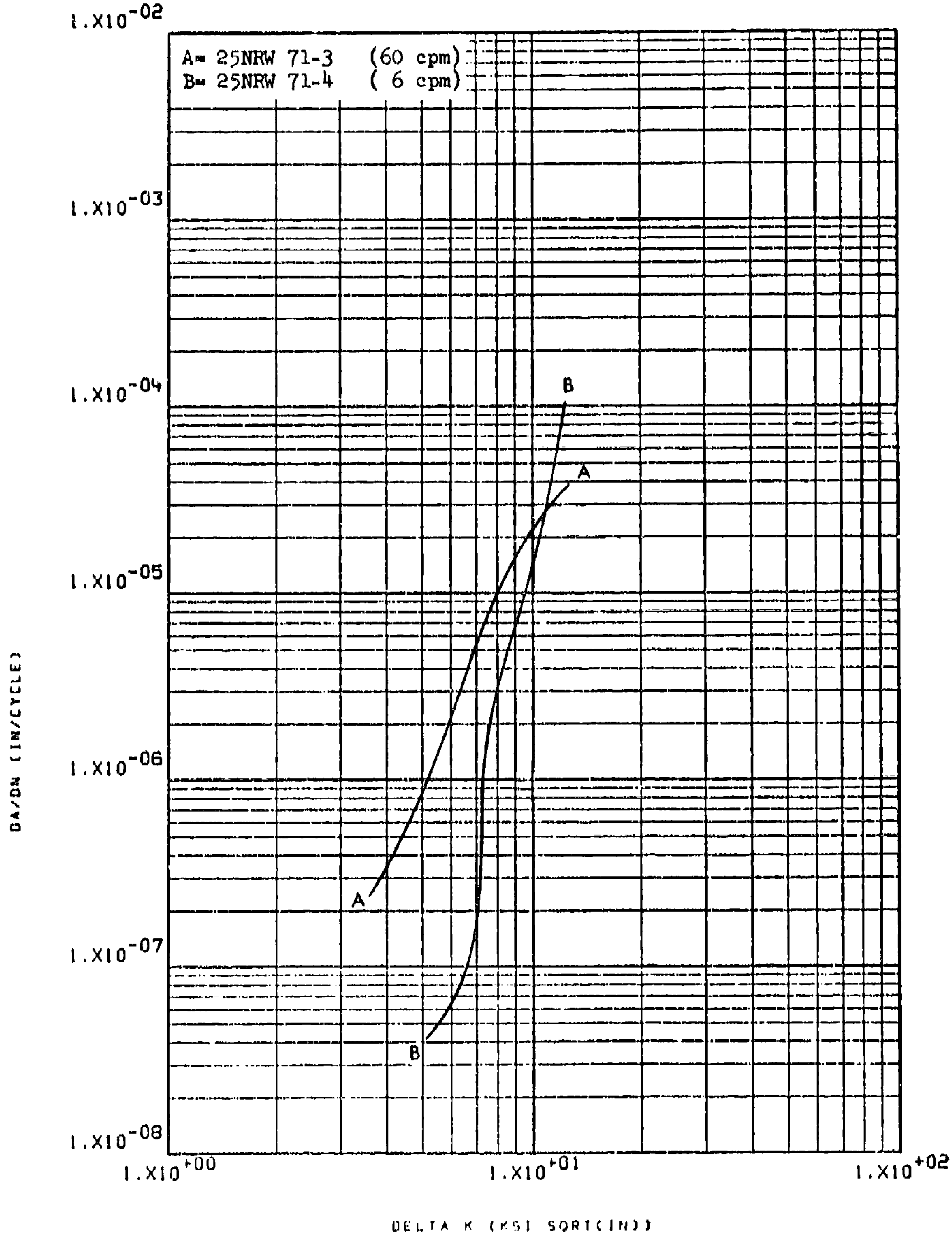

Figure 8.2.5.1-1 Effect of cyclic rate on STW-FCGR at R.T., R=0.08, RW direction, in 7049-T7352 3" x 24" x 48" forging

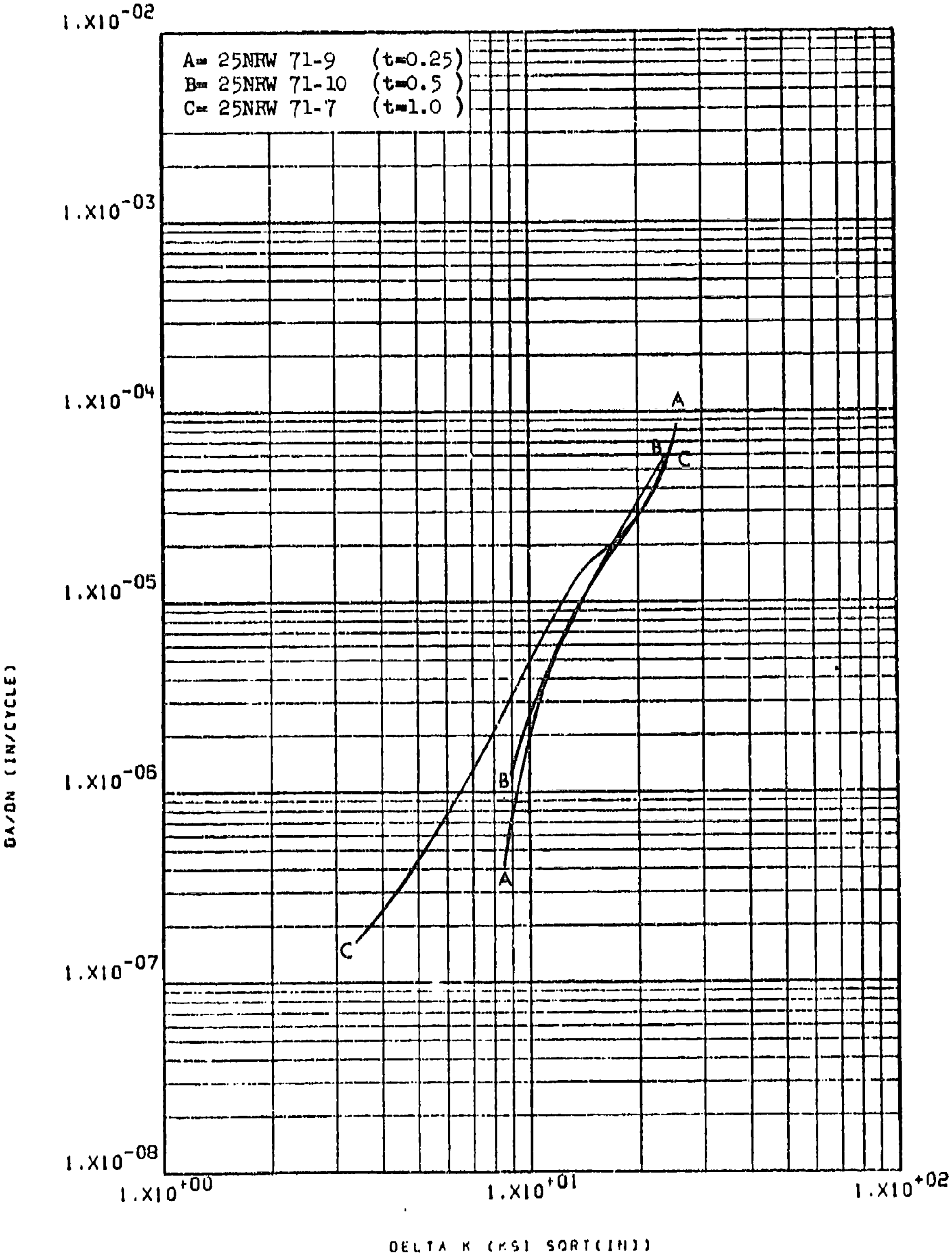

Figure 8.2.5.3-1 Effect of specimen thickness on LHA-FCGR at R.T., R=0.08, 360 cpm, RW direction, in 7049-T7352 3" x 24" x 48" forging

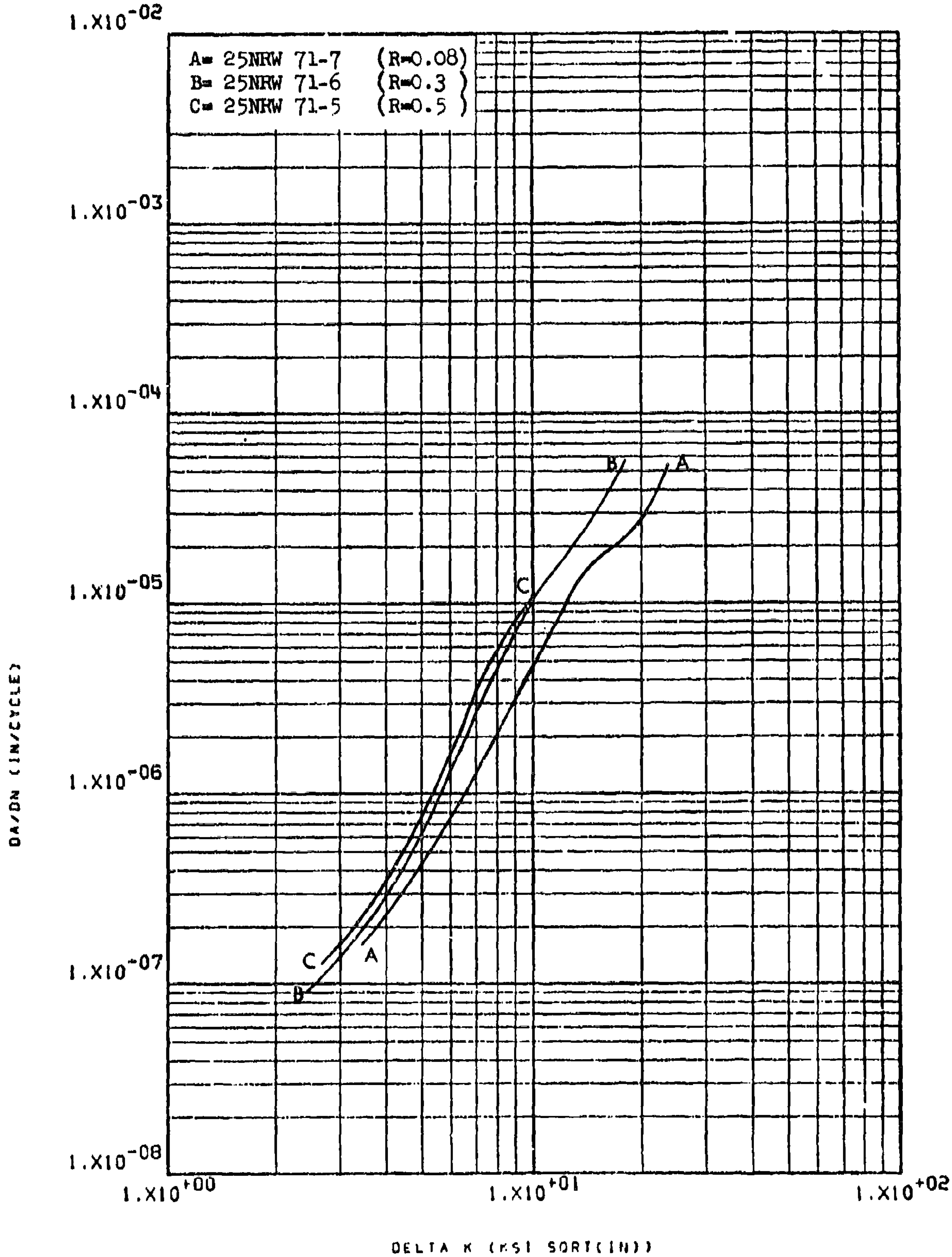

Figure 8.2.5.4-1 Effect of R factor on LHA-FCGR at R.T., 360 cpm, RW direction, in 7049-T7352 3" x 24" x 48" forging

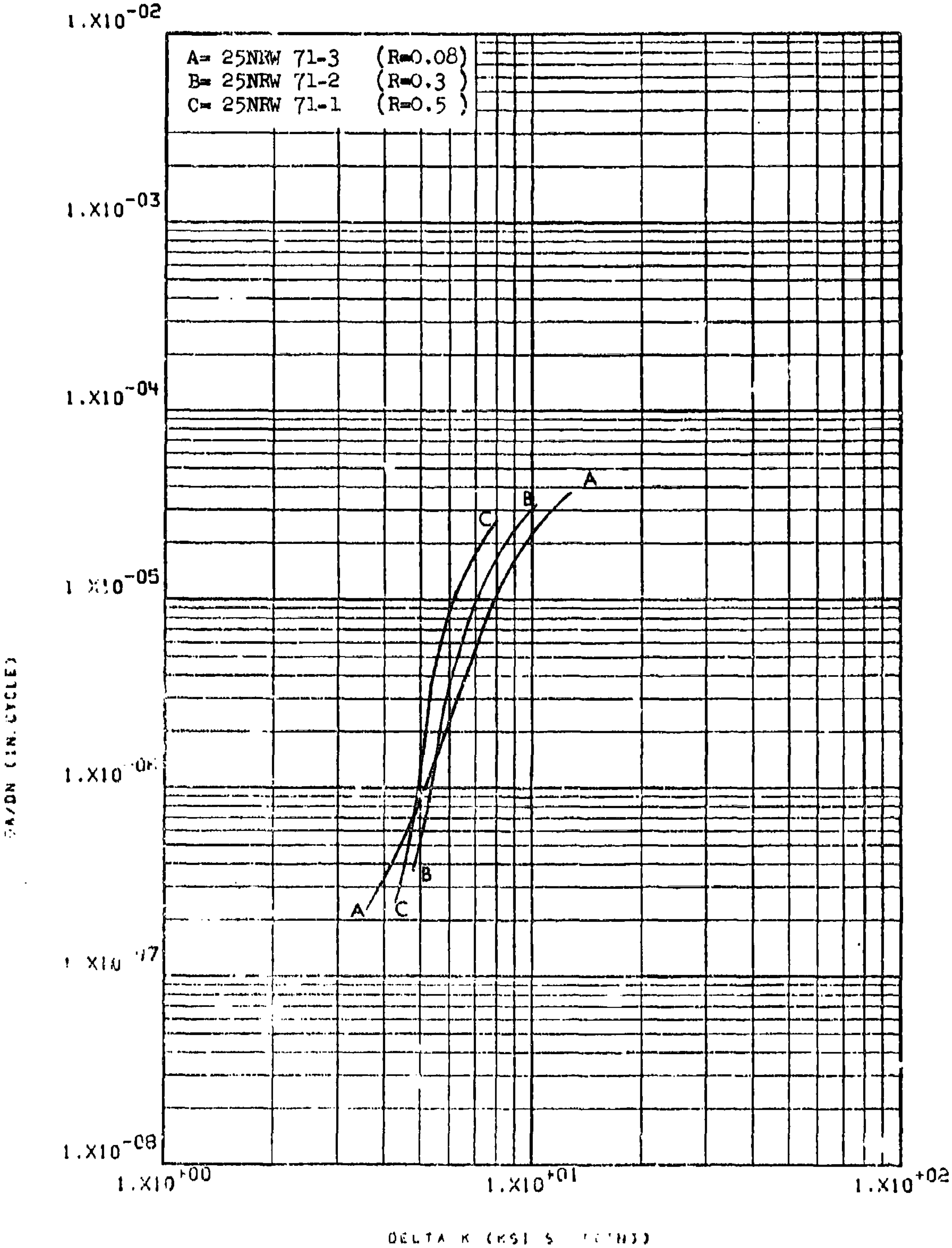

Figure 8.2.5.4-2 Effect of R factor on STW-FCGR at R.T., 60 cpm, RW direction, in 7049-T7352 3" x 24" x 48" forging

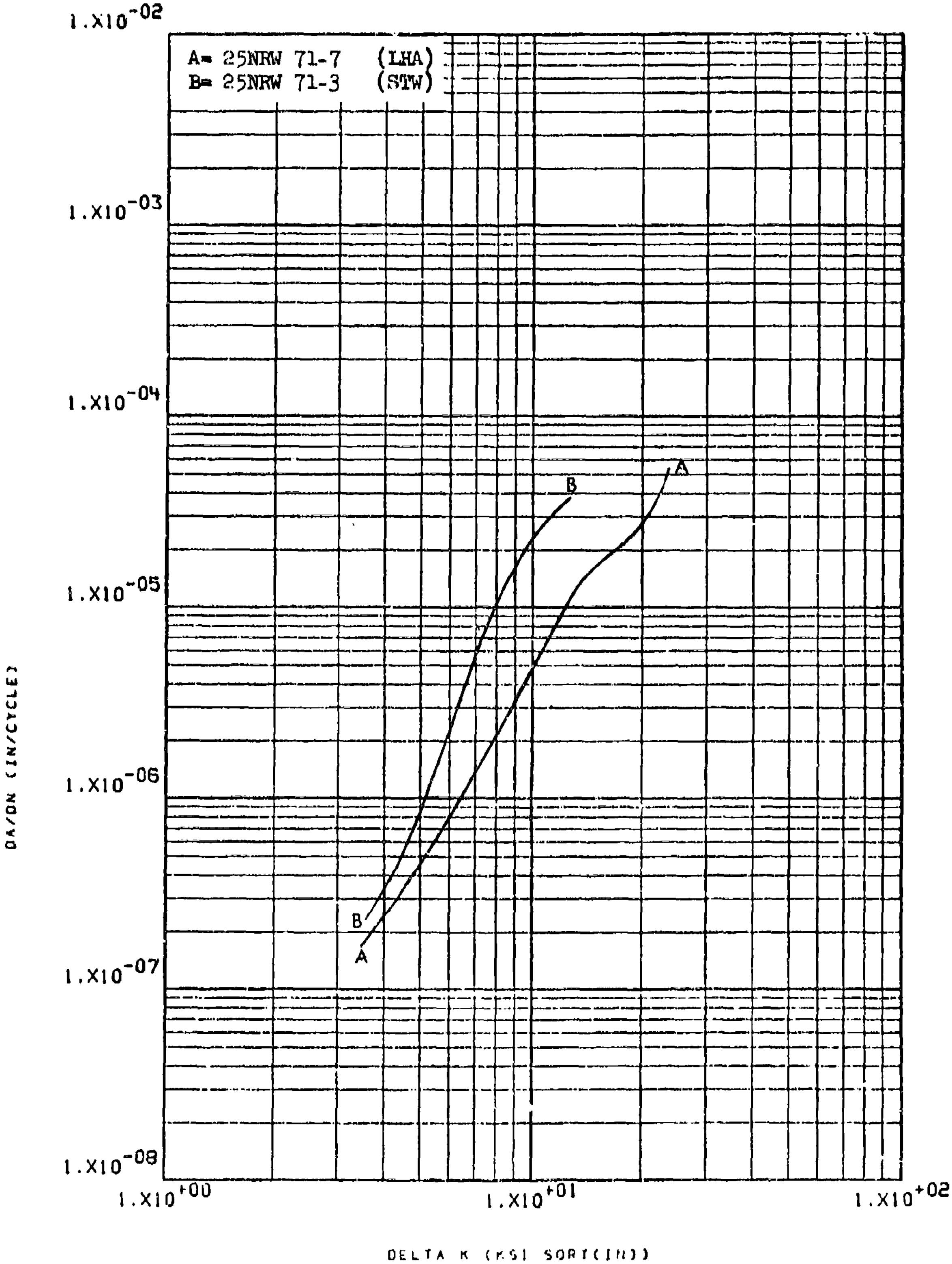

Figure 0.2.5.5-1 Effect of environment on FCGR at R.T., R=0.08, RW direction, in 7049-T7352 3" x 24" x 48" forging

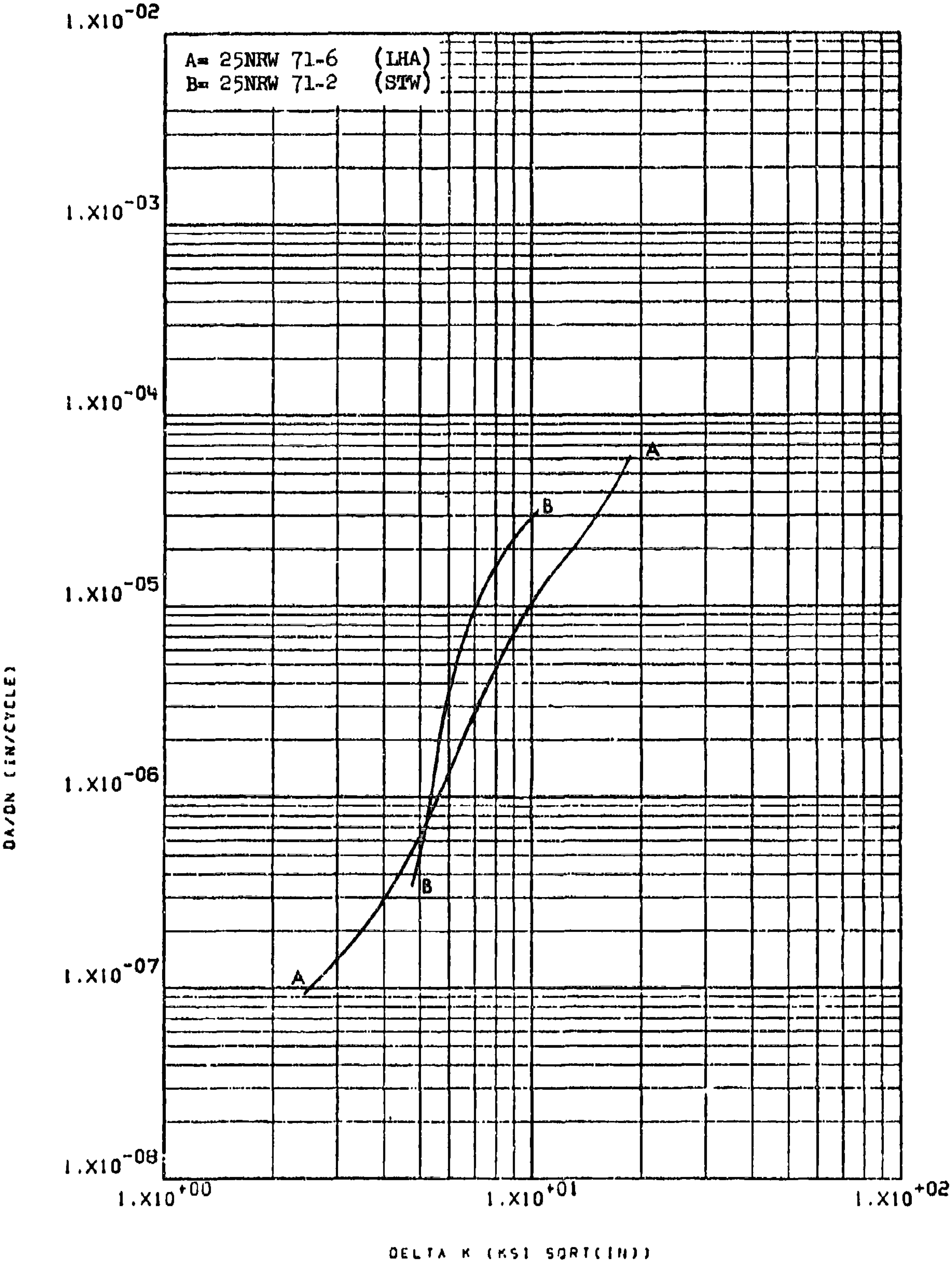

Figure 8.2.5.5-2 Effect of environment on FCGR at R.T., R=0.3, RW direction, in 7049-T7352 3" x 24" x 48" forging

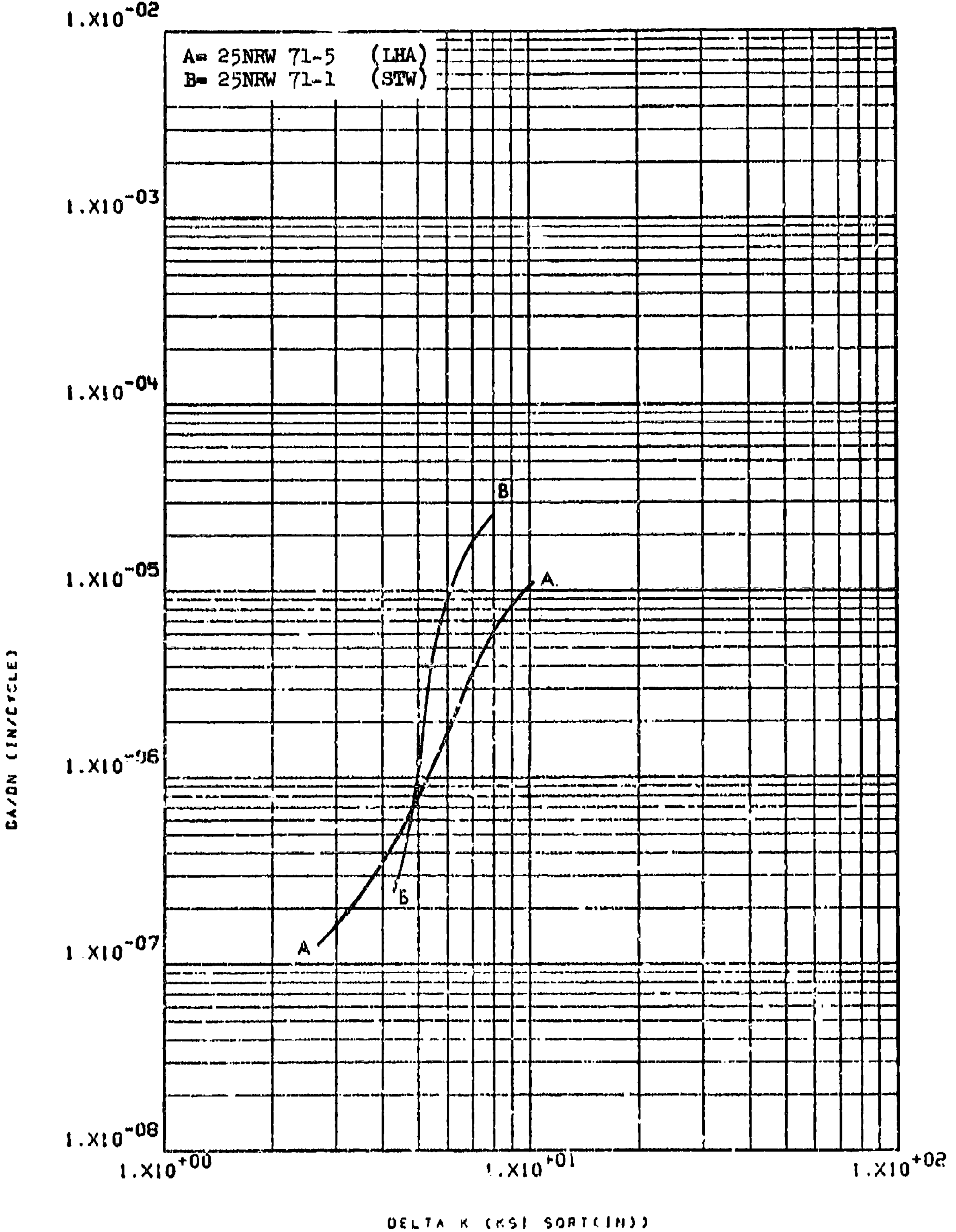

Figure 8.2.5.5-3 Effect of environment on FCGR at R.T., R=0.5, RW direction, in 7049-T7352 3" x 24" x 48" forging

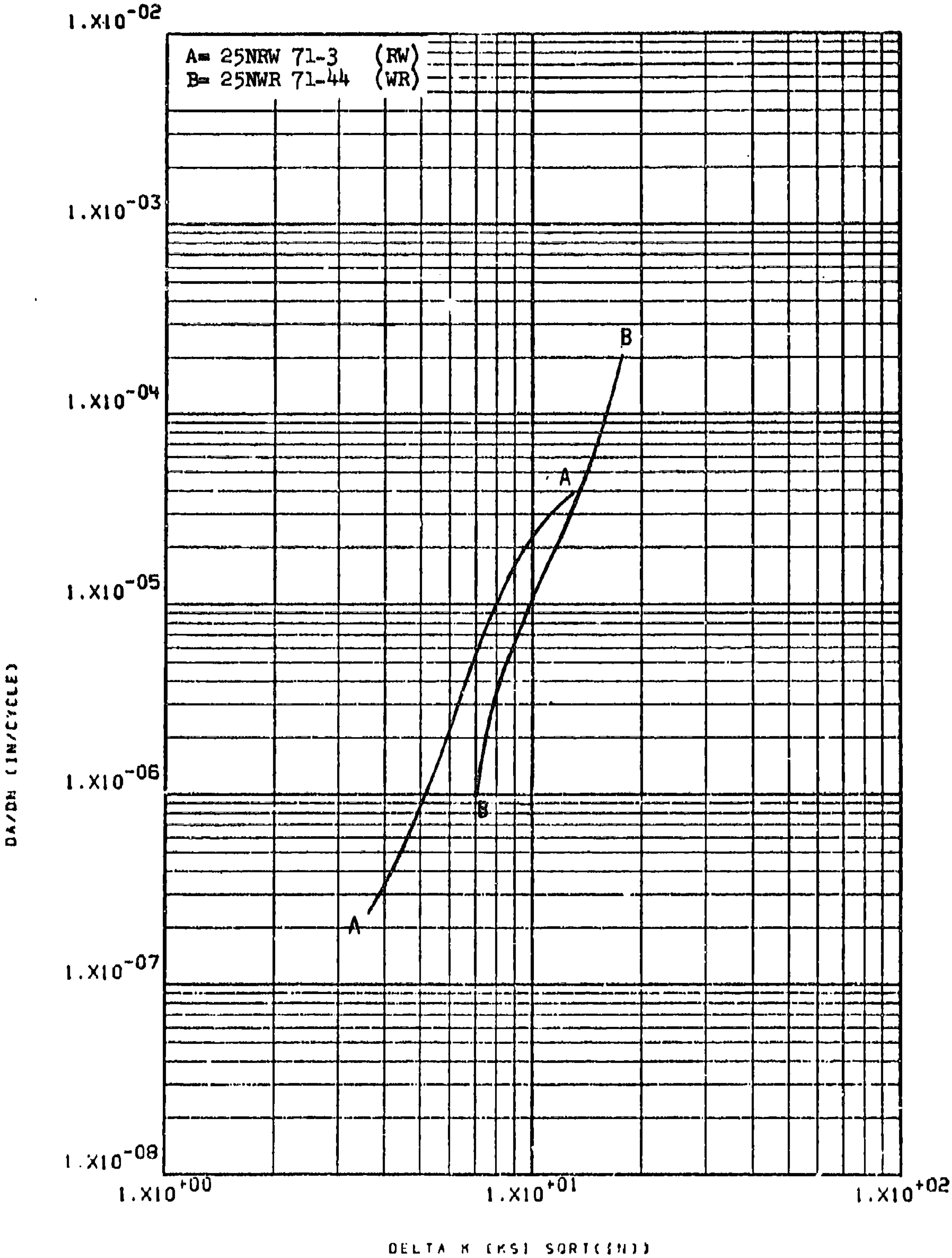

Figure 8.2.5.6-1 Effect of test direction on STW-FCGR at R.T., R=0.08, 60 cpm, in 7049-T7352 3" x 24" x 48" forging

8.2.6 Aluminum Alloy 7050

8.2.6.1 Cyclic Frequency - Not evaluated.

8.2.6.2 Test Temperature - Not evaluated.

8.2.6.3 Specimen Thickness - Not evaluated.

8.2.6.4 R Factor - The crack growth rate of this material was seen to increase significantly as R was increased from 0.08 to 0.3 to 0.5 (Figure 8.2.6.4-1). The magnitude of these increases was also seen to increase with increasing delta K levels.

8.2.6.5 Environment - Growth rates of this material in sump tank water and low humidity air were seen to be essentially equivalent at a delta K level of 5.5 ksi $\sqrt{in.}$ Above this level, however, the growth rate in sump tank water was seen to be significantly greater than in low humidity air (Figure 8.2.6.5-1).

8.2.6.6 Test Direction - There was no consistently significant difference between the growth rates of this material in the RW and WR directions (Figure 8.2.6.6-1).

8.2.6.7 Product Form - Not evaluated.

8.2.6.8 Heat Treat Condition - Not evaluated.

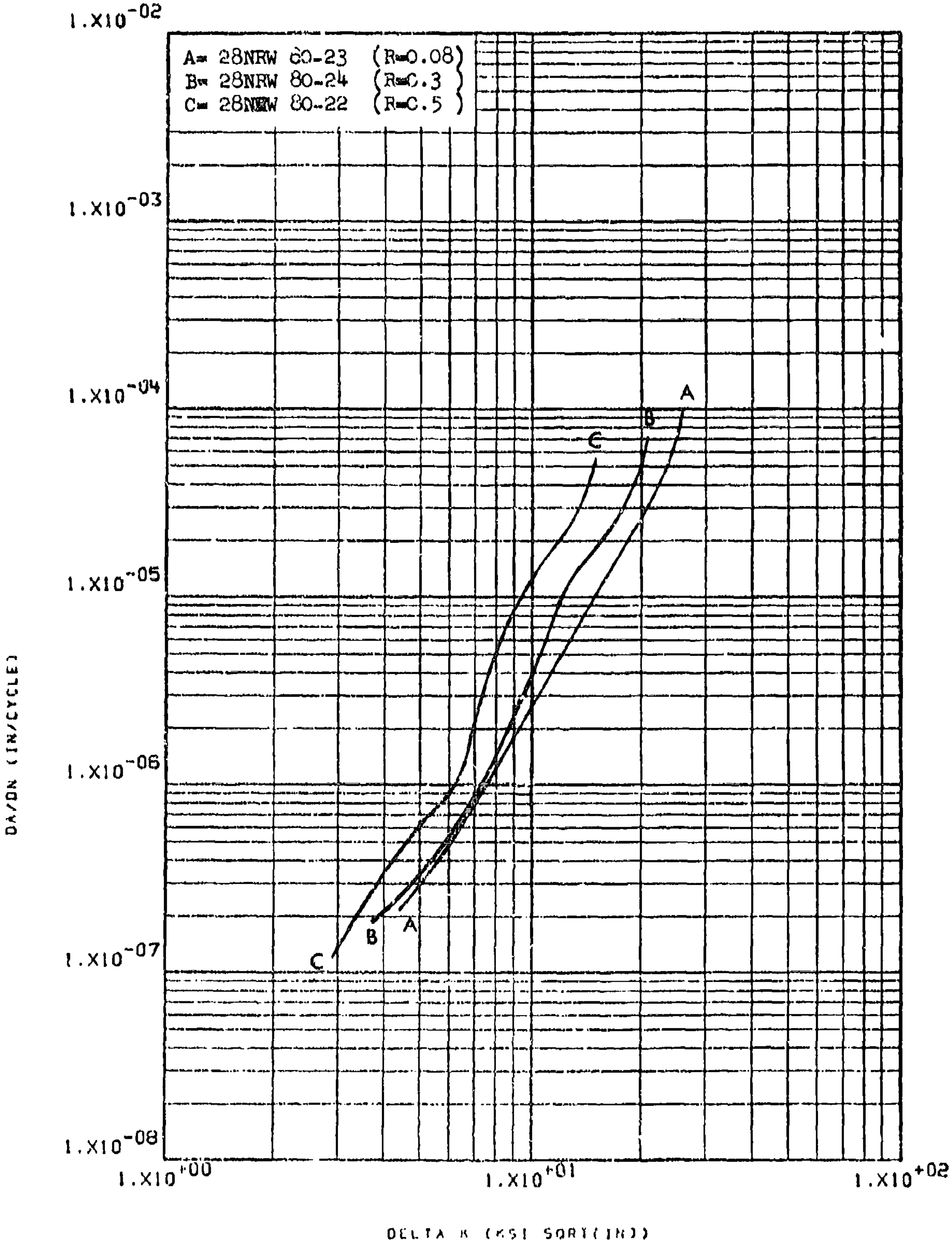

Figure 8.2.6.4-1 Effect of R factor on LHA-FCGR at R.T., 360 cpm, RW direction, in 7050-T73651 4" plate

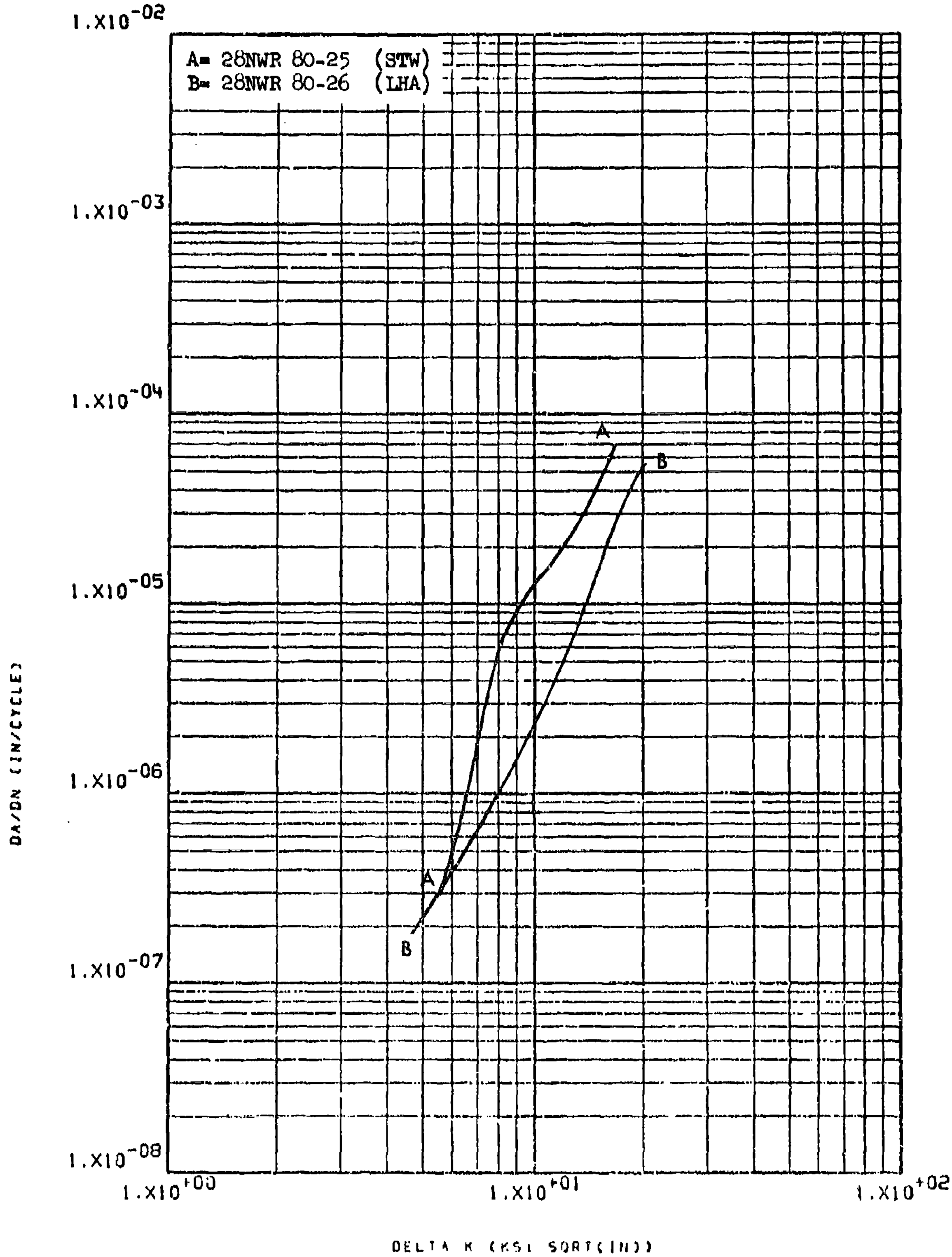

Figure 8.2.6.5-1 Effect of environment on FCGR at R.T., R=0.08, WR direction, in 7050-T73651 4" plate

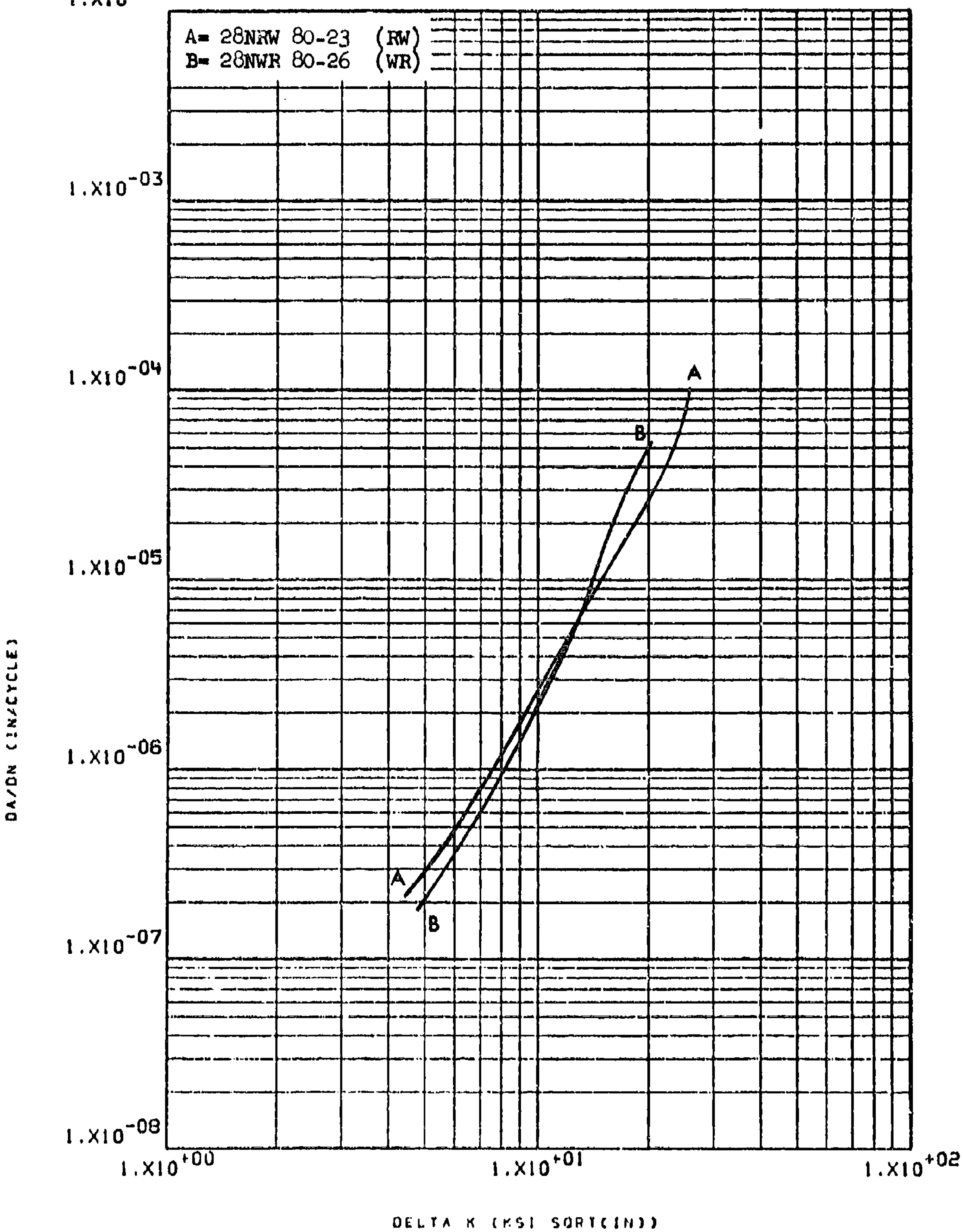

Figure 8.2.6.6-1 Effect of test direction on LHA-FCGR at R.T., 360 cpm, R=0.08, in 7050-T73651 4" plate

8.2.7 Aluminum Alloy 7075

8.2.7.1 Cyclic Frequency - In the T7351 condition low humidity air growth rates were seen to increase slightly when the cyclic frequency of test was decreased from 360 to 60 cpm, but no further increases were observed when the frequency was further decreased to 6 cpm (Figure 8.2.7.1-1). In the T7651 condition the effects of changing cyclic frequency in low humidity air at ambient temperature and 265°F were inconsistent from test to test, and essentially insignificant (Figures 8.2.7.1-2 through -4). In sump tank water, however, growth rates were seen to be significantly accelerated when the frequency was dropped from 60 to 6 cpm, particularily at low delta K levels. As delta K was increased this effect became less pronounced until at ~11 ksi $\sqrt{in}$ the rates were seen to be essentially equivalent (Figure 8.2.7.1-5).

8.2.7.2 Test Temperature - In the T7351 condition growth rates of this material at moderate delta K levels in low humidity air were significantly greater at 265°F than at ambient temperature (Figure 8.2.7.2-1). The magnitude of difference between the growth rates at these two temperatures decreased as delta K was increased up to approximately 15 ksi $\sqrt{in}$, and also at low levels of delta K as delta K was decreased. In the T7651 condition growth rates were seen to be significantly greater at 265°F than at room temperature while at low levels of delta K (Figure 8.2.7.2-2). This temperature effect became less pronounced, however, as delta K was increased and non-existent at ~10 ksi $\sqrt{in}$ (Figure 8.2.7.2-3).

8.2.7.3 Specimen Thickness - There was no consistently significant effect observed of specimen thickness on fatigue crack growth rates of this material in the T7351 condition (Figures 8.2.7.3-1 and -2), and in the T7651 condition (Figures 8.2.7.3-3 and -4).

8.2.7.4 R Factor - Significant increases in crack growth rates were observed in the T7351 condition of this material when the R factor was increased from 0.08 to 0.3 to 0.5 to 0.7 in low humidity air and sump tank water (Figures 8.2.7.4-1 through -3). Similar increases in growth rate were observed in the T7651 condition (Figures 8.2.7.4-4 and -5).

8.2.7.5 Environment - In the T7351 condition, growth rates in sump tank water were seen to be slightly greater than those in low humidity air in plate stock (Figure 8.2.7.5-1) and significantly greater in extrusions (Figure 8.2.7.5-2). The magnitude of difference between rates in sump tank water and low humidity air was seen to decrease as delta K was decreased (Figures 8.2.7.5-2 through -6). Growth rates in shop cleaning solvent were seen to be slightly greater than those in low humidity air in the RW direction (Figure 8.2.7.5-2) and significantly greater than in low humidity air in the WR direction (Figure 8.2.7.5-6). In both directions, the magnitude of difference in rates tended to decrease as delta K was increased, until at ~16 ksi $\sqrt{in}$ they were essentially equivalent. In the T7651 condition growth rates were also seen to be greater in sump tank water than in low humidity air at low levels of delta K (Figures 8.2.7.5-7 through -11). The magnitude of this effect diminished in all cases except at R=0.3 (Figure 8.2.7.5-9) as delta K was increased. Growth rates in shop cleaning solvent were seen to be essentially the same as those in sump tank water (Figure 8.2.7.5-8).

8.2.7.6 Test Direction - There was no consistently observable effect of test direction on the crack growth rates of this material in either the plate or extrusions (Figures 8.2.7.6-1 through -5).

8.2.7.7 Product Form - In each test performed in this material in the T7351 condition crack growth rates were seen to be greater in extrusions than in plate (Figures 8.2.7.7-1 through -5). The magnitude of difference between rates was seen to be most significant at delta K levels below ~9.5 ksi $\sqrt{\text{in.}}$ Growth rates in forged stock were significantly greater than those in extruded stock throughout the delta K range (Figure 8.2.7.7-5). In the T7651 condition growth rates of this material were also seen to be greater in extrusions than in plate at low levels of delta K in sump tank water and low humidity air environments in both the RW and WR directions (Figures 8.2.7.7-6 through -9). The magnitude of difference in rates between the two forms were seen to diminish as delta K was increased, and became non-existent at ~10 to 20 ksi $\sqrt{\text{in.}}$

8.2.7.8 Heat Treat Condition - The difference in crack growth rates of this material in the T73 and T76 conditions was seen to be insignificant (Figures 8.2.7.8-1 through -4).

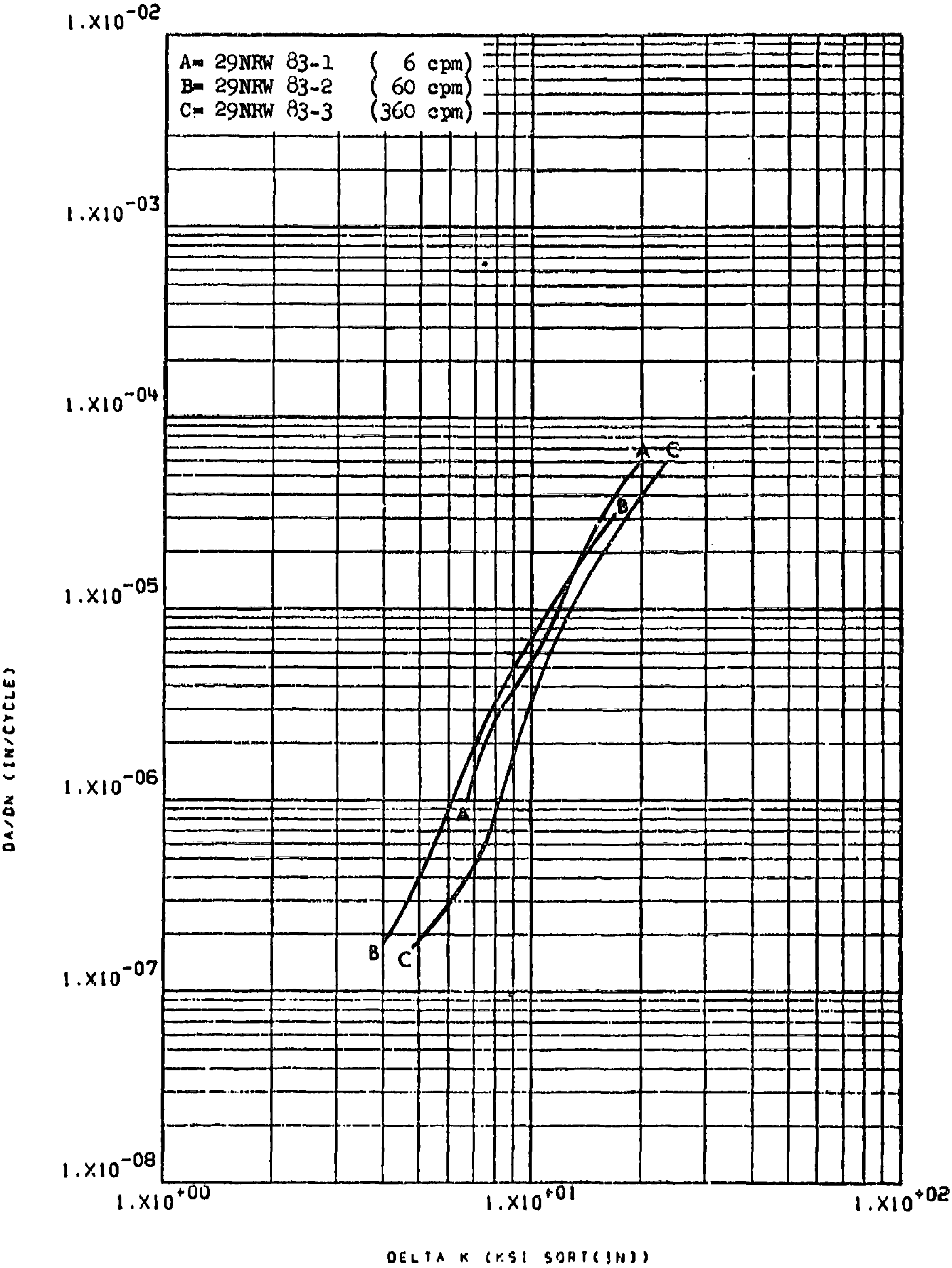

Figure 8.2.7.1-1 Effect of cyclic frequency on LHA-FCGR at R.T., R=0.08, RW direction in 7075-T73511 3" x 17" extrusion

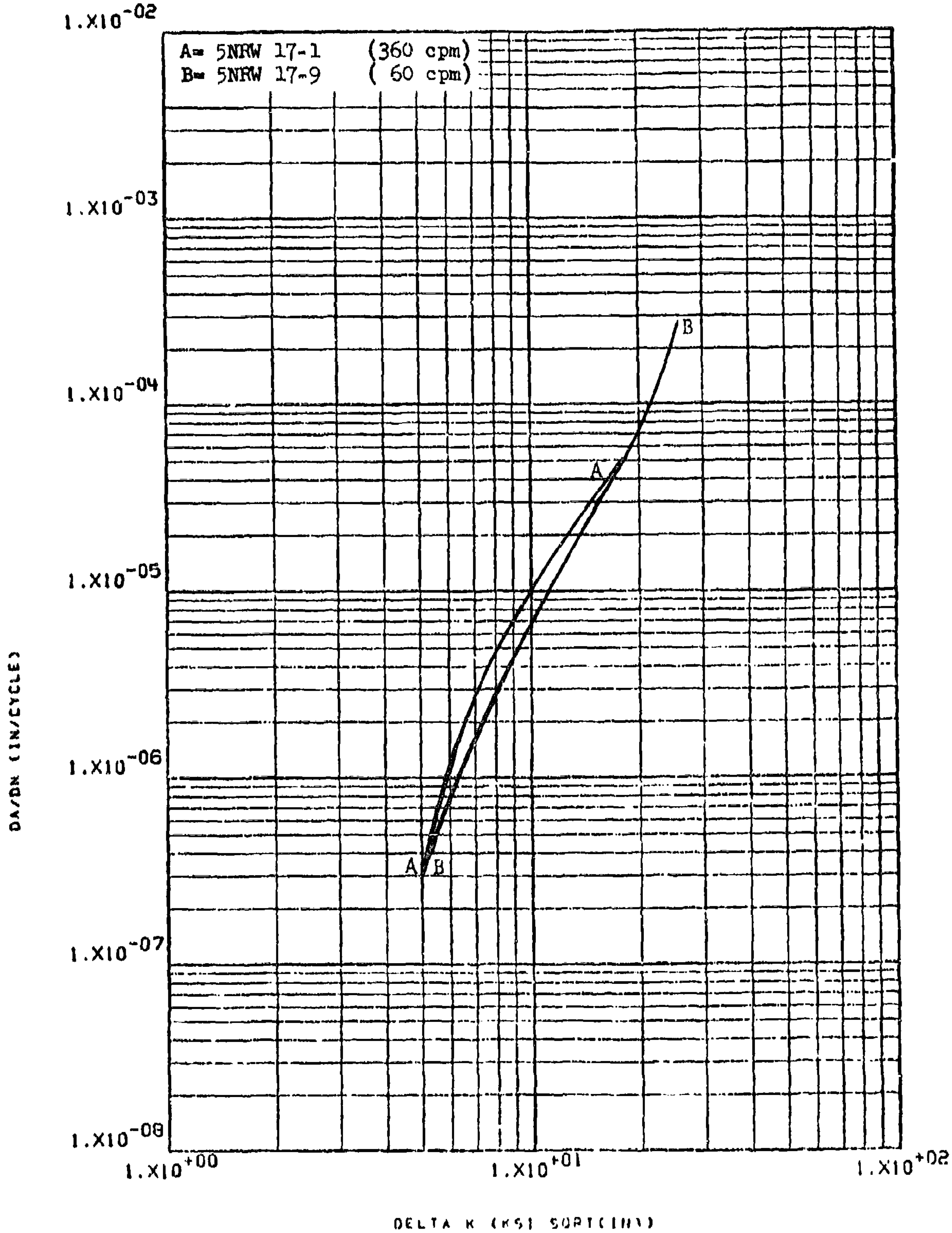

Figure 8.2.7.1-2 Effect of cyclic frequency on IHA-FCGR at R.T., R=0.08, RW direction in 7075-T7651 2" plate

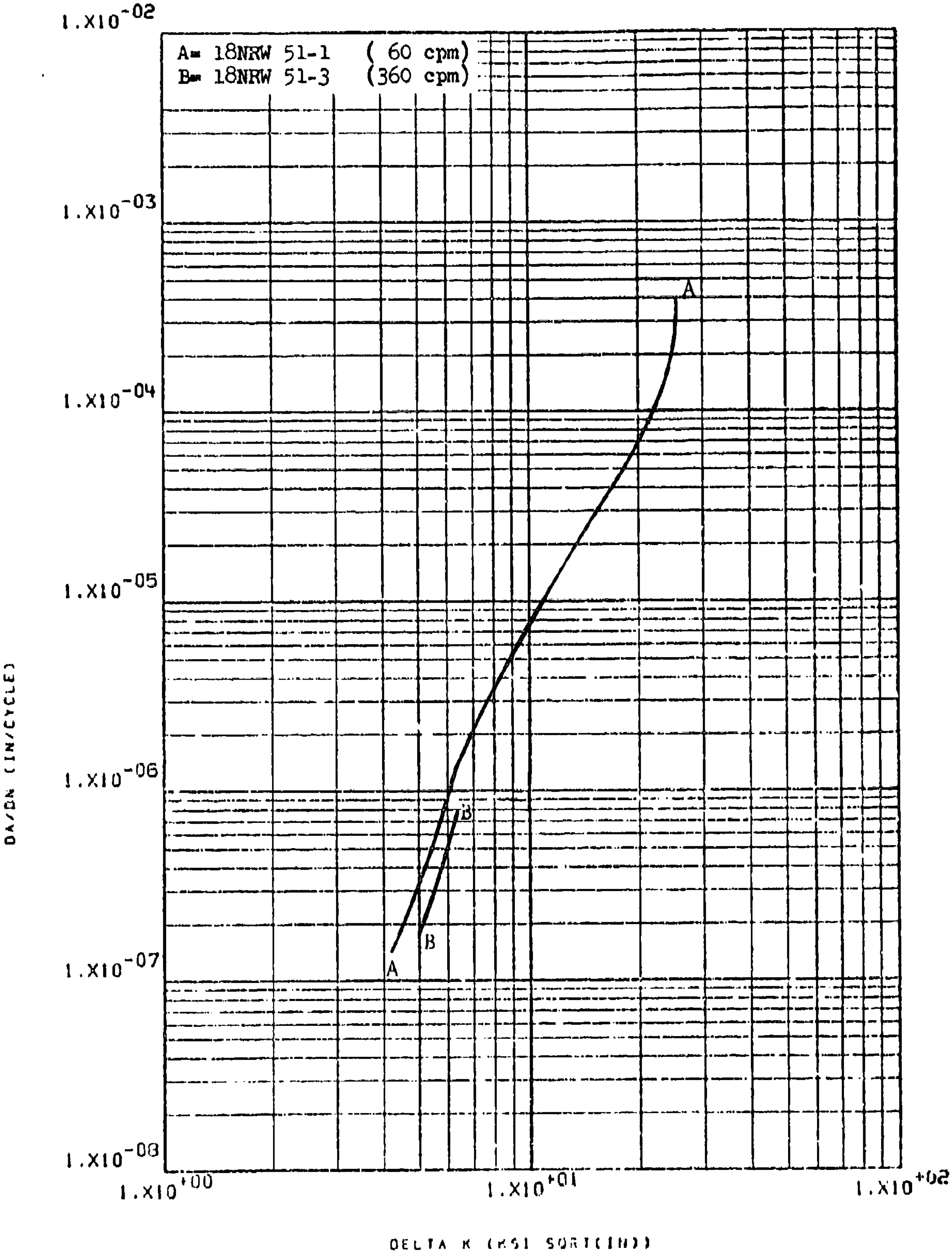

Figure 8.2.7.1-3 Effect of cyclic frequency on LHA-FCGR at R.T., R=0.08, RW direction in 7075-T7651 2" plate

Table 7-2 (Page 1 of 2)

DIFFUSION BONDED 6-4 TITANIUM K_{Iscc} TEST RESULTS

Specimen No.'s	Orientation	Environment	K_I (Test Time in Hrs), Specimen Crack Traces	$K_{Ii} - K_{If}$ (Crack Growth, In), Crack Front Measurements	K_{Iscc}, KSI $\sqrt{In}$	Specimen Plane Strain Capability K_I, KSI $\sqrt{In}$
Mat'l 74 - Billet of 1.5" Plate (Mat'l 70) Laminations						
			As Bonded			
52-11	TW/TW	STW	89 (0), 87 (1-983)	86 - 71(.23)	71	72
-9	TW/TW	STW	74 (0-1), 73 (4-1273)	71 - 65(.11)	65	72
-10	TW/TW	STW	63 (0), 62 (1-1271)	60 - 53(.15)	53	72
-8	TW/TW	STW	56 (0-1601)	-----	--	72
-8RT	TW/TW	STW	65 (0-1012)	65 - 46(.34)	46	72
					59	
			As Bonded +2 DB Thermal Cycles			
53-7	TW/TW	STW	79 (0-1274)	76 - 71(.09)	71	72
-6	TW/TW	STW	57 (0-1434)	-----		72
-6RT	TW/TW	STW	73 (0), 72 (5-1012)	69 - 54(.27)	54	72
					62	
			As Bonded +4 DB Thermal Cycles			
54-7	TW/TW	STW	86 (0), 85 (1-1274)	82 - 76(.09)	76	70
-6	TW/TW	STW	57 (0), 56 (25-1434)	54 - 52(.03)	53	70
					65	
1.5" (WR) and 2.5" (TR) Plate Material, Diffusion Bonded with Intentional Bond Plane Anomalies						
			As Bonded With Fine Porosity in Bond Plane (Dia.-.0015", Freq-10,000/in^2)			
4KSA31	WR/TR	STW	56 (0), 41 (1-4), 40 (46-1033)	54-37(.39)	37	76
			As Bonded With Intermediate Porosity in Bond Plane (Dia.-.002", Freq-2500/in^2)			
4KSA31	WR/TR	STW	69 (0), 40 (1-4), 39 (46-1033)	66 - 37(.65)	37	75

Table 7-2 (Page 2 of 2)

DIFFUSION BONDED 6-4 TITANIUM K_{Iscc} TEST RESULTS

Specimen No.'s	Orientation	Environment	K_I (Test Time in Hrs), Specimen Crack Traces	K_{Ii} - K_{If} (Crack Growth, In), Crack Front Measurements	K_{Iscc}, KSI $\sqrt{In}$	Specimen Plane Strain Capability K_I, KSI $\sqrt{In}$
1.5" (WR) and 2.5" (TR) Plate Material, Diffusion Bonded with Intentional Bond Plane Anomalies (Cont'd)						
			As Bonded with Coarse Porosity in Bond Plane (Dia.-.004", Freq-2500/in^2)			
4KSA41	WR/TR	STW	60 (0), 54 (1-4), 53 (46-1033)	57 - 43 (.31)	43	75
			As Bonded With Oxygen Enriched Bond Plane (Medium)			
3KSA61	WR/TR	STW	51 (0), 26 (1-1033)	49 - 21 (1.03)	21	75

Table 7-3 (Page 1 of 2)

6-4 TITANIUM GTA OR PA BUTT WELD JOINTS K_{Iscc} TEST RESULTS

Specimen No.'s	B, In	Notch Location	Environment	K_I (Test Time in Hrs), Specimen Crack Traces	K_{Ii} - K_{If} (Crack Growth, In), Crack Front Measurements	K_{Iscc}, KSI $\sqrt{In}$	Specimen Plane Strain Capability K_I, KSI $\sqrt{In}$
Mat'l 88, 1-1/4" Plate, Preweld - Cond RA							
				Postweld - 1400F, 1 HR (GTAW)			
B624	1/8	HAZ(RW)	STW	64 (0-1392)	62 - 62	>62	27
				Postweld - 1200F, 1 HR (GTAW)			
B623	1/8	HAZ(RW)	STW	69 (0-1392)	67 - 67	>67	27
				Postweld - 1400F, 1/2 HR (GTAW)			
B618	1/4	HAZ(RW)	STW	73 (0-1392)	70 - 70	>70	38
19	1/4	HAZ(RW)	STW	69 (0-1392)	67 - 67	>67	38
						>70	
				Postweld - 1200F, 1/2 HR (GTAW)			
B620	1/4	HAZ(RW)	STW	66 (0-1392)	66 - 66	>66	38
21	1/4	HAZ(RW)	STW	65 (0-1392)	62 - 62	>62	38
						>66	
				Postweld - 1100F, 2 HR (GTAW)			
B654	1/2	WELD(RW)	STW	104 (0), 102 (1-1870)	100 - 93 (.07)	93	54
51	1/2	WELD(RW)	STW	74 (0-1392)	71 - 71	>71	54
52	1/2	WELD(RW)	STW	65 (0-1251)	62 - 62	>62	54
53	1/2	WELD(RW)	STW	65 (0-1251)	62 - 62	>62	54
55	1/2	WELD(RW)	STW	65 (0-1251)	61 - 61	>61	54
50	1/2	WELD(RW)	STW	58 (0-1434)	59 - 59	>59	54
						93	
B602	1/2	HAZ(RW)	STW	49 (0-1419)	50 - 50	>50	54
3	1/2	HAZ(RW)	STW	49 (0-1419)	53 - 53	>53	54
4	1/2	HAZ(RW)	STW	44 (0-1419)	48 - 48	>48	54
						>53	

Table 7-3 (Page 2 of 2)

6-4 TITANIUM GTA OR PA BUTT WELD JOINTS K_{Iscc} TEST RESULTS

Specimen No.'s	B, In	Notch Location	Environment	K_I (Test Time in Hrs), Specimen Crack Traces	$K_{Ii} - K_{If}$ (Crack Growth, In), Crack Front Measurements	K_{Iscc}, KSI $\sqrt{In}$	Specimen Plane Strain Capability K_I, KSI $\sqrt{In}$
Mat'l 88, 1-1/4" Plate, Preweld - Cond RA (Cont'd)							
				Postweld - 1100F, 2 HR (GTAW)			
B606	1/2	HAZ(RW)	FCS	49 (0-1419)	48 - 48	>48	54
-7	1/2	HAZ(RW)	FCS	48 (0-1419)	46 - 46	>46	54
-5	1/2	HAZ(RW)	FCS	46 (0-1419)	44 - 44	>44	54
						>48	
B609	1/2	HAZ(RW)	SCS	63 (0-1251)	64 - 64	>64	54
-08	1/2	HAZ(RW)	SCS	47 (0-1491)	48 - 48	>48	54
-10	1/2	HAZ(RW)	SCS	47 (0-1419)	47 - 47	>47	54
						>64	
B614	3/4	HAZ(RW)	STW	105 (0), 83 (1-1869)	95 - 71 (.31)	71	66
-16	3/4	HAZ(RW)	STW	97 (0), 87 (1-93), 86 (190-1870)	89 - 76 (.17)	76	66
						74	
B600	1	HAZ(RW)	STW	60 (0), 59 (0-1434)	64 - 58 (.09)	58	76
				Postweld - 1100F, 2HR (PAW)			
B656	1/2	WELD(RW)	STW	75 (0-1028)	73-73	>73	54
57	1/2	WELD(RW)	STW	71 (0-1028)	70-70	>70	54
						>73	
B628	1/2	HAZ(RW)	STW	92 (0-1028)	89-89	>89	54
Mat'l 75, T-Shape Extrusion (Beta Extruded & Mill Annealed), Preweld - Mill Annealed							
				Postweld - 1200F, 1 HR (GTAW)			
B626	1/2	HAZ(RW)	STW	75 (0), 70 (1-1006)	75 - 60 (.22)	60	54
-27	1/2	HAZ(RW)	STW	60 (0-1906)	59 - 57 (.03)	57	54
						59	

Table 7-4

2024 ALUMINUM ALLOY - K_{Iscc} TEST RESULTS

Specimen No.'s	Orientation	Environment	K_I (Test Time in Hrs), Specimen Crack Traces	K_{Ii} - K_{If} (Crack Growth, In), Crack Front Measurements	K_{Iscc}, KSI $\sqrt{In}$	Specimen Plane Strain Capability K_I, KSI $\sqrt{In}$
Material 27 - 2024, 3 x 18 x 35" Forged Block, T852						
75-93	WR	STW	22.0(0-2228)	20.7-20.5(.01)	20.5	34
-94	"	"	22.0(0-2228)	21.6-19.8(.10)	19.8	"
-95	"	"	22.0(0-2228)	21.0-21.0	>21.0	"
-96	"	"	21.5(0-2228)	21.0-21.0	>21.0	"
					20.5	
75-85	RW	SCS	37.0(0-1028)	35.6-34.0(.05)	34.0	34
-82	"	"	23.0(0-1082)	22.5-22.1(.01)	22.1	"
					28.0	
Material 19 - 2024, 3 x 18 x 23" Forged Block, T852						
64-23	RW	STW	24.5(0-1269)	23.5-23.5	> 23.5	37
-24	"	"	24.5(0-1269)	23.5-22.5(.07)	22.5	"
-25	"	"	24.0(0-1269)	23.0-22.5(.04)	22.5	"
					22.5	
64-21	TR	STW	23.0(0-2228)	21.5-20.0(.10)	20.0	37
-20	"	"	14.0(0-2228)	13.5-13.5	>13.5	"
					20.0	

Table 7-5

2124 ALUMINUM ALLOY - K_{Iscc} TEST RESULTS

Specimen No.'s	Orientation	Environment	K_I (Test Time in Hrs), Specimen Crack Traces	K_{Ii} - K_{If} (Crack Growth, In), Crack Front Measurements	K_{Iscc}, KSI $\sqrt{In}$	Specimen Plane Strain Capability K_I, KSI $\sqrt{In}$
Material 12 - 2124, 3" Plate, T851						
35-98	RW	STW	29.5(0-1172)	28.4-27.8(.02)	27.8	41
-99	"	"	28.0(0-1172)	27.1-26.7(.015)	26.7	"
-100	"	"	26.5(0-1005)	26.0-26.0	> 26.0	"
-97	"	"	26.5(0-906)	25.5-25.2(.01)	25.2 26.5	"
35-82	TR	STW	32(0), 31(66-281), 30(335-1315), 29(1488-2177)	30.5-26.0(.17)	26.0	40
-83	"	"	25.5(0-906)	25.0-21.0(.19)	21.0	"
-81	"	"	25.5(0-5), 25.0(30-862)	25.0-25.0	>25.0	"
-84	"	"	23.5(0-906)	22.5-21.0(.06)	21.0 23.0	"

Table 7-6

2219 ALUMINUM ALLOY - K_{Iscc} TEST RESULTS

Specimen No.'s	Orientation	Environment	K_I (Test Time in Hrs), Specimen Crack Traces	K_{Ii} - K_{If} (Crack Growth, In), Crack Front Measurements	K_{Iscc}, KSI $\sqrt{In}$	Specimen Plane Strain Capability K_I, KSI $\sqrt{In}$
Material 7, 1-3/4" Plate, T851						
23-92	RW	STW	39.0(0-1392)	38.0-36.0(.07)	36.0	32
-91	"	"	35.0(0-862)	33.5-33.0(.02)	33.0	"
-93	"	"	21.0(0-596)	20.0-20.0	>20.0	"
-95	"	"	14.0(0-596)	12.9-12.9	>12.9	"
					35.0	
23-120	RW	SCS	44.0(0-1028	41.0-39.0(.05)	39.0	32
-103	"	"	44.0(0-985)	42.0-37.0(.11)	37.0	"
-100	"	"	30.5(0-1254)	29.0-27.0(.07)	27.0	"
					34.0	
23-102	RW	FCS	32.5(0-1254)	31.5-30.5(.04)	30.5	32
-101	"	"	30.5(0-1254)	29.0-27.5(.05)	27.5	"
					29.0	
23-81	WR	STW	29.5(0), 29.0(5-862)	27.5-27.0(.02)	27.0	30
-78	"	"	18.5(0-596)	17.5-17.5	>17.0	"
-79	"	"	12.5(0-596)	12.0-12.0	>12.0	"
					27.0	
23-133	TW	STW	32.5(0-1392)	32.0-29.5(.08)	29.5	30
-132	"	"	31.5(0-862)	30.5-29.5(.03)	29.5	"
-131	"	"	13.0(0-596)	13.0-13.0	13.0	"
					29.5	

Table 7-7

7049 ALUMINUM ALLOY - K_{Iscc} TEST RESULTS

Specimen No.'s	Orientation	Environment	K_{I} (Test Time in Hrs), Specimen Crack Traces	K_{Ii} - K_{If} (Crack Growth, In), Crack Front Measurements	K_{Iscc}, KSI $\sqrt{In}$	Specimen Plane Strain Capability K_{I}, KSI $\sqrt{In}$
Material 25, 3 x 4 x 48" Forged Block, T7352						
71-27	RW	STW	21.5(0),15.0(2228), Crack Angle of 60°	21.0-<21.0	<21.0	41
-28	"	"	21.5(0-2228)	21.0-21.0	21.0	"
					21.0	
71-29	RW	SCS	29.0(0-1270)	27.7-27.6(.005)	27.6	41
-30	"	"	26.0(0-1270)	25.5-25.5	>25.5	"
					27.6	
71-34	RW	FCS	29.0(0-1269)	28.5-28.5	>28.5	41
-33	"	"	28.5(0-1270)	27.5-27.5	>27.5	"
					>28.5	
71-40	WR	STW	22.5(0-215), 20.5(383-2228)	* -19.5	19.5	41
-41	"	"	20.5(0-2228)	20.0-20.0	>20.0	"
-42	"	"	22.5(0-215), 20.0(383-2228)	* -19.0	19.0	"
-39	"	"	22.5(0-2228)	21.5-21.5	>21.5	"
					20.0	
71-36	TR	STW	18.0(0-1390), 17.5 (1557-2228)		17.5	39
-36 RT**	"	"	23.0(0-1028)	22.5-22.5	>22.5	"
-37	"	"	19.5(0-215), 18.0 (549-2228)	* -17.0	17.0	"
-38	"	"	18.0(0-2228)	17.5-17.5	>17.5	"
					18.5	

* Unable to distinguish precrack front because of general corrosion.

** RT = Retest

Table 7-8

7050 ALUMINUM ALLOY - K_{Iscc} TEST RESULTS

Specimen No.'s	Orientation	Environment	K_i (Test Time in Hrs), Specimen Crack Traces	K_{Ii} - K_{If} (Crack Growth, In), Crack Front Measurements	K_{Iscc}, KSI $\sqrt{In}$	Specimen Plane Strain Capability K_I, KSI $\sqrt{In}$
Material 28, 4" Plate, T73651						
80-10	WR	STW	31.0(0-215), 30.5(383-718), 30.0(887-2228)	30.0-27.5(.09)	27.5	43
80-11	"	"	30.5(0-2228)	30.0-28.0(.07)	28.0 27.5	43

Table 7-9 (Page 1 of 2)

7075 ALUMINUM ALLOY - K_{Iscc} TEST RESULTS

Specimen No.'s	Orientation	Environment	K_I (Test Time in Hrs), Specimen Crack Traces	K_{Ii} - K_{If} (Crack Growth, In), Crack Front Measurements	K_{Iscc}, KSI $\sqrt{In}$	Specimen Plane Strain Capability K_I, KSI $\sqrt{In}$
Material 18, 2" Plate, T7651						
50-19	RW	STW	23.5(0-1269)	22.0-22.0	>22.0	40
-18	"	"	23.0(0-1392)	21.5-21.5	>21.5 >22.0	"
51-25	RW	SCS	28.0(0-1003)	26.5-26.5	> 26.5	40
-22	"	"	25.5(0-1254)	23.5-23.5	> 23.5 >26.5	"
51-20	RW	FCS	25.5(0-1254)	24.0-24.0	>24.0	40
51-71	TR	STW	14.0(0-1392)	13.3-13.1(.02)	13.1	40
-27	"	"	13.5(0-1269)	13.3-12.7(.05)	12.7	"
-28	"	"	13.5(0-1269)	13.0-12.6(.03)	12.7	"
-29	"	"	13.5(0-1269)	13.2-12.8(.03)	12.8 12.8	"
Material 18, 2" Plate, T7351						
51-73	TR	STW	13.5(0-1269)	13.1-13.1	>13.1	37
-72	"	"	13.5(0-1269)			"
-72 RT	"	"	20.0(0), 18.5(1-73), 18(474-1028)	18.6-15.0(.23)	15.0 15.0	"
Material 22, Forging, T73						
68-8	WR	STW	26.0(0-1082)	25.0-25.0	>25.0	42

Table 7-9 (Page 2 of 2)

7075 ALUMINUM ALLOY - K_{Iscc} TEST RESULTS

Specimen No.'s	Orientation	Environment	K_I (Test Time in Hrs), Specimen Crack Traces	$K_{Ii} - K_{If}$ (Crack Growth, In), Crack Front Measurements	K_{Iscc}, KSI $\sqrt{In}$	Specimen Plane Strain Capability K_I, KSI $\sqrt{In}$
Material 29, 3 x 17" Extruded Bar, T73511						
83-42	TR	STW	22.2(0-1002)	21.3-21.3	>21.3	41
-41	"	"	22.0(0-984)	21.0-21.0	>21.0	"
-39	"	"	19.5(0-1870)	19.5-19.5	>19.5 >21.3	"
83-46	RW	SCS	37.5(0-1254)	35.7-35.6(.005)	35.6	41
83-45	RW	FCS	37.0(0-1254)	34.0-34.0	>34.0	41

Table 7-10

7175 ALUMINUM ALLOY - K_{Iscc} TEST RESULTS

Specimen No.'s	Orientation	Environment	K_I (Test Time in Hrs), Specimen Crack Traces	K_{Ii} - K_{If} (Crack Growth, In), Crack Front Measurements	K_{Iscc}, KSI $\sqrt{In}$	Specimen Plane Strain Capability K_I, KSI $\sqrt{In}$
Material 26, 6 x 14 x 48" Forged Block, T73652						
72-11	RW	STW	22.5(0-2228)	21.5-21.5	>21.5	44
-12	"	"	22.5(0-2228)	21.5-21.5	>21.5	"
-13	"	"	22.5(0-2060)	22.5-22.5	>22.5	"
-14	"	"	22.5(0-2228)	22.5-22.5	>22.5	"
					>22.5	
72-15	RW	SCS	29.5(0-1270)	27.7-27.5(.01)	27.5	44
-16	"	"	29.0(0-1270)	27.9-27.7(.01)	27.7	"
					27.6	
72-20	RW	FCS	29.0(0-1269)	27.6-26.6	>27.6	44
-21	"	"	29.0(0-1269)	27.8-27.8	>27.8	"
					>27.8	
72-26	WR	STW	23.0(0-2228)	22.2-22.0(.01)	22.0	40
-23	"	"	19.0(0-2228)	18.0-18.0	>18.0	"
-24	"	"	19.0(0-2228)	18.5-18.5	>18.5	"
-25	"	"	19.0(0-1006), 18.5(1223-2228)	18.5-18.5	> 18.5	"
					22.0	

Table 7-11 (Page 1 of 3)

9-4-20 STEEL ALLOY K_{Iscc} TEST RESULTS

Specimen No.'s	Orientation	Environment	K_I (Test Time in Hrs), Specimen Crack Traces	$K_{Ii} - K_{If}$ (Crack Growth, In), Crack Front Measurements	K_{Iscc}, KSI $\sqrt{In}$	Specimen Plane Strain Capability K_I, KSI $\sqrt{In}$
Material 37 2.5" Plate, HT 190-210 ksi						
30-30	RW	STW	111(0-95), 109(214-431), 107(596-768), 106(934-1438)*	110-103(.08)	103	119
-31	"	"	111(0-23), 110(95), 106 (214-934), 105(1271-1438)*	109-105(.04)	105	119
-32	"	"	113(0-95), 111(214-596), 109(768-1438)*	111-107(.04)	107/105	119
30-28	WR	STW	118(0-23), 114(95), 110 (214), 109(431), 105 (768-934), 104(1271-1438)	117-97 117-97(.23)	97 97	119
-27	"	"	117(0-23), 113(95-214), 112(431), 108(596-1438)	116-92(.29)	92	119
-26	"	"	117(0-23), 112(95), 109 (214-431), 108(596-1438)	115-93(.25)	93	119
-29	"	"	108(0-23), 107(95-431), 105(596-1438)	107-104(.04)	104	119
-25	"	"	117(0),116(23),109(95) 108(214-1438)	116-96(.23)	96/96	119

*Bifurcated crack traces at end of precrack (~45° angle). The crack path in the interior of the specimen was horizontal.

Table 7-11 (Page 2 of 3)

9-4-20 STEEL ALLOY K_{Iscc} TEST RESULTS

Specimen No.'s	Orientation	Environment	K_I (Test Time in Hrs), Specimen Crack Traces	$K_{Ii} - K_{If}$ (Crack Growth, In), Crack Front Measurements	K_{Iscc}, KSI $\sqrt{In}$	Specimen Plane Strain Capability K_I, KSI $\sqrt{In}$
Material 43, 4 x 18 x L Forged Bar, HT 190 - 210 ksi						
60-71	RW	STW	127(0), 123(23), 117(95-214), 114(431), 110(596-1438), Crack angle of ~70°	126-<126	<126	118
-72	"	"	130(0), 125(23), 116(95), 112(214), 109(431-934), 106(1271-1436), Crack angle of ~60°	129-<129	<129	"
-73	"	"	126(0), 124(23), 116(95-214), 111(431-934), 108(1271-1438) *	125-110(.16)	110 / 110	"
60-79	RW	SCS	124(0-1011)	122-122	> 122	
-77	"	"	132(0-1003)	129-129	> 129 / > 129	
60-20	WR	STW	126(0), 123(23), 117(95-214), 113(431-596), 110(768-1271), 108(1438)*	125-109(.16)	109	118
22	"	"	126(0), 124(33), 114(105-224), 110(441-944), 105(1281) *	125-105(.21)	105	"
21	"	"	117(0), 112(23-214), 109(431-934), 106(1271-1438), Crack angle of ~60°	117-<117	<117 / 107	118

*Bifurcated crack traces at end of precrack (~45° angle). The crack path in the interior of the specimen was horizontal.

Table 7-11 (Page 3 of 3)

9-4-20 STEEL ALLOY K_{Iscc} TEST RESULTS

Specimen No.'s	Orientation	Environment	K_I (Test Time in Hrs), Specimen Crack Traces	K_{Ii} - K_{If} (Crack Growth, In), Crack Front Measurements	K_{Iscc}, KSI $\sqrt{In}$	Specimen Plane Strain Capability K_I, KSI $\sqrt{In}$
Material 43 (Cont'd.)						
60-40	TW	STW	96(0), 86(100-266), 80 (434-1947)	96-75(.31)	75	118 "
-41	"	"	96(0-23), 90(95-431), 86(596-934), 85(1271-1438)	94-81(.18)	81	"
-42	"	"	96(0-214), 95(431-596), 92(768-934), 88(1271-1438)	96-79-(.24)	79	"
-43	"	"	97(0-23), 86(95-214), 83(431-1271), 80(1438) **Crack angle of 70°**	97-<97	<97 / 78	"

Table 7-12

9-4-20 STEEL GTA BUTT WELD JOINTS K_{Iscc} TEST RESULTS

Specimen No.'s	B, In	Notch Location	Environment	K_I (Test Time in Hrs), Specimen Crack Traces	$K_{Ii} - K_{If}$ (Crack Growth, In), Crack Front Measurements	K_{Iscc}, KSI $\sqrt{In}$	Specimen Plane Strain Capability K_I, KSI $\sqrt{In}$
Material 57, 1.5" Plate, Preweld - HT 190 to 210 ksi, Postweld - 950F, 2 Hrs.							
A650	1/2	Weld, RW	STW	108(0-7), 91(57), 87(177-984)	107-84(.25)	84	85
1	"	"	"	104(0-1), 102(7), 86(57) 81(176-984)	103-81(.25)	81	"
2	"	"	"	97(0-1), 96(7), 79(57) 76(176-984)	97-76(.26)	76/80	"
A602	1/2	HAZ, RW	STW	78(0), 68(76-1251)	76-70(.11)	68	
0	"	"	"	76(0), 66(76), 62(244-1251)	75-62(.24)	62	"
1	"	"	"	75(0), 69(76), 66(244-1251)	74-66(.13)	66	"
A615	"	"	"	62(0-1419)	61-58(.03)	58/64	"
A616	1/2	HAZ, RW	FCS	77(0-1251)	77-77	>77	85
Material 33, 4 x 18 x 36" Forged Block, Preweld - HT 190 to 210 ksi, Postweld - 950F, 2 Hrs.							
A619	1/2	HAZ, RW	STW	90(0), 89(1-91), 85(166), 76(622), 75(1006)	87-81(.08)	81	85
20	"	"	"	70(0-51), 67(166), 63(622-1006)	68-62(.09)	62/72	"
A621	1/4	HAZ, RW	STW	90(0-4), 80(51), 61(166), 38(622), 36(1006)	90-36(1.08)	*	60
22	"	"	"	70(0-4), 68(51-166), 66(622), 62(1006)	69-63(.10)	63/63	"

(*) Discarded, crack front shape indicated eccentric loading.

Table 7-13 (Page 1 of 4)

PH13-8MO STEEL ALLOY - K_{Iscc} TEST RESULTS

Specimen No.'s	Orientation	Environment	K_I (Test Time in Hrs), Specimen Crack Traces	K_{Ii} - K_{If} (Crack Growth, In), Crack Front Measurements	K_{Iscc}, KSI $\sqrt{In}$	Specimen Plane Strain Capability K_I, KSI $\sqrt{In}$
Material 36, 4 x 5" Forged Bar, H950						
24-26	RW	STW	52(0-1392)	50-49.5(.01)	50	130
-27	"	"	52(0-24), 51(216-1392	51-46(.15)	46	"
-23	"	"	50(0), 49(5-862)	48-48	>48	"
-22	"	"	50(0), 40(5), 31(30), 26 (53), 23(75), 18(339-862)*		44**	"
-24	"	"	49(0-813)	48-48	>48	"
-25	"	"	50(0-813)	49-49	>49	
					48	
24-38	RW	STW	52(0-1438)	50-50	>50	131
-36	"	"	50(0-1392)	48-48	>48	"
-31	"	"	47(0-862)	46-46	>46	"
-32	"	"	47(0-30), 46(53-862)	46-46	>46	"
-39	"	"	41(0-1438)	40-40	>40	"
					>50	
Material 36, 4 x 5" Forged Bar, H1000						
24-29	RW	STW	83(0-1392)	80-80	>80	127
-28	"	"	76(0-862)	74-74	>74	"
					>80	
24-40	WR	STW	73(0-5), 72(30-862)	71-71	>71	125
-41	"	"	72(0-862)	68-68	>68	"
-42	"	"	49(0-1392)	49-49	>49	"
-43	"	"	49(0-1392)	49-49	>49	"
-44	"	"	47(0-1392)	46-46	>46	"
					>71	

*Crack curves out of notch zone at a K_I of 22.
**Discarded test result because of inability to duplicate in repeat tests.

Table 7-13 (Page 2 of 4)

PH13-8Mo STEEL ALLOY - K_{Iscc} TEST RESULTS

Specimen No.'s	Orientation	Environment	K_I (Test Time in Hrs), Specimen Crack Traces	$K_{Ii} - K_{If}$ (Crack Growth, In), Crack Front Measurements	K_{Iscc}, KSI $\sqrt{In}$	Specimen Plane Strain Capability K_I, KSI $\sqrt{In}$
Material 40, 1-1/2 x 12" Rolled Bar, H1000						
56-48	RW	STW	76(0-1438)	73-73	>73	132
-49	"	"	76(0-1947)	73-73	>73	"
-50	"	"	75(0-1947)	73-70(.06)	70	"
-51	"	"	76(0-1947)	73-73	$\frac{>73}{72}$	"
56-57	RW	SCS	72(0-1254)	70-70	>70	132
-53	"	"	90(0-1003)	87-87	$\frac{>87}{>87}$	"
56-58	RW	FCS	78(0-1253)	75-75	>75	132
56-45	WR	STW	66(0-1947)	63-63	>63	133
-46	"	"	66(0-1947)	63-63	>63	"
-47	"	"	66(0-1947)	63-63	>63	"
-44	"	"	65(0-1438)	63-63	$\frac{>63}{>63}$	"
Material 41, 1.5 x 8" Extrusion, H1000						
57-42	RW	STW	56(0-431), 45(596), 44 (768), 38(934-1438)*	54-<54	<54	132
-43	"	"	56(0-940), 54(1107), 42(1275-1947)*	53-<53	<53	"
-44	"	"	56(0-1947)	53-53	$\frac{>53}{53}$	"
57-49	WR	STW	56(0-1443), 42(1779), 41(1947) *	53-<53	<53	132
-50	"	"	56(0-1947	54-54	>54	"
-52	"	"	56(0-1947)	53-53	$\frac{>53}{53}$	"

*Crack bifurcates at end of precrack (~50° angle)

Table 7-13 (Page 3 of 4)

PH13-8Mo STEEL ALLOY - K_{Iscc} TEST RESULTS

Specimen No.'s	Orientation	Environment	K_I (Test Time in Hrs), Specimen Crack Traces	K_{Ii} - K_{If} (Crack Growth, In), Crack Front Measurements	K_{Iscc}, KSI $\sqrt{In}$	Specimen Plane Strain Capability K_I, KSI $\sqrt{In}$
Material 41, 1.5 x 8" Extrusion, Re-Solutioned +H1000						
57-55	RW	STW	58(0-2014)	56-55(.02)	55	132
-54	"	"	57(0-2014)	52-52	$>\underline{52}$ $\underline{\underline{55}}$	"

Table 7-13 (Page 4 of 4)

PH13-8Mo STEEL ALLOY - K_{Iscc} TEST RESULTS

Specimen No.'s	Orientation	Environment	K_I (Test Time in Hrs), Specimen Crack Traces	K_{Ii} - K_{If} (Crack Growth, In), Crack Front Measurements	K_{Iscc}, KSI $\sqrt{In}$	Specimen Plane Strain Capability K_I, KSI $\sqrt{In}$
Material 54, 1.5" Dia. Bar (K_{Ic} Specimen Configuration)						
			RH 950			
105-7	RT	STW	No Change (0-2016)	54-54	>54	97
-8	RT	STW	No Change (0-2016)	56-56	>56	97
					>56	
			RH 975			
105-9	RT	STW	No Change (0-2016)	67-67	>67	97
-10	RT	STW	No Change (0-2016)	67-67	>67	97
					>67	
			RH 1000			
105-11	RT	STW	No Change (0-2016)	92-92	>92	96
-12	RT	STW	No Change (0-2016)	101-101	>101	96
					>101	
Material 56, 1.5" Dia. Bar (K_{Ic} Specimen Configuration)						
			RH 950			
108-5	RT	STW	No Change (0-2016)	50-50	>50	98
-6	RT	STW	No Change (0-2016)	51-51	>51	98
					>51	
			RH 975			
108-7	RT	STW	No Change (0-2016)	58-58	>58	98
			RH 1000			
108-8	RT	STW	No Change (0-2016)	85-85	>85	97

Table 7-14 (Page 1 of 2)

PH13-8Mo GTA BUTT WELD JOINTS K_{Iscc} TEST RESULTS

Specimen No.'s	B, In	Notch Location	Environment	K_I (Test Time in Hrs), Specimen Crack Traces	$K_{Ii} - K_{If}$ (Crack Growth, In), Crack Front Measurements	K_{Iscc}, KSI $\sqrt{In}$	Specimen Plane Strain Capability K_I, KSI $\sqrt{In}$
Material 40, 1.5 x 12" Rolled Bar, Preweld - H1000, Postweld - 950F, 2 Hrs.							
C654	1/4	Weld, RW	STW	90(0-1), 88(4), 64(51) 62(166), 60(622), 55 (1006)	90-56(.50)	56	54
C655	"	"	"	70(0-1006)	69-69	>69 62	"
C600	1/4	HAZ, RW	STW	83(0-1006)	83-83	>83	54
1	"	"	"	69(0-1006)	69-69	>69 >83	"
C602	1/4	HAZ, RW	SCS	84(0-1006)	83-83	>83	54
3	"	"	"	70(0-1006)	69-69	>69 >83	"
C608	1/8	HAZ, RW	STW	90(0), 40(0-1006)	83-39(.98)	*	38
9	"	"	"	70(0-4), 57(51), 62(166), 38(622), 34(1006)	69-34(.79)	*	"
Material 41, 1.5 x 8" Extruded Bar, Preweld - Cond A, Postweld - H1000							
C650	1/4	Weld, RW	STW	76(0-1392)	73-73	>73	58
1	"	"	"	78(0-1392)	77-77	>77	"
2	"	"	"	74(0-1392)	74-74	>74	"
3	"	"	"	64(0-1392)	64-64	>64 >77	"

(*) Discarded, specimen testing suspected.

Table 7-14 (Page 2 of 2)

PH13-8Mo GTA BUTT WELD JOINTS K_{Iscc} TEST RESULTS

Specimen No.'s	B, In	Notch Location	Envir-onment	K_I (Test Time in Hrs), Specimen Crack Traces	K_{Ii} - K_{If} (Crack Growth, In), Crack Front Measurements	K_{Iscc}, KSI $\sqrt{In}$	Specimen Plane Strain Capability K_I, KSI $\sqrt{In}$
Material 41 (Cont'd.)							
C610	1/4	HAZ, RW	STW	101(0-1006)	100-95(.06)	95	58
11	"	" "	"	90(0-1006)	89-86(.04)	86	"
12	"	" "	"	80(0-1006)	79-76(.02)	76/86	"
C613	1/4	HAZ, RW	SCS	101(0-1006)	101-97(.04)	97	58
14	"	" "	"	90(0-1006)	90-90	>90	"
15	"	" "	"	80(0-1006)	79-76(.03)	76/87	"
C616	1/8	HAZ, RW	STW	90(0-1006)	90-85(.05)	85	41
17	"	" "	"	80(0-1006)	80-79(.01)	79	"
18	"	" "	"	69(0-1006)	69-69	>69/82	"

Table 7-15

300M STEEL ALLOY K_{Iscc} TEST RESULTS

Specimen No.'s	Orientation	Environment	K_I (Test Time in Hrs), Specimen Crack Traces	$K_{Ii} - K_{If}$ (Crack Growth, In), Crack Front Measurements	K_{Iscc}, KSI $\sqrt{In}$	Specimen Plane Strain Capability K_I, KSI $\sqrt{In}$
Material 39, 3 x 36 x 72" Forged Block, HT 280-300ksi						
55-19	RW	STW	46(0), Failed(96) Crack Curves at K_I of 25		<25	150
55-20	"	"	46(0), Failed(96) Crack Curves at K_I of 21		$\frac{<21}{<21}$	"
55-21	RW	FCS	46(0), Failed(96) Crack Curves at K_I of 29		<29	150
55-22	"	"	46(0), Failed(96) Crack Curves at K_I of 21.		<21	"
55-23	"	"	46(0), Failed(96) Crack Curves at K_I of 30		$\frac{<30}{<21}$	
55-24	RW	SCS	46(0-602), 45(770-1443), 44(1609-1946)	45-39(.21)	39	150
55-25	"	"	46(0-602), 45(770-1443), 44(1609-1946)	45-39(.20)	39	"
55-26	"	"	46(0-434), 44(602-770), 42(938-1443), 40(1609-1946)	45-36(.27)	$\frac{36}{38}$	"
55-31	TR	STW	46(0), Failed(96) Crack Curves at K_I of 25		<25	150
55-32	"	"	46(0), Failed(96) Crack Curves at K_I of 25		<25	"
55-30	"	"	46(0), 17(26-1270)	45-15.9(1.66)	16	"
55-33	"	"	46(0), 17(26-94), 16 (265-1270)	45-15.4(1.76)	$\frac{15}{15}$	"

NOTE: On the failed specimens the crack ran straight for approximately .7" and then it curved and intersected the 1x6" specimen edge.

Table 7-16

INCONEL 718 ALLOY K_{Iscc} TEST RESULTS

Specimen No.'s	Orientation	Environment	K_I (Test Time in Hrs), Specimen Crack Traces	K_{Ii} - K_{If} (Crack Growth, In), Crack Front Measurements	K_{Iscc}, KSI $\sqrt{In}$	Specimen Plane Strain Capability K_I, KSI $\sqrt{In}$
Material 51, 4 x 8 x 144" Forged Bar, HT 192 ksi						
82-27	RW	STW	189(0-1985)	180-180	>180	103
82-34	"	"	95(0-1001)	86-86	> 86	103
					>180	
82-37	RW	SCS	179(0-1003)	166-166	> 166	103
82-33	"	"	95(0-1003)	86-86	> 86	"
					> 166	
82-39	WR	STW	135(0-1985)	128-121(.07)	121	104
82-38	"	"	95(0-1001)	89-89	> 89	"
					121	
82-25	TR	STW	103(0-1273)	99-99	> 99	104
82-22	"	"	96(0-1002)	87-87	> 87	"
					> 99	

Table 7-17

K_{Iscc} TEST RESULTS - MP 35 N ALLOY

Specimen No.'s	Orientation	Environment	K_I In KSI $\sqrt{In}$ to (Test Time In Hours) Crack Side Measurements	Crack Front Measurements	K_{Iscc}, KSI $\sqrt{In}$	Specimen Plane Strain Capability K_I, KSI $\sqrt{In}$
MAT'L 55, 1.5" DIA BAR, HT-236 KsI (Kic Specimen Configuration)						
106-3	RT	STW	No Change (0-2016)	86 - 86	>86	104
106-4	RT	STW	No Change (0-2016)	96 - 96	>96	104
					>96	

B-1 Part Test

(1) Part: 13004248-003 support beam stud (1" diameter x 10" long) containing a semi-circular fatigue crack (a = .17, c = .16) at the root of one of the threads at the ends (RT crack orientation).

(2) Loading: In a Ti-6Al-4V block by torquing end nuts to a torque of 6,500 in-lbs which produced a stress in the shank section of the stud of 36 ksi (strain gage measurements).

(3) Environment: STW for 1 year.

(4) Results: Examination of the crack surface did not reveal any evidence of stress corrosion cracking.

TABLE 7-18 (Page 1 of 2)

Ti-6Al-4V Alloy - SUMMARY OF K_{Iscc} VALUES

Alloy	Form and Condition	Mat'l No.	Orientation	K_{Ic}, $KSI\sqrt{in.}$ Mat'l	K_{Ic}, $KSI\sqrt{in.}$ Req'd	Environment	K_{Iscc} % of Mat'l K_{Ic}	K_{Iscc} % of Reqd K_{Ic}	K_{Iscc} K_I $KSI\sqrt{in.}$
Parent Metal	Plate, RA	67	RW	90	70	STW	72	92	65
		68	WR	100	70	STW	58	83	58
		72	RW	78	70	STW	78	87	61
		72	WR	95	70	STW	64	87	61
		77	RW	78	70	STW	76	84	59
									61 Ave
		72	WR	95	70	SCS	73	98	69
		72	WR	95	70	FCS	74	100	70
	Plate, RA + Hot Formed	9012	WR	--	70	STW	--	79	55
	Plate, RA + Exposed to DB Thermal Cycle	67	WR	--	70	STW	--	86	60
		68	WR	--	70	STW	--	76	53
		70	RW	--	70	STW	--	96	67
		72	WR	92	70	STW	48	63	44
		76	WR	--	70	STW	--	76	53
		77	WR	--	70	STW	--	79	55
		253	WR	--	70	STW	--	83	58
		294	WR	--	70	STW	--	83	58
									56 Ave
	Forging, RA	79	TR	--	70	STW	--	80	56
		82	WR	102	70	STW	52	76	53
		84	TR	83	70	STW	67	80	56
		85	TR	105	70	STW	>68	>101	>71
									59 Ave
Weld Joints	Plate. GTA Butt Weld, Preweld - Cond RA								
	1/8" Thick Joint, Postweld-1400F, 1/2 hr	88	RW(HAZ)	--	60	STW	--	--	>27, (>62)[a]
	1/8" Thick Joint, Postweld-1200F, 1 hr	88	RW(HAZ)	--	60	STW	--	--	>27, (>67)[a]
	1/4" Thick Joint, Postweld-1400F, 1/2 hr	88	RW(HAZ)	--	60	STW	--	--	>38, (>70)[a]
	1/4" Thick Joint, Postweld-1200F, 1 hr	88	RW(HAZ)	--	60	STW	--	--	>38, (>66)[a]
	1/2" Thick Joint, Postweld-1100F, 2 hr	88	RW (WELD)	(100)[a]	60	STW	--	--	>54, (93)[a]
	1/2" Thick Joint, Postweld-1100F, 2 hr	88	RW(HAZ)	73	60	STW	>73	--	>53
	1/2" Thick Joint, Postweld-1100F, 2 hr	88	RW(HAZ)	73	60	SCS	--	--	>54, (>64)[a]
	3/4" Thick Joint, Postweld-1100F, 2 hr	88	RW(HAZ)	--	60	STW	--	--	>66, (74)
	1" Thick Joint, Postweld-1100F, 2 hr	88	RW(HAZ)	--	60	STW	--	97	58

ABLE 7-18 (Page 2 of 2)

Ti-6Al-4V Alloy - SUMMARY OF K_{Iscc} VALUES

Alloy	Form and Condition	Mat'l No.	Orientation	K_{Ic}, $KSI\sqrt{in}$ Mat'l	K_{Ic}, $KSI\sqrt{in}$ Req'd	Environment	K_{Iscc} % of Mat'l K_{Ic}	K_{Iscc} % of Reqd K_{Ic}	K_{Iscc} K_I, $KSI\sqrt{in.}$
Weld Joints	Extruded Bar, GTA Butt Weld, Preweld - Cond RA 1/2" Thick Joint, Postweld - 1100F, 2 hrs	75	RW(HAZ)	76	60	STW	--	--	>54,(59)[a]
Diffusion Bond Joints	Plate, Diffusion Bond Joint								
	As Bonded	74	TW/TW	88	70	STW	67	84	59
	As Bonded + 2DB Thermal Cycles	74	TW/TW	94	70	STW	66	89	62
	As Bonded + 4DB Thermal Cycles	74	TW/TW	92	70	STW	71	93	65
	Plate, Diffusion Bond Joints Containing Anomalies, As Bonded								
	Porosity, Dia. - .0015, Freq - 10,000/in^2	--	WR/TR	63	70	STW	59	53	37
	Porosity, Dia. - .002, Freq - 2,500/in^2	--	WR/TR	89	70	STW	42	53	37
	Porosity, Dia. - .004, Freq - 2,500/in^2	--	WR/TR	70	70	STW	61	61	43
	Oxygen Enrichment, Medium	--	WR/TR	--	70	STW	--	30	21

[a] Value in parentheses is for a mixed mode stress state $[B<2.5\,(K_I/TY)^2]$

TABLE 7-19 (Page 1 of 2)

Aluminum Alloys -SUMMARY OF K_{Iscc} VALUES

Alloy	Form and Condition	Mat'l No.	Orientation	K_{Ic}, $KSI\sqrt{in}$ Mat'l	K_{Ic}, $KSI\sqrt{in}$ Req'd	Environment	K_{Iscc} % of Mat'l K_{Ic}	K_{Iscc} % of Reqd K_{Ic}	K_{Iscc} K_I, $KSI\sqrt{in.}$
2024	3x18x23" Forged Block, T852	19	RW	28	23	STW	80	98	22.5
			TR	--	17	STW	--	118	20.0
	3x18x35" Forged Block, T852	27	WR	27	19	STW	76	108	20.5
			RW	37	23	SCS	76	122	28.0
2124	3" Plate, T851	12	RW	32	25	STW	83	106	26.5
			TR	--	18	STW	--	128	23.0
2219	1 3/4" Plate, T851	7	RW	43	33	STW	>74	>97	>32,(35)[a]
						SCS	>74	>97	>32,(34)[a]
						FCS	67	88	29.0
			WR	36	30	STW	75	90	27.0
			TW	--	20	STW	--	148	29.5
7049	3x4x48" Forged Block, T73	25	RW	38	30	STW	55	70	21.0
						SCS	73	92	27.6
						FCS	>75	>95	>28.5
			WR	23	25	STW	87	80	20.0
			TR	23	25	STW	80	74	18.5
7050	4" Plate, T73651	28	WR	28	--	STW	98	--	27.5
7075	2" Plate, T7651	18	RW	28	27	STW	>79	>81	>22.0
						SCS	>95	>98	>26.5
						FCS	>86	>89	>24.0
		18	TR	16	18	STW	80	71	12.8
	2" Plate, T7351	18	TR	18	20	STW	83	75	15.0

TABLE 7-19 (Page 2 of 2)

Aluminum Alloys - SUMMARY OF K_{Iscc} VALUES

Alloy	Form and Condition	Mat'l No.	Orien-tation	K_{Ic}, KSI$\sqrt{in}$ Mat'l	K_{Ic}, KSI$\sqrt{in}$ Req'd	Environ-ment	K_{Iscc} % of Mat'l KIc	K_{Iscc} % of Reqd KIc	K_{Iscc} K_I, KSI$\sqrt{in.}$
7075	Forging, T73	22	WR	--	26	STW	--	>96	25.0
	3x17" Extrusion, T73511	29	TR	22	20	STW	>97	>123	>21.3
			RW	39	30	SCS	91	119	35.6
			RW	39	30	FCS	>87	>113	>34.0
7175	Forging, T73652	26	RW	35	33	STW	>64	>68	>22.5
						SCS	79	84	27.6
						FCS	>79	>84	>27.8
			WR	27	28	STW	81	79	22.0

[a] Value in parentheses is for a mixed mode stress state $[B<2.5\,(K_I/TY)^2]$

TABLE 7-20

9-4-20 Steel - SUMMARY OF K_{Iscc} VALUES

Alloy	Form and Condition	Mat'l No.	Orientation	K_{Ic}, $KSI\sqrt{in}$ Mat'l	K_{Ic}, $KSI\sqrt{in}$ Req'd	Environment	K_{Iscc} % of Mat'l K_{Ic}	K_{Iscc} % of Reqd K_{Ic}	K_{Iscc} K_I, $KSI\sqrt{in}$.
9-4-20 Parent Metal	2.5" Plate, Ht 190-210 ksi	37	RW	124	120	STW	85	87	105
			WR	128	120	STW	75	80	96
	4x18xL Forged Bar, Ht 190-210 ksi	43	RW	141	120	STW	78	92	110
			RW	141	120	SCS	>91	106	>129
			WR	126	120	STW	85	89	107
			TW	115	120	STW	69	65	78
9-4-20 Weld Joints	TIG Butt Weld Joints, 1 1/2" Plate Stock, Preweld-HT 190 to 210 KSI, Postweld - 950F, 2 Hrs								
	1/2" Thick Joint	57	Weld,RW	97	90	STW	82	89	80
	1/2" Thick Joint		HAZ,RW	105	90	STW	61	71	64
	1/2" Thick Joint		HAZ,RW	105	90	FCS	>73	80	>77
	TIG Butt Weld Joints, 4x18"xL Forged Bar, Preweld - HT 190 to 210 KSI, Postweld - 950F, 2 Hrs								
	1/4" Thick Joint	33	HAZ,RW	--	90	STW	—	>67	>60,(63)[a]
	1/2" Thick Joint	33	HAZ,RW	95	90	STW	76	80	72

[a] Value in parentheses is for a mixed mode stress state $[B<2.5\ (K_I/TY)^2]$

ABLE 7.21 (Page 1 of 2)

PH13-8Mo Steel - SUMMARY OF K_{Iscc} VALUES

Alloy	Form and Condition	Mat'l No.	Orientation	K_{Ic}, KSI$\sqrt{in}$ Mat'l	K_{Ic}, KSI$\sqrt{in}$ Req'd	Environment	K_{Iscc} % of Mat'l KIc	K_{Iscc} % of Reqd KIc	K_{Iscc} K_I, KSI$\sqrt{in.}$
PH13-8Mo Parent Metal	4x5" Forged Bar, H950	36	RW	60	60	STW	80	80	48
			WR	57	60	STW	>88	>83	>50
	4x5" Forged Bar, H1000	36	RW	95	90	STW	>84	>89	>80
			WR	90	90	STW	>79	>79	>71
	1.5x12" Rolled Bar, H1000	40	RW	90	90	STW	80	80	72
			RW	90	90	SCS	>97	>97	>87
			RW	90	90	FCB	>83	>83	>75
			WR	75	90	STW	>84	>70	>63
	1.5x8" Extrusion, H1000	41	RW	67	90	STW	79	59	53
			WR	66	90	STW	80	59	53
	1.5x8" Extrusion, Resolutioned + H1000	41	RW	74	90	STW	74	61	55
	1.5" Dia. Bar, RH950	54	RF	62	60	STW	>90	>93	>56
	RH975		RF	72	75	STW	>93	>89	>67
	RH1000		RF	111	90	STW	--	--	>95,(>101)a
	1.5" Dia. Bar, RH950	56	RF	58	60	STW	>88	>85	>51
	RH975		RF	66	75	STW	>88	>77	>58
	RH1000		RF	95	90	STW	>89	>94	>85
PH13-8Mo Weld Joints	TIG Butt Weld Joints in 1.5"x12" Rolled Bar Stock, Preweld-H1000, Postweld - 950F, 2 Hrs								
	1/4" Thick Joint	40	Weld, RW	--	80	STW	--	--	>54,(62)a
	1/4" Thick Joint		HAZ, RW	88	80	STW	--	--	>54,(>83)a
	1/4" Thick Joint		HAZ, RW	88	80	SCS	--	--	>54,(>83)a

TABLE 7.21 (Page 2 of 2)

PH13-8Mo Steel - SUMMARY OF K_{Iscc} VALUES

Alloy	Form and Condition	Mat'l No.	Orientation	K_{Ic}, KSI$\sqrt{in}$ Mat'l	K_{Ic}, KSI$\sqrt{in}$ Req'd	Environment	K_{Iscc} % of Mat'l K_{Ic}	K_{Iscc} % of Reqd K_{Ic}	K_{Iscc} K_I, KSI$\sqrt{in.}$
PH13-8Mo Weld Joints	TIG Butt Weld Joints in 1.5x8" Extruded Bar Stock, Preweld - Cond A, Postweld - H1000								
	1/4" Thick Joint	41	Weld,RW	(140)[a]	80	STW	--	--	>58,(>77)[a]
	1/4" Thick Joint		HAZ,RW	93	80	STW	--	--	>58,(86)[a]
	1/4" Thick Joint		HAZ,RW	93	80	SCS	--	--	>58,(87)[a]
	1/8" Thick Joint		HAZ,RW	--	80	STW	--	--	>41,(82)[a]

[a] Value in parentheses is for a mixed mode stress state $[B<2.5\ (K_I/TY)^2]$

TABLE 7-22

SUMMARY OF K_{Iscc} VALUES

300M Steel, Inconel 718 Alloy, MP35N Alloy

Alloy	Form and Condition	Mat'l No.	Orientation	K_{Ic}, KSI$\sqrt{in}$ Mat'l	K_{Ic}, KSI$\sqrt{in}$ Req'd	Environment	K_{Iscc} % of Mat'l KIc	K_{Iscc} % of Reqd KIc	K_{Iscc} K_I, KSI$\sqrt{in.}$
300M	3x36x72" Forged Block, HT 287 ksi	39	RW	55	60	STW	<36	<35	<21
			RW	55	60	FCS	<38	<35	<21
			RW	55	60	SCS	65	60	36
			TR	54	60	STW	28	25	15
Inconel 718	4x8x144" Forged Bar, HT 192 ksi	51	RW	(212)	85	STW	--	121	>103,(>180)[a]
			RW	(212)	85	SCS	--	121	>103,(>166)[a]
			WR	134	85	STW	>78	122	>104,(121)[a]
			TR	108	85	STW	>92	116	>99
MP35N	1.5" Dia. Bar, HT 236 ksi	55	RT	129	90	STW	>74	107	>96

[a] Value in parentheses is for a mixed mode stress state $[B<2.5\ (K_I/TY)^2]$

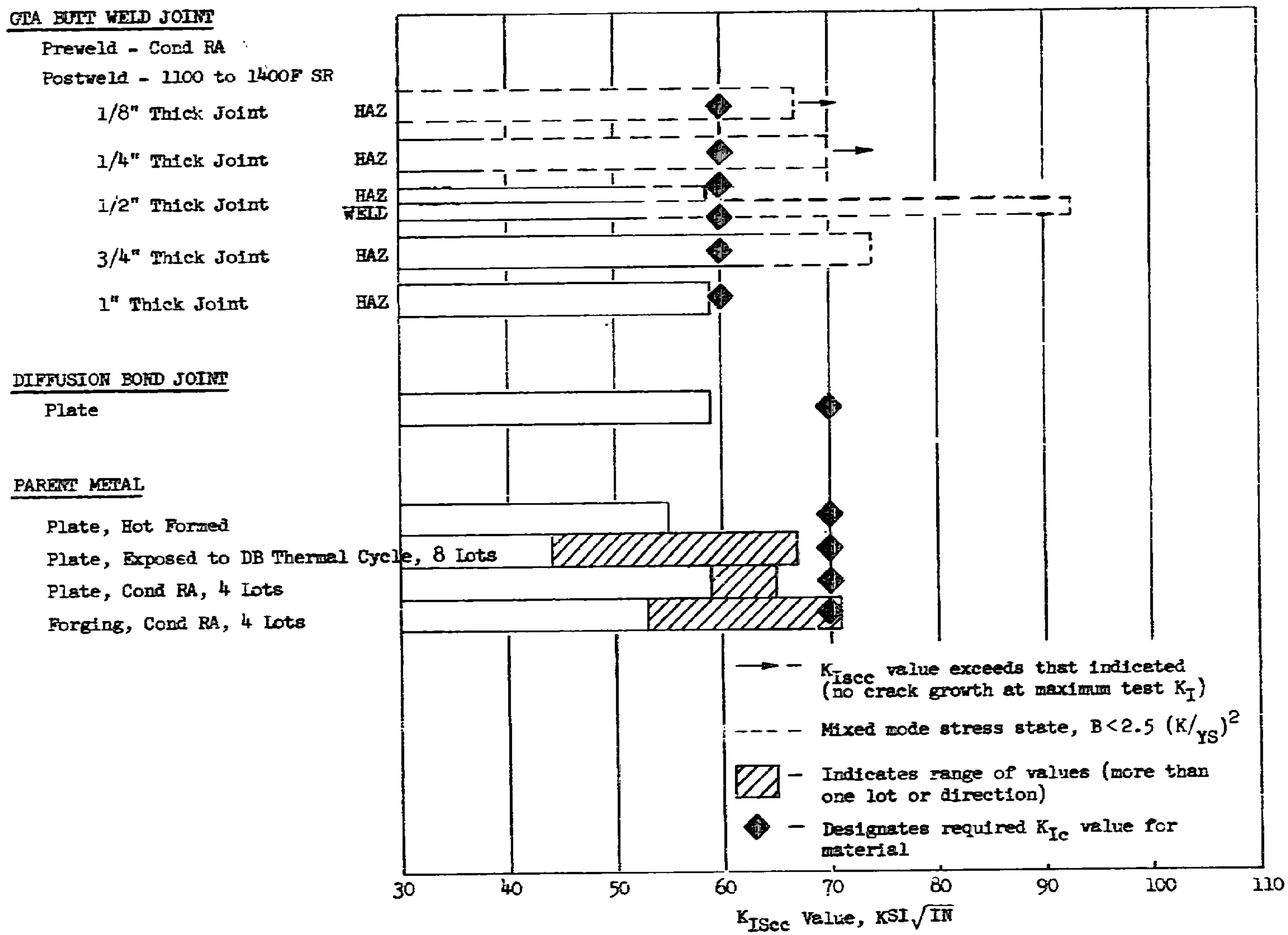

Figure 7-1 Comparison of K_{ISCC} Values for Ti-6Al-4V in Sump Tank Residue Water (welds, D.B. joint, plate, forging)

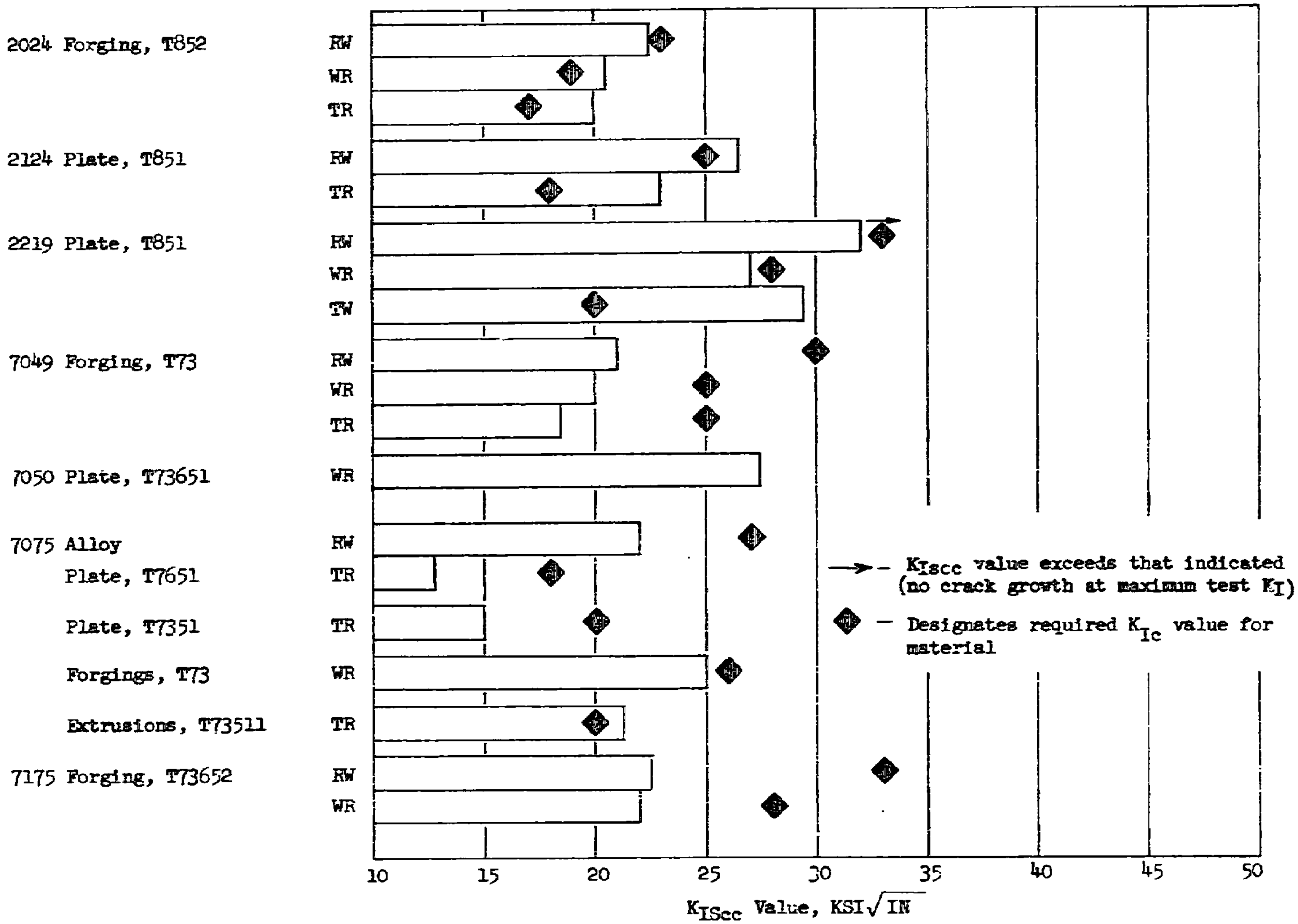

Figure 7-2. Comparison of K_{ISCC} Values for Aluminum Alloys in Sump Tank Residue Water

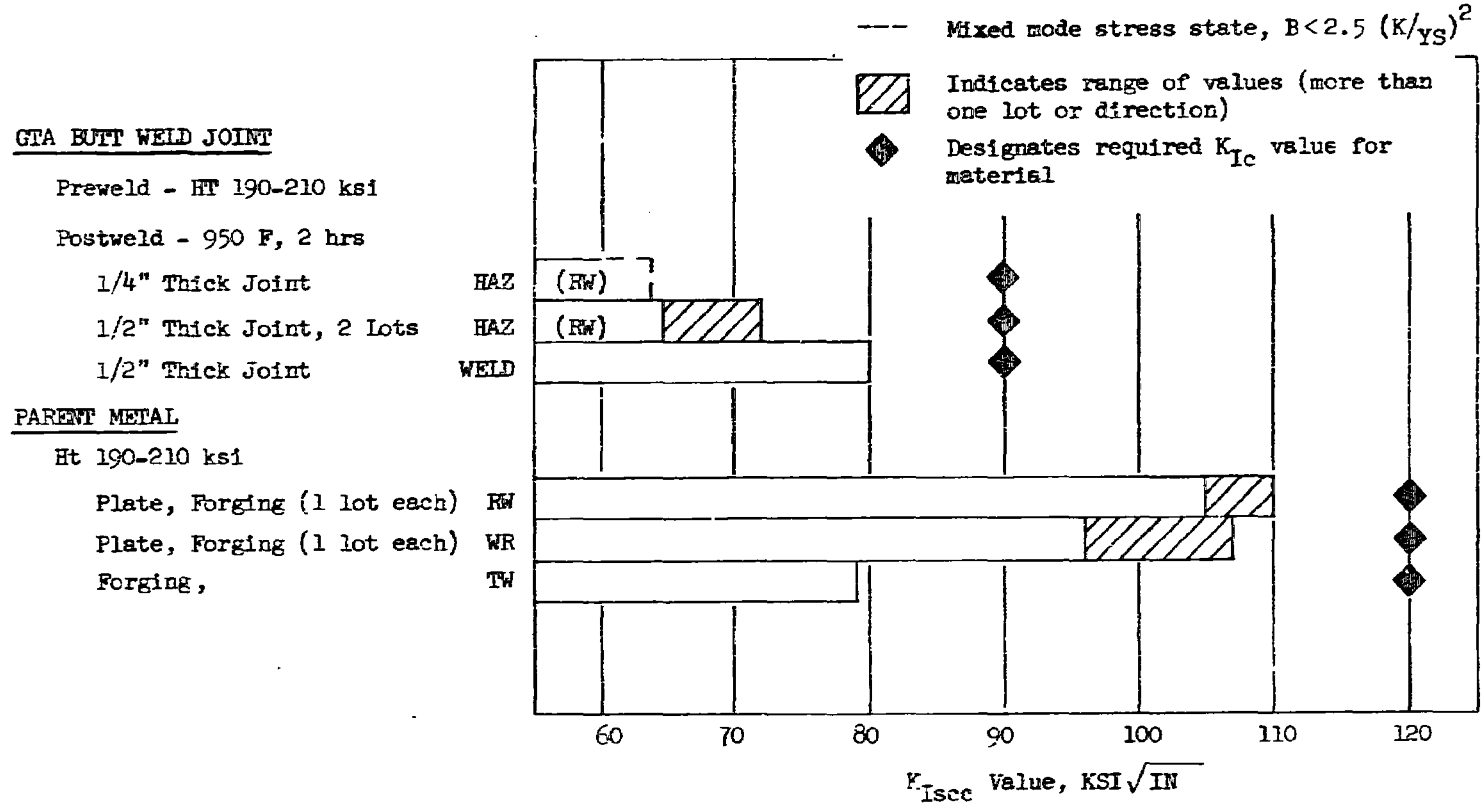

Figure 7-3 Comparison of K_{Iscc} Values for 9-4-20 Steel in Sump Tank Residue Water (welds, parent metal)

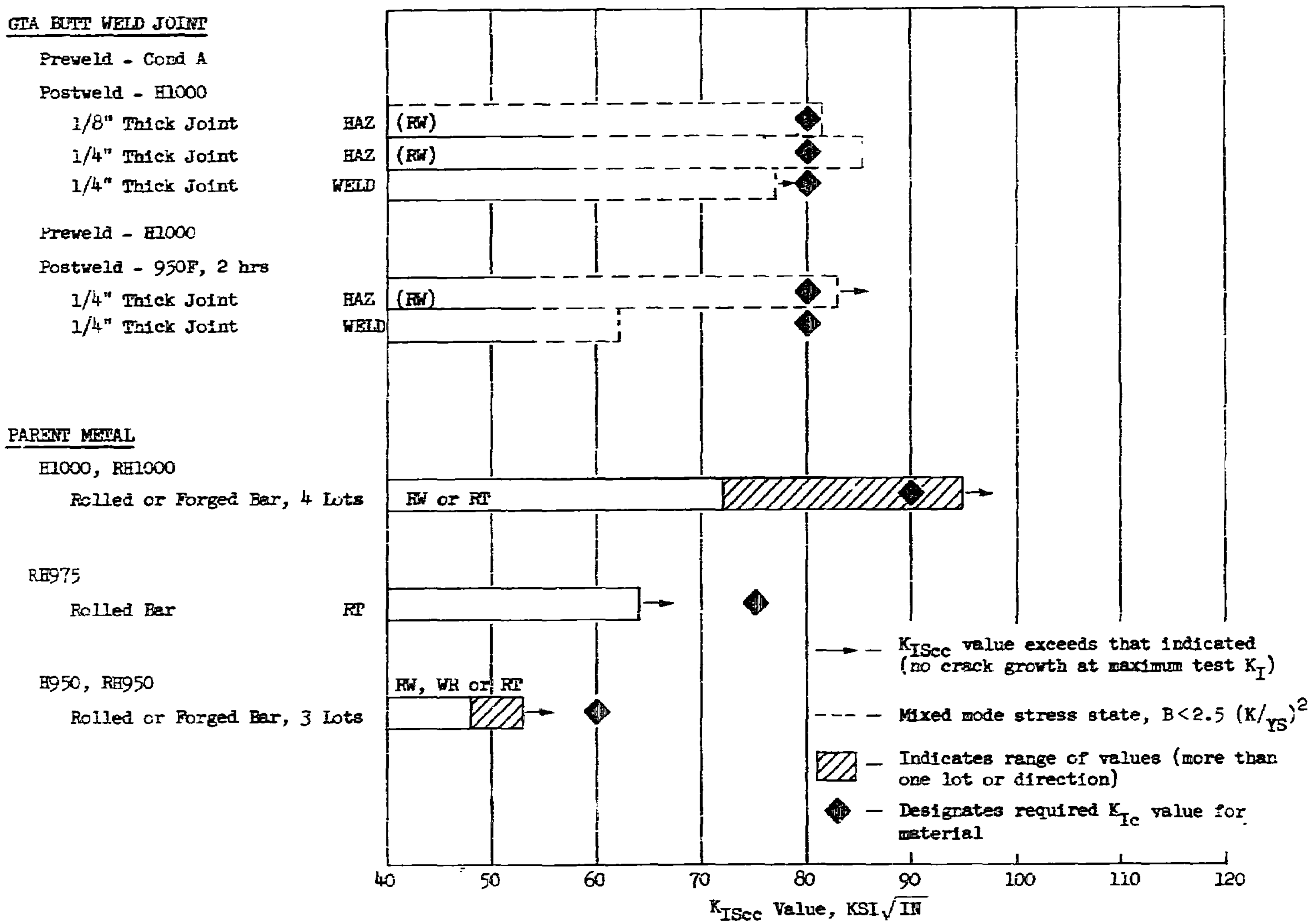

Figure 7-4 Comparison of K_{IScc} Values for PH13-8Mo in Sump Tank Residue Water (welds, parent metal)

Fracture face on specimen 84ETR103-3 tested in STW. Before breaking specimen open, it was heated at 900F for 1 hour to mark corrosion crack front.

Notch Edge

Precrack Front

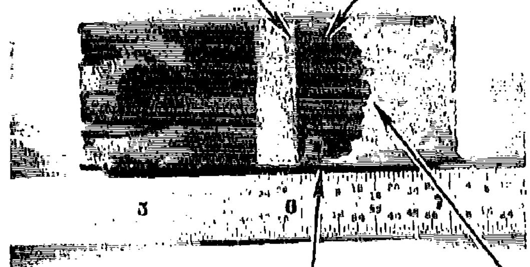

Note crack growth is least at the edges

and highest at the center(where the lateral restraint was greatest)

Figure 7-5 Corrosion Crack Growth Pattern in Ti-6Al-4V K_{Iscc} Specimens

SECTION 8 - FATIGUE CRACK GROWTH RATE TEST DATA

8.1 TEST RESULTS

Due to the large number of da/dN tests performed in this program, a plot of da/dN vs ΔK for each test is presented in an appendix. Plots for Ti-6Al-4V are presented in Appendix A, aluminum alloys in Appendix B, steels and Inconel 718 in Appendix C, and all weldments in Appendix D. Computer print-out tabulations of raw data (crack lengths, loads, and cycles) for all tests performed on compact tension specimens are presented in reference (M) together with computed values of ΔK and da/dN corresponding to each test point shown in the plots of Appendices A through D for this type of specimen.

8.2 DISCUSSION OF TEST RESULTS

To facilitate evaluation of test parameter effects (R factor, environment, cyclic frequency, test temperature, test direction, and specimen thickness) and make possible inter-alloy and intra-alloy (product form and heat to heat) comparisons the individual data points of each da/dN vs ΔK plot in Appendices A through D were connected manually using French curves (i.e., computer enhanced curve fitting techniques were not employed in this presentation). Overlays were then made of appropriate combinations of the resultant curves, to graphically demonstrate effects of test parameter variations, product forms, etc. These comparative curves are presented in sections 8.2.1 through 8.2.17 together with discussions of these results.

8.2.1 <u>Titanium Alloy Ti-6Al-4V</u>

8.2.1.1 Cyclic Frequency - The low humidity air fatigue crack growth rates of this material were seen to be essentially unaffected by varying the cyclic frequency of test through the range of 60 to 3600 cpm. This was true for diffusion bonded plate, beta processed plus mill annealed extrusions, mill annealed plate and sheet, recrystallization annealed hand forgings, and recrystallization annealed plate (Figures 8.2.1.1-1 through -7). Sump tank water growth rates in recrystallization annealed plate were seen to be equally unaffected by changing the frequency of test from 60 to 6 cpm (Figure 8.2.1.1-8).

8.2.1.2 Test Temperature - The low humidity air fatigue crack growth rates of recrystallization annealed plate were not significantly nor consistently affected by increases in test temperature from ambient to 265°F, but were noticeably decreased at low levels of delta K (below ~15 ksi $\sqrt{in}$) when the test temperature was dropped from ambient to -65°F (Figure 8.2.1.2-1 and -2).

8.2.1.3 Specimen Thickness - The growth rates of recrystallization annealed plate in low humidity air were seen to be unaffected by **decreases in** specimen thickness from 1.0" to 0.25" (Figure 8.2.1.3-1).

8.2.1.4 R Factor - Fatigue crack growth rates were seen to increase with increasing R factors for all conditions evaluated except that of 0.1" thick mill annealed sheet (Figure 8.2.1.4-1). In low humidity air, substantial rate increases were seen as R was increased through the range 0.08 to 0.7 in beta processed plus mill annealed extrusions, recrystallization annealed hand forgings, and recrystallization annealed plates (Figure 8.2.1.4-2 through -5). In sump tank water the growth rates of recrystallization annealed plate were seen to increase significantly as R was increased from 0.08 to 0.5 (Figure 8.2.1.4-6).

8.2.1.5 Environment - Fatigue crack growth rates in this material were seen to be significantly greater in sump tank water than in low humidity air, while rates in jet fuel were essentially equivalent to those in low humidity air for all forms and conditions evaluated. Specifically, sump tank water rates were seen to be greater than low humidity air rates at an R factor of 0.08 in the RW direction of recrystallization annealed plates, mill annealed sheet, and beta processed plus mill annealed extrusions (Figure 8.2.1.5-1 through -4). These figures also demonstrate the rate equivalencies in jet fuel and low humidity air. Sump tank water growth rates were similarly greater, in the RW direction, than those in low humidity air at R factors of 0.3 and 0.5 for these product forms (Figures 8.2.1.5-5 through -7) and in diffusion bond thermal cycled plate (Figure 8.2.1.5-8). In the WR direction of this material environmental effects were not seen to be as significant as in the RW direction. In two heats of recrystallization annealed plate (1.5" conventionally rolled, and 2.5" ring rolled) growth rates in sump tank water and low humidity air were seen to be essentially equivalent (Figures 8.2.1.5-9 and -10) while in a third plate (1.5" conventionally rolled) growth rates in sump tank water were slightly greater than those in low humidity air (Figure 8.2.1.5-11). Again, growth rates in low humidity air and jet fuel were seen to be essentially equivalent (Figure 8.2.1.5-11). In a beta processed plus mill annealed "L" extrusion sump tank water growth rates were seen to be slightly greater than those in low humidity air (Figure 8.2.1.5-12) while in 0.1" mill annealed sheet they were significantly greater (Figure 8.2.1.5-13).

8.2.1.6 Test Direction - Of all the material forms and test conditions evaluated for this alloy only one form and condition displayed a marked difference between RW and WR direction fatigue crack growth rate characteristics; that of beta rolled plus mill annealed plate in low humidity air (Figure 8.2.1.6-1). The remaining nineteen comparisons did not demonstrate a consistently significant effect of test direction on growth rates (Figures 8.2.1.6-2 through 8.2.1.6-20). These evaluations included comparisons in recrystallization annealed plates and hand forgings, beta processed plus mill annealed extrusions, mill annealed sheet, diffusion bonded plate, and diffusion bond thermal cycled plate.

8.2.1.7 Product Form - In the recrystallization annealed condition of this material low humidity air fatigue crack growth rates in the RW direction were seen to increase with decreasing plate thicknesses. Noticeable increases in rates were seen to occur when these plate thickness was decreased from

3.5" to 2.0" at delta K levels below ~25 ksi $\sqrt{in}$ and again to 1.5" throughout the entire delta K range (Figure 8.2.1.7-1). Growth rates in a 4" x 10" x 34" hand forged block were seen to be equivalent to those in the 2.0" plate. In the WR direction of this material condition, differences in growth rates between 1.5" and 2.5" plate were seen to occur only at delta K levels below ~20 ksi $\sqrt{in}$, while rates in both plates were seen to be significantly greater than in the hand forging (Figure 8.2.1.7-2). At 60 cpm, however, the low humidity air fatigue crack growth rates of 1.5" plate were seen to be only slightly greater than those of the hand forging in the RW direction (Figure 8.2.1.7-3). There was little difference observed between the low humidity air fatigue crack growth rates of two different beta processed plus mill annealed extrusions (Figure 8.2.1.7-4) or between one of these extrusions and 1.5" beta rolled plus mill annealed plate at an R factor of 0.3 (Figure 8.2.1.7-5). Under these same test conditions (low humidity air, R=0.3) growth rates in one 0.625" diffusion bond thermal cycled plate (Material #62) were seen to be noticeably greater than those of a second diffusion bond thermal cycled plate (Material 61) from the same heat (Figure 8.2.1.7.6).

The effect of original plate thickness on fatigue crack growth rates of this material in sump tank water was seen to be inconsistent from test to test throughout the range of delta K (Figures 8.2.1.7-7 and -8). The results of these tests all fell within a fairly narrow scatter band bounded on the fast growth rate side by 0.375" plate, and on the slow growth rate side by 1.5" plate (Figure 8.2.1.7-8).

8.2.1.8 Heat Treat Condition - The low humidity air and sump tank water growth rates of 1.5" plate in the recrystallization annealed condition and in the diffusion bond thermal cycled condition were seen to be essentially equivalent when measured in both the RW and WR directions (Figures 8.2.1.8-1 through -5). In one set of comparative curves, however, the sump tank water growth rates at R=0.08 of recrystallization annealed material were seen to be slightly greater than those of the diffusion bond thermal cycled material, particularly at delta K levels below ~17 ksi $\sqrt{in}$ (Figure 8.2.1.8-5).

The low humidity air fatigue crack growth rates of 0.625" plate were seen to be substantially greater in a mill annealed condition and in a solution treated and overaged condition than in a diffusion bond thermal cycled condition, while growth rates in a beta annealed condition were seen to be moderately slower than in the diffusion bond thermal cycled condition (Figure 8.2.1.8-6). There were essentially no differences observed in sump tank water between the fatigue crack growth rates in diffusion bonded material and material which had been diffusion bonded plus thermally repaired (Figure 8.2.1.8-7). Similarly, no differences in sump tank water or low humidity air rates were observed between diffusion bonded material and material which had been diffusion bonded plus subjected to multiple diffusion bond thermal cycles (Figures 8.2.1.8-8 and -9). There was no significant difference observed between the sump tank water growth rates of plate which had been diffusion bonded with simulated microporosities and those of plate which had been diffusion bonded with oxygen enrichment at the bond line interface (Figure 8.2.1.8-10).

The sump tank water fatigue crack growth rates in the RW direction of 2.5" plate containing a diffusion bond line were seen to be slightly greater at a delta K level of ~20 ksi $\sqrt{in}$ than those in recrystallization annealed

material containing no bond line, and the magnitude of this effect was seen to increase with decreasing levels of delta K (Figure °.2.1.8-11). This effect was also seen to occur in sump tank water in the WR direction, where growth rates of recrystallization annealed material were seen to be slightly greater than those in diffusion bond thermal cycled plus thermally repaired plate which did not contain a bond line (Figure 8.2.1.8-12).

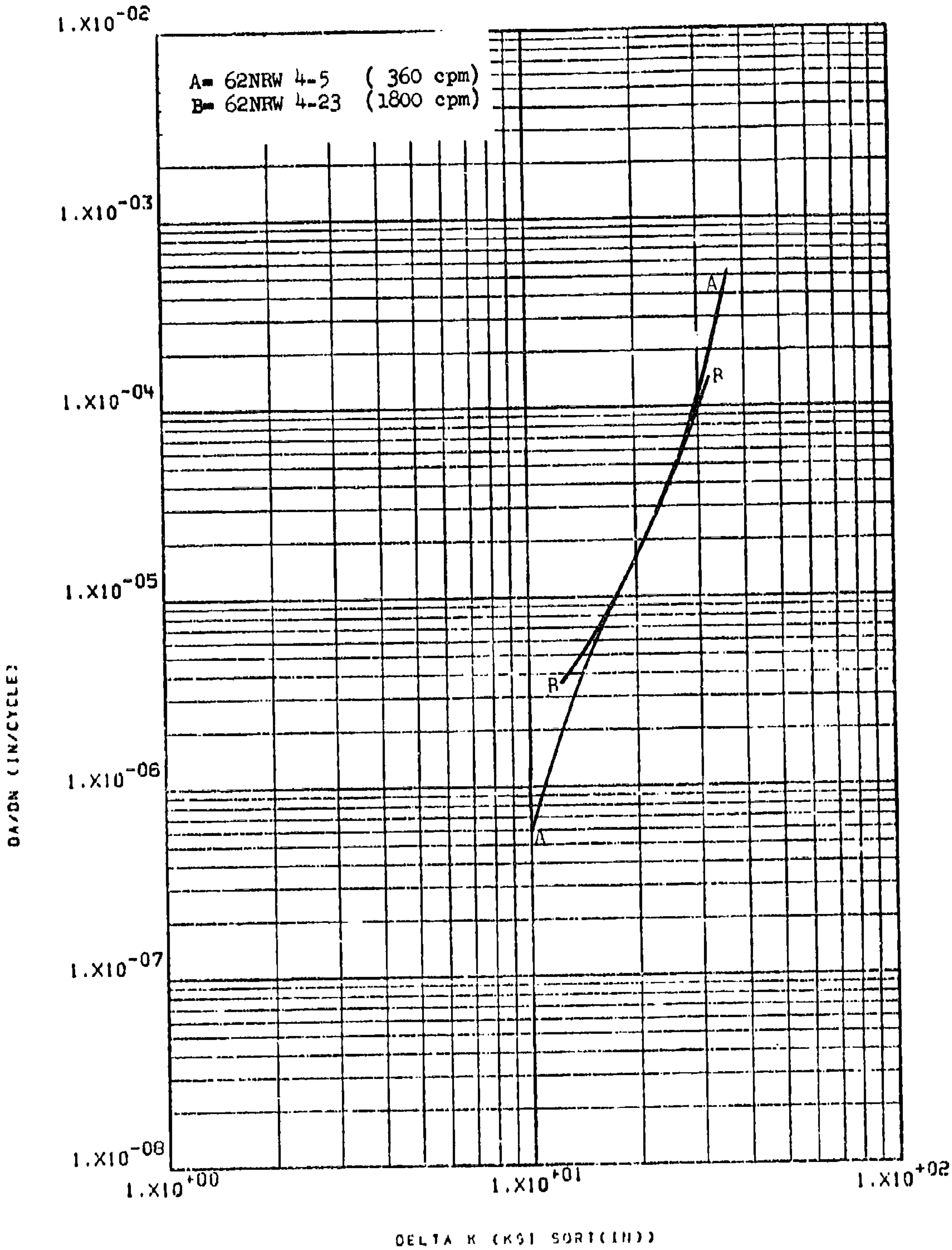

Figure 8.2.1.1-1 Effect of cyclic frequency on LHA-FCGR at R.T., R-0.3, RW direction in 0.625" Ti-6-4 diffusion bonded plate

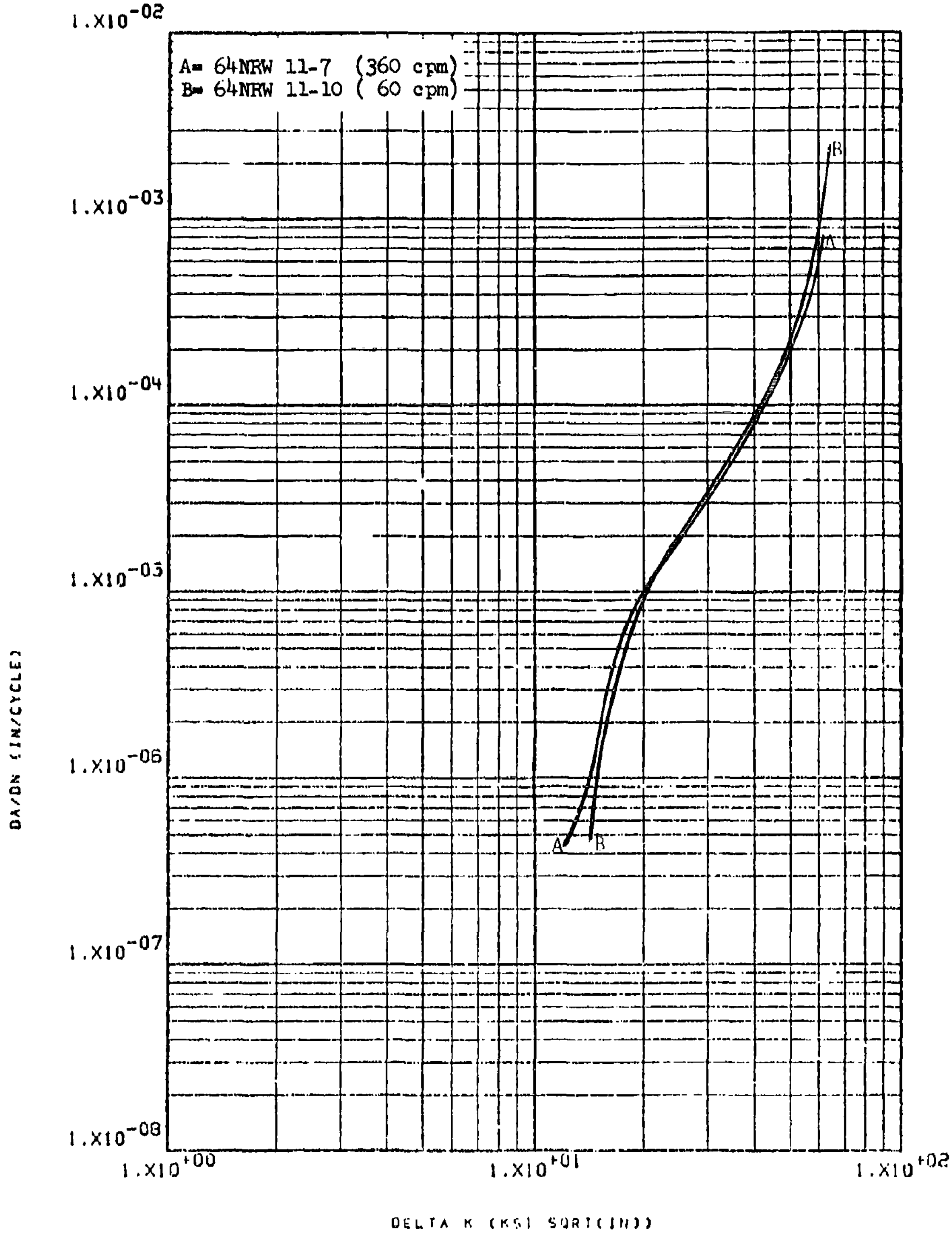

Figure 8.2.1.1-2 Effect of cyclic frequency on LHA-FCGR at R.T., R-0.08, RW direction in beta processed plus mill annealed Ti-6-4 "L" extrusion

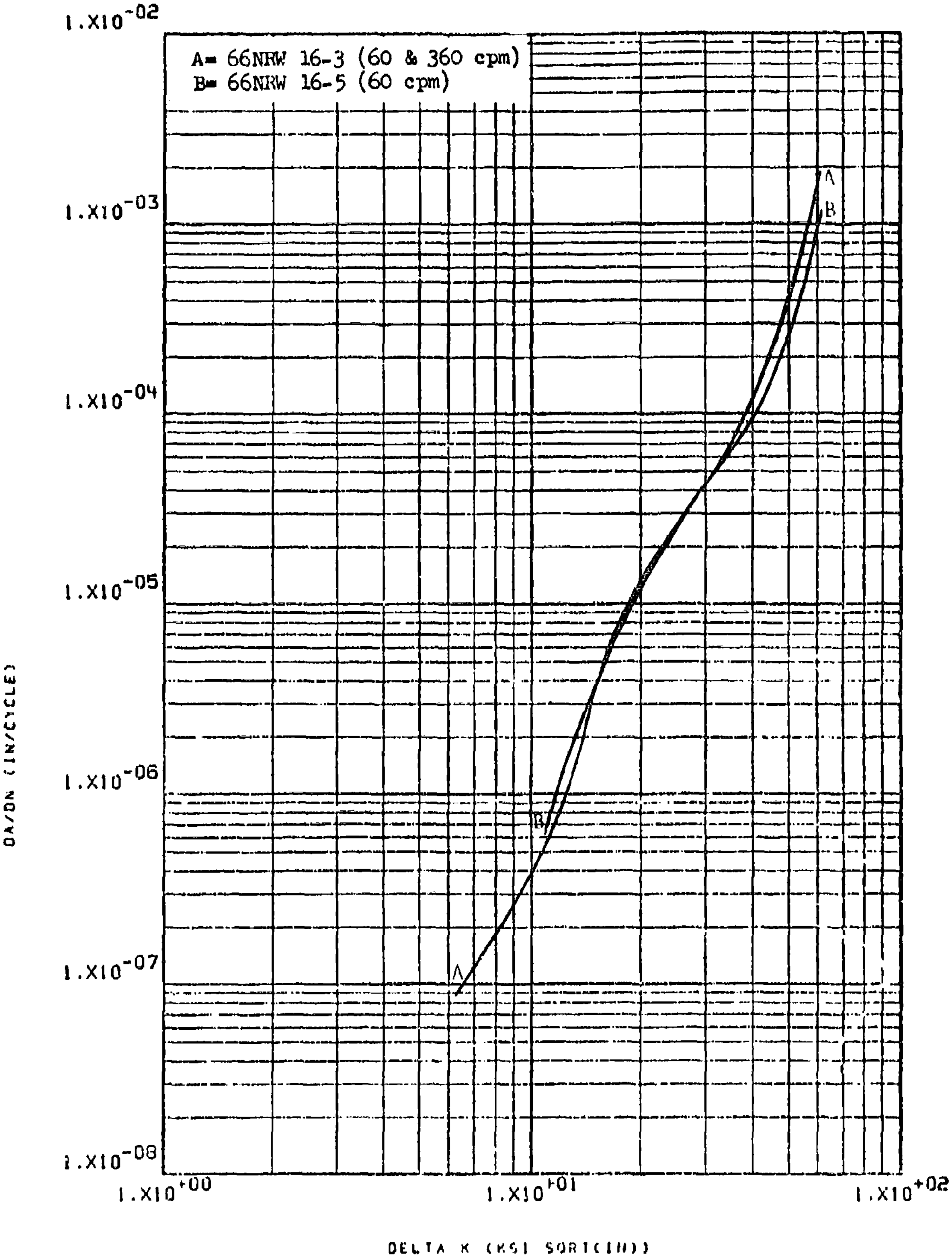

Figure 8.2.1.1-3 Effect of cyclic frequency on LHA-FCGR at R.T., R=0.3, RW direction in 1.5" beta processed plus mill annealed Ti-6-4 plate

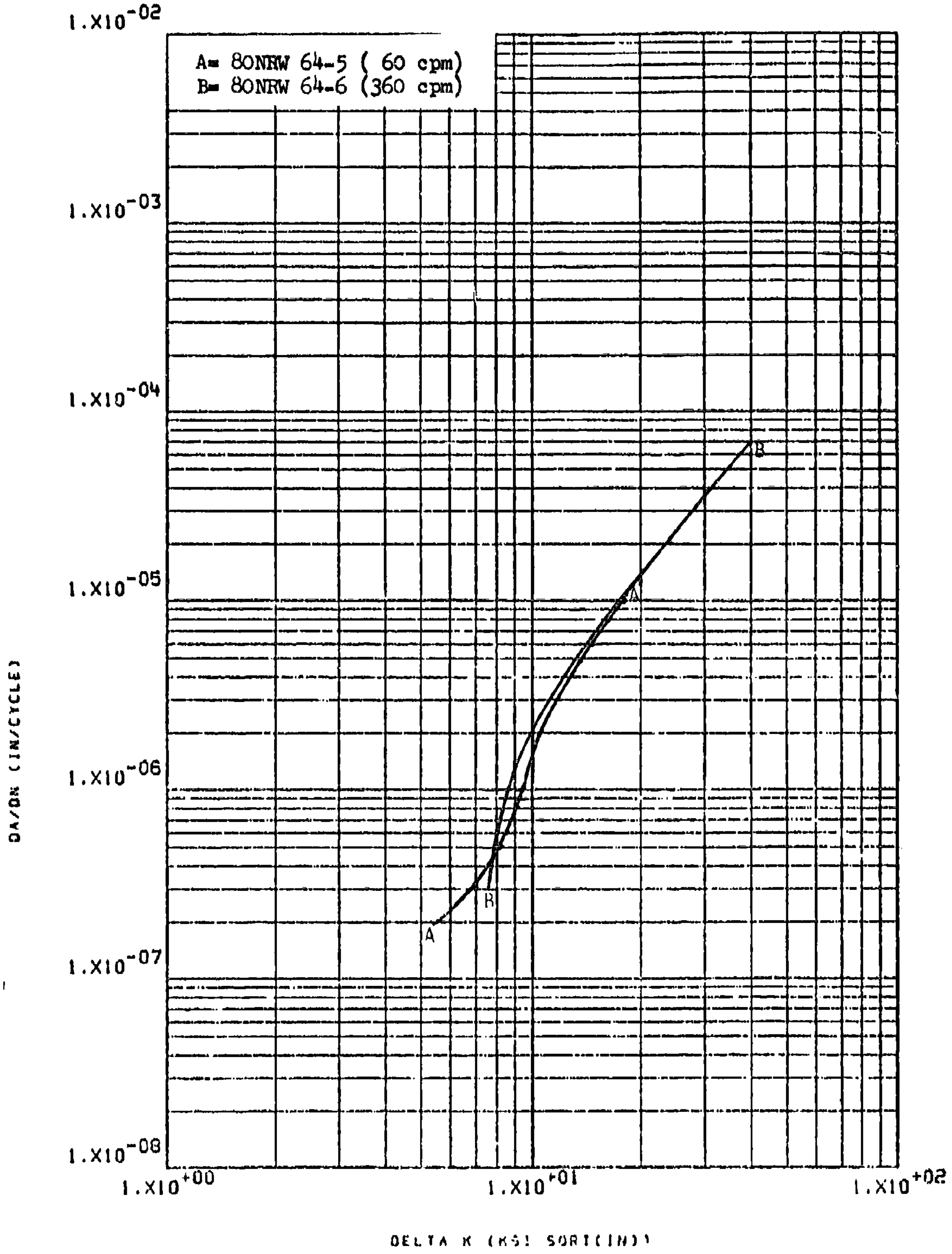

Figure 8.2.1.1-4 Effect of cyclic frequency on LHA-FCGR at R.T., R=0.08, RW direction in 0.1" mill annealed Ti-6-4 sheet

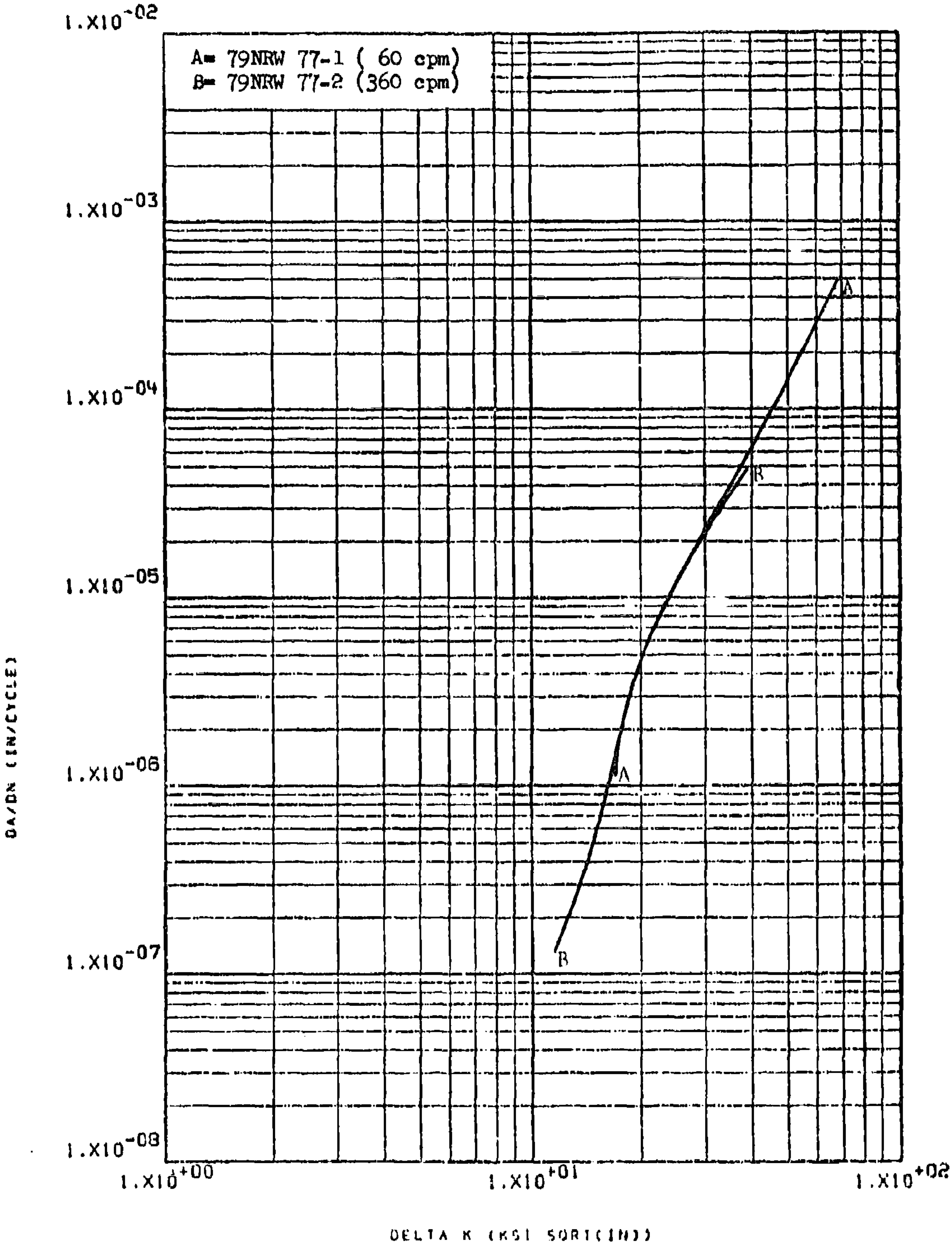

Figure 8.2.1.1-5 Effect of cyclic frequency on LHA-FCGR at R.T., R=0.08, RW direction in recrystallization annealed 4" x 10" x 34" Ti-6-4 forged block

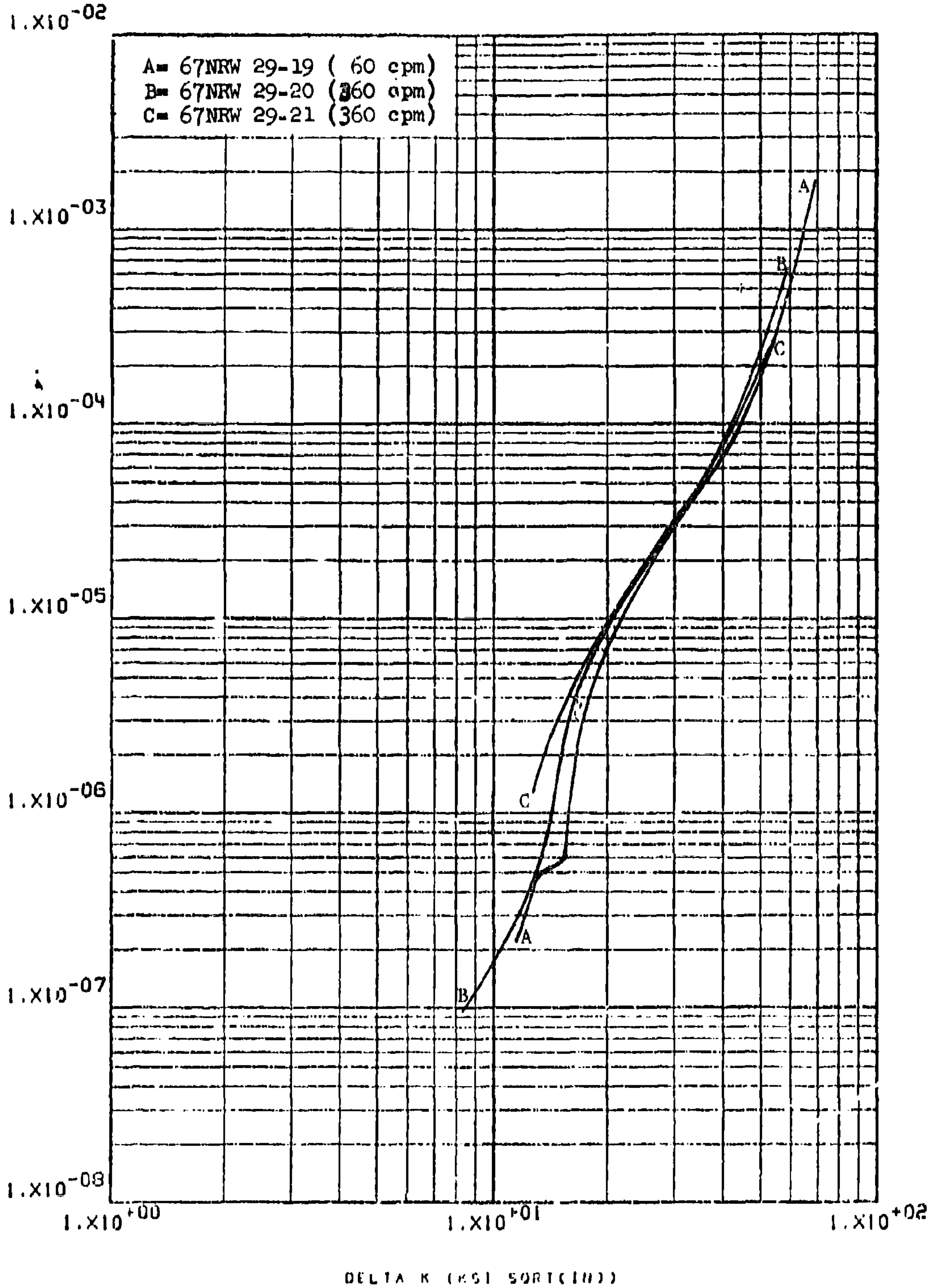

Figure 8.2.1.1-6 Effect of cyclic frequency on LHA-FCGR at R.T., R=0.08, RW direction in recrystallization annealed 1.5" Ti-6-4 plate

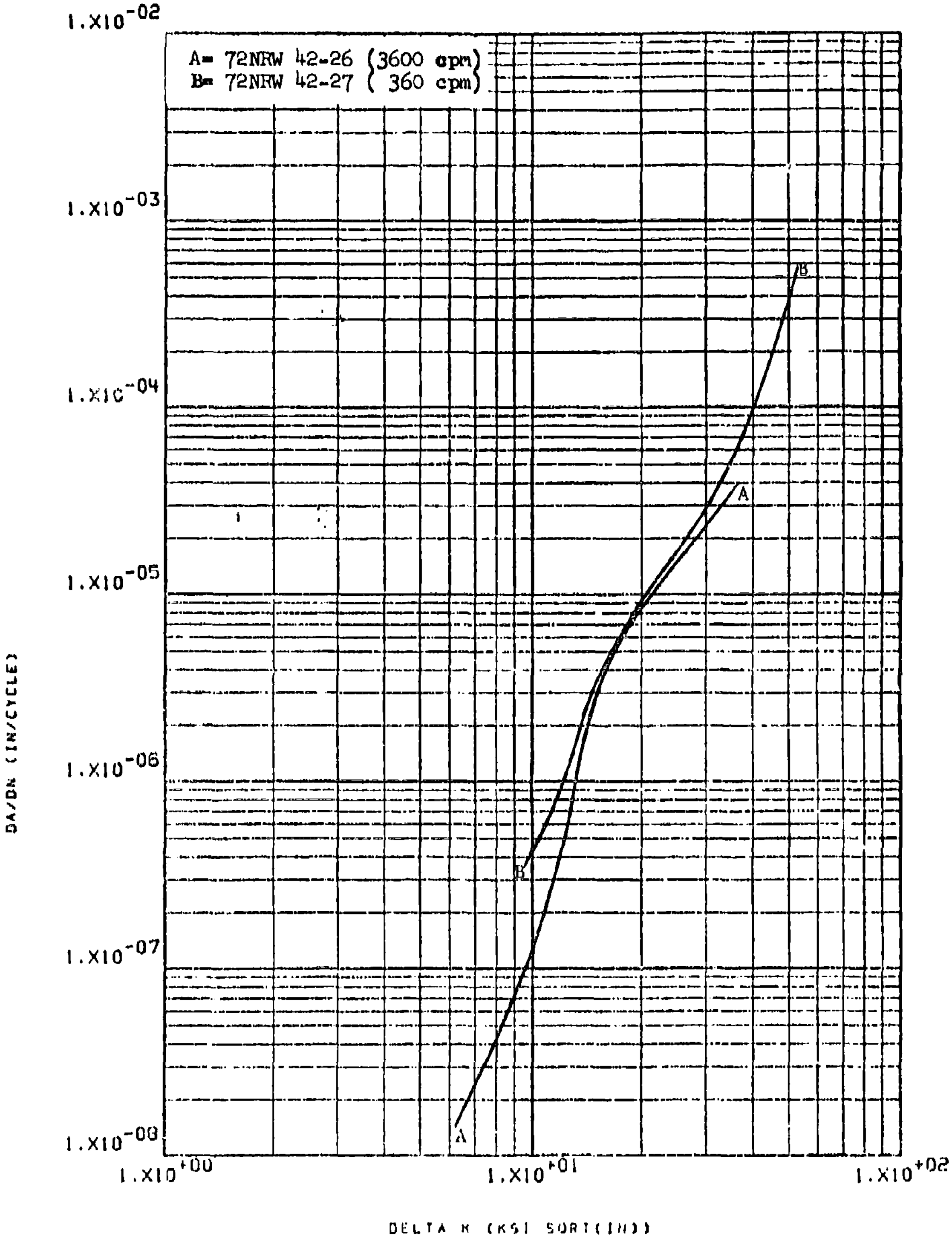

Figure 8.2.1.1-7 Effect of cyclic frequency on LHA-FCGR at R.T., R=0.08, RW direction in recrystallization annealed 1.5" Ti-6-4 plate

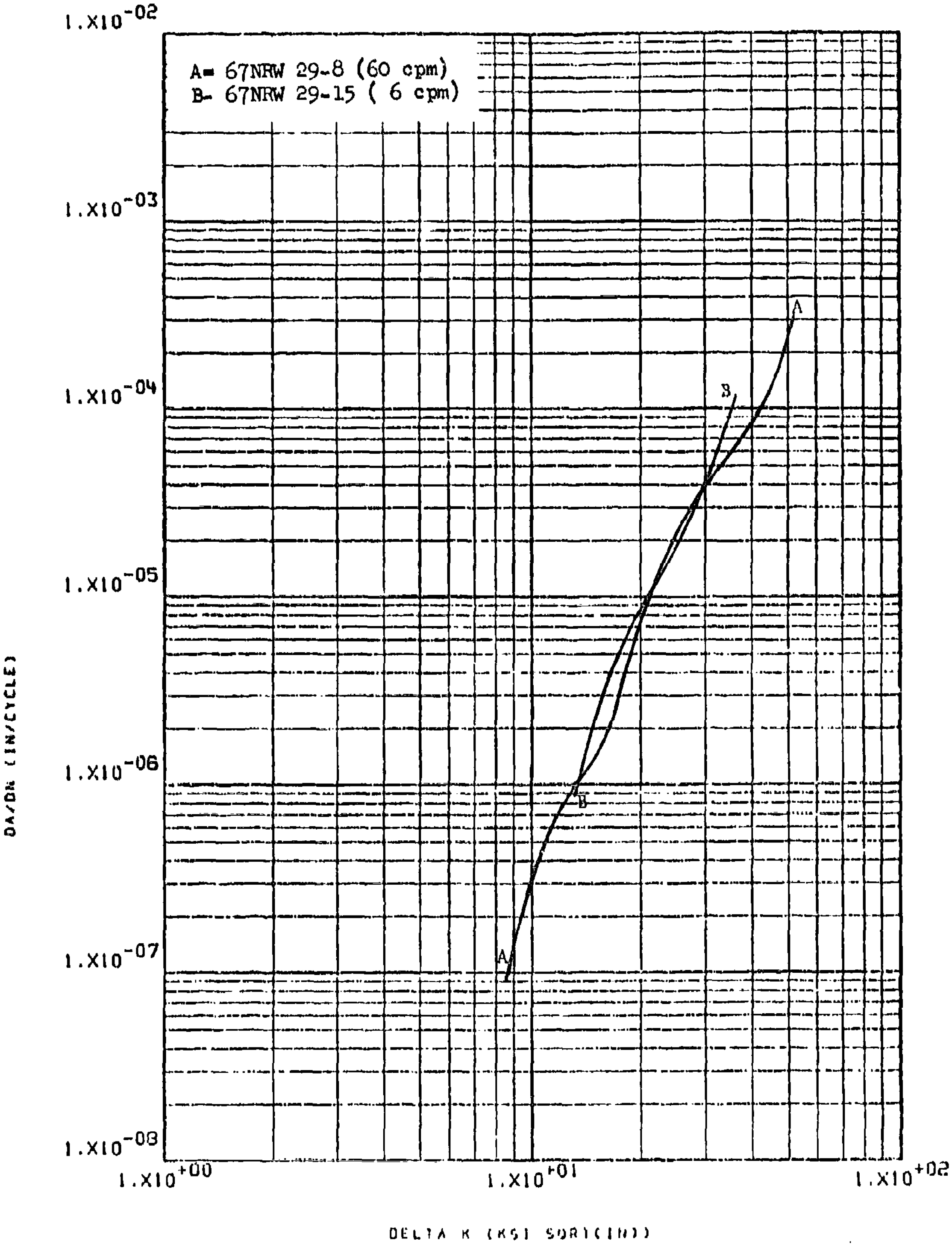

Figure 8.2.1.1-8 Effect of cyclic frequency on STW-FCGR at R.T., R=0.08 RW direction in recrystallization annealed 1.5" Ti-6-4 plate

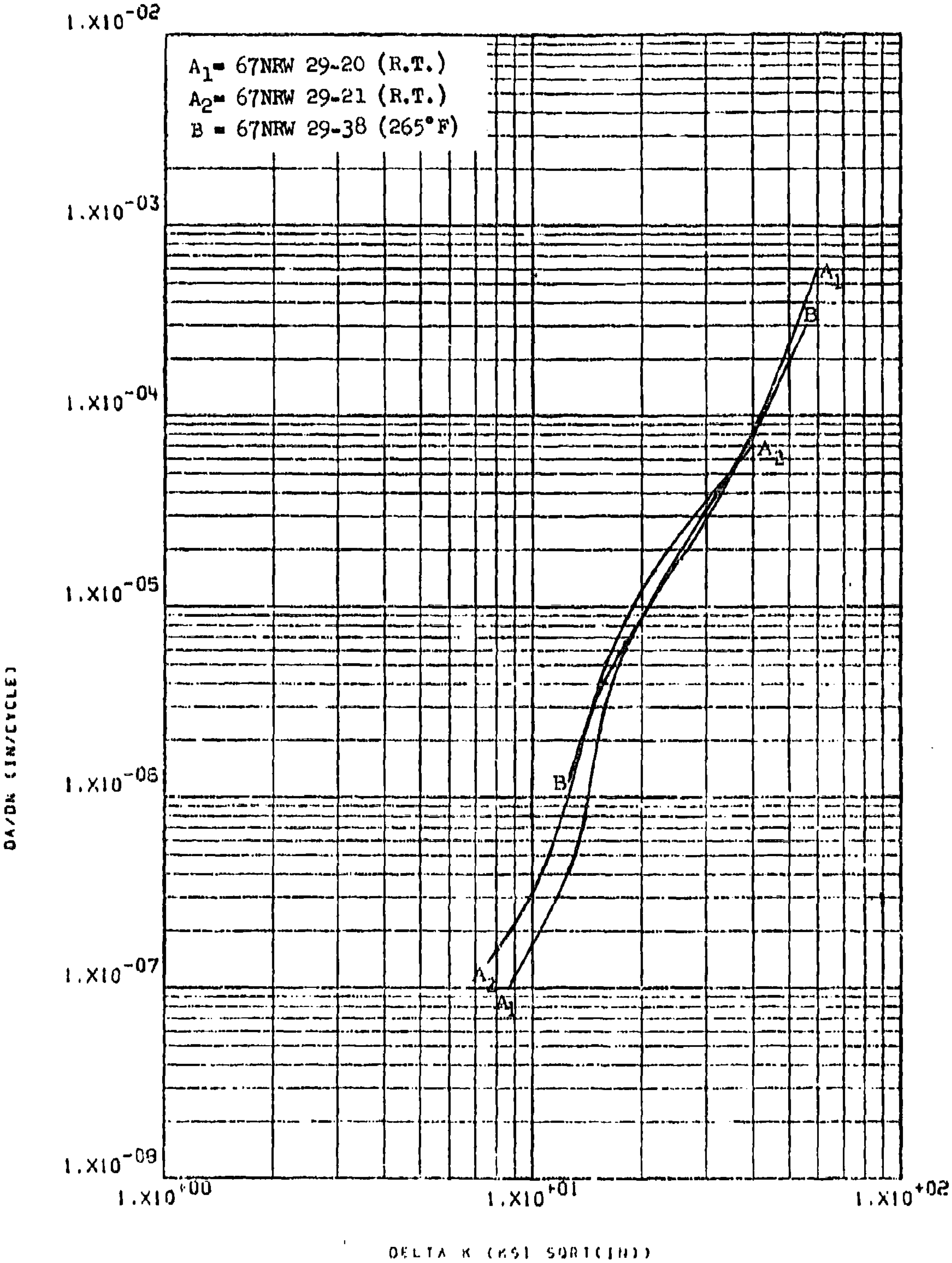

Figure 8.2.1.2-1 Effect of test temperature on LHA-FCGR at R=0.08, 360 cpm, RW direction in 1.5" Ti-6-4 R.A. plate

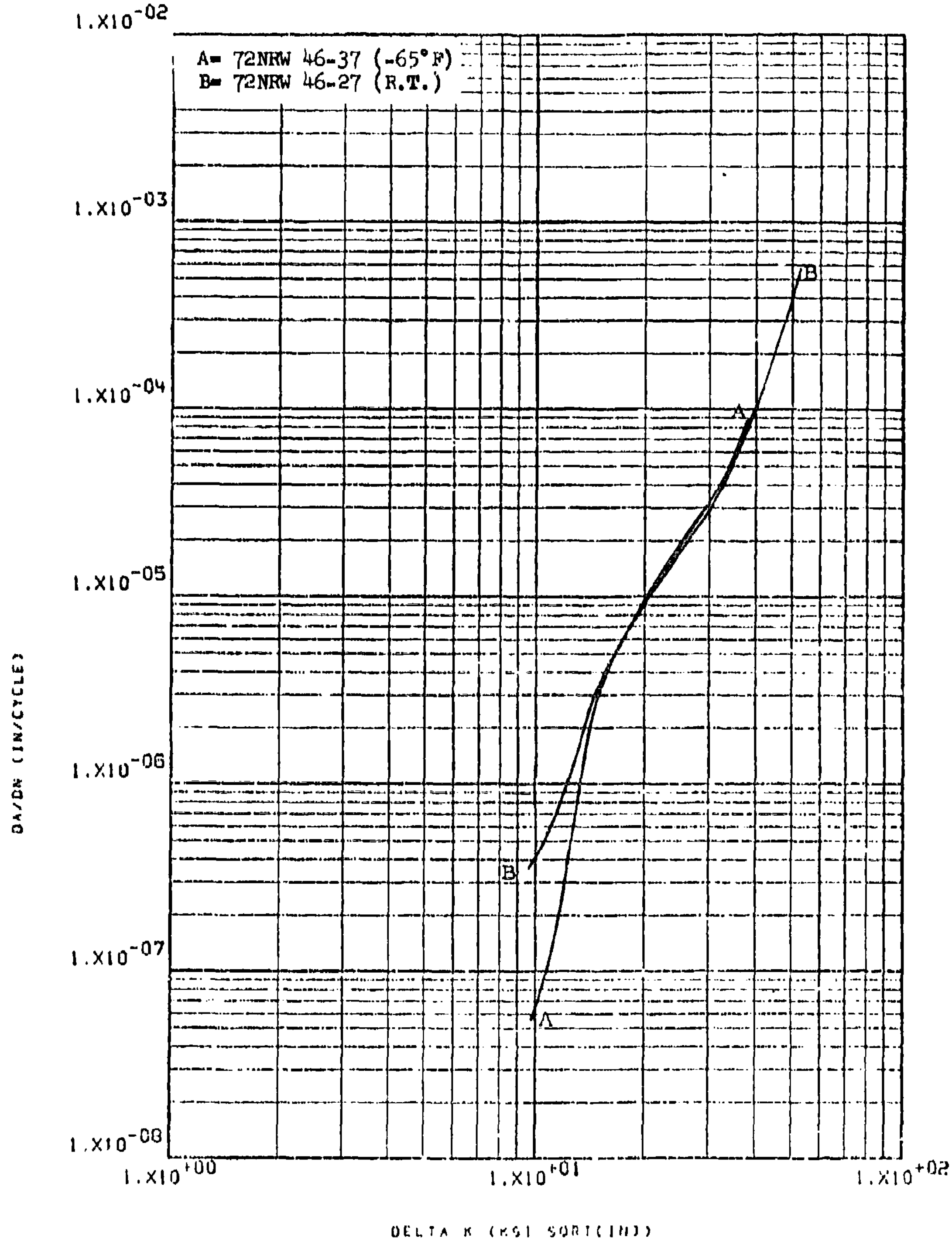

Figure 8.2.1.2-2 Effect of test temperature on LHA-FCGR at R=0.08, 360 cpm, RW direction in 1.5" Ti-6-4 R.A. plate

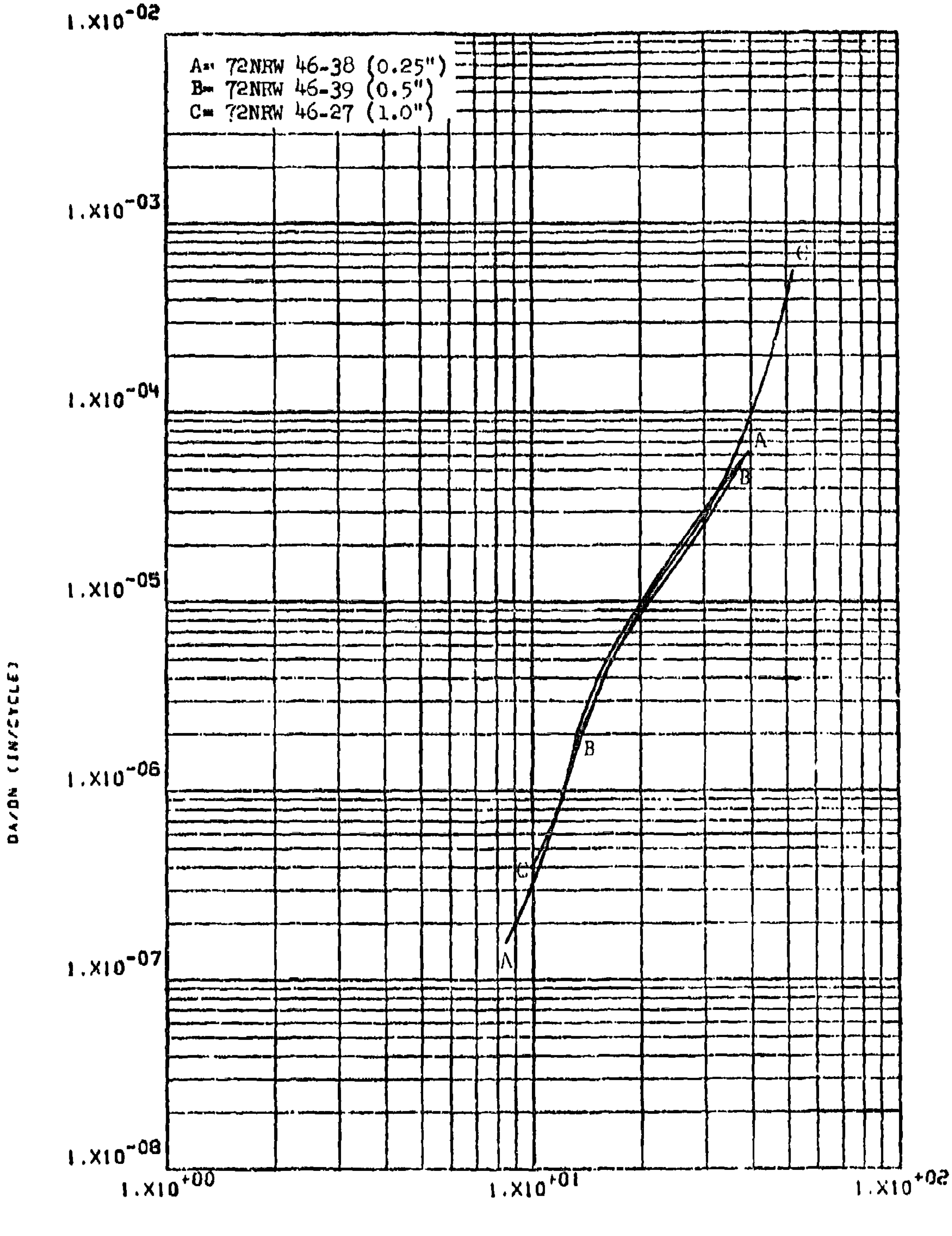

Figure 8.2.1.3-1 Effect of specimen thickness of LHA-FCGR at R.T., R=0.08, 360 cpm, RW direction in 1.5" Ti-6-4 R.A. plate

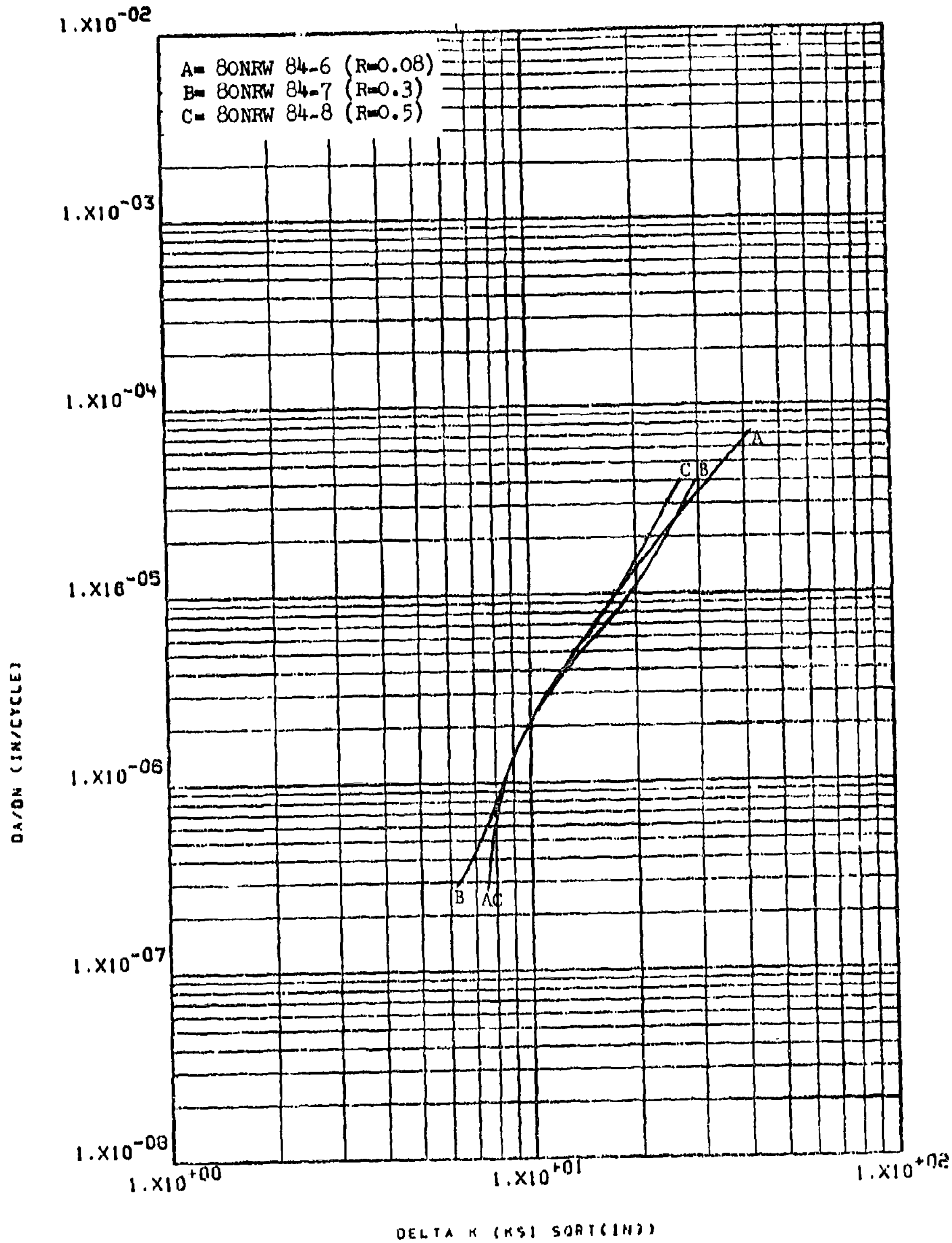

Figure 8.2.1.4-1 Effect of R factor on LHA-FCGR at R.T., R=0.08, 360 cpm, RW direction in 0.1" Ti-6-4 M.A. sheet

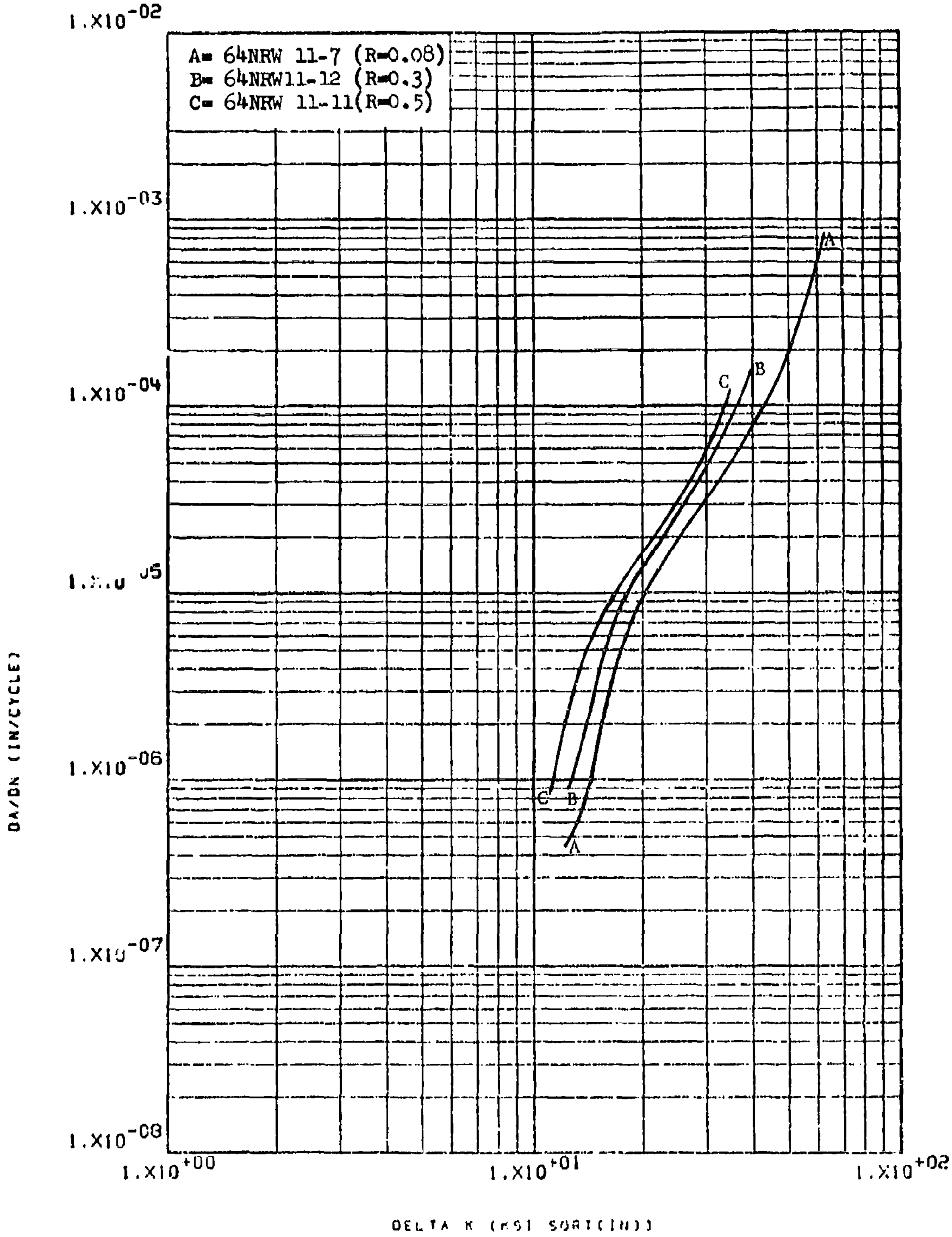

Figure 8.2.1.4-2 Effect of R factor on IHA-FCGR at R.T., 360 cpm, RW direction in beta processed plus mill annealed Ti-6-4 "L" extrusion

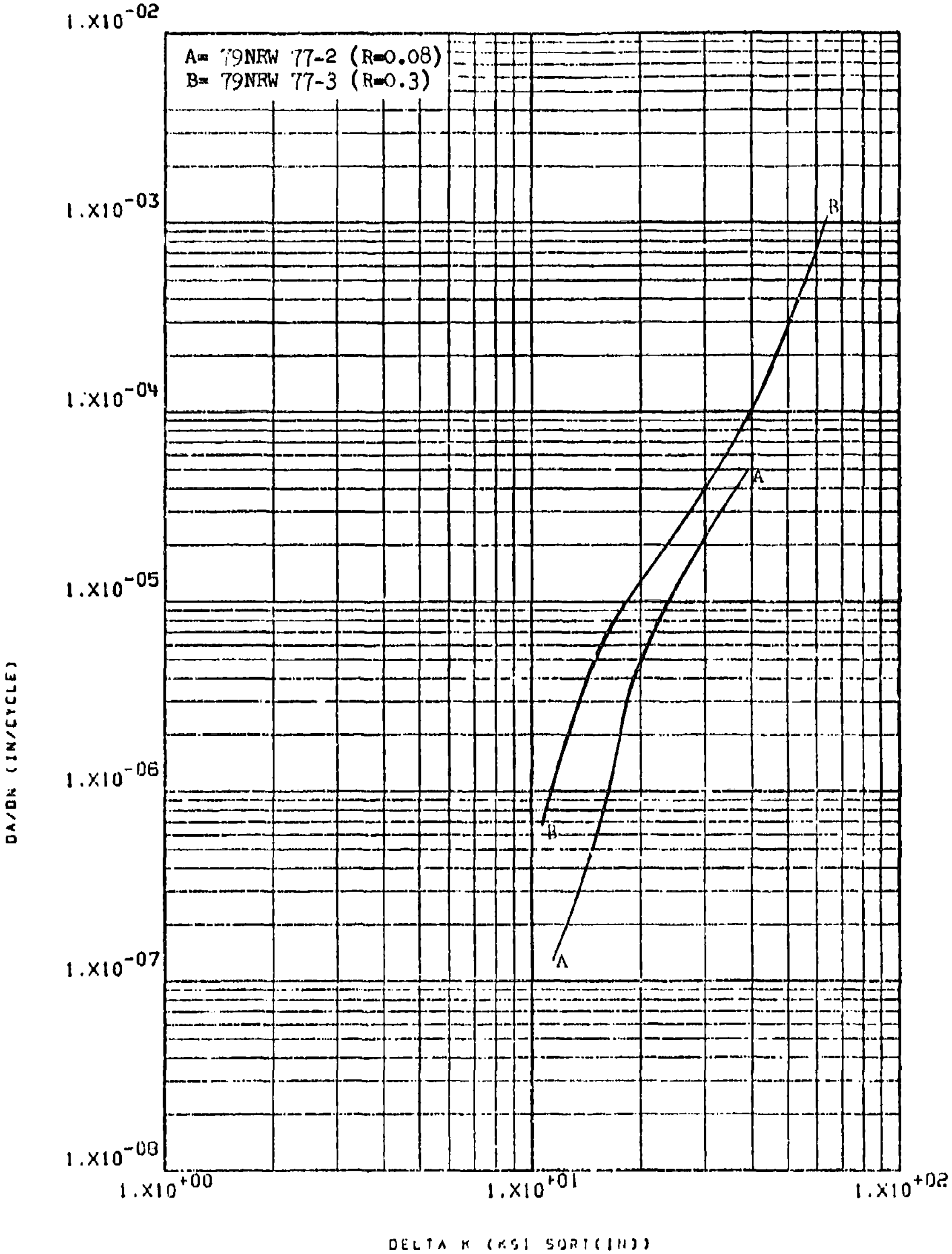

Figure 8.2.1.4-3 **Effect** of R **factor on LHA-FCGR at R.T.,** 360 cpm, RW direction in 4" x 10" x 34" Ti-6-4 R.A. hand forged block

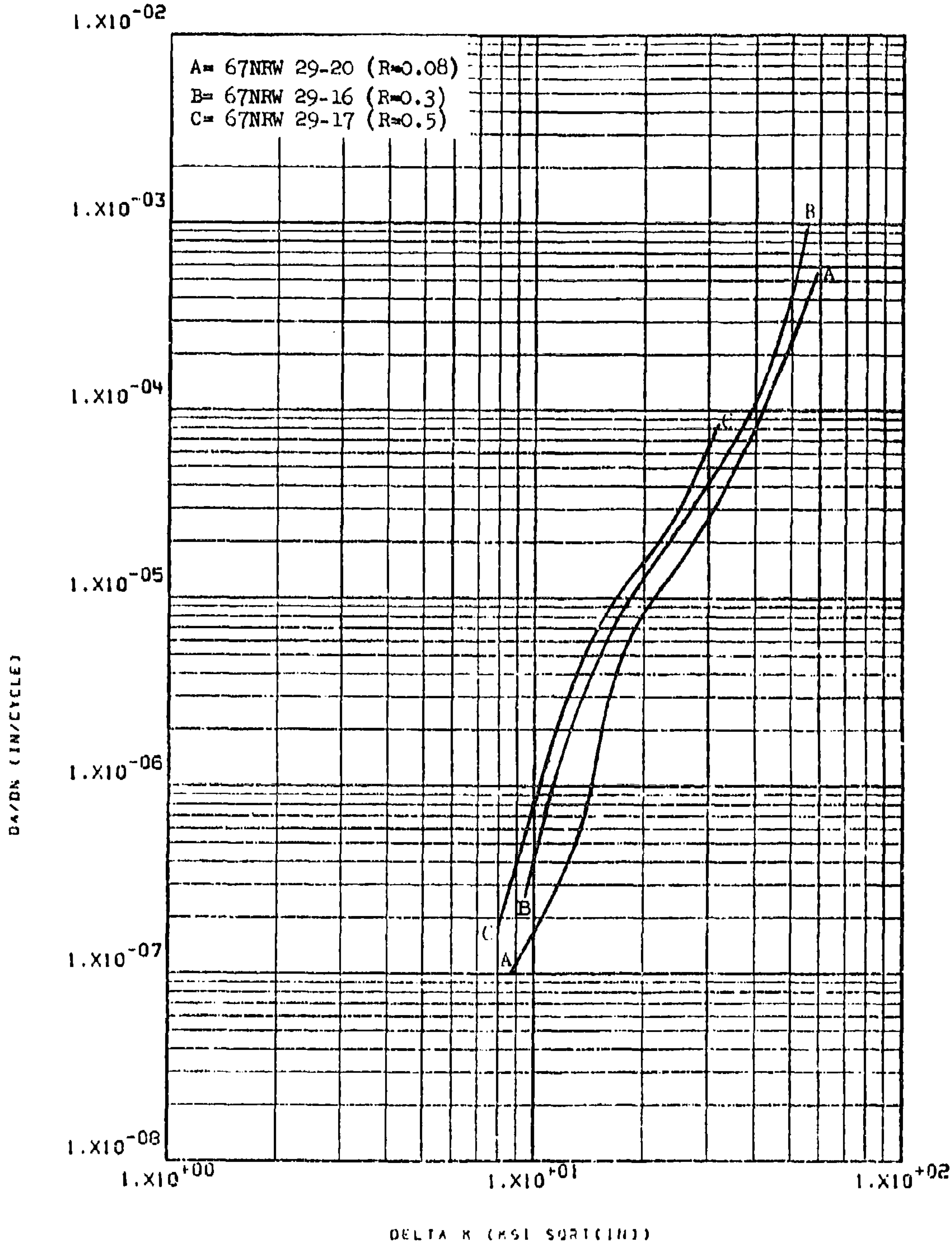

Figure 8.2.1.4-4 Effect of R factor on LHA-FCGR at R.T., 360 cpm, RW direction in 1.5" Ti-6-4 R.A. plate

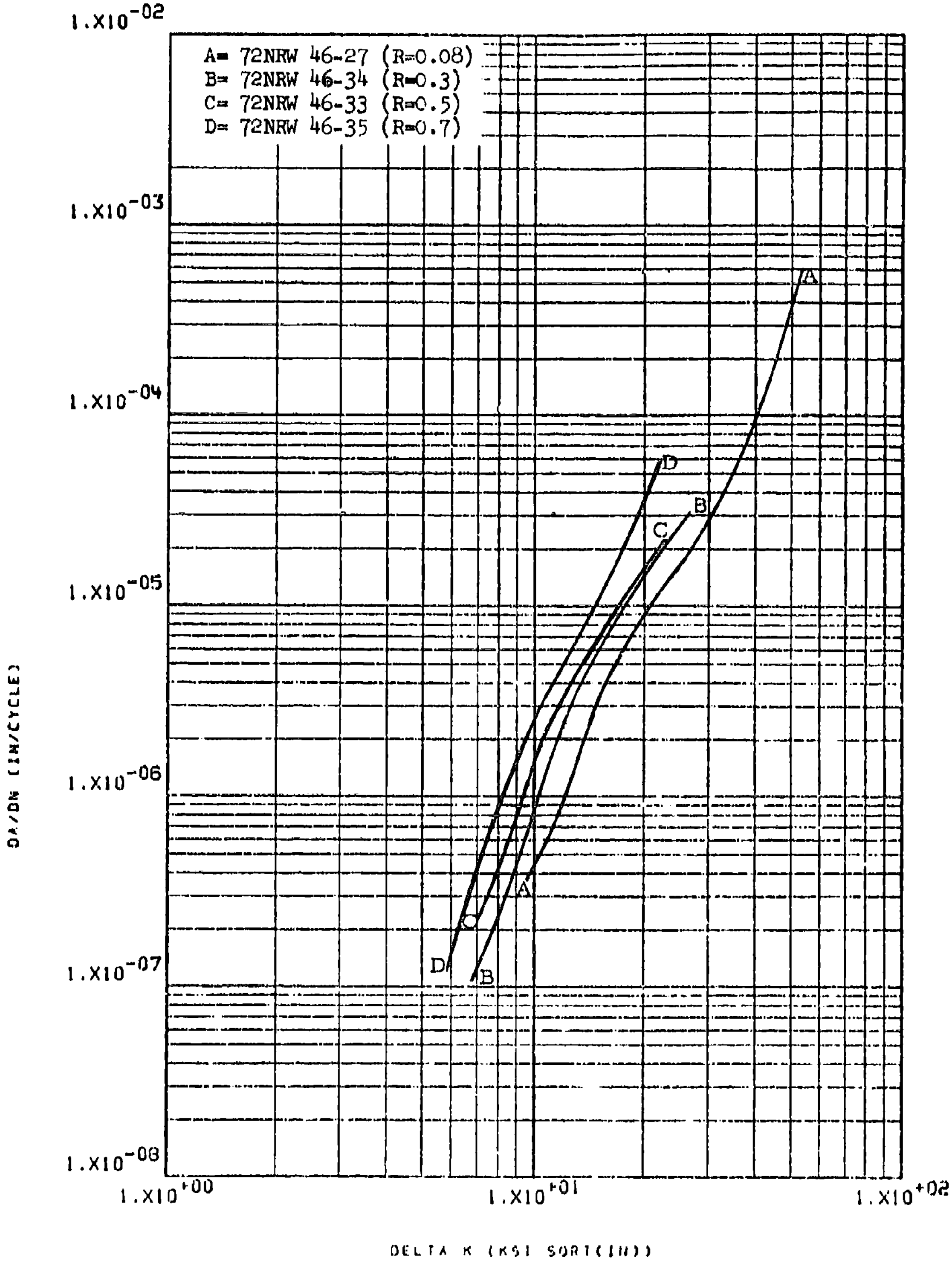

Figure 8.2.1.4-5 Effect of R factor on IHA-FCGR at R.T., 360 cpm, RW direction in 1.5" Ti-6-4 R.A. plate

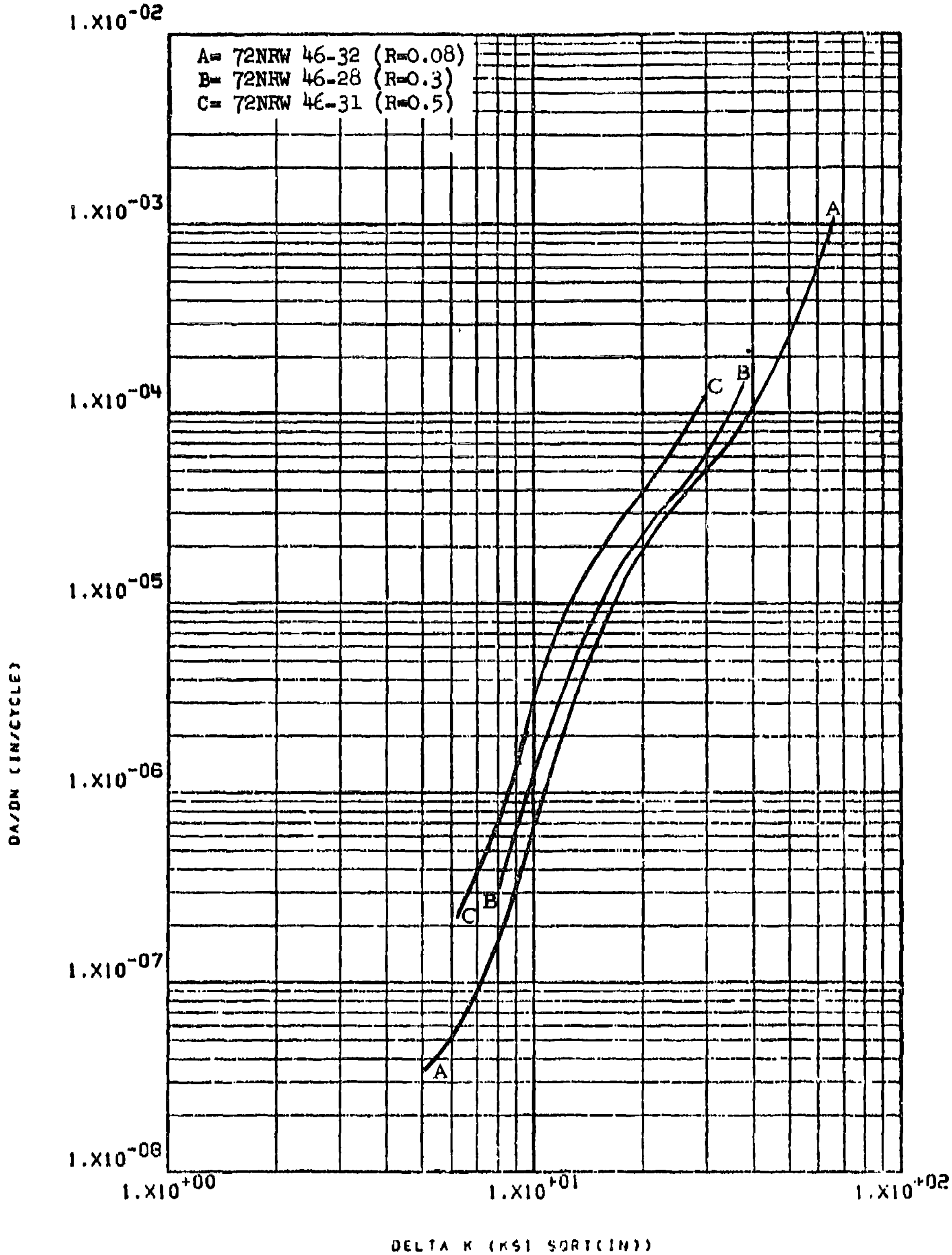

Figure 8.2.1.4-6 Effect of R factor on STW-FCGR at R.T., 60 cpm, RW direction in 1.5" Ti-6-4 R.A. plate

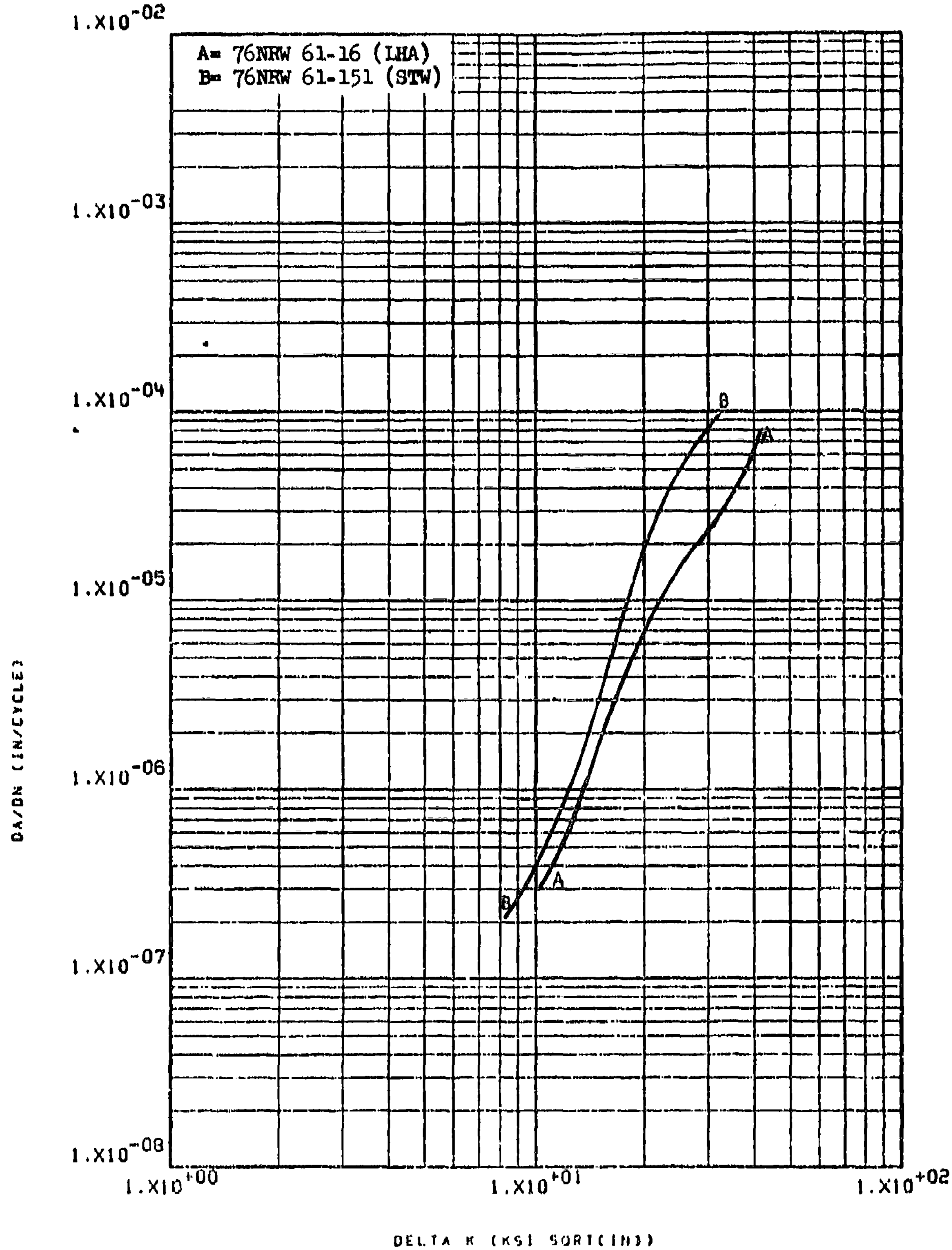

Figure 8.2.1.5-1 Effect of environment on FCGR at R.T., R=0.08, RW direction in 1.5" Ti-6-4 R.A. plate

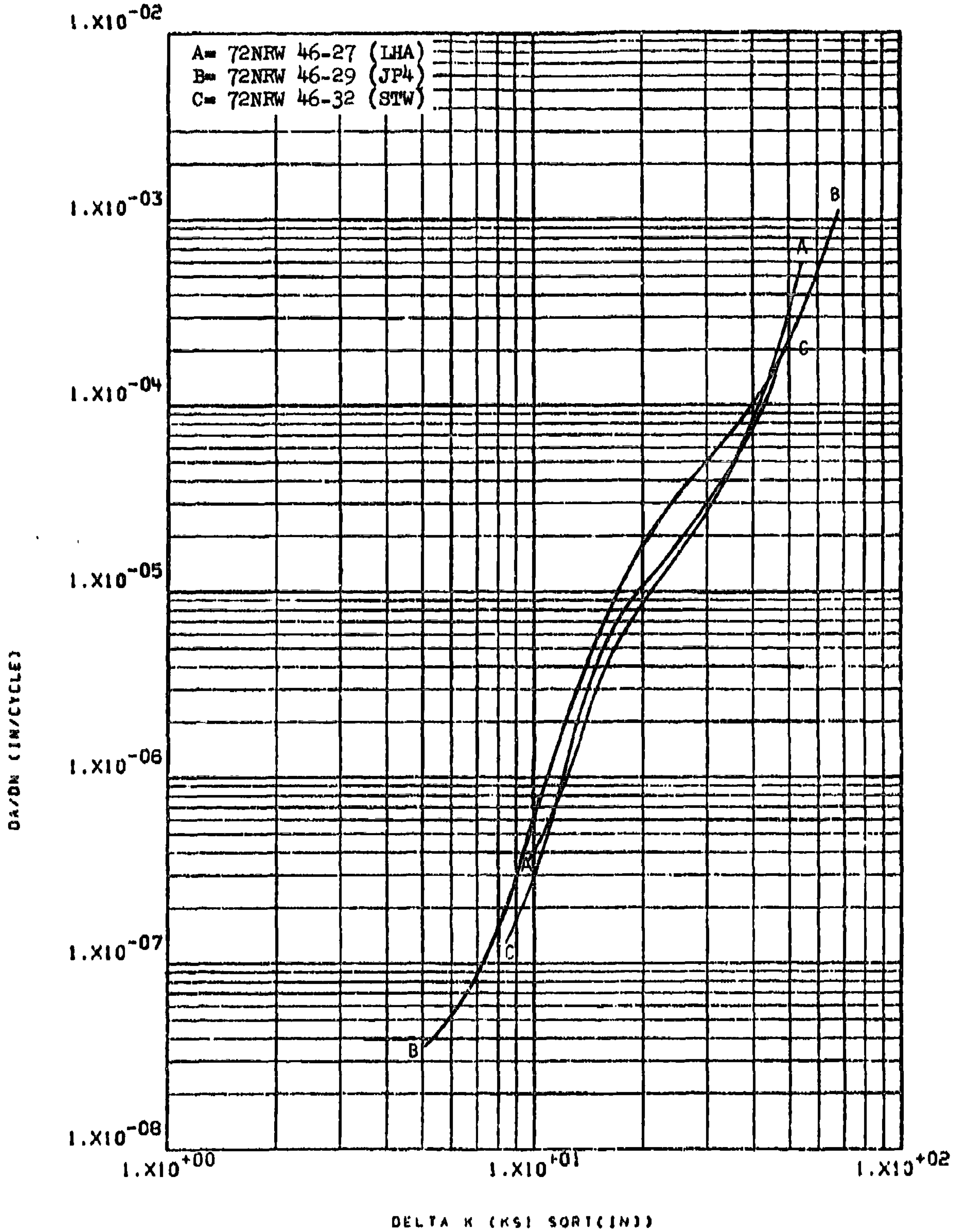

Figure 8.2.1.5-2 Effect of environment on FCGR at R.T., R=0.08, RW direction in 1.5" Ti-6-4 R.A. plate

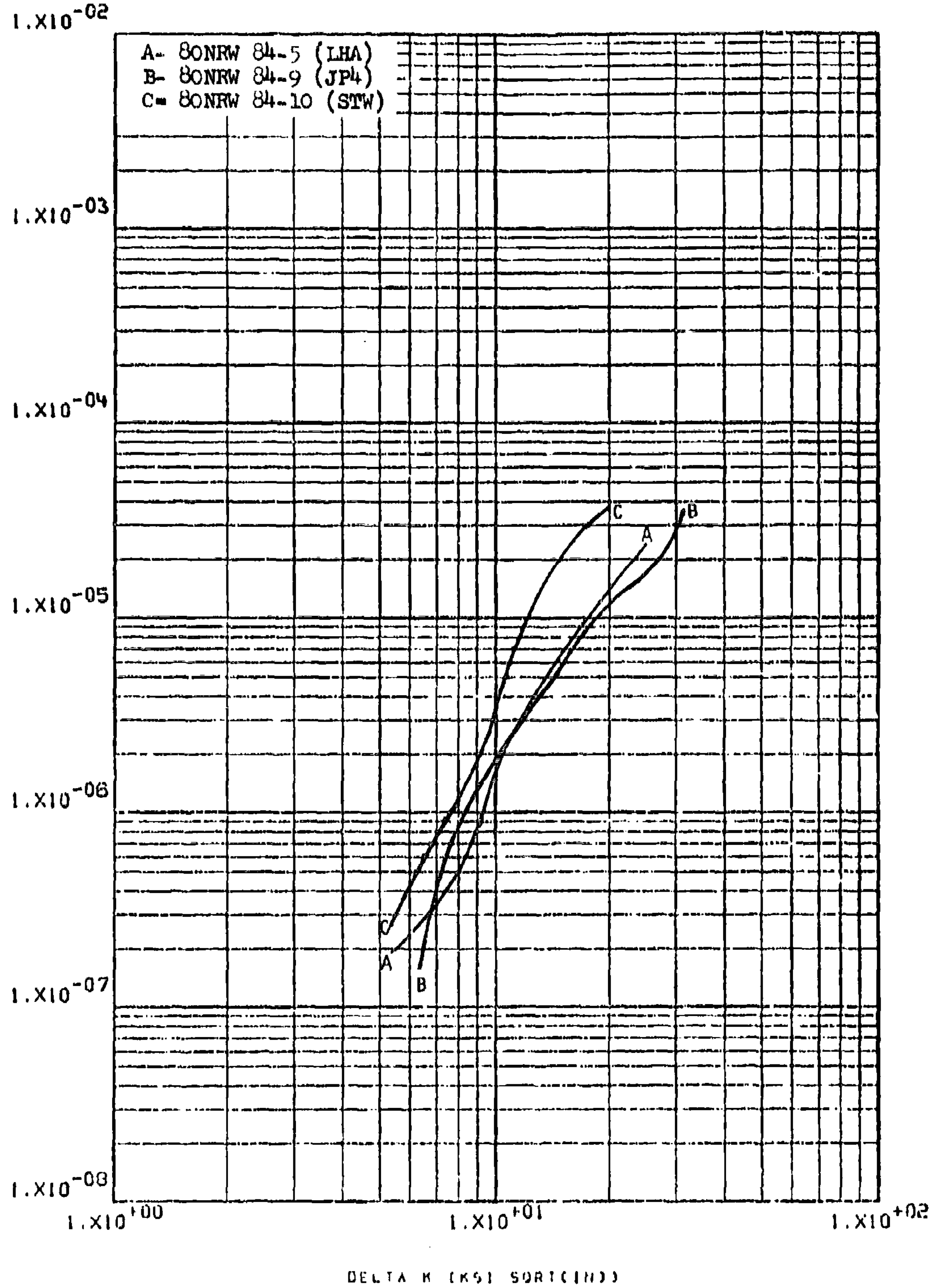

Figure 8.2.1.5-3 Effect of environment on FCGR at R.T., R-0.08, RW direction in 0.1" Ti-6-4 M.A. sheet

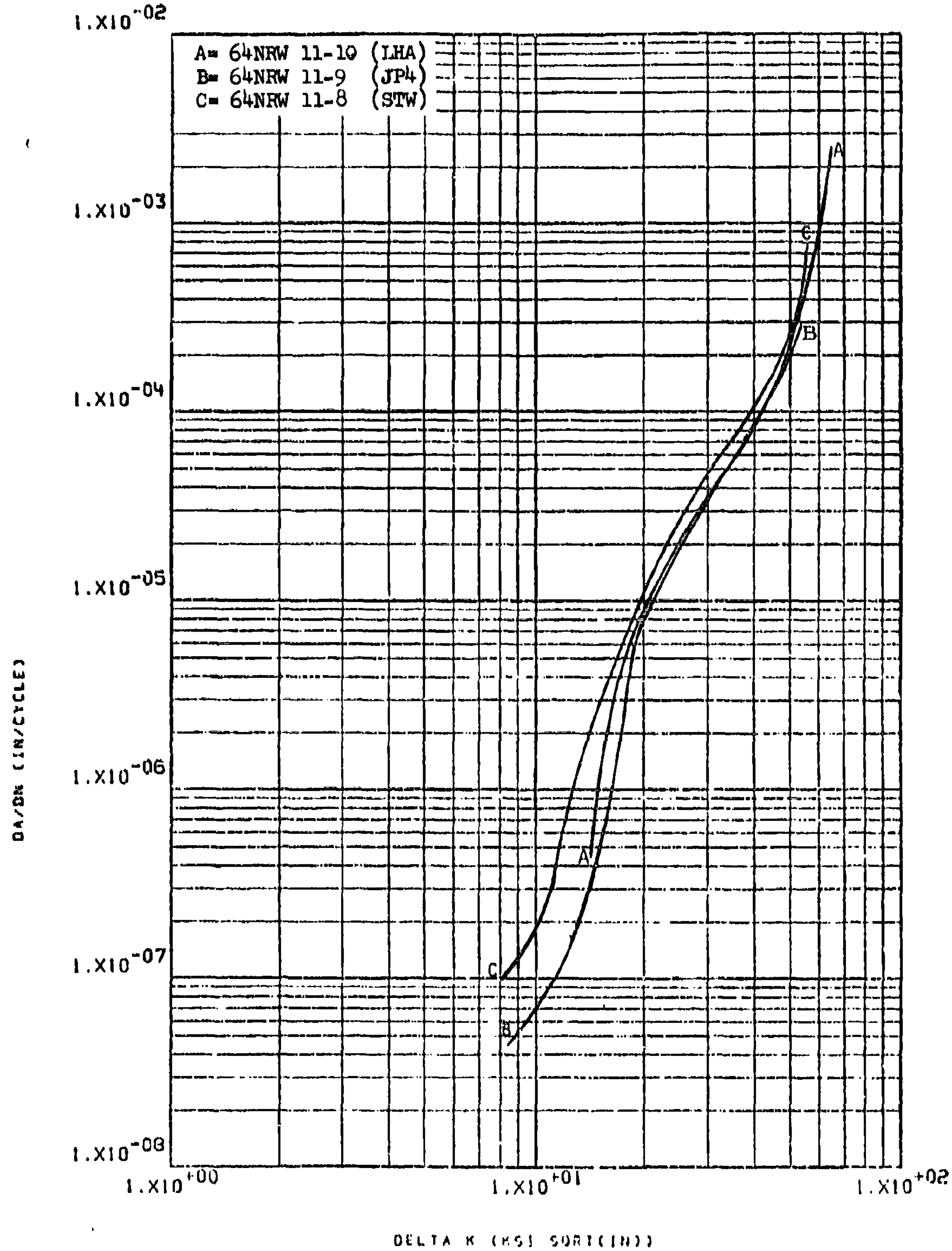

Figure 8.2.1.5-4 Effect of environment on FCGR at R.T., R=0.08, 60 cpm, RW direction in beta processed plus mill annealed Ti-6-4 "L" extrusion

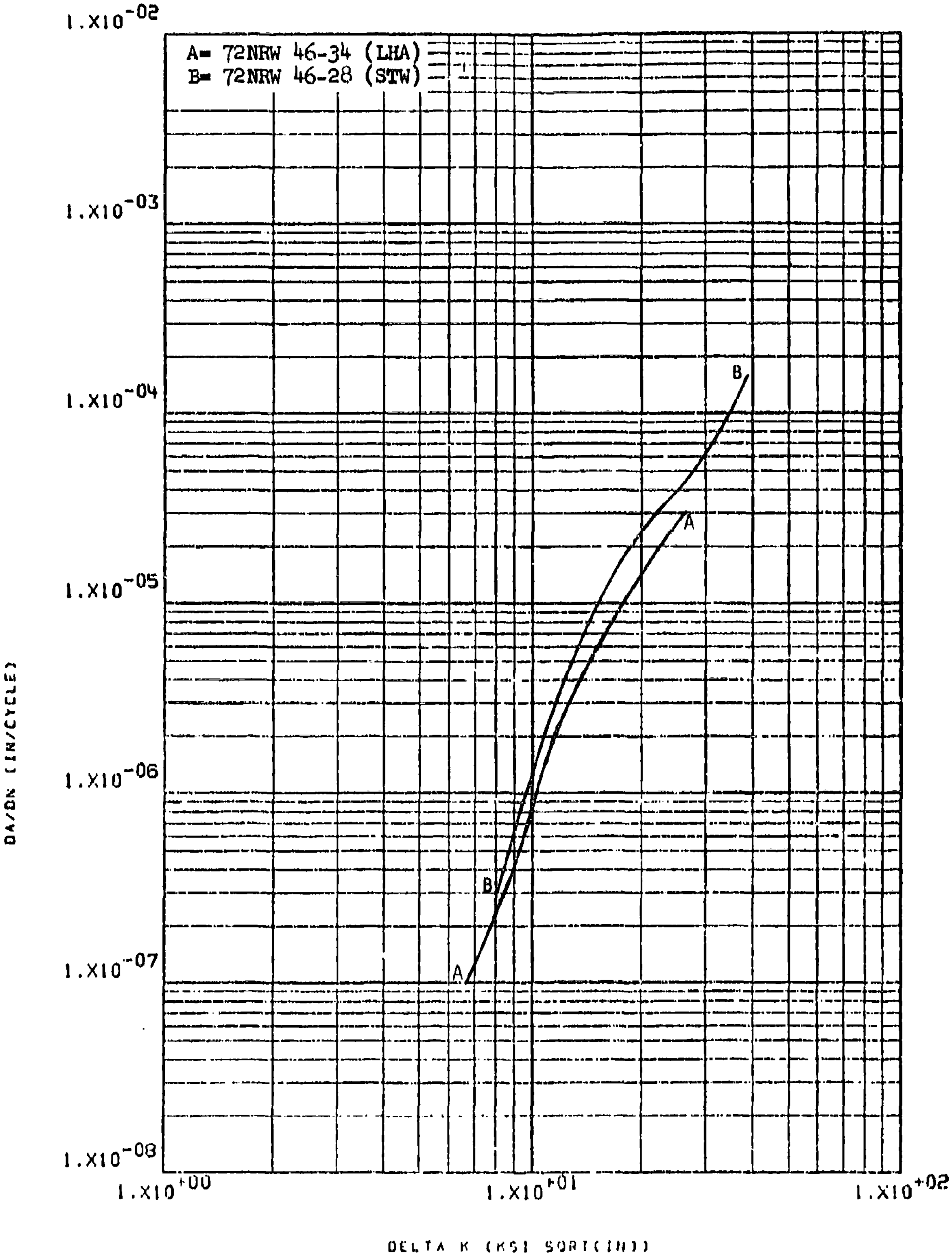

Figure 8.2.1.5-5 Effect of environment on FCGR at R.T., R=0.3, RW direction in 1.5" Ti-6-4 R.A. plate

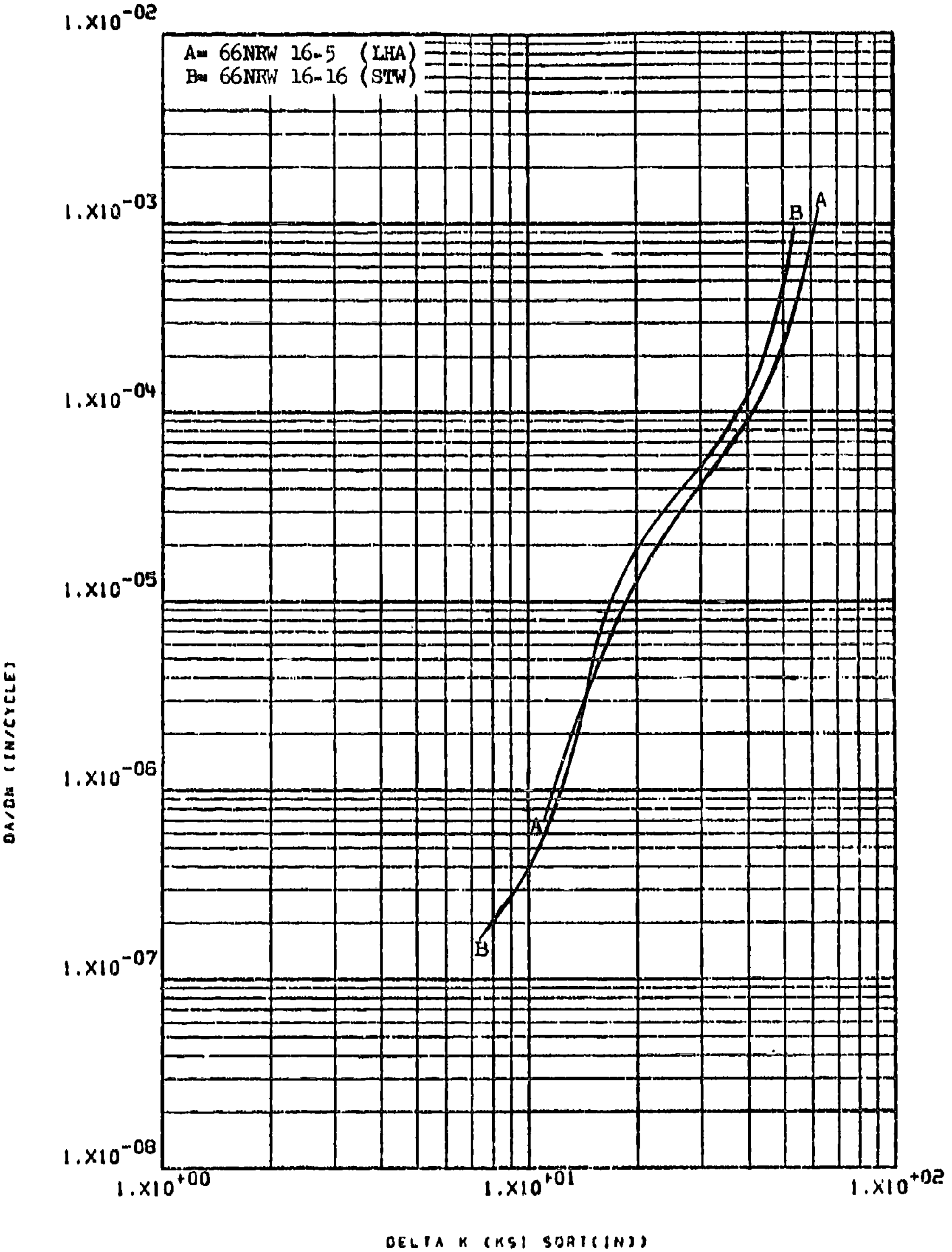

Figure 8.2.1.5-6 Effect of environment on FCGR at R.T., R=0.3, 60 cpm, RW direction in 1.5" beta rolled plus mill annealed Ti-6-4 plate

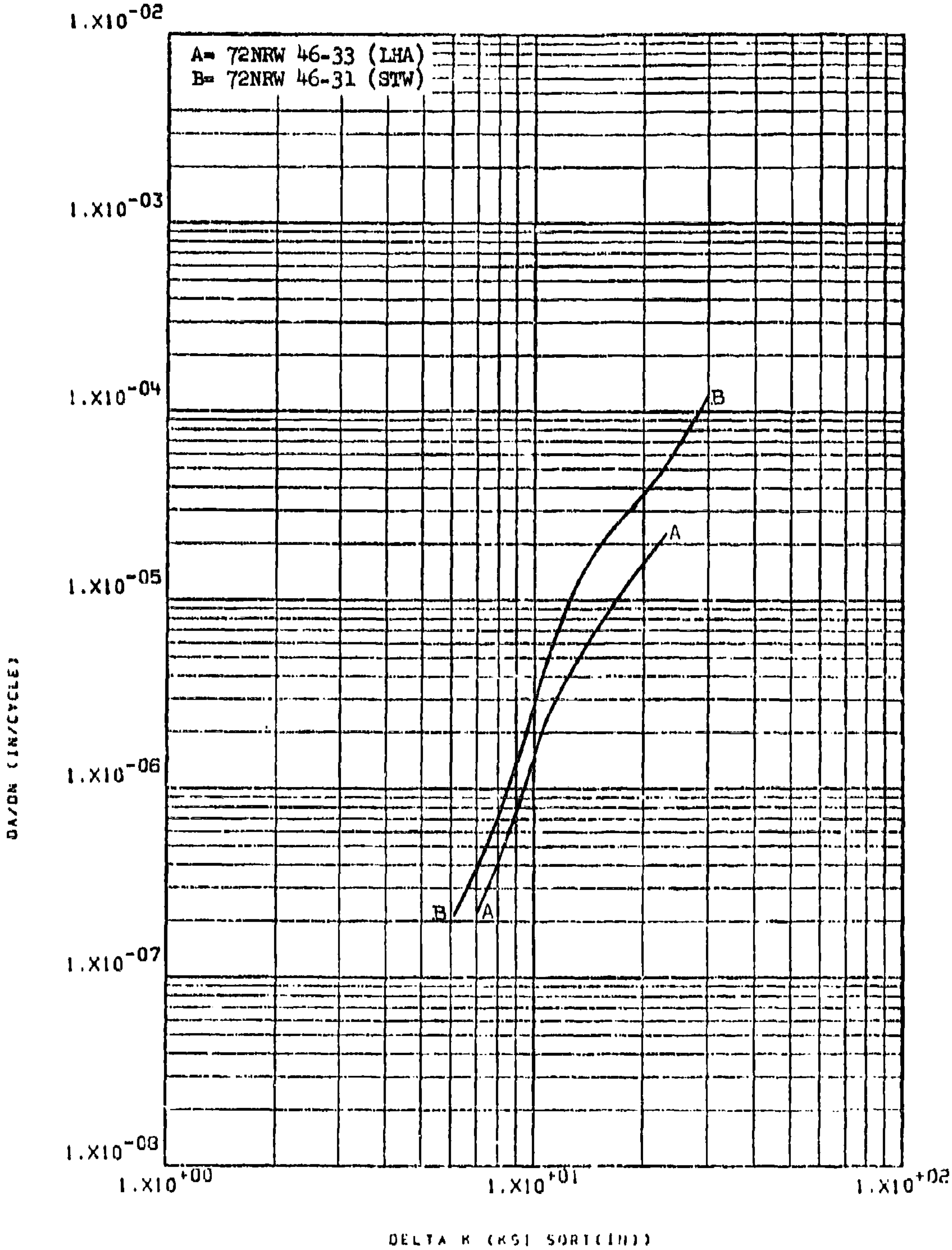

Figure 8.2.1.5-7 Effect of environment on FCGR at R.T., R=0.5, RW direction in 1.5" Ti-6-4 R.A. plate

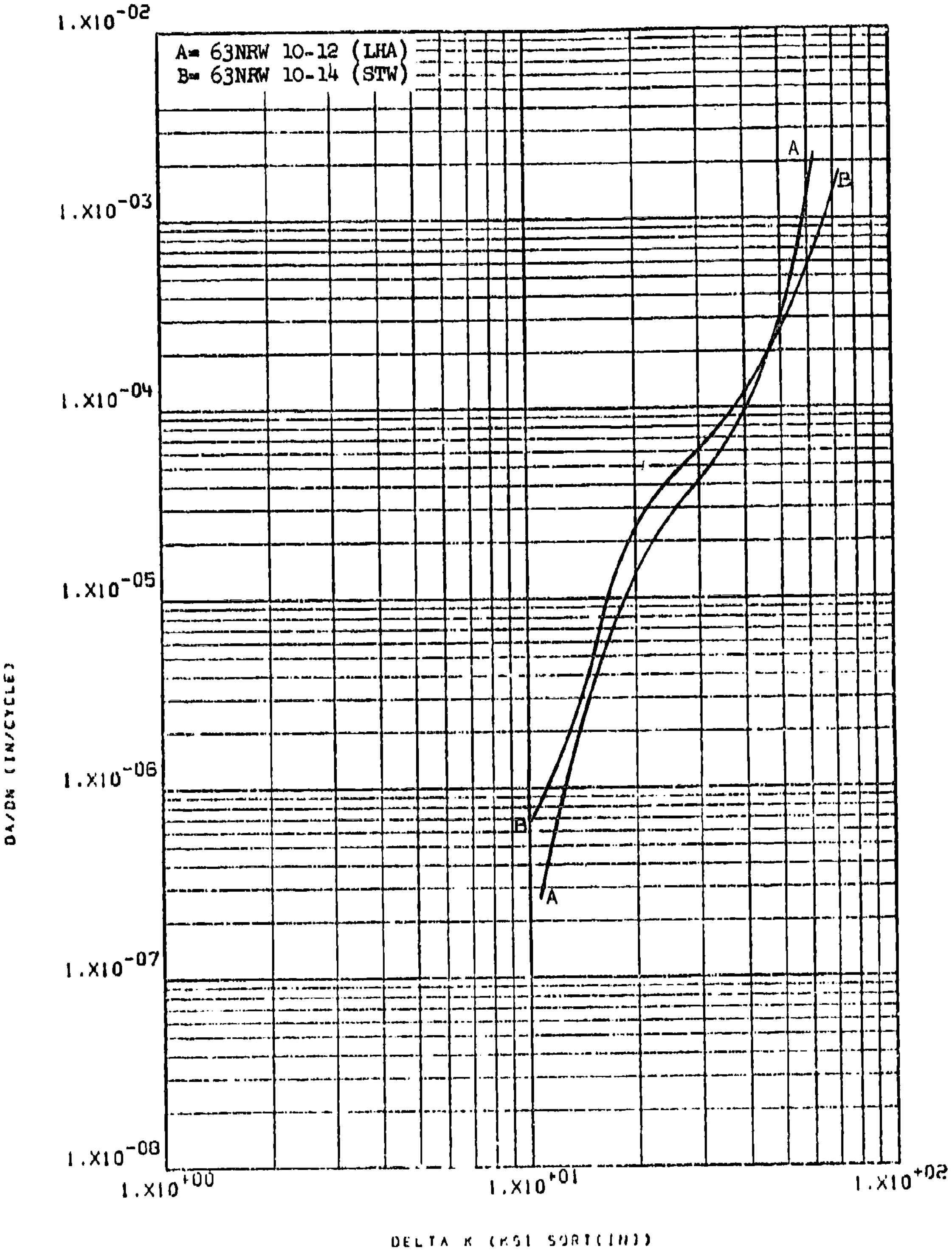

Figure 8.2.1.5-8 Effect of environment on FCGR at R.T., R=0.3, RW direction in 1.25" Ti-6-4 diffusion bond thermal cycled plate

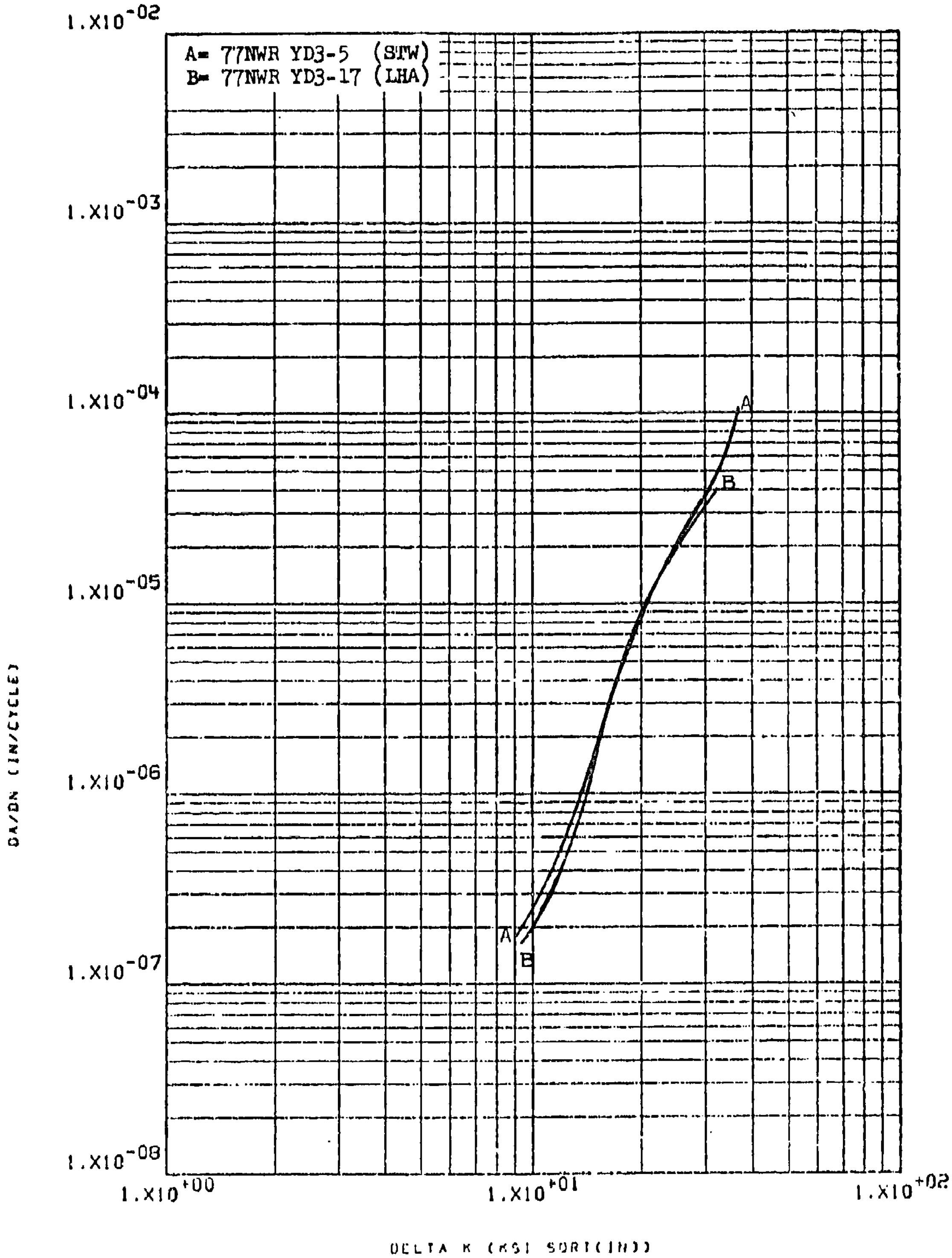

Figure 8.2.1.5-9 Effect of environment on FCGR at R.T., R=0.08, WR direction in 2.5" Ti-6-4 ring rolled plus R.A. plate

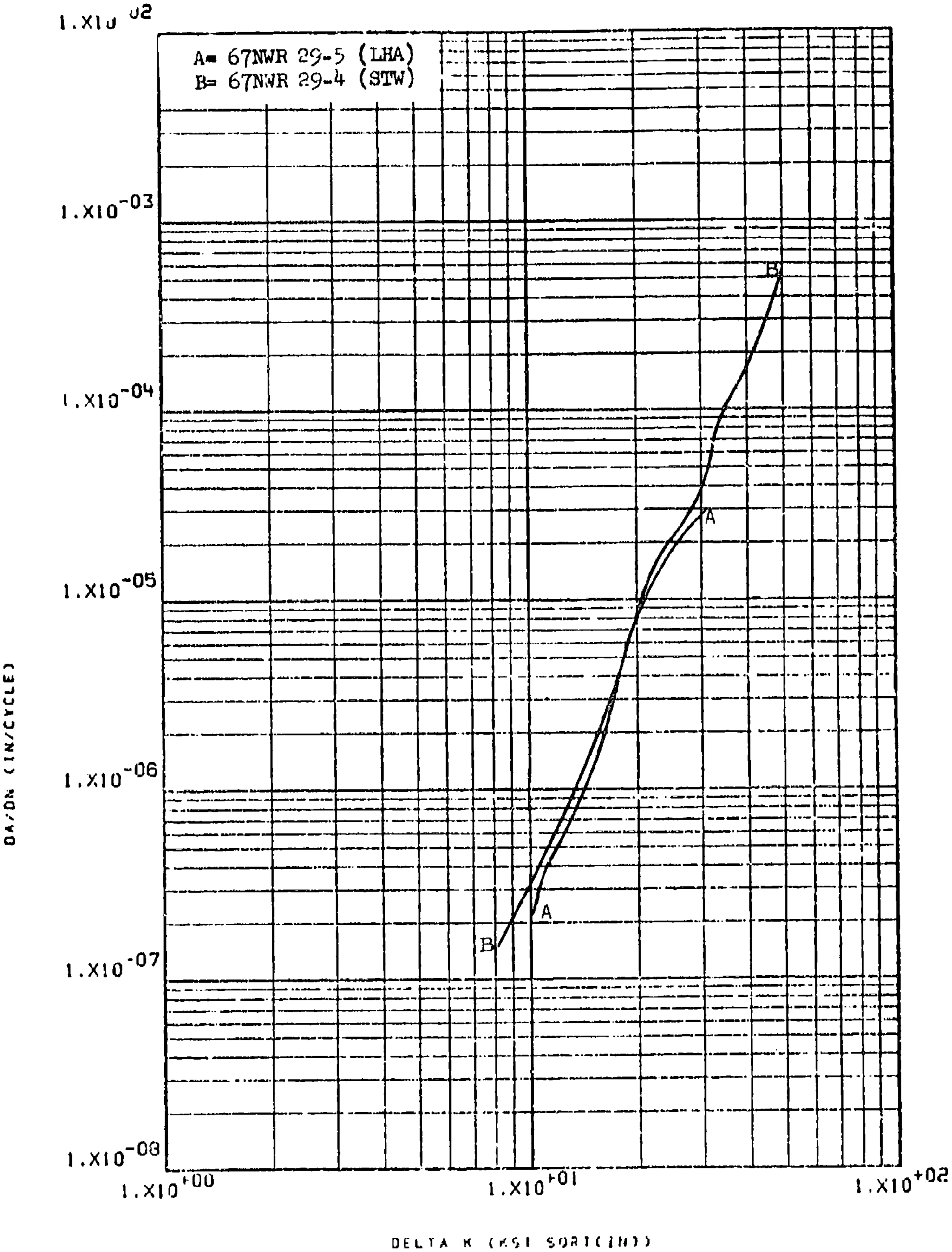

Figure 8.2.1.5-10 Effect of environment on FCGR at R.T., R=0.08, WR direction 1.5" Ti-6-4 R.A. plate

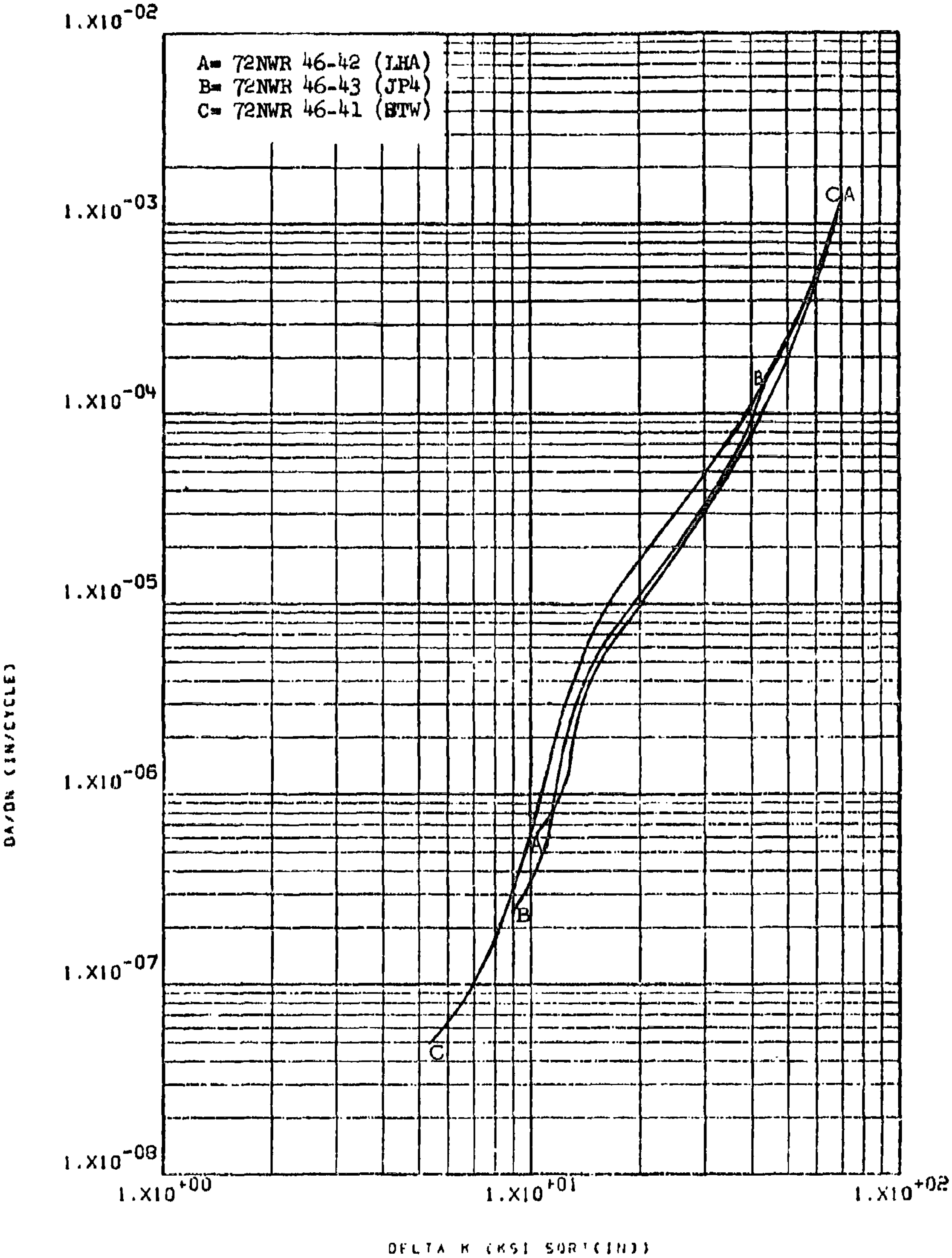

Figure 8.2.1.5-11 Effect of environment on FCGR at R.T., R=0.08, WR direction in 1.5" Ti-6-4 R.A. plate

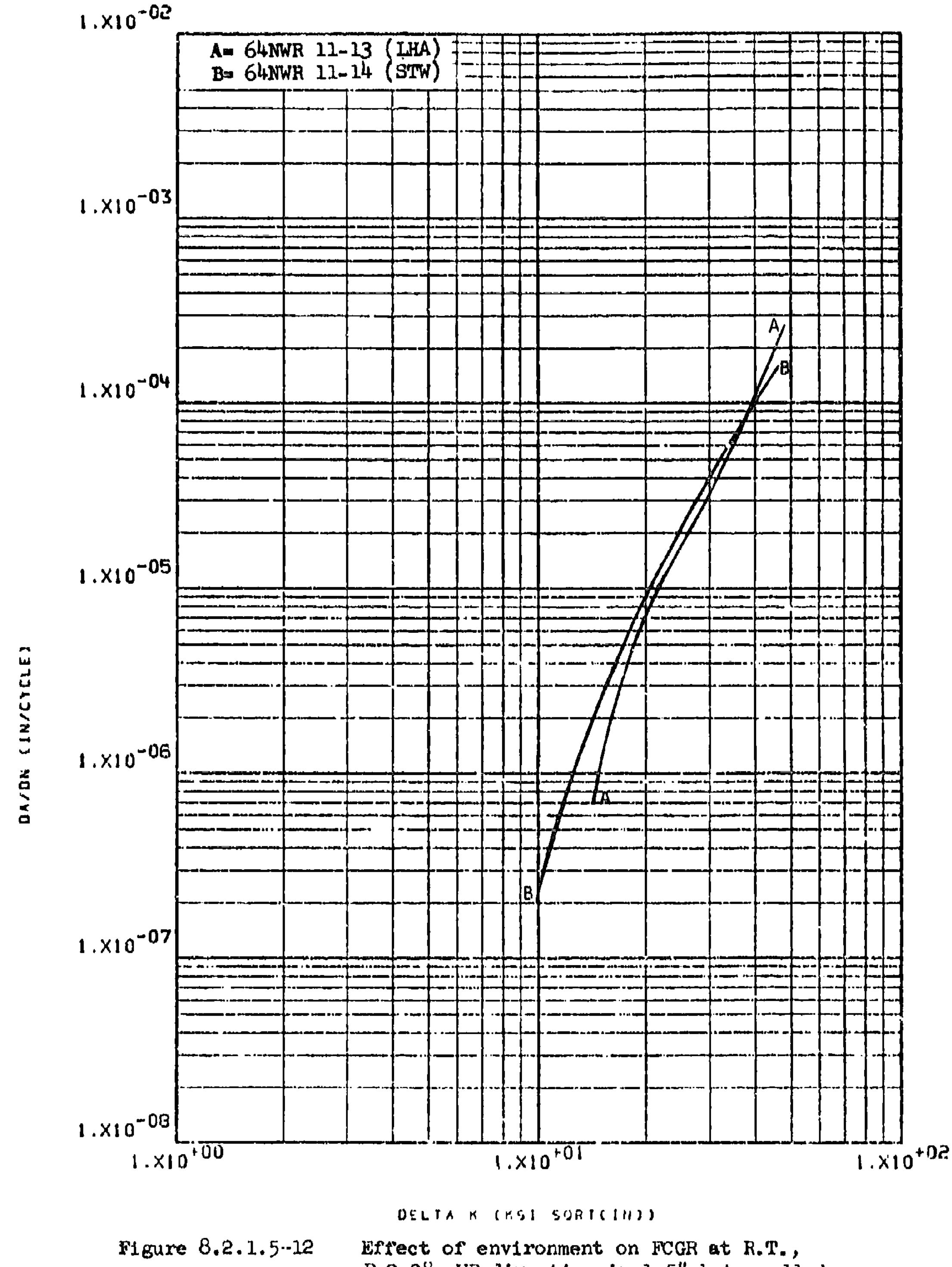

Figure 8.2.1.5-12 Effect of environment on FCGR at R.T., R=0.08, WR direction in 1.5" beta rolled plus mill annealed Ti-6-4 plate

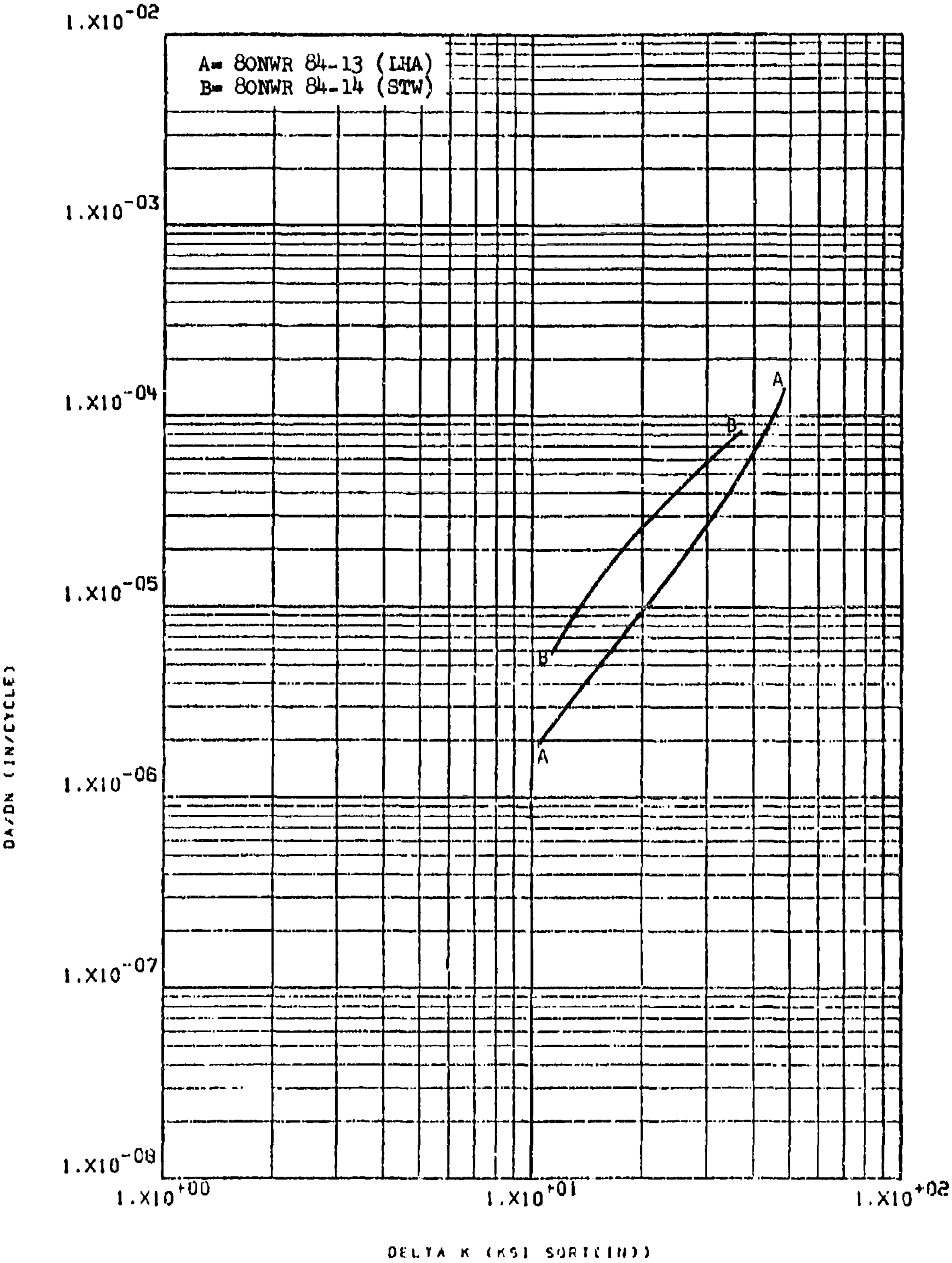

Figure 8.2.1.5-13 Effect of environment on FCGR at R.T., R-0.08, 360 cpm, WR direction in 0.1" Ti-6-4 M.A. sheet

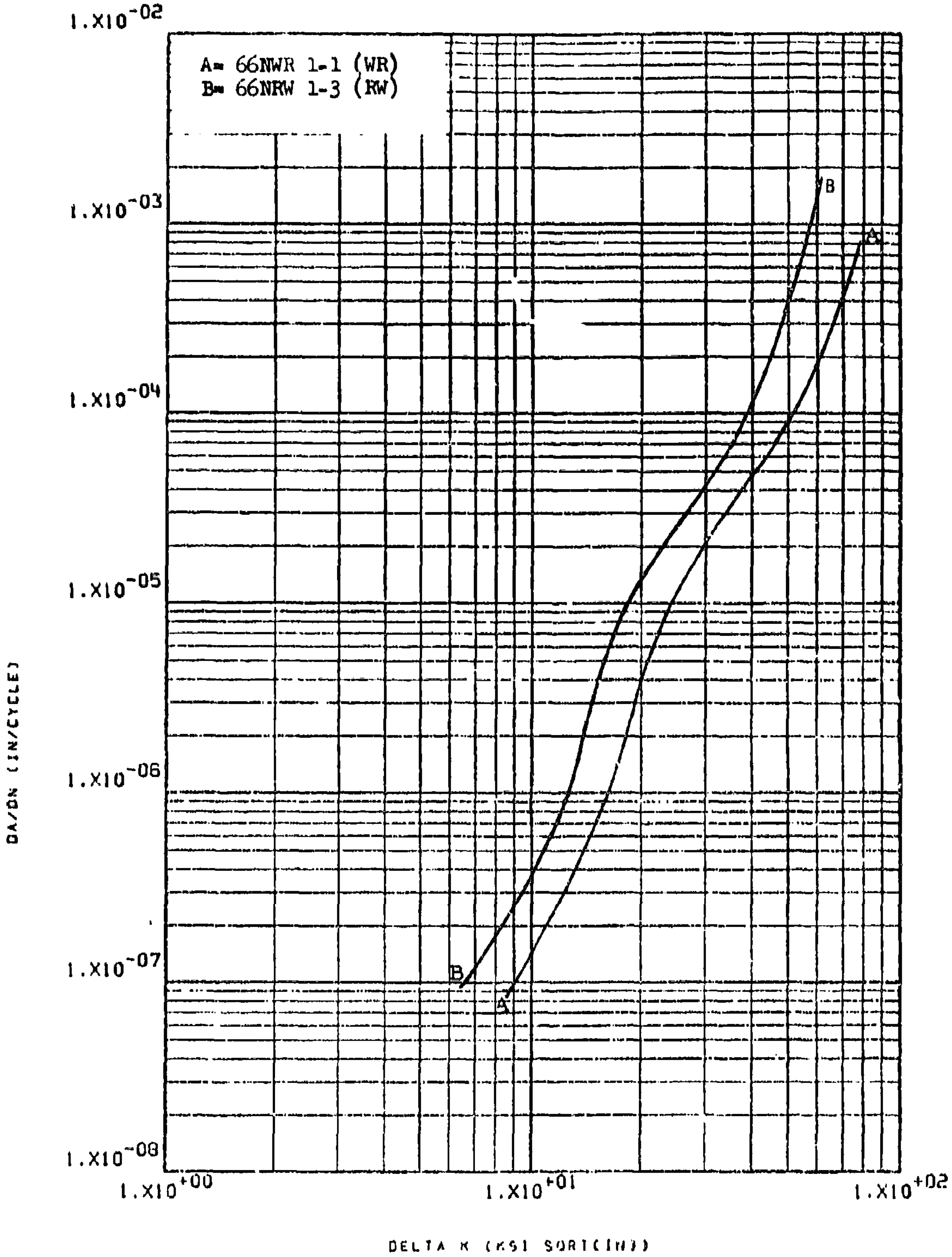

Figure 8.2.1.6-1 Effect of test direction on LHA-FCGR at R.T., R=0.3, in 1.5" beta rolled plus mill annealed Ti-6-4 plate

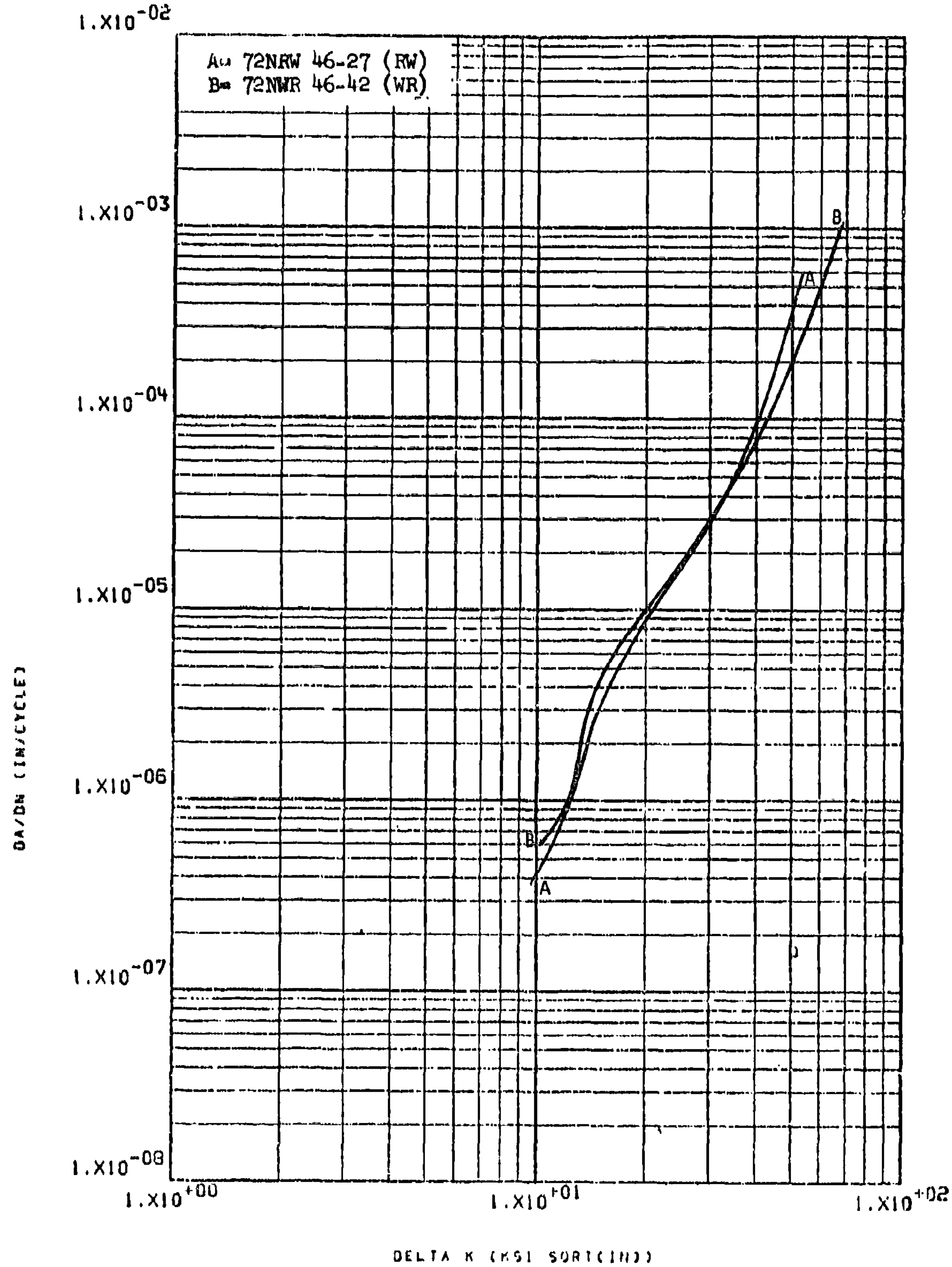

Figure 8.2.1.6-2 Effect of test direction on LHA-FCGR at R.T., R=0.08, 360 cpm in 1.5" Ti-6-4 R.A. plate

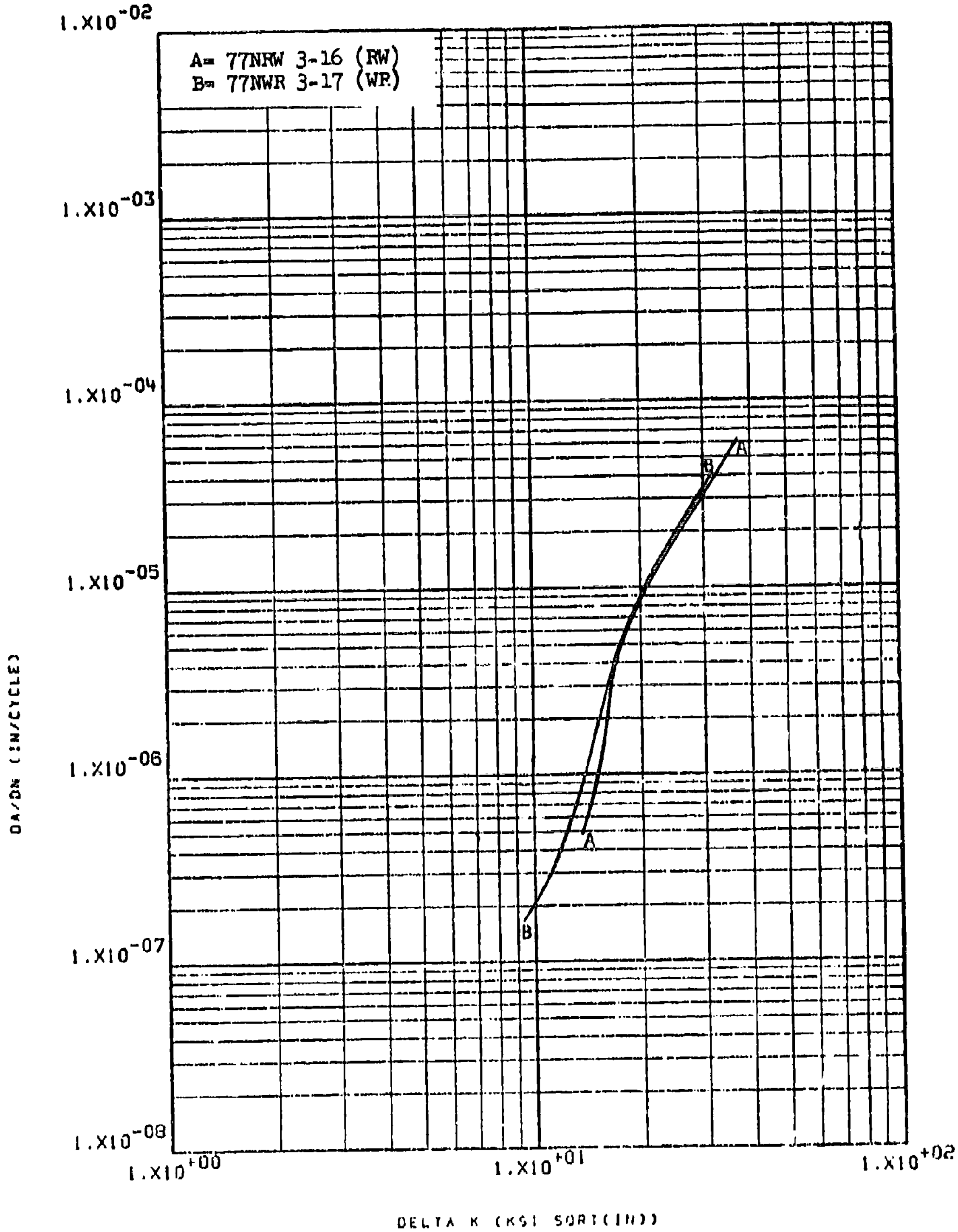

Figure 8.2.1.6-3 Effect of test direction on LHA-FCGR at R.T., R=0.08, 360 cpm in 2.5" Ti-6-4 ring rolled plus R.A. plate

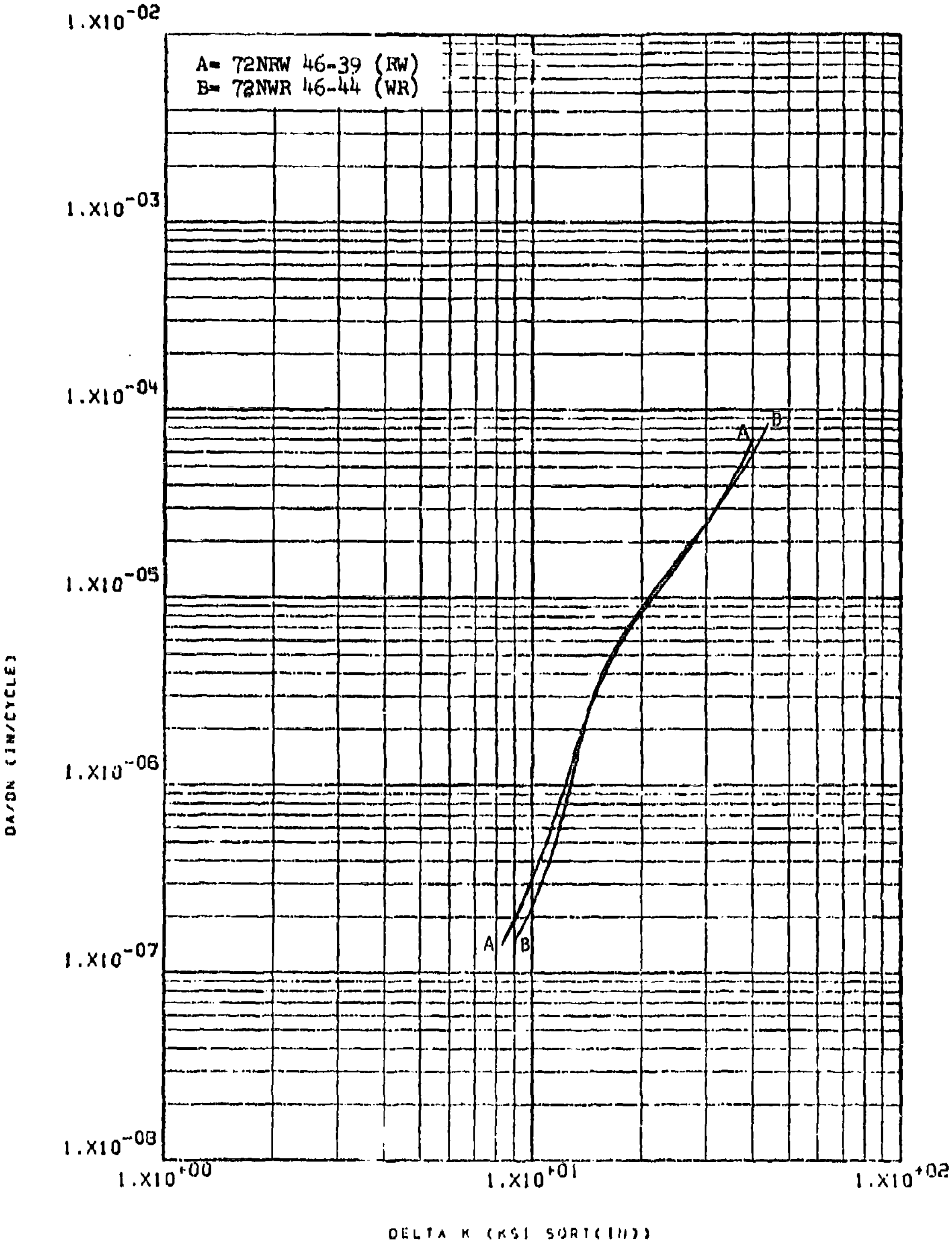

Figure 8.2.1.6-4 Effect of test direction on LHA-FCGR at R.T., R=0.08, 360 cpm in 1/2" thick specimens of 1.5" Ti-6-4 R.A. plate

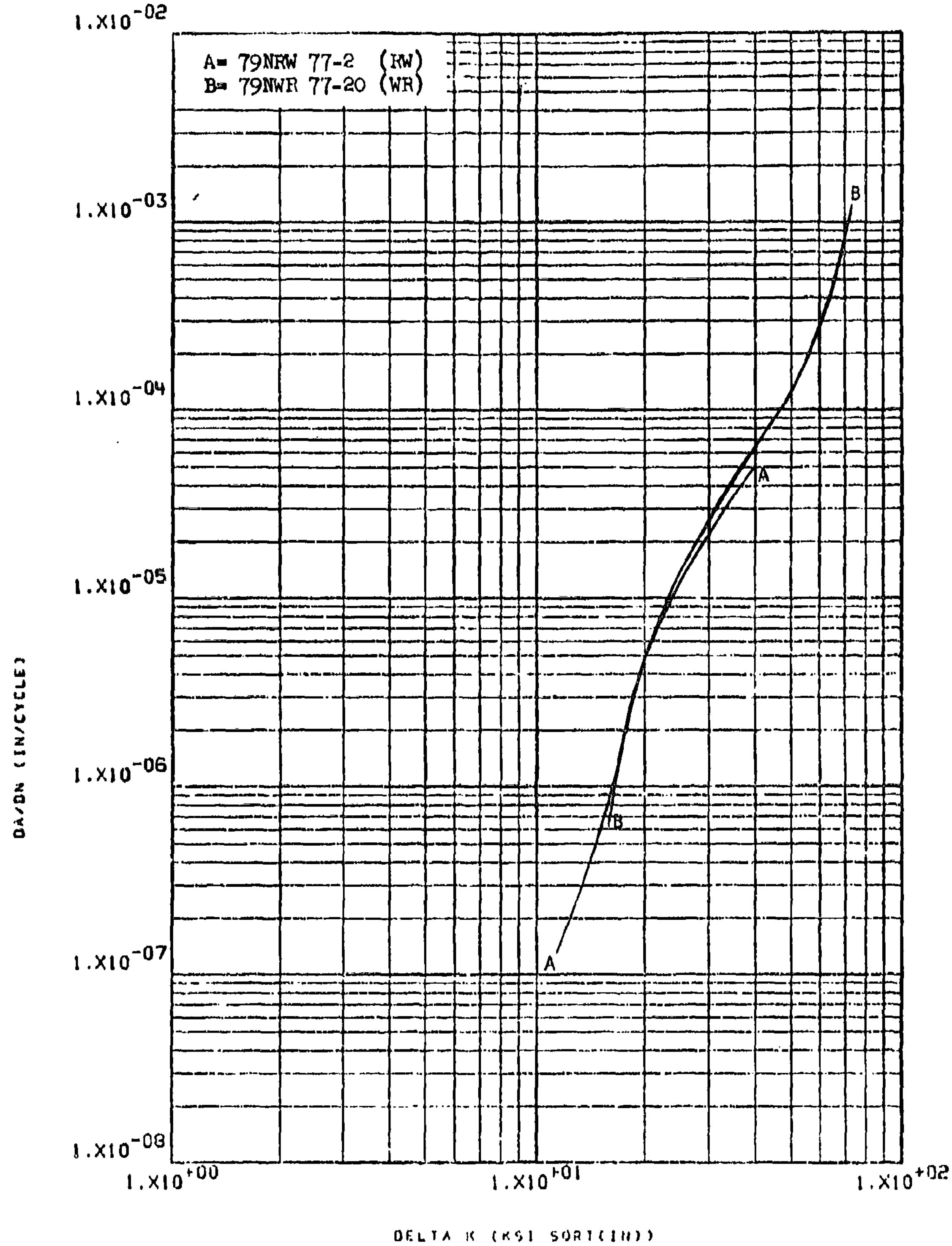

Figure 8.2.1.6-5 Effect of test direction on LHA-FCGR at R.T., R=0.08, 360 cpm in 4" x 10" x 34" Ti-6-4 R.A. hand forging

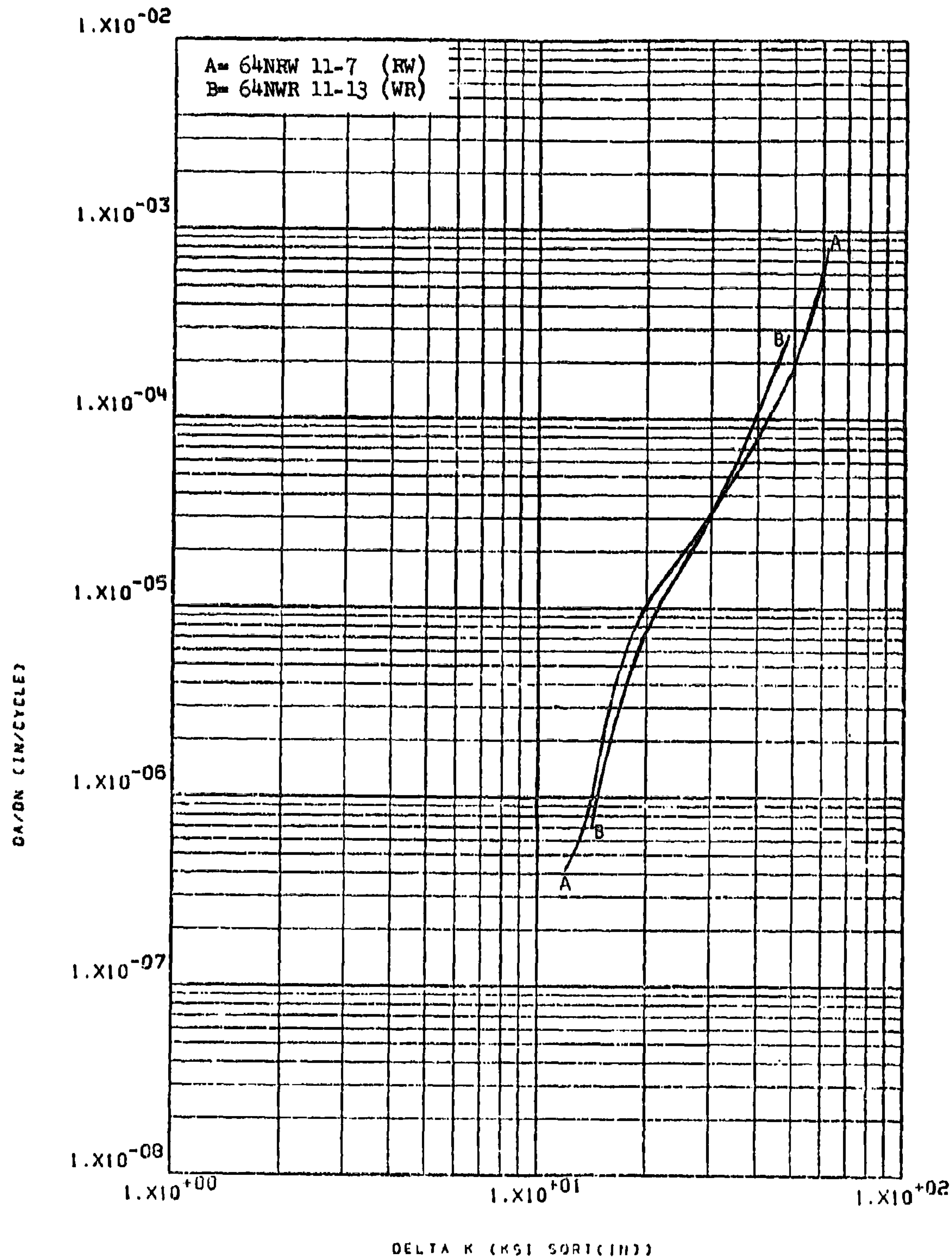

Figure 8.2.1.6-6 Effect of test direction on LHA-FCGR at R.T., R=0.08, 360 cpm in beta processed plus mill annealed Ti-6-4 "L" extrusion

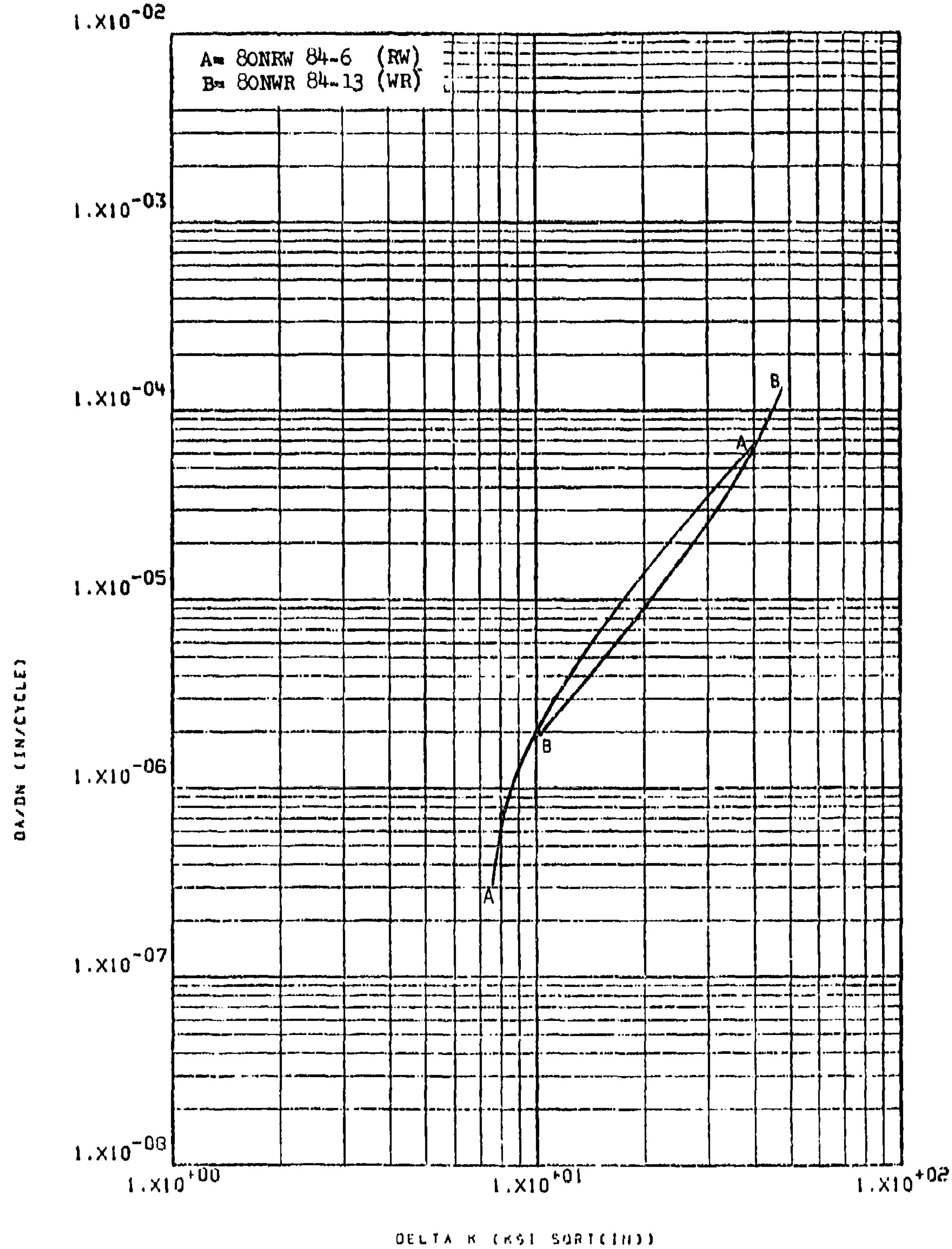

Figure 8.2.1.6-7 Effect of test direction on LHA-FCGR at R.T., R=0.08, 360 cpm in 0.1" Ti-6-4 M.A. sheet

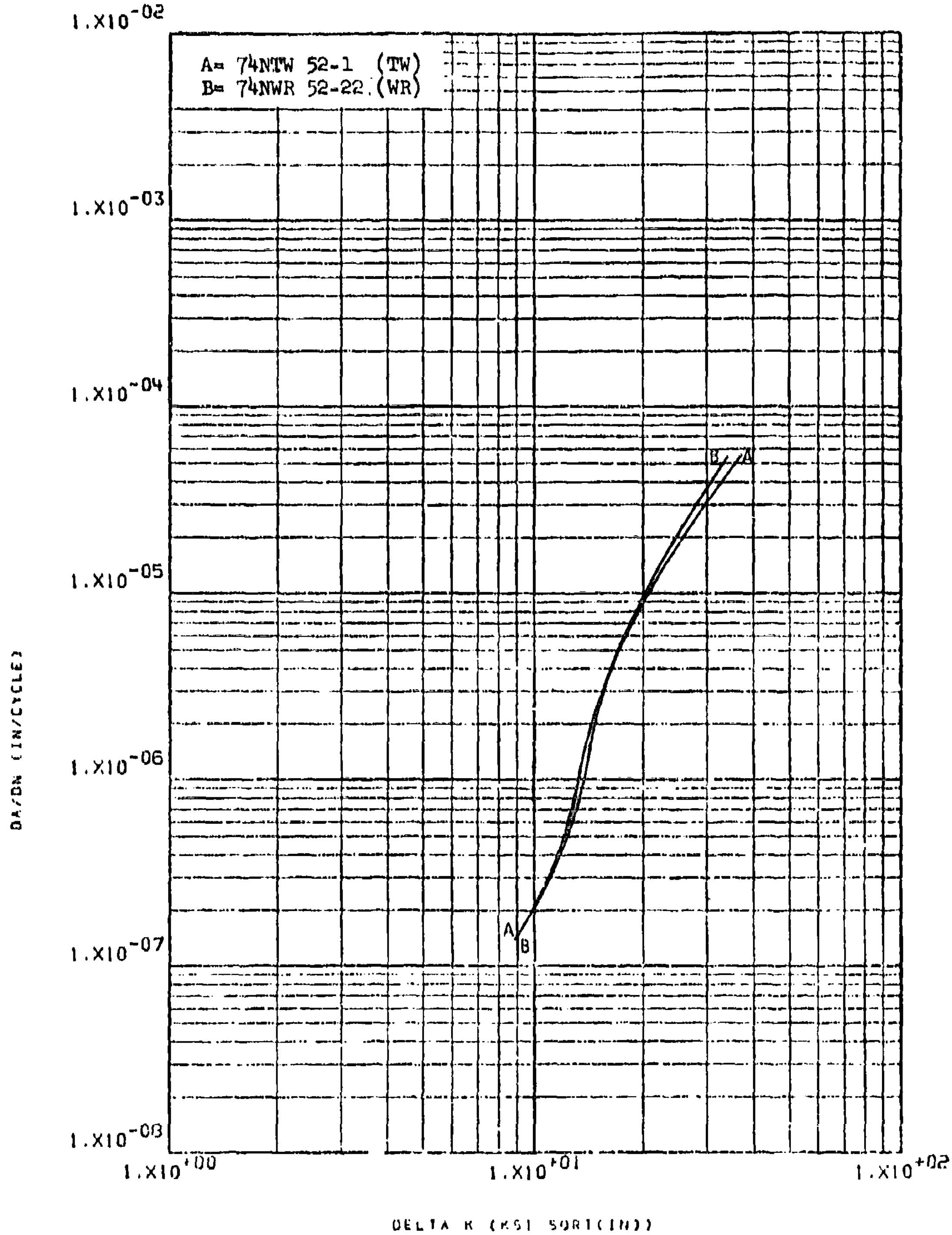

Figure 8.2.1.6-8 **Effect of test direction on LHA-FCGR at R.T., R=0.08,360 cpm in 1.5" Ti-6-4 diffusion bonded plate**

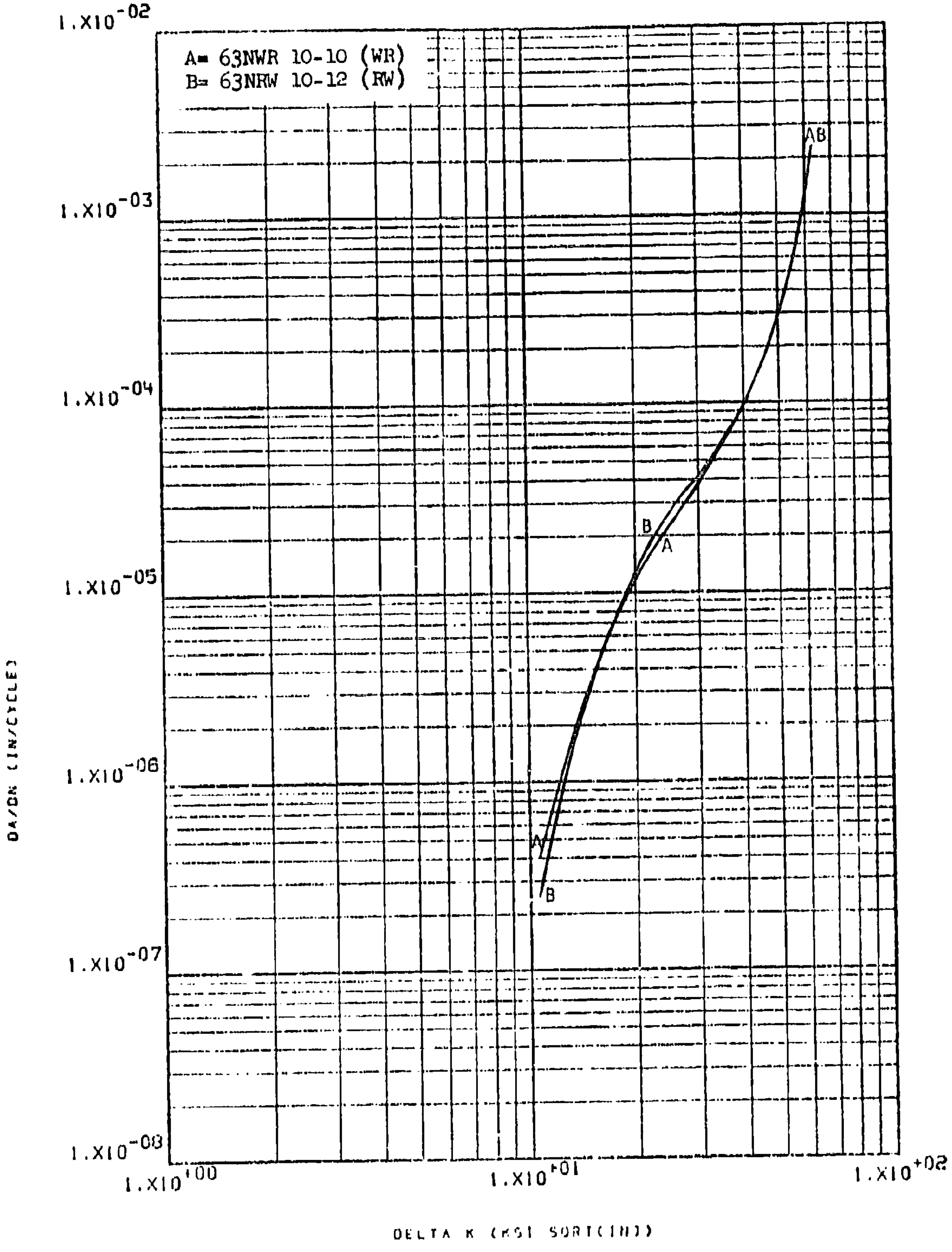

Figure 8.2.1.6-9 Effect of test direction on LHA-FCGR at R.T., R=0.3, 60 cpm in 1.25" Ti-6-4 diffusion bond thermal cycled plate

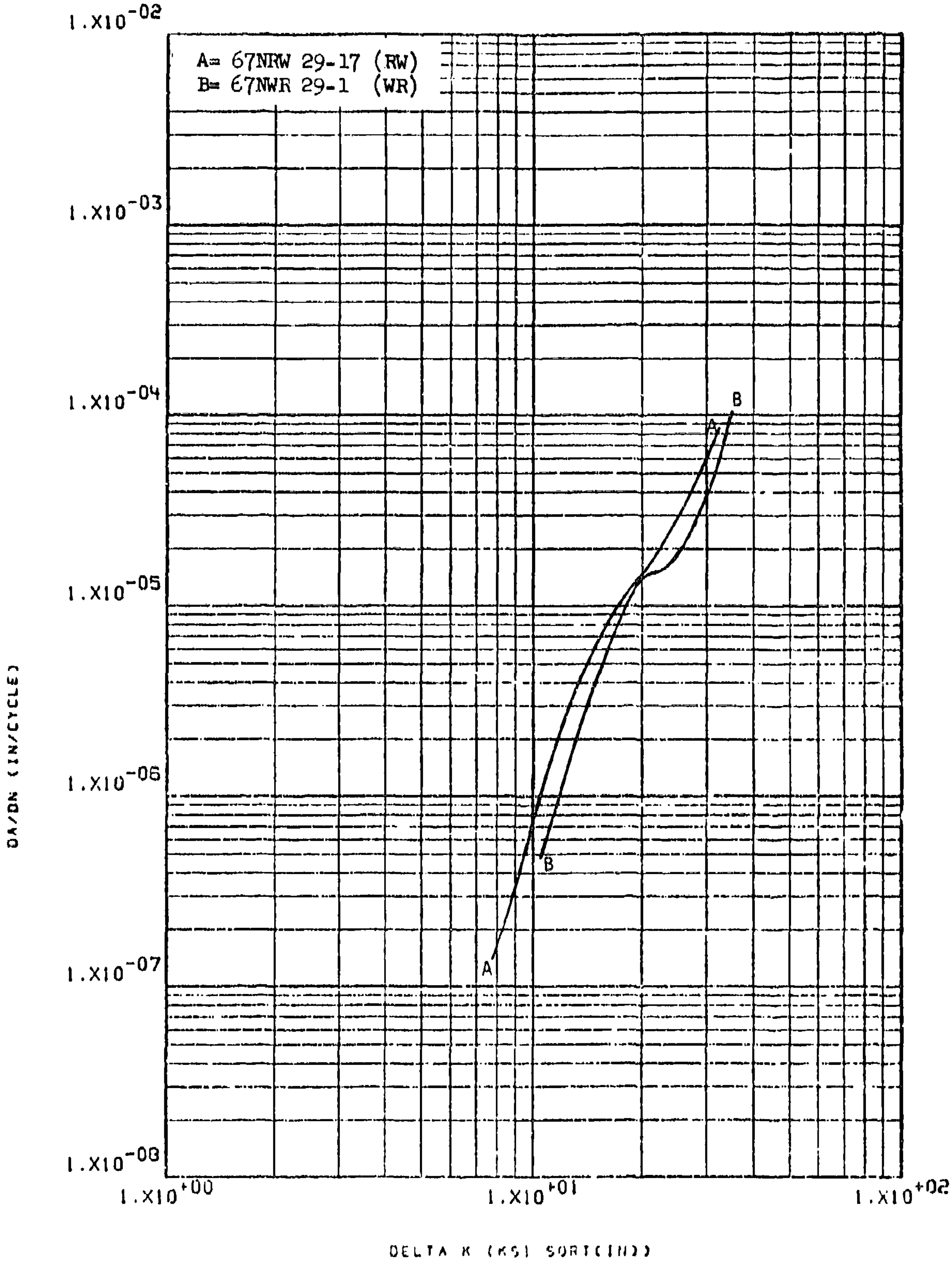

Figure 8.2.1.6-10 Effect of test direction on LHA-FCGR at R.T., R=0.5, 360 cpm in 1.5" Ti-6-4 R.A. plate

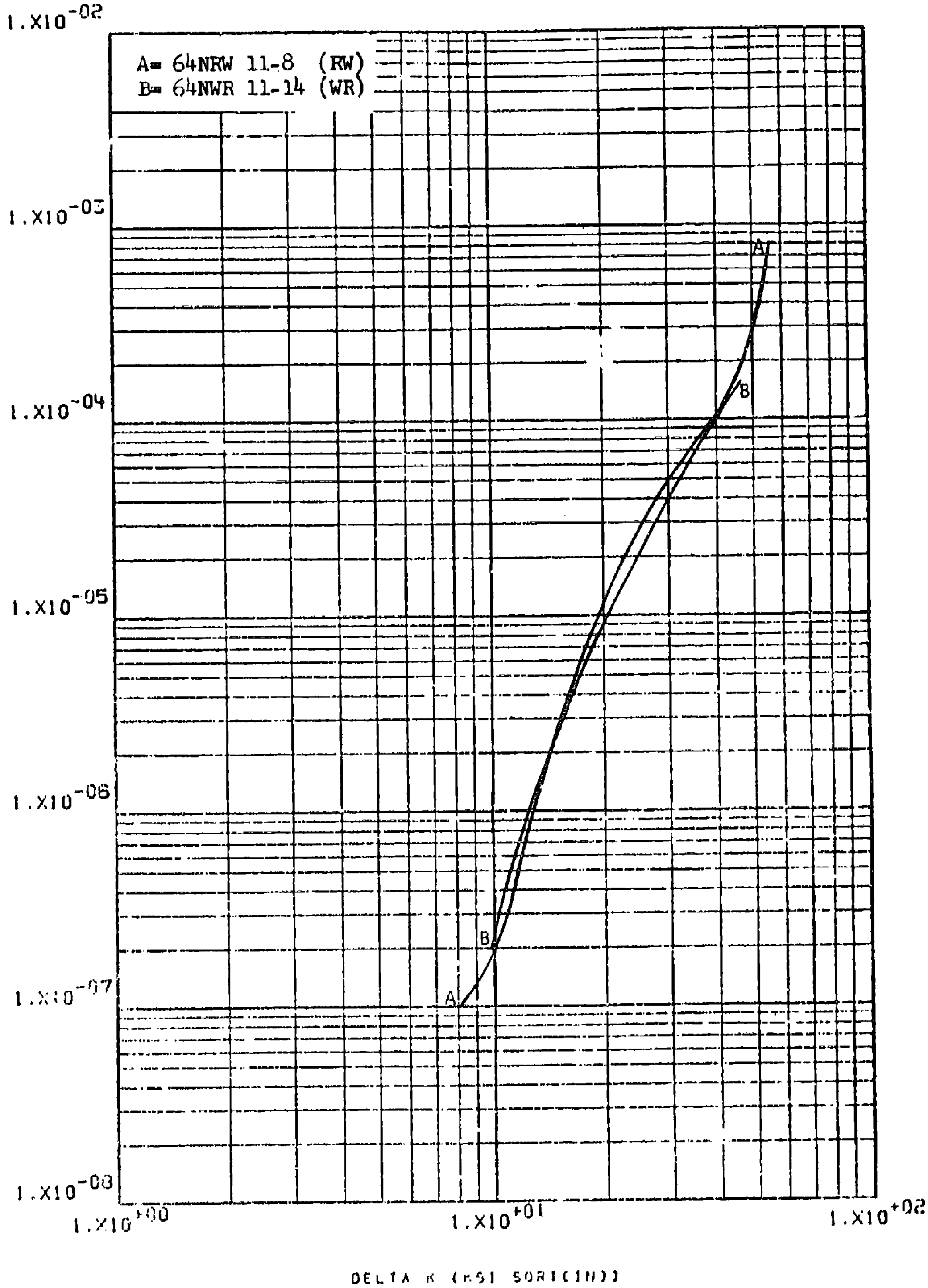

Figure 8.2.1.6-11 Effect of test direction on STW-FCGR at R.T., R=0.08, 60 cpm in beta processed plus mill annealed Ti-6-4 "L" extrusion

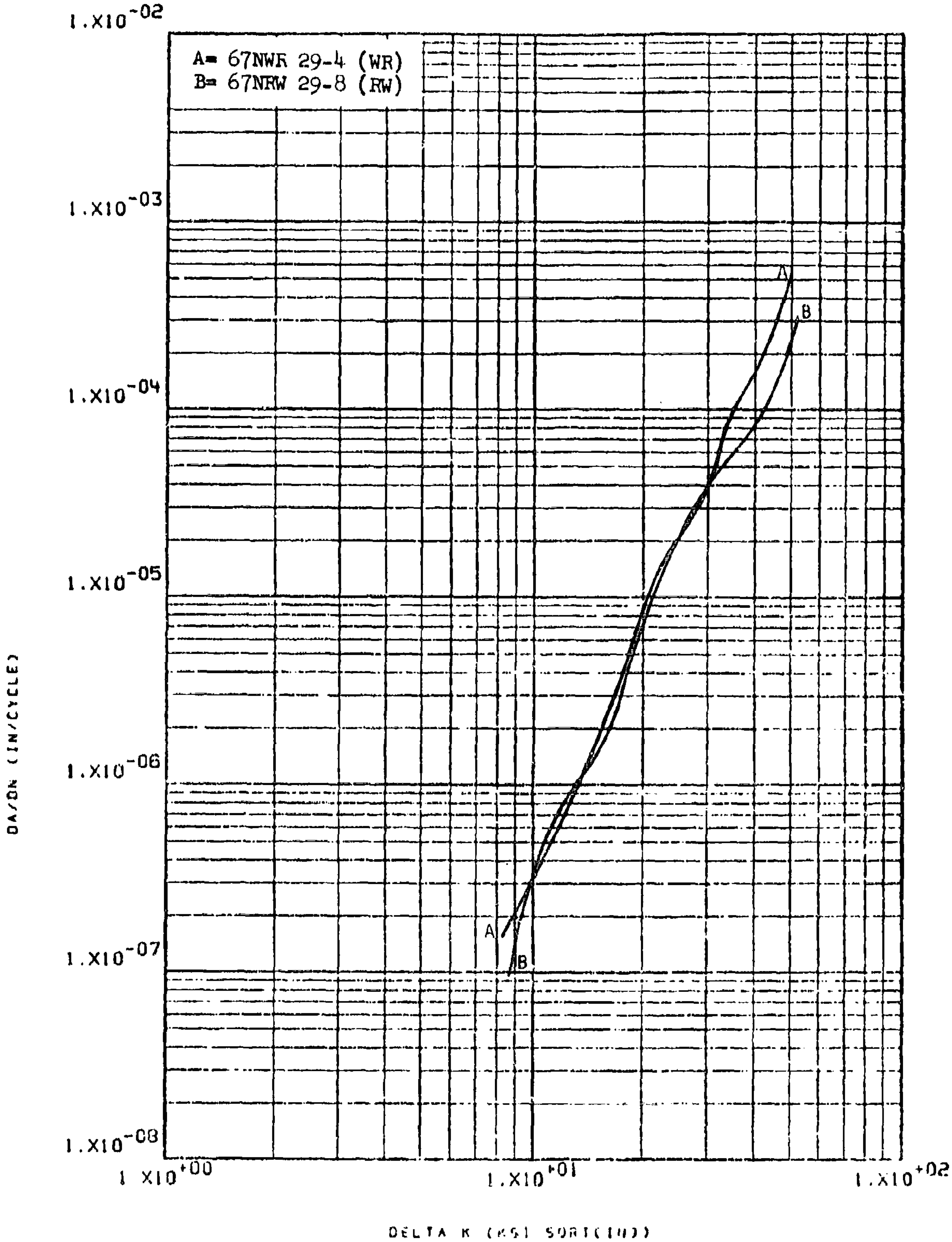

Figure 8.2.1.6-12 Effect of test direction on STW-FCGR at R.T., R=0.08, 60 cpm in 1.5" Ti-6-4 R.A. plate

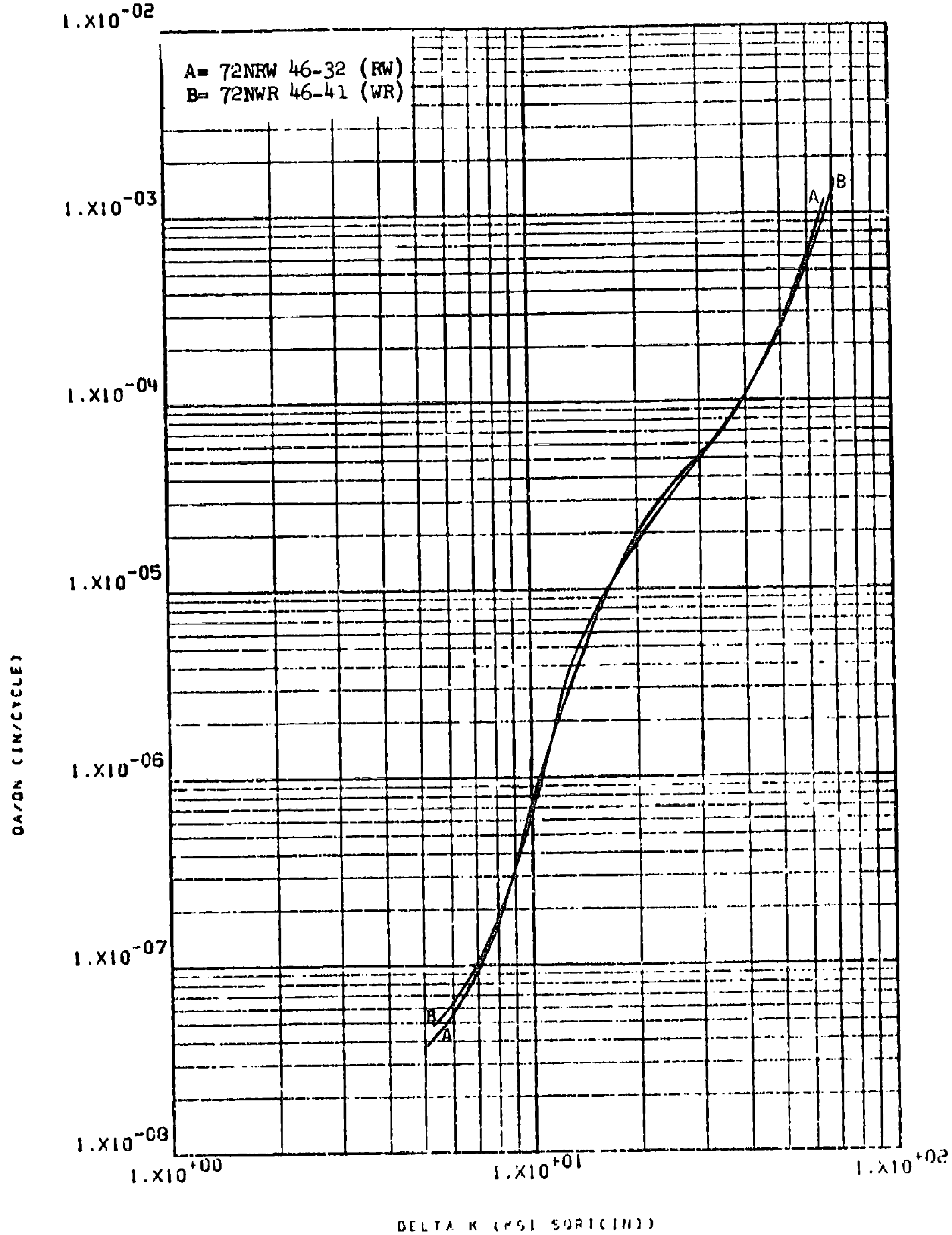

Figure 8.2.1.6-13 **Effect of test direction on STW-FCGR at R.T., R-0.08, 60 cpm in 1.5" Ti-6-4 R.A. plate**

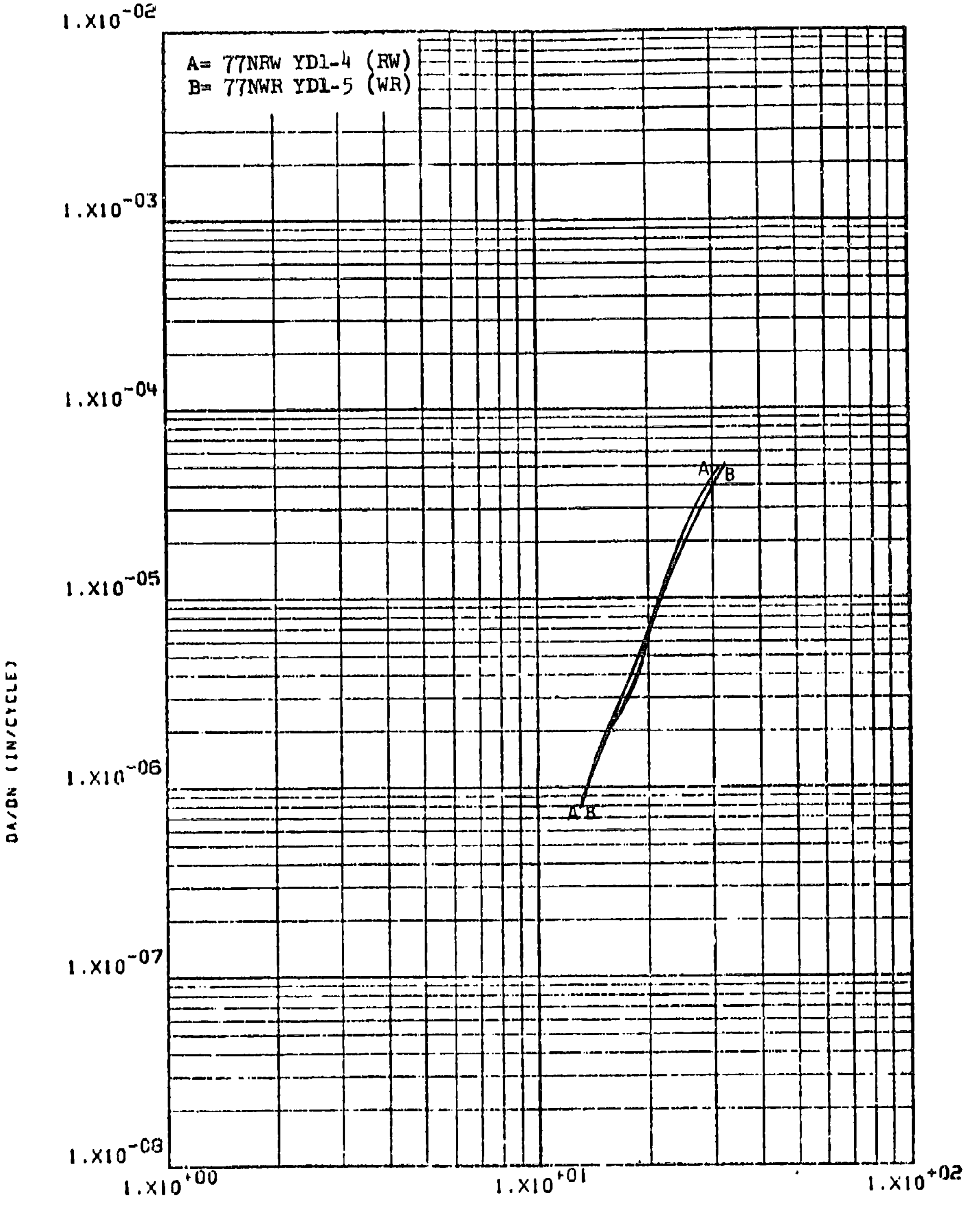

Figure 8.2.1.6-14 Effect of test direction on STW-FCGR at R.T., R=0.08, 60 cpm in 2.5" Ti-6-4 ring rolled plus R.A. plate

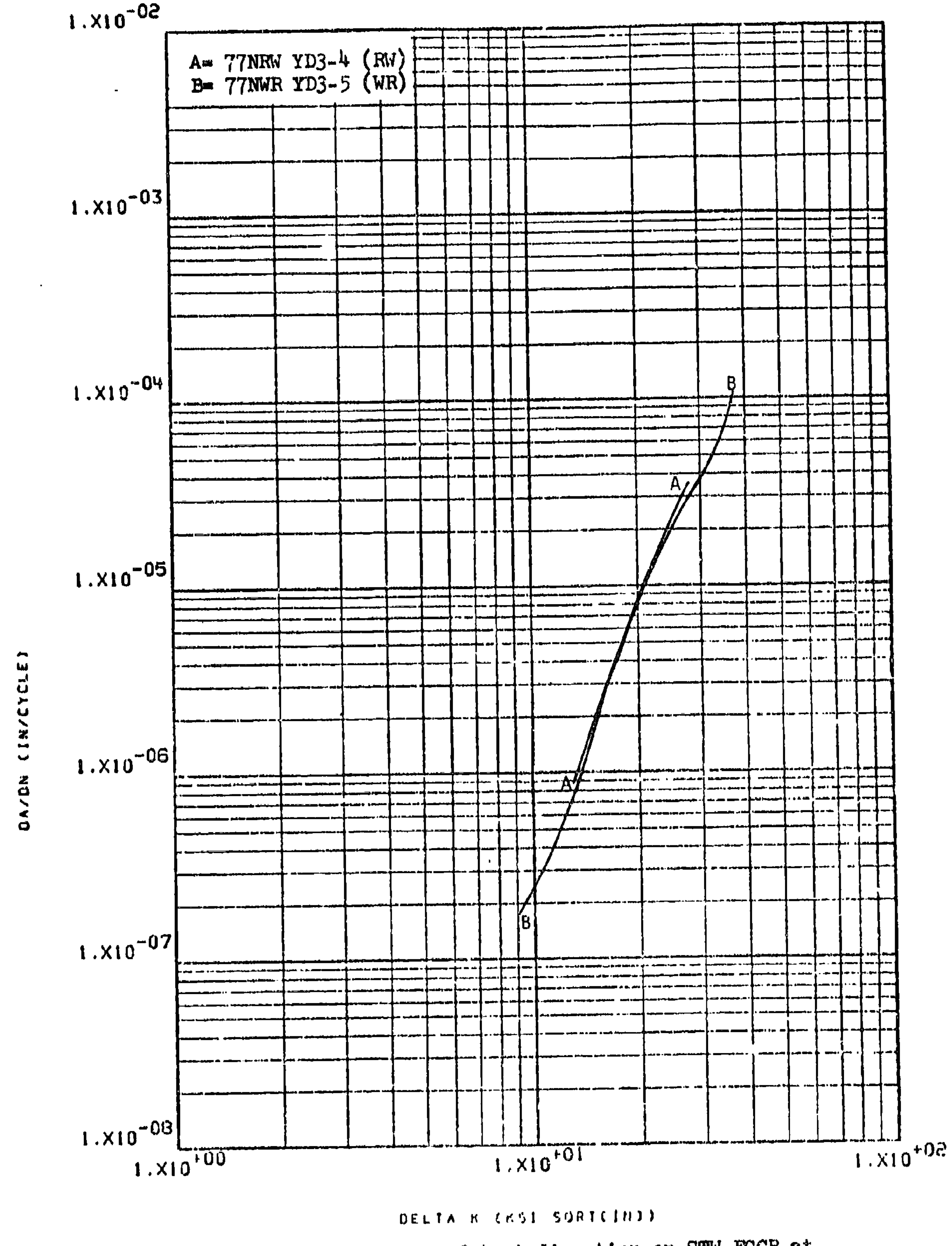

Figure 8.2.1.6-15 Effect of test direction on STW-FCGR at R.T., R-0.08, 60 cpm in 2.5" Ti-6-4 ring rolled plus R.A. plate

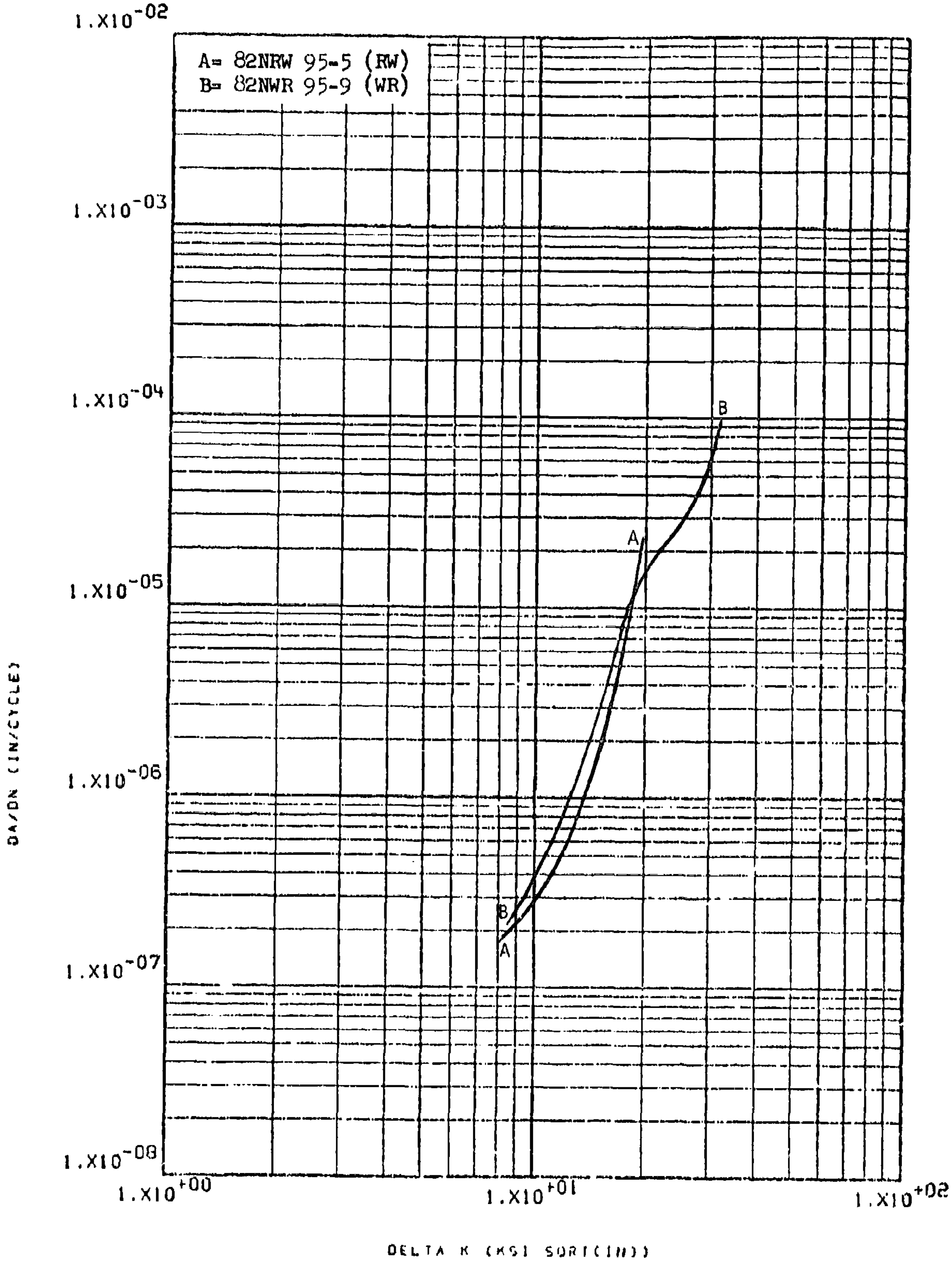

Figure 8.2.1.6-16 Effect of test direction on STW-FCGR at R.T., R=0.08, 60 cpm in 4" x 10" x 34" Ti-6-4 R.A. hand forged block

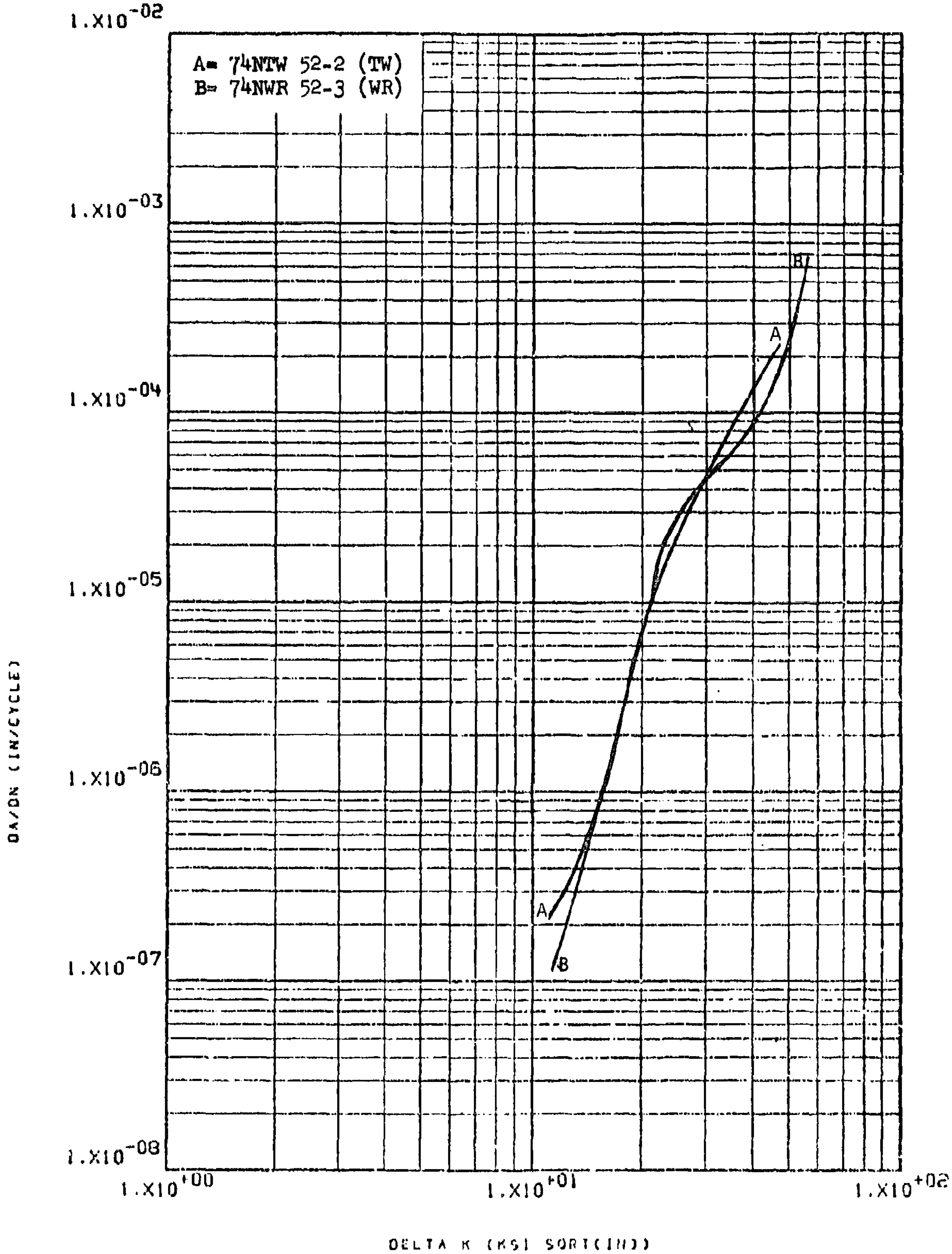

Figure 8.2.1.6-17 Effect of test direction on STW-FCGR at R.T., R=0.08, 60 cpm in 1.5" diffusion bonded Ti-6-4 plate

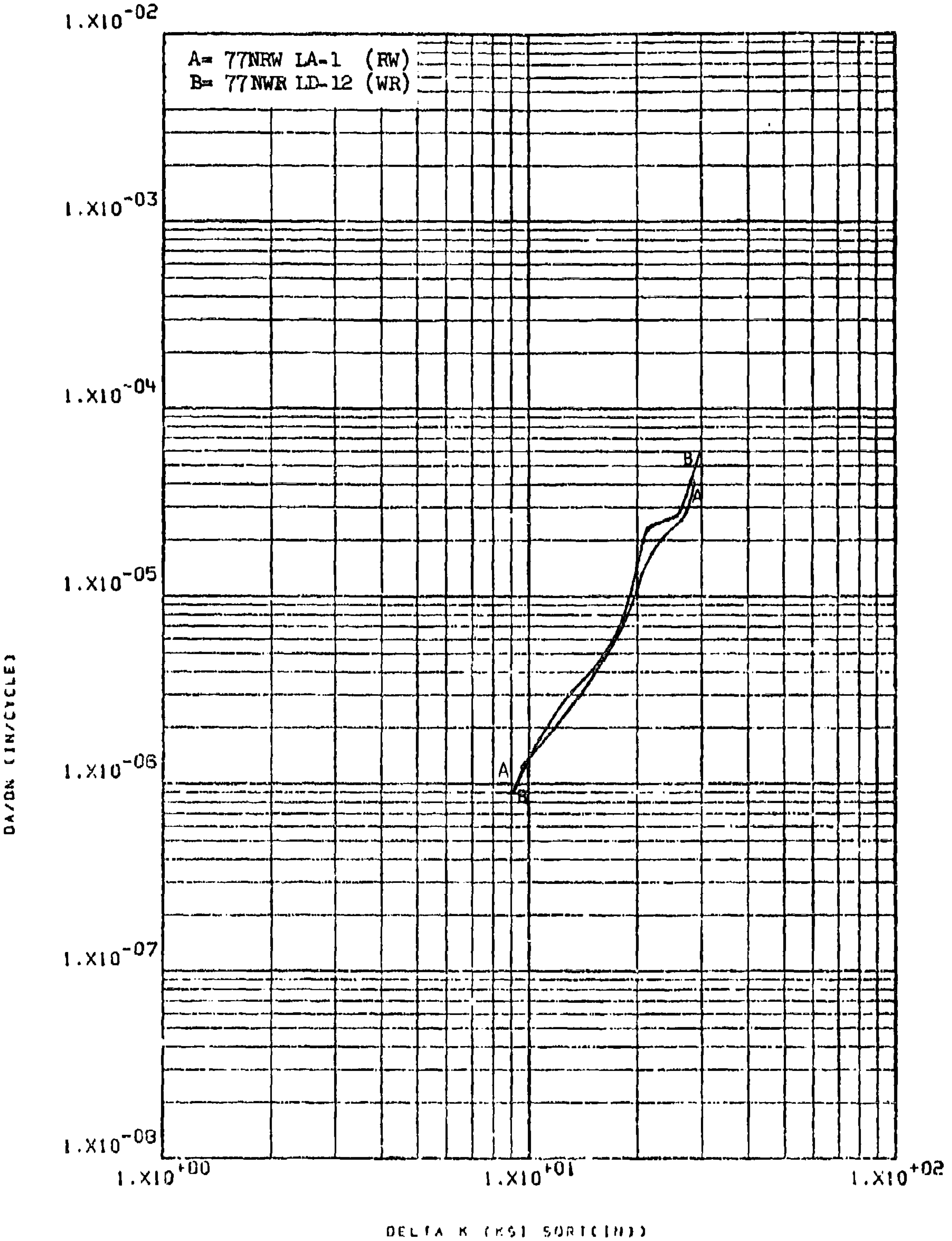

Figure 8.2.1.6-18 Effect of test direction on STW-FCGR at R.T., R=0.08, 60 cpm in 2.5" Ti-6-4 ring rolled plus diffusion bonded plate

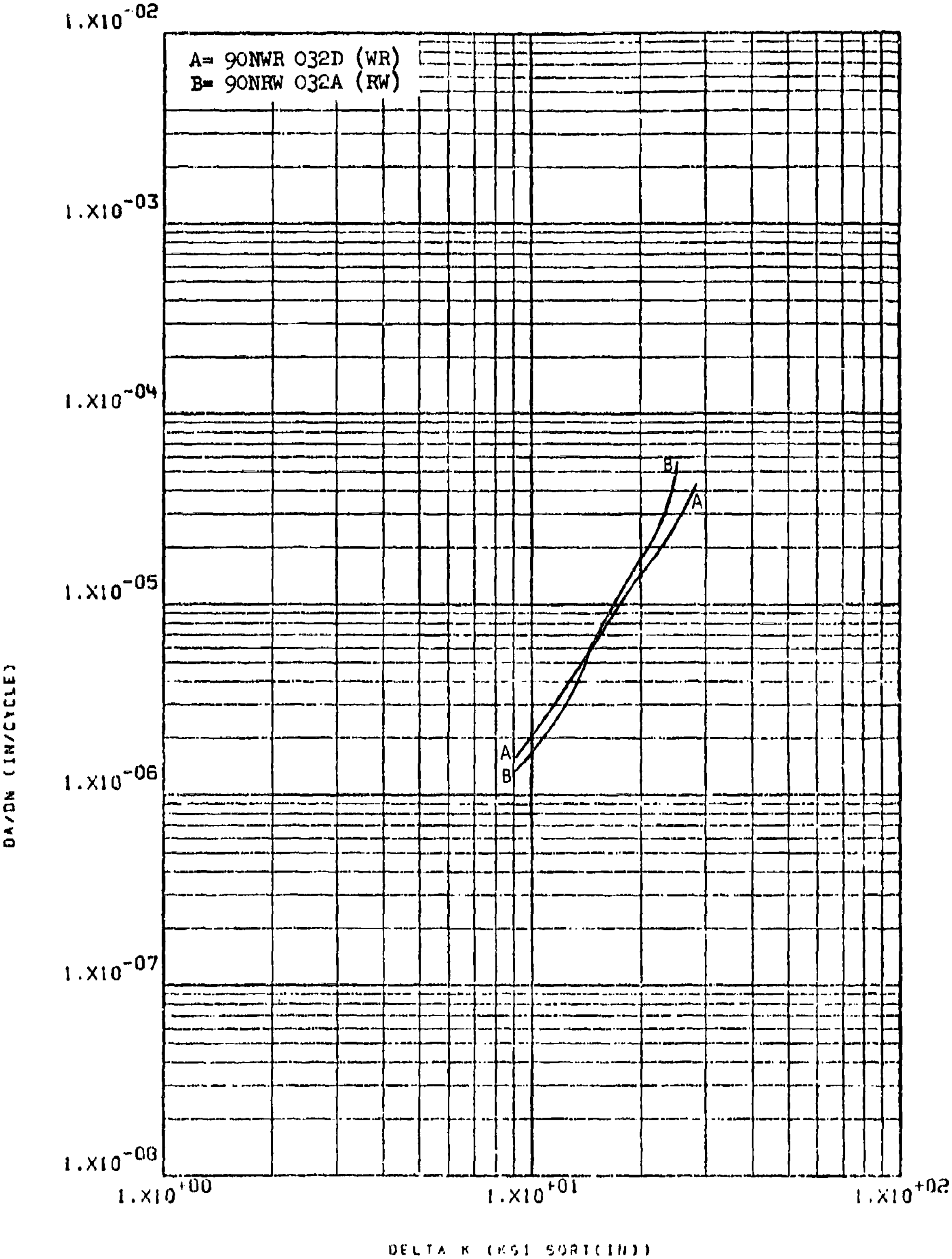

Figure 8.2.1.6-19 Effect of test direction on STW-FCGR at R.T., R=0.08, 60 cpm in 2.5" Ti-6-4 ring rolled plus diffusion bonded plate

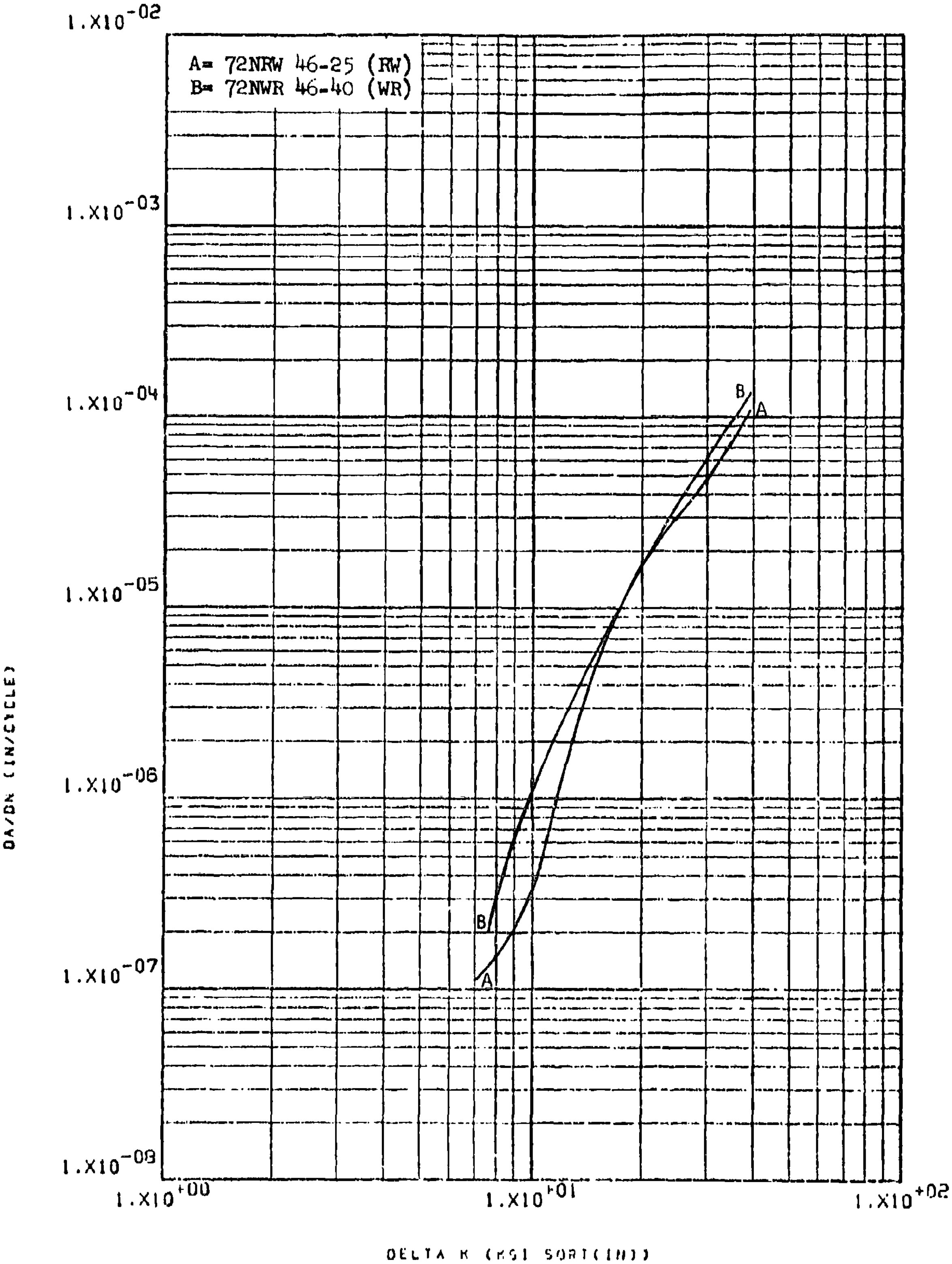

Figure 8.2.1.6-20 Effect of test direction on STW-FCGR at R.T., R=0.08, 60 cpm in 1.5" Ti-6-4 diffusion bond thermal cycled plate

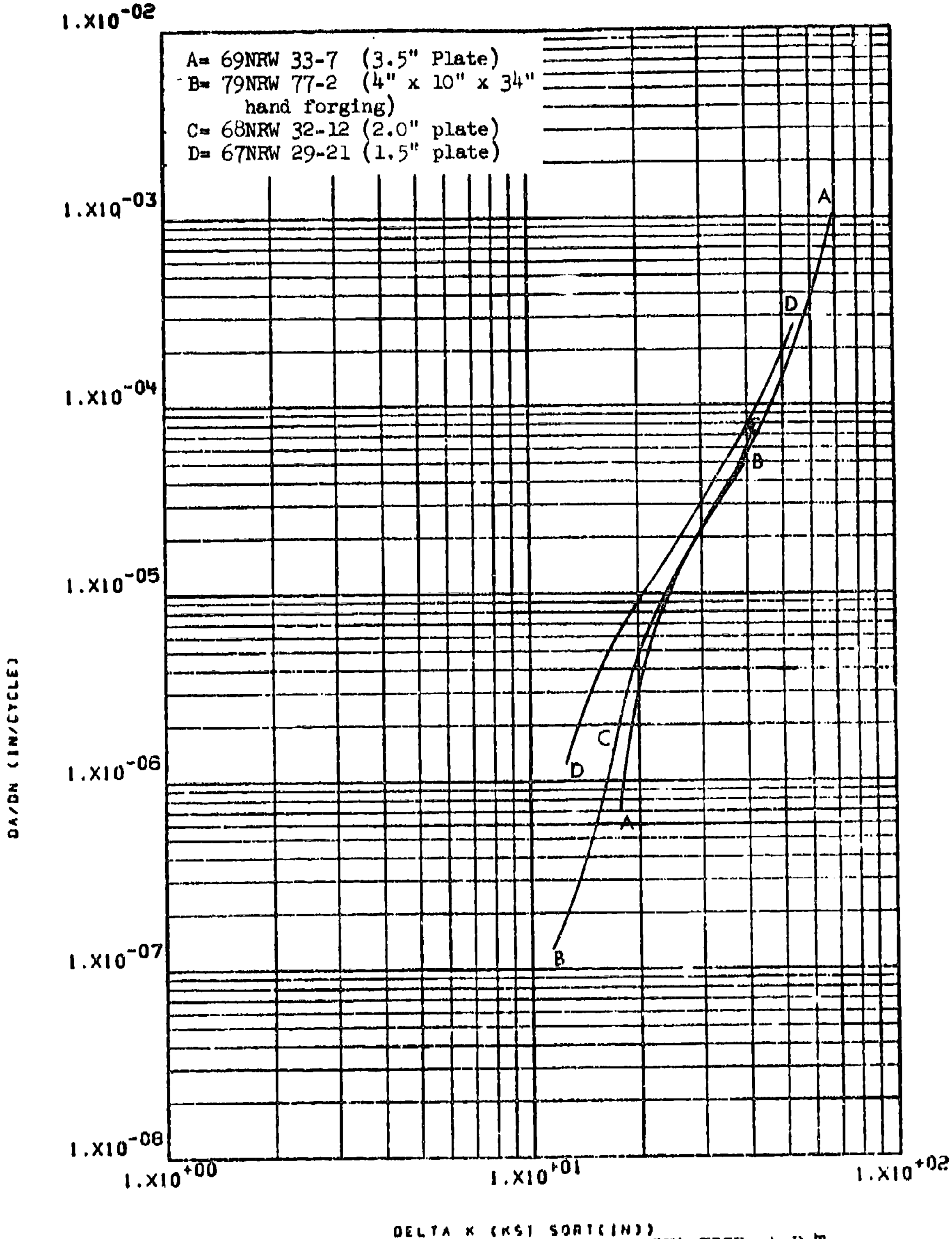

Figure 8.2.1.7-1 Effect of product form on LHA-FCGR at R.T., R=0.08, 360 cpm, RW direction in recrystallization annealed Ti-6-4

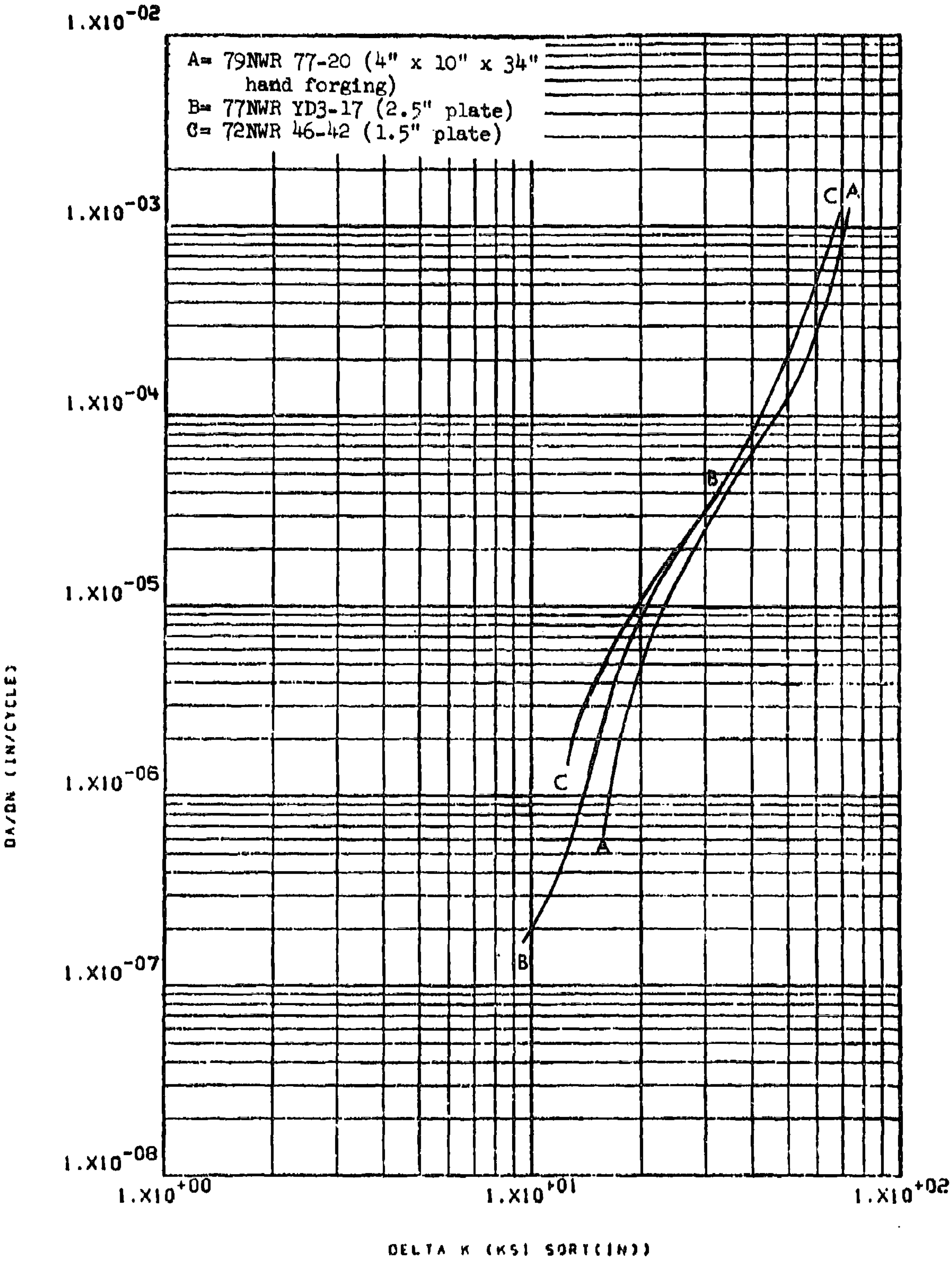

Figure 8.2.1.7-2 Effect of product form on LHA-FCGR at R.T., R=0.08, 360 cpm, WR direction in recrystallization annealed Ti-6-4

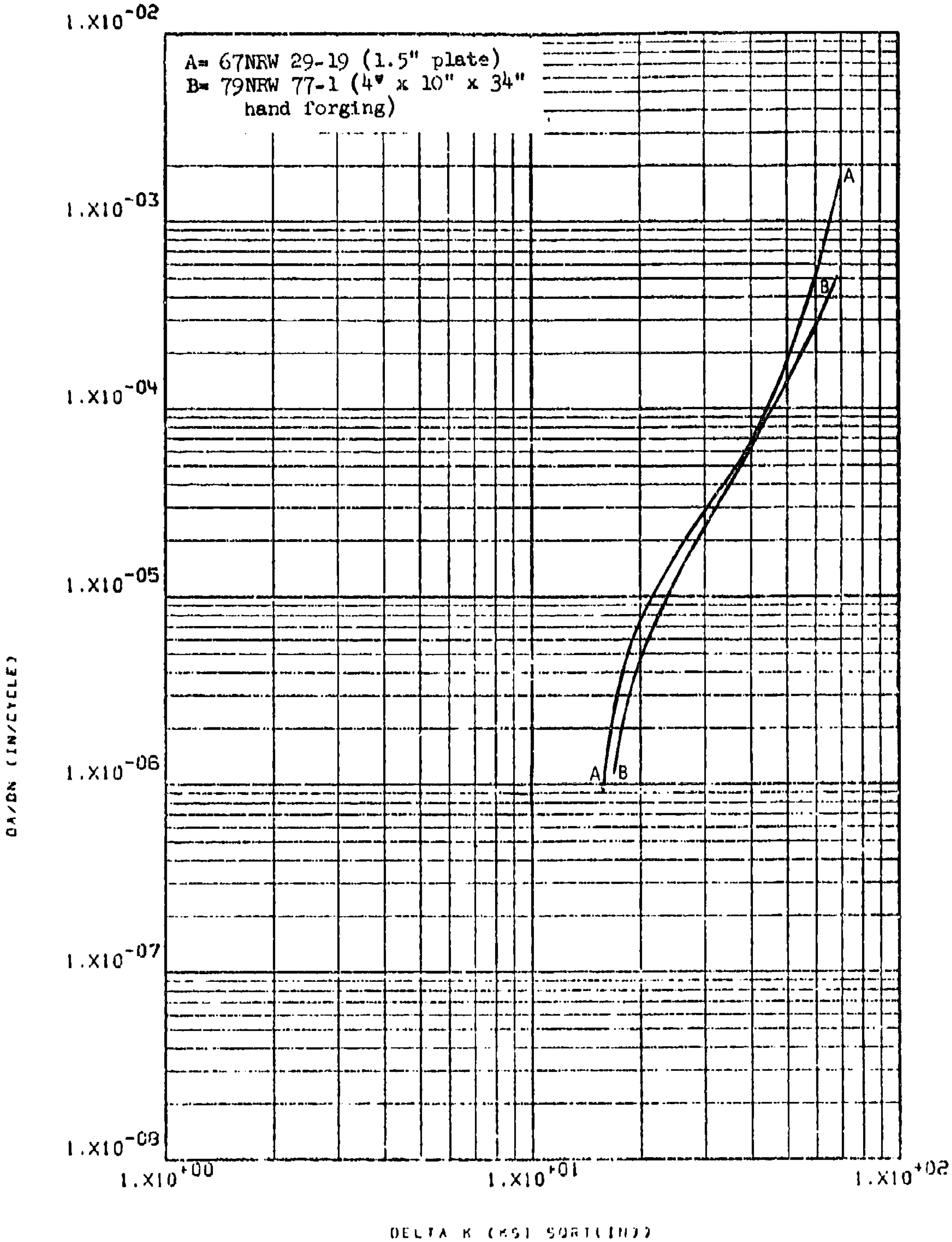

Figure 8.2.1.7-3 Effect of product form on LHA-FCGR at R.T., R=0.08, 60 cpm, RW direction in recrystallization annealed Ti-6-4

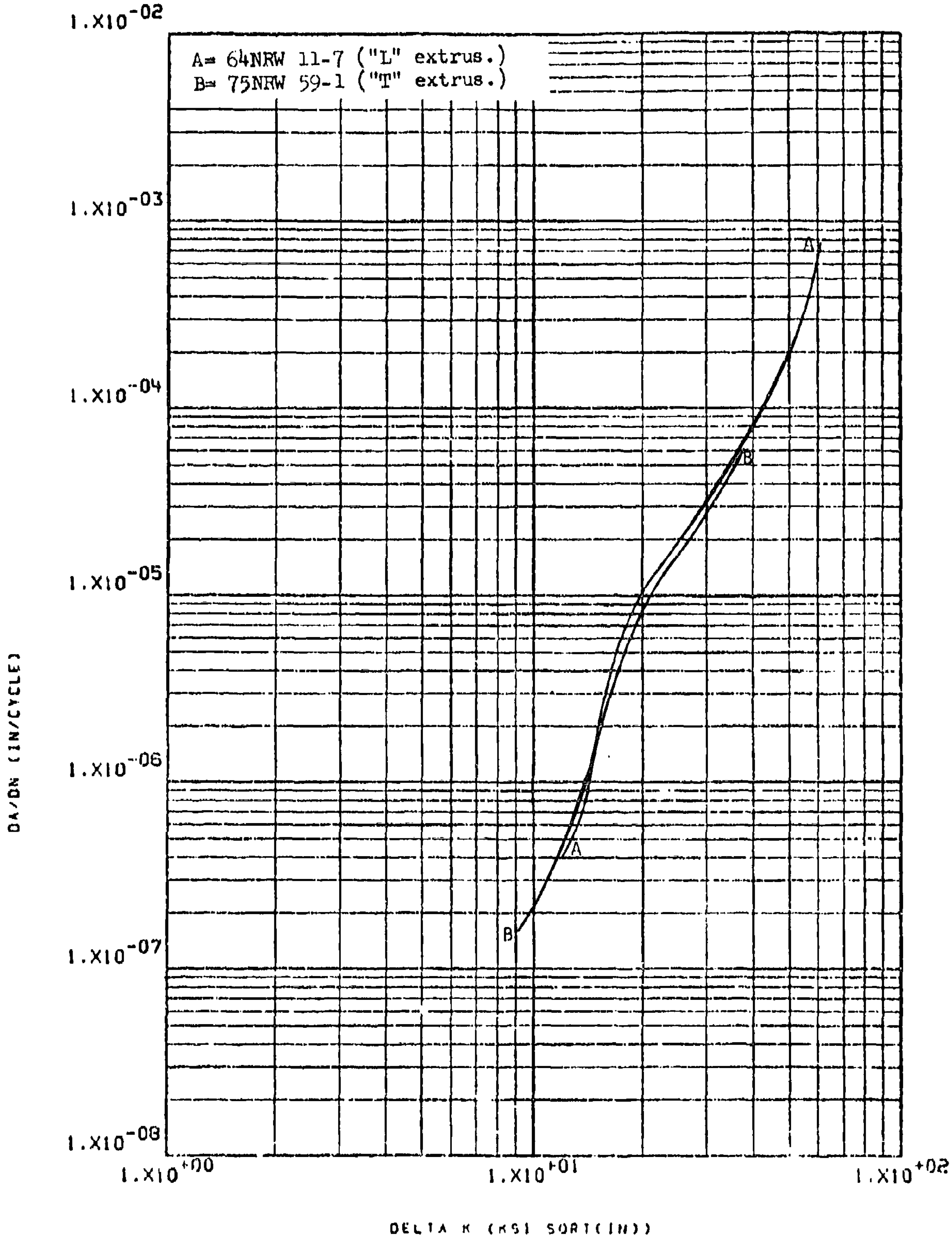

Figure 8.2.1.7-4 Effect of product form on LHA-FCGR at R.T., R=0.08, 360 cpm, RW direction in beta processed plus mill annealed Ti-6-4

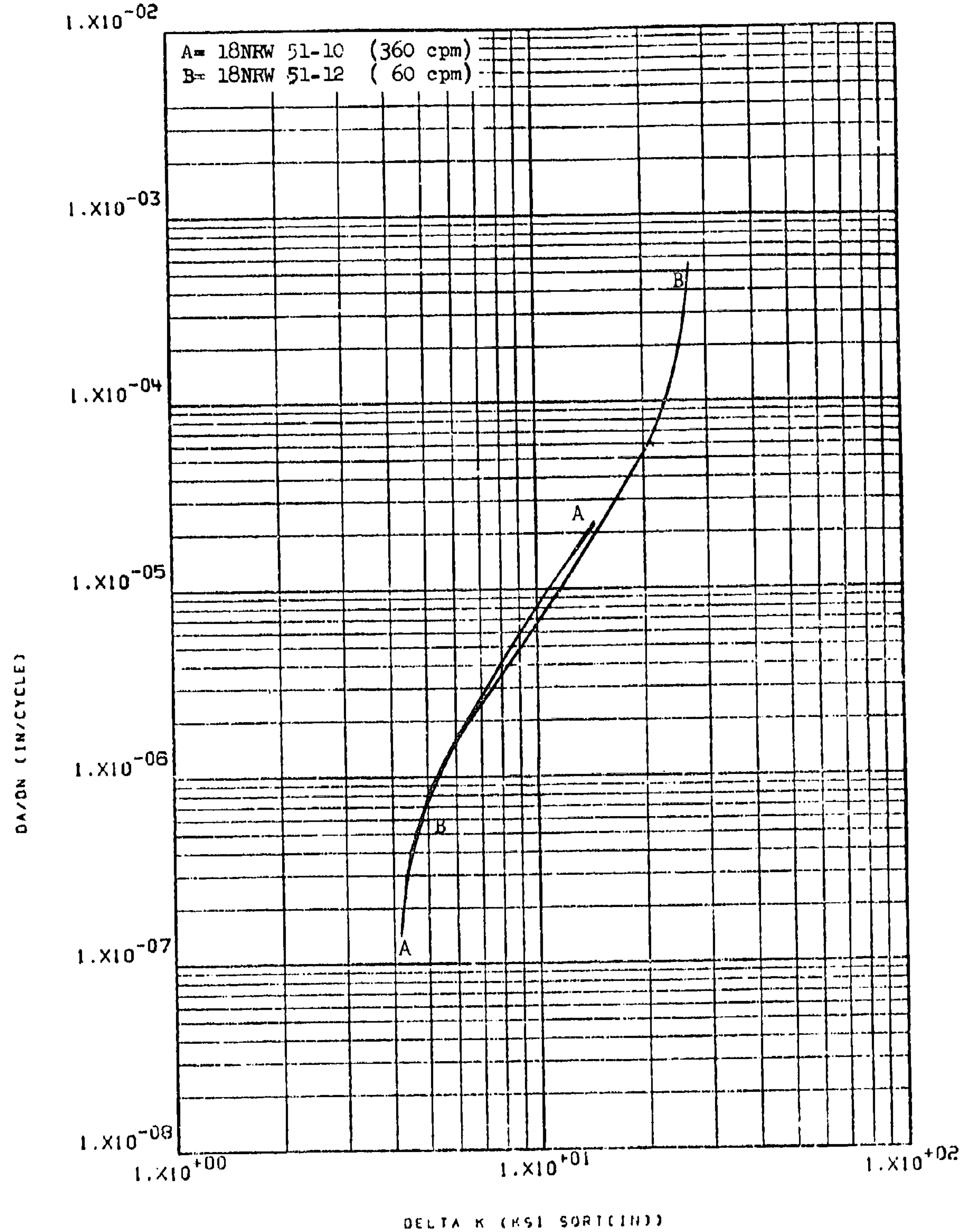

Figure 8.2.7.1-4 Effect of cyclic frequency on LHA-FCGR at 265°F, R=0.08, RW direction in 7075-T7651 2" plate

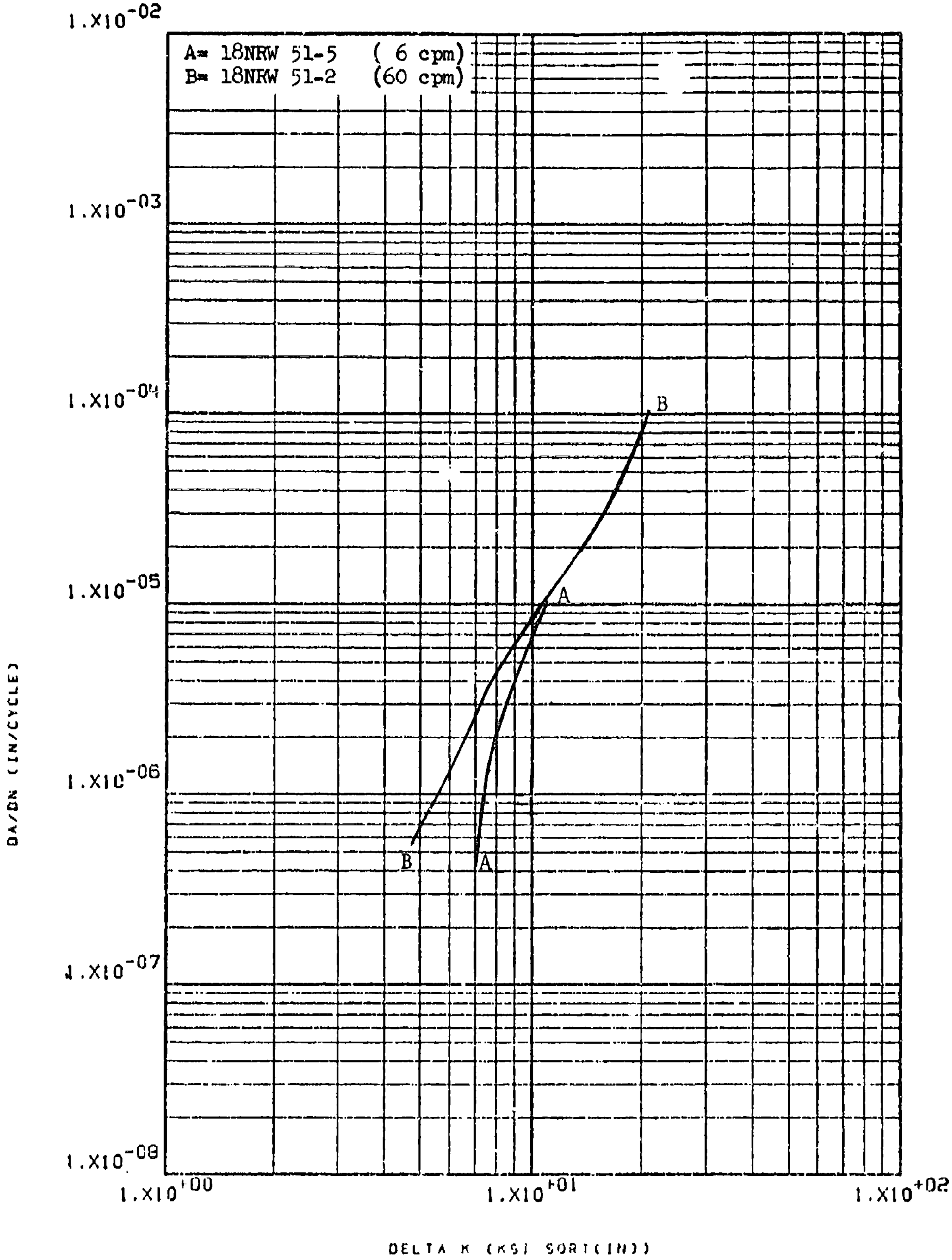

Figure 8.2.7.1-5 Effect of cyclic frequency on STW-FCGR at R.T., R=0.08, RW direction in 7075-T7651 2" plate

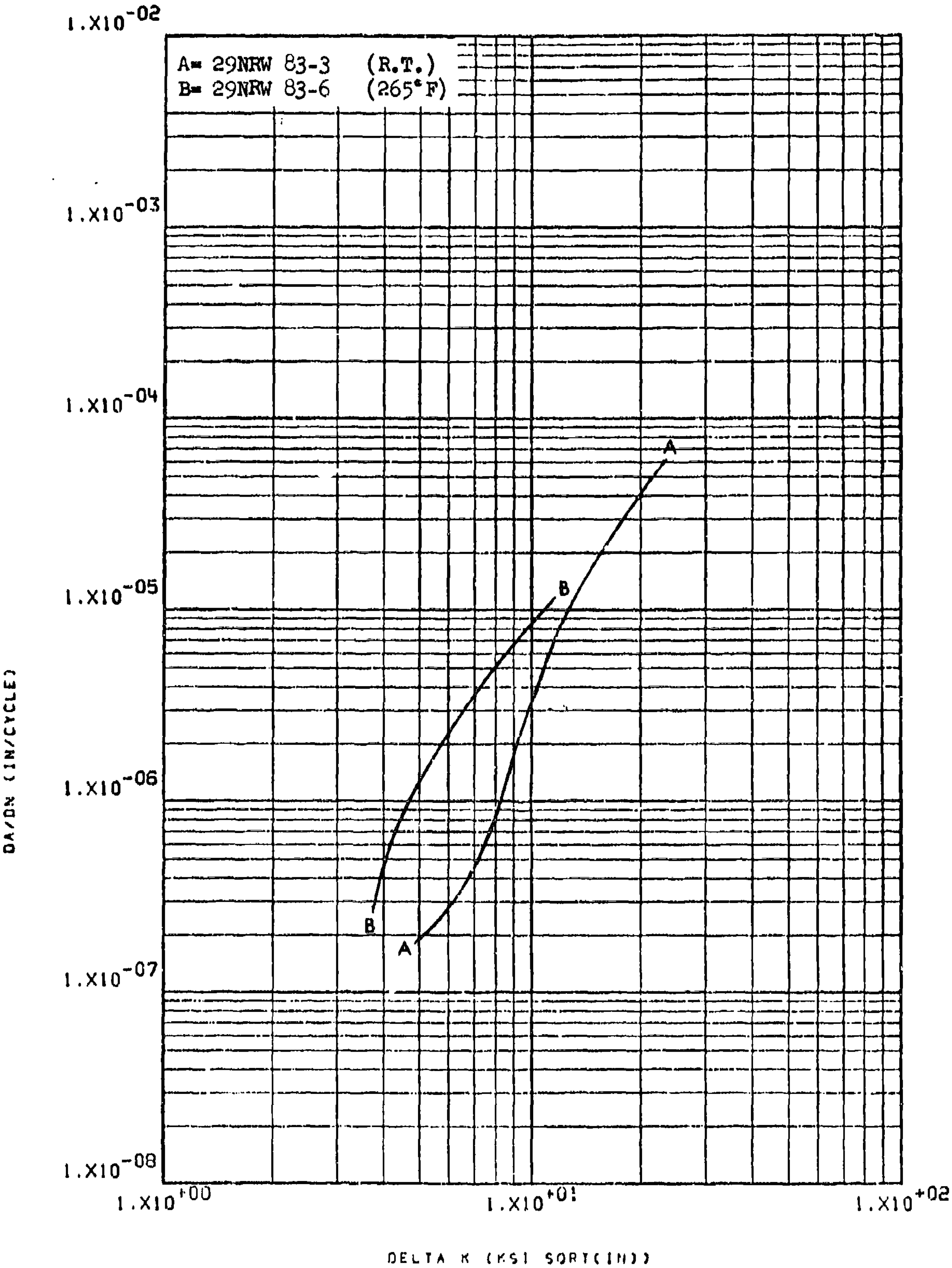

Figure 8.2.7.2-1 Effect of test temperature on LHA-FCGR at R=0.08, 360 cpm, RW direction in 7075-T73511 3" x 17" extrusion

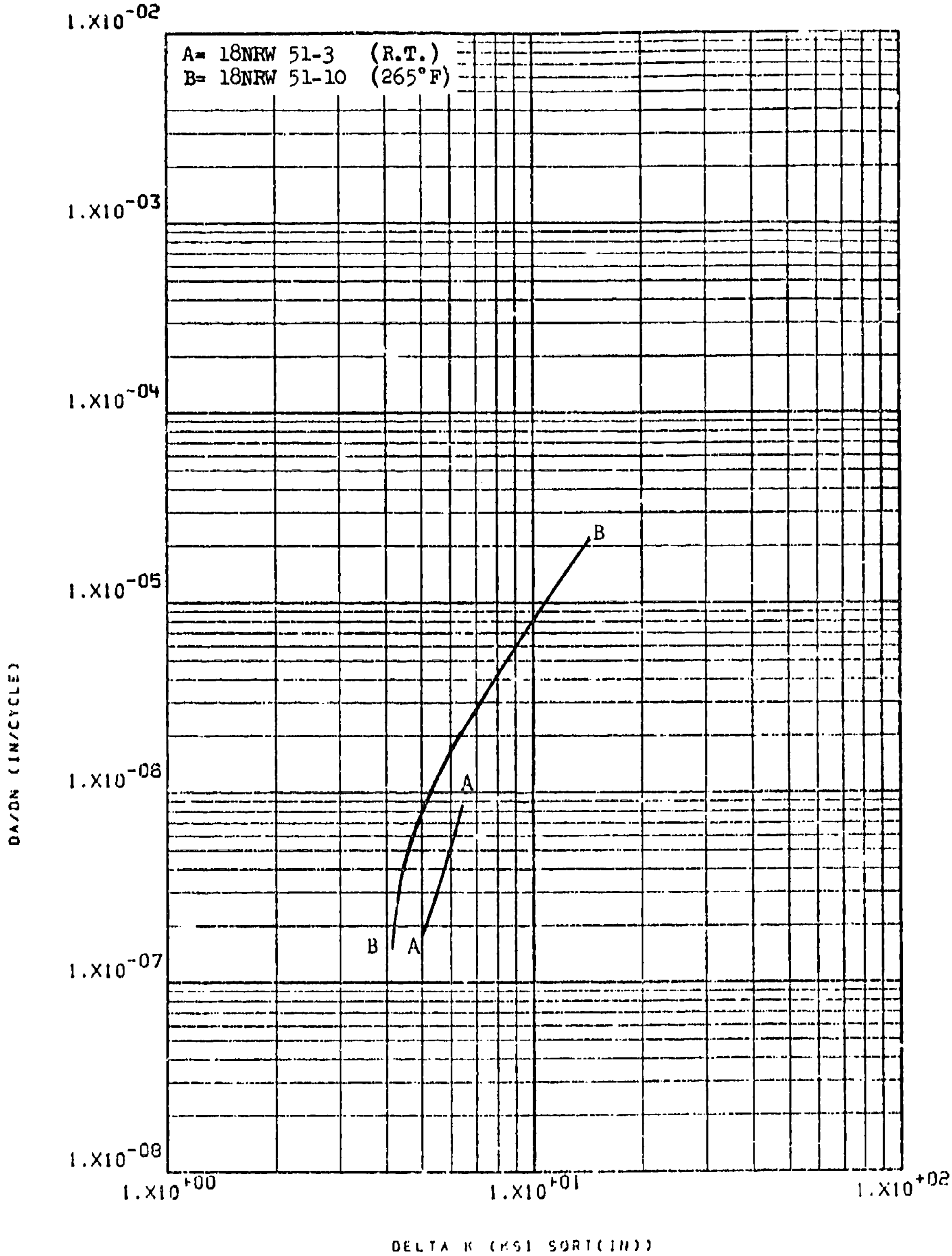

Figure 8.2.7.2-2 Effect of test temperature on LHA-FCGR at R=0.08, 360 cpm, RW direction in 7075-T7651 2" plate

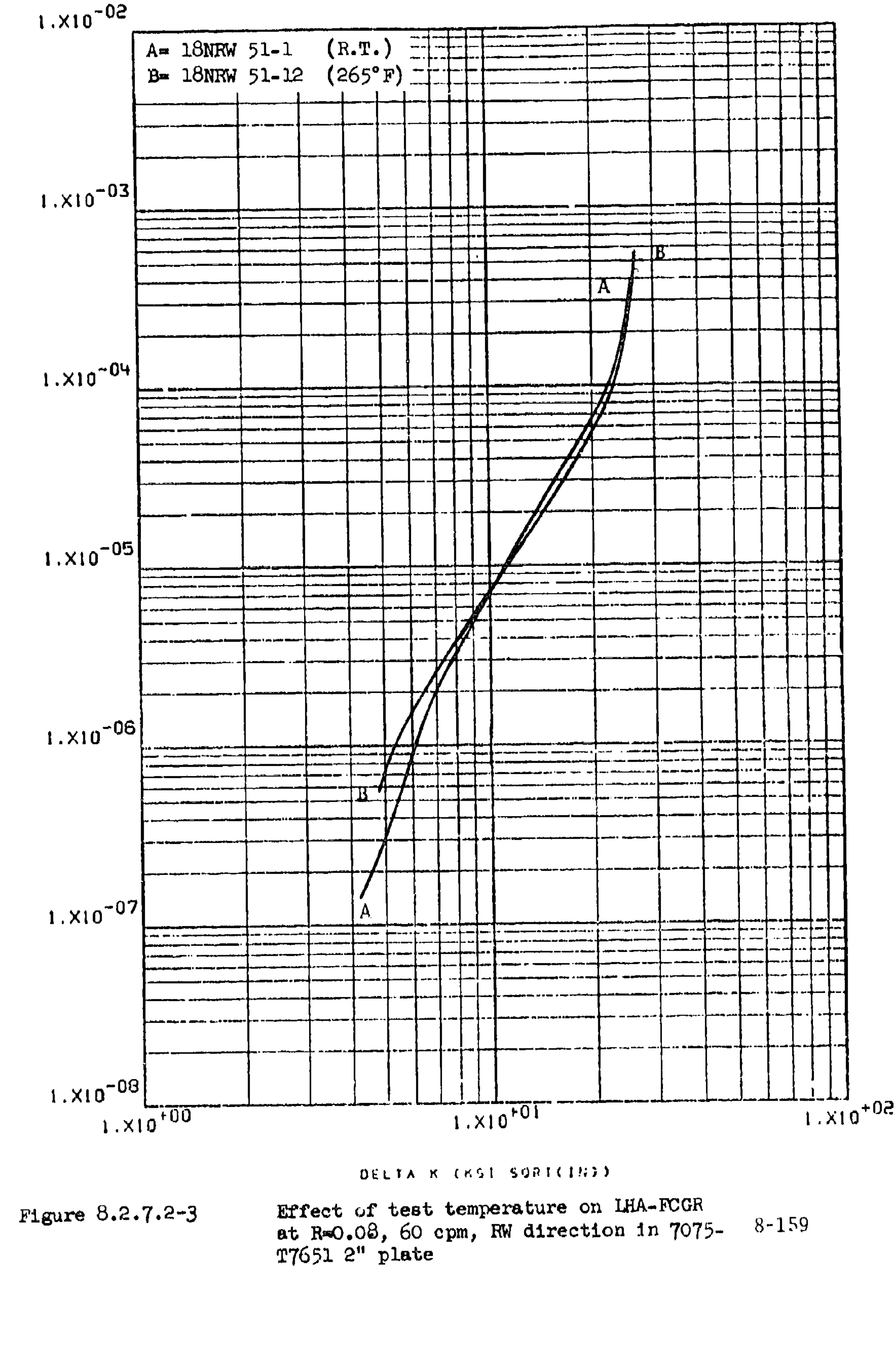

Figure 8.2.7.2-3 Effect of test temperature on LHA-FCGR at R=0.08, 60 cpm, RW direction in 7075-T7651 2" plate

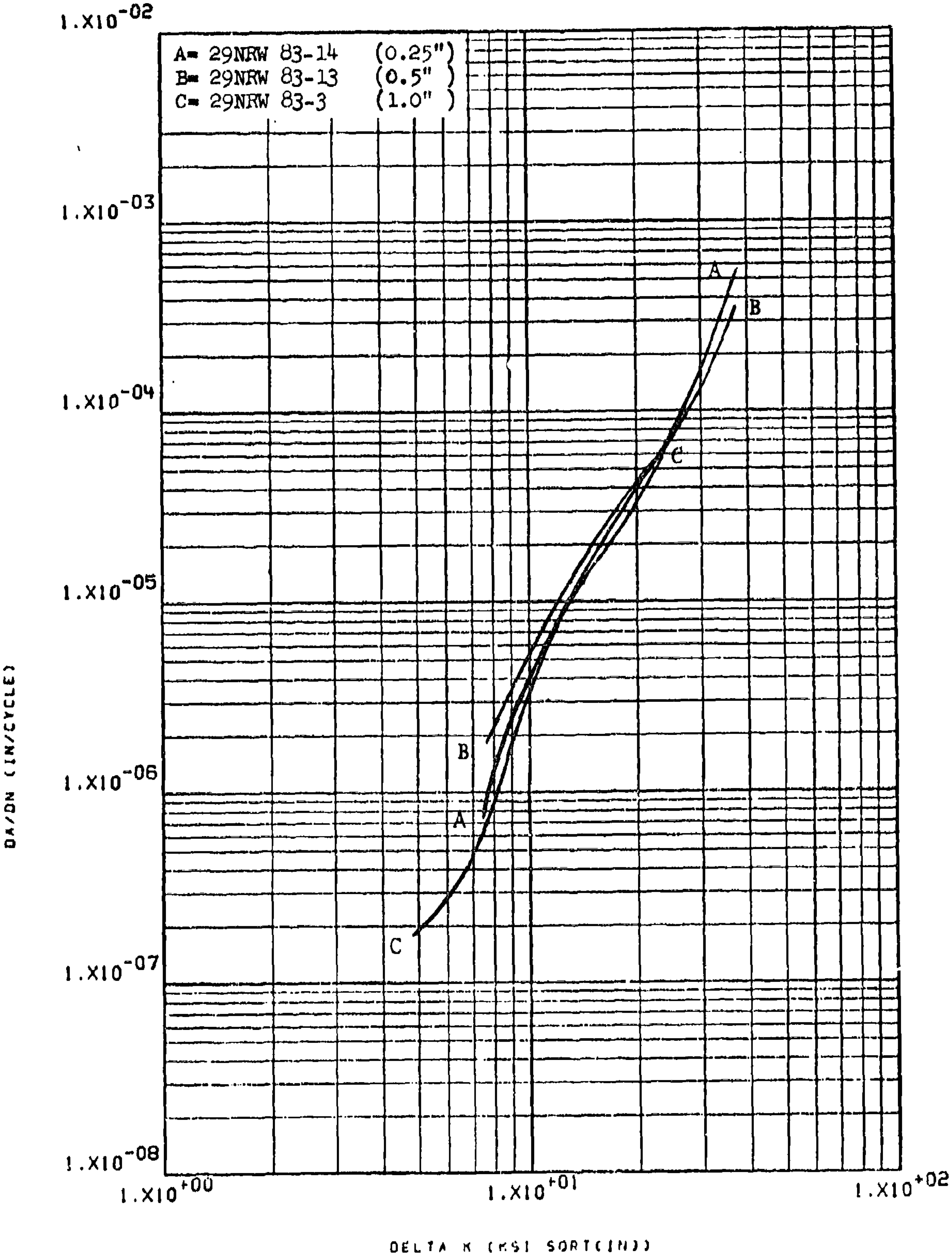

Figure 8.2.7.3-1 Effect of specimen thickness on LHA-FCGR at R.T., R=0.08, 360 cpm, RW direction in 7075-T73511 3" x 17" extrusion

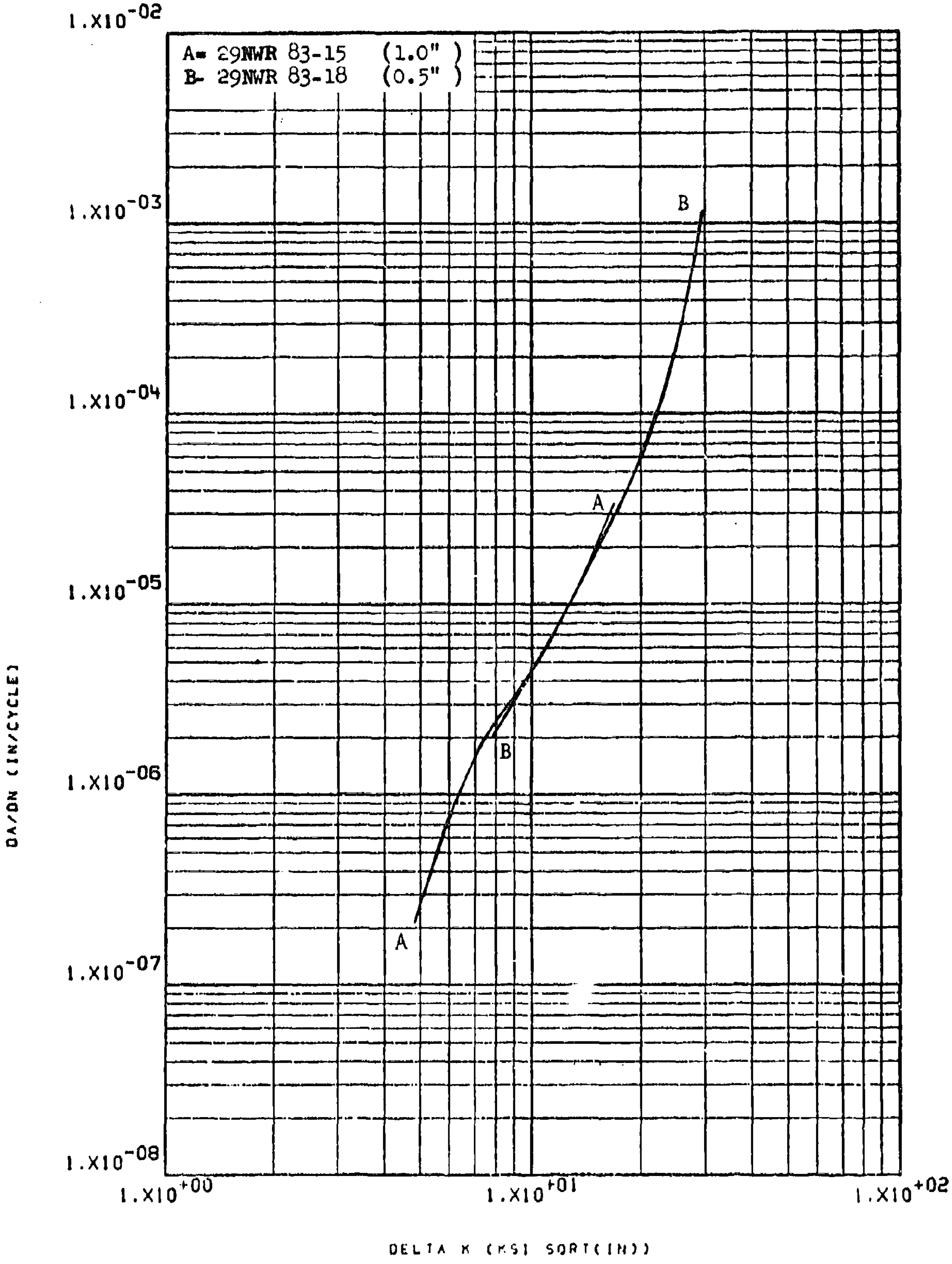

Figure 8.2.7.3-2 Effect of specimen thickness on LHA-FCGR at R.T., R=0.08, 360 cpm, WR direction in 7075-T73511 3" x 17" extrusion

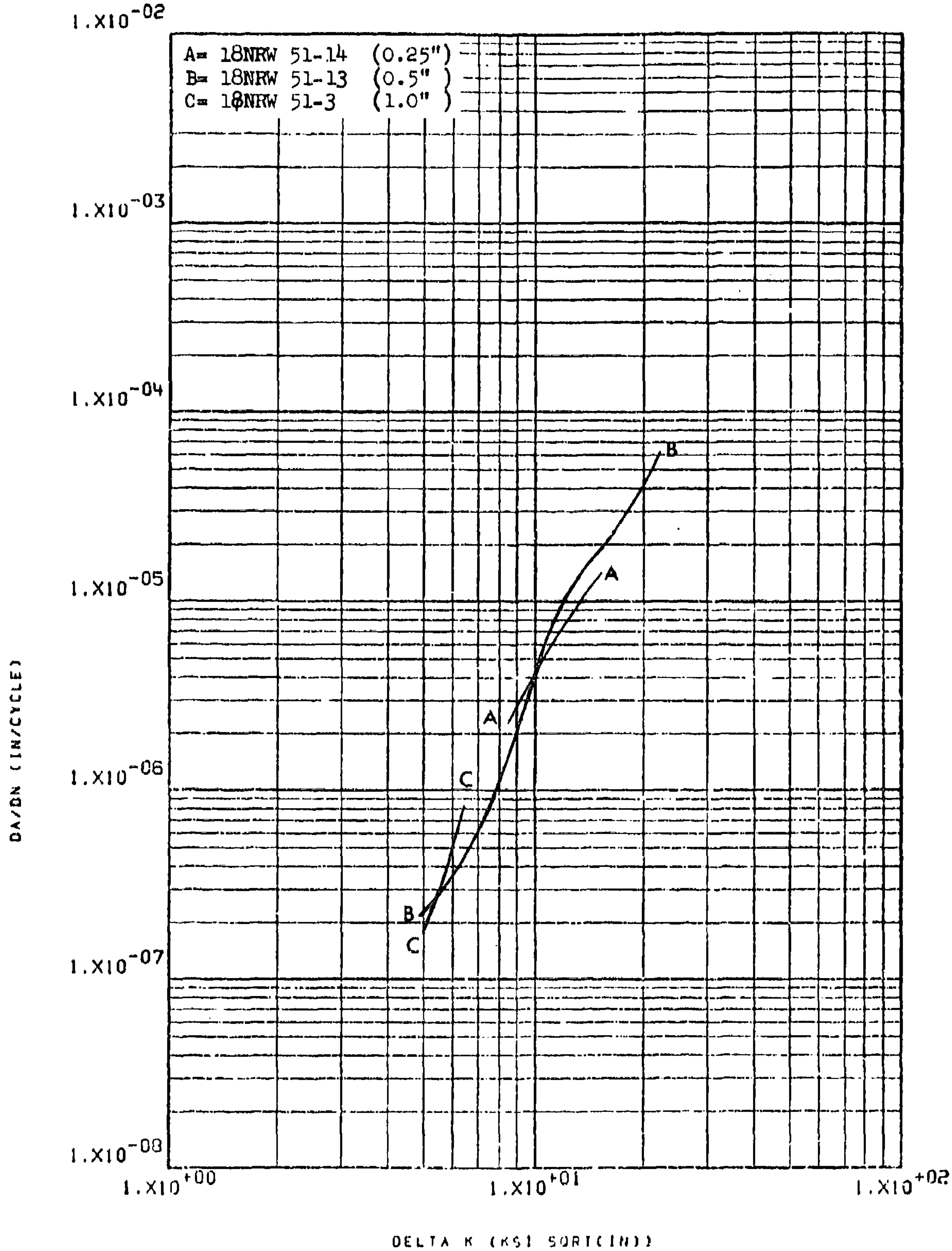

Figure 8.2.7.3-3 Effect of specimen thickness on LHA-FCGR at R.T., R=0.08, 360 cpm, RW direction in 7075-T7651 2" plate

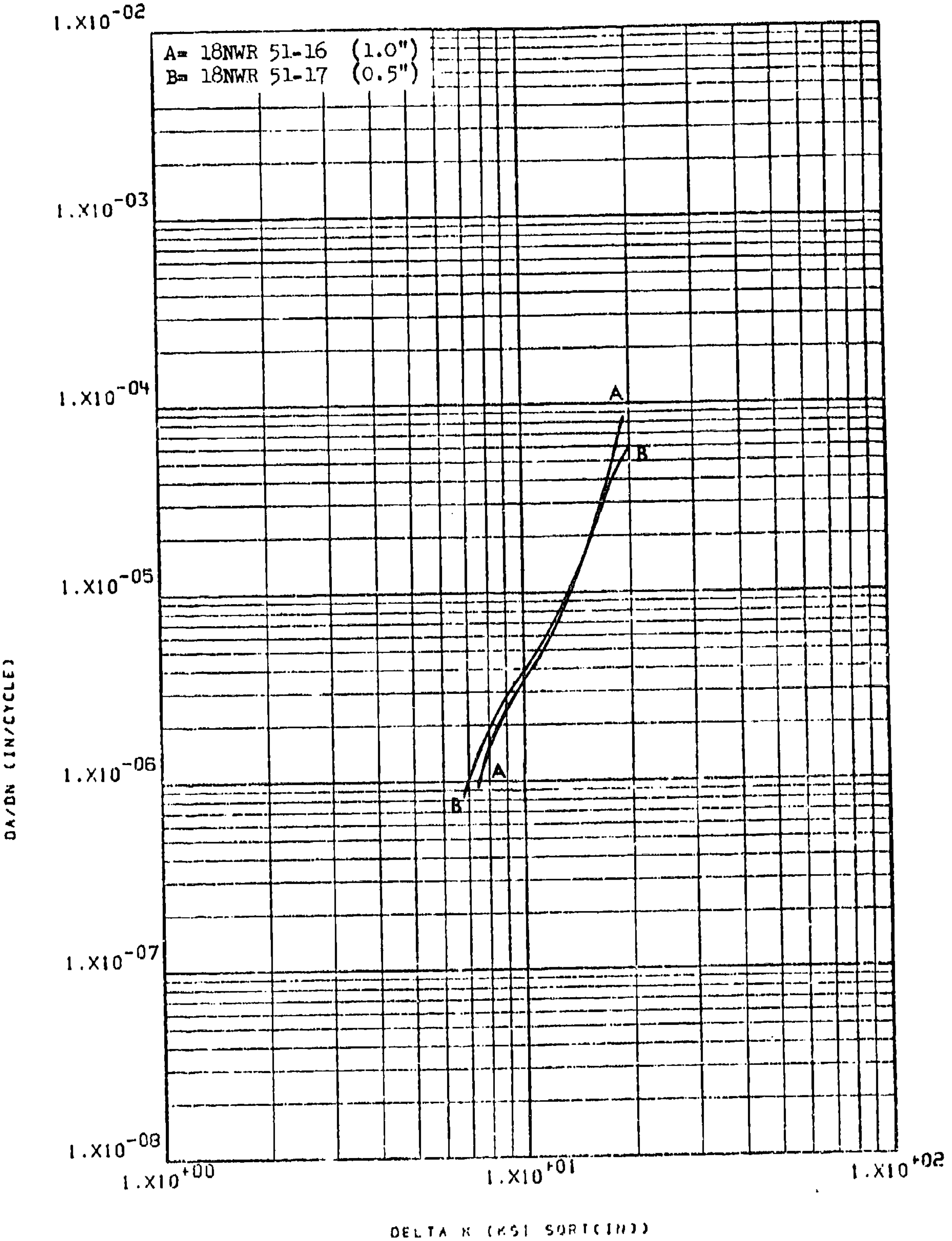

Figure 8.2.7.3-4 Effect of specimen thickness on LHA-FCGR at R.T., R=0.08, 360 cpm, WR direction in 7075-T7651 2" plate

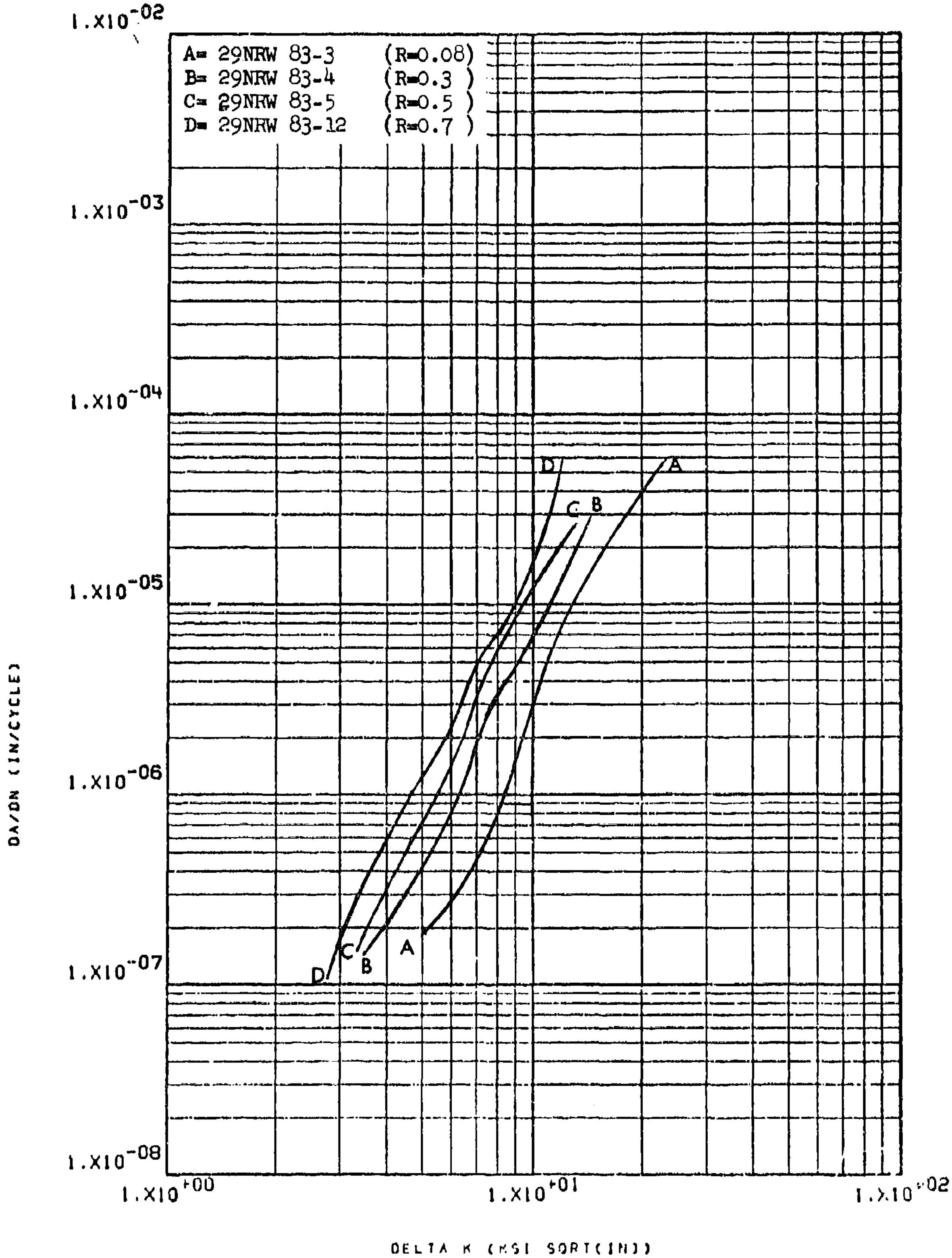

Figure 8.2.7.4-1. Effect of R factor on LHA-FCGR at R.T., 360 cpm, RW direction in 7075-T73511 3" x 17" extrusion

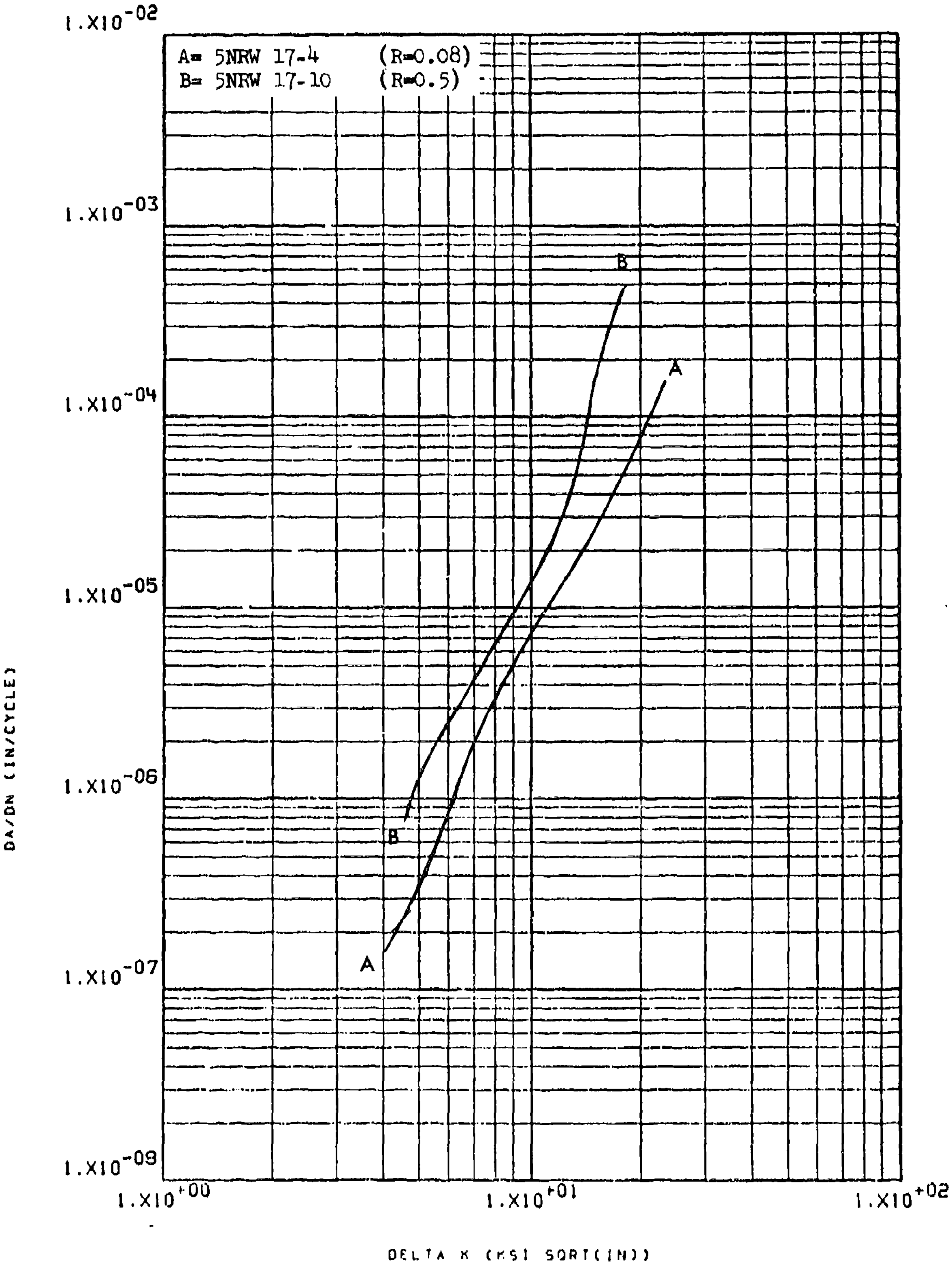

Figure 8.2.7.4-2 Effect of R factor on LHA-FCGR at R.T., 360 cpm, RW direction in 7075-T7351 2" plate

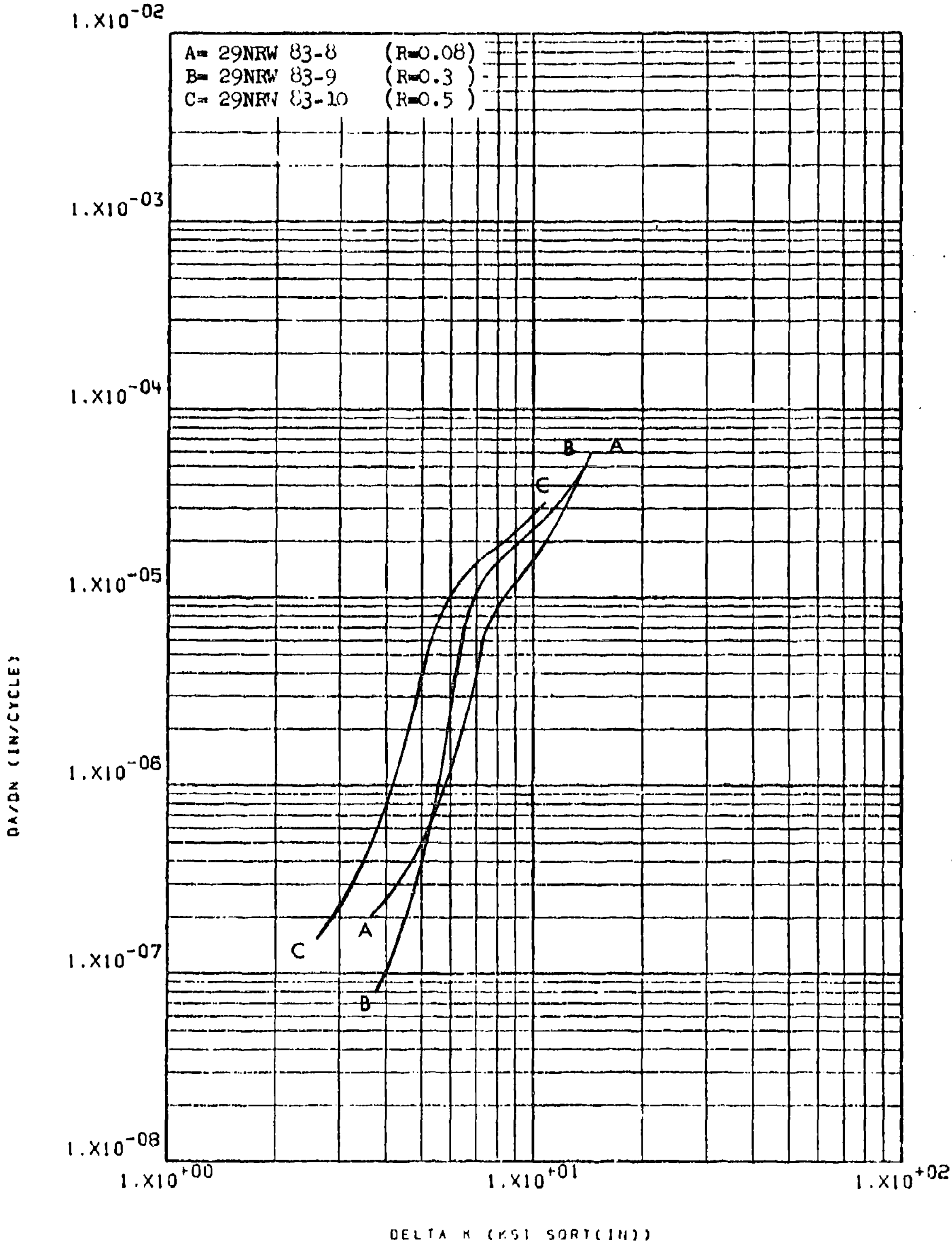

Figure 8.2.7.4-3 Effect of R factor on STW-FCGR at R.T., 60 cpm, RW direction in 7075-T73511 3" x 17" extrusion

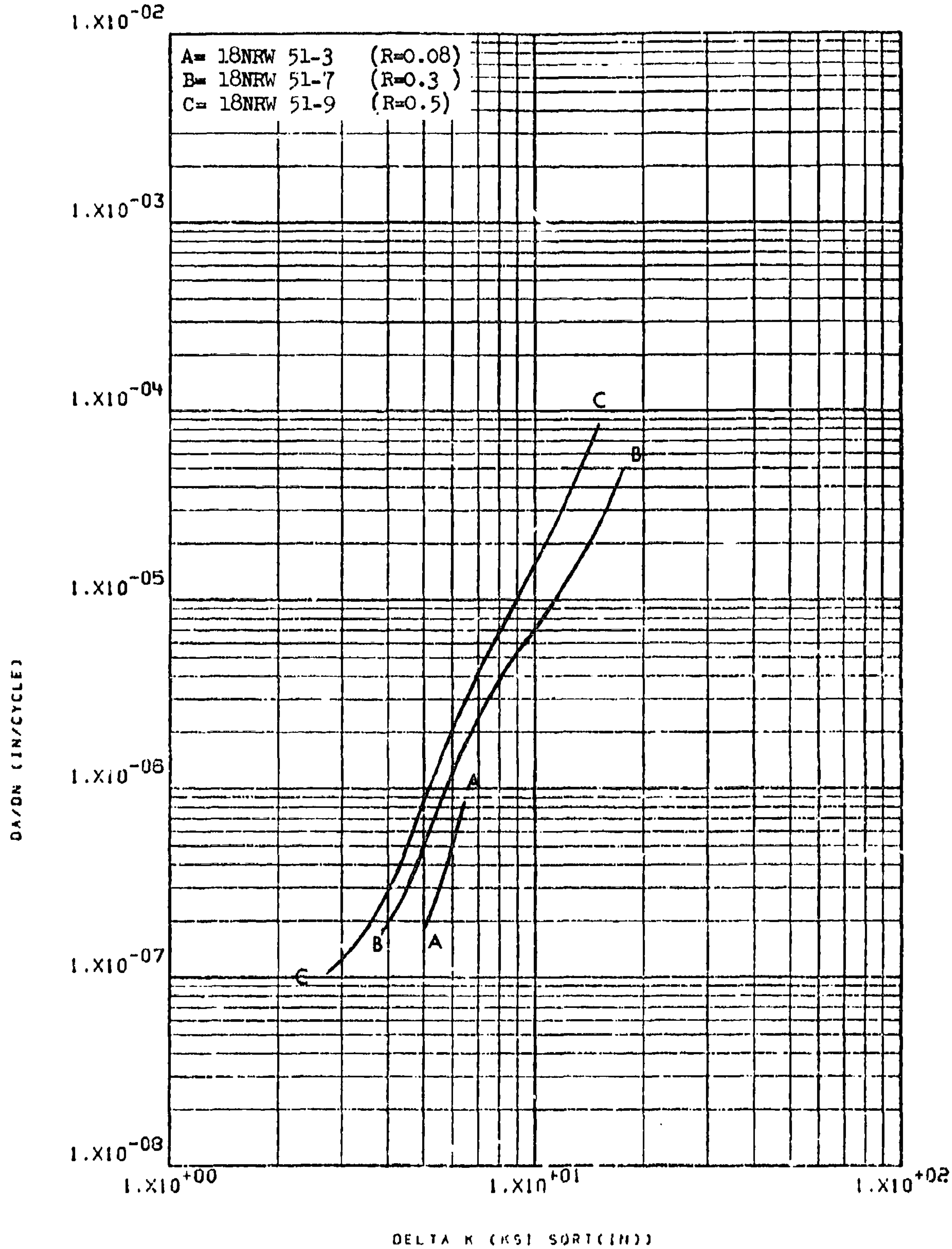

Figure 8.2.7.4-4 **Effect of R factor on LHA-FCGR at R.T., 360 cpm, RW direction in 7075-T7651 2" plate**

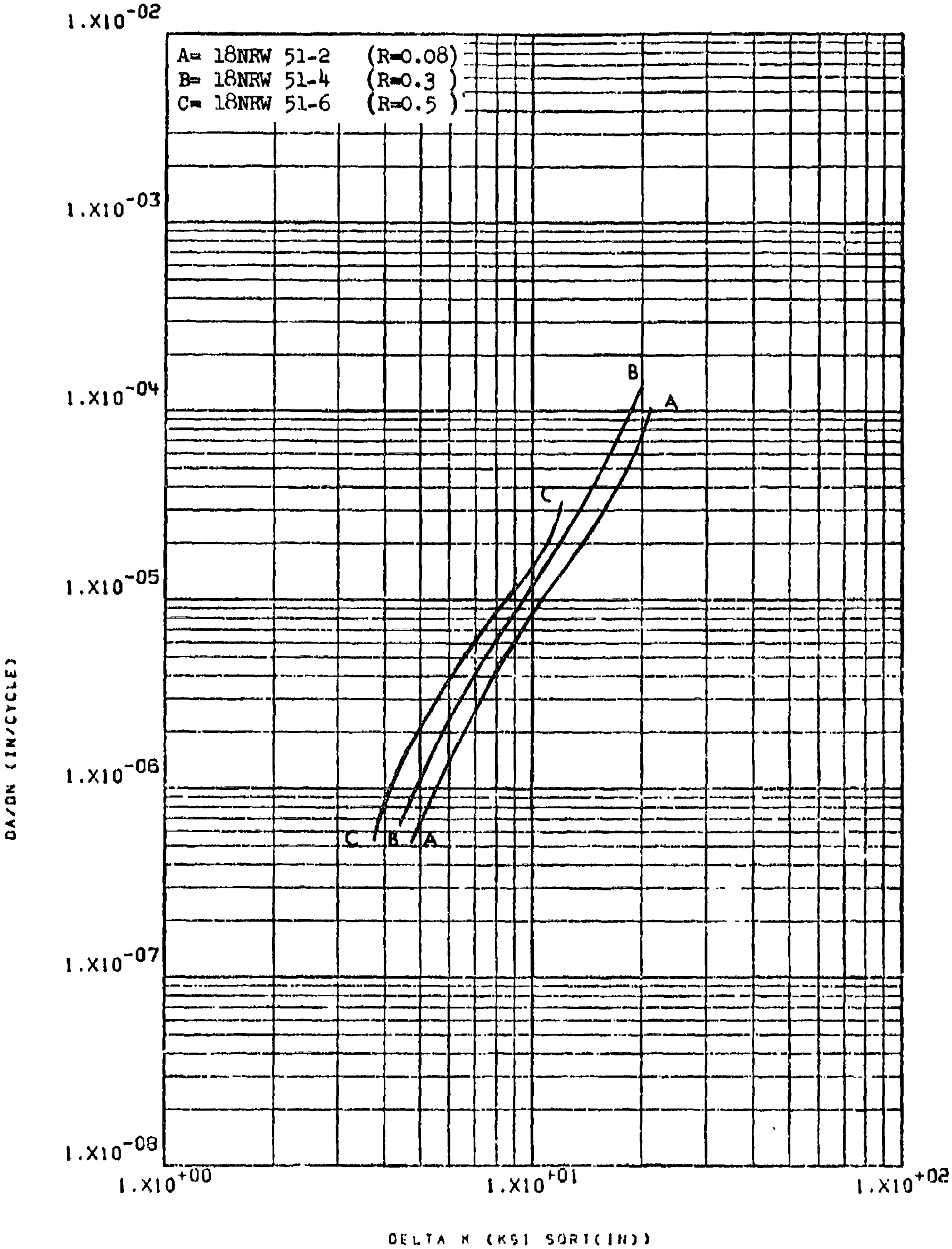

Figure 8.2.7.4-5 Effect of R factor on STW-FCGR at R.T., 60 cpm, RW direction in 7075-T7651 2" plate

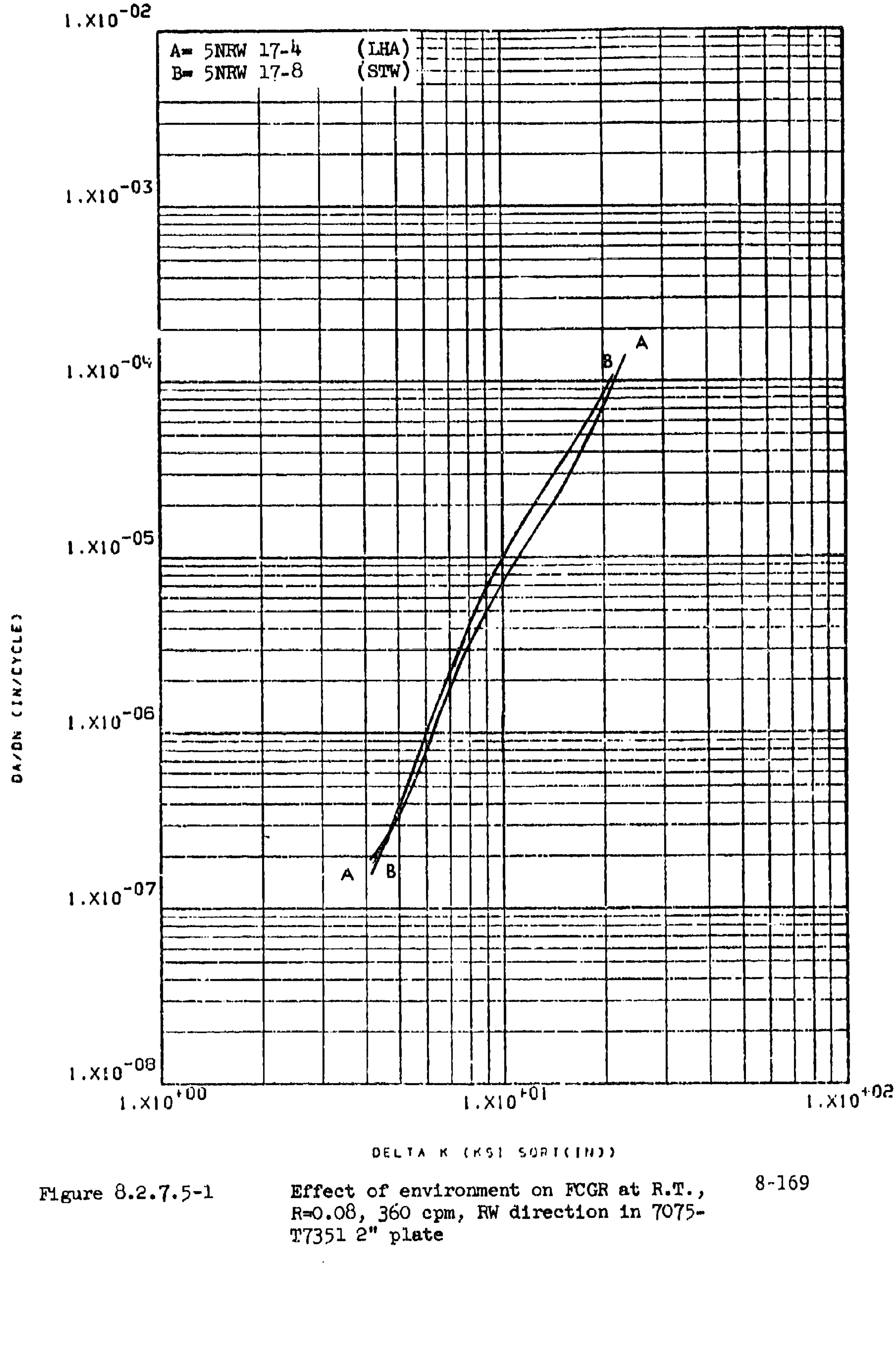

Figure 8.2.7.5-1 Effect of environment on FCGR at R.T., R=0.08, 360 cpm, RW direction in 7075-T7351 2" plate

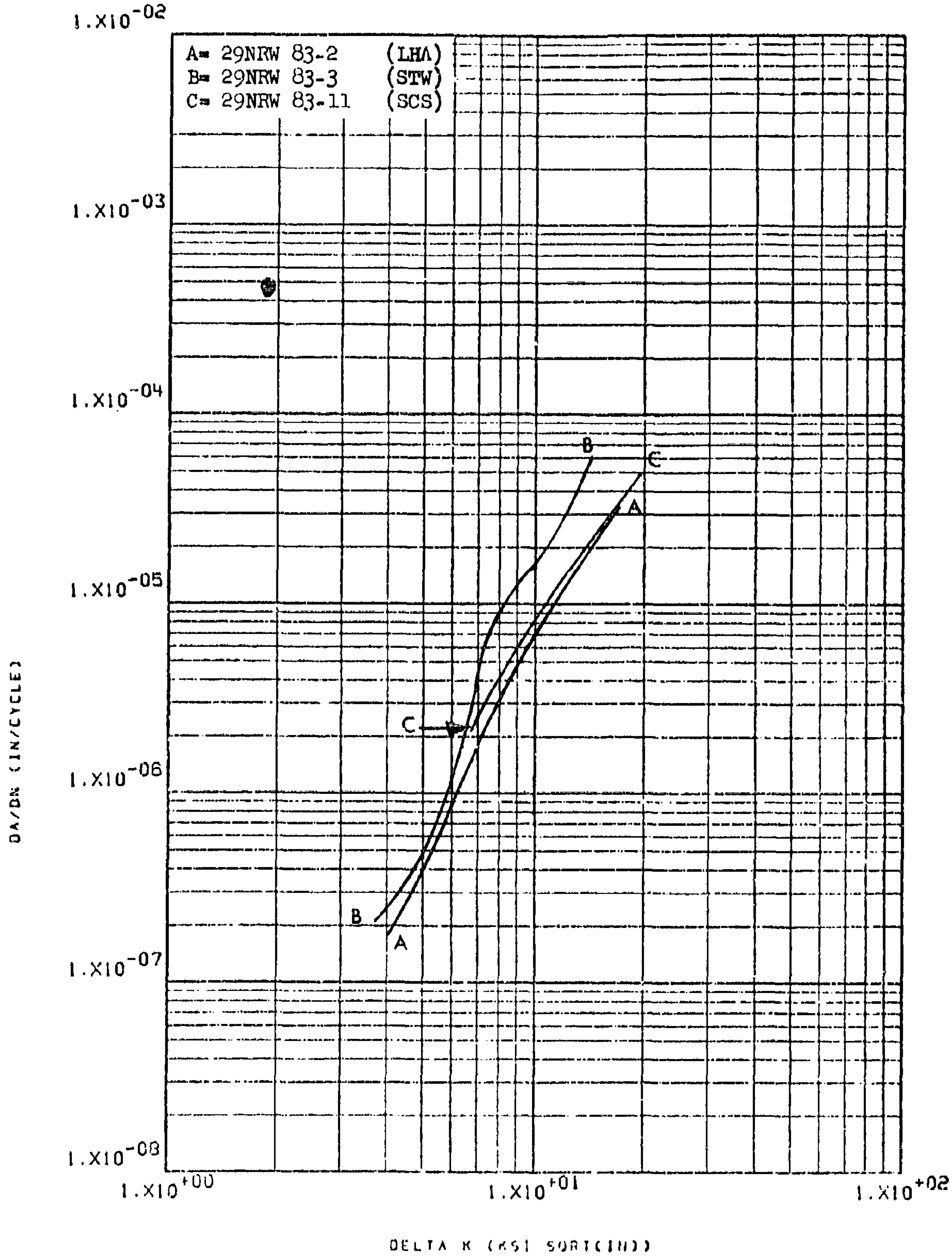

Figure 8.2.7.5-2 Effect of environment on FCGR at R.T., R=0.08, 60 cpm, RW direction in 7075-T73511 3" x 17" extrusion

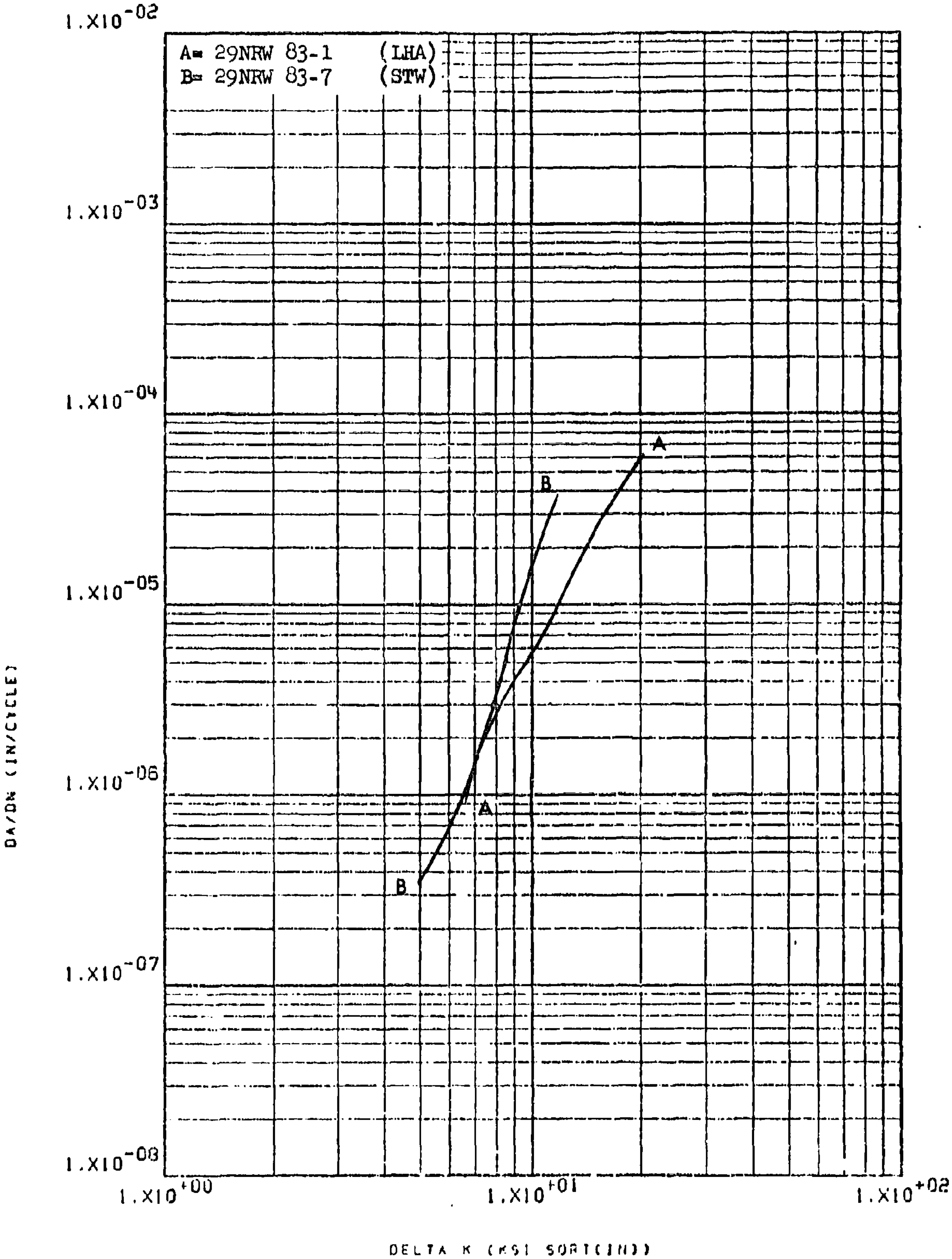

Figure 8.2.7.5-3 Effect of environment on FCGR at R.T., R=0.08, 6 cpm, RW direction in 7075-T73511 3" x 17" extrusion

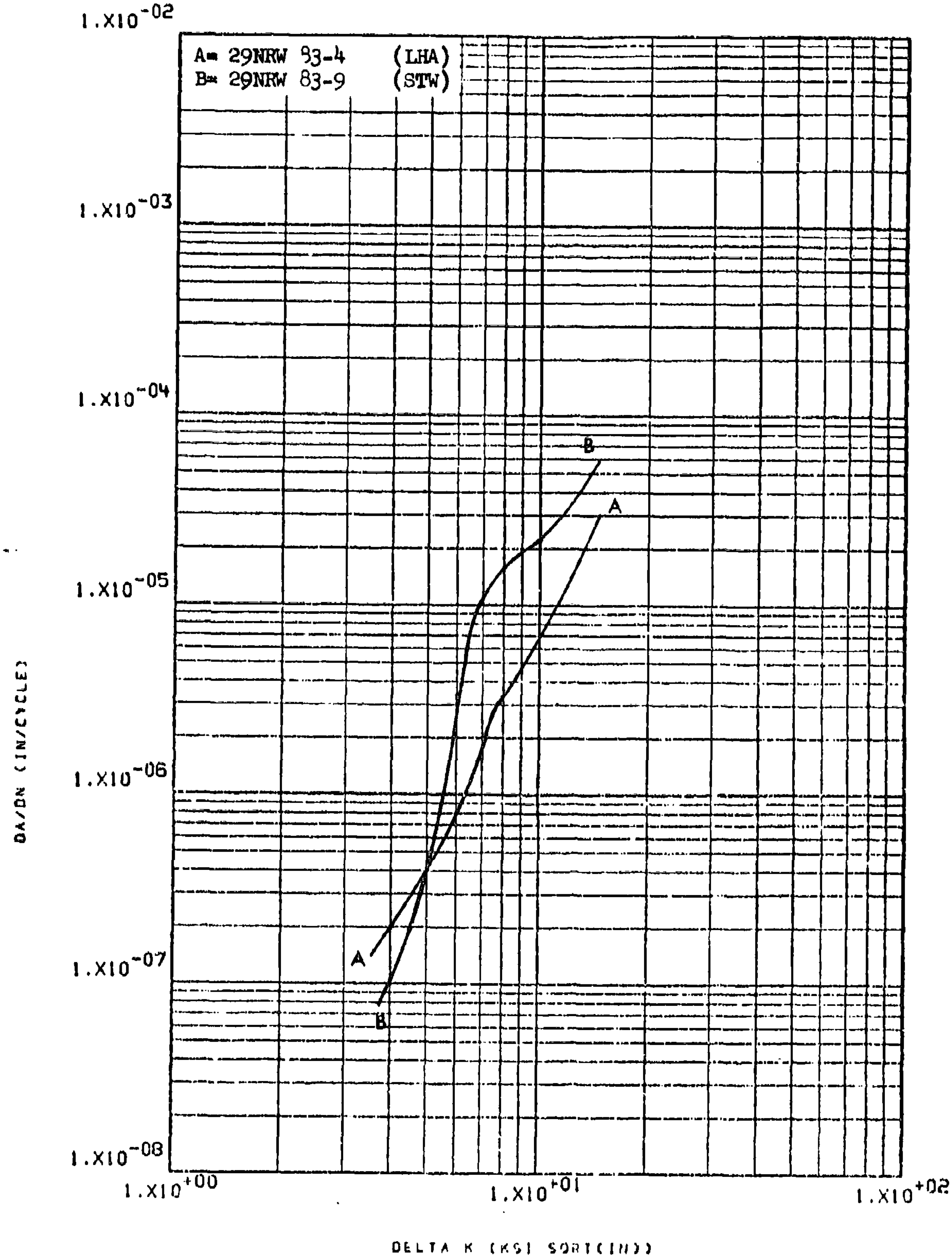

Figure 8.2.7.5-4 Effect of environment on FCGR at R.T., R=0.3, 60 cpm, RW direction in 7075-T73511 3" x 17" extrusion

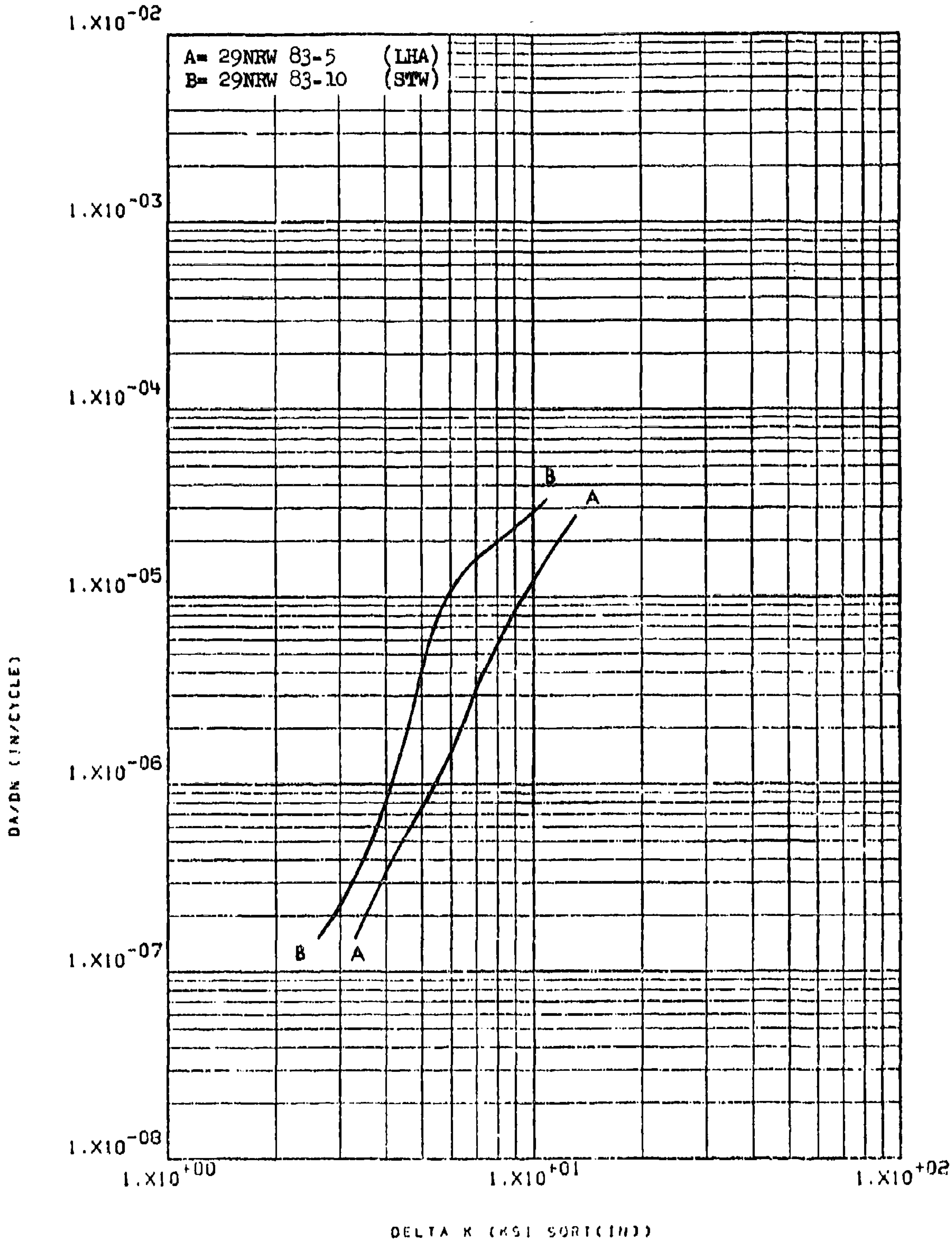

Figure 8.2.7.5-5 Effect of environment on FCGR at R.T., R=0.5, 60 cpm, RW direction in 7075-T73511 3" x 17" extrusions

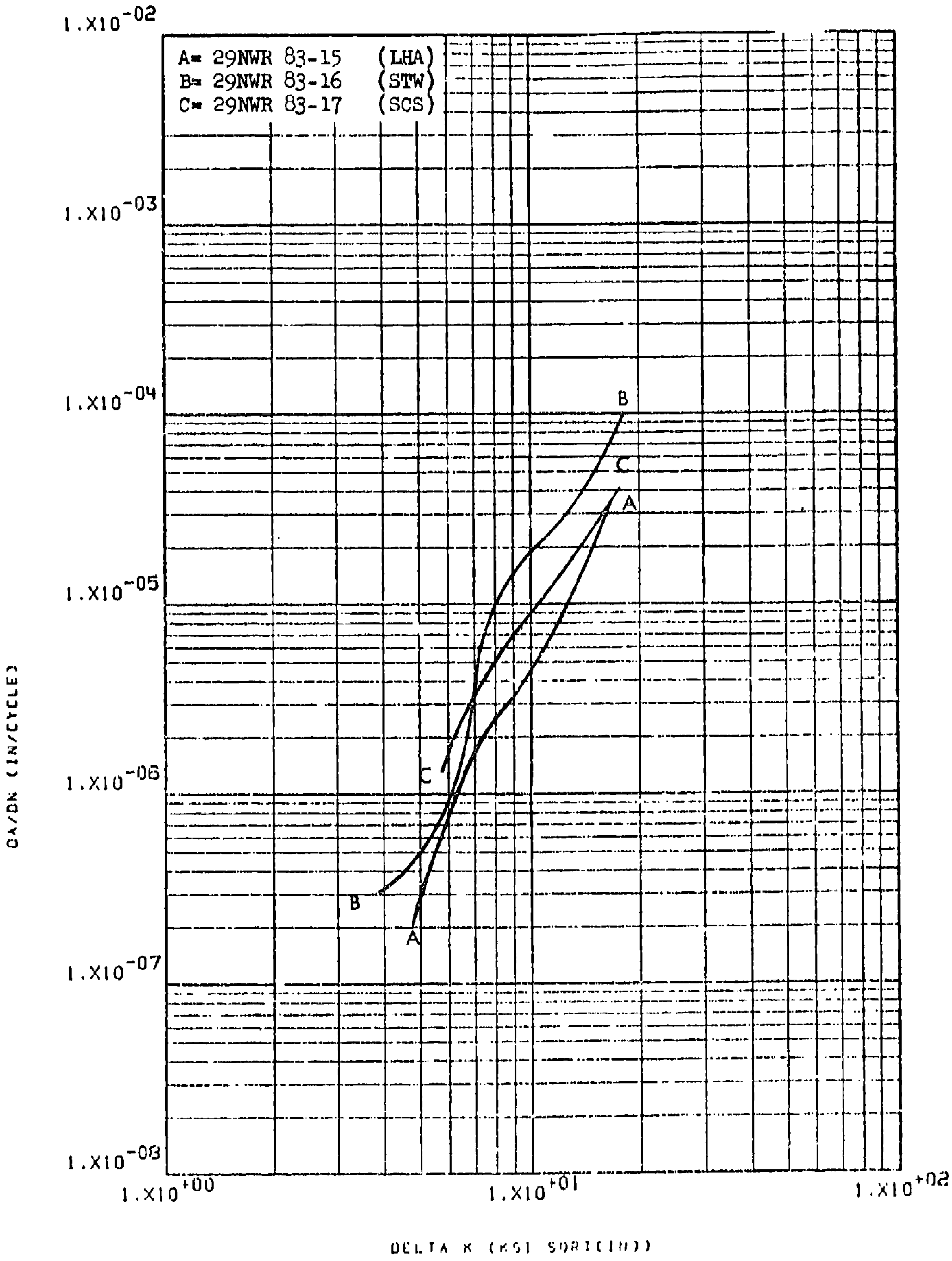

Figure 8.2.7.5-6 Effect of environment on FCGR at R.T., R-0.08, WR direction in 7075-T73511 3" x 17" extrusion

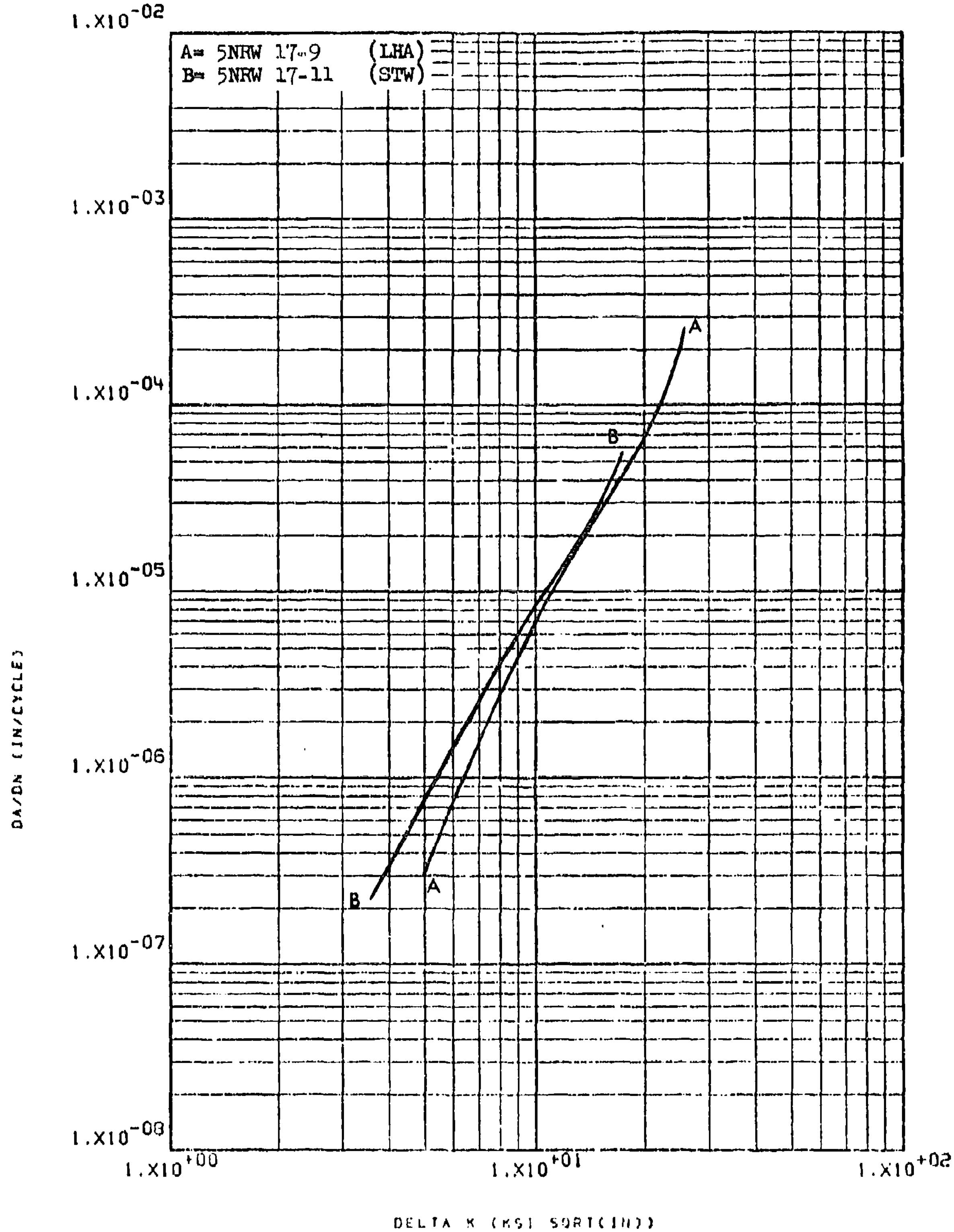

Figure 8.2.7.5-7 Effect of environment on FCGR at R.T., R=0.08, 60 cpm, RW direction in 7075-T7651 2" plate

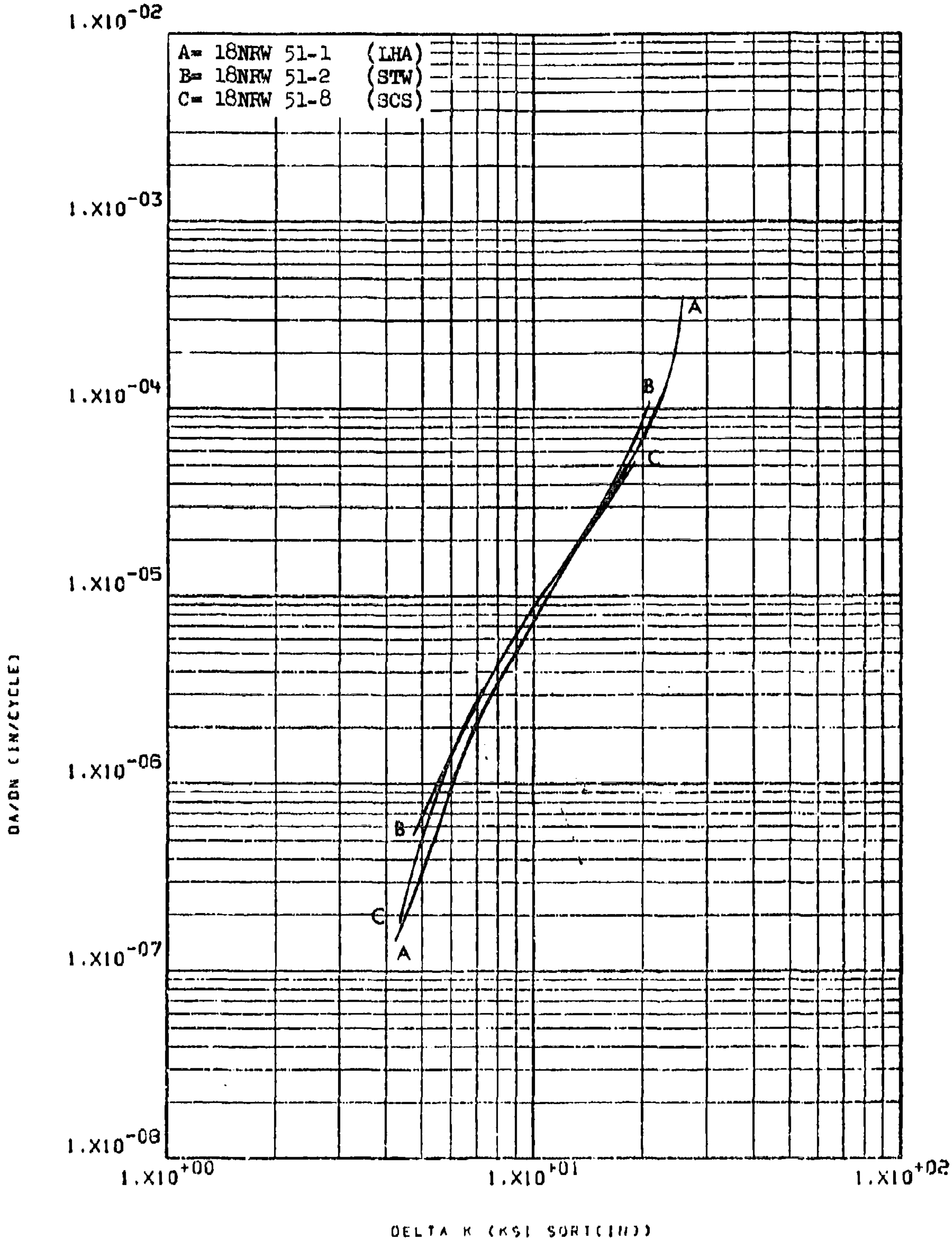

Figure 8.2.7.5-8 Effect of environment on FCGR at R.T., R=0.08, 60 cpm, RW direction in 7075-T7651 2" plate

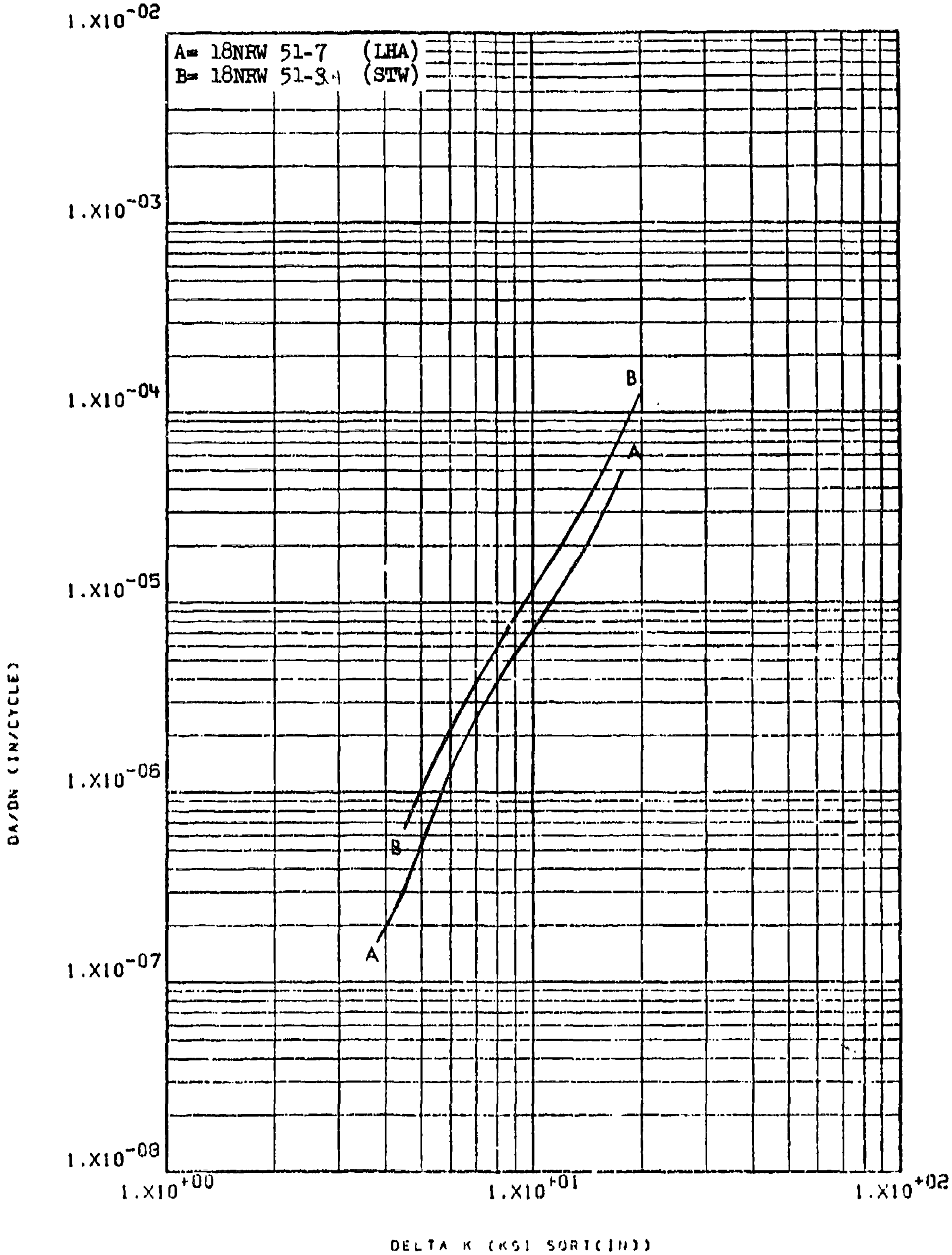

Figure 8.2.7.5-9 Effect of environment on FCGR at R.T., R=0.3, RW direction in 7075-T7651 2" plate

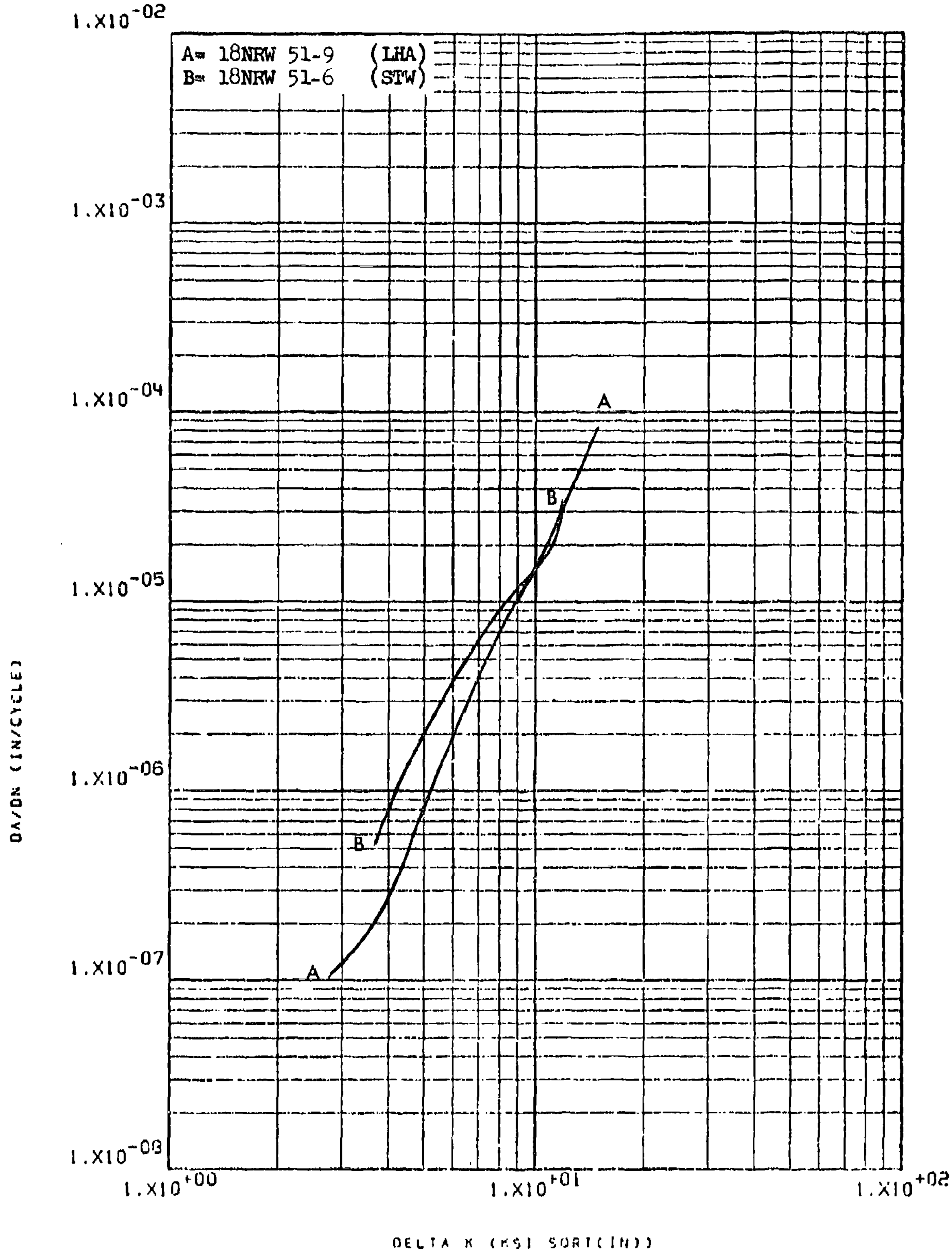

Figure 8.2.7.5-10 Effect of environment on FCGR at R.T., R=0.5, RW direction in 7075-T7651 2" plate

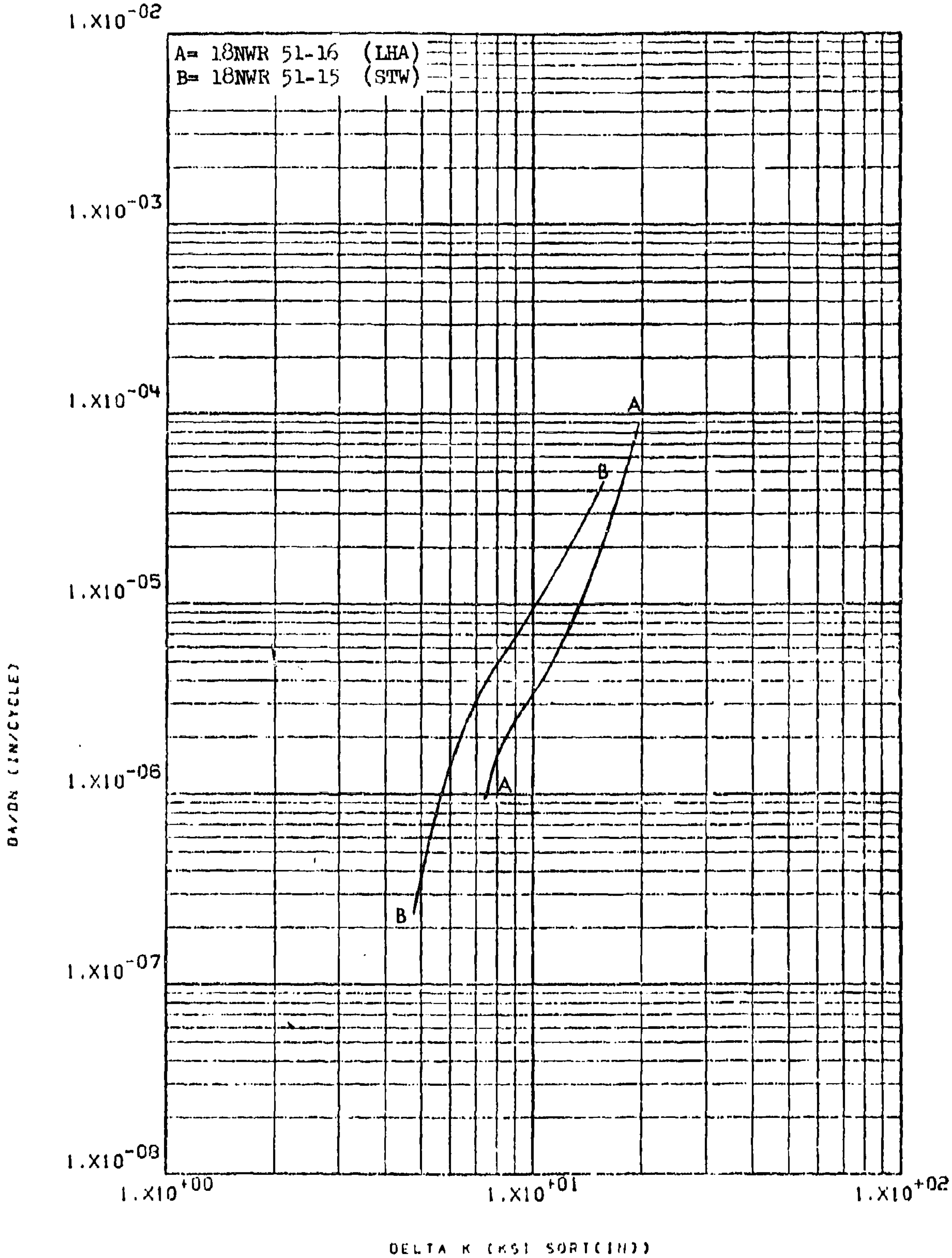

Figure 8.2.7.5-11 Effect of environment on FCGR at R.T., R=0.08, WR direction in 7075-T7651 2" plate

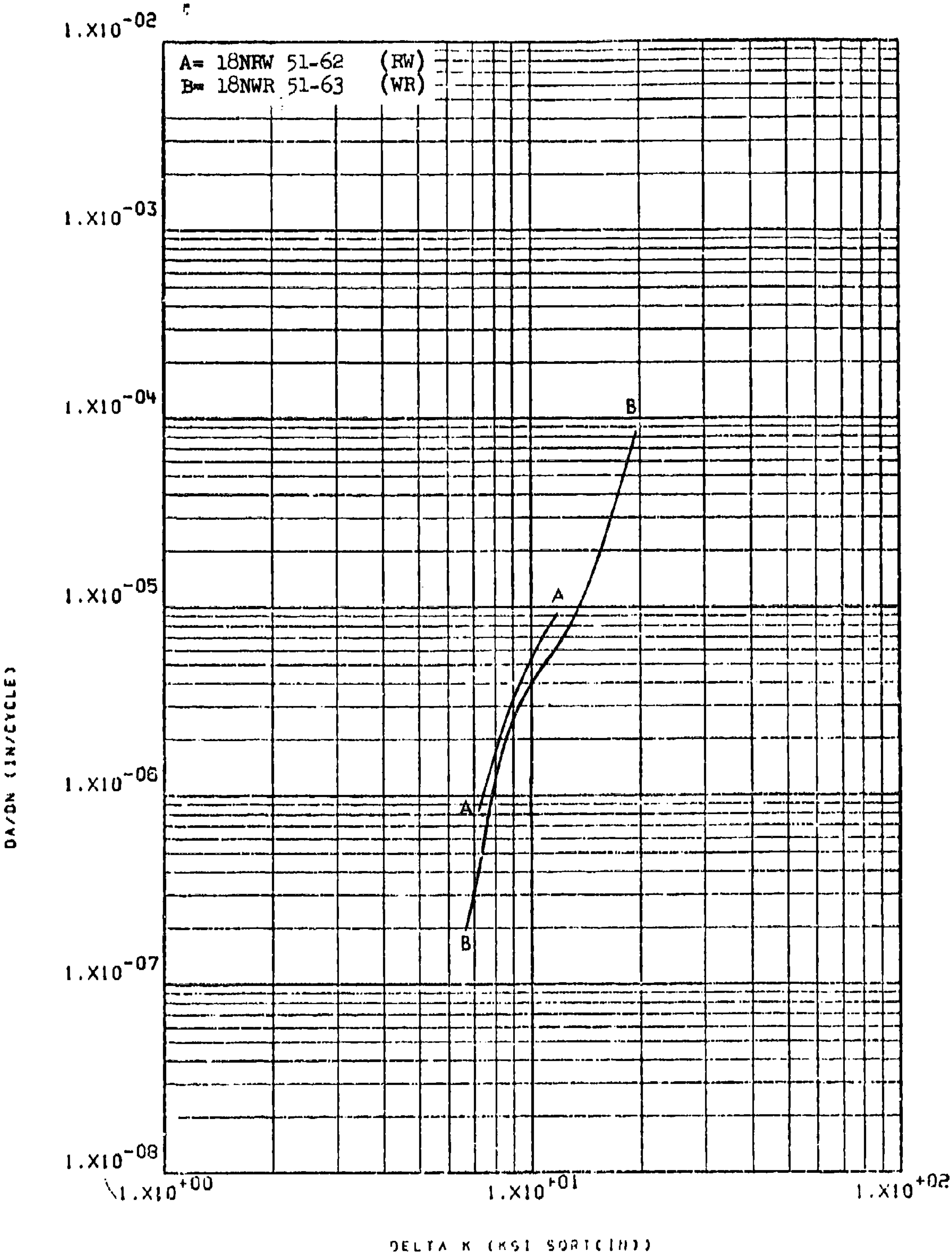

Figure 8.2.7.6-1 Effect of test direction on LHA-FCGR at R.T., R=0.08, 360 cpm in 7075-T7351 2" plate

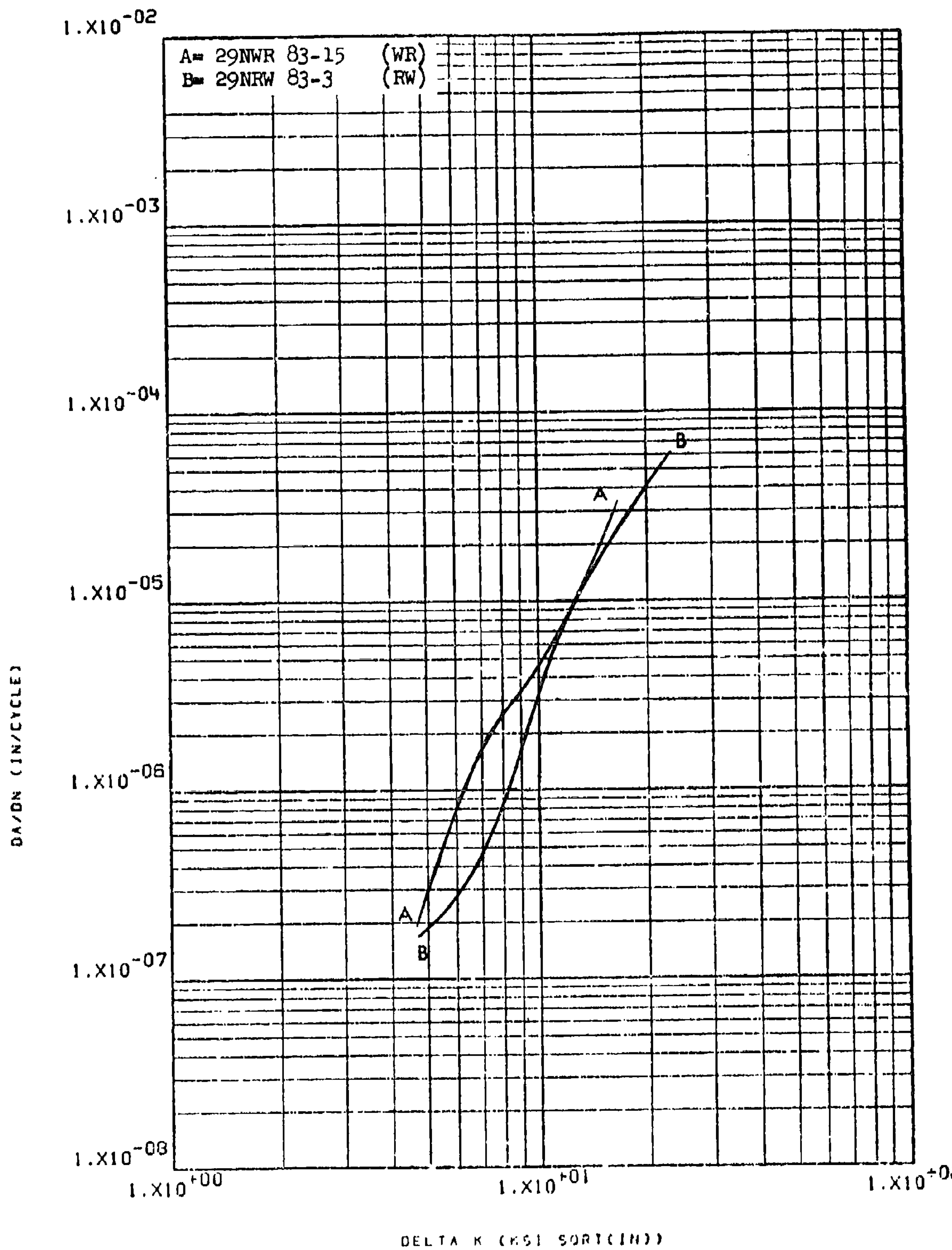

Figure 8.2.7.6-2 Effect of test direction on LHA-FCGR at R.T., R=0.08, 360 cpm in 7075-T73511 3" x 17" extrusion

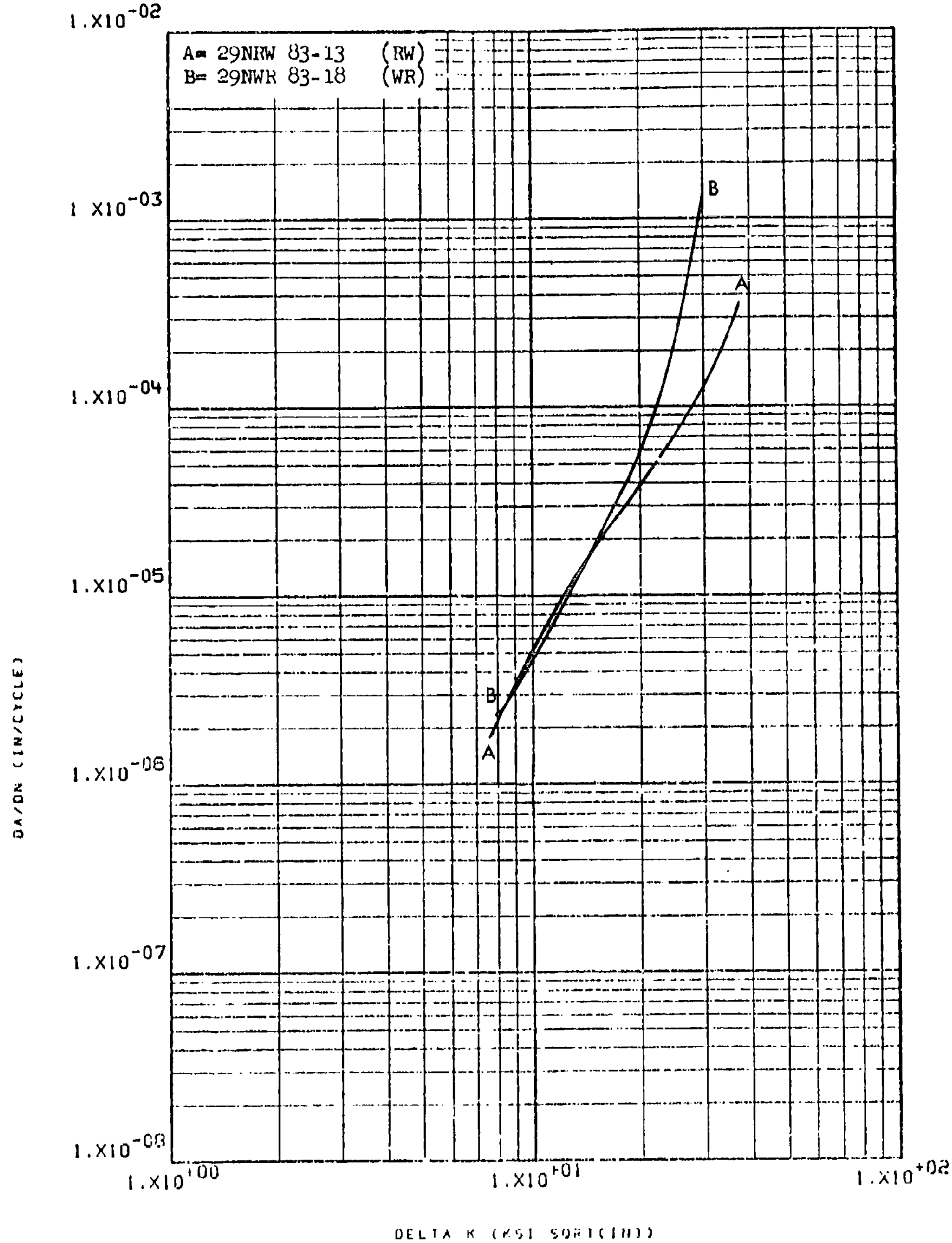

Figure 8.2.7.6-3 Effect of test direction on LHA-FCGR at R.T., R=0.08, 360 cpm in 1/2" thick specimens of 7075-T73511 3" x 17" extrusions

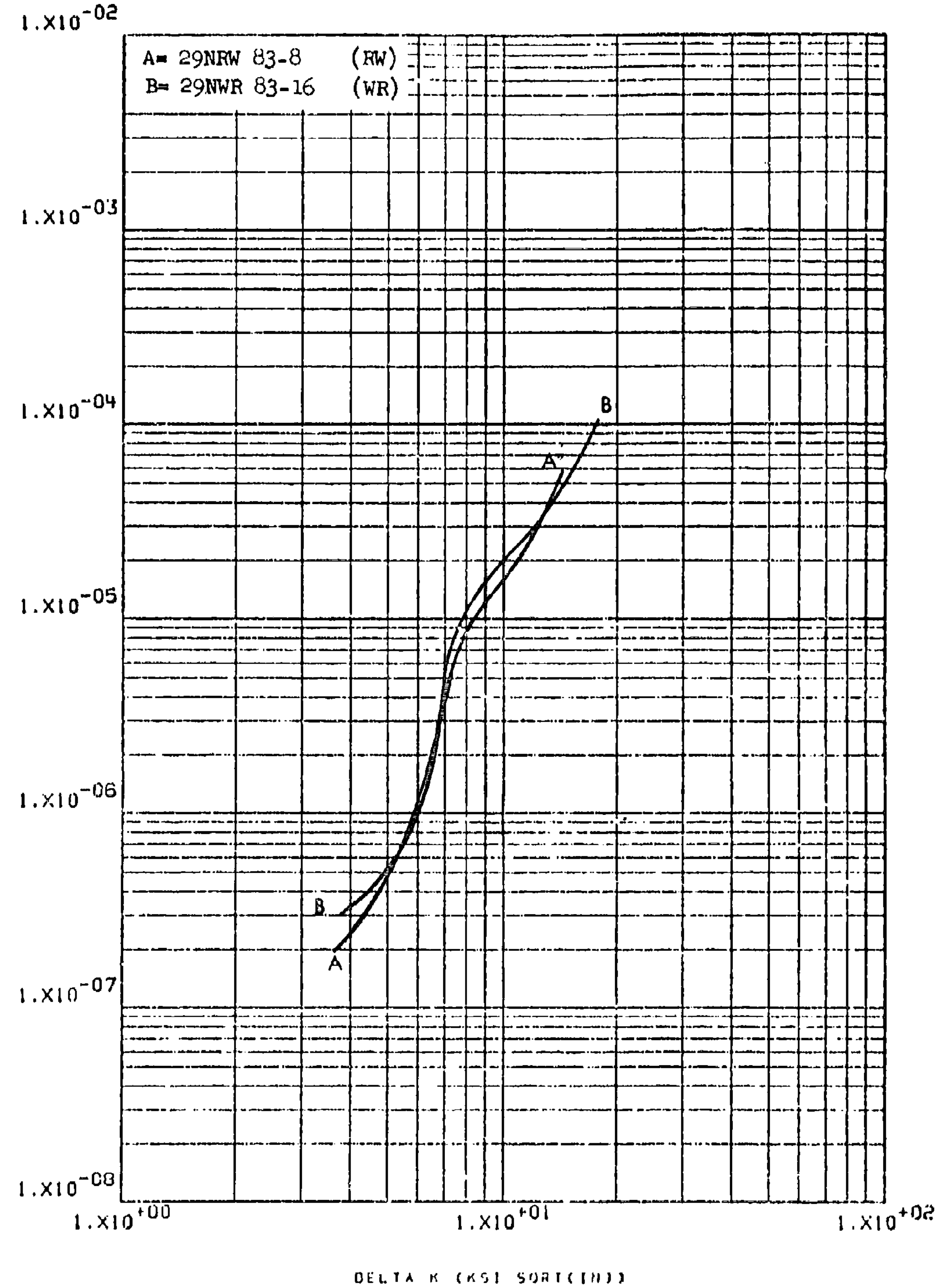

Figure 8.2.7.6-4 Effect of test direction on STW-FCGR at R.T., R=0.08, 60 cpm in 7075-T73511 3" x 17" extrusions

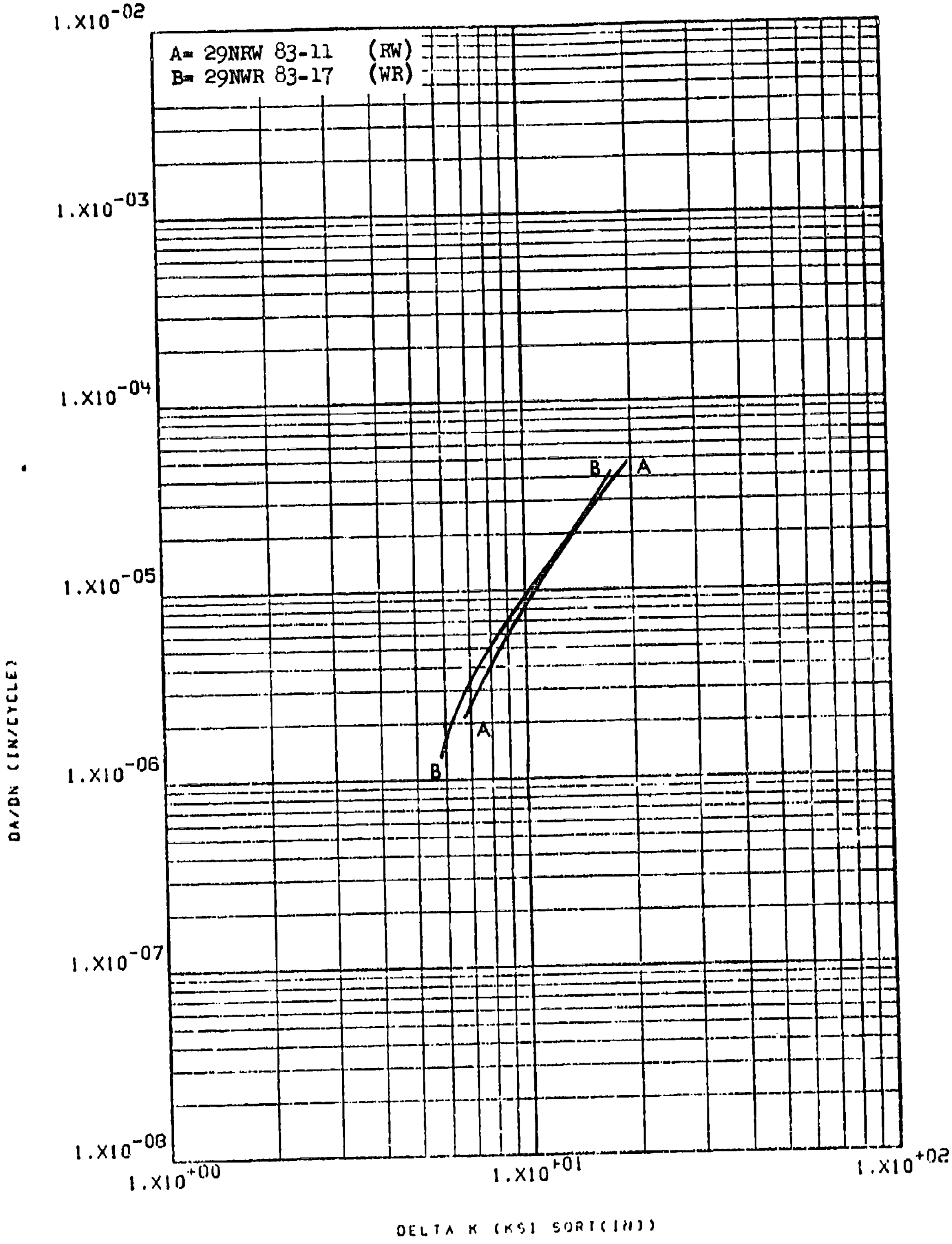

Figure 8.2.7.6-5 Effect of test direction on SCS-FCGR at R.T., R=0.08, 60 cpm in 7075-T73511 3" x 17" extrusion

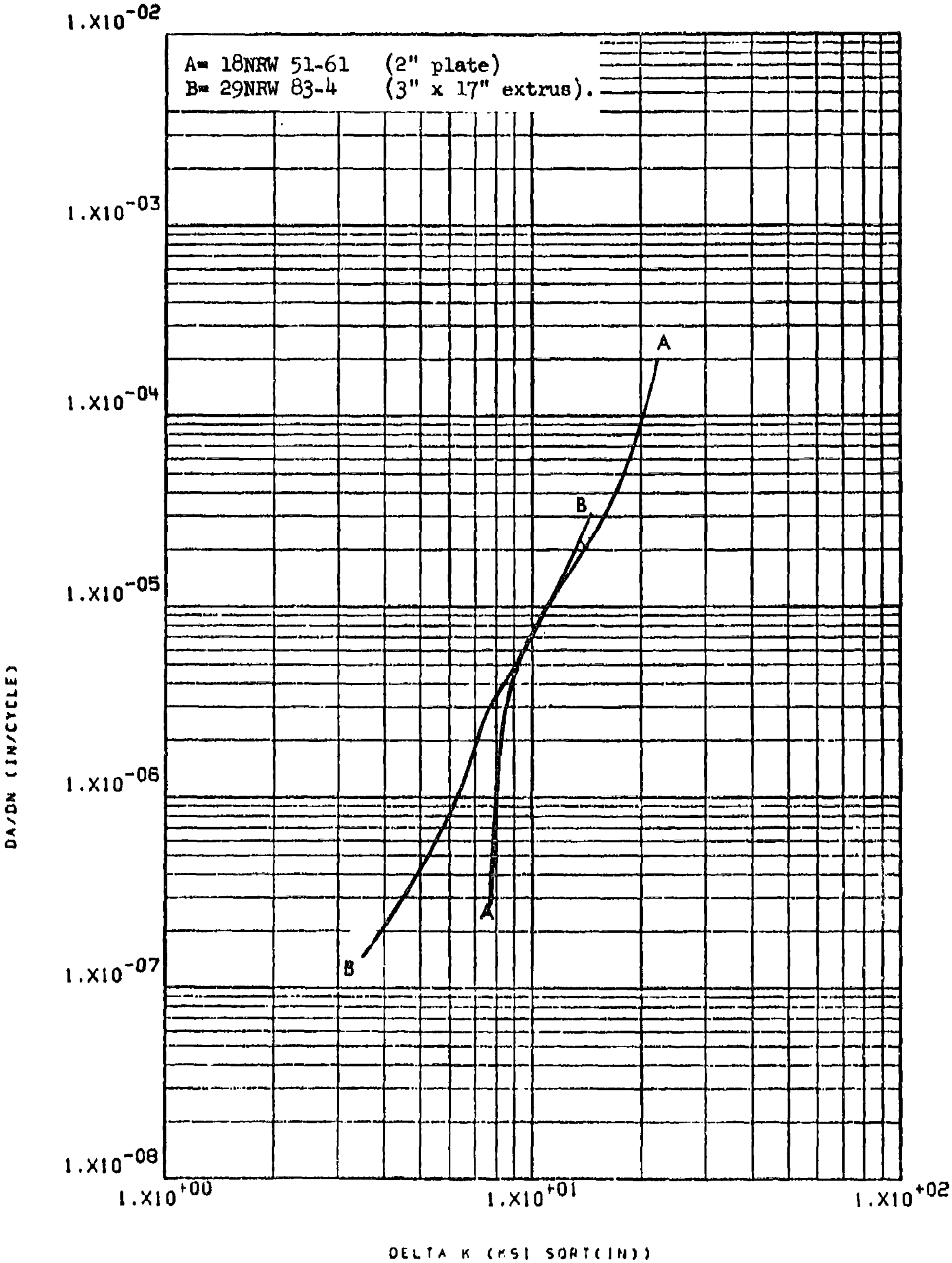

Figure 8.2.7.7-1 Effect of product form on LHA-FCGR at R.T., R=0.3, 360 cpm, RW direction in 7075 Al.

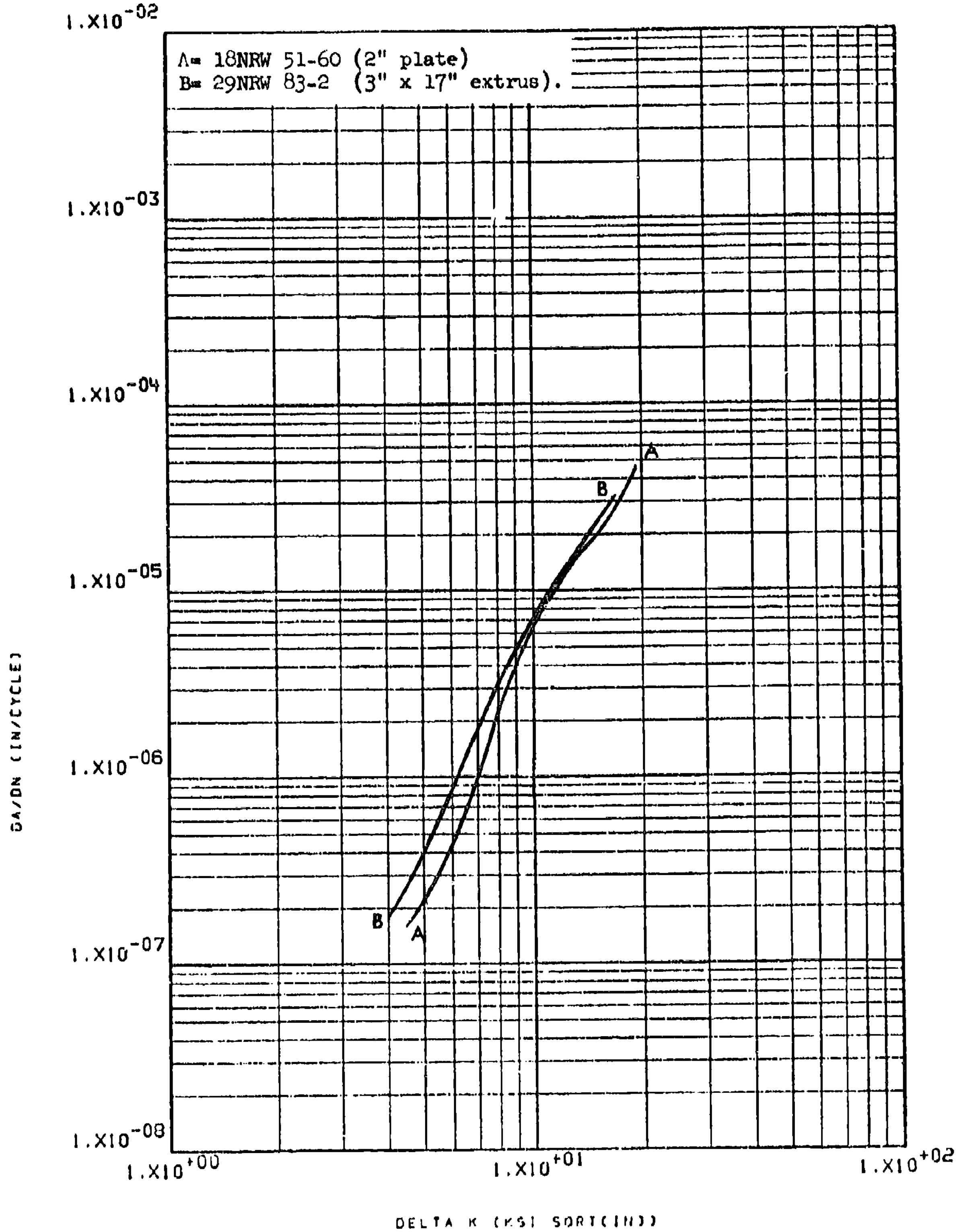

Figure 8.2.7.7-2 Effect of product form on LHA-FCGR at R.T. R=0.08, 60 cpm, RW direction in 7075 Al.

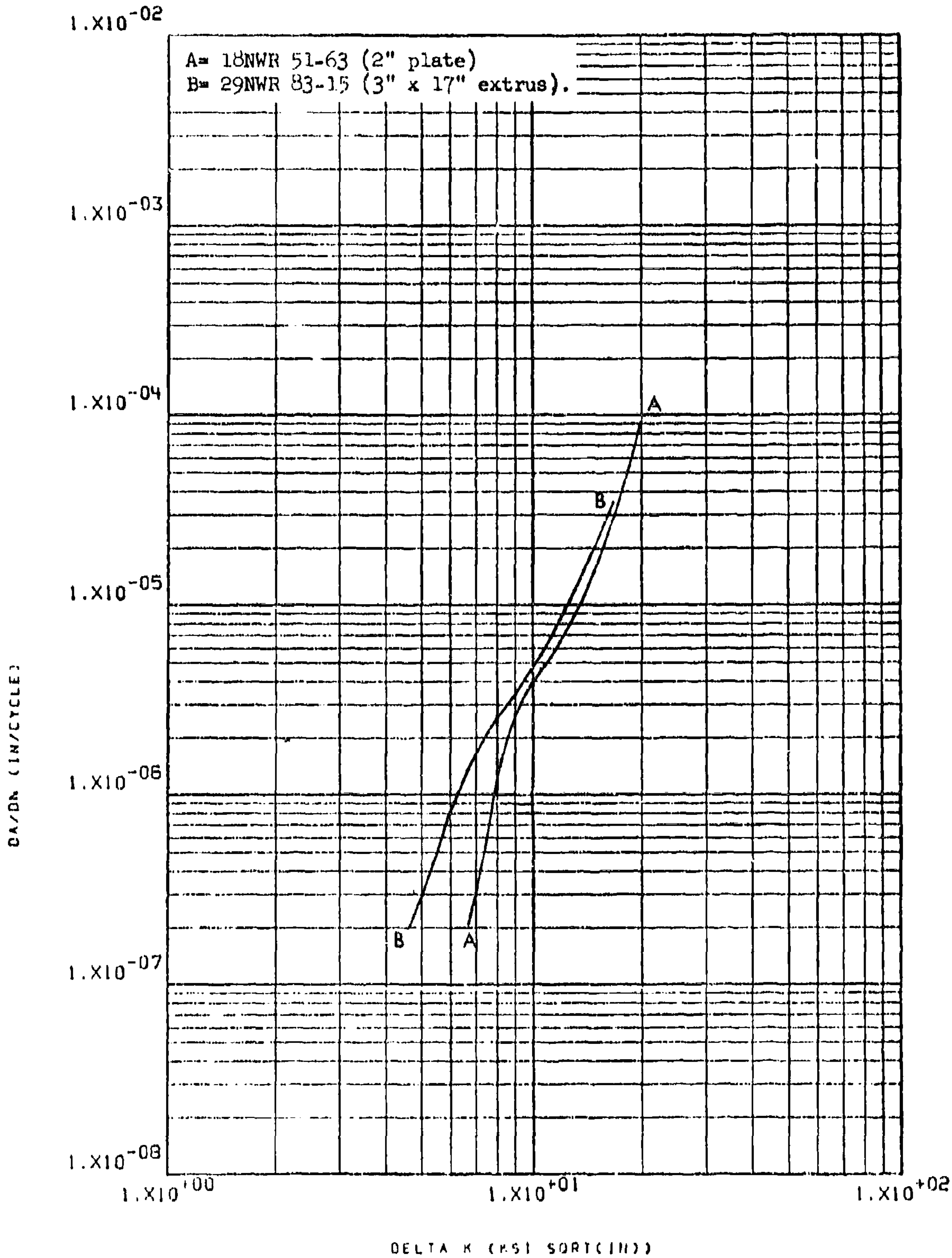

Figure 8.2.7.7-3 Effect of product form on LHA-FCGR at R.T., R=0.08, 360 cpm, WR direction in 7075 Al.

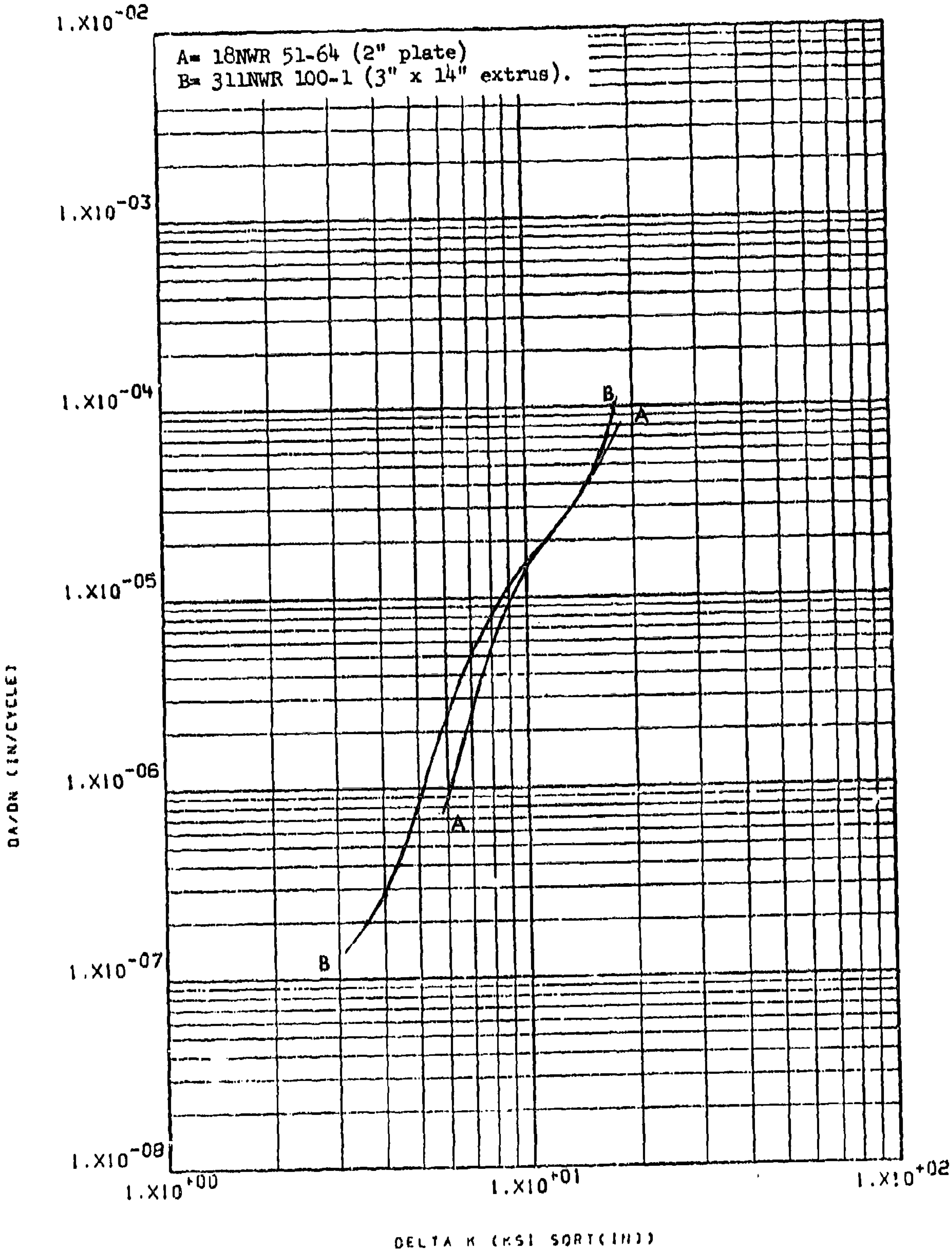

Figure 8.2.7.7-4 Effect of product form on STW-FCGR at R.T., R=0.08, 60 cpm, WR direction in 7075 Al.

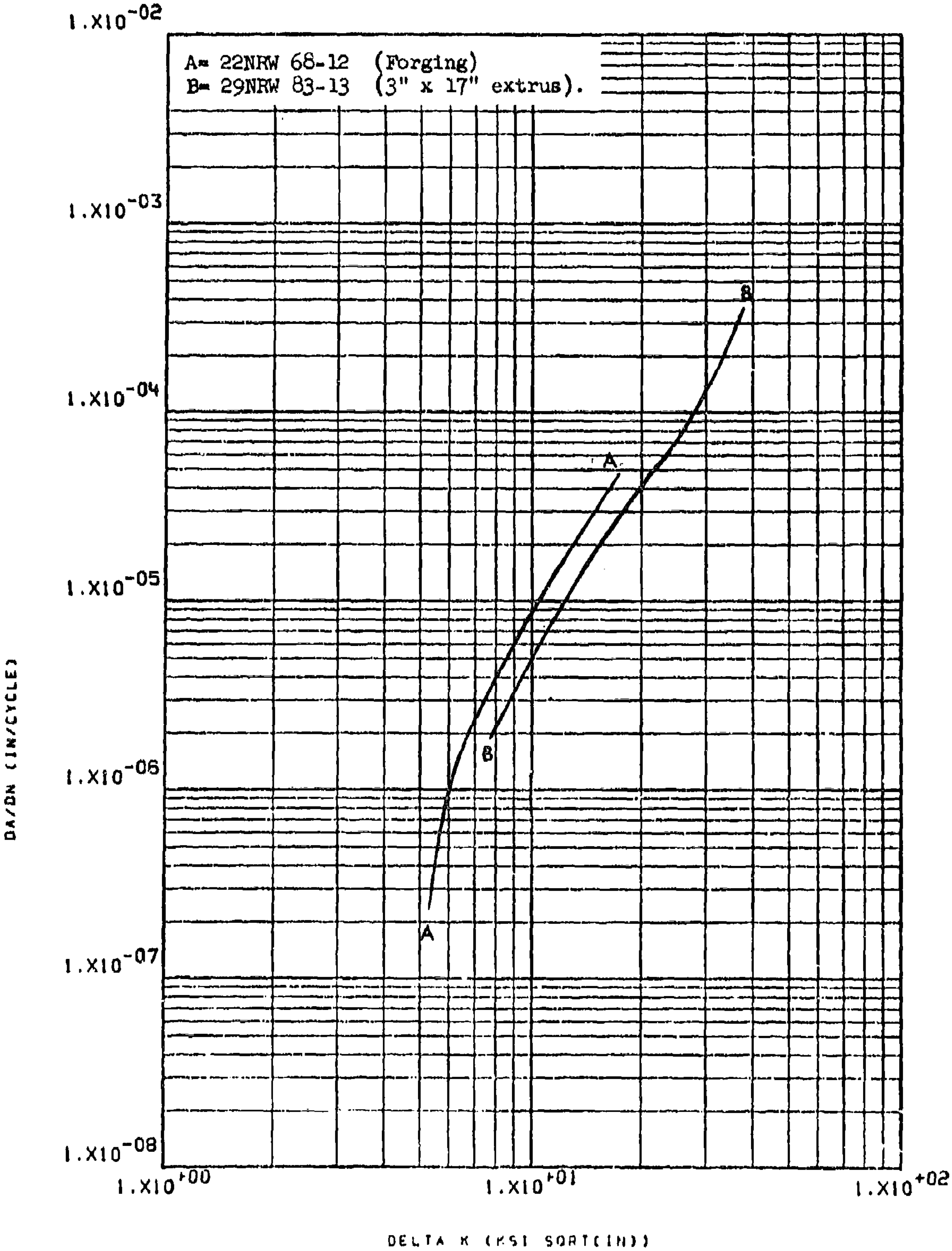

Figure 8.2.7.7-5 Effect of product form on LHA-FCGR at R.T., R=0.08, 360 cpm, RW direction in 7075 Al.

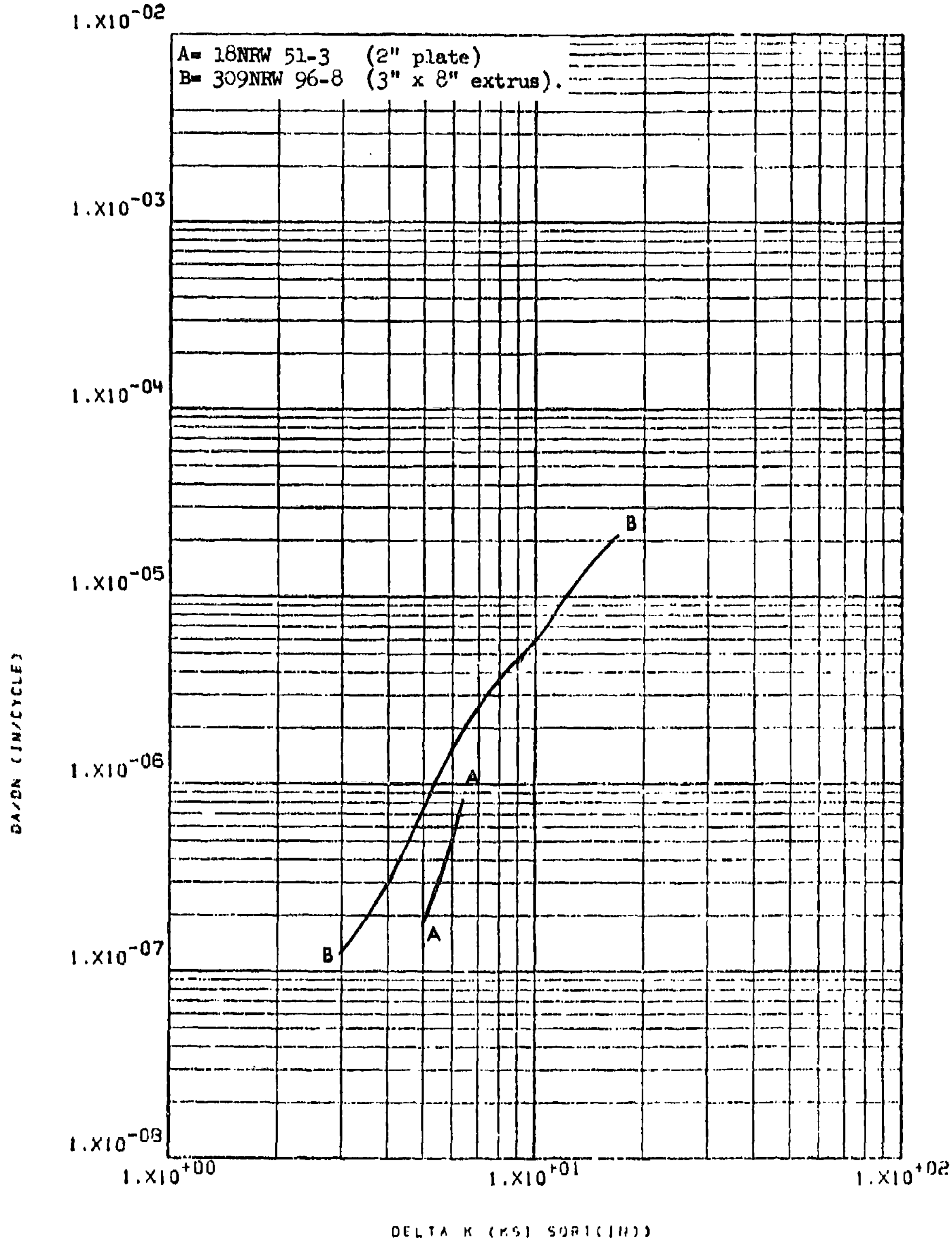

Figure 8.2.7.7-6 Effect of product form on LHA-FCGR at R.T., R=0.08, 360 cpm, RW direction in 7075-T76XX Al.

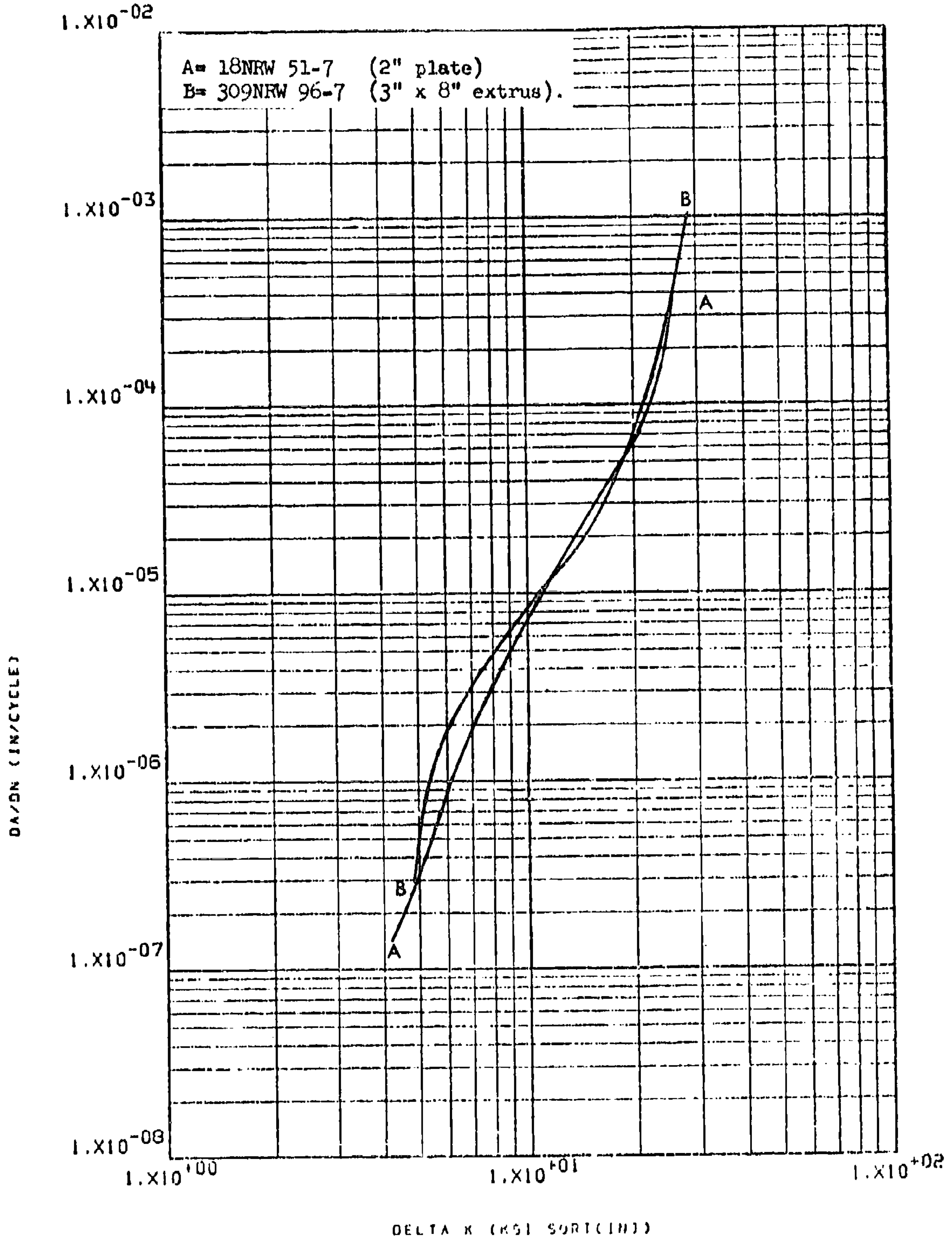

Figure 8.2.7.7-7 Effect of product form on LHA-FCGR at R. T., R=0.3, 360 cpm, RW direction in 7075-T76XX Al.

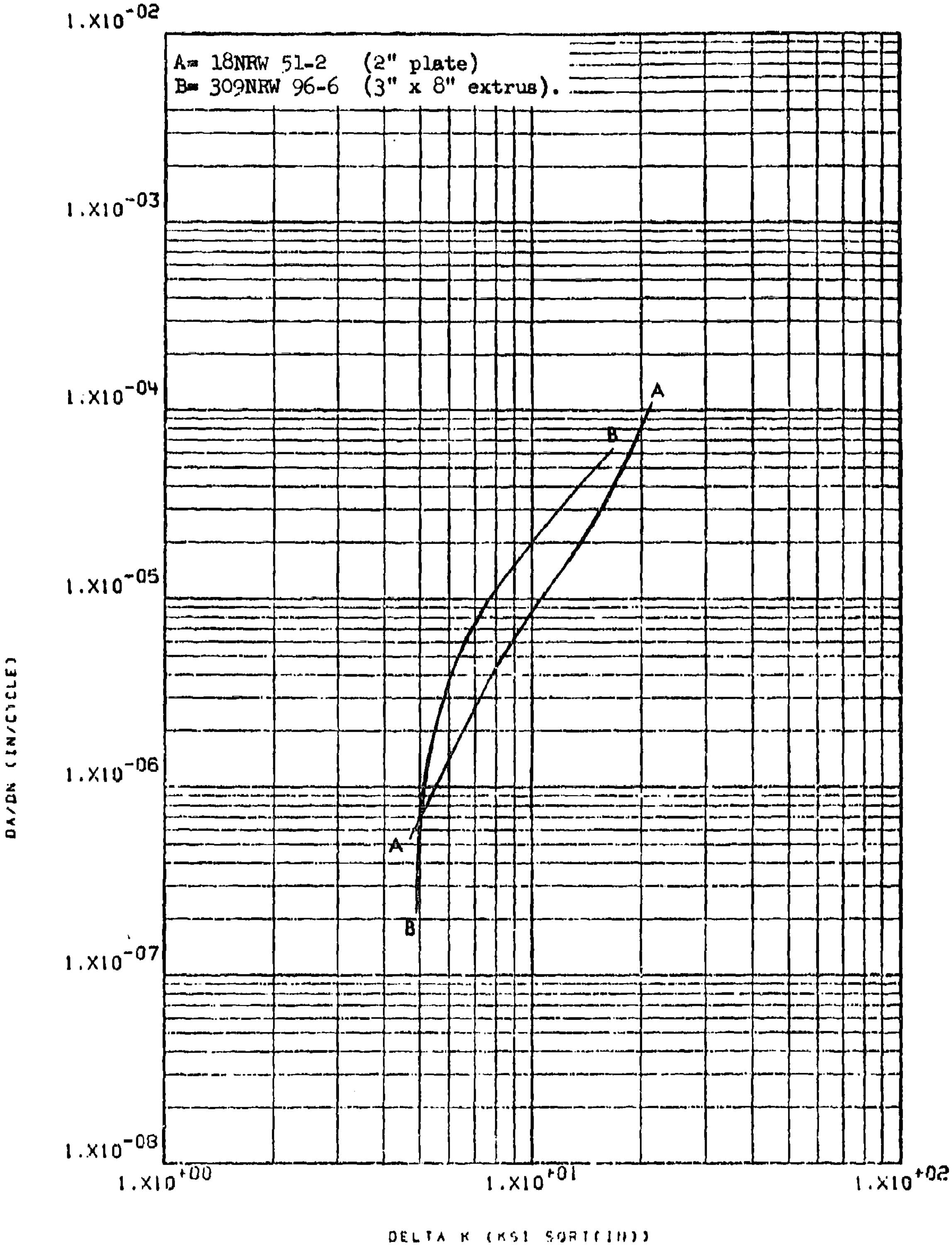

Figure 8.2.7.7-8 Effect of product form on STW-FCGR at R.T., R=0.08, 60 cpm, RW direction in 7075-T76XX Al.

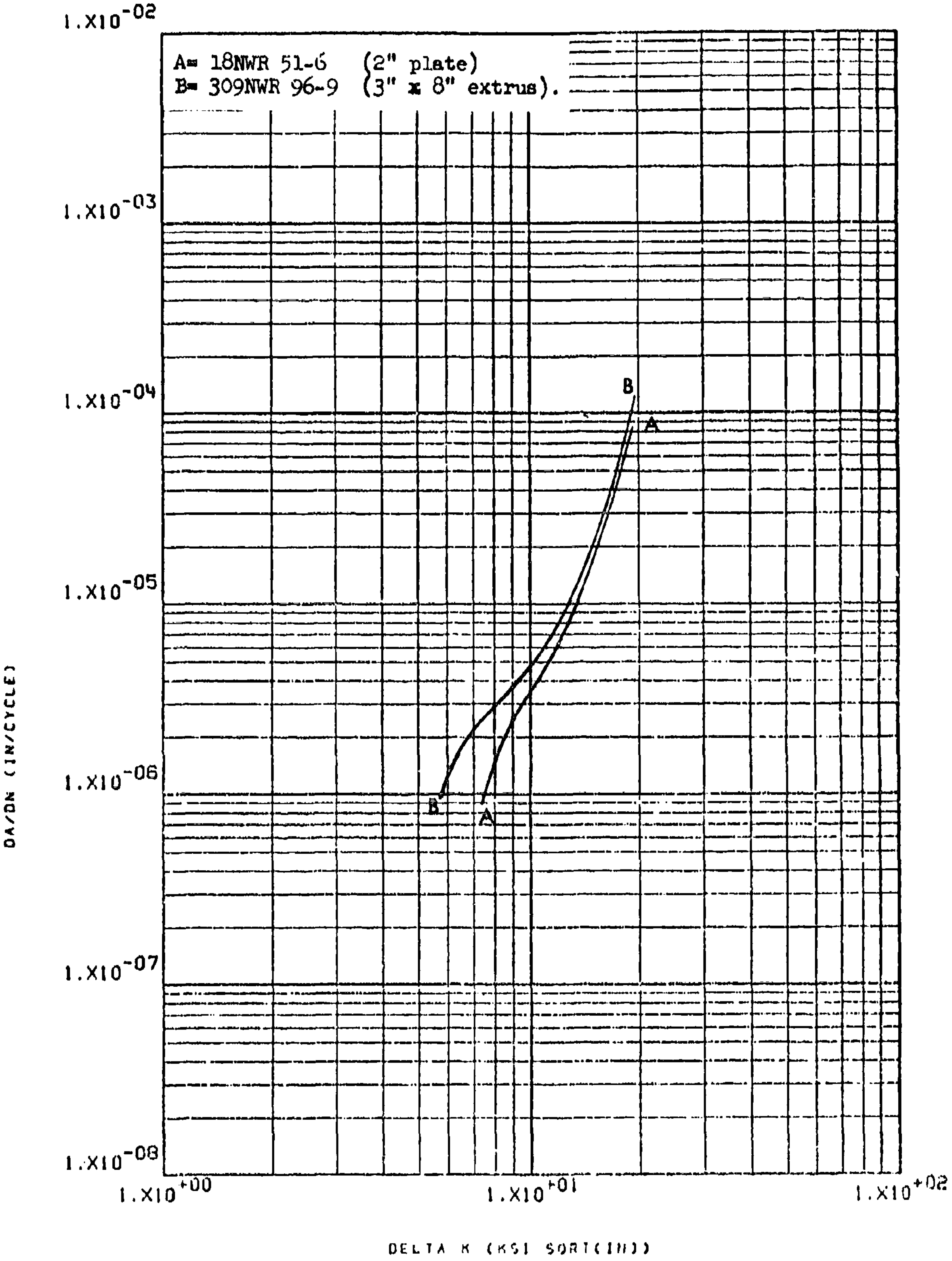

Figure 8.2.7.7-9 Effect of product form on LHA-FCGR at R.T., R=0.08, 360 cpm, WR direction in 7075-T76XX Al.

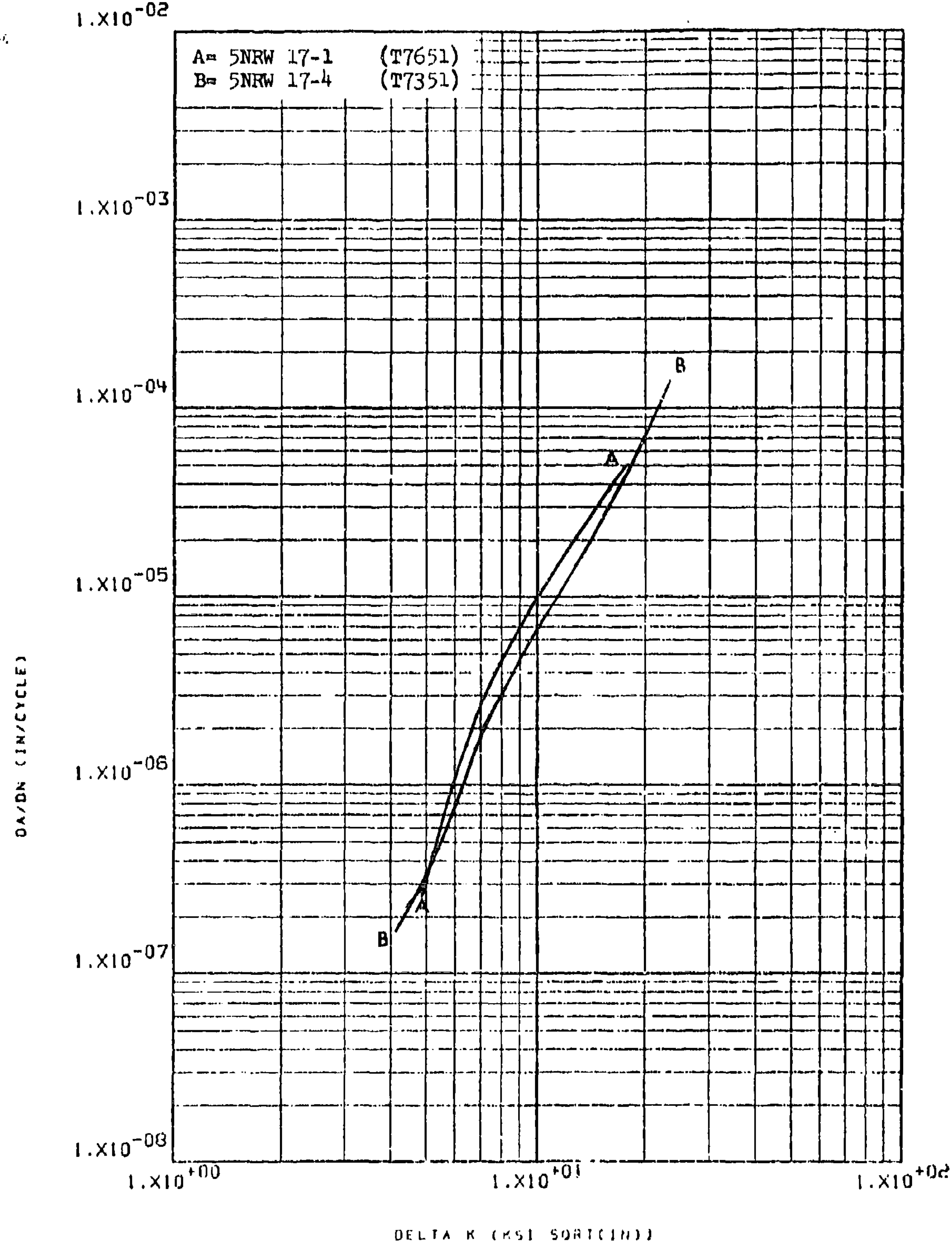

Figure 8.2.7.8-1 **Effect of temper condition on LHA-FCGR at R.T., R=0.08, 360 cpm, RW direction in 7075 Al 2" plate**

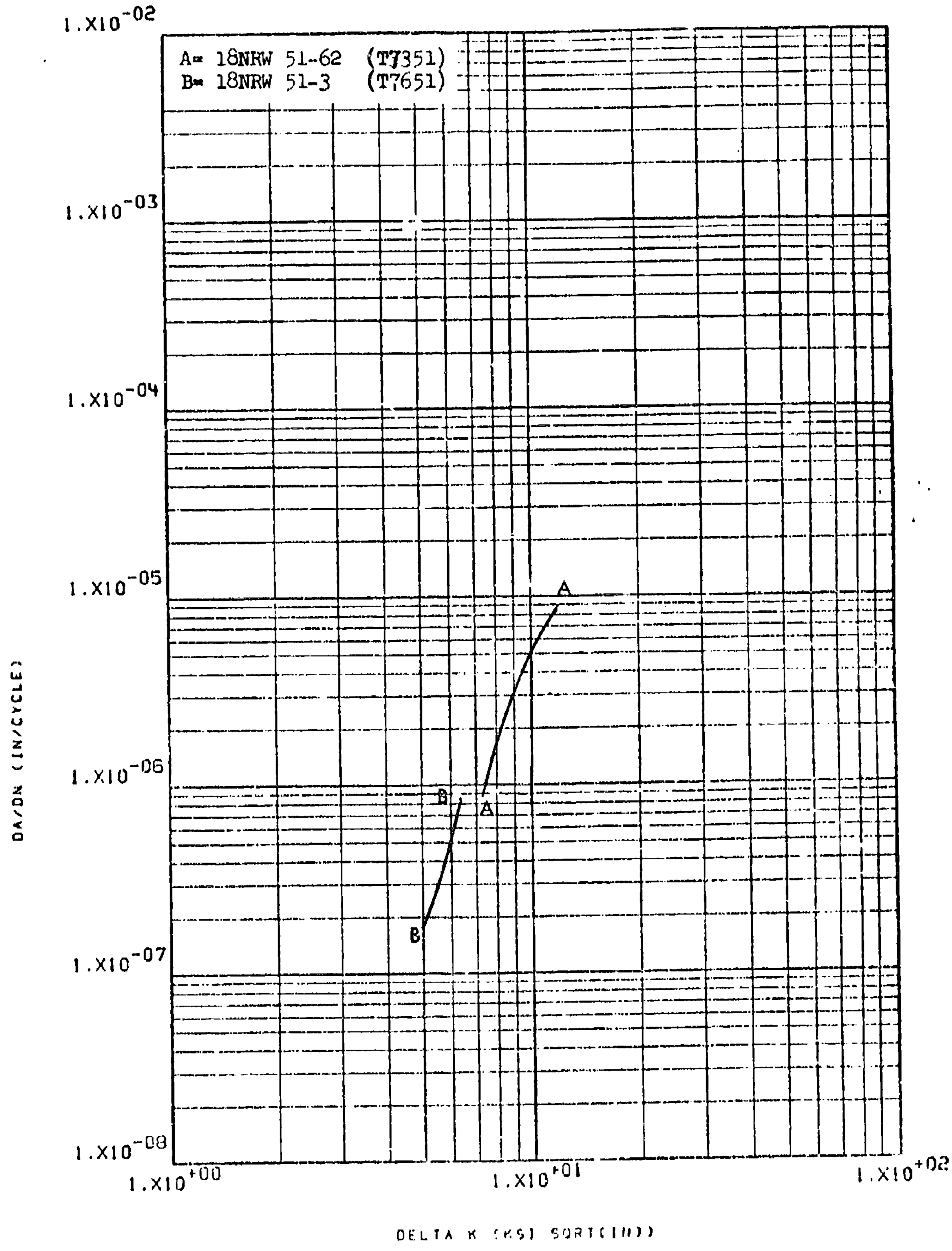

Figure 8.2.7.8-2 Effect of temper condition on LHA-FCGR at R.T., R=0.08, 360 cpm, RW direction in 7075 Al 2" plate

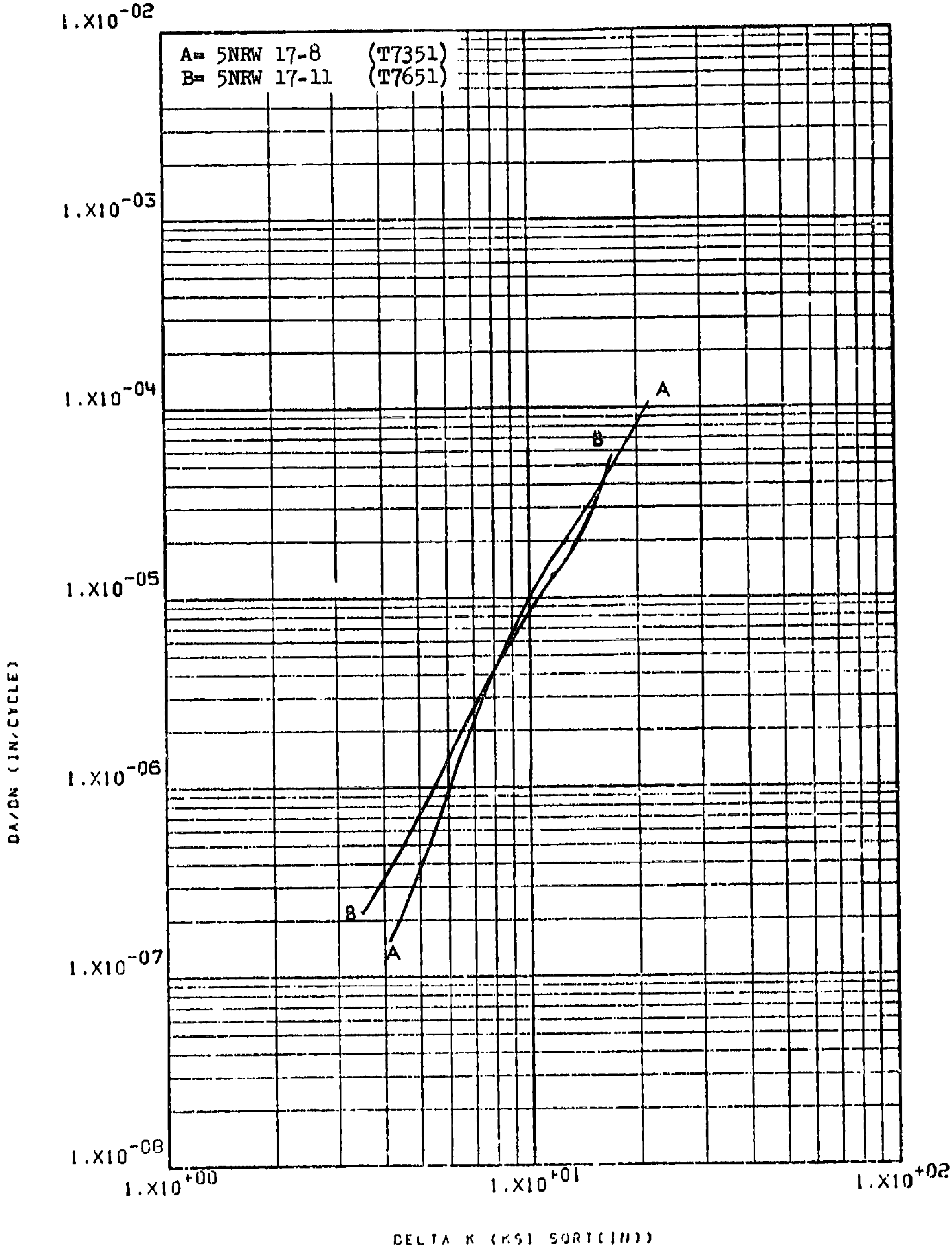

Figure 8.2.7.8-3 Effect of temper condition on STW-FCGR at R.T., R=0.08, RW direction in 7075 Al 2" plate

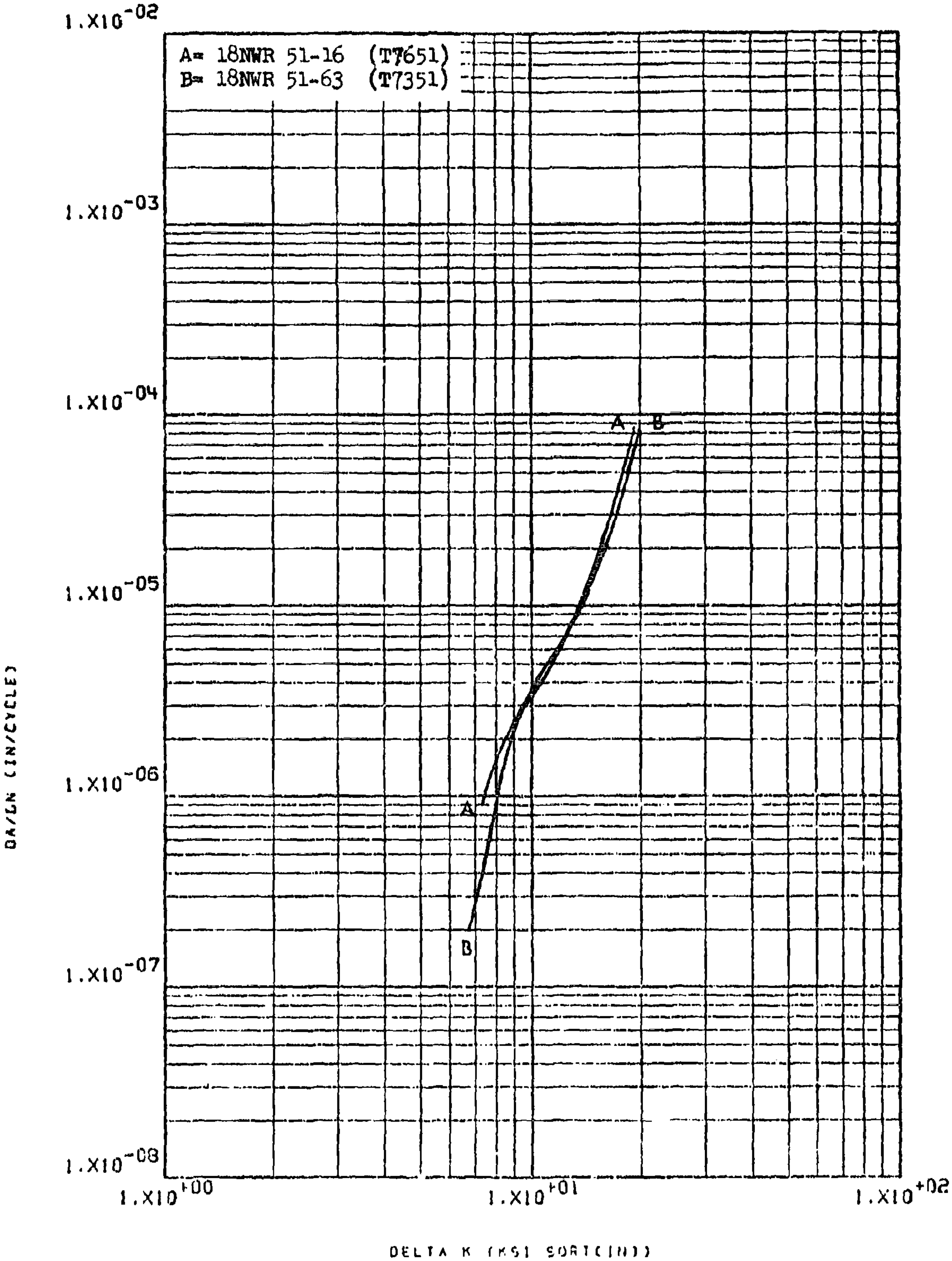

Figure 8.2.7.8-4 Effect of temper condition on LHA-FCGR at R.T., R=0.08, 360 cpm, WR direction in 7075 Al 2" plate

8.2.8 Aluminum Alloy 7175

8.2.8.1 Cyclic Frequency - In low humidity air there was no apparent effect on crack growth rates of increasing cyclic frequency from 6 to 60 to 360 cpm (Figure 8.2.8.1-1). In sump tank water, however, growth rates were seen to be significantly increased when the test frequency was dropped from 60 to 6 cpm (Figure 8.2.8.1-2).

8.2.8.2 Test Temperature - There was no significant effect on growth rates in this material of increasing the temperature of test from room temperature to 265°F (Figure 8.2.8.2-1).

8.2.8.3 Specimen Thickness - Growth rates were seen to be very slightly greater in 1.0 inch thick specimens of this material than in 0.25 inch and in 0.5 inch specimens, when measured in the RW direction (Figure 8.2.8.3-1). This effect was not seen to be consistent in the WR direction, however (Figure 8.2.8.3-2).

8.2.8.4 R Factor - In low humidity air, crack growth rates were increased slightly when R was increased from 0.08 to 0.3, and significantly increased when R was increased from 0.3 to 0.5 (Figure 8.2.8.4-1). In sump tank water, on the other hand, the significant increase in rate was seen to occur when R was increased from 0.08 to 0.3, while the rate increase associated with R being raised from 0.3 to 0.5 was only slight (Figure 8.2.8.4-2).

8.2.8.5 Environment - Crack growth rates of this material in shop cleaning solvent and field cleaning solvent were seen to be essentially equivalent with both rates being substantially greater than low humidity air growth rates at delta K levels up to ~ 11 ksi $\sqrt{in.}$ At this level of delta K growth rates in all three environments were essentially the same (Figure 8.2.8.5-1). Growth rates in sump tank water were seen to be greater than those in low humidity air only when above particular delta K levels ranging from 6.5 to 9.5 ksi $\sqrt{in}$, depending on test frequency and direction (Figure 8.2.8.5-1 through -3).

8.2.8.6 Test Direction - In both low humidity air and sump tank water, fatigue crack growth rates of this material were seen to be greater in the RW direction than in the WR direction at low levels of delta K (Figures 8.2.8.6-1 and -2). The magnitude of this effect diminished, however, as delta K was increased up to ~ 15 ksi $\sqrt{in}$, where the rates were seen to be approximately equal. The magnitude of this directional effect was seen to be decreased by decreasing specimen thickness from 1.0 to 0.5 inch (Figures 8.2.8.6-1 and -3).

8.2.8.7 Product Form - Based on very limited comparative data, low humidity air crack growth rates in a compressive stress relieved forged block appeared to be significantly greater than those in a non-stress relieved die forging (Figure 8.2.8.7-1).

8.2.8.8 Heat Treat Condition - Not evaluated.

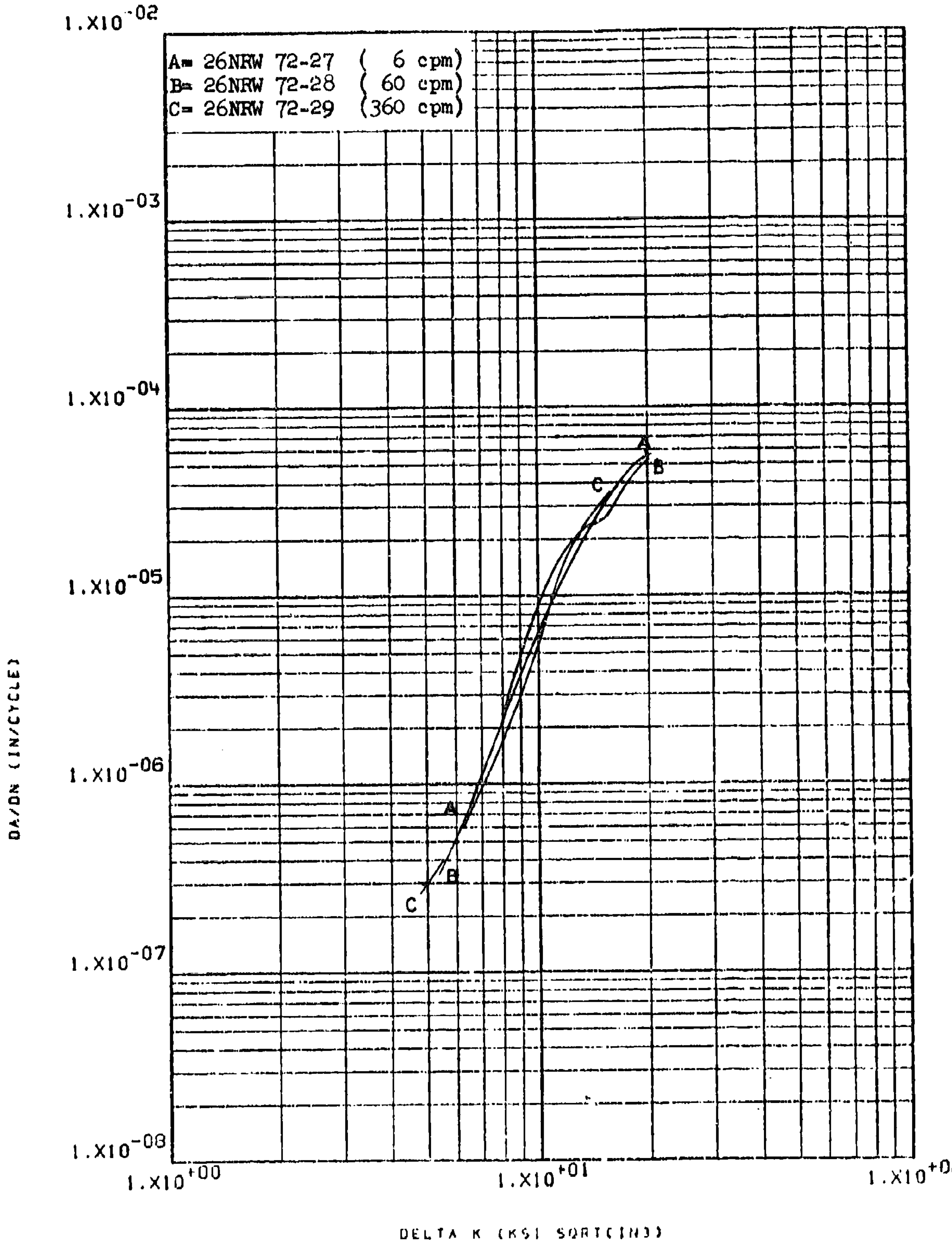

Figure 8.2.8.1-1 Effect of cyclic frequency on LHA-FCGR at R.T., R=0.08, RW direction in 7175-T73652 6" x 14" x 48" forged block

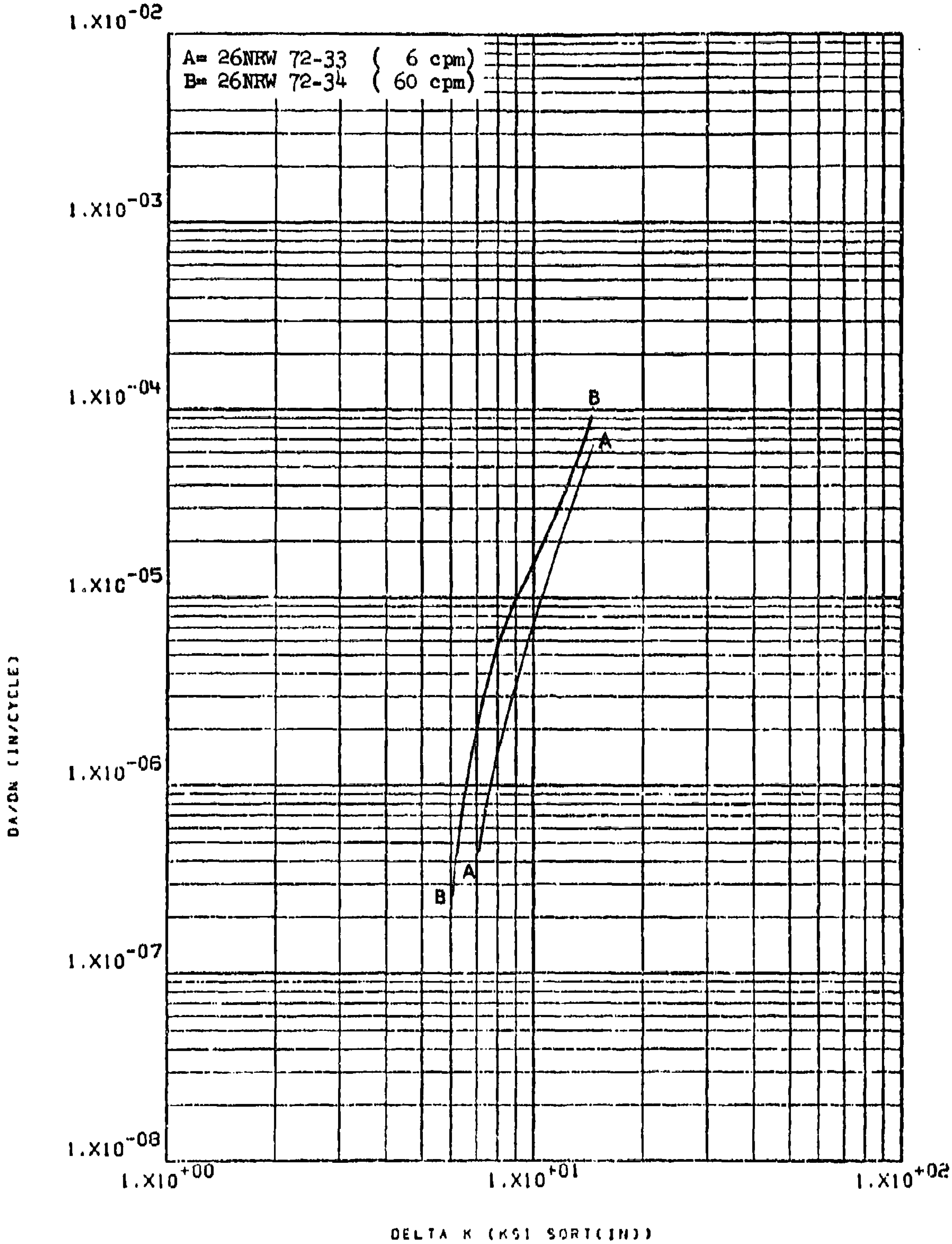

Figure 8.2.8.1-2 Effect of cyclic frequency on STW-FCGR at R.T., R=0.08, RW direction in 7175-T73652 6" x 14" x 48" forged block

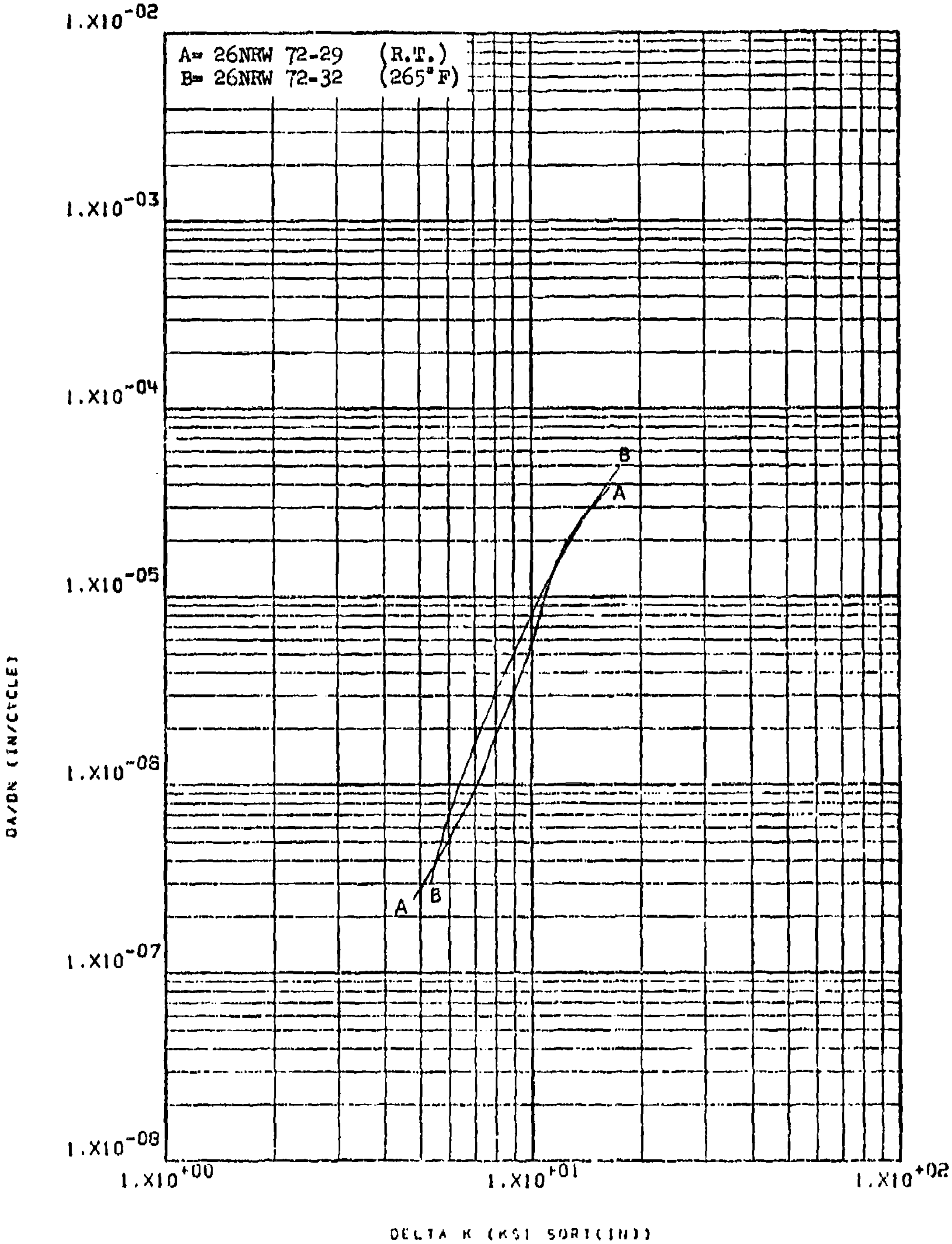

Figure 8.2.8.2-1 Effect of test temperature on LHA-FCGR at R=0.08, 360 cpm, RW direction in 7175-T73652 6" x 14" x 48" forged block

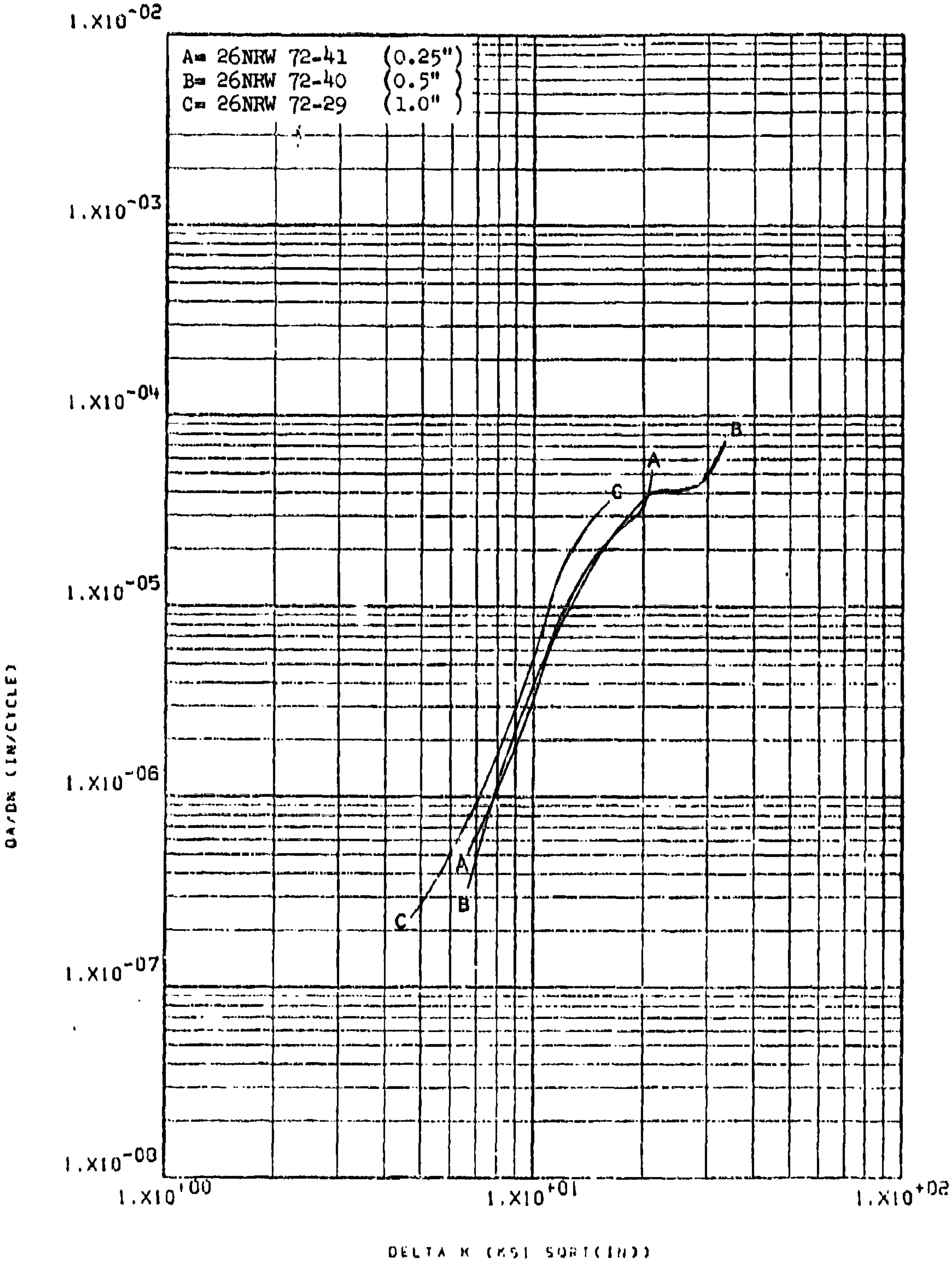

Figure 8.2.8.3-1 Effect of specimen thickness on LHA-FCGR at R.T., R=0.08, 360 cpm, RW direction in 7175-T73652 6" x 14" x 48" forged block

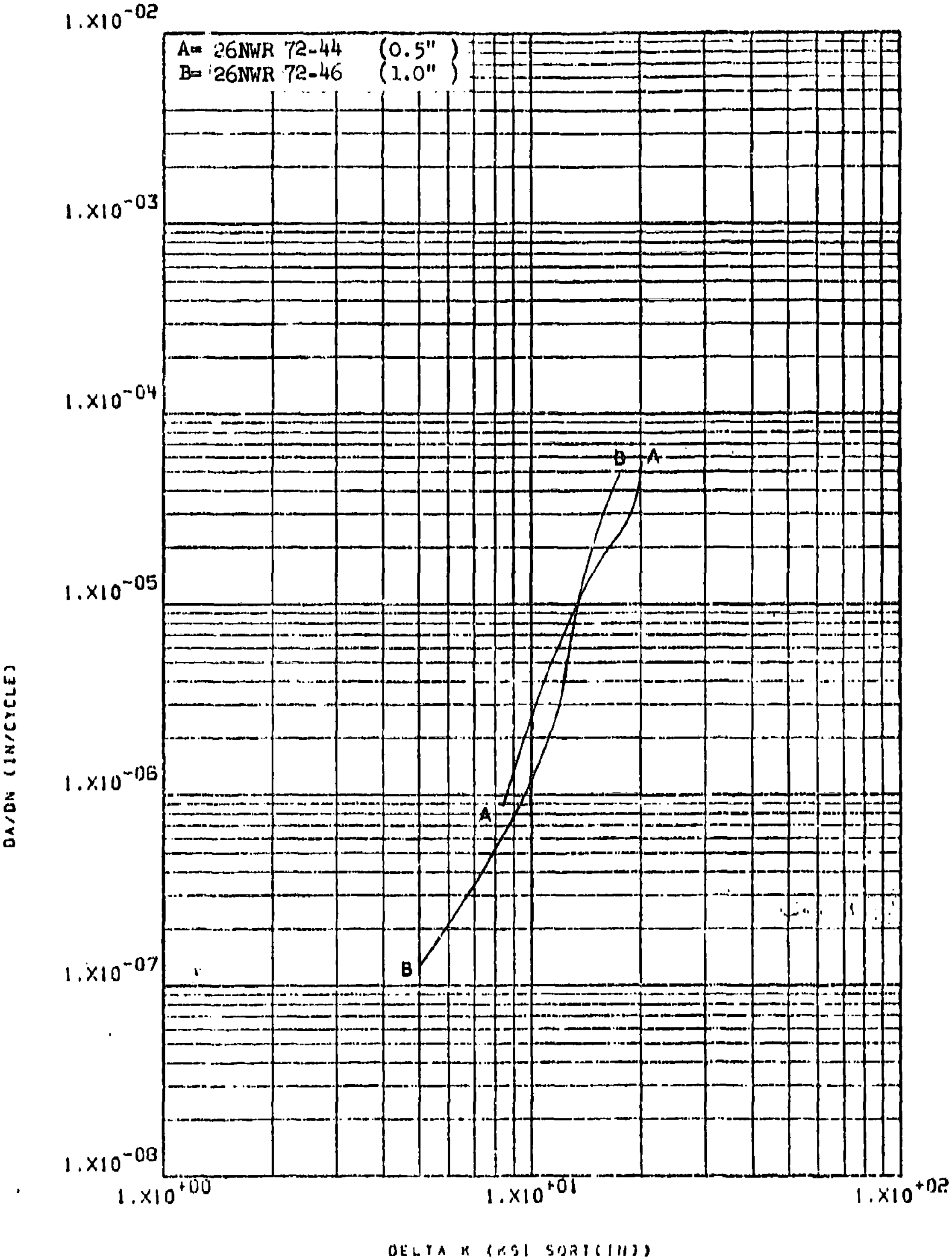

Figure 8.2.8.3-2 Effect of specimen thickness on LHA-FCGR at R.T., R=0.08, 360 cpm, WR direction in 7175-T73652 6" x 14" x 48" forged block

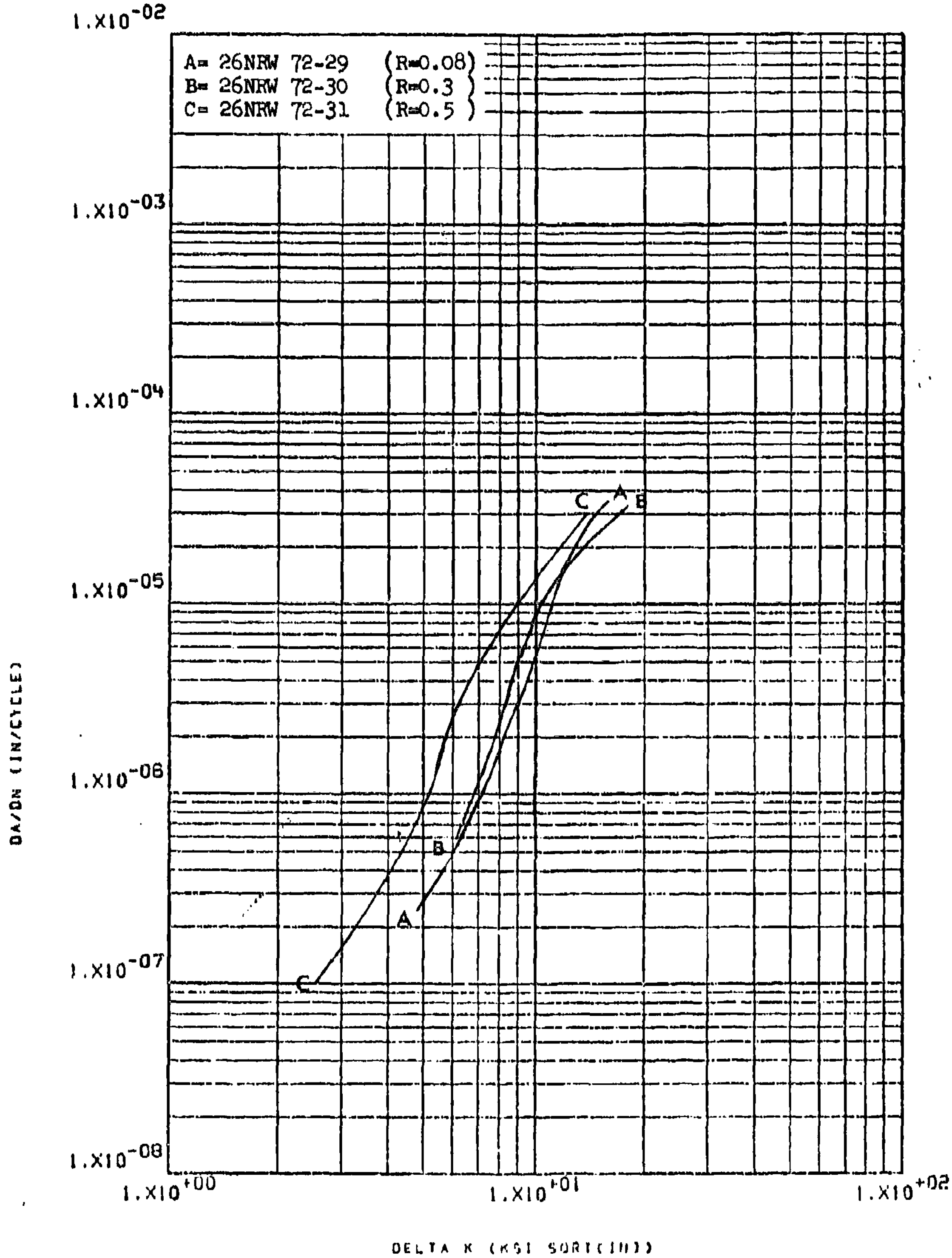

Figure 8.2.8.4-1 Effect of R factor on LHA-FCGR at R.T., 360 cpm, RW direction in 7175-T73652 6" x 14" x 48" forged block

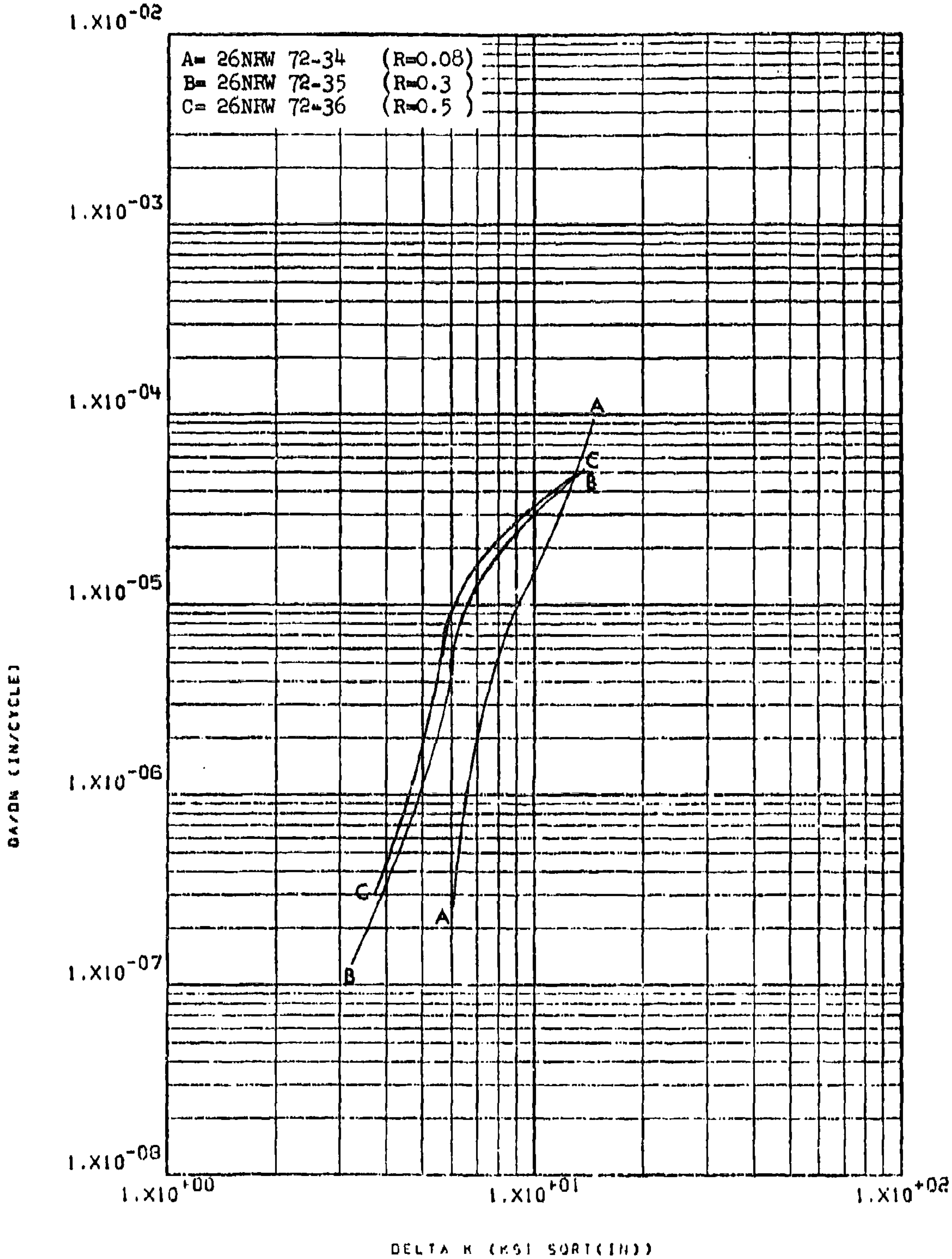

Figure 8.2.8.4-2 Effect of R factor on STW-FCGR at R.T., 60 cpm, RW direction in 7175-T73652 6" x 14" x 48" forged block

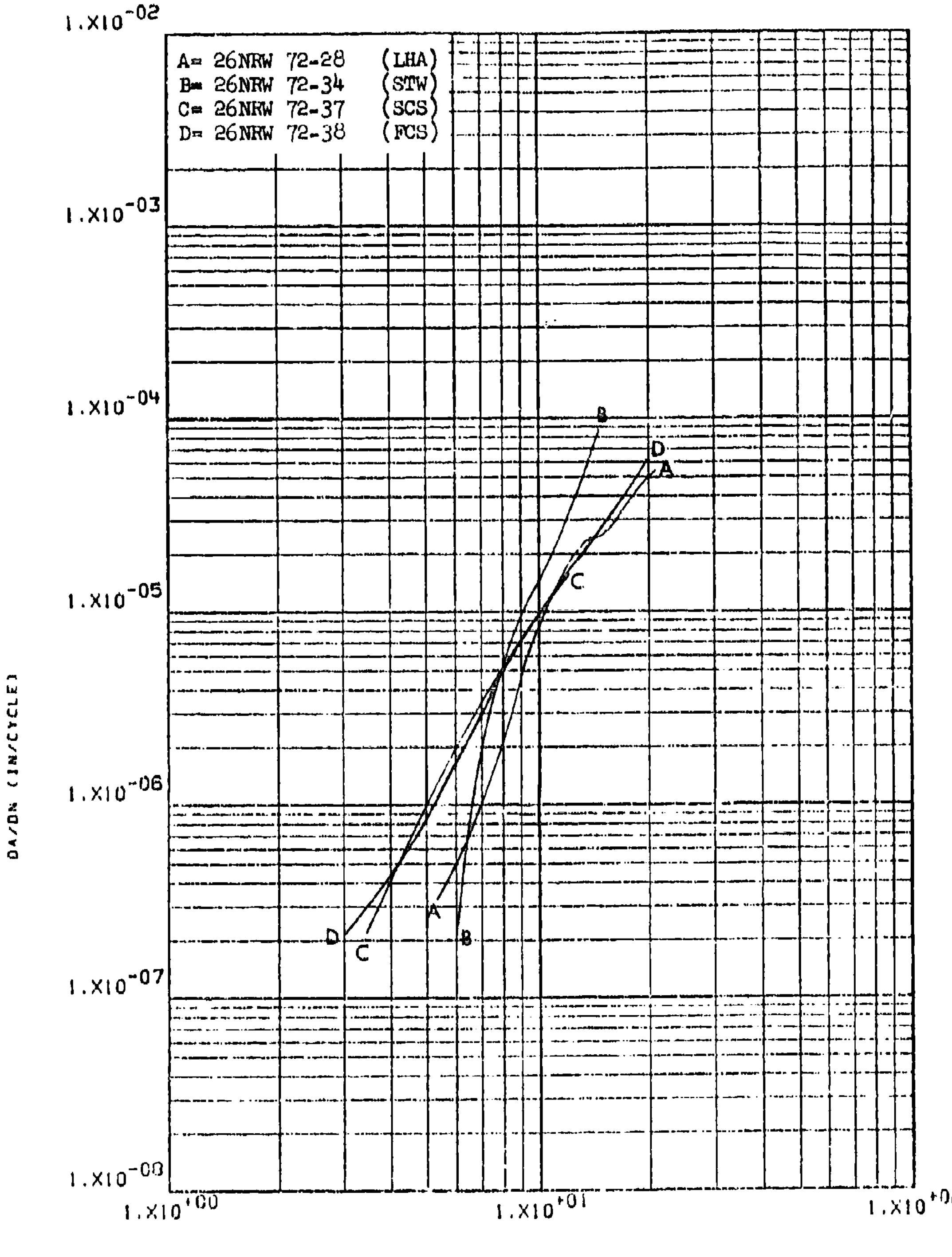

Figure 8.2.8.5-1 Effect of environment on FCGR at R.T., 60 cpm, R=0.08, RW direction in 7175-T73652 6" x 14" x 48" forged block

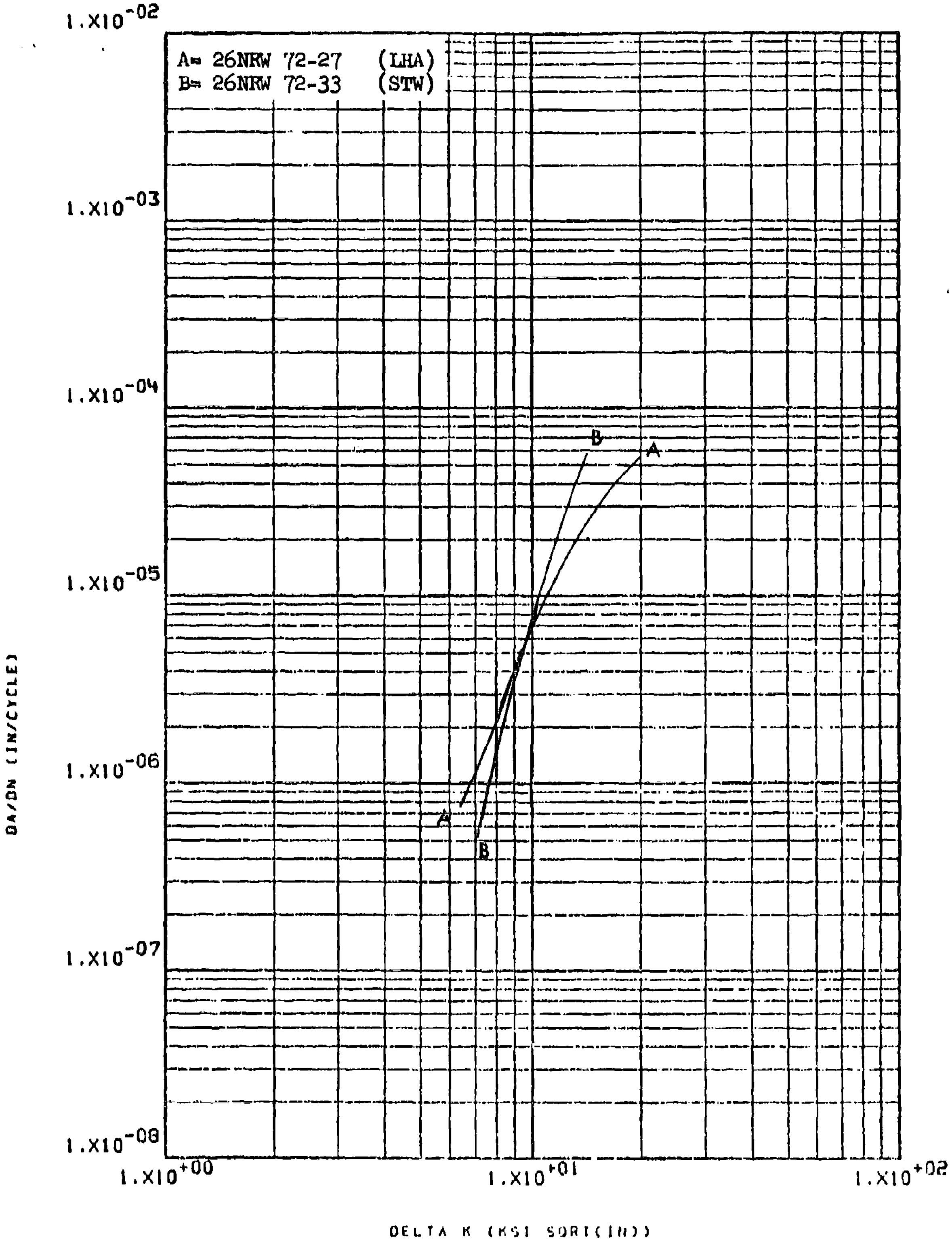

Figure 8.2.8.5-2 Effect of environment on FCGR at R.T., 6 cpm, R=0.08, RW direction in 7175-T73652 6" x 14" x 48" forged block

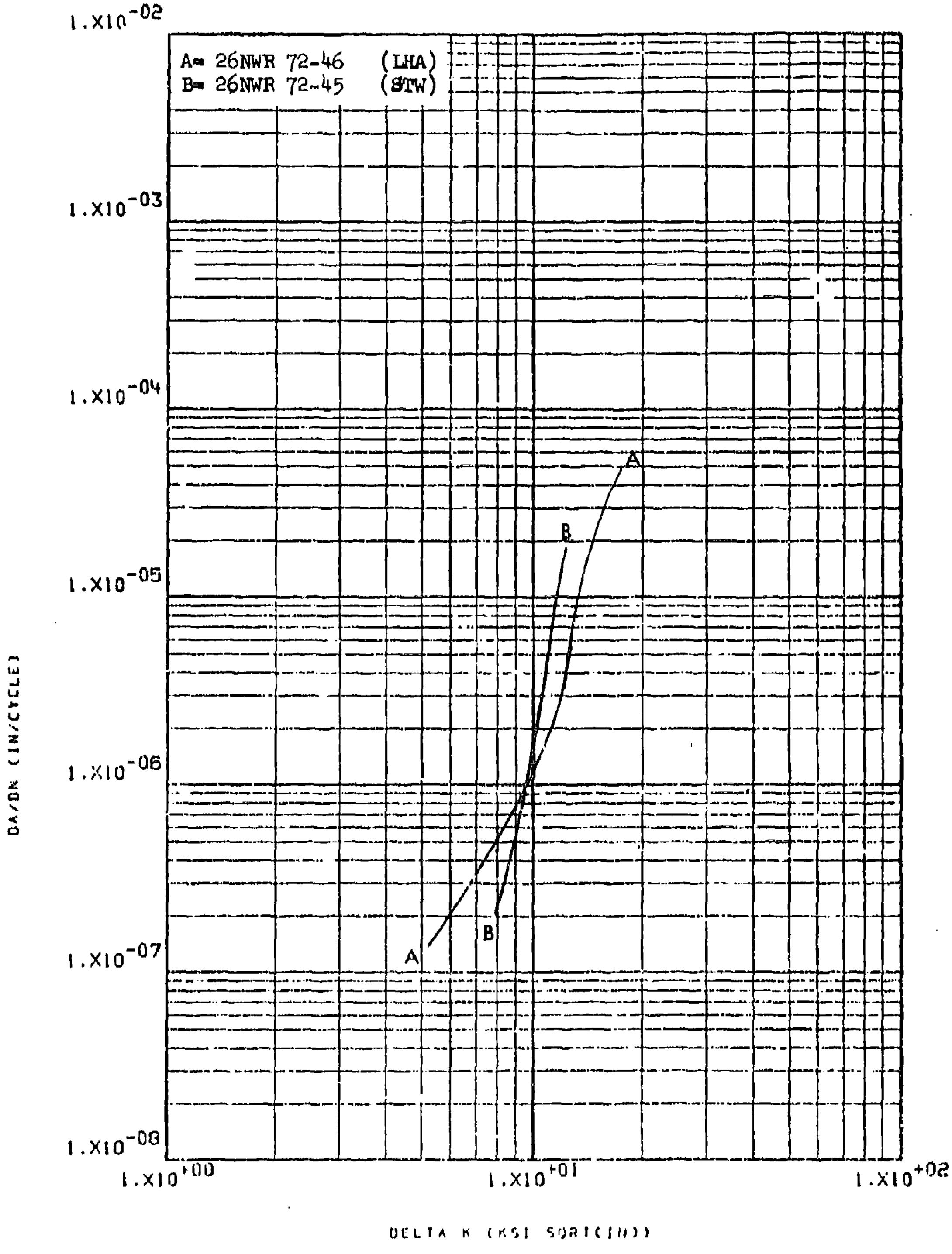

Figure 8.2.8.5-3 Effect of environment on FCGR at R.T., R=0.08, WR direction in 7175-T73652 6" x 14" x 48" forged block

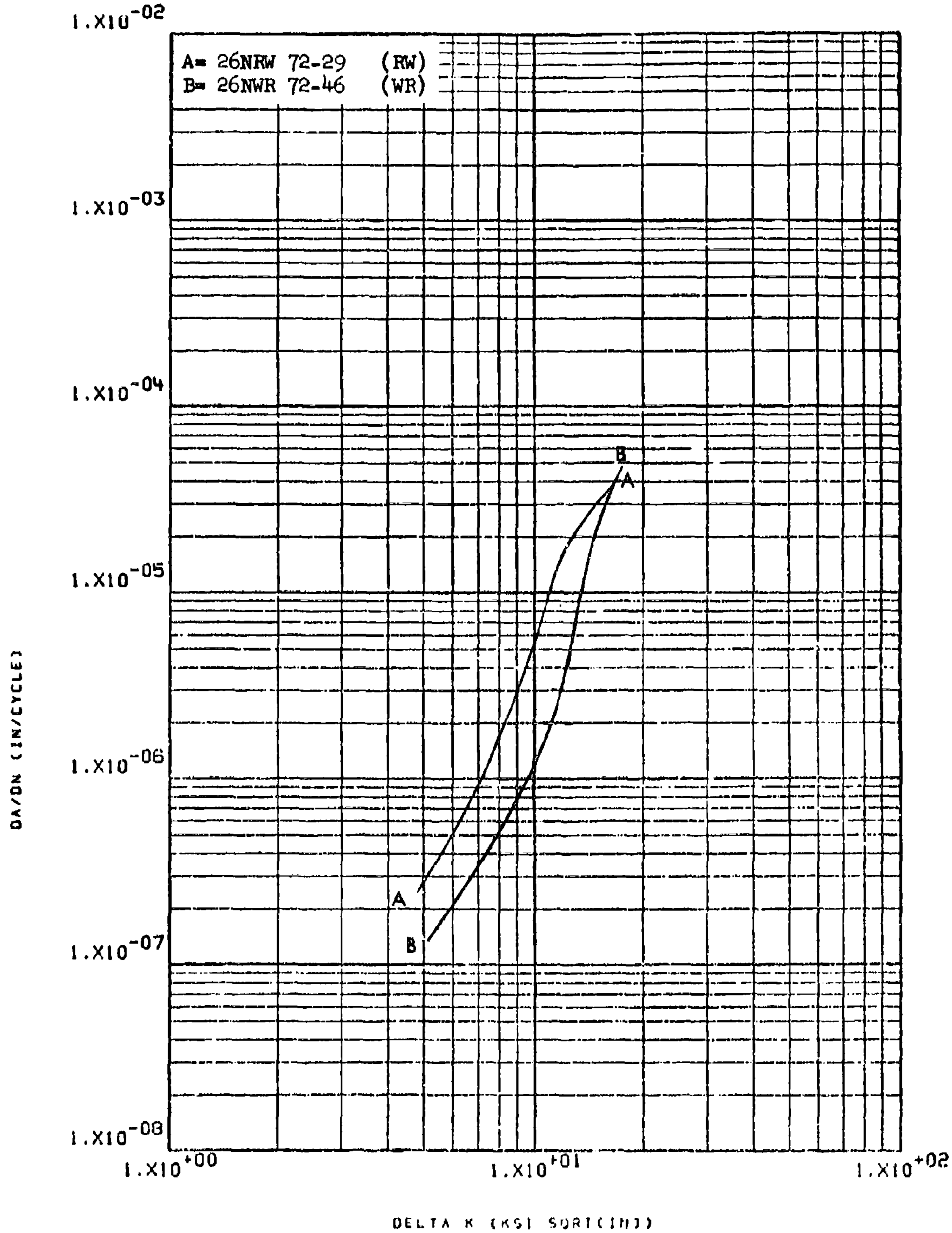

Figure 8.2.8.6-1 Effect of test direction on LHA-FCGR at R.T., R=0.08, 360 cpm in 7175-T73652 6" x 14" x 48" forged block

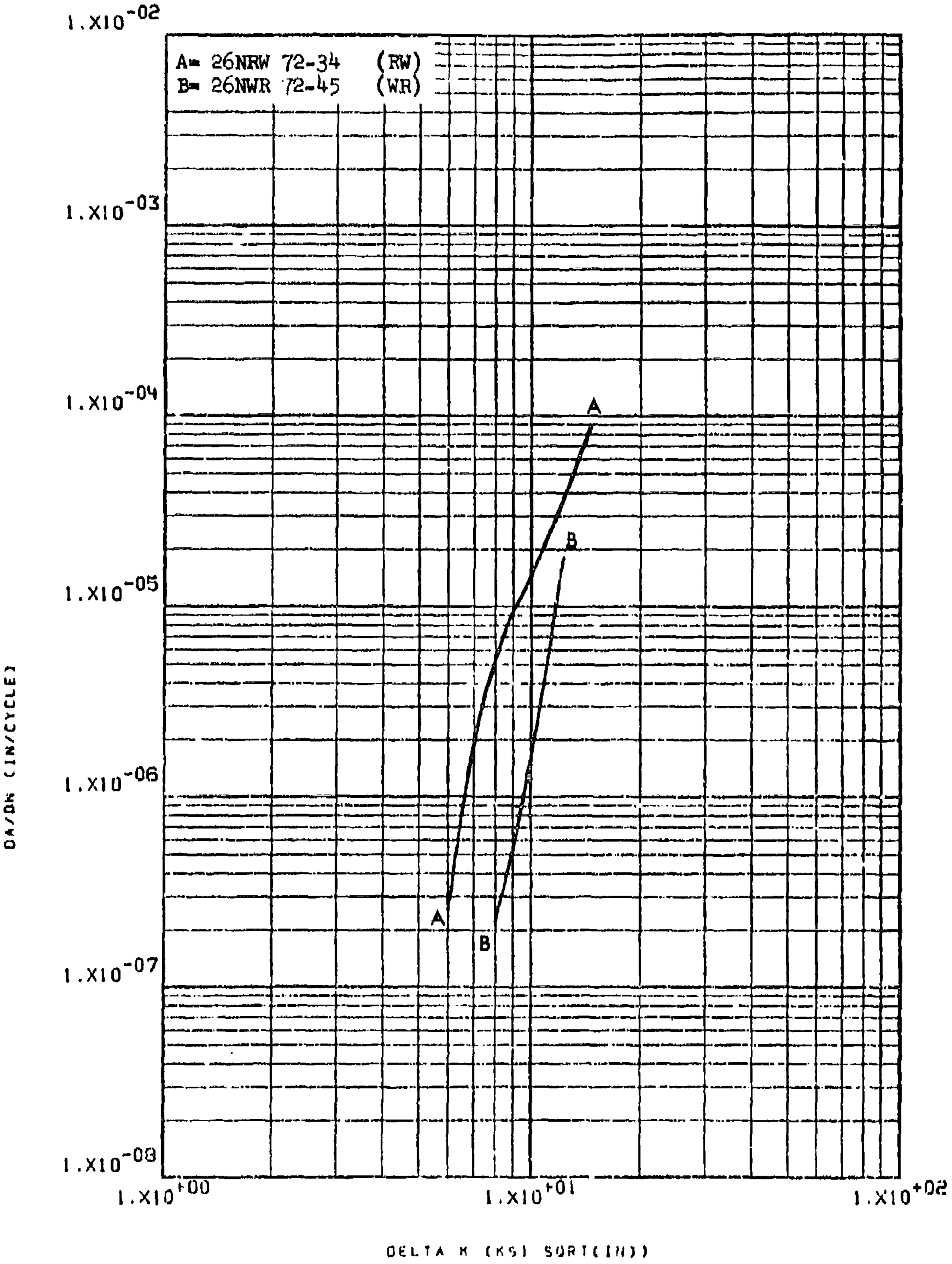

Figure 8.2.8.6-2 Effect of test direction on STW-FCGR at R.T., R=0.08, 60 cpm in 7175-T73652 6" x 14" x 48" forged block

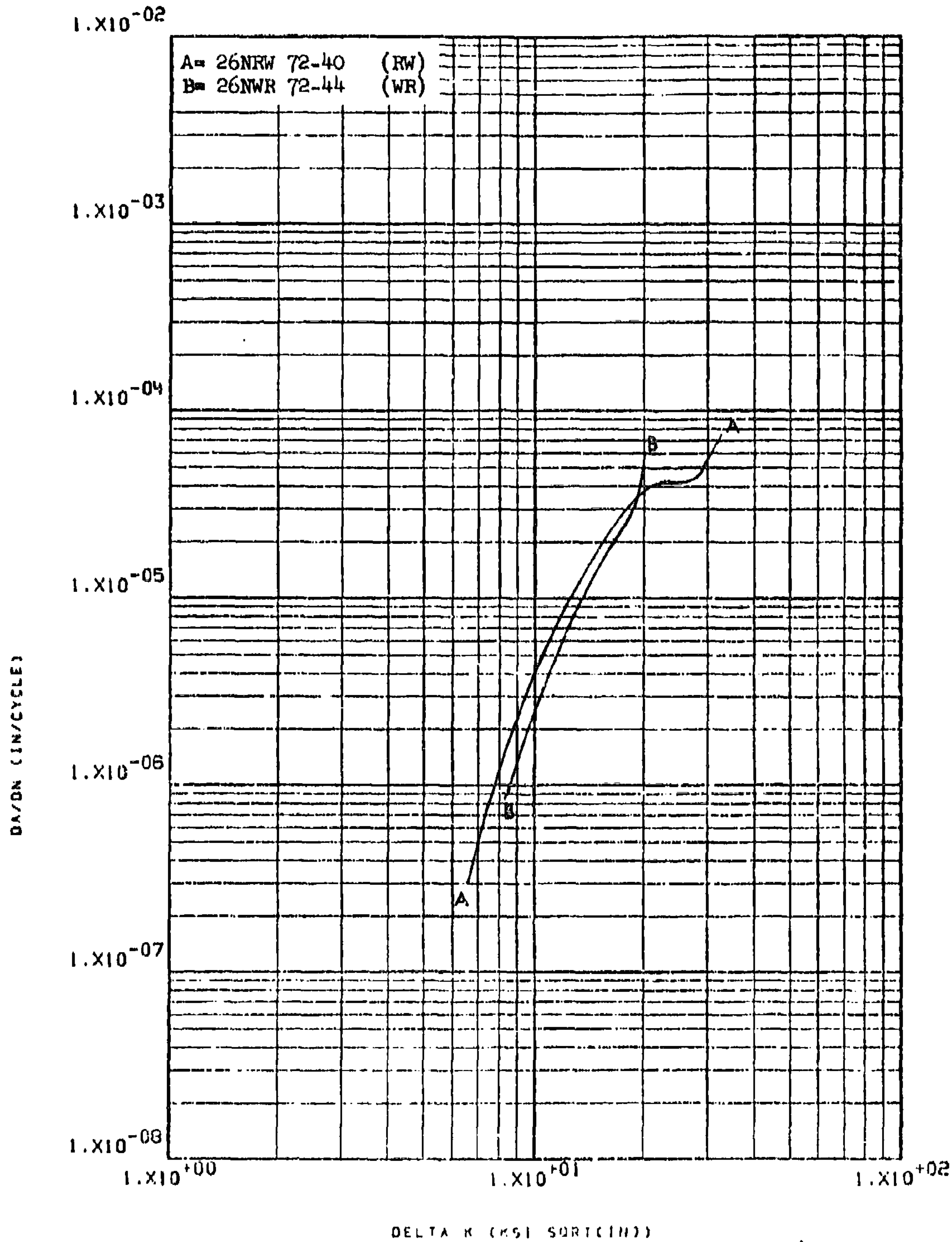

Figure 8.2.8.6-3 Effect of test direction on LHA-FCGR at R.T., R=0.08, 360 cpm, in 1/2" thick specimens of 7175-T73652,6" x 14" x 48" forged block

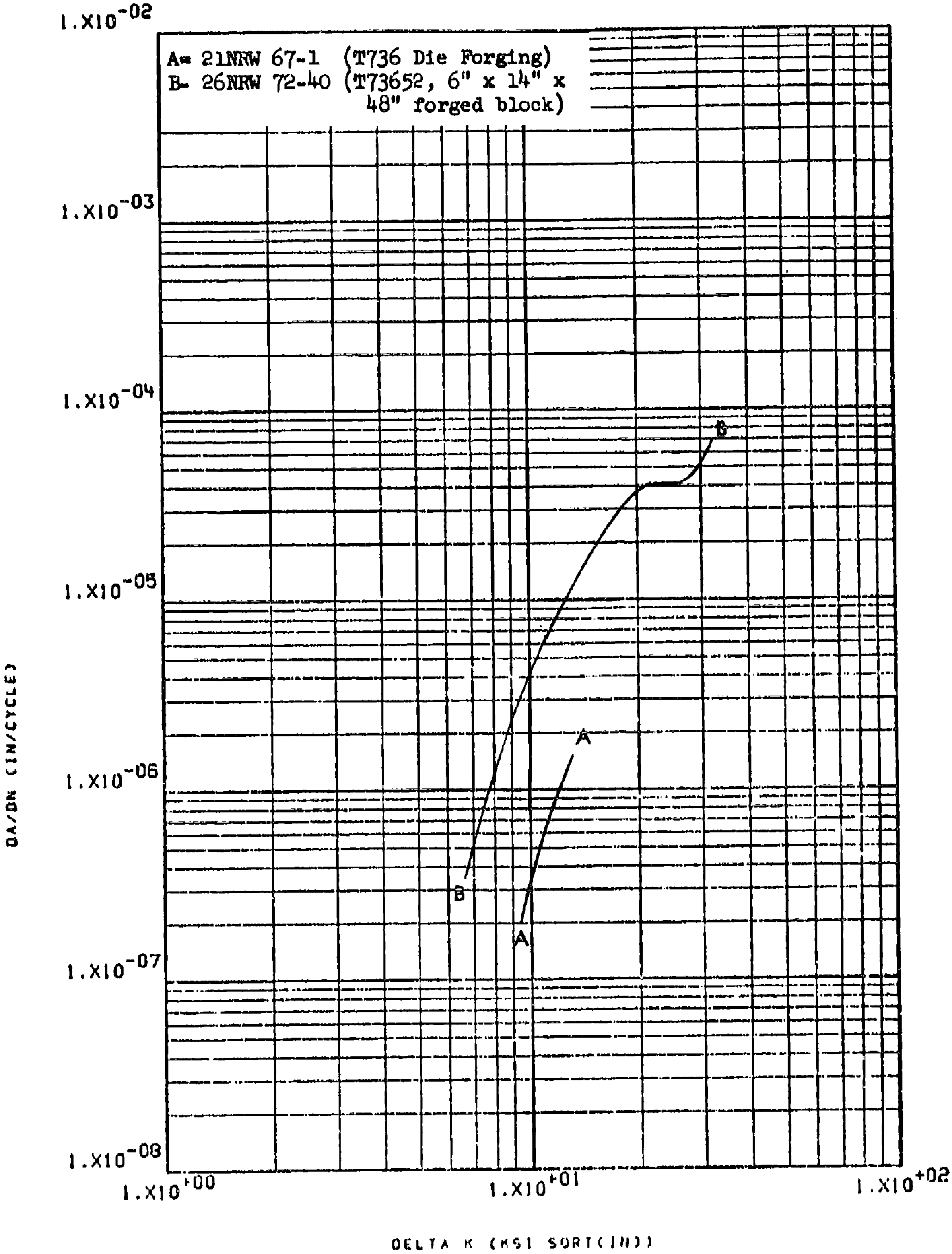

Figure 8.2.8.7-1 Effect of product form on IHA-FCGR at R.T., R=0.08, 360 cpm, RW direction in 1/2"thick specimens of 7175 Al.

8.2.9 9Ni-4Co-0.20C Steel

8.2.9.1 Cyclic Frequency - The effect of changing cyclic frequency on low humidity air fatigue crack growth rates was seen to be inconsistent from material to material. In one forged bar, for example, growth rates at 60 and 360 cpm were essentially equivalent (Figure 8.2.9.1-1). In another bar no effect was seen of changing the cyclic frequency from 6 to 60 cpm throughout the delta K range, or from changing the frequency from 60 to 540 cpm at low delta K levels up to $\sim$15 ksi$\sqrt{\text{in.}}$ Above this level, however, growth rates at 540 cpm were seen to be noticeably greater than at 6 or 60 cpm (Figure 8.2.9.1-2).

8.2.9.2 Test Temperature - Low humidity air fatigue crack growth rates of this material were seen to be slightly greater at ambient temperature than at -65°F in both the RW and WR directions of rolled plate (Figures 8.2.9.2-1 through -3). This effect was even more noticeable in forged bar (Figure 8.2.9.2-4).

8.2.9.3 Specimen Thickness - A very slight increase in low humidity air fatigue crack growth rates of this material was seen to result from increasing the specimen thickness from 0.825" to 1.0" (Figure 8.2.9.3-1). No increase was seen to result, however, when thickness was increased from 0.25" to 0.5" (Figure 8.2.9.3-2).

8.2.9.4 R Factor - Low humidity air and 100% humidity fatigue crack growth rates of this material were essentially unchanged by increases in R factor from 0.08 to 0.3. In low humidity air, further increases in R to 0.5 did not affect growth rates (Figure 8.2.9.4-1) while in 100% humidity, this increase in R resulted in a very slight increase in growth rates (Figure 8.2.9.4-2).

8.2.9.5 Environment - The fatigue crack growth rates of this material in a 100% humidity environment were seen to be slightly greater than those in low humidity air. The magnitude of this environmental effect was also seen to decrease with increasing R factors until at R=0.5 the difference in rates was negligible (Figure 8.2.9.5-1 through -3). Growth rates in shop cleaning solvent and sump tank water were seen to be essentially equivalent to those in low humidity air, although at the high and low ends of delta K rates in sump tank water were very slightly greater than those in low humidity air and shop cleaning solvent (Figure 8.2.9.5-4).

8.2.9.6 Test Direction - There was no significant difference observed between the growth rates in the RW and WR directions for this material in any of the conditions evaluated (Figures 8.2.9.6-1 through -5).

8.2.9.7 Product Form - There was no significant or consistent effect of product form on the fatigue crack growth rate characteristics of this material when tested in low humidity air, 100% humidity and sump tank water in the RW and WR directions at ambient temperature and -65°F, and at frequencies of 60 and 360 cpm (Figures 8.2.9.7-1 through -7). Forms tested included forged block and rolled plate.

8.2.9.8 Heat Treat Condition - Not evaluated.

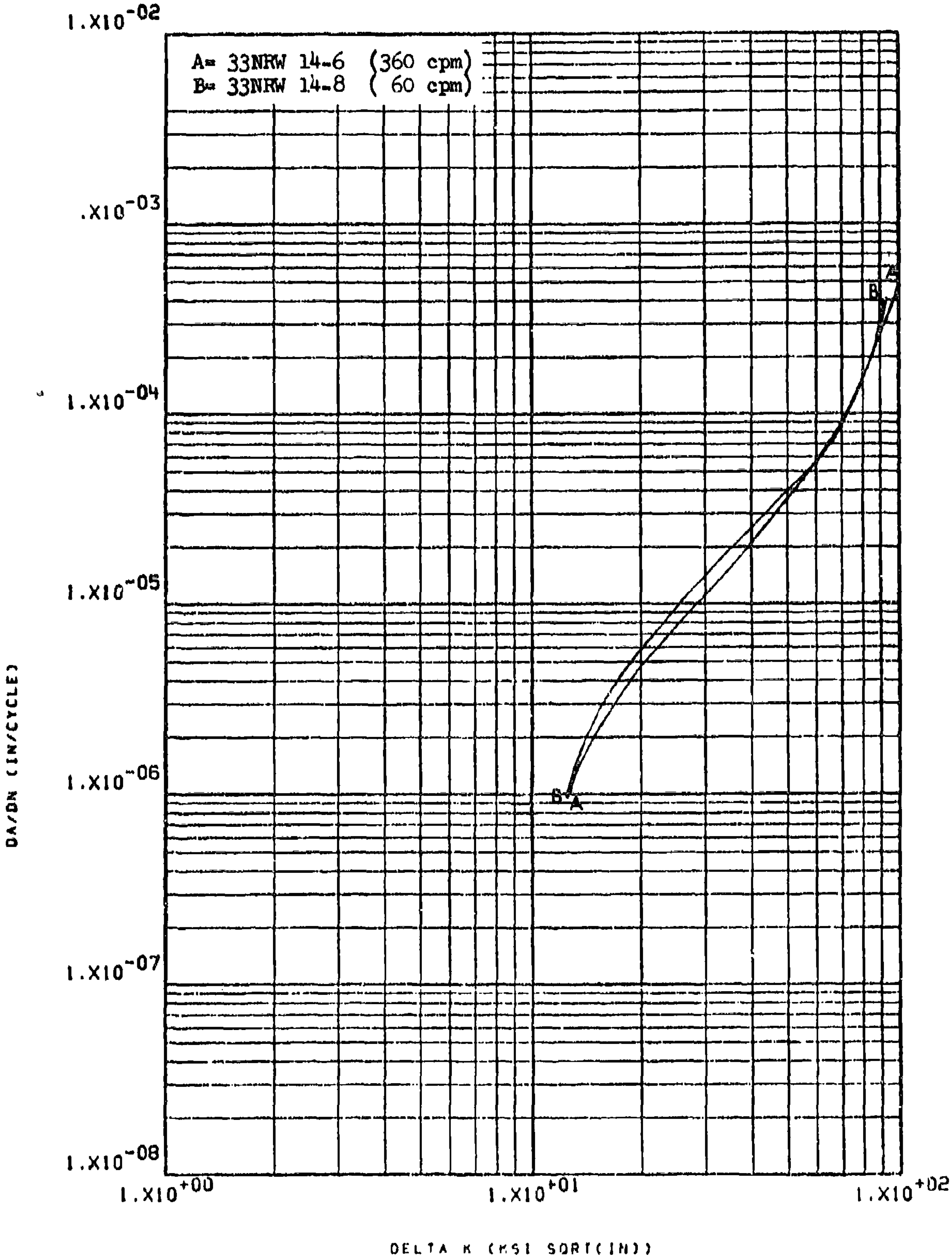

Figure 8.2.9.1-1 Effect of cyclic frequency on LHA-FCGR at R.T., R=0.08, RW direction in 4" x 18" x 36" HP-.9-.4-.20 forged bar

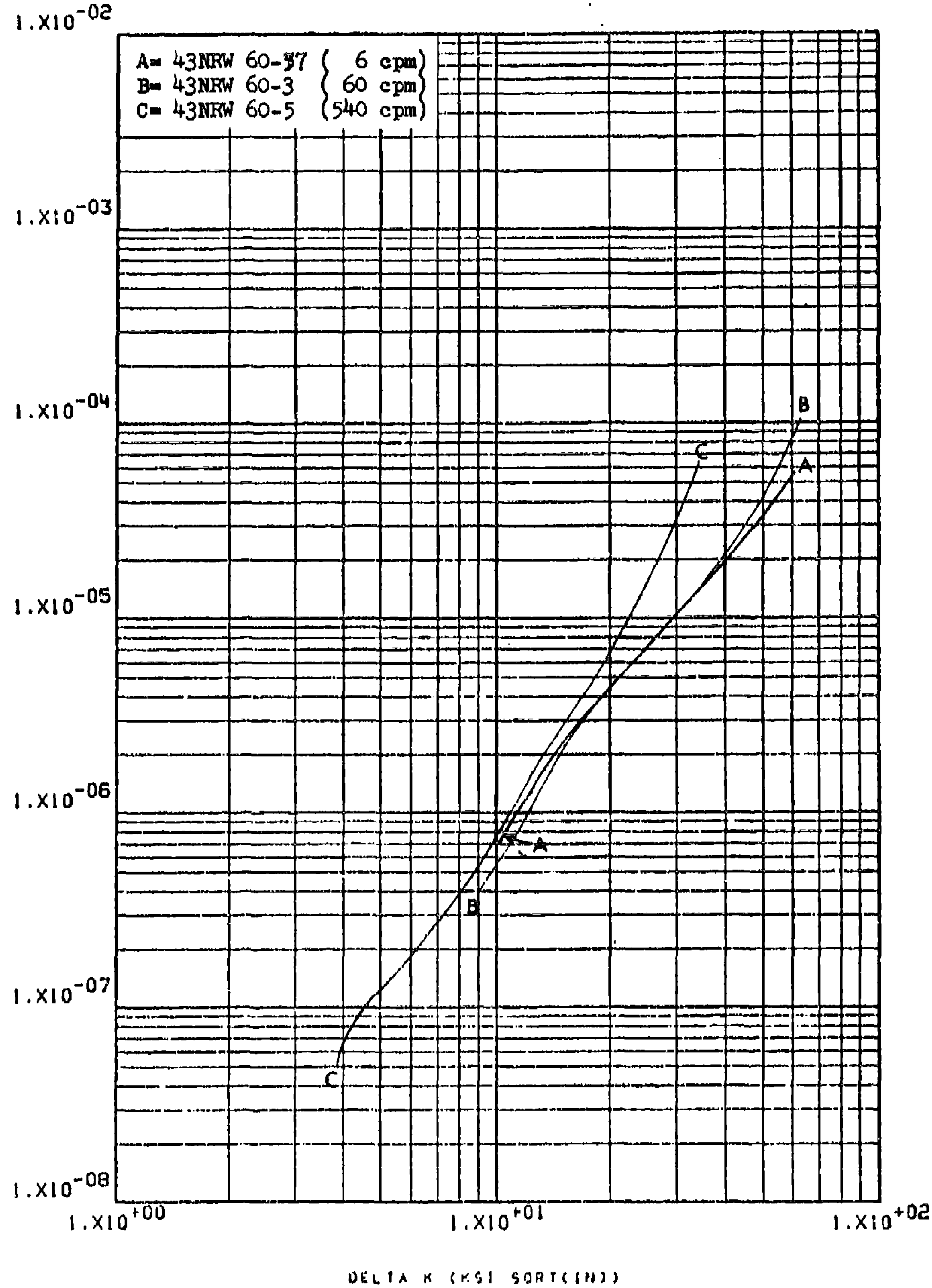

Figure 8.2.9.1-2 Effect of cyclic frequency on LHA-FCGR at R.T., R=0.08, RW direction in 4" x 18" x 36" HP-94-.20 forged bar

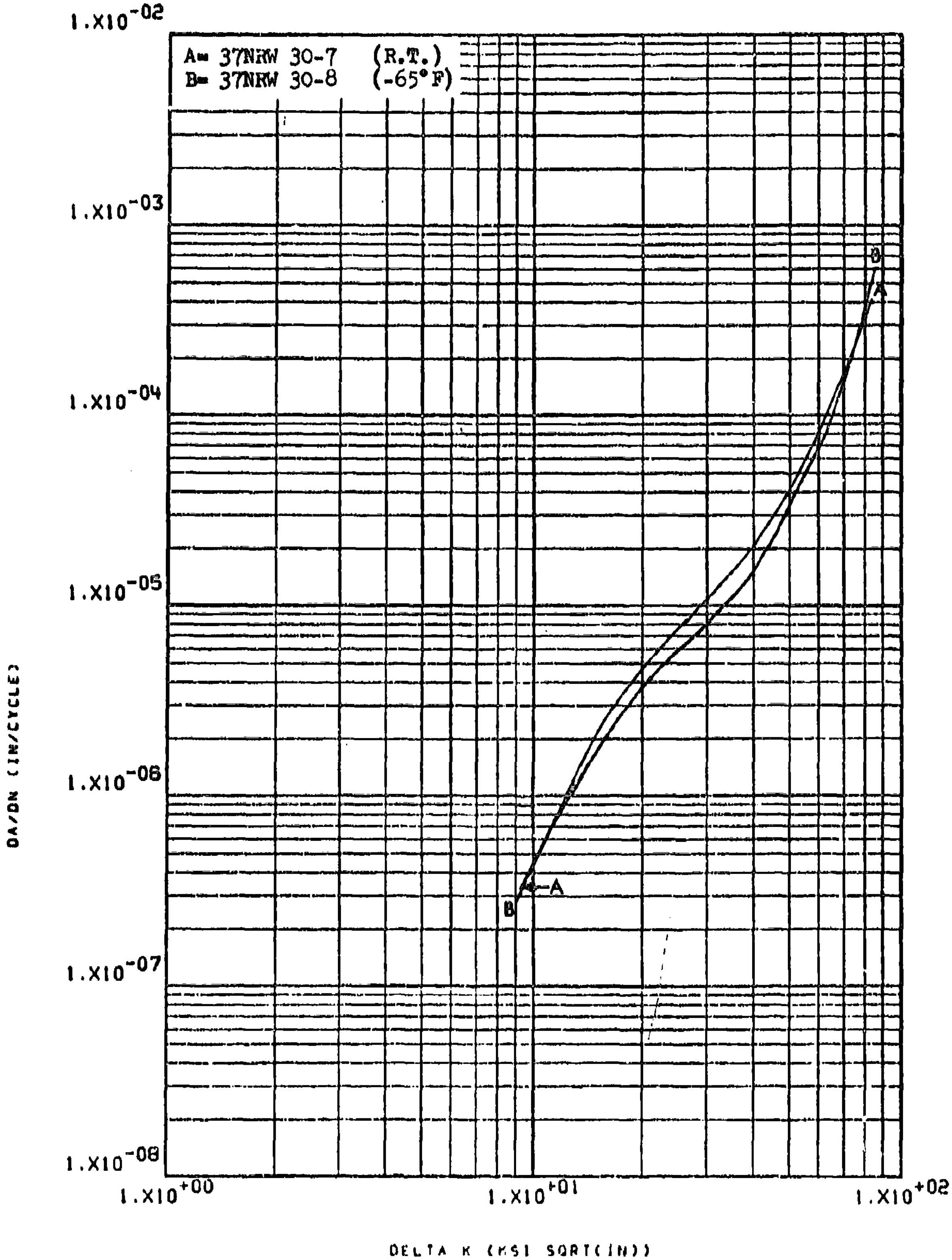

Figure 8.2.9.2-1 Effect of test temperature on LHA-FCGR at R=0.08, RW direction in 2.5" HP-9-4-.20 rolled plate

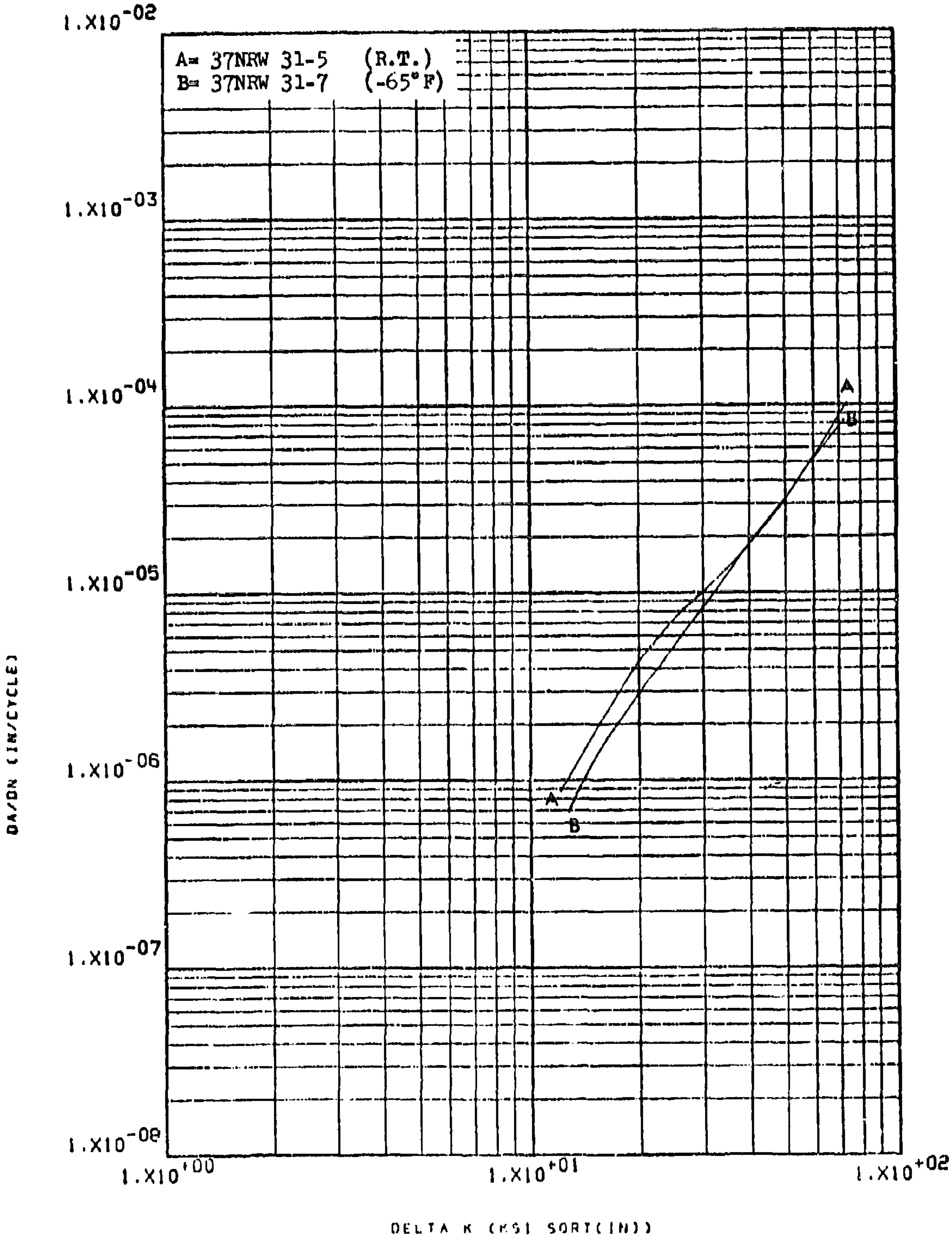

Figure 8.2.9.2-2 Effect of test temperature on LHA-FCGR at R=0.08, RW direction in 2.5" HP-9-4-.20 rolled plate

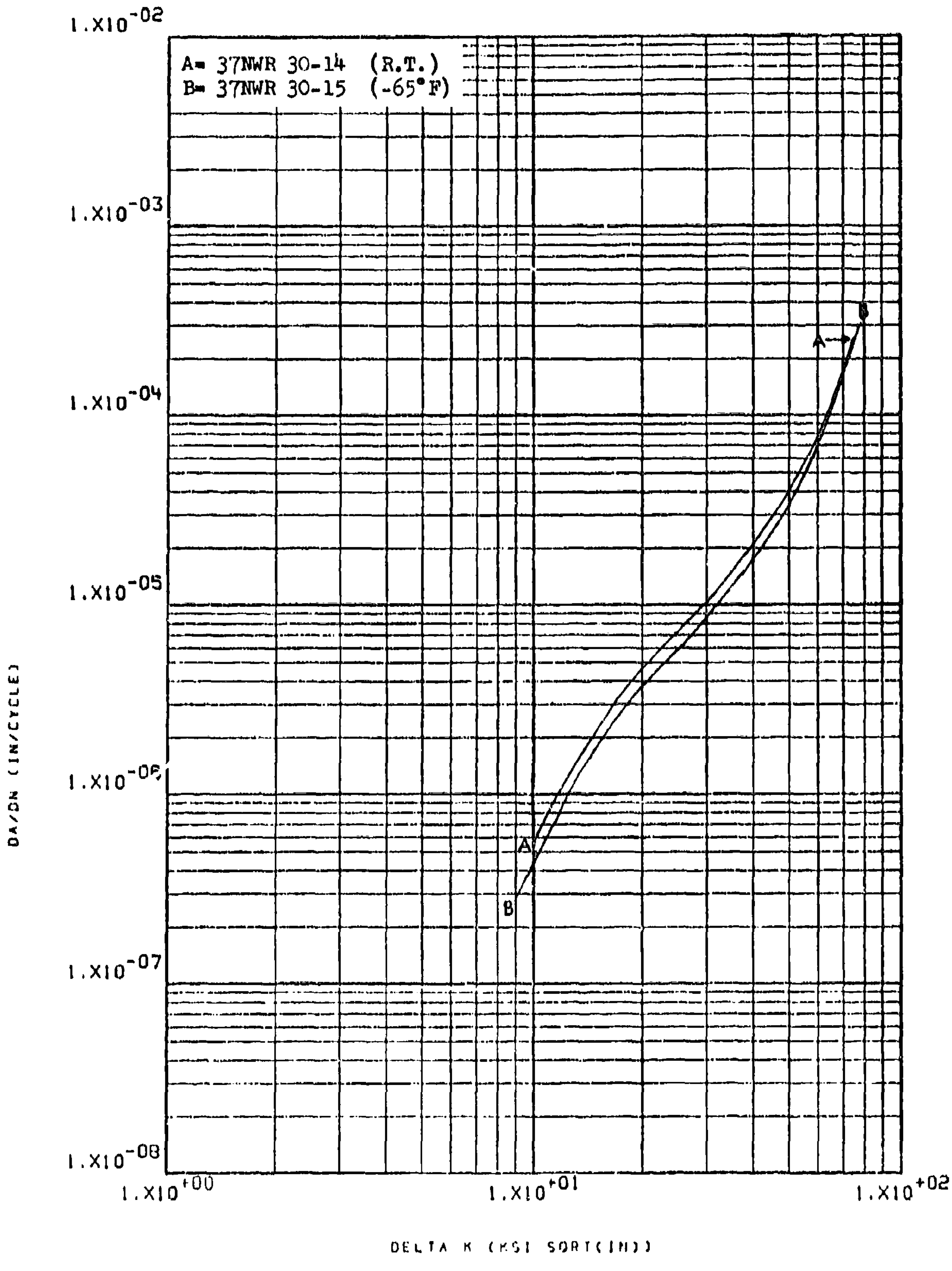

Figure 8.2.9.2-3 Effect of test temperature on LHA-FCGR at R=0.08, WR direction in 2.5" HP-9-4-.20 rolled plate

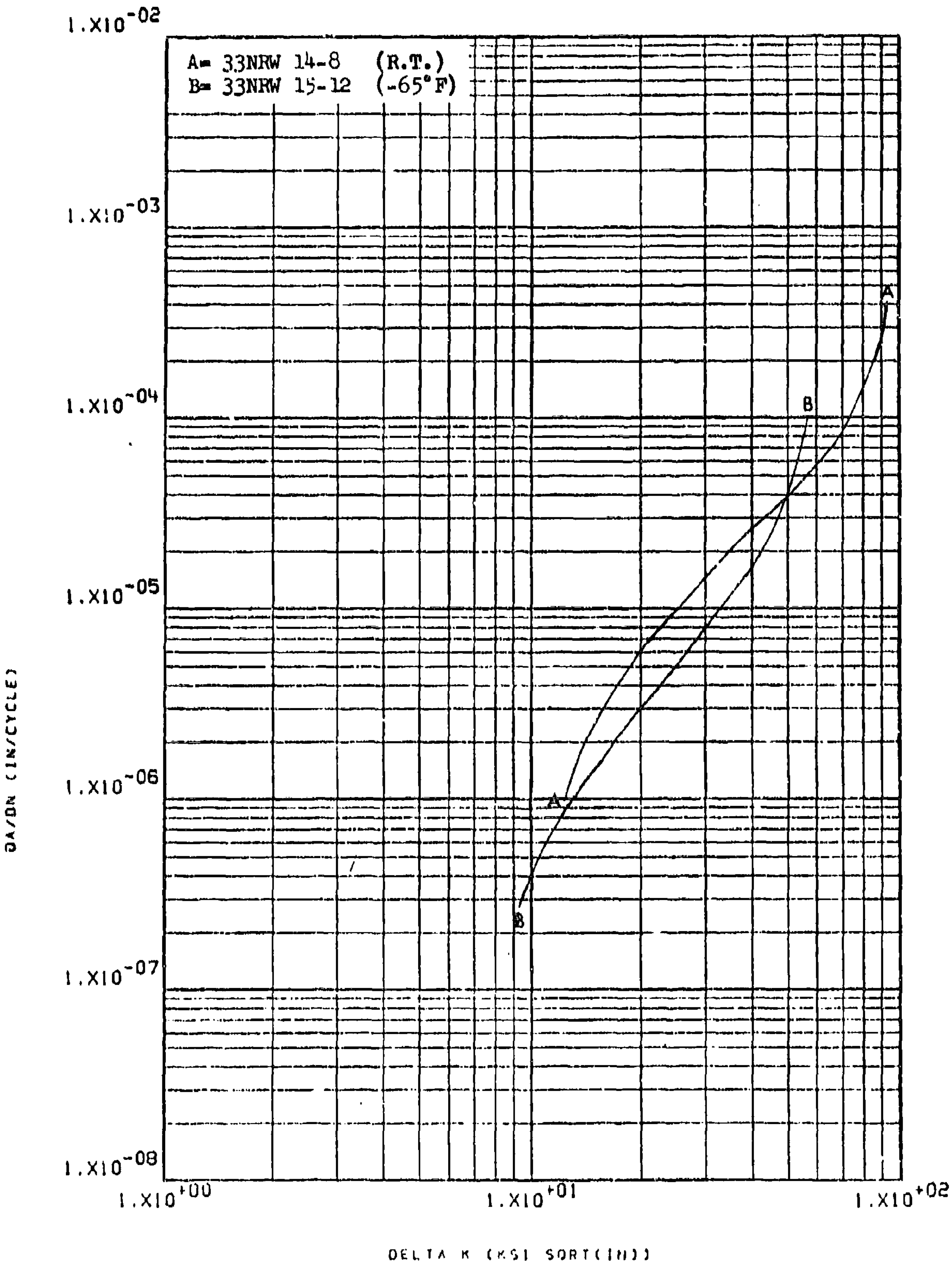

Figure 8.2.9.2-4 Effect of test temperature on LHA-FCGR at R=0.08, 60 cpm, RW direction in 4" x 18" x 36" HP-9-4-.20 forged bar

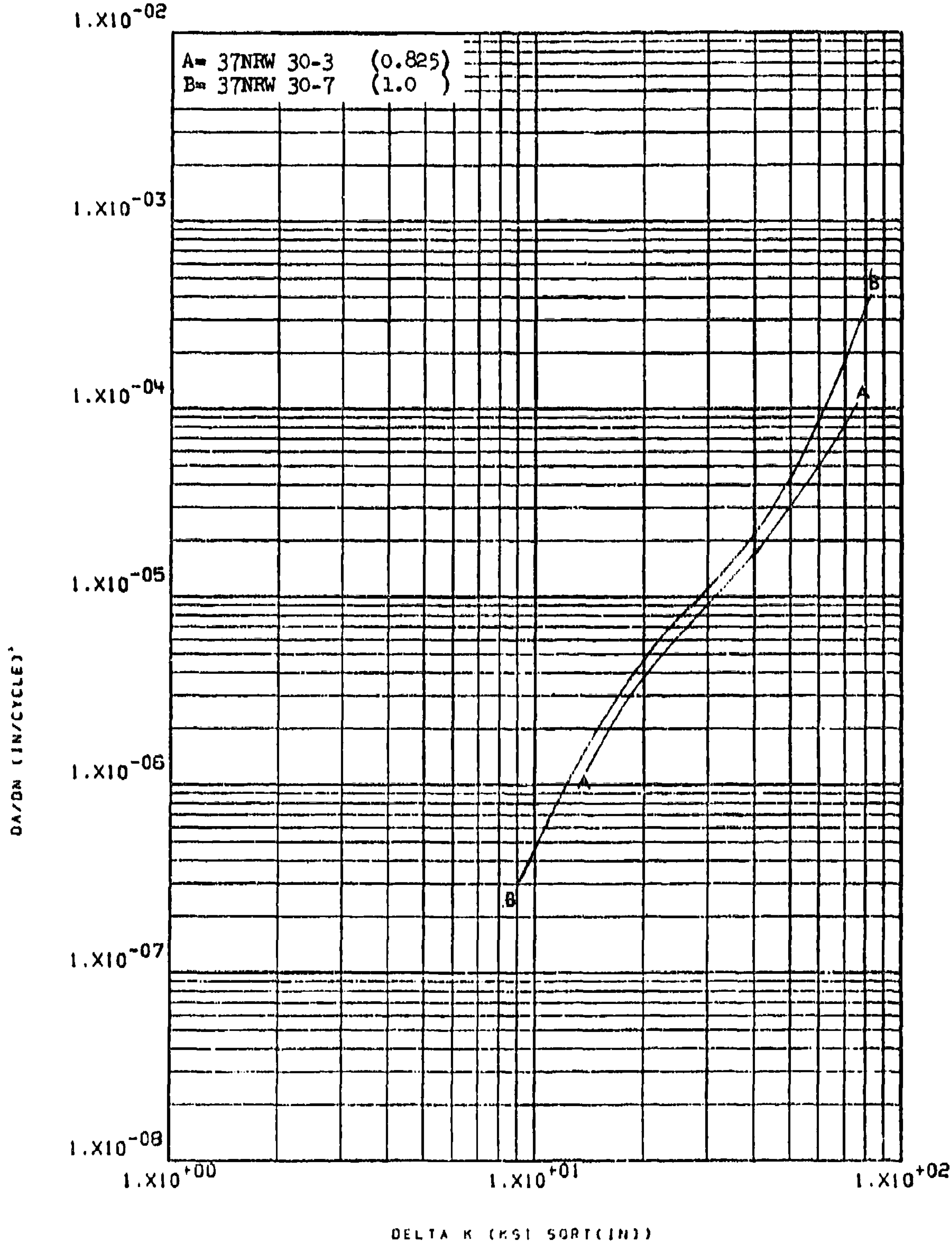

Figure 8.2.9.3-1 Effect of specimen thickness on LHA-FCGR at R.T., R=0.08, 360 cpm, RW direction in 2.5" HP-9-4-.20 rolled plate

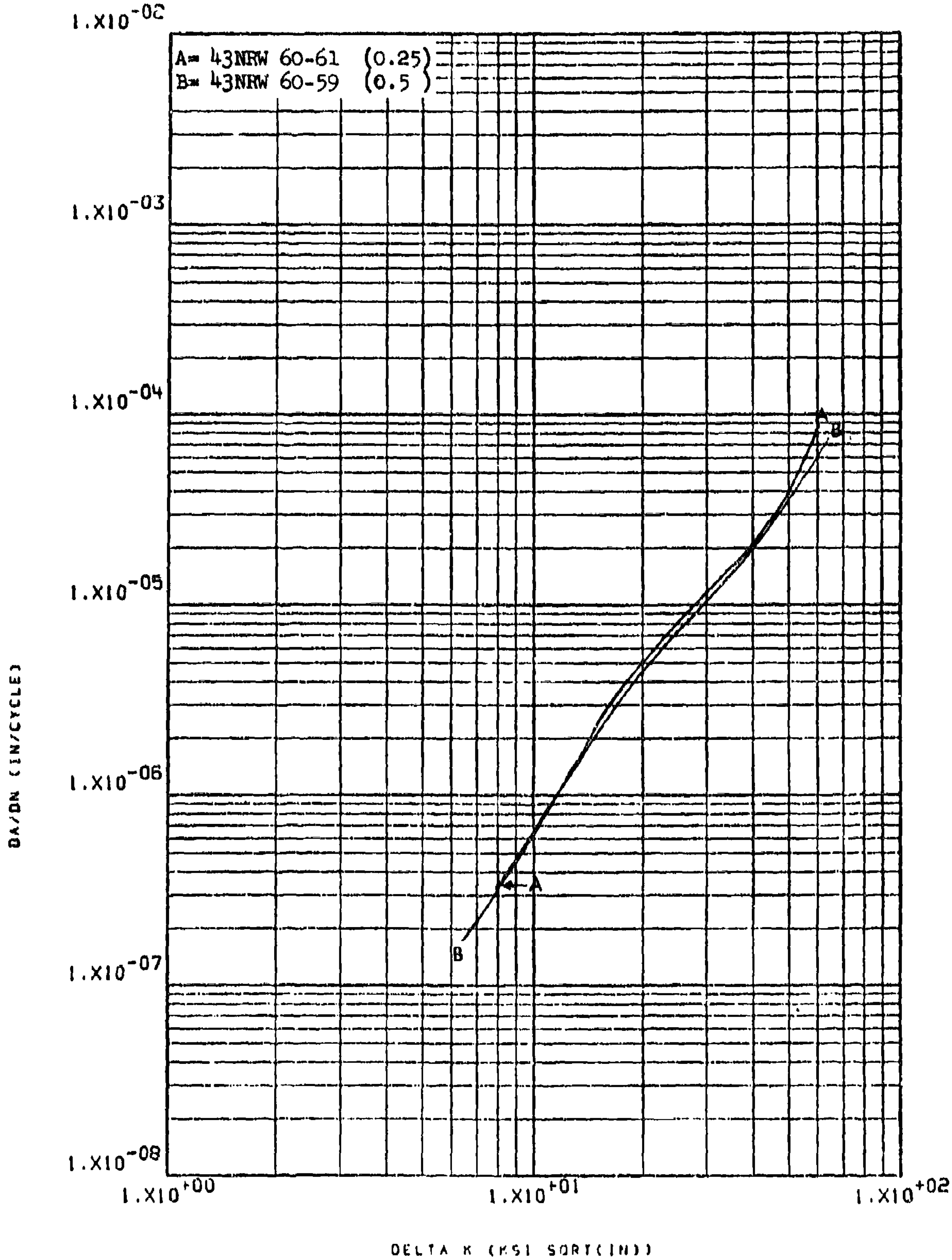

Figure 8.2.9.3-2 Effect of specimen thickness on LHA-FCGR at R.T., R=0.08, 360 cpm, RW direction in 4" x 18" x 36" HP-9-4-.20 forged bar

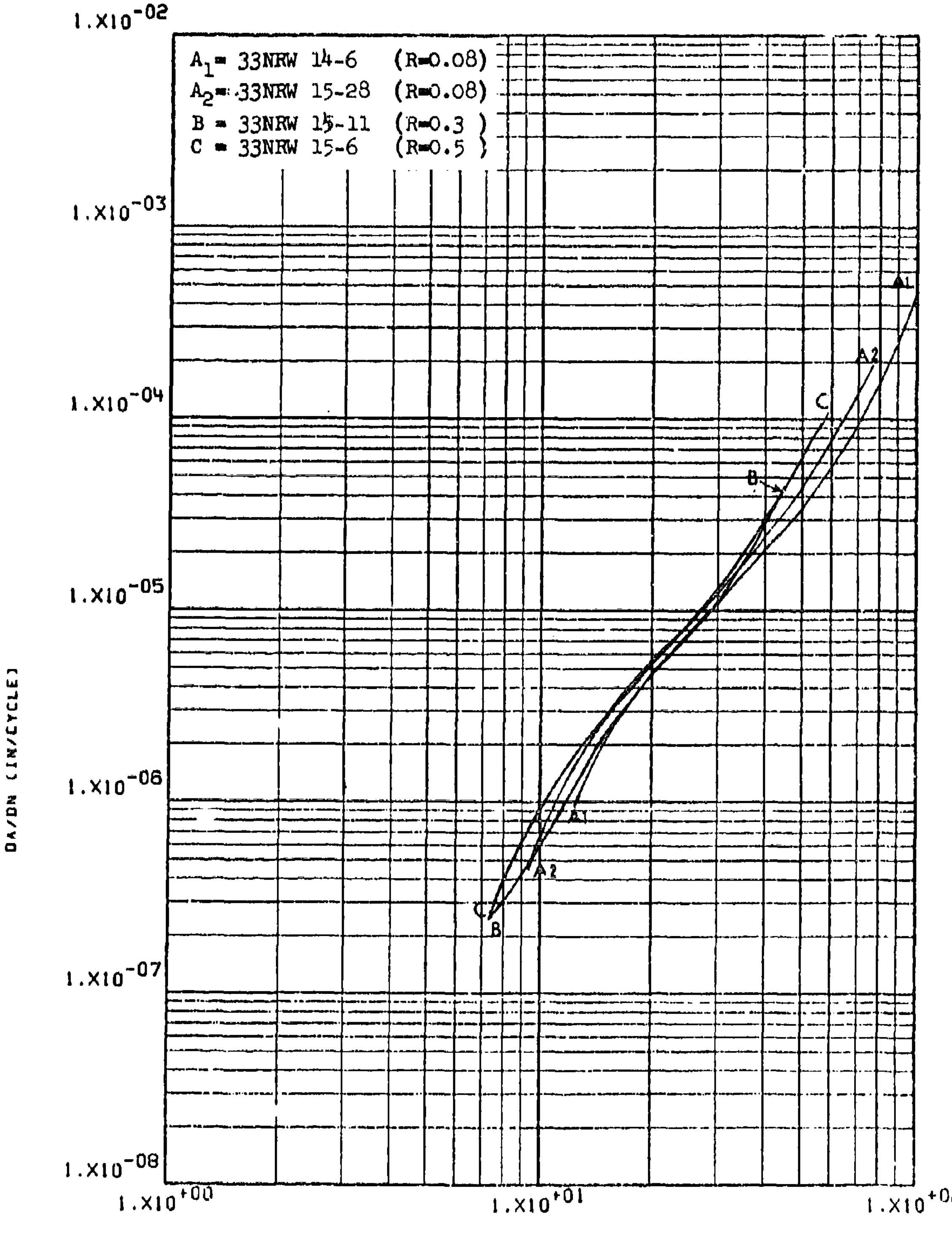

Figure 8.2.9.4-1 Effect of R factor on LHA-FCGR at R.T., 360 cpm, RW direction in 4" x 18" x 36" HP-9-4-.20 forged bar

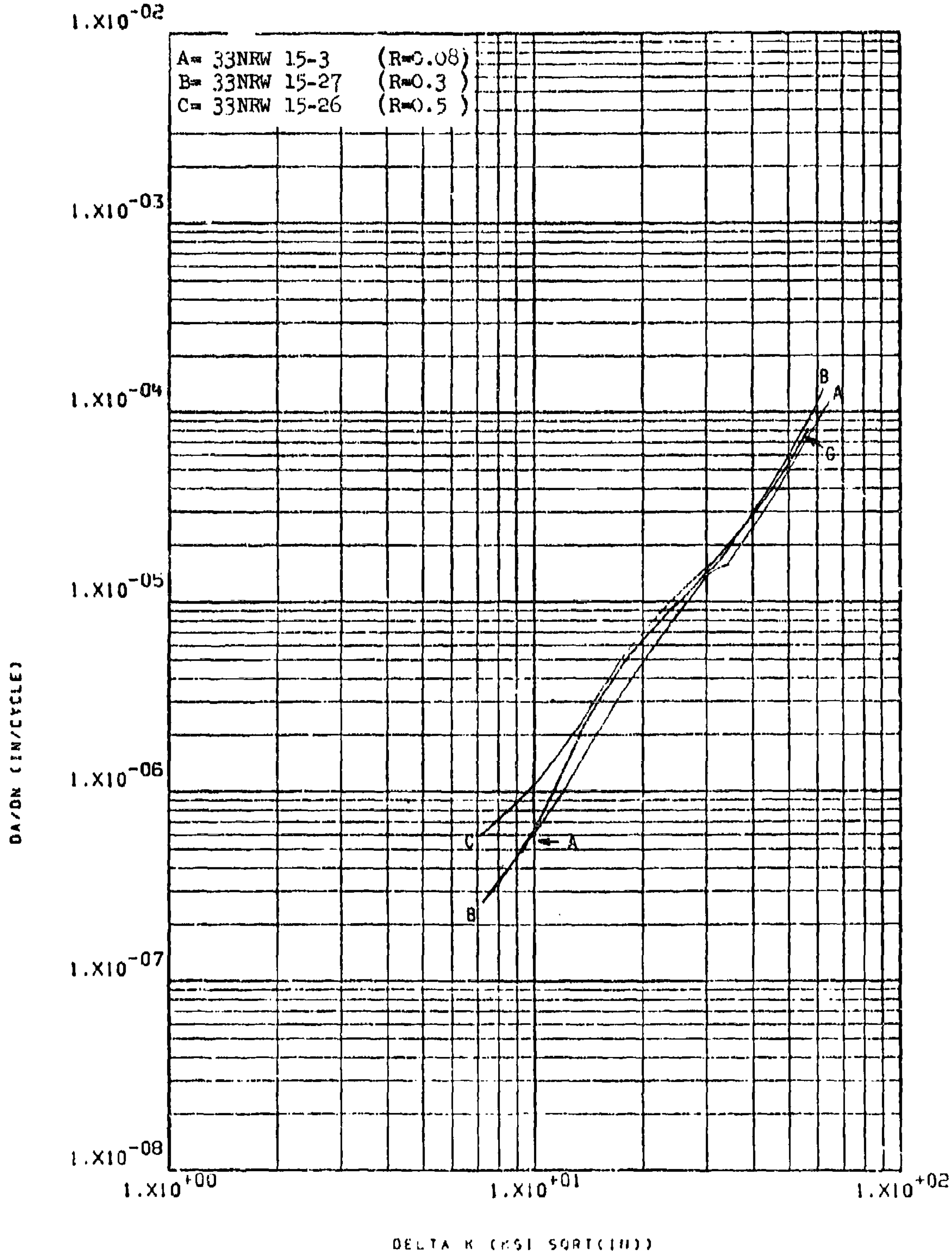

Figure 8.2.9.4-2 Effect of R factor on 100% humidity-FCGR at R.T., 60 cpm, RW direction in 4" x 18" x 36" HP-9-4-.20 forged bar

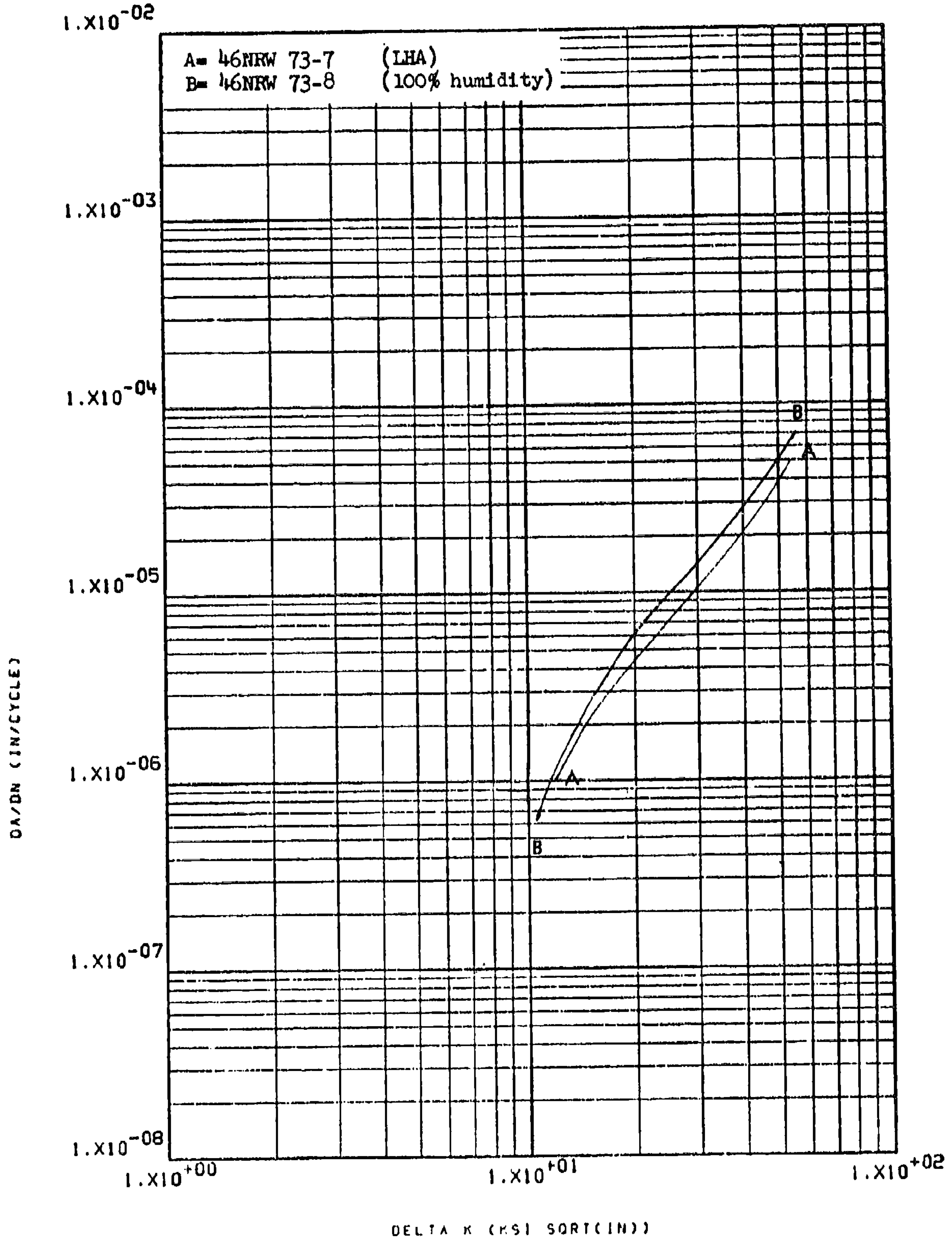

Figure 8.2.9.5-1 Effect of environment on FCGR at R.T., R=0.08, RW direction in 4" x 8" HP-9-4-.20 forged bar

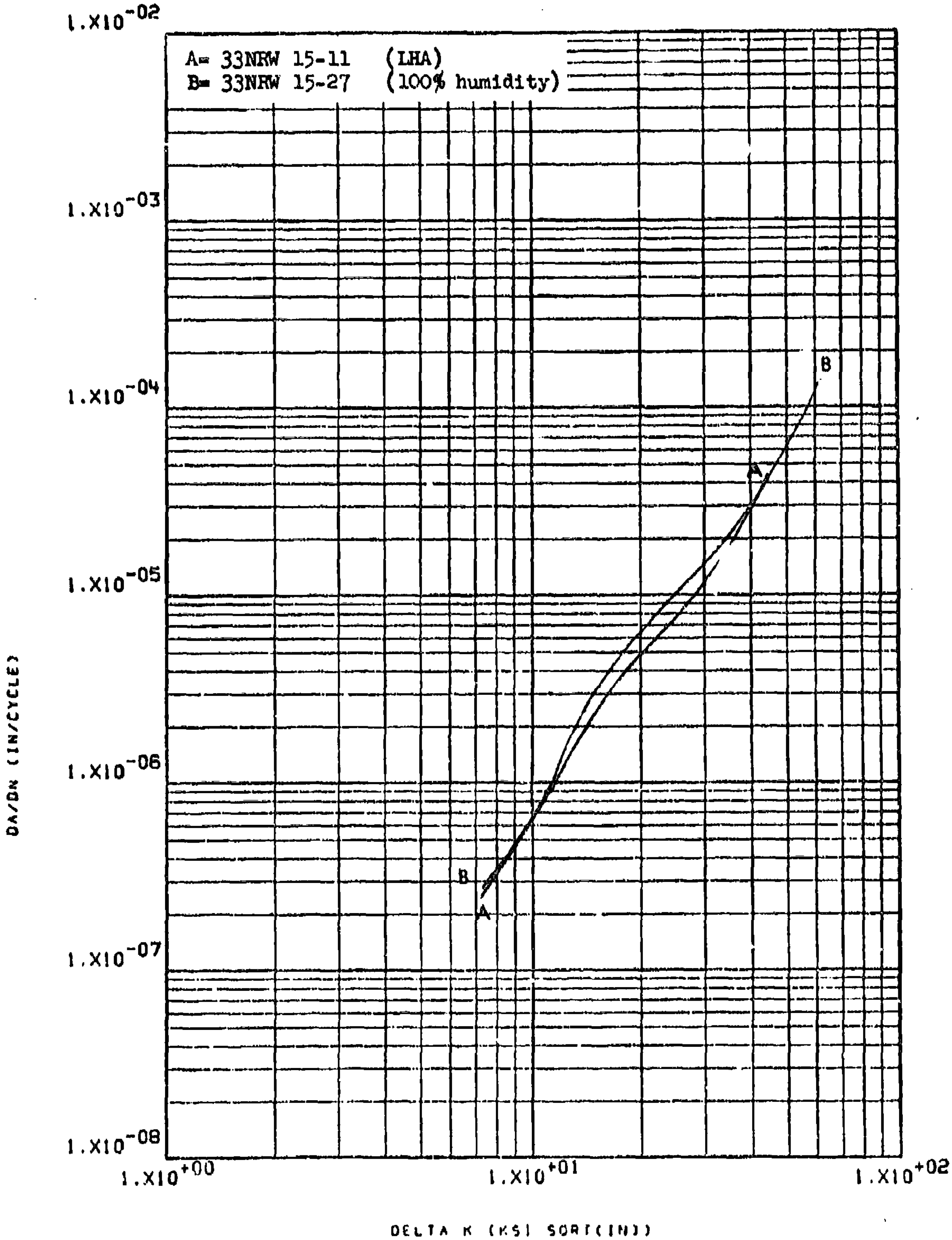

Figure 8.2.9.5-2 Effect of environment on FCGR at R.T., R=0.3, RW direction in 4" x 18" x 36" HP-9-4-.20 forged bar

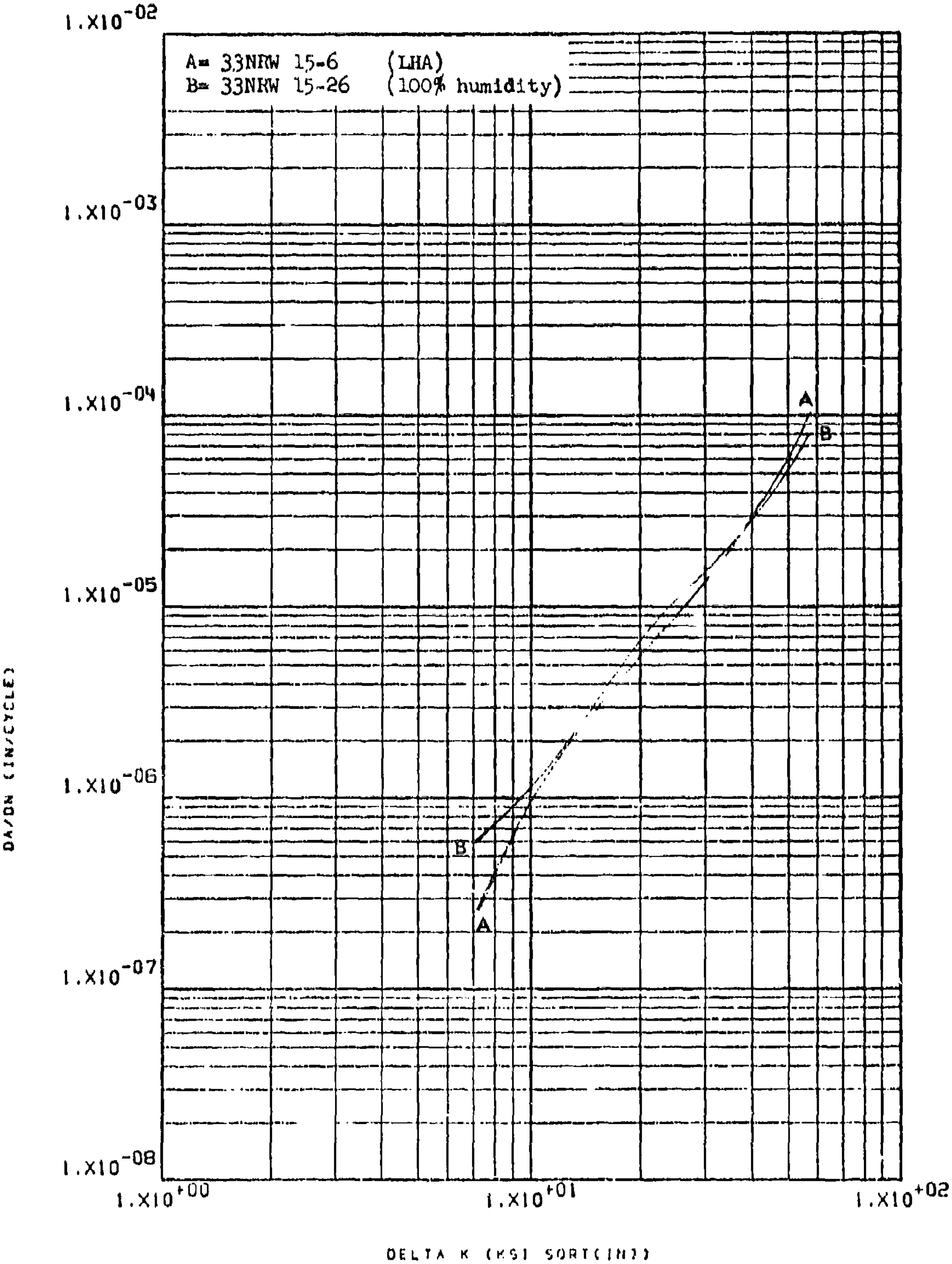

Figure 8.2.9.5-3 Effect of environment on FCGR at R.T., R=0.5, RW direction in 4" x 13" x 36" HP-9-4-.20 forged bar

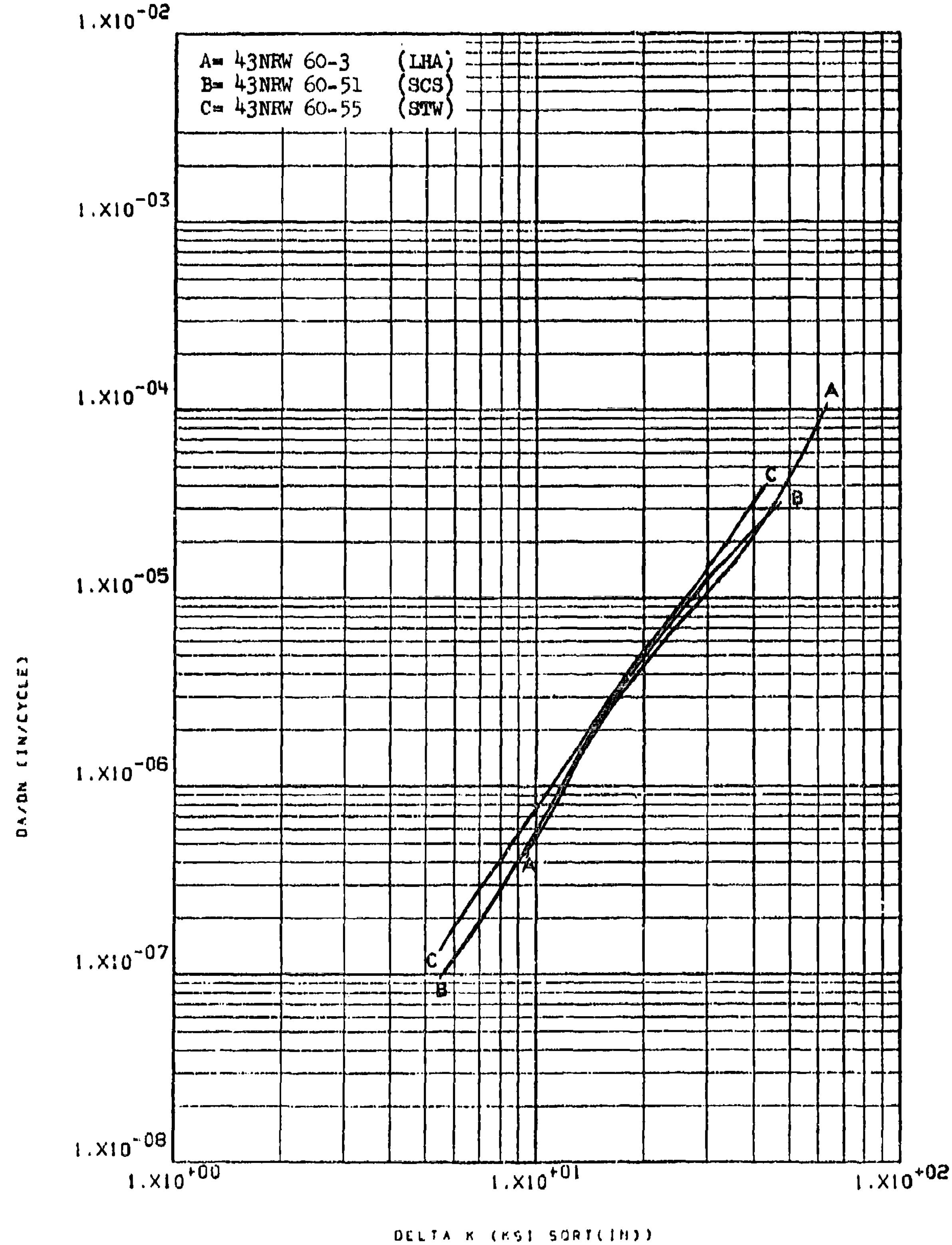

Figure 8.2.9.5-4 Effect of environment on FCGR at R.T., R=0.08, RW direction in 4" x 18" x 36" HP-9-4-.20 forged bar

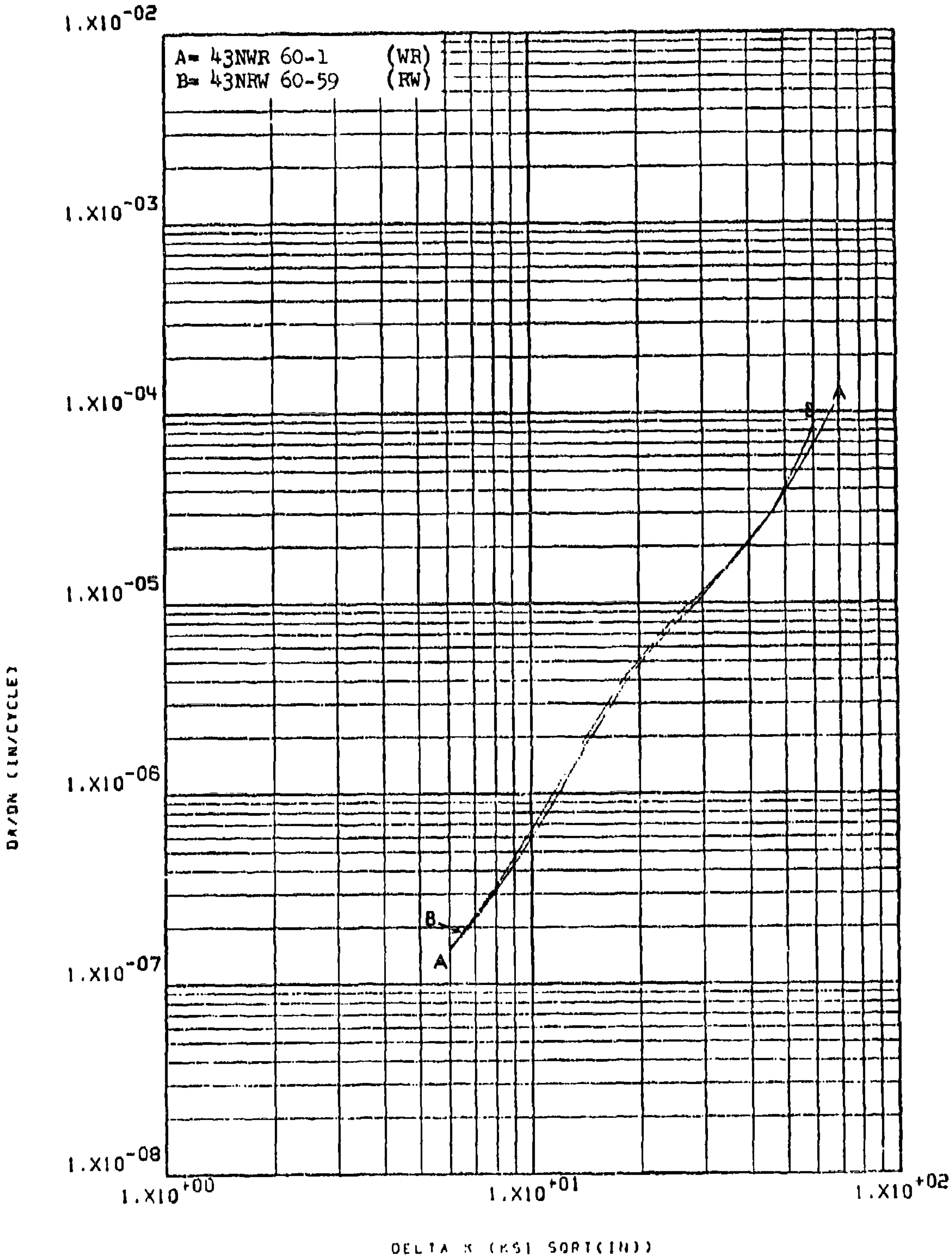

Figure 8.2.9.6-1 Effect of test direction on LHA-FCGR at R.T., R=0.08, 360 cpm, 1/2" thick specimens in 4" x 18" x 36" HP-9-4-.20 forged bar

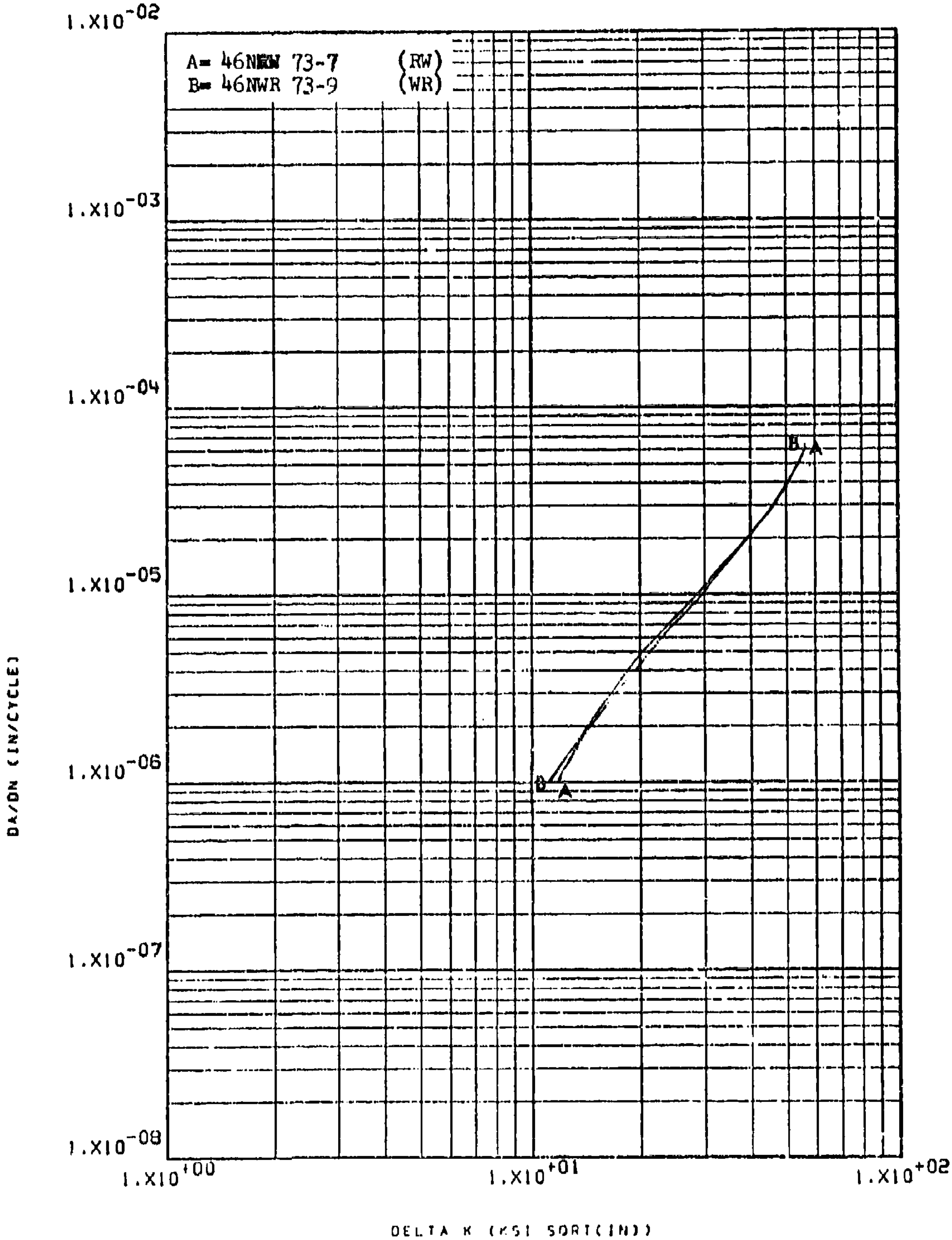

Figure 8.2.9.6-2 Effect of test direction on LHA-FCGR at R.T., R=0.08, 360 cpm in 4" x 8" HP-9-4-.20 forged bar

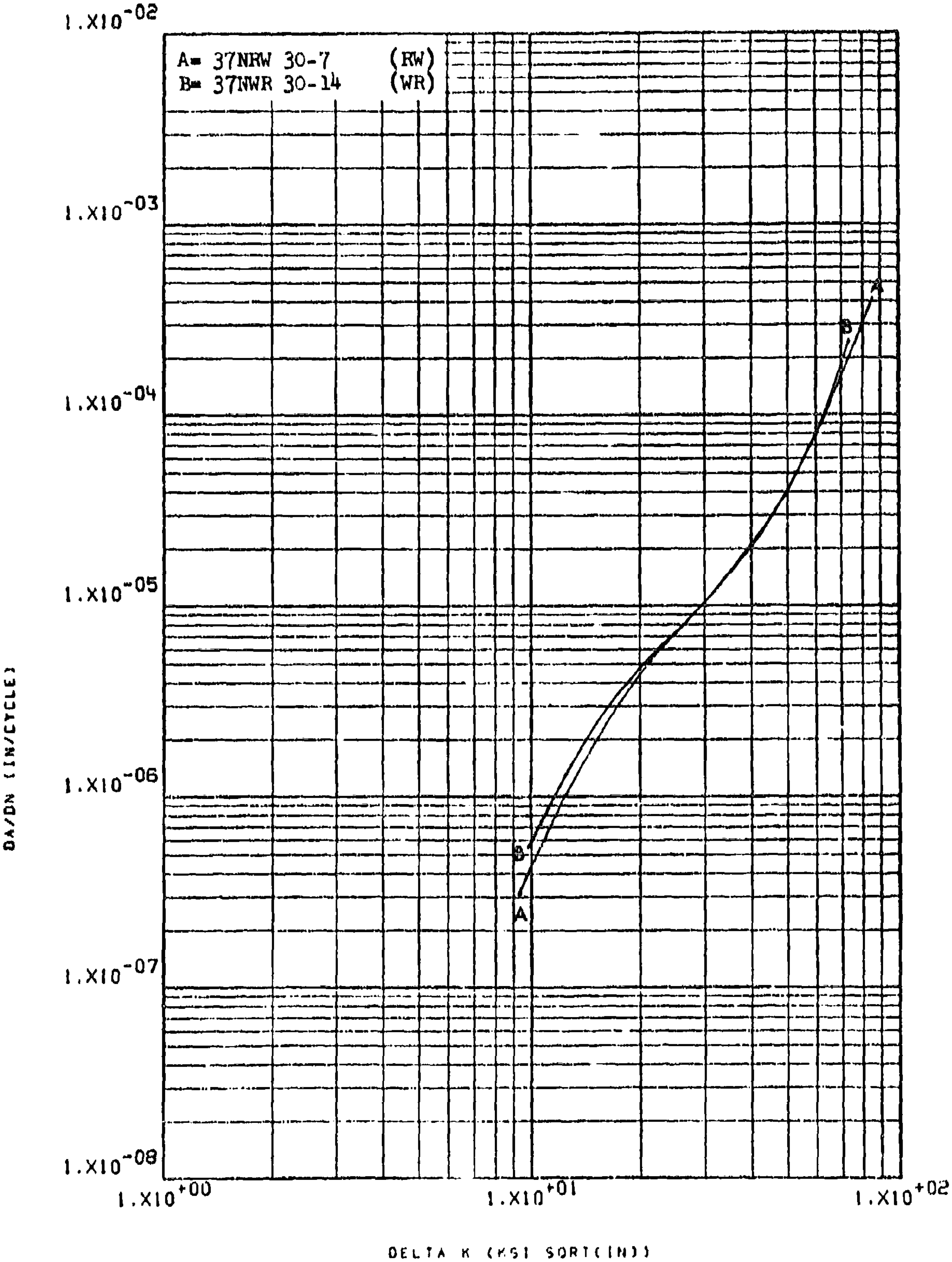

Figure 8.2.9.6-3 Effect of test direction on LHA-FCGR at R.T., R=0.08, 360 cpm in 2.5" HP-9-4-.20 rolled plate

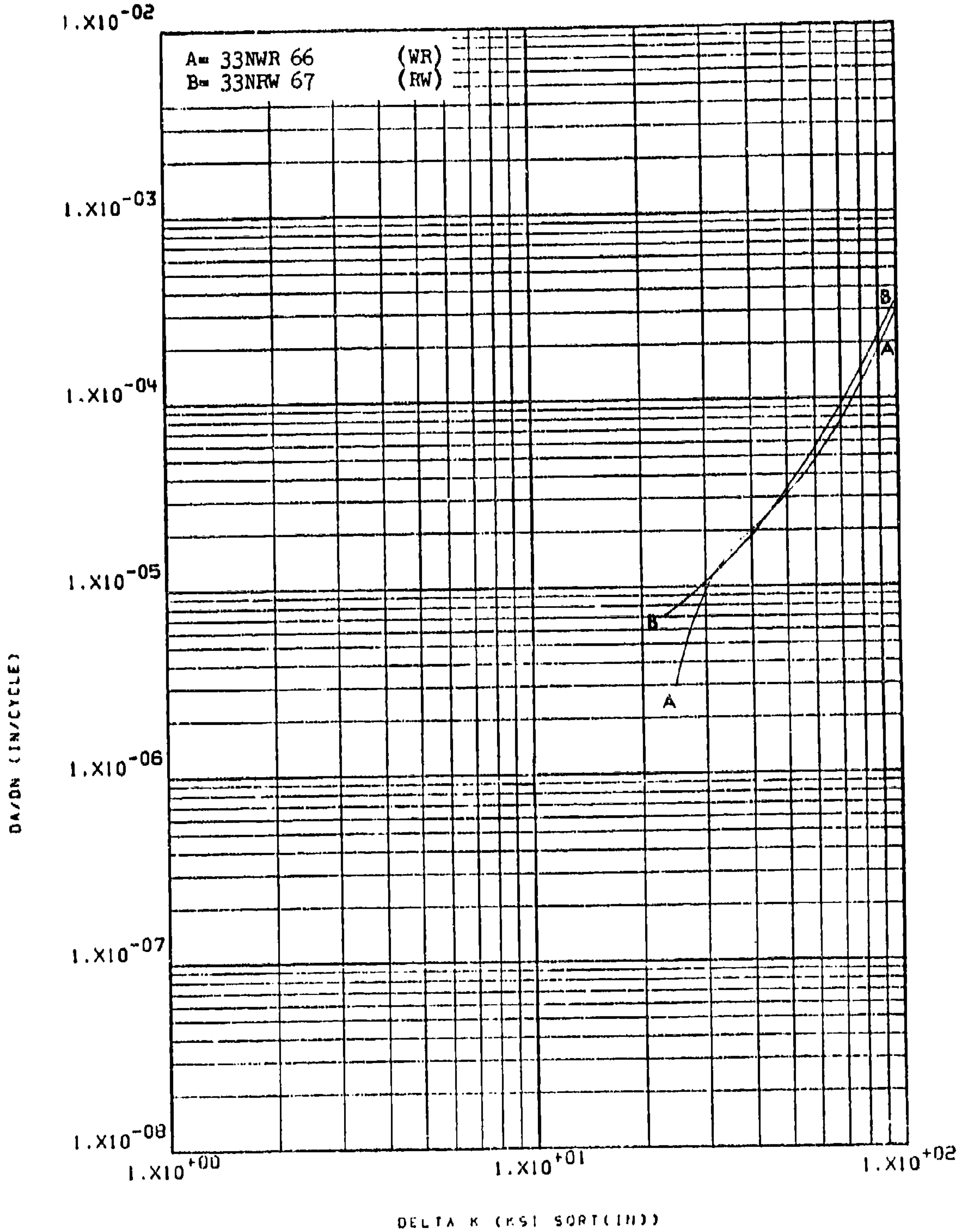

Figure 8.2.9.6-4 Effect of test direction on LHA-FCGR at R.T., R=0.05, 60 cpm in 4" x 18" x 36" HP-9-4-.20 forged bar

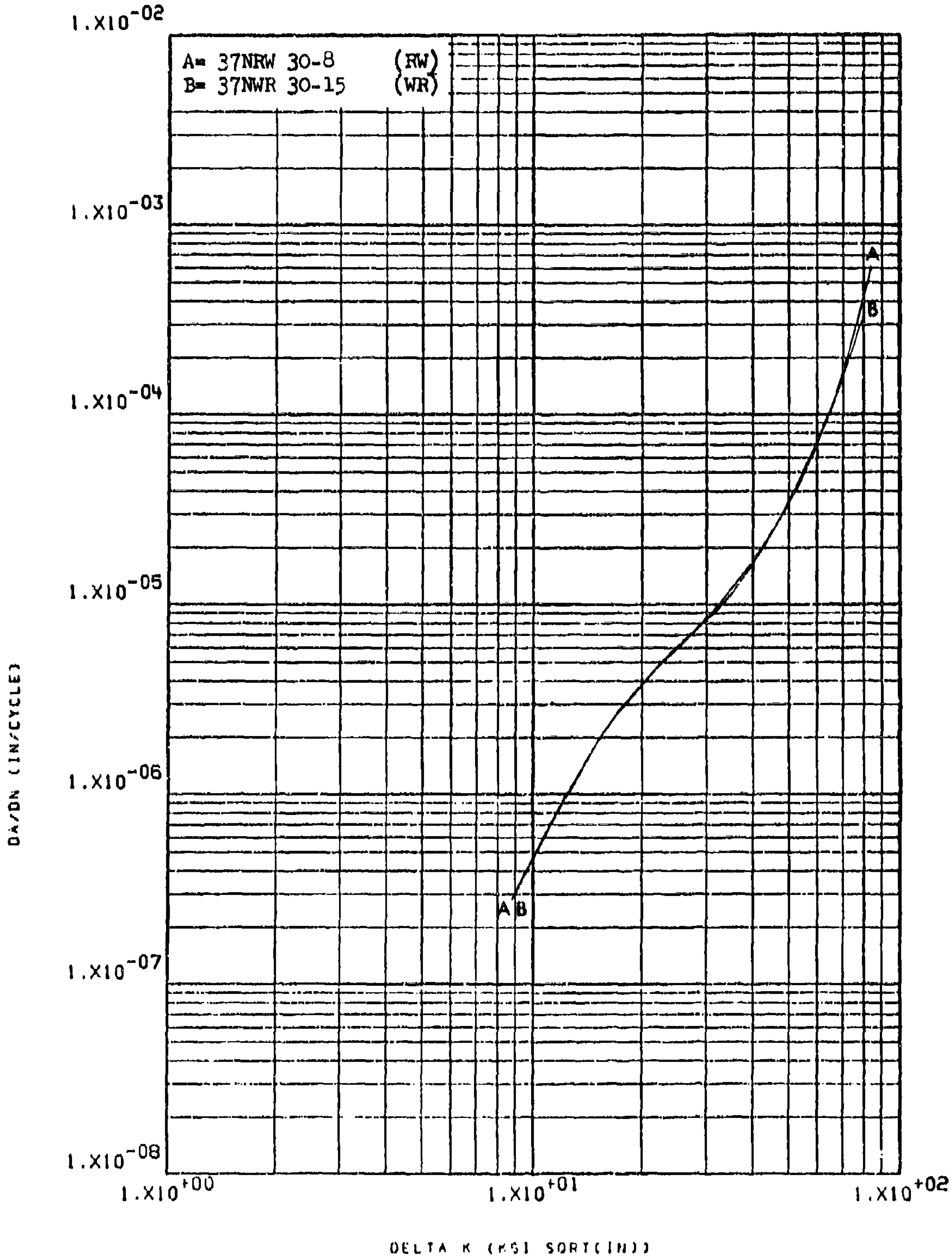

Figure 8.2.9.6-5 Effect of test direction on LHA-FCGR at -65°F, R=0.08, 60 cpm in 2.5" HP-9-4-.20 rolled plate

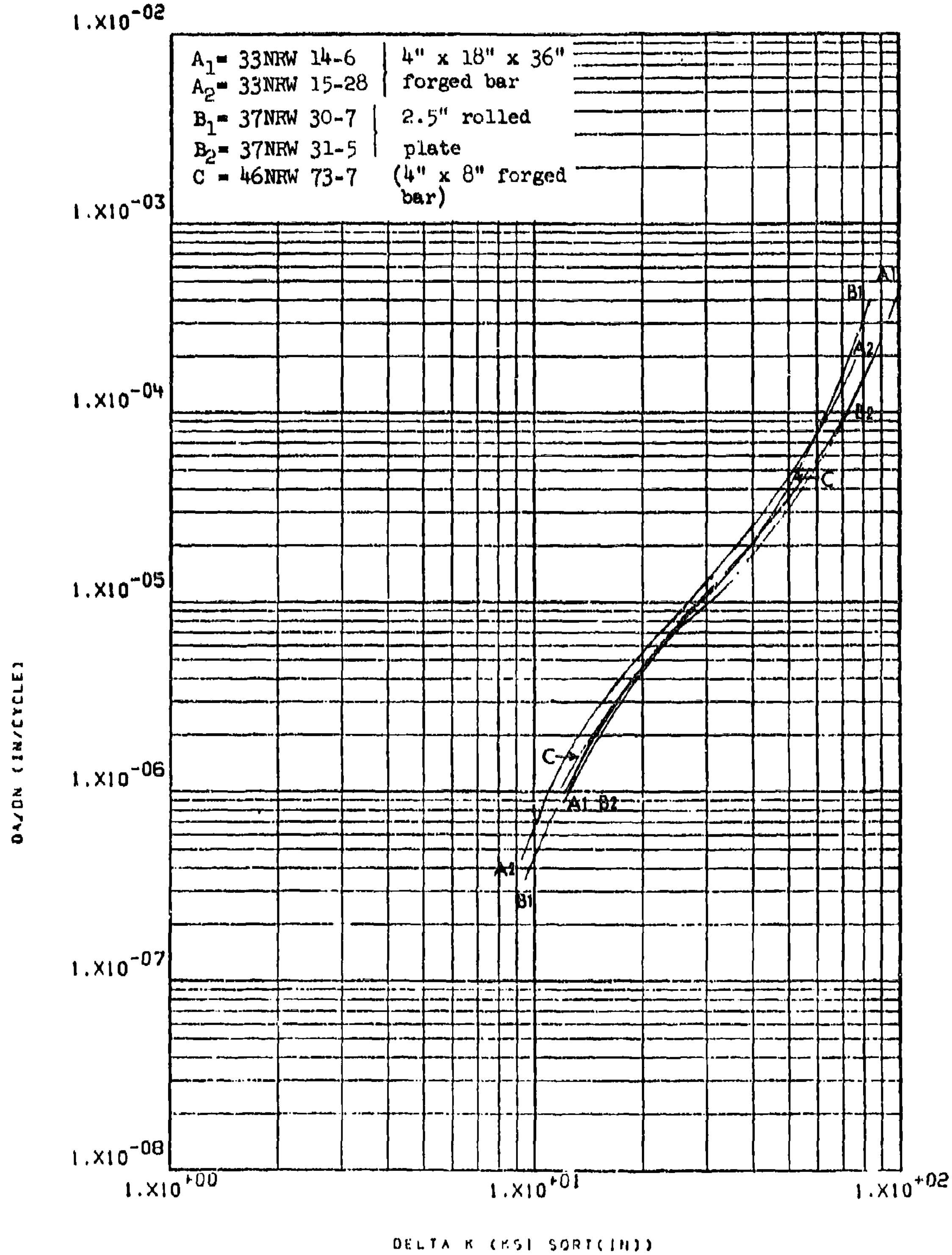

Figure 8.2.9.7-1 Effect of product form on LHA-FCGR at R.T., R=0.08,360 cpm, RW direction in HP-9-4-.20

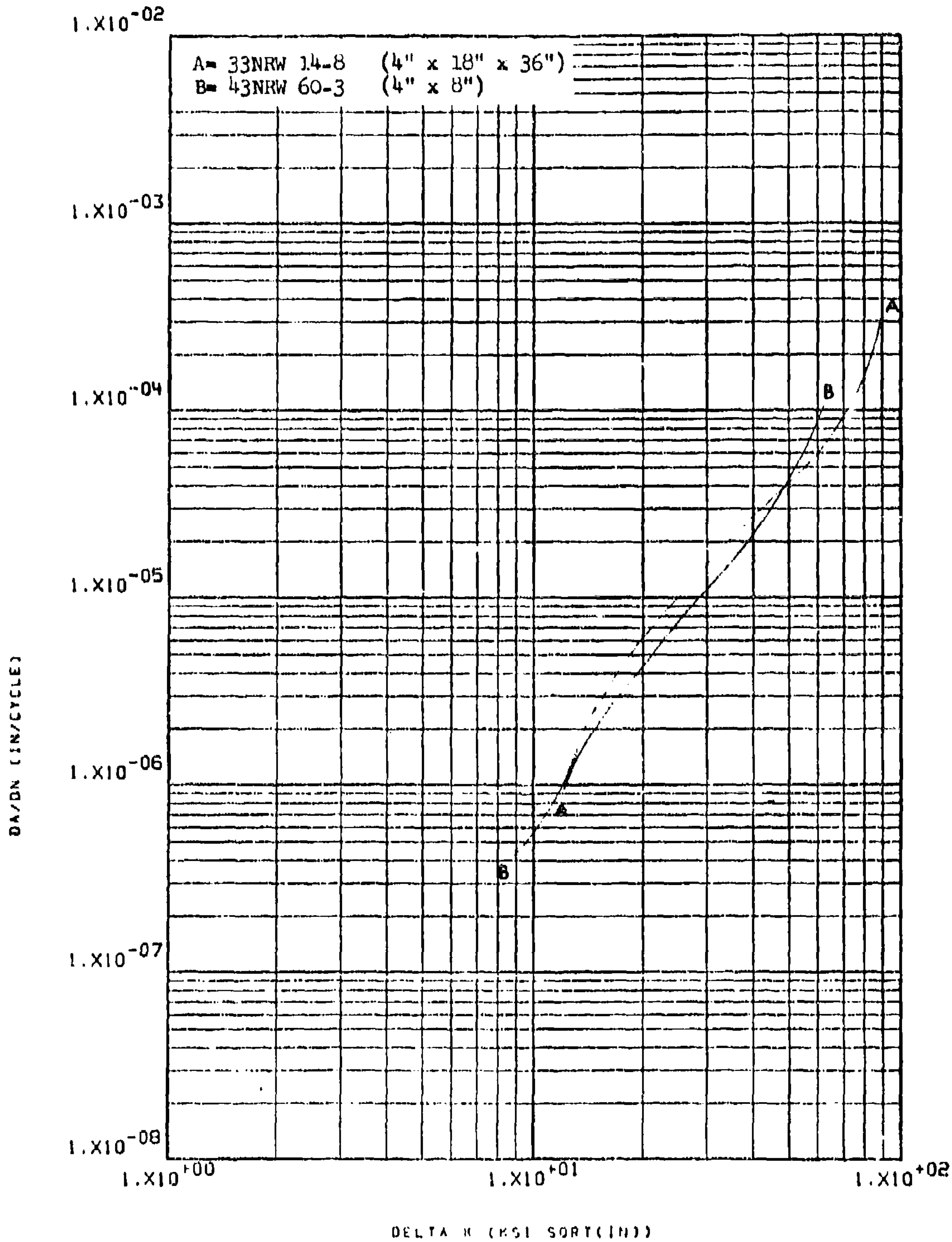

Figure 8.2.9.7-2 Effect of product form on LHA-FCGR at R.T., R=0.08, 60 cpm, RW direction in HP-9-4-.20 forged bar

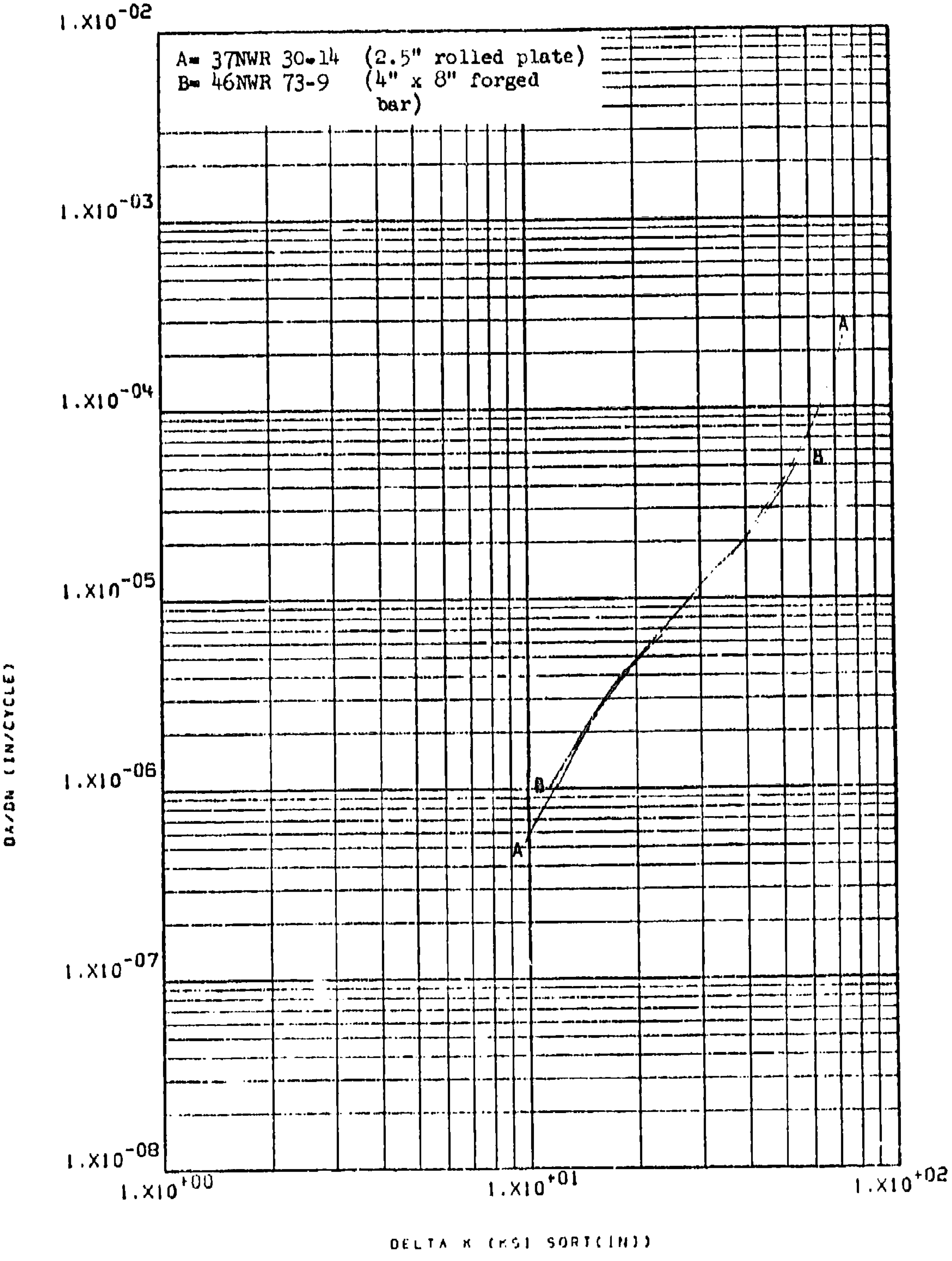

Figure 8.2.9.7-3 Effect of product form on LHA-FCGR at R.T., R=0.08, 360 cpm, WR direction in HP-9-4-.20

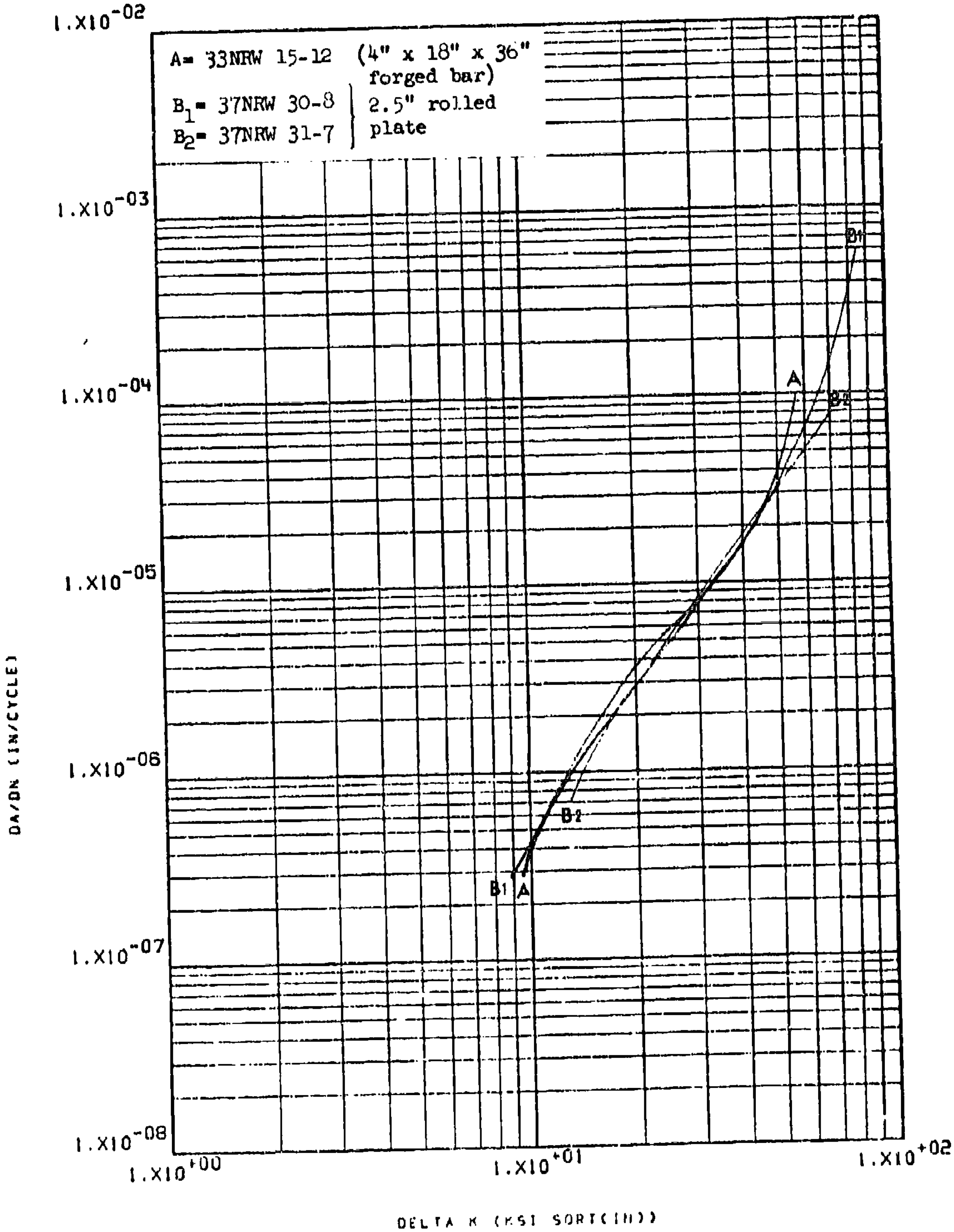

Figure 8.2.9.7-4 Effect of product form on LHA-FCGR at -65°F, R=0.08, 60 cpm, RW direction in HP-9-4-.20

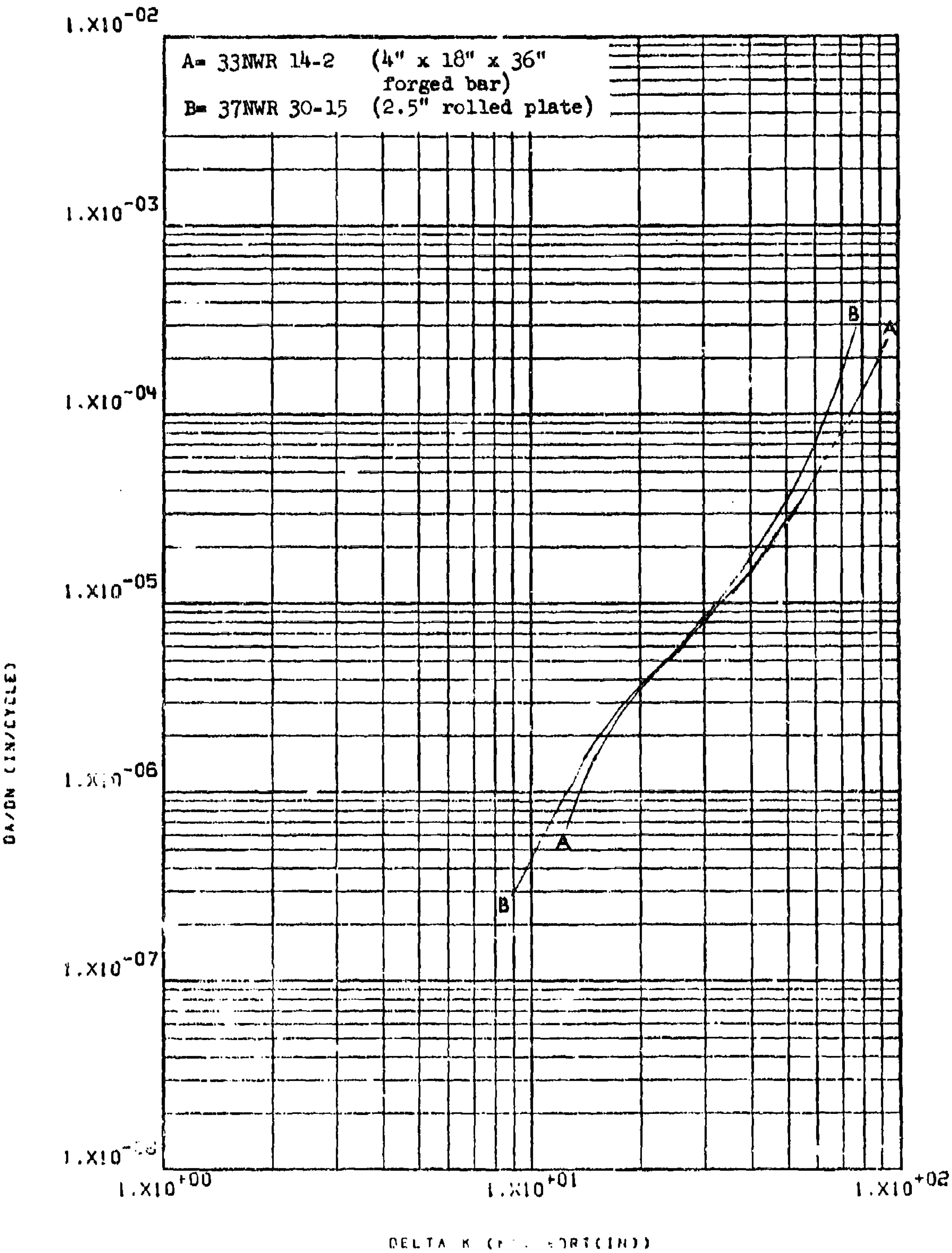

Figure 8.2.9.7-5 Effect of product form on LHA-FCGR at -65°F, R=0.08, 60 cpm, WR direction in HP-9-4-.20

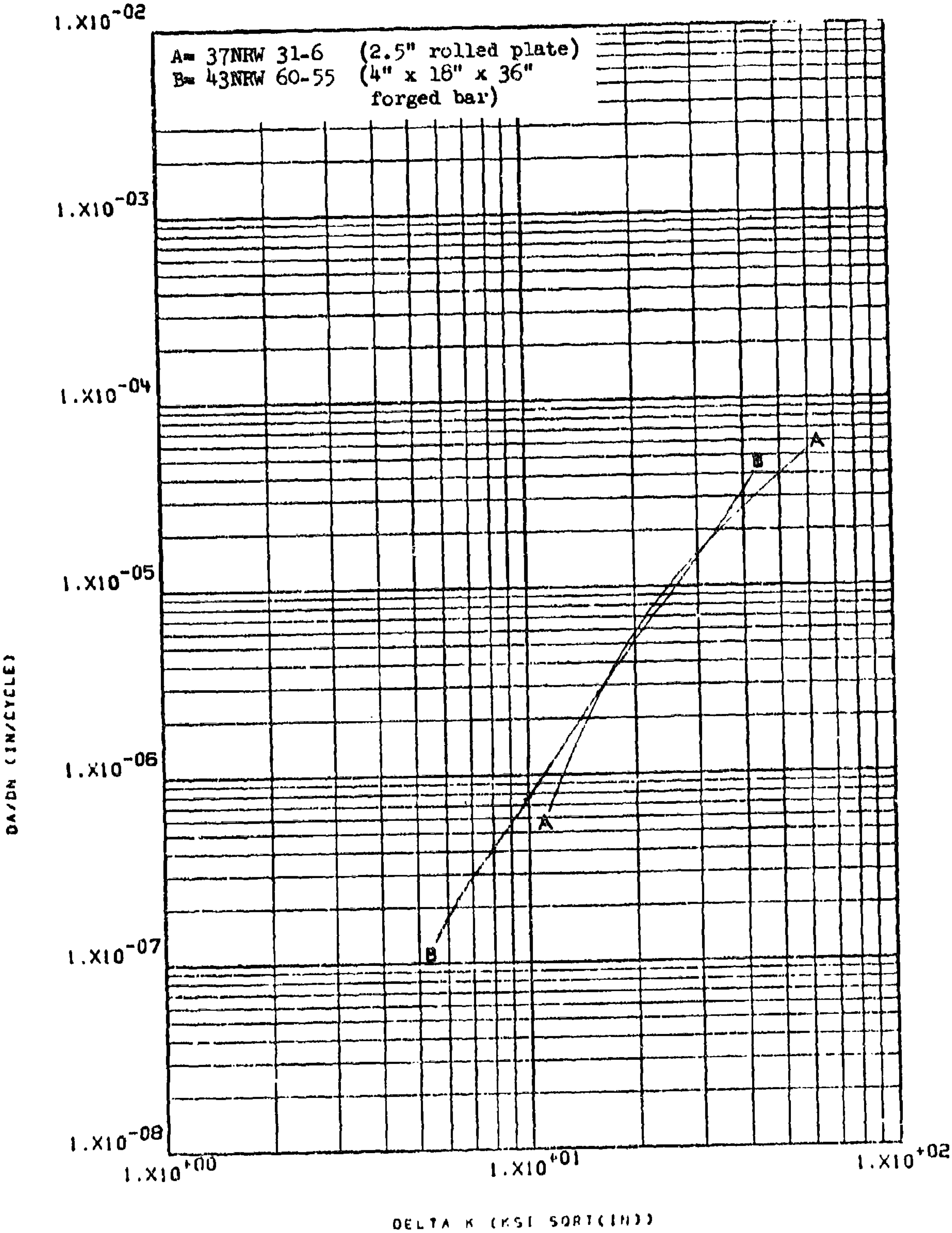

Figure 8.2.9.7-6 Effect of product form on STW-FCGR at R.T., R=0.08, 60 cpm, RW direction in HP-9-4-.20

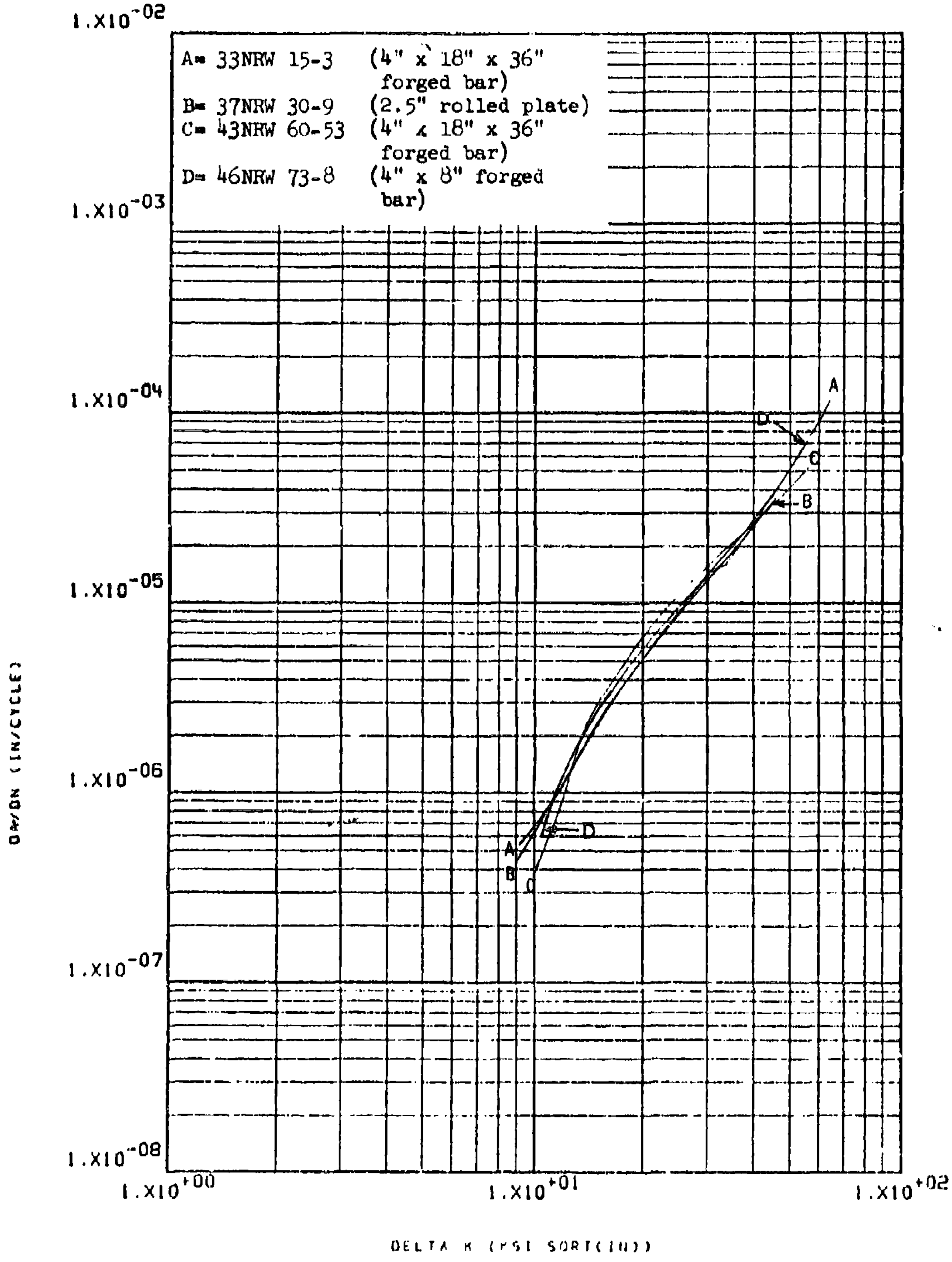

Figure 8.2.9.7-7 Effect of product form on 100% humidity - FCGR at R.T., R=0.08, 60 cpm, RW direction in HP-9-4-.20

8.2.10 9Ni-4Co-0.30C Steel

8.2.10.1 Cyclic Frequency - No changes in fatigue crack growth rates were observed in this material in low humidity air when the cyclic frequency of test was changed from 360 to 60 cpm (Figure 8.2.10.1-1).

8.2.10.2 Test Temperature - The low humidity air fatigue crack growth rates of this material were slightly, but noticeably reduced when the test temperature was decreased from ambient to -65°F (Figure 8.2.10.2-1).

8.2.10.3 Specimen Thickness - There was no noticeable difference in sump tank water growth rates of this material when measured using 0.75" and 1.0" thick specimens (Figure 8.2.10.3-1).

8.2.10.4 R Factor - A slight increase in low humidity air fatigue crack growth rates was observed in this material when R was increased from 0.08 to 0.3, while no further increase was evident when R was further increased to 0.5 (Figure 8.2.10.4-1). Similarly slight increases in sump tank water growth rates were observed when R was increased from 0.3 to 0.5 (Figure 8.2.10.4-2).

8.2.10.5 Environment - Fatigue crack growth rates of this material were essentially equivalent in low humidity air and sump tank water at delta K levels of $\sim$15 ksi $\sqrt{in}$ and above, but were seen to differ in an inconsistent manner below this level (Figures 8.2.10.5-1 through -3).

8.2.10.6 Test Direction - The low humidity air fatigue crack growth rates of this material in the RW and WR directions were seen to be equivalent (Figure 8.2.10.6-1).

8.2.10.7 Product Form - The low humidity air fatigue crack growth rates of the two different 3" x 18" x 36" forged blocks were seen to be essentially equivalent in the WR direction at R=0.08 (Figure 8.2.10.7-1) and the RW direction at R=0.3 (Figure 8.2.10.7-2).

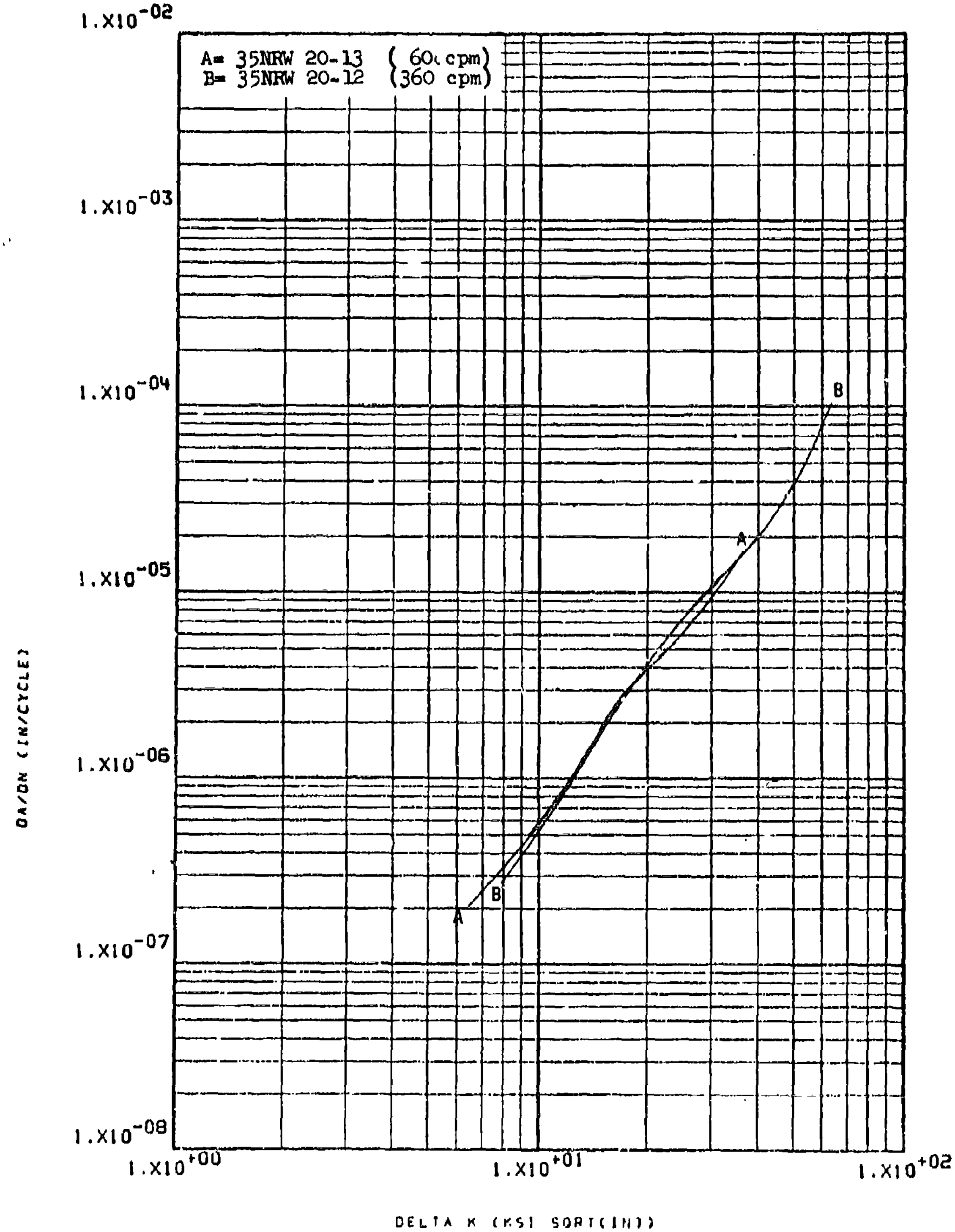

Figure 8.2.10.1-1 **Effect of cyclic frequency on LHA-FCGR at R.T., R=0.08, RW direction in 3" x 18" x 36" HP-9-4-.30 forged block**

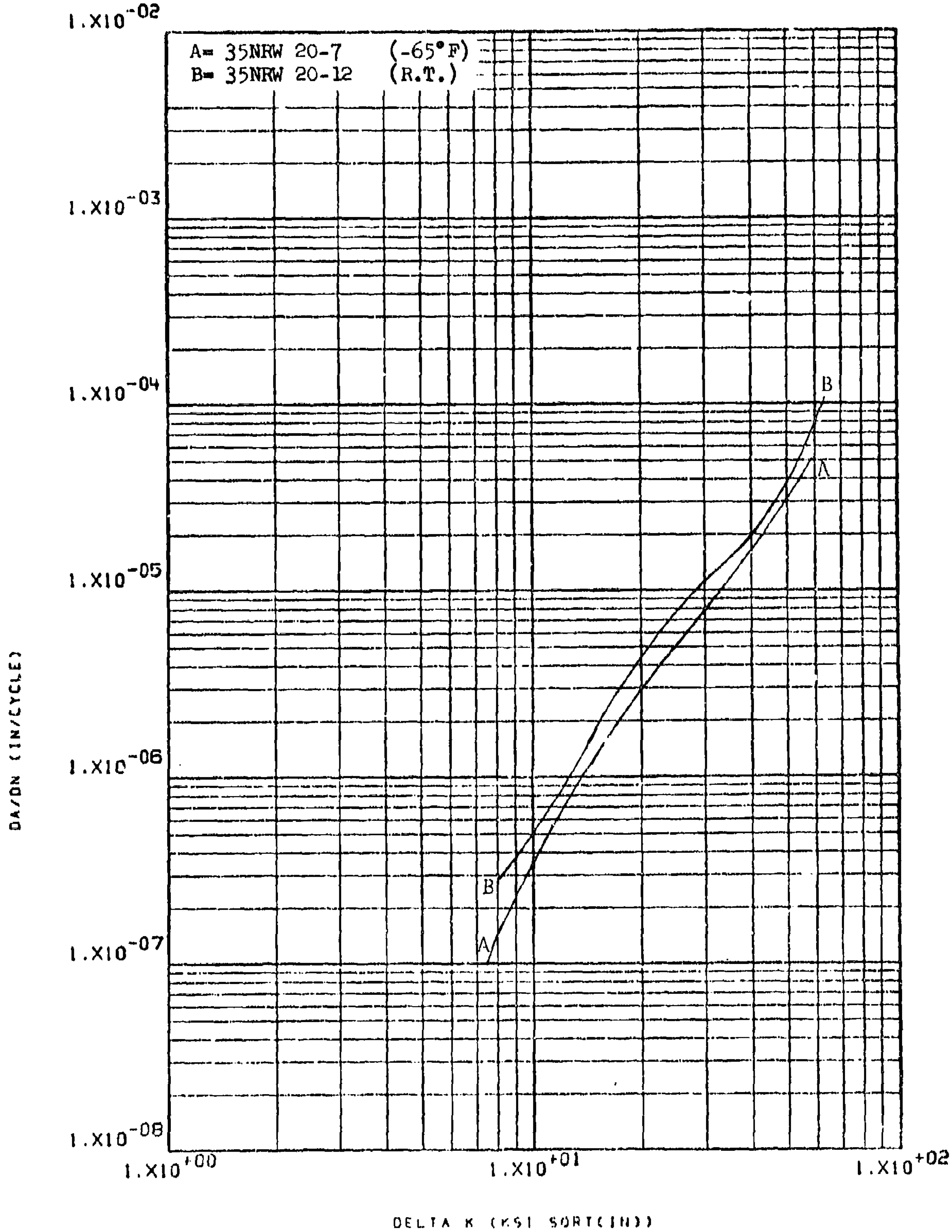

Figure 8.2.10.2-1 Effect of test temperature on LHA-FCGR at R=0.08, 360 cpm, RW direction in 3" x 18" x 36" HP-9-4-.30 forged block

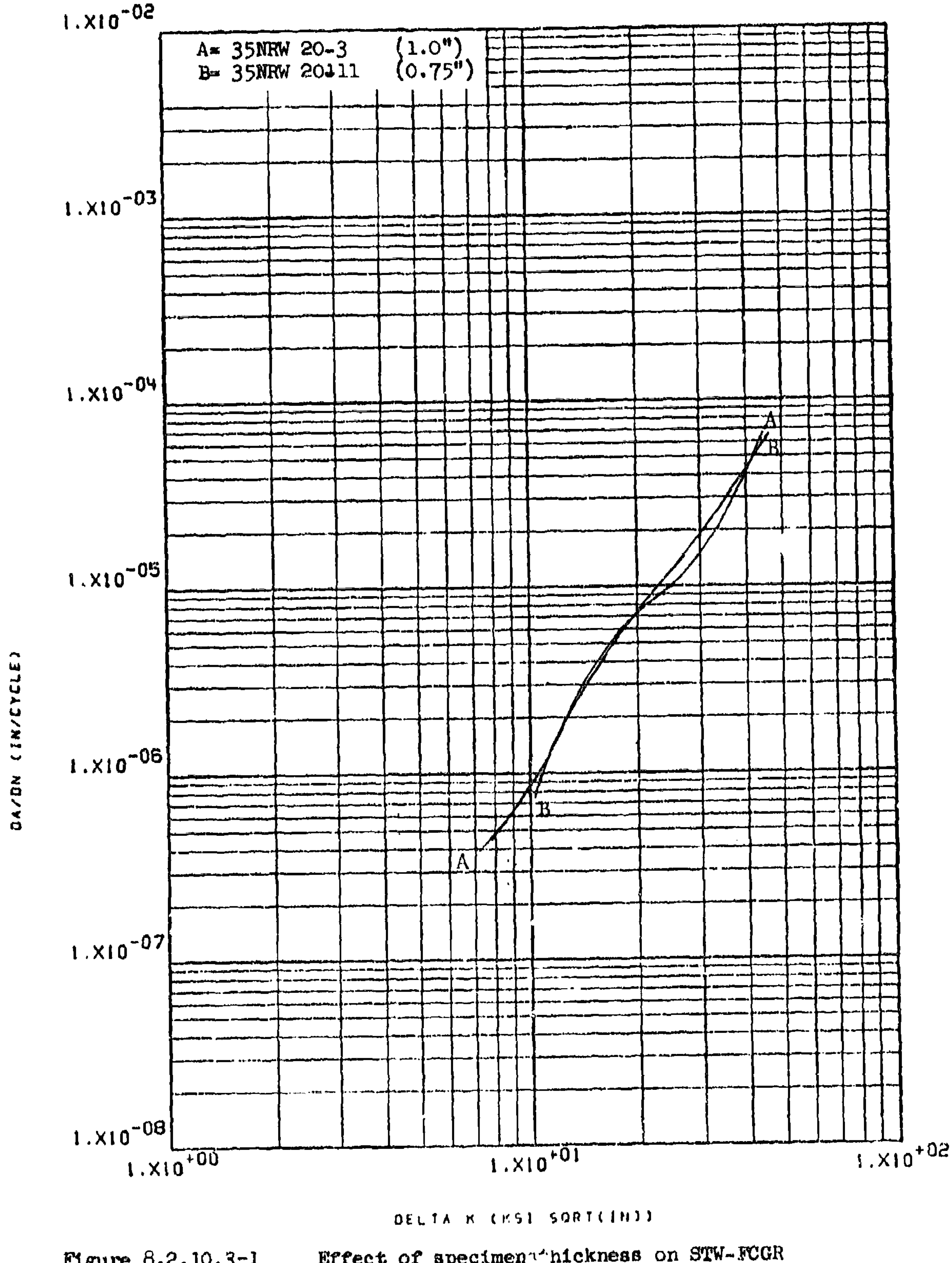

Figure 8.2.10.3-1 Effect of specimen thickness on STW-FCGR at R.T., R=0.5, RW direction in 3" x 18" x 36" HP-9-4-.30 forged block

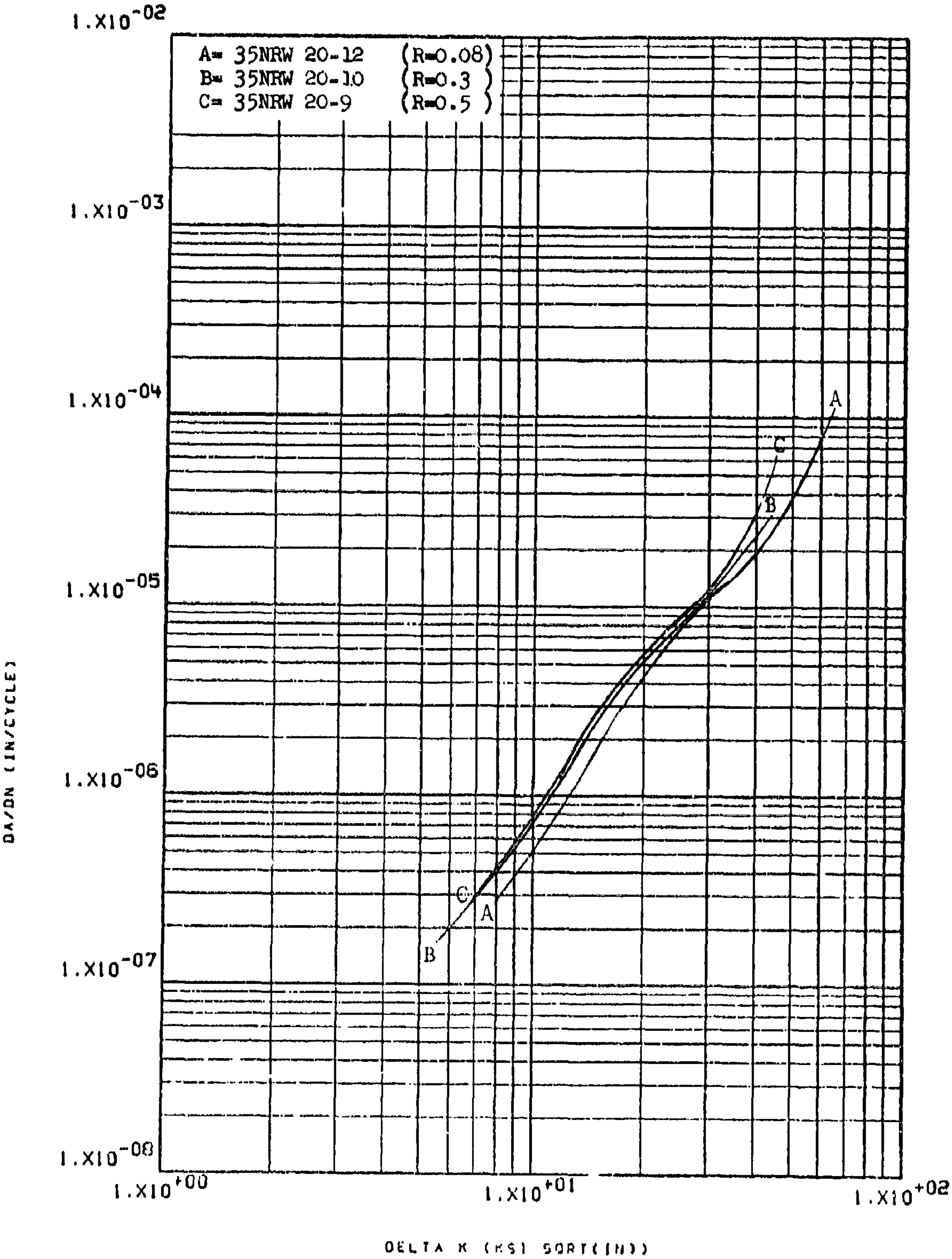

Figure 8.2.10.4-1 Effect of R factor on LHA-FCGR at R.T., 360 cpm, RW direction in 3" x 18" x 36" HP-9-4-.30 forged block

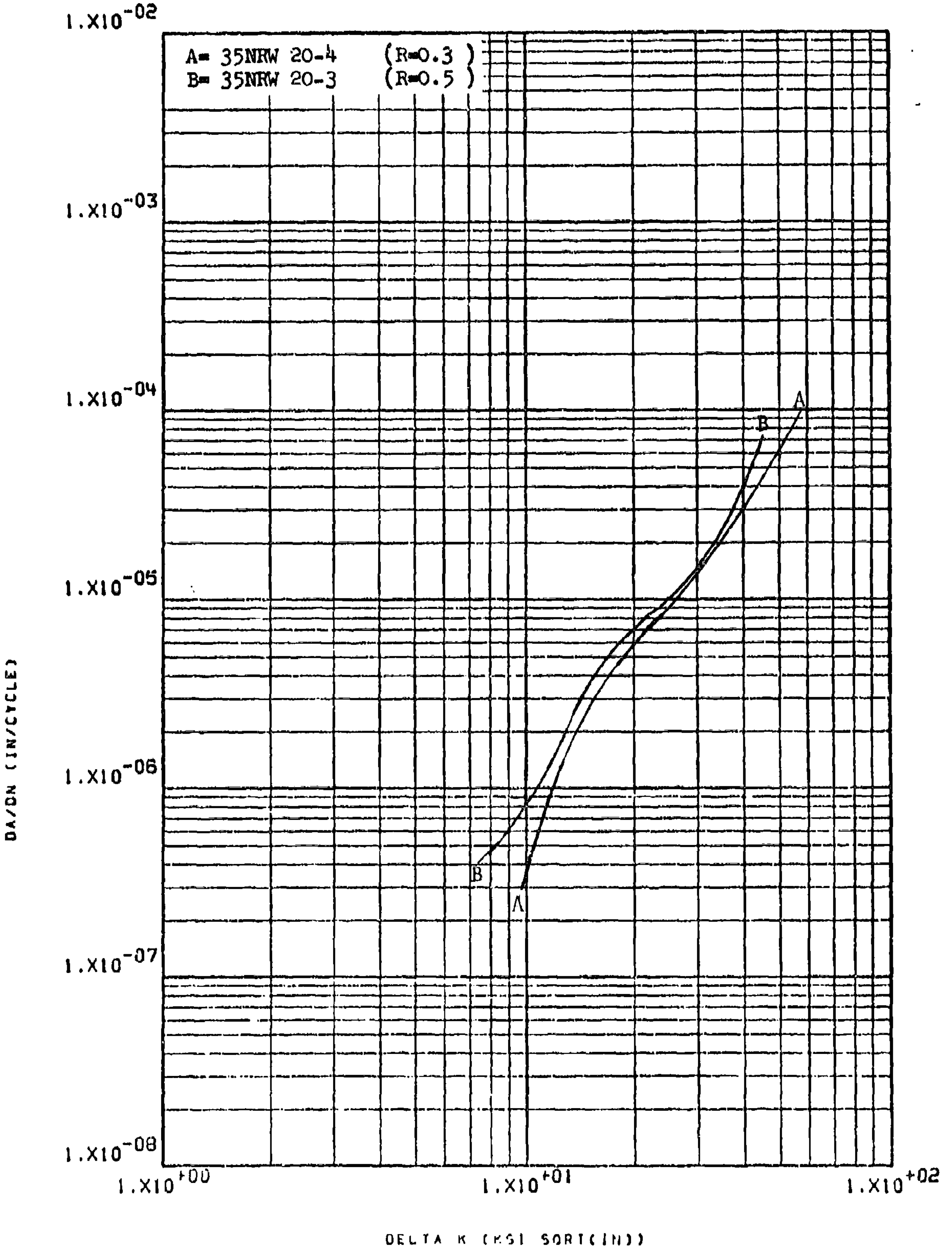

Figure 8.2.10.4-2 Effect of R factor on STW-FCGR at R.T., 60 cpm, RW direction in 3" x 18" x 36" HP-9-4-.30 forged block

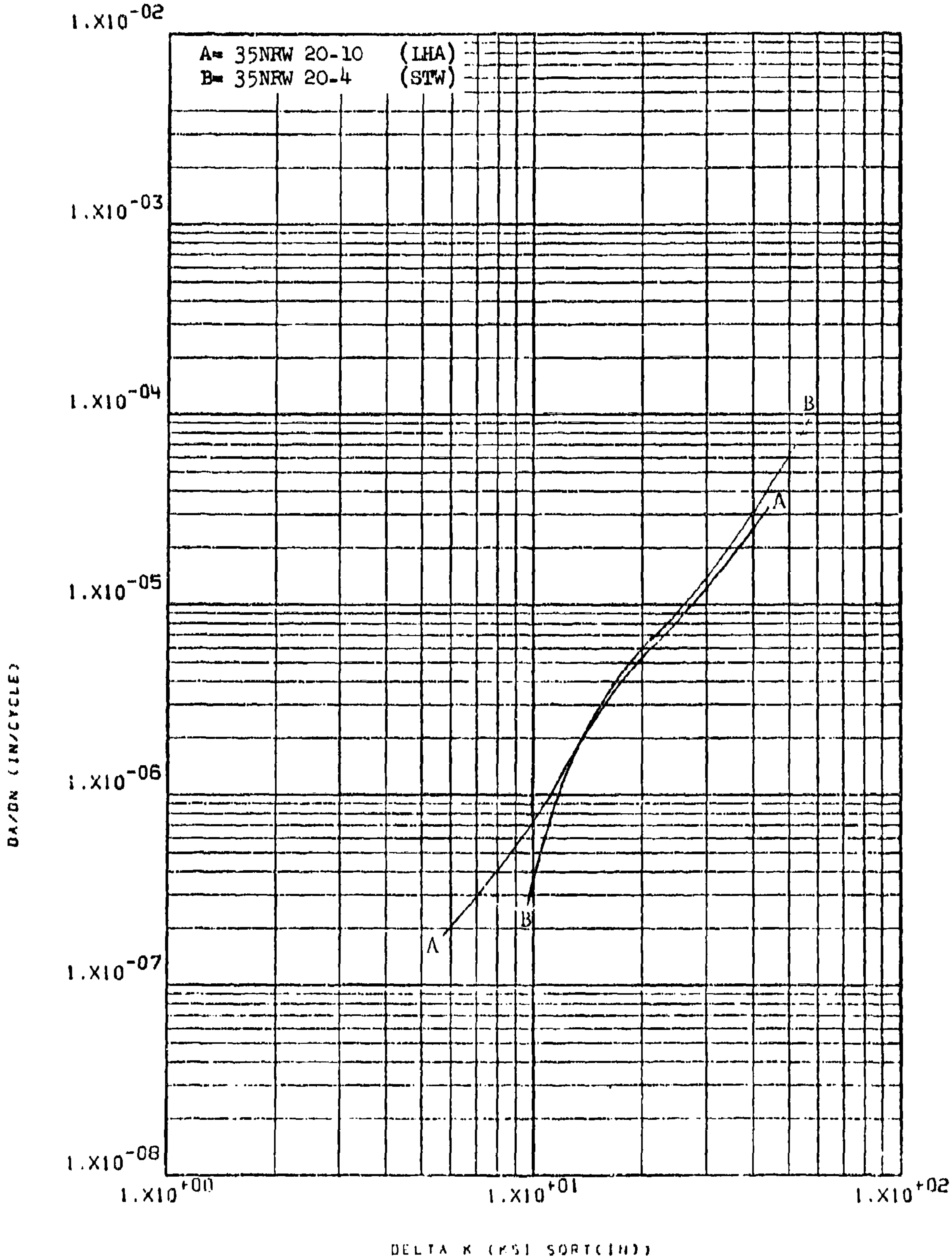

Figure 8.2.10.5-1 Effect of environment on FCGR at R.T., R=0.3, RW direction in 3" x 18" x 36" HP-9-4-.30 forged block

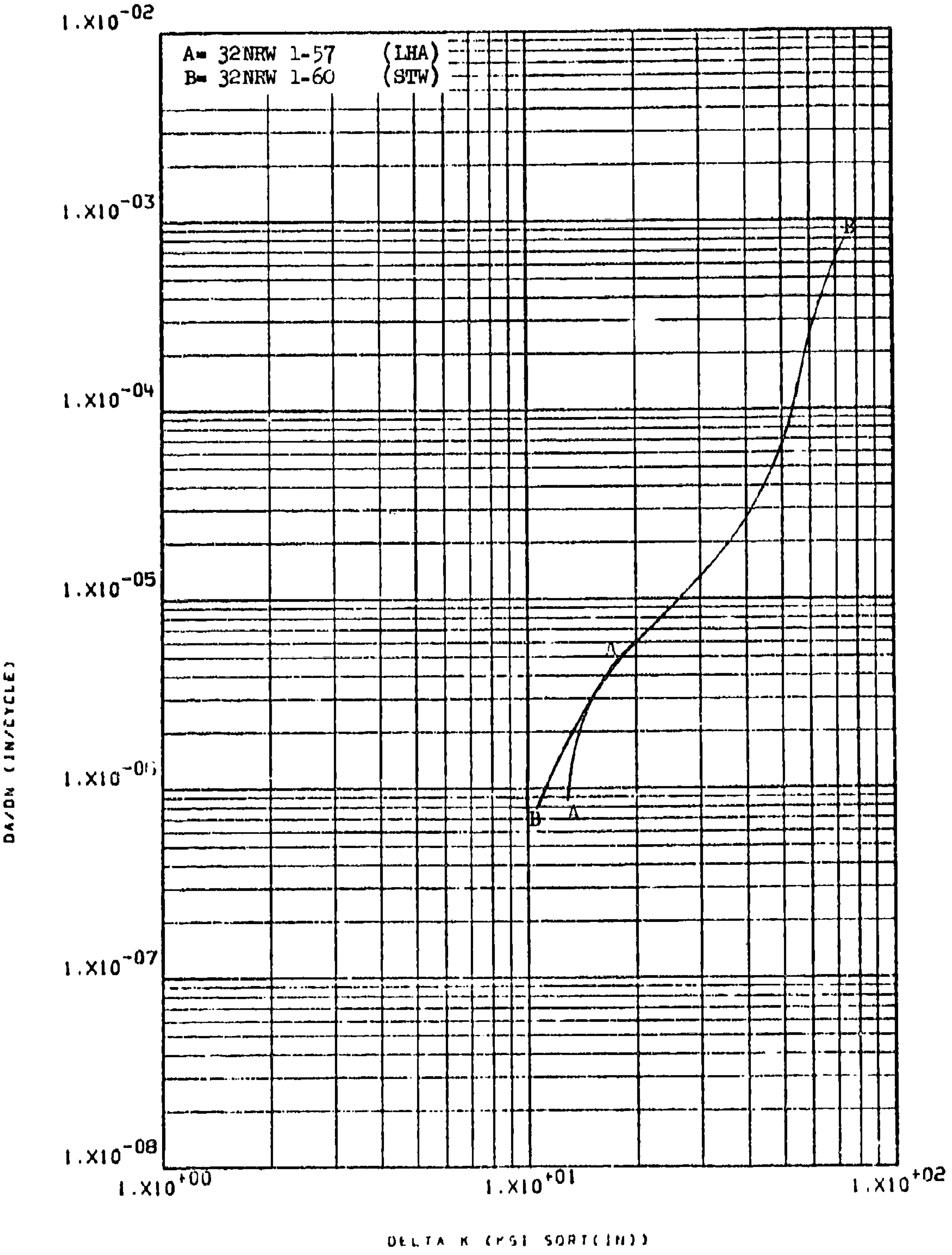

Figure 8.2.10.5-2 Effect of environment on FCGR at R.T., R=0.08, 60 cpm, RW direction in 3" x 18" x 36" HP-9-4-.30 forged block

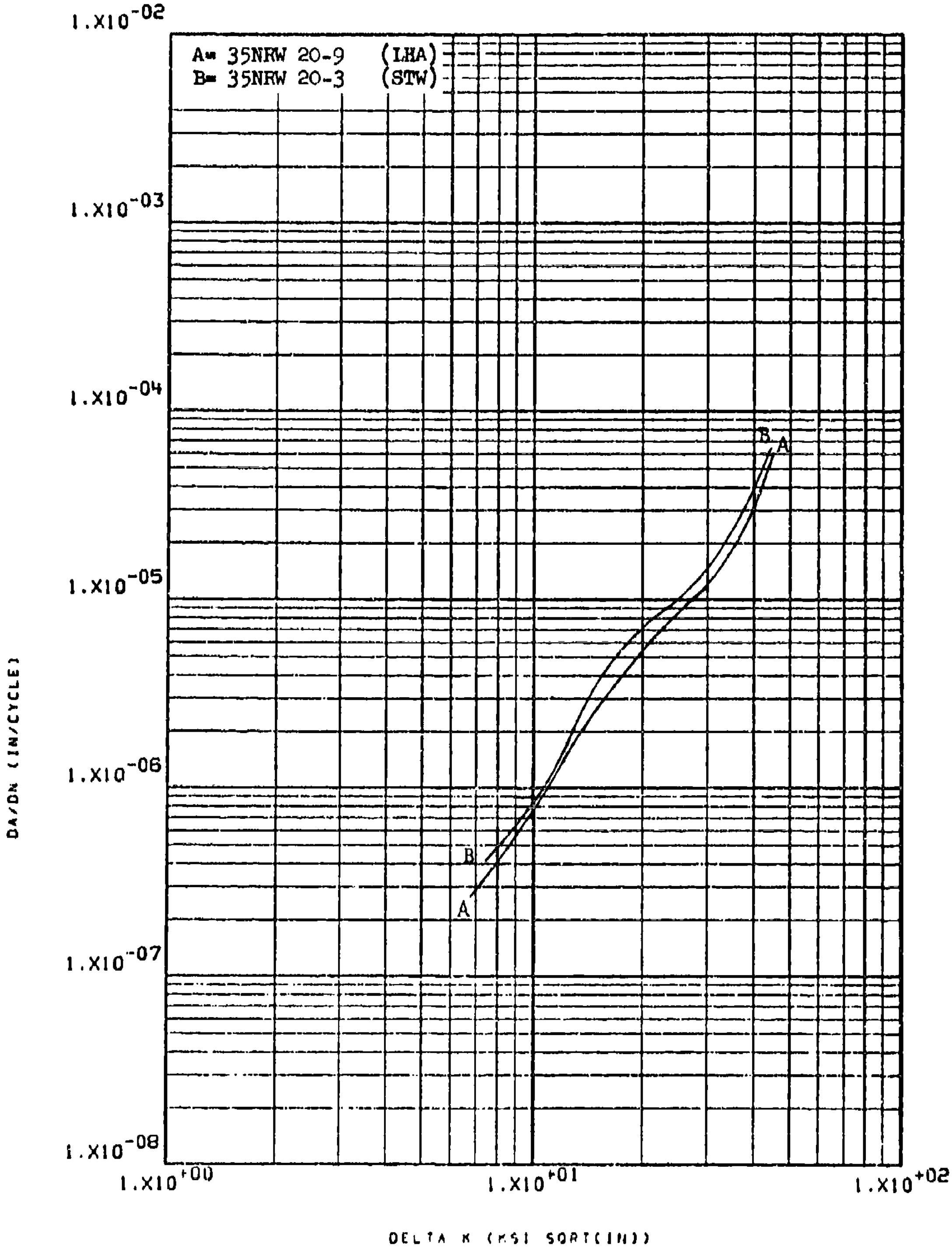

Figure 8.2.10.5-3 Effect of environment on FCGR at R.T., R=0.5, RW direction in 3" x 18" x 36" HP-9-4-.30 forged block

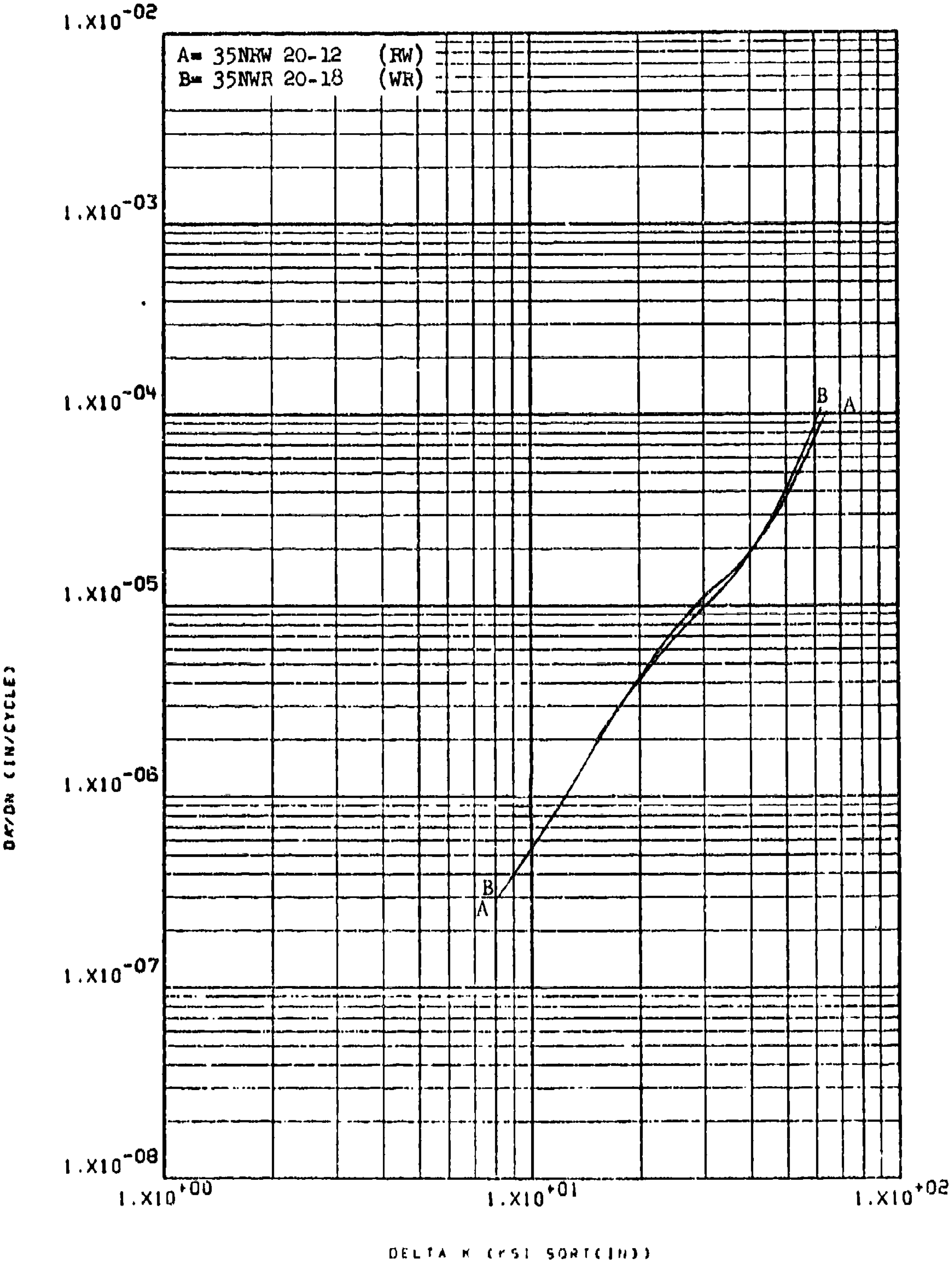

Figure 8.2.10.6-1 Effect of test direction on LHA-FCGR at R.T., R=0.08, 360 cpm in 3" x 18" x 36" HP-9-4-.30 forged block

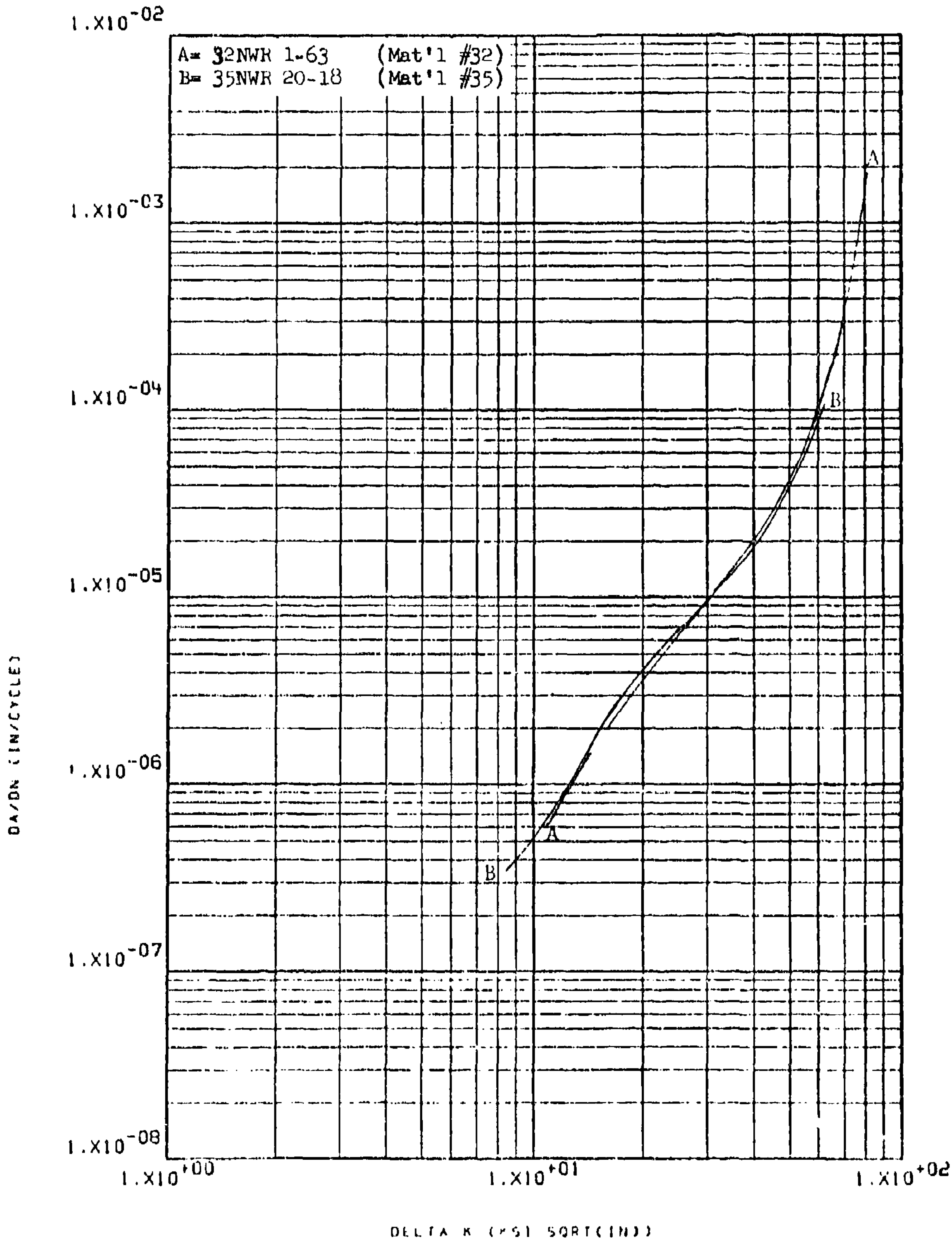

Figure 8.2.10.7-1 Effect of product form on LHA-FCGR at R.T., R=0.08, 360 cpm, WR direction in 3" x 18" x 36" HP-9-4-.30 forged block

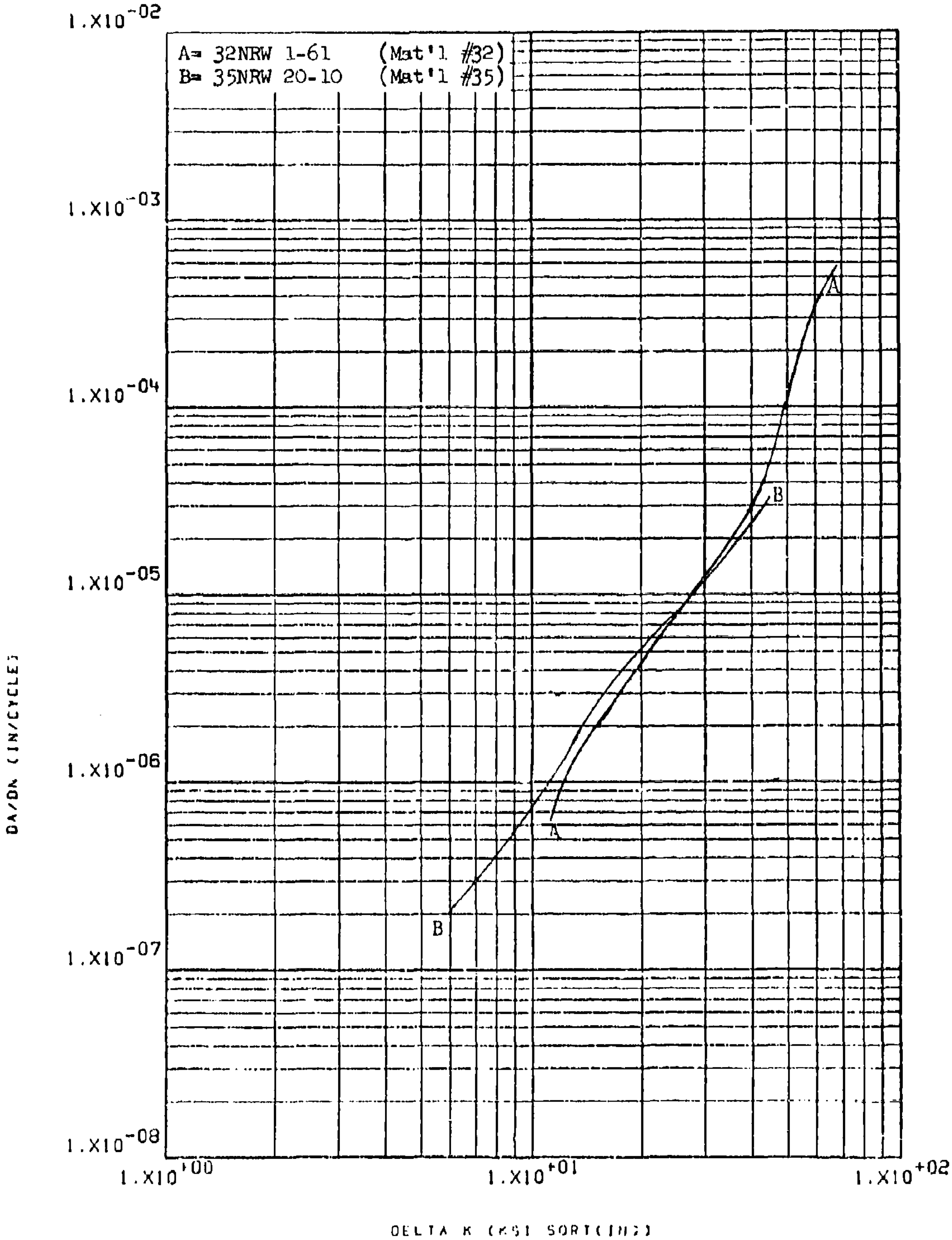

Figure 8.2.10.7-2 Effect of product form on LHA-FCGR at R.T., R=0.3, 360 cpm, RW direction in 3" x 18" x 36" HP-9-4-.30 forged block

8.2.11 PH 13-8Mo Steel

8.2.11.1 Cyclic Frequency - There was no consistently significant effect observed in the fatigue crack growth rate characteristics of this material when the cyclic frequency of test was reduced from 360 to 60 cpm in low humidity air, and from 60 to 6 in sump tank water (Figures 8.2.11.1-1 and -2).

8.2.11.2 Test Temperature - The effects of variations in test temperatures on the fatigue crack growth rate characteristics of this material were inconsistent (Figures 8.2.11.2-1 and -2), although one set of comparative curves for rolled bar indicated substantially increased growth rates at ambient temperature than at -65°F (Figure 8.2.11.2-3).

8.2.11.3 Specimen Thickness - In the WR direction the low humidity air growth rates of this material measured in a 1.0 inch thick specimen were seen to be very slightly greater than those measured in a 0.5 inch thick specimen (Figure 8.2.11.3-1). This thickness effect was also observed in the RW direction, although it was not consistent throughout the entire range of delta K. In this direction, however, growth rates measured in both 0.5" and 1.0" thick specimens were seen to be greater than those measured in an 0.25" thick specimen (Figure 8.2.11.3-2).

8.2.11.4 R Factor - The effects of increasing R factors on the low humidity air fatigue crack growth rate characteristics of this material in the RW direction were inconsistent throughout the delta K range in 4" x 5" forged bar (Figure 8.2.11.4-1) and 1.5" x 12" rolled bar (Figure 8.2.11.4-2). In 0.5" x 8" extruded stock, on the other hand, trends were demonstrated toward slight acceleration of growth rates when R was increased from 0.08 to 0.5 (Figure 8.2.11.4-3), and in sump tank water growth rates of the rolled bar stock were significantly accelerated when R was increased from 0.08 to 0.3 (Figure 8.2.11.4-4).

8.2.11.5 Environment - Fatigue crack growth rates of 1.5" x 12" rolled bar stock in sump tank water and shop cleaning solvent were seen to be essentially equivalent throughout the range of delta K and both were equivalent to low humidity air growth rates at delta K levels below ~20 ksi $\sqrt{in}$ and an R factor of 0.08 (Figure 8.2.11.5-1). Above this level, however, growth rates in sump tank water and shop cleaning solvent were significantly greater than those in low humidity air. At an R=0.3 in this same material,sump tank water growth rates were significantly greater than those in low humidity air at delta K levels as low as ~15 ksi $\sqrt{in}$ (Figure 8.2.11.5-2). Similar equivalencies in rates at low delta K levels were observed in 0.5" x 8" extrusions at R=0.08 (Figure 8.2.11.5-3). In 4" x 5" forged bar stock at R=0.08 and R=0.3, and in the WR direction at R=0.08 of the 1.5" x 12" rolled bar,sump tank water growth rates were seen to be noticeably greater than low humidity air rates throughout the entire range of delta K (Figures 8.2.11.5-4 through -6).

8.2.11.6 Test Direction - In general, fatigue crack growth rates in this material were seen to be slightly greater in the RW direction than in the WR direction (Figures 8.2.11.6-1 through -5). In low humidity air at -65°F, however, this trend was seen to be reversed (Figure 8.2.11.6-6).

8.2.11.7 Product Form - No significant differences in low humidity air crack growth rate characteristics were observed between forged bar, rolled bar, extrusions and upset forgings (Figures 8.2.11.7-1 through 8.2.11.7-4). In sump tank water at R=0.08, however, growth rates in forged bar were noticeably greater than those in rolled bar (Figures 8.2.11.7-5 and -6), while at R=0.3 this trend was reversed (Figure 8.2.11.7-7). At -65°F in low humidity air the crack growth rate of extruded stock was seen to be substantially greater than the rate of rolled bar at a delta K level of 15 ksi$\sqrt{\text{in}}$. These rates tended to converge on each other, however, as delta K was increased to ~35 ksi$\sqrt{\text{in}}$ (Figure 8.2.11.7-8).

8.2.11.8 Heat Treat Condition - Not evaluated.

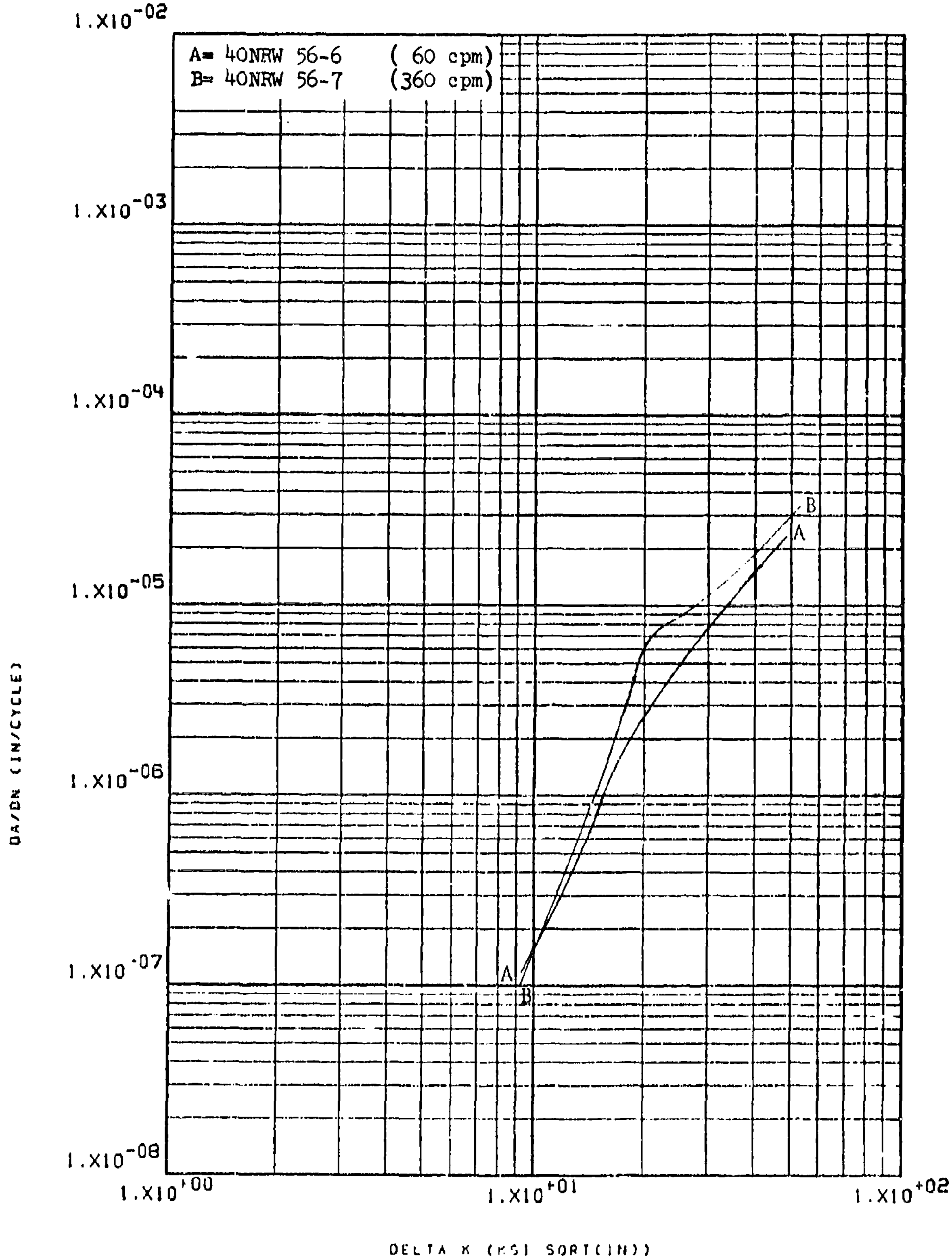

Figure 8.2.11.1-1 Effect of cyclic frequency on LHA-FCGR at R.T., R=0.08, RW direction in 1.5" x 12" PH13-8Mo rolled bar

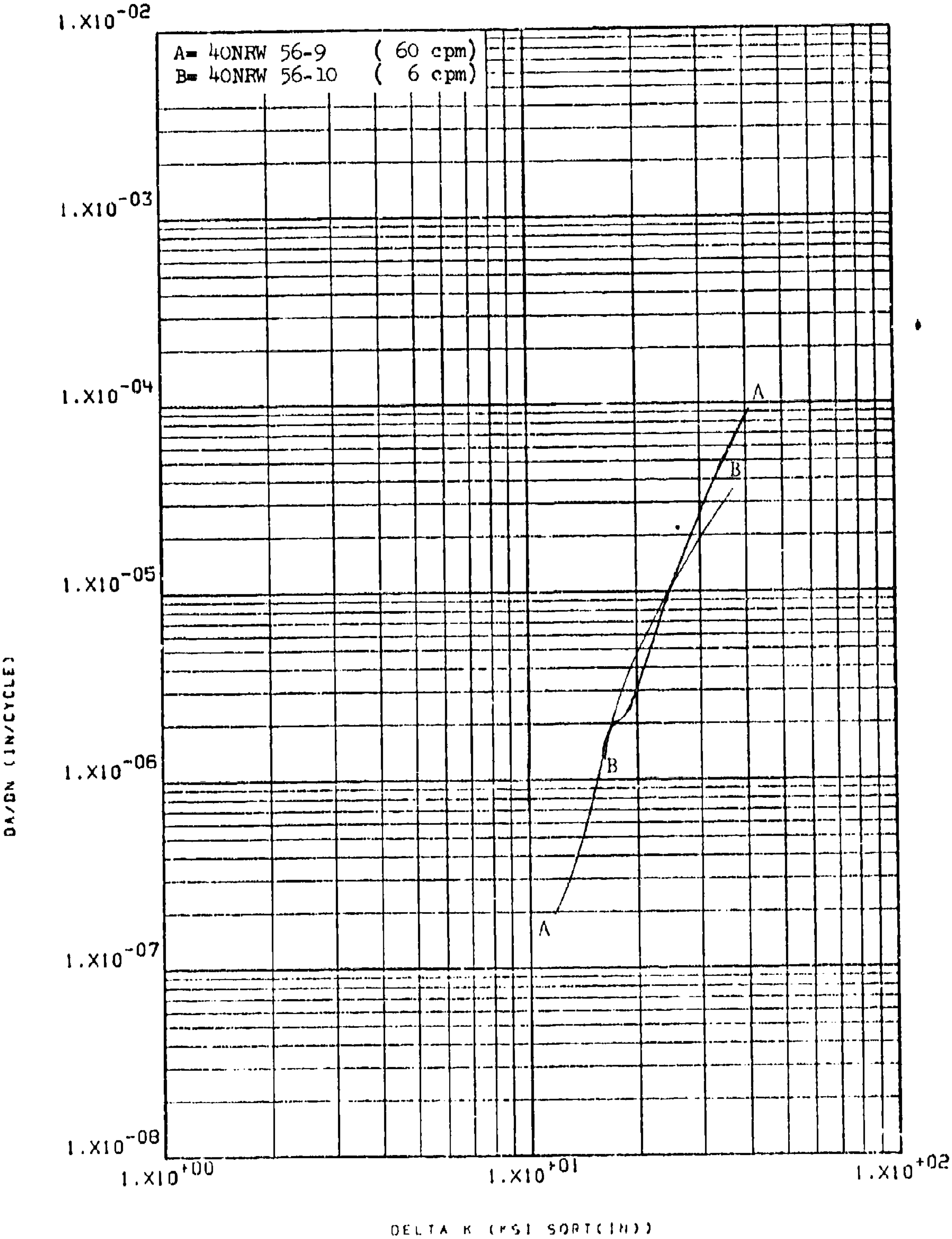

Figure 8.2.11.1-2 Effect of cyclic frequency on STW-FCGR at R.T., R=0.08, RW direction in 1.5" x 12" PH13-8Mo rolled bar

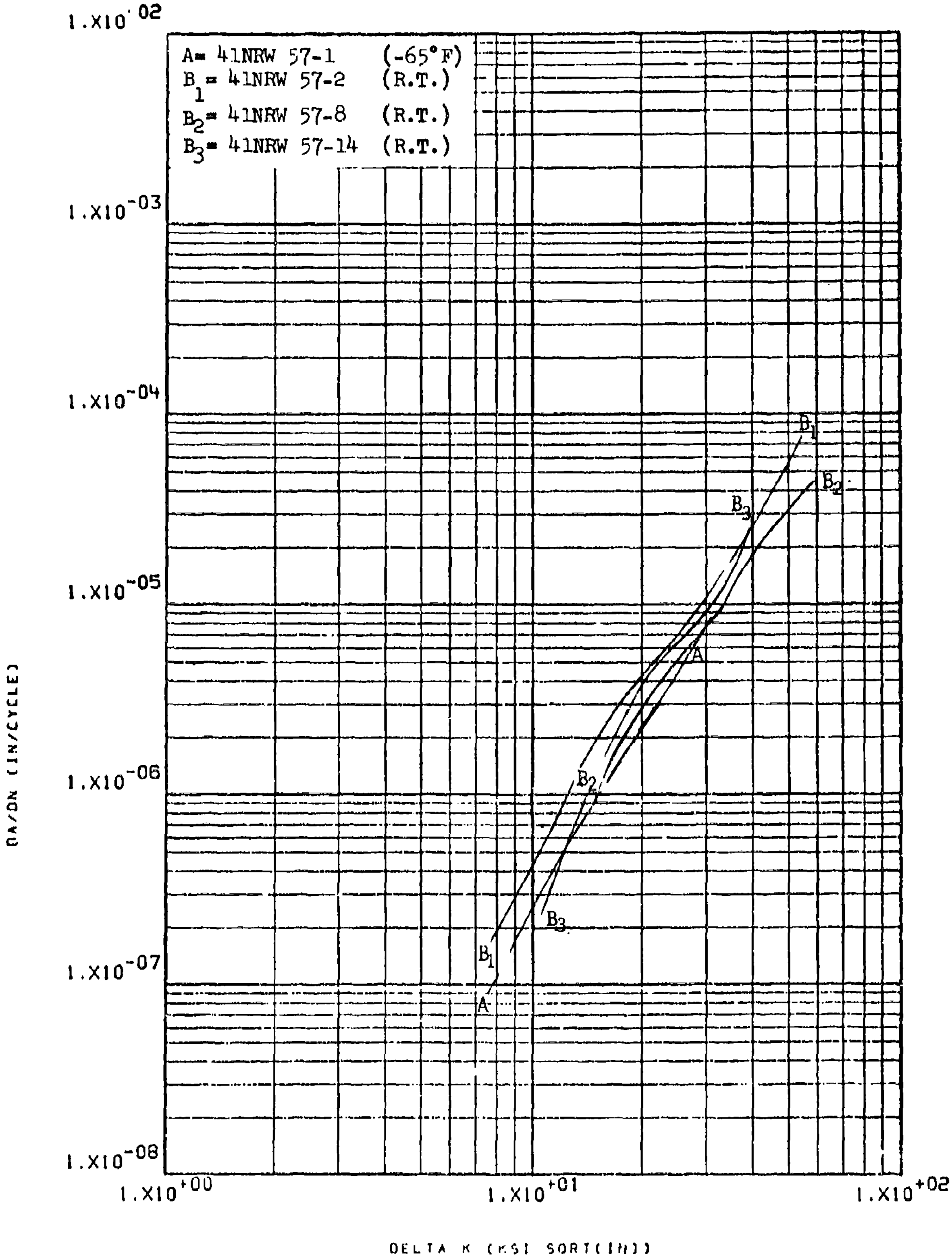

Figure 8.2.11.2-1 Effect of test temperature on LHA-FCGR at R=0.08, 360 cpm, RW direction in 0.5" x 8" PH13-8Mo extrusion

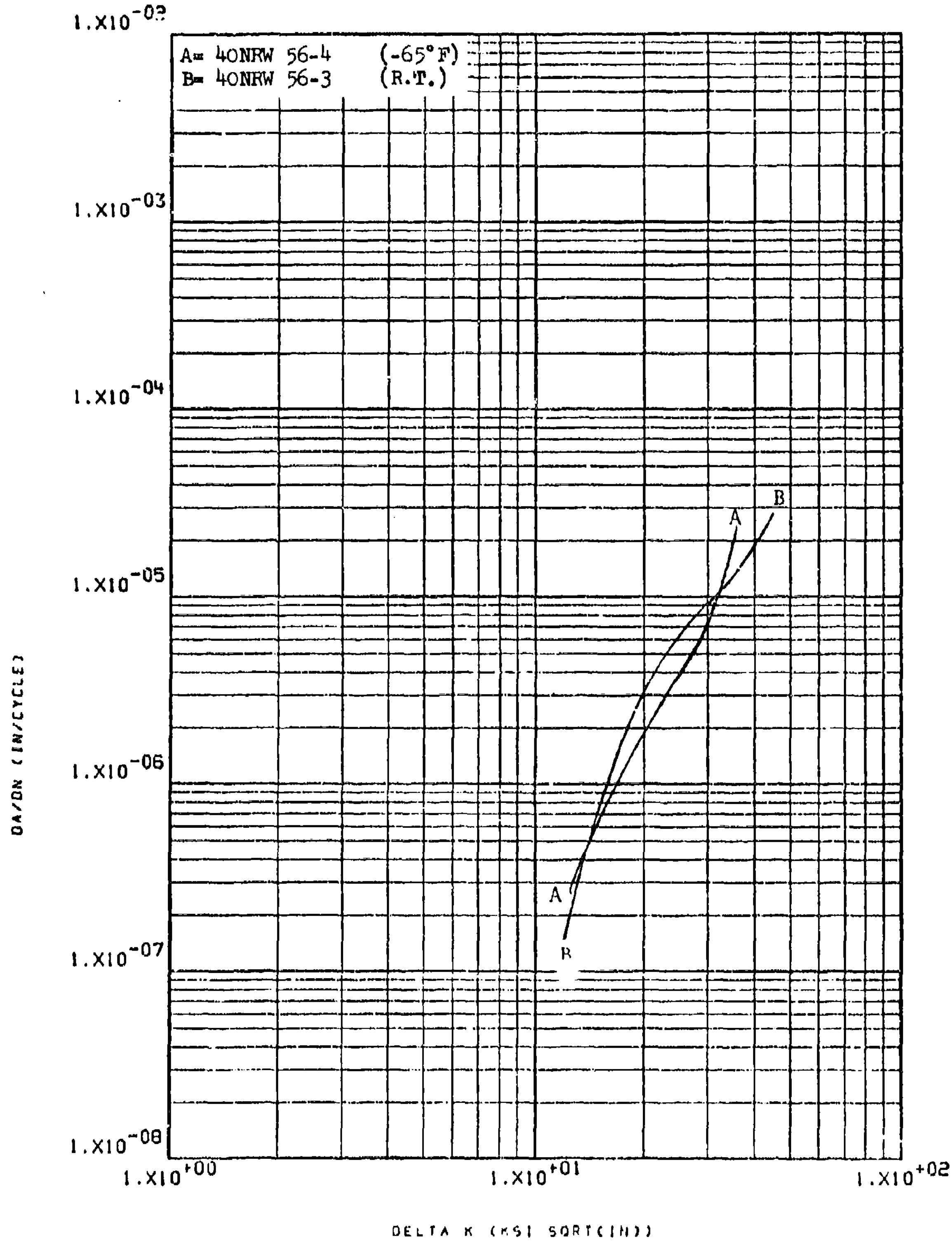

Figure 8.2.11.2-2 Effect of test temperature on LHA-FCGR at R=0.08, 360 cpm, WR direction in 1.5" x 12" PH13-8Mo rolled bar

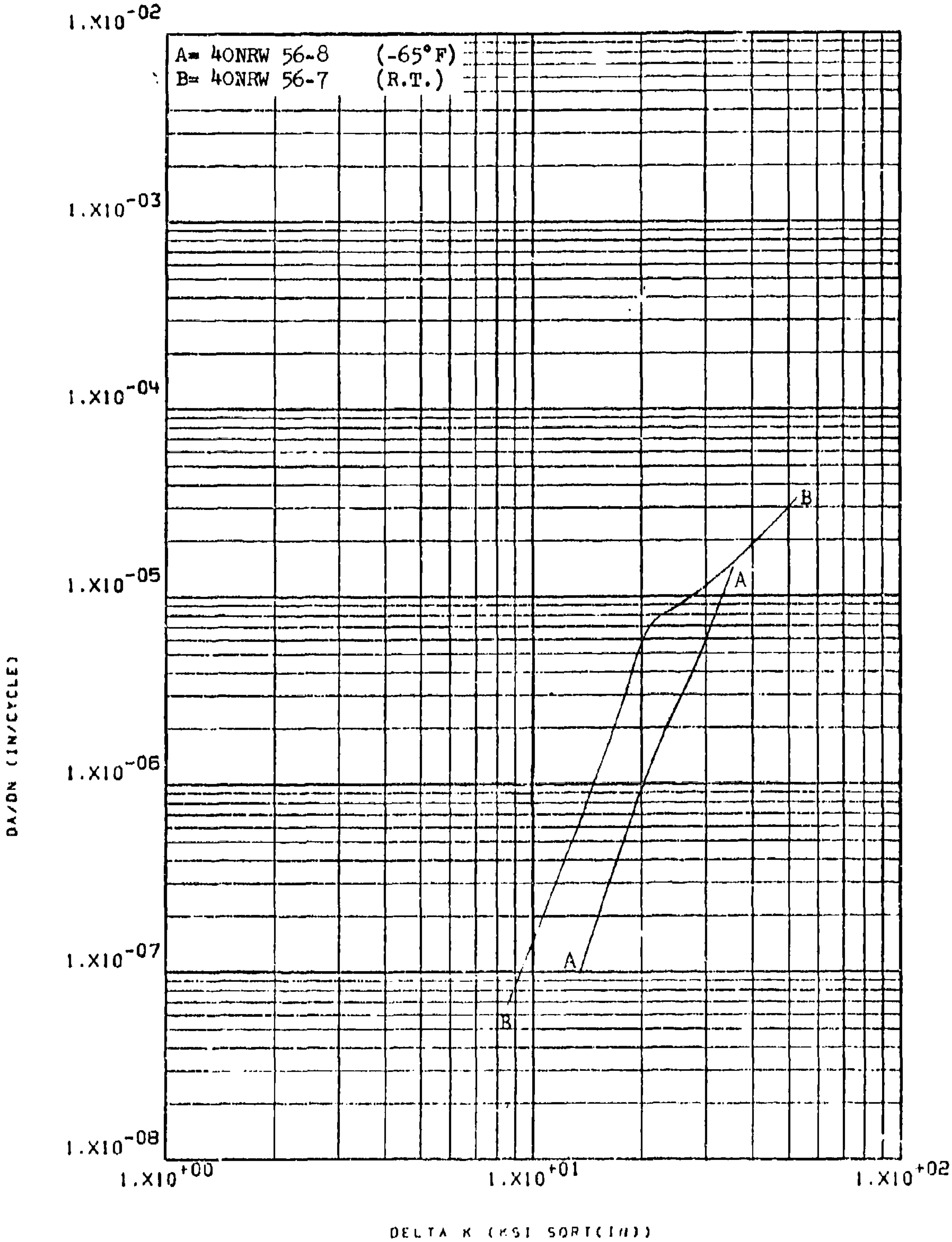

Figure 8.2.11.2-3 Effect of test temperature on LHA-FCGR at R=0.08, 360 cpm, RW direction in 1.5" x 12" PH13-8Mo rolled bar

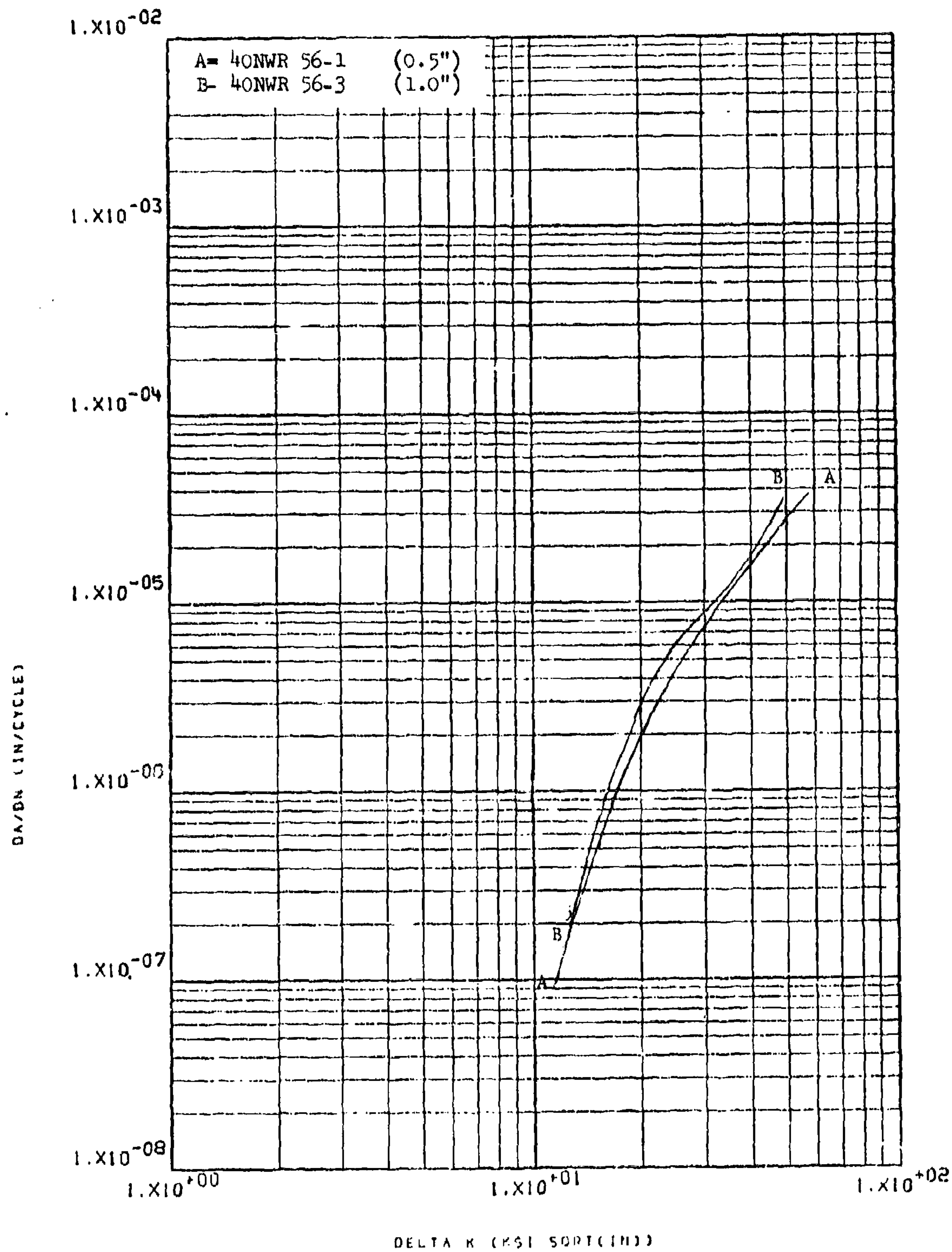

Figure 8.2.11.3-1 Effect of specimen thickness on LHA-FCGR at R.T., R=0.08, 360 cpm, WR direction in 1.5" x 12" PH13-8Mo rolled bar

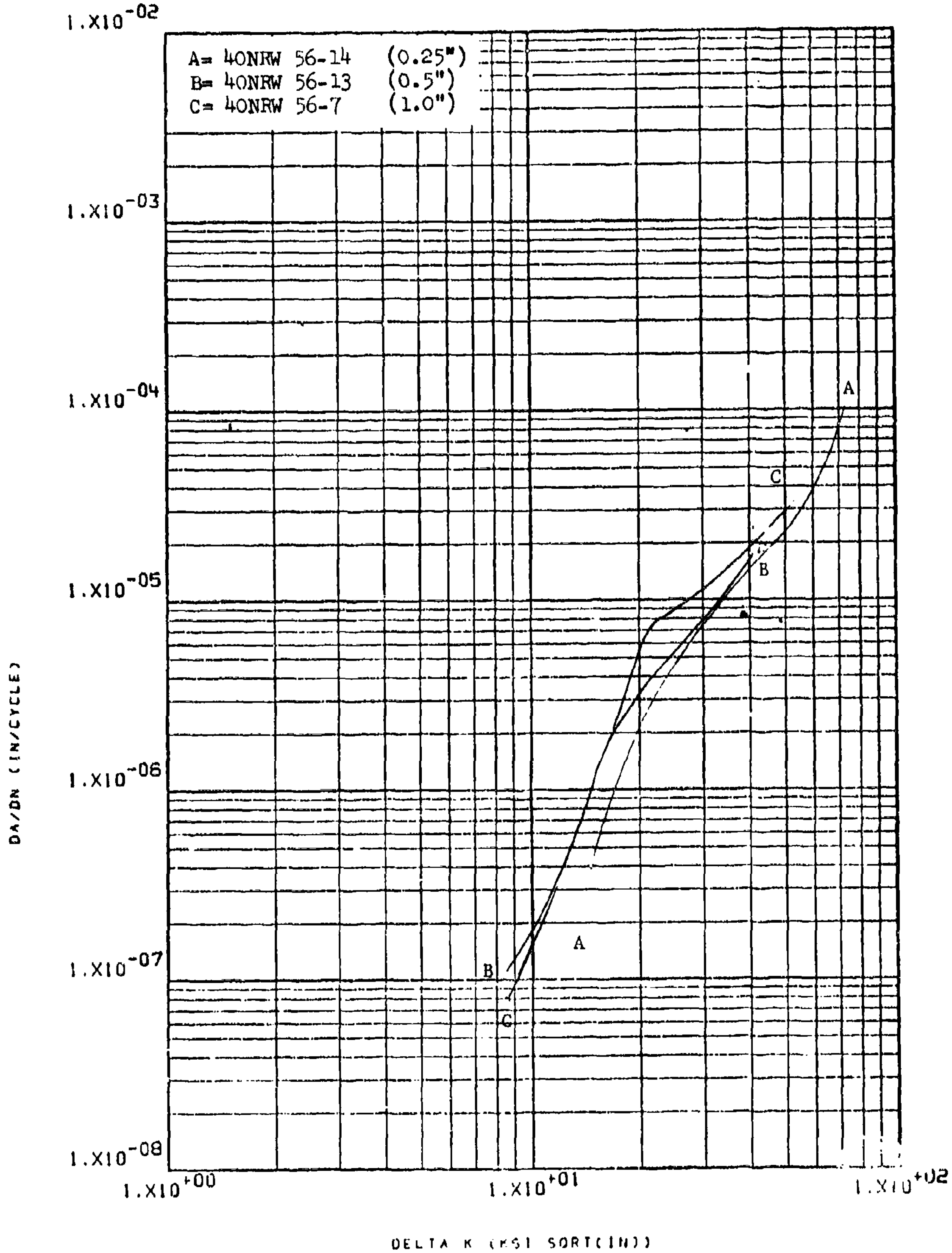

Figure 8.2.11.3-2 Effect of specimen thickness on LHA-FCGR at R.T., R=0.08, 360 cpm, RW direction in 1.5" x 12" PH13-8Mo rolled bar

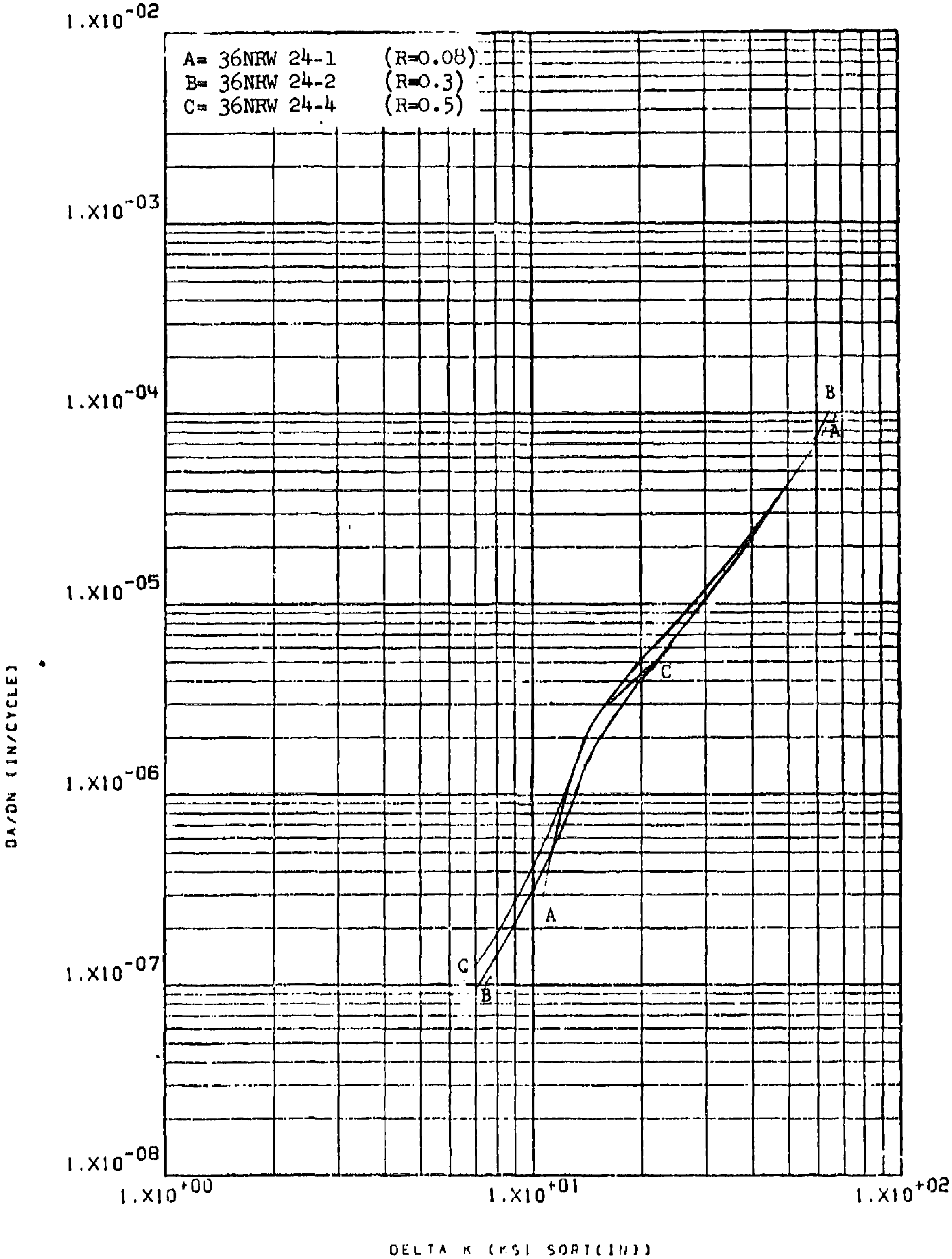

Figure 8.2.11.4-1 Effect of R factor on LHA-FCGR at R.T., 360 cpm, RW direction in 4" x 5" PH13-8Mo forged bar

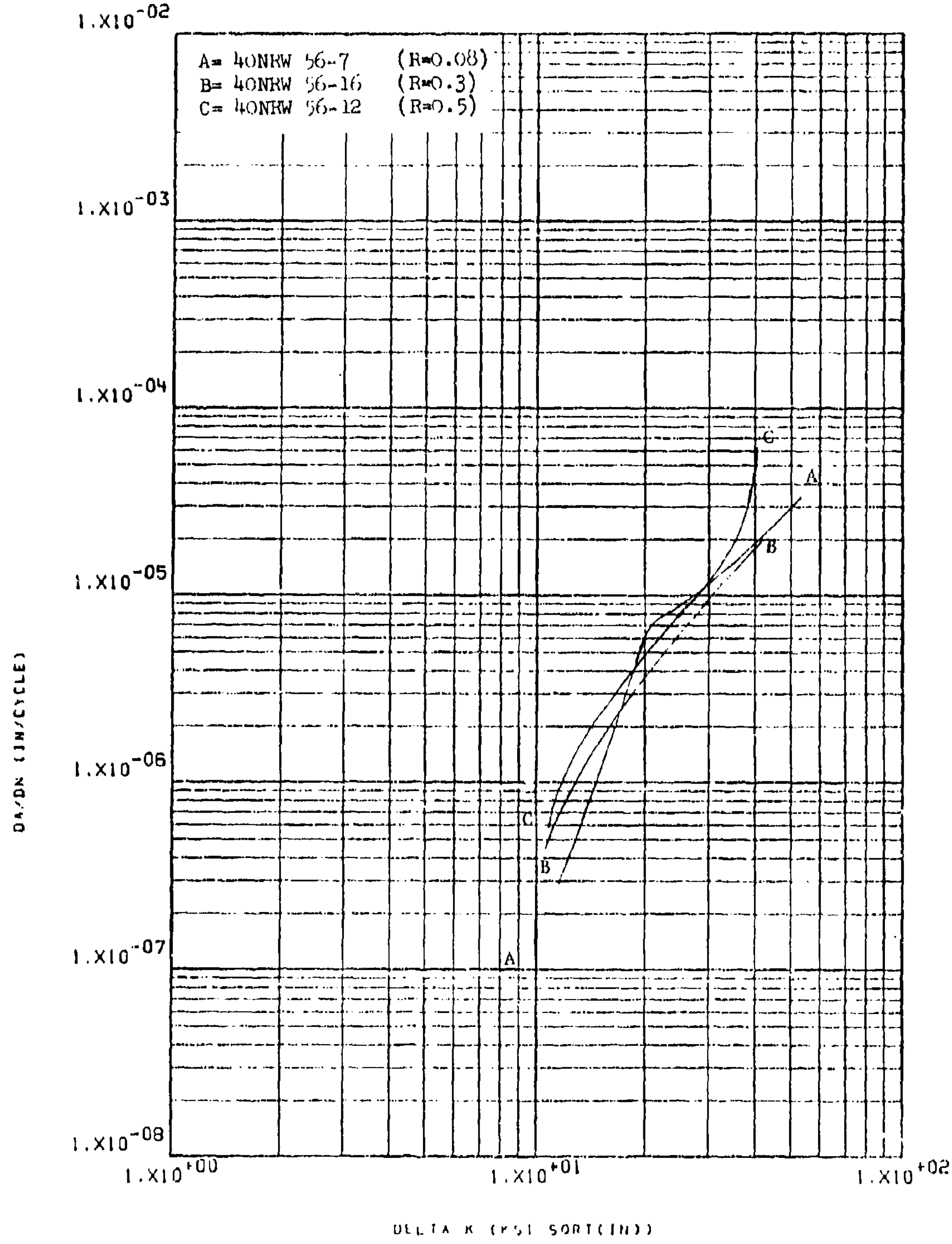

Figure 8.2.11.4-2 Effect of R factor on LHA-FCGR at R.T., 360 cpm, RW direction in 1.5" x 12" PH13-8Mo rolled bar

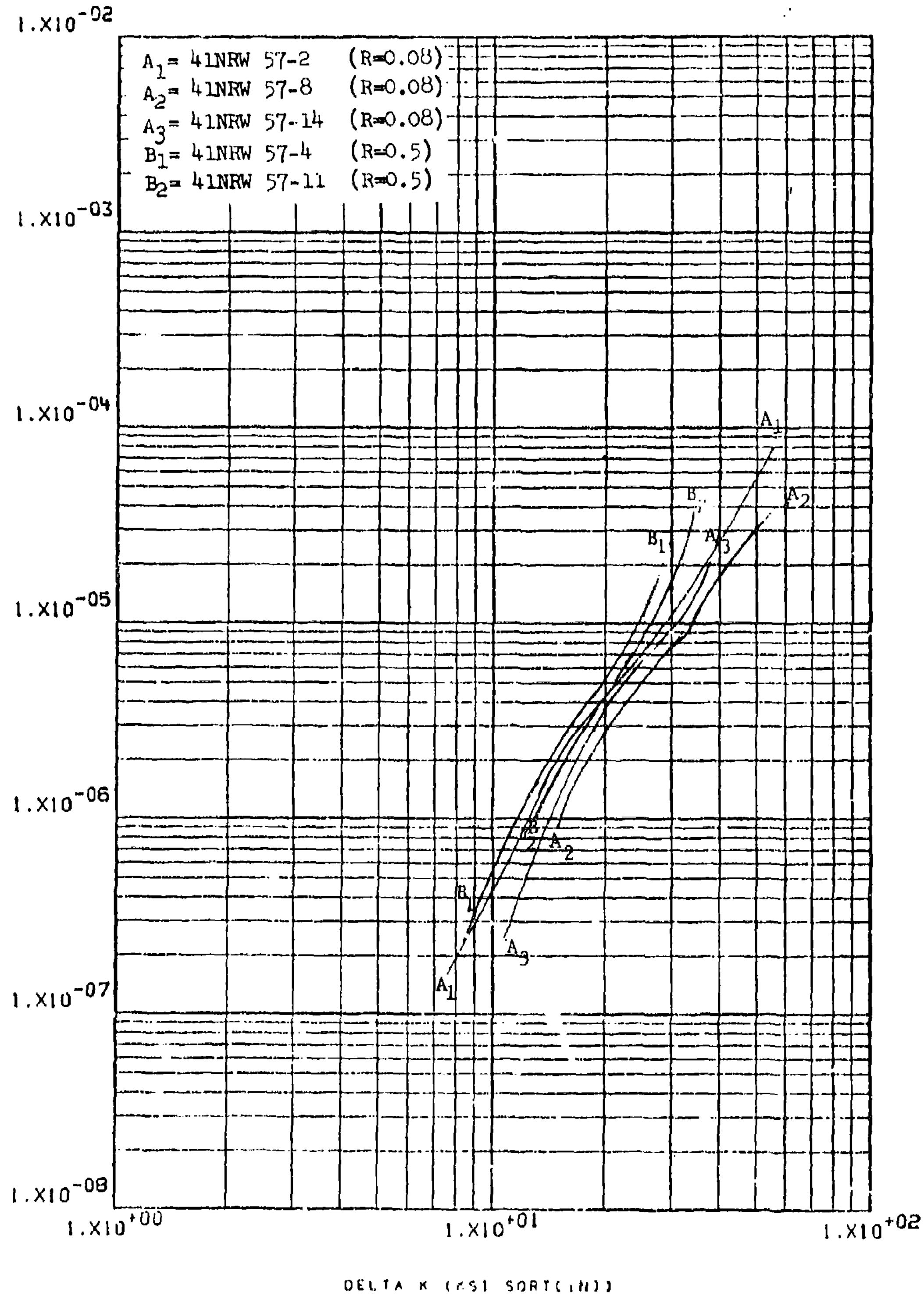

Figure 8.2.11.4-3 Effect of R factor on LHA-FCGR at R.T., 360 cpm, RW direction in 0.5" x 8" PH13-8Mo extrusion

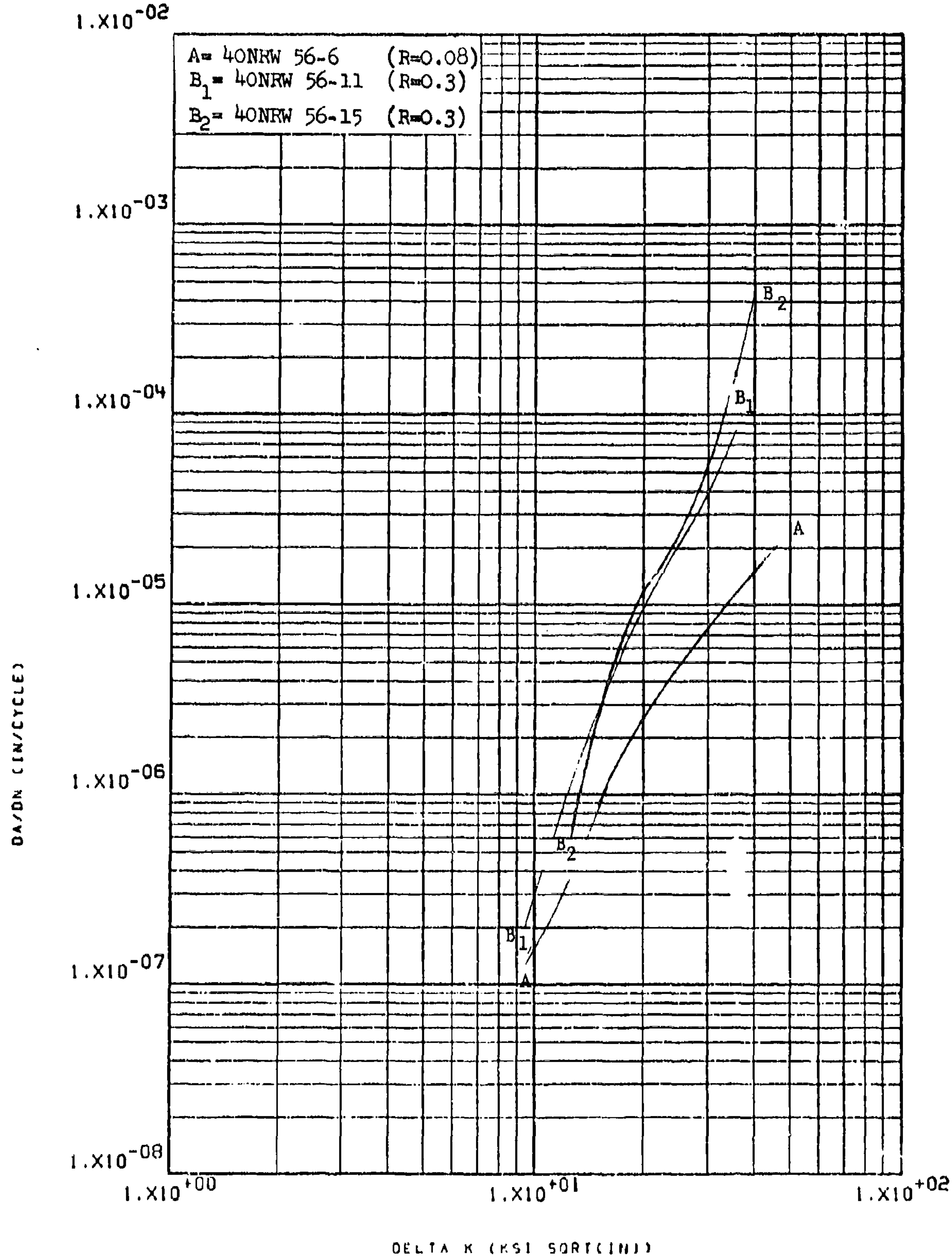

Figure 8.2.11.4-4 Effect of R factor on STW-FCGR at R.T., 60 cpm, RW direction in 1.5" x 12" PH13-8Mo rolled bar

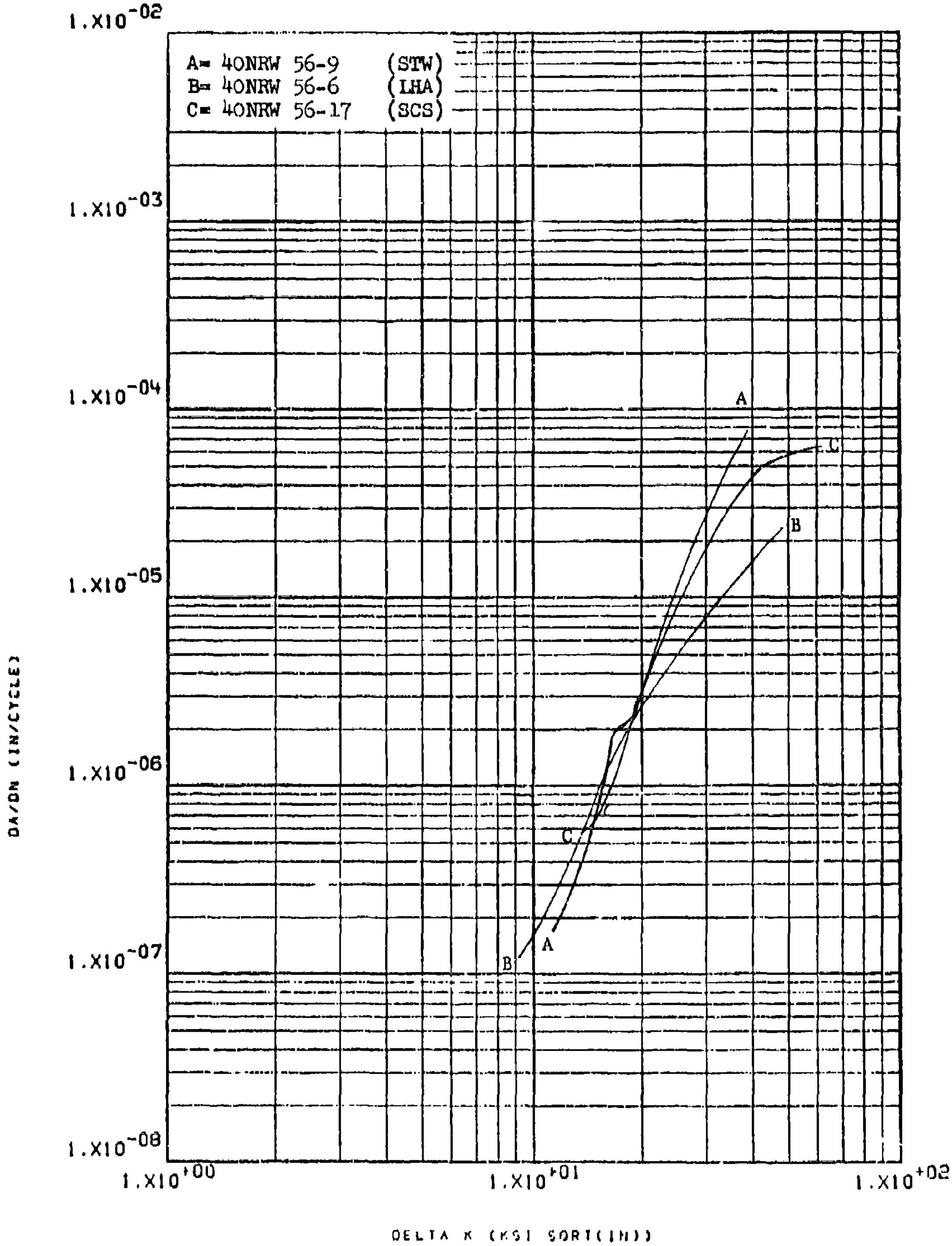

Figure 8.2.11.5-1 Effect of environment on FCGR at R.T., R=0.08, 60 cpm, RW direction in 1.5" x 12" PH13-8Mo rolled bar

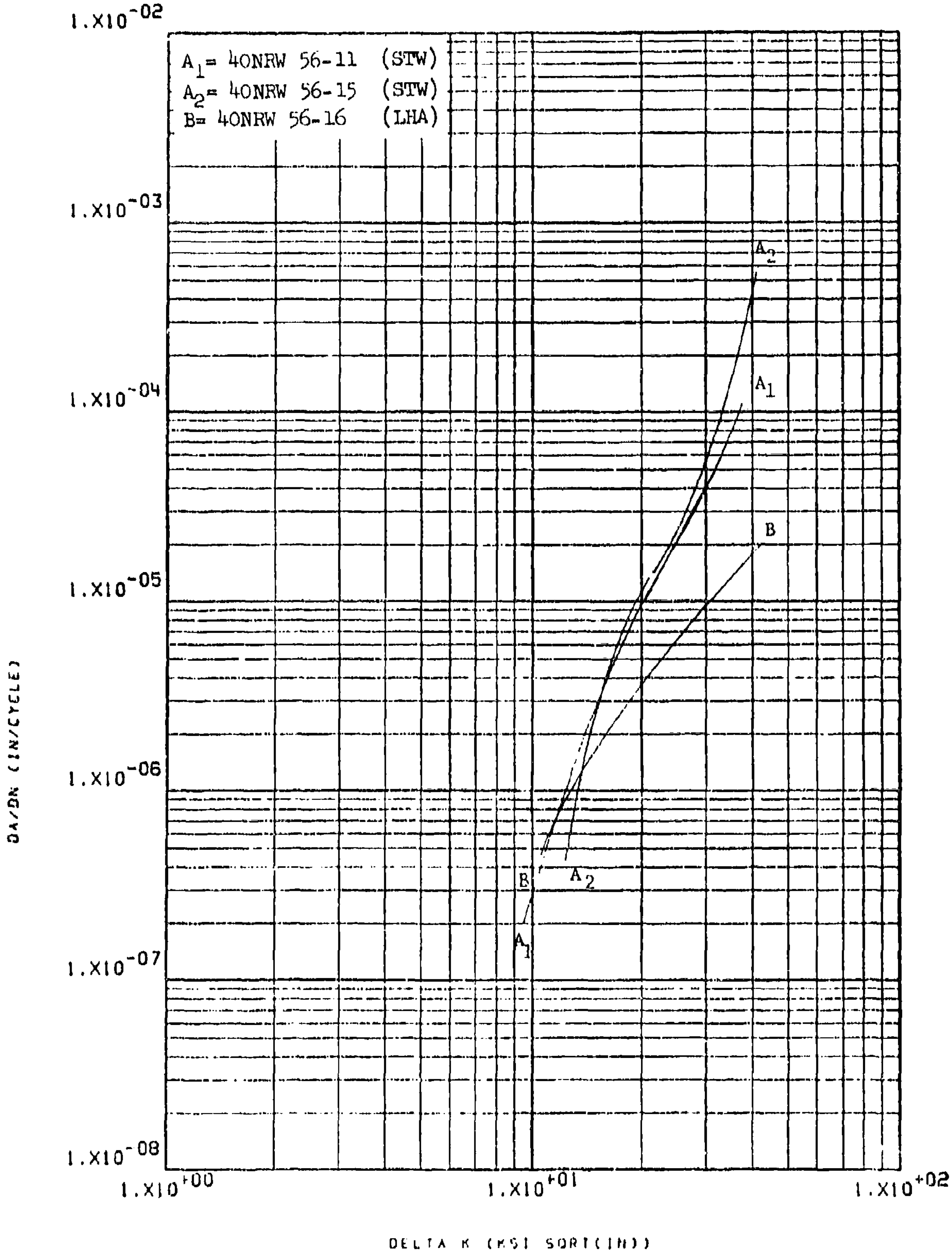

Figure 8.2.11.5-2 **Effect of environment on FCGR at R.T., R=0.3, RW direction in 1.5" x 12" PH13-8Mo rolled bar**

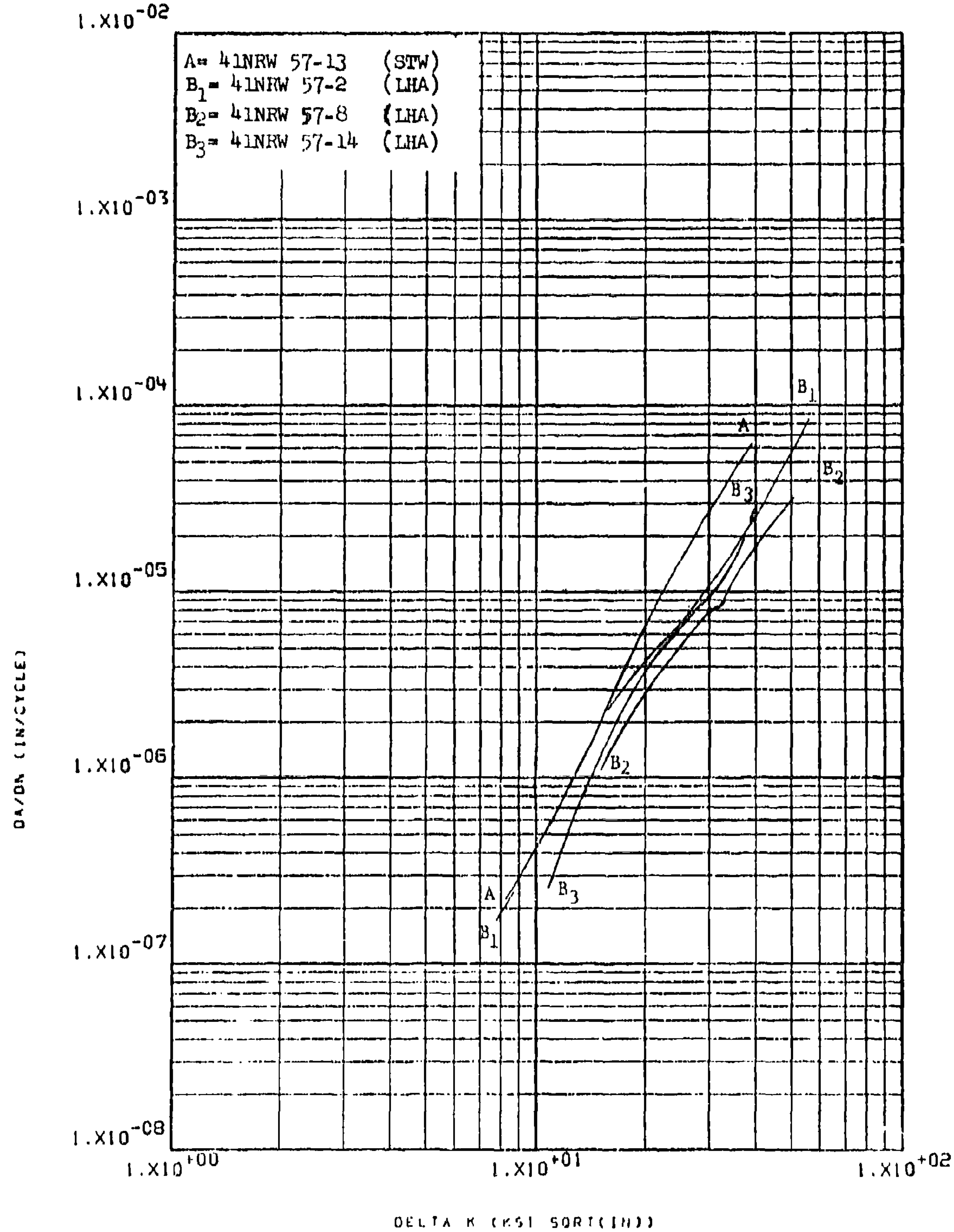

Figure 8.2.11.5-3 Effect of environment on FCGR at R.T., R=0.08, RW direction in 0.5" x 8" PH13-8Mo extrusion

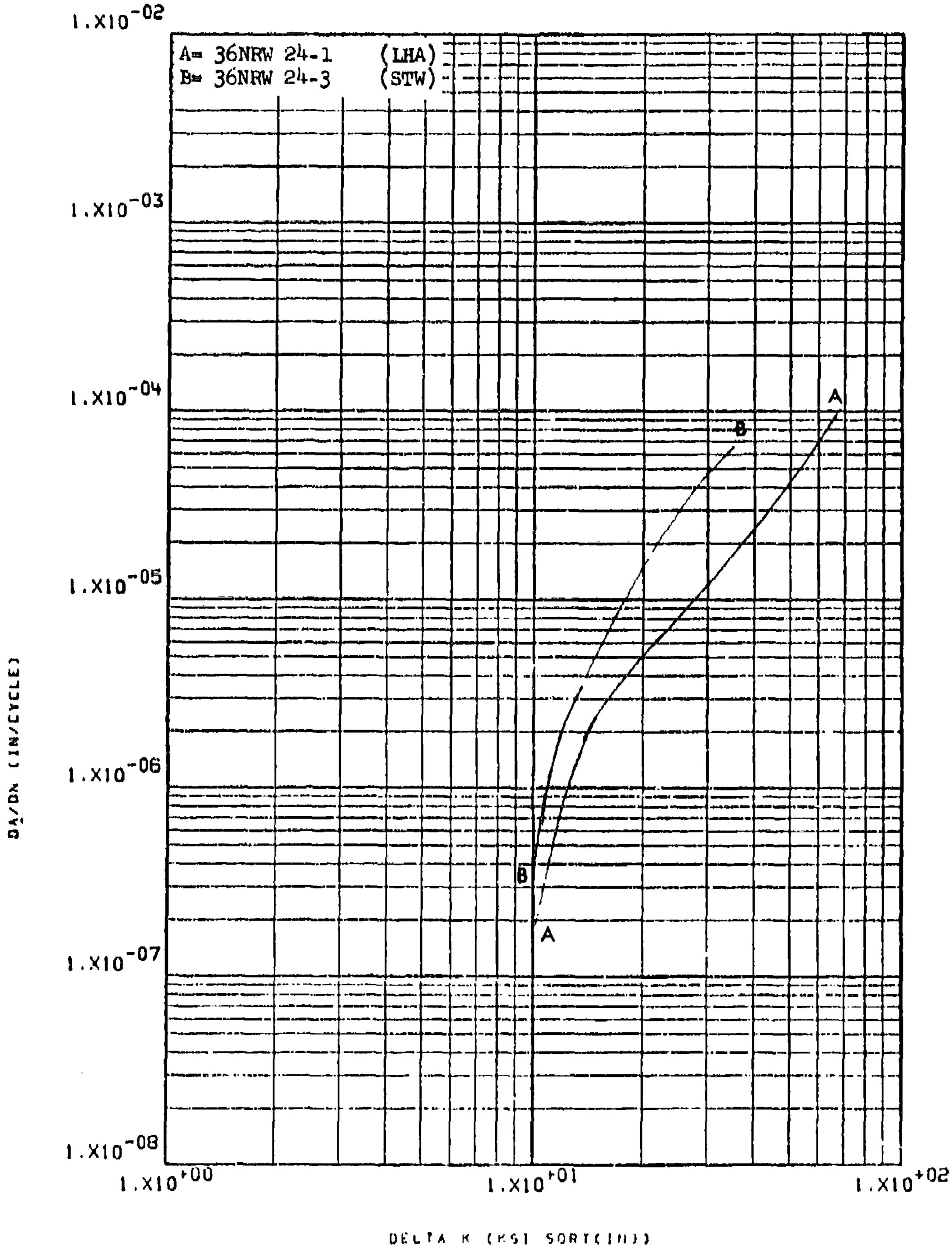

Figure 8.2.11.5-4 Effect of environment of FCGR at R.T., R=0.08, RW direction in 4" x 5" PH-13-8Mo forged bar

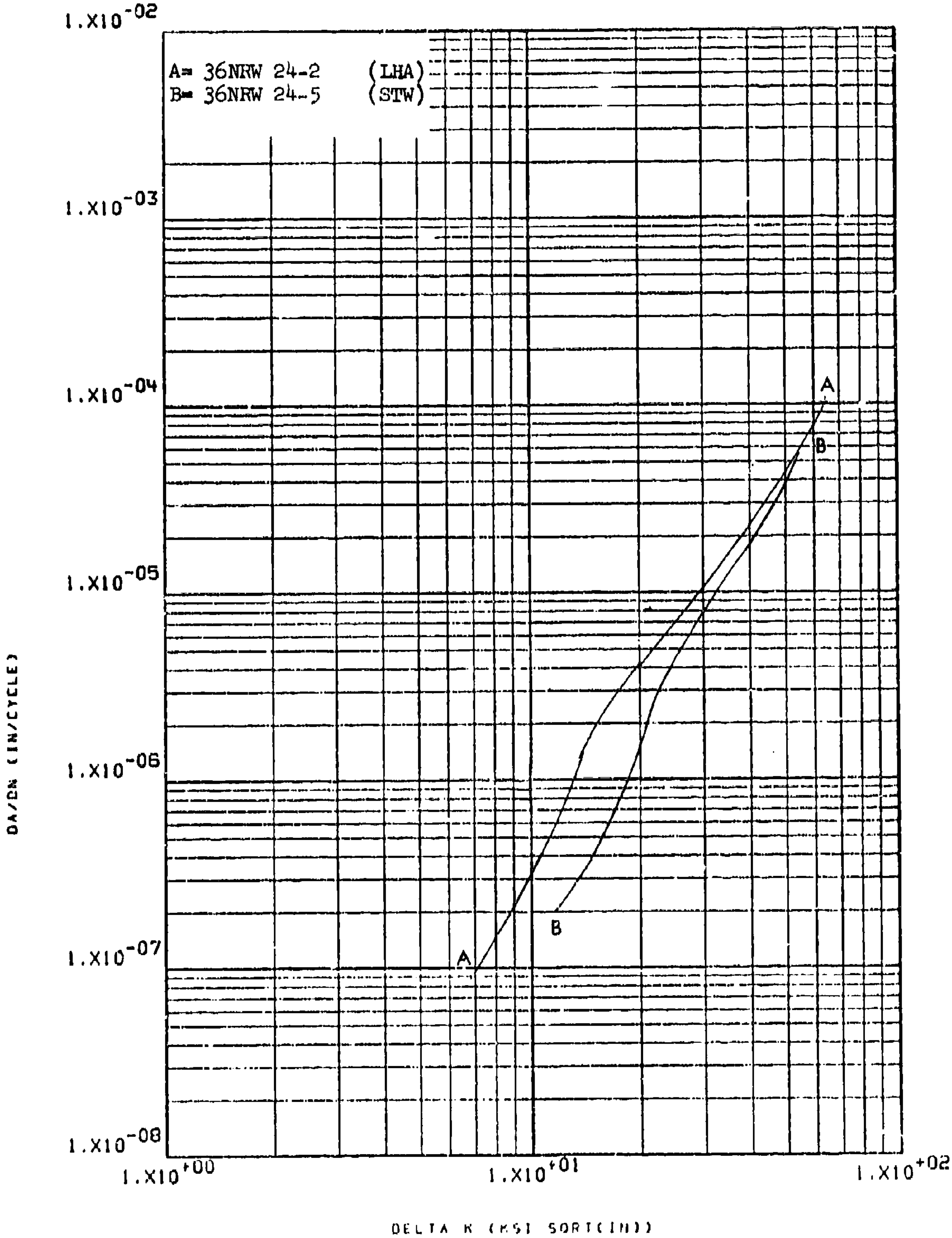

Figure 8.2.11.5-5 Effect of environment on FCGR at R.T., R=0.3, RW direction in 4" x 5" PH13-8Mo forged bar

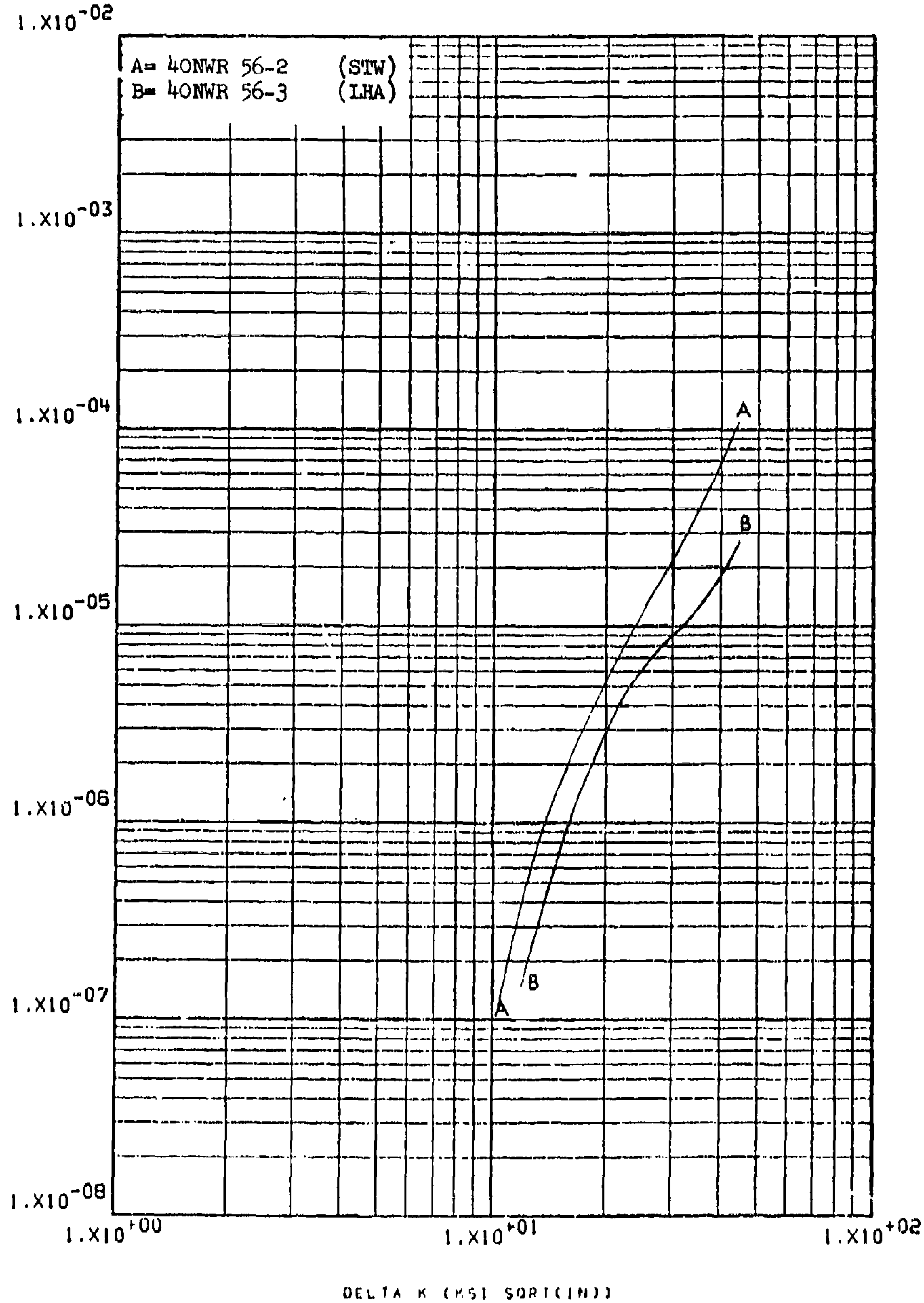

Figure 8.2.11.5-6 Effect of environment on FCGR at R.T., R=0.08, WR direction in 1.5" x 12" PH13-8Mo rolled bar

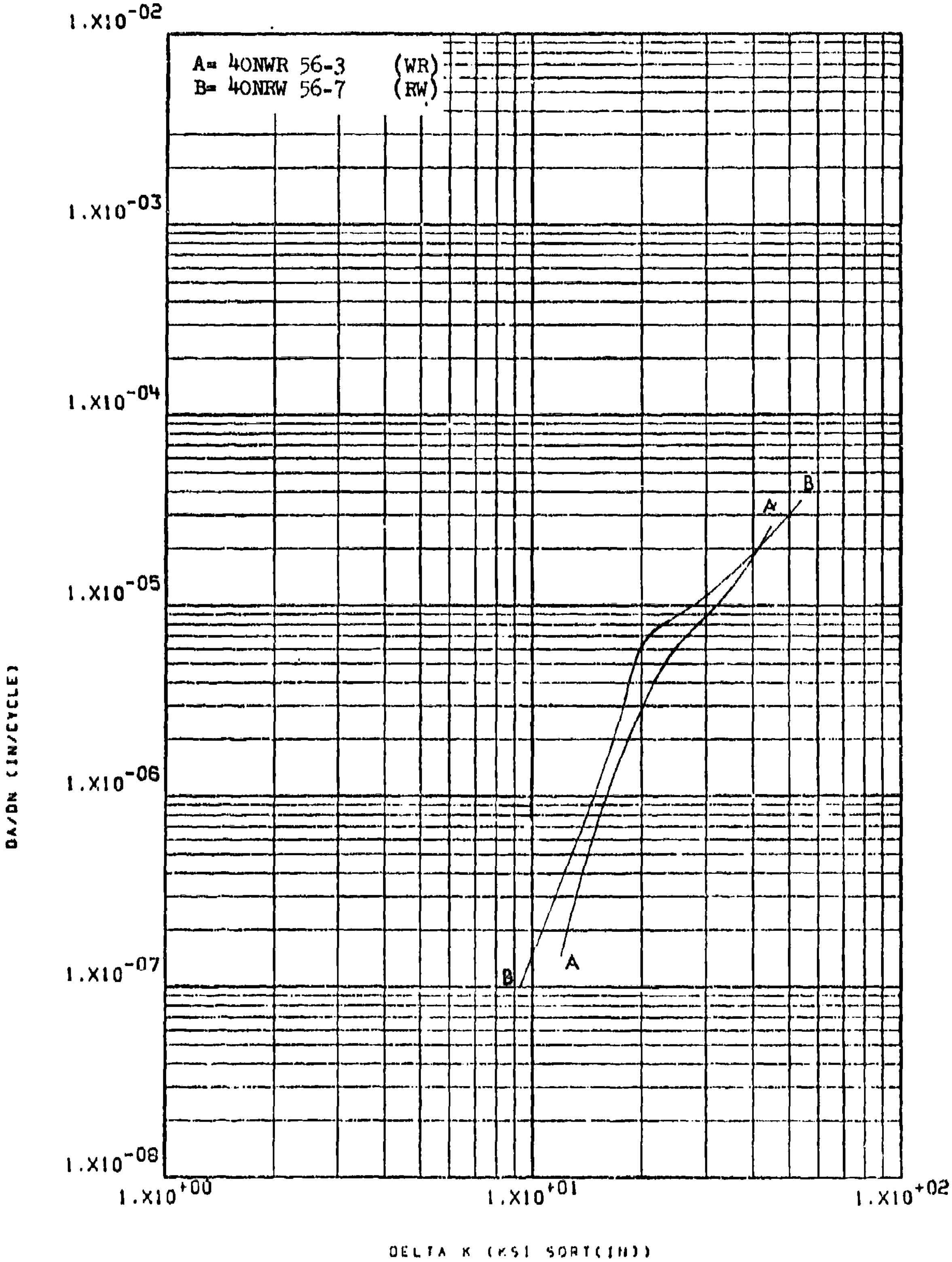

Figure 8.2.11.6-1 Effect of test direction on LHA-FCGR at R.T., R=0.08, 360 cpm in 1.5" x 12" PH13-8Mo rolled bar

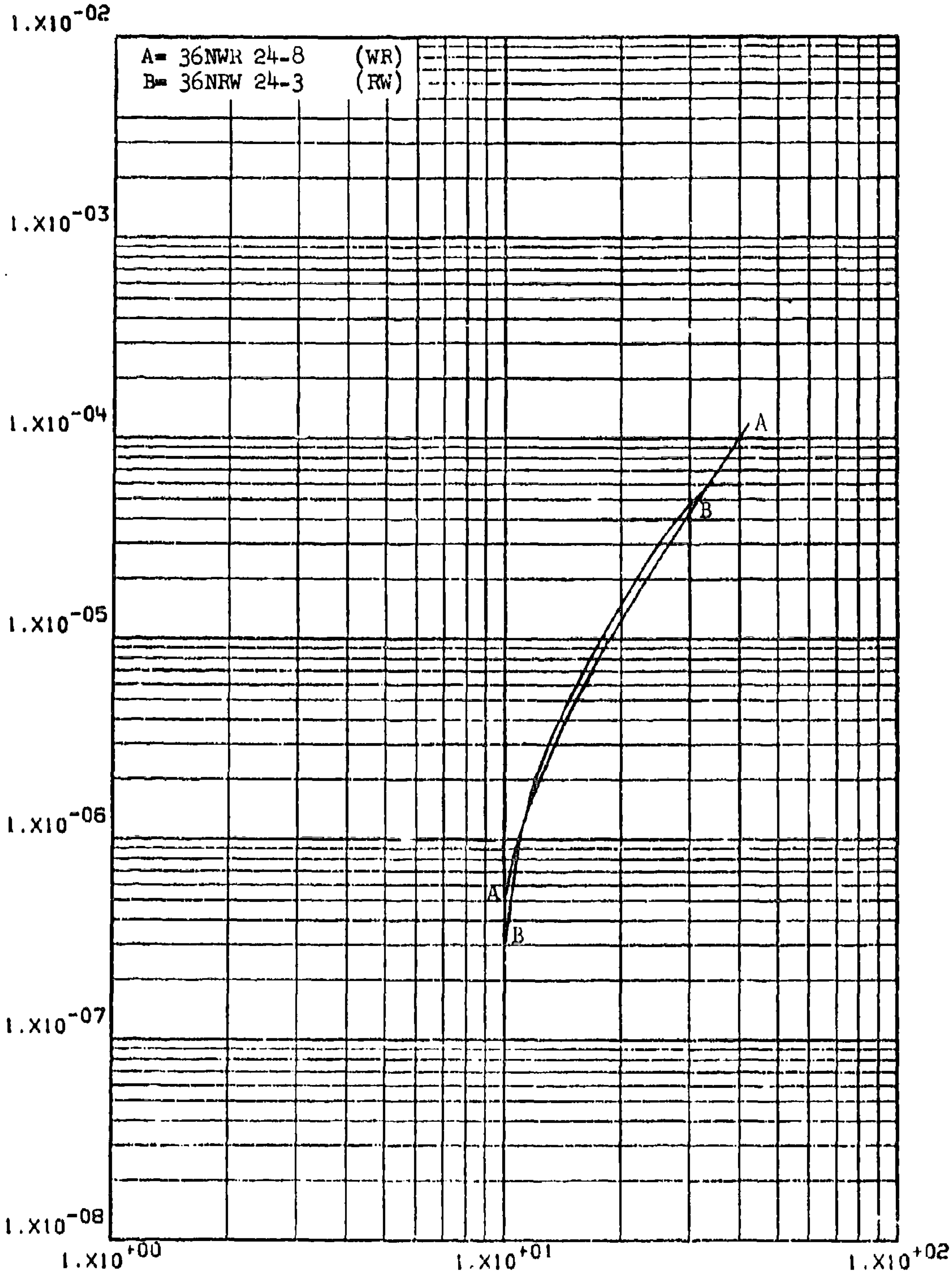

Figure 8.2.11.6-2 Effect of test direction on STW-FCGR at R.T., R=0.08, 60 cpm in 4" x 5" PH13-8Mo forged bar

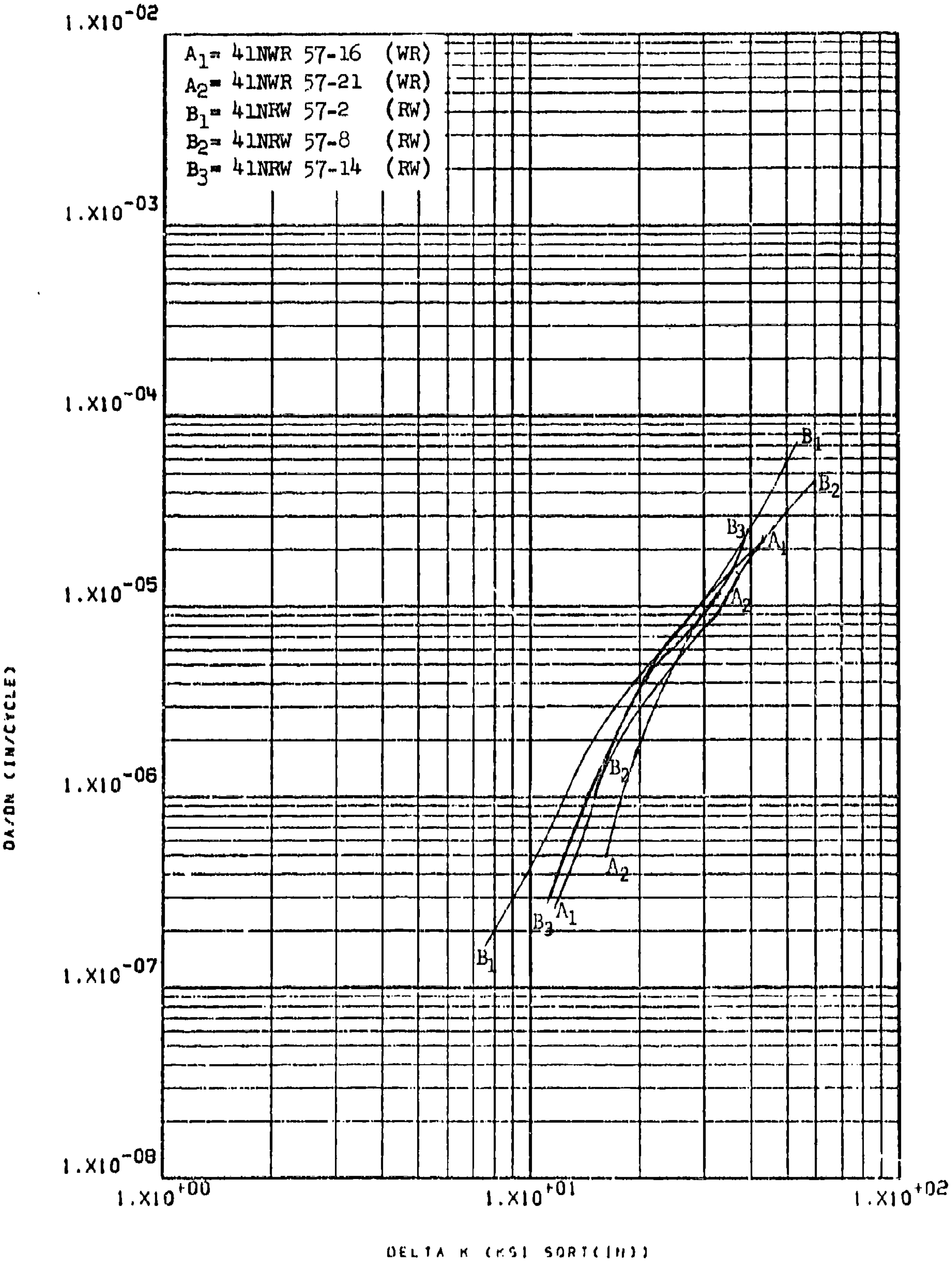

Figure 8.2.11.6-3 Effect of test direction on LHA-FCGR at R.T., R=0.08, 360 cpm in 0.5" x 8" PH13-8Mo extrusion

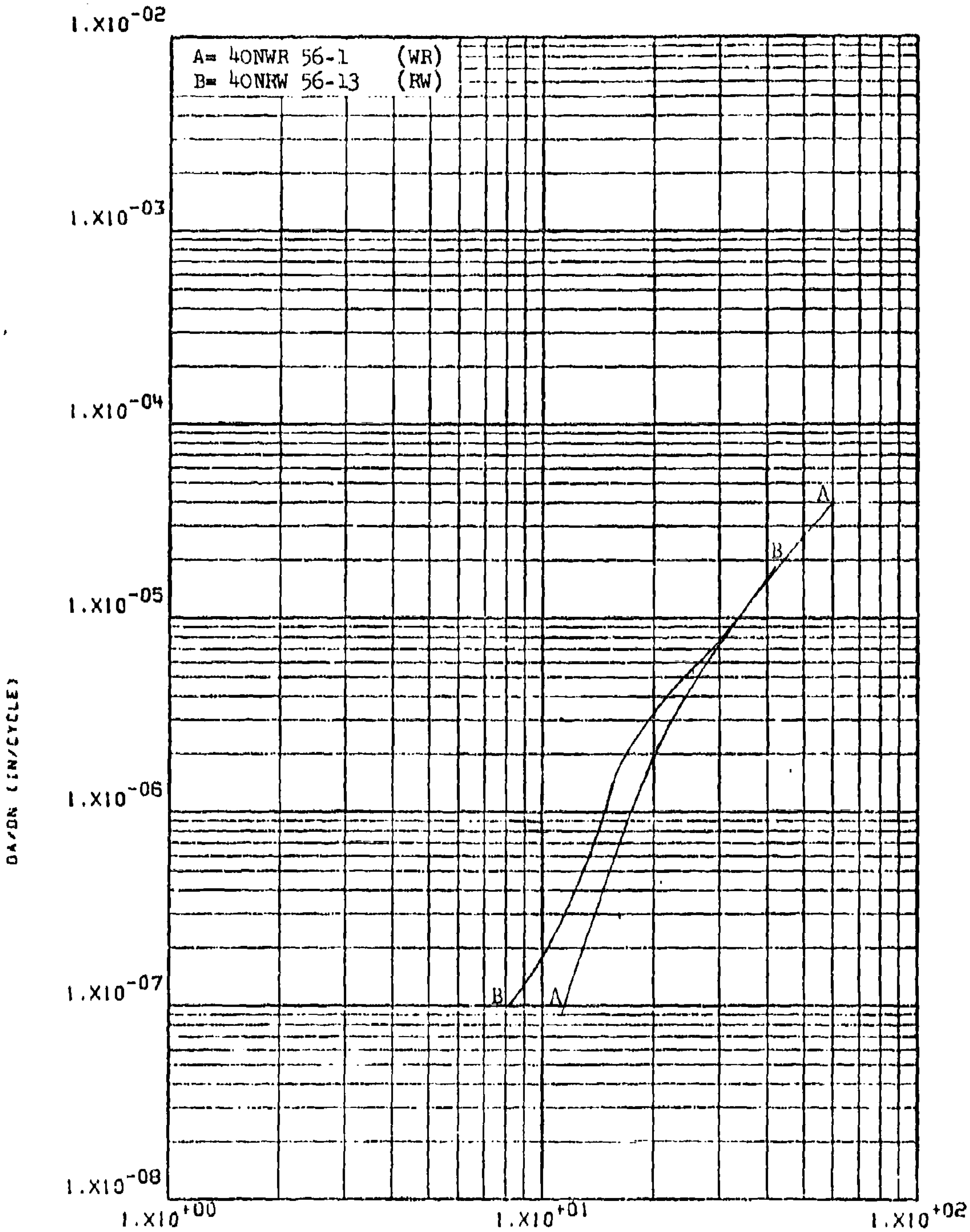

Figure 8.2.11.6-4 Effect of test direction on LHA-FCGR at R.T., R=0.08, 360 cpm in 1/2" thick specimens of 1.5" x 12" PH13-8Mo rolled bar

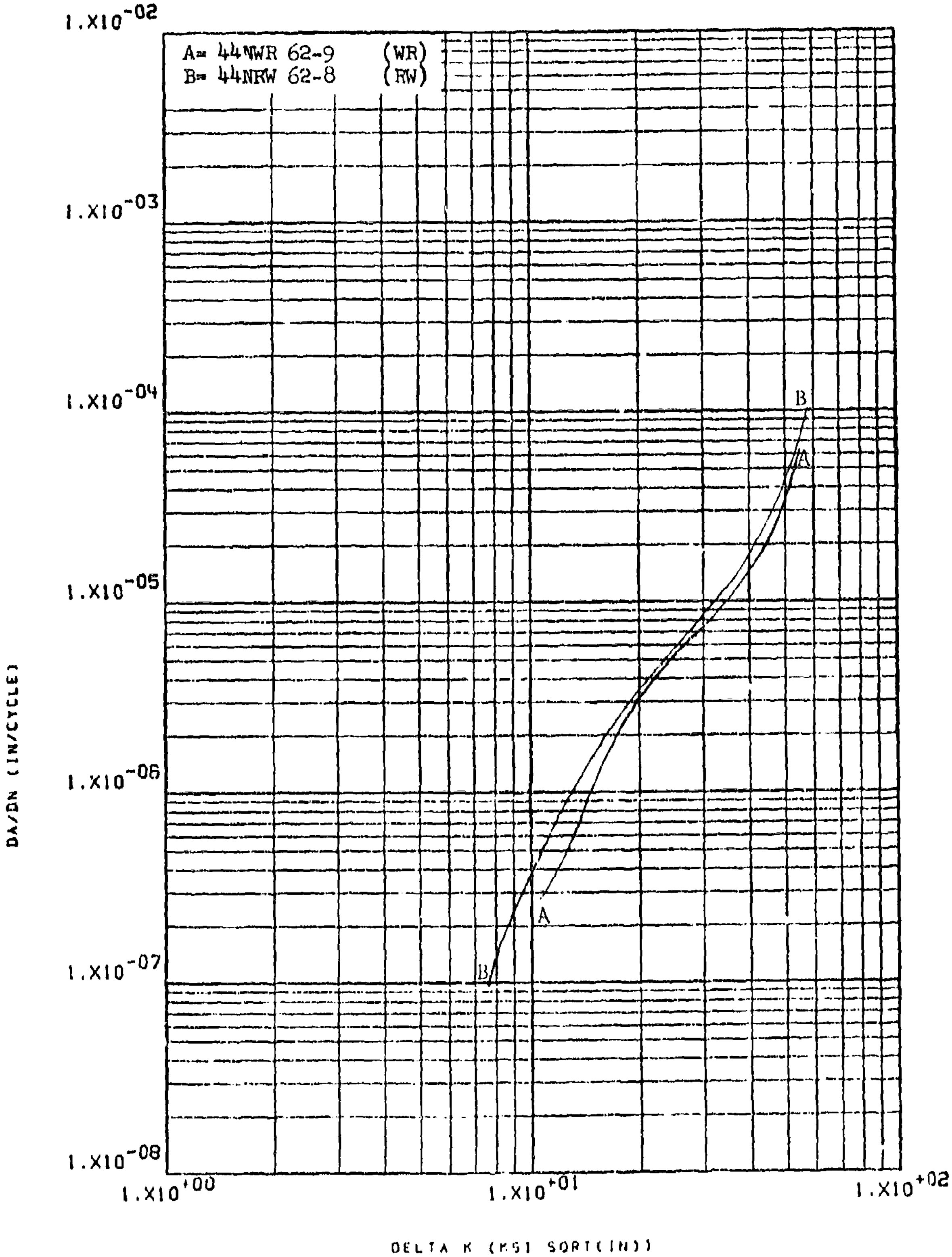

Figure 8.2.11.6-5 Effect of test direction on LHA-FCGR at R.T., R=0.08, 360 cpm in 4" x 24" diameter PH13-8Mo upset forging

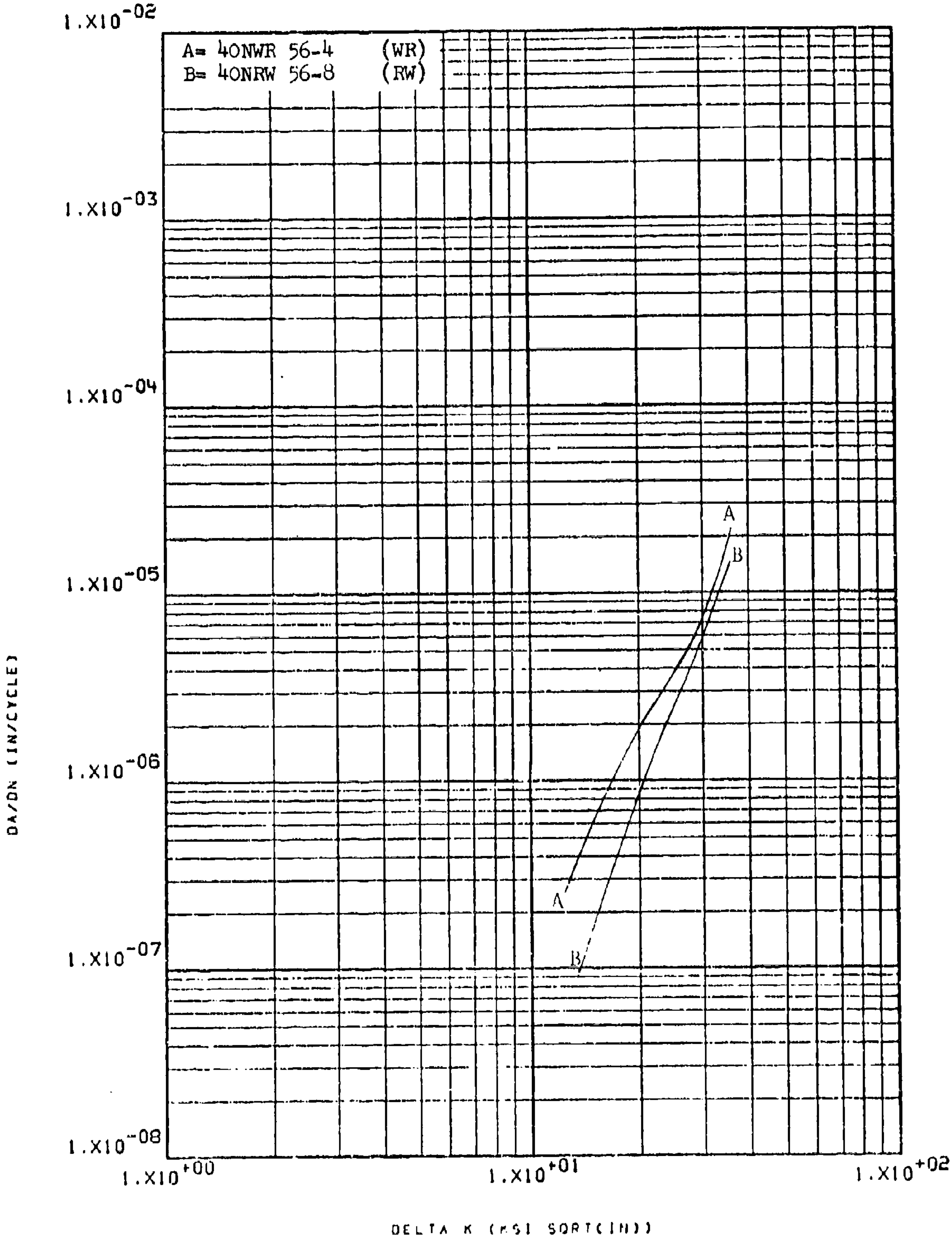

Figure 8.2.11.6-6 Effect of test direction on LHA-FCGR at -65°F, R=0.08, 360 cpm in 1.5" x 12" PH13-8Mo rolled bar

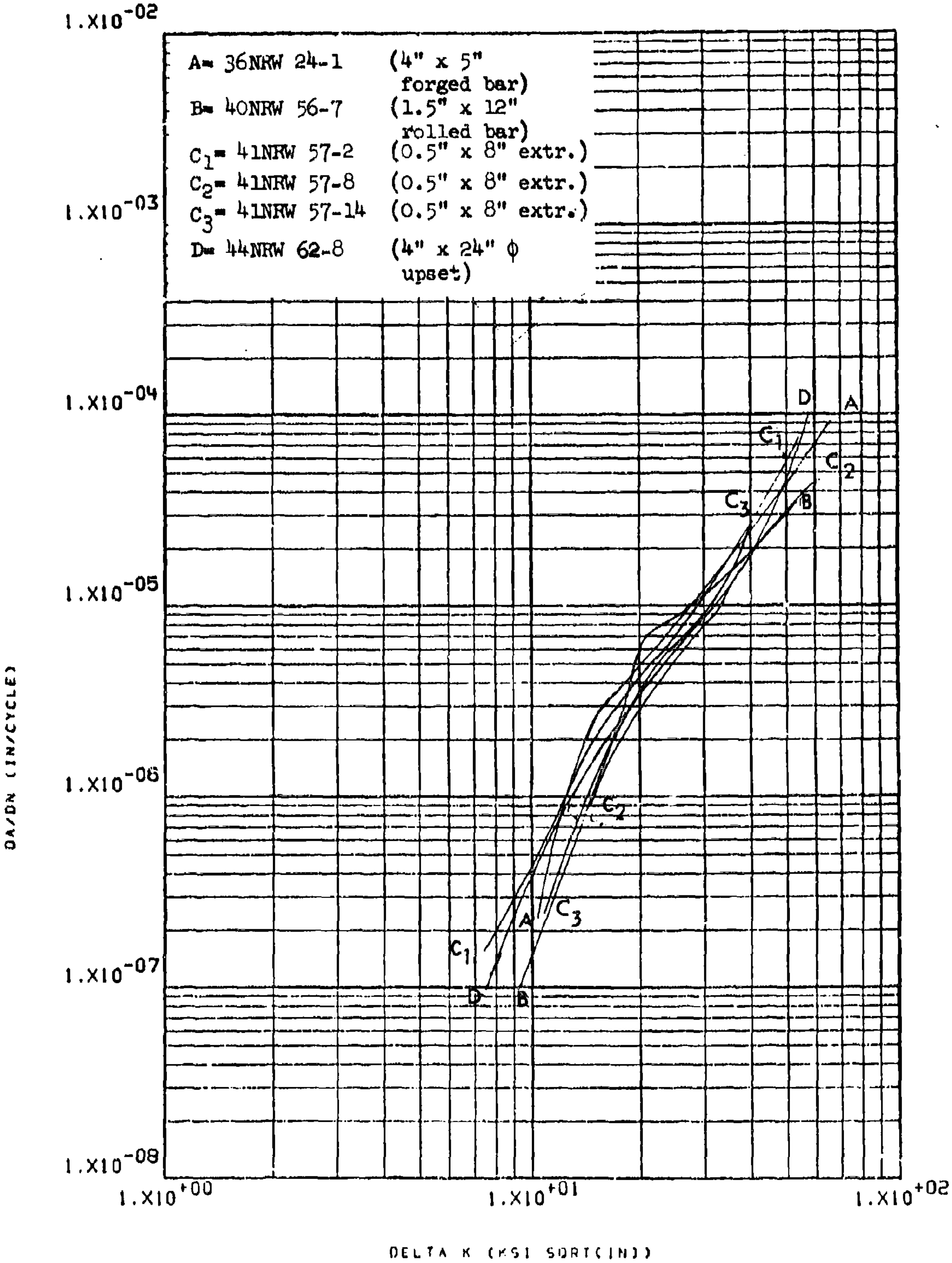

Figure 8.2.11.7-1 **Effect of product form on LHA-FCGR at R.T., R=0.08, 360 cpm, RW direction in PH13-8Mo.**

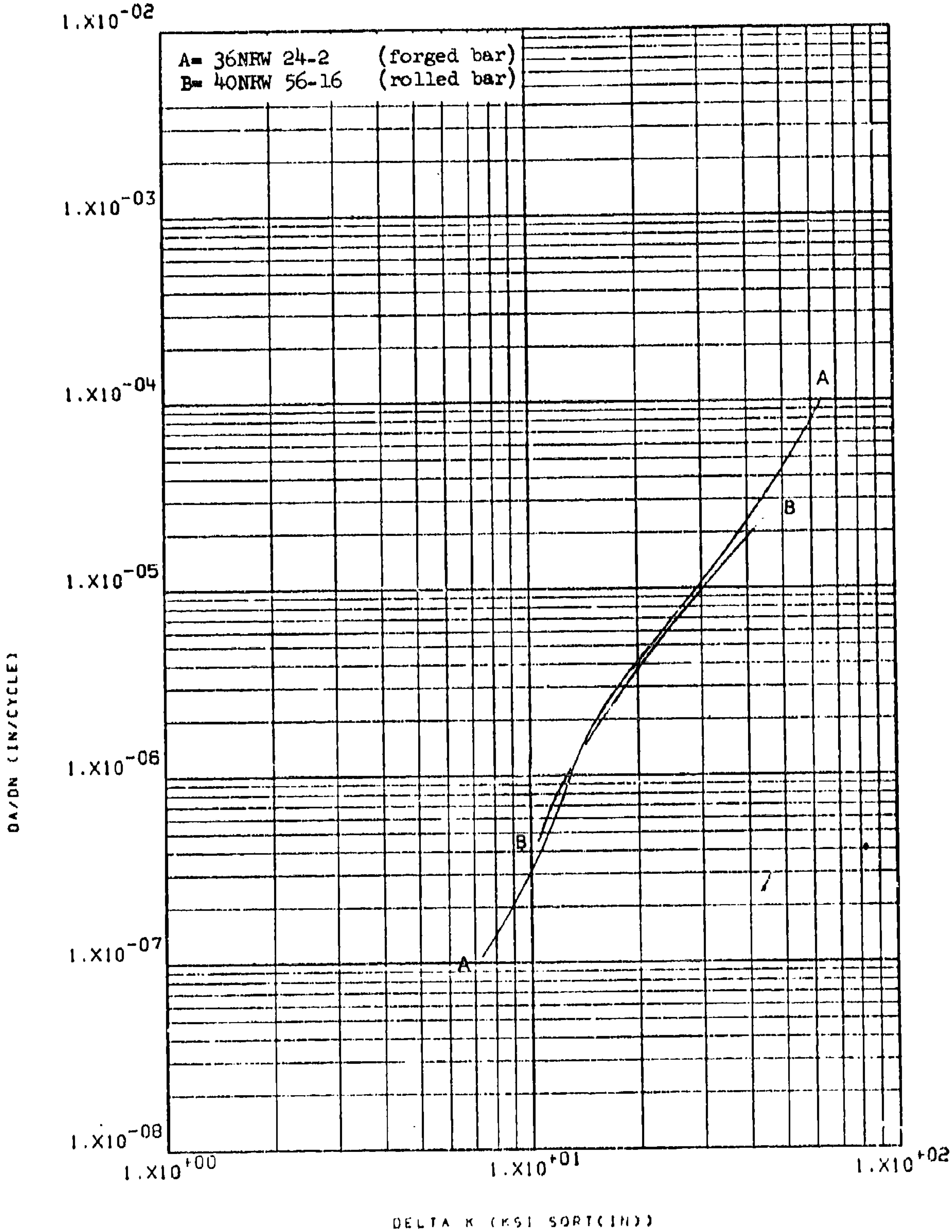

Figure 8.2.11.7-2 Effect of product form on LHA-FCGR at R.T., R=0.3, 360 cpm, RW direction in PH13-8Mo

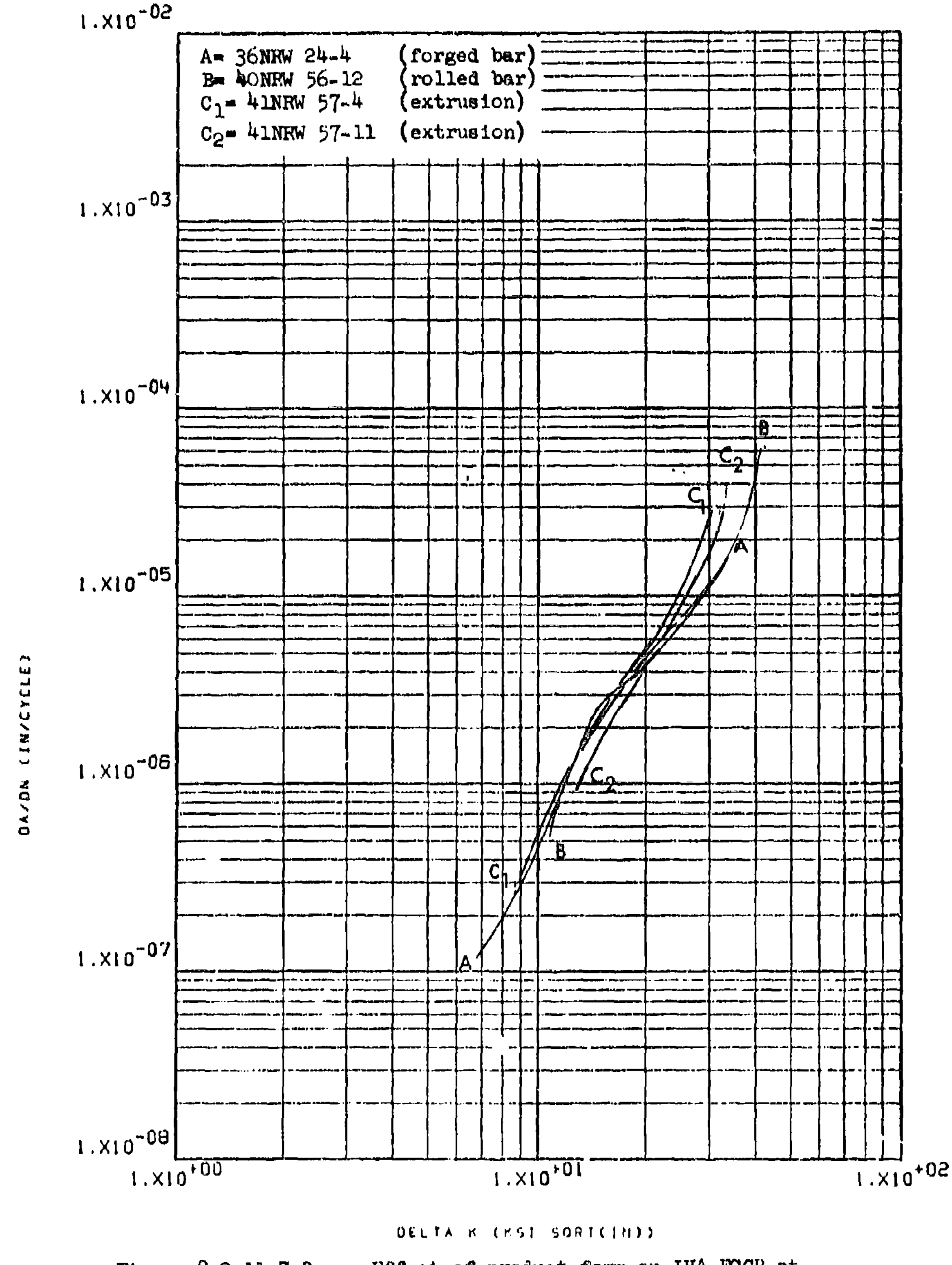

Figure 8.2.11.7-3 Effect of product form on LHA-FCGR at R.T., R=0.5, 360 cpm, RW direction in PH13-8Mo

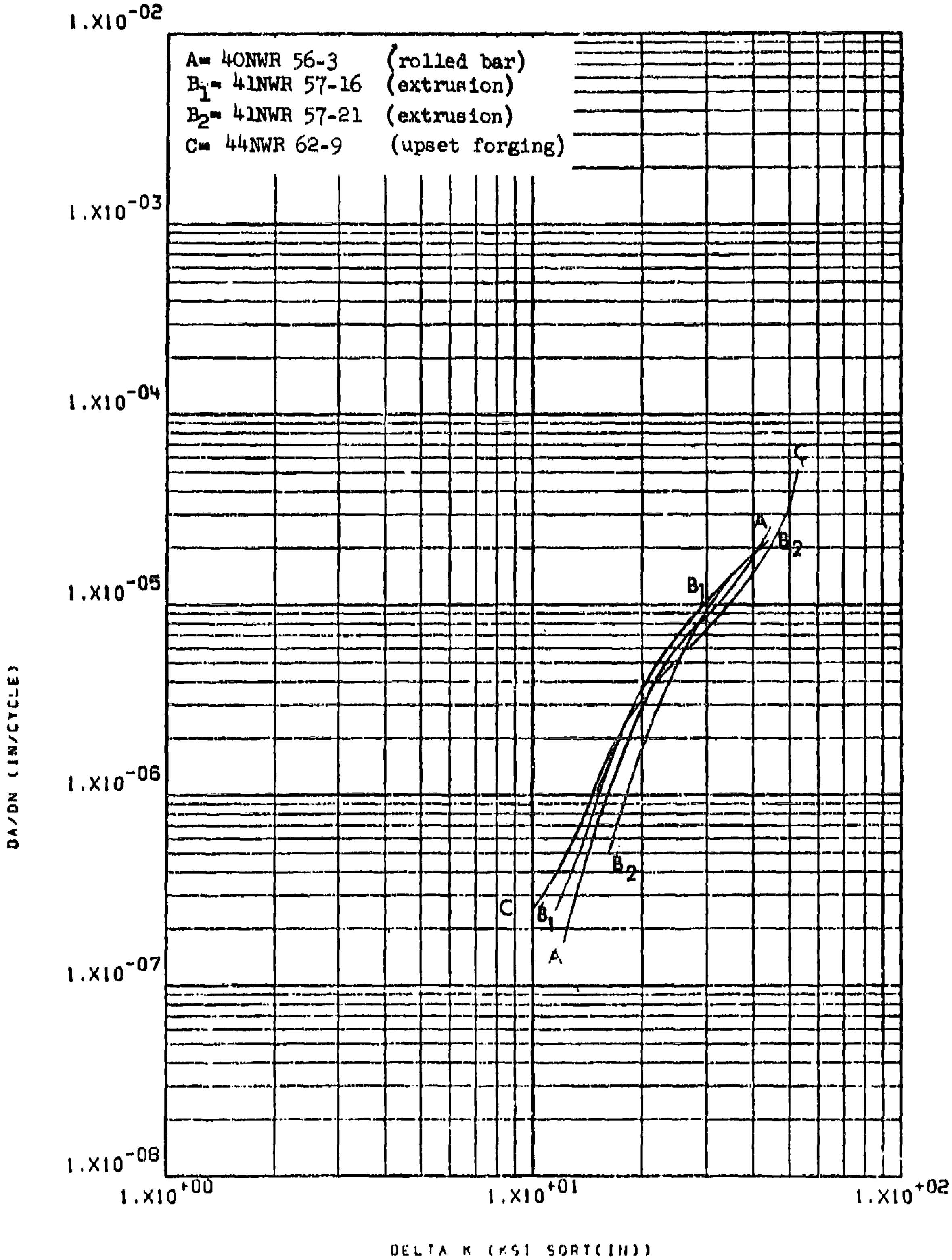

Figure 8.2.11.7-4 Effect of product form on LHA-FCGR at R.T., R=0.08, 360 cpm, WR direction in PH13-8Mo

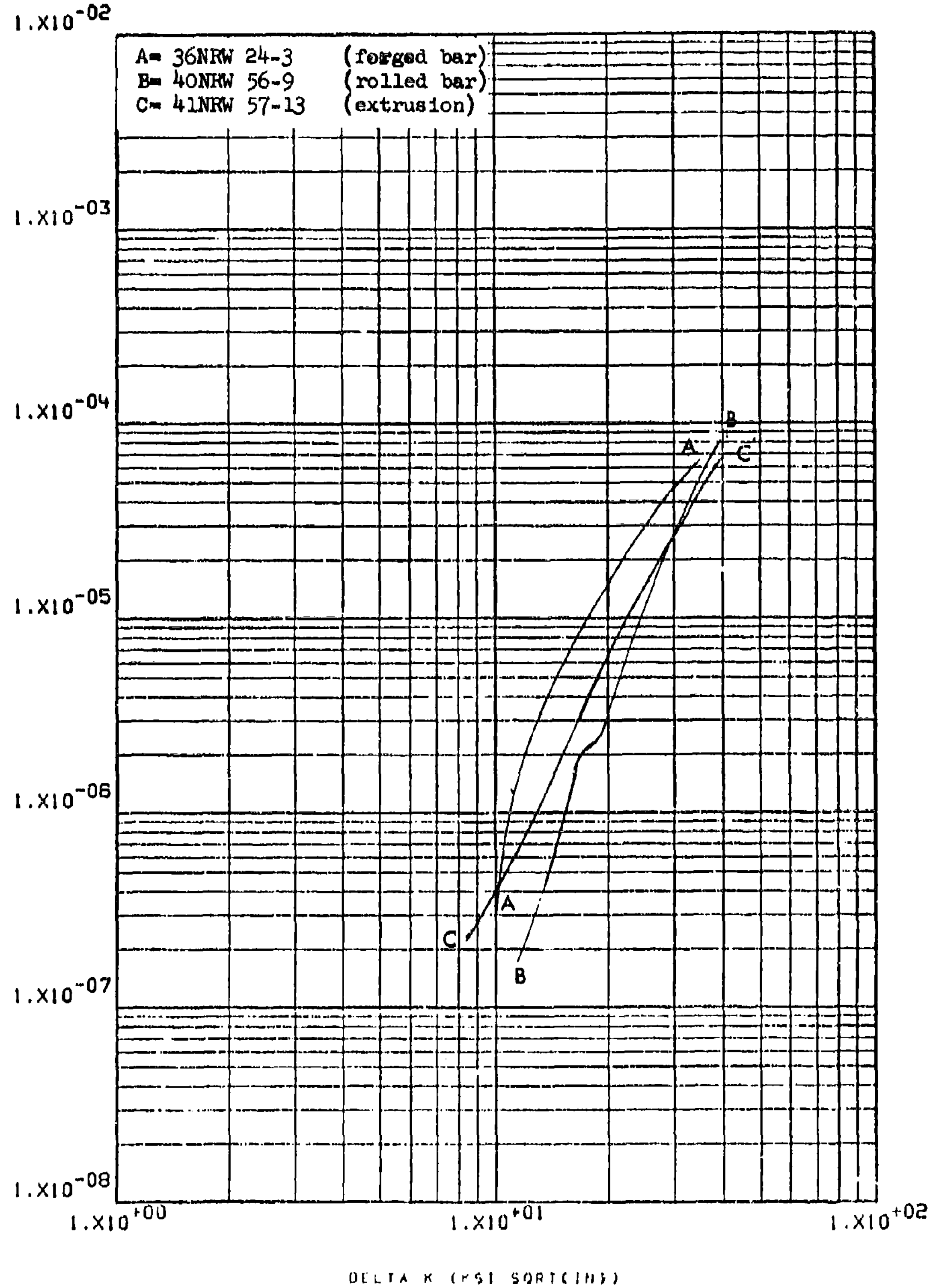

Figure 8.2.11.7-5 Effect of product form on STW-FCGR at R.T., R=0.08, 60 cpm, RW direction in PH13-8Mo

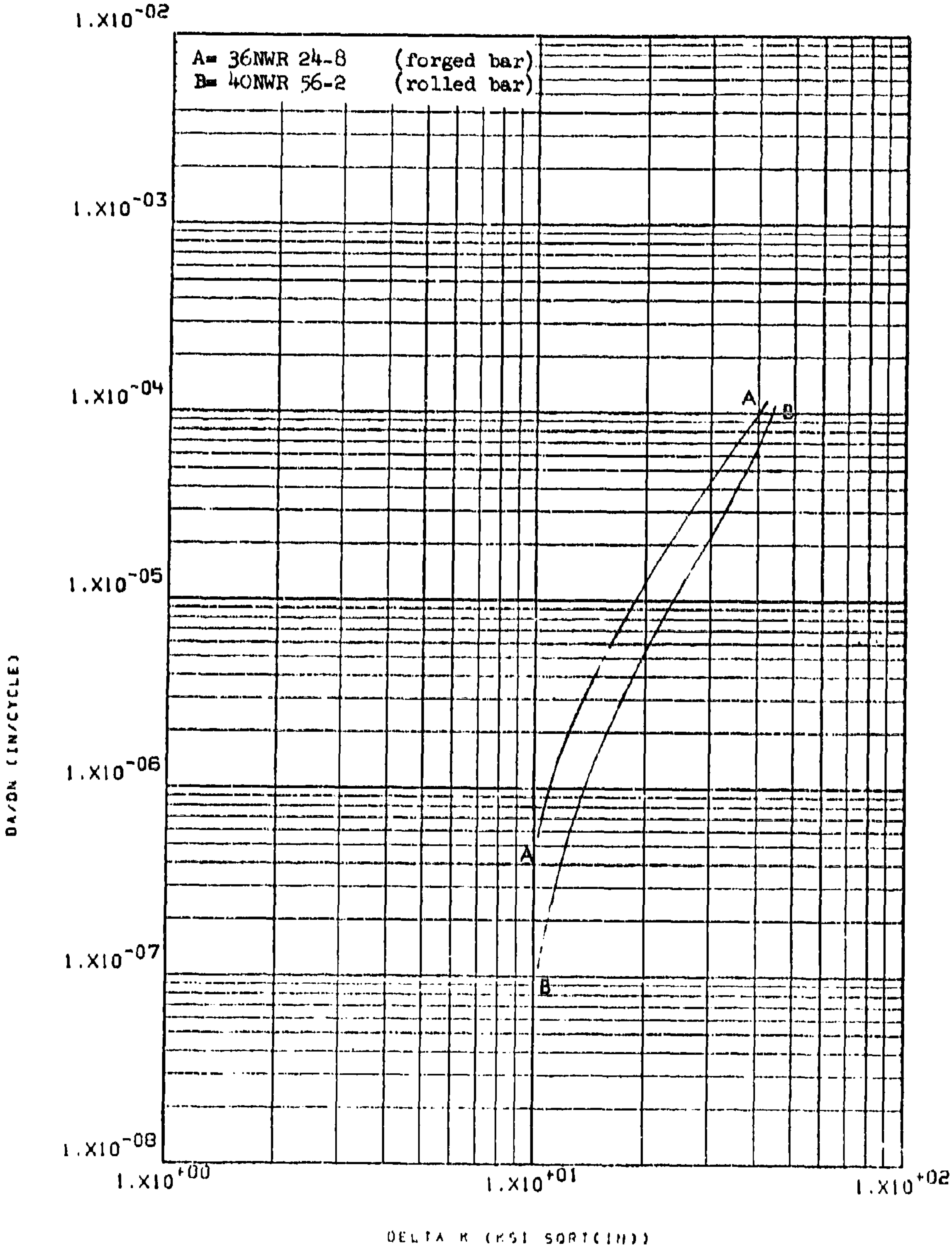

Figure 8.2.11.7-6 Effect of product form on STW-FCGR at R.T., R=0.08, 60 cpm, WR direction in PH13-8Mo

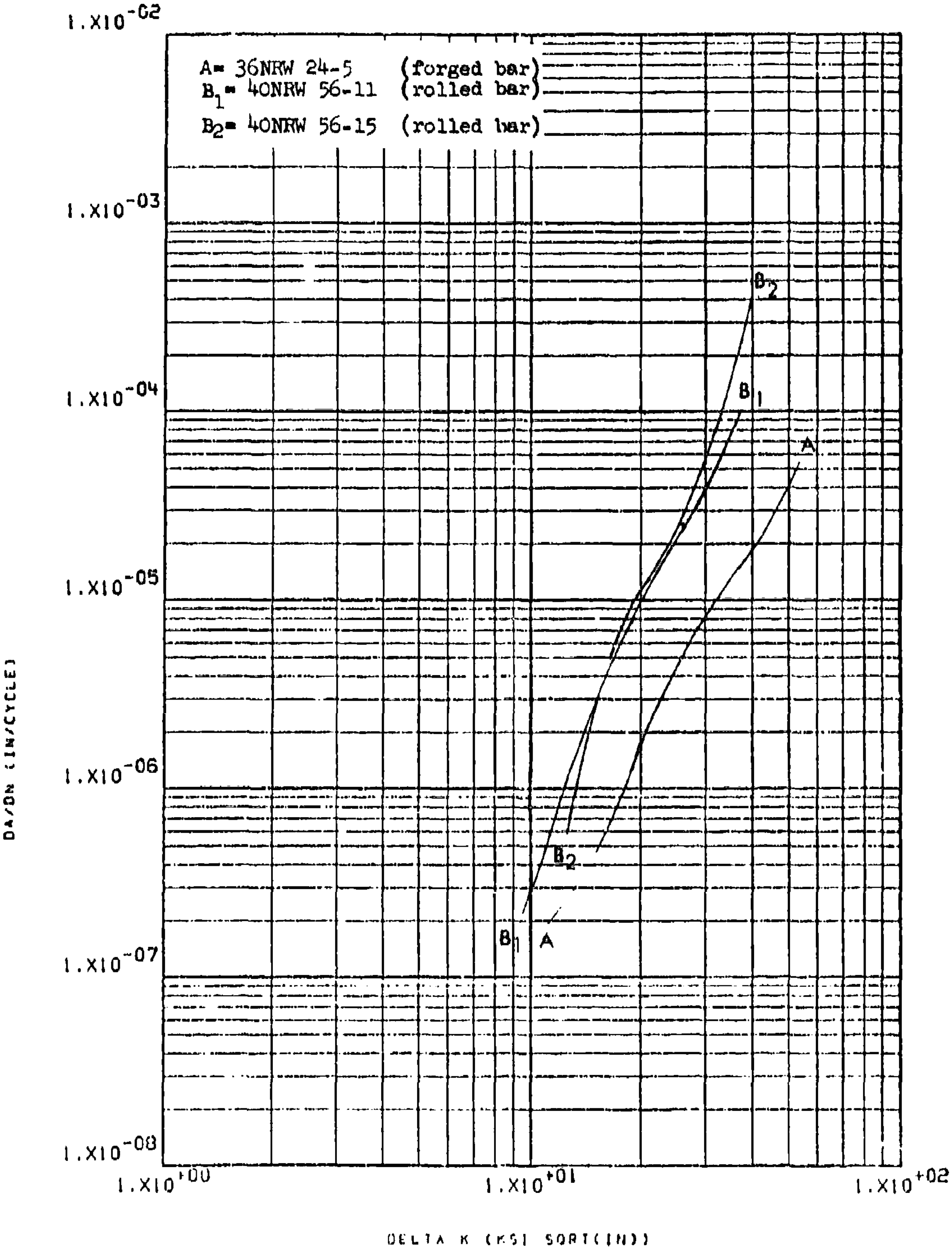

Figure 8.2.11.7-7 Effect of product form on STW-FCGR at R.T., R=0.3, 60 cpm, RW direction in PH13-8Mo

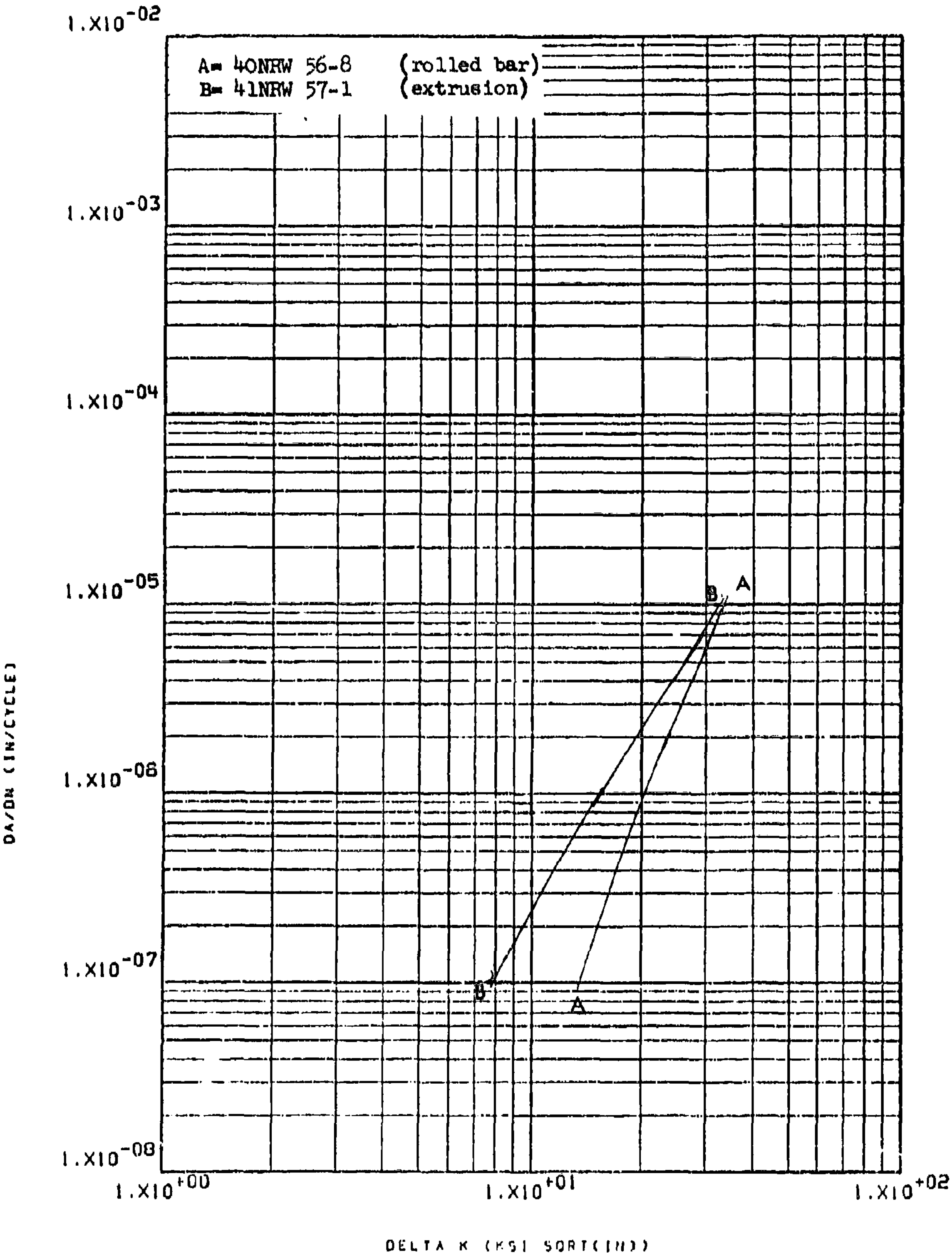

Figure 8.2.11.7-8 Effect of product form on LHA-FCGR at -65°F, R=0.08, 360 cpm, RW direction in PH13-8Mo

8.2.12 300M Steel

8.2.12.1 Cyclic Rate - Increasing the cyclic frequency of tests from 60 to 360 cpm did not significantly alter the crack growth rate characteristics of this material in low humidity air at room temperature (Figure 8.2.12.1-1).

8.2.12.2 Test Temperature - Slight increases in growth rates were observed in this material when the test temperature was increased from -65°F to ambient at low levels of delta K in both the RW and TR directions (Figures 8.2.12.2-1 and -2). This effect became less pronounced as delta K was increased until at approximately 30 ksi $\sqrt{in}$ the rates were essentially equivalent at both temperatures.

8.2.12.3 Specimen Thickness - Not evaluated.

8.2.12.4 R Factor - At low values of delta K (~10 ksi $\sqrt{in}$) the crack growth rates of this material were seen to be approximately equal when tested at R=0.08, 0.3 and 0.5 in low humidity air (Figure 8.2.12.4-1). As delta K was increased, however, crack growth rates were seen to increase with increasing values of R. In sump tank water, similar increases in rates with increasing values of R were apparent throughout the range of delta K (Figure 8.2.12.4-2). Of particular interest in the sump tank water test results was the relatively large amount of test-to-test scatter encountered.

8.2.12.5 Environment - Despite the large amount of data scatter incurred in testing, the growth rates of this material were seen to be clearly greater in sump tank water than in low humidity air. This effect was seen to be true in the RW direction at R factors of 0.08, 0.3, and 0.5 (Figures 8.2.12.5-1 through -3) and at an R factor of 0.08 in the WR and TR directions (Figures 8.2.12.5-4 and -5).

8.2.12.6 Test Direction - Crack growth rates were seen to be essentially equivalent in all three directions (RW, WR, and TR) in low humidity air and sump tank water (Figures 8.2.12.6-1 and -2).

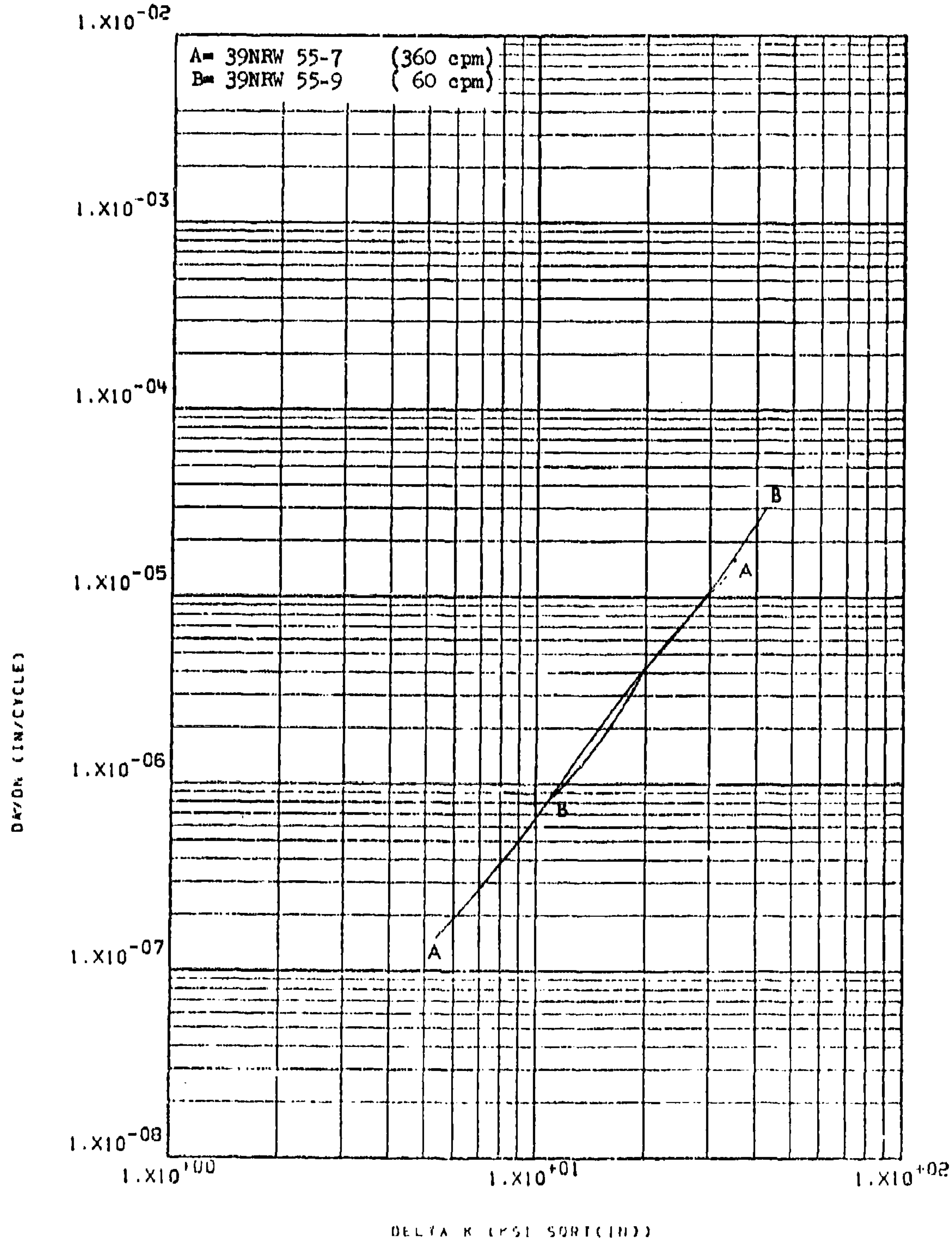

Figure 8.2.12.1-1 Effect of cyclic frequency on LHA-FCGR at R.T., R=0.08, RW direction in 3" x 36" x 72" 300M forged block

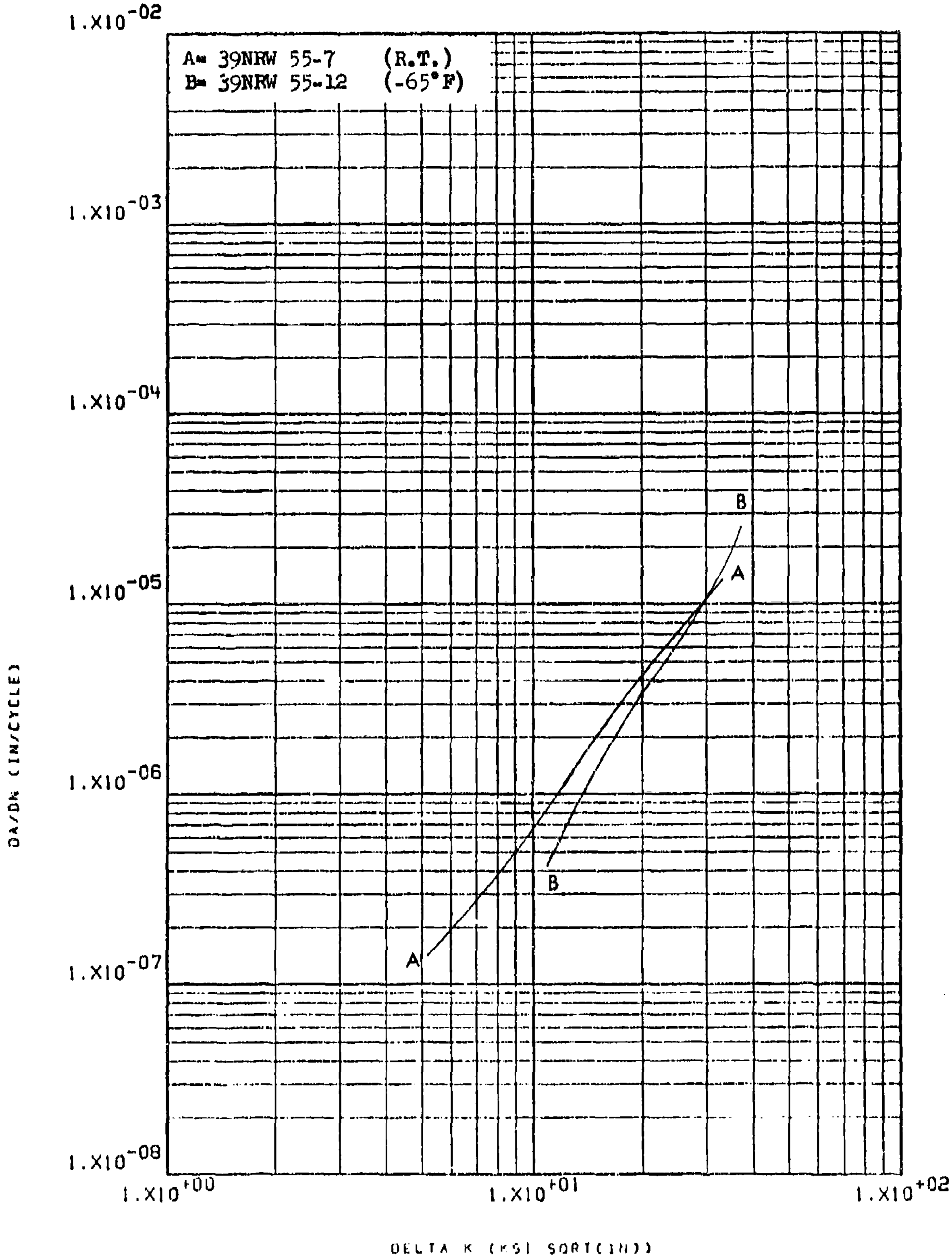

Figure 8.2.12.2-1 Effect of test temperature on LHA-FCGR at R=0.08, 360 cpm, RW direction in 3" x 36" x 72" 300M forged block

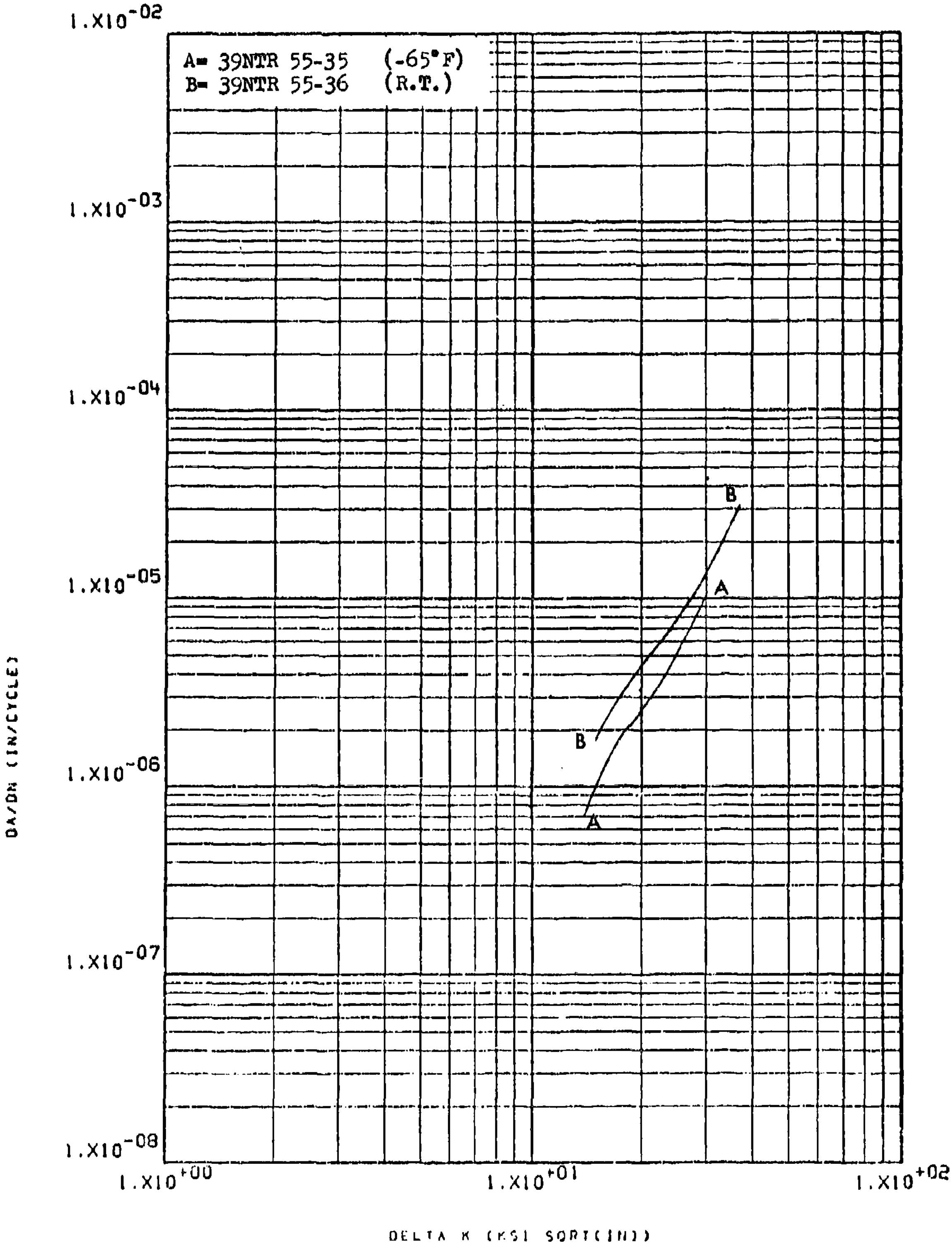

Figure 8.2.12.2-2 Effect of test temperature on LHA-FCGR at R=0.08, 360 cpm, TR direction in 3" x 36" x 72" 300M forged block

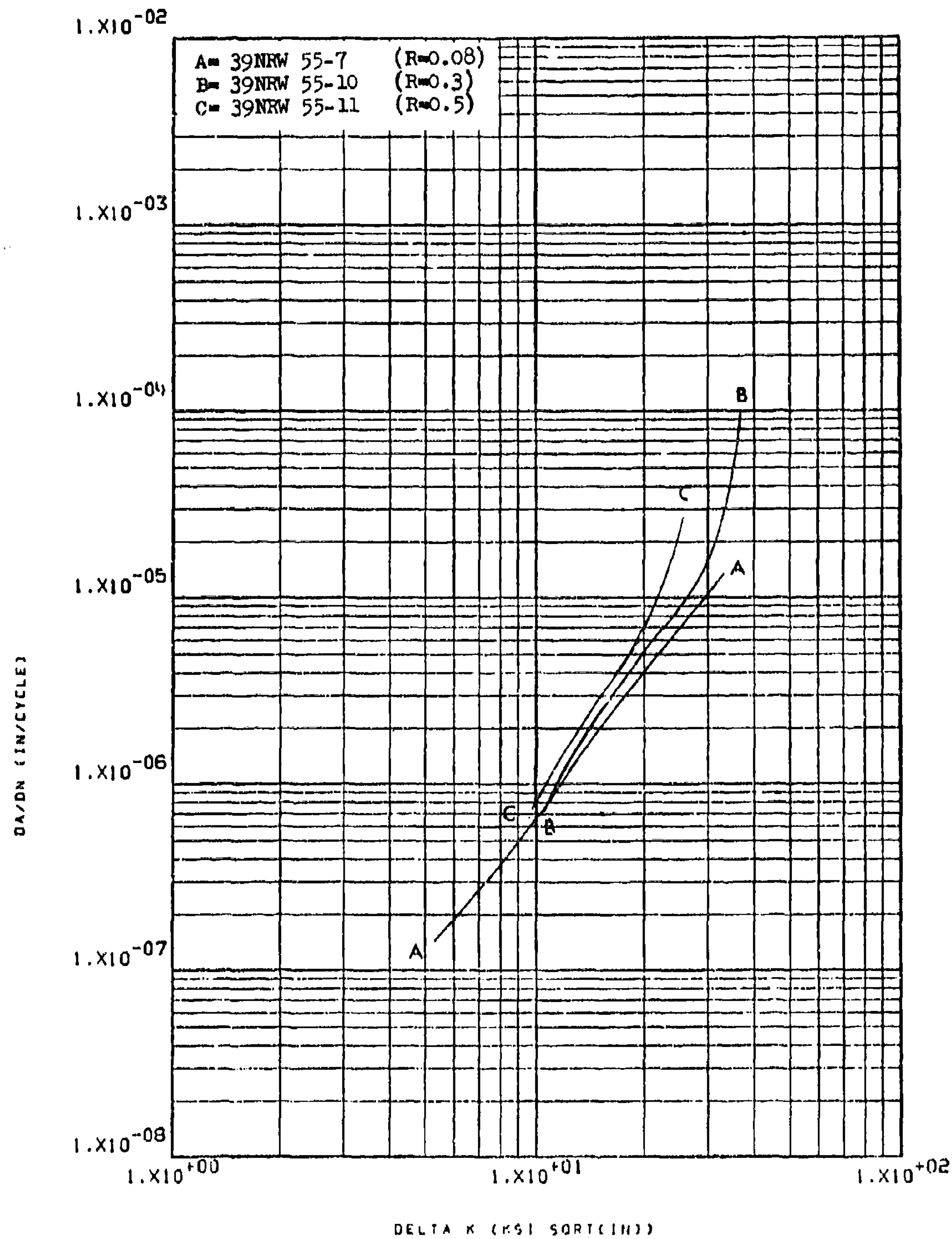

Figure 8.2.12.4-1 Effect of R factor on LHA-FCGR at R.T., 360 cpm, RW direction in 3" x 36" x 72" 300M forged block

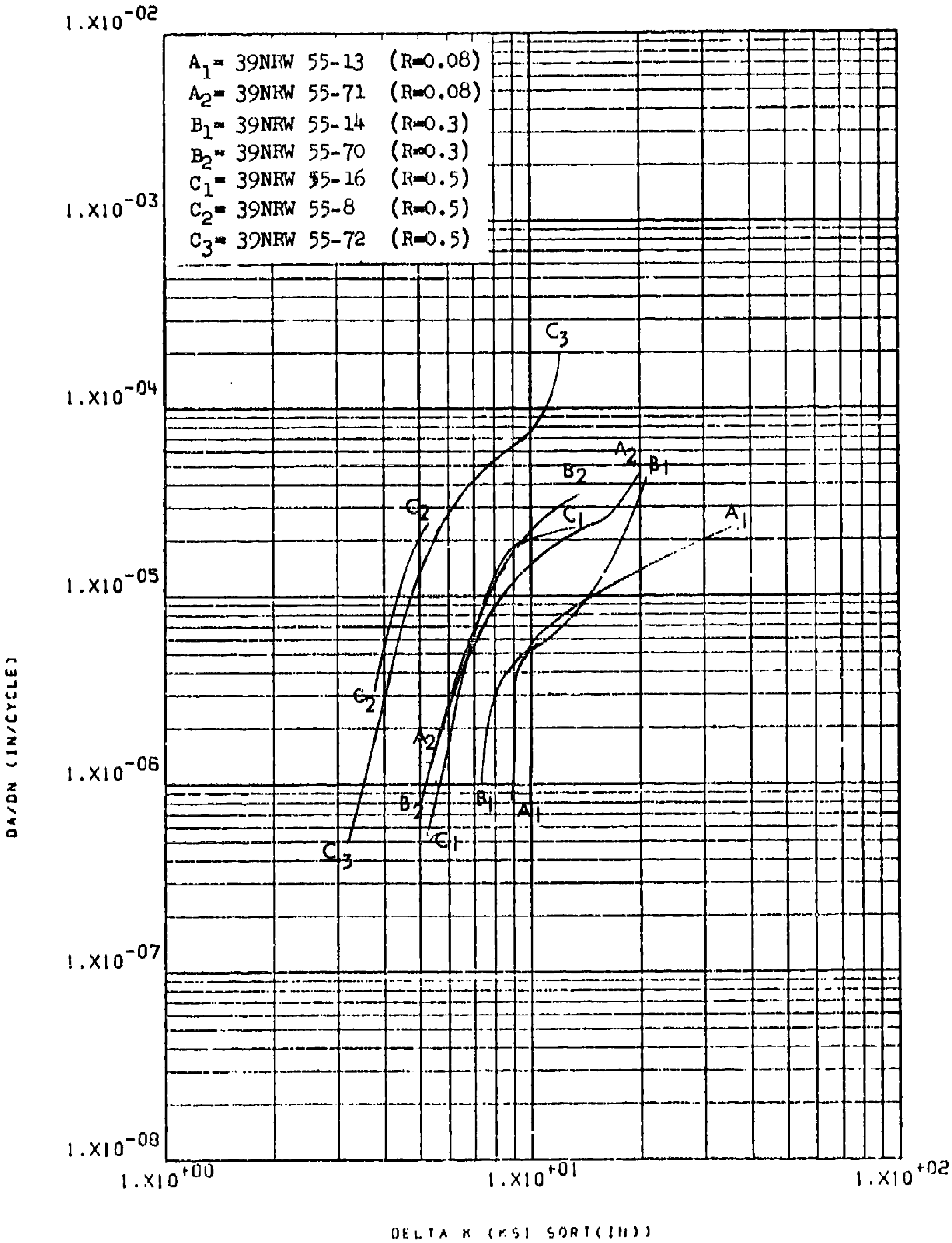

Figure 8.2.12.4-2 Effect of R factor on STW-FCGR at R.T., 60 cpm, RW direction in 3" x 36" x 72" 300M forged block

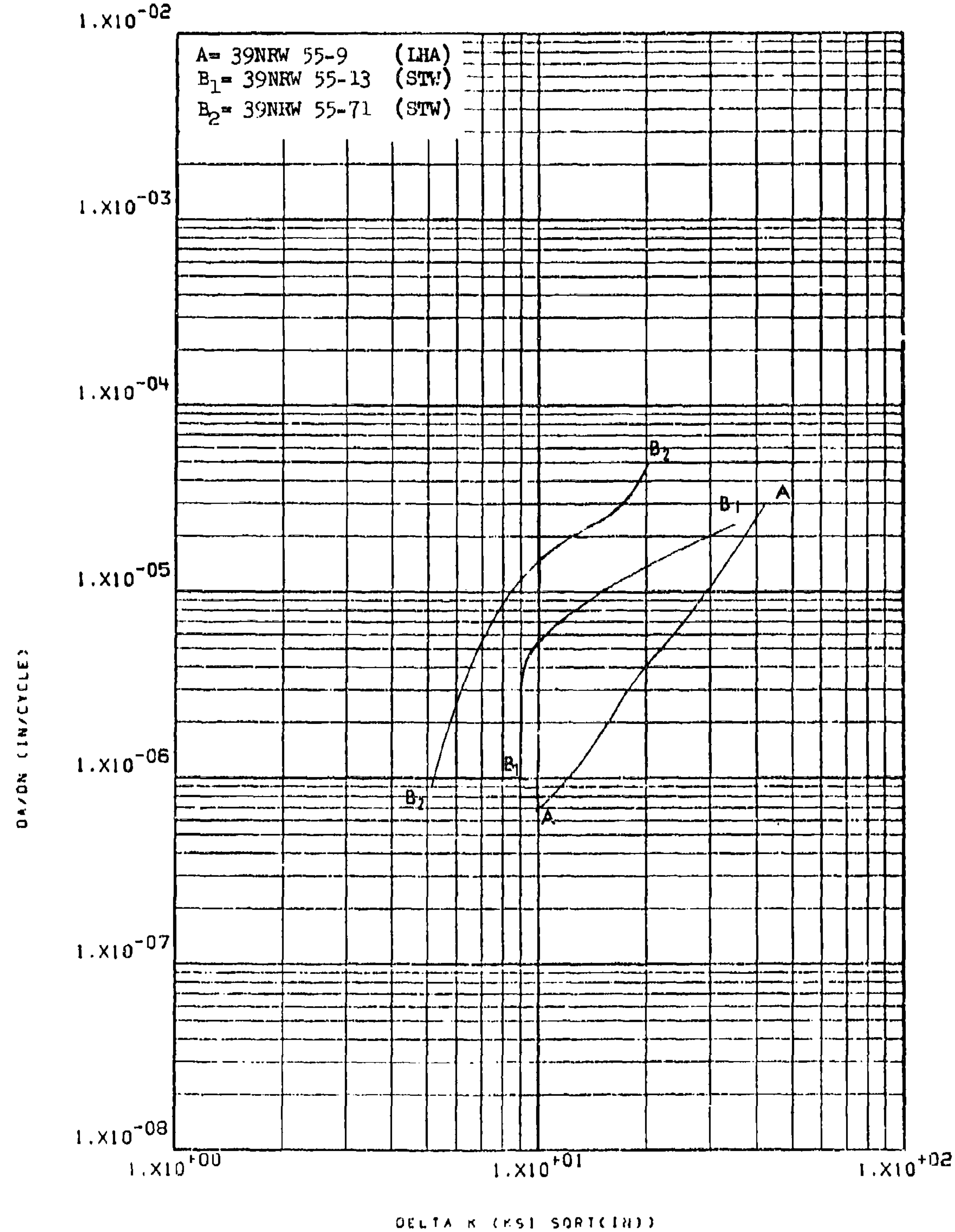

Figure 8.2.12.5-1 Effect of environment on FCGR at R.T., R=0.08, 60 cpm, RW direction in 3" x 36" x 72" 300M forged block

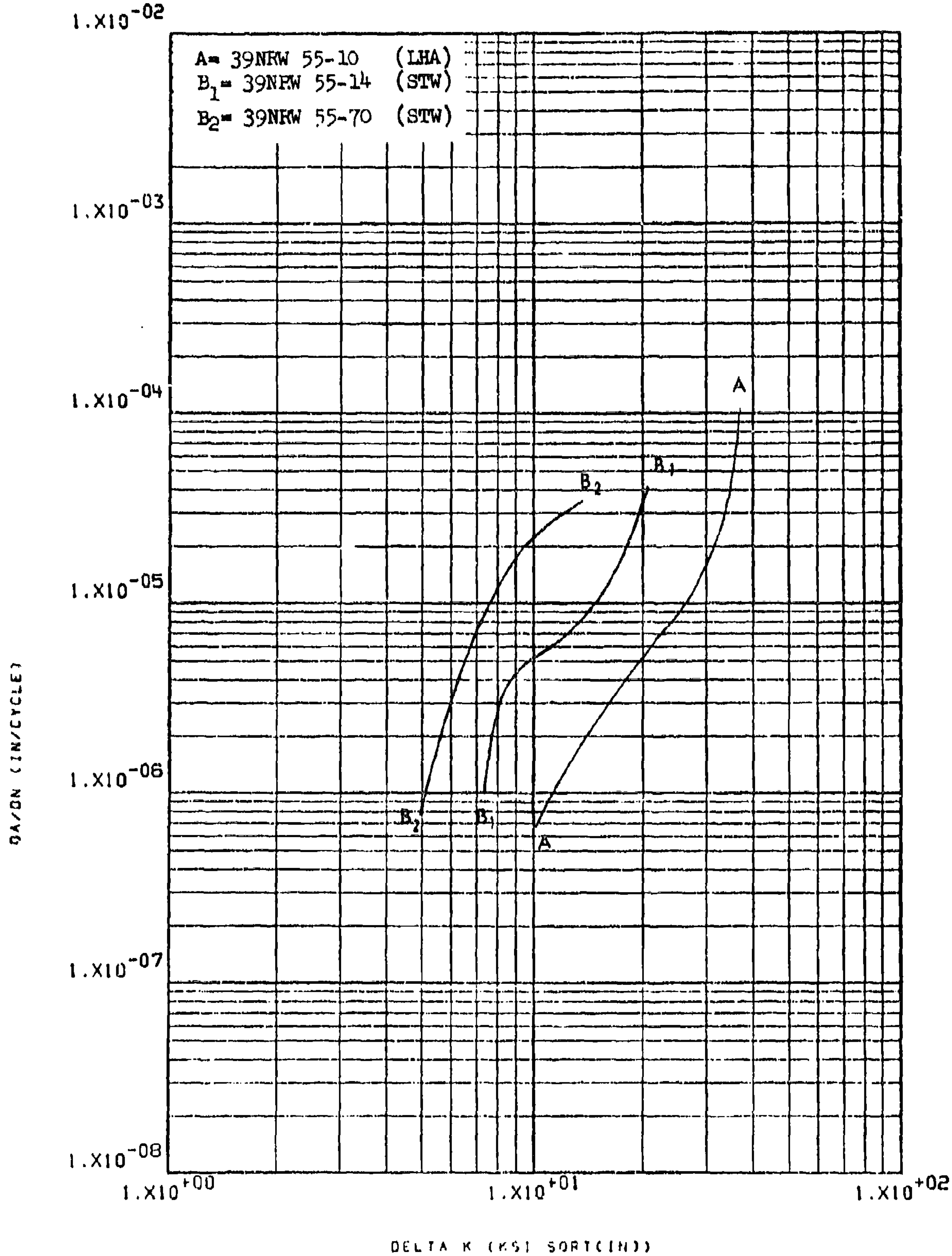

Figure 8.2.12.5-2 Effect of environment on FCGR at R.T., R=0.3, RW direction, in 3" x 36" x 72" 300M forged block

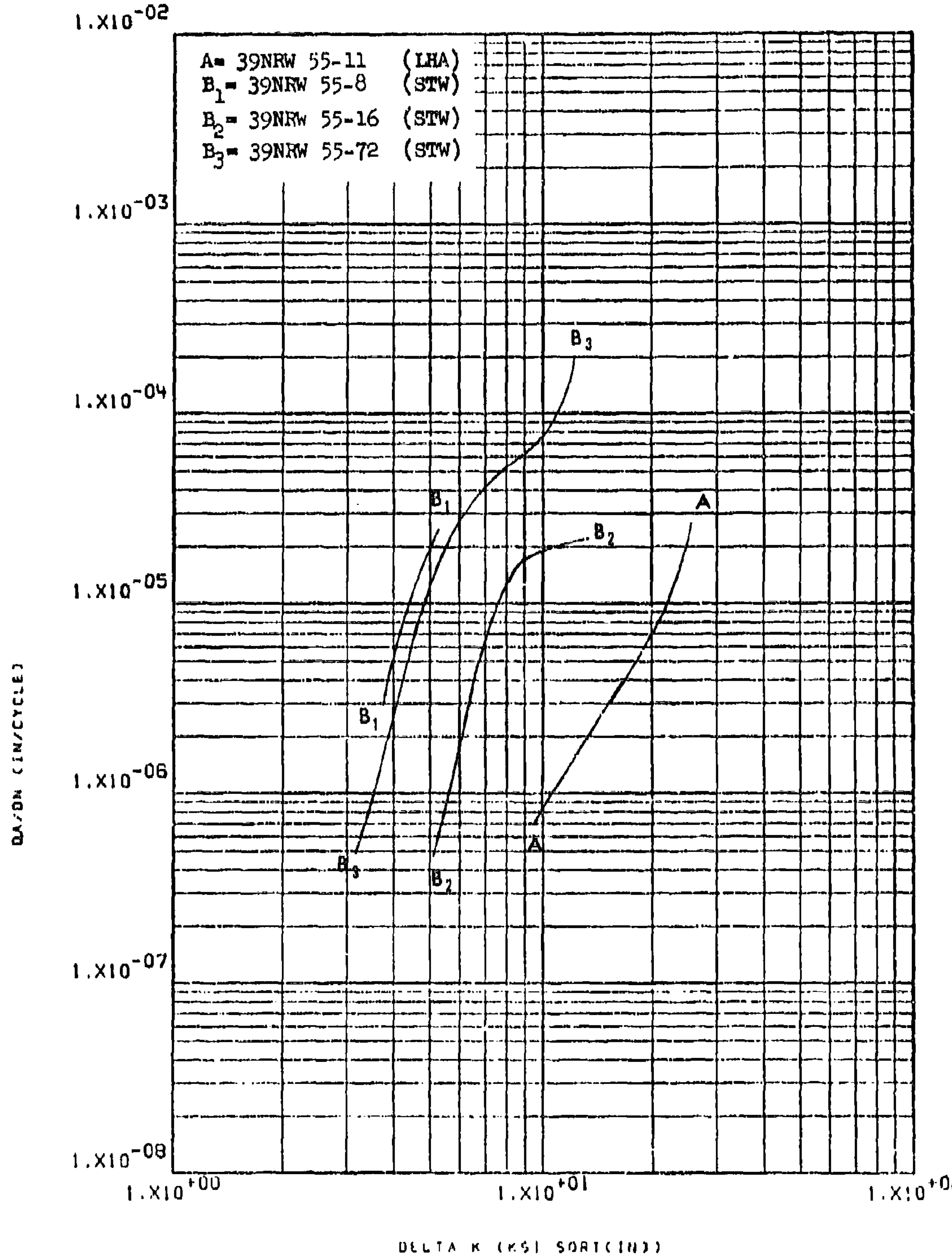

Figure 8.2.12.5-3 Effect of environment on FCGR at R.T., R=0.5, RW direction in 3" x 36" x 72" 300M forged block

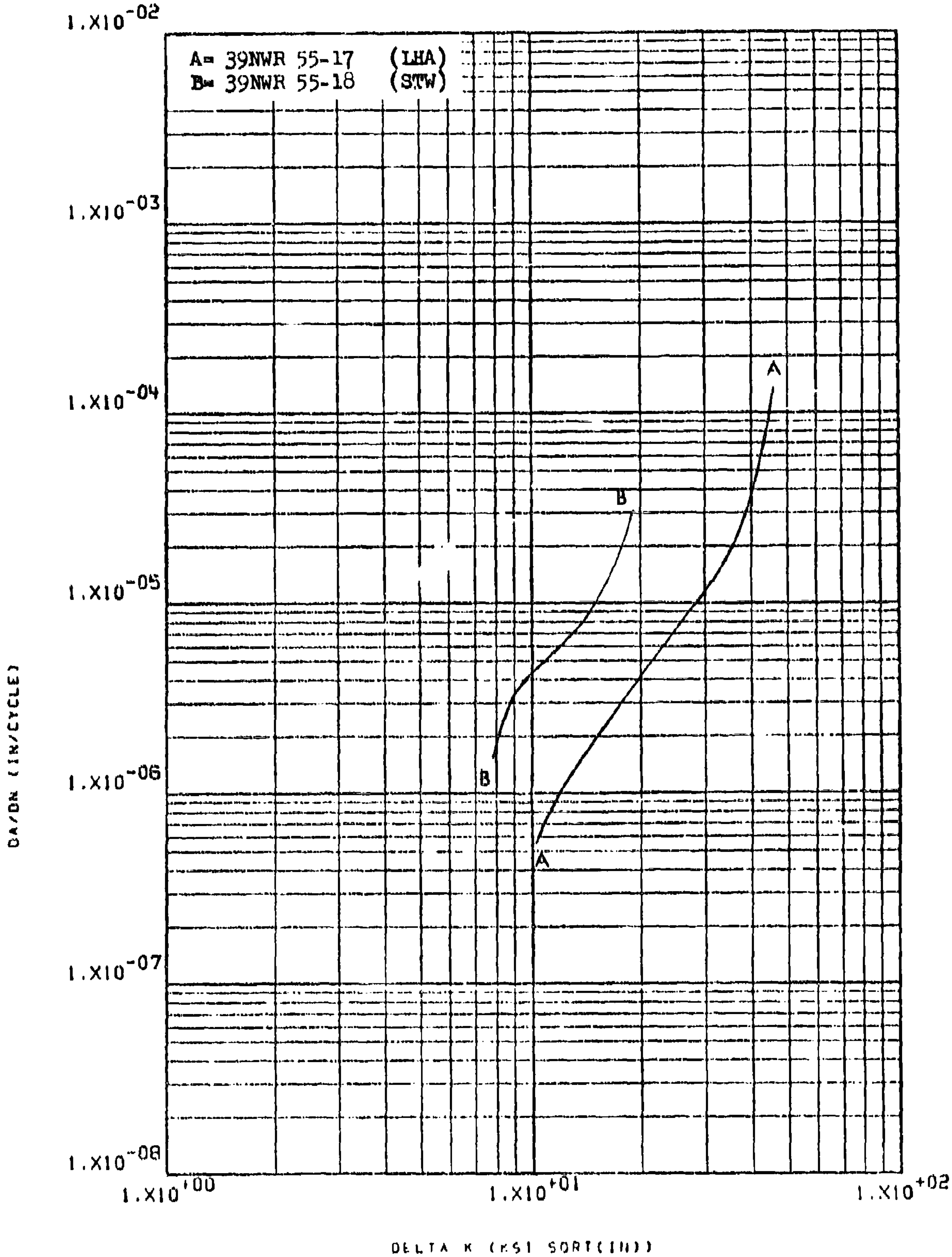

Figure 8.2.12.5-4 Effect of environment on FCGR at R.T., R=0.08, WR direction in 3" x 36" x 72" 300M forged block

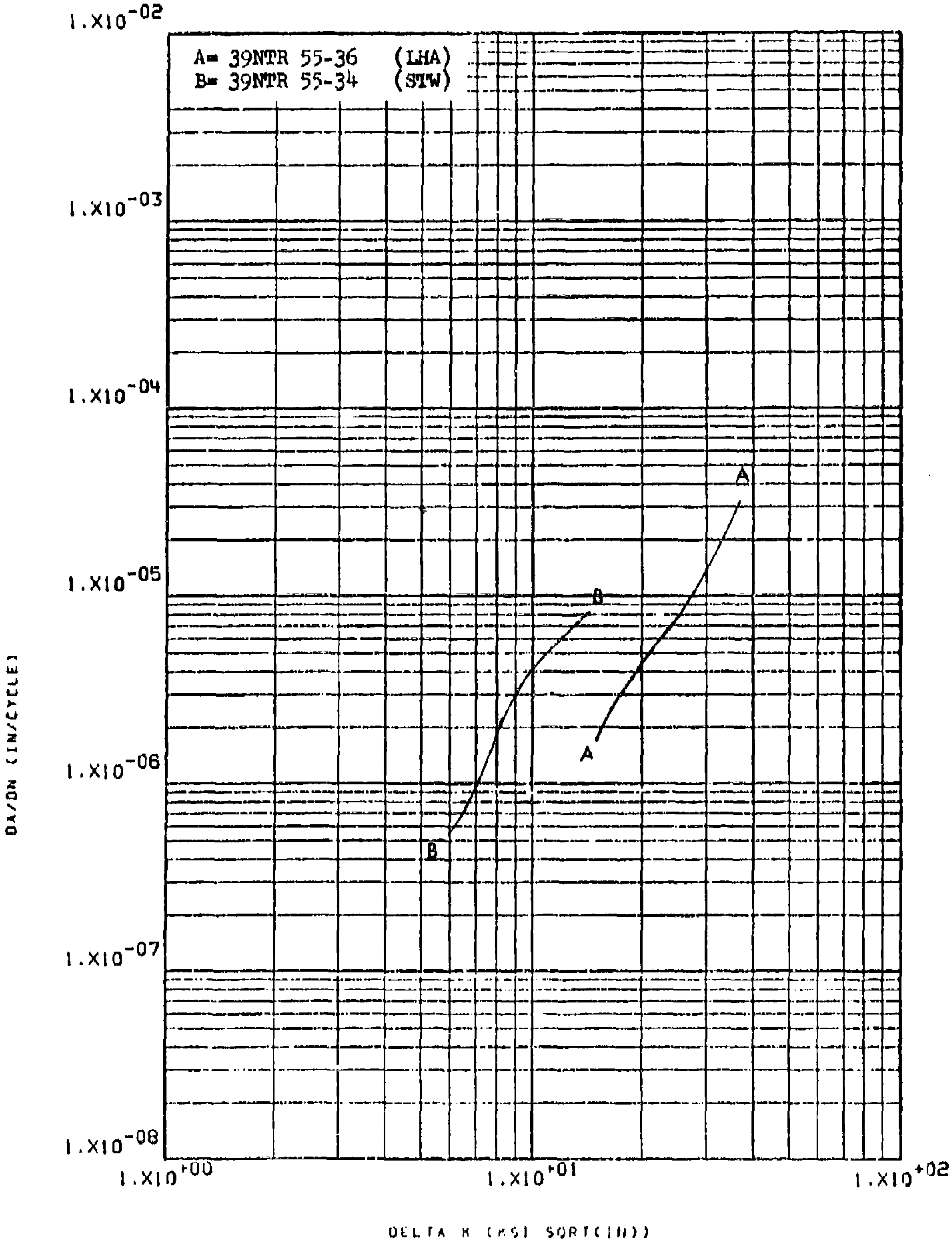

Figure 8.2.12.5-5 Effect of environment on FCGR at R.T., R=0.08, TR direction in 3" x 36" x 72" 300M forged block

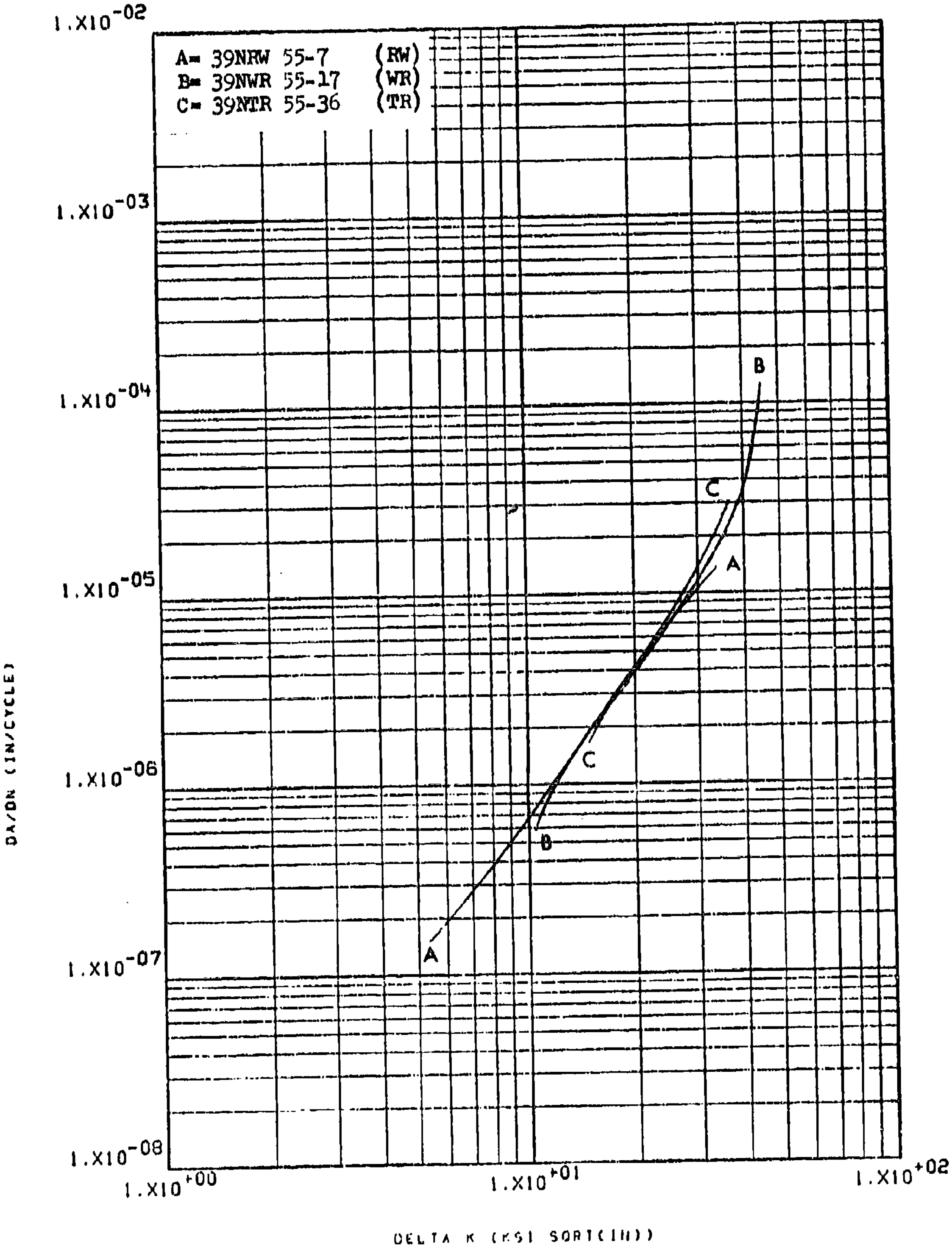

Figure 8.2.12.6-1 Effect of test direction on LHA-FCGR at R.T., R=0.08, 360 cpm in 3" x 36" x 72" 300M forged block

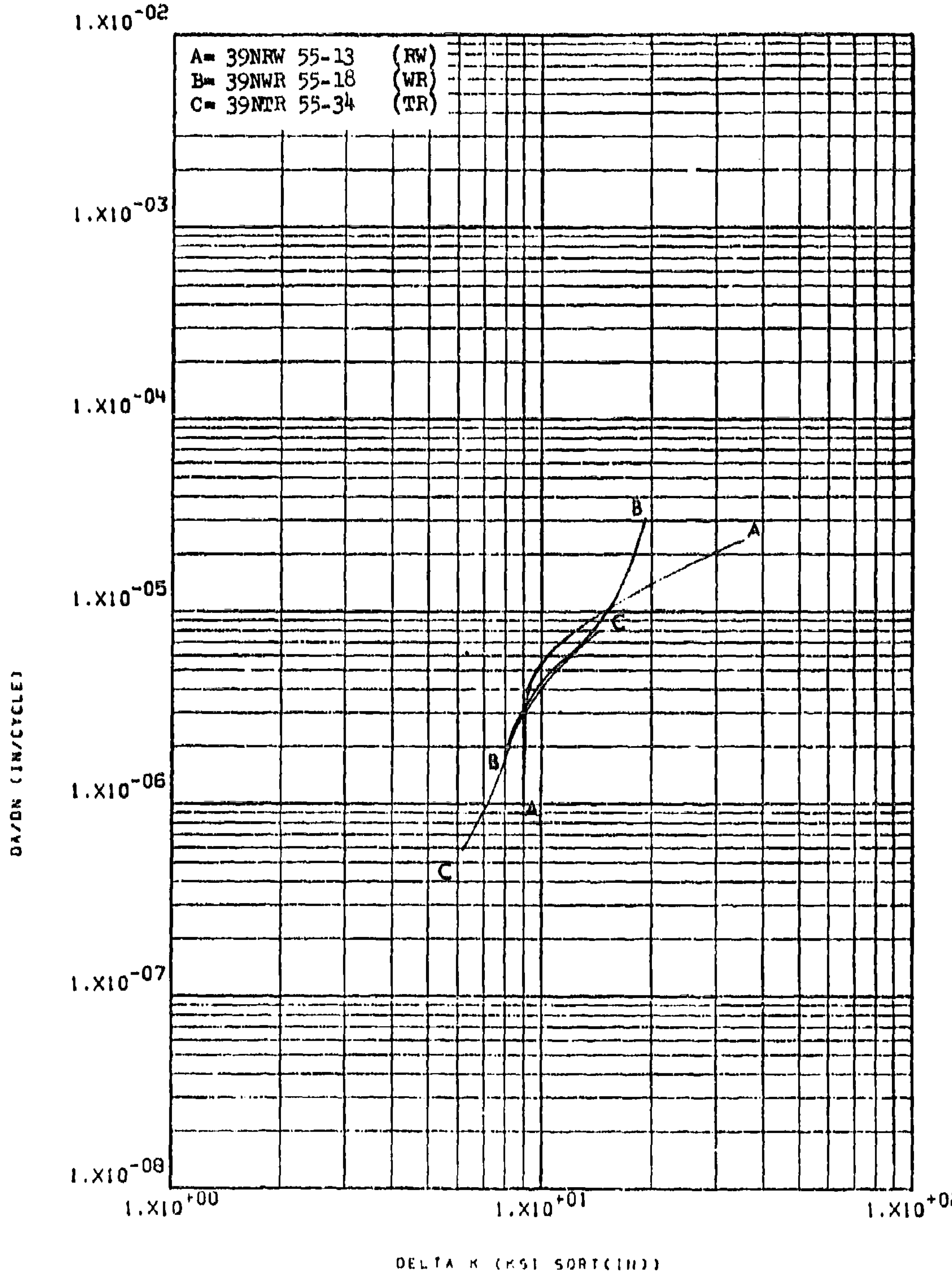

Figure 8.2.12.6-2 Effect of test direction on STW-FCGR at R.T., R=0.08, 60 cpm in 3" x 36" x 72" 300M forged block

8.2.13 Nickel Alloy Inconel 718

8.2.13.1 Cyclic Frequency - Not evaluated.

8.2.13.2 Test Temperature - No significant increases in low humidity air fatigue crack growth rates in the TR direction of this material were observed when raising the test temperature, at an R factor of 0.08, from ambient to 400°F (Figure 8.2.13.2-1). A slight increase in growth rates was observed, however, in the RW direction (Figure 8.2.13.2-2), which was even more significant at an R factor of 0.5 (Figure 8.2.13.2-3).

8.2.13.3 Specimen Thickness - Not evaluated.

8.2.13.4 R Factor - Increasing R factors from 0.08 to 0.5 resulted in a significant increase in the low humidity air fatigue crack growth rates of the forged bar at room temperature and 400°F (Figures 8.2.13.4-1 and -2), while resulting in only a slight increase in growth rates in the hot die forging at room temperature (Figure 8.2.13.4-3).

8.2.13.5 Environment - There was no consistently significant effect on crack growth rates of varying environments from low humidity air to sump tank water or shop cleaning solvent (Figures 8.2.13.5-1 through -3).

8.2.13.6 Test Direction - The low humidity air fatigue crack growth rates of the forged block material were seen to be essentially equivalent in both the RW and WR directions (Figure 8.2.13.6-1), while in the hot die forged materials growth rates in the WR direction were slightly greater than those in the RW direction (Figure 8.2.13.6-2). In sump tank water growth rates of the forged block in the RW direction were greater than those in the WR direction (Figure 8.2.13.6-3).

8.2.13.7 Product Form - Fatigue crack growth rates of this material in low humidity air were seen to be significantly greater in both the RW and WR directions of hot die forgings as compared to forged bars at an R factor of 0.08 (Figures 8.2.13.7-1 and -2). At an R factor of 0.5, however, this effect was not observed, and growth rates of the two product forms were seen to be essentially equivalent (Figure 8.2.13.7-3). The heat treatment cycle for the two products forms differed in that a 1850F solution treatment temperature was used for the forged bar as compared to 1750F for the die forging. This may have contributed to the difference observed in crack growth rates between the two product forms.

8.2.13.8 Heat Treat Condition - Not evaluated.

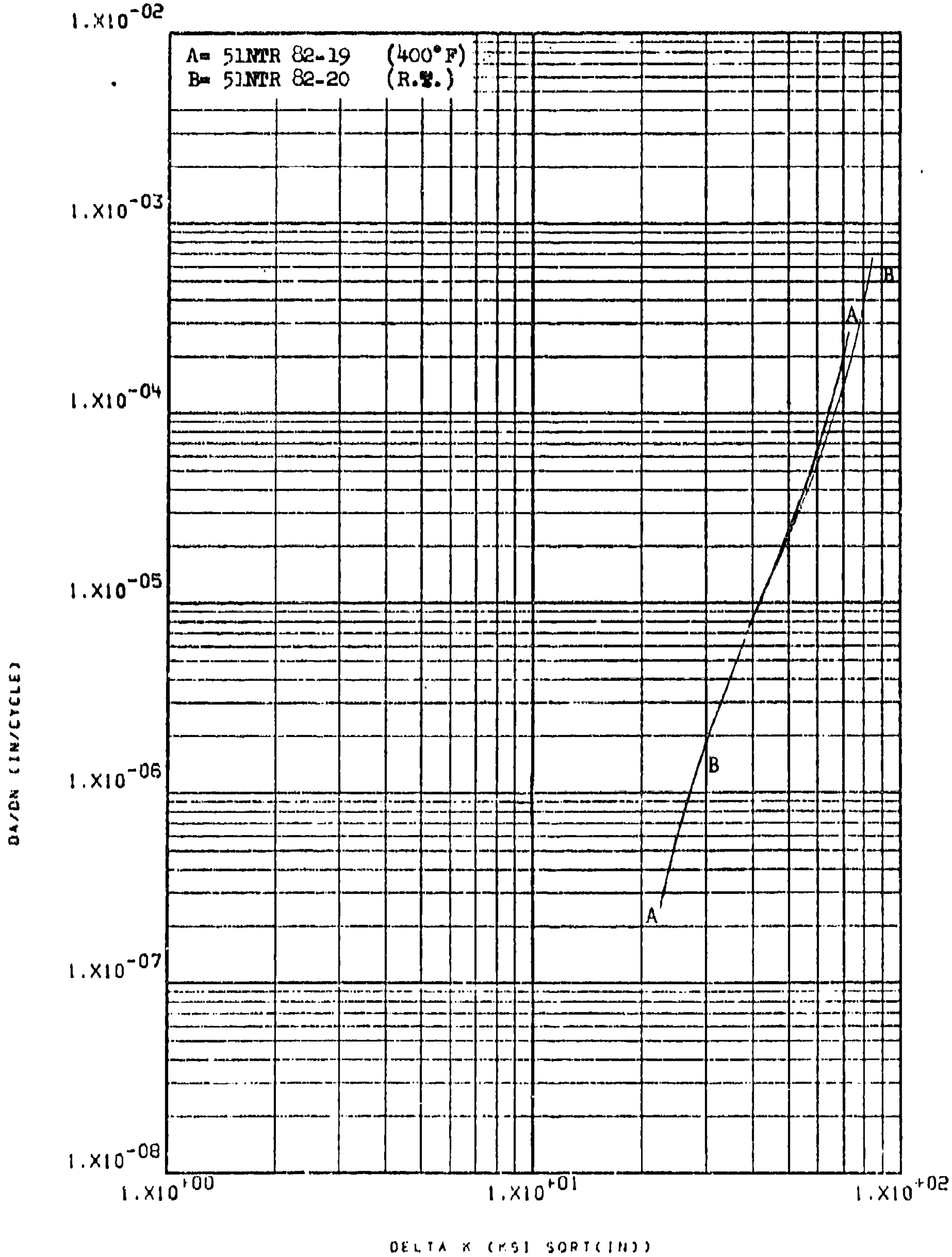

Figure 8.2.13.2-1 Effect of test temperature on LHA-FCGR at R=0.08, 360 cpm, TR direction in Inconel 718 forged bar

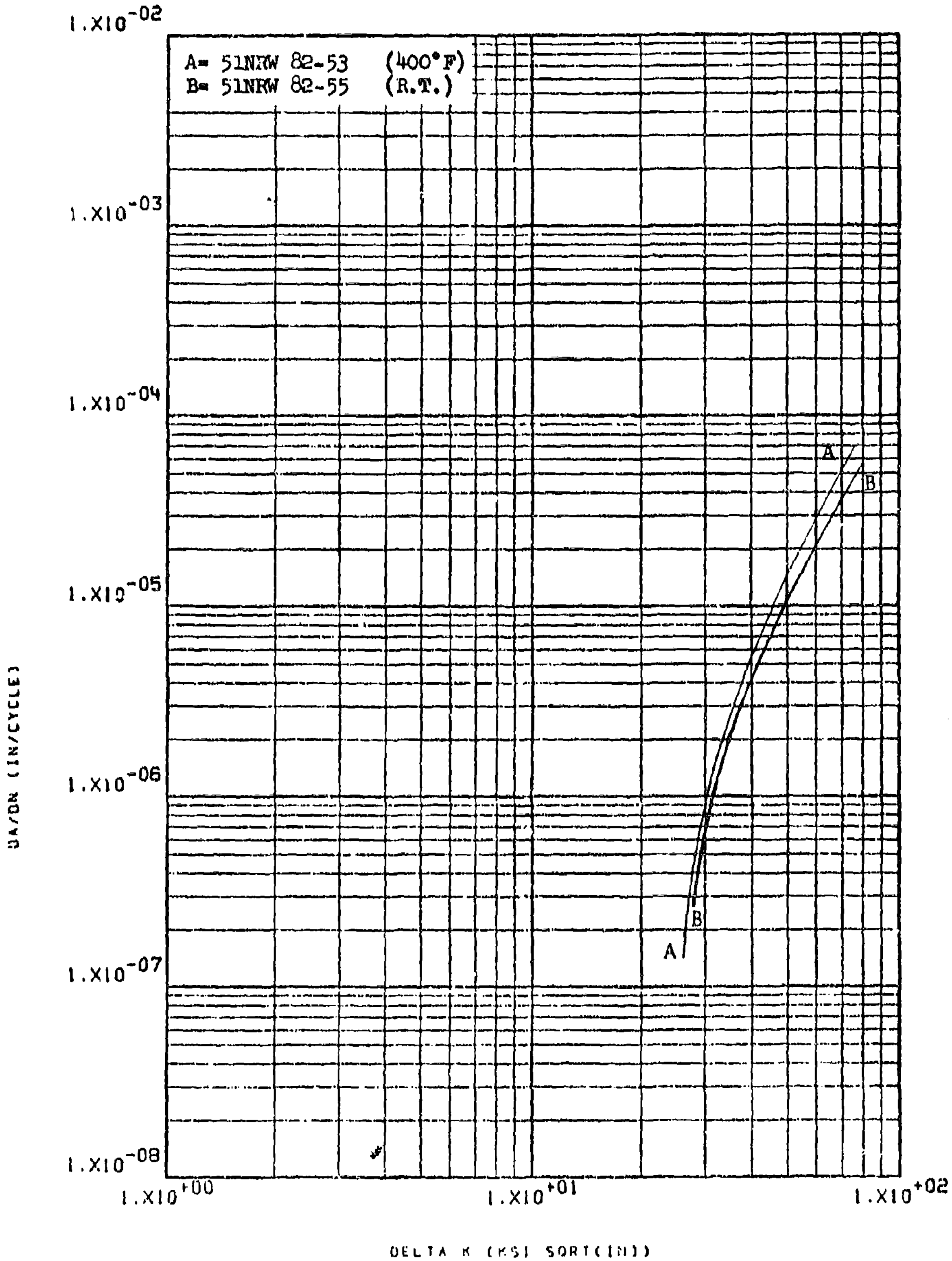

Figure 8.2.13.2-2 Effect of test temperature on LHA-FCGR at R=0.08, 360 cpm, RW direction in Inconel 718 forged bar

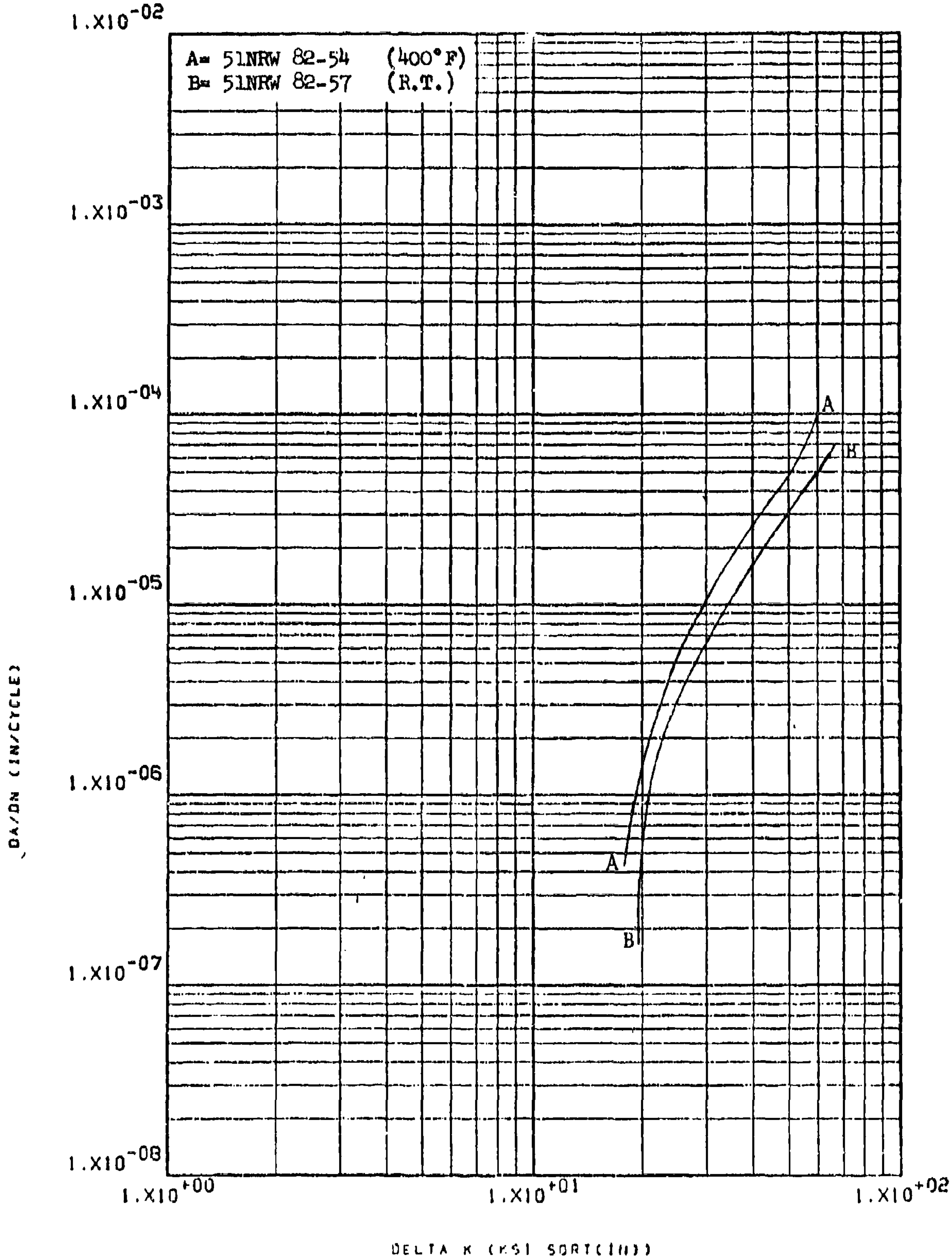

Figure 8.2.13.2-3 Effect of test temperature on LHA-FCGR at R=0.5, 360 cpm, RW direction in Inconel 718 forged bar

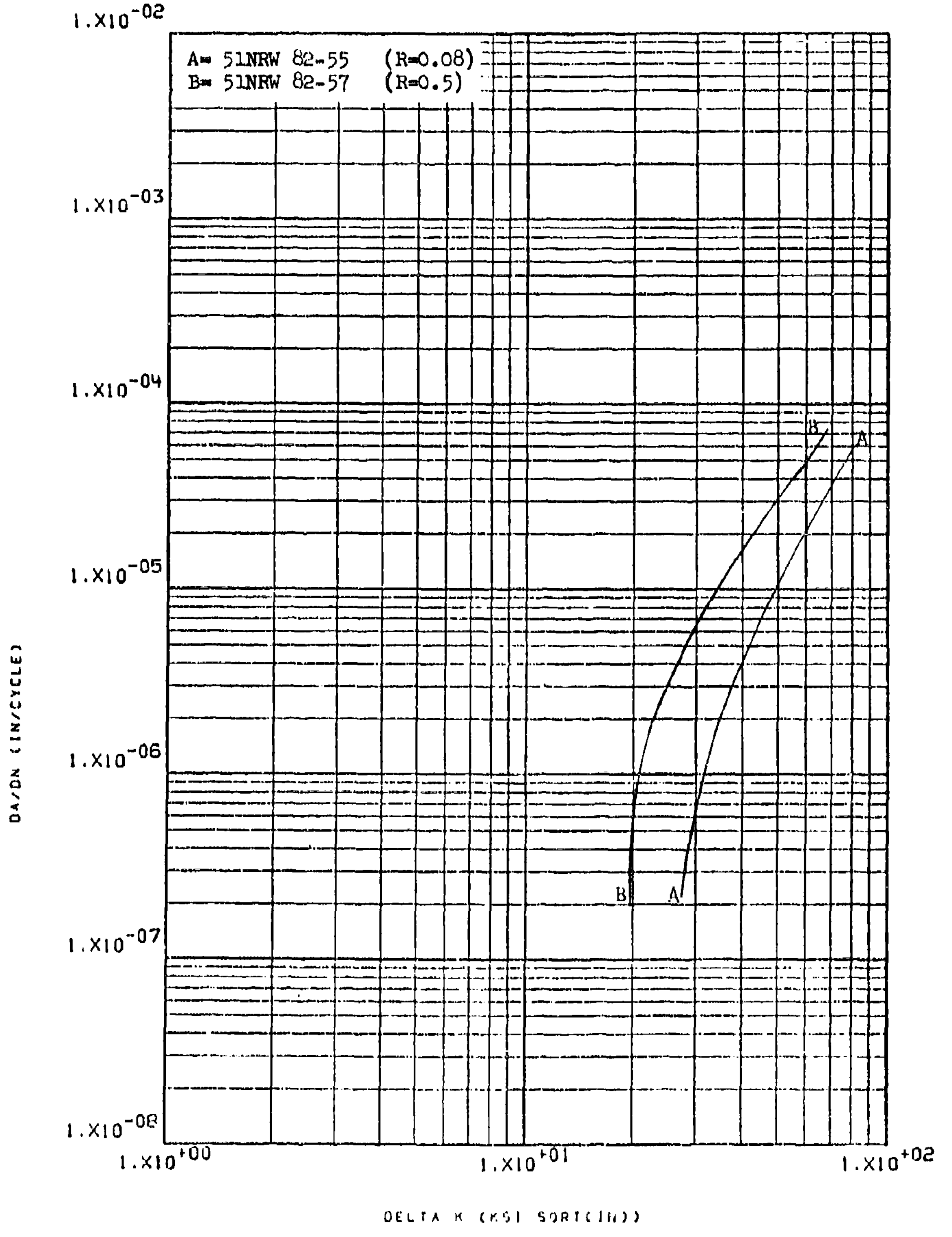

Figure 8.2.13.4-1 Effect of R factor on LHA-FCGR at R.T. 360 cpm, RW direction in Inconel 718 forged bar

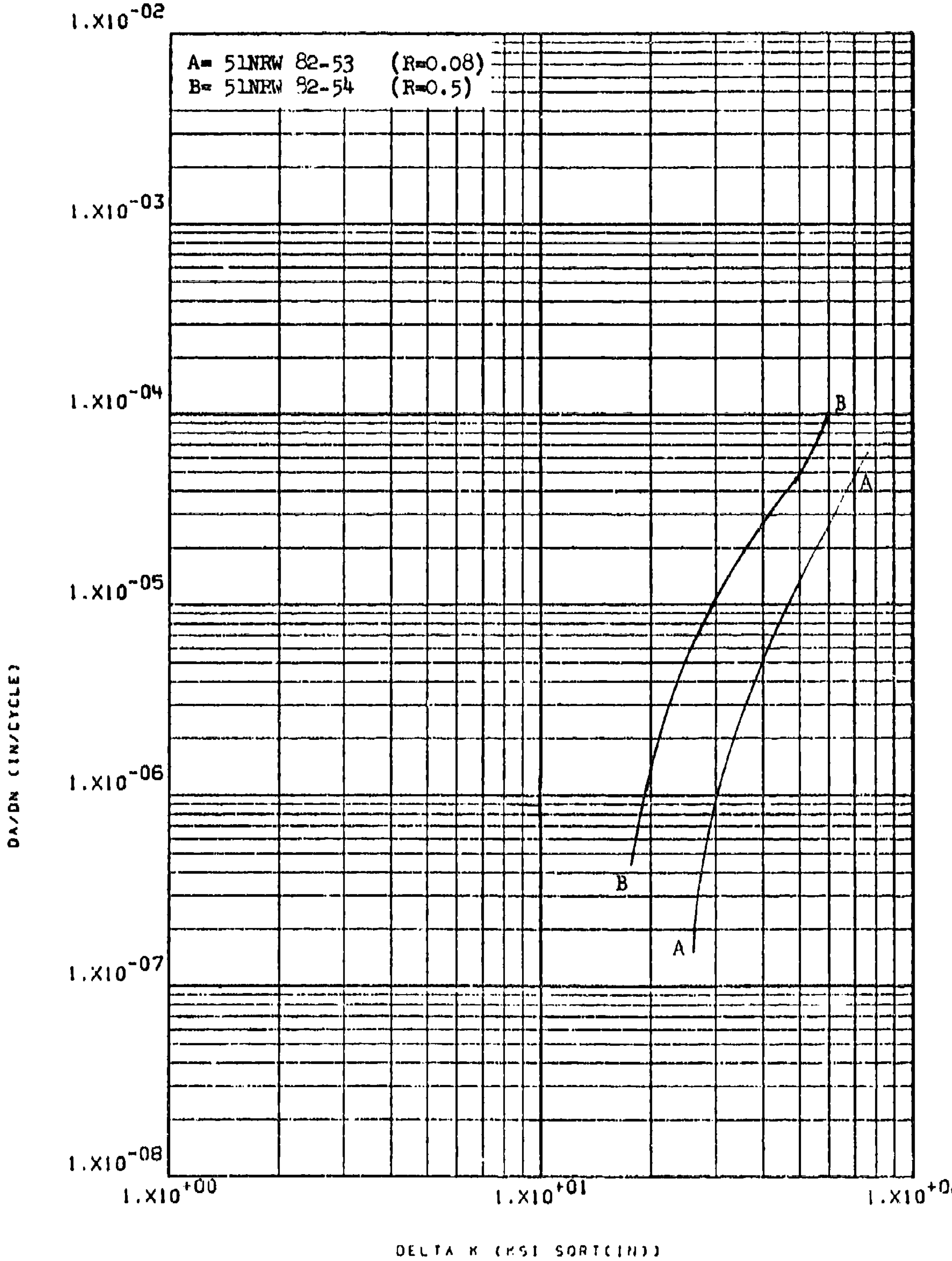

Figure 8.2.13.4-2 Effect of R factor on LHA-FCGR at 400°F, 360 cpm, RW direction in Inconel 718 forged bar

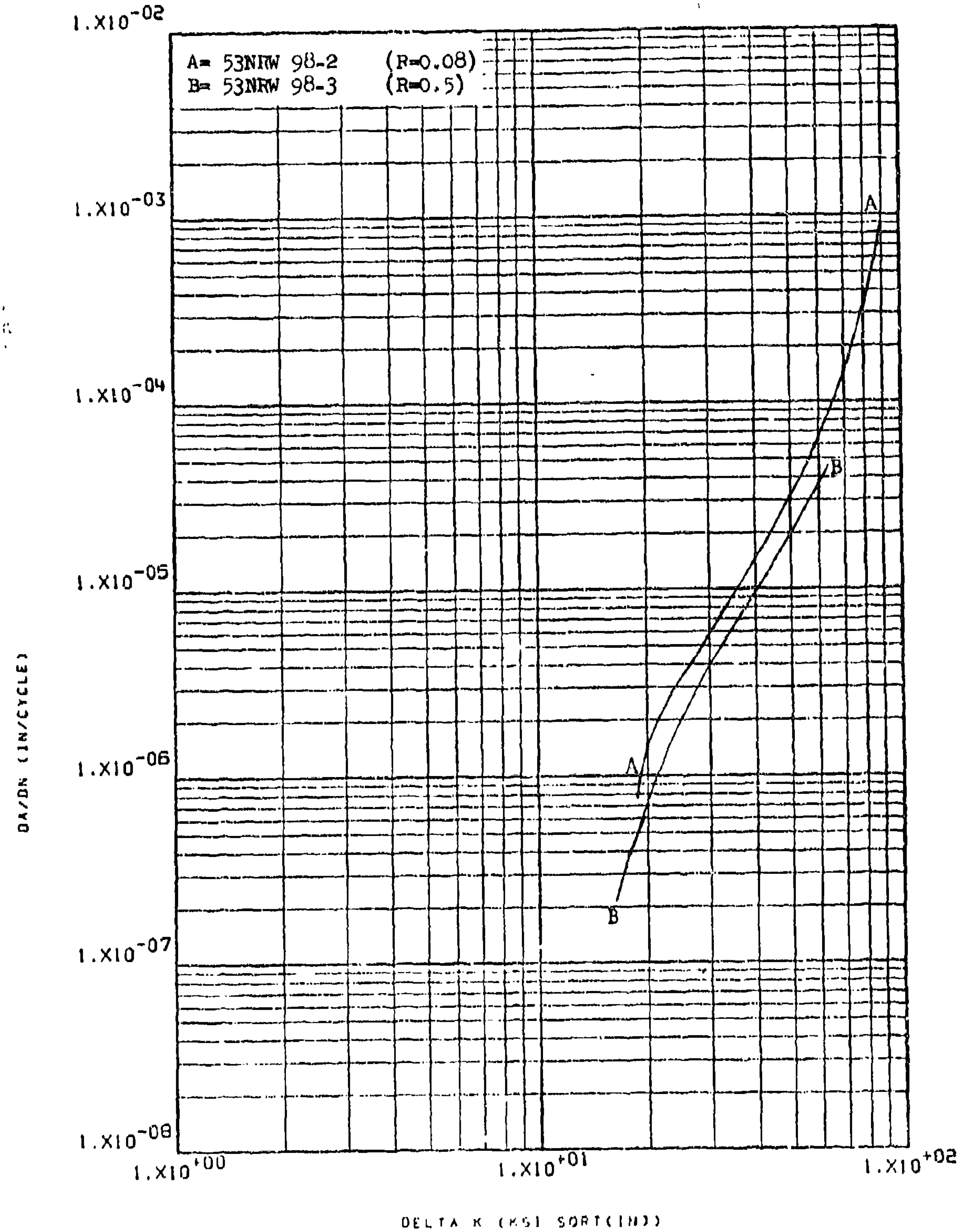

Figure 8.2.13.4-3 Effect of R factor on LHA-FCGR at R.T., 360 cpm, RW direction in Inconel 718 hot die forging

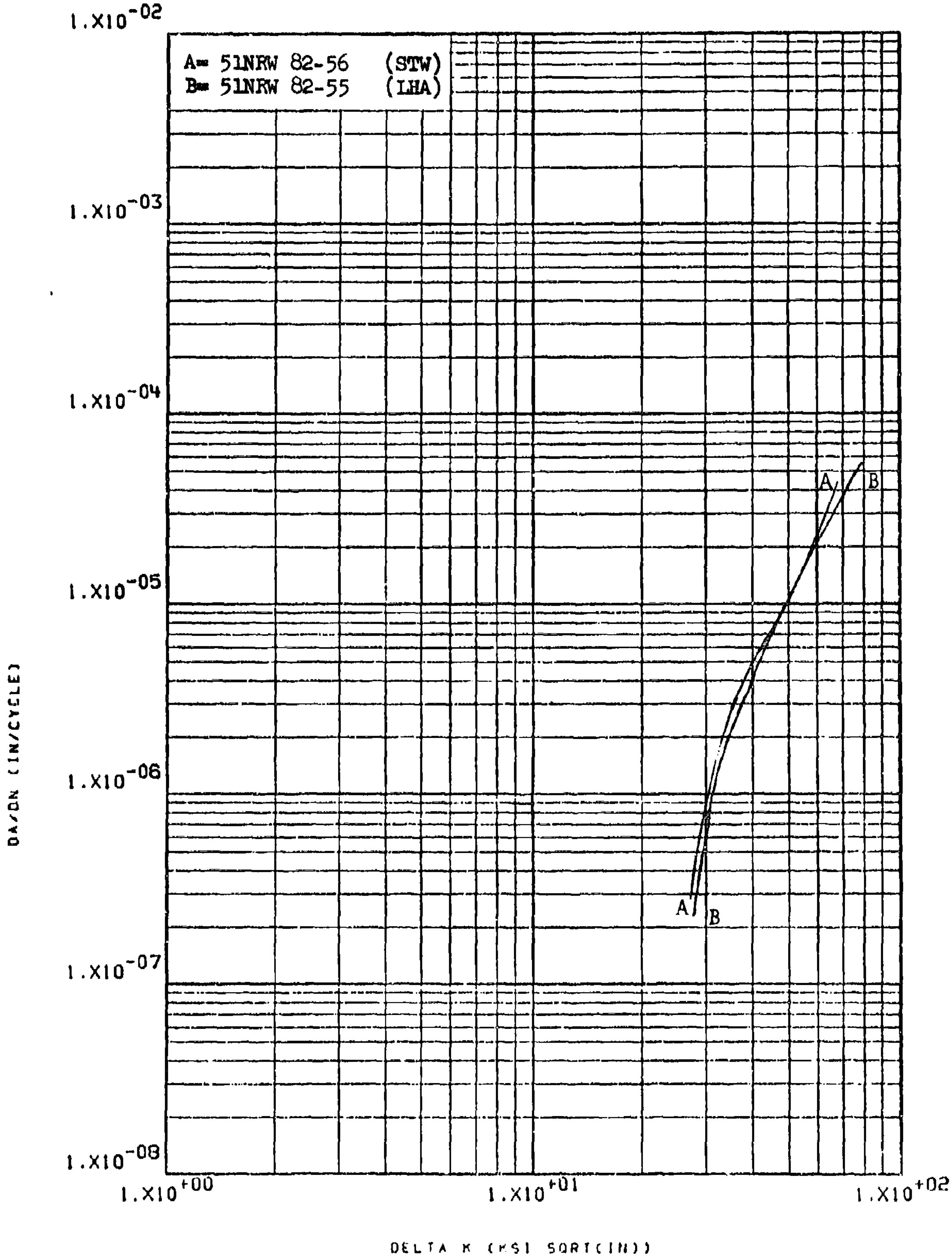

Figure 8.2.13.5-1 Effect of environment on FCGR at R.T., R=0.08, RW direction in Inconel 718 forged bar

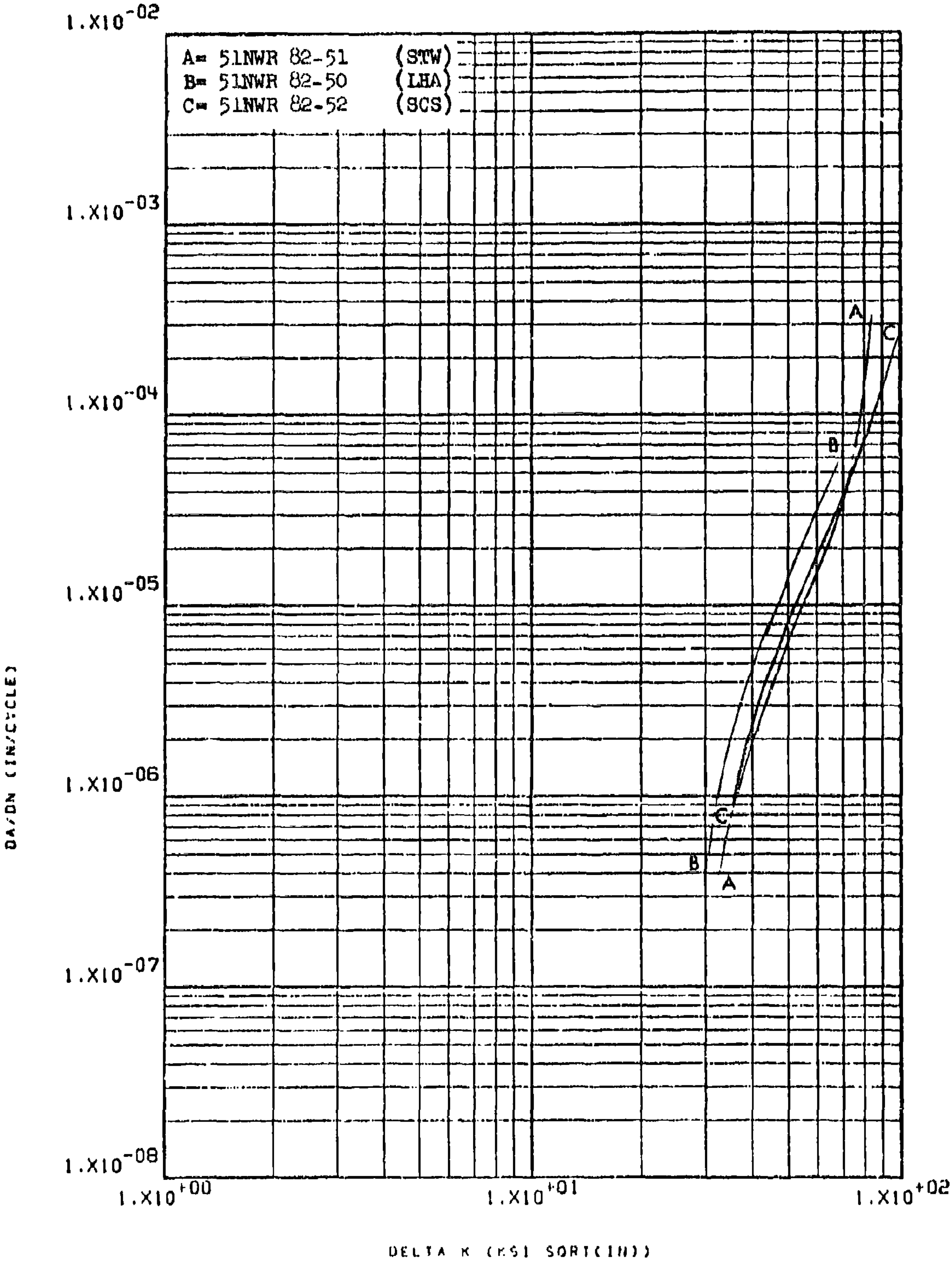

Figure 8.2.13.5-2 Effect of environment on FCGR at R.T., R=0.08, WR direction in Inconel 718 forged bar

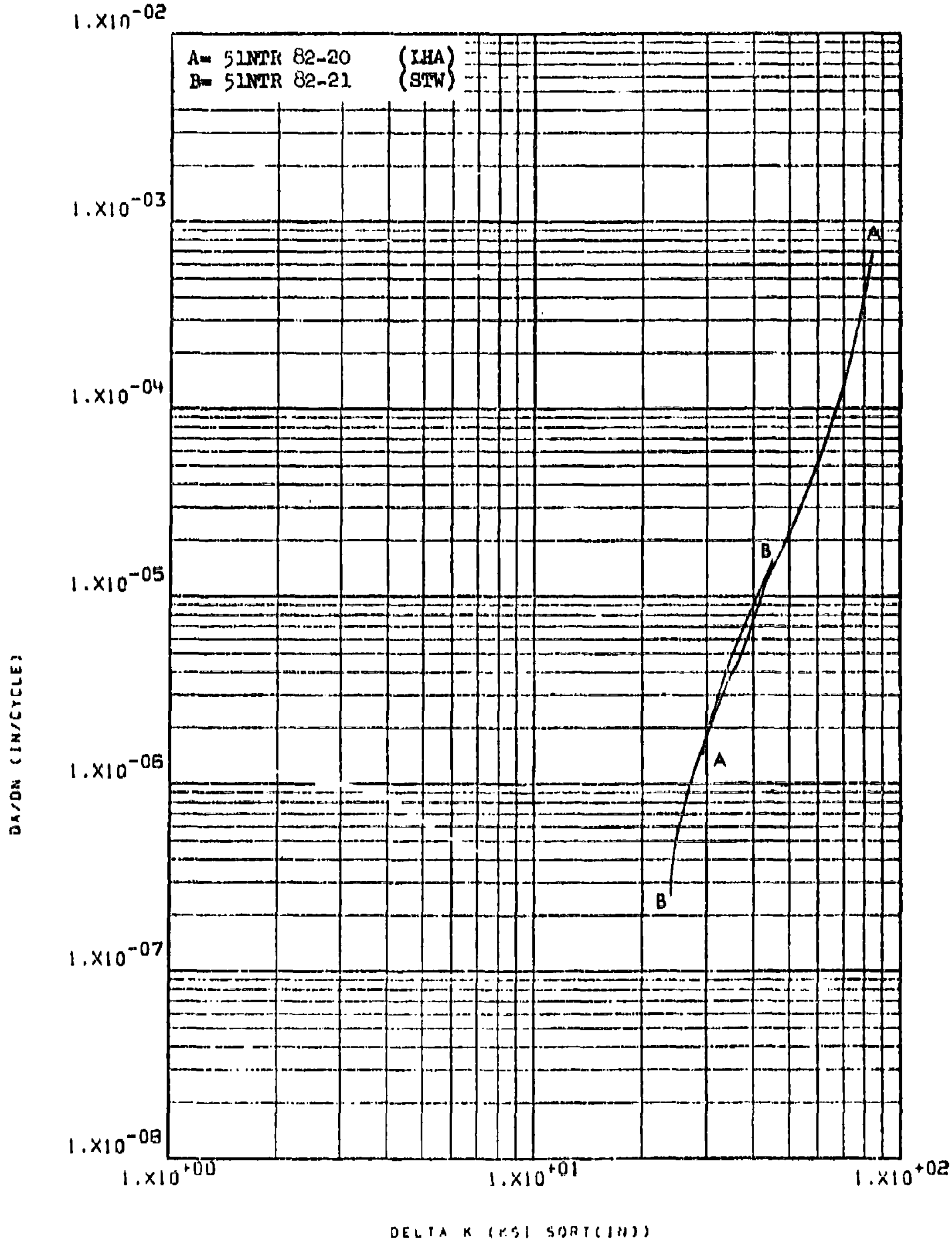

Figure 8.2.13.5-3 Effect of environment on FCGR at R.T., R=0.08, TR direction in Inconel 718 forged bar

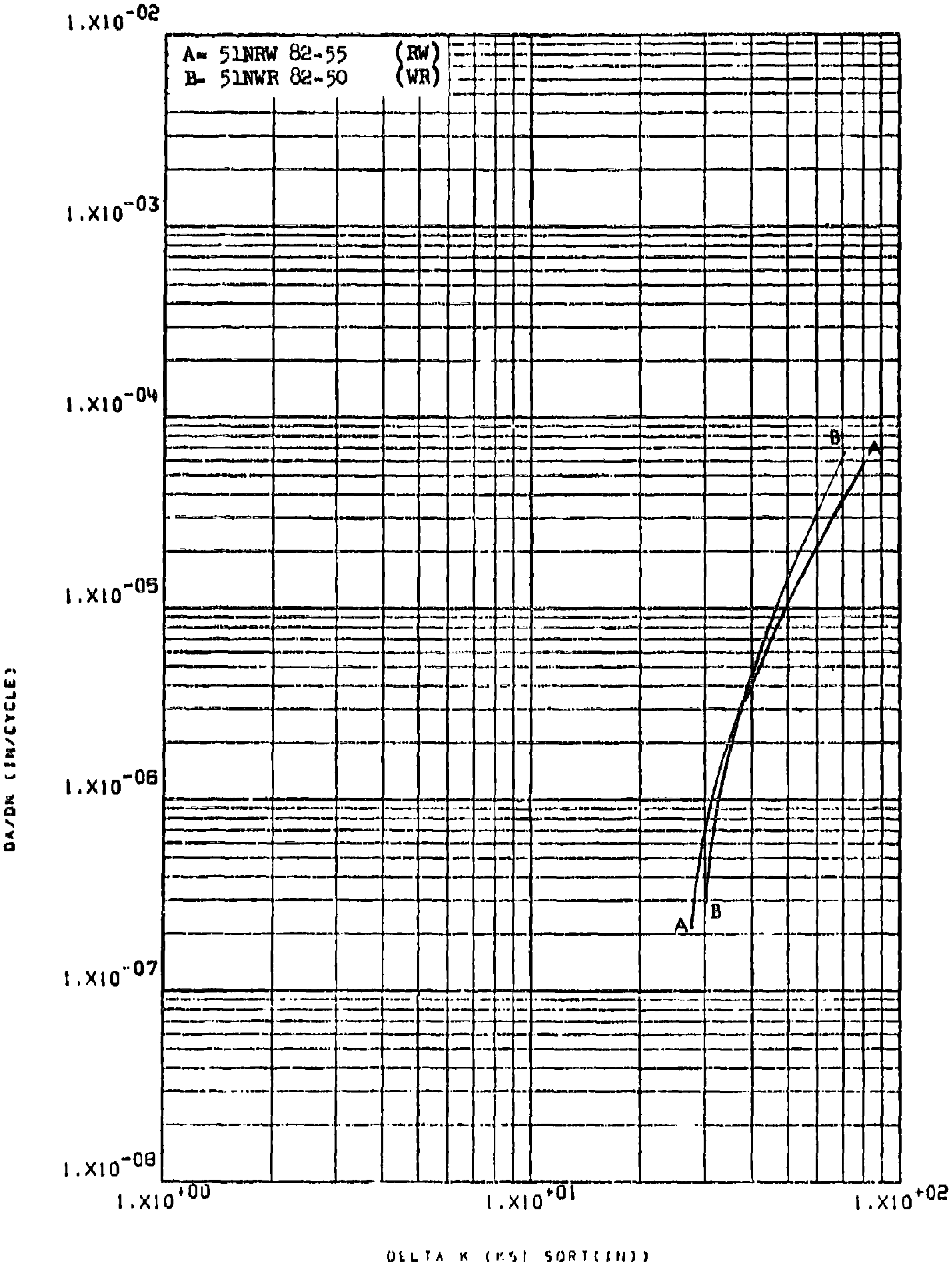

Figure 8.2.13.6-1 Effect of test direction on LHA-FCGR at R.T., R=0.08, 360 cpm, in Inconel 718 forged bar

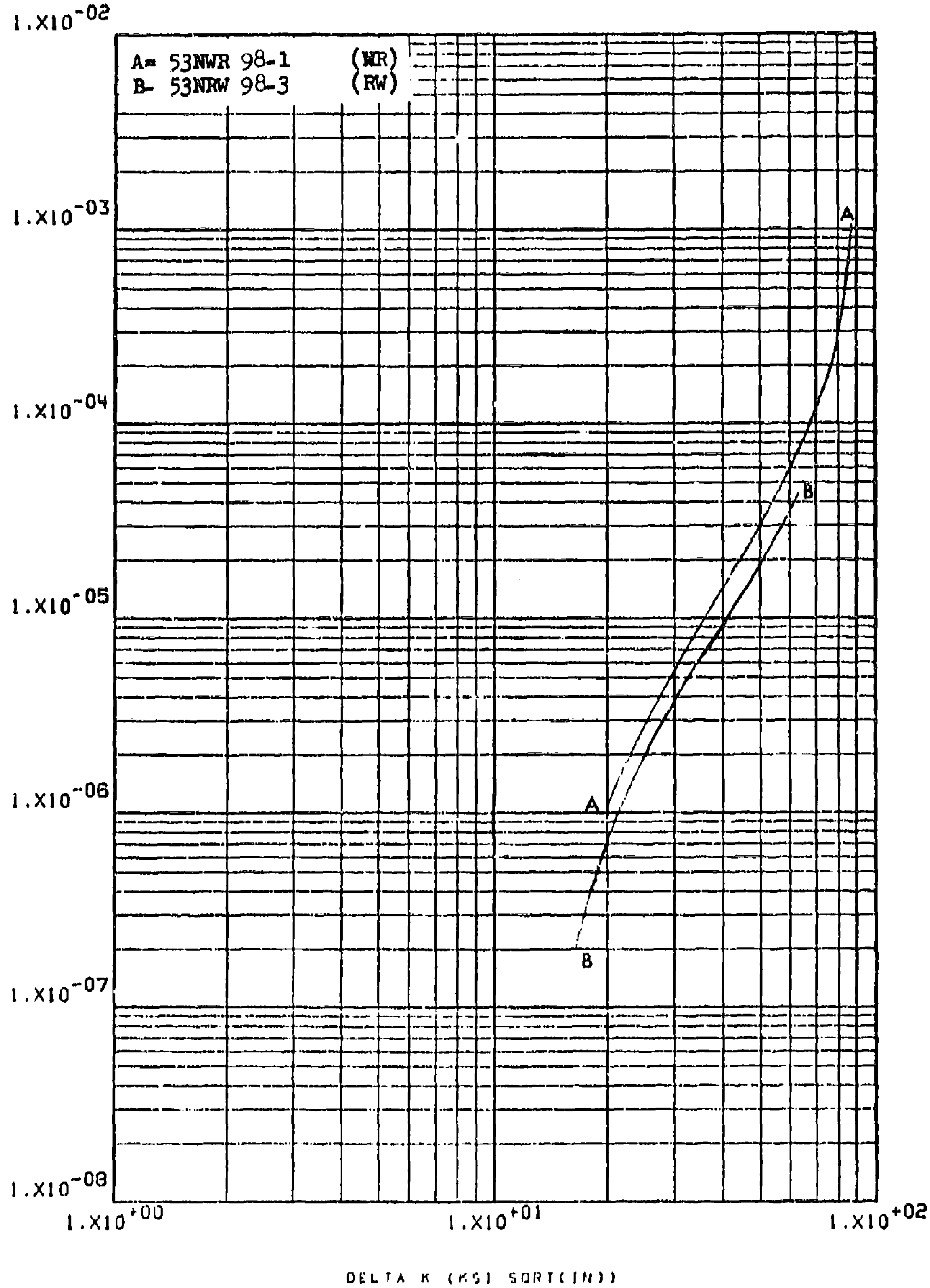

Figure 8.2.13.6-2 Effect of test direction on LHA-FCGR at R.T., R=0.08, 360 cpm in Inconel 718 hot die forging

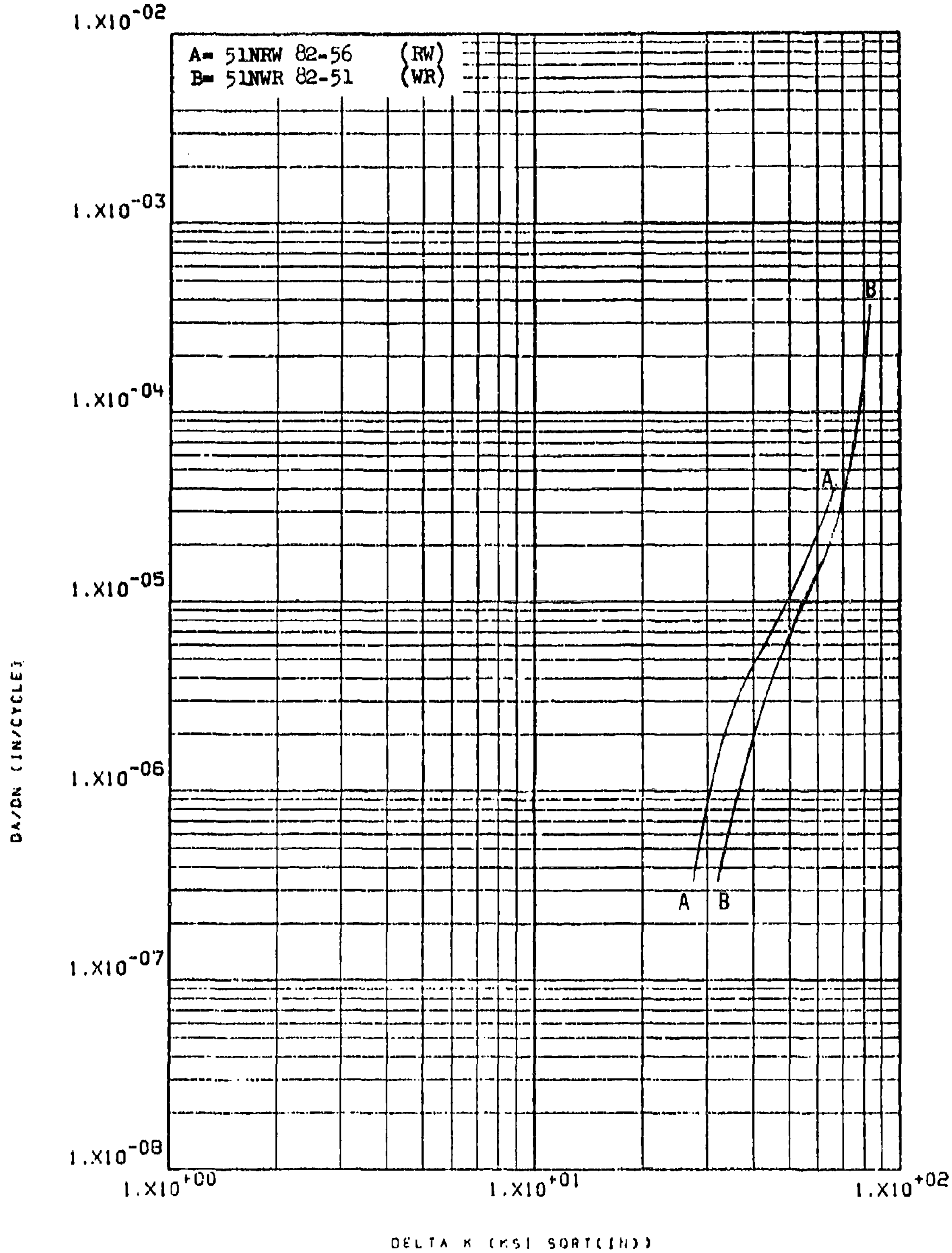

Figure 8.2.13.6-3 Effect of test direction on STW-FCGR at R.T., R=0.08, 60 cpm in Inconel 718 forged bar

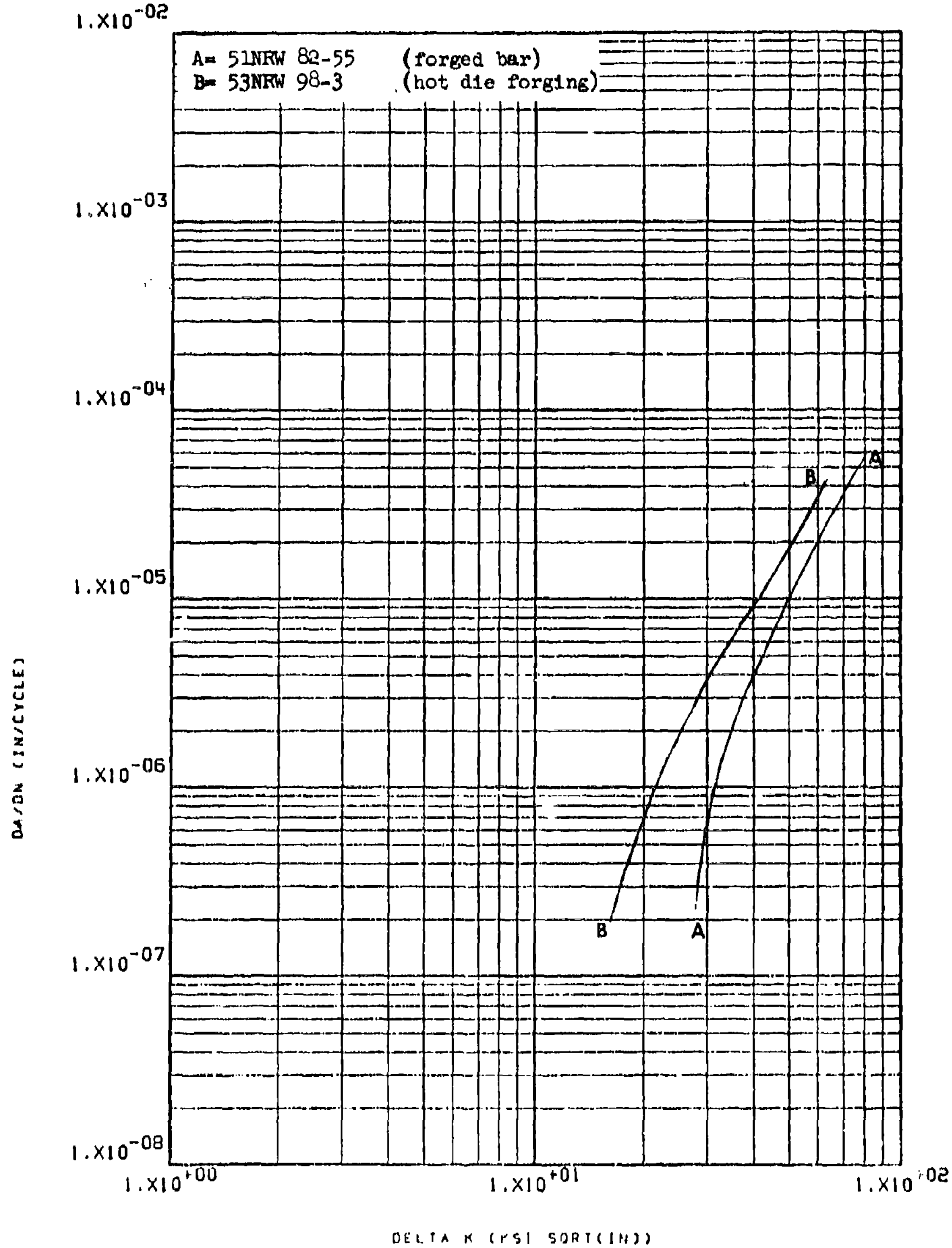

Figure 8.2.13.7-1 Effect of product form on LHA-FCGR at R.T. R=0.08, 360 cpm, RW direction in Inconel 718

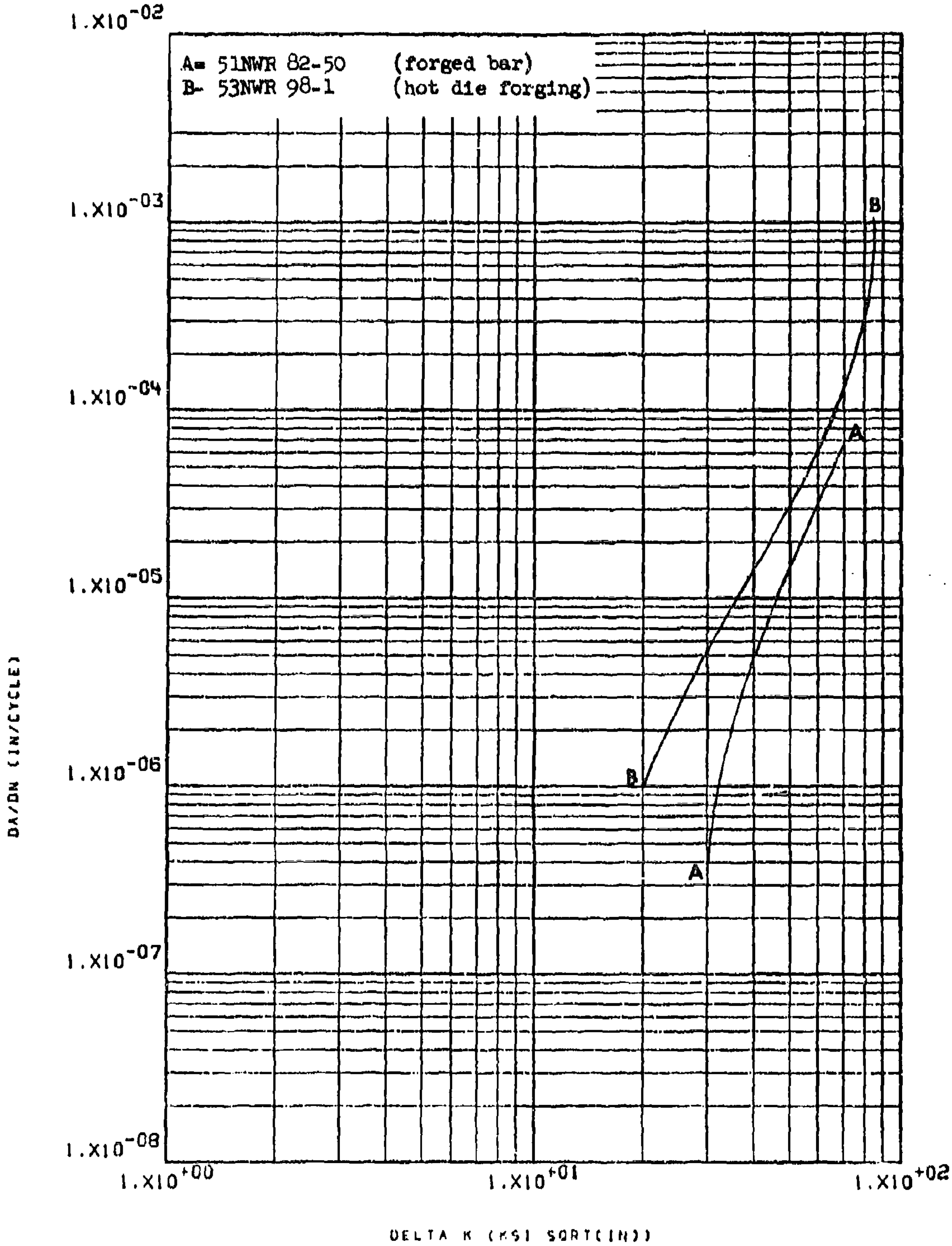

Figure 8.2.13.7-2 Effect of product form on LHA-FCGR at R.T., R=0.08, 360 cpm, WR direction in Inconel 718

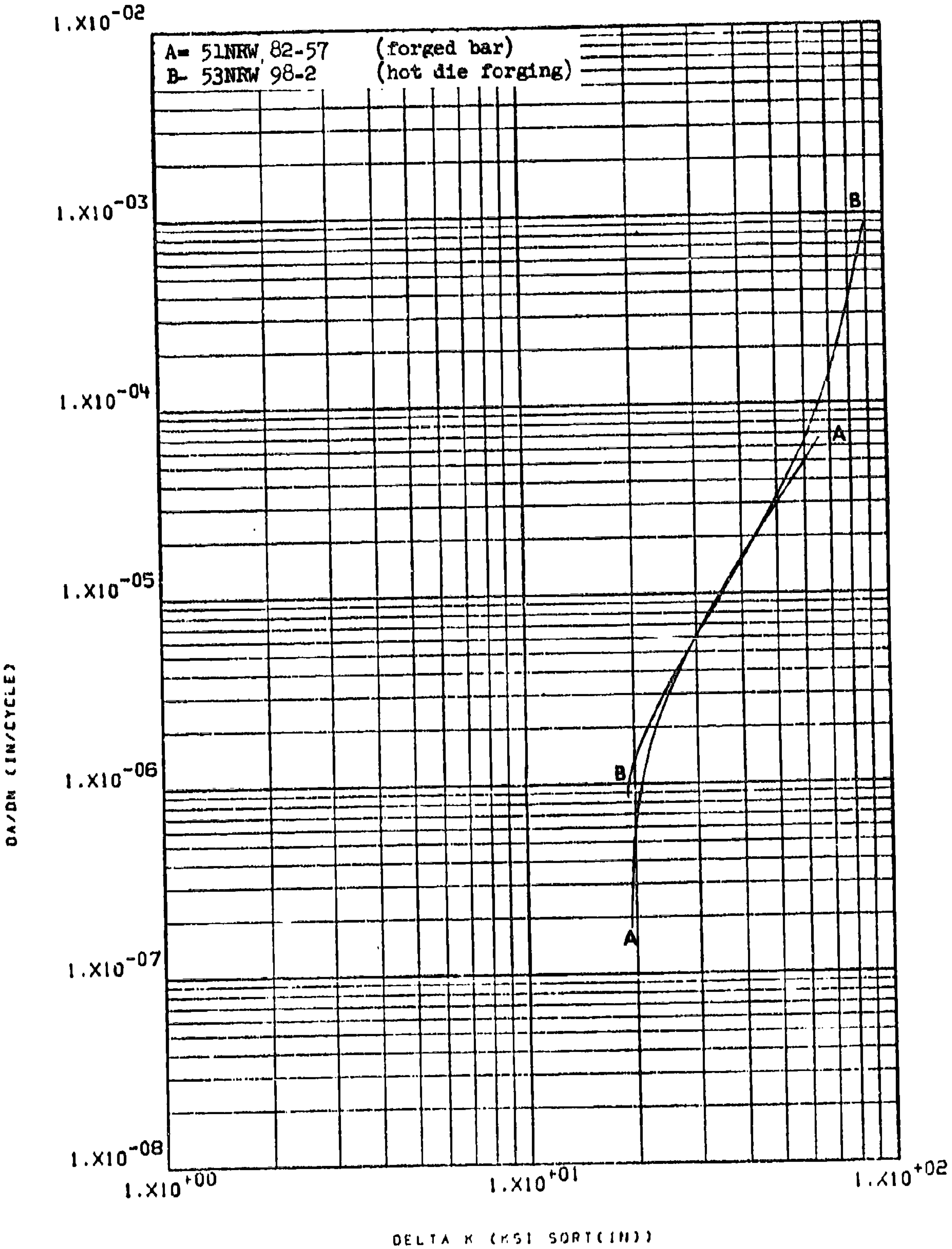

Figure 8.2.13.7-3 Effect of product form on LHA-FCGR at R.T., R=0.5, 360 cpm, RW direction in Inconel 718

8.2.14 ALL WELDMENTS

Unlike most raw material tests, which utilized a compact tension (CT) specimen configuration, fatigue crack growth rate testing of weldments was conducted primarily using part through crack (PTC) specimens, augumented by some center cracked tension (CCT) specimens and a few CT specimens. While the PTC and CCT specimens provide only a minimal number of data points per test, the data are usually sufficient to define the growth rate characteristics of weldments over the major area of concern for design applications; i.e. da/dn values of 5×10^{-7} up to 1×10^{-5} inch/cycle at Δk levels from ~ 10 to 40 ksi $\sqrt{in}$.

The results of each weldment test conducted in this program are presented in Appendix D. Interweld comparisons have also been made, and are presented below:

8.2.14.1 Ti-6Al-4V Weldments

Unless otherwise indicated, all results refer to tests performed in PTC specimens fabricated from weldments which had been stress relieved for 2 hours at 1100°F.

8.2.14.1.1 Cyclic Frequency - Low humidity air growth rates in both the heat affected zone and the weld of this material were seen to be essentially unaffected by changing the cyclic frequency of test from 60 to 360 cpm (Figure 8.2.14.1.1-1 and -2) In the HAZ growth rates were very slightly greater at 60 cpm than at 360 cpm, while in the weld of material which had been mill annealed prior to welding there was virtually no difference in rates at the two frequencies.

8.2.14.1.2 Test Temperature - Low humidity air growth rate in the heat affected zone of both welded R.A. plate and a welded extrusion (beta processed plus mill annealed prior to welding) were seen to be essentially unaffected by decreasing the test temperature from ambient to -65°F. (Figure 8.2.14.1.2-1 and -2) In the case of the plate material, rates were seen to be very slightly greater at ambient temperature than at -65°F, while the opposite was seen to be true in the case of the extrusion.

8.2.14.1.3 Specimen Thickness - Although the data was insufficient to be conclusive, it appeared to indicate that the low humidity air growth rates in the heat affected zone of a 0.5" thick specimen were slightly greater than those of a 0.25" thick specimen (Figure 8.2.14.1.3-1).

8.2.14.1.4 R-Factor - Low humidity air fatigue crack growth rates in the heat affected zone were seen to be virtually unaffected as R was increased from 0.08 to 0.3 (Figure 8.2.14.1.4-1). In sump tank water,

on the other hand, growth rates were noticeably accelerated by the same increase in R. (Figure 8.2.14.1.4-2)

8.2.14.1.5 Environment - Fatigue crack growth rates in both the weld and the heat affected zone were seen to be significantly accelerated when the test environment was changed from low humidity air to sump tank water (Figures 8.2.14.1.5-1 through -4). In the case of the weld, this was seen to be true in plate material which had been mill annealed prior to welding (Figure 8.2.14.1.5-1). In the heat affected zone, this was seen to be true in an extrusion which had been beta processed plus mill annealed prior to welding, (Figure 8.2.14.1.5-2) a sheet which had been mill annealed prior to welding (Figure 8.2.14.1.5-3), and in R.A. plate which had been stress relieved at 1200^{O}F for 1 hour after welding (Figure 8.2.14.1.5-4). In RA plate material which had been plasma arc welded, or which had been post-weld stress relieved at 1400^{O}F for 1 hour this affect was not so significant, but still noticeable (Figures 8.2.14.1.5-5 and -6). Growth rates in the heat affected zone of welded plate which had been post-weld stress relieved for 2 hours at 1100^{O}F were seen to be essentially equivalent in sump tank water, shop cleaning solvent, and Freon TF (Figure 8.2.14.1.5-7).

8.2.14.1.6 Product Form - At low levels of ΔK there was very little differnce observed between the low humidity air growth rates in the heat affect zones of three different plates evaluated. As delta K was increased to above ~10 ksi $\sqrt{in}$, however, the 1.5" plate showed a marked acceleration in growth rate as compared to the two thinner (1.25") plates. (Figure 8.2.14.1.6-1)

8.2.14.1.7 Test Direction - Not Evaluated

8.2.14.1.8 Heat Treat Condition - Sump tank water growth rates in the weld bead of a grindout-reweld in plate material were seen to be very slightly greater if no post-weld stress relief cycle was used than if a 2 hour long cycle at 1100^{O}F was used (Figure 8.2.14.1.8-1). Sump tank water growth rates in the heat affected zone of welded plate were seen to be essentially equivalent after post-weld stress reliefs at 1100^{O}F for 2 hours or 1400^{O}F for 1 hour. (Figure 8.2.14.1.8-2) The low humidity air growth rates in the heat affected zone of this material were seen to be similarly unaffected when the stress relief cycles was revised from 1100^{O}F/2 hours to either 1200^{O} or 1400^{O}F/1 hour. (Figure 8.2.14.1.8-3)

8.2.14.1.9 Crack Plane Location - Low humidity air crack propogation rates were seen to be significantly greater in the weld than in the heat affected zone of a beta processed plus mill annealed extrusion. (Figure 8.2.14.1.9-1). Sump tank water rates were similarly seen to be greater in the weld of a plate which had been stress relieved for 1 hour at 1200°F (Figure 8.2.14.1.9-2). Low humidity air growth rates in the heat affected zone of a plasma arc welded plate, on the other hand, were seen to noticeably greater than those in the weld. (Figure 8.2.14.1.9-3). Wether this reversal of effects is real or not, or may be attributed to the differences in welding procedure was not within the scope of this investigation.

8.2.14.1.10 Welding Procedure - Low humidity air and sump tank water growth rates in the heat affected zones of welded plate were seen to be unaffected by the weld procedure or joint preparation technique, when comparing GTAW standard double U edge butt welds with plasma arc welds with a square butt edge preparation (Figure 8.2.14.1.10 1) and additionally with a GTAW single U edge preparation (Figure 8.2.14.1.10-2). Low humidity air growth rates in the weld bead of a plasma arc weld with a square butt edge preparation were seen to be significantly slower than those in the bead of a GTAW overlay (Figure 8.2.14.1.10-3). This effect may be associated with the observations made in section 8.2.14.1.9.

8.2.14.2 HP-9Ni-4Co - .20C Weldments

All comparisons made in this material represent weldments with a 950°F/2hr. stress-relief. Unless otherwise specified in the figure captions, tests were performed in PTC specimens.

8.2.14.2.1 Cyclic Frequency - Low humidity air fatigue crack growth rates in the weld of this material when tested at 60 cpm were seen to be slightly greater than the fastest of two tests performed at 360 cpm (Figure 8.2.14.2.1-1). There was no apparent cause for the large test-to test variation observed between the two specimens run at 360 cpm.

8.2.14.2.2 Test Temperature - Low humidity air growth rates in the heat affected zone of welded plate were seen to be noticeably greater at ambient temperature than at -65°F (Figure 8.2.14.2.2-1).

8.2.14.2.3 Specimen Thickness - Changing specimen thickness from 0.25" to 0.5" resulted in virtually no effect on the low humidity air fatigue crack growth rates in the heat affected zones of welded plate (Figure 8.2.14.2.3-1). Similarly, increasing the thickness from 0.25" to 0.75", had no affect on the distilled water growth rates in the heat affected zone (Figure 8.2.14.2.3-2)

8.2.14.2.4 R Factor - Low humidity air fatigue crack growth in the weld bead were seen to increase significantly as the R factor was increased from 0.08 to 0.3 and again to 0.5 (Figure 8.2.14.2.4-1). Again, as in section 8.2.14.2.1, there was no apparent reason for the rapid growth rate observed in specimen A552.

8.2.14.2.5 Environment - The results of environmental evaluations on weldments in this material were seen to be inconsistent with observations made in raw material evaluations. In the heat affected zone, for example, growth rates were seen to be very slightly faster in low humidity air than in sump tank water (Figure 8.2.14.2.5-1), and significantly faster, at low delta K levels, than in distilled water (Figure 8.2.14.2.5-2). In the weld, growth rates observed in one low humidity air test were seen to be equivalent to those observed in a 100% humidity test, while second test in low humidity air showed significantly lower growth rates. (Figure 8.2.14.2.5-3) The cause of these inconsistencies was not determined.

8.2.14.2.6 Test Direction - Not Evaluated

8.2.14.2.7 Product Form - There was virtually no difference observed between the low humidity air growth rates in the heat affected zones of welded plate and a welded forged block (Figure 8.2.14.2.7-1).

8.2.14.2.8 Heat Treat Condition - Not evaluated

8.2.14.2.9 Crack Plane Location - Low humidity air fatigue crack growth rates were seen to be noticeably greater in the heat affected zone than in the base metal in welded plate (Figure 8.2.14.2.9-1).

8.2.14.2.10 Weld Procedure - Distilled water fatigue crack growth rates were seen to be significantly greater in the bead of a weld overlay than in the bead of a grindout-reweld. This effect was seen to be true in both the stress relieved and as-welded conditions (Figures 8.2.14.2.10-1 and -2, respectively).

8.2.14.3 PH13-8Mo Weldments

Unless otherwise specified in figure captions, testing was performed in PTC specimens.

8.2.14.3.1 Cyclic Frequency - Not Evaluated.

8.2.14.3.2 Test Temperature - Not Evaluated.

8.2.14.3.3 Specimen Thickness - Not Evaluated.

8.2.14.3.4 R Factor - Lab air fatigue crack growth rates in the weld bead of a welded bar extrusion were seen to be noticeably increased as the R factor was increased from 0.08 to 0.3 (Figure 8.2.14.3.4-1).

8.2.14.3.5 Environment - Growth rates in both the weld bead of a welded extruded bar and the heat affected zone of a welded rolled bar were seen to be significantly increased when test environments were changed from lab air to sump tank water (Figures 8.2.14.3.5-1 and -2).

8.2.14.3.6 Test Direction - Not Evaluated.

8.2.14.3.7 Product Form - Not Evaluated.

8.2.14.3.8 Heat Treat Condition - Not Evaluated.

8.2.14.3.9 Crack Plane Location - Sump tank water growth rates of welded rolled bar in both the weld bead and the heat affected zone were seen to be essentially equivalent (Figure 8.2.14.3.9-1).

8.2.14.3.10 Weld Procedure - Not Evaluated.

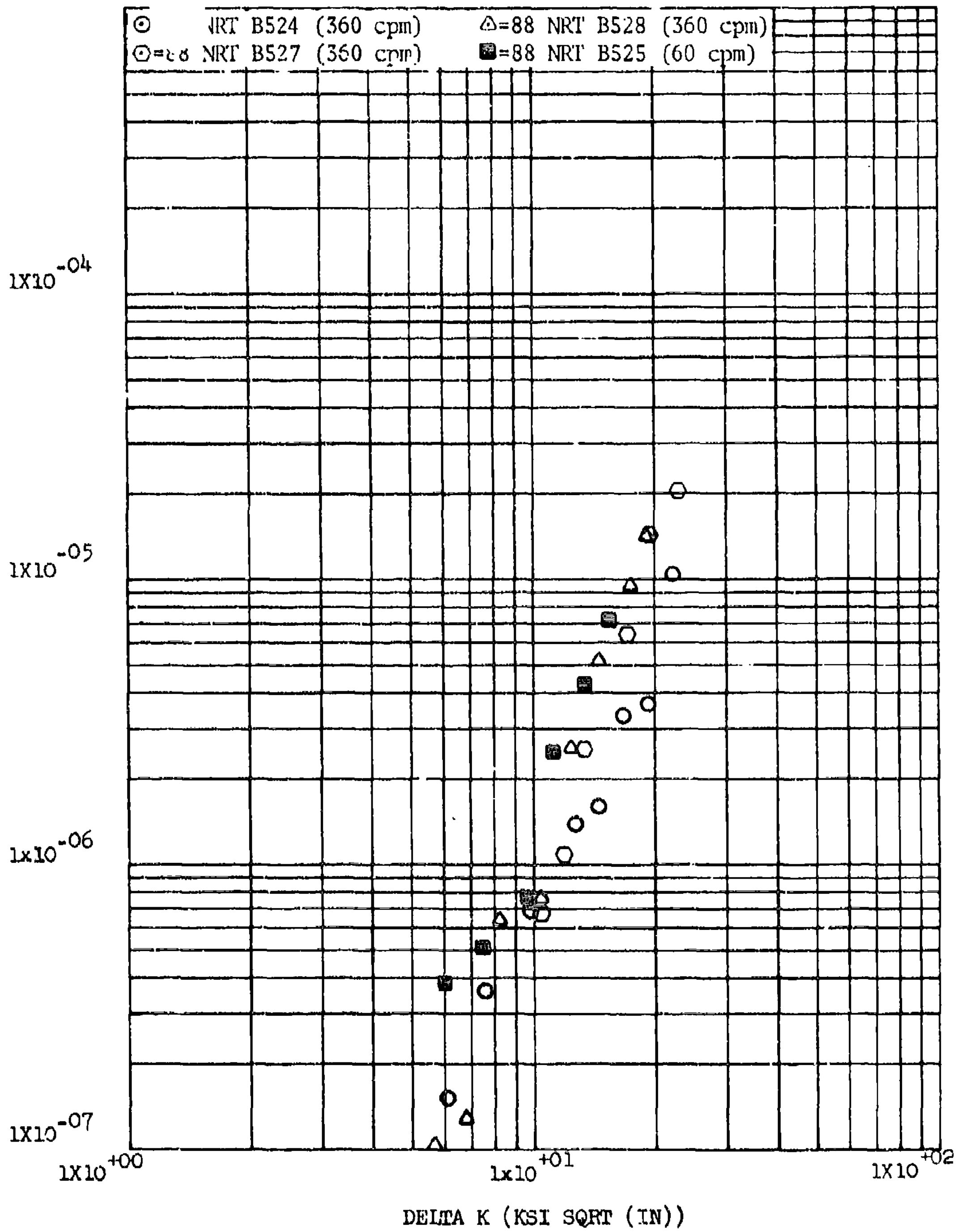

Figure 8.2.14.1.1-1 Effect of cyclic frequency on LHA-FCGR in HAZ of welded Ti-6Al-4V plate at R.T., R=0.08, in RT Direction

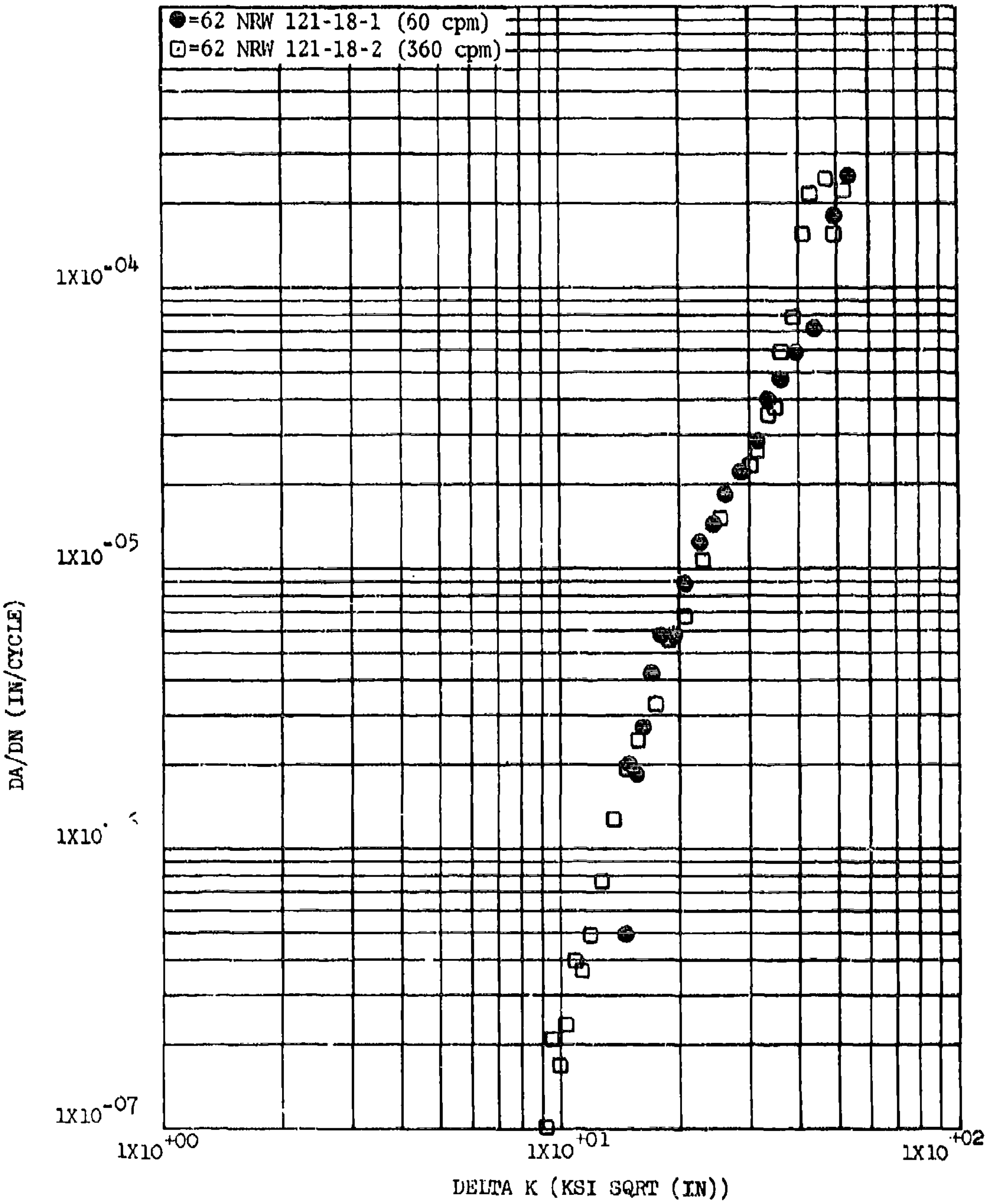

Figure 8.2.14.1.1-2 Effect of cyclic frequency on LHA-FCGR in weld of Ti-6Al-4V plate (MA pre-weld) at R.T., R=0.08, in RW Direction (CT Specimens)

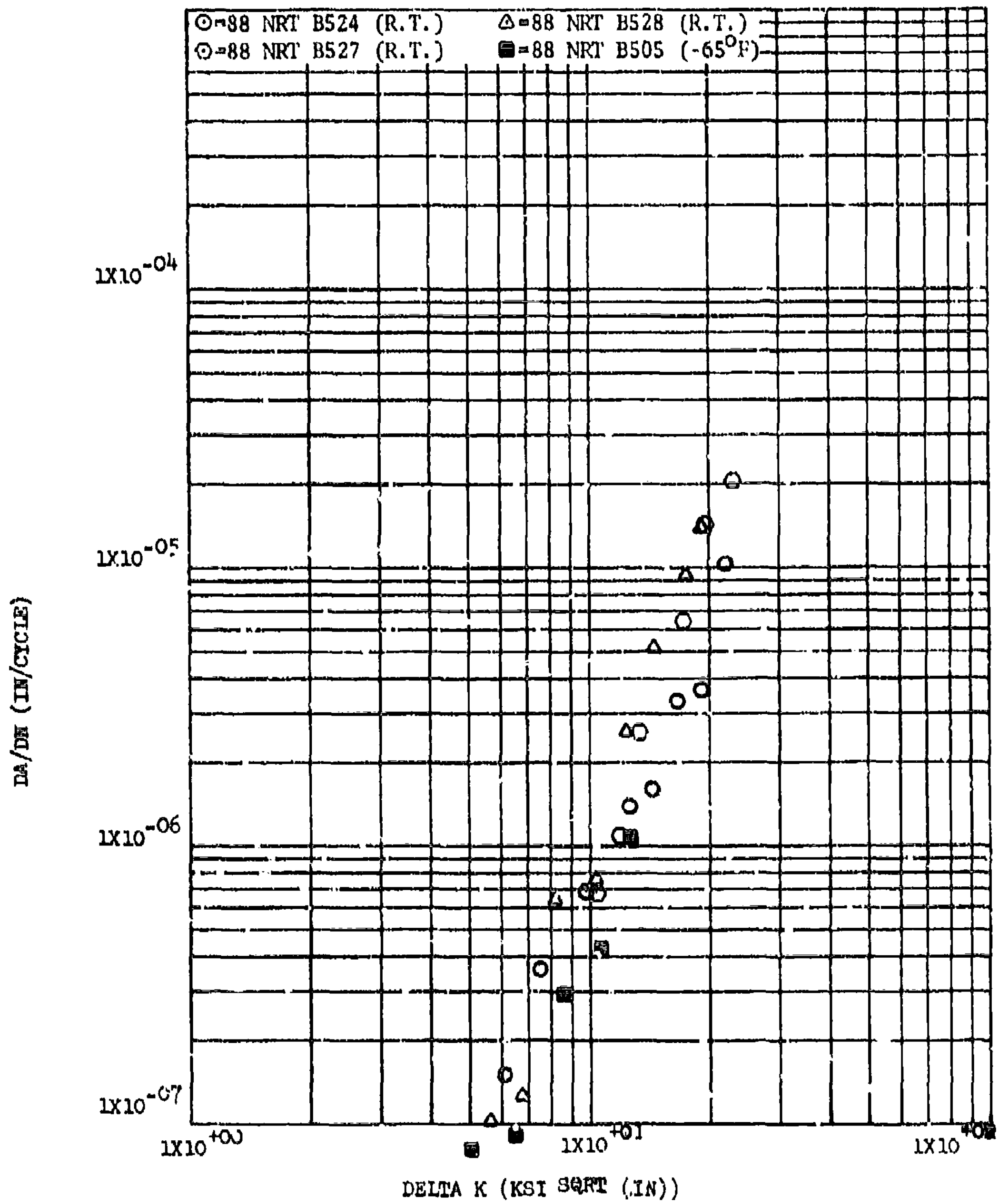

Figure 8.2.14.1.2-1 Effect of test temperature on LHA-FCGR in HAZ of welded Ti-6Al-4V plate at R=0.08, 360 cpm in RT Direction

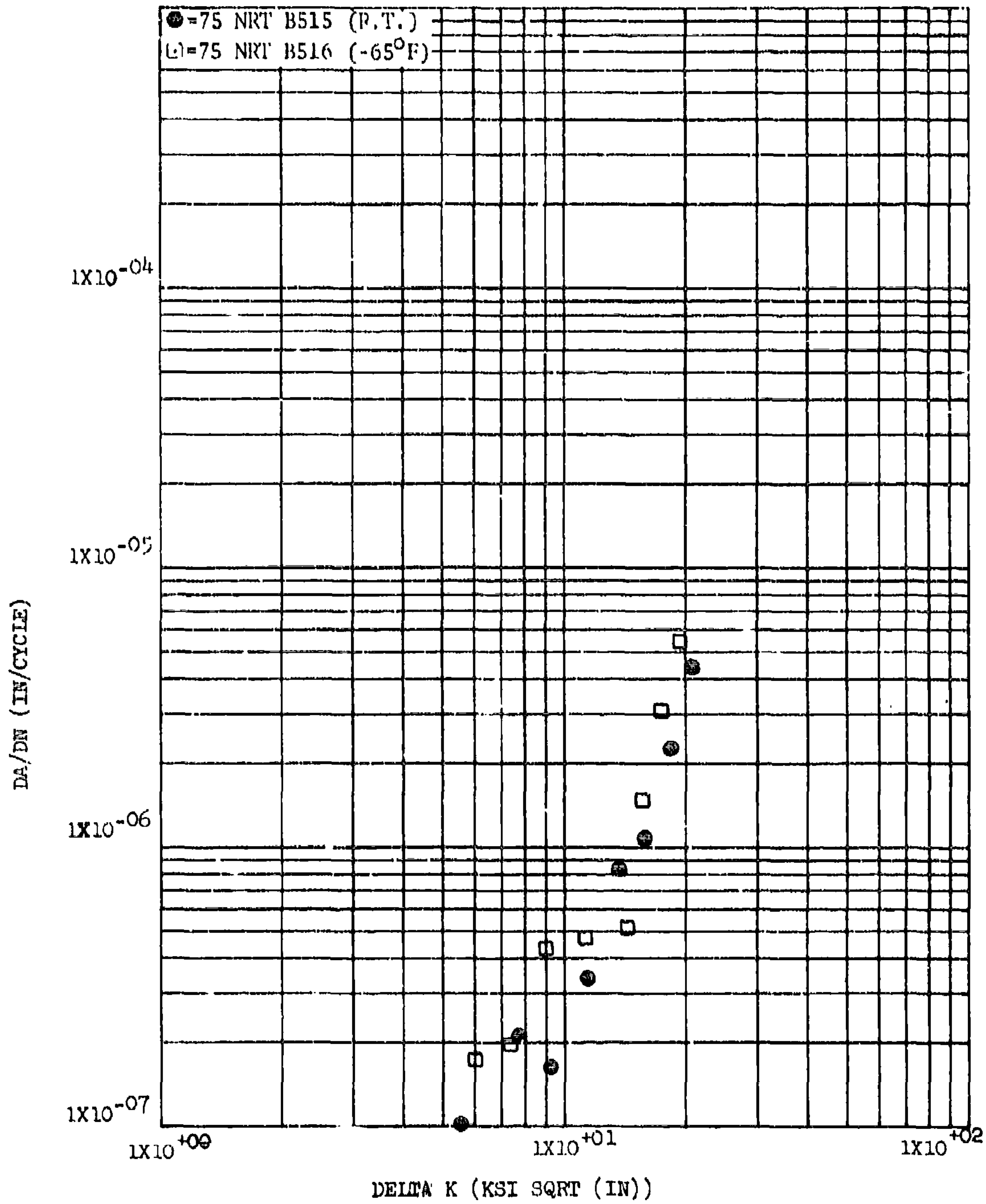

Figure 8.2.14.1.2-2 Effect of test temperature on LHA-FCGR in HAZ of welded Ti-6Al-4V beta processed plus mill annealed extrusion at R=0.08, 360 cpm in RT Direction

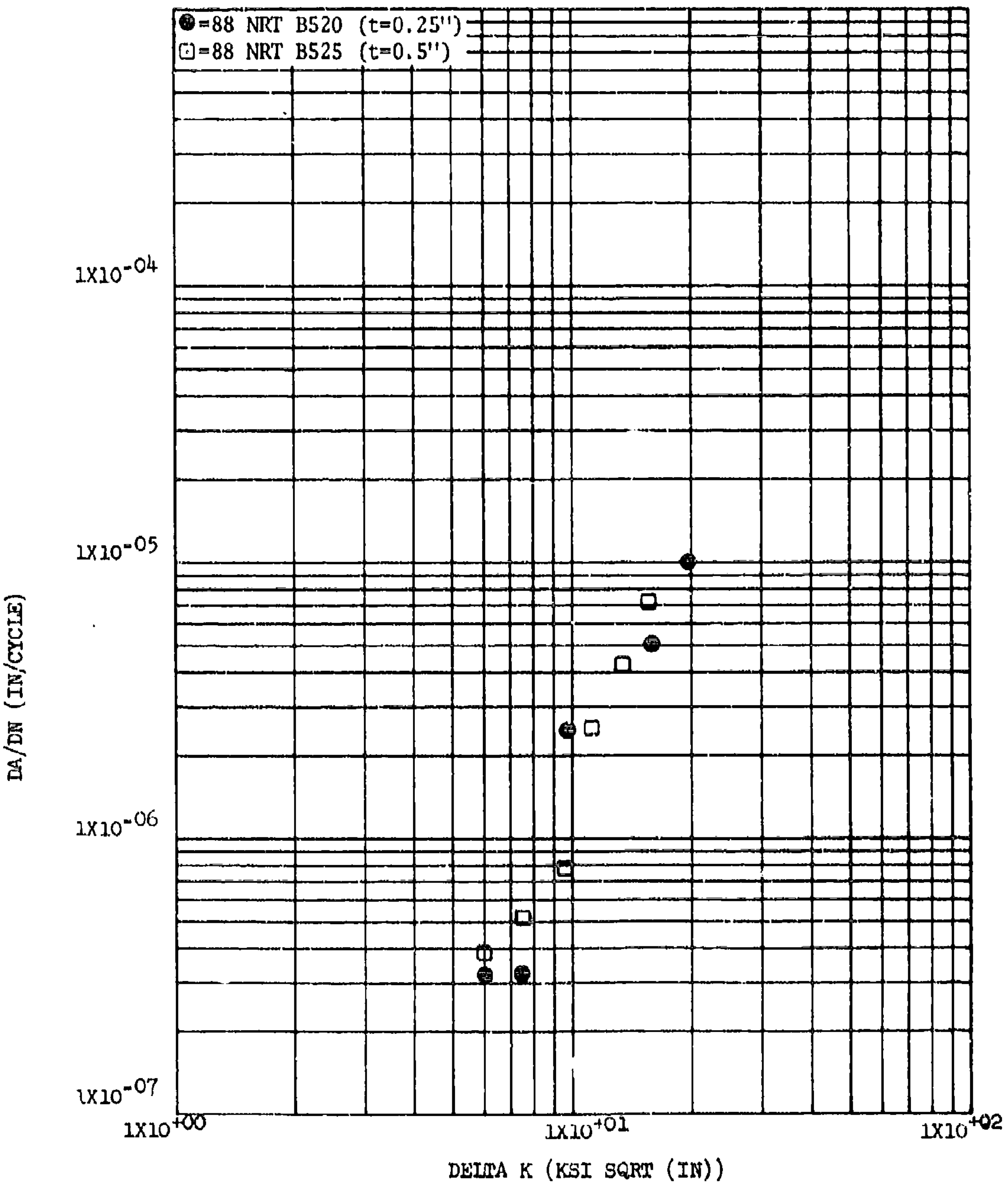

Figure 8.2.14.1.3-1 Effect of specimen thickness on LHA-FCGR in HAZ of welded Ti-6Al-4V plate at R.T., R=0.08, 60 cpm in RT Direction

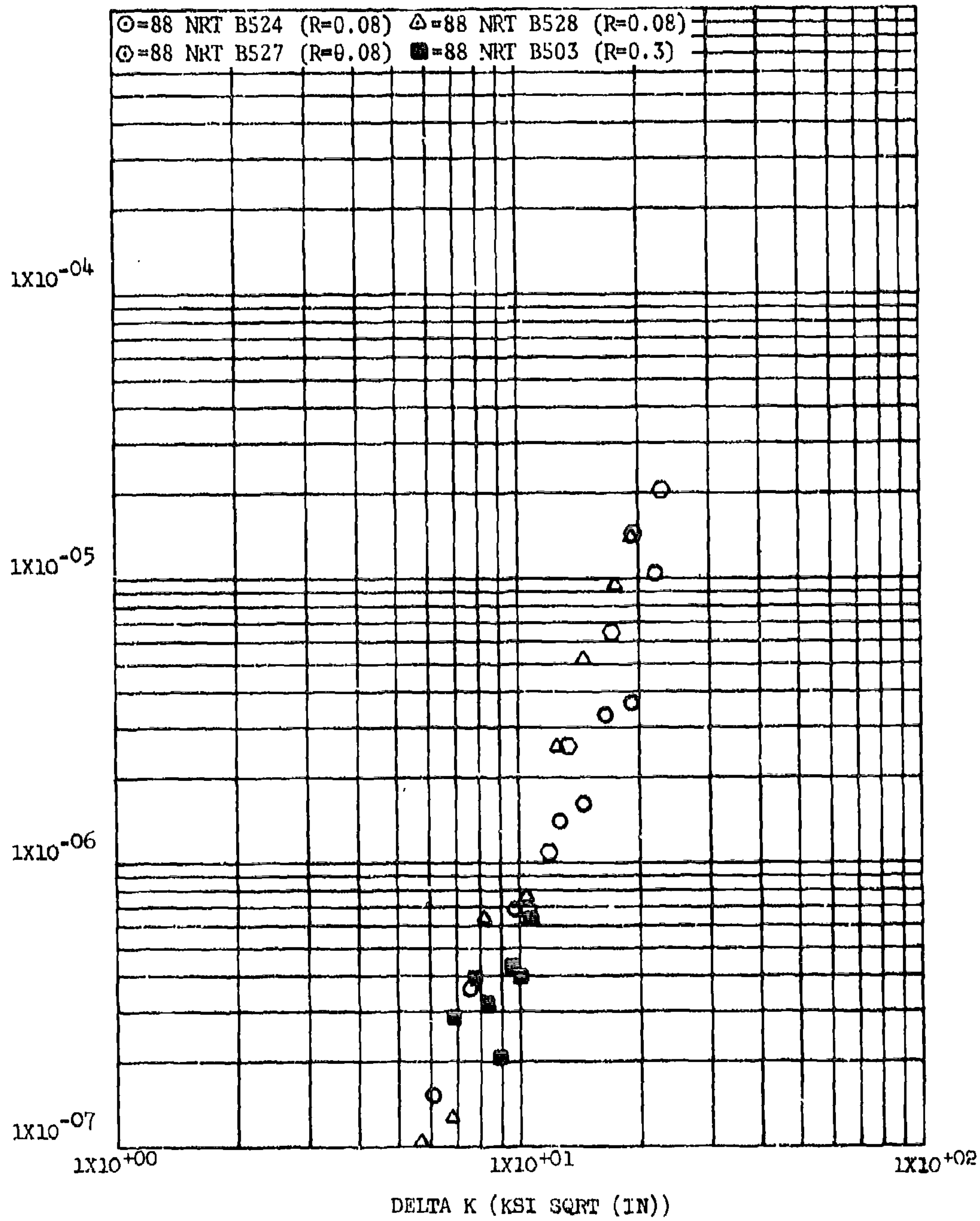

Figure 8.2.14.1.4-1 Effect of R factor on LHA-FCGR in HAZ of welded Ti-6Al-4V plate at R.T., 360 cpm in RT Direction

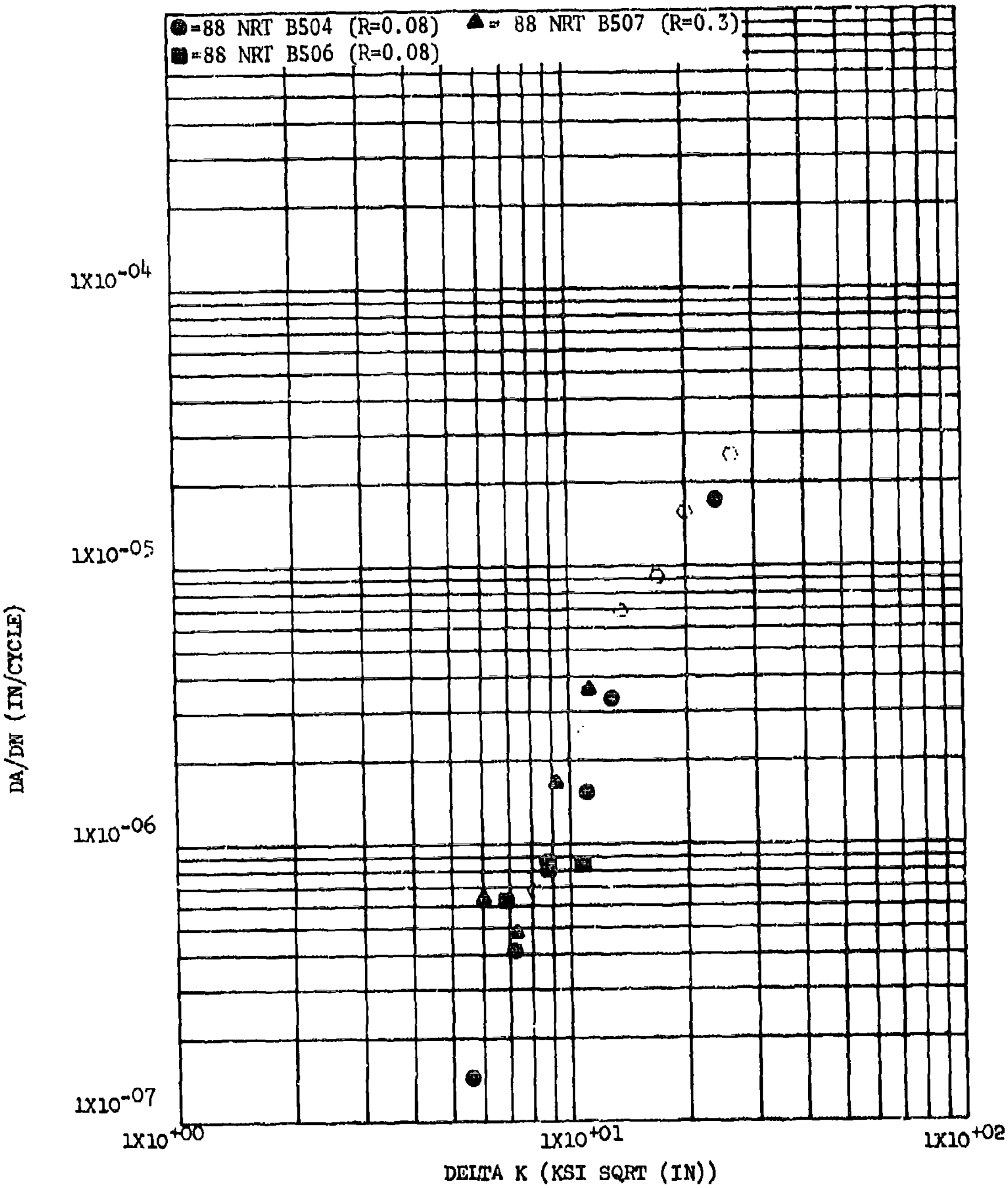

Figure 8.2.14.1.4.2 Effect of R factor on STW-FCGR in HAZ of welded Ti-6Al-4V plate at R.T., 60 cpm in RT Direction

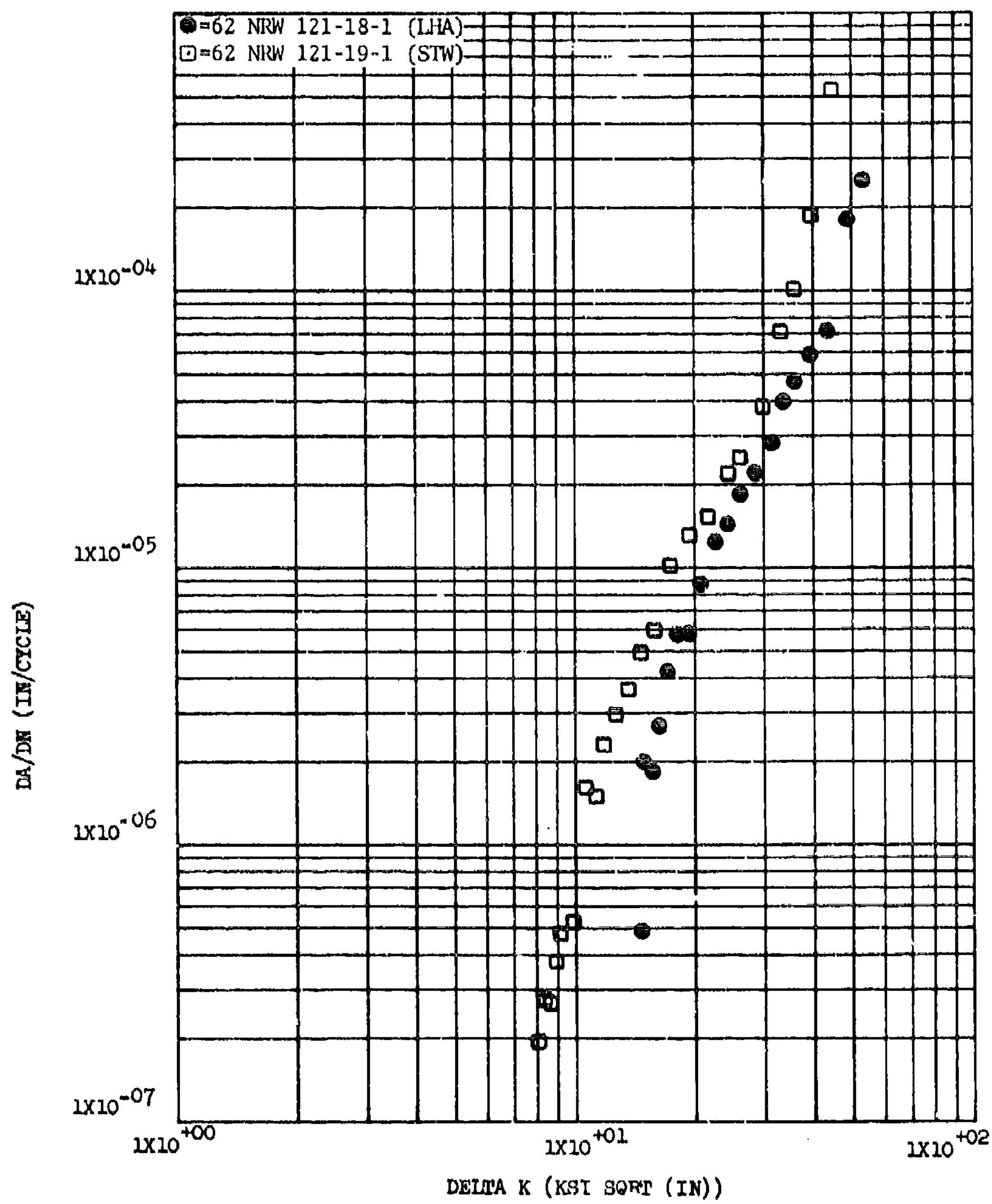

Figure 8.2.14.1.5-1 Effect of environment on FCGR in weld of Ti-6Al-4V plate (MA pre-weld) at R.T., R=0.08, 60 cpm in RW Direction (CT Specimens)

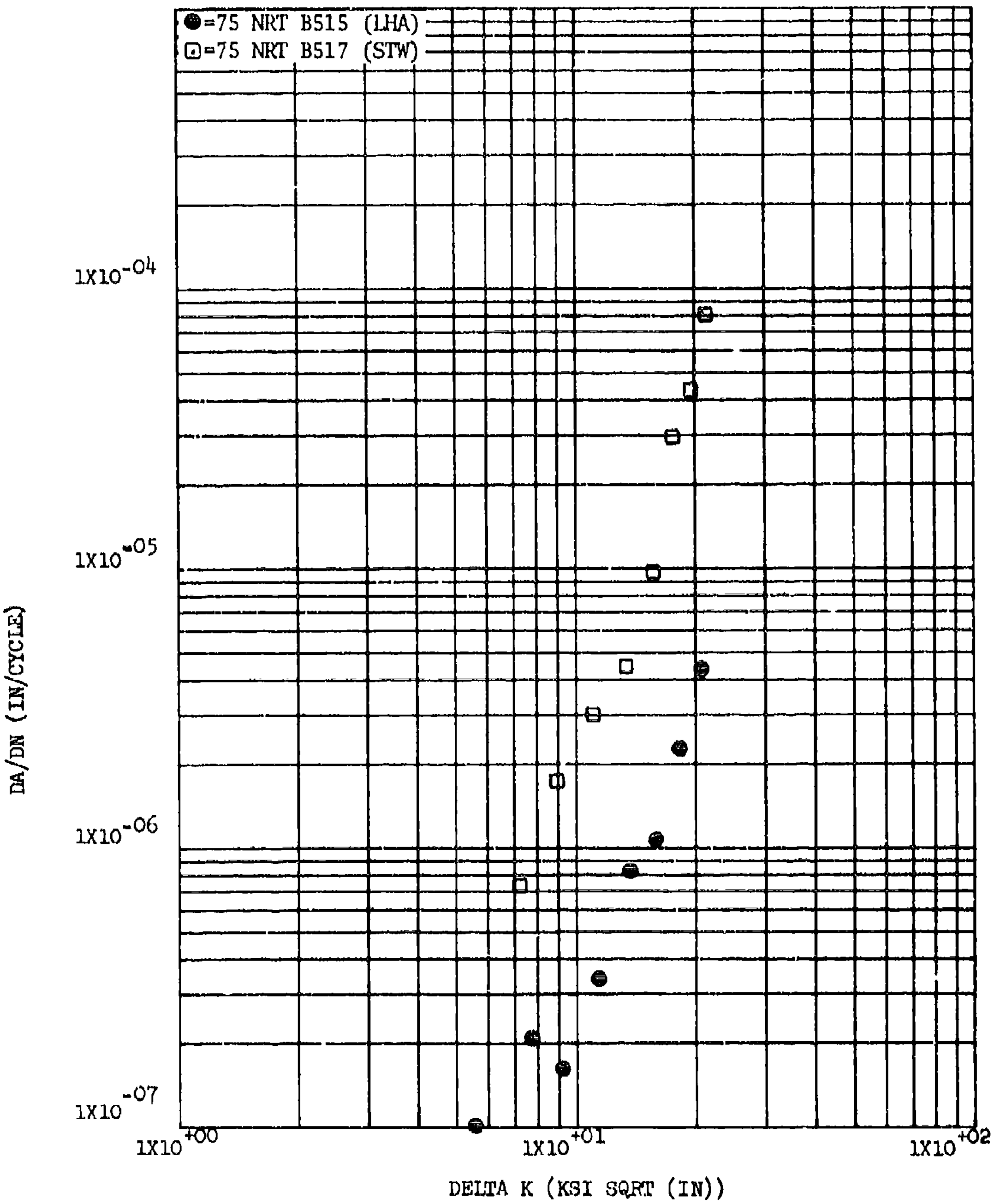

Figure 8.2.14.1.5-2 Effect of environment on FCGR in HAZ of welded Ti-6Al-4V beta processed plus mill annealed extrusion at R.T., R=0.08, in RT Direction

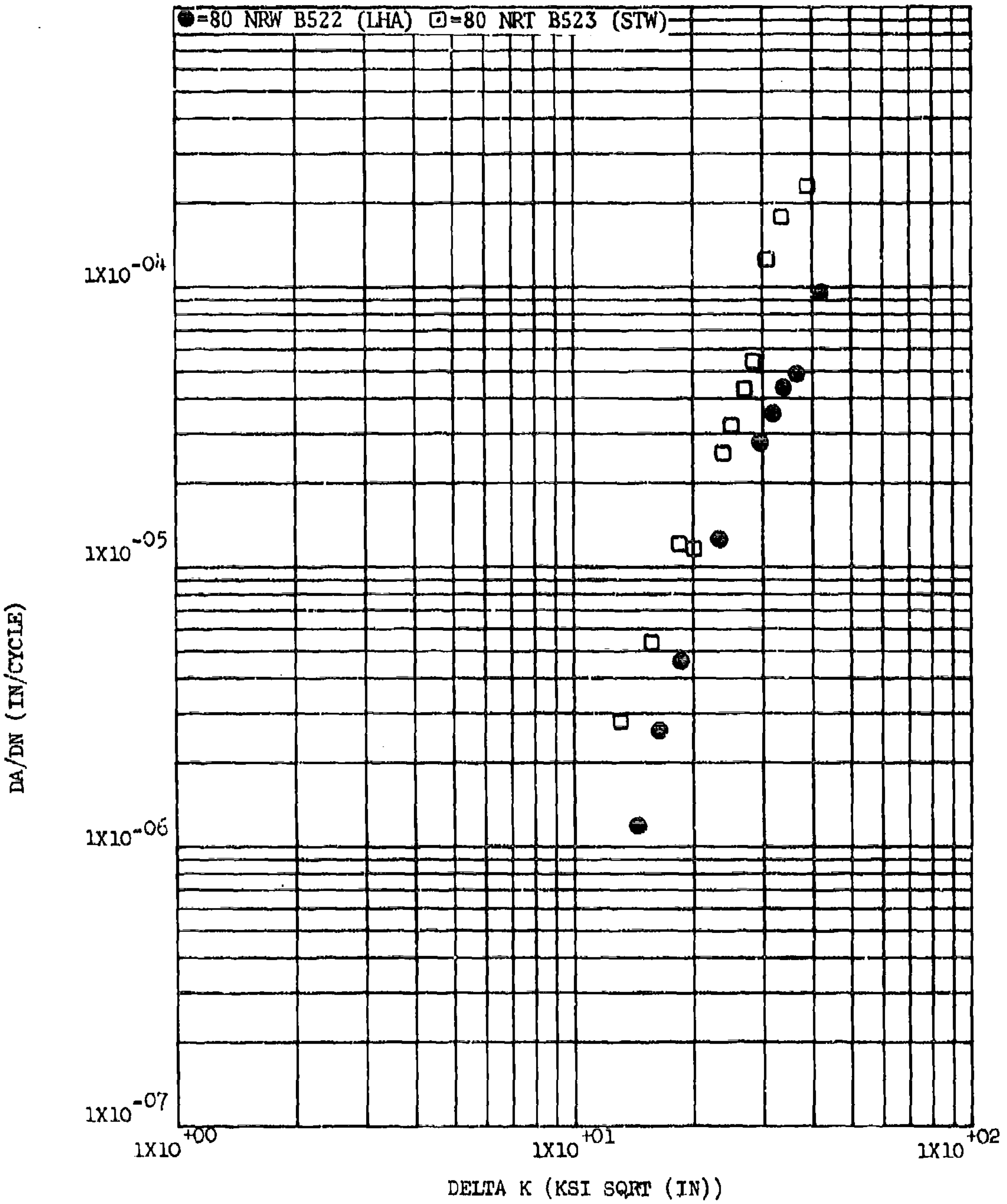

Figure 8.2.14.1.5-3 Effect of environment on FCGR in HAZ of welded Ti-6Al-4V sheet (MA pre-weld) at R.T., R=0.08, 60 cpm in RW Direction (CCT Specimens)

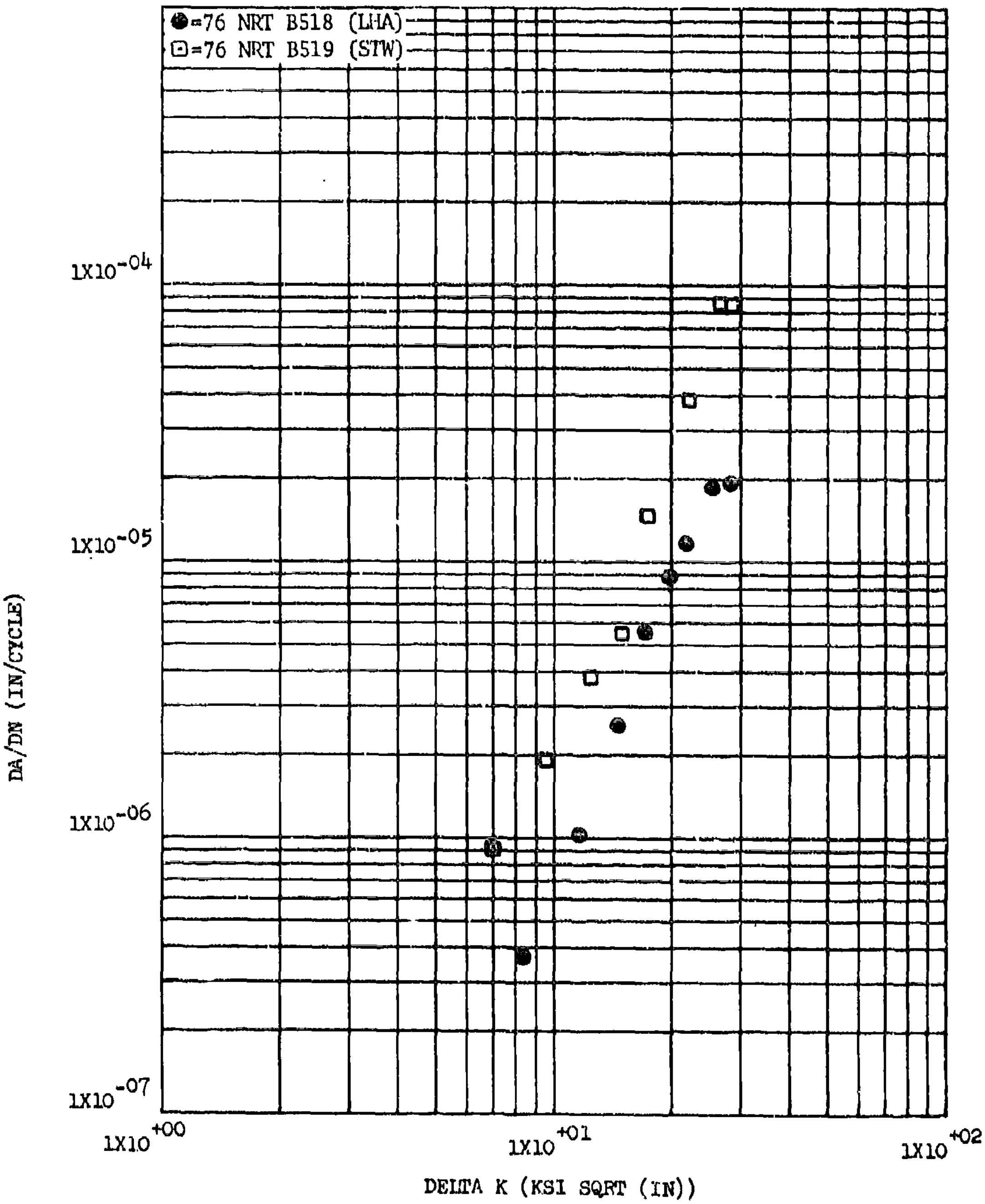

Figure 8.2.14.1.5-4 Effect of environment on FCGR in HAZ of Ti-6Al-4V plate at R.T., R=0.08, 60 cpm in RT Direction

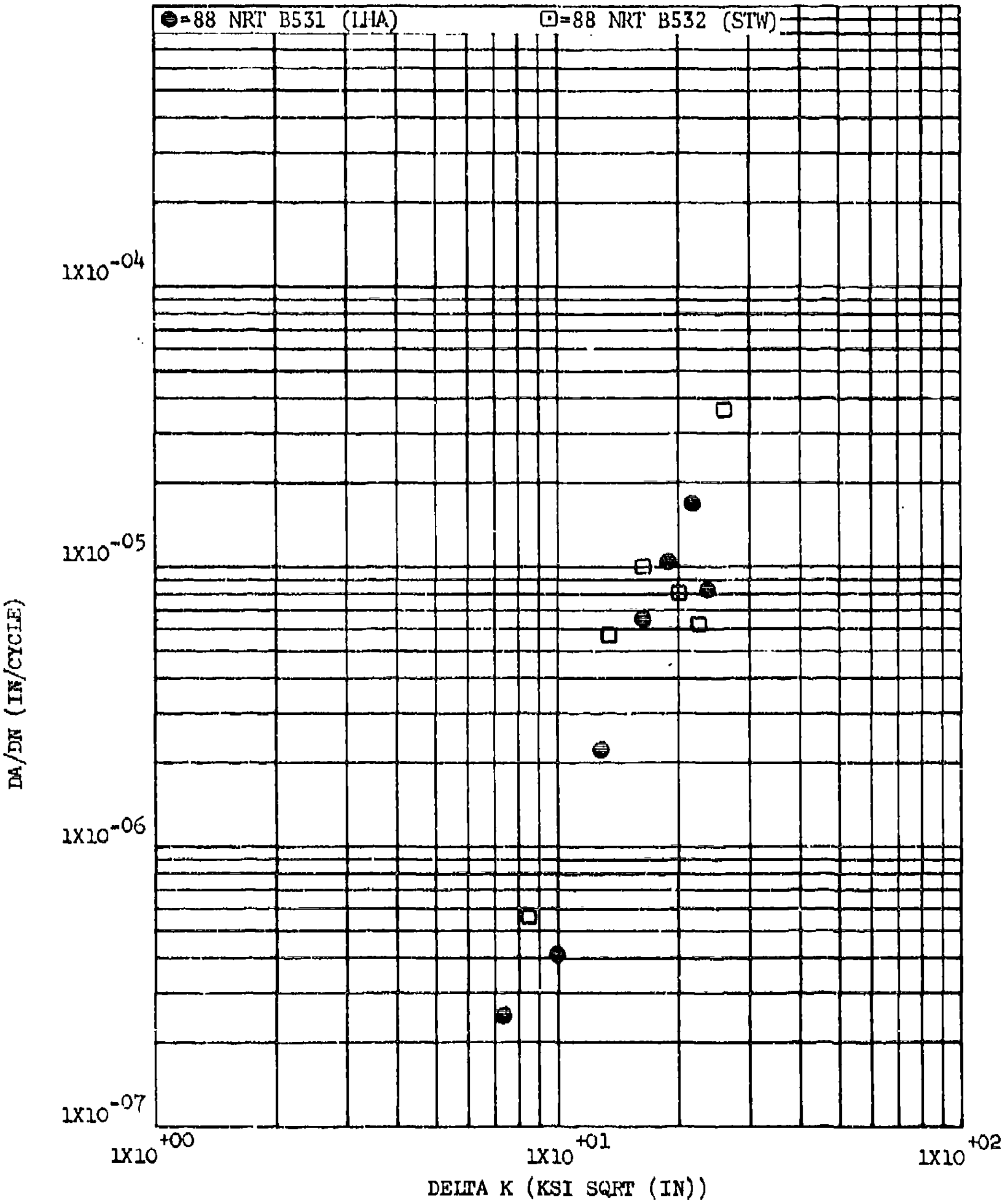

Figure 8.2.14.1.5-5 Effect of environment on FCGR in HAZ of PAW Ti-6Al-4V plate at R.T., R=0.08, 360 cpm in RT Direction

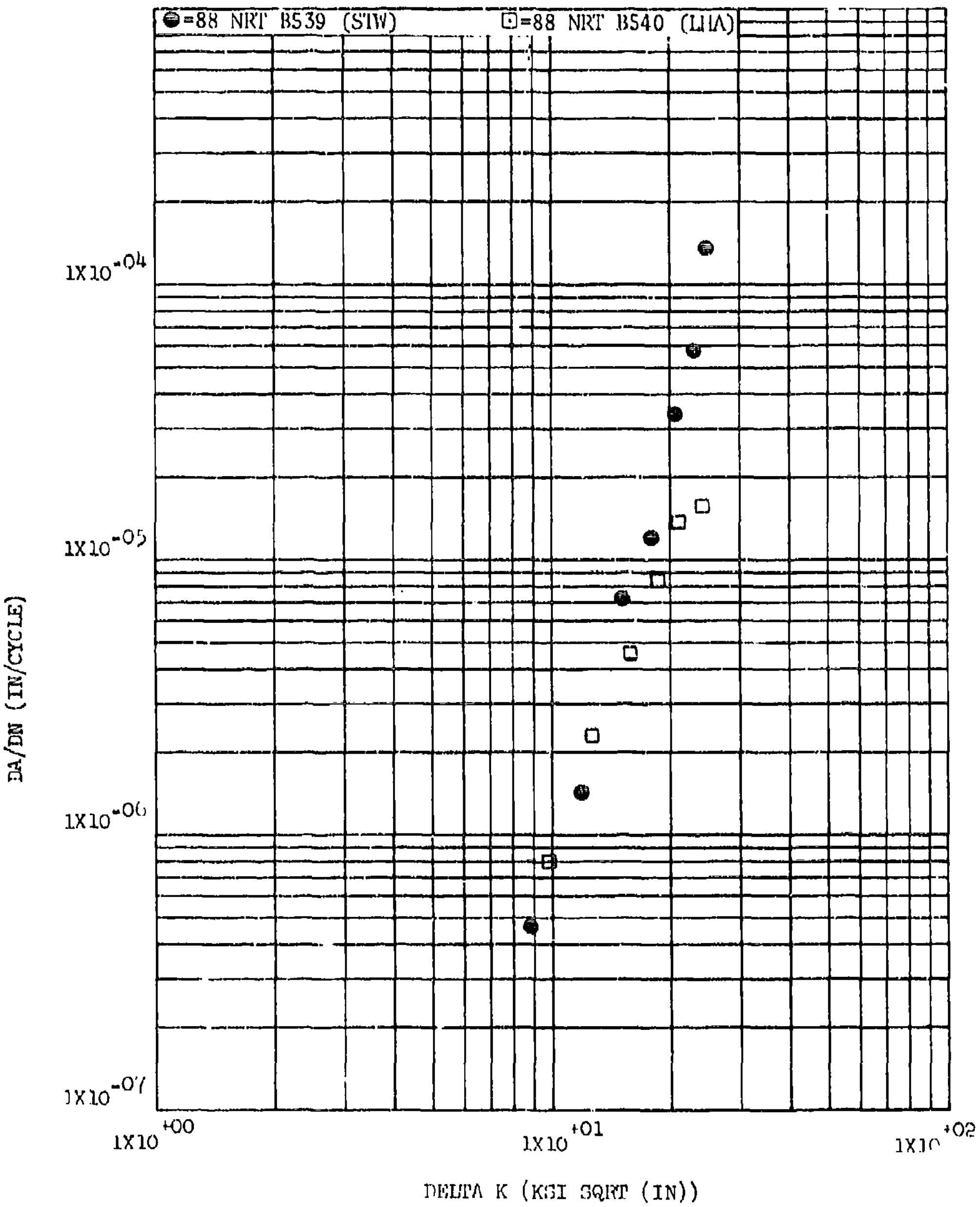

Figure 8.2.14.1.5-6 Effect of environment on FCGR in HAZ of welded + 1400°F/1 hr stress relieved Ti-6Al-4V plate at R.T., R=0.08, in RT Direction

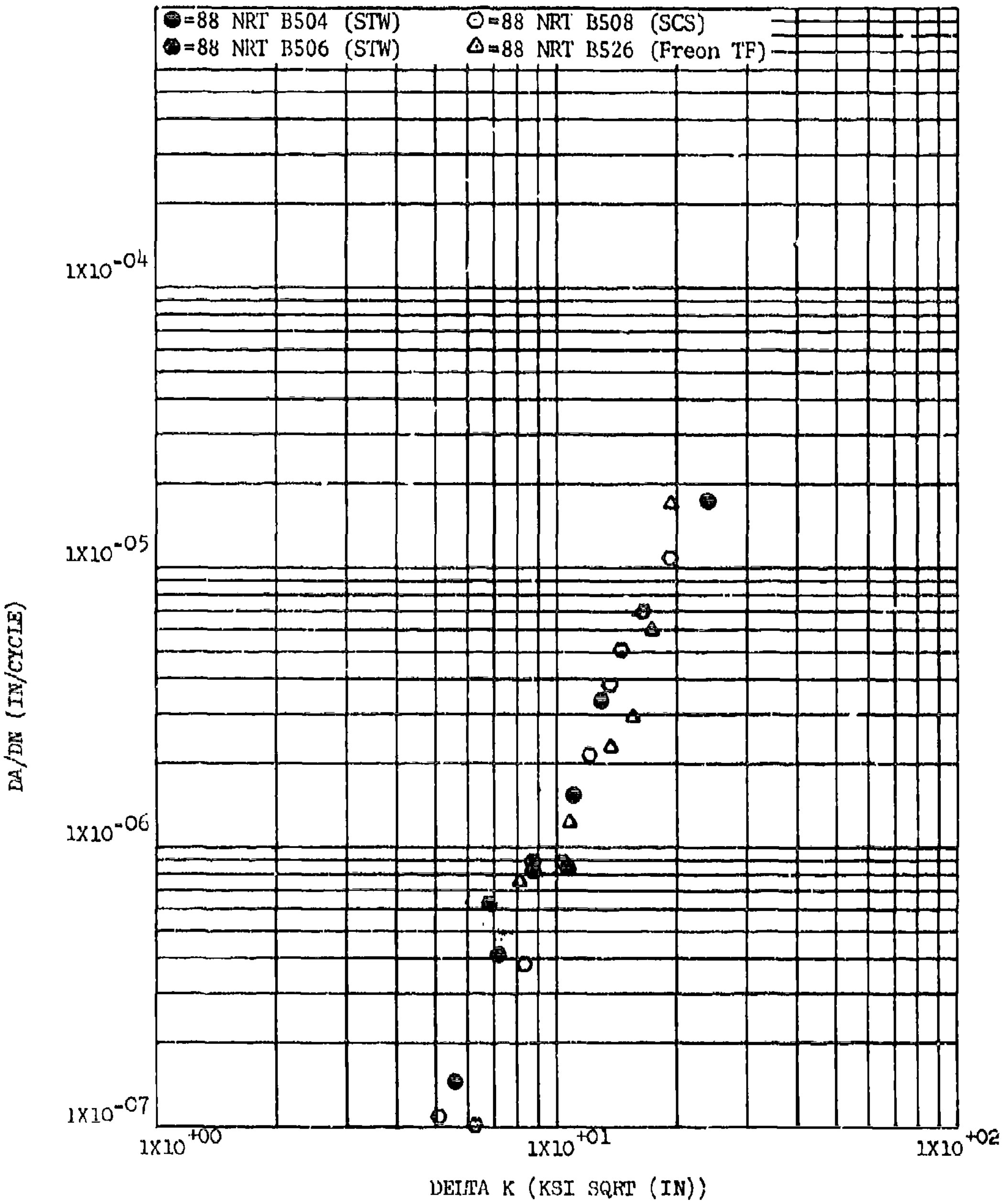

Figure 8.2.14.1.5-7 Effect of environment on FCGR in HAZ of welded Ti-6Al-4V plate at R.T., R=0.08, 60 cpm in RT Direction

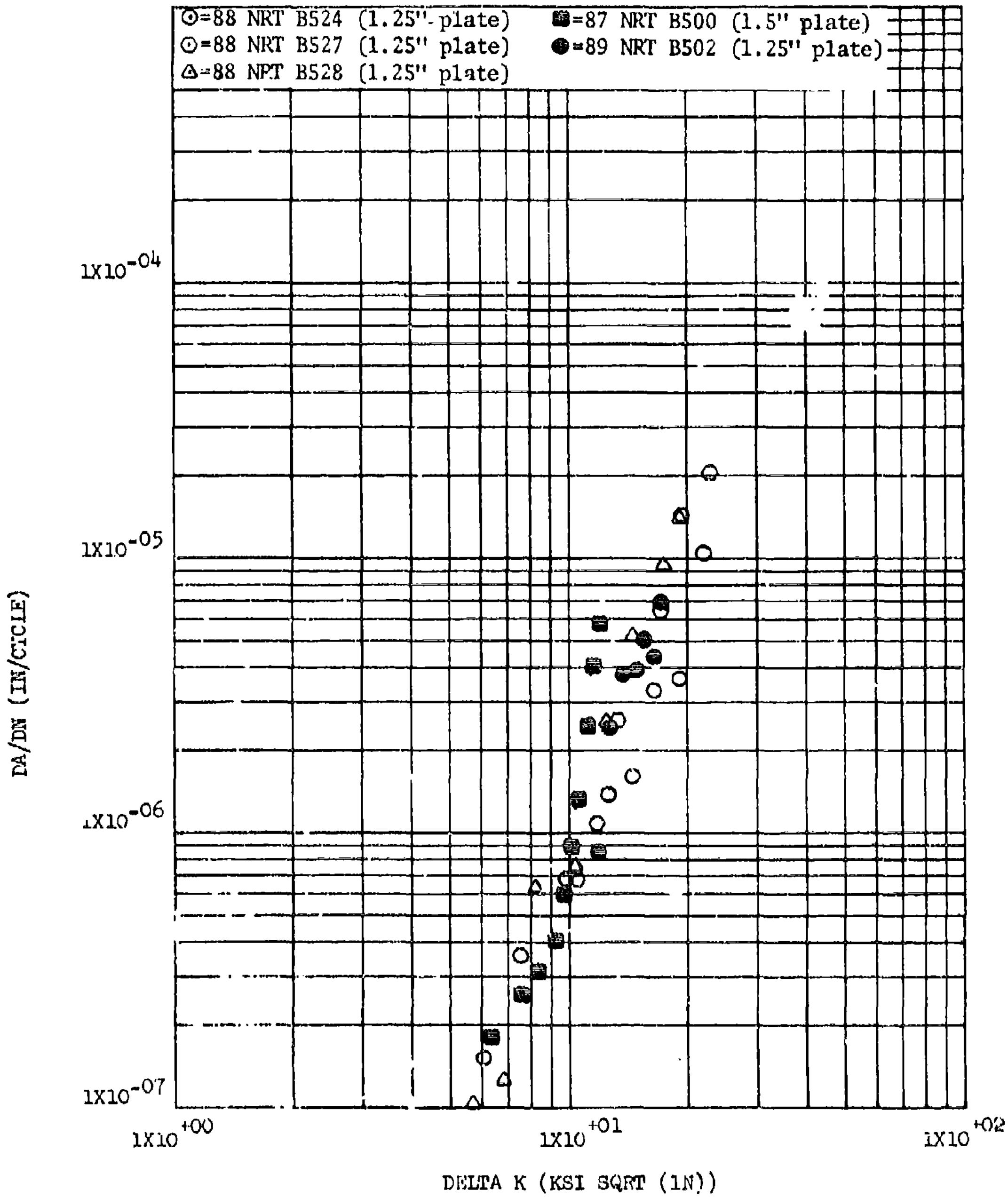

Figure 8.2.14.1.6-1 Effect of product form (material variances) on LHA-FCGR in HAZ of welded Ti-6Al-4V plate at R.T., R=0.08, 360 cpm in RT Direction

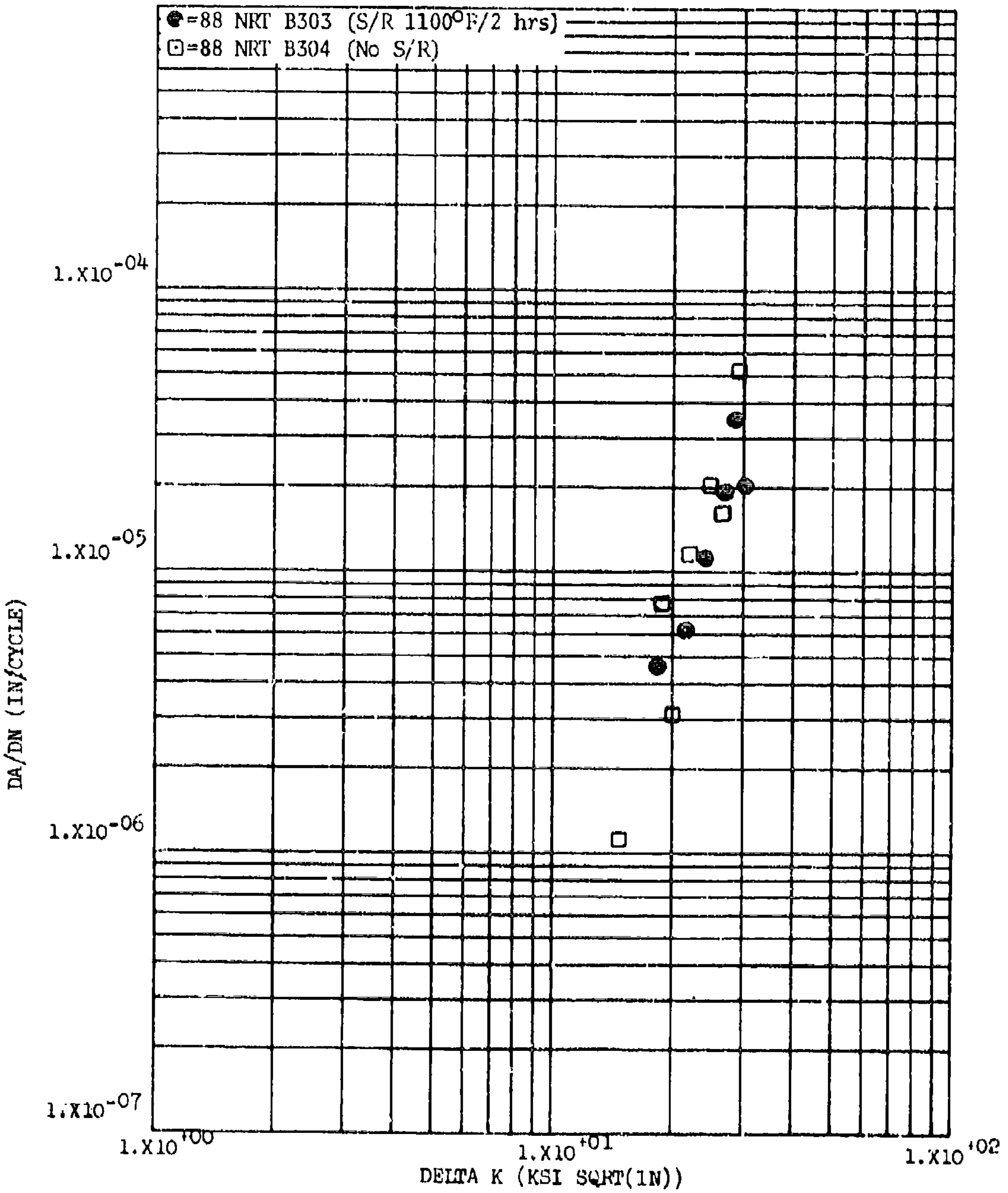

Figure 8.2.14.1.8-1 Effect of post-weld stress relief on SIW-FCGR in weld bead of grindout reweld in Ti-6Al-4V plate at R.T., R=0.08, 60 cpm, in RT Direction

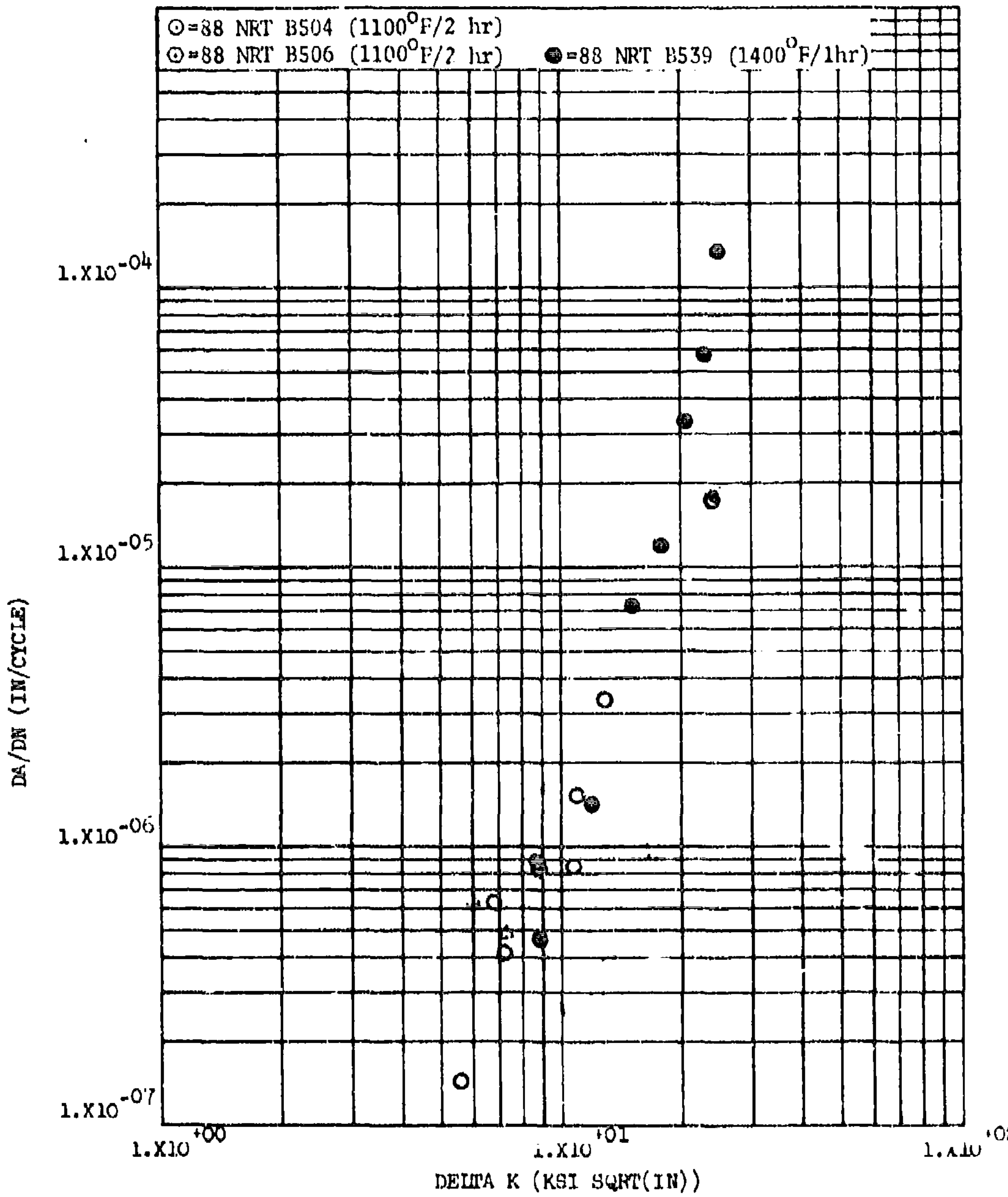

Figure 8.2.14.1.8-2 Effect of post-weld stress relief on STW-FCGR in HAZ of welded Ti-6Al-4V plate at R.T., R=0.08, 60 cpm in RT Direction

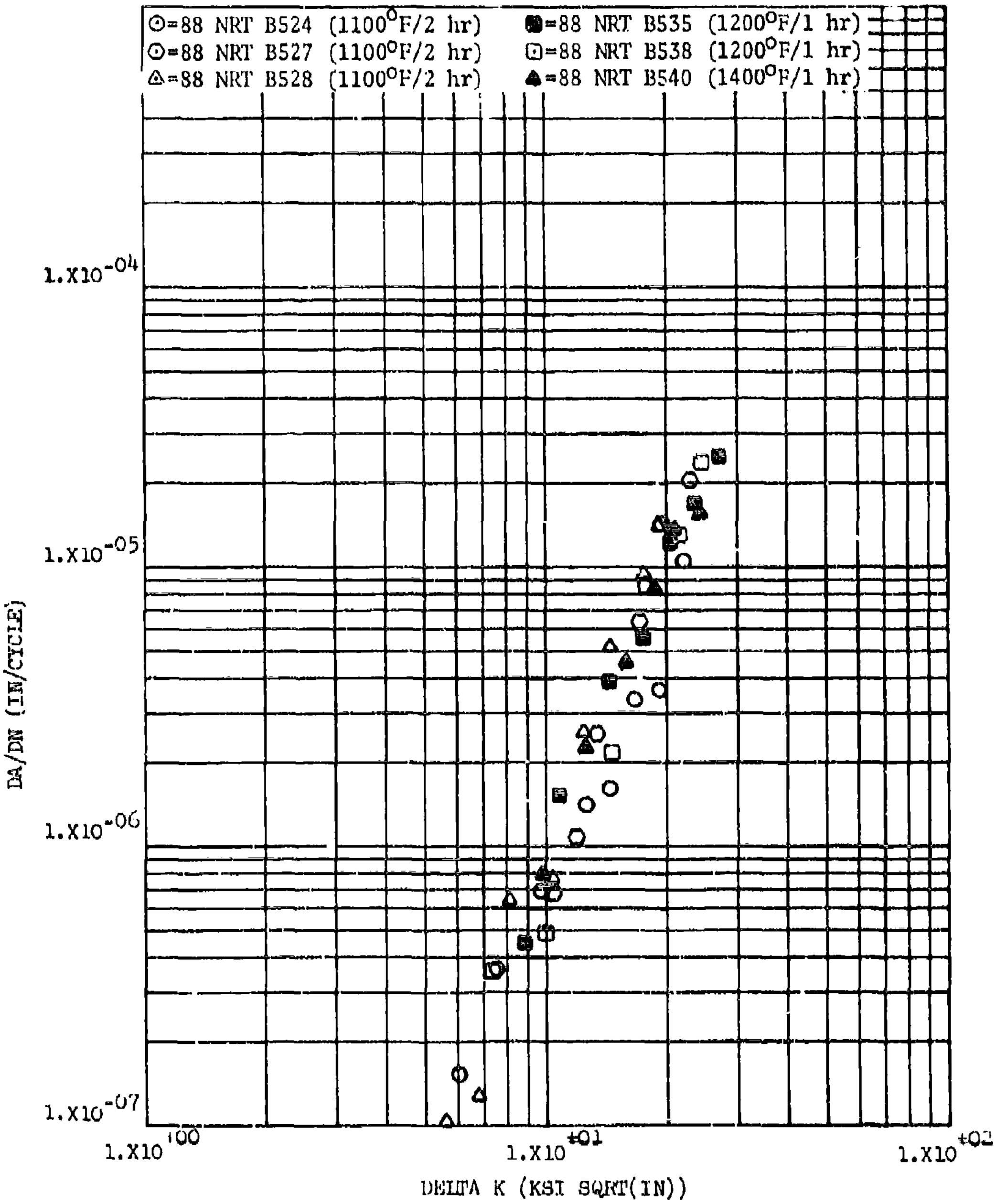

Figure 8.2.14.1.8-3 Effect of post-weld stress relief on LHA-FCGR in HAZ of welded Ti-6Al-4V plate at R.T., R=0.08, 360 cpm in RT Direction

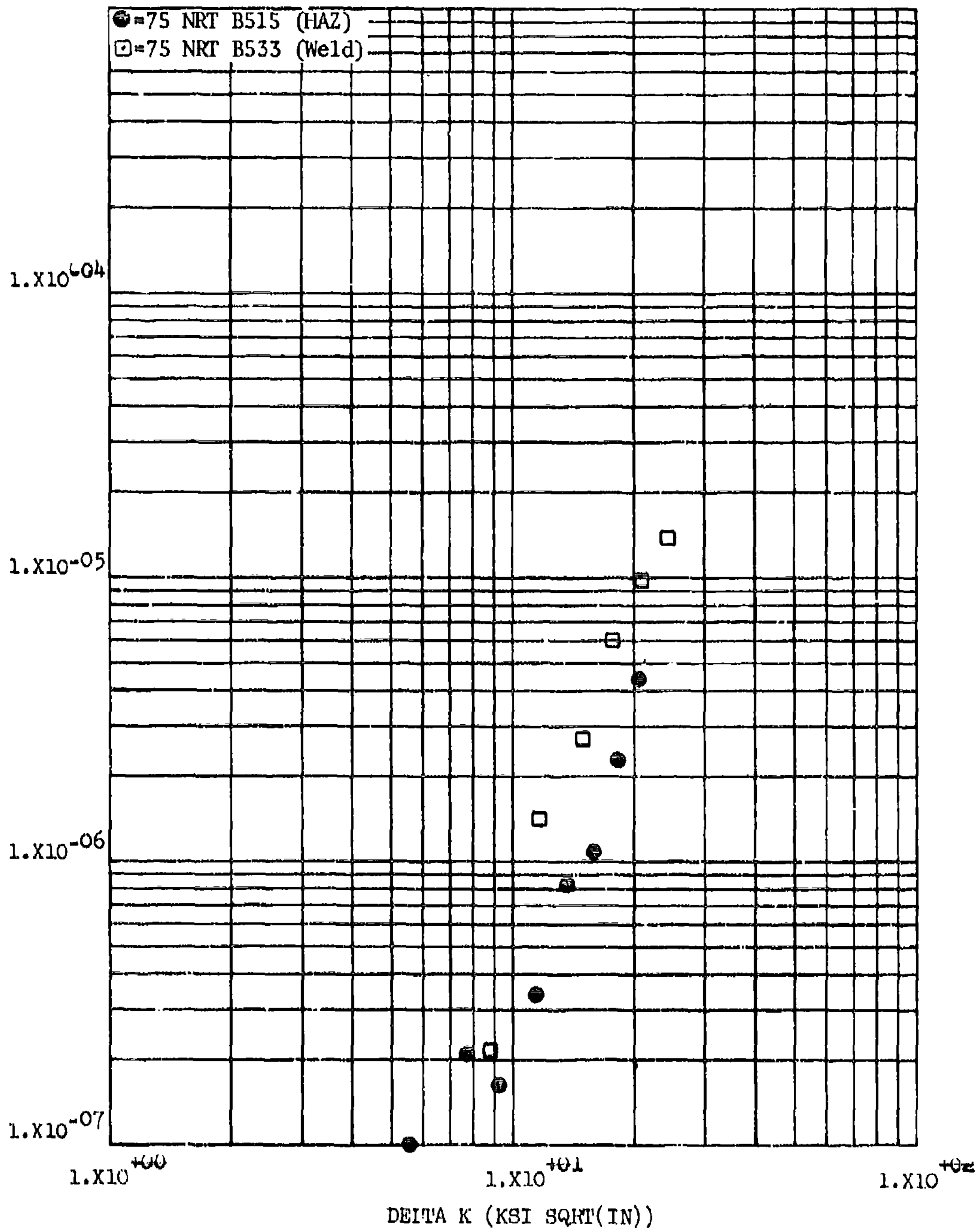

Figure 8.2.14.1.9-1 Effect of crack plane location on LHA-FCGR in welded Ti-6Al-4V beta processed plus mill annealed extrusion at R.T., R=0.08, 360 cpm in RT Direction

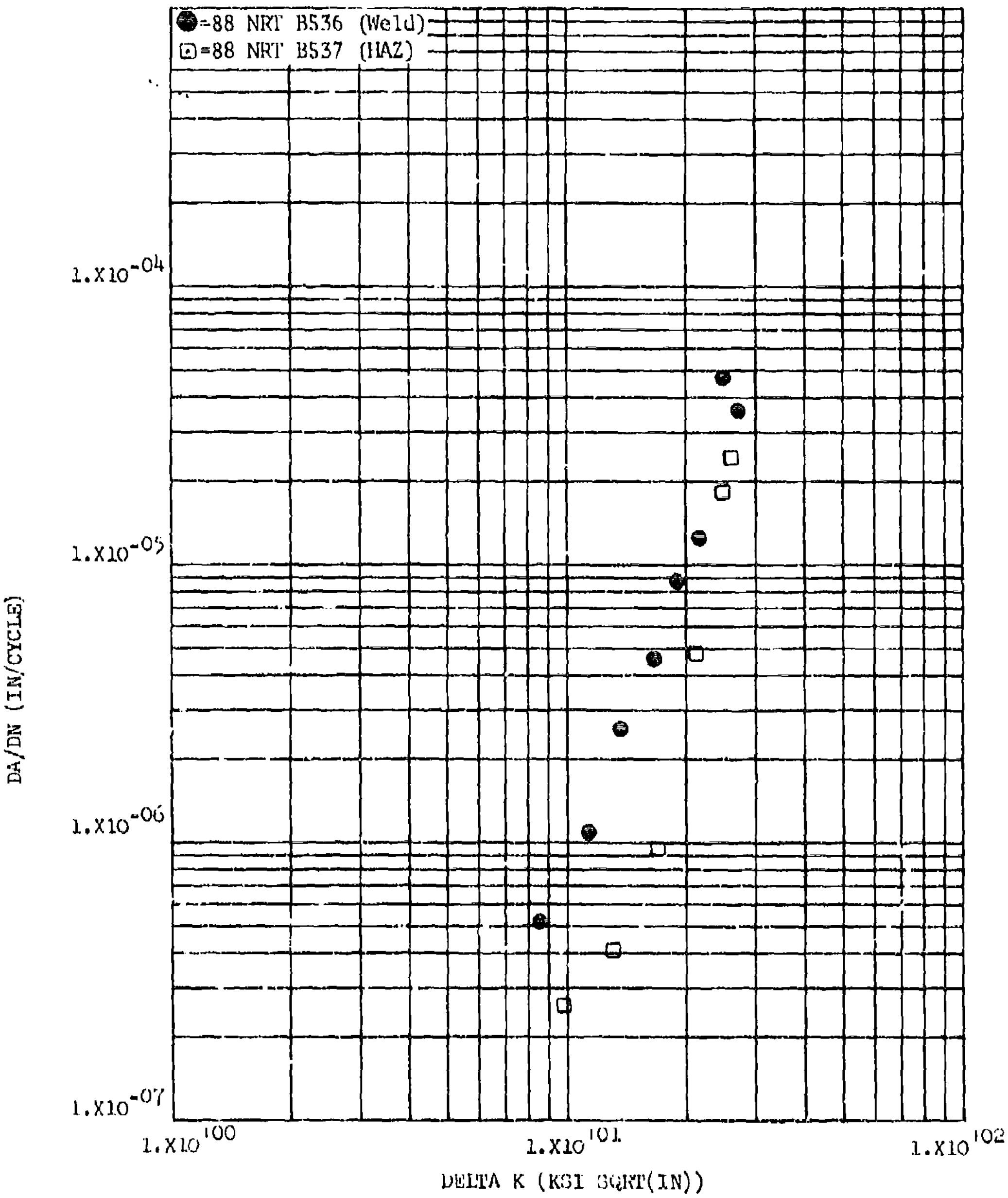

Figure 8.2.14.1.9-2 Effect of crack plane location on STW-FCGR in welded + 1200°F/1 hr. stress relieved Ti-6Al-4V plate at R.T., R=0.08, 60 cpm in RT Direction

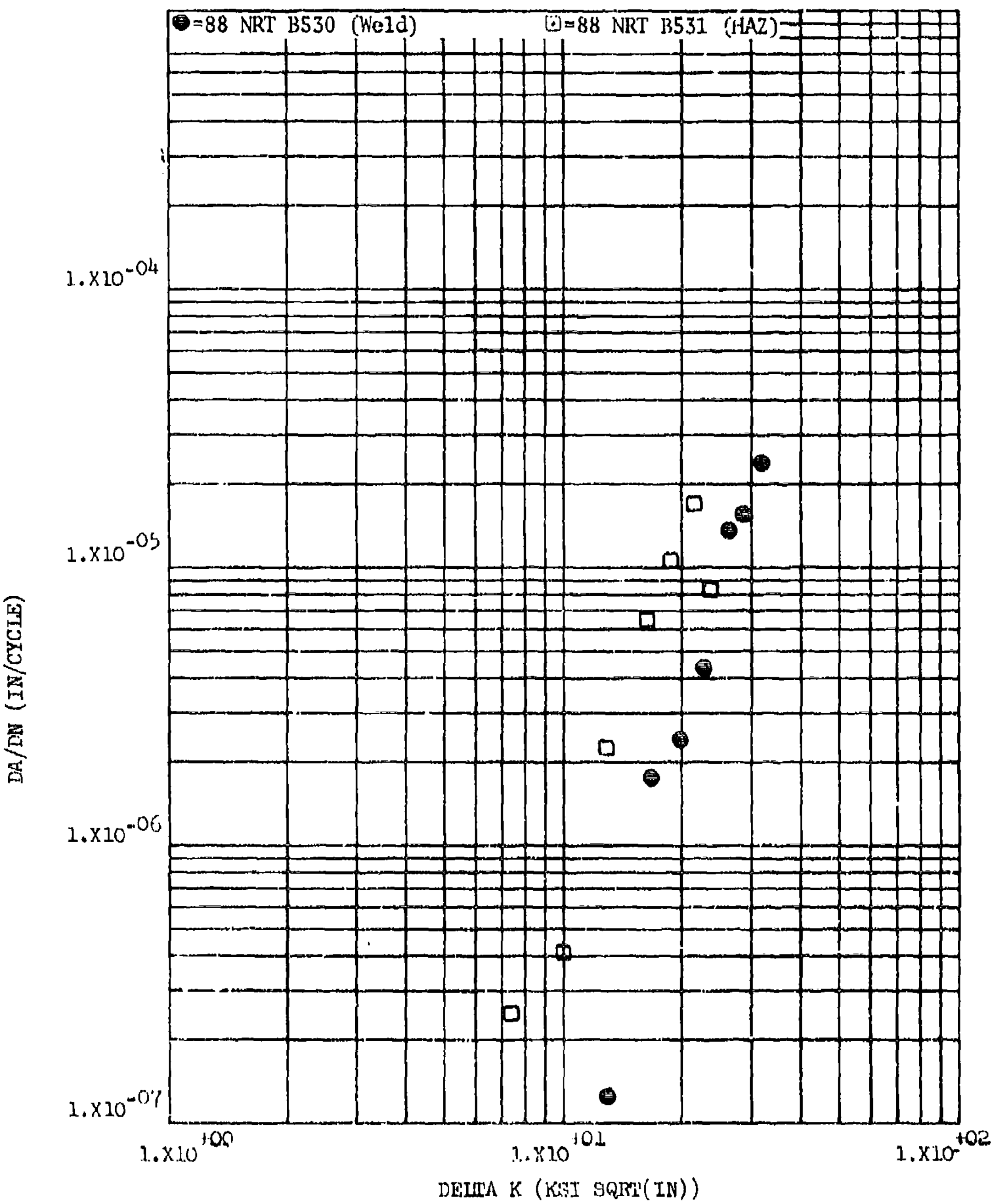

Figure 8.2.14.1.9-3 Effect of crack plane location on LHA-FCGR in PAW Ti-6Al-4V plate at R.T., R=0.08, 360 cpm in RT Direction

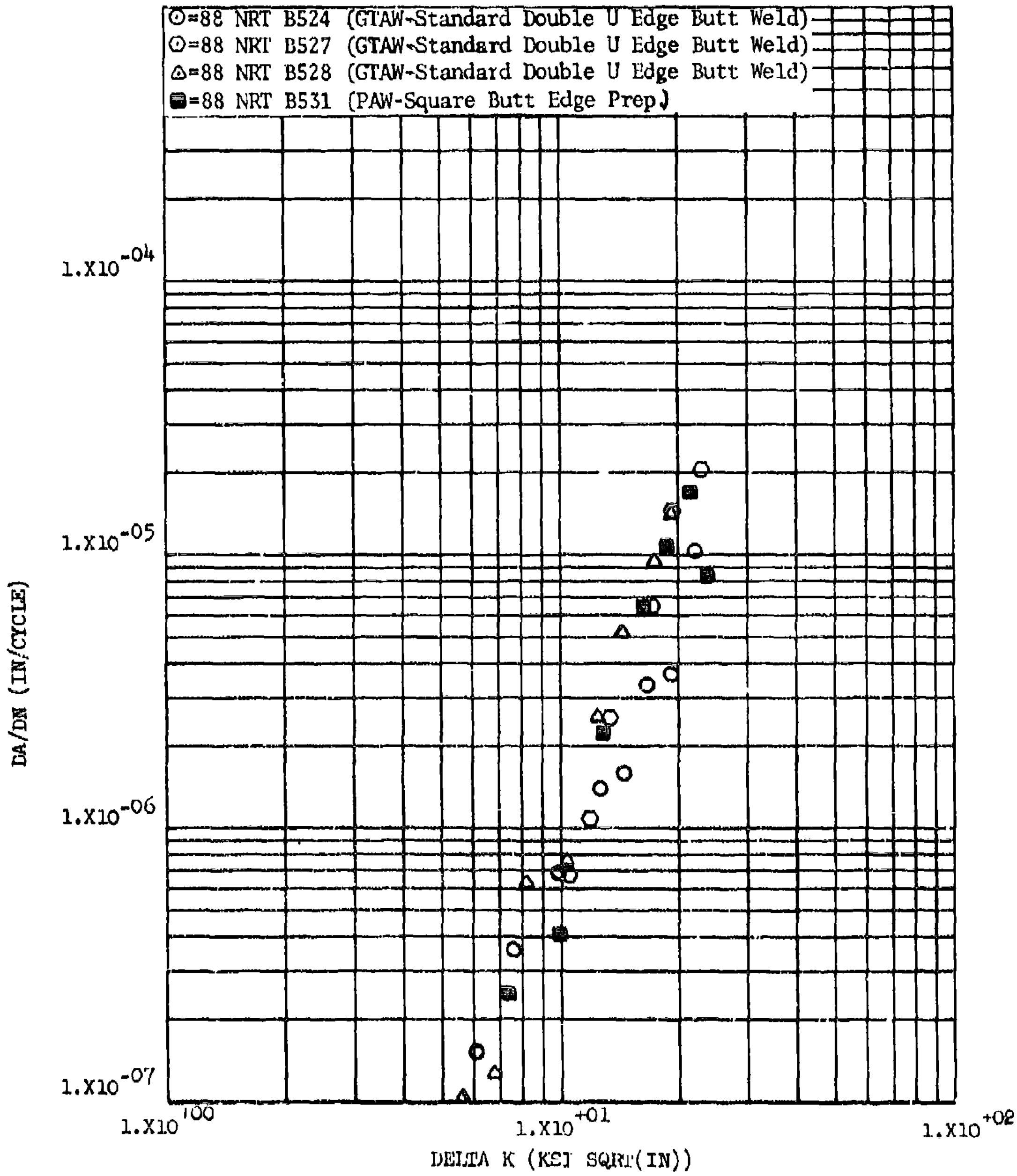

Figure 8.2.14.1.10-1 Effect of welding procedure on LHA-FCGR in HAZ of welded Ti-6Al-4V plate at R.T., R=0.08, 360 cpm in RT Direction

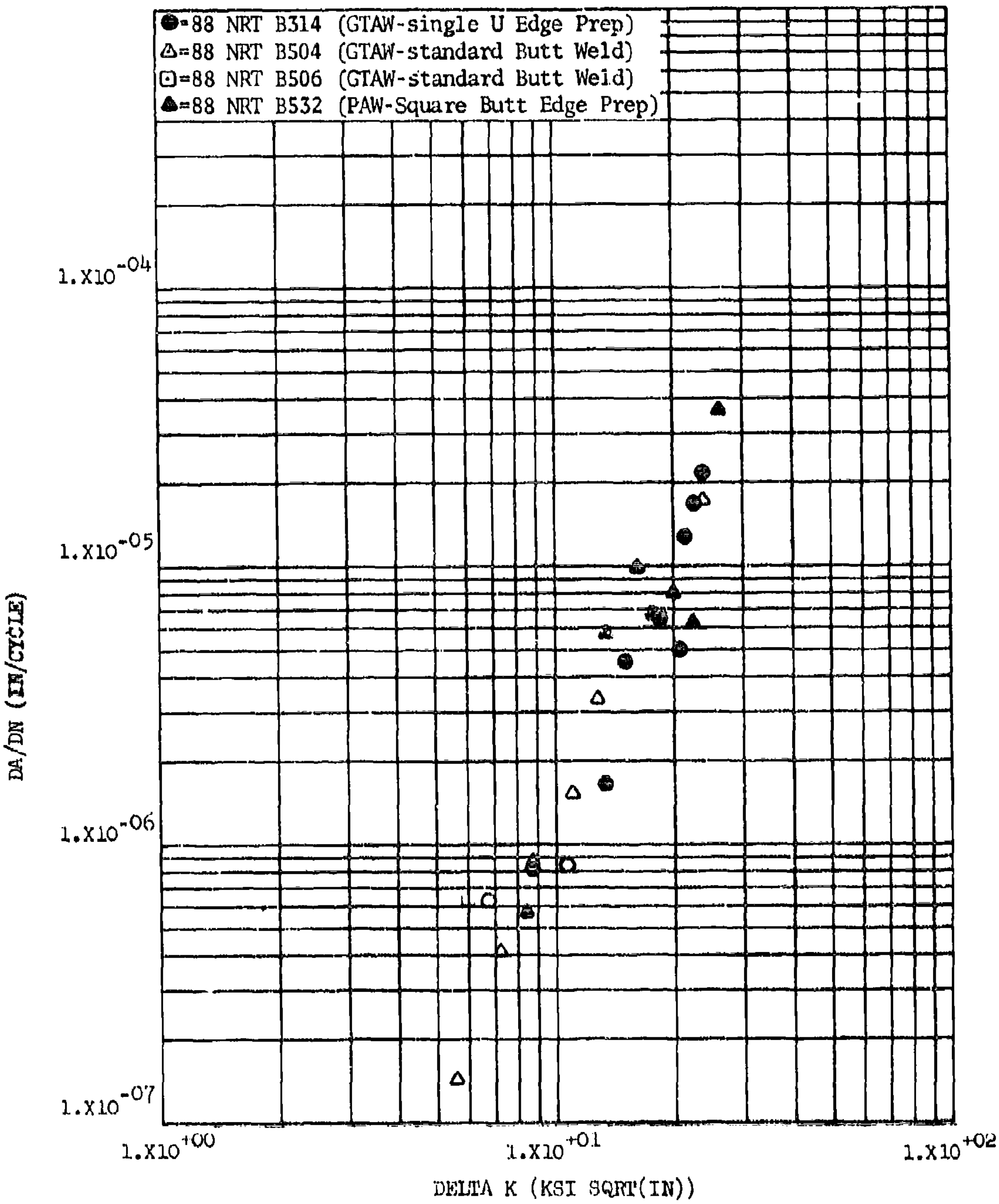

Figure 8.2.14.1.10-2 Effect of welding procedure on STW-FCGR in HAZ of welded Ti-6Al-4V plate at R.T., R=0.08, 60 cpm in RT Direction

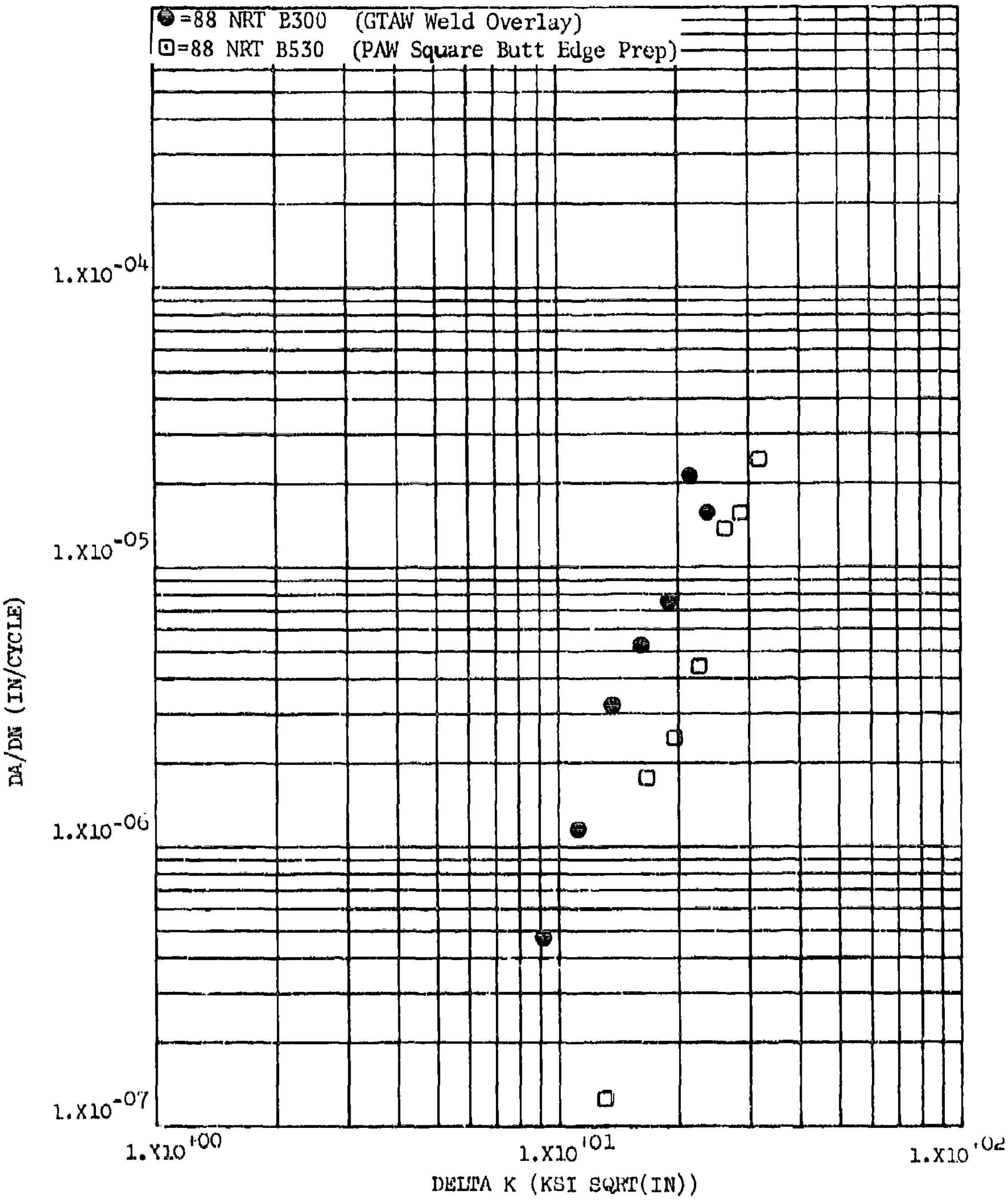

Figure 8.2.14.1.10-3 Effect of welding procedure on LHA-FCGR in weld bead of Ti-6-4 plate at R.T., R=0.08, 360 cpm in RT Direction

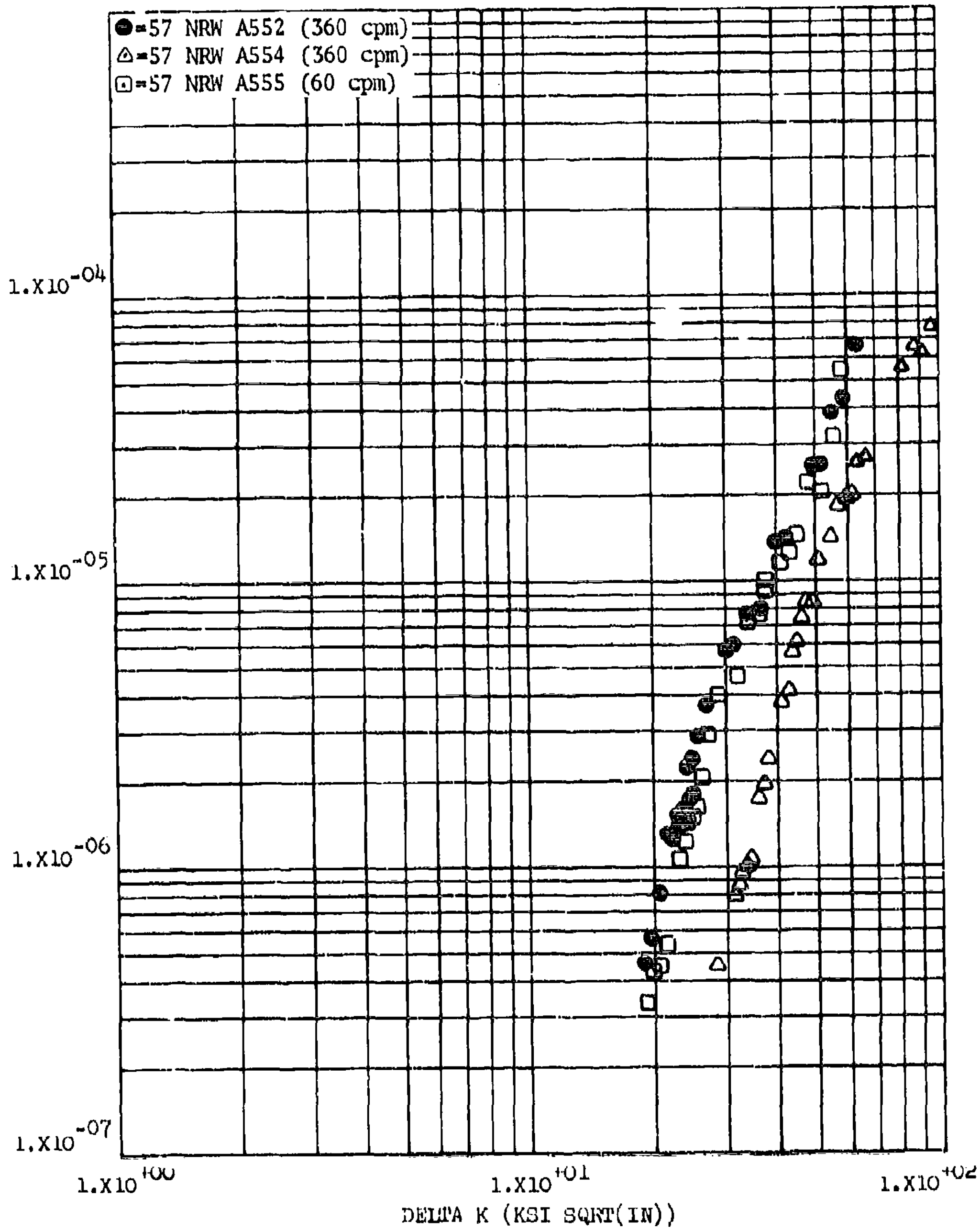

Figure 8.2.14.2.1-1 Effect of cyclic frequency on LHA-FCGR in weld of HP-9-4-.20 plate at R.T., R=0.08, in the RW Direction (CT Specimen)

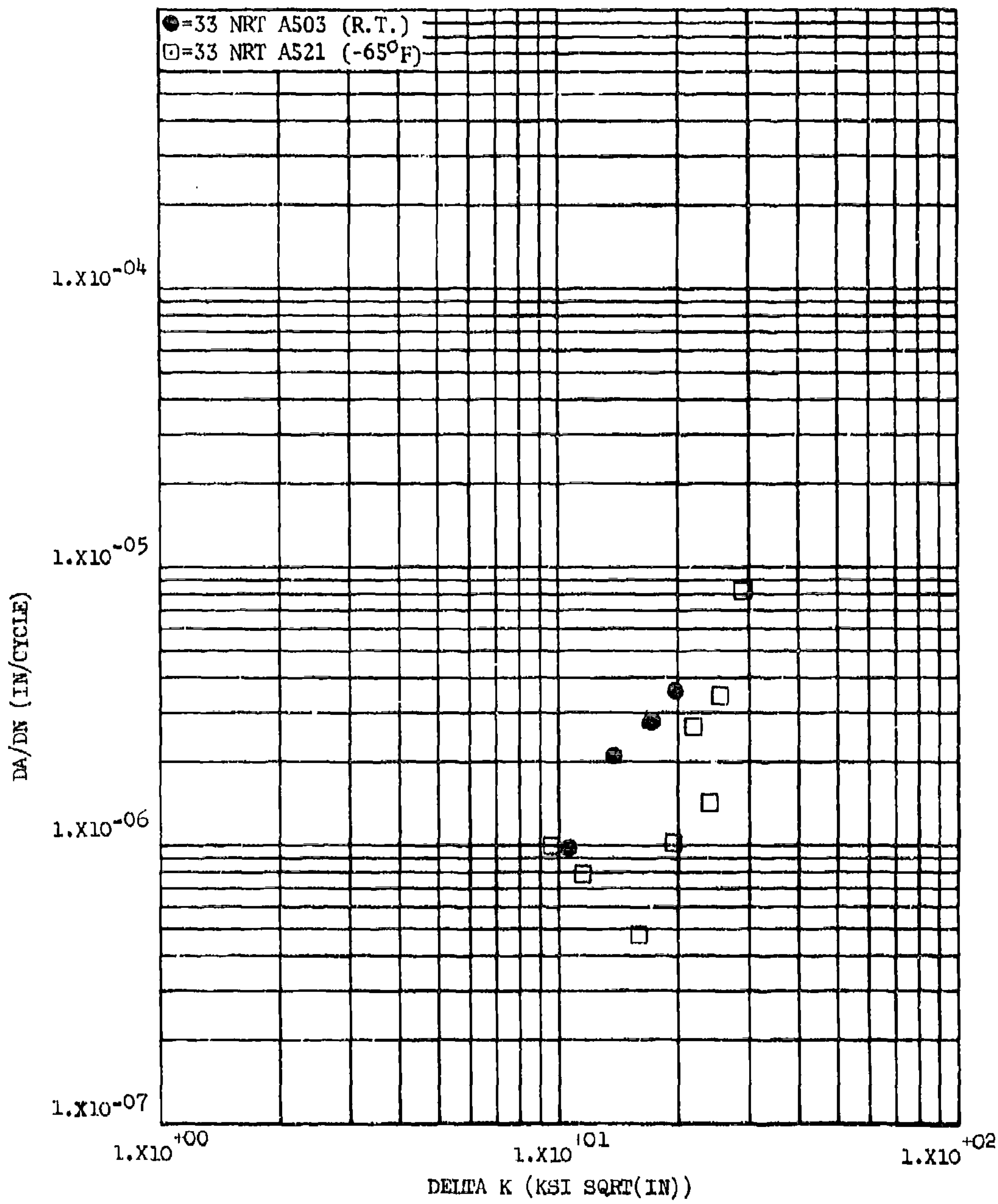

Figure 8.2.14.2.2-1 Effect of test temperature on LHA-FCGR in the HAZ of welded HP-9-4-.20 forged block at R=0.08, 60 cpm in the RT Direction

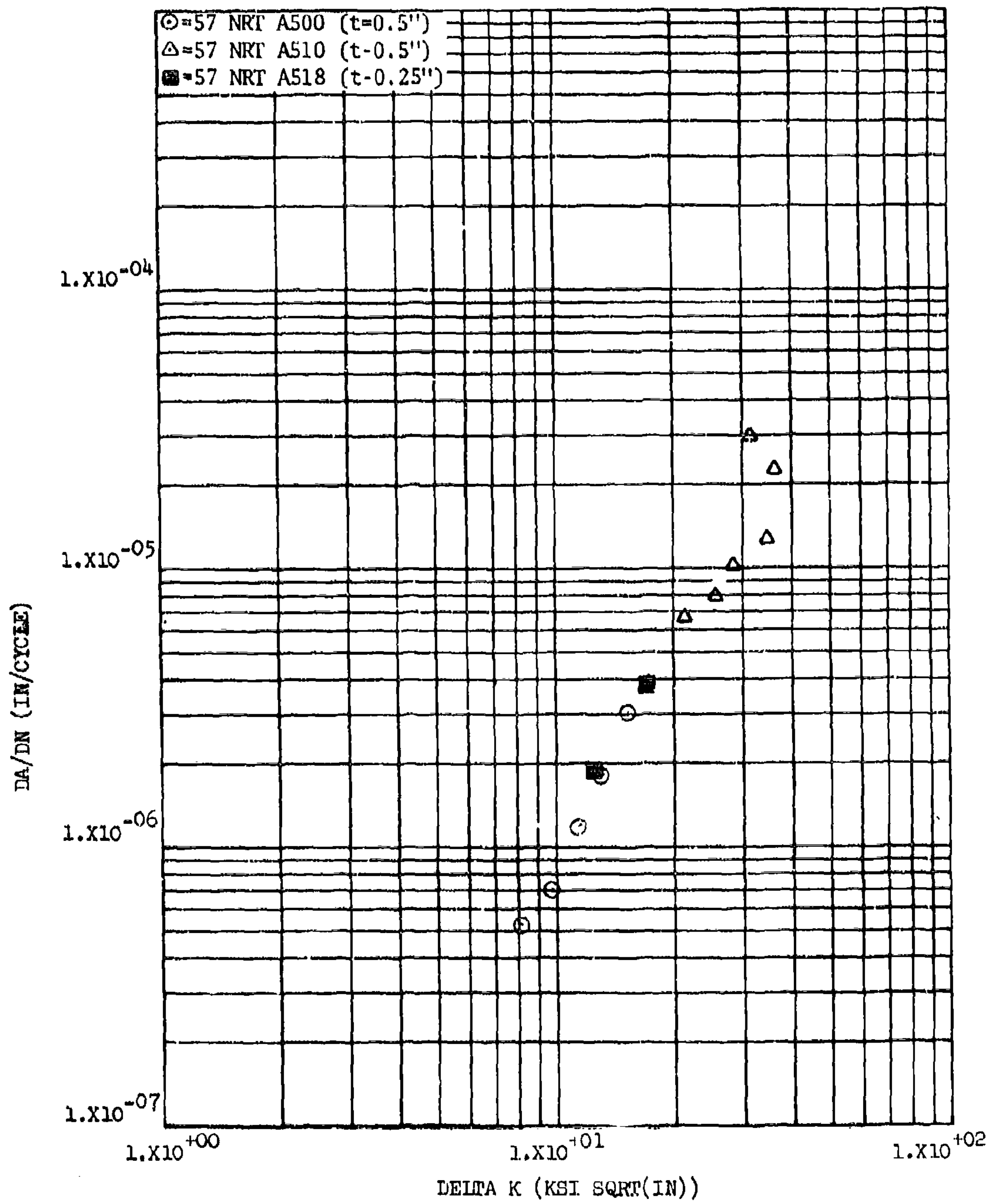

Figure 8.2.14.2.3.1 Effect of specimen thickness on LHA-FCGR in the HAZ of welded HP-9-4-.20 plate at R.T., R=0.08, 60 cpm in the RT Direction

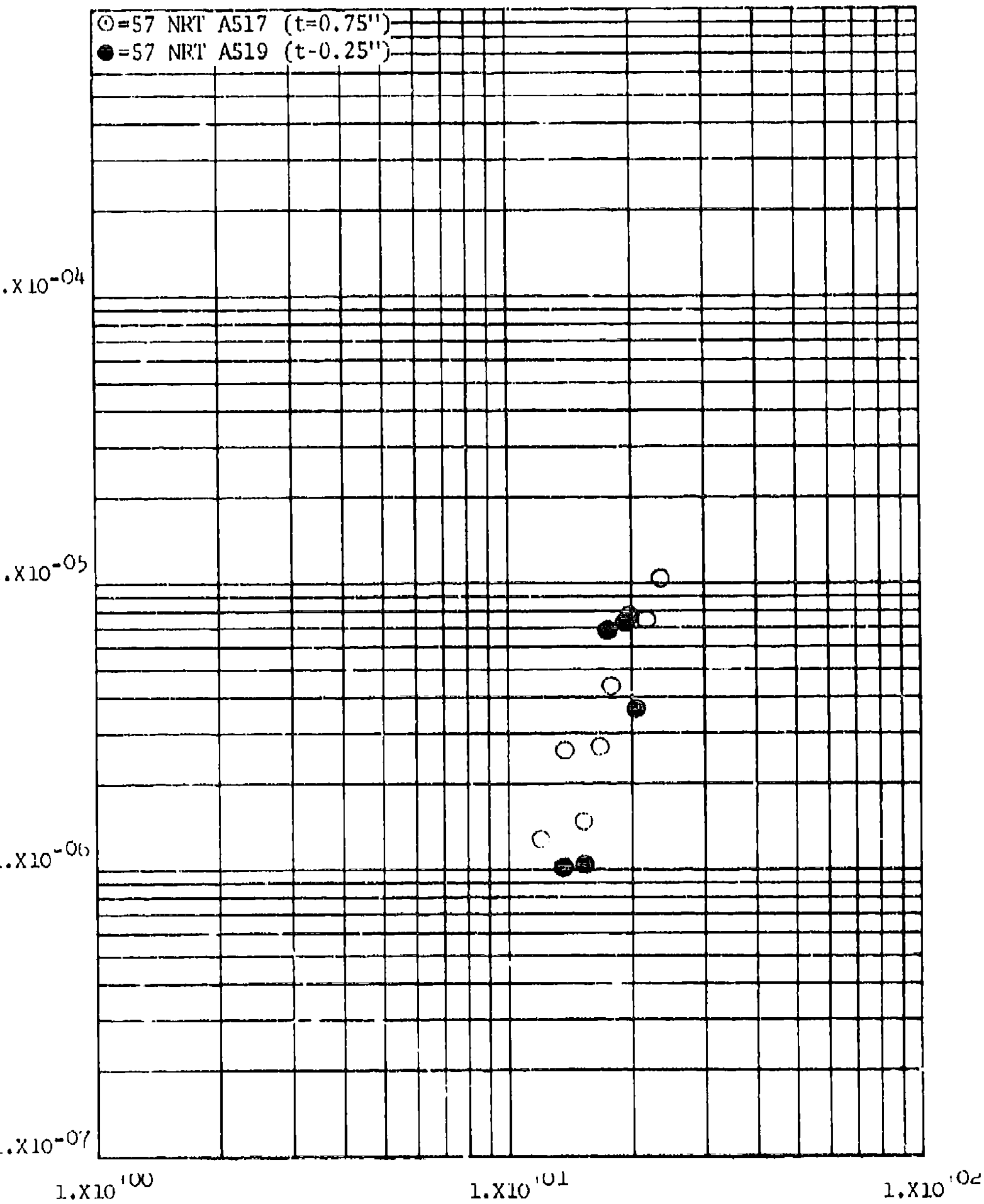

Figure 8.2.14.2.3-2 Effect of specimen thickness on Distilled Water - FCGR in the HAZ of welded HP 9-4-.20 plate at R.T., R=0.08, 60 cpm in the RT Direction

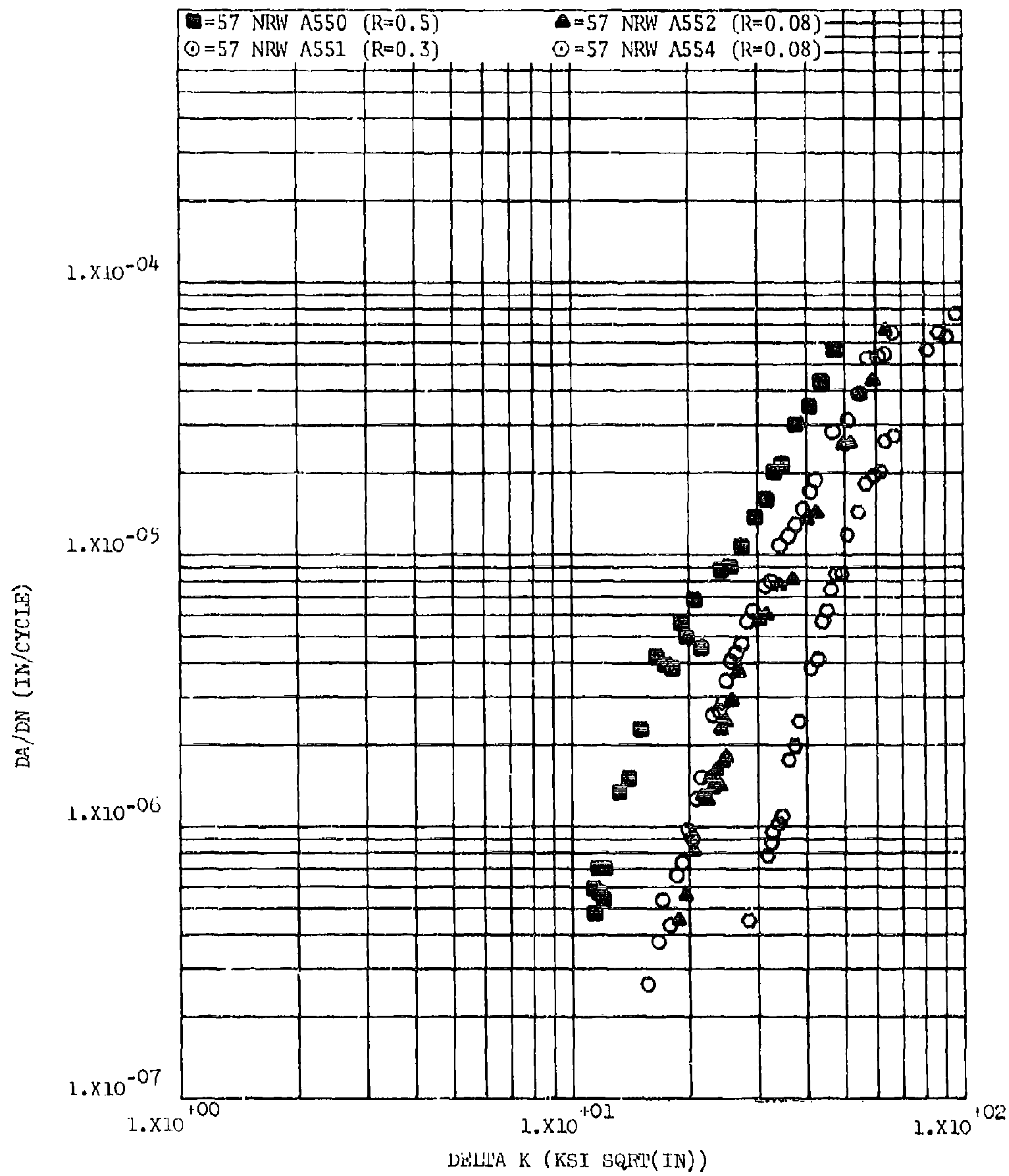

Figure 8.2.14.2.4-1 Effect of R factor on LHA-FCGR in the weld of HP-9-4-.20 plate at R.T., 360 cpm, in the RW Direction (CT Specimens)

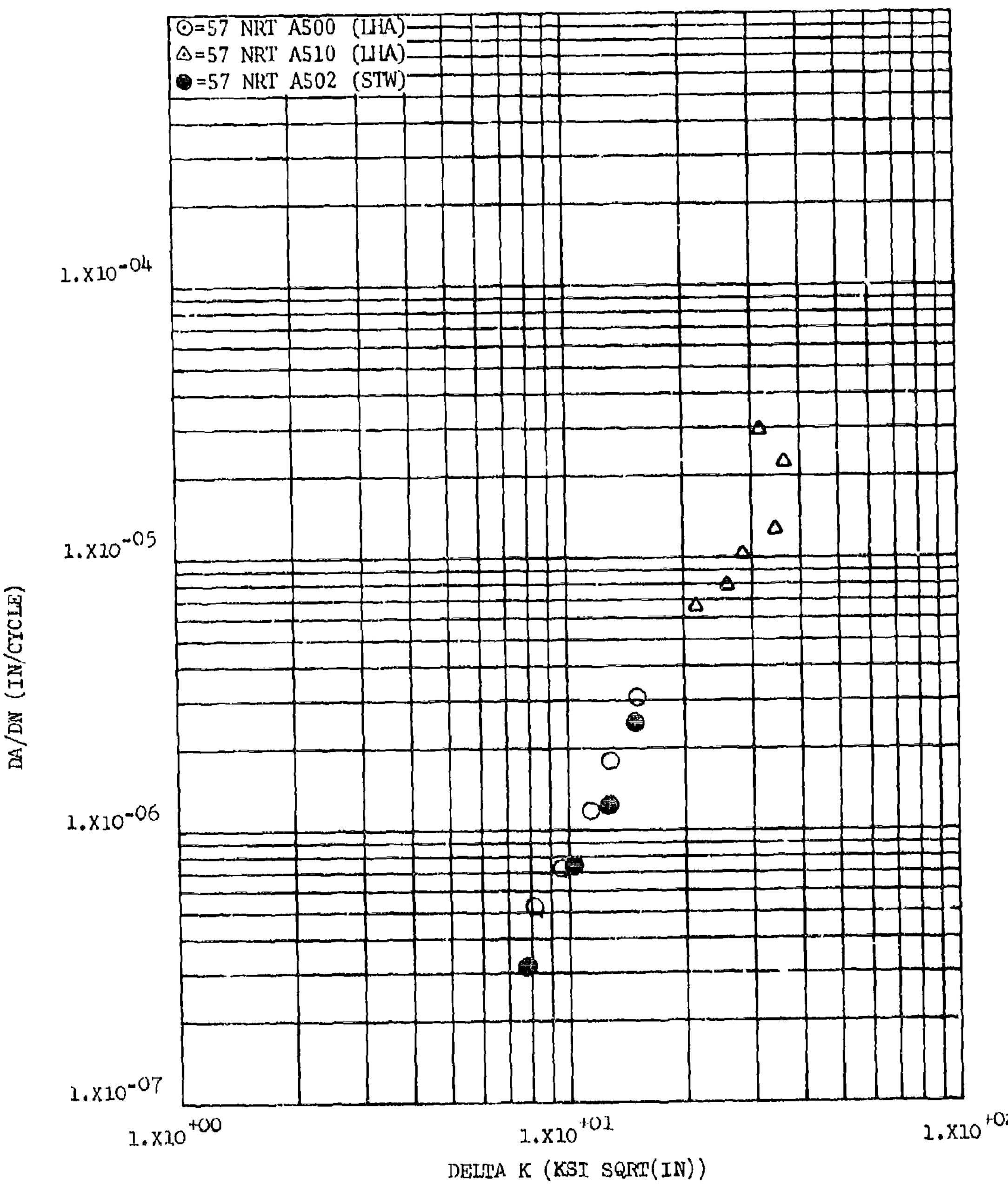

Figure 8.2.14.2.5-1 Effect of environment on FCGR in the HAZ of welded HP-9-4.20 plate at R.T., R=0.08, 60 cpm in the RT Direction

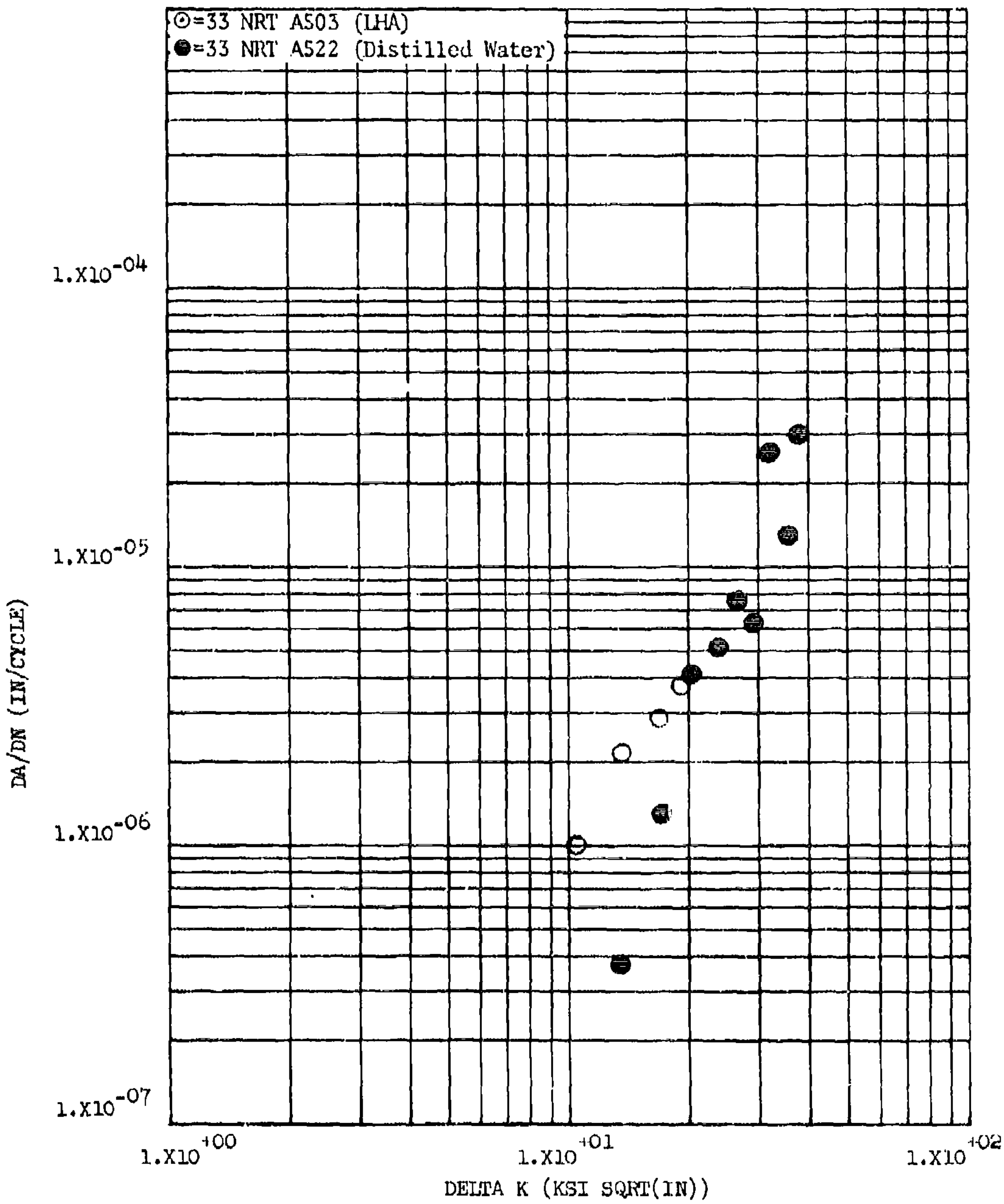

Figure 8.2.14.2.5-2 Effect of environment on FCGR in the HAZ of welded HP-9-4-.20 forged block at R.T., R=0.08, 60 cpm in the RT Direction

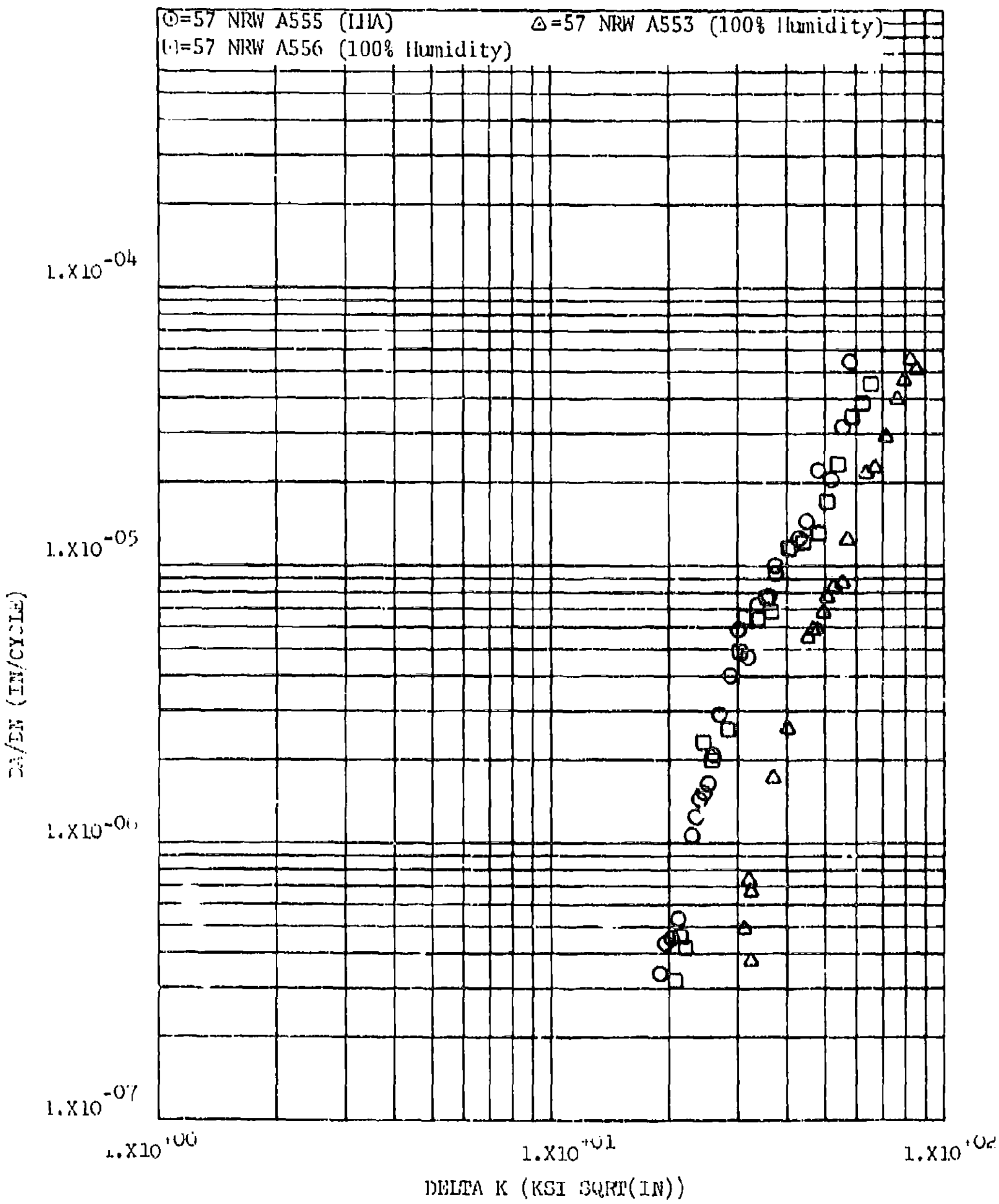

Figure 8.2.14.2.5-3 Effect of environment on FCGR in the weld of HP-9-4.20 plate at R.T., R 0.08, 60 cpm in the RW Direction (CT Specimen)

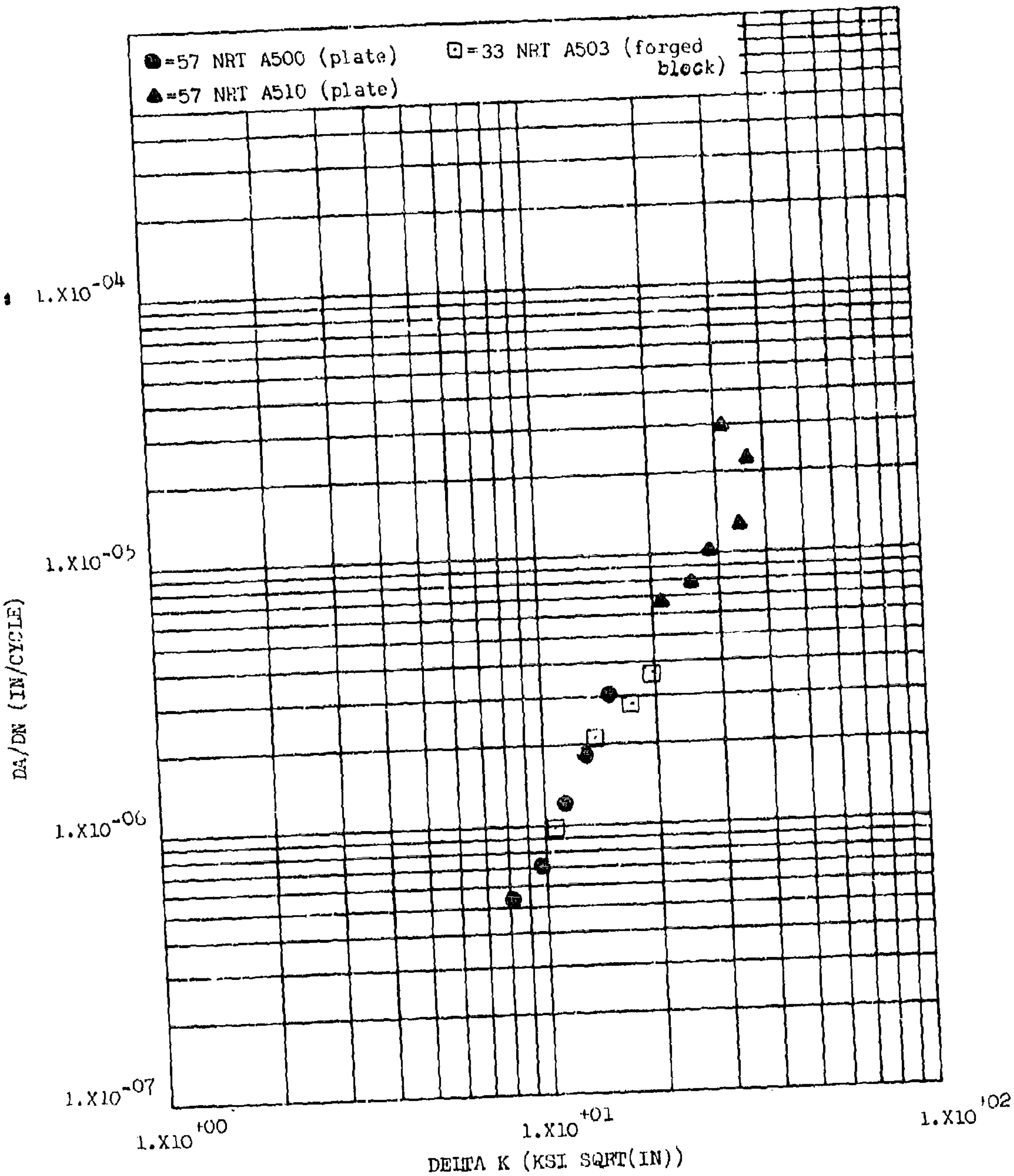

Figure 8.2.14.2.7-1 Effect of Product form on LHA-FCGR in HAZ of welded HP-9-4-.20 at R.T., R=0.08, 60 cpm in RT Direction

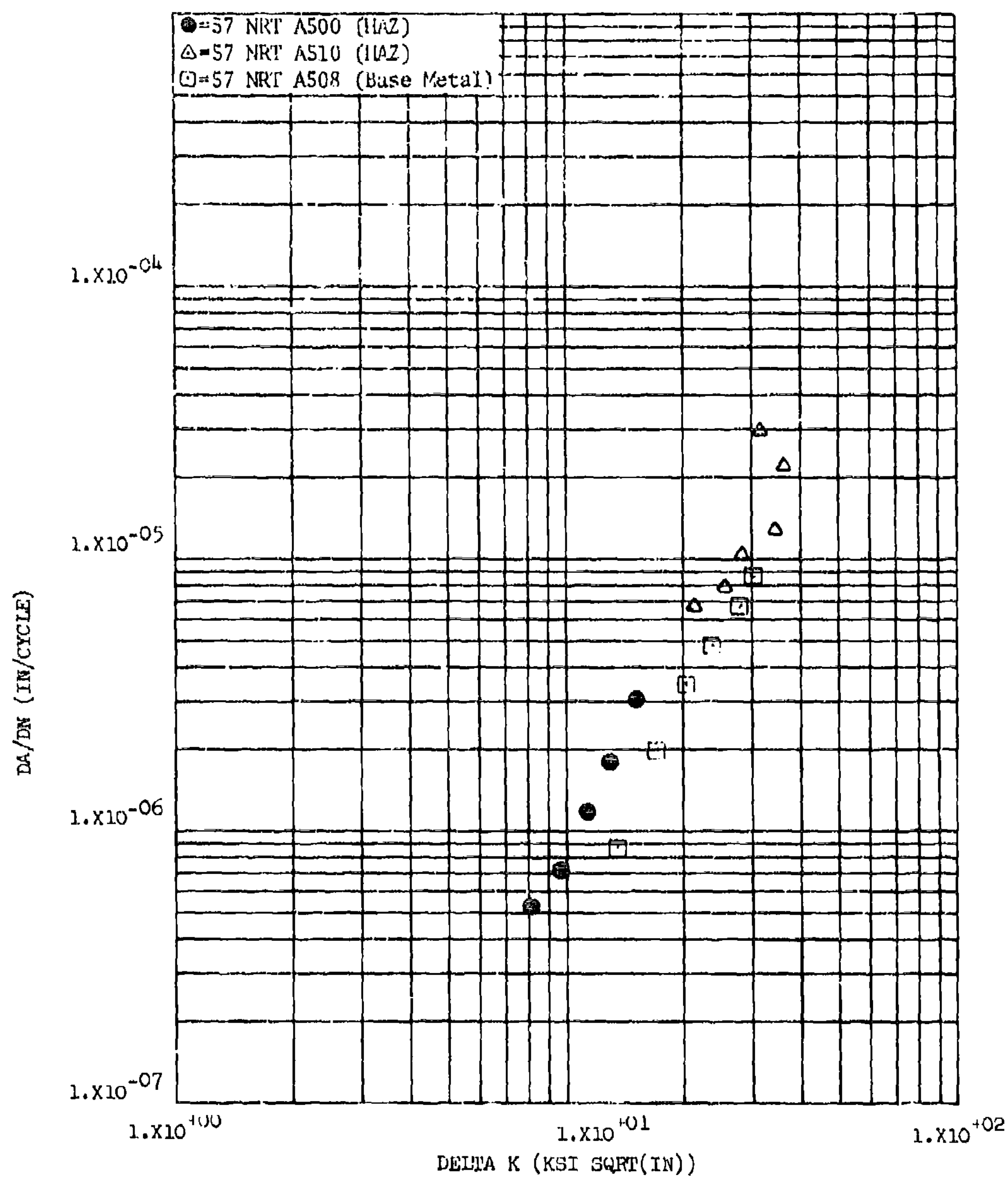

Figure 8.2.14.2.9-1 Effect of crack plane location on LHA-FCGR in welded HP-9-4-.20 plate at R.T., R=0.08, 60 cpm in the RT Direction

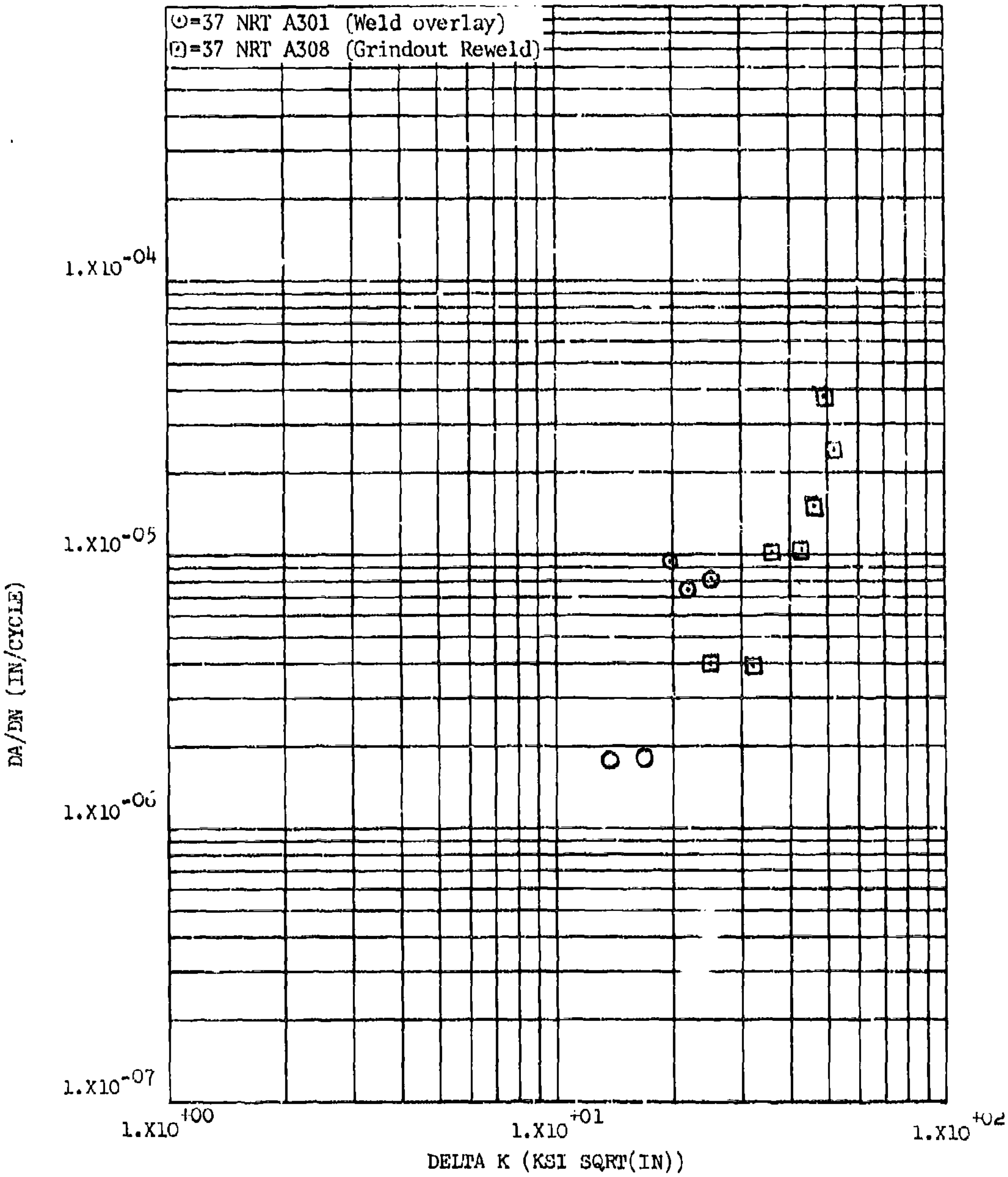

Figure 8.2.14.2.10-1 Effect of weld type on Distilled Water - FCGR in stress relieved weld bead of HP-9-4-.20 plate at R.T., R=0.08, 60 cpm in RT Direction

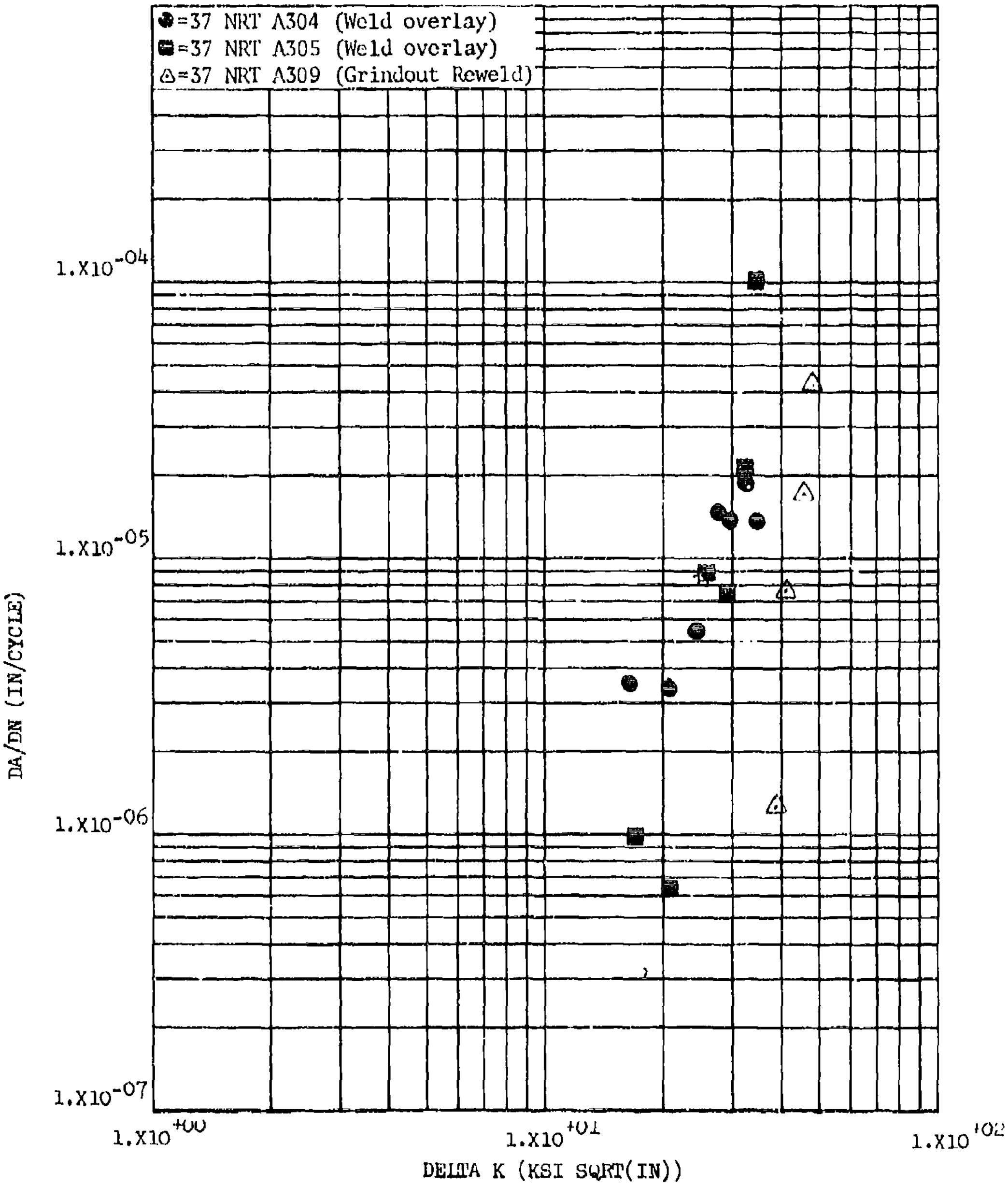

Figure 8.2.14.2.10-2 Effect of weld type on Distilled Water - FCGR in un-stress-relieved weld bead of HP-9-4-.20 plate at R.T., R=0.08, 60 cpm in the RT Direction

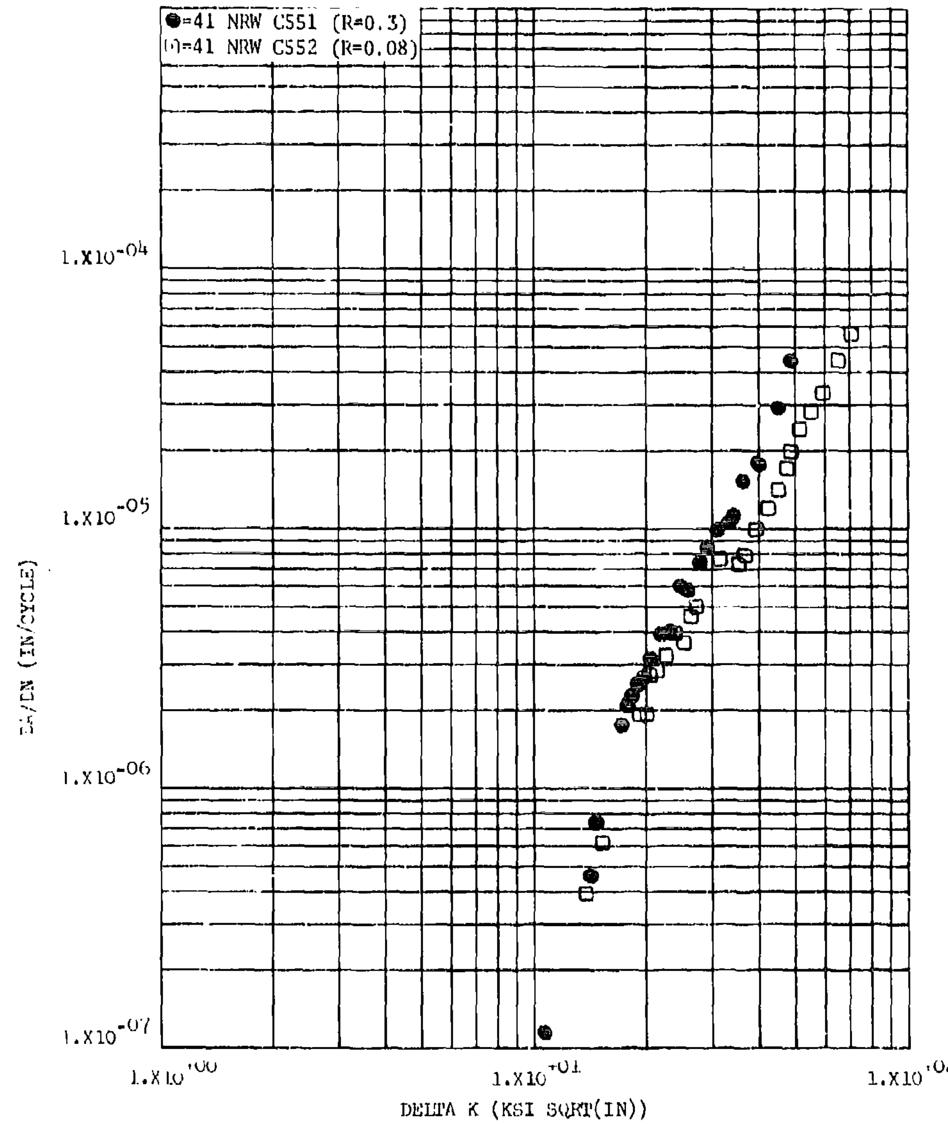

Figure 8.2.14.3.4-1 Effect of R factor on Lab Air - FCGR in the weld of PH13-8Mo extruded bar at R.T., 360 cpm, in the RW Direction (CT Specimen)

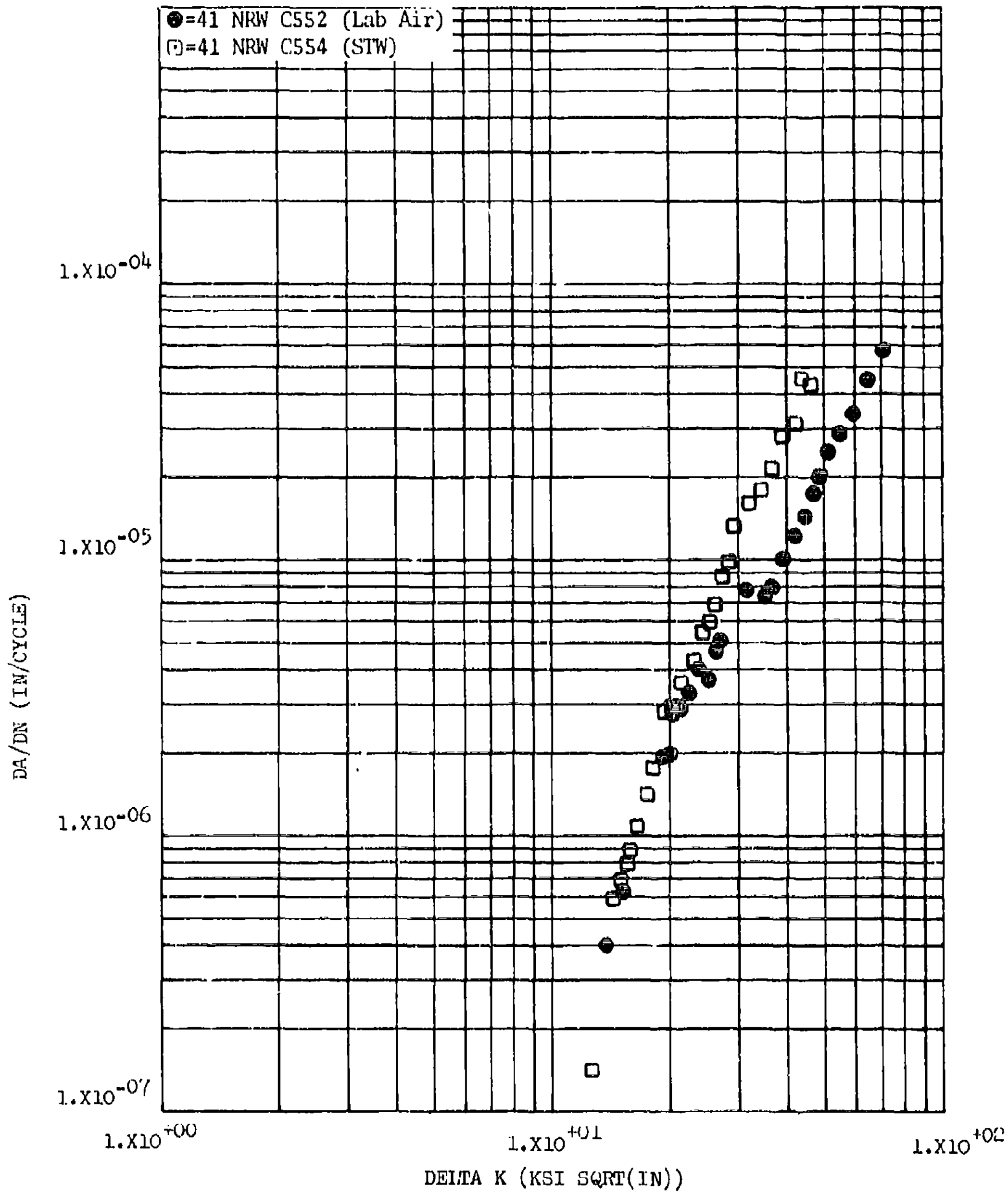

Figure 8.2.14.3.5-1 Effect of environment on FCGR in the Weld of PH13-8Mo extruded bar at R.T., R=0.08, 60 cpm, in the RW Direction (CT Specimen)

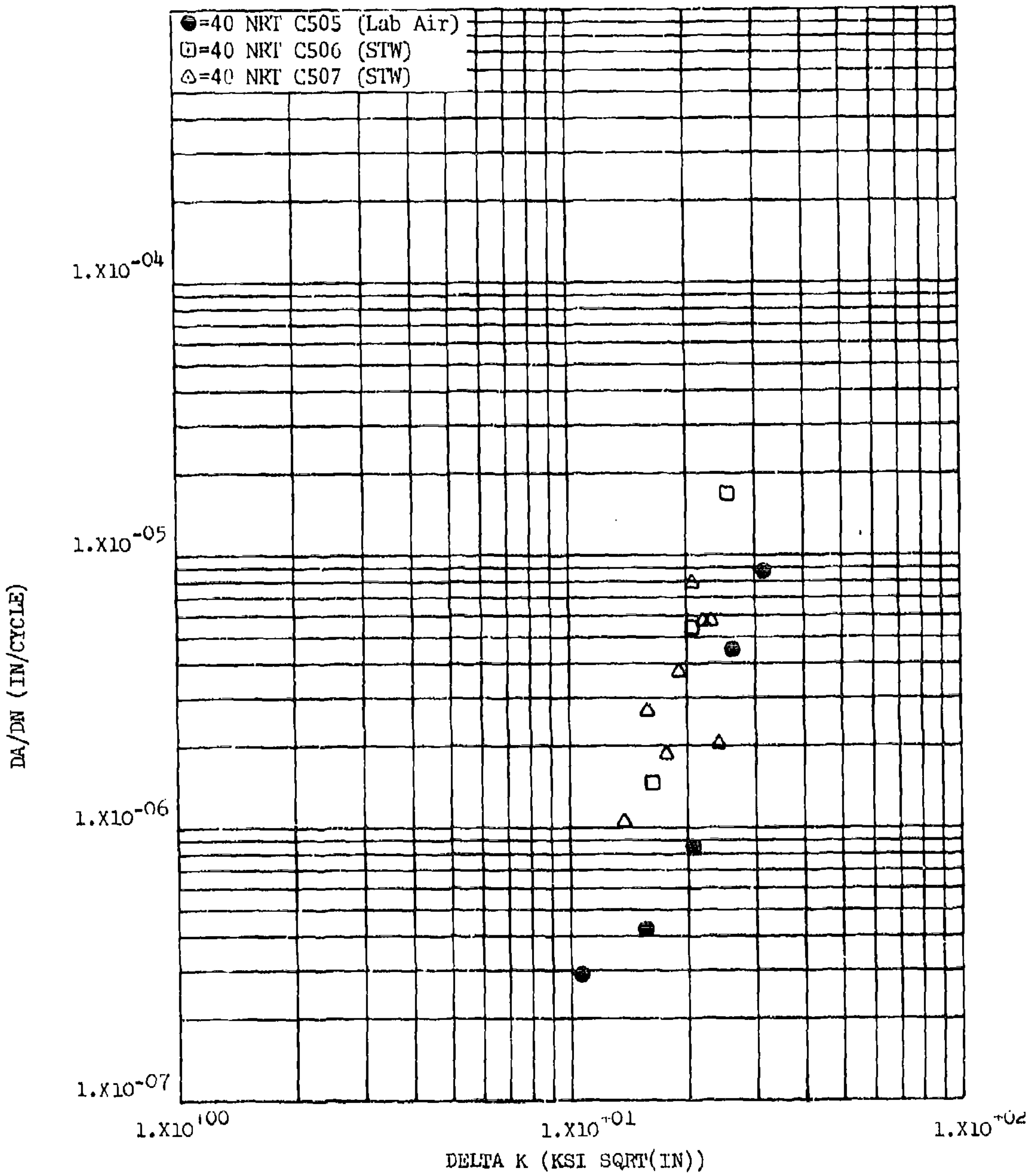

Figure 8.2.14.3.5-2 Effect of environment on FCGR in the HAZ of welded PH13-8Mo rolled bar at R.T., R=0.08, 60 cpm in the RT Direction

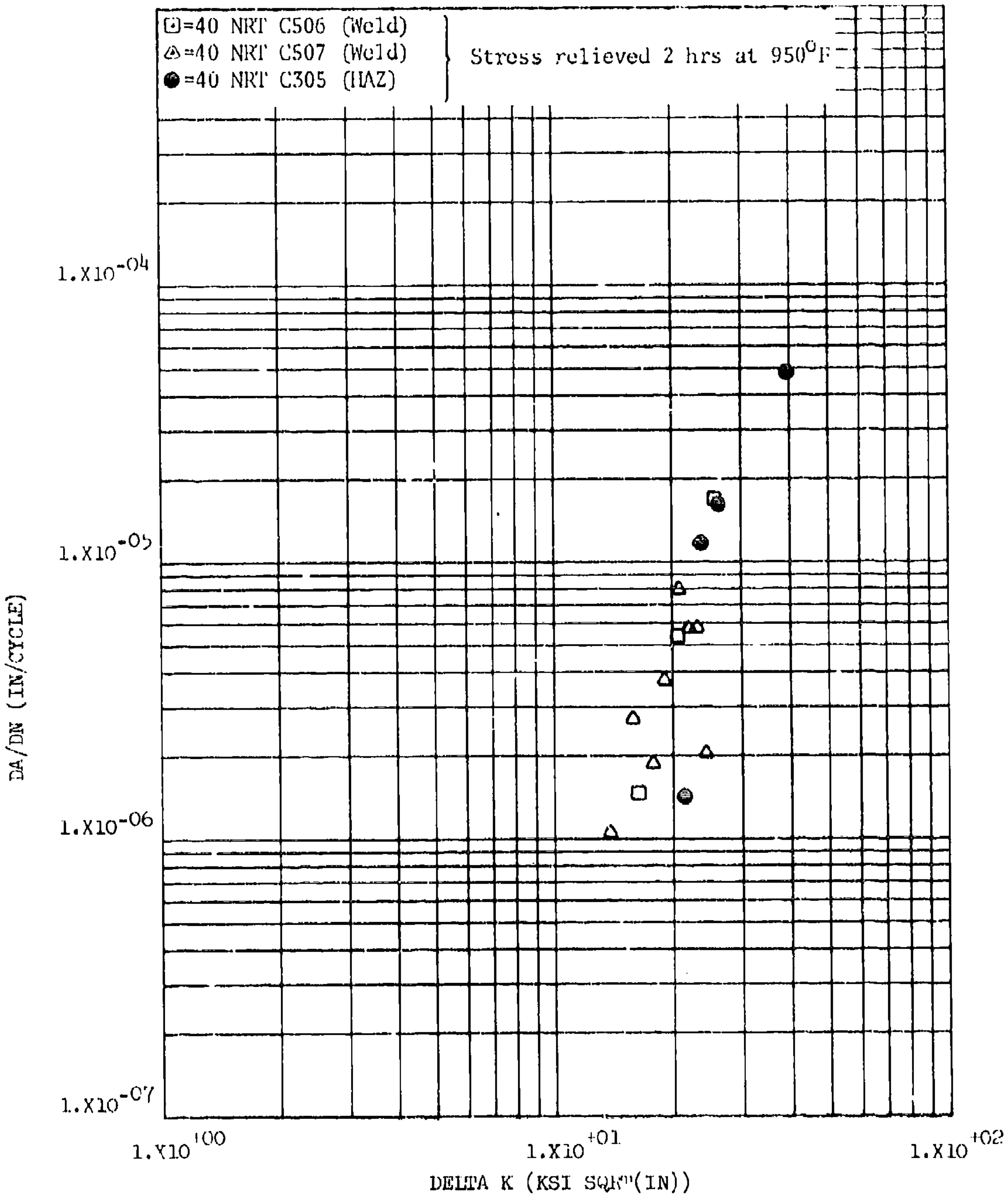

Figure 8.2.14.3.9-1 Effect of crack plane location on the STW-FCGR of welded PH13-8Mo rolled bar at R.T., R=0.08, 60 cpm in the RT Direction

8.2.15 All Aluminum Alloys

To facilitate comparisons of fatigue crack growth rates of the various aluminum alloys evaluated in this program, overlays were prepared of each da/dN curve generated in each alloy system at a fixed set of test parameters. In some instances, a number of curves were available for each alloy representing minor variations in either product form or alloy heat. In these cases, scatter bands are presented rather than individual curves to simplify presentation and analysis. These comparisons are described below in terms of test parameters under which comparisons were made. One set of test parameters (LHA, R.T., R=0.08, 360 cpm, RW direction) was arbitrarily chosen as a standard test condition. Variances from this standard have then been underlined in the section title.

8.2.15.1 Standard Conditions - LHA, R.T., R=0.08, 360 cpm, RW direction - Fatigue crack growth rates in 2024-T851 plate were seen to be significantly greater than those in either 2124-T851 or 2219-T851 plate at delta K levels above ~10 ksi $\sqrt{in}$ (Figure 8.2.15.1-1). At delta K levels of ~15 ksi $\sqrt{in}$ and above the scatter bands for the latter two alloys indicated equivalent growth rates. Below this level, however, growth rates in the 2219-T851 plate were seen to be slightly greater than in the 2124-T851 plate material (Figure 8.2.15.1-1). The scatter band for 2124-T851 plate shown in Figure 8.2.15.1-1 was replotted in Figure 8.2.15.1-2 for comparison with growth rates in a 2024-T852 forging, a 2219-T852 forging and a 2219-T851 extrusion. While there was little difference in rates observed in this comparison, the da/dN curves for the forgings and extrusion all fell to the right hand edge of the plate scatter band, indicating slower growth rates in these product forms than in the plate. Care should be taken, however, in generalizing on the basis of single curves vs. scatter bands. This trend could well be reversed or at least negated with additional tests.

In the 7000 series aluminum alloys growth rates of 7075-T7651 plate were seen to be slightly greater than those of 7075-T7351 plate, while rates in 7050-T73651 plate were seen to be slower than those of the 7075-T7351 plate (Figure 8.2.15.1-3). Again, these generalizations are based on single curves vs. scatter bands, and therefore should be interpreted with caution. The 7075-T7351 plate scatter band in Figure 8.2.15.1-3 is duplicated in Figure 8.2.15.1-4 for comparison with a 7049-T7352 forging, a 7175-T73652 forging, a 7075-T7351 extrusion and a 7075-T7651 extrusion. The growth rates of both forgings and both extrusions were seen to be essentially comparable to those of the 7075-T7351 plate, although at low levels of delta K (below 8 ksi $\sqrt{in}$) rates in the T7651 condition of the 7075 extrusion were seen to be slightly greater than those of the other alloys and product forms evaluated.

8.2.15.2 LHA, R.T., R=0.08, 360 cpm, WR Direction - In the WR direction of the 2000 series aluminum alloys fatigue crack growth rates of 2024-T852 forgings were seen to be significantly lower than the rates of 2219-T851

plate, while rates in a 2219-T851 extrusion were shown to be essentially equivalent to those in the 2219-T851 forgings (Figure 8.2.15.2-1). Growth rates in 2024-and 2124-T851 plates were essentially equivalent to each other, and fell within the scatter band for 2219-T851 plate at delta K levels below 12-13 ksi $\sqrt{in.}$ Above this level, however, rates in both the 2024 and 2124 plates were noticeably greater than those in the 2219 plate (Figure 8.2.15.2-1).

Fatigue crack growth rates in the 7000 series aluminum alloys evaluated were all seen to be essentially equivalent at delta K levels above ~13 ksi $\sqrt{in.}$ Below this level, however, the rates were seen to differ noticeably with those in a 7075-T7651 extrusion being the greatest. In order of decreasing growth rates below this delta K level were those of a 7075-T7351 extrusion, then a 7075-T7651 plate, then a 7050-T73651 plate, and finally, a 7175-T73652 forging representing the lowest growth rate (Figure 8.2.15.2-2).

8.2.15.3 LHA, R.T., R=0.3, 360 cpm, RW direction - At an R factor of 0.3 the low humidity air fatigue crack growth rate of a 2024-T852 forging was seen to be substantially lower than the remaining 2000 series aluminum alloys and product forms evaluated (Figure 8.2.15.3-1). The growth rates of a 2219-T851 plate, a 2219-T851 extrusion, and a 2124-T851 plate all fell within a fairly narrow scatter band which demonstrated growth rates just slightly lower than those of 2024-T62 plate (Figure 8.2.15.3-1).

In the 7000 series aluminum alloys at an R factor of 0.3 growth rates of all alloy types, product forms and temper conditions fell within a fairly narrow scatter band with the possible exception of one 7075-T7651 plate, which demonstrated somewhat lower growth rates at a delta K level below ~8.5 ksi $\sqrt{in}$ (Figure 8.2.15.3-2). Conditions evaluated included a 7049-T7352 forging, a 7050-T73651 plate, three 7075-T7651 plates, a 7075-T7351 extrusion, a 7075-T7651 extrusion, and a 7175-T73652 forging.

8.2.15.4 LHA, R.T., R=0.5, 360 cpm, RW direction - At an R factor of 0.5, the low humidity air fatigue crack growth rates in all product forms and alloy types for both the 2000 series and 7000 series aluminu alloys all fell within a relatively narrow scatter band (Figure 8.2.15. -1). Growth rates of the 2000 series alloys did fall on the right hand (lower growth rate) edge of this band. Those materials compared in this evaluation consisted of 7075-T7351 and T7651 plates, a 7075-T7351 extrusion, a 7050-T73651 plate, a 7175-T73652 forging, a 2219-T851 plate, and a 2124-T851 plate.

8.2.15.5 STW, R.T., R=0.08, 60 cpm, RW direction - At an R factor of 0.08, the sump tank water growth rates in 2024-, 2124-, and 2219-T851 plate stock all fell within a fairly narrow scatter band throughout the entire delta K range with the exception of one test in 2124 plate which exhibited substantially reduced growth rates at delta K levels below ~11 ksi $\sqrt{in}$

(Figure 8.2.15.5-1). The results of this single test broadened the scatter band considerably at the low end of the delta K range. The total scatter band in Figure 8.2.15.5-1 has been reconstructed in Figure 8.2.15.5-2 ignoring the broadening effect at low delta K levels for the purpose of comparing product forms. In this comparison the growth rates of one 2024-T852 forging were seen to be substantially lower than those of a similar 2024-T852 forging, and a 2219-T851 extrusion. The growth rates of the latter forging and the extrusion were seen to be comparable to growth rates observed in the plate stock at delta K levels above ~10 ksi $\sqrt{in}$, while being slightly lower than the plate stock growth rates at delta K levels lower than ~ 10 ksi $\sqrt{in}$.

In the 7000 series aluminum alloys, sump tank water fatigue crack growth rates at R=0.08 were again seen to vary inconsistently with product form and delta K level, all falling within a 15 to 25 ksi $\sqrt{in}$ wide scatter band (Figure 8.2.15.5-3).

8.2.15.6 STW, R.T., R=0.08, 60 cpm, WR direction - The sump tank water fatigue crack growth rates in the WR direction of a 2124-T851 plate were seen to be slightly greater than those of 2219-T851 plate at delta K levels above 6 ksi $\sqrt{in}$, while being essentially equivalent to growth rates in the 2219 plate below this level (Figure 8.2.15.6-1). Growth rates in a 2219-T851 extrusion were seen to be equivalent to those of the 2219 plate throughout the range of delta K. Growth rates of a 2024-T852 forging were seen to be noticeably lower at delta K levels below ~11 ksi $\sqrt{in}$ than those of the 2219-T851 plates and extrusion, and the 2124-T851 plate under these test conditons (Figure 8.2.15.6-1).

Sump tank water fatigue crack growth rates in the WR direction of 7000 series aluminum alloys were all seen to fall within a relatively narrow scatter band with the exception of one test performed in a 7175-T73652 forging, which demonstrated substantially lower growth rates than the other product forms and alloys evaluated (Figure 8.2.15.6-2).

8.2.15.7 STW, R.T., R=0.3, 60 cpm, RW direction - With the exception of one test run in 7075-T7651 plate, the sump tank water fatigue crack growth rates of all 7000 series alloys and product form evaluated at R=0.3 fell within a narrow scatter band (Figure 8.2.15.7-1). Those forms and alloys included in this comparison were, in addition to the 7075-T7651 plate, a 7049-T7352 forging, a 7075-T7351 extrusion, and a 7175-T73652 forging. The growth rates of the 7075-T7651 plate were noticeably lower than the remaining 7000 series tests, and more closely resembled the growth rates observed in 2219-T851 plate. Growth rates of a 2024-T852 forging under these test conditions were seen to be substantially lower than either the 2219-T851 plate or any of the 7000 series alloys evaluated (Figure 8.2.15.7-1).

8.2.15.8 STW, R.T., R=0.5, 60 cpm, RW direction - While the growth rates in sump tank water of the 7000 series aluminum alloys varied inconsistently with respect to one another depending on delta K level, all were seen to be noticeably greater than growth rates in either a 2219-T851 plate or a 2024-T852 forging under these test conditions (Figure 8.2.15.8-1). In this comparison the growth rates in both the 2219 plate and the 2024 forging were seen to be essentially equivalent at low levels of delta K (4 ksi $\sqrt{in}$), while at higher levels of delta K growth rates in the 2219 plate were seen to be roughly 8 times faster than in the 2024 extrusion (ΔK= 10 ksi $\sqrt{in}$).

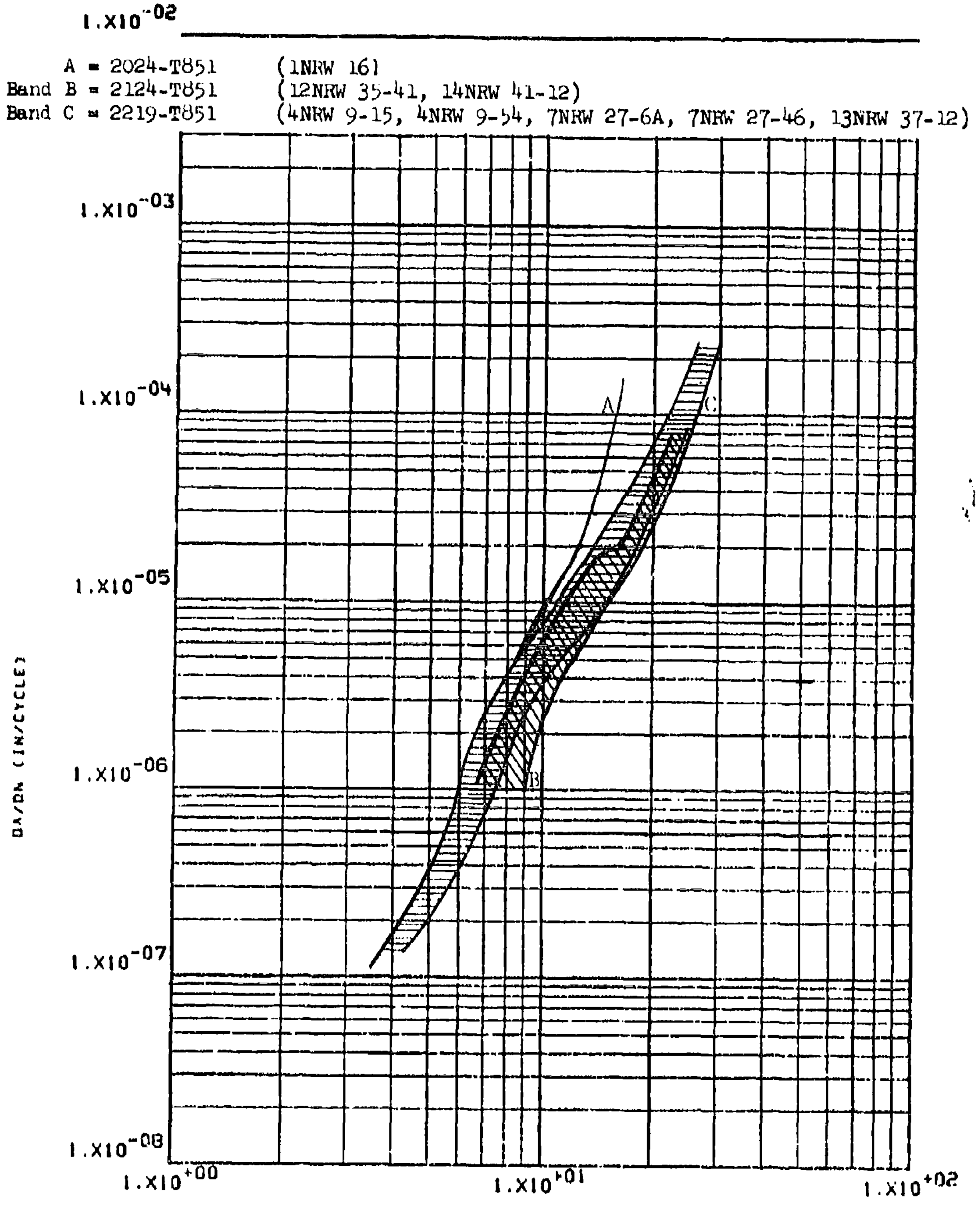

Figure 8.2.15.1-1 Effect of alloy type on LHA-FCGR at R.T., R=0.08, 360 cpm, RW direction in 2000 series aluminum alloy plate.

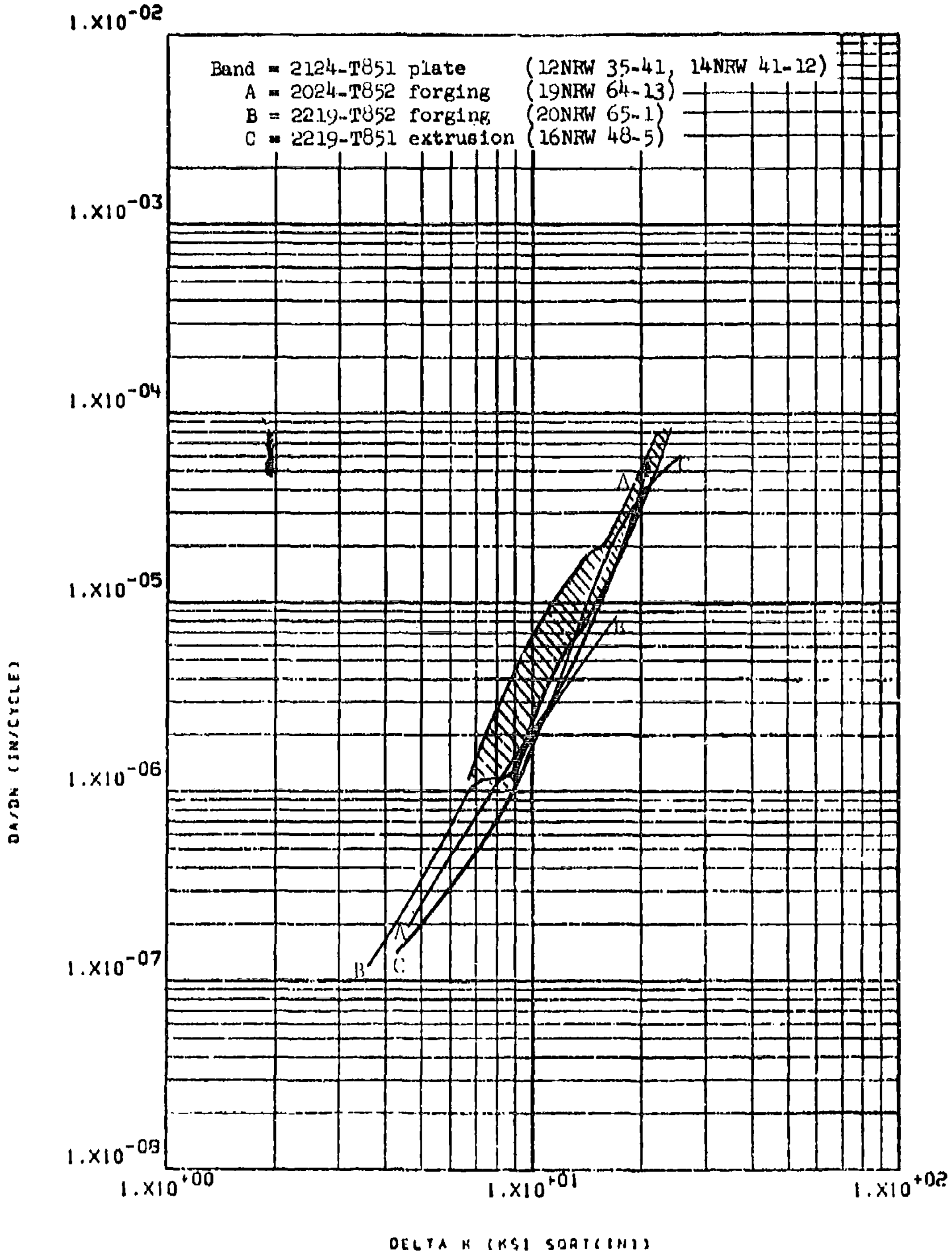

Figure 8.2.15.1-2 Effect of alloy type and product form on LHA-FCGR at R.T., R=0.08, 360 cpm, RW direction in 2000 series aluminum alloys.

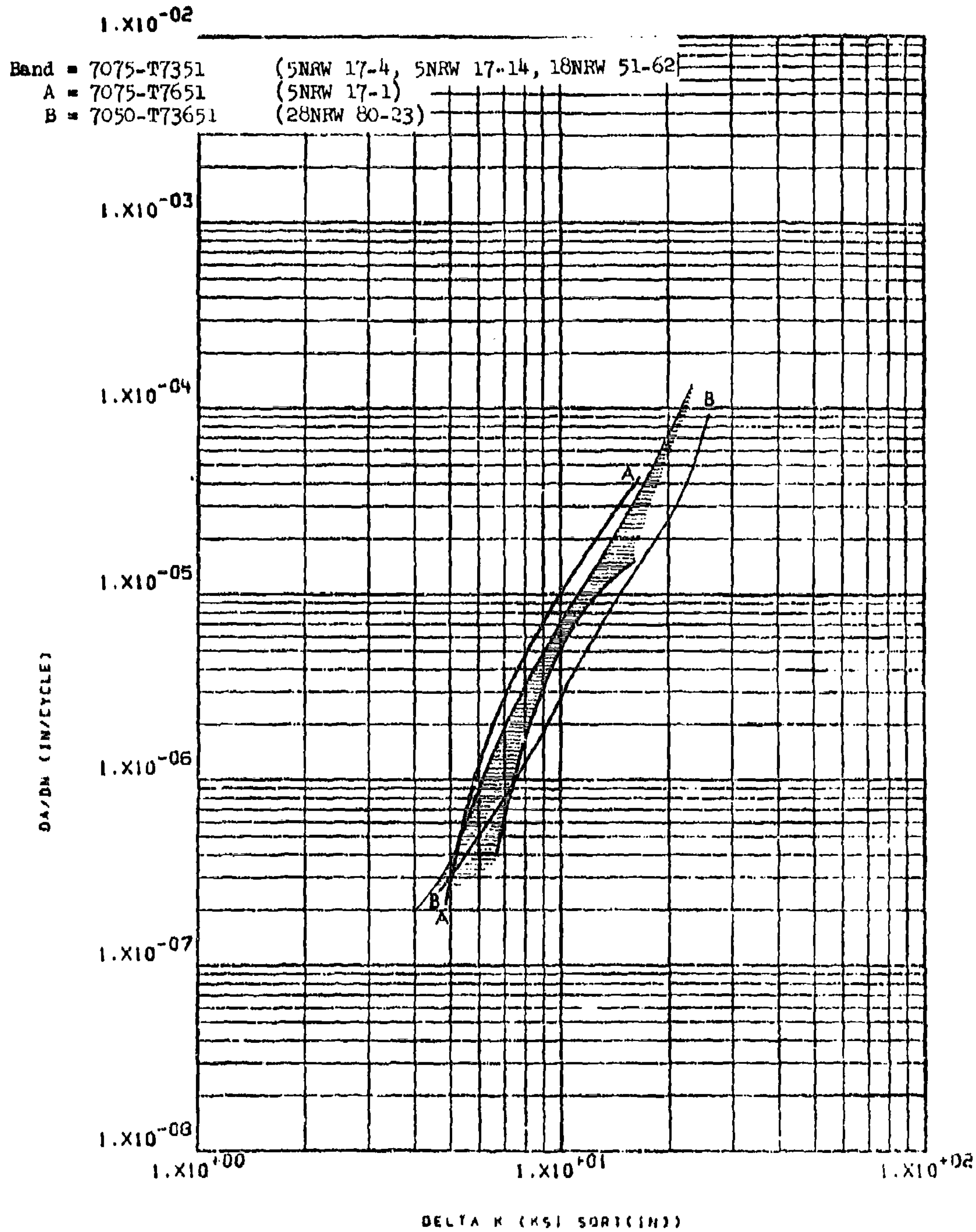

Figure 8.2.15.1-3 Effect of alloy type and temper condition on LHA-FCGR at R.T., R=0.08, 360 cpm, RW direction in 7000 series aluminum alloy plate.

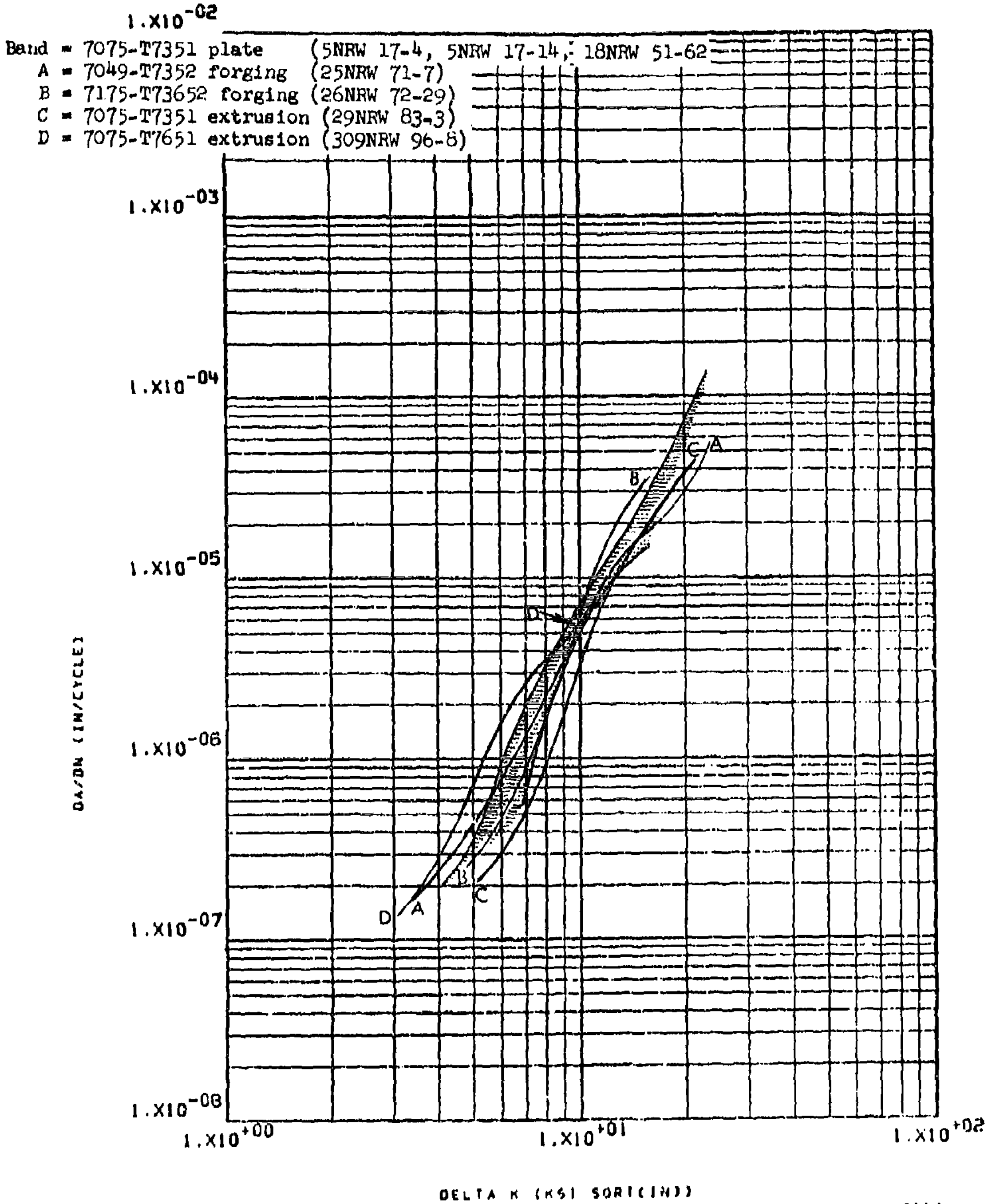

Figure 3.2.15.1-4 Effect of alloy type, product form and temper condition on LHA-FCGR at R.T., R=0.08, 360 cpm, RW direction in 7000 series aluminum alloys.

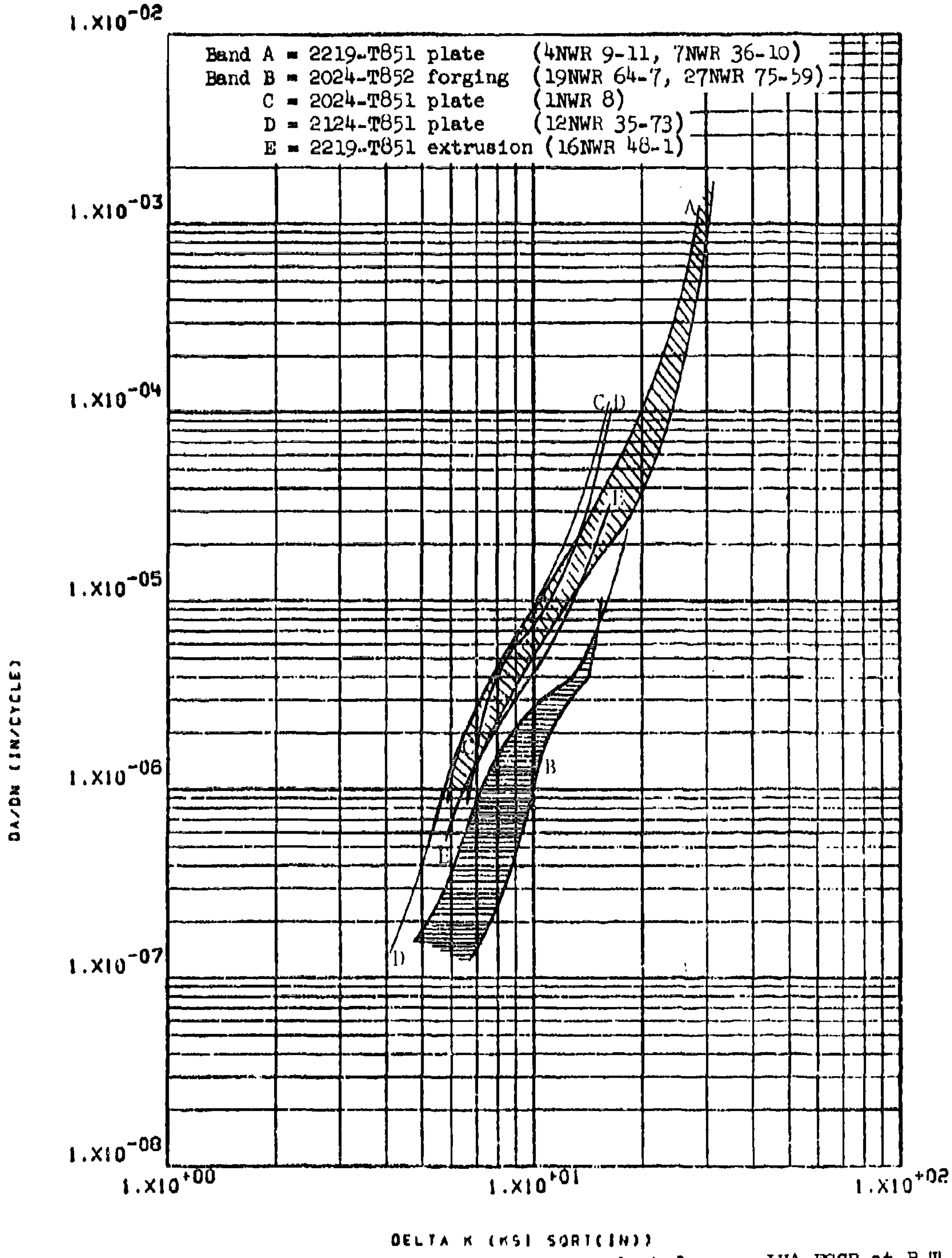

Figure 8.2.15.2-1 Effect of alloy type and product form on LHA-FCGR at R.T., R=0.08, 360 cpm, WR direction in 2000 series aluminum alloys.

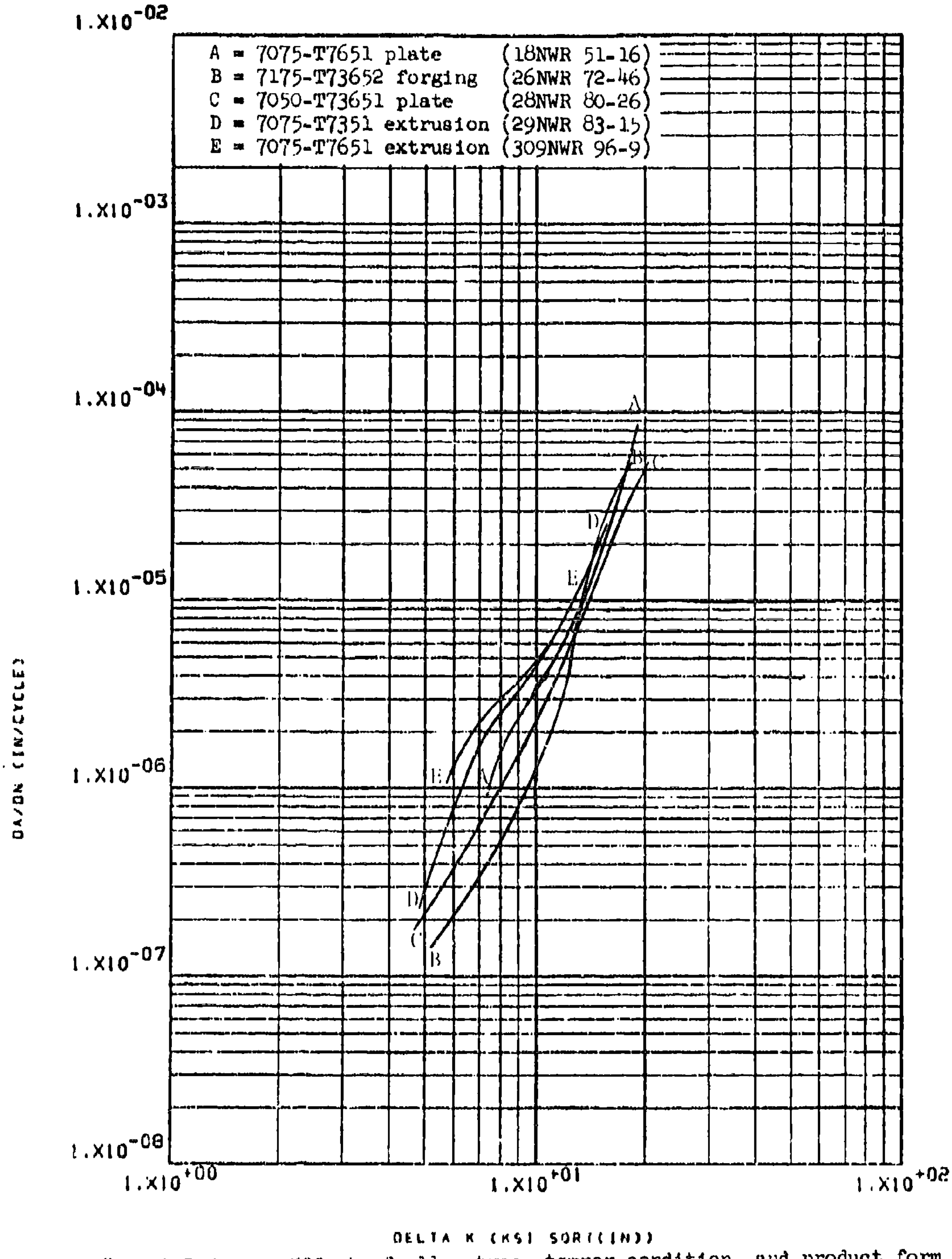

Figure 8.2.15.2-2 Effect of alloy type, temper condition, and product form on LHA-FCGR at R.T., R=0.08, 360 cpm, WR direction in 7000 series aluminum alloys.

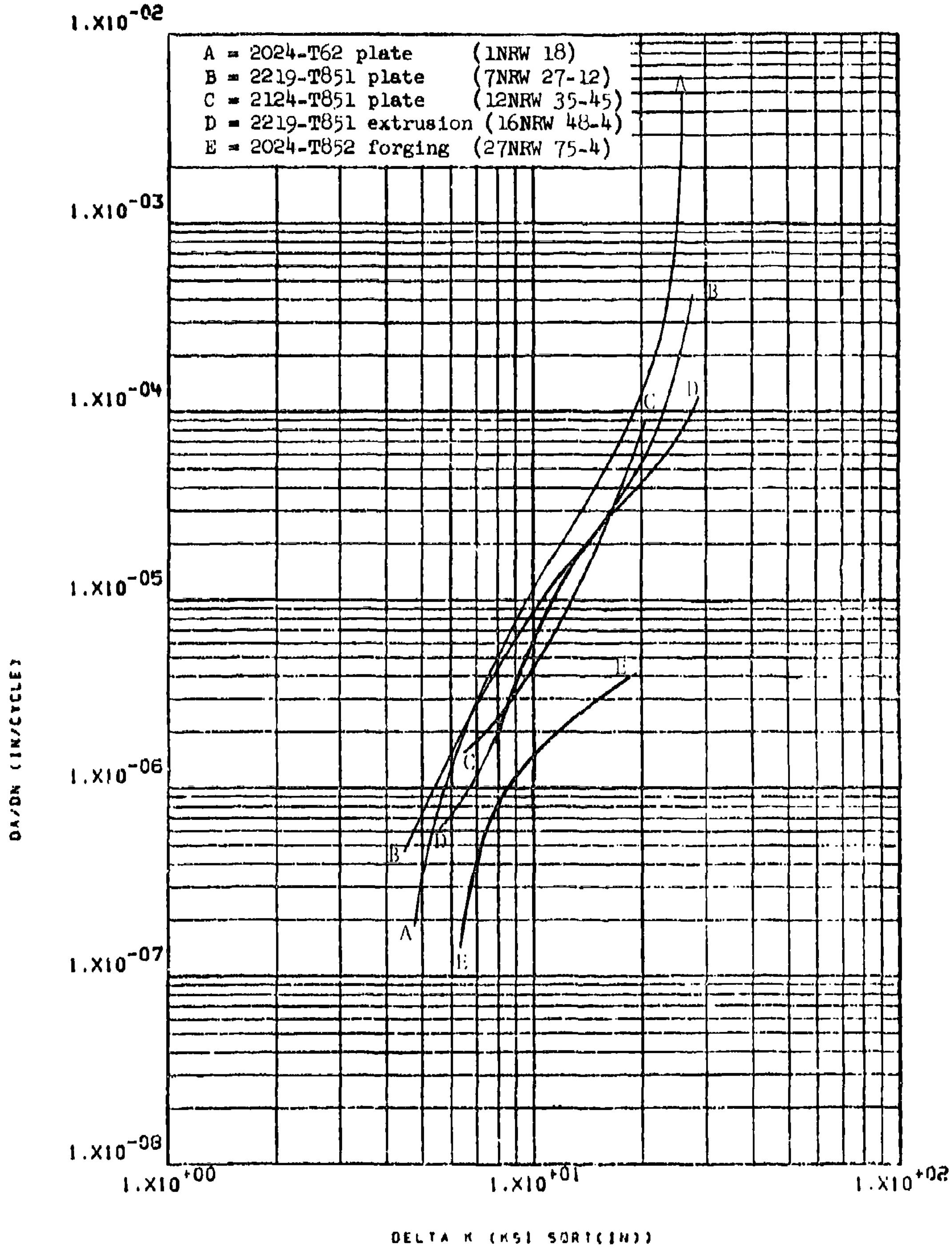

Figure 8.2.15.3-1 Effect of alloy type and product form on LHA-FCGR at R.T., R=0.3, 360 cpm, RW direction in 2000 series aluminum alloys

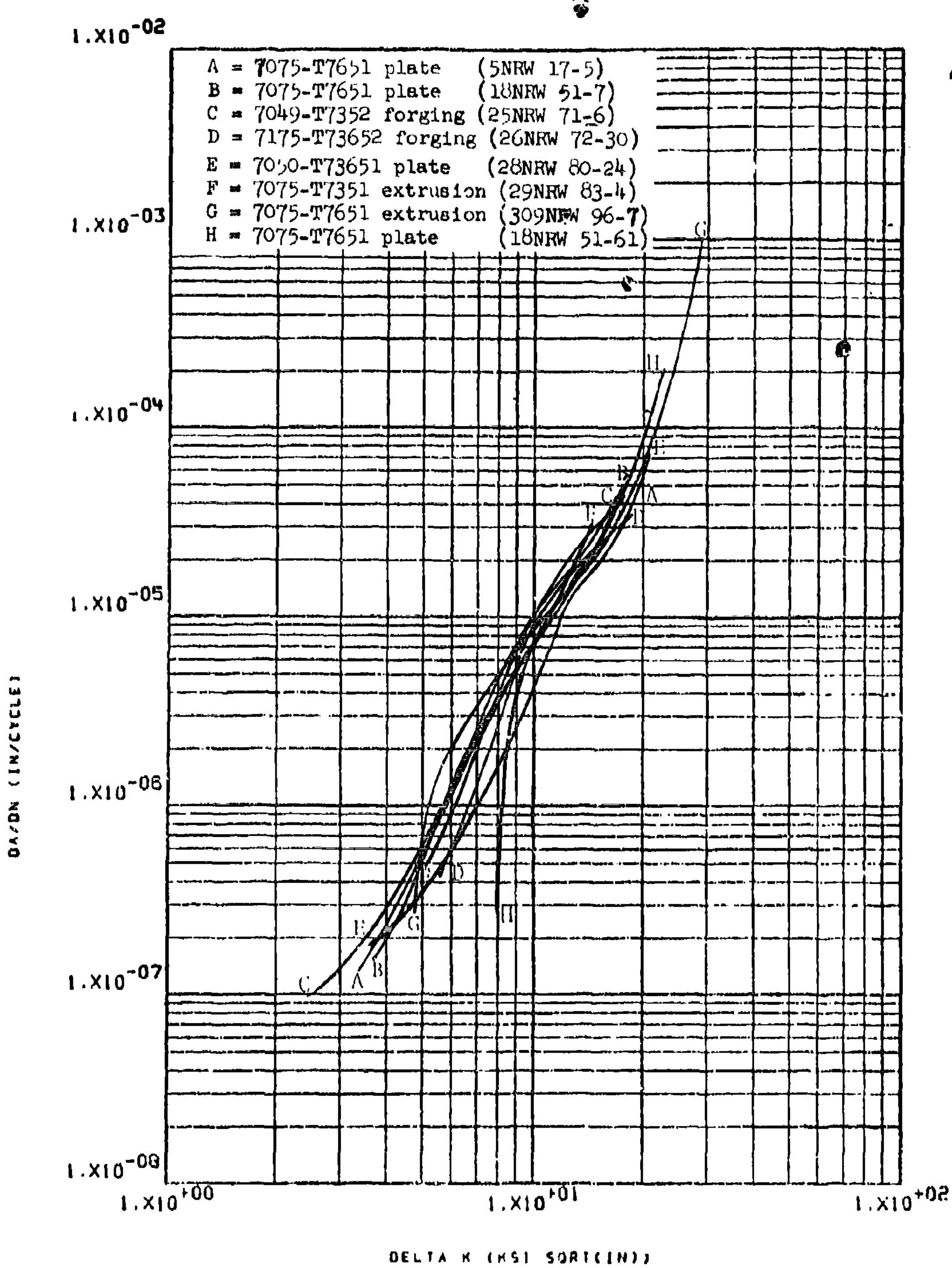

Figure 8.2.15.3-2 Effect of alloy type, temper condition and product form on LHA-FCGR at R.T., R=0.3, RW direction in 7000 series aluminum alloys.

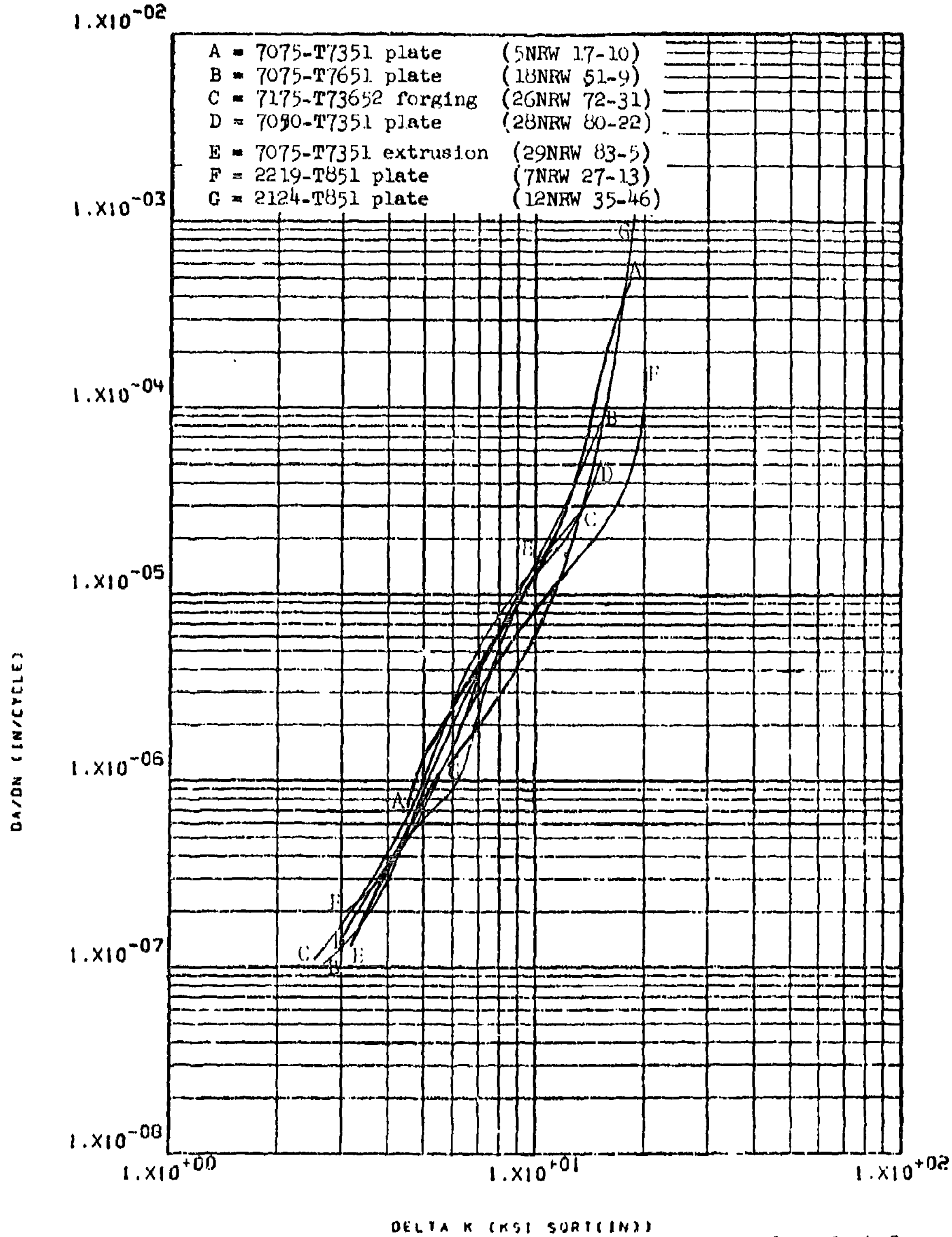

Figure 8.2.15.4-1 Effect of alloy type, temper condition and product form on LHA-FCGR at R.T., R=0.5, RW direction in aluminum alloys.

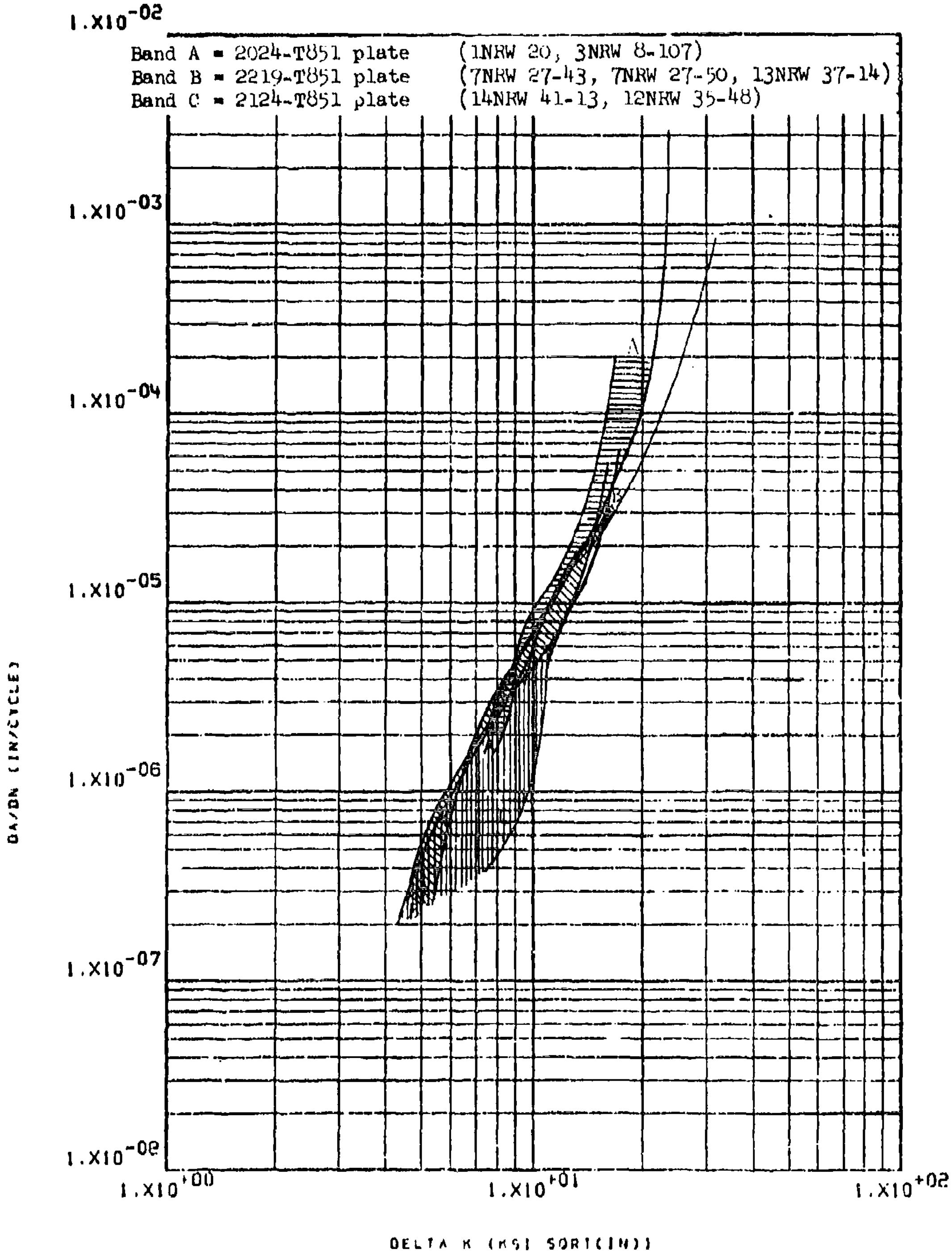

Figure 8.2.15.5-1 Effect of alloy type on the STW-FCGR at R.T., R=0.08, 60 cpm, RW direction in 2000 series aluminum alloy plate.

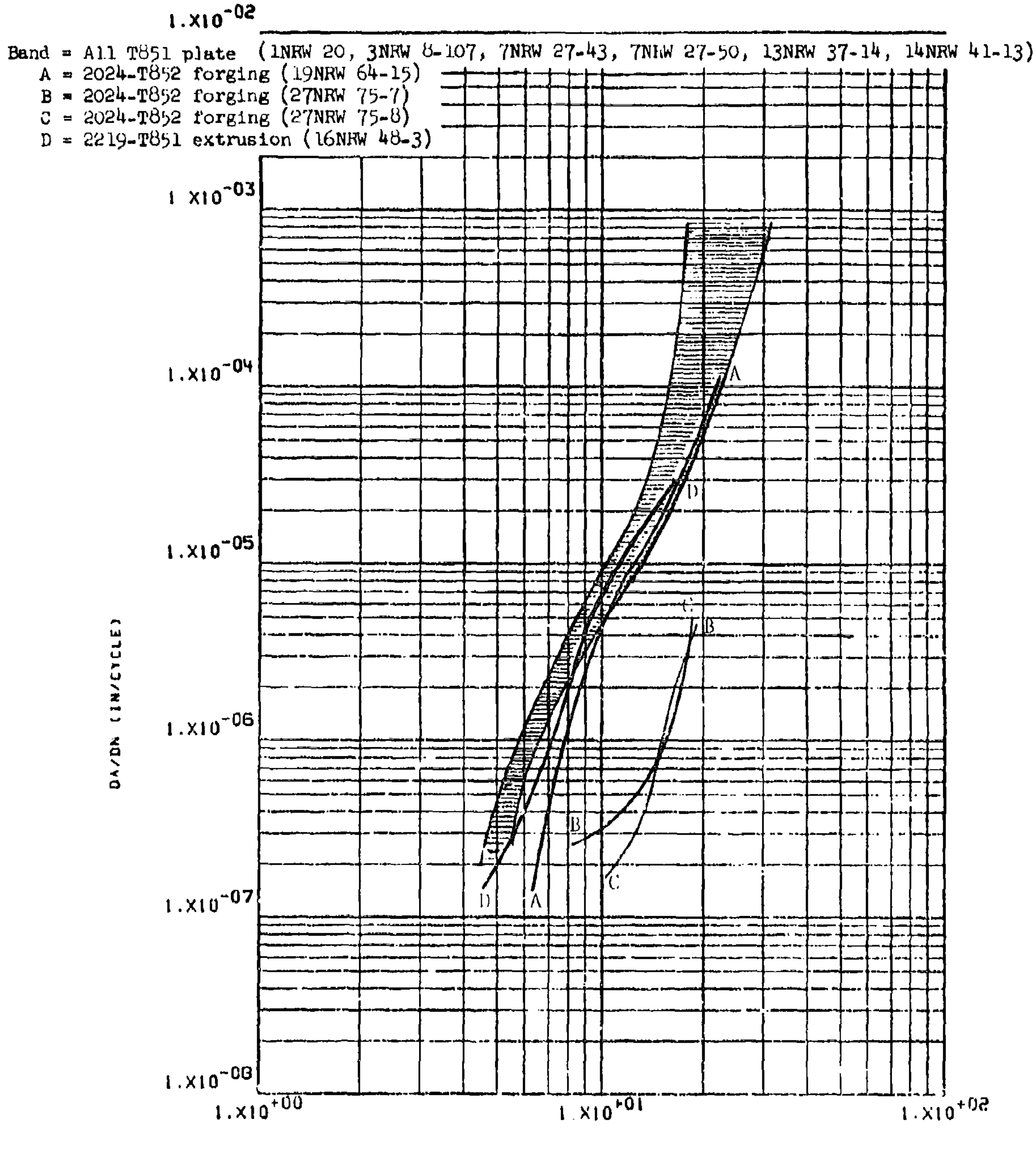

Figure 8.2.15.5-2 Effect of alloy type and product form on the STW-FCGR at R.T., R=0.08, 60 cpm, RW direction in 2000 series aluminum alloys.

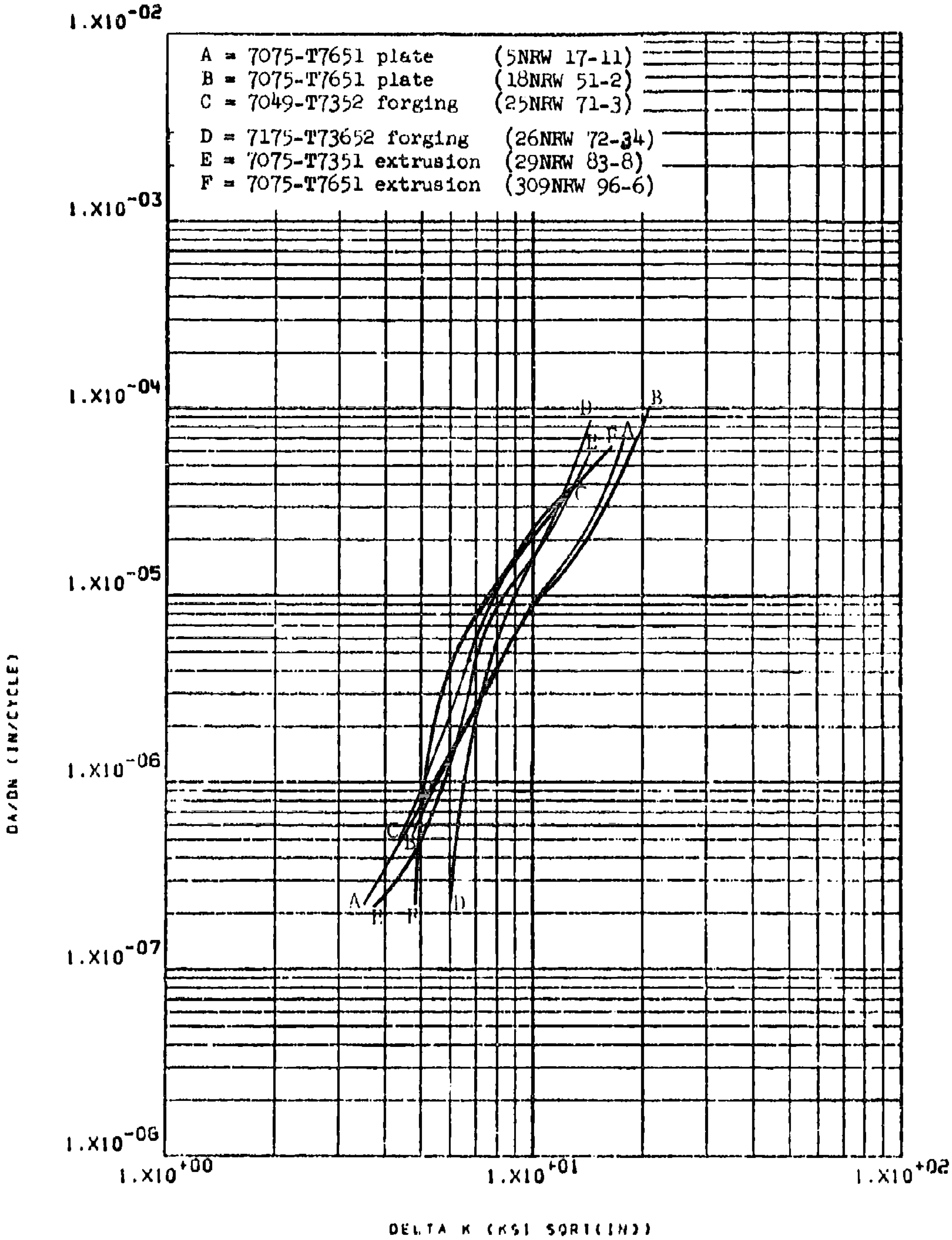

Figure 8.2.15.5-3 Effect of alloy type, temper condition, and product form on STW-FCGR at R.T., R=0.08, 60 cpm, RW direction in 7000 series aluminum alloys.

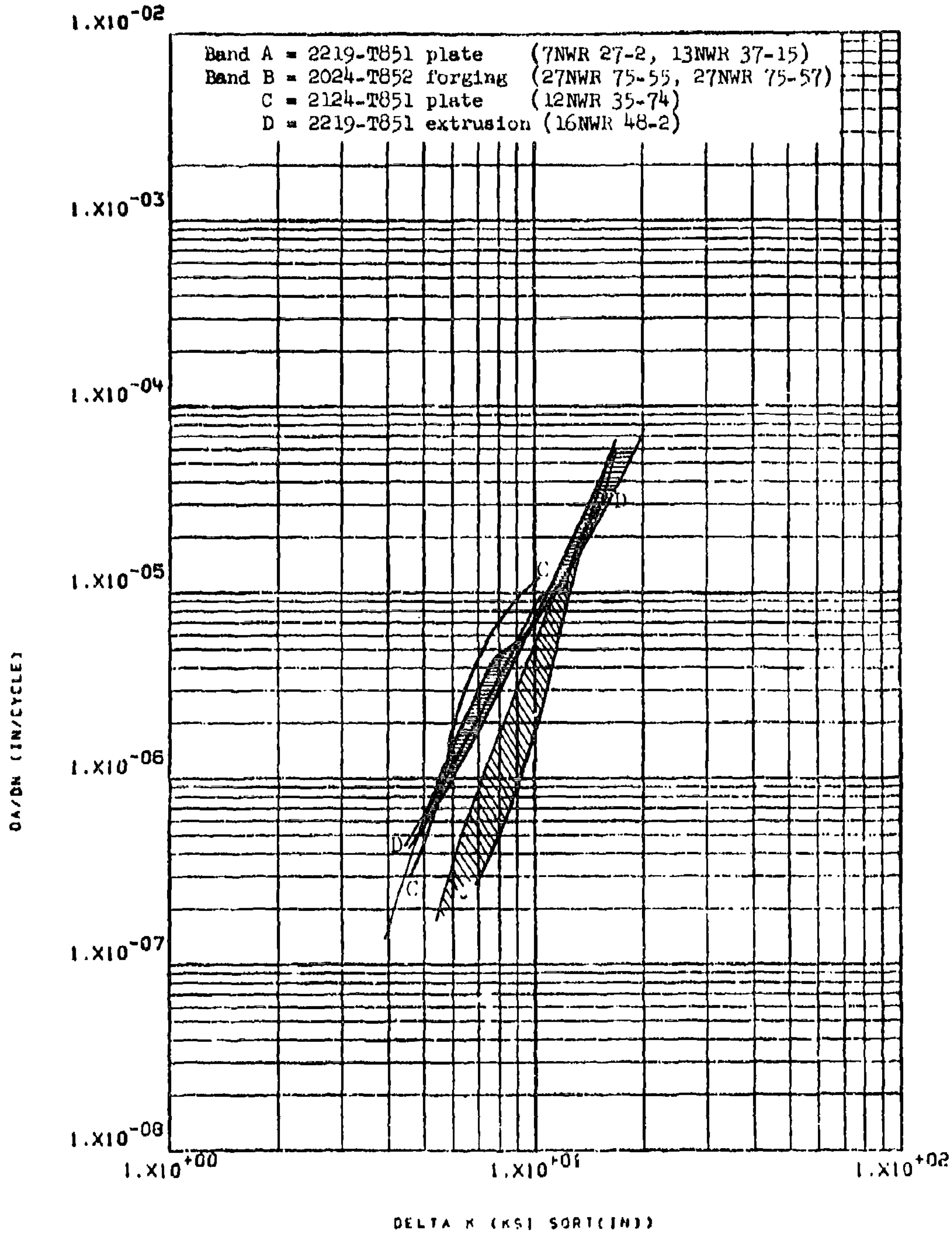

Figure 8.2.15.6-1 Effect of alloy type and product form on the STW-FCGR at R.T., R=0.08, 60 cpm, WR direction in 2000 series aluminum alloys.

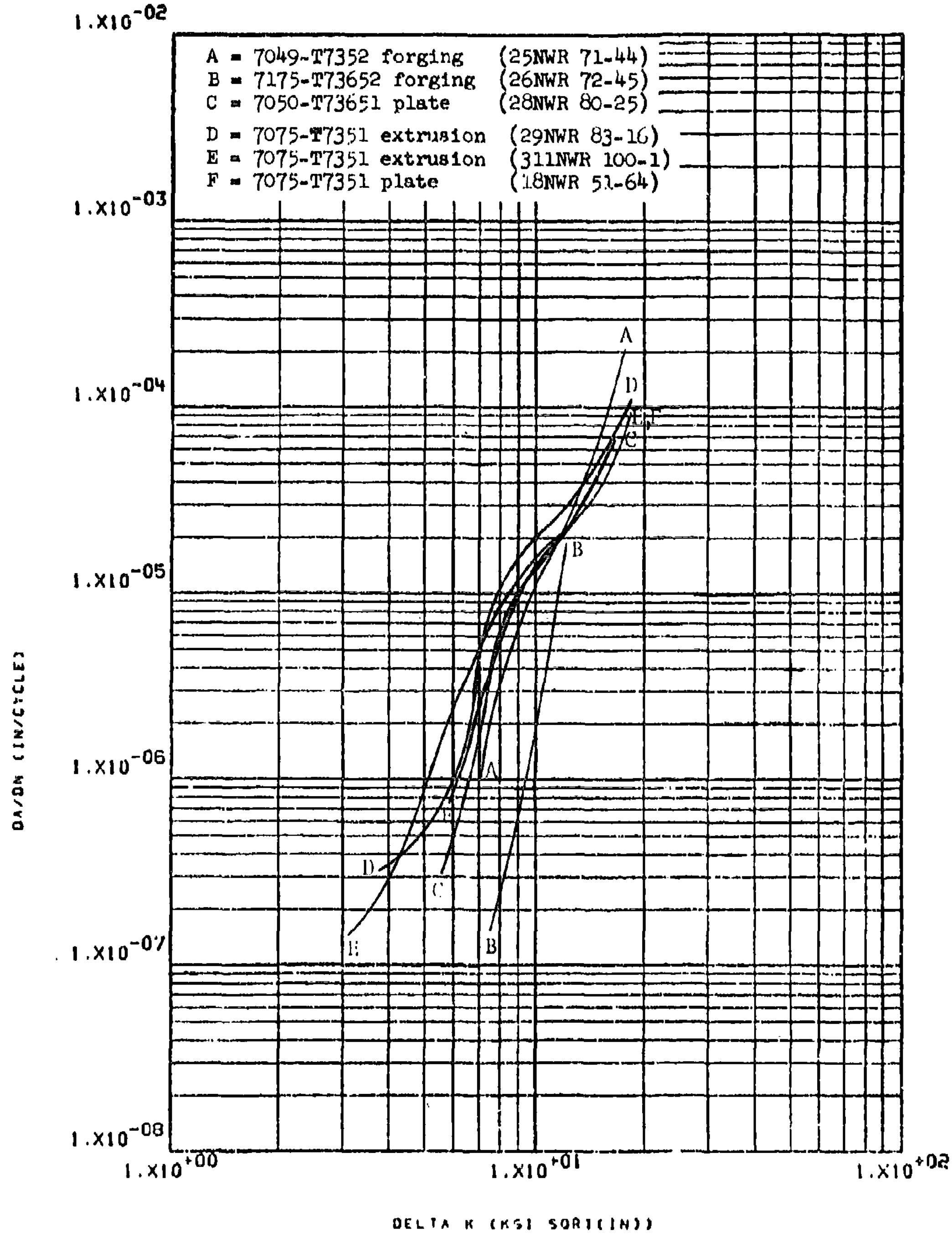

Figure 8.2.15.6-2 Effect of alloy type and product form on STW-FCGR at R.T., R=0.08, 60 cpm, WR direction in 7000 series aluminum alloys.

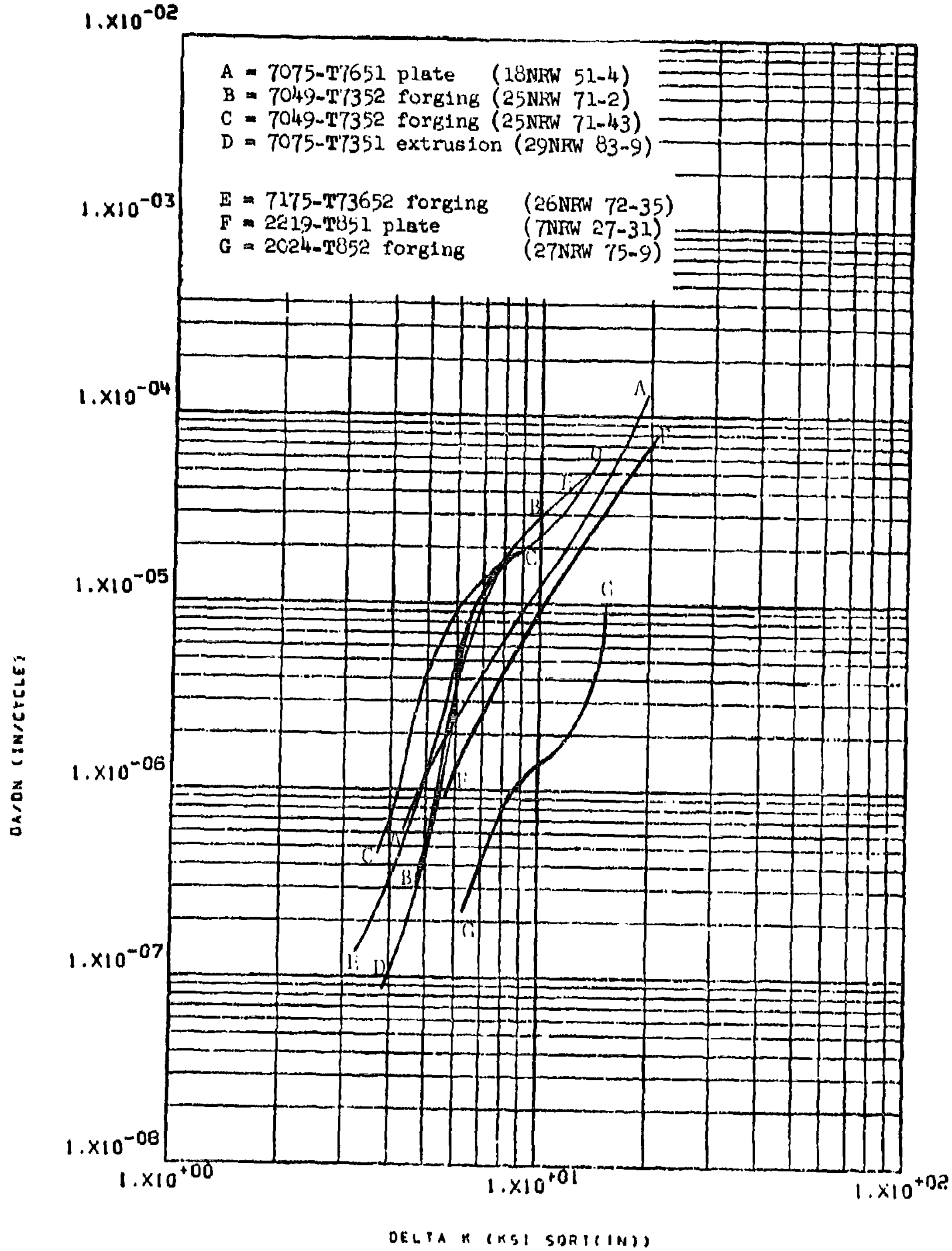

Figure 8.2.15.7-1 Effect of alloy type and product form on STW-FCGR at R.T., R=0.3, 60 cpm, RW direction in aluminum alloys.

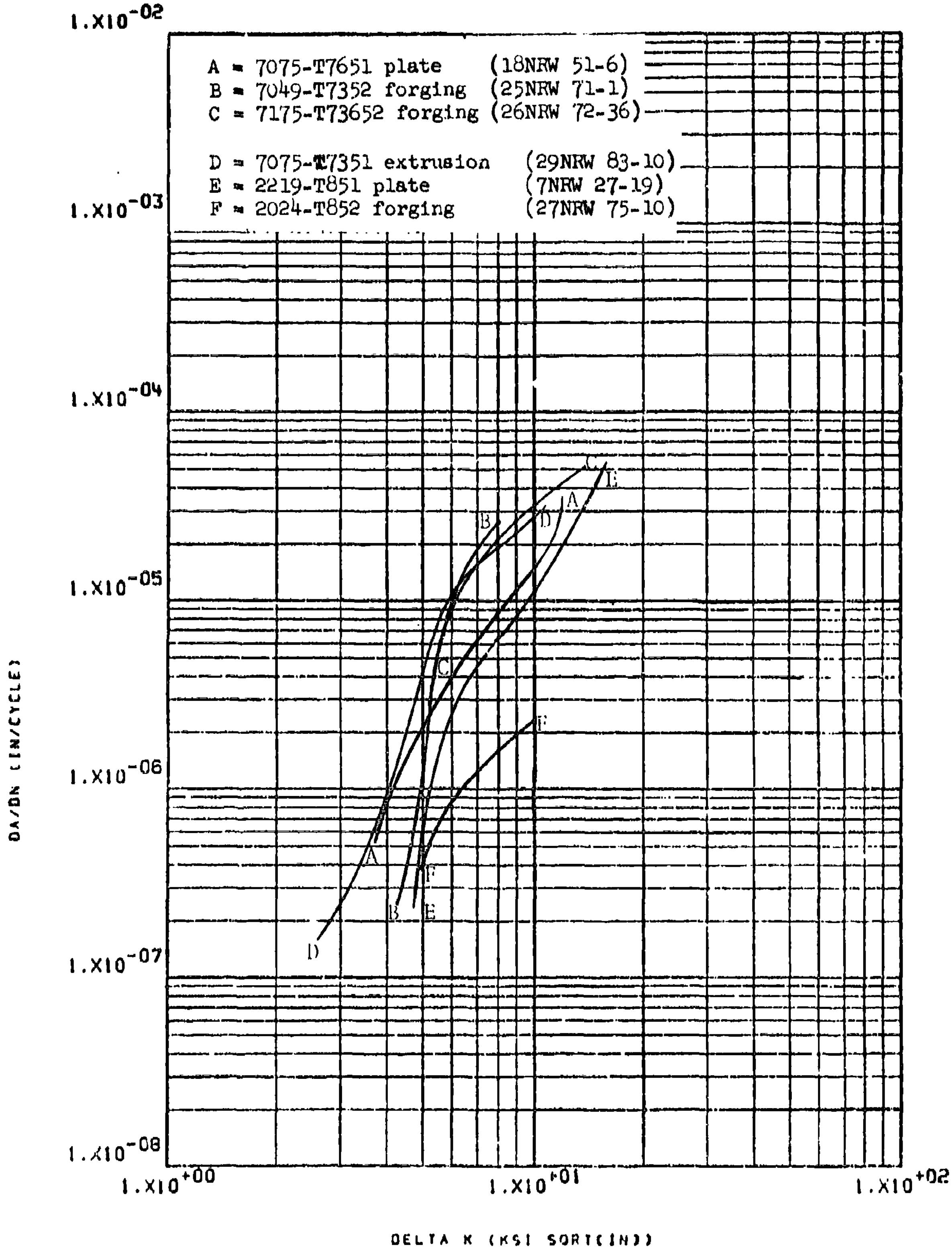

Figure 8.2.15.8-1 Effect of alloy type and product form on the STW-FCGR at R.T., R=0.5, 60 cpm, RW direction in aluminum alloys.

8.2.16 <u>All Steels and Inconel 718</u>

In a manner similar to that presented in Section 8.2.15, overlays were prepared of each da/dN curve generated in each alloy system at a fixed set of test parameters, to facilitate comparisons of fatigue crack growth rates between the various steels evaluated in this program. These comparisons have been made without regard to the ultimate strength level of each material, which might well influence fatigue crack growth rate characteristics. Each material evaluated in this program was, however, heat treated to its most commonly used condition prior to testing.

8.2.16.1 Standard Conditions - LHA, R.T., R=0.08, 360 cpm, RW direction - There was surprisingly little difference between the low humidity air fatigue crack growth rate characteristics of all forms of HP-9-4-.20, HP-9-4-.30, and 300M. The results from six different tests performed on HP-9-4-.20 forged block and plate all fell within a very narrow scatter band, which also contained the curves of a 300M forged block, an HP-9-4-.30 forged block and an HP-9-4-.30 rolled block (Figure 8.2.16.1-1). Similarly the curves for six different tests performed on PH13-8Mo forged block, rolled block, extrusion and upset forging all fell within a narrow scatter band (Figure 8.2.16.1-2), though not so narrow as that for the 300M, 9-4-.20 and 9.4.-30. Both of these scatter bands have been replotted in Figure 8.2.16.1-3 for comparison with each other, and with growth rate characteristics of Inconel 718. At delta K levels above approximately 16 ksi $\sqrt{in}$ the two scatter bands were seen to be essentially congruent, while below this delta K level growth rates in PH13-8Mo were seen to be very slightly lower than those of the 300M, HP-9-4-.20, and HP-9-4.-30. Growth rates of Inconel 718 were seen to be substantially lower than rates in any of the steels evaluated throughout the entire range of delta K.

8.2.16.2 LHA, R.T., R=0.08, 360 cpm, <u>WR direction</u> - Similar to the observations made in the RW direction, the low humidity air fatigue crack growth rates in the WR direction of 300M forged bar, HP-9-4-.20 plate and forged block, and HP-9-4-.30 forged and rolled blocks all fell within a very narrow scatter band (Figure 8.2.16.2-1). One peculiarity was observed, however, in the growth rate curve generated from 300M, which displayed substantially accelerated growth rates at delta K levels above 20 ksi $\sqrt{in}$, when compared with the HP-9-4-.20 and HP-9-4-.30 curves. The scatter band for PH13-8Mo material in the WR direction was again seen to be narrow, but not as narrow as the band for the HP-9-4.-20 and HP-9-4-.30 (Figure 8.2.16.2-2). Both of these bands have been replotted in Figure 8.2.16.2-3 for comparison with each other, and with the fatigue crack growth rate characteristics of 300M and Inconel 718. Again the growth rates in Inconel 718 were seen to be substantially lower than in any of the steels evaluated.

8.2.16.3 LHA, R.T., <u>R=0.3</u>, 360 cpm, RW direction - Under these test conditions again very little difference was observed between the fatigue crack growth rate characteristics of HP-9-4-.20 forged block, HP-9-4.-30 forged block and rolled block, and PH13-8Mo forged block and rolled block (Figure 8.2.16.3-1). At delta K levels below ~25 ksi $\sqrt{in}$, growth rates in

300M were again seen to be equivalent to those of the other steels listed above, while at higher levels of delta K growth rates in 300M were seen to be significantly greater than in the remaining steels evaluated in this program. No tests were performed in Inconel 718 at an R factor of 0.3.

8.2.16.4 LHA, R.T., R=0.5, 360 cpm, RW direction - At an R factor of 0.5, a slight broadening of the scatter band for all steels was observed with growth rates in PH13-8Mo exhibiting the slowest growth rates at delta K levels below 15-17 ksi $\sqrt{in}$ (Figure 8.2.16.4-1). There was no distinct trend of one alloy system being faster or slower than any other alloy system in growth rate characteristics throughout the range of delta K, although growth rates in 300M forged block were again observed to be greater than the other steels at delta K levels above ~15 ksi $\sqrt{in}$. Growth rates in Inconel 718 were again observed to be substantially lower than in any of the steels evaluated. At this R factor, little difference was observed between the growth rates in the Inconel 718 forged block and those in the Inconel 718 die forging, in contrast to the differences observed at lower R factors.

8.2.16.5 STW, R.T., R=0.08, 60 cpm, RW direction - The difference between fatigue crack growth rate characteristics of the various steels evaluated in this program became distinctly apparent when testing was conducted in sump tank water. At the same time, the magnitude of scatter bands associated with each alloy system was greatly increased from that observed in low humidity air tests. Of all the steels evaluated, 300M exhibited the fastest growth rates, being almost an order of magnitude faster than rates observed in PH13-8Mo, 9-4-.20 and 9-4-.30 at a delta K level of 10 ksi $\sqrt{in}$ (Figure 8.2.16.5-1). The curves of Figure 8.2.16.5-1 are replotted as scatter bands in Figure 8.2.16.5-2 to clearly show the difference in rates experienced in these alloy systems. At delta K levels above 20 ksi $\sqrt{in}$ the bands of PH13-8Mo and 300M were seen to overlap. The bands of PH13-8Mo and 9-4-.20 and -.30 were seen to be essentially congruent below a delta K level of 25 ksi $\sqrt{in}$ while rates in the 9-4-.20 and -.30 steels were noticeably lower than those in PH13-8Mo at delta K values above this level. Again, growth rates in Inconel 718 were seen to be substantially lower than any of the steels evaluated throughout the entire range of delta K.

8.2.16.6 STW, R.T., R=0.08, 60 cpm, WR direction - While only limited sump tank water testing was performed in the WR direction of steels, growth rates in 300M forged bar were again seen to be noticeably greater than in PH13-8Mo forged block and rolled block, and growth rates in Inconel 718 forged block were almost two orders of magnitude slower than the slowest PH13-8Mo test (Figure 8.2.16.6-1).

8.2.16.7 STW, R.T., R=0.3, 60 cpm, RW direction - At an R factor of 0.3, the sump tank water growth rates of 300M forged block were again seen to be substantially greater than those observed in 9-4-.30 rolled block and

PH13-8Mo rolled block and forged block (Figure 8.2.16.7-1). At delta K levels below ~15 ksi$\sqrt{in}$ growth rates in the rolled block of 9-4-.30 and PH13-8Mo were seen to be essentially equivalent, while at delta K values above this level growth rates in the PH13-8Mo material were substantially greater than those in the 9-4-.30. Growth rates in a PH13-8Mo forged block were seen to be noticeably lower than those in the 9-4-.30 rolled block throughout the entire range of delta K.

8.2.16.8 STW, R.T., R=0.5, 60 cpm, RW direction - The effect of increasing the R factor of test from 0.3 to 0.5 on the sump tank water growth rates of steels is clearly exemplified by the broadened scatter band of 300M, together with significantly increased growth rates of this material (Figure 8.2.16.8-1 compared with Figure 8.2.16.7-1). Again 300M growth rates are significantly greater than those in 9-4-.30, being up to two orders of magnitude greater at a delta K level of 10 ksi$\sqrt{in}$.

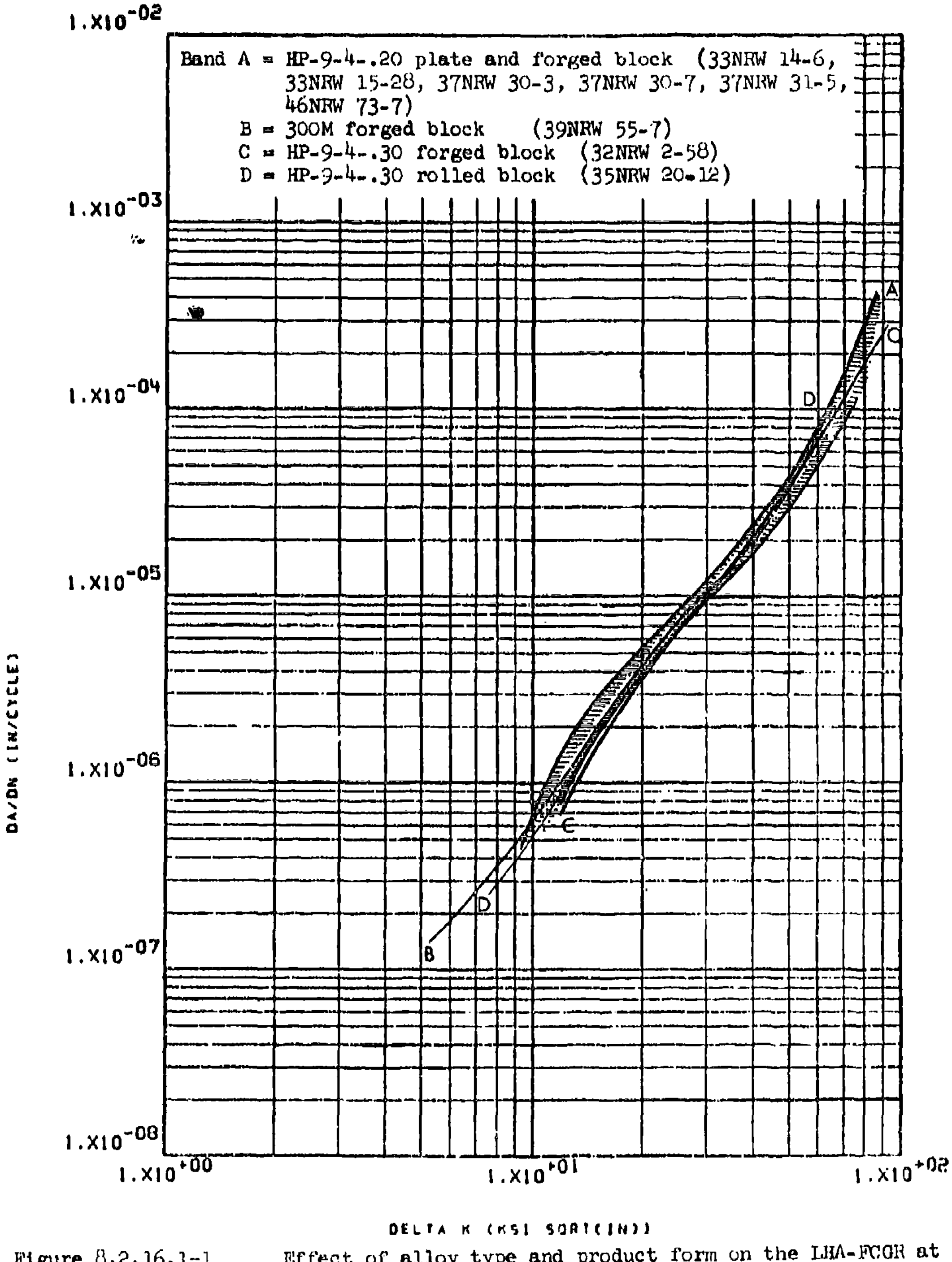

Figure 8.2.16.1-1 Effect of alloy type and product form on the LHA-FCGR at R.T., R=0.08, 360 cpm, RW direction of HP-9-4-.20, HP-9-4-.30 and 300M.

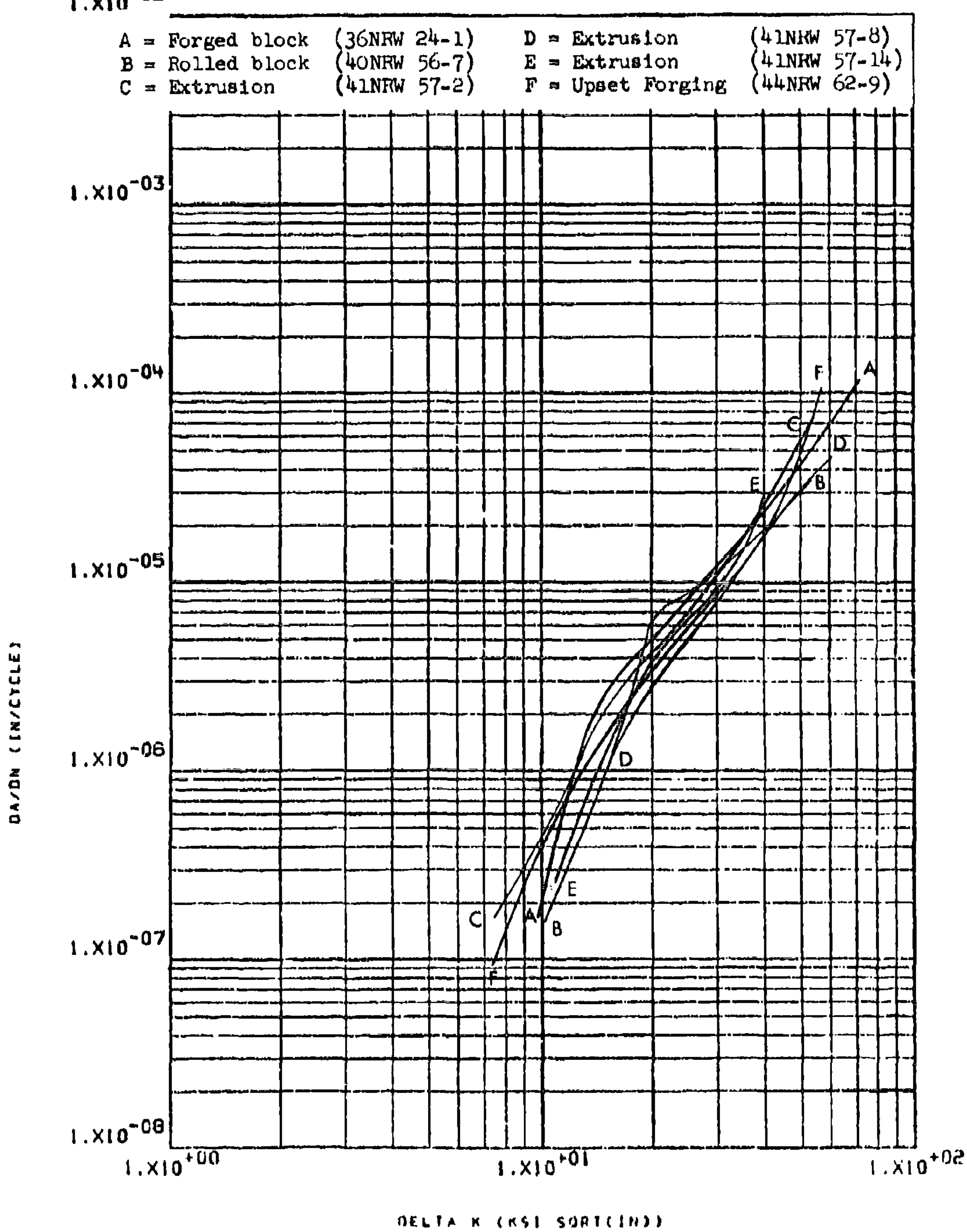

Figure 8.2.16.1-2 Effect of product form on LHA-FCGR at R.T., R=0.08, 360 cpm, RW direction of PH13-8Mo

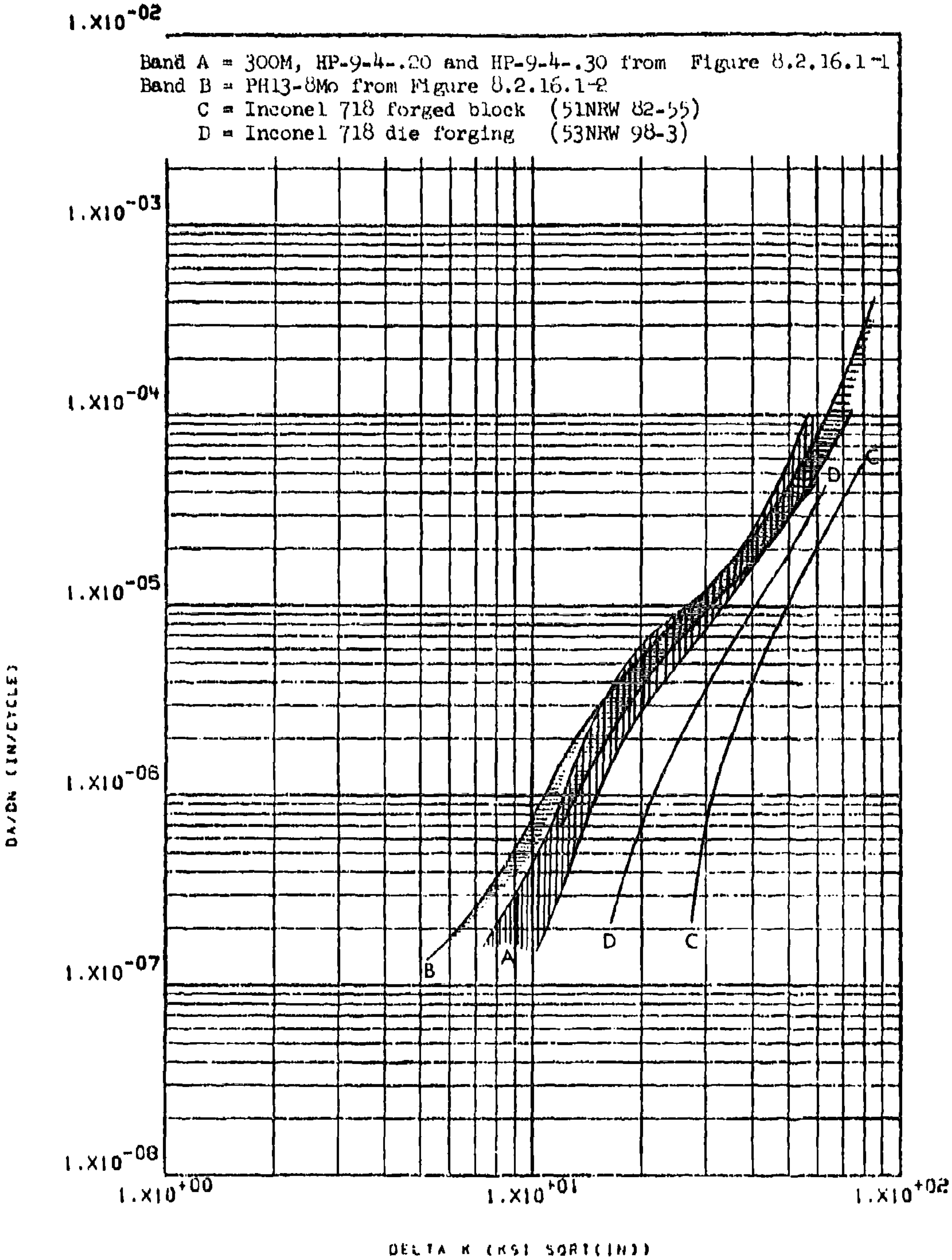

Figure 8.2.16.1-3 Effect of alloy type and product form on LHA-FCGR at R.T., R=0.08, 360 cpm, RW direction in 300M, HP-9-4-.20, HP-9-4-.30, PH13-8Mo, and Inconel 718

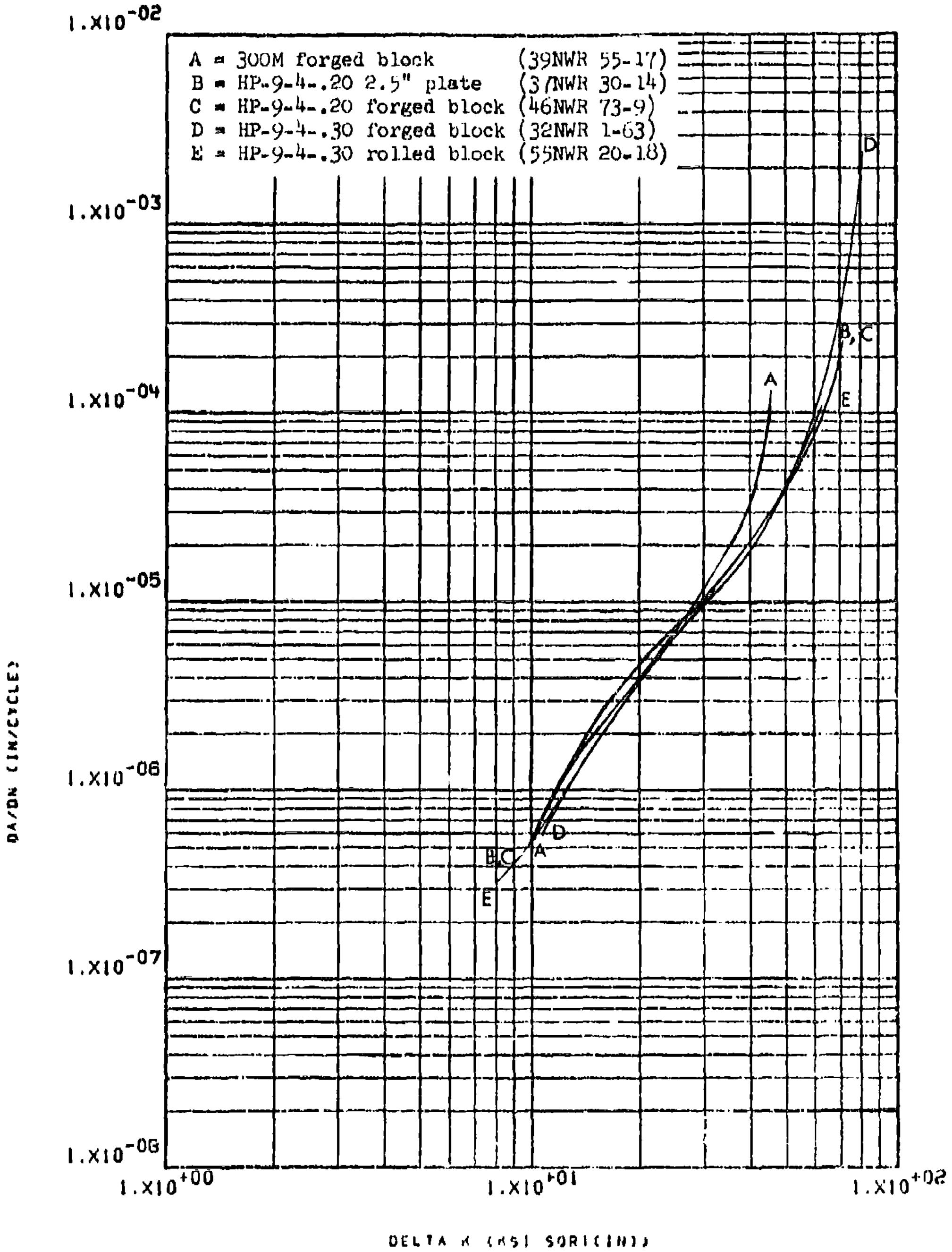

Figure 8.2.16.2-1 Effect of alloy type and product form on the LHA-FCGR at R.T., R=0.08, 360 cpm, WR direction in 300M, HP-9-4-.20, and HP-9-4-.30

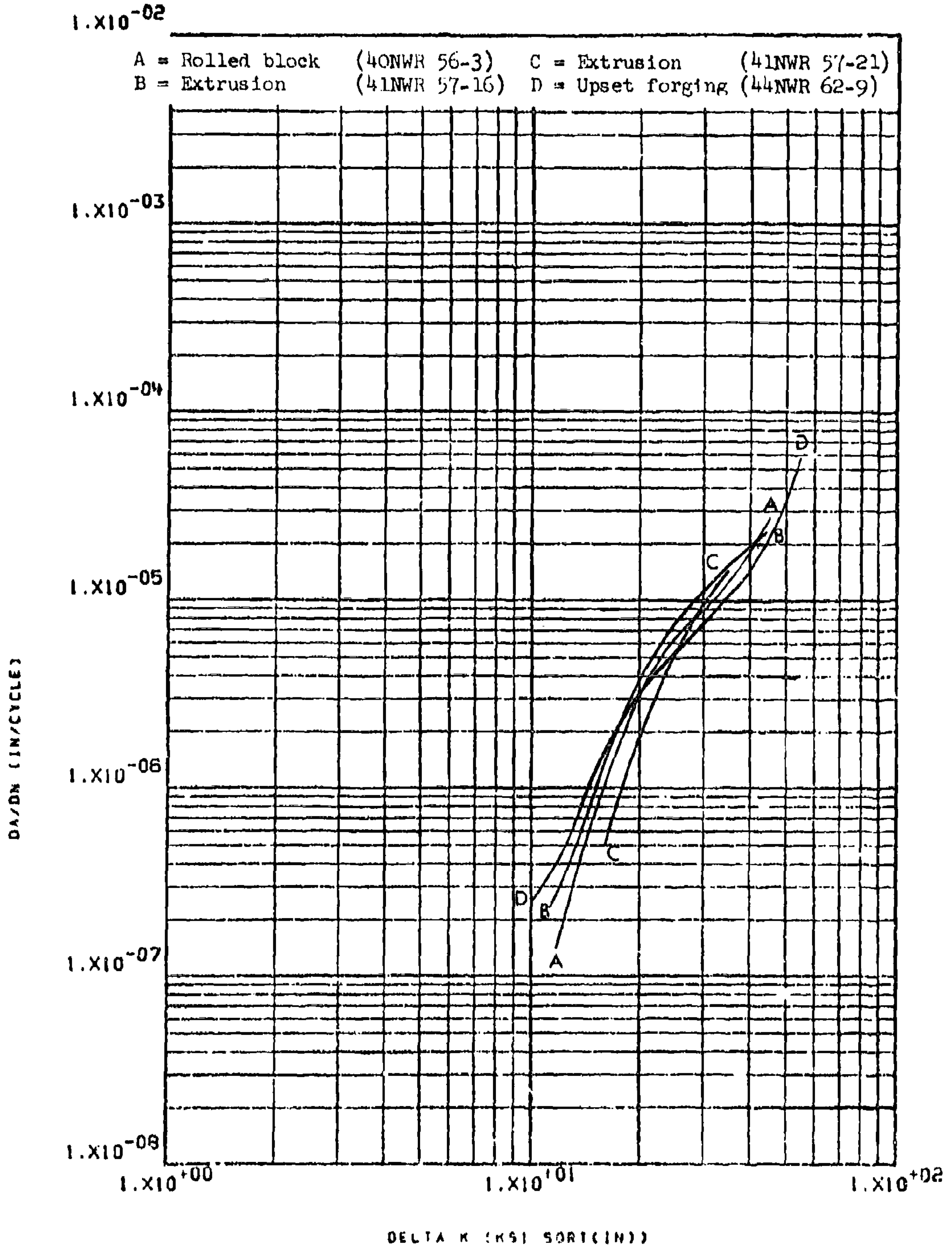

Figure 8.2.16.2-2 Effect of product form on the LHA-FCGR at R.T., R=0.08, 360 cpm, WR direction in PH13-8Mo.

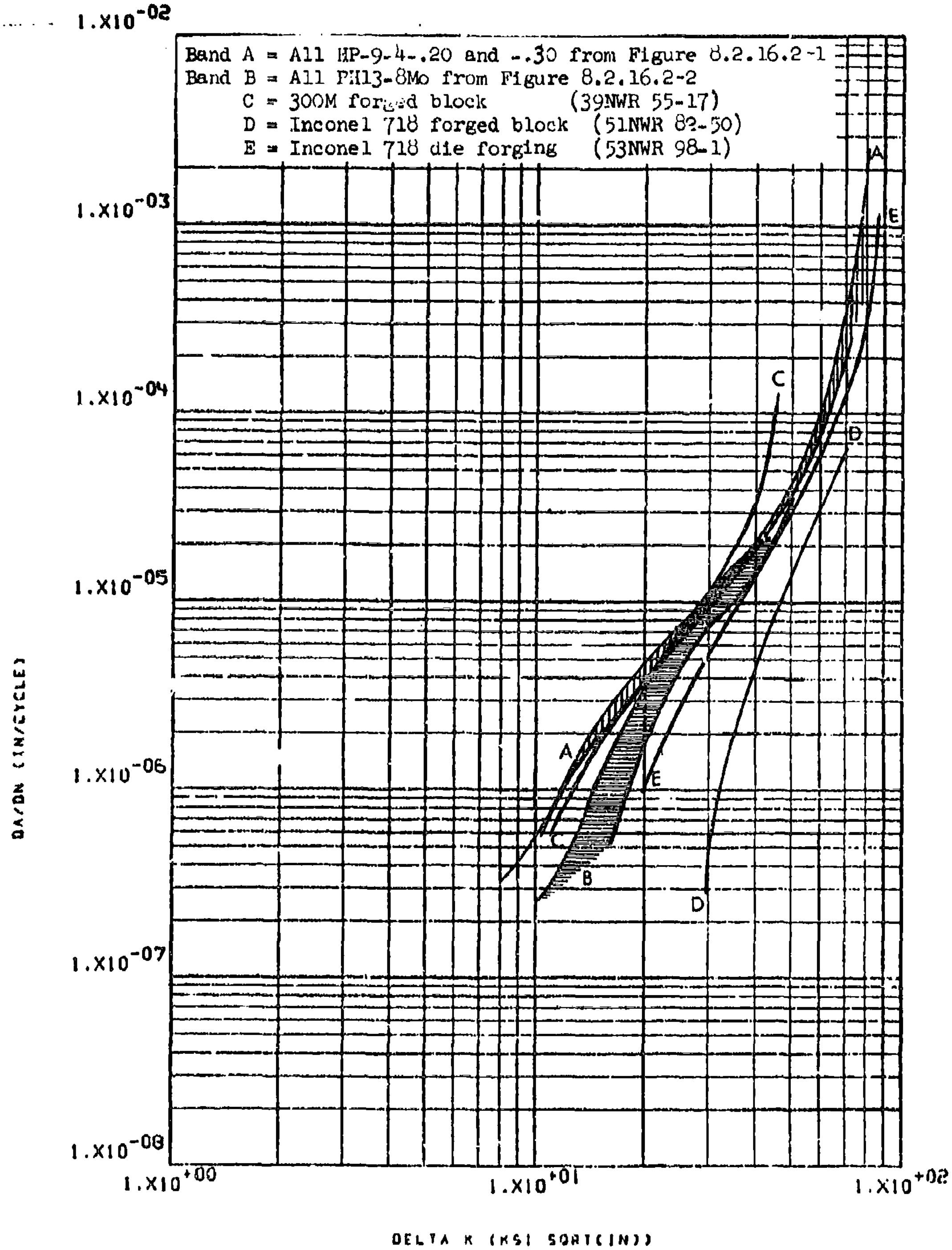

Figure 8.2.16.2-3 Effect of alloy type and product form on the LHA-FCGR at R.T., R=0.08, 360 cpm, WR direction in 300M, HP-9-4-.20, HP-9-4-.30, PH13-8Mo and Inconel 718

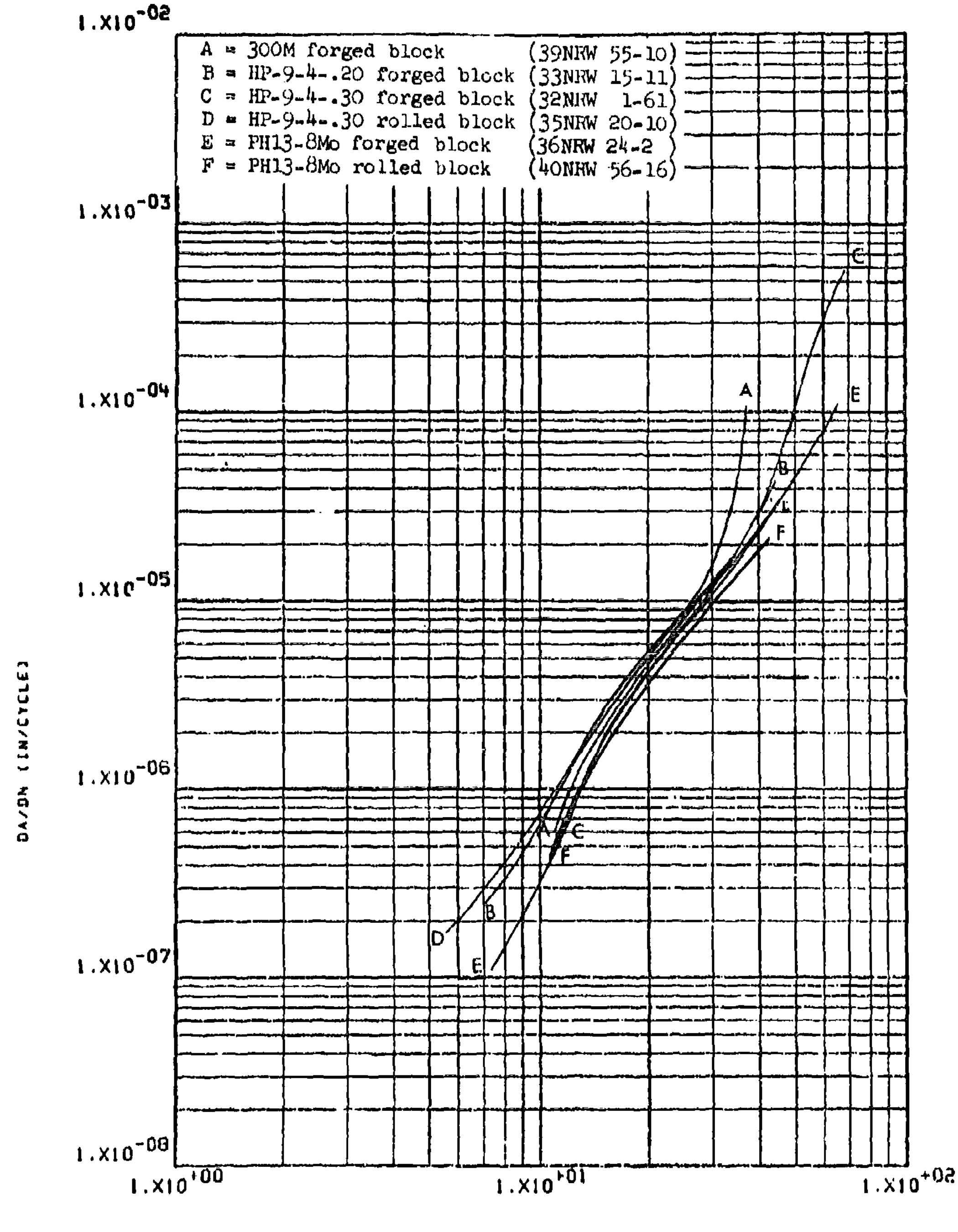

Figure 8.2.16.3-1 Effect of alloy type and product form on the LHA-FCGR at R.T., R=0.3, 360 cpm, RW direction in 300M, HP-9-4-.20, HP-9-4-.30, and PH13-8Mo

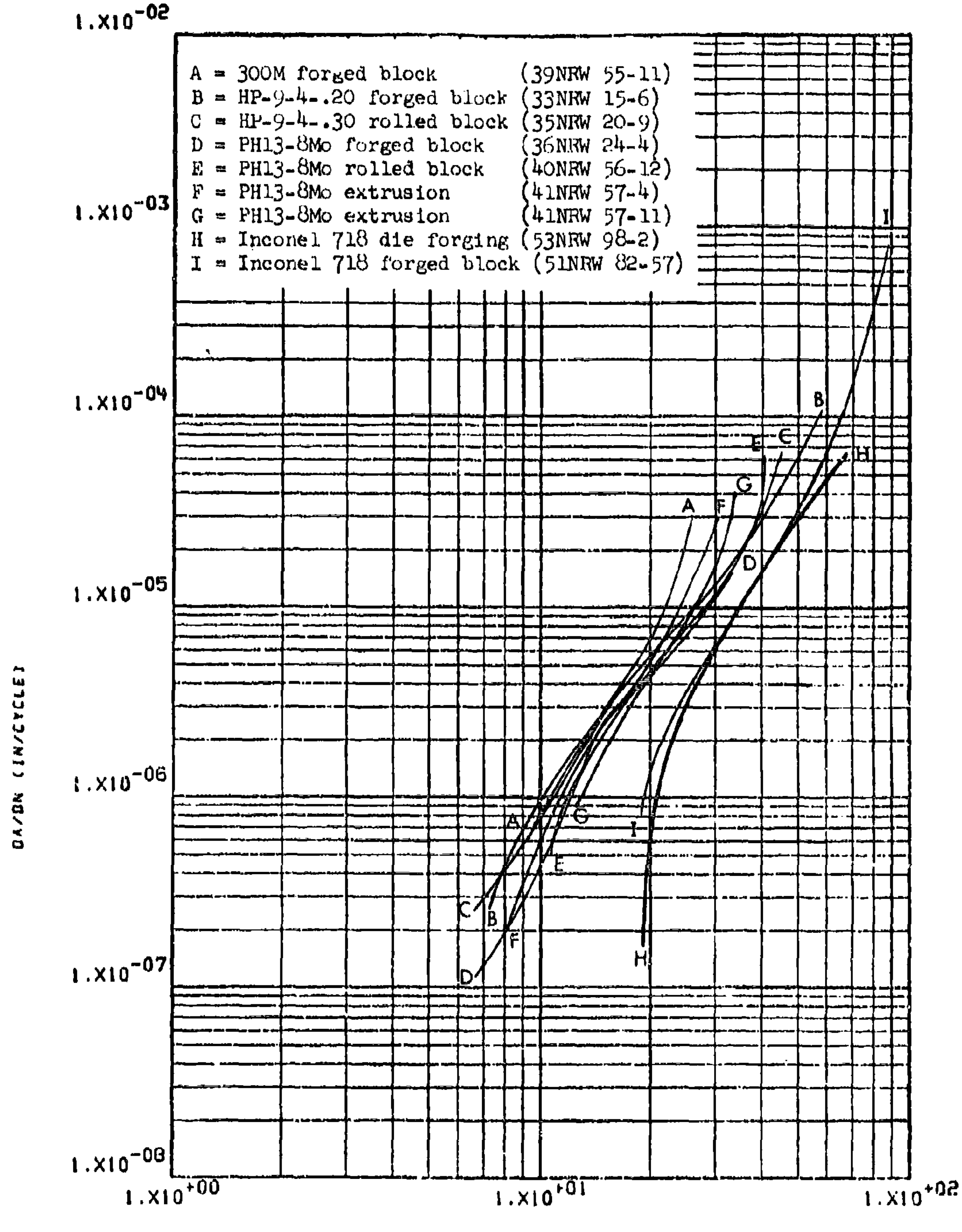

Figure 8.2.16.4-1 Effect of alloy type and product form on the LHA-FCGR at R.T., R=0.5, 360 cpm, RW direction in 300M, HP-9-4-.20, HP-9-4-.30, PH13-8Mo, and Inconel 718

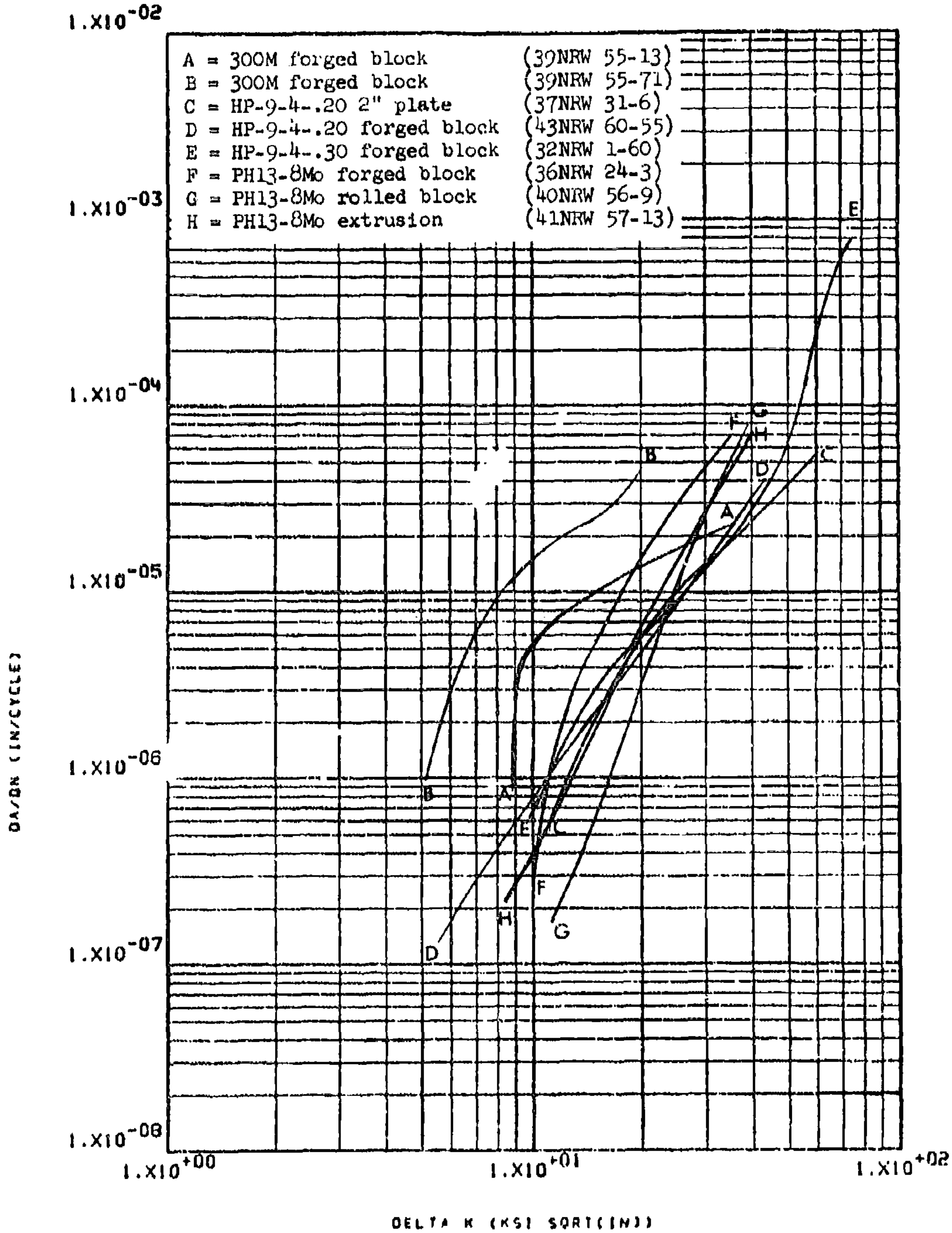

Figure 8.2.16.5-1 Effect of alloy type and product form on the STW-FCGR at R.T., R=0.08, 60 cpm, RW direction in 300M, HP-9-4-.20, HP-9-4-.30 and PH13-8Mo.

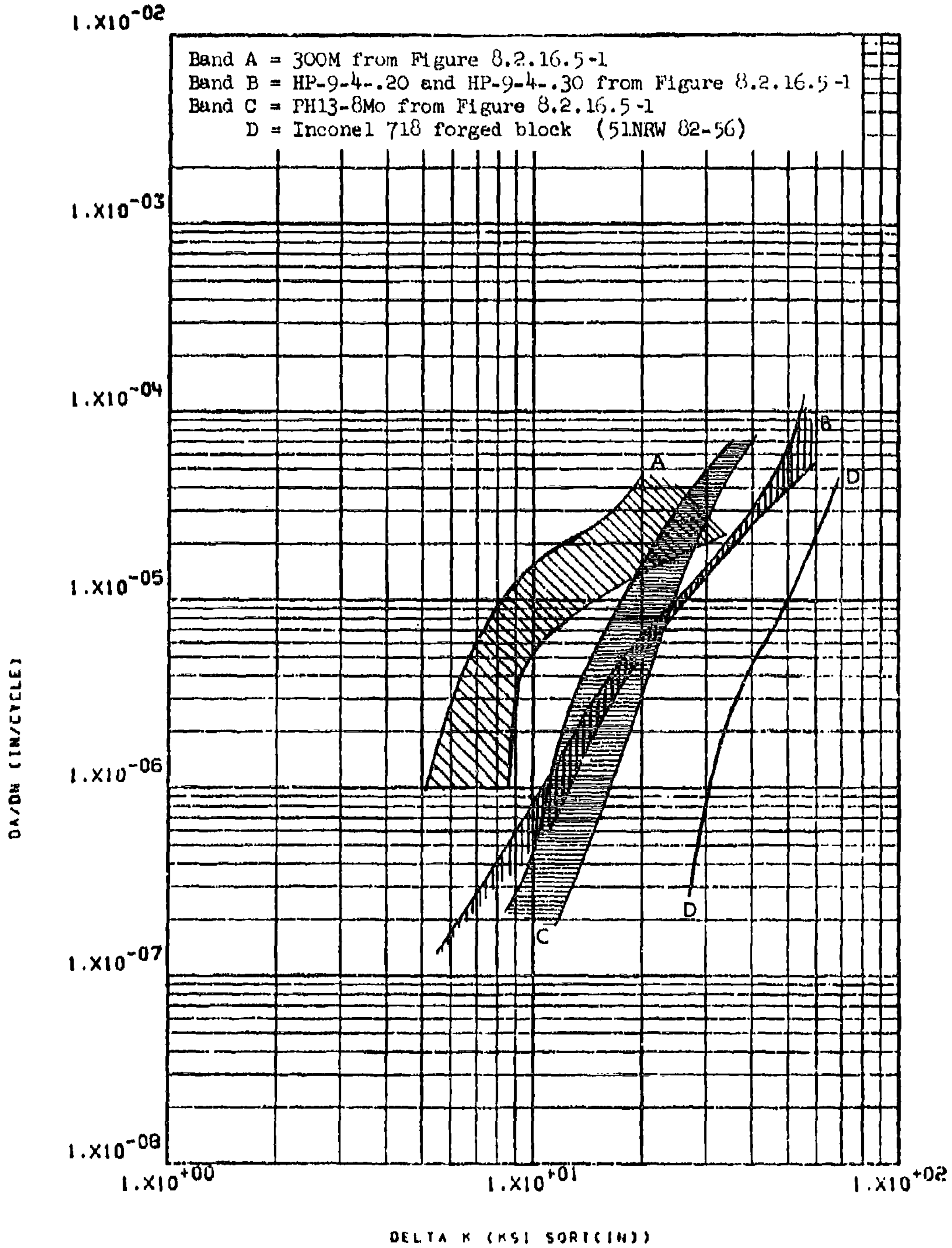

Figure 8.2.16.5-2 Effect of alloy type and product form on the STW-FCGR at R.T., R=0.08, 60 cpm, RW direction in 300M, HP-9-4-.20, HP-9-4-.30, PH13-8Mo, and Inconel 718.

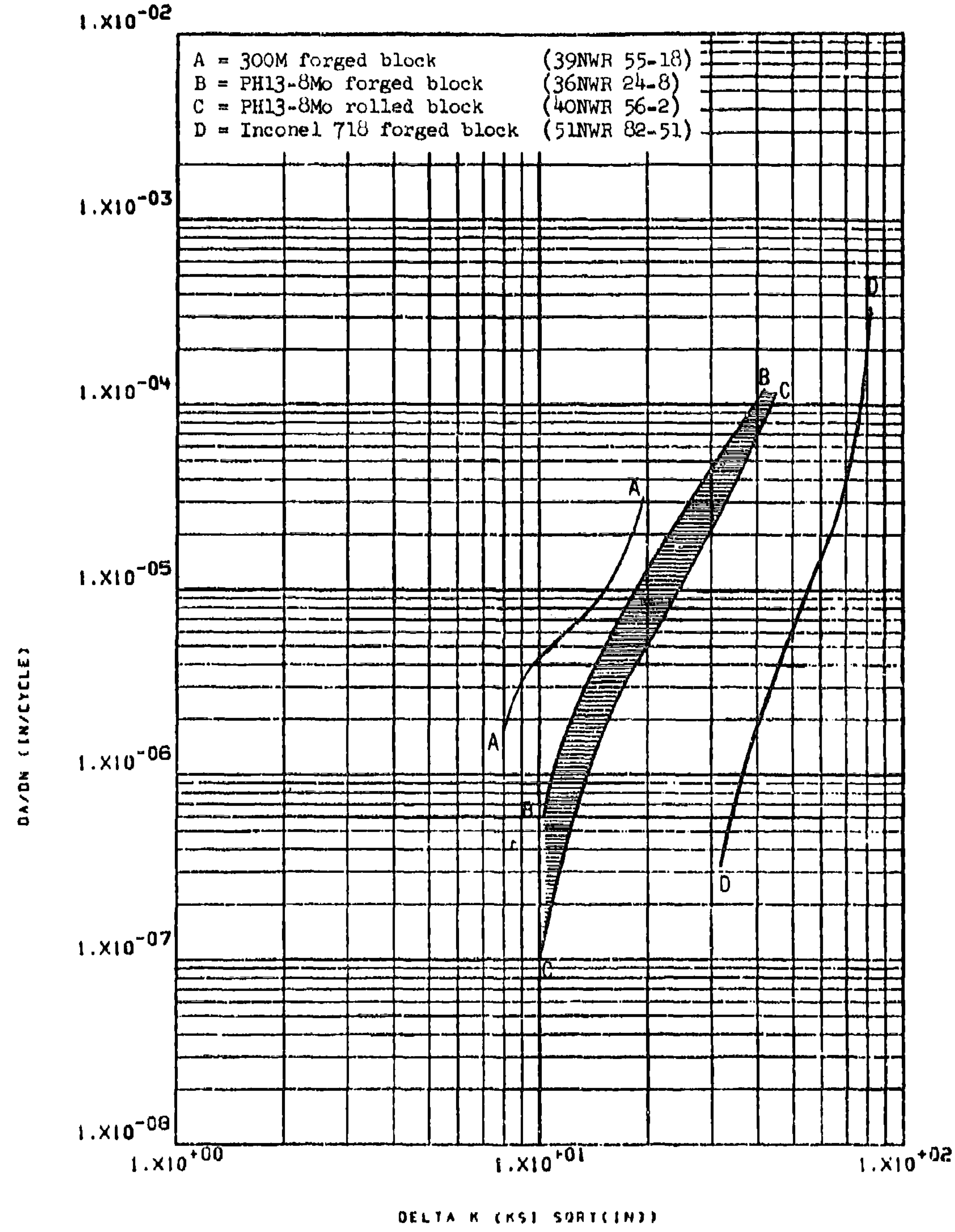

Figure 8.2.16.6-1 Effect of alloy type and product form on the STW-FCGR at R.T., R=0.08, 60 cpm, WR direction in 300M, PH13-8Mo and Inconel 718.

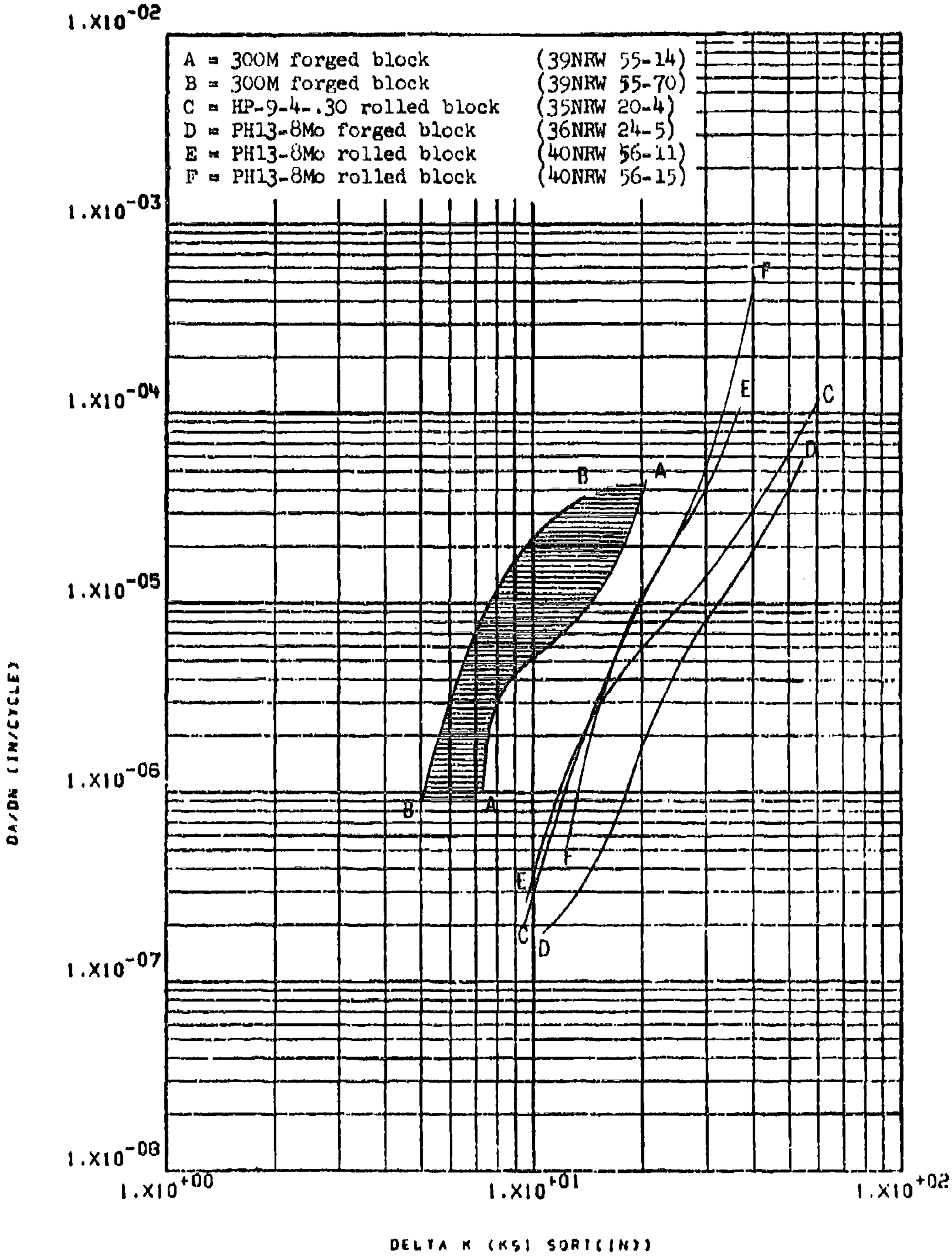

Figure 8.2.16.7-1 Effect of alloy type and product form on the STW-FCGR at R.T., R=0.3 , 60 cpm, RW direction in 300M, PH13-8Mo and HP-9-4-.30

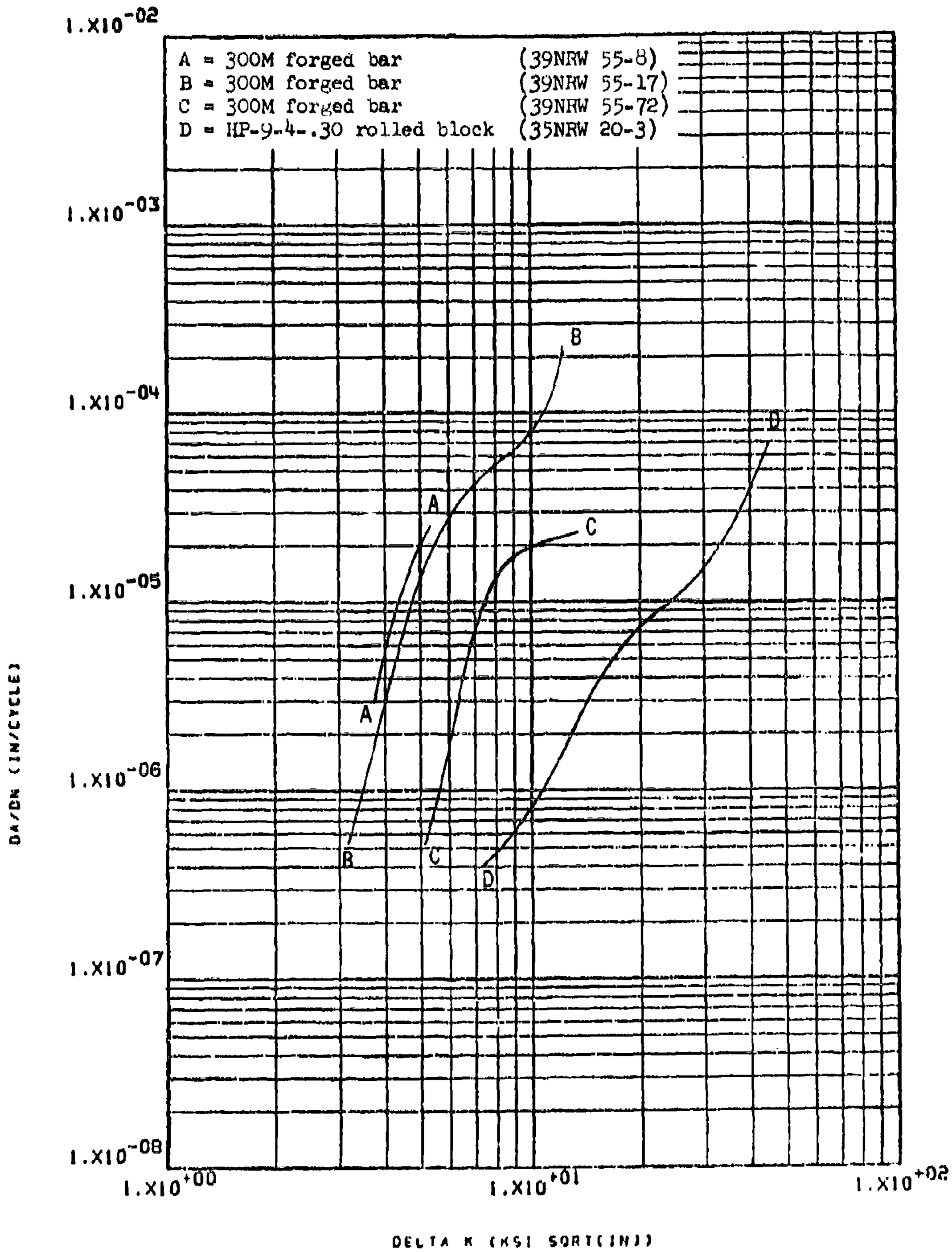

Figure 8.2.16.8-1 Effect of alloy type and product form on the STW-FCGR at R.T., R=0.5, 60 cpm, RW direction in 300M and HP-9-4-.30

8.2.17 All Titanium (Ti-6Al-4V)

8.2.17.1 Standard Conditions - LHA, R.T., R=0.08, 360 cpm, RW direction - The low humidity air fatigue crack growth rates of four tests in three different 1.5" thick recrystallization annealed plates all fell within a very narrow scatter band (Figure 8.2.17.1-1). Growth rates in a 2" thick RA plate and in a 3.5" thick RA plate were seen to be slower than those observed in the 1.5" thick plates throughout the entire range of delta K, with growth rates tending to increase as plate thickness decreased (Figure 8.2.17.1-1). The curves for 1.5" thick plate have been replotted as a scatter band in Figure 8.2.17.1-2 for comparison with other product forms and heat treat conditions of this material. Figure 8.2.17.1-2 reveals that as delta K increases the reduction in growth rates associated with increases in plate thickness becomes less pronounced. Above ~25 ksi$\sqrt{in}$ the 2" and 3.5" curves coincide, although throughout the entire delta K range both remain lower than the curves for the 1.5" thick plate. Growth rates in two beta processed plus mill annealed extrusions were seen to be essentially equivalent to those in the 1.5" thick plate (falling within the scatter band for that material) while growth rates in a 4" x 10" x 34" RA hand forging were seen to be equivalent to those in the 2" thick plate.

8.2.17.2 LHA, R.T., R=0.08, 360 cpm, WR direction - In the WR direction the low humidity air growth rates of 1.5" thick diffusion bonded plate, a beta processed plus mill annealed extrusion, and a 2.5" thick recrystallization annealed plate all fell within the scatter band of the 1.5" thick RA plate, while growth rates in a 4" x 10" x 34" RA hand forging were seen to be slightly lower than those in the above forms and conditions (Figure 8.2.17.2-1).

8.2.17.3 LHA, R.T., R=0.3, 360 cpm, RW direction - At an R factor of 0.3, the scatter band for low humidity air growth rates in 1.5" RA plate was again seen to be very narrow, and enveloped the growth rate curve of 0.625" diffusion bonded plate up to a delta K level of ~17 ksi $\sqrt{in}$ (Figure 8.2.17.3-1). At higher levels of delta K, however, growth rates in this diffusion bonded plate were seen to be significantly greater than those in 1.5" RA plate, a 1.5" beta processed plus mill annealed plate, a 4" x 10" x 34" RA hand forging, and a beta processed plus mill annealed extrusion. Growth rates in the beta processed plus mill annealed plate and extrusion were somewhat slower than the remaining product forms and conditions over the delta K range of 10-15 ksi $\sqrt{in}$ (Figure 8.2.17.3-1).

8.2.17.4 LHA, R.T., R=0.5, 360 cpm, RW direction - At delta K levels of ~17 ksi $\sqrt{in}$ the low humidity air growth rates in 1.5" RA plates, a 4" x 10" x 34" RA hand forging and a beta processed plus mill annealed extrusion were essentially equivalent when the R factor of test was at 0.5 (Figure 8.2.17.4-1). Below this level of delta K, however, the growth rates in the hand forging and extrusion were seen to be very slightly lower than those in the plate.

8.2.17.5 STW, R.T., R=0.08, 60 cpm, RW direction - In sump tank water there was no apparent effect of original plate thickness on growth rates at an R factor of 0.08 in the RW direction, with the results from nine different tests falling within a single, fairly narrow scatter band (Figure 8.2.17.5-1). This band has been replotted in Figure 8.2.17.5-2 for comparison with growth rates in two RA die forgings, an RA hand forging, and a beta processed plus mill annealed extrusion. The latter figure indicates essentially equivalent growth rates in all of these product forms and conditions under these test conditions. The RA plate scatter band has also been replotted in Figure 8.2.17.5-3 for comparison with diffusion bonded plate, and with diffusion bond thermal cycled plate, the scatter bands of which have also been shown in this figure. At delta K levels below ~15-17 ksi$\sqrt{in}$, growth rates in diffusion bonded material are seen to be noticeably greater than those in either the RA plate or the diffusion bond thermal cycled plate, while over the delta K range of ~11-18 ksi $\sqrt{in}$ growth rates in diffusion bond thermal cycled plate are only slightly greater than those in RA plate (Figure 8.2.17.5-3).

8.2.17.6 STW, R.T., R=0.08, 60 cpm, WR direction - In the WR direction there again was no observed consistent effect of original plate thickness on sump tank water growth rates. Results of six different tests all fell within a scatter band which was fairly broad at low delta K levels, but narrowed considerably as delta K increased (Figure 8.2.17.6-1). Sump tank water growth rates in the WR direction of diffusion bonded plate were slightly greater than those in diffusion bond thermal cycled plate at delta K levels below ~15 ksi $\sqrt{in}$ (Figure 8.2.17.6-2). This effect was similar to that observed in the RW direction (compare with Figure 8.2.17.5-3). Figure 8.2.17.6-2 also reveals that inclusion of post-bonding thermal cycles tended to reduce sump tank water fatigue crack growth rates to levels even below those in diffusion bond thermal cycled material (no bond line present). The scatter bands of Figure 8.2.17.6-2 are seen to converge to a single band as delta K is increased from low levels up to ~25 ksi $\sqrt{in}$, where rates could be represented by a single band-that of the diffusion bond thermal cycled plate. In most cases of tests in diffusion bonded material, early stages of crack propagation (low ΔK) were seen to be contained within the plane of the bond, whereas at later stages the crack deviated from the bond plane into the parent material. The exact cause of this deviation has not yet been identified, but material texture is suspect at this time.

The scatter band of Figure 8.2.17.6-1 has been replotted for comparison with the bands in Figure 8.2.17.6-2 (Figure 8.2.17.6-3). From this figure it is seen that while growth rates in diffusion bonded material are slightly greater than those in RA plate at low levels of delta K, implementation of post-bonding thermal cycles can shift the growth rate scatter band to lower levels commensurate with those of the RA plate.

8.2.17.7 STW, R.T., R=0.3, 60 cpm, RW direction - Only limited sump tank water testing was performed on Ti-6Al-4V at an R factor of 0.3. Those specimens tested indicated no significant difference between growth rates in 1.5" thick diffusion bond thermal cycled plate and those in 1.5" beta processed plus mill annealed plate (Figure 8.2.17.7-1). Both of these rates were slightly lower at delta K levels below ~17 ksi $\sqrt{in}$ than were those in 1.5" RA plate.

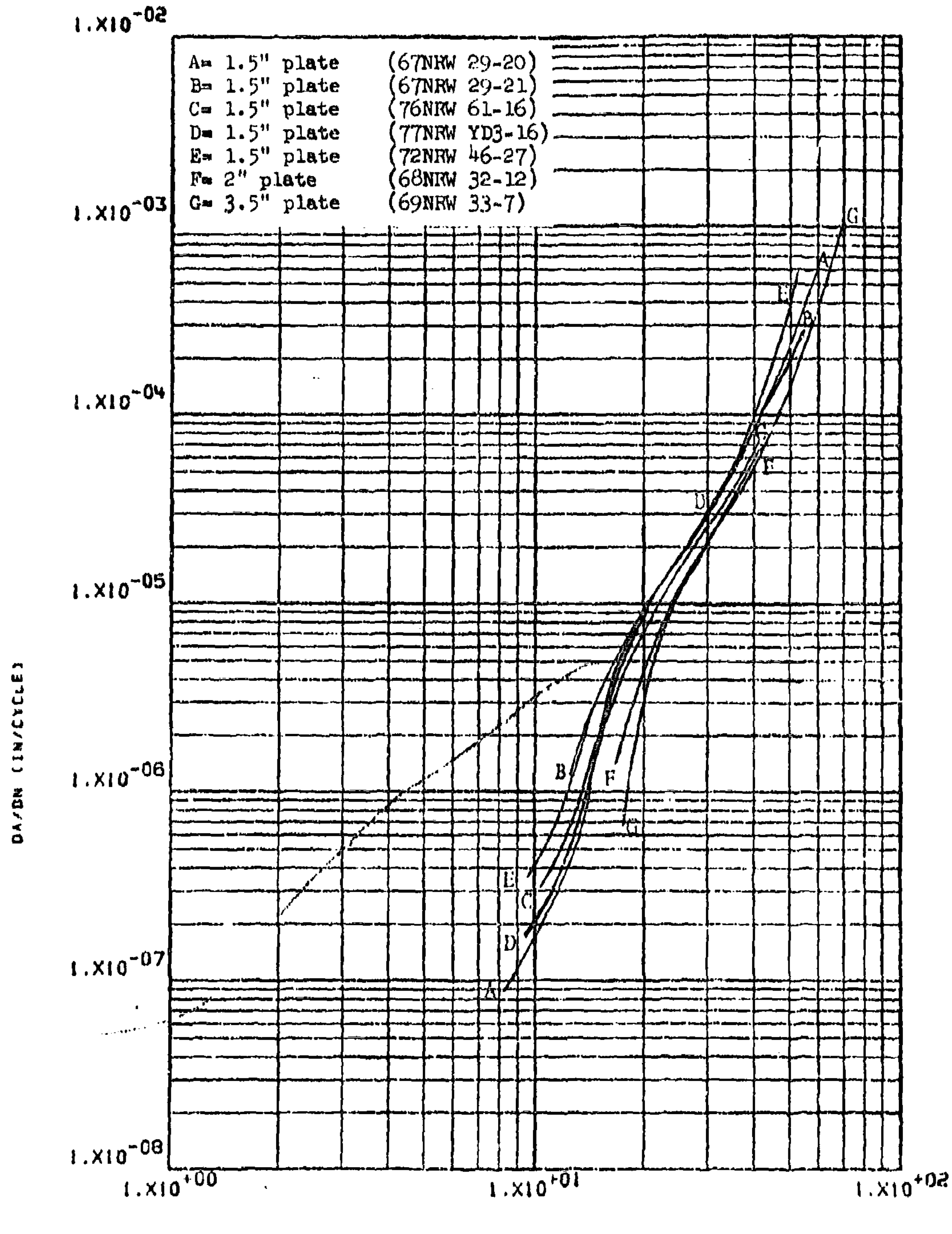

Figure 8.2.17.1-1 Effect of product form on the LHA-FCGR at R.T., R=0.08, 360 cpm, and RW direction in Ti-6Al-4V recrystallization annealed plate

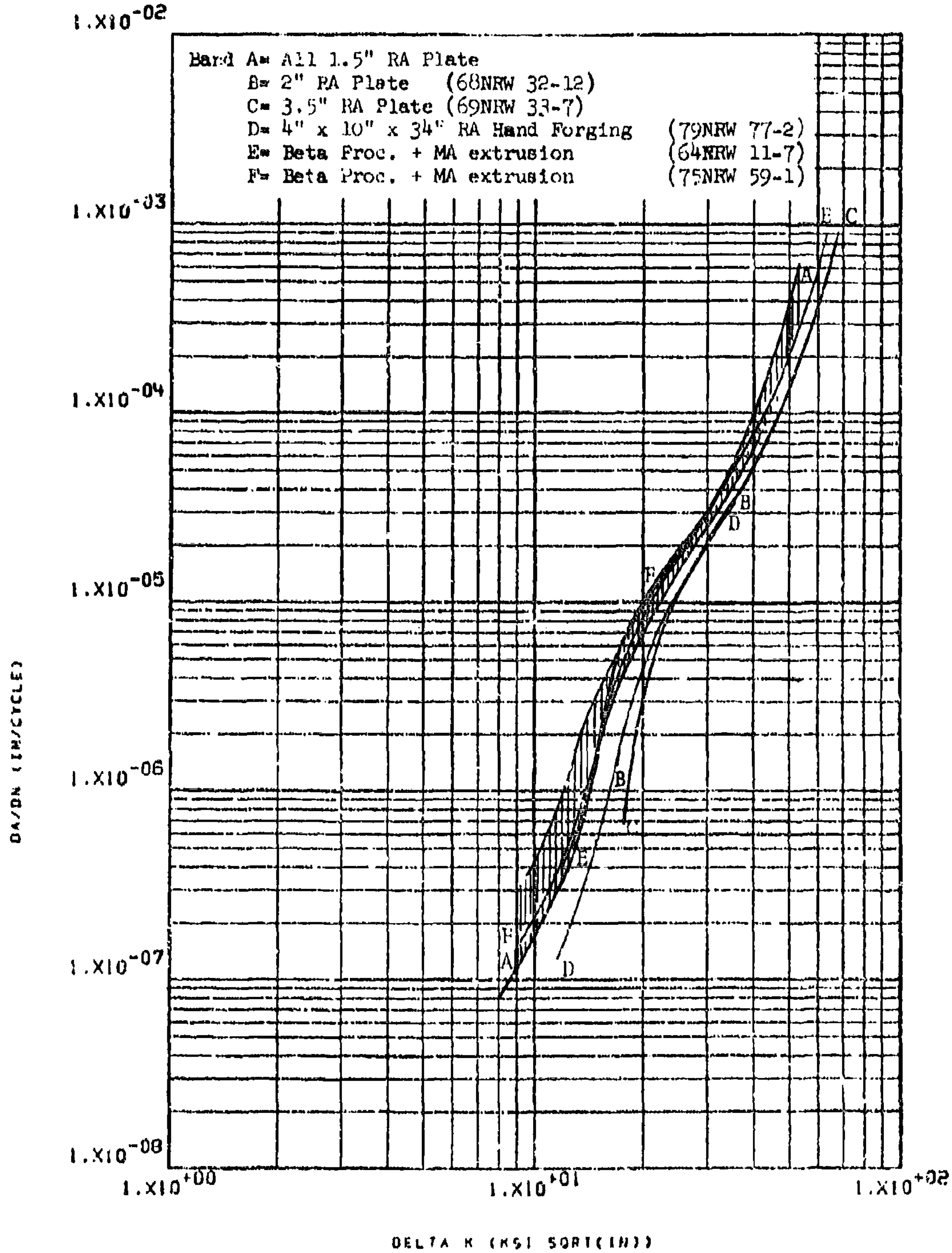

Figure 8.2.17.1-2 Effect of product form and heat treat condition on the LHA-FCGR at R.T., R=0.08, 360 cpm, and RW direction in Ti-6Al-4V

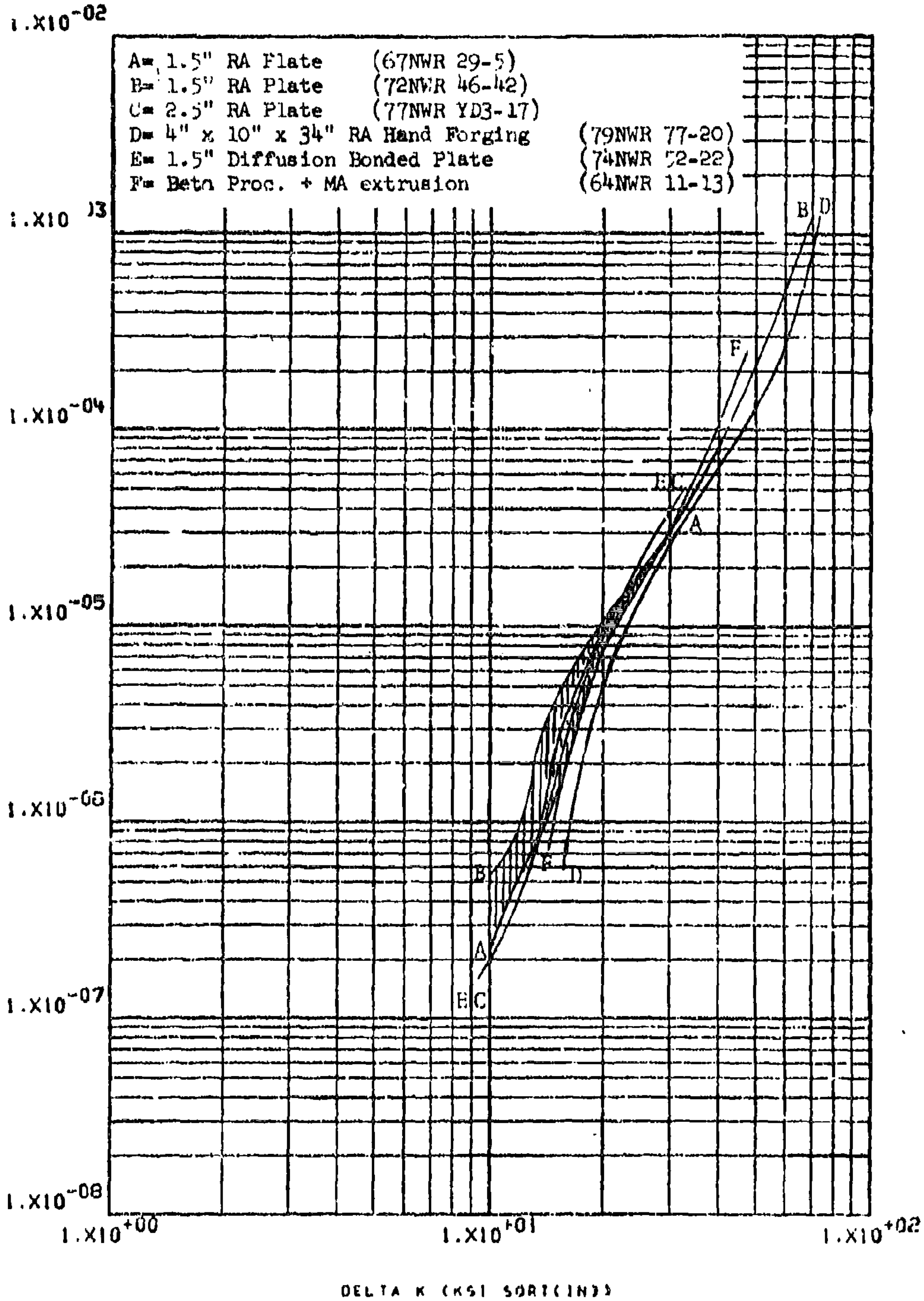

Figure 8.2.17.2-1 Effect of product form and heat treat condition on the LHA-FCGR at R.T., R=0.08, 360 cpm, and WR direction in Ti-6Al-4V

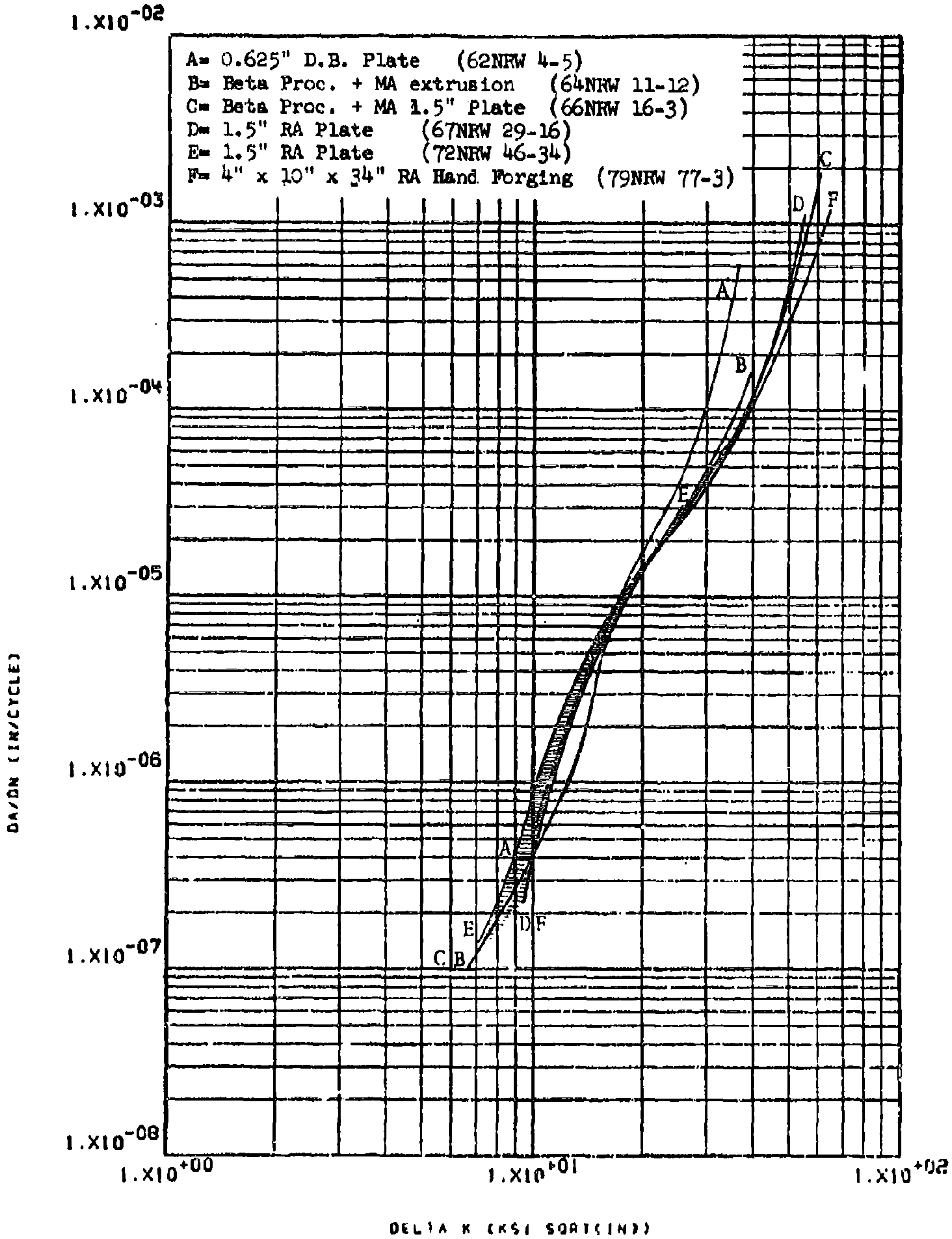

Figure 8.2.17.3-1 Effect of product form and heat treat condition on the LHA-FCGR at R.T., R=0.3, 360 cpm, and RW direction in Ti-6Al-4V

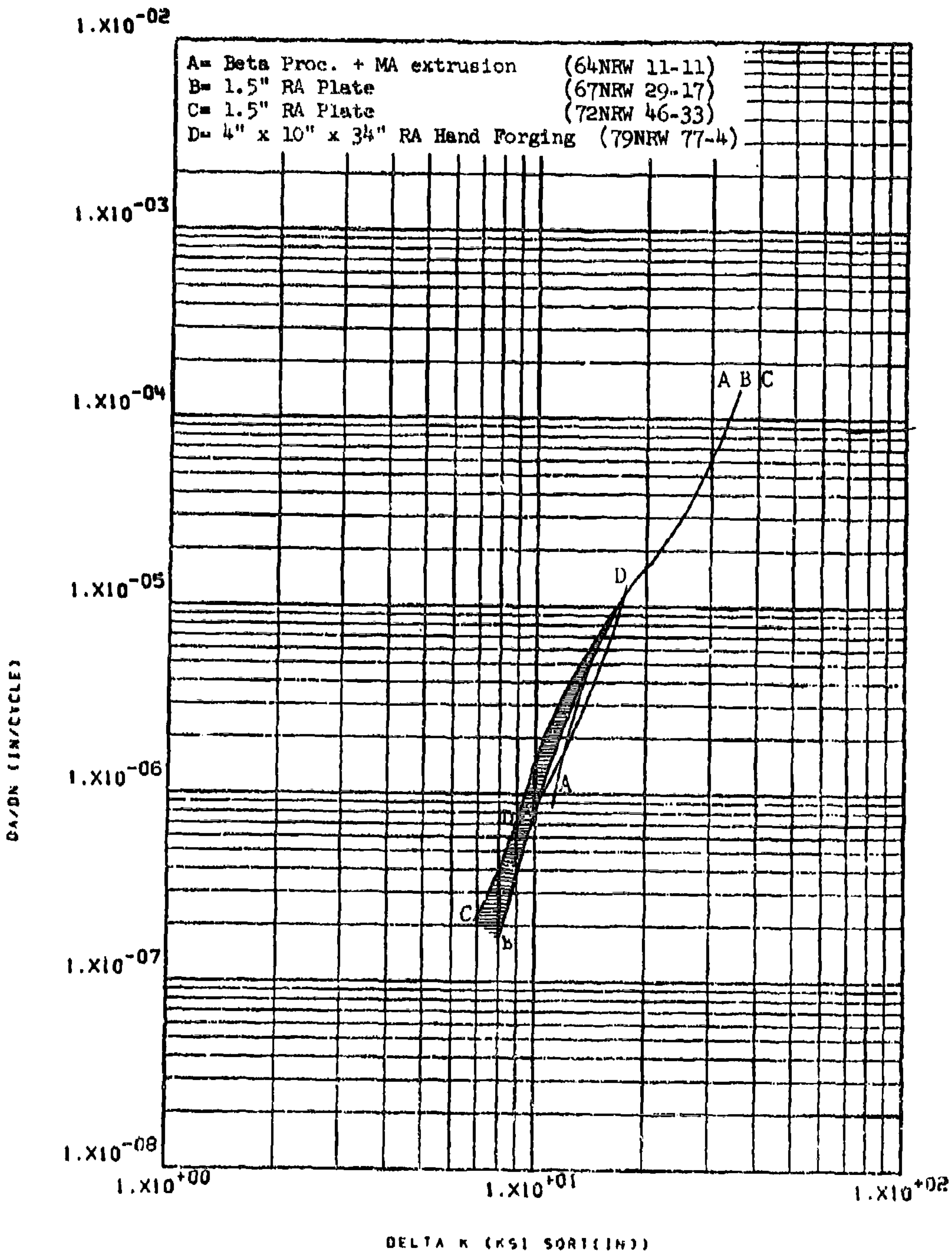

Figure 8.2.17.4-1 Effect of product form and heat treat condition on the LHA-FCGR at R.T., R=0.5, 360 cpm, and RW direction in Ti-6Al-4V

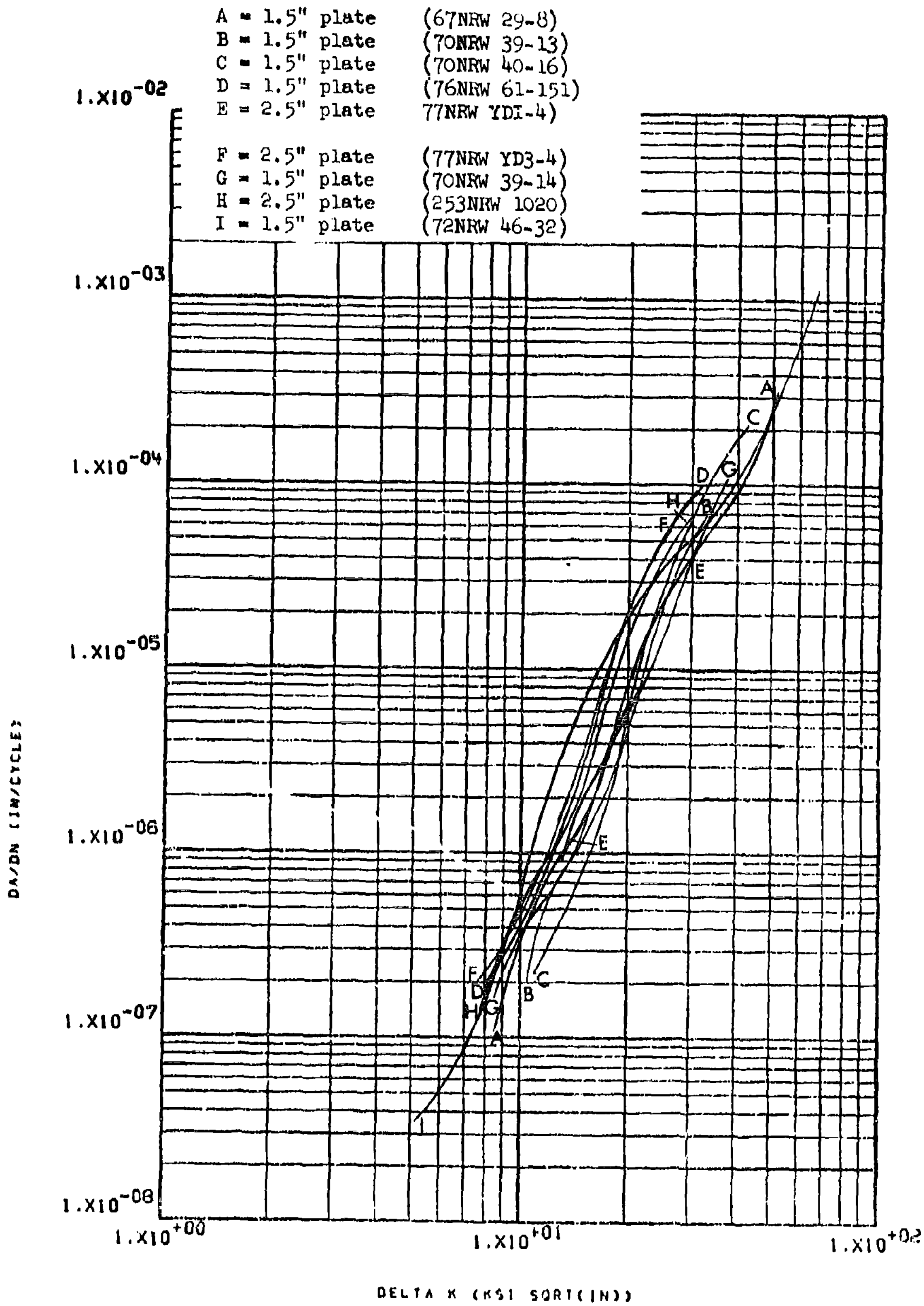

Figure 8.2.17.5-1 Effect of Product Form on the STW-FCGR at R.T., R=0.08, 60 cpm, and RW Direction in Ti-6Al-4V RA Plate

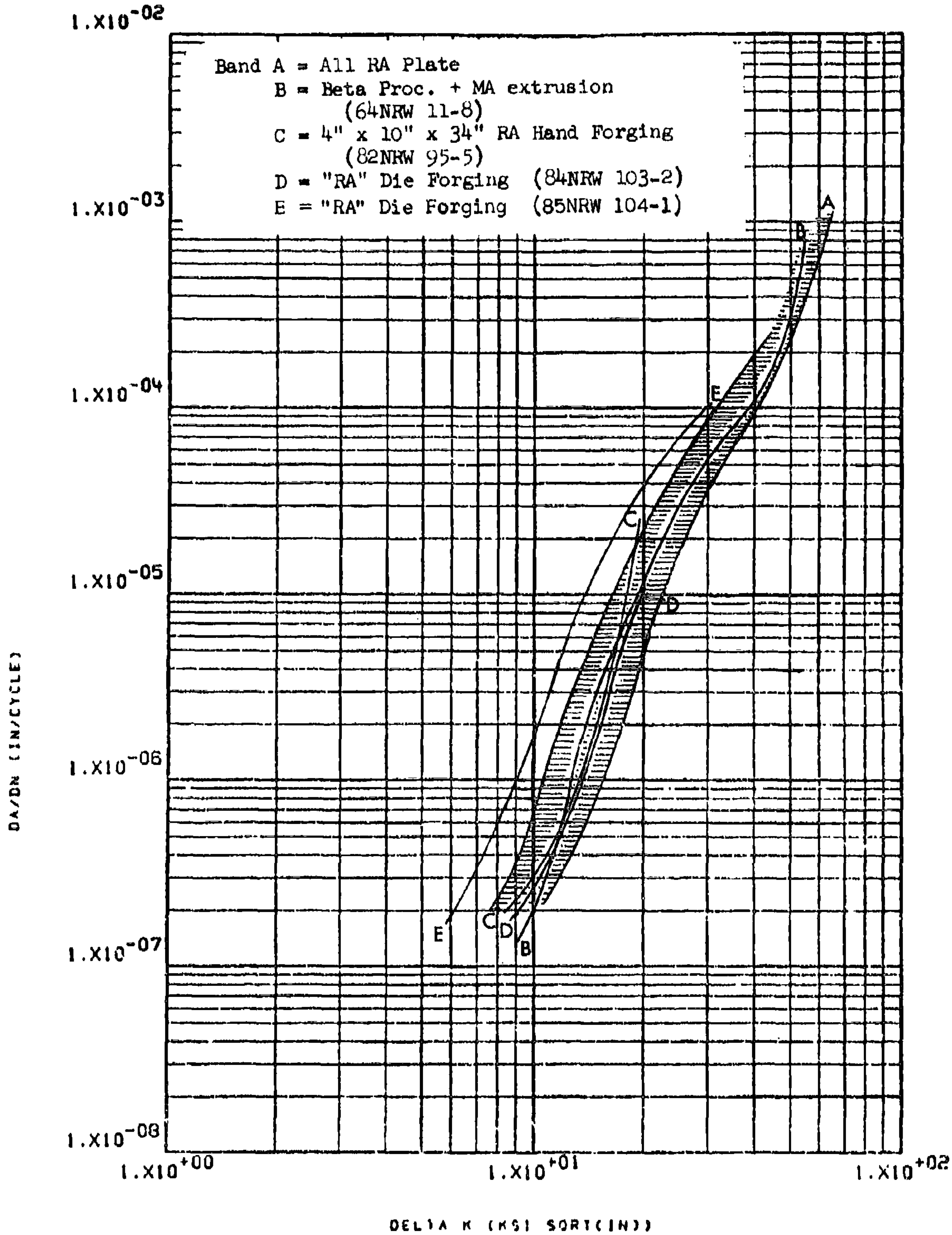

Figure 8.2.17.5-2 Effect of Product Form and Heat Treat Condition on the STW-FCGR at R.T., R= 0.08, 60 cpm, and RW Direction in Ti-6Al-4V

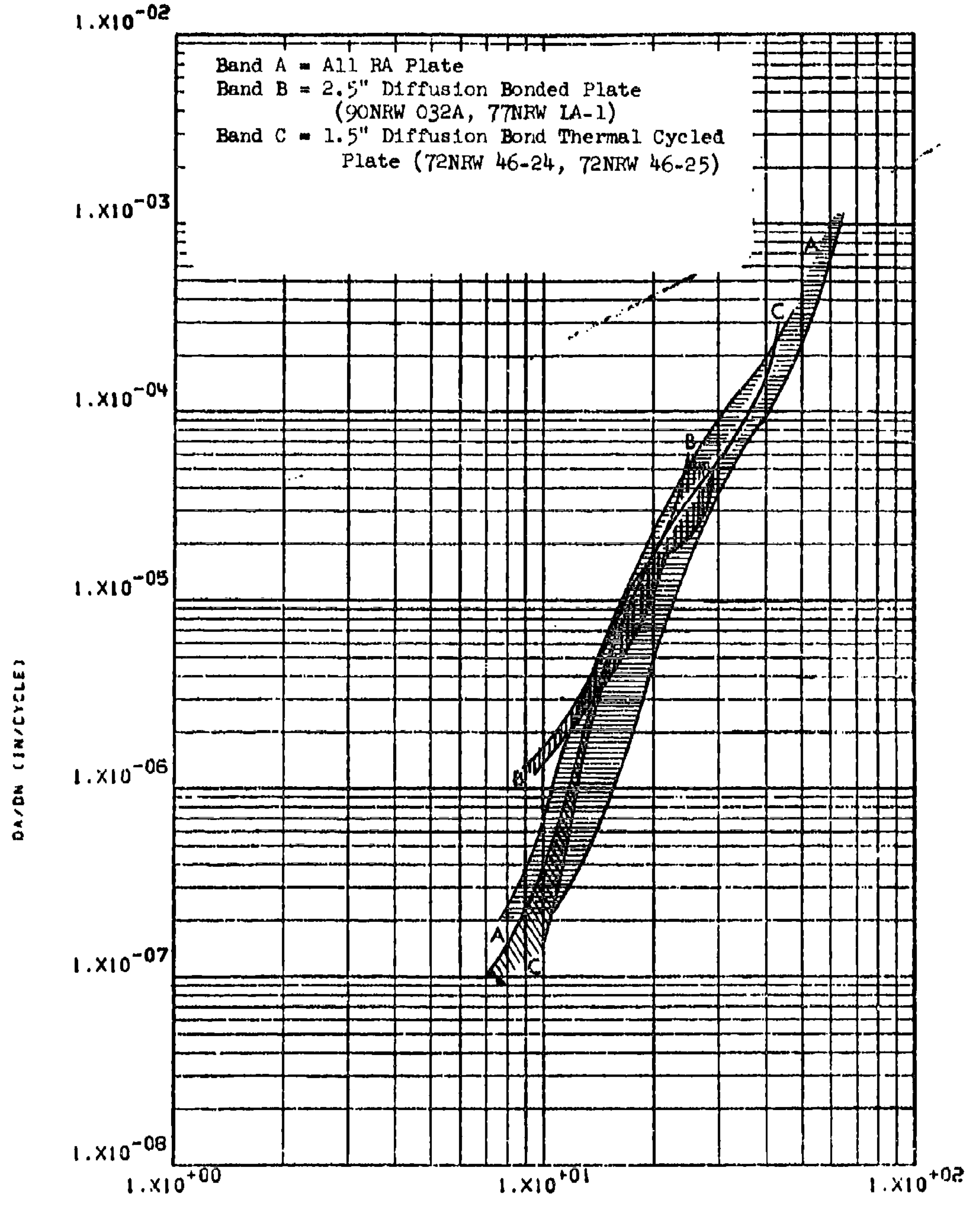

Figure 8.2.17.5-3 Effect of Heat Treat Condition and Product Form on the STW-FCGR at R.T., R=0.08, 60 cpm, and RW Direction in Ti-6Al-4V

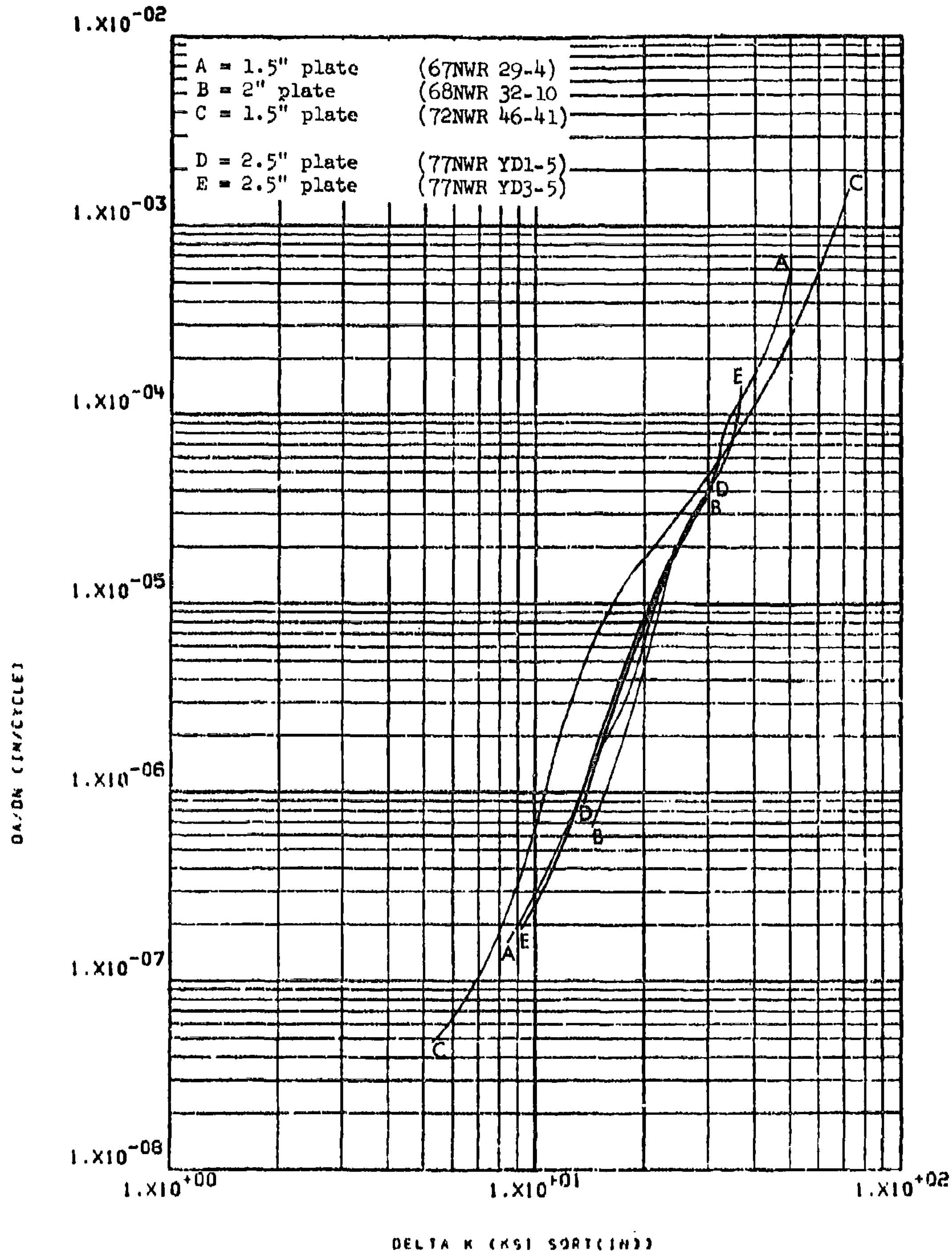

Figure 8.2.17.6-1 Effect of Product Form on the STW-FCGR at R.T., R=0.08, 60 cpm, and WR Direction in Ti-6Al-4V RA 1.5" to 2.5" Thick Plate

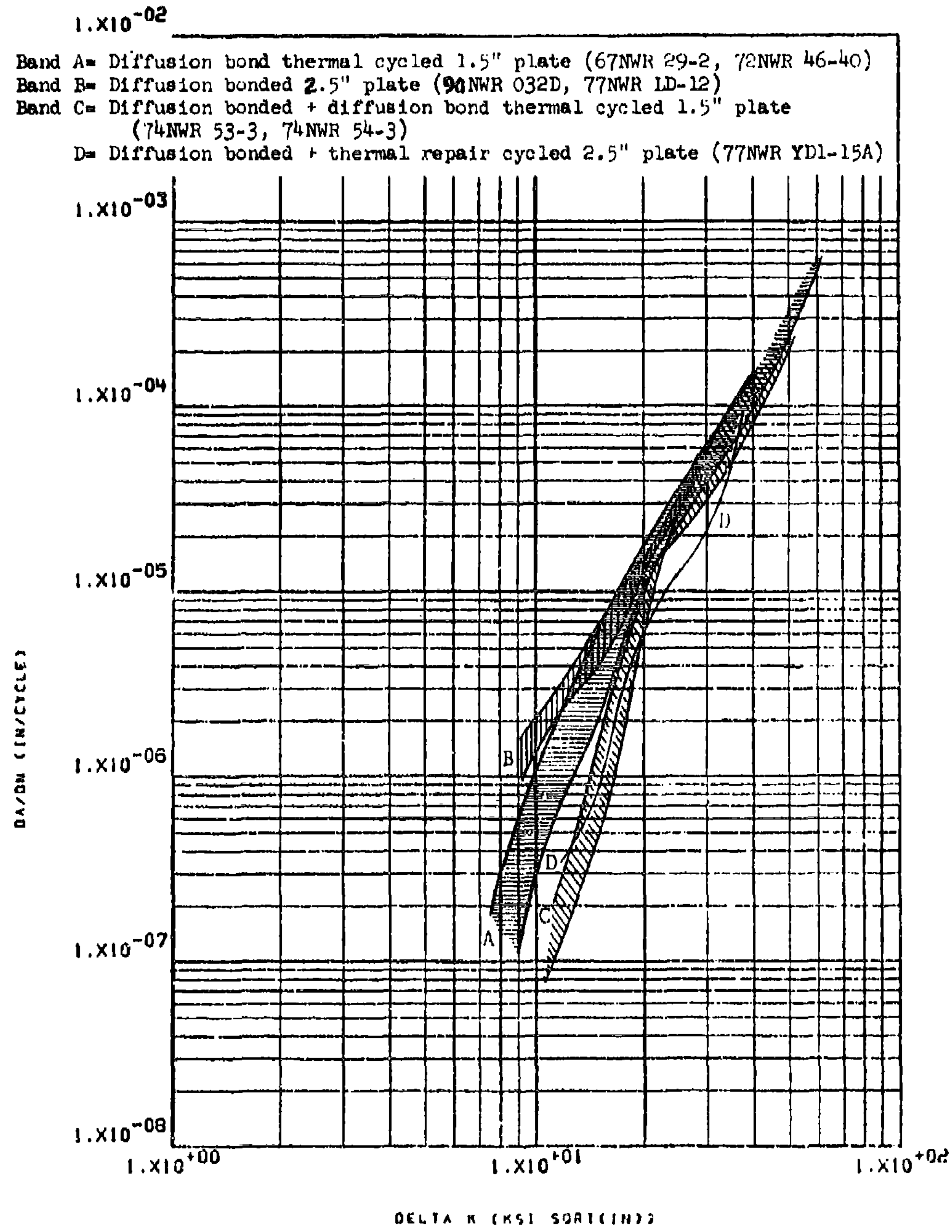

Figure 8.2.17.6-2 Effect of product form and heat treat condition on the STW-FCGR at R.T., R=0.08, 60 cpm, and WR direction in Ti-6Al-4V plate

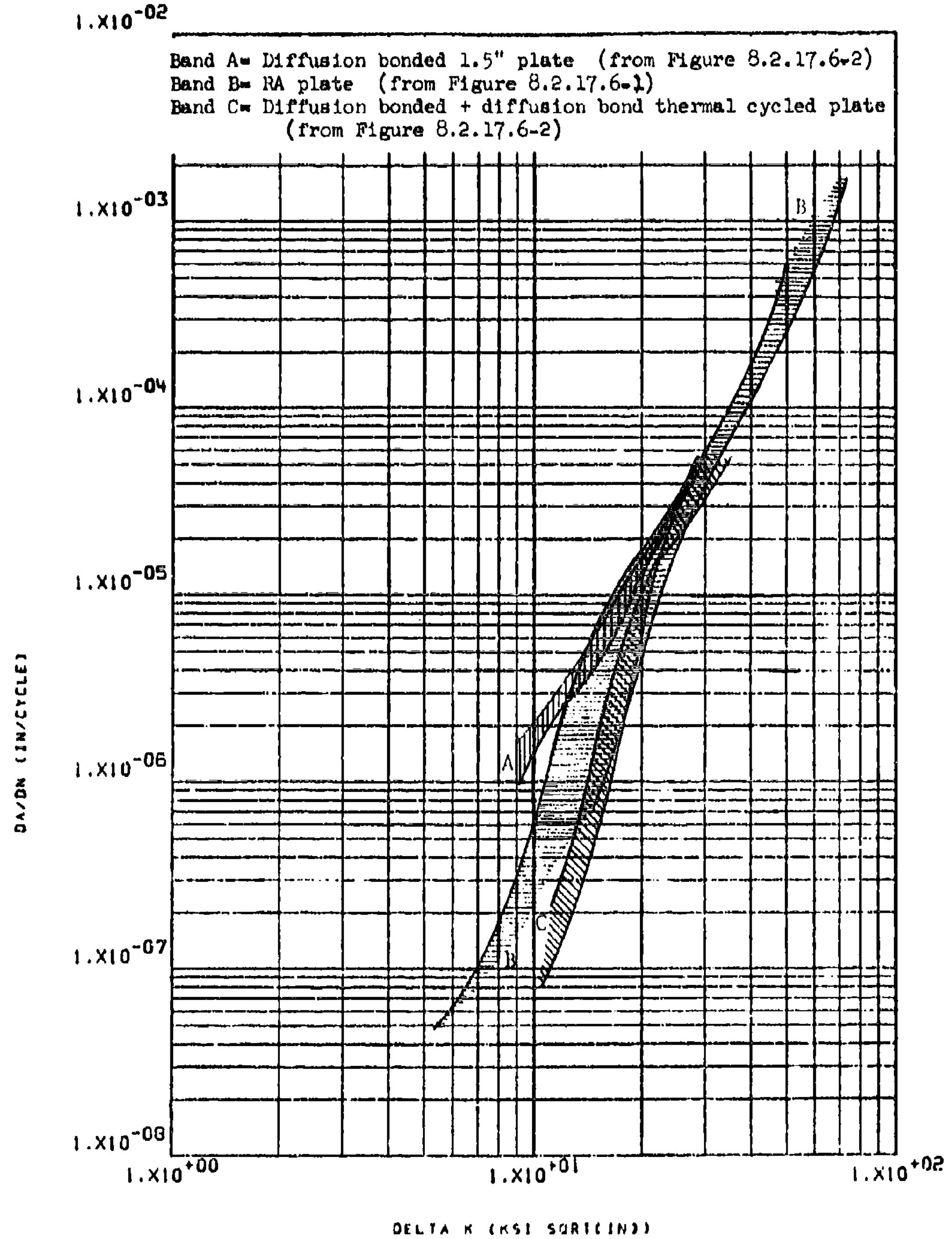

Figure 8.2.17.6-3 Effect of product form and heat treat condition on the STW-FCGR at R.T., R=0.08, 60 cpm, and WR direction in Ti-6Al-4V plate

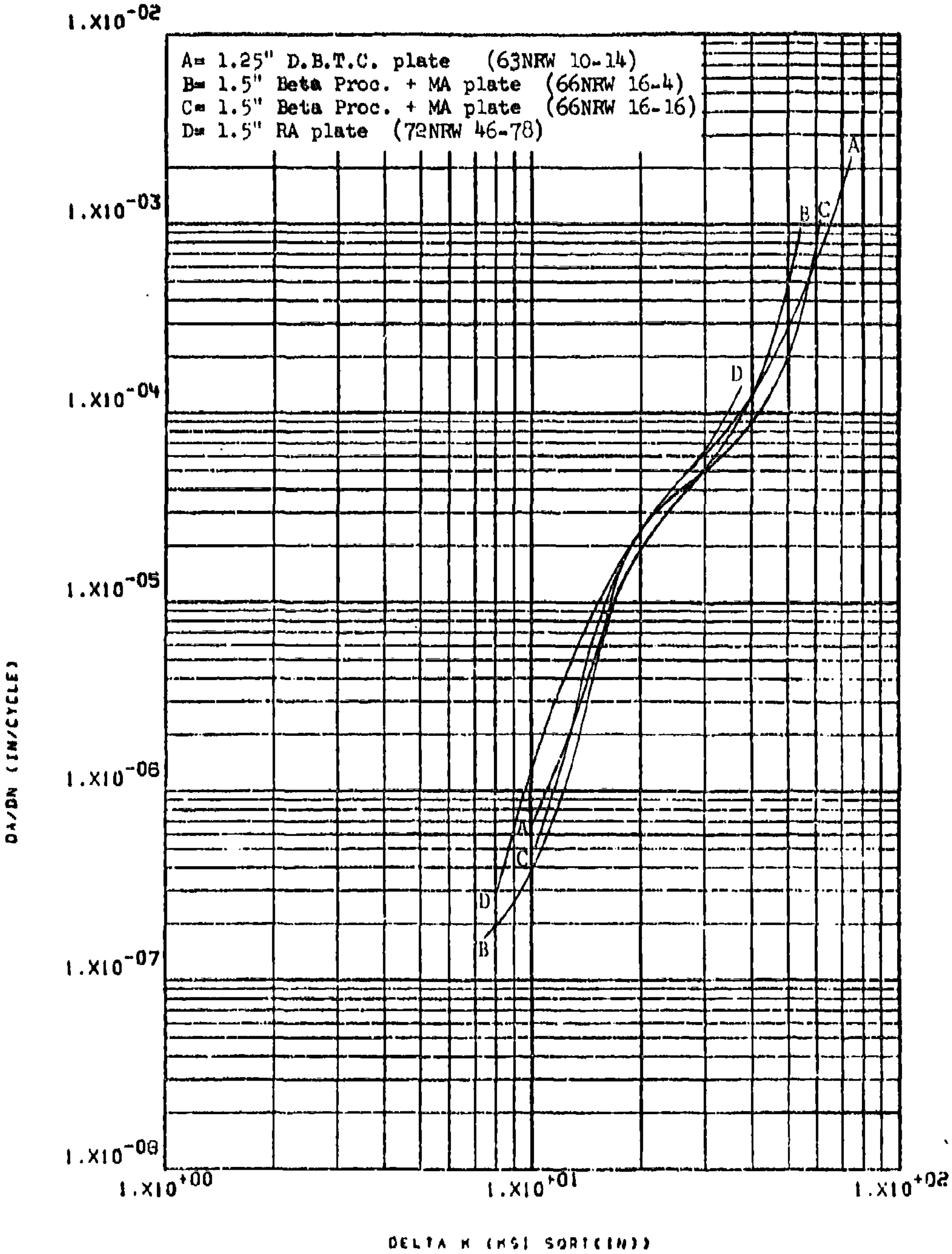

Figure 8.2.17.7-1 Effect of product form and heat treat condition on the STW-FCGR at R.T., R=0.3, 60 cpm, and RW direction in Ti-6Al-4V plate

8.3 Summary and Conclusions

8.3.1 In light of the number of testing variables associated with fatigue crack growth rate testing, a summary of test results must inherently be in the form of generalizations, and conclusions drawn from this summary must be interpretted cautiously. With this word of caution, an attempt has been made to present the salient features of this growth rate characterization study, realizing that in certain instances what may be true for one alloy system may not necessarily be true for another system under the same circumstances, but rather represents a general trend for all material systems.

8.3.2 Cyclic Frequency - Low humidity air fatigue crack growth rates in parent material and welds of Ti-6Al-4V and the steels were essentially unaffected by changing test frequency from 360 to 60 cpm, as were sump tank water growth rates when the frequency was decreased from 60 to 6 cpm. In the aluminum alloys, however, growth rates were significantly increased in low humidity air when the frequency was decreased from 360 cpm to 60 cpm, and in sump tank water when the frequency was decreased from 60 to 6 cpm. These results suggest that environmental crack growth acceleration may be operative in the aluminum alloys even in low humidity air environments where moisture content is limited.

8.3.3 Test Temperature - Low humidity air fatigue crack growth rates in Ti-6Al-4V, Inconel 718 and the steels were essentially unchanged when the test temperature was increased from ambient to 265°F (or 400°F in the case of Inconel 718), but were noticeably decreased as the temperature was dropped from ambient to -65°F in Ti-6Al-4V and steel parent materials and HP-9-4-.20 weld HAZ. In the case of Ti-6Al-4V weld HAZ this latter effect ranged from slight to non-existent depending on the product form evaluated. Low humidity air growth rates in the aluminum alloys 2024, 2219, and 7075 were seen to be significantly accelerated when the temperature of test was increased from ambient to 265°F, and sump tank water rates were similarly accelerated in 2024 when the temperature was increased to 150°F. 7175 was the only aluminum alloy observed to be unaffected in low humidity air growth rates by increasing the temperature from ambient to +265°F. These effects are consistent with general effects of temperature on material strengths over the temperature ranges investigated.

8.3.4 Specimen Thickness - The effects of specimen thickness on low humidity air fatigue crack growth rates were seen to be dependent on material type. When an effect was seen to exist growth rates were generally seen to be greater in the thicker specimens. This was seen to be true in 7049 and 7175 aluminum alloys, HP-9-4-.20, PH13-8Mo steels (parent metals) and Ti-6Al-4V weld HAZ. Specimen thickness effects in remaining materials were either non-existent, not significant or not evaluated.

8.3.5 R Factor - Growth rates in low humidity air and sump tank water were generally seen to increase significantly with increasing values of stress ratio, R. In one system, however, that of the aluminum alloy 2219, an R factor cut-off was observed in low humidity air wherein growth rates were accelerated by increasing R from 0.08 to 0.3, but no further increases in growth rates were observed as R was increased from 0.3 to 0.5. This cut-off effect was not observed to occur for 2219 in sump tank water, indicating that its probable cause, crack closure phenomena, as presented by numerous investigators, is either non-existent in, or severely affected by aggressive environments.

8.3.6 Environment - Changing test environments from low humidity air to sump tank water was seen to result in fatigue crack growth rate accelerations ranging from slight to substantial in Ti-6Al-4V, 300M steel, and welded Ti-6Al-4V and PH13-8Mo. STW growth rates were also seen to be substantially greater than LHA growth rates in PH13-8Mo and the 7000 series aluminum alloys only when above particular levels of ΔK. In 2000 series aluminum alloys, Inconel 718, HP-9-4-.20, and HP-9-4-.30 steels growth rates in both environments were essentially equivalent.

Shop cleaning solvent was seen to be essentially a non-aggressive environment, in comparison with low humidity air growth rates, with respect to 2219 aluminum alloy, Inconel 718, and HP-9-4-.20. Growth rates in this environment were seen to be accelerated over those in low humidity air for 7075 and 7175 aluminum alloys, PH13-8Mo (above a particular level of ΔK), and Ti-6Al-4V welds.

Distilled water was also seen to be a non-aggressive environment with respect to Ti-6Al-4V and 2219 aluminum alloy, as was jet fuel with respect to Ti-6Al-4V and 2024 aluminum alloy.

Field cleaning solvent was seen to be non-aggressive with respect to 2219 aluminum alloy, while causing some acceleration of growth rates in 7175 aluminum alloy at low ΔK levels.

In light of the above summary and that associated with cyclic frequency effects (Section 8.3.2), particularly with respect to the aluminum alloys, it appears that growth rates are more substantially affected by the time that the environment has to act on the crack tip region than by the nature of the environment itself. Note that while no difference is observed between STW and LHA growth rates in 2219 at 60 cpm, substantial differences in growth rates are observed between LHA tests run at 60 and 360 cpm, and between STW tests run at 6 and 60 cpm. The comparison would suggest that STW is non-aggressive with respect to LHA, while the latter two comparisons show that both STW and LHA may be aggressive under appropriate test conditions.

8.3.7 Test Direction - Fatigue crack growth rates in low humidity air and sump tank water were seen to be independent of test direction in 7050 and 7075 aluminum alloys, HP-9-4-.20, HP-9-4-.30, and 300M steels, Inconel 718 forged block, and for all practical purposes, Ti-6Al-4V (one of twenty product forms demonstrated some directionality). In the 2000 series aluminum alloys (2024, 2124, and 2219) growth rates in both environments were faster in WR specimens than in RW specimens, while in 7049 and 7175 the opposite was found to be true up to ΔK levels of 11-13 ksi $\sqrt{in}$, above which the rates were seen to be equivalent. In PH13-8Mo, LHA growth rates were faster in RW specimens at ambient temperature than in WR specimens, while at -65°F this observation was reversed. Inconel 718 hot die forgings also demonstrated a reversal with rates in WR specimens being faster than those in RW specimens in low humidity air, but slower than those in RW specimens in sump tank water.

8.3.8 Product Form - The dependence of fatigue crack growth rates on product form was seen to be a function of each alloy system so that no generalizations were made for this variable.

8.3.9 Heat Treat Condition - As above the effect of heat treat condition on fatigue crack growth rates was seen to be a function of each alloy system. Attention is therefore directed to individual sections (8.2.1.8, 8.2.7.8, and 8.2.14.1.8).

8.3.10 Alloy Type - In comparing entire alloy systems with each other under fixed sets of test parameters, certain trends were evident which allowed ranking of these systems with respect to their fatigue crack growth rate characteristics under those parameters. A summary of those trends is presented in Table 8.3.10-1. Again, caution must be exercised in the interpretation of this summary, realizing that it represents trends and that exceptions to these trends were observed within almost every alloy system. In ranking each alloy system, comparative curves presented in Sections 8.2.15 through 8.2.17 were utilized. If growth rates of two or more alloy systems were seen to be essentially equivalent over the entire ΔK range, under a particular set of test parameters, they were listed in the same rank column for that test condition. If, however, growth rates in one system were slightly greater than another they were listed in separate rank columns, accordingly, separated by "approximately equal" ($\approx$) signs. Where differences in growth rates were slight but noticeable they were separated by "less than" ($<$) signs, and where significant differences were observed these differences were denoted by "much less than" ($\ll$) signs.

In all cases where comparisions with Inconel 718 could be made, the growth rates in this material were seen to be substantially slower than in all other materials evaluated. This included the RW and WR directions in low humidity air and sump tank water at an R factor of 0.08, and the RW direction in low humidity air at an R factor of 0.5.

In low humidity air, growth rates of all the steels were generally equivalent to each other and significantly faster than those of Inconel 718. Growth rates in Ti-6Al-4V were usually observed to be greater than those of steels in low humidity air but the magnitude of this difference decreased as ΔK levels were dropped until at ~10-20 ksi $\sqrt{in}$ the rates in Ti-6Al-4V and the steels were essentially equivalent. In all low humidity air comparisons, growth rates of all aluminum alloys were observed to be significantly greater than those of Ti-6Al-4V, all steels and Inconel 718.

The ranking of materials, particularly 300M steel and the 7000 series aluminum alloys was significantly influenced by test environment. In low humidity air growth rates of the 2000 series and 7000 series aluminum alloys were all essentially equivalent, whereas in sump tank water growth rates of the 7000 series were significantly faster than those of the 2000 series. 300M steel was similarly shifted backward in the ranking order, when tested in sump tank water, from having one of the slowest crack growth rates to having one of the fastest growth rates.

Test direction was seen to effect this material ranking system only slightly by reflecting slower sump tank water growth rates in the WR direction of PH13-8Mo and Ti-6Al-4V than in the RW direction. Trends were not observed to change by increasing R factors.

TABLE 8.3.10-1

SUMMARY RANKING OF ALLOY SYSTEMS WITH RESPECT TO FATIGUE CRACK GROWTH RATE CHARACTERISTICS UNDER FIXED TEST PARAMETERS

Test Conditions	Growth Rate Ranking: 1 (Slowest)	2	3	4	5	6	7 (Fastest)
LHA, R.T., R= .08, RW Dir.	Inconel 718 ≪	300M, 9-4-.20, 9-4-.30 ≈	PH13-8Mo <	Ti-6-4(1) ≪	All Aluminum		
STW, R.T., R=0.08, RW Dir.	Inconel 718 ≪	9-4-.20, 9-4-.30 <	PH13-8Mo ≈	Ti-6-4 ≪	2000 Sers. Aluminum ≈	300M ≈	7000 Sers. Aluminum
LHA, R.T., R=0.08, WR Dir.	Inconel 718 ≪	PH13-8Mo <	300M ≈	9-4-.20, 9-4-.30 <	Ti-6-4(2) <	All Aluminum	
STW, R.T., R=0.08, WR Dir.	Inconel 718 ≪	PH13-8Mo, Ti-6-4 ≪	2000 Sers. Aluminum ≈	300M ≈	7000 Sers. Aluminum		
LHA, R.T., R=0.3, RW Dir.	300M, 9-4-.20, 9-4-.30, PH13-8Mo <	Ti-6-4 ≪	All Aluminum				
STW, R.T., R=0.3, RW Dir.	9-4-.30, PH13-8Mo	Ti-6-4 ≪	2000 Sers. Aluminum ≈	300M ≈	7000 Sers. Aluminum		
LHA, R.T., R=0.5, RW Dir.	Inconel 718 ≪	9-4-.20, 9-4-.30, PH13-8Mo, 300M <	Ti-6-4 ≪	All Aluminum			
STW, R.T., R=0.5, RW Dir.	9-4-.30 ≪	2000 Sers. Aluminum ≈	300M ≈	7000 Sers. Aluminum			

(1) at $\Delta K > 11\text{-}15$ ksi $\sqrt{in.}$

(2) at $\Delta K > 15\text{-}20$ ksi $\sqrt{in.}$

Section 9: References and Nomenclature

9.1 References:

(a) Rockwell International Corporation, B-1 Division, "Crack Growth Retardation Under Aircraft Spectrum Loads," NA-72-374, 26 Jan. 1973.

(b) Rockwell International Corporation, B-1 Division, "Effect of R Factor and Crack Closure on Fatigue Crack Growth for Aluminum and Titanium Alloys," NA-73-724, 22 October 1973.

(d) Rockwell International Corporation, B-1 Division, "B-1 Fracture Mechanics Material Property Test Results," NA-71-373, 28 Aug. 1971.

(e) Piper, D.E.,"Proposed Method of Test for Stress-Corrosion Cracking Using a Single-Edge-Cracked Plate Specimen Crackline Loaded by Constant Deflection," specification submitted to ASTM Sub-committee G-01.06, 4 August 1970.

(f) Battelle - Columbus Laboratories, Damage Tolerant Design Handbook MCIC-HB-01, 1973, p 11.1.1-3.

(g) "Plane-Strain Fracture Toughness of Metallic Materials", ASTM Specification E399-72.

(h) "Proposed Recommended Standard for R-Curve Determination", ASTM E-24.01.04 Task Group on Crack Growth Resistance Curves, Jan. 1973.

(i) Irwin, G.R., "Theoretical Aspects of Fracture Failure Analysis," Metals Engineering Quarterly, Feb. 1963.

(j) Air Force Flight Dynamics Laboratory, Fracture Mechanics Guidelines for Aircraft Structural Applications, by D. P. Wilhem, Feb. 1970, p. 124.

(k) Plane Strain Crack Toughness Testing, ASTM STP 410, Mar. 1969, p. 77.

(l) Hyatt, M.V, "Use of Precracked Specimens in Stress Corrosion Testing of High Strength Aluminum Alloys," Corrosion, vol. 26, no. 11, Nov. 1970.

(m) Rockwell International Corporation, B-1 Division "Computer Tabulated Fatigue Crack Growth Data Generated from CT Specimens Tested in the B-1 Fracture Mechanics Program," TFD-74-449, 2 April 1975.

9.2 Nomenclature

a	Crack length as measured from load line for CT and DCB specimens. Crack depth as measured from specimen surface for PTC specimens. One-half total crack length as measured from crack tip to crack tip for CCT specimens.
a_o	Initial crack length
a_f	Final crack length
AC	Air Cool
B	Specimen Thickness
BA	Beta annealed
C	Specimen compliance, COD/P
2c	Surface length of a part-through-crack
CCT	Center-cracked-tension
COD	Crack opening displacement
cpm	Cycles per minute
CT	Compact Tension
da/dn	Cyclic crack growth rate
DB	Diffusion bonded
DBTC	Diffusion bond thermal cycle
DCB	Double Cantilever beam
E	Elastic modulus
EDM	Electrical discharge machining
Extr	Extrusion
FCGR	Fatigue crack growth rate
FCS	Field Cleaning solvent
GTA.	Gas Tungsten arc weld
H	Half-height of a CT or DCB specimen
HT	Heat Treated
HAZ	Heat affected zone
K	Stress Intensity
K_I	Stress-intensity
K_{Ii}	Initial stress-intensity
K_{If}	Final stress-intensity
K_c	Failure stress intensity
K_{Ic}	Plane-strain fracture toughness stress intensity
K_{Iscc}	Stress-corrosion cracking arrest stress-intensity

9.2 Nomenclature - Continued

K_Q	Invalid stress intensity K_{Ic} test value
LA	Laboratory Air
LHA	Low Humidity Air
N	Cycles
MA	Mill Annealed
Man'l	Manual
Mach	Machine
Mat'l	Material
OQ	Oil quench
P	Load
PAW	Plasma arc weld
PTC	Part-through-crack
R	Load ratio, Pmax/Pmin
RA	Recrystallization annealed
RT	Room temperature
SCS	Shop cleaning solvent
SR	Stress Relief
STOA	Solution Treated and overaged
STW	Sump tank water
t	Thickness
TR	Thermal repair heat treatment consisting of 1400F, 1 hr. AC
TY	0.2% offset tensile yield strength
TU	Tensile ultimate strength
W	Specimen width as measured from loadline for CT and DCB specimens and as measured from edge to edge for CCT specimen.

☆ U. S. GOVERNMENT PRINTING OFFICE: 1977 — 757-001/596